ISSN 0021-9673

ISHED
TNIGHTLY

VOL. 126 NOVEMBER 3, 1976

COMPLETE IN ONE ISSUE

Advances in Chromatography 1976
Houston, Texas, November 1–5, 1976

RNAL OF

CHROMATOGRAPHY

ERNATIONAL JOURNAL ON CHROMATOGRAPHY, ELECTROPHORESIS AND RELATED METHODS

EDITOR, Michael Lederer (Rome)
ASSOCIATE EDITOR, K. Macek (Prague)
EDITORIAL BOARD
W. A. Aue (Halifax)
V. G. Berezkin (Moscow)
A. Bevenue (Honolulu, Hawaii)
P. Boulanger (Lille)
A. A. Boulton (Saskatoon)
G. P. Cartoni (Rome)
K. V. Chmutov (Moscow)
G. Duyckaerts (Liège)
L. Fishbein (Jefferson, Ark.)
A. Frigerio (Milan)
C. W. Gehrke (Columbia, Mo.)
E. Gil-Av (Rehovot)
G. Guiochon (Palaiseau)
I. M. Hais (Hradec Králové)
N. G. L. Harding (Cambridge)
E. Heftmann (Berkeley, Calif.)
S. Hjertén (Uppsala)
E. C. Horning (Houston, Texas)
J. F. K. Huber (Vienna)
A. T. James (Sharnbrook)
J. Janák (Brno)
A. I. M. Keulemans (Eindhoven)
K. A. Kraus (Oak Ridge, Tenn.)
E. Lederer (Gif-sur-Yvette)
A. Liberti (Rome)
H. M. McNair (Blacksburg, Va.)
Y. Marcus (Jerusalem)
G. B. Marini-Bettòlo (Rome)
R. Neher (Basel)
G. Nickless (Bristol)
J. Novák (Brno)
O. Samuelson (Göteborg)
G.-M. Schwab (Munich)
G. Semenza (Zürich)
L. R. Snyder (Tarrytown, N.Y.)
A. Zlatkis (Houston, Texas)
EDITORS, BIBLIOGRAPHY SECTION
K. Macek (Prague), J. Janák (Brno), Z. Deyl (Prague)
EDITOR, BOOK REVIEW SECTION
R. Amos (Abingdon)
EDITOR, NEWS SECTION
J. F. K. Huber (Vienna)
COORD. EDITOR, DATA SECTION
J. Gasparič (Hradec Králové)

ELSEVIER SCIENTIFIC PUBLISHING COMPANY
AMSTERDAM

CONTENTS

Eleventh International Symposium on Advances in Chromatography, Houston, Texas (U.S.A), November 1–5, 1976

Contents VII

Foreword XI

Winners of the M. S. Tswett Chromatography Medal XIII

New horizons

Continuous and ultrasensitive apparatus for the measurement of air-borne tracer substances
by P. G. Simmonds (Ringwood, Great Britain) and A. J. Lovelock and J. E. Lovelock (Bowerchalke, Great Britain) 3

Heater-displacement chromatography
by C. M. A. Badger, J. A. Harris, K. F. Scott, M. J. Walker and C. S. G. Phillips (Oxford, Great Britain) 11

Particle size, pressure and analysis time in routine high-performance liquid chromatography
by I. Halász, H. Schmidt and P. Vogtel (Saarbrücken, G.F.R.) 19

Thin-layer chromatographic transport detector for high-performance liquid chromatography
by P. R. Boshoff, B. J. Hopkins and V. Pretorius (Pretoria, South Africa) 35

Development and use of carbon adsorbents in high-performance liquid–solid chromatography. I. Carbon-coated silica particles
by H. Colin and G. Guiochon (Palaiseau, France) 43

A tailor-made C_{87} hydrocarbon as a possible non-polar standard stationary phase for gas chromatography
by F. Riedo, D. Fritz, G. Tarján and E. sz. Kováts (Lausanne, Switzerland) 63

Theoretical and practical aspects of gas chromatography

A study of column performances in gas chromatography. A C_{87} hydrocarbon on chemically modified supports
by L. Boksányi and E. sz. Kováts (Lausanne, Switzerland) 87

N-Acyl derivatives of chiral amines as novel, readily prepared phases for the separation of optical isomers by gas chromatography
by S. Weinstein, B. Feibush and E. Gil-Av (Rehovot, Israel) 97

"Selectivity" of high-temperature liquid phases for gas chromatography
by R. D. Schwartz and R. G. Mathews (Shreveport, La., U.S.A.) 113

© ELSEVIER SCIENTIFIC PUBLISHING COMPANY — 1976

All rights reserved. No part of this publication may be reproduced, stored in a retrieval system or transmitted in any form or by any means, electronic, mechanical, photocopying, recording or otherwise, without the prior written permission of the publisher, Elsevier Scientific Publishing Company, P.O. Box 330, Amsterdam, The Netherlands.

Submission of an article for publication implies the transfer of the copyright from the author to the publisher and is also understood to imply that the article is not being considered for publication elsewhere.

Printed in The Netherlands

Preparation of glass capillary columns coated with polar phase for high-temperature gas chromatography. I. Study of roughening of the glass surface
by J. J. Franken, G. A. F. M. Rutten and J. A. Rijks (Eindhoven, The Netherlands) . . . 117

Preparation and application of surface-modified high-resolution wall-coated open tubular columns
by F. I. Onuska and M. E. Comba (Burlington, Canada) 133

Effect of etching with gaseous hydrogen chloride on the quality of glass capillary columns
by J. Krupčík, M. Kristín, M. Valachovičová and Š. Janiga (Bratislava, Czechoslovakia) 147

New method for the preparation of highly stable polysiloxane-coated glass open-tubular capillary columns and application to the analysis of hormonal steroids
by C. Madani and E. M. Chambaz (La Tronche, France) and M. Rigaud, J. Durand and P. Chebroux (Limoges, France) 161

New perspectives in the prediction of Kováts indices
by J. R. Chrétien and J.-É. Dubois (Paris, France) 171

Chromatographic solute identification using peak shape analysis
by S. D. Mott and E. Grushka (Buffalo, N.Y., U.S.A.) 191

Application of gas chromatographic headspace analysis to the characterization of chemical equilibria in solutions
by A. G. Vitenberg, B. V. Ioffe, Z. St. Dimitrova and T. P. Strukova (Leningrad, U.S.S.R.) 205

Characterization of coal-derived fluids by capillary column gas chromatography–mass spectrometry
by W. Bertsch and E. Anderson (University, Ala., U.S.A.) and G. Holzer (Houston, Texas, U.S.A.) 213

Comprehensive interfaced pyrolysis gas chromatographic peak identification system
by P. C. Uden, D. E. Henderson and R. J. Lloyd (Amherst, Mass., U.S.A.) 225

Quantitative pyrolysis studies of styrene, acrylate ester systems, and their α-methyl-substituted homologs
by J. K. Haken and D. K. M. Ho (Kensington, Australia) 239

Analysis of pyrolysis gas chromatograms using pattern recognition techniques
by E. Küllik, M. Kaljurand and M. Koel (Tallinn, U.S.S.R.) 249

Possibility of increasing the selectivity of chromatographic separation under the action of laser radiation
by K. I. Sakodynski, R. I. Sokolovski, N. N. Tunitzki and S. A. Volkov (Moscow, U.S.S.R.) 257

A semi-specific flame-ionization detection system
by J. Ševčík, R. E. Kaiser and R. Rieder (Bad Duerkheim, G.F.R.) 263

Continuous stirred reactor model as basis for optimisation of electron capture detector operation in coulometric and constant current modes
by E. Broś and F. M. Page (Birmingham, Great Britain) 271

Effects of digital filters on chromatographic signals
by S. P. Cram (Walnut Creek, Calif., U.S.A.), S. N. Chesler (Gainesville, Fla., U.S.A.) and A. C. Brown, III (Walnut Creek, Calif., U.S.A.) 279

Totally pneumatic gas chromatographic process stream analyzer
by R. Annino (Buffalo, N.Y., U.S.A.) and J. Curren, Jr., R. Kalinowiski, E. Karas, R. Lindquist and R. Prescott (Foxboro, Mass., U.S.A.) 301

Theoretical and practical aspects of liquid column chromatography

Fluorescence enhancement. New selective detection principle for liquid chromatography
by P. A. Asmus, J. W. Jorgenson and M. Novotný (Bloomington, Ind., U.S.A.) 317

Variables affecting precision and accuracy in high-performance liquid chromatography
by S. R. Bakalyar and R. A. Henry (Santa Clara, Calif., U.S.A.) 327

(Continued overleaf)

Contents (continued)

New mini-computer automated linear photodiode array spectrometer system for high-resolution liquid chromatography
by R. E. Dessy (Blacksburg, Va., U.S.A.), W. D. Reynolds (Jefferson, Ark., U.S.A.), W. G. Nunn and C. A. Titus (Blacksburg, Va., U.S.A.) and G. F. Moler (Jefferson, Ark., U.S.A.) 347

A flow controller for high-performance liquid chromatography and its applications
by K. Asai, Y.-I. Kanno, A. Nakamoto and T. Hara (Kyoto, Japan) 369

Pressurized, annular chromatograph for continuous separations
by C. D. Scott, R. D. Spence and W. G. Sisson (Oak Ridge, Tenn., U.S.A.) 381

Movement and band spreading of unsorbed solutes in liquid chromatography
by C. Horvath and H.-J. Lin (New Haven, Conn., U.S.A.) 401

Chromatographic reproducibility in high-performance liquid chromatographic gradient elution
by S. R. Abbott, J. R. Berg, P. Achener and R. L. Stevenson (Walnut Creek, Calif., U.S.A.) 421

Preparative liquid chromatography using radially compressed columns
by J. N. Little, R. L. Cotter, J. A. Prendergast and P. D. McDonald (Milford, Mass., U.S.A.) 439

High-performance thin-layer chromatography

Computer-controlled evaluation in thin-layer chromatography. Results and possibilities by S. Ebel and J. Hocke (Marburg, G.F.R.) 449

Use of a gaseous electrical discharge to induce fluorescence in organic compounds separated by thin-layer chromatography
by H. Shanfield, F. Hsu and A. J. P. Martin (Houston, Texas, U.S.A.) 457

Biomedical applications of gas and liquid chromatography

Rapid quantitative microanalysis of ketones in urine by gas chromatography–mass fragmentography
by H. M. Liebich and G. Huesgen (Tübingen, G.F.R.) 465

Column elution and concentration of volatile compounds in biological fluids
by A. Zlatkis and K. Kim (Houston, Texas, U.S.A.) 475

Application of glass capillary-column gas chromatography–mass spectrometry to the studies of human diseases
by E. Jellum, P. Størseth, J. Alexander, P. Helland, O. Stokke and E. Teig (Oslo, Norway) 487

Profiles of volatile metabolites in body fluids
by M. Stafford, M. G. Horning and A. Zlatkis (Houston, Texas, U.S.A.) 495

Picogram analysis of free triiodothyronine and free thyroxine hormones in serum by equilibrium dialysis and electron capture gas chromatography
by B. A. Petersen, R. N. Hanson, R. W. Giese and B. L. Karger (Boston, Mass., U.S.A.). 503

Determination of hydralazine and its metabolites by gas chromatography–mass spectrometry
by K. D. Haegele, H. B. Skrdlant, N. W. Robie, D. Lalka and J. L. McNay, Jr. (San Antonio, Texas, U.S.A.). 517

Gas chromatographic study of free polyols and aldoses in cataractous human lens tissue
by C. D. Pfaffenberger, J. Szafranek and E. C. Horning (Houston, Texas, U.S.A.) . . . 535

Gas chromatographic–mass spectrometric–computer methods in the study of drug metabolism
by R. N. Stillwell and W. G. Stillwell (Houston, Texas, U.S.A.) 547

Analysis of the acidic fraction of marijuana smoke condensate by capillary gas chromatography–mass spectrometry
by M. P. Maskarinec, G. Alexander and M. Novotný (Bloomington, Ind., U.S.A.) . . . 559

Study of the intestinal tyrosine metabolism using stable isotopes and gas chromatography–mass spectrometry
by H. Ch. Curtius, M. Mettler and L. Ettlinger (Zürich, Switzerland) 569

Aldehyde condensation products as derivatives for the vapor phase analysis of biogenic amines
by B. S. Middleditch (Houston, Texas, U.S.A.) 581

Applications of boronate derivatives in the study of ceramides by gas–liquid chromatography–mass spectrometry
by S. J. Gaskell, C. G. Edmonds and C. J. W. Brooks (Glasgow, Great Britain) 591

Electron capture and multiple ion detection of benzodiazepine esters in pharmacokinetic studies
by M. C. Sánchez, J. Colomé and E. Gelpí (Barcelona, Spain) 601

Chemical ionization mass spectrometry for rapid assay of drugs in serum
by M. Lehrer and A. Karmen (Bronx, N.Y., U.S.A.) 615

Solubility factors in gas–liquid chromatography. Comparison between two approaches and application to some biological studies
by P. Laffort and F. Patte (Gif-sur-Yvette, France) 625

Structure–gas chromatographic electron capture sensitivity relationships of some substituted 17α-acetoxyprogesterones
by K. T. Koshy (Kalamazoo, Mich., U.S.A.) 641

Application of gas–liquid chromatography and high-performance liquid chromatography to the analysis of trace amounts of salicylic acid, acetylsalicylic anhydride and acetylsalicyl-salicylic acid in aspirin samples and aspirin formulations
by S. L. Ali (Eschborn/Ts, G.F.R.) 651

Post-column fluorescence derivatization of peptides. Problems and potential in high-performance liquid chromatography
by R. W. Frei, L. Michel and W. Santi (Basle, Switzerland) 665

Evaluation of microparticle chemically bonded reversed-phase packings in the high-pressure liquid chromatographic analysis of nucleosides and their bases
by R. A. Hartwick and P. R. Brown (Kingston, R. I., U.S.A.) 679

High-performance liquid chromatographic analysis of the isomerization products of carbohydrates
by W. Voelter and H. Bauer (Tübingen, G.F.R.) 693

Selective liquid chromatographic isolation procedure for gas chromatographic–mass spectrometric analysis of 3-ketosteroids in biological materials
by M. Axelson and J. Sjövall (Stockholm, Sweden) 705

Analysis of benzoylecgonine in urine by high-performance liquid chromatography and gas chromatography–mass spectrometry
by A. P. Graffeo, D. C. K. Lin and R. L. Foltz (Columbus, Ohio, U.S.A.) 717

Identification of organic compounds by an elution gas chromatography–reactor–frontal gas chromatography system
by V. Rezl and J. Bursa (Brno, Czechoslovakia) 723

Separation of carbohydrates on a new polar bonded phase material
by F. M. Rabel, A. G. Caputo and E. T. Butts (Clifton, N.J., U.S.A.) 731

Environmental applications of gas and liquid chromatography

Microdetermination of nitrates and nitrites in saliva, blood, water, and suspended particulates in air by gas chromatography
by J. W. Tesch, W. R. Rehg and R. E. Sievers (Boulder, Colo., U.S.A.) 743

Evaluation of organic pollutants in the open air and atmospheres in industrial sites using graphitized carbon black traps and gas chromatographic–mass spectrometric analysis with specific detectors
by P. Ciccioli, G. Bertoni, E. Brancaleoni, R. Fratarcangeli and F. Bruner (Rome, Italy) 757

Gas chromatographic–mass spectrometric evaluation of exhaled tobacco smoke
by G. Holzer and J. Oró (Houston, Texas, U.S.A.) and W. Bertsch (University, Ala., U.S.A.) 771

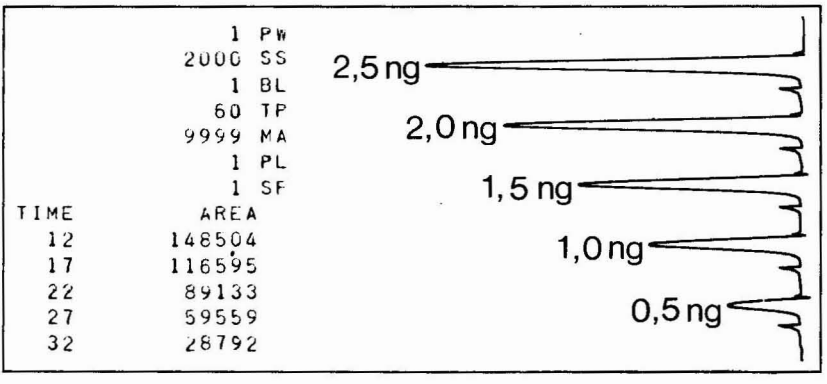
(Continued overleaf)

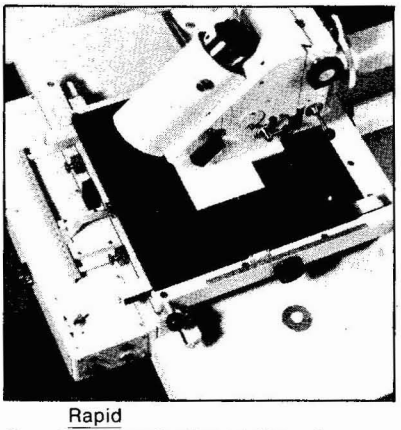
Contents (continued)

Application of high-speed liquid chromatography to the analysis of polyoxyethylene surfactants and their decomposition products in industrial process waters
by R. M. Cassidy and C. M. Niro (Chalk River, Canada) 787
Author Index 795

TLC and High-Performance TLC (HPTLC)
Reflectance, transmission, simultaneous* reflectance and transmission, fluorescence, fluorescence quenching.
ZEISS KM 3 TLC Spectrophotometer – a high-performance instrument for routine and research. From 185 nm–2500 nm.

* US Pat. No. 3746869





Rapid
Quantitative evaluation of 10 tracks in less than 10 minutes.

Easy to operate
Few controls – clearly arranged.
Automatic 100 % control for background correction and rapid plotting of spectra.
Easy and precise sample positioning, even in HPTLC.
Capable of optical integration when using fluorescence mode.
Data processing by computer-integrator.
Computer-compatible. Program-controlled scanning stage as an accessory.

Sensitive
Typical detection limits for TLC:
10 ng caffeine, 40 ng vitamin E, 5 ng sudan red, 0.01 ng rhodamine B, 0.1 ng aflatoxin B_1.

Precise
Photometric reproducibility 0.1 %.
Instrument reproducibility 0.3 %.
Reproducibility for the method 1–2 %.
Considerably reduced exposure of sample.

Tested
More than 100 publications of measurements with the ZEISS chromatogram spectrophotometer.
Information service:
Compendia of References – Application and Method Sheets.

Applications
Pharmacology, Organic chemistry, Foodstuffs chemistry, Clinical chemistry, Forensic chemistry, Biochemistry, Biology, Pollution control and . . .

Accessories
Capillaries for TLC and HPTLC, Applicator, Recorder, Computer-integrator.

If you would like more information, please write to: CARL ZEISS, D 7082 Oberkochen, West Germany

CARL ZEISS, Inc., 444 Fifth Avenue, New York, N.Y. 10018

ZEISS
West Germany

Focus on the future

ref.no.249

Fast high-performance liquid chromatography with new Chromosorb® LC-2 packing

Johns-Manville Technology brings you the second in the Chromosorb LC support series.

Now with Chromosorb LC-2 adsorbent, J-M has developed a pellicular packing having active porous silica layers permanently bonded to an inert spherical solid glass core. (The scanning electron micrograph below shows one of these spheres magnified 1500 times.)

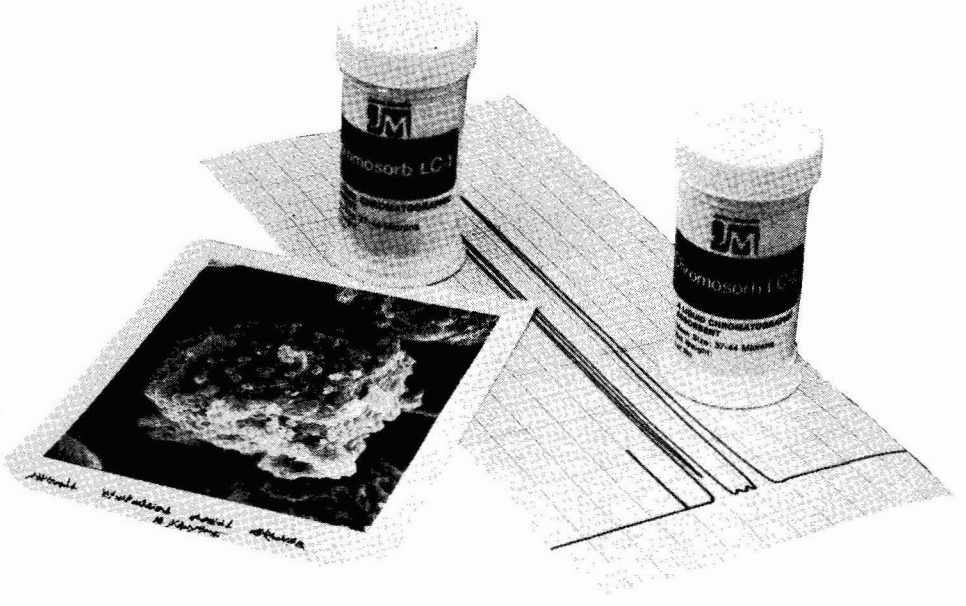
Columns packed with high-speed Chromosorb LC-2 support provide high efficiency and rapid mass transfer, with exceptional resolution and quick equilibration. The result: reproducible retention data of various classes of compounds.

Chromosorb LC-2 adsorbent carries on the consistent quality you expect from J-M. This Chromosorb support has a narrow particle size of 37/44 microns, uniform pore size and a surface area of 15/30 m^2/g. Because of its spherical shape and narrow particle size distribution, Chromosorb LC-2 adsorbent easily packs to a uniform density by tapping, and provides low column pressures and high column efficiency.

Chromosorb LC-2 is the newest Chromosorb support in the LC series, following LC-1, the first diatomite-based support for liquid chromatography. For information about LC-2, LC-1 or the complete line of Chromosorb supports for gas chromatography, write Ed Hammel, Johns-Manville International, P.O. Box 5108, Denver, Colorado 80217.

JM

Johns-Manville



Johns-Manville International Corporation: Denver/New York/Miami/San Francisco. Affiliated Companies: Beirut/Buenos Aires/Caracas/Ghent/Goteborg/Husavik/Johannesburg/London/Mexico City/Milan/Mol/Nairobi/Paris/San Juan/Sao Paulo/Singapore/Sydney/Teheran/Tokyo/Wiesbaden. Other Representation: Lima.

ref. no. 209



Make any LC more versatile with Du Pont columns and packings.

Whether you own a Du Pont liquid chromatograph or any other make, you can enjoy these advantages of Du Pont columns and packings:

Outstanding resolution over wide range of compounds with columns based on microparticulate ZORBAX™ chromatographic packings, adsorption, reversed phase and ion exchange chromatography.

Rapid size separations (GPC) without the solvent and pressure restrictions of gels with new Size Exclusion columns.

New special slurry loading techniques providing maximum stability and performance for both ZORBAX™ and Size Exclusion columns.

Exceptional performance with columns based on pellicular ZIPAX® chromatographic support over a range of chemically modified surfaces. This material can be dry loaded by the user.

Rapid, high-efficiency gram-size separations with preparative columns.

All columns available with standard 1/16″ end fittings.

For information on Du Pont columns and packings, a free subscription to our newsletter, and new literature as it becomes available, write to Du Pont Instruments, Room 24020, Wilmington, DE 19898.

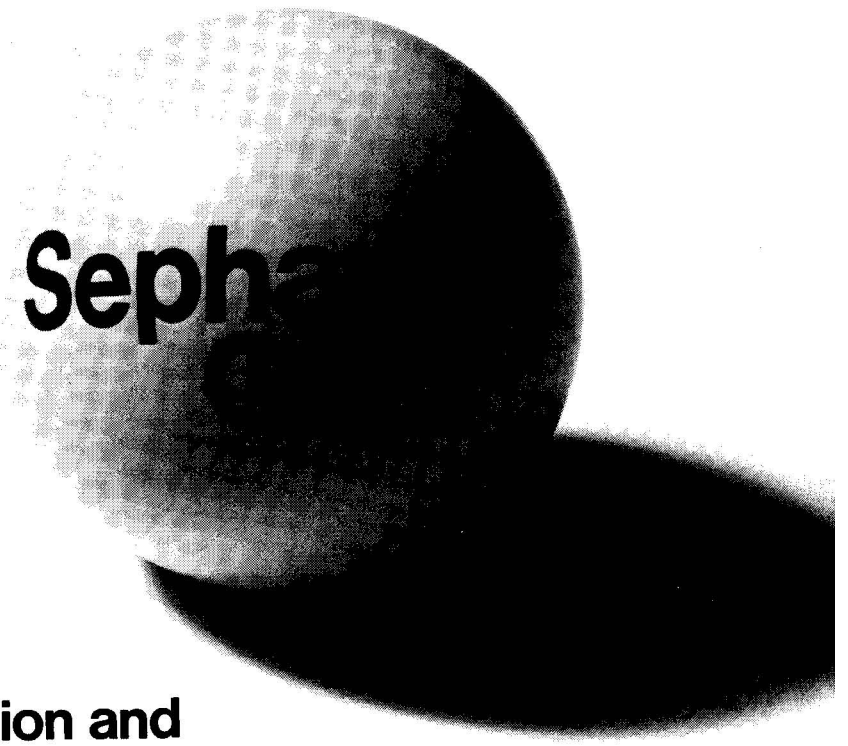
Du Pont Instruments

DU PONT

REG. U.S. PAT. & TM. OFF.

Ref. no. 201

And now.....



Gel filtration and Affinity chromatography even in 6M GuHCl, organic solvents, 8M urea, 3M KSCN at pH3, pH12, 80°C

CROSS-LINKED SEPHAROSE is a new beaded agarose chromatographic medium with exceptional stability and extremely low non-specific adsorption. It can be used with confidence in the most extreme dissociating media including strong solutions of urea, guanidine hydrochloride and chaotropic salts. Sepharose CL can also be used in organic solvents.

You can sterilize Sepharose CL repeatedly by autoclaving at 110°C - 120°C. Cross-linked Sepharose is available in three types: Sepharose® CL-2B, CL-4B and CL-6B.

Ask for the free booklet with data and details of new techniques, from your supplier of Sephadex®, Sepharose® and other separation media.

Pharmacia Fine Chemicals
Box 175
S-751 04 Uppsala 1
Sweden

ref. nr. 354

Pharmacia Fine Chemicals

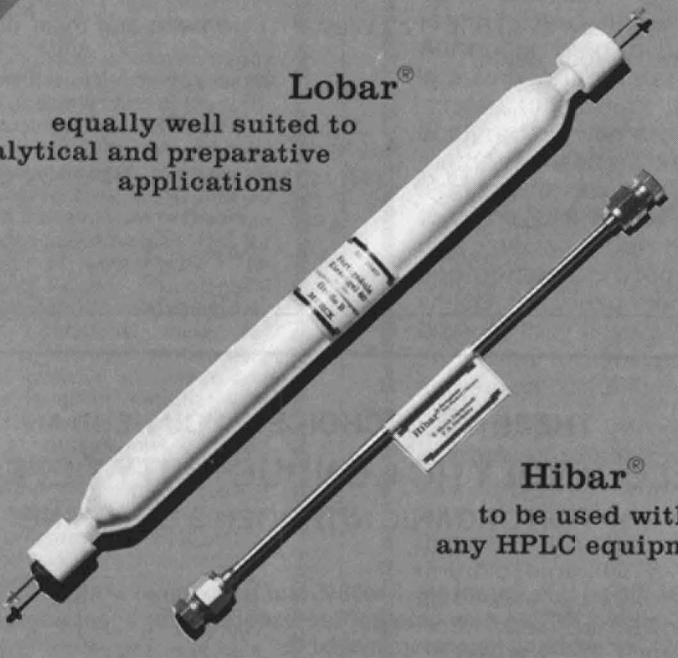
Reagents

MERCK

Pre-packed columns

for High-performance liquid chromatography

Lobar®
equally well suited to analytical and preparative applications



Hibar®
to be used with any HPLC equipment

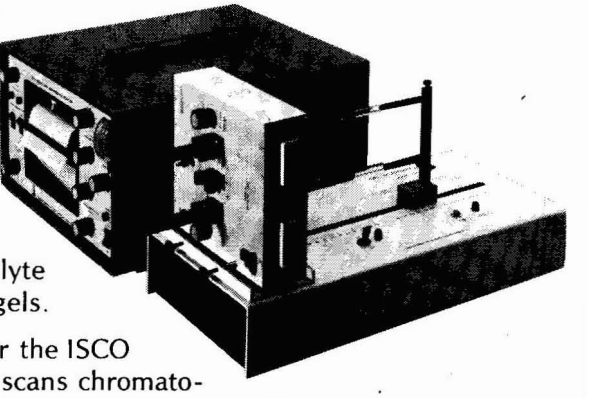
- No filling problems
- Highly reproducible separations
- High separation efficiency
- Rapid separation
- Filled with standardised sorbents

Easy to use · Reliable · Economical
Please send for special prospectus

E. Merck, Darmstadt, Federal Republic of Germany ref.no. 400

Scan gels with or without staining

Gels polymerized and electrophoresed in UV-transparent tubes up to 10'' long can be scanned in the same tubes at 280 nm without staining. Stained tubular or slab gels can be scanned at visible wavelengths with sensitivity and resolution equal to gel-scanning spectrophotometers. Dual beam scanning subtracts ampholyte absorbance in isoelectrically focused gels.



The scanner is a low cost accessory for the ISCO UA-5 absorbance monitor, which also scans chromatographic effluents and centrifuged gradients at 13 wavelengths.

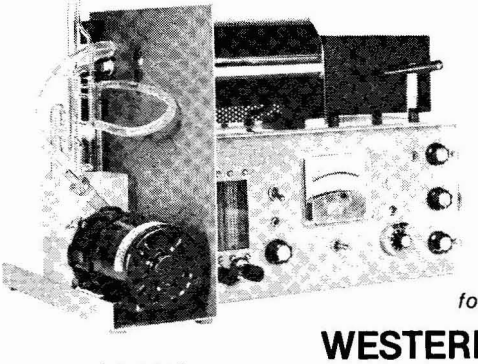
Local sales and service are available in all Western European and most other countries. Write for the name of your dealer.

ISCO BOX 5347 LINCOLN, NEBRASKA 68505 U.S.A.

ref. no. 610

THERE IS A CHOICE IF YOU NEED AN
ELECTROLYTIC CONDUCTIVITY DETECTOR
FOR ORGANIC NITROGEN & CHLORINE

Based on U.S. Patent No. 3309845 and the original work of Dr. Dale M. Coulson, WSA's new detector represents a significant advance over similar systems heretofore available.



- Total sample reduction assured by 8 inch furnace
- All-glass/quartz system for delicate compounds
- Sub-nanogram sensitivity
- Built-in electronics and gas controls
- Easily interfaced with most gas chromatographs
- Simple, reliable DC bridge with high-low sensitivity switch
- Highest specificity

for complete information, contact:

WESTERN SCIENTIFIC ASSOCIATES

Box 698, Danville, CA 94526 USA (415) 837-4622

Only **$2850**

ref no.501

Instrumental Liquid Chromatography

A practical manual on high-performance liquid chromatographic methods

by **N.A. PARRIS**

JOURNAL OF CHROMATOGRAPHY LIBRARY, Vol. 5.

1976 x+329 pages. US $38.50/Dfl. 100.00
ISBN 0-444-41427-4

Available texts on liquid chromatography have tended to emphasize the developments in the theoretical understanding of the technique and methodology or to list numerous applications, complete with experimental details. The present work is intended to bridge the gap between these two treatments by providing, with the minimum of theory, a practical guide to the use of the technique for the development of separations. The material is based largely on practical experience and high-lights details which may have important operational value for laboratory workers. Information regarding the usefulness of available equipment and column packings is given, together with chapters devoted to the methodology of each separation method. Applications of liquid chromatography are described with reference to the potential of the technique for qualitative, quantitative and trace analysis as well as for preparative applications. Numerous applications from the literature are tabulated and cross-referenced to sections concerned with the optimisation procedures of the particular methods. In addition, many of the figures have been drawn from hitherto unpublished work. Although written primarily for workers currently involved with the application or the development of liquid chromatographic methods, the book will also be of value to those who seek to establish whether methods for their particular interests have been reported or seem feasible.

ELSEVIER SCIENTIFIC PUBLISHING COMPANY
P.O. Box 211, Amsterdam,
The Netherlands

Distributor in the U.S.A. and Canada:
ELSEVIER/NORTH-HOLLAND INC.,
52 Vanderbilt Ave., New York., N.Y. 10017

The Dutch guilder price is definitive.
US $ prices are subject to exchange rate fluctuations.

1933 E

Chromatography of Steroids

by E. HEFTMANN

JOURNAL OF CHROMATOGRAPHY LIBRARY, Vol. 8

1976. about 225 pages
US $34.75/Dfl. 90.00
ISBN 0-444-41441-X

Written by one of the pioneers in the field, this is the only complete and up-to-date book on steroid chromatography currently available.
Although some theory is included, it is mainly a laboratory handbook, arranged according to the steroids analyzed as well as according to the methods used. The subject index, along with extensive tables of *R* values and a list of requisite chemicals, permits the reader to select appropriate procedures, many of which are described in detail. The bibliography covers 1200 of the most important articles published on this subject since 1964.

CONTENTS: 1. Introduction. 2. Liquid column chromatography. 3. Paper and thin-layer chromatography. 4. Gas chromatography. 5. Relations between structure and chromatographic mobility. 6. Sterols. 7. Bile acids and alcohols. 8. Estrogens. 9. Androstane derivatives. 10. Pregnane derivatives. 11. Corticosteroids. 12. Miscellaneous steroid hormones. 13. Vitamins D. 14. Molting hormones. 15. Steroid sapogenins and alkaloids. 16. Cardenolides and bufadienolides. Subject index.

ELSEVIER SCIENTIFIC PUBLISHING COMPANY
P.O. Box 211, Amsterdam,
The Netherlands

Distributor in the U.S.A. and Canada:
ELSEVIER/NORTH-HOLLAND, INC.,
52 Vanderbilt Ave., New York, N.Y. 10017

The Dutch guilder price is definitive.
US $ prices are subject to exchange rate fluctuations.

1939 E

Chemical Derivatization in Liquid Chromatography

by J.F. LAWRENCE *and* R.W. FREI

JOURNAL OF CHROMATOGRAPHY LIBRARY, Vol. 7

1976 viii + 214 pages
US $34.50/Dfl. 90.00
ISBN 0-444-41429-0

This book is intended for all investigators concerned with the use of physical separation techniques for solving complex analytical problems. It is the first publication to provide a comprehensive account of modern derivatization in liquid chromatography with special emphasis on the practical aspects. Many examples are given in sufficient detail to permit the worker to reproduce a method without resorting to the original literature. Thus, the book will be particularly useful on the bench top of the laboratory, as well as in practically-oriented courses.

CONTENTS: INTRODUCTION: Pre-separation techniques. Post-separation techniques. BACKGROUND: Chromatographic principles. Spectrometry. Direct measurements from solid surfaces. Further reading. INSTRUMENTATION: TLC equipment. HPLC equipment. Further reading. APPLICATIONS: UV-visible derivatization. Fluorimetric derivatization. Radiochemical derivatization. Derivatization and mass spectrometry. Subject index.

ELSEVIER SCIENTIFIC PUBLISHING COMPANY
P.O. Box 211, Amsterdam,
The Netherlands

Distributor in the U.S.A. and Canada:
ELSEVIER/NORTH-HOLLAND INC.,
52 Vanderbilt Ave., New York., N.Y. 10017

The Dutch guilder price is definitive.
US $ prices are subject to exchange rate fluctuations.

1938 E

Isotachophoresis

Theory, Instrumentation and Applications

by F.M. EVERAERTS, J.L. BECKERS *and* TH. P.E.M. VERHEGGEN.

JOURNAL OF CHROMATOGRAPHY LIBRARY, Vol. 6

1976 xiv + 418 pages
US $61.50/Dfl. 160.00
ISBN 0-444-41430-4

This book is the only text currently avai able providing full information on the ne separation technique known as Isotach phoresis, which competes with liquid ar gas chromatography. All kinds of ion materials can be separated and sever classes of components can be analyse in quick succession as a proper rinsir of the equipment is all that is neede between separations. The various cha ters of the book can be referred to mo or less independently by scientists inte ested in fundamental aspects, by resea chers intending to construct an instr ment and by workers mainly concerne with analytical aspects.

CONTENTS: 1. Historical review. THEOR 2. Principles of electrophoretic techniques. Concept of mobility. 4. Mathematical mod for isotachophoresis. 5. Choice of electroly systems. INSTRUMENTATION: 6. Detectic systems. 7. Instrumentation. APPLICATION 8. Introduction. 9. Practical aspects. 10. Qua titative aspects. 11. Separation of cation species in aqueous solutions. 12. Separatic of anionic species in aqueous solutions. 1 Amino acids, peptides and proteins. 14. Sep ration of nucleotides in aqueous systems. 1 Enzymatic reactions. 16. Separations in no aqueous systems. 17. Counter flow of electr lyte. APPENDICES: A. Simplified model moving-boundary electrophoresis for t measurement of effective mobilities. Diameter of the narrow-bore tube, appli for separation. C. Literature. Symbols ar abbreviations. Subject index.

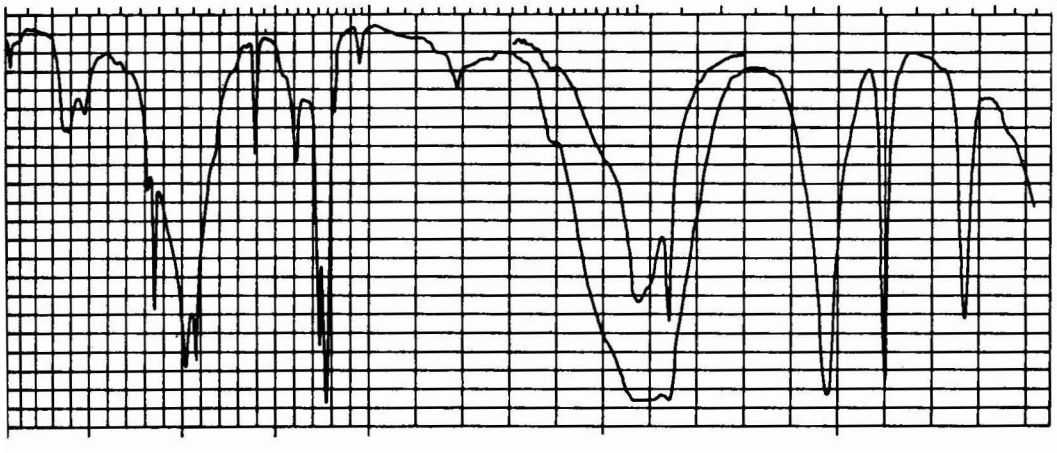
ELSEVIER SCIENTIFIC PUBLISHING COMPANY
P.O. Box 211, Amsterdam,
The Netherlands

Distributor in the U.S.A. and Canada
ELSEVIER/NORTH-HOLLAND, INC.,
52 Vanderbilt Ave., New York, N.Y. 10017

The Dutch guilder price is definitive.
US $ prices are subject to exchange rate fluctuations.

1937 E

RS solvents for UV and IR spectrophotometry



Acetone UV and IR
Acetonitrile UV and IR
Benzene UV and IR
Carbonium sulfide UV and IR
Carbonium tetrachloride UV and IR
Chloroform UV and IR
Cyclohexane UV and IR
N-N-Dimethylformamide UV and IR
Dichloroethane IR
Dimethylsulfoxide UV
Dioxane UV
Ethyl acetate IR
Ethyl alcohol UV 95° and abs.
Ethyl ether UV
n-Heptane UV
n-Hexane UV
Isoctane UV and IR
Isopropyl alcohol UV
Methylene chloride UV and IR
Methyl Alcohol UV
n-Pentane UV
Potassium bromide IR
Tetrachloroethylene IR
Tetrahydrofuran UV and IR
Toluene IR
Trichloroetilene IR

MONTEDISON GROUP
CARLO ERBA

CHEMICALS DIVISION
P.O. Box 3996/20159 Milano/Via Imbonati 24 (Italy)
Telex Erba Mi 36314/Tel. 6995

MONTEDISON S.p.A. REG. TRADEMARK

no. 224



INTRODUCING THE ANALYTICAL MODULE WITH MODEL 428 GC

The Analytical Module is an integral assembly comprising a rapidly interchangeable column oven cover complete with dual injection ports, dual detector block, and columns.
With additional Analytical Modules for the model 428 GC the user can, within minutes, completely alter the chromatography parameters with regard to columns, detectors, and even injectors thus providing unique flexibility for both routine laboratories with requirements for many gas chromatographs as well as the individual researcher. The Analytical Module provides 360° accessability to each set of column connections, at eye level, and is therefore particularly well suited for the mounting of fragile columns, including glass capillary columns.

All temperature control and monitoring electronics, as well as detector measurement and control electronics are of uniform size modular plug-in construction, thus providing the user with the flexibility to change the instrument capabilities economically.

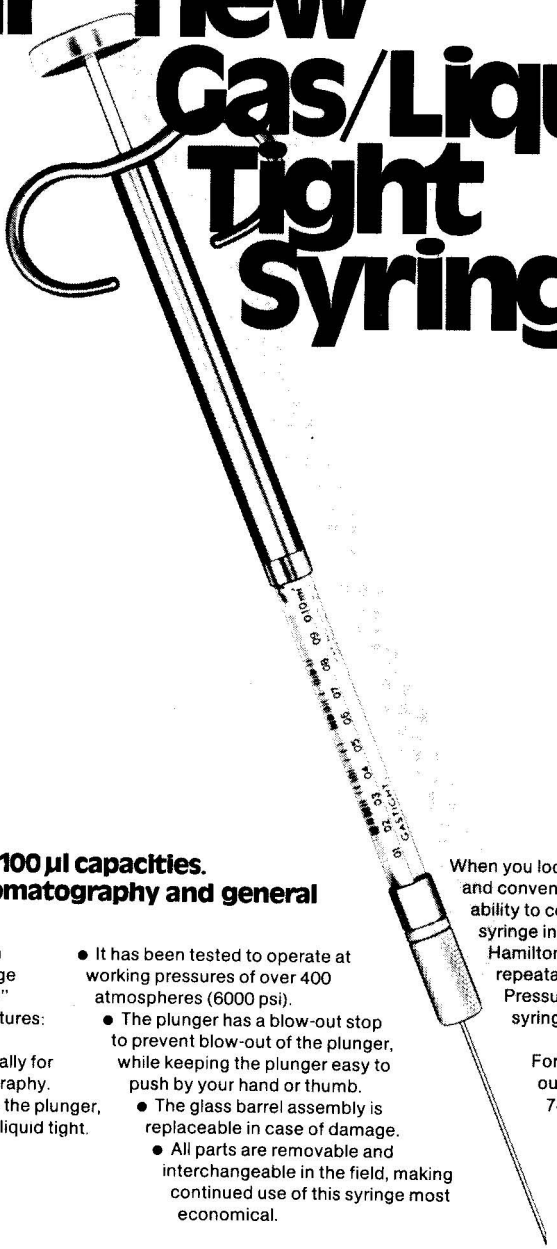
Packard

PACKARD - BECKER B.V.
VULCANUSWEG 259 - P.O. BOX 519, DELFT, NETHERLANDS
PACKARD INSTRUMENT INTERNATIONAL S.A.
TALSTRASSE 39, 8001 ZURICH, SWITZERLAND
PACKARD INSTRUMENT COMPANY, INC.
2200 WARRENVILLE RD. DOWNERS GROVE, IL. 60515, U.S.A.
SUBSIDIARIES OF AMBAC INDUSTRIES, INC.

Packard

ref no 254

Four new Gas/Liquid Tight Syringes



10 µl, 25 µl, 50 µl and 100 µl capacities.
r high pressure chromatography and general urpose use.

This is the syringe that has been called "the most modern syringe available for chromatography" because of its advanced features:

- It was designed specifically for high pressure chromatography.
- There's a Teflon* tip on the plunger, making it both gas and liquid tight.
- It has been tested to operate at working pressures of over 400 atmospheres (6000 psi).
- The plunger has a blow-out stop to prevent blow-out of the plunger, while keeping the plunger easy to push by your hand or thumb.
- The glass barrel assembly is replaceable in case of damage.
- All parts are removable and interchangeable in the field, making continued use of this syringe most economical.

When you look at all the features and conveniences, the unique ability to continually rebuild the syringe in the field, and the traditional Hamilton high precision and repeatability... Hamilton's High Pressure Syringes may be the only syringes you'll ever need.

For additional information contact our local dealer or Micromesure A.G., 7402 Bonaduz, Switzerland.

HAMILTON

* Du Pont registered trademark.

ref.no.144

Chemistry and Biochemistry of Natural Waxes

edited by **P.E. KOLATTUKUDY,** Department of Agricultural Chemistry, Washington State University, Pullman, Washington.

1976 xx+460 pages US $49.75/Dfl. 129.00 ISBN 0-444-41470-3 LC 76-18140

In recent years, the development of modern analytical techniques has led to significant advances in the understanding of the components of natural waxes. Since these advances are relevant to those who deal with a variety of biological problems from agriculture to dermatology, it appeared that a research level book on this subject was needed. This book, the first of its kind, fulfills this need, and provides comprehensive information on the chemistry and biochemistry of natural waxes from bacteria, fungi, algae, higher plants, insects, birds, marine organisms, and mammals including man. It will be especially useful as a research level reference book for biologists, biochemists, and lipid chemists.

CONTENTS: Chapters 1. Introduction to Natural Waxes (P.E. Kolattukudy). 2. Mammalian Waxes (D.T. Downing). 3. Marine Waxes (J.R. Sargent, R.F. Lee and J.C. Nevenzel). 4. Bird Waxes (J. Jacob). 5. Biochemistry of Bird Waxes (J.S. Buckner and P.E. Kolattukudy). 6. Insect Waxes (L.L. Jackson and G.J. Blomquist). 7. Chemistry of Waxes of Higher Plants (A.P. Tulloch). 8. Biochemistry of Plant Waxes (P.E. Kolattukudy, R. Croteau and J.S. Buckner). 9. Algal and Fungal Waxes (J.D. Weete). 10. Bacterial Waxes (P.W. Albro). Subject Index.

ELSEVIER SCIENTIFIC PUBLISHING COMPANY

P.O. Box 211, Amsterdam, The Netherlands

Distributor in the U.S.A. and Canada:
ELSEVIER/NORTH-HOLLAND, INC.,
52 Vanderbilt Ave., New York, N.Y. 10017



The Dutch guilder price is definitive. US $ prices are subject to exchange rate fluctuations.

1979 E

Advances in Chromatography 1975

Proceedings of the Tenth International Symposium, held in Munich, November 3-6, 1975

Special volume: Reprinted from the Journal of Chromatography, Vol. 112
edited by **A. ZLATKIS.**

associate editors: E. BAYER, L.S. ETTRE and I. HALÁSZ.

1975. 752 pages. US $74.95/Dfl. 180.00. ISBN 0-444-41382-0.

This volume represents the proceedings of the Tenth International Symposium on the Advances in Chromatography. All aspects of chromatography are covered by the 61 papers presented by scientists from 15 different countries. The increased importance of combined techniques such as GC-MS is evidenced by more than a dozen papers describing various advanced systems and their application in biochemical-clinical and environmental analysis. Following the renaissance of liquid column chromatography, a similar upsurge is appearing in thin-layer chromatography. The papers on further advances in selective detectors, high-performance open tubular colomns and special techniques such as head-space analysis demonstrate the still-continuing development of gas chromatography.

CONTENTS: **Foreword** (A. Zlatkis). **Winners of the M.S. Tswett Chromatography Medal. The development of gas chromatography** (L.S. Ettre). **New Horizons.** *Main Contributors:* I. Halász, J.E. Lovelock, C.S.G. Phillips, V. Pretorius, J.H. Purnell and J. Ripphahn. **Chromatographic columns and stationary phases.** *Main Contributors:* J. Garaj, E. Gil-Av, E. Grushka, J.K. Haken, H. kelker, J.H. Knox, R.D. Schwartz and A. Zlatkis. **Theoretical and practical aspects of chromatography.** *Main Contributors:* W.A. Aue, V.G. Berezkin, W. Bruening, S.P. Cram, S.N. Deming, H. Engelhardt, D.C. Fenimore, G. Guiochon, J.F.K. Huber, B.V. Ioffe, R.E. Kaiser, J.J. Kirkland, B. Kolb, E. Küllik, J.N. Little, C. Merritt Jr., J. Novák, B.A. Rudenko, G. Schomburg, R.P.W. Scott and A. Zlatkis. **Biomedical applications of chromatography.** *Main Contributors:* C.J.W. Brooks, P.R. Brown, H.Ch. Curtius, A. Frigerio, E. Grushka, E.C. Horning, M.G. Horning, E. Jellum, A. Karmen, H.M. Liebich, B.F. Maume, C.W. Moss, M. Novontny, C.D. Pfaffenberger, K. Tsuji, W.J.A. Van den Heuvel, W. Voelter and A. Zlatkis. **Environmental applications of chromatography.** *Main Contributors:* W. Bertsch, J.L. Monkman and W.D. Ross.

Advances in Chromatography 1974

Proceedings of the Ninth International Symposium held in Houston, Texas, November 4-7, 1974.
Special volume: Reprinted from the Journal of Chromatography, Vol. 99.

edited by **A. ZLATKIS,** and **L.S. ETTRE.**

1974. 789 pages. US $66.75/Dfl. 160.00. ISBN 0-444-41267-0

ELSEVIER SCIENTIFIC PUBLISHING COMPANY
P.O. Box 211, Amsterdam, The Netherlands

Distributed in the U.S.A. and Canada by:
AMERICAN ELSEVIER PUBLISHING COMPANY
52 Vanderbilt Ave., New York, N.Y. 10017, U.S.A.



The Dutch guilder price is definitive. US $ prices are subject to exchange rate fluctuations.

Quadrupole Mass Spectrometry and its Applications

edited by **PETER H. DAWSON,** National Research Council of Canada.

1976. xxii + 350 pages. US $49.75/Dfl. 129.00. ISBN 0-444-41345-6

This is the first comprehensive account of quadrupole mass spectrometry. While its many contributors provide a broader-than-usual viewpoint, it is, nevertheless, a systematic text. It begins with simple qualitative descriptions of the mass filter, the monopole, the quadrupole ion trap and related time-of-flight spectrometers. It proceeds to an exploration of their particular advantages, disadvantages and applications. Experimental design and performance is discussed in detail. The theoretical treatment includes computational design techniques such as the recently developed utilisation of phase-space dynamics. Although there have been countless routine applications of quadrupole mass spectrometry, there are an unusual number of individualized applications in both science and technology which require specially designed or modified instruments. This book will therefore be of interest and value to many users for whom a knowledge of quadrupole design, performance and limitations may be essential.

CONTENTS: Chapters: I. Introduction *(P.H. Dawson).* II. Principles of Operation *(P.H. Dawson).* III. Analytical Theory *(P.H. Dawson).* IV. Numerical Calculations *(P.H. Dawson).* V. Fringing Fields and Other Imperfections *(P.H. Dawson).* VI. The Mass Filter: Design and Performance *(W.E. Austin, A.E. Holme and J.H. Leck).* VII. The Monopole: Design and Performance *(R.F. Herzog).* VIII. Quadrupole Ion Traps *(J.F.J. Todd, G. Lawson and R.F. Bonner).* IX. Time-of-Flight Spectrometers *(J.P. Carrico).* X. Applications in Atomic and Molecular Physics *(J.F.J. Todd).* XI. Applications to Upper Atmosphere Research *(G.R. Carignan).* XII. Applications to Gas Chromatography *(M.S. Story).* XIII. Medical and Environmental Applications *(G. Lawson).*

ELSEVIER SCIENTIFIC PUBLISHING COMPANY

P.O. Box 211, Amsterdam, The Netherlands

Distributor in the U.S.A. and Canada:
ELSEVIER/NORTH-HOLLAND, INC.,
52 Vanderbilt Ave., New York, N.Y. 10017



The Dutch guilder price is definitive. US $ prices are subject to exchange rate fluctuations.

1999 E

JOURNAL OF CHROMATOGRAPHY
VOL. 126 (1976)

JOURNAL *of* CHROMATOGRAPHY

INTERNATIONAL JOURNAL ON CHROMATOGRAPHY, ELECTROPHORESIS AND RELATED METHODS

EDITOR

MICHAEL LEDERER (Rome)

ASSOCIATE EDITOR

K. MACEK (Prague)

EDITORIAL BOARD

W. A. Aue (Halifax), V. G. Berezkin (Moscow), A. Bevenue (Honolulu, Hawaii), P. Boulanger (Lille), A. A. Boulton (Saskatoon), C. P. Cartoni (Rome), K. V. Chmutov (Moscow), G. Duyckaerts (Liège), L. Fishbein (Jefferson, Ark.), A. Frigerio (Milan), C. W. Gehrke (Columbia, Mo.), E. Gil-Av (Rehovot), G. Guiochon (Palaiseau), I. M. Hais (Hradec Králové), N. G. L. Harding (Cambridge), E. Heftmann (Berkeley, Calif.), S. Hjertén (Uppsala), E. C. Horning (Houston, Texas), J. F. K. Huber (Vienna), A. T. James (Sharnbrook), J. Janák (Brno), A. I. M. Keulemans (Eindhoven), K. A. Kraus (Oak Ridge, Tenn.), E. Lederer (Gif-sur-Yvette), A. Liberti (Rome), H. M. McNair (Blacksburg, Va.), Y. Marcus (Jerusalem), G. B. Marini-Bettòlo (Rome), R. Neher (Basel), G. Nickless (Bristol), J. Novák (Brno), O. Samuelson (Göteborg), G.-M. Schwab (Munich), G. Semenza (Zürich), L. R. Snyder (Tarrytown, N.Y.), A. Zlatkis (Houston, Texas)

EDITORS, BIBLIOGRAPHY SECTION

K. Macek (Prague), J. Janák (Brno), Z. Deyl (Prague)

EDITOR, BOOK REVIEW SECTION

R. Amos (Abingdon)

EDITOR, NEWS SECTION

J. F. K. Huber (Vienna)

COORDINATING EDITOR, DATA SECTION

J. Gasparič (Hradec Králové)

VOL. 126 1976



The Alamo — an historical landmark of Texas independence

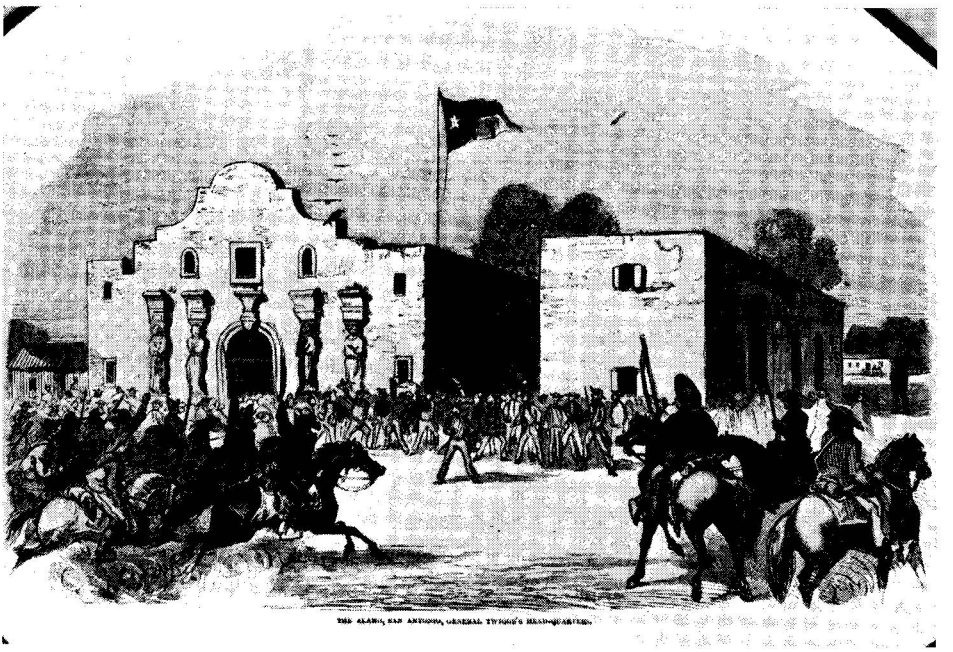
© ELSEVIER SCIENTIFIC PUBLISHING COMPANY — 1976

All rights reserved. No part of this publication may be reproduced, stored in a retrieval system or transmitted in any form or by any means, electronic, mechanical, photocopying, recording or otherwise, without the prior written permission of the publisher, Elsevier Scientific Publishing Company, P.O. Box 330, Amsterdam, The Netherlands.

Submission of an article for publication implies the transfer of the copyright from the author to the publisher and is also understood to imply that the article is not being considered for publication elsewhere.

Printed in The Netherlands

SPECIAL VOLUME



ADVANCES IN CHROMATOGRAPHY 1976

Proceedings of the Eleventh International Symposium
held in Houston, Texas, November 1–5, 1976

Edited by:

A. ZLATKIS
Professor of Chemistry
University of Houston
Houston, Texas, U.S.A.

Associate Editors:

H. SHANFIELD
Chemistry Department
University of Houston
Houston, Texas, U.S.A.

L. S. ETTRE
The Perkin-Elmer Corporation
Norwalk, Conn., U.S.A.

CONTENTS

ELEVENTH INTERNATIONAL SYMPOSIUM ON ADVANCES IN CHROMATOGRAPHY, HOUSTON, TEXAS (U.S.A.), NOVEMBER 1–5, 1976

A. Zlatkis, Foreword XI

Winners of the M. S. Tswett Chromatography Medal XIII

New horizons

P. G. Simmonds, A. J. Lovelock and J. E. Lovelock, Continuous and ultrasensitive apparatus for the measurement of air-borne tracer substances 3

C. M. A. Badger, J. A. Harris, K. F. Scott, M. J. Walker and C. S. G. Phillips, Heater-displacement chromatography 11

I. Halász, H. Schmidt and P. Vogtel, Particle size, pressure and analysis time in routine high-performance liquid chromatography 19

P. R. Boshoff, B. J. Hopkins and V. Pretorius, Thin-layer chromatographic transport detector for high-performance liquid chromatography 35

H. Colin and G. Guiochon, Development and use of carbon adsorbents in high-performance liquid–solid chromatography. I. Carbon-coated silica particles 43

F. Riedo, D. Fritz, G. Tarján and E. sz. Kováts, A tailor-made C_{87} hydrocarbon as a possible non-polar standard stationary phase for gas chromatography 63

Theoretical and practical aspects of gas chromatography

L. Boksányi and E. sz. Kováts, A study of column performances in gas chromatography. A C_{87} hydrocarbon on chemically modified supports 87

S. Weinstein, B. Feibush and E. Gil-Av, N-Acyl derivatives of chiral amines as novel, readily prepared phases for the separation of optical isomers by gas chromatography 97

R. D. Schwartz and R. G. Mathews, "Selectivity" of high-temperature liquid phases for gas chromatography 113

J. J. Franken, G. A. F. M. Rutten and J. A. Rijks, Preparation of glass capillary columns coated with polar phase for high-temperature gas chromatography. I. Study of roughening of the glass surface 117

F. I. Onuska and M. E. Comba, Preparation and application of surface-modified high-resolution wall-coated open tubular columns 133

J. Krupčík, M. Kristín, M. Valachovičová and Š. Janiga, Effect of etching with gaseous hydrogen chloride on the quality of glass capillary columns 147

C. Madani, E. M. Chambaz, M. Rigaud, J. Durand and P. Chebroux, New method for the preparation of highly stable polysiloxane-coated glass open-tubular capillary columns and application to the analysis of hormonal steroids 161

J. R. Chrétien and J.-É. Dubois, New perspectives in the prediction of Kováts indices 171

S. D. Mott and E. Grushka, Chromatographic solute identification using peak shape analysis . 191

A. G. Vitenberg, B. V. Ioffe, Z. St. Dimitrova and T. P. Strukova, Application of gas chromatographic headspace analysis to the characterization of chemical equilibria in solutions . 205

W. Bertsch, E. Anderson and G. Holzer, Characterization of coal-derived fluids by capillary column gas chromatography–mass spectrometry 213

P. C. Uden, D. E. Henderson and R. J. Lloyd, Comprehensive interfaced pyrolysis gas chromatographic peak identification system 225

J. K. Haken and D. K. M. Ho, Quantitative pyrolysis studies of styrene, acrylate ester systems, and their α-methyl-substituted homologs 239

E. Küllik, M. Kaljurand and M. Koel, Analysis of pyrolysis gas chromatograms using pattern recognition techniques 249

K. I. Sakodynski, R. I. Sokolovski, N. N. Tunitzki and S. A. Volkov, Possibility of increasing the selectivity of chromatographic separation under the action of laser radiation 257

J. Ševčík, R. E. Kaiser and R. Rieder, A semi-specific flame-ionization detection system 263

E. Broš and F. M. Page, Continuous stirred reactor model as basis for optimisation of electron capture detector operation in coulometric and constant current modes 271

S. P. Cram, S. N. Chesler and A. C. Brown, III, Effects of digital filters on chromatographic signals 279

R. Annino, J. Curren, Jr., R. Kalinowiski, E. Karas, R. Lindquist and R. Prescott, Totally pneumatic gas chromatographic process stream analyzer 301

Theoretical and practical aspects of liquid column chromatography

P. A. Asmus, J. W. Jorgenson and M. Novotný, Fluorescence enhancement. New selective detection principle for liquid chromatography 317

S. R. Bakalyar and R. A. Henry, Variables affecting precision and accuracy in high-performance liquid chromatography 327

R. E. Dessy, W. D. Reynolds, W. G. Nunn, C. A. Titus and G. F. Moler, New mini-computer automated linear photodiode array spectrometer system for high-resolution liquid chromatography 347

K. Asai, Y.-I. Kanno, A. Nakamoto and T. Hara, A flow controller for high-performance liquid chromatography and its applications 369

C. D. Scott, R. D. Spence and W. G. Sisson, Pressurized, annular chromatograph for continuous separations 381

C. Horvath and H.-J. Lin, Movement and band spreading of unsorbed solutes in liquid chromatography 401

S. R. Abbott, J. R. Berg, P. Achener and R. L. Stevenson, Chromatographic reproducibility in high-performance liquid chromatographic gradient elution 421

J. N. Little, R. L. Cotter, J. A. Prendergast and P. D. McDonald, Preparative liquid chromatography using radially compressed columns 439

High-performance thin-layer chromatography

S. Ebel and J. Hocke, Computer-controlled evaluation in thin-layer chromatography. Results and possibilities 449

H. Shanfield, F. Hsu and A. J. P. Martin, Use of a gaseous electrical discharge to induce fluorescence in organic compounds separated by thin-layer chromatography 457

Biomedical applications of gas and liquid chromatography

H. M. Liebich and G. Huesgen, Rapid quantitative microanalysis of ketones in urine by gas chromatography–mass fragmentography 465

A. Zlatkis and K. Kim, Column elution and concentration of volatile compounds in biological fluids 475

E. Jellum, P. Størseth, J. Alexander, P. Helland, O. Stokke and E. Teig, Application of glass capillary-column gas chromatography–mass spectrometry to the studies of human diseases 487

M. Stafford, M. G. Horning and A. Zlatkis, Profiles of volatile metabolites in body fluids . . . 495

B. A. Petersen, R. N. Hanson, R. W. Giese and B. L. Karger, Picogram analysis of free triiodothyronine and free thyroxine hormones in serum by equilibrium dialysis and electron capture gas chromatography 503

K. D. Haegele, H. B. Skrdlant, N. W. Robie, D. Lalka and J. L. McNay, Jr., Determination of hydralazine and its metabolites by gas chromatography–mass spectrometry 517

C. D. Pfaffenberger, J. Szafranek and E. C. Horning, Gas chromatographic study of free polyols and aldoses in cataractous human lens tissue 535

R. N. Stillwell and W. G. Stillwell, Gas chromatographic–mass spectrometric–computer methods in the study of drug metabolism 547

M. P. Maskarinec, G. Alexander and M. Novotný, Analysis of the acidic fraction of marijuana smoke condensate by capillary gas chromatography–mass spectrometry 559

H. Ch. Curtius, M. Mettler and L. Ettlinger, Study of the intestinal tyrosine metabolism using stable isotopes and gas chromatography–mass spectrometry 569

B. S. Middleditch, Aldehyde condensation products as derivatives for the vapor phase analysis of biogenic amines 581

S. J. Gaskell, C. G. Edmonds and C. J. W. Brooks, Applications of boronate derivatives in the study of ceramides by gas–liquid chromatography–mass spectrometry 591

M. C. Sánchez, J. Colomé and E. Gelpí, Electron capture and multiple ion detection of benzodiazepine esters in pharmacokinetic studies 601

M. Lehrer and A. Karmen, Chemical ionization mass spectrometry for rapid assay of drugs in serum 615

P. Laffort and F. Patte, Solubility factors in gas–liquid chromatography. Comparison between two approaches and application to some biological studies 625

K. T. Koshy, Structure–gas chromatographic electron capture sensitivity relationships of some substituted 17α-acetoxyprogesterones 641

S. L. Ali, Application of gas–liquid chromatography and high-performance liquid chromatography to the analysis of trace amounts of salicylic acid, acetylsalicylic anhydride and acetylsalicylsalicylic acid in aspirin samples and aspirin formulations 651

R. W. Frei, L. Michel and W. Santi, Post-column fluorescence derivatization of peptides. Problems and potential in high-performance liquid chromatography 665

R. A. Hartwick and P. R. Brown, Evaluation of microparticle chemically bonded reversed-phase packings in the high-pressure liquid chromatographic analysis of nucleosides and their bases 679

W. Voelter and H. Bauer, High-performance liquid chromatographic analysis of the isomerization products of carbohydrates 693

M. Axelson and J. Sjövall, Selective liquid chromatographic isolation procedure for gas chromatographic–mass spectrometric analysis of 3-ketosteroids in biological materials . 705

A. P. Graffeo, D. C. K. Lin and R. L. Foltz, Analysis of benzoylecgonine in urine by high-performance liquid chromatography and gas chromatography–mass spectrometry . . . 717

V. Rezl and J. Bursa, Identification of organic compounds by an elution gas chromatography–reactor–frontal gas chromatography system 723

F. M. Rabel, A. G. Caputo and E. T. Butts, Separation of carbohydrates on a new polar bonded phase material 731

Environmental applications of gas and liquid chromatography

J. W. Tesch, W. R. Rehg and R. E. Sievers, Microdetermination of nitrates and nitrites in saliva, blood, water, and suspended particulates in air by gas chromatography 743

P. Ciccioli, G. Bertoni, E. Brancaleoni, R. Fratarcangeli and F. Bruner, Evaluation of organic pollutants in the open air and atmospheres in industrial sites using graphitized carbon black traps and gas chromatographic–mass spectrometric analysis with specific detectors 757

G. Holzer, J. Oró and W. Bertsch, Gas chromatographic–mass spectrometric evaluation of exhaled tobacco smoke 771

R. M. Cassidy and C. M. Niro, Application of high-speed liquid chromatography to the analysis of polyoxyethylene surfactants and their decomposition products in industrial process waters 787

Author Index 795

FOREWORD

This volume represents the proceedings of the Eleventh International Symposium on Advances in Chromatography held in Houston, Texas, November 1–5, 1976. The 63 articles represent contributions of scientists from 18 countries. The subject of the papers is related to all aspects of chromatography, involving questions of theory and practice. Today, there is probably no branch of science where chromatography is not utilized and this is well demonstrated by the broad spectrum of the subjects of the symposium. Biochemistry–clinical chemistry and environmental control are two fields where the application of chromatography is particularly important.

A number of papers deal with the practice of glass open tubular columns and their applications. It was 20 years ago that M. J. E. Golay presented his first theoretical discussion at the gas chromatography symposium of the American Chemical Society held in Dallas, Texas which led to the development of the theory and practice of open tubular columns. The papers presented at this symposium show that Dr. Golay's invention is still steadily increasing in importance and it is a particular pleasure to recognize his merits at this anniversary.

In the present volume and in other presentations during the meeting, particular emphasis is given to the papers dealing with high-performance thin-layer chromatography. Generally, the Fifth Symposium held January 1969, in Las Vegas, Nevada, is credited as the real start of modern high-performance liquid column chromatography; it is believed that the present papers on modern TLC will be referred to in the years ahead as the renaissance of this technique.

1976 is being celebrated as the bicentennial of the United States of America. Science is international, unrestricted by political boundaries, and its cultivation belongs to one of the universal rights of mankind. Indeed, the importance of this event, the 200th anniversary of the Declaration of Independence which first drew attention to the unalienable rights of all men to life, liberty and the pursuit of happiness should be emphasized.

I would like to express my gratitude to Dr. L. S. Ettre for his cooperation in the organization of this Symposium. The editor has been fortunate in securing the contributions of the distinguished authors who have made these Advances in Chromatography. In particular, thanks are due to Dr. M. Lederer for his help in making the publication of this volume possible.

University of Houston
Houston, Texas (U.S.A.)

A. ZLATKIS


FOR DISTINGUISHED RESEARCH IN CHROMATOGRAPHY
M.S.TSWETT
1872-1919

THE M. S. TSWETT CHROMATOGRAPHY MEDAL

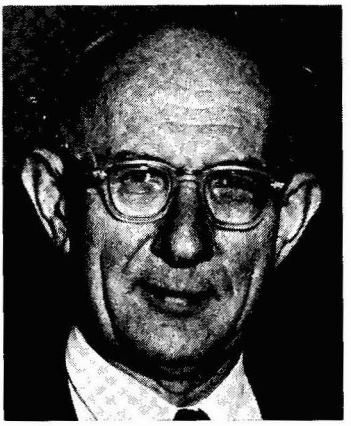
The Eleventh International Symposium on Advances in Chromatography awards the M. S. Tswett Chromatography Medal to

M. J. E. GOLAY	for the invention of open tubular (capillary) columns and the development of their theory;
G. GUIOCHON	for his many contributions to the progress of gas and liquid chromatography;
A. T. JAMES	for his pioneering work in the invention of gas–liquid partition chromatography and its application to biochemistry;
E. LEDERER	for his life work in chromatography;
V. PRETORIUS	for his invention of the flame ionization detector and for his numerous contributions to the development of chromatography.

These distinguished scientists have furthered the advancement of chromatography, for the benefit of us all.

Houston, Texas, November 1, 1976

A. ZLATKIS
Symposium Chairman



Marcel Jules Edouard Golay was born in 1902, in Neuchâtel, Switzerland. He studied at the Eidgenössische Technische Hochschule (the Federal Technical University) in Zurich, receiving his Licentiate in Electrical Engineering in 1924. He then joined the staff of Bell Telephone Laboratories where he worked until 1928 when he entered the University of Chicago to pursue graduate studies. He received his Ph.D. in 1931 with a thesis in atomic physics. On graduation, Dr. Golay joined the U.S. Signal Corps Engineering Laboratories at Fort Monmouth, N.J., where he remained until 1955. His last position there was that of the chief scientist of the Components Division. Between 1955 and 1961 Dr. Golay served as consultant to the Philco Corporation, Philadelphia, Pa., and to the Perkin-Elmer Corporation, Norwalk, Conn. In 1961–1962 he was a visiting professor at the Technische Hogeschool in Eindhoven, The Netherlands, and since 1963, he has been a senior scientist at Perkin-Elmer.

Dr. Golay has made significant contributions in various scientific disciplines such as information theory, computer science, radio communications, infrared and nuclear magnetic resonance spectroscopy. His activities in gas chromatography started in 1956 with theoretical studies leading to the development of the open tubular columns which are generally acknowledged as the greatest singular theoretical and technological advance since the introduction of the technique. Other activities in the field of gas chromatography include the development of the theory of preparative chromatography and the utilization of mixing washers; investigations on the effect of various parameters on the efficiency of sample introduction systems; and various theoretical considerations aimed at the improvement of the separation ability of gas chromatographic columns.

Dr. Golay has received various awards during his professional career, among them the American Chemical Society Award in Chemical Instrumentation and the Distinguished Achievement Award of the Instrument Society of America.



Georges Guiochon was born in 1931, in Nantes, France, and studied at the École Polytechnique and the University of Paris where he received his Ph.D. in 1958. Between 1954 and 1968, he worked with professor Leon Jacqué at the École Polytechnique and, after the death of professor Jacqué, he became the head of the Laboratoire de Chimie Analytique Physique of this school. He was appointed associate professor at the École Polytechnique and the University of Paris in 1958 and 1968, respectively, and in 1974 professor of chemistry at both schools. He is vice-president of G.A.M.S., the French analytical chemistry society, and a honorary member of the Chromatography Discussion Group.

Dr. Guiochon has made numerous contributions to the development of both gas and modern high-performance liquid chromatography, including investigations on the effect of gas compressibility, the influence of various analytical parameters on the accuracy and reproducibility of chromatographic measurements, the performance of high-efficiency columns and the theory of the techniques. He is the author (with C. Pommier) of two books, one on the use of gas chromatography in inorganic chemistry and the other on the use of the technique in the analysis of organics and organo-metallics.



Anthony Trafford James was born in 1922, in Canton, Cardiff, Wales. He studied in London, at Northern Polytechnic and at the University College receiving

his Ph.D. in 1946. This was followed by a Medical Research Council Studentship at Bedford College, London, and association with the Lister Institute of Preventive Medicine. In 1950, he joined Dr. A. J. P. Martin at the National Institute for Medical Research where he remained until 1962 when he became associated with Unilever's Research Laboratories in Sharnbrook, Bedfordshire, serving first as divisional manager and head of the Biosynthesis Unit and later as the head of the Division of Plant Products and Biochemistry. Since 1969 he has been manager of the Biosciences Group at Unilever. Between 1966 and 1971 he was also industrial professor of chemistry at Loughborough University of Technology.

Dr. James has been very active in the scientific community. During his student days he was president of the Joint University of Wales and University College Student Representative Council and president of the National Union of Students. He is a member of the Council and the Board of the Science Research Council of the United Kingdom, chairman of the Food Science and Technology Committee of the Ministry of Food and Agriculture Research Council and president of the International Conferences on the Biochemistry of Lipids. Dr. James received a number of awards, among them the John Price Wetherill Medal of the Franklin Institute, the Lipid Award of the Americal Oil Chemists' Society and the bronze medal of the French Biochemical Society. He is the author and coauthor of a number of scientific publications and also wrote a book in cooperation with M. I. Gurr on lipid biochemistry, published in 1972.

Dr. James' activities in gas chromatography started in 1951 when, working with A. J. P. Martin, they jointly developed the technique of gas–liquid partition chromatography. He pioneered in demonstrating the applications of the technique in biochemistry, particularly in the analysis of lipids.

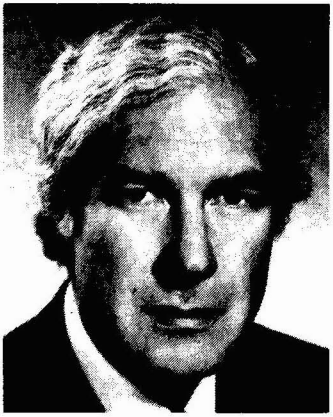


Edgar Lederer was born in 1909, in Vienna, Austria. He studied chemistry at the University of Vienna receiving his Ph.D. in 1930. From September 1930 on he worked at the Kaiser Wilhelm Institut für Medizinische Forschung, in Heidelberg, Germany, under the direction of Dr. Richard Kuhn. After the advent of nazism in Germany he went to France where he worked for two years in various research laboratories. In 1935–1937 he was research director at the Vitamin Institute of Leningrad, U.S.S.R. In 1938, he returned to France and started to work as a research associate

at the École Normale Supérieure. In 1940, after the French armistice, he joined professor Claude Fromageot at the University of Lyon. In 1947, Dr. Lederer moved once more to Paris, continuing his research activities there. In 1958, he became full professor of Biochemistry at the Sorbonne; this chair was transferred in 1963 with part of his team to the Faculté des Sciences of Orsay. Since 1960, he has also been the director of the Institut de Chimie des Substances Naturelles, at Gif-sur-Yvette.

Dr. Lederer's involvement in chromatography started in 1930, in Heidelberg, where he introduced Tswett's chromatographic method to the investigation of natural substances. He has been active in chromatography during his whole professional career. He has published over 300 original papers dealing with various aspects of the technique and its applications, and with investigations of natural products. He also authored and coauthored several books on chromatography, carotenoids and lipid biochemistry; the French monograph published in 1949–1952 and its English edition published in 1955 written in cooperation with M. Lederer, his cousin, belong to the classics of chromatography.

Dr. Lederer has received a number of awards for his achievements. He is a chevalier of the Legion d'Honneur and an officer of the Ordre National du Mérite; he has honorary doctorates from the Universities of Aberdeen and Liège and has been elected as the member of the academies of sciences of a number of countries and various scientific societies. He received the Fritzsche Award and the gold medal of the American Chemical Society, two awards from the Académie des Sciences of Paris, the August Wilhelm von Hoffmann gold medal of the German Chemical Society, the Paul Karrer gold medal of the Swiss Chemical Society and the gold medal of the Centre National de la Recherche Scientifique.



Victor Pretorius was born in 1928, in Randfontein, Transvaal, South Africa. He studied at the University of Pretoria receiving his B.Sc. and M.Sc. degrees in 1949 and 1951, respectively. In 1952 he was awarded a Rhodes Scholarship to Oxford University, England, where he worked under the Nobel Laurate Sir Cyril Hinshelwood. He finished his studies there receiving the Ph.D. in 1955. Returning to the University of Pretoria Dr. Pretorius was appointed a senior lecturer in 1957 and professor and head of the Department of Physical Chemistry in 1960. In 1966 he became director

of the Research Unit for Chromatography and in 1973 the director of the Institute for Chromatography of the University of Pretoria.

Dr. Pretorius' research interests have centered almost exclusively around chromatography. In 1958 he pioneered in the development of the flame ionization detector. Besides this, his contributions range from the theoretical aspects of both gas and liquid chromatography to preparative gas chromatography. He is the author of over 70 scientific papers and coedited with A. Zlatkis a monograph on preparative gas chromatography. Dr. Pretorius is member of various official committees in the Republic of South Africa. He has served as president of the South African Chemical Institute (1966–1967), the Joint Council of South African Scientific Societies (1969–1970), the Chemistry Section of the Suid-Afrikaanse Akademie vir Wetenskap en Kuns (1971–1972) and the Associated Scientific and Technical Societies of South Africa (1974–1975).

Dr. Pretorius was awarded the gold medal of the South African Chemical Institute in 1975.

NEW HORIZONS

Journal of Chromatography, 126 (1976) 3–9
© Elsevier Scientific Publishing Company, Amsterdam — Printed in The Netherlands

CHROM. 9411

CONTINUOUS AND ULTRASENSITIVE APPARATUS FOR THE MEASUREMENT OF AIR-BORNE TRACER SUBSTANCES

P. G. SIMMONDS

International Science Consultants, The Pines, The Chase, Hurn Rd, Ringwood, Hants. (Great Britain)

and

A. J. LOVELOCK and J. E. LOVELOCK

Brazzos Ltd., Bowerchalke, Nr Salisbury, Wilts. (Great Britain)

SUMMARY

An apparatus is described for the continuous and ultrasensitive measurement of air-borne tracer substances, based on direct analysis with an electron capture detector which uses ambient air as the carrier gas following the chemical conversion of indigenous oxygen to water. Optimal sensitivity and stability are achieved by the use of synchronous detection. The apparatus has potential application in the increasingly important study of the transport and diffusion of gases both on a local scale and over continental distances.

INTRODUCTION

The use of the electron capture detector with air as the carrier gas is hindered by atmospheric oxygen. The presence of this weak electron absorber, at a concentration of 21% in the carrier gas is sufficient to cause a 94% reduction in the detector saturation current[1]. Although the detector may function in this mode, the sensitivity and dynamic range are drastically reduced. An alternative approach which employs frontal chromatography coupled with electron capture detection for the semi-continuous determination of sulphur hexafluoride (SF_6) has been described by Dietz and Cote[2]. In this, the SF_6 is eluted in the nitrogen of the air for up to 60 sec before the oxygen emerges from the column.

The electron capture detector may be adapted, however, to operate as a continuous device by sampling air through a simple catalytic reactor where all substances other than nitrogen, carbon dioxide, SF_6 and some perfluorocarbons are converted to elemental hydrides. Atmospheric oxygen is changed to water, and chlorocarbons including the "Freons" produce HCl and HF, respectively, while nitrogen compounds are converted either to nitrogen or ammonia. Water formed in the reaction is removed conveniently by low-temperature condensation. The reactor, which is a palladium–gold alloy tube containing palladised asbestos, selectively transmits only SF_6 and some perfluorocarbons. This modified electron capture detector provides a continuous

signal in real time over the concentration range 10^{-9} to 4×10^{-14} parts by volume, without the need for chromatographic separation of SF_6 and oxygen[3 11].

EXPERIMENTAL

The general arrangement of the apparatus is illustrated in Fig. 1. In practice, air is driven into the apparatus from any convenient pump (A) at a flow-rate of 35–40 ml min^{-1}. A metal bellows pump (Model 21 E: Metal Bellows, Boston, Mass., U.S.A.) is an excellent non-contaminating pump for this purpose. A constant flow is achieved by metering the input air delivered by the pump through a control valve (B) (Type B1SA needle valve; Nupro, Cleveland, Ohio, U.S.A.). The incoming air is mixed with hydrogen gas supplied from a pressurized cylinder (C) and preset to flow at a rate of 20 ml min^{-1} via a capillary restrictor (D). The mixed gases then pass into the reactor (E), which consists of a palladium–gold (6:4) alloy tube 10 cm long × 3 mm in diameter (Englehard Ind., Cinderford, Gloucs., Great Britain). The reactor is heated electrically by means of an externally wound nichrome resistance heater (F) to a temperature of 300 ± 20°. The first 3.0 cm of the tube are loosely filled with 20% palladium on asbestos fibre (Englehard Ind.) which serves to combust the air–hydrogen mixture with the direct formation of water as steam. In addition, this catalyst promotes the conversion of all substances other than nitrogen, CO_2, and perfluorinated compounds to their elemental hydrides. Hydrogen in excess of that required for stoichiometric combination with oxygen and reduction of trace organics escapes through the walls of the reactor tube and is converted to water by catalytic reaction with atmospheric oxygen at the outer surface.

The gases leaving the reactor are a mixture of nitrogen, steam, traces of hydrogen halides, CO_2, and inert gases. This gas mixture is passed along a stainless-steel tube (0.159 cm O.D. by 0.76 mm I.D.) exposed to the air, in which it cools to about the condensation temperature of the steam. It is then passed into a 10 cm long

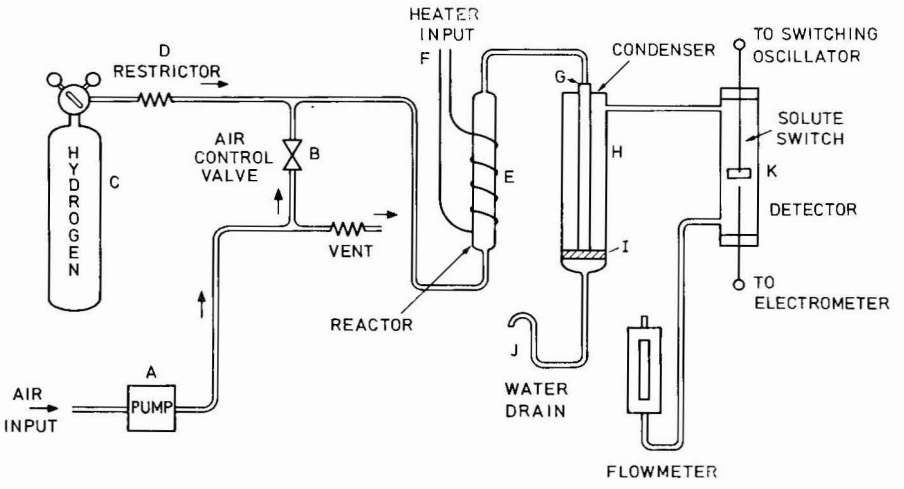


Fig. 1. Basic arrangement of continuous electron capture detection system.

× 3 mm diameter vertical pipe (G), which forms the inner member of a condenser, and is mounted axially inside a second pipe 6 mm in diameter (H). This outer pipe is firmly attached to a thermoelectric cooler (Model 801-2001-01; Cambion, Cambridge, Mass., U.S.A.) which is thermostatically controlled to maintain a temperature of approximately 3°.

The condensed water flows to a glass frit (I) (Sinterglass 531; Gallenkamp, London, Great Britain) which closes the bottom of the condenser. In this simple condenser system the water vapour is reduced in concentration to that set by the water vapour pressure at 3°. The bulk of the water which is condensed flows through the frit and away along a drain pipe (J) carrying with it, in dilute solution, the hydrogen acids and bases produced in the reactor. The capillary forces of the water in the pores of the frit are sufficient to seal the frit against the passage of gas. The gas stream leaving the condenser is now almost pure nitrogen with only the rare gases, CO_2 of the air, and traces of water vapour as contaminants. None of these react with or affect free electrons at thermal energy, and consequently this gas can serve as the background of an electron capture detector. When SF_6 is present in the gas stream it is detectable in the usual way by the capture of free electrons.

However, in the present apparatus a substantial gain in detectivity is achieved by passing the catalytically purified air into a specially modified electron capture detector (K), with solute switching and synchronous demodulation[12].

Electron capture detector with solute switching and synchronous demodulation

If the gas from the condenser is connected to a conventional electron capture detector, then it is only possible to observe trace concentrations down to about 1 in 10^{12} by volume. Noise and drift due to small changes of pressure, temperature, and gas flow-rate prevent the detection of even smaller concentrations. However, by using a solute switch[12], it is possible coherently to modulate the concentration of SF_6, for example, in the carrier stream, and then to recover any weak signals by synchronous demodulation. This not only provides a gain in detectivity but is impressively effective in eliminating baseline drift.

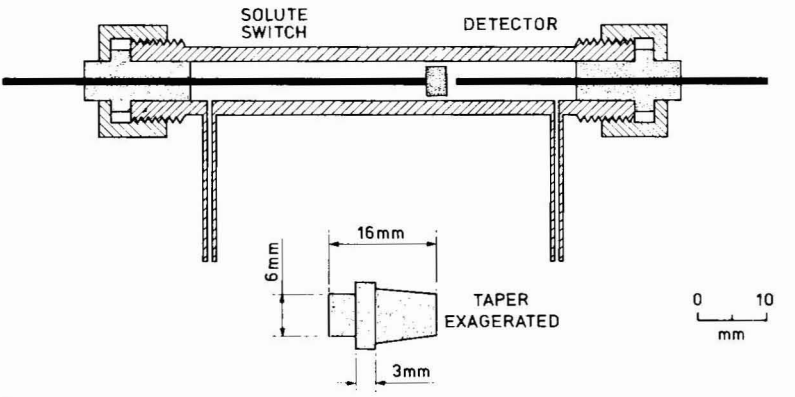


Fig. 2. Detail of dual-chamber electron capture detector with solute switching and synchronous demodulation.

The detailed design of the electron capture detector which incorporates these features is illustrated in Fig. 2. Two unequal chambers, in a ratio of 2:1, are provided in a single detector body by means of a PTFE separator. The detector is constructed from brass with PTFE insulators at each end and contains a single 300 mCi tritium radioactive source, size 5.0 × 1.5 × 0.025 mm thick (Radiochemical Center, Amersham, Great Britain). Gas from the condenser first enters the longer section of the detector, which operates as the solute switch. In this the SF_6 is alternately allowed to pass unhindered or destroyed by reaction with free electrons. The switch operates with an applied potential of 15 V positive, at a constant periodicity of 3 sec on and 3 sec off. The gas from the solute switch section of the detector passes around the PTFE separator and enters the shorter chamber which functions as a conventional electron capture detector. This senses the presence of SF_6 only when the switch allows it to pass, so that the output from this detector is therefore a low-frequency a.c. signal at the switching frequency. The amplitude of this signal is amplified fifteenfold and then converted to a steady d.c. level by means of a synchronous demodulator which is switched at the same phase and frequency as the solute switch. The basics of this electronic processing are illustrated in Fig. 3. The amplified signal is then passed through a low pass filter to remove any spurious noise generated by the switching process and continuously recorded to indicate the atmospheric SF_6 concentration. The entire system from the vapour switch to the output of the low pass filter achieves amplification of the SF_6 signal under conditions where noise and drift are rejected. Consequently the sensitivity of detection is increased by approximately 30 times, so that SF_6 can be detected at levels down to 4 parts in 10^{14} by volume.

Response to possible interferences

The ability of the apparatus to measure both continuously and specifically SF_6 and similar substances clearly depends on the special properties of the palladium catalyst and the temperature at which the reactor is operated, for there are various atmospheric contaminants which are also known to be strong electron absorbers. The most important class of electron absorbing trace compounds in the atmosphere are

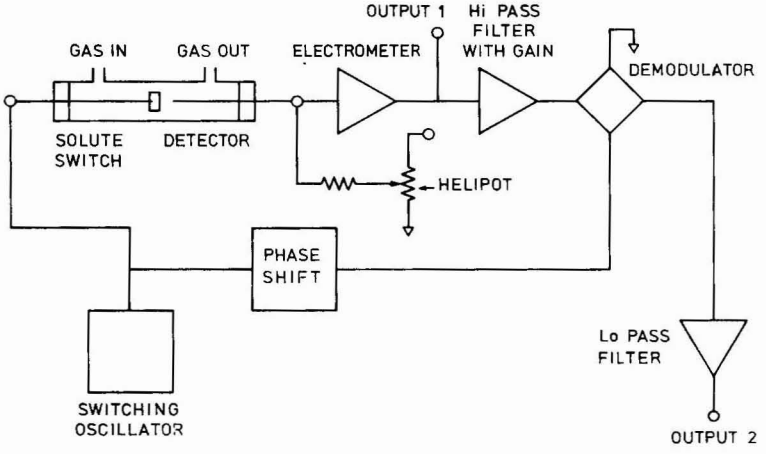


Fig. 3. Block diagram of electronic processing for dual-chamber electron capture detector.

TABLE I

RESPONSE OF CONTINUOUS APPARATUS TO POSSIBLE ATMOSPHERIC INTERFERENCES

Compound	*Normal ambient conc. (ppt)**	*Concentration of standard X (ambient conc.)*	*Instrument response*
Freon 12 (CCl_2F_2)	115	7×10^6	+
		10^5	–
Freon 11 (CCl_3F)	87	5×10^7	+
		10^6	–
Freon 113 (CCl_2FCClF_2)	1	10^6	+
		10^5	–
CCl_4	138	10^8	+
		2×10^7	–
$CHCl_3$	19	1×10^5	–
CH_3CCl_3	75	5×10^5	–
$CHCl=CCl_2$	5	5×10^8	–
		10^{10}	+
$CCl_2=CCl_2$	21	5×10^6	–
		4×10^8	+

* ppt = parts per 10^{12} by volume.

the chlorocarbons and the chlorofluorocarbons ("Freons"). The high thermal and chemical stability of the Freons, in particular, suggests that they possibly might survive transport through the catalyst. To test for this possible source of interference high vapour concentrations of Freons and other industrial chlorinated solvents were injected directly into the apparatus. The results of these tests are listed in Table I, which also includes literature values for the global background concentrations of the substances tested[13,14]. None of the compounds listed in Table I gave a response at concentrations of 10^5 times their global background. However, dichlorodifluoromethane (Freon 12) and 1,1,2-trichloro-1,2,2-trifluoroethane (Freon 113) did give small signals when the concentration injected exceeded about 100 ppm and 1 ppm, respectively. Although this reflects the known stability of these particular Freons to palladium-type catalysts[15], it is anticipated that even higher concentrations of contaminants might be tolerated if the bed length of catalyst within the reactor were to be increased. In a second experiment to test the ability of the catalyst to continuously destroy unwanted Freon, several microliters of liquid Freon 11 (monofluorotrichloromethane) were added to a small room containing a high-speed fan to give an approximate vapour concentration of 1 ppm. The apparatus was then allowed to sample the air from this room at an input flow-rate of 40 ml min^{-1} for about 45 min; and during this period there was no change in the baseline of the synchronously demodulated channel.

PERFORMANCE

The performance of the apparatus is illustrated in Fig. 4. Trace A is the output from the conventional pulsed detector electronics, while trace B is the synchronously

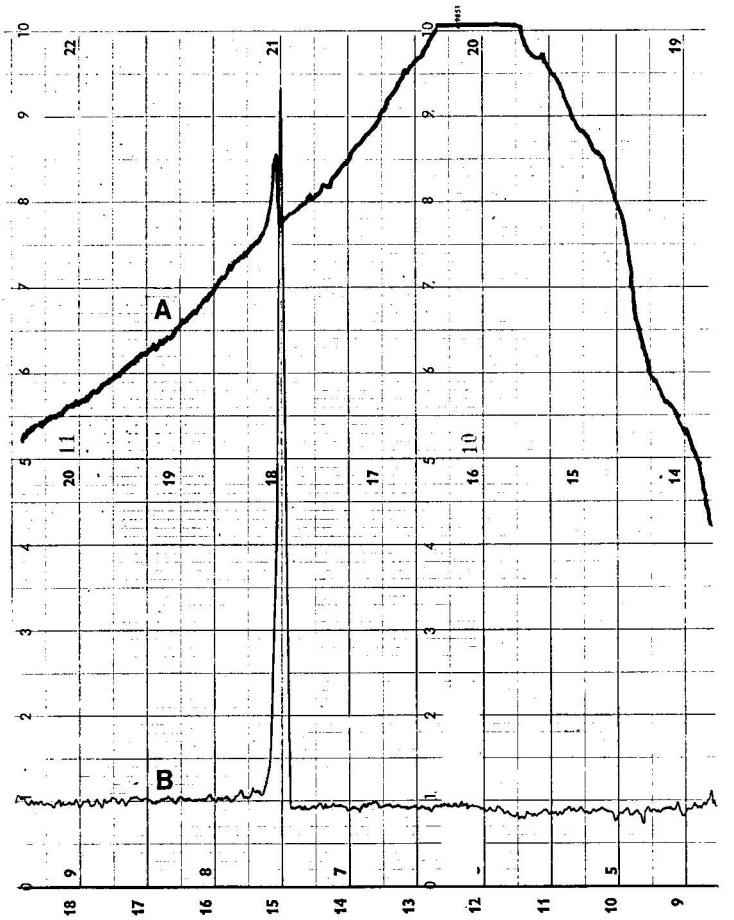


Fig. 4. Performance of continuous electron capture apparatus. Channel A: conventional pulsed detector output (4×10^{-10} A.f.s.d.); channel B: synchronously demodulated output (1.7×10^{-11} A.f.s.d.).

demodulated channel. The very stable baseline of this demodulated channel is particularly striking compared to trace A, where the baseline has drifted off-scale and back on again in response to a deliberately imposed change of about 10° in the ambient temperature of the laboratory. The 10 mV offset from electrical zero observed on trace B represents the normal background SF_6 concentration of approximately 5×10^{-13} by volume.

The signals observed on both channels are in response to a brief increase in SF_6 concentration to about 1 ppt (1 part in 10^{12} by volume). The substantial gain in sensitivity on the synchronously demodulated channel is readily apparent. Thus far the ambient background of SF_6 is small and steady enough in concentration not to interfere with the use of SF_6 as an air-borne tracer. The apparatus can also be used with perfluorocarbon tracers but the sensitivity to these substances is less than with SF_6.

The apparatus described thus provides both a continuous and ultrasensitive monitor which is also highly selective. The design is simple and is easily adapted as a self-contained portable instrument. It should find practical applications in the study of atmospheric dispersion problems, including hurricane dynamics, and the experimental verification of theoretical models which describe complicated patterns of air flow. Moreover, the basic apparatus should be useful in conducting long-range tracer experiments to study transport and diffusion of gaseous plumes over continental distances.

ACKNOWLEDGEMENT

We gratefully acknowledge the assistance of Dr B. Foulger.

REFERENCES

1 G. G. Guilbault and C. Herrin, *Anal. Chim. Acta*, 36 (1966) 252.
2 R. N. Dietz and E. A. Cote, *Environ. Sci. Technol.*, 7 (1973) 338.
3 G. F. Collins, F. E. Bartlett, A. Turk, S. M. Edmonds and H. L. Mark, *J. Air Pollut. Control Ass.*, 15 (1965) 109.
4 L. E. Niemeyer and R. A. McCormick, *J. Air Pollut. Control Ass.*, 18 (1968) 403.
5 A. Turk, S. M. Edmonds and H. L. Mark, *Environ. Sci. Technol.*, 2 (1968) 44.
6 C. A. Clemons, A. I. Coleman and B. E. Saltzman, *Environ. Sci. Technol.*, 2 (1968) 551.
7 H. F. Hawkins, K. R. Kurfis, B. M. Lewis and H. G. Ostlund, *J. Appl. Meteorol.*, 11 (1972) 221.
8 P. G. Simmonds, G. R. Shoemake, J. E. Lovelock and H. C. Lord, *Anal. Chem.*, 44 (1972) 860.
9 P. J. Drivas, P. G. Simmonds and F. H. Shair, *Environ. Sci. Technol.*, 6 (1972) 609.
10 B. E. Saltzman, A. I. Coleman and C. A. Clemons, *Anal. Chem.*, 38 (1966) 753.
11 L. Zoccolillo and A. Liberti, *J. Chromatogr.*, 108 (1975) 219.
12 J. E. Lovelock, *J. Chromatogr.*, 112 (1975) 29.
13 J. E. Lovelock, *Nature (London)*, 241 (1975) 194.
14 E. P. Grimsrud and R. A. Rasmussen, *Atmos. Environ.*, 9 (1975) 1014.
15 F. W. Williams and H. G. Eaton, *Anal. Chem.*, 46 (1974) 179.

Journal of Chromatography, 126 (1976) 11–18
© Elsevier Scientific Publishing Company, Amsterdam — Printed in The Netherlands

CHROM. 9430

HEATER-DISPLACEMENT CHROMATOGRAPHY

C. M. A. BADGER, J. A. HARRIS, K. F. SCOTT, M. J. WALKER and C. S. G. PHILLIPS
Inorganic Chemistry Laboratory, Oxford University, Oxford (Great Britain)

SUMMARY

The classical displacement gas chromatographic method has been modified by using a moving heater which eliminates the need for the displacer substance normally required pure and in large quantity. The technique is particularly suitable for trace concentration and for preparative work on a continuous basis, and by using catalysts as adsorbents it is also possible to carry out reaction and separation in one operation.

INTRODUCTION

There have been many examples of the use of elution gas chromatography (GC) for preparative work[1], of which the most successful (*e.g.*, ref. 2) would appear to be that of the ERAP-SRTI process (ELF, Solaize, France) now used for the production of high-purity products on the scale of up to 3 kg/h. As was shown some years ago, displacement GC is a powerful alternative and has certain peculiar advantages[3]. These include:

(1) The fact that displacement chromatography operates best under conditions of high vapour concentration where there is competition between molecules, for, *e.g.*, surface sites on an adsorbent, *i.e.*, in the region of marked curvature in the Langmuir-type adsorption isotherm. Thus 50-g samples are readily separated on 350 g of activated charcoal adsorbent[3].

(2) The enhanced selectivity of adsorbents over normal GC liquids which makes possible the tailoring of columns for particular difficult separations. This selectivity can usually be determined most rapidly first of all by simple elution experiments.

(3) The use of these adsorbents at lower temperatures in displacement than in elution chromatography. This will in general enhance the separations, but is most important in reducing the risk of chemical reactions occurring on a column packed with an active adsorbent.

(4) The possibility of using buffer substances (*e.g.*, added artificially to the mixture to be separated) which will form displacement bands between the substances to be separated, and which can then be easily removed, *e.g.*, by some simple chemical or solution methods.

(5) The concentration of trace impurities (*e.g.*, of alkenes in alkanes by a factor of 10^8) (ref. 3).

The original displacement method suffers, however, from two disadvantages:

(1) A large quantity of pure displacer material is required to displace the sample from the column.

(2) The column needs to be regenerated and the displacer material recovered by heating up the column after the end of the displacement experiment. These two disadvantages can be overcome, as we have now shown, by use of a heater moving along the column. The function of the heater is to drive all the sample substances ahead of it along the column in a manner similar to the analytical device of Turner[4] as distinct from having the sample within the heater zone as in the chromatothermographic technique of Turkeltaub[5]. In this manner the most strongly adsorbed component of the mixture displaces the next most strongly adsorbed component, etc. In the case of a thermolabile sample, it may be necessary to add a small amount of a displacer substance (more strongly adsorbed than any of the components of the sample) which serves to protect the thermolabile substances from the heater by ensuring that they will always be in the colder parts of the column some distance ahead of the heater.

It is also possible to use the heater to induce reactions on the column itself so that reaction and separation of products can be effected in one operation on the preparative and possibly on the production scale. Some preliminary examples of this mode of operation and using catalysts as adsorbents are described in the latter part of the paper, while the earlier part is concerned with examples involving preparative separation only.

EXPERIMENTAL AND RESULTS

The experiments quoted in this paper have been carried out using a small-scale prototype heater-displacement apparatus with a glass column of 1 m length and 1 cm I.D. This has been packed or partly packed with adsorbents such as activated charcoal, activated alumina, silica (Porasil), $Pt–Al_2O_3$, $Ni–SiO_2$, and porous polymer (Porapak). The column is mounted vertically in an air oven which can be maintained at controlled temperatures between room temperature and 130°. An electrical-resistance heater, 6 cm long, fits loosely around the column and moves downwards under its own weight on slide rails attached to the side of the oven. The rate of movement of the heater is controlled by a motor and pulley system between 10 and 80 cm h^{-1}. The heater temperature can be varied between 100 and 500°, and thermocouple measurements inside the column show that the temperature rises quite sharply (over about 3 cm) into the heater zone. Better and more efficient operation would be expected using direct dielectric heating of the adsorbent. Carrier gas flow-rates have been varied between 10 and 300 cm^3 min^{-1}. The effluent from the column passes through a heated sampling valve which is operated automatically so as to inject samples via a splitter into a rapid GC analytical column consisting of a 20 ft. × 1/100 in. stainless-steel capillary column coated with squalane.

Samples have been introduced to the column either by direct injections or via a saturator. With single injections of relatively large samples great care has to be taken to avoid liquid running down the inside wall of the column. The majority of runs have been made with batch introduction of sample, but it has proved possible to continue to introduce fresh sample on to the cooled parts of the column while the heater is still

moving down the rest of the column. This means that the process can be carried out on a continuous basis, as is envisaged schematically in Fig. 1. Sample (*e.g.*, directly from a reactor) is fed on to the column continuously in carrier gas at a concentration somewhat less than it will eventually leave the column in the displacement band. A number of heaters then pass along the column, and in front of each heater some concentration and then displacement separation takes place. The different components leaving the column can be collected by a valving sequence suitably timed in relation to the movement of the heaters. In this way most of the column can be utilised all the time, provided that, as is likely in practice, the process is used for a relatively close range of substances so that none of these elute ahead of the displacement bands.

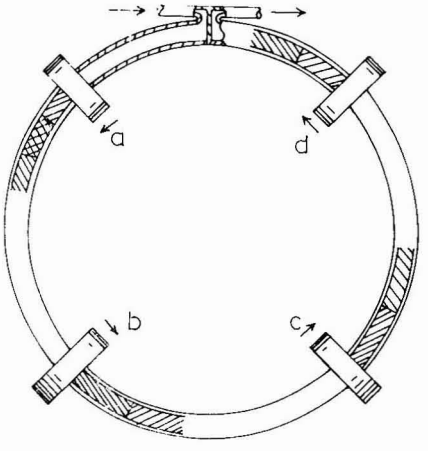


Fig. 1. Schematic heater-displacement apparatus with continuous operation. Sample is introduced continuously at top left and collects on column until it is displaced forward by one of the moving heaters, a, b, c, or d. Individual components are taken off at top right via valves suitably synchronised with the moving heaters.

The experiments which we have so far conducted have been limited to sample sizes not greater than 5 g leaving the column over a period of about 100 min. Reasonable increases in heater speed and carrier gas flow-rate and in particular increase in column diameter (say to 12.5 cm, which has proved entirely feasible in the ERAP-SRTI process) would lead to productive rates of a kilogram or more per hour per unit.

Examples of separation only

Figs. 2–4 illustrate the kinds of separation which have been achieved with the simple heater-displacement apparatus. Activated charcoal (as in Fig. 2) has a high sample capacity but is not as selective for alkane isomers as, *e.g.*, Al_2O_3 (Fig. 3). Terpenes have been found to be too strongly retained on charcoal and to undergo extensive reactions on unmodified Al_2O_3 or SiO_2 surfaces. They can, however, be separated satisfactorily with porous polymer (Fig. 4) as adsorbent. In this case undecane has been used as a "thermal buffer". It displaces the terpenes and thus protects them from reaction in the heater zone. Figs. 3 and 4 show the manner in which various impurities (so far unidentified in the case of the terpene samples) are concentrated in

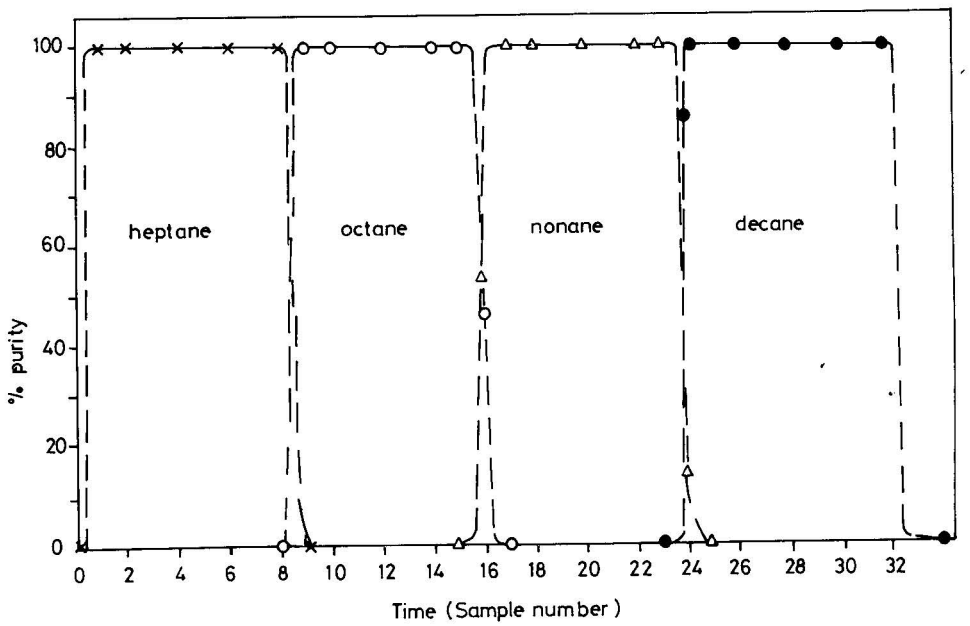


Fig. 2. Separation of a 4-g mixture of *n*-alkanes. Column, 90 × 1 cm I.D.; adsorbent, activated charcoal (Sutcliffe-Speakman 207C) at 100°; nitrogen flow-rate, 120 cm^3 min^{-1}; heater temperature, 450°; heater speed, 20 cm h^{-1}. Samples taken for analysis every 5 min after a 2-h running time.

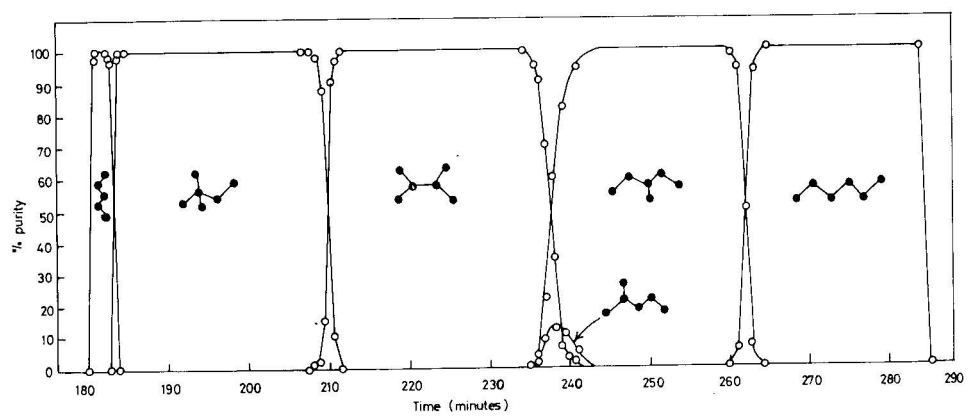


Fig. 3. Separation of a 2-g mixture of equal quantities of four isomeric hexanes (with *n*-pentane and 2-methylpentane impurities). Column, 100 × 1 cm I.D.; adsorbent, γ-Al_2O_3 (Phase Separations, Queensferry, Great Britain) at 18°; nitrogen flow-rate, 70 cm^3 min^{-1}; heater temperature, 110°; heater speed, 21 cm h^{-1}.

front of or between the main displacement bands. It should be noted that increasing both the length of the column and the sample size will normally lead to broader bands without any increase in the width of the overlap zones. In general, gas flow-rates and heater speeds have to be adjusted to avoid elution (which will occur at high gas flow-rates and/or low heater speeds) on the one hand or condensation (which will occur at low gas flow-rates and/or high heater speeds) on the other.

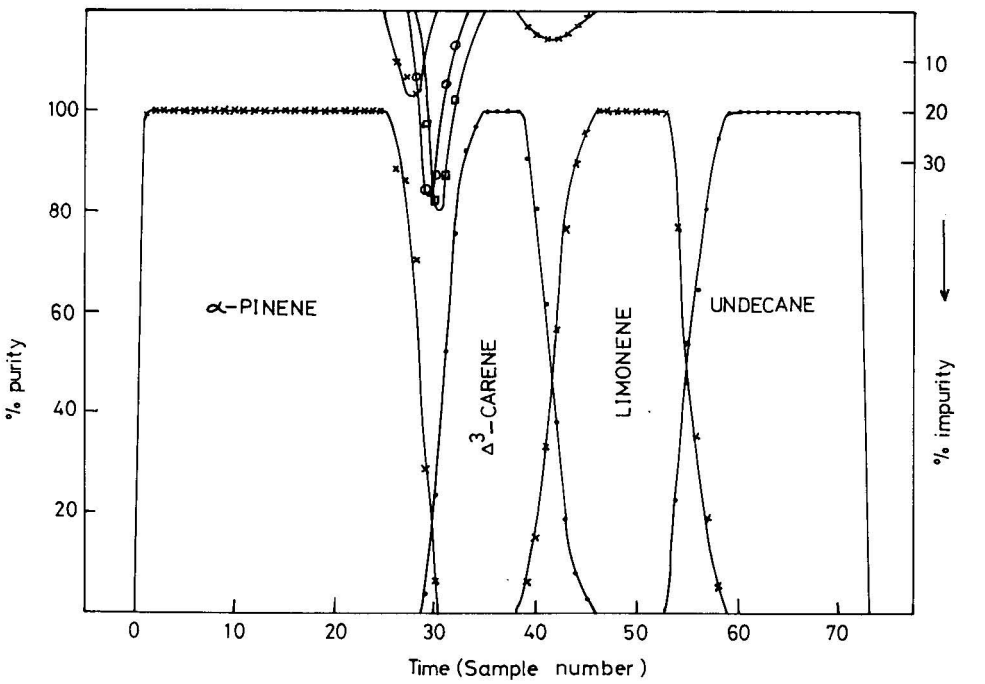


Fig. 4. Separation of a 1.5-g mixture of α-pinene, Δ^3-carene, and limonene with concentration of four unidentified impurities. Undecane was added to act as "thermal buffer". Column, 50 × 1 cm I.D.; adsorbent, Porapak Q at 85°; nitrogen flow-rate, 200 cm^3 min^{-1}; heater temperature, 300°; heater speed, 20 cm h^{-1}.

Reaction and separation

Further variations on the heater displacement principle are possible if the column adsorbent is a catalyst on which reactions take place at the temperature induced by the moving heater while only separation takes place ahead of the heater in the cooler parts of the column. It should thus be possible to carry out reaction and separation on the preparative scale in one single operation. We have as yet done relatively few experiments in this particular mode of operation, and it has become clear that in most cases a rather delicate choice of the conditions (thus the gas flow-rate, heater temperature, and heater speed markedly affect the amount of reaction occurring in the heater zone), and the catalyst and the adsorbent may be necessary to achieve optimum results. The general principles may, however, be illustrated by the chromatograms of Figs. 5–7.

Fig. 5. shows the results of a dehydrochlorination reaction on Al_2O_3 modified with KCl. The three olefins formed in the reaction in the heater are reasonably separated on the same material in the parts of the column ahead of the heater which were kept at room temperature. One interesting feature of this chromatogram is the combination of two of the products of the reaction, namely HCl and 1,1-dichloroethylene, to give 1,1,1-trichloroethane which emerges as a peak between the *cis*- and *trans*-1,2-dichloroethylene isomers. Fig. 6 shows the reaction of a sample of *n*-decane on a Ni–SiO_2 column under hydrogen carrier gas. Hydrocracking of the *n*-decane occurs

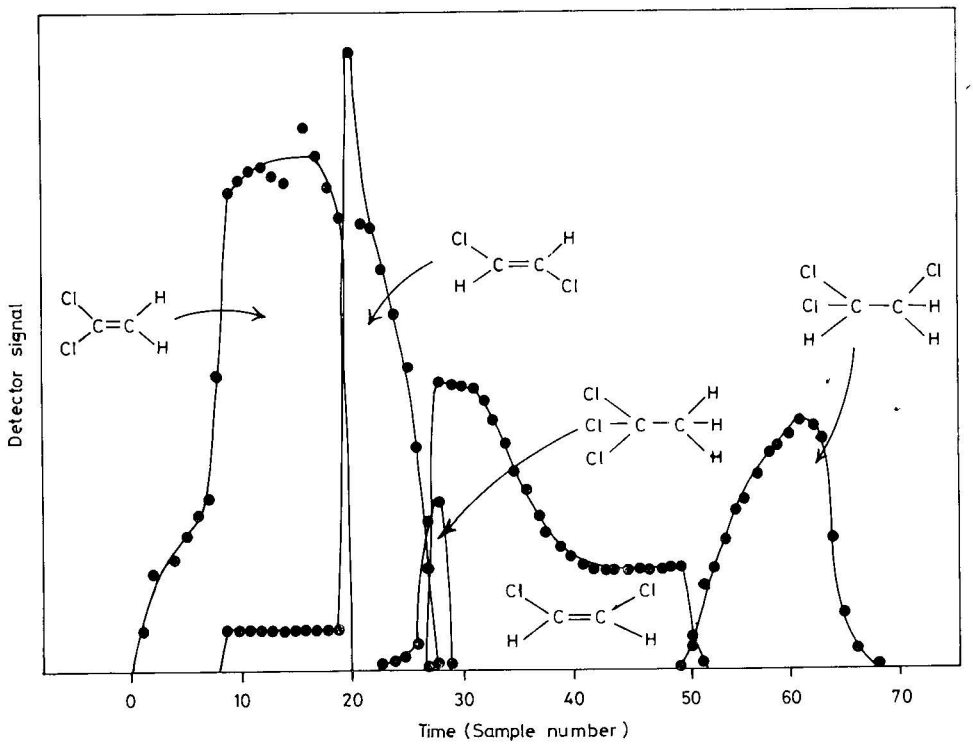


Fig. 5. Reaction (dehydrochlorination) of 1,1,2-trichloroethane (0.3 g) followed by partial separation of products on 5% KCl–Al_2O_3. Column, 30 × 1 cm I.D. at 18°; heater temperature, 500°.

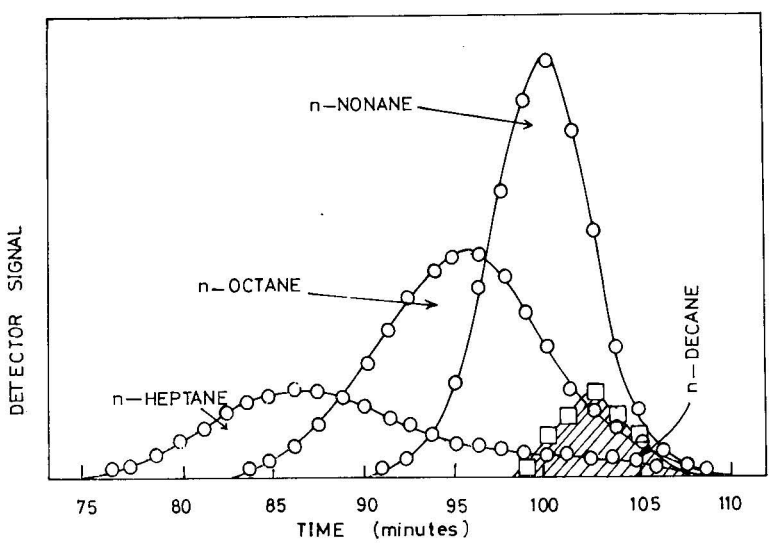


Fig. 6. Reaction (hydrocracking) of *n*-decane (0.02 g) followed by partial separation of products on 2.3% Ni–SiO_2. Column, 33 × 1 cm I.D. at 125°; hydrogen flow-rate, 10 ml min^{-1}; heater temperature, 180°; heater speed, 20 cm h^{-1}.

largely by successive steps[6] to *n*-nonane, *n*-octane, etc., and these are then partially separated on the catalyst ahead of the heater. However, by packing the lower part of the column with a catalytically inactive adsorbent (which need not even be in the same oven as the catalyst) the reaction could be made to cease when the heater reaches the end of the $Ni–SiO_2$, so that only separation occurs in the last part of the column.

A particularly interesting possibility arises when the catalysed reaction involves an isomerisation, because the continuing sequence of reaction, separation, and re-reaction then offers the potential of driving the reaction beyond its thermodynamic equilibrium position and eventually to the production of only one isomer in high yield. The result of a preliminary experiment on the isomerisation of *n*-hexane is illustrated in Fig. 7. The original *n*-hexane is isomerised to a mixture of *n*-hexane, 2-methylpentane, 3-methylpentane, 2,3-dimethylbutane, and 2,2-dimethylbutane (there is also some hydrocracking to *n*-pentane, etc.) on the $Pt–Al_2O_3$ catalyst in the heater zone. The isomers then begin to separate ahead of the heater, but the *n*-hexane and the less branched isomers lie at the rear of the displacement sequence and thus come into

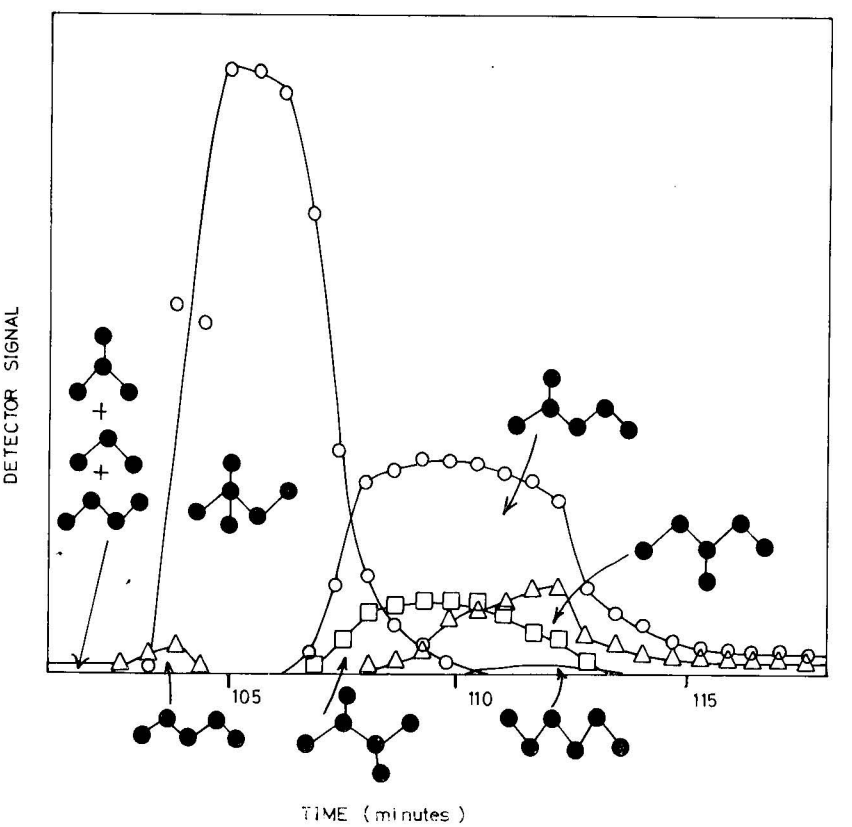


Fig. 7. Continuous reaction (isomerisation) and partial separation of products from *n*-hexane (0.7 g) on $Pt–Al_2O_3$ (Engelhard RD-290C activated with CCl_4). Column, 100 × 1 cm I.D. at 18°; hydrogen flow-rate, 30 cm^3 min^{-1}; heater temperature, 120°; heater speed, 50 cm h^{-1}. Reaction has so far proceeded to 99.5% conversion of the *n*-hexane with a 46% yield of 2,2-dimethylbutane. 4.5% of the *n*-hexane has been hydrocracked to lighter material, eluting ahead of the displacement bands.

repeated contact with the active (hight-temperature) part of the catalyst, so that the doubly branched isomers are continuously increased at the expense of the less branched isomers. Eventually the reaction should give rise to 2,2-dimethylbutane as almost the only product. As the highly branched alkane isomers have much higher octane (anti-knock rating) values, this might be of some commercial application.

ACKNOWLEDGEMENTS

The work is supported in part by a grant from the Petroleum Research Fund of the American Chemical Society. One of us (K.F.S.) is the holder of a British Petroleum Research Studentship. U.K. Patent Application 29491/74 and corresponding applications in the U.S.A. and other foreign territories, rights in which are assigned to National Research and Development Corporation.

REFERENCES

1 A. Zlatkis and V. Pretorius, *Preparative Gas Chromatography*, Wiley-Interscience, New York, 1971.
2 P. Valentin, G. Hagenbach, B. Roz and G. Guiochon, in S. G. Perry (Editor), *Gas Chromatography 1972*, Applied Science and Institute of Petroleum, London, 1973, p. 157.
3 C. G. Scott and C. S. G. Phillips, in A. Goldup (Editor), *Gas Chromatography 1964*, Institute of Petroleum, London, 1965, p. 266.
4 N. C. Turner, *Oil Gas J.*, 29 April (1943) 48.
5 N. M. Turkeltaub, *Zavod. Lab.*, 15 (1949) 653.
6 K. F. Scott and C. S. G. Phillips, *J. Chromatogr.*, 112 (1975) 61.

Journal of Chromatography, 126 (1976) 19–33
© Elsevier Scientific Publishing Company, Amsterdam — Printed in The Netherlands

CHROM. 9428

PARTICLE SIZE, PRESSURE AND ANALYSIS TIME IN ROUTINE HIGH-PERFORMANCE LIQUID CHROMATOGRAPHY*

ISTVÁN HALÁSZ, HEINRICH SCHMIDT and PETER VOGTEL
Angewandte Physikalische Chemie, Universität des Saarlandes, Saarbrücken (G.F.R.)

SUMMARY

The maximum number of theoretical plates that can be generated in a column can be calculated from the empirical equations $u_{min}\, d_p = 10$ and $h_{min} = 4\, d_p$ (where the minimum linear velocity of the eluent, u_{min}, is given in mm/sec and the average size, d_p, in μm), if the average particle size d_p is based entirely on chromatographic particle measurements. It was demonstrated experimentally that 30-cm silica or reversed-phase columns having over 7000 plates could be packed with $d_p = 10\,\mu$m. Such columns can resolve, with baseline peak separation, mixtures that possess relative retentions greater than 1.12. In routine work, the relative retentions are usually greater and it is advantageous to use only 7.5-cm long columns. Analysis times of 10 min or less can be achieved even with velocities around u_{min}. Consequently, most routine separations require column pressures of less than 50 atm. For research studies and for the optimization of conditions for routine work, columns packed with 5-μm particles are often necessary. The reproducibility of column packing with $d_p < 5\,\mu$m is poor. It was shown that up to 600 plates/cm and over 100 plates/sec (capacity ratio = 1) can be generated on silica columns with $d_p = 3.2\,\mu$m. Such small particle sizes are particularly advantageous for trace analysis because, as our experience indicates, these short and efficient columns can be loaded with samples larger than the amount calculated from the weight of the stationary phase present.

INTRODUCTION

It is well known that the separation time in high-performance liquid chromatography (HPLC) decreases with decreasing particle size. If the pressure drop, Δp, along a column is kept constant (because of equipment limitations), the maximum number of theoretical plates, n_{max}, available at u_{min} (the linear velocity at the minimum of an *h versus u* curve) decreases with decreasing particle size. Furthermore, with decreasing particle size (1) u_{min} increases, (2) the pneumatic resistance for a given column length increases, (3) packing of the column becomes more difficult and (4) the heat of friction due to the high pressure drop cannot always be neglected. These problems were discussed in

* Part of a lecture presented at the 10th International Symposium on Advances in Chromatography, Munich, G.F.R., November, 1975.

previous publications[1-3], and it was demonstrated that a sieve fraction with a particle size of about 10 μm seems to be an optimal compromise. The main objective of this paper is to demonstrate that most routine separations can be carried out with columns packed with 10-μm particles.

Column packing

During column packing, the sedimentation of the support particles must be minimized, particularly if their diameter is less than 25 μm, and all successful packing procedures make use of this fact. It is well known that the sedimentation velocity, dx/dt, is given by

$$\frac{dx}{dt} = \frac{2r^2 (\varrho_s - \varrho_l)}{9\eta} \qquad (1)$$

where r is the radius and ϱ_s the true specific gravity of the support particles, and ϱ_l is the specific gravity and η the viscosity of the dispersing liquid. The differences in the sedimentation velocity due to variations in the particle size can be minimized by: (1) minimizing the difference in both densities, *i.e.*, ϱ_s and ϱ_l, (2) "maximizing" the viscosity η, or (3) using an appropriate combination of both.

The first of these procedures is the balanced density method[1,4-8], which gives good results only when the wetting of the solid by the dispersing liquid is very good (*i.e.*, the wetting angle is approximately zero). If the wetting angle is high, the required specific gravity of the slurry, ϱ_l, can become a function of the pore size distribution (and, sometimes, of the particle size distribution) of the packing material. The wetting angle between a given solid support and a liquid frequently changes from batch to batch, and it is therefore essential to check visually the sedimentation rate of each support sample. Among other factors, the wetting angle is a function of the polarity of the support (*e.g.*, it is different for silica and reversed-phase supports).

The second packing procedure is the viscosity method[8], which is more universally applicable than the first and the choice of dispersing agents is extensive. This aspect can be of special interest if chemically bonded phases are to be packed. However, with increasing viscosity of the dispersing agent, the time required for packing increases. Therefore, as a third alternative, a compromise between the "balanced density" and "viscosity" methods is sometimes the best solution. The columns discussed in this paper were packed by the first two methods[8].

The quality of a column is determined by its efficiency and its lifetime, and our experience indicates that the lifetime of a column is governed primarily by its packing density. This factor is especially important for columns packed with reversed phases. If the packing density is low, the initial efficiency can be up to two times that of a well packed column (to be quantitatively defined later). However, the lifetime of such columns is frequently very short (on the order of 1 h to 5 days). If the packing density is very high, it is almost impossible to destroy the column efficiency by mechanical means. The price for such a long lifetime is a high pneumatic resistance, *i.e.*, the pressure drop along the column is up to twice that of a well packed column. Yet the differences in packing density are small and hard to determine. To produce well packed columns consistently requires both experience and intuition and, furthermore, the problems increase with decreasing particle size. In fact, based on our experience and

that of others, using the packing techniques described above, it can be simply stated that packing columns with 10-μm particles is routine, packing those with about 5-μm particles requires "art", and for packing those with particles smaller than 5 μm nothing short of "black magic" is enough (the rate of success being less than 10%).

Average particle size, d_p

Column efficiency is a function of the narrowness of the particle size range (width of a sieve fraction) and the average particle size, d_p, of the stationary phase. Unfortunately, d_p is not an unambiguously defined quantity, but depends on the way in which it is determined (sieving, air-classification, sedimentation, centrifugation, measurement with a Coulter counter, microscopy, light scattering, etc.) and the way its average is expressed (number-, volume- or weight-average). Such d_p determinations are carried out on the unpacked stationary phase, and it is questionable whether the values thus obtained characterize realistically the stationary phase inside the column. It is well known that the specific surface area and therefore the surface energy of solids increase essentially linearly with decreasing particle size. To decrease this surface energy, the particles can agglomerate. Thus, the surface energy of 5- to 10-μm particles can become a significant factor during packing, and for particles of size <1 μm agglomeration ("particle bridging") is almost inevitable if the solid is at least partially dry. As an illustration, let us consider two columns packed with a narrow sieve fraction of about 10 μm, but with one of them containing an additional *ca.* 1% by number of 0.1-μm particles. The weight- and volume-averaged d_p values would be virtually identical for both packings, but the efficiency of the column containing the 0.1-μm particles would be lowered considerably.

From the above discussion, it follows that an unambiguous definition of d_p is very important. We have previously proposed[1–3] a definition of d_p that is based entirely on chromatographic measurements:

$$d_p = 41 \sqrt{\frac{F \eta L}{r^2 \pi \Delta p}} \tag{2}$$

where the parameters are given in convenient units, *i.e.*, d_p in μm, flow-rate, F, in ml/min, viscosity η in cP, column length, L, in cm, column radius, r, in mm, and pressure drop, Δp, in atm (if the c.g.s. system is used, the proportionality factor becomes $\sqrt{1000} = 31.6$ instead of 41 in eqn. 2).

Definition of a well packed column

Based on literature data and our experience with 4–40-μm (or perhaps even 3–80-μm) particles, a tolerable definition[2,3] for a "well packed column" seems to be a column whose h *versus* u curve can be described by the following equation, provided that d_p is defined by eqn. 2:

$$h = 3 d_p + \frac{2 D}{u} + \frac{d_p^2 u}{5.3 D} \tag{3}$$

where the height equivalent to a theoretical plate, h, and d_p are in μm, the diffusion coefficient, D, of the sample in the eluent in 10^{-5} cm^2/sec and the linear velocity of

the eluent, u, in mm/sec. To obtain a valid value for h, all three terms must be summed because the individual terms themselves tend to compensate each other. Eqn. 3 is valid in the velocity range in which virtually all routine separations are carried out, the limitations being imposed by the capabilities of the currently available commercial equipment.

A typical value of D for HPLC in non-aqueous solvents and for samples with molecular weights of roughly 200–600 is $3 \cdot 10^{-5}$ cm^2/sec. Substituting this value of D into eqn. 3 yields

$$h = 3\,d_p + \frac{6}{u} + \frac{d_p^2\,u}{16} \tag{4}$$

Eqn. 3 or 4, in conjunction with eqn. 2, defines a well packed column to within $\pm 20\%$ in h at commonly used linear velocities. These velocities, of course, vary with d_p.

Eqns. 3 and 4 can be expressed in dimensionless parameters, in terms of the reduced plate height, h/d_p, and the reduced velocity, $\nu = ud_p/D$:

$$\frac{h}{d_p} = 3 + \frac{2}{\nu} + \frac{\nu}{5.3} \tag{5}$$

Eqn. 4 can be rewritten as

$$\frac{h}{d_p} = 3 + \frac{6}{u\,d_p} + \frac{d_p\,u}{16} \tag{6}$$

Plots of eqns. 5 and 6 are given in Fig. 1. Experience shows that in LC the reduced parameters, to a good approximation, are independent of d_p, as predicted by theory. It should be pointed out again, however, that agreement between theory and practice is valid only for velocities that are typical at present for routine separations. Differentiation of eqn. 6 yields

$$d_p\,u_{\min} \approx 10\left(\mu\text{m} \cdot \frac{\text{mm}}{\text{sec}}\right) \tag{7}$$

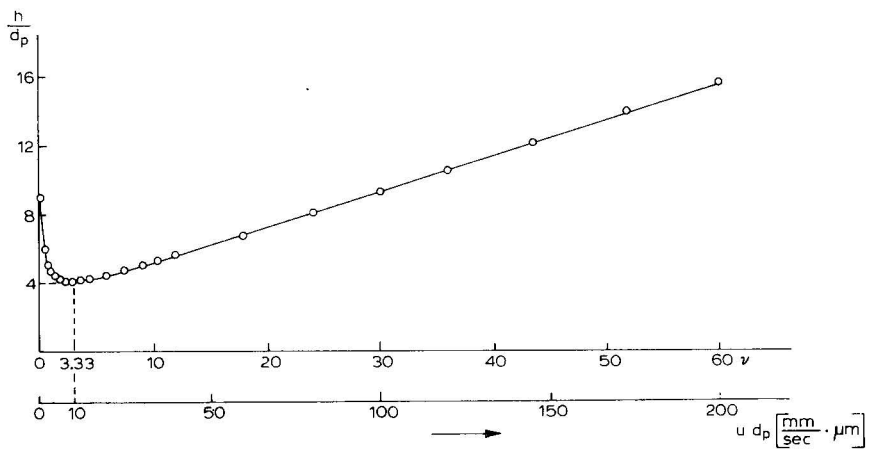


Fig. 1. Plot of reduced plate height, h/d_p, *versus* reduced velocity, ν, as calculated from eqns. 5 and 6. For the ud_p-axis, it is assumed that $D = 3 \cdot 10^{-5}$ cm^2/sec.

if d_p is given in μm and the linear velocity at the minimum of the curve in Fig. 1, u_{min}, in mm/sec. For example, if $d_p = 10\ \mu$m the minimum of the curve occurs at $u_{min} = 1$ mm/sec. As this a slower velocity than is commonly used, only the ascending branch of the *h versus u* curve used to be presented, which is, of course, linear. Such linearity is particularly true for columns packed with particles with $d_p \geqslant 10\ \mu$m. From the constants in eqn. 4, it is evident that at typical velocities h is, to a first approximation, linear in d_p if $d_p \leqslant 5\ \mu$m and $h \approx d_p^2$ if $d_p > 50\ \mu$m. By substituting u_{min} from eqn. 7 into eqn. 6, we obtain for the h value at the minimum of the *h versus u* curve

$$h_{min} \approx 4\ d_p \tag{8}$$

The specific permeability of a packed column is proportional to d_p^2. Consequently, for $d_p < 10\ \mu$m, h increases approximately linearly with d_p, but the pneumatic resistance of a given column increases with d_p^2. For small particles, therefore, the maximum number of theoretical plates that can be generated with a given maximum pressure decreases with decreasing particle size[2].

The efficiency and analysis time at u_{min}

It will now be demonstrated that most routine separations can be effected with columns packed with 10-μm particles. It should be pointed out again that d_p is not the average particle size claimed by the manufacturer, but rather the value calculated from eqn. 2. A comparison of commercially available "10-μm" silicas revealed a d_p range of 6–12 μm or even greater. The variation in d_p from batch to batch from the same manufacturer is usually smaller, but seldom negligible.

Tables I and II present typical data for routine separations. For the purpose of the following discussion, it will be assumed that the eluent viscosity is 0.4 cP (non-polar eluents), the total porosity, ε_T, of the column is 0.8, and the column diameter

TABLE I

CALCULATED PARAMETERS FOR COLUMNS OPERATED AT MAXIMUM EFFICIENCY

The following typical parameters were used in the calculations: viscosity of the eluent, 0.4 cP; inner diameter of the column, 4.2 mm; total porosity of the column, 0.8.

d_p (μm)	L (cm)	h_{min} (μm)	u_{min} (mm/sec)	F_{min} (ml/min)	n_{max}	Δp (atm)
10	30	40	1	0.68	7500	12
5	30	20	2	1.35	15000	96

TABLE II

CALCULATED PARAMETERS FOR COLUMNS OPERATED AT MAXIMUM EFFICIENCY

d_p (μm)	k'	N_{max}	R	α	t_R (min) ($k' = 2$)
10	2	3333	1.5	1.12	15
10	2	3333	1.0	1.07	15
5	2	6666	1.5	1.08	7.5
5	2	6666	1.0	1.05	7.5

and length are 4.2 mm and 30 cm, respectively. From the data, it can be seen that for $d_p = 10\ \mu m$ at $u_{min} = 1$ mm/sec, about 7500 theoretical plates (corresponding to 3333 effective plates, N, for $k' = 2$) are generated with a pressure drop of only 12 atm for a flow-rate of less than 0.7 ml/min. If the compounds to be separated have capacity ratios, k', of about 2, samples with a relative retention, α, of 1.12 can be separated if a resolution $R = 1.5$ (*i.e.*, baseline separation) is required. The analysis time is 15 min. With $N_{max} = 3333$, even compounds with $\alpha = 1.07$ can be separated if $R = 1$ is sufficient. For smaller relative retentions, the best approach would be to change the properties of the eluent (*i.e.*, change the eluent) and look for higher relative retentions. Only if this approach fails should a column with $d_p = 5\ \mu m$ be tried. With such a column ($L = 30$ cm), a pair of sample components with $\alpha = 1.05$ can be separated, provided $R = 1$ is adequate. Alternatively, a longer 10-μm particle column can be used if a longer analysis time can be tolerated. Most of the separations published recently have involved mixtures in which adjacent peaks had relative retentions of 1.15–1.6 (and greater). As Tables I and II demonstrate, the analysis time, of course, decreases with decreasing particle size. It is questionable, however, whether analysis times shorter than 5–10 minutes are always of great interest in routine work.

APPARATUS AND MATERIALS

Home-built equipment with a UV detector[2] was used. Commercially available eluents were purified by distillation. The stationary phase consisted of porous silica with an average pore size of 100 Å (SI 100, E. Merck, Darmstadt, G.F.R.). The silica was used as received or was chemically bonded with C_{18} bristles (*i.e.*, reversed phase).

RESULTS AND DISCUSSION

In Fig. 2, the column efficiencies obtained with samples having capacity ratios between 0.34 and 1.03 are plotted against the linear velocity. The eluent was methy-

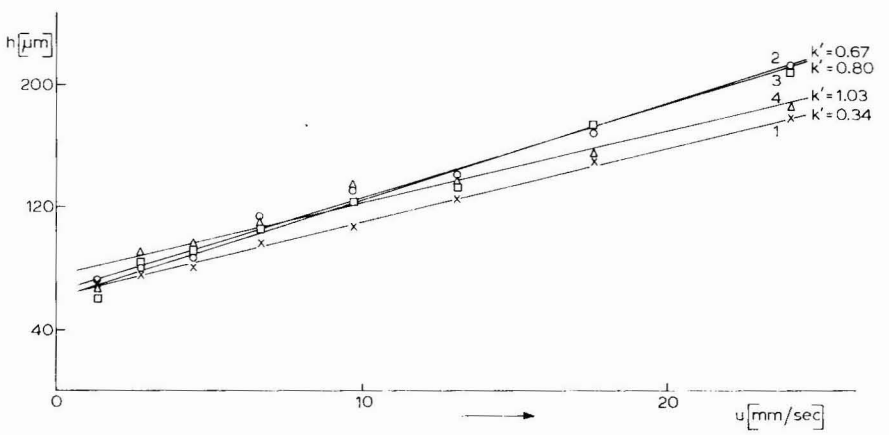


Fig. 2. Plots of h *versus* u on silica SI 100 ($d_p = 13.5\ \mu m$). Column length, 30 cm; I.D., 4.2 mm. Eluent, methylene chloride–propanol-2 (95:5, v/v). Samples: 1, thiogenal ($k' = 0.34$); 2, secobarbital ($k' = 0.67$); 3, vinylbarbital ($k' = 0.80$); 4, barbital ($k' = 1.03$). $K_F = 1.8 \cdot 10^{-9}$ cm². Temperature, ambient.

lene chloride–propanol-2 (95:5, v/v), and the average particle size (eqn. 2) was 13.5 μm. All measurements were carried out at ambient temperature. The linear velocity was varied from 1 to 25 mm/sec, which is typical for routine applications with d_p = 13.5 μm. The value of u_{min} is 0.74 mm/sec (eqn. 7).

As expected, the curves display acceptable linearity and are more or less independent of the k' values. It is an empirical fact, for which at present there is no theoretical basis, that for "excellent" columns the h *versus* u curves are independent of k' for a wide range of capacity ratios. But even for experts in column packing the probability of producing an "excellent" column is less than 10%. The results shown in Fig. 2 were obtained with an above-average, but not "excellent", column. The data points in Fig. 2 are replotted in Fig. 3 in terms of the (dimensionless) reduced plate height, h/d_p. The solid line represents the values calculated by means of eqn. 5, where $u = Dv/d_p = 3v/13.5$, assuming that $D = 3 \cdot 10^{-5}$ cm^2/sec and $d_p = 13.5$ μm. It is evident that acceptable agreement exists between the calculated and measured values in the commonly used velocity range. The pressure required to achieve a particular velocity is also shown in Fig. 3.

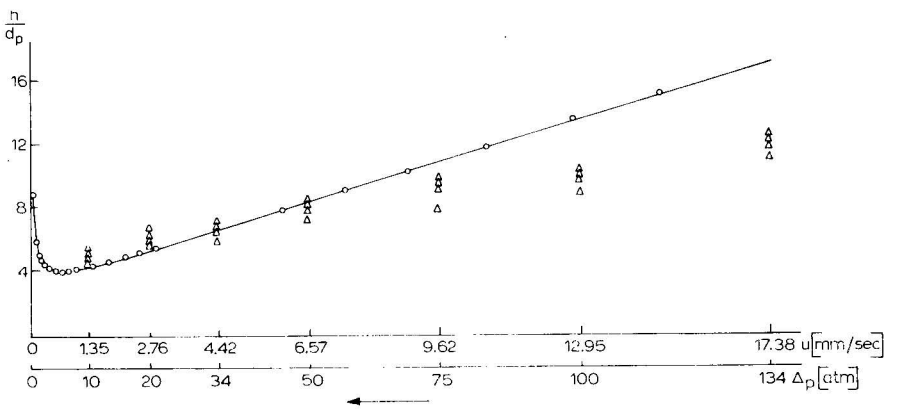


Fig. 3. Plots of h/d_p *versus* u. Parameters as in Fig. 2. The solid line was calculated by means of eqn. 5, assuming that $D = 3 \cdot 10^{-5}$ cm^2/sec and $d_p = 13.5$ μm.

A separation of barbiturates on the same column is illustrated in Fig. 4. The linear velocity was 1.1 mm/sec, *i.e.*, 50% higher than u_{min}, and the pressure drop was only 7.5 atm. For the pair of compounds with the smallest relative retention (α = 1.19), secobarbital and vinylbarbital, the resolution $R_{2,3}$ was 1.62, *i.e.*, better than baseline resolution. In general, if the resolution exceeds 1.5 only time is wasted. To optimize the separation time, the resolution should be reduced, *i.e.*, the column efficiency is actually excessive. To reduce the column efficiency, either the column length can be decreased or the linear velocity increased. Based on experience, the minimum column length should be greater than 7 cm if $d_p \leq 10$ μm. Otherwise, the inlet and outlet turbulences inside the column reduce its efficiency, as calculated from an h *versus* u curve determined with a longer column.

Unfortunately, packed columns 7–10 cm in length are almost unavailable from commercial sources. Therefore, a more practical means of optimizing the analysis

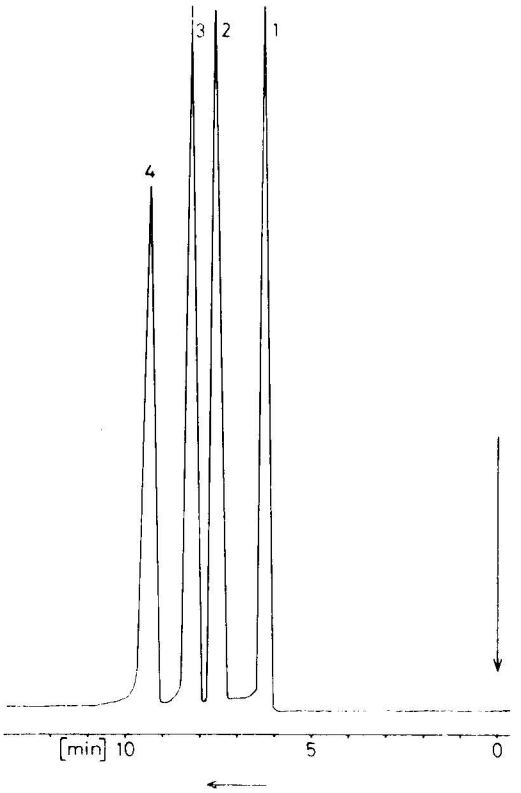


Fig. 4. Separation of barbiturates on silica. Parameters as in Fig. 2, except: u = 1.1 mm/sec, Δp = 7.5 atm and $R_{2,3}$ = 1.62.

time, t_R, is to keep the column length the same but to decrease the efficiency by using a faster flow-rate. Such optimization can be achieved only at the expense of increased pressure (Figs. 5–7). In Fig. 5, $R_{2,3}$ = 1.47 (essentially a baseline separation) is attained with Δp = 10 atm in 8 min. In Fig. 6, the analysis time is only 45 sec, but the pressure has risen to 100 atm. Of course, t_R can be reduced even further (25 sec), at the expense of a higher pressure (185 atm) and lower resolution (0.71), as shown in Fig. 7.

All of the results discussed above are well known, and perhaps trivial, but these facts are seldom applied in routine work. Thus:

(1) The maximum number of plates, n_{max}, is generated at u_{min}. Both can be estimated from eqns. 7 and 8.

(2) For conventional columns (L = 30 cm or 1 ft.) and typical relative retentions ($\alpha > 1.2$), peak separation better than baseline resolution is generally attained if the linear velocity is u_{min}. The analysis time can be optimized by reducing the column efficiency by using faster flow-rates. This is usually done intuitively, and the result is a high pressure drop over the column. It is for this reason that commercial equipment sometimes includes excessively high pressure pumps and attendant fittings, injection system, etc., which increase its price considerably.

(3) It would be better to reduce the conventional column length because sepa-

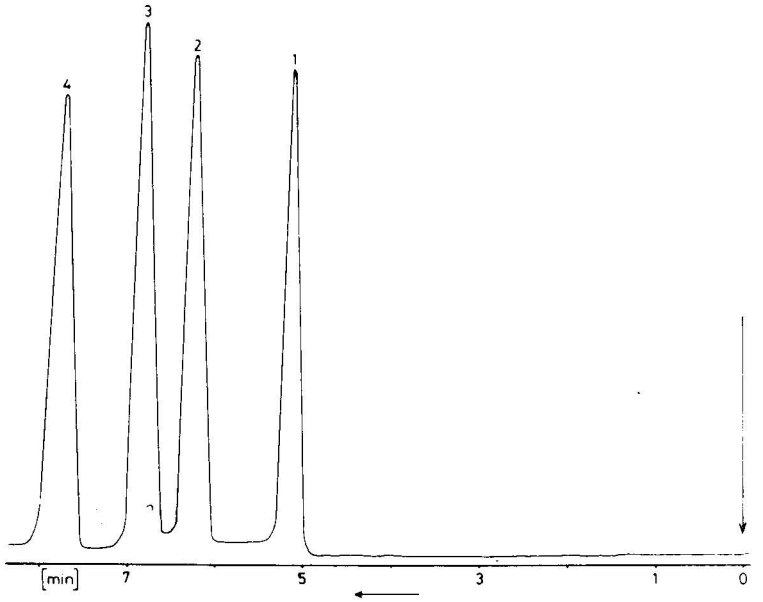


Fig. 5. Separation of barbiturates on silica. Parameters as in Fig. 2, except u = 1.33 mm/sec, Δp = 10 atm and $R_{2,3}$ = 1.47.

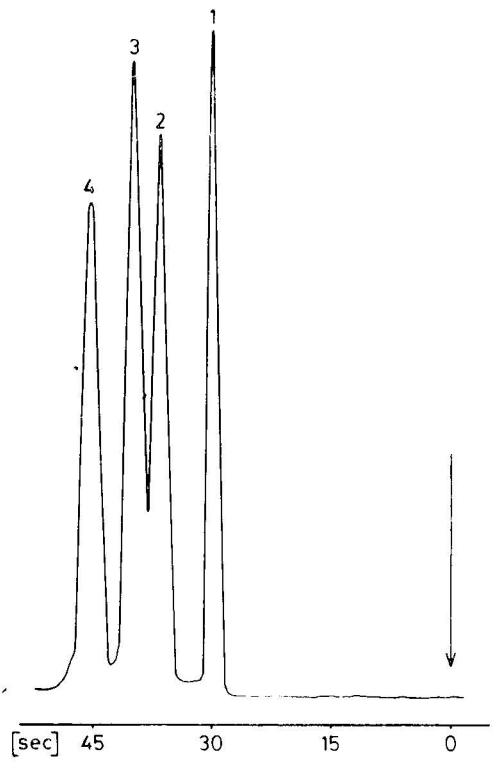


Fig. 6. Separation of barbiturates on silica.. Parameters as in Fig. 2, except u = 13.6 mm/sec, Δp = 100 atm and $R_{2,3}$ = 0.89.

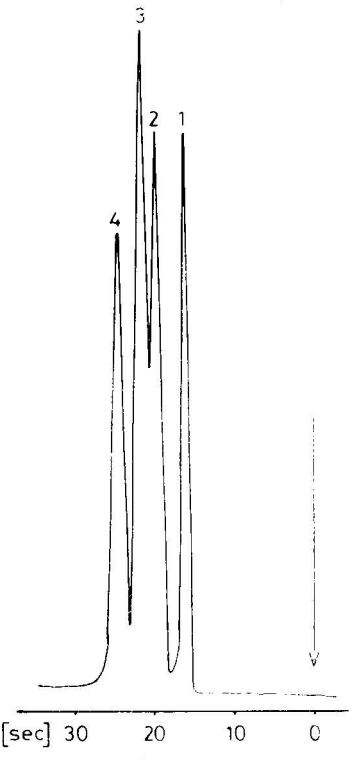


Fig. 7. Separation of barbiturates on silica. Parameters as in Fig. 2, except u = 24.6 mm/sec, Δp = 185 atm and $R_{2,3}$ = 0.71.

rations with $\alpha = 1.2$ could still be accomplished on a 10-cm column packed with particles with $d_p = 10\ \mu$m in a reasonable period of time (< 5 min) and the required pressure would be less than 50 atm.

(4) A short column has a further advantage over a "long" column. Identical resolution would be achieved with both columns if they possessed equal plate numbers, but h would be smaller for the short column. Moreover, since a decrease in peak height is a concomitant effect of peak broadening, which varies directly with column length, for equal h values higher peaks would be generated with the shorter column. The consequence of the overall result, which is a product of both of these effects, is that the minimum detectable sample concentration decreases with decreasing column length if the columns are loaded with identical sample sizes. This result is always an important consideration in quantitative and qualitative trace analyses.

(5) A third means of reducing the required pressure for optimal resolution is to increase the particle size. A 1-ft. column can be dry-packed with 30-μm particles as in gas chromatography[9]. Although this column packing technique is simple, the increased detection sensitivity discussed above would be lost.

(6) If the relative retention, α, and the required resolution, R, are fixed, the number of theoretical plates, n, needed for such a separation increases with decreasing capacity ratios, k', because to a good approximation

$$R = \frac{\alpha - 1}{\alpha} \cdot \frac{k'}{1 + k'} \sqrt{n} = \frac{\alpha - 1}{\alpha} \sqrt{N} \tag{9}$$

Hence, the resolution is proportional to the square root of the effective plate number, N. Figs. 4–7 demonstrate, however, that even with relatively small capacity ratios ($k' = 0.3$–1.0), the analysis can be completed within 15 min.

(7) The diffusion coefficient, D, of a given sample component decreases with increasing eluent viscosity, η. In a given eluent, D varies approximately inversely with $\sqrt{M}$, the molecular weight of the solute. In the analytically important velocity range where $u > u_{min}$, h increases with decreasing D, as can be seen from eqn. 3. For high values of M or η (*e.g.*, water), or especially of both, more efficient columns (for example, those packed with 5-μm particles) may be required. Such efficient columns are necessary, of course, for research work and for the development of optimal conditions for routine analyses.

To demonstrate the effect of increasing eluent viscosity on h *versus* u curves, some organic acids were eluted with a water–methanol–acetic acid mixture on a C_{18} chemically bonded stationary phase, with $d_p = 10.9$ μm (compare Fig. 8 and Figs. 4–7). Experience shows the efficiencies of silica and reversed-phase columns to be essentially the same under otherwise identical conditions. The data in Fig. 8 are in reasonable accord with the values calculated from eqn. 3.

A separation of five acids at $u_{min} = 1$ mm/sec is displayed in Fig. 9. A pressure drop of only 25 atm was sufficient and the analysis took less than 20 min, although the resolution was unnecessarily high ($R = 1.71$). A somewhat less than baseline separation ($R = 1.38$) required less than 3 min (Fig. 10), although the inlet pressure had increased to 220 atm.

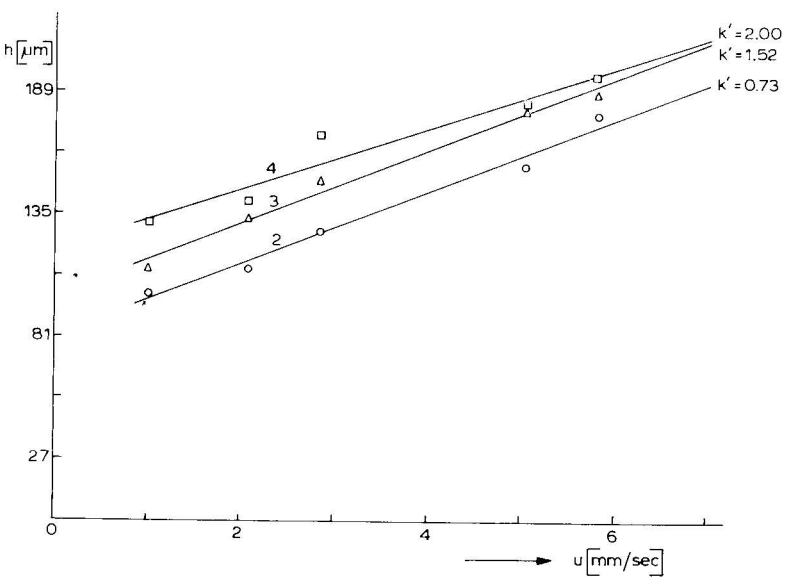


Fig. 8. Plots of h *versus* u on a reversed phase ($d_p = 10.9$ μm). Stationary phase, C_{18} chemically bonded on silica (SI 100). Column length, 30 cm; I.D., 4.2 mm. Eluent, water–methanol–acetic acid (55:30:15, v/v/v). Samples: 2, caffeic acid ($k' = 0.73$); 3, p-coumaric acid ($k' = 1.52$); 4, m-coumaric acid ($k' = 2.0$). $K_F = 1.2 \cdot 10^{-9}$ cm^2. Temperature, ambient.

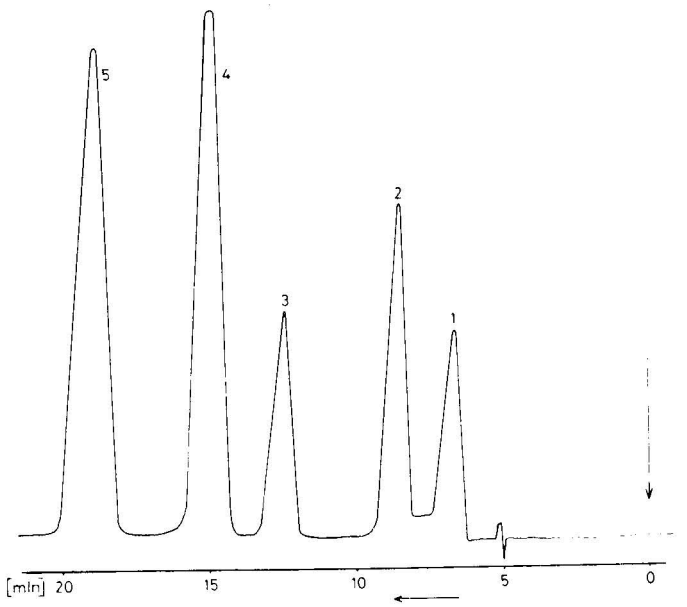


Fig. 9. Separation of organic acids on a reversed phase. Parameters as in Fig. 8, except for the following. Samples: 1, chlorogenic acid ($k' = 0.38$); 2, caffeic acid ($k' = 0.73$); 3, *p*-coumaric acid ($k' = 1.52$); 4, *m*-coumaric acid ($k' = 2.0$); 5, *o*-coumaric acid ($k' = 2.82$). $u = 1$ mm/sec; $\Delta p = 25$ atm; $R_{3,4} = 1.71$.

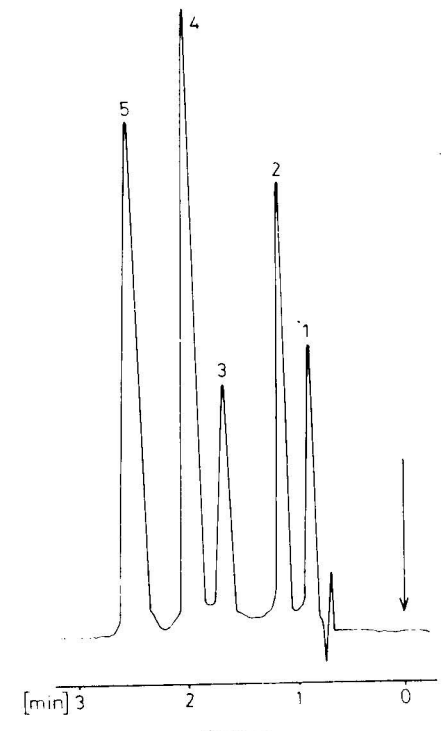


Fig. 10. Separation of organic acids on a reversed phase. Parameters as in Fig. 9, except $u = 7.5$ mm/sec, $\Delta p = 220$ atm and $R_{3,4} = 1.38$.

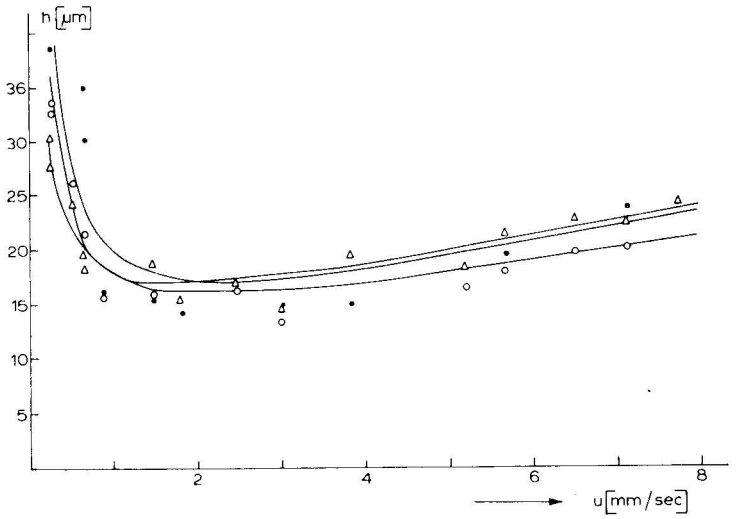


Fig. 11. Plots of h *versus* u on spherical silica (d_p = 3.2 μm). Column length, 7.5 cm; I.D., 4.2 mm. Eluent, *n*-heptane. Samples: △, *o*-terphenyl; ○, diphenyl; ●, inert. $K_F = 1 \cdot 10^{-10}$ cm². Temperature, ambient.

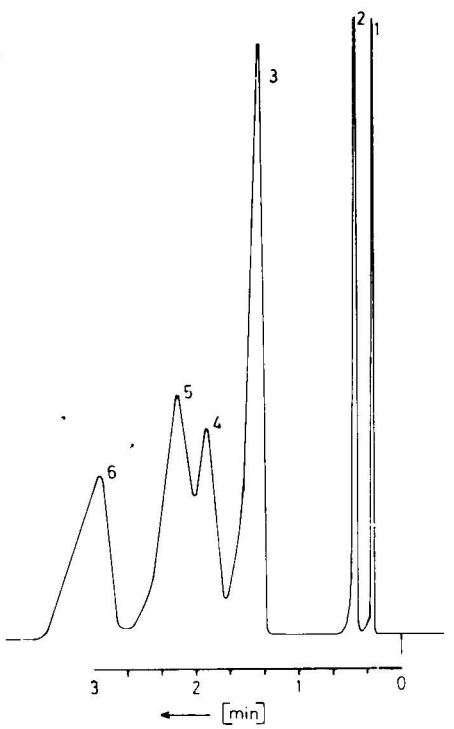


Fig. 12. Separation of barbiturates on spherical silica (d_p = 3.2 μm). Column length, 7.5 cm; I.D., 4.2 mm. Eluent, methylene chloride–ethyl acetate (95:5, v/v). Samples: 1, inert; 2, thiobarbital; 3, secobarbital; 4, amobarbital; 5, vinylbarbital; 6, barbital. $K_F = 1 \cdot 10^{-10}$ cm². Temperature, ambient. u = 4.2 mm/sec; Δp = 105 atm.

Efficiency of columns packed with 3.2-μm silica

The low rate of success (less than 10%) in packing a "good" column with 3.2-μm silica was pointed out earlier. The data for the best of about 15 columns packed are presented in Fig. 11. Because of its low specific permeability, the column was only 7.5 cm long. As the viscosity of the eluent (*n*-heptane) and the molecular weights of the sample components were low, more than 600 theoretical plates/cm were generated at u_{min}. As predicted by eqn. 7, the small particle size causes u_{min} to shift to higher values (u_{min} = 3.3 mm/sec). The high column efficiency in this instance (Fig. 12) would have permitted more barbiturates to be separated than on a column packed with 13.5-μm silica (Figs. 4–7). The analysis was carried out at u = 4.2 mm/sec with a pressure drop of only 105 atm in about 3 min. The lifetime of such highly efficient columns is as long as that of more conventional columns (d_p = 10 μm). Because of the sophisticated packing techniques required, however, columns with $d_p < 5$ μm are not recommended for routine applications.

The loadability (*i.e.*, the maximum sample size that causes no loss in efficiency) of silica columns is about 10^{-4} g per gram of support. In our experience, highly efficient columns such as those described in Figs. 11 and 12 have a higher loadability, and hence are very suitable for use in trace analysis.

LIST OF SYMBOLS

d_p (μm)	average particle size as defined in eqn. 2
h (μm)	height equivalent to a theoretical plate
h_{min} (μm)	h at the minimum of the h *versus* u curve
k'	capacity ratio $\left(= \frac{t_R - t_0}{t_0}\right)$
n	number of theoretical plates
n_{max}	n at u_{min}
Δp (atm)	pressure drop over the column
r (mm)	radius of the column
t_R (sec)	time of analysis
t_0	hold-up time of the inert peak
u (mm/sec)	linear velocity of the eluent
u_{min} (mm/sec)	u at the minimum of the h *versus* u curve
$\bar{w}$ (sec)	average peak width
D (10^5 cm^2/sec)	interdiffusion coefficient in the mobile phase
F (cm^3/min)	flow-rate
K_F (cm^2)	specific permeability $\left(= \frac{F \eta L}{r^2 \pi \Delta p}\right)$
L (cm)	column length
M	molecular weight of the sample
N	number of effective plates
N_{max}	N at u_{min}
R	resolution $\left(= \frac{\Delta t_R}{\bar{w}}\right)$

α	relative retention $\left(= \frac{k'_2}{k'_1}\right)$
ϱ_l (g/cm^3)	specific gravity of the dispersing liquid
ϱ_s (g/cm^3)	true specific gravity of the support
ν	reduced velocity $(= ud_p/D)$
η (cP)	viscosity of the eluent
ε_T	total porosity

ACKNOWLEDGEMENTS

The authors thank the Deutsche Forschungsgemeinschaft for financial furtherance of this research work. We acknowledge the help of Dr. G. Gutnikov (California State Polytechnic University, Pomona, Calif., U.S.A.) in the preparation of the manuscript.

REFERENCES

1 R. Endele, I. Halász and K. Unger, *J. Chromatogr.*, 99 (1974) 377.
2 I. Halász, R. Endele and J. Asshauer, *J. Chromatogr.*, 112 (1975) 37.
3 I Halász, *Z. Anal. Chem.*, 277 (1975) 257.
4 R. E. Majors, *Anal. Chem.*, 44 (1972) 1722.
5 G. J. Kennedy and J. H. Knox, *J. Chromatogr. Sci.*, 10 (1972) 549.
6 J. J. Kirkland, *J. Chromatogr. Sci.*, 10 (1972) 593.
7 W. Strubert, *Chromatographia*, 6 (1973) 50.
8 J. Asshauer and I. Halász, *J. Chromatogr. Sci.*, 12 (1974) 139.
9 F. H. Huyten, W. van Beersum and G. W. A. Rijnders, in R. P. W. Scott (Editors), *Gas Chromatography 1960*, Butterworths, London, 1960, p. 224.

Journal of Chromatography, 126 (1976) 35–41
© Elsevier Scientific Publishing Company, Amsterdam — Printed in The Netherlands

CHROM. 9508

THIN-LAYER CHROMATOGRAPHIC TRANSPORT DETECTOR FOR HIGH-PERFORMANCE LIQUID CHROMATOGRAPHY*

P. R. BOSHOFF, B. J. HOPKINS and VICTOR PRETORIUS
Institute of Chromatography, Pretoria University, Pretoria (South Africa)

SUMMARY

A procedure for the detection and quantitation of compounds in high-performance liquid chromatography (HPLC) is described. Solutes from the column are transferred on to a moving chromatoplate and subsequently detected according to well established thin-layer chromatographic methods. The performance compares favourably with existing methods of detection in HPLC and in particular has a universal and more linear response to organic compounds.

INTRODUCTION

Despite a great deal of research, detectors still remain the weakest component of high-performance liquid chromatography (HPLC). One approach has attempted to devise a means of interfacing the liquid chromatograph with a well-proven gas chromatographic detector such as the flame-ionisation or electron-capture detector. In most instances some form of transport device, *e.g.* a moving wire[1], belt[2] or disc[3] is involved.

Segura and Gotto[4] recently described a general-purpose fluorescent technique for detection of compounds separated by thin-layer chromatography (TLC) at the nanogram level. This prompted us to explore TLC plates as a transport mechanism for HPLC. The device described here resembles in principle the one devised by Janák[5] for gas chromatography but differs in that it is applied to column liquid chromatography.

EXPERIMENTAL

Chromatograph–chromatoplate interface

The most crucial factor determining band spreading lies in the extent to which the solutes may be confined to their point of application on the chromatoplate. It is therefore necessary to remove the solvent as rapidly as possible once it has made contact with the adsorbent, without removing any of the solute material.

* *Editor's note*: The performance of the assembly seems to be in the order of the new high-performance thin-layer chromatographic (HPTLC) method. One asks oneself therefore, why the authors do not chromatograph directly on the new fast thin layers. *Editor of J. Chromatogr.*

Authors' reply: The comment about using the new HPTLC plates from Merck appears to us to be irrelevant. The device we describe is an interface for column liquid chromatography.

For this purpose, the eluent was transferred with a fine steel capillary tube (0.5 mm O.D. × 0.25 mm I.D.) to the surface of the chromatoplate. The actual gap between the tube and adsorbent was adjustable in the region of 0.25 mm. Regular application of the eluent to the plate could be achieved only by maintaining a continous eluent bridge between the capillary and the adsorbent surface. It was necessary to decide upon a compromise among a number of parameters: sample size, length and speed of the chromatoplate, the solvent flow-rate, volatility and surface tension, the temperature of the plate, the rate at which the solvent vapour was to be removed and the amount of solute material, if any, lost in the process.

Standard 20 × 5 cm chromatoplates were used as they are readily available and a plate speed of 2 cm/min was chosen so as to provide 8–10 min in which to record the chromatogram. For most applications a flow-rate of 1 ml/min would thus be

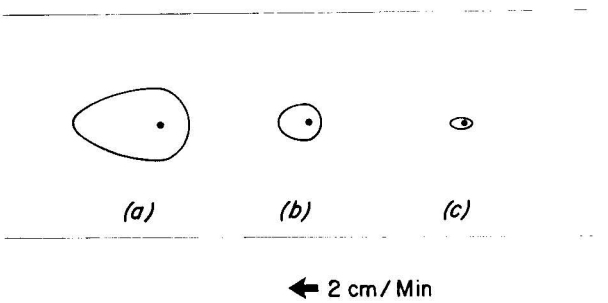


Fig. 1. Effect of temperature on band spreading. Temperature: (a) ambient; (b) 50°; (c) 90°.

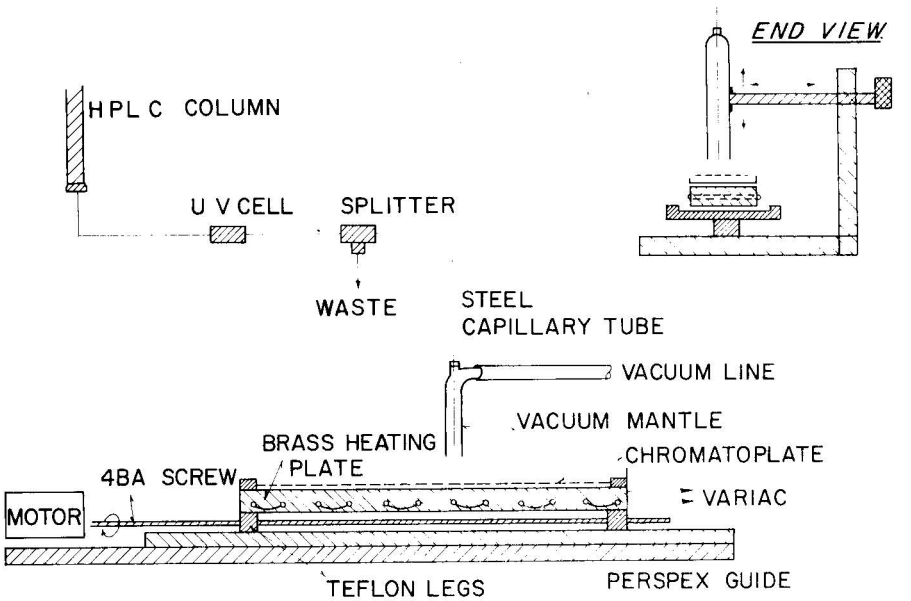


Fig. 2. Diagram of apparatus.

required and, as this could not be coped with efficiently, an eluent splitter was introduced.

The chromatoplate was evenly heated on a brass plate, whose temperature was regulated with a 5-A Variac. An indication of the effect of chromatoplate temperature on the degree of solvent spreading in the adsorbent material may be gained from Fig. 1.

The solvent vapour was removed from the adsorbent by positioning a glass tube of 8 mm diameter concentrically about the capillary, at a height of 6 mm above the chromatoplate. A vacuum line connected this tube to a strong venturi pump. The latter facility is not only essential to prevent band spreading but also avoids a possible health hazard.

The chromatoplate and heating carriage were driven by a small reversible and variable-speed motor, which was coupled to a 25-cm long 4 BA screw, which was in turn threaded to the Teflon legs on the carriage assembly (Fig. 2).

Chromatoplates. Pre-coated 20 × 5 cm silica gel plates with a 0.25-mm coating, both with and without F254 fluorescent indicator, were obtained from E. Merck (Darmstadt, G.F.R.). Anasil®-H chromatoplates were obtained from Analabs (North Haven, Conn., U.S.A.). An attempt was made to remove possible organic impurities by continous development of the plates with methanol for 12 h.

Fluorescence measurements. These measurements were made after the compounds on the chromatoplates had been derivatized according to Segura and Gotto's method. In this method the chromatoplates (without fluorescent indicator) containing the eluted compounds were placed on a plate holder which was transferred to a 4-gal capacity tank to which 6 g of ammonium hydrogen carbonate had been added. The tank was placed into an oven and heated at 110–150° for 3–12 h. Steroids usually form the required fluorescent derivatives after 3 h at 110°.

A relatively inexpensive TLC scanning instrument, constructed in our laboratory, was used to measure the chromatoplates. Working in the absorption mode, plates containing F254 were measured directly. Only UV-active compounds are detectable in this manner (Fig. 3a).

For chromatoplates treated according to Segura and Gotto's method, the derivatized products were activated at 360 nm and the subsequent fluorescent emission, with a maximum close to 450 nm, was detected and recorded with a photomultiplier and a strip-chart recorder (Fig. 3b).

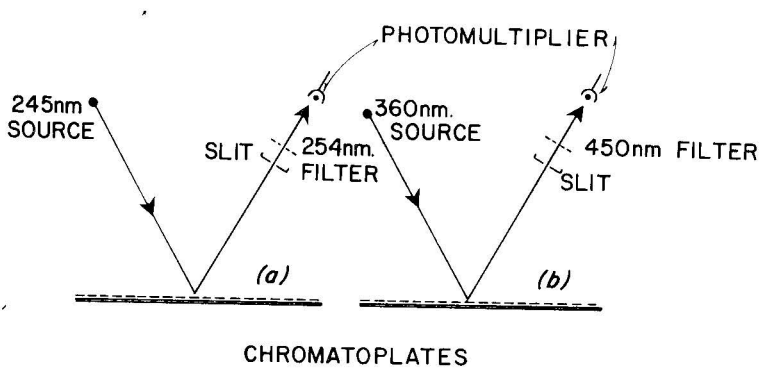


Fig. 3. Optics for plate scanning: (a) absorption mode; (b) emission mode.

RESULTS

As a rule, eluent flow-rates in excess of 0.6 ml/min on to the chromatoplate resulted in band spreading, due mainly to sporadic backwashing of the excess of solvent across the saturated adsorbent.

Increasing the adsorbent thickness caused problems with detection owing to the tendency of the solute to advance with the solvent front. Although heating of the chromatoplate had a marked effect on band spreading, care was necessary not to reduce the volume of solvent between the capillary and chromatoplate as this bridge had to be maintained and, further, the passage of solutes across this bridge caused visible boiling. This was a particular problem with solvents of low surface tension or when excessive air was present in the solvent supply.

It was found that washing the chromatoplate with methanol improved the stability of this solvent bridge. This improvement is possibly due to the displacement of water from the adsorbent particles, thus permitting a miscible interface. Chromatoplates were therefore washed by continuous development with methanol for 12 h, allowed to dry at room temperature and activated at 80° for 15 min *in situ* prior to use.

Because the solutes tend to advance with the solvent front, they tend also to be deposited on the adsorbent at the solvent perimeter. The result of this effect is that the chromatoplates appear as depicted in Fig. 4a.

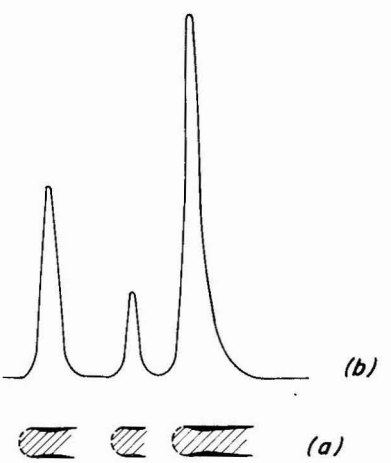


Fig. 4. (a) Appearance of chromatographic spots. (b) Strip-chart recording of (a).

The strip-chart recording in Fig. 4b was obtained by scanning the plate with a spectrofluorimeter with a 1 cm × 1 mm slit image at the plate.

The analysis of a synthetic mixture of steroids is shown in Fig. 5. A 10-mg amount of each of progesterone, testosterone, cortisone and 17β-estradiol were diluted to give solute concentrations of 100 ng/μl. A 2-μl volume of this solution was introduced on to a 25-cm Partisil (5 μm) column and eluted with dichloromethane–methanol (95:5, v/v) at a flow-rate of 1 ml/min. The eluent was split in the ratio 2:1 after passing through a UV detector. A 66-ng amount of each solute was thus deposited on the chromatoplate. The plate temperature was 80°.

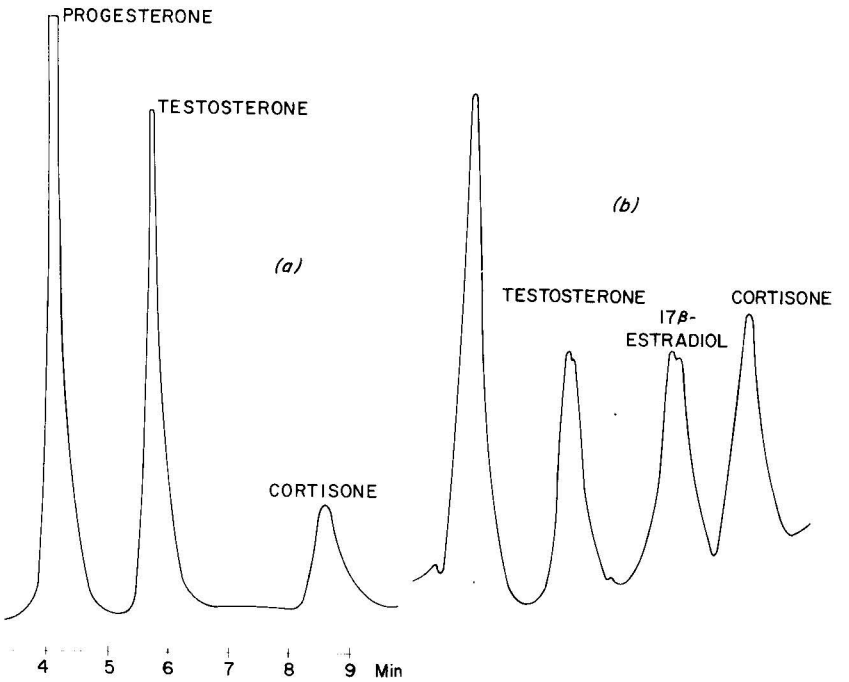


Fig. 5. Synthetic steroid mixture: (a) recording from UV photometric detector, (b) fluorescence emission recording obtained from HPLC–TLC.

Fluorescent products were prepared according to Segura and Gotto's method. Three of the four compounds had absorption maxima at 240 nm and were strongly UV active ($E^{1\%}_{1\,cm}$ = 390–540), while 17β-estradiol was UV inactive at 254 nm (λ_{max} = 280 nm, $E^{1\%}_{1\,cm}$ = 50). Progesterone was very soluble in the solvent system while the other three steroids were only slightly soluble.

The analysis of a mixture of nine steroids is shown in Fig. 6. The same conditions were used as in the previous example except that the solvent system was chloroform–methanol (97:3, v/v), the splitting ratio was 1:1 and the flow-rate was 0.6 ml/min.

The analysis of insecticides produces unexpected difficulties relating to Segura and Gotto's method. Although organochlorine compounds produced excellent fluorescent products, the organophosphorus compounds examined did not. In such instances, F254 chromatoplates, or alternatively some other method of detection such as esterase inhibition, can be used. The analysis of a mixture of three insecticides is shown in Fig. 7. The chromatoplate contained F254 indicator. A 25-cm Partisil (5 μm) column was used, the solvent was pentane–chloroform (1:1, v/v), the flow-rate was 0.7 ml/min and the splitting ratio was 1:1.

Sensitivity

Methoxychlor was diluted to give a solution of 1 ng/μl concentration, 2 μl (2 ng) were then introduced on to a 25-cm Partisil (5 μm) column and the column was eluted with chloroform–methanol (95:5, v/v). The effluent was split after passing through the UV photometer cell in the ratio 1:2. The chromatoplate thus contained

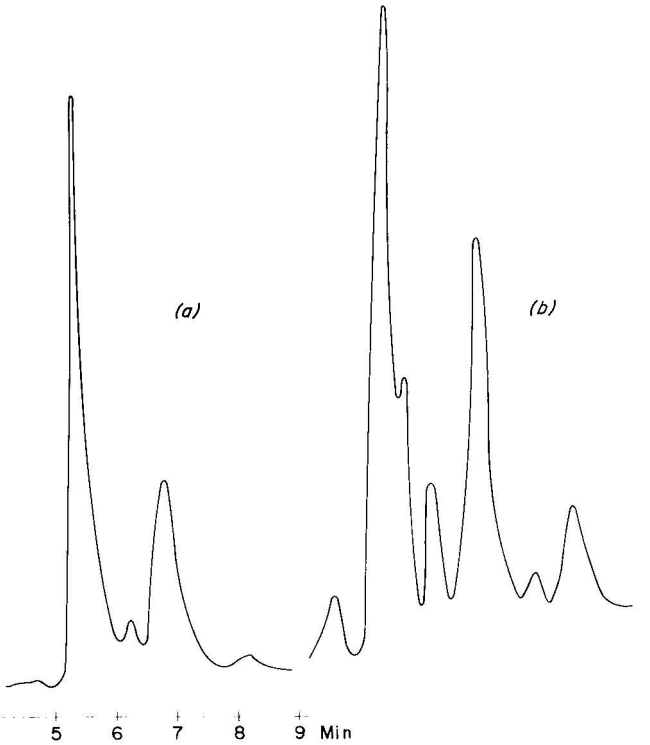


Fig. 6. Complex steroid mixture: (a) UV detector recording; (b) HPLC–TLC recording.

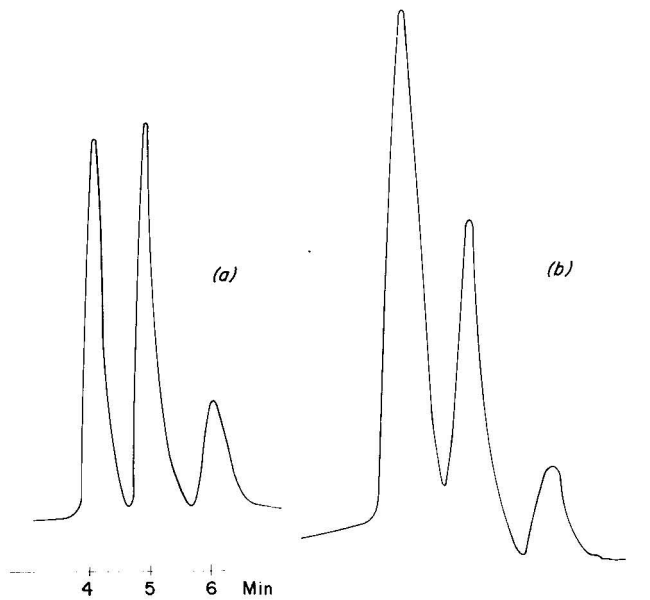


Fig. 7. Organochlorine insecticide mixture: (a) UV detector recording; (b) absorption recording obtained from HPLC–TLC (F254).

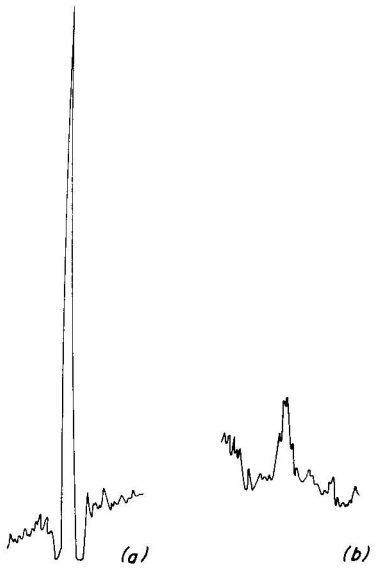


Fig. 8. Recording of methoxychlor: (a) 2-ng sample recorded with a UV detector, sensitivity 0.05 a.u.f.s.; (b) 0.66-ng fluorescence emission recording from chromatoplate, recorded at maximum available sensitivity, 1 mV f.s.d.

0.66 ng of methoxychlor. The UV response was recorded at 0.05 a.u.f.s. (Fig. 8a) and the chromatoplate was treated according to Segura and Gotto's method with ammonium hydrogen carbonate for 10 h at 110°. The spectrofluorimeter recording was obtained at the maximum available sensitivity on a 1-mV f.s.d. strip-chart recorder (Fig. 8b). The maximum available sensitivity of the UV photometric detector was 0.01 a.u.f.s. and a recorder of 1 mV f.s.d. was used. As the signal to noise ratios were of a similar order, these results indicate the UV photometric method to be one order of magnitude better in sensitivity for methoxychlor (λ_{max} = 220 nm, $E^{1\%}_{1\,cm}$ = 460) than that obtained for the fluorescent method.

CONCLUSION

It has been demonstrated that solutes eluted in HPLC can be transferred to a chromatoplate without serious loss of resolution and that suitable methods are available for subsequent detection at the lower nanogram level.

In particular, when this approach is used in conjunction with Segura and Gotto's method, sensitivities of the same order as those found for the UV photometric method are possible and, in addition, a wider range of compounds respond favourably to detection.

REFERENCES

1 A. T. James, J. R. Ravenhill and R. P. W. Scott, *Chem. Ind.*, 18 (1964) 746.
2 E. Haahti, T. Nikkari and J. Kërkainen, *J. Gas Chromatogr.*, 4 (1966) 12.
3 J. J. Szakasits and R. E. Robinson, *Anal. Chem.*, 46 (1974) 1648.
4 R. Segura and A. M. Gotto, Jr., *J. Chromatogr.*, 99 (1974) 643.
5 J. Janák, *J. Gas Chromatogr.*, 1 (1963) 20.

Journal of Chromatography, 126 (1976) 43–62
© Elsevier Scientific Publishing Company, Amsterdam — Printed in The Netherlands

CHROM. 9383

DEVELOPMENT AND USE OF CARBON ADSORBENTS IN HIGH-PERFORMANCE LIQUID–SOLID CHROMATOGRAPHY

I. CARBON-COATED SILICA PARTICLES

H. COLIN and G. GUIOCHON

Laboratoire de Chimie Analytique Physique, École Polytechnique, Route de Saclay, 91120 Palaiseau (France)

SUMMARY

The technique for coating silica particles with a layer of pyrocarbon is described. The conditions of preparation are important as they determine both the chromatographic performance and the degree of agglomeration of particles during coating.

The effect of the coating was studied in terms of both efficiency and retention data. For the silica studied (Spherosil XOB 75), moderate amounts of pyrocarbon (less than 15%) gave the best results; greater degrees of coating give a large decrease in efficiency with increasing retention, while smaller degrees of coating give very small retentions and polar adsorbents.

Some simple separations are shown to illustrate the analytical characteristics of these adsorbents.

INTRODUCTION

Reversed-phase chromatography is based on non-specific intermolecular interactions between (1) adsorbent and solute and (2) adsorbent and eluent. A chromatographic process based only on dispersive (non-specific) forces needs a non-specific and,consequently non-polar adsorbent. As recently pointed out by Bebris *et al.*[1], the basic foundations are identical in classical liquid–solid chromatography (LSC) (using silica or alumina) and in reversed-phase chromatography. In particular, all interactions (adsorbent–solute, adsorbent–solvent and solvent–solute) must be taken into account in order to understand the mechanism of retention.

However, contrary to Bebris *et al.*[1], we do not think that it is unreasonable or misleading to continue to use the term "reversed-phase". It allows a more precise definition of the type of interactions that will be responsible for the retention and consequently for the separations. Obviously, we must always bear in mind that no basic difference exists between the two instances. The retention of a solute is due to its positive adsorption and consequently to negative adsorption of the solvent. However, at the molecular level, the difference between reversed-phase and classical LSC is that only non-specific interactions occur in the former while specific interactions are important in the latter. This aspect is important.

TABLE I

EXPERIMENTAL CONDITIONS FOR THE PREPARATION OF CARBON-COATED SILICA PARTICLES

L = column length; d_c = column diameter; d_p = particle size.

Column	*L (cm)*	*d_c (cm)*	*d_p (μm)*	*Support*	*Coating (%)*	*Pyrolysis temperature (°C)*	*Benzene saturator temperature (°C)*	*Flow-rate (cm^3/min)*	*Reaction time (min)*	*Amount treated (g)*
A	65	2.17	31.5–40	Spherosil (XOB 75)	0.3*	900	29	34.6	1	3.51
B	65	2.17	31.5–40	Spherosil (XOB 75)	0.8*	900	29	34.6	3	3.51
C	65	2.17	31.5–40	Spherosil (XOB 75)	1.5*	900	29	63.15	3	3.52
D	65	2.17	31.5–40	Spherosil (XOB 75)	4.0	900	29	63.15	10	3.52
E	65	2.17	31.5–40	Spherosil (XOB 75)	15.4	900	29	63.15	31	3.56
F	65	2.17	31.5–40	Spherosil (XOB 75)	53**	947	30.5	57.9	40	3.23
G	65	2.17	31.5–40	Spherosil (XOB 75)	140**	947	30.5	57.9	100	3.40
H***	11.5	4.17	6	Partisil 5	4.1	904	36.5	64	3	0.70
I***	12	4.17	6	Partisil 5	13.6	904	36.5	65.8	4	0.76
J***	11.3	4.17	6	Partisil 5	24.8	904	36.5	65.8	10	0.76
R	75	2.17	31.5–40	Sterling FT.FF	13 (graphitized)	947	39	98	30	24

* Calculated from previous experiments.

** The precision is low as the particles stick to the wall.

*** Silica coated with the first set-up (without stirring particles, see ref. 2).

We have described in previous papers[2,3] the treatment of carbon black (CB) particles to obtain a mechanically stable adsorbent for LSC and various chromatographic applications. It has been mentioned[3] that the problem of obtaining small particles that are hard enough to stand the high pressure drop that is commonly used in packing techniques and in many experiments could be solved by coating silica particles with carbon. Bebris *et al.*[1] have published some preliminary results. This paper describes the results we have obtained recently with different silica particles. One of the most important results is that it has proved possible to prepare a new adsorbent that exhibits chromatographic properties that are similar to those of pure carbon.

Carbon black-coated silica is thermally very stable and is not sensitive to pH insofar as the silica is not destroyed and can be used in any solvent. As for pure carbon, the equilibration time when changing the solvent is very small and the reproducibility of the chromatographic data obtained is very good. It is also possible to change the chromatographic properties by decreasing the amount of pyrocarbon coated on the silica particles. It is thus possible to adjust retention and to optimize efficiency.

PREPARATION OF CARBON-COATED SILICA PARTICLES (CCSP)

It is well known that high efficiencies in high-performance liquid–solid chromatography (HPLSC) are achieved by the use of small particles (*ca.* 5 μm in diameter), and we have mentioned previously the difficulties encountered in trying to make carbon particles in that range[3]. We thought that coating fine silica particles with pyrocarbon would be a means of avoiding these problems. In their recent paper, Bebris *et al.*[1] gave little information about the preparation technique and the properties of the product obtained, and no chromatograms were shown.

The coating procedure used in this work is identical with that described previously for carbon-black hardening[2–4]. The set-up provides for continuous stirring of the powder during the pyrolysis process, which increases both the production and the homogeneity of the final product. More details will be given in a later paper[5]. Four different silica gels were used: Partisil 5 (Reeve Angel, Clifton, N.J., U.S.A.), Lichrosorb Si 60 5 μm (Merck, Darmstadt, G.F.R.) and Spherosil XOA 600 and XOB 75 (Rhone-Progil, Antony, France). Only systematic results obtained with large (30–40-μm Spherosil) and small (*ca.* 5-μm Partisil) particles are reported here (*cf.*, Table I).

In order to make possible an exact measurement of the amount of pyrocarbon coated, the silica was first dehydrated at 900° for 3 h under a stream of pure nitrogen. It is strongly advised that fine silica particles (5 μm) should not be stirred during this step, as large particles (up to several hundred microns) would be formed by pelletization; these pellets are then hardened by the pyrocarbon coating (*cf.*, Fig. 1).

Carbon coating was carried out at 950, 900 and 875°. While the weight loss during dehydration is approximately the same at all three temperatures, it seems that the agglomeration is less important at 875°. Moreover, we observed that the pyrolysis reaction gives better results at the lowest temperature. The experimental conditions under which ten different samples and a reference sample of pure carbon were prepared are given in Table I.

The carbon layer should cover completely all of the silica surface and be thick enough to offset the sorption properties of silica. Hence it would seem that a large

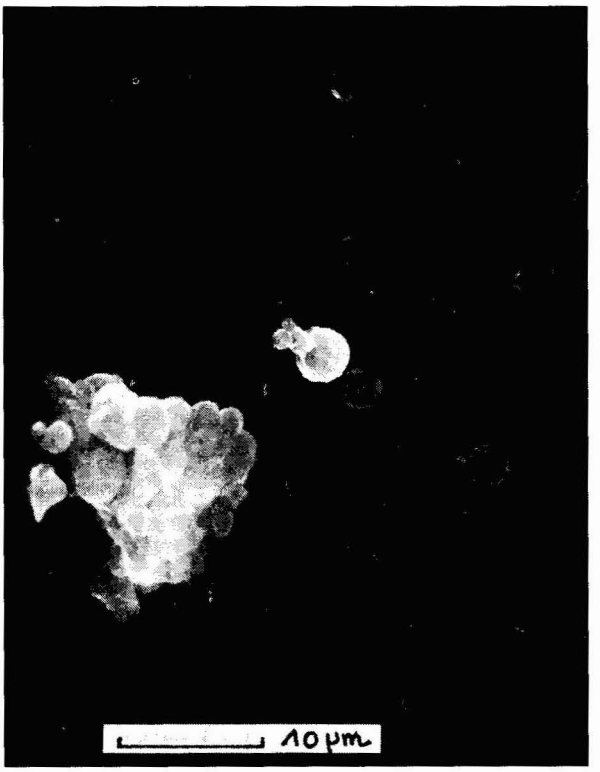


Fig. 1. Scanning electron microscope photograph of carbon-coated silica. Agglomerate of Spherosil particles made during dehydration.

amount of pyrocarbon is necessary. However, it rapidly became clear to us that it is impossible to coat more than about 50–55% (w/w) of carbon on any of the 5-μm silica particles used, otherwise all of the particles become stuck together into hard, compact agglomerates that cannot be broken down into the individual particles. At present we do not know whether this limit results from a property of carbon formation or of the experimental set-up.

The upper limit of the degree of pyrocarbon coating is sharp; 5-μm particles have been coated with 41% and 53% of pyrocarbon without any notable agglomeration (observation under optical microscope), while all attempts to coat more than 60% produced particles that were agglomerated to a large extent, if not completely. When coating larger particles, this problem is much less critical. For instance, using a 31.5–40-μm sieve fraction, coatings exceeding 140% were possible without agglomeration, although the particles stuck to the pyrolysis tube wall. For hardened carbon black[2], the greater is the degree of coating, the more metallic grey were the particles; at low degrees of coating they were black.

Photographs of particles of carbon-coated silica obtained with a scanning electron microscope are shown in Figs. 2, 3 and 4. Unfortunately, the secondary emission coefficients of silicon and carbon are very similar, so these substances cannot be readily distinguished on the photographs.



Fig. 2. Detail of a particle of Spherosil coated with 0.84% of pyrocarbon (*cf.*, Table I, B).

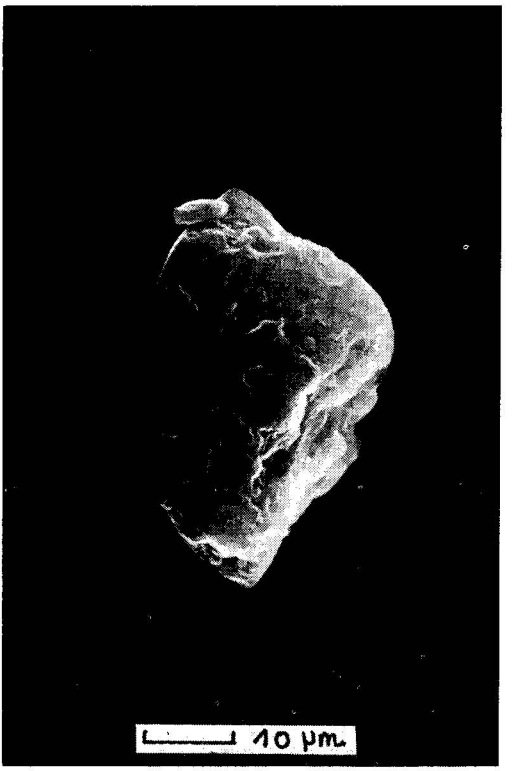


Fig. 3. Detail of a particle of Spherosil coated with 15.4% of pyrocarbon (*cf.*, Table I, E).

The clear spots in Fig. 2, showing a silica with a low carbon coating (0.8%), are probably carbon. This is in agreement with the generally accepted assumption that benzene pyrolysis does not produce carbon layers directly on the whole silica surface but various substances of higher molecular weight that eventually give droplets and condense further in the liquid state. Figs. 3 and 4 show that at high degrees of coating the particles lose their spherical shape. Large amounts of carbon form around the particle core but, as will be shown later, the porosity and specific surface area remain large.

STUDY OF COLUMN EFFICIENCY

All columns are packed using the slurry technique. The slurry liquid is a mixture of dibromoethane and acetonitrile (*ca.* 76:24, v/v), accurate adjustments being made, depending on the degree of coating. A suspension is prepared with 10% (w/w) of coated silica particles. The packing pressures are 300 bar for larger particles and 600 bar for the smaller. Some experimental data are shown in Fig. 5 for two columns, B and G (*cf.*, Tables I and II). The curves are very similar for non-retained solutes, showing that the packing technique is reproducible, but are different for retained solutes.



Fig. 4. Detail of the centre of particle shown in Fig. 3.

Usually it can be assumed that the reduced plate height h ($= H/d_p$), and the reduced velocity ν ($= ud_p/D_m$) are related by the equation of Knox and co-workers[6–8]:

$$h = \frac{B}{\nu} + A\nu^{0.33} + C\nu \tag{1}$$

which is an approximation of the original rigorous Giddings equation[9]:

$$h = \frac{B'}{\nu} + \frac{A'}{D' + \frac{1}{\nu}} + C'\nu \tag{2}$$

In a previous paper[3], HETP curves were fitted by eqns. 1 and 2 assuming that $B = B' = 2$, as it is difficult and time consuming to make HETP measurements in the range of flow-rates where B (and B') are the controlling terms, especially when using large particles. We used the well known non-linear least-squares fitting technique in order to calculate the parameters. The diffusion coefficients that appear in the expression of the reduced velocity are derived from the classical Wilke and Chang equation[9]:

$$D_m = \frac{7.4 \cdot 10^{-10} (\psi M)^{\frac{1}{2}} T}{\eta V^{0.6}} \tag{3}$$

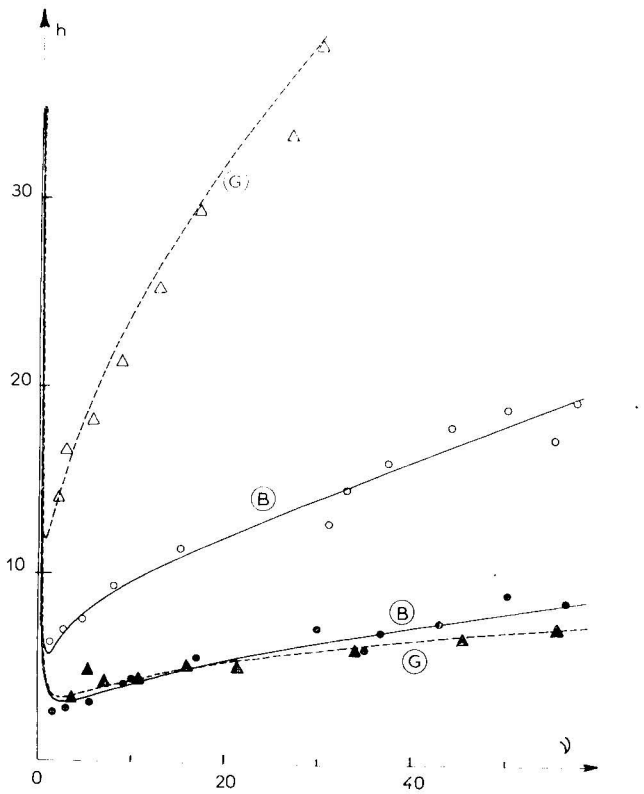


Fig. 5. Reduced plate height (h) *versus* reduced velocity (v) for columns B and G in acetonitrile. Broken lines, column G; ▲, benzene; △, 1,8-dimethylnaphthalene. Solid lines, column B; ●, benzene; ○, 2,3,5-trimethylnaphthalene.

We previously used a value of 1.5 for the association parameter ψ of acetonitrile[2,3]. Recently, Fawcett and Caton[10] measured the diffusion coefficient of anthracene in acetonitrile, and it appears from their data that a better estimate of ψ in eqn. 3 is 2,14. This value is used here for the calculation of the reduced velocity.

The results are summarized in Table II, and show that by using the slurry technique it is possible to pack good columns with either small or large particles. With large particles, we packed long columns and obtained $h_{min.}$ values of between 2.4 and 3.5 and A values of about 2 (*cf.*, columns A–G). Obviously, with such columns high efficiencies correspond to very low flow-rates of the eluent (typically *ca.* $7 \cdot 10^{-3}$ cm/sec) and consequently time-consuming analyses. With small particles (columns H, I and J), although the packing is less good ($h_{min.} = 4$–5.5), high efficiencies are obtained at large solvent flow-rates (*ca.* $5 \cdot 10^{-2}$ cm/sec), which permits good separations to be effected in a short time (see below).

The increase in $h_{min.}$ is probably due to the formation of some small agglomerates of the particles during pyrolysis. No attempt was made to eliminate agglomerates smaller than 20 μm.

It can also be seen from Table II that the best results in terms of efficiency are

TABLE II

HETP EQUATIONS FOR THE DIFFERENT COLUMNS

Column	*Unretained solute*						
	Equation 1	h_{min}	v_{opt}	*Equation 2*		h_{min}	v_{opt}
A*	$2/\nu + 1.92\,\nu^{0.33} + 5.26\,10^{-2}\,\nu$	3.52	2.20	$2/\nu + \frac{0.85}{0.12 + 1/\nu} + 7.16\,10^{-2}\,\nu$		2.50	1.80
B*	$2/\nu + 1.67\,\nu^{0.33} + 3.81\,10^{-2}\,\nu$	3.16	2.40	$2/\nu + \frac{0.93}{0.16 + 1/\nu} + 5.71\,10^{-2}\,\nu$		2.51	1.70
C*	$2/\nu + 1.97\,\nu^{0.33} + 9.46\,10^{-2}\,\nu$	3.67	2.00	$2/\nu + \frac{1.53}{0.29 + 1/\nu} + 13.89\,10^{-2}\,\nu$		3.15	1.60
D*	$2/\nu + 1.87\,\nu^{0.33} + 6.45\,10^{-2}\,\nu$	3.48	2.10	$2/\nu + \frac{1.22}{0.22 + 1/\nu} + 9.71\,10^{-2}\,\nu$		2.85	1.60
E*	$2/\nu + 1.23\,\nu^{0.33} + 4.18\,10^{-2}\,\nu$	2.55	2.90	$2/\nu + \frac{1.475}{0.51 + 1/\nu} + 7.39\,10^{-2}\,\nu$		2.60	2.30
F*	$2/\nu + 3.11\,\nu^{0.33} + 1.71\,10^{-2}\,\nu$	4.91	1.60	$2/\nu + \frac{0.76}{0.05 + 1/\nu} + 3.77\,10^{-2}\,\nu$		2.43	1.70
G**	$2/\nu + 1.92\,\nu^{0.33} + 0.00\,10^{-2}\,\nu$	3.40	2.40	$2/\nu + \frac{1.10}{0.16 + 1/\nu} + 2.19\,10^{-2}\,\nu$		2.68	1.70
H**	$2/\nu + 2.12\,\nu^{0.33} + 66.22\,10^{-2}\,\nu$	4.71	1.30	$2/\nu + \frac{5282.2}{2816.2 + 1/\nu} + 95.26\,10^{-2}\,\nu$		4.64	1.40
I**	$2/\nu + 3.60\,\nu^{0.33} + 0.00\,10^{-2}\,\nu$	5.45	1.50	$2/\nu + \frac{4379.8}{1018.2 + 1/\nu} + 0.00\,10^{-2}\,\nu$		4.3	–
J**	$2/\nu + 2.48\,\nu^{0.33} + 0.00\,10^{-2}\,\nu$	4.11	2.00	$2/\nu + \frac{4985.4}{1677 + 1/\nu} + 0.00\,10^{-2}\,\nu$		3.0	–

* Injection of 2 μl.
** Injection of 1 μl.

obtained with degrees of coating between 1 and 15% (columns B–E). On the one hand, one should expect that for non-retained compounds the larger the degree of coating, the better the column. This would be for mechanical reasons and because of a decrease in the intraparticle resistance to mass transfer. It is explained by the reduction in pore depth as thicker layers of pyrocarbon are coated on the silica surface and the obstruction of finer pores. However, as already observed[2,3] with carbon black, the efficiency is closely related to the retention and depends on the solvent used and the solute for a given column. The ratio of the numbers of theoretical plates for two solutes with different retentions depends on the flow-rate, generally being smallest near the minimum of the HETP curve. The coefficients C and C' are much more important for retained than for non-retained solutes and even A and A' are larger. The variation increases with increase in the degree of coating. It appears, however, that moderate amounts of pyrocarbon provide the best columns.

Retained solute							
	Equation 1	h_{min}	ν_{opt}	*Equation 2*		h_{min}	ν_{opt}
.08	$2/\nu + 9.15\,\nu^{0.33} + 3.79\,10^{-2}\,\nu$	11.01	0.70	$2/\nu + \frac{9.06}{0.42 + 1/\nu} + 29.78\,10^{-2}\,\nu$		7.86	0.60
.60	$2/\nu + 4.07\,\nu^{0.33} + 6.35\,10^{-2}\,\nu$	6.06	1.30	$2/\nu + \frac{6.05}{0.69 + 1/\nu} + 19.10\,10^{-2}\,\nu$		5.75	0.90
69	$2/\nu + 4.90\,\nu^{0.33} + 9.68\,10^{-2}\,\nu$	6.99	1.10	$2/\nu + \frac{4.71}{0.40 + 1/\nu} + 22.87\,10^{-2}\,\nu$		5.54	0.80
85	$2/\nu + 3.61\,\nu^{0.33} + 12.76\,10^{-2}\,\nu$	5.65	1.30	$2/\nu + \frac{3.57}{0.41 + 1/\nu} + 22.60\,10^{-2}\,\nu$		5.05	1.60
025	$2/\nu + 2.19\,\nu^{0.33} + 25.47\,10^{-2}\,\nu$	4.22	1.60	$2/\nu + \frac{21.21}{6.077 + 1/\nu} + 36.06\,10^{-2}\,\nu$		4.95	2.00
13	$2/\nu + 4.36\,\nu^{0.33} + 14.53\,10^{-2}\,\nu$	6.47	1.20	$2/\nu + \frac{2.03}{0.13 + 1/\nu} + 20.0\,10^{-2}\,\nu$		3.99	1.00
11	$2/\nu + 9.83\,\nu^{0.33} + 28.15\,10^{-2}\,\nu$	11.80	0.70	$2/\nu + \frac{13.44}{0.52 + 1/\nu} + 46.47\,10^{-2}\,\nu$		9.56	0.50

Finally it should be noted that the values of the parameters A, B and C obtained by the fitting technique should be used with care. For instance, 0.00 is sometimes obtained for C in eqn. 1, and such a value obviously has no physical meaning. A realistic calculation of the parameters is possible only if measurements of h over very large range of ν values are carried out, which is generally not done because of the experimental difficulties. This is especially so for columns H, I and J; for these small-particle columns, measurements of h have been made only around the minimum. If the values derived for A are meaningful, this is not so for C, the contribution of the corresponding term being small in this region.

RETENTION ON CARBON-COATED SILICA PARTICLES

The comparison of the columns is made using three solvents with widely dif-

ferent polarities: high (a 1:1 mixture of water and acetonitrile), medium (pure acetonitrile) and no polarity (*n*-heptane). This choice allows the study of retention patterns in a large range of eluotropic strength, ε° (ref. 3). The influence of the silica skeleton, if it remains, will show up differently for polar and non-polar solutes and depends on the solvent.

Polar solvent

Polar solvents generally have a weak eluotropic strength on carbon[3,11]. If specific interactions can take place between the solvent and the adsorbent, ε° would be even larger than with pure carbon. This decrease can be explained as follows.

The pyrolysis is accompanied by thermal treatment of the silica. Adsorption on thermally modified silica is much weaker than on ordinary silica, although it remains high for polar compounds[12]. Adsorption on carbon is very substantial[2,3], but if the layer of pyrocarbon is too thin, the silica located under it can influence the retention on carbon. In this way, a polar solvent may be more strongly adsorbed than on carbon because of specific interactions with the underlying silica, and hence ε° is larger. This effect also happens near the edges of carbon spots in the case of partial coverage, where solvent molecules will be more retained because of the interactions with the silica.

If a monolayer of pyrocarbon is expected to be coated on the silica, the corresponding amount of carbon (weight-% increase) is high (*cf.*, Table III). In practice, as the coating is not homogeneous, much larger degrees of coating are necessary than the values given in Table III. In our work, for instance, we used Spherosil XOB 75. The specific surface area before dehydration was 108 m^2/g (stated by the manufacturer) and after dehydration 99 m^2/g (measured). In fact, it is possible that the pyrocarbon does not cover all of the silica surface but plugs some pores, reducing the surface area. This may happen only seldom, as shown by the measurements reported in Table IV. These results are surprising as they show that the specific surface area does not decrease regularly with increase in the degree of coating, as happens for carbon black. Possibly the pyrocarbon coating is porous and in the range 0–15% of carbon the two effects, reduction of the skeleton surface area and increase in the pyrocarbon pore surface area, cancel each other. The surface measurements are in excellent agreement with the results of retention data measurements.

TABLE III

DEGREE OF COATING NECESSARY TO OBTAIN A MONOLAYER OF CARBON ON SILICA

Average density of graphite, 2.25 g/cm^3.

Specific surface area (m^2/g)	*Weight-% increase*
10	0.77
50	3.85
100	7.69
400	30.78

TABLE IV

SPECIFIC SURFACE AREA OF SILICA (SPHEROSIL XOB 75) COATED WITH PYROCARBON

Degree of coating (%)	*Specific surface area (m^2/g)*
0	99.8
0.3	85
0.8	99.5
4.0	74
15.4	90

Concerning the adsorption of a non-polar solute, two effects can modify the column capacity factor (k') when increasing the degree of coating: the surface area available for carbon solute interaction increases, and the eluotropic strength of the solvent tends towards the value observed on pure carbon. For a polar solute, it may be necessary to take into account specific adsorption on silica. However, it is impossible to make any quantitative prediction as we are dealing with two very different adsorbents, giving rise to adsorption forces that are difficult to compare, and we do not even know how the ratio of the surface areas of silica and carbon varies with the degree of coating.

The results of a comparison between retention data on different columns using various solutes are given in Table V. We should point out that the retentions on column A were very small and difficult to measure accurately (especially relative retentions). Table V includes the column capacity (k') and the relative retention (α), the reference solute being 1,2,3-trimethylbenzene, the retention of which can be measured with good precision on the different columns. The use of α allows a more significant comparison to be made between the columns as it eliminates the possible effect of surface area. The corresponding retention data on pure carbon (Sterling FT.FF hardened with 13% of pyrocarbon and graphitized) are also given. However, as will be pointed out in a forthcoming paper, these data must be used with caution. Indeed, it will be seen that even columns of carbon are difficult to compare when packed with adsorbents of different specific surface areas. We chose a carbon giving retentions similar to those on CCSP. Capacity factors of some solutes are plotted *versus* the amount of pyrocarbon in Fig. 6. It seems that the results for column D are too low, while the other results are self-consistent. The same effect does not occur with column D when the other solvents are used (see below). For this reason, it is not possible to exclude an error in the composition of the solvent mixture used in this instance (too much acetonitrile). However, the general form of the plot shows that the retention first increases very rapidly with increase in the degree of coating and then tends towards a limit. The data for column G are in agreement with the other data and a large reduction in specific surface area.

The relative retentions are only slightly different from those measured on column R, suggesting that the effect of the variation of apparent eluotropic strength is not very important: ε° drifts slowly towards the values on pure carbon. The effect of ε° is better illustrated in Fig. 7 which is a plot of log k' *versus* the number of methyl groups for two homologous series (methylbenzenes and methylphenols). Nearly

TABLE V

COMPARISON BETWEEN RETENTION DATA ON DIFFERENT COLUMNS (*cf.*, TABLE I) WITH WATER–ACETONITRILE (1:1) AS SOLVENT

*Solute**	*Parameter*	*Column*							
		A	*B*	*C*	*D*	*E*	*F*	*G*	*R*
Benzene	k'	0.03	0.16	0.08	0.13	0.18	0.46	0.19	0.18
	α	0.50	0.41	0.17	0.13	0.10	0.07	0.11	0.06
Phenol	k'	0.00	0.12	0.06	–	0.12	0.24	0.08	0.13
	α	0.00	0.32	0.12	–	0.07	0.04	0.05	0.04
2,4-Xylenol	k'	0.03	0.15	0.13	0.23	0.52	–	0.35	0.88
	α	0.50	0.39	0.26	0.23	0.29	–	0.20	0.28
2,3,4-TMP	k'	0.06	0.28	0.37	0.67	1.74	4.74	1.03	3.44
	α	1.00	0.73	0.76	0.66	0.97	0.73	0.60	1.08
2,3,4,6-TeMP	k'	0.12	–	0.74	1.90	3.33	12.26	2.85	8.77
	α	2.00	–	1.50	1.86	1.86	1.88	1.66	2.75
β-Naphthol	k'	0.11	0.39	0.58	1.07	2.17	8.17	1.11	4.85
	α	1.90	1.03	1.18	1.05	1.21	1.25	0.65	1.52
Naphthalene	k'	0.12	0.60	0.96	1.80	3.13	–	2.00	5.03
	α	2.00	1.57	1.94	1.76	1.75	–	1.17	1.58
n-Propylbenzene	k'	0.00	–	0.23	0.41	0.75	2.20	0.79	0.89
	α	0.00	–	0.46	0.40	0.42	0.34	0.46	0.28
n-Butylbenzene	k'	0.00	0 33	0.36	0.75	1.26	4.22	1.51	1.60
	α	0.00	0.86	0.72	0.74	0.71	0.64	0.88	0.50
1,2,3-TMB	k'	0.06	0.38	0.49	1.02	1.79	6.54	1.72	3.19
	α	1.00	1.00	1.00	1.00	1.00	1.00	1.00	1.00
1,2,3,4-TeMB	k'	0.19	0.83	1.14	2.87	5.15	19.11	4.86	11.63
	α	3.15	2.17	2.31	2.81	2.88	2.92	2.83	3.65

* TMP = trimethylphenol; TMB = trimethylbenzene; TeMP = tetramethylphenol; TeMB = tetramethylbenzene.

parallel straight lines are obtained in all instances and the two lines corresponding to each column are close to each other. The larger the degree of coating, the larger are the slopes, suggesting a small decrease in ε°.

In conclusion, with this polar solvent, the chromatographic properties of CCSP are similar to those of carbon when the degree of coating is large enough.

Medium-polarity solvent

The variation of solvent strength with degree of coating and its effect on retention is less important when the polarity of the eluent is lower. The retentions of some solutes for the different columns are given in Fig. 8, and results for more compounds are given in Table VI. The curves are very similar to those in Fig. 6, but their initial slopes are smaller. This is in agreement with a smaller variation in the apparent eluotropic strength of the solvent, and is confirmed by the results in Table VI.

Owing to malfunction of the equipment, column D was accidentally destroyed during these measurements so some results in acetonitrile and all results in *n*-heptane are lacking for this column.

Non-polar solvent

Although this is of little direct analytical interest, experiments using a non-

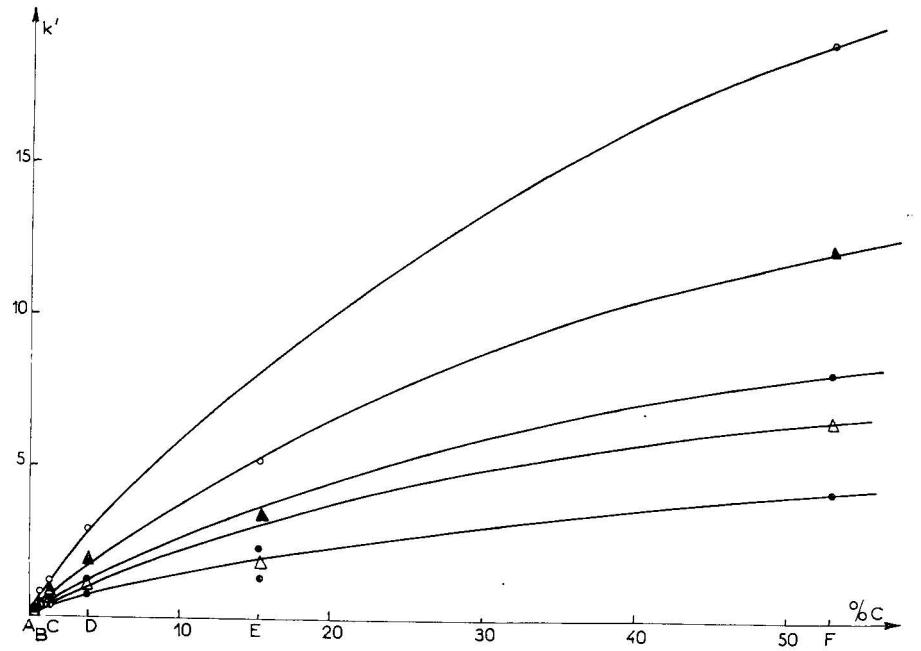


Fig. 6. Capacity factors (k') of various solutes *versus* degree of carbon coating with water–acetonitrile (1:1) as solvent. ○, 1,2,3,4-tetramethylbenzene; ▲, 2,3,4,6-tetramethylphenol; ●, β-naphthol; △, *n*-butylbenzene; ◐, 1,2,3-trimethylbenzene.

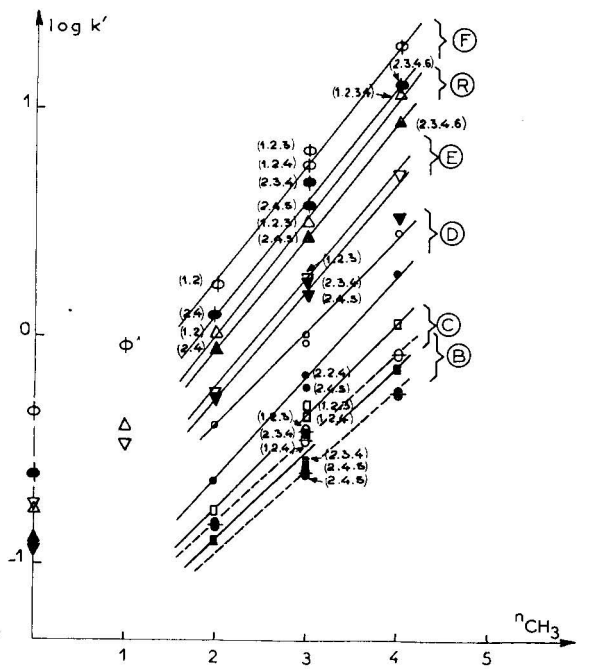


Fig. 7. Variation of log k' in homologous series. Open symbols, methylbenzenes; closed symbols, methylphenols.

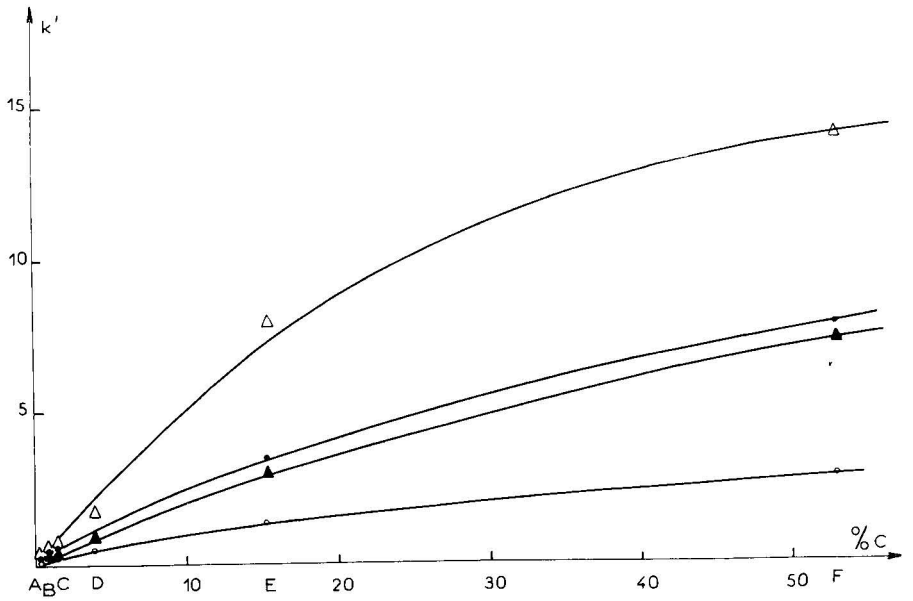


Fig. 8. Capacity factors (k') of various solutes *versus* degree of carbon coating with acetonitrile as solvent. △, 2,3,5-Trimethylnaphthalene; ●, hexamethylbenzene; ▲, 1,8-dimethylnaphthalene; ○, 2-methylnaphthalene.

polar solvent are the best means of testing the influence of the silica substrate, which is well measured by the retention of polar compounds. Indeed, a non-polar solvent is very weakly adsorbed on the silica surface. Conversely, a polar solute, for which interactions with the solvent are small while specific interactions with the adsorbent are large, will be strongly adsorbed on the silica. The retentions of such compounds will increase with the surface area of the uncovered silica. On the other hand, the retention of non-polar solutes will increase with increasing area of the carbon-liquid interface and with an increase in the degree of coating.

The results are reported in Table VII and Fig. 9. As expected, the relative retention of polar compounds decreases with increase in the degree of coating.

As can be seen in Fig. 10, the elution peaks of polar solutes are asymmetric and accurate measurements are not possible. As their adsorption takes place essentially on silica, the linear capacity of the adsorbents is necessarily very small, especially at large degrees of coating, and hence the columns are easily overloaded. No further effort was made to assess the influence of column overloading and its variation with increasing retention and degree of coating. Nevertheless, it appears from Table VII that polar solutes are slightly retained on pure carbon.

The values obtained with column A, which contains virtually no pyrocarbon, are much smaller than those reported by Scott and Kucera[12]. As an example, for Partisil 5, the lowest degree of coating used was 4.12%, and for this column (H) the k' value of naphthalene was 0.25 while that given by Scott and Kucera was 1.25. Although this effect might result in part from a lower specific surface area of our silica particles, it also demonstrates the dehydration effect of the thermal treatment that

TABLE VI

COMPARISON BETWEEN RETENTION DATA ON DIFFERENT COLUMNS (*cf.*, TABLE I) WITH ACETONITRILE AS SOLVENT

*Solute**	*Parameter*	*Column*							
		A	*B*	*C*	*D*	*E*	*F*	*G*	*R*
Naphthalene	k'	0.04	0.06	0.06	—	0.44	1.38	0.12	0.45
	α	0.11	0.09	0.09	—	0.06	0.10	0.07	0.05
2-MMN	k'	0.09	0.12	0.18	0.45	1.30	2.82	0.28	1.18
	α	0.25	0.20	0.26	0.27	0.21	0.20	0.17	0.11
1,8-DMN	k'	0.18	0.29	0.38	0.85	2.97	7.32	0.71	2.75
	α	0.50	0.47	0.55	0.51	0.37	0.52	0.44	0.32
2,3,5-TMN	k'	0.36	0.61	0.69	1.68	7.94	14.00	1.60	8.52
	α	1.00	1.00	1.00	1.00	1.00	1.00	1.00	1.00
Acenaphthylene	k'	0.10	0.22	0.27	0.63	2.94	5.40	0.57	2.24
	α	0.28	0.37	0.39	0.38	0.37	0.39	0.36	0.26
Fluorene	k'	0.25	0.51	0.58	1.26	6.50	13.10	0.94	5.70
	α	0.78	0.84	0.84	0.75	0.82	0.94	0.59	0.67
β-Naphthol	k'	0.09	0.10	—	0.45	0.71	1.40	0.17	1.45
	α	0.24	0.17	—	0.27	0.09	0.10	0.11	0.17
2,4-Xylenol	k'	0.04	0.00	0.03	0.05	0.13	0.29	0.04	0.19
	α	0.11	0.00	0.04	0.03	0.02	0.02	0.02	0.02
2,3,4-TMP	k'	0.03	0.05	0.05	—	0.31	0.98	0.13	0.69
	α	0.07	0.09	0.07	—	0.04	0.07	0.08	0.08
1,2,3-TMB	k'	0.00	0.02	0.04	—	0.14	0.41	0.07	0.20
	α	0.00	0.04	0.07	—	0.02	0.03	0.04	0.02
2,3,4,6-TeMP	k'	0.05	0.08	0.11	0.37	0.64	1.68	0.28	1.22
	α	0.13	0.12	0.15	0.22	0.08	0.12	0.17	0.14
1,2,3,4-TeMB	k'	0.03	0.06	0.08	—	0.46	1.10	0.22	0.60
	α	0.08	0.10	0.11	—	0.06	0.08	0.14	0.07
PMB	k'	0.07	0.14	0.14	—	1.06	2.46	0.58	1.66
	α	0.20	0.23	0.20	—	0.13	0.18	0.36	0.19
HMB	k'	0.17	0.40	0.40	—	3.54	7.74	1.93	6.40
	α	0.48	0.64	0.58	—	0.45	0.55	1.20	0.75

* MMN, DMN and TMN = mono-, di- and trimethylnaphthalene, respectively; PMB, HMB = pentamethyl- and hexamethylbenzene, respectively. Other abbreviations as in Table V.

TABLE VII

COMPARISON BETWEEN RETENTION DATA ON DIFFERENT COLUMNS (*cf.*, TABLE I) WITH *n*-HEPTANE AS SOLVENT

Solute	*Parameter*	*Column*							
		A	*B*	*C*	*D*	*E*	*F*	*G*	*R*
Naphthalene	k'	0.05	0.09	0.14	—	0.37	0.92	0.09	0.16
	α	0.15	0.16	0.20	—	0.16	0.15	0.19	0.09
Acenaphthylene	k'	0.13	0.18	0.23	—	0.86	2.24	0.21	0.58
	α	0.38	0.31	0.34	—	0.38	0.36	0.46	0.32
Fluorene	k'	0.34	0.59	0.68	—	2.26	6.11	0.45	1.84
	α	1.00	1.00	1.00	—	1.00	1.00	1.00	1.00
Phenol	k'	16.4	16.0	13.4	—	6.05	9.40	2.56	0.23
	α	48.0	27.0	19.7	—	2.68	1.54	5.64	0.12
o-Cresol	k'	Too high	6.2	8.4	—	3.83	5.72	1.62	0.18
	α		23.7	12.3	—	1.70	0.94	3.56	0.09
2,4-Xylenol	k'	Too high	6.2	8.3	—	3.83	5.95	1.62	0.16
	α		23.7	12.2	—	1 70	0.97	3.56	0.09

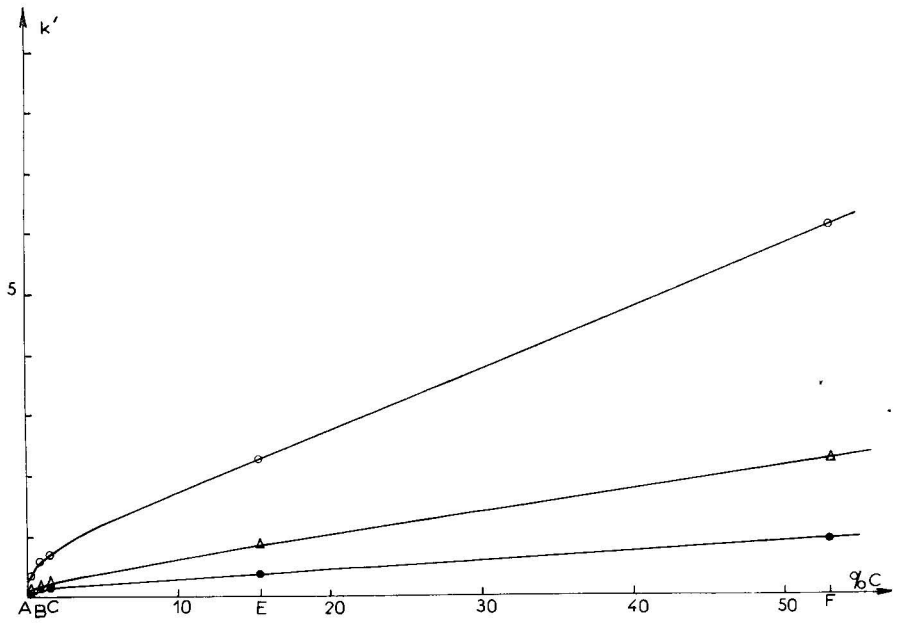


Fig. 9. Capacity factors (k') of various solutes *versus* degree of carbon coating with *n*-heptane as solvent. ○, fluorene; △, acenaphthylene; ●, naphthalene.

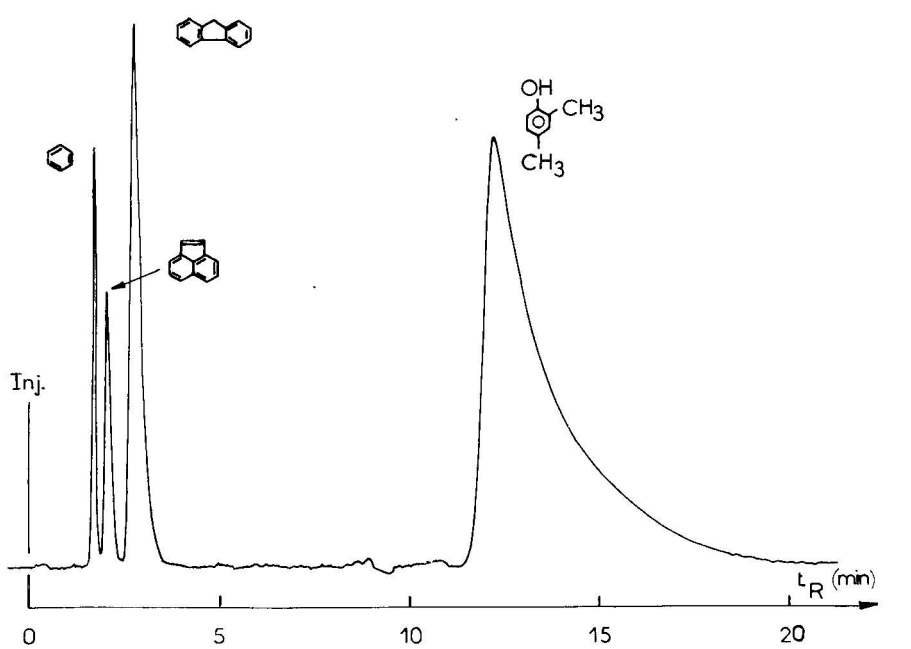


Fig. 10. Elution of non-polar and polar solutes in *n*-heptane. Column B; 0.98 cm³/min; UV detector.

accompanies the pyrolysis. No column of thermally treated uncoated silica has been packed.

These results are in agreement with those of Bebris *et al.*[1]. It does not seem possible to mask the properties of the underlying silica completely. This does not make it difficult, however, to obtain good analytical results with polar eluents.

ANALYTICAL PROPERTIES OF CARBON-COATED SILICA PARTICLES

A few simple separations are considered here in order to illustrate some characteristics of CCSP.

The three chromatograms in Fig. 11 represent the separations of a mixture of phenol and alkylbenzenes. The solvent was water–acetonitrile (1:1) and the flow-rate 0.4 cm³/min in all instances. Chromatogram I was obtained with column R, and II and III with columns E and B, respectively. Separations I and II are very similar, the resolution of phenol and benzene, however, being better on CCSP. When injected alone, the capacity factors for these solutes are 0.18 and 0.13 on column R. The k' values are

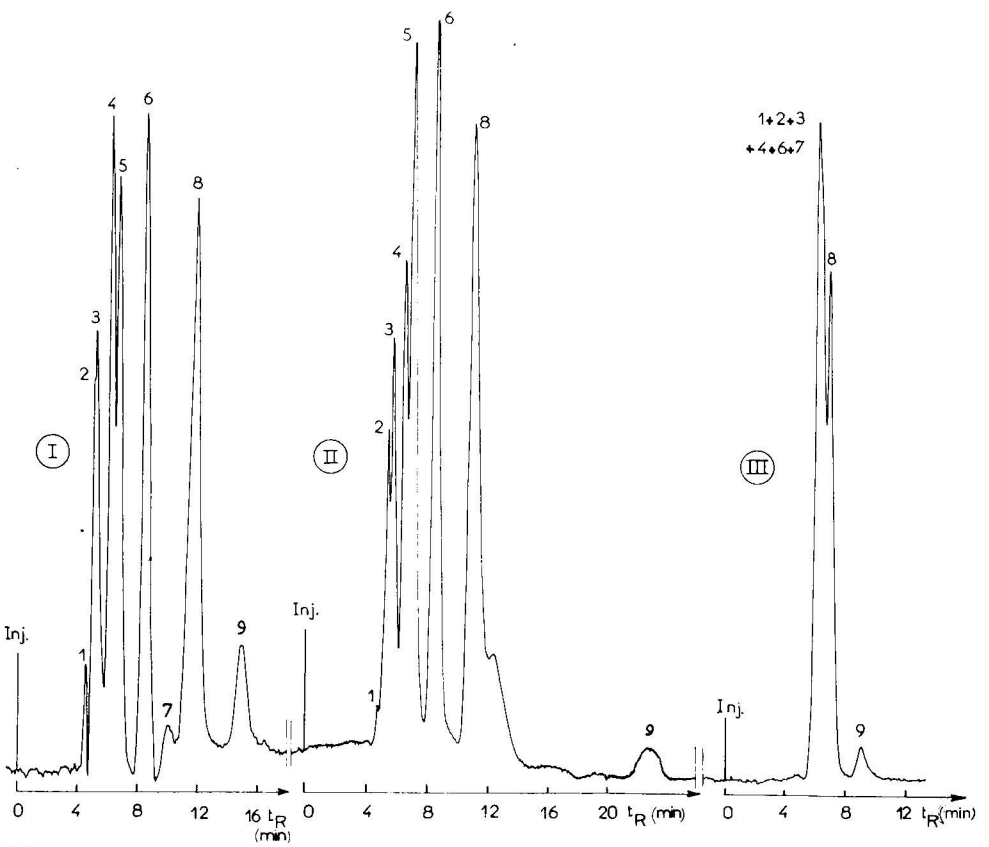
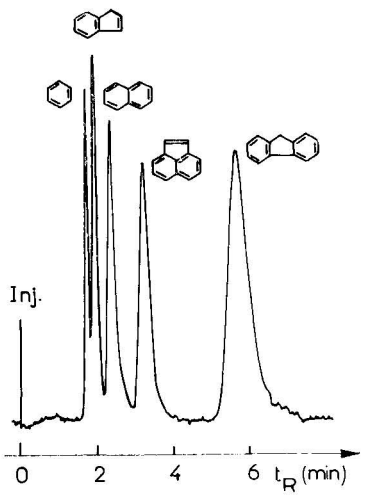


Fig. 11. Separations of phenol and alkylbenzenes on different adsorbents: I, column R; II, column E; III, column B. Solvent, water–acetonitrile (1:1); flow-rate, 0.4 cm³/min; UV detector. Peaks: 1 = acetonitrile (solvent for sample); 2 = phenol; 3 = benzene; 4 = toluene; 5 = ethylbenzene; 6 = *n*-propylbenzene; 7 = impurity; 8 = *n*-butylbenzene; 9 = impurity.

0.15 and 0.10 when the measurements are made from the chromatogram I. This effect, which is probably due to local column overloading during the beginning of the chromatographic process, is currently under investigation. Chromatogram III suggests, on the other hand, that the degree of carbon coating (0.84%) is insufficient: only *n*-butylbenzene is slightly retained and can be identified in the mixture.

Fig. 12 shows the separation of some polynuclear aromatic compounds with *n*-heptane as eluent. The decrease in efficiency with increasing retention is very important, as illustrated in Fig. 13. This effect is due in part to the large flow-rate used ($u = 0.54$ cm/sec, $\nu = 90$). For $k' = 2.2$, the column exhibits three-fold fewer theoretical plates than for a non-retained solute. When dealing with the mixture water–acetronitrile, however, the decrease in efficiency is lower: only 1.7-fold fewer plates for $k' = 2.1$ (*n*-pentylbenzene) than for $k' = 0$. On the other hand, the peak symmetry seems to be good in all instances.



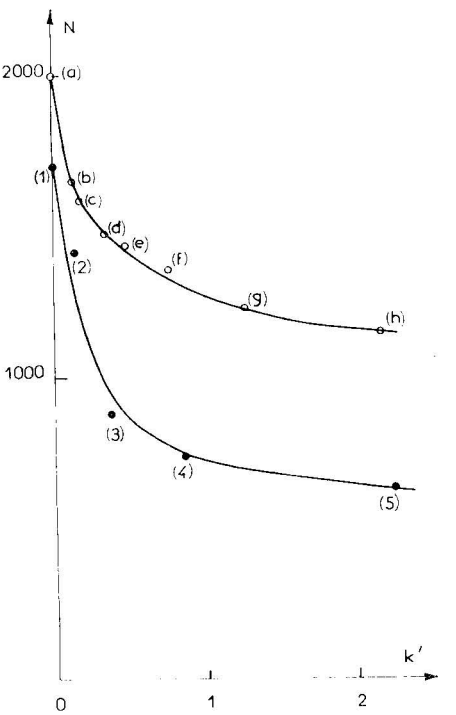


Fig. 12. Separation of polynuclear aromatic compounds. Column E. Solvent, *n*-heptane; flow-rate, 1.2 cm³/min; UV detector.

Fig. 13. Variation of the number of theoretical plates (N) with retention (k') at constant flow-rate. Column E. Solvent: open symbols, water–acetonitrile (1:1) (0.4 cm³/min); closed symbols, *n*-heptane (1.2 cm³/min).

The separation shown in Fig. 14 has been performed previously using water–acetonitrile (6:4) on carbon black[3]; we carried it out here with the 1:1 mixture on column F. The retention of aromatic nitro compounds is twice as great on column F, while those of benzene and toluene are only 1.3-fold greater. This effect is due in part to the fact that all retentions are higher on column F than on column R. Furthermore,

a decrease in the water content of the mixture sometimes increases the retention of polar compounds[5].

Finally, the separations of a mixture of polymethylphenols is shown in Fig. 15. It is, in fact, the analysis of a "pure" commercial 2,3,5,6-tetramethylphenol sample. Peaks 2, 3 and 4 have been tentatively identified as those of other methylphenols. This separation was performed on Partisil 5 coated with 14% of pyrocarbon (column I). The efficiency is not high ($N = 1110$ for 2,3,5,6-tetramethylphenol; $k' = 1.0$; $h = 15$), but the time of analysis is very short. Also, as pointed out previously, the coating of fine powders is tedious and is accompanied to some extent by agglomeration of particles, resulting in an increase in the HETP values.

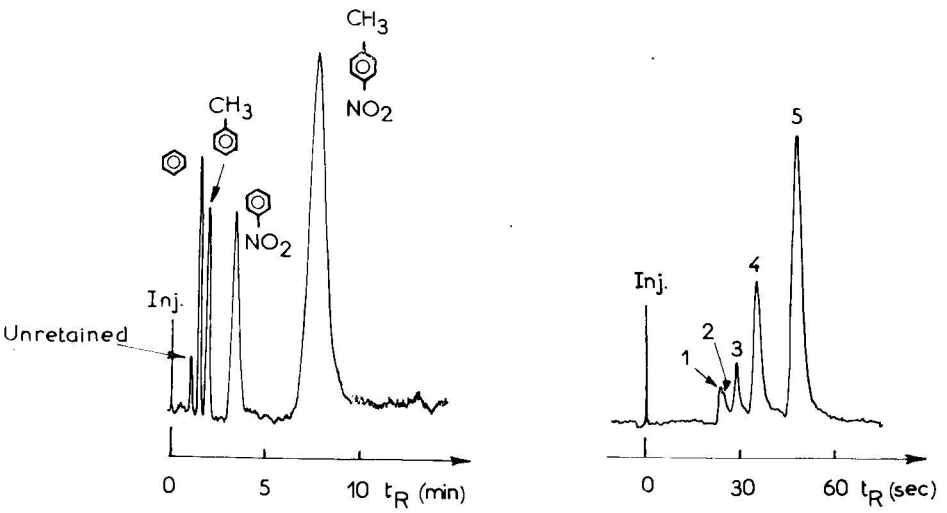


Fig 14. Separation of a mixture of compounds of very different polarities. Column F. Solvent, water–acetonitrile (1:1); flow-rate, 2 cm³/min; UV detector.

Fig. 15. Separation of methylphenols. Column I. Solvent, acetonitrile; Flow-rate, 2.55 cm³/min ($v = 3.5$); UV detector. Peaks: 1 = unretained; 2 = 2,4-xylenol (?); 3 = 2,4,6-trimethylphenol; 4 = 2,3,4,6-tetramethylphenol; 5 = 2,3,5,6-tetramethylphenol.

CONCLUSION

The coating of silica particles with pyrocarbon can be a good method for providing suitable adsorbents for reversed-phase HPLSC. The correct amount of carbon to be deposited depends on the type of silica used, and the experimental conditions of preparation seem to be very important. Moreover, the optimal conditions are probably not the same for all types of silica particles.

This work was carried out essentially using Spherosil XOB 75, which explains why the few results obtained with Partisil 5 were not very good.

It is possible to modify fine particles of 5-μm diameter, which would permit very efficient columns to be packed. This possibility is attractive insofar as it is extremely difficult to prepare pure carbon particles in this size range. The silica particles have very good mechanical properties and can be regularly shaped, which makes packing

easy. On the other hand, carbon-coated silica cannot be graphitized. Although we have not yet assessed the consequences of this treatment, our preliminary results seem to show that it improves the chromatographic performances of the packings.

Work will be carried out on the use of other silica and aluminosilicate materials. The main drawback, however, seems to be the virtual impossibility of completely eliminating the influence of silica: at low degrees of coating a large part of the silica surface is not covered. It seems that at high degrees of coating the coating does not adhere well to the underlying material and peels off during the cooling, leaving part of the silica exposed. This would explain the results in Table IV and the polarity of the adsorbent in column G.

ACKNOWLEDGEMENT

We thank Mr. A. Ansel (Thomson C. S. F., Corbeville, France) for the photographs obtained with scanning electron microscope.

REFERENCES

1 N. K. Bebris, R. G. Vorobieva, A. V. Kiselev, Yu. S. Nikitin, L. V. Tarasova, I. I. Frolov and Ya. I. Yashin, *J. Chromatogr.*, 117 (1976) 257.
2 H. Colin, C. Eon and G. Guiochon, *J. Chromatogr.*, 119 (1976) 41.
3 H. Colin, C. Eon and G. Guiochon, *J. Chromatogr.*, 122 (1976) 223.
4 T. V. Barmakova, A. V. Kiselev and N. V. Kovaleva, *Kolloid. Zh.*, 36 (1974) 133.
5 H. Colin and G. Guiochon, to be published.
6 G. J. Kennedy and J. H. Knox, *J. Chromatogr. Sci.*, 10 (1972) 549.
7 J. H. Knox and G. Vasvari, *J. Chromatogr.*, 83 (1973) 181.
8 J. H. Knox and A. Pryde, *J. Chromatogr.*, 112 (1975) 171.
9 J. C. Giddings, *Dynamics of Chromatography, Part I*, Marcel Dekker, New York, 1965.
10 N. C. Fawcett and R. D. Caton, Jr., *Anal. Chem.*, 48 (1976) 600.
11 L. R. Snyder, *Principles of Adsorption Chromatography*, Marcel Dekker, New York, 1968.
12 R. P. W. Scott and P. Kucera, *J. Chromatogr. Sci.*, 13 (1975) 337.

Journal of Chromatography, 126 (1976) 63–83
© Elsevier Scientific Publishing Company, Amsterdam — Printed in The Netherlands

CHROM. 9415

A TAILOR-MADE C_{87} HYDROCARBON AS A POSSIBLE NON-POLAR STANDARD STATIONARY PHASE FOR GAS CHROMATOGRAPHY

F. RIEDO, D. FRITZ, G. TARJÁN and E. sz. KOVÁTS

Laboratoire de Chimie Technique de l'École Polytechnique Fédérale de Lausanne, Lausanne (Switzerland)

SUMMARY

A hydrocarbon of empirical formula $C_{87}H_{176}$ has been found to have advantageous properties for use as a stationary phase in gas chromatography. It is a non-polar solvent with a working temperature range from 30°C to about 280°C. Being a pure substance, it has reproducible properties. The information necessary for determining the precise position of the starting point of the chromatogram is given, and its separation properties are discussed, taking as examples the chromatographic behaviour of *n*-alkanes and other selected compounds. With the aid of these data, this hydrocarbon is compared with squalane and the methylsilicones, and proved to show most of the advantages of both of these phases.

INTRODUCTION

Alkanes are thought to be the least polar organic solvents and are therefore accepted as "non-polar" stationary phases in gas chromatography in the absence of a hypothetical, non-polar substance[1–3]. In fact, experimental evidence shows that the retention properties of such liquids can be explained by assuming that they can interact with solutes by dispersion forces only. Hence their retention character is considered as the basis of comparison for all other stationary phases. By examining the additional retention of a series of substances on a polar phase compared with that on an alkane, the "polarity" of the polar stationary phase can be characterized in an empirical way[2–4]. However, the retention character of hydrocarbons as a group can be spoken of only as a first approximation, as there are differences between the solvent properties of the individual substances, with the retention data depending mainly on the molecular weight[5–8]. Solvents of higher molecular weight appear to be slightly polar if compared with squalane, a liquid repeatedly proposed and accepted as a non-polar standard[1,3,4,9,10].

Such a choice is prejudicial to high-temperature work as the upper temperature limit of the use of squalane is only 100–120°C. Note also that squalane is a mixture of varying amounts of diastereoisomers. Therefore, the use of methylsilicones has been advanced as a standard or as one of a set of "preferred phases"[11,12], as they are almost non-polar and stable up to 300°C. This choice may also be criticised for several

reasons. Firstly, they are polymers and as such their molecular weight changes from batch to batch, thus affecting retention data. Secondly, sp^3-hybridized silicon atoms are Lewis acids capable of forming weak complexes by $\pi(p,d)$-bonds with bases such as ethers and alcohols. Finally, methylsilicones are always altered during the preparation of the column packing. During conditioning, the column is heated to higher temperatures for a given period of time in order to allow the methylsilicone chains to substitute the surface hydroxyl groups of the support[13]. Volatiles formed in these reactions and those present in the original polymer evaporate, resulting in a serious loss of weight of the applied polymer. Such a liquid cannot be accepted as a standard if well defined experimental conditions and reproducibility of retention data are required[14].

In this paper, we describe the properties of a "tailor-made" hydrocarbon that combines most of the advantages of the two above-mentioned liquids. It has nearly optimal properties if it is accepted that the following, partly contradictory, conditions have to be fulfilled: (1) the hydrocarbon should be a pure substance with no chiral centres; (2) its melting point should be as low as possible; (3) it should be of low viscosity; (4) the upper temperature limit of its use should be determined by its pyrolytic stability and not by volatility; and (5) the price of the substance should not be prohibitive for its use as a stationary phase.

Obviously, points (2) and (3) imply a hydrocarbon of low molecular weight, consequently too volatile to be used as a stationary phase. Therefore, the lowest admissible molecular weight to satisfy condition (4) had to be estimated. For this purpose, a series of 1,1,6,6-tetraalkylhexanes of general formula I, where R = alkyl, ranging from $C_{30}H_{62}$ to $C_{78}H_{158}$ have been synthesized in our laboratory. By investigating their thermal behaviour, we concluded that for a hydrocarbon to be nonvolatile up to 300°C, a minimum molecular weight (M) of about 1200 is required[7].

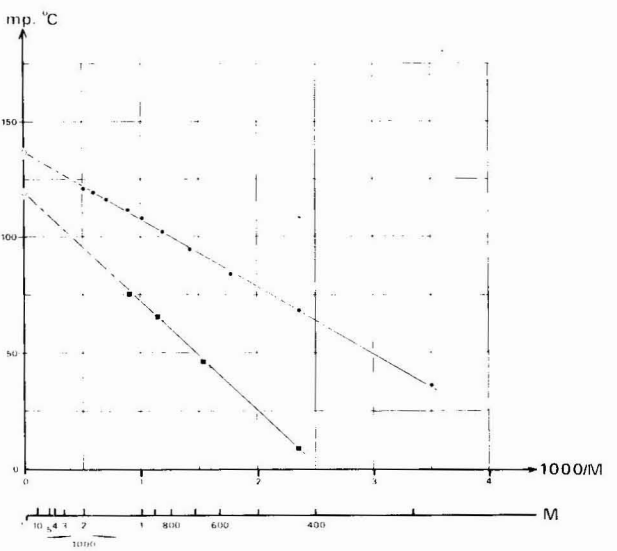
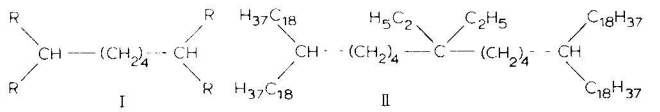


Fig. 1. Melting points of n-alkanes and branched hydrocarbons of structure I as a function of the reciprocal of the molecular weight (from ref. 15). For the melting points of n-alkanes of higher molecular weight, see ref. 16.

Fig. 1 shows that an *n*-alkane of the same molecular weight melts at about 112°C and that even the melting point of a branched alkane of structure I would be too high (80°C)[15]. Therefore, the synthesis of the hydrocarbon of structure II ($C_{87}H_{176}$, 24,24-diethyl-19,29-dioctadecylheptatetracontane; mol. wt. = 1222.37) was undertaken, assuming that it has the necessary degree of branching to bring about the desired melting point[17]. Its physical properties are summarized in Table I.



I II

TABLE I

PHYSICAL PROPERTIES OF HYDROCARBON II, $C_{87}H_{176}$

For the determination of the melting points, see Fig. 2. Sample P, dissolved and precipitated substance; sample M, crystallized from the melt at 21–22 °C. Confidence limits at the 95% significance level.

Property	*Sample*	*Value*
Melting point	P	33.3 ± 0.6 °C
	M	28.3 ± 0.3 °C
Enthalpy of fusion	P	28.7 ± 0.4 cal·g^{-1}
	M	23.3 ± 1.2 cal·g^{-1}
Density at 130 °C		0.776 ± 0.001 g·cm^{-3}
Specific volume at 130 °C		1.289 ± 0.002 cm^3·g^{-1}
Coefficient of cubic thermal expansion		(0.746 ± 0.007) 10^{-3} °C^{-1}
Molecular weight		1222.37 g·mole^{-1}
Molecular weight by vapour osmometry		1217 ± 30 g·mole^{-1}
Lower temperature limit of use as stationary phase		30 °C
Higher temperature limit of use as stationary phase (estimated)		280–300 °C

In Fig. 2, two melting curves of the same sample of hydrocarbon II are depicted. Trace P refers to the substance obtained in the last purification step. The hydrocarbon was dissolved in *n*-hexane and precipitated at 0°C by the addition of propanol-1. The white powder obtained by this procedure showed a shoulder of widely varying area on the melting curve at about 31° and a sharper peak at 33.3 ± 0.6°C. The previous handling largely determines the magnitude of the pre-melting effect, which might be due to structural defects introduced by mechanical shearing in the course of handling. By cooling the molten substance at different cooling rates, it always solidified at 21–22°. Trace M in Fig. 2 is the melting curve of such a solidified sample, whereby transitions were observed at *ca.* 25.6 (shoulder, sometimes missing), 26.6 ± 0.2 and 28.3 ± 0.3°C with varying areas under the individual peaks. It is interesting to note that substances once molten never again showed the high melting point of the precipitated substance.

The hydrocarbon has been used as the stationary phase in two packed columns for 8 months. During this period, about 500 chromatograms have been measured on each of them, the columns having also been heated overnight at 30–250°C. Subse-

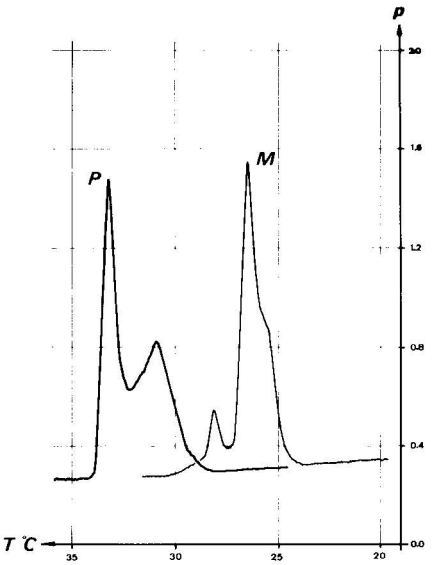


Fig. 2. Melting curves of a sample of the hydrocarbon II (4.52 mg) in a differential scanning calorimeter. Curve P, substance precipitated from its solution in *n*-hexane with propanol-1 at 0 °C; curve M, after crystallisation in the calorimeter at a cooling rate of 1–2 °C·min^{-1} at 21–22 °C. The power, p, is in mcal·sec^{-1}.

quently, the unchanged hydrocarbon was recovered from the column packing by extraction in nearly quantitative yield.

In conclusion, we felt that this substance can be proposed as a standard stationary phase, and its gas chromatographic properties were therefore investigated. The results are reported below.

EXPERIMENTAL

The substances used as solutes were obtained from Fluka (Buchs, Switzerland), and the rare gases and light hydrocarbons were products of Air Liquide (Paris, France).

The chromatographic data were measured with a Packard-Becker (Delft, The Netherlands) Model 419 apparatus, the thermostated oven of which was slightly modified. By inserting an additional box of aluminium plates to regulate the circulation of the hot air, the temperature gradient, originally 1.5°C between extreme points, could be reduced to 0.3–0.5°C for isothermal work. The flow-rate of the helium carrier gas was regulated by a thermostated (25 ± 0.5°C) Brooks (Hatfield, Pa., U.S.A.) valve. The temperature of the column oven was constant to within ± 0.1°C over 8 h. The flow-rate was determined twice daily with a soap-film device and controlled continuously with the aid of a precision flow meter[18]. The support was prepared from Chromosorb G (Johns-Manville, Denver, Colo., U.S.A.), which was made to react with trimethylsilanol in the presence of ammonia vapour at 100°C for 24 h in three successive treatments[13]. Two column packings were prepared by wetting the silanized support (particle diameter 180–220 μm) with a solution of hydrocarbon II in *n*-hexane and evaporating the solvent. The columns were Pyrex tubes (length 240

cm, I.D. 0.4 cm). Column A contained 2.583 g of stationary phase (column packing ratio, Chromosorb:hydrocarbon $\approx$ 90:10, w/w) and column B contained 4.017 g of stationary phase (packing ratio $\approx$ 86:14, w/w).

The melting curves of hydrocarbon II were recorded on a Perkin-Elmer Model DSC-1B differential scanning calorimeter. The measurements were made on samples of 1–4 mg in a nitrogen atmosphere at a heating rate of $1°C \cdot min^{-1}$. The molecular weight was determined with a Knauer (Berlin, G.F.R.) vapour-pressure osmometer in toluene solution (standard: benzil).

The specific volume and thermal dilatation of the hydrocarbon were determined in a home-made pyknometer on three samples of 800 mg each at different temperatures between 30 and 190°C. With the experimental specific volumes, v, (corrected for vacuum) the coefficients of the equation $\ln v = \ln v(T^\dagger) + \kappa(T - T^\dagger)$, where T is the temperature and $T^\dagger = 130°C$, were determined by linear regression. For the values of the specific volume at 130° $[v(T^\dagger)]$ and the coefficient of thermal expansion, κ, see Table I.

All of the necessary calculations were made on a Control Data Model Cyber 7326 computer at the École Polytechnique Fédérale de Lausanne. The programs were written in Fortran. The coefficients of the various equations were determined by the least-squares method, using the routines CARLIN, IMGC, LSQ1Z, LSQ2Z and PSQ3Z of the numerical analysis library POLYFTN, developed in the Department of Mathematics (under the responsibility of Prof. J. Descloux). Prior to calculations, some of the experimental results were first rejected by means of adequate statistical tests.

RESULTS AND DISCUSSION

The starting point of the chromatogram

For the determination of chromatographic data, the retention property X (distance on the chart, time, volume) of a hypothetical, non-retained substance is necessary. By working with a thermal conductivity detector, nitrogen is accepted as a substitute for such a substance. If a flame-ionization detector is used, methane is commonly assumed to approximate to the ideal properties, which is certainly an unsatisfactory assumption for precision work. The true zero can easily be determined if the relative retentions of a pair of substances are known with the necessary precision.

Let us choose one of the solutes to be methane, as it appears near to the true zero and it is detected by currently used detectors. Let us further assume that it is injected together with a second substance, A, (see Fig. 3) which is sufficiently separated from methane. The relative retention of A with respect to methane is then given by

$$r_{A/CH_4} = \frac{X'_R(A)}{X'_R(CH_4)} = \frac{X_R(A) - X_m}{X_R(CH_4) - X_m} \tag{1}$$

where X is the retention property of the solute (distance, d; time, t; volume, V) and X'_R, X_R and X_m represent the gross, corrected (net) and dead retention properties, respectively. Eqn. 1 gives, after the necessary transformations:

$$X_m = X_R(CH_4) - \frac{X_R(A) - X_R(CH_4)}{r_{A/CH_4} - 1} = X_R(CH_4) - \delta \tag{2}$$

TABLE II

GROSS RETENTION VOLUMES OF NEON AND NET RETENTION VOLUMES OF PERMANENT GASES AND LIGHT HYDROCARBONS

All volumes in millilitres, referred to mean column conditions (mean pressure and column temperature). Net retentions calculated with neon as non-retained substance. Column B with 4.017 g of stationary phase; thermal conductivity detector; helium carrier gas. Data for neon, averages of 4–6 experiments; all other data, averages of 3–4 determinations. In italics: values for neon calculated with the aid of the coefficients of a linear regression; for the other substances, values calculated with the data listed in Table IV.

Compound	*Temperature (°C)*										
	30	*50*	*70*	*90*	*110*	*130*	*150*	*170*	*190*	*210*	*230*
Neon	26.49	26.54	26.13	26.33	26.31	26.14	26.09	26.09	26.11	25.97	25.67
	26.49	*26.43*	*26.37*	*26.30*	*26.24*	*26.17*	*26.11*	*26.04*	*25.98*	*25.92*	*25.85*
Nitrogen	0.15	0.07	0.06	0.10	0.11	0.18	0.08	0.14	0.15	0.05	0.19
	0.10	*0.10*	*0.10*	*0.10*	*0.10*	*0.11*	*0.11*	*0.12*	*0.12*	*0.12*	*0.13*
Hydrogen	0.33	0.19	0.14	0.18	0.13	0.19	0.18	0.22	0.35	0.35	0.36
	0.27	*0.20*	*0.17*	*0.16*	*0.16*	*0.17*	*0.19*	*0.22*	*0.27*	*0.33*	*0.43*
Argon	0.42	0.51	0.43	0.44	0.45	0.49	0.47	0.58	0.47	0.47	0.58
	0.45	*0.45*	*0.45*	*0.46*	*0.47*	*0.47*	*0.48*	*0.50*	*0.51*	*0.52*	*0.54*
Krypton	2.33	1.80	1.62	1.61	1.45	1.52	1.39	1.44	1.43	1.38	1.49
	1.96	*1.77*	*1.65*	*1.56*	*1.50*	*1.46*	*1.43*	*1.43*	*1.43*	*1.43*	*1.45*
Xenon	8.89	7.60	6.47	5.84	5.13	4.83	4.35	4.09	3.71	3.57	3.54
	8.96	*7.55*	*6.53*	*5.76*	*5.18*	*4.72*	*4.35*	*4.06*	*3.82*	*3.62*	*3.46*
Methane	1.15	1.14	1.07	1.04	1.00	1.00	0.94	0.91	0.98	0.96	1.00
	1.20	*1.12*	*1.06*	*1.02*	*0.99*	*0.97*	*0.96*	*0.96*	*0.96*	*0.97*	*0.98*
Ethane	9.04	7.13	6.40	5.36	4.69	4.27	3.71	3.50	3.23	3.02	—
	8.98	*7.36*	*6.21*	*5.35*	*4.71*	*4.21*	*3.81*	*3.49*	*3.23*	*3.01*	*2.83*
Propane	29.60	21.48	16.90	13.33	10.84	9.16	7.74	6.88	6.04	5.47	—
	29.57	*21.74*	*16.69*	*13.27*	*10.87*	*9.13*	*7.83*	*6.84*	*6.07*	*5.45*	*4.96*
Butane	103.81	66.19	45.73	33.25	25.06	19.85	15.95	13.32	11.34	9.77	—
	103.16	*66.61*	*45.83*	*33.22*	*25.15*	*19.74*	*15.99*	*13.29*	*11.30*	*9.81*	*8.65*
Neopentane	107.91	70.10	48.73	35.69	26.79	21.07	17.35	14.20	12.21	10.42	—
	107.77	*70.32*	*48.74*	*35.50*	*26.96*	*21.20*	*17.17*	*14.26*	*12.11*	*10.48*	*9.21*
Tetramethylsilane	148.21	90.92	60.15	42.92	31.53	23.95	19.27	15.65	13.00	11.15	—
	147.24	*91.34*	*60.69*	*42.68*	*31.45*	*24.12*	*19.12*	*15.61*	*13.05*	*11.15*	*9.71*

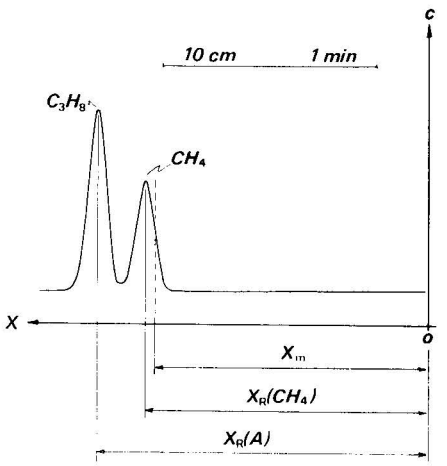


Fig. 3. Chromatogram of a mixture of methane and propane. Column B with 4.017 g of the hydrocarbon II; 210 °C; helium carrier gas. Concentration, c, in arbitrary units.

For calculation of the value of δ, a precise knowledge of the relative retention $r_{A/CH4}$ is necessary. To provide this, we equipped the chromatograph with a thermal conductivity detector, and on column B, containing 4.017 g of hydrocarbon II, we determined the gross retention volume of a series of permanent gases and light hydrocarbons. The results, summarized in Table II, show that neon has the smallest gross retention volume. We accepted tentatively that this value corresponds to the dead volume of the column, which implies that neon is supposed to be insoluble in the stationary phase, which is obviously not true. The systematic error introduced by this assumption at 25°C can be estimated as follows. From Henry's coefficient, h, reported in the literature for permanent gases and methane in several n-alkanes for 25°C[19–25], Henry's molal coefficient, $g^{(m)}$, was calculated as

$$g^{(m)} = M\,h/1000 \tag{3}$$

where M is the molecular weight of the solvent. The coefficients h and $g^{(m)}$ are defined by

$$p = h\,x = g^{(m)}m \tag{4}$$

where p is the partial pressure of the solute over the solution, x is its mole fraction and m is its concentration in the solvent expressed in molality (moles of substance per kilogram of solvent). From Henry's molal coefficient, the related standard chemical potential was calculated, given by

$$\Delta\mu^{(m)} = RT \ln g^{(m)} \tag{5}$$

where Δ is the difference between the ideally dilute solution and the ideal gaseous state. Finally, by using the equation

$$V_q = \frac{RT_c}{1000\,g^{(m)}} \tag{6}$$

the specific retention volume of the solute can be calculated by assuming that the solvent in question is used as the stationary phase.

It has been shown[6,7] that, in agreement with the Flory[26] and Huggins[27] theory for mixtures of molecules of unequal size, the dependence of a quantity such as $\Delta\mu^{(m)}$ on the reciprocal of the molecular weight of the solvent is linear, to a first approximation. The data plotted in Fig. 4 confirm this linear relationship. Extrapolation to the molecular weight of hydrocarbon II shows that our values are of the right order of magnitude and, further, that neon might have a specific retention volume of about 0.02 ml at 25°C. In Table III, this value is compared with those of the permanent gases and of methane measured from neon as zero. If the estimated value of the retention volume of neon is correct, its neglect would introduce an error of about 7% in the specific retention volume of methane. Other permanent gases such as hydrogen and nitrogen have even higher retentions than neon.

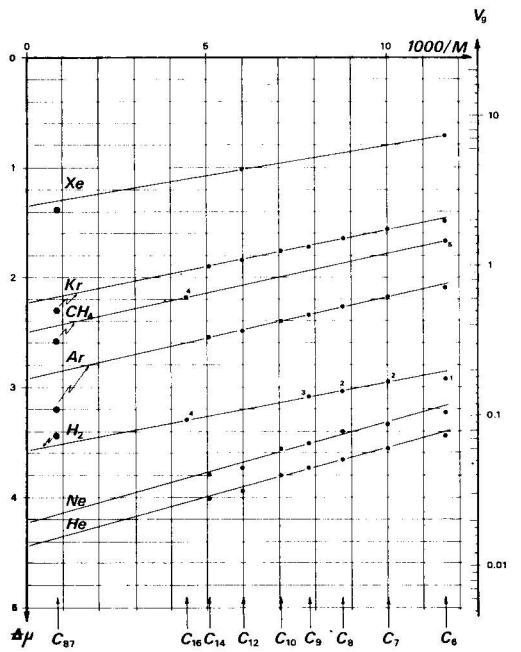


Fig. 4. Chemical potential related to Henry's molal coefficient, $\Delta\mu$, of several gases in *n*-alkanes and in hydrocarbon II. The logarithmic scale of the specific retention volume ($ml \cdot g^{-1}$) is also shown. Data for xenon, see ref. 19; for krypton, argon, neon and helium, see ref. 20; for hydrogen and methane point marked by 1, see ref. 21, by 2 see ref. 22, by 3 see ref. 23, by 4 see ref. 24 and by 5 see ref. 25. Data on hydrocarbon II were extrapolated to 25 °C with the aid of the regression coefficients listed in Table IV.

Unfortunately, we cannot use the value of 0.02 ml g^{-1} for neon as a correction for the whole temperature range. A substance with a positive free enthalpy difference will be more soluble at higher temperatures, and the correction will therefore be greater. Obviously, static measurements of the solubility of neon in the presence of helium would permit the calculation of the precise value of this correction and thus enhance the precision.

TABLE III

SPECIFIC RETENTION VOLUMES ON HYDROCARBON II

Values (ml·g^{-1}) extrapolated to 25 °C by using the coefficients in Table IV. For details, see text.

Estimated from Fig. 3	*Measured from neon as starting point*						
Ne	*Ne*	*Ar*	*Kr*	*Xe*	H_2	N_2	CH_4
0.02	0	0.12	0.50	2.33	0.074	0.024	0.304

In the absence of such data, we compared the temperature dependence of the dead volume of the column measured for neon with that calculated from the thermal expansion of the stationary phase. The dead volume of the column obviously changes with temperature because of the thermal expansion of the stationary phase as

$$V_m = V_m(T^\dagger) + V_{SP}(T^\dagger)\,[1 - e^{\kappa(T - T^\dagger)}] \qquad (7)$$

where $T^\dagger$ is a chosen temperature, κ the coefficient of cubic thermal expansion of the stationary phase and $V_{SP}(T^\dagger)$ the volume of the stationary phase at the temperature $T^\dagger$. In Fig. 5, the experimental gross retention volumes of neon are plotted as a function of the column temperature. The broken line is the linear regression calculated from the experimental data, while the full line was calculated from eqn. 7 by using the data in Table I. The agreement is very satisfactory.

In conclusion, the bias of the net retention volumes shown in Table II can be considered to be not too serious; even for a value of 0.8 ml (corresponding to a specific retention volume of 0.20 ml·g^{-1}) it is not more than 10%.

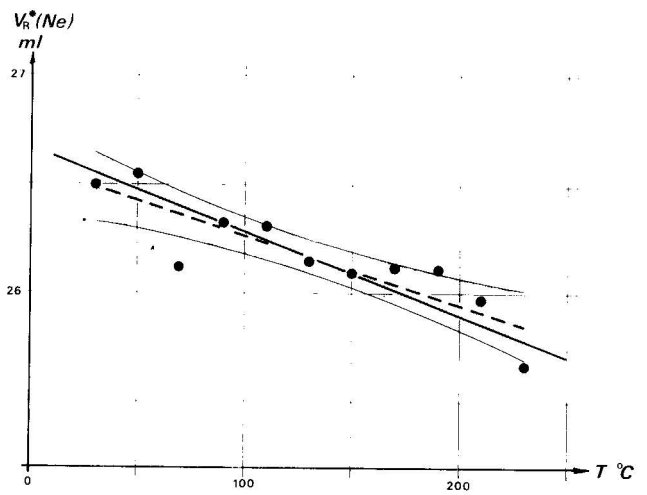


Fig. 5. The dead volume of column B (4.017 g of stationary phase) as measured by the gross retention volume of neon *versus* column temperature. Broken line, linear regression $V_m = V_m(T^\dagger) + b(T - T^\dagger)$ with slope of 0.0032 ± 0.0013 ml·°K^{-1}; solid line, trace of eqn. 7, where the value of $V_m(T^\dagger)$ was taken from the linear regression; its slope at 130 °C is 0.00386 ml·°K^{-1}. $T^\dagger$ = 130 °C. The shaded area shows the confidence limits of the linear regression at the 95% confidence level.

Neglecting this bias, the chemical potential related to Henry's molal coefficient was calculated by the least-squares method using eqns. 6 and 8:

$$RT \ln g_j^{(m)} = \Delta\mu_j^{(m)} = \Delta H_j(T^\dagger) - T\Delta S_j(T^\dagger) + \Delta C_{P,j}\left(T - T^\dagger - T \ln \frac{T}{T^\dagger}\right) \quad (8)$$

$T^\dagger = 403.15°K$ (= 130°C), where T is the absolute temperature, $\Delta H_j(T^\dagger)$ the molar enthalpy difference, $\Delta S_j(T^\dagger)$ the molar entropy difference of the solute, j, between the ideal dilute solution and the perfect gaseous state at 130°C; $\Delta C_{P,j}$ is the difference of the molar specific heat in these two states and is assumed to be constant over the whole temperature range (Kirchoff's method). The results are shown in Table IV.

TABLE IV

DIFFERENCES IN MOLAR ENTHALPY, ΔH_j, MOLAR ENTROPY, ΔS_j, BETWEEN IDEAL DILUTE SOLUTION AND PERFECT GASEOUS STATE AT 130 °C AND DIFFERENCE IN MOLAR SPECIFIC HEAT, $\Delta C_{P,j}$

Calculated with eqn. 8 and the retention volumes shown in Table II, by taking neon as non-retained substance.

Compound	$\Delta H_j(T^\dagger)$ (kcal·mole^{-1})	$\Delta S_j(T^\dagger)$ (cal·mole·°K^{-1})	$\Delta C_{P,j}$ (cal·mole^{-1}·°K^{-1})
Nitrogen*	−0.214	−14.69	+3.75
Hydrogen*	+0.669	−22.57	+45.75
Argon*	−0.555	−12.33	+1.78
Krypton	−1.139	−11.79	+4.93
Xenon	−2.192	−12.07	+1.06
Methane	−1.018	−12.29	+3.22
Ethane	−2.509	−13.08	+0.47
Propane	−3.441	−13.86	+1.92
Butane	−4.444	−14.81	+4.82
Neopentane	−4.430	−14.64	+3.85
Tetramethylsilane	−4.803	−15.30	+5.17

* Probably with heavy bias.

With the aid of the regression coefficients [$\Delta H_j(T^\dagger)$, $\Delta S_j(T^\dagger)$ and $\Delta C_{P,j}$], the relative retentions of ethane, propane and butane were re-calculated with respect to methane. The results (Fig. 6) give the necessary information for the determination of the starting point of the chromatogram by the method summarized in eqn. 2.

As an example, the chromatogram of a mixture of methane and propane at 210°C is shown in Fig. 3 (column B). We measured 15.4 and 13.2 cm for the gross retention distances of propane and methane, respectively. From Fig. 6, we read off 5.7 as the relative retention of the propane, and so we calculate

$$d_m = 13.2 - \frac{15.4 - 13.2}{5.7 - 1} = 13.2 - 0.47 = 12.7 \text{ cm} \quad (9)$$

for the distance corresponding to the dead volume of the column.

Retention behaviour of n-alkanes

During an 8-month period, about 1500 retention values of *n*-alkanes from pentane to pentadecane were determined on columns A and B between 30 and 250°C. The net retention volumes did not change with time, and the relative error of a single determination amounted to about ± 1%. The specific retention volumes calculated

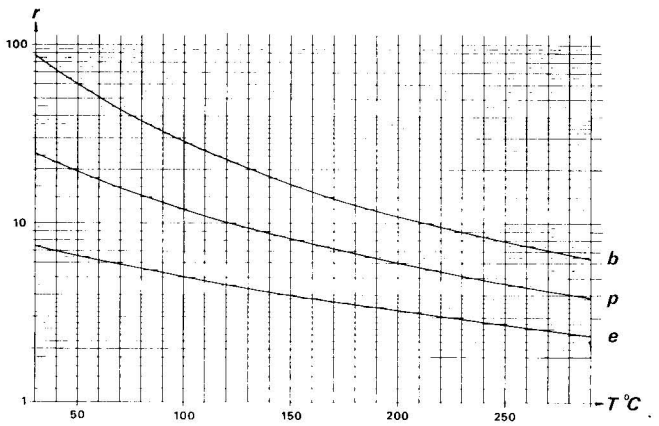


Fig. 6. Relative retention of ethane (e), propane (p) and butane (b) with respect to methane as a function of temperature. For details, see text. Values over 230 °C are extrapolated.

from the results showed a systematic difference of *ca.* 3%, the values being smaller on column B, which could be due to the error in the determination of the weight of the stationary phase. Therefore, the parameters of eqn. 8 were calculated with the average of the specific retention volumes. The regression coefficients of the higher homologues showed a systematic variation. By fitting the equation

$$\Delta\mu_z^{(m)} = (\alpha_0 + \alpha_1 z + \alpha_2(z^2 - z)/2) - T(\beta_0 + \beta_1 z) + \left(T - T^\dagger - T \ln \frac{T}{T^\dagger}\right)(\gamma_0 + \gamma_1 z) \quad (10)$$

where z ($\geqslant 8$) is the carbon number of the *n*-alkane C_zH_{2z+2}, to the experimental points for the *n*-alkanes from octane to pentadecane, the deviations of the experimental points (averages) were of the order of 0.6% [Δ_{rel} (95%) = ±1.3%]. This regression permits extrapolation to a few higher homologues. The results listed in Table V are

TABLE V

SOLUBILITY PARAMETERS OF *n*-ALKANES

Experiments in the temperature range indicated; m = number of experimental points. For details see Table IV and text. $T^\dagger$ = 403.15 °K (= 130.0 °C).

Compound	*Temperature range (°C)*	*m*	$\Delta H_J(T^\dagger)$ *(kcal·mole^{-1})*	$\Delta S_J(T^\dagger)$ *(cal·mole^{-1}·°K^{-1})*	$\Delta C_{P,J}$ *(cal·mole^{-1}·°K^{-1})*
Pentane	50–250	257	−5.418	−15.78	+7.02
Hexane	50–250	271	−6.438	−16.99	+9.16
Heptane	50–250	245	−7.445	−18.20	+10.58
Octane	90–250	223	$\alpha_0 + \alpha_1 z +$		
Nonane	90–250	188	$\alpha_2(z^2 - z)/2$	$\beta_0 + \beta_1 z$	$\gamma_0 + \gamma_1 z$
Decane	130–250	143	with	with	with
Undecane	130–250	121	α_0 = −0.143	β_0 = −9.12	γ_0 = −1.79
Dodecane	190–250	63	α_1 = 1.0444	β_1 = −1.277	γ_1 = +1.632
Tridecane	190–250	63	α_2 = +0.00282		
Tetra-decane	210–250	39			
Penta-decane	230–250	17			

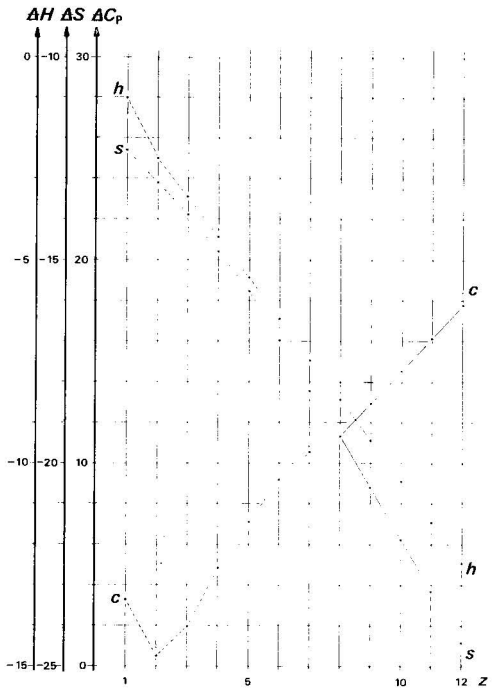


Fig. 7. Solubility parameters for *n*-alkanes as a function of the carbon number, *z*. Values for methane to heptane are calculated for each hydrocarbon by using eqn. 7. ΔH (trace h–h) in kcal·mole^{-1}, ΔS (trace s–s) and ΔC_P (trace c–c) in cal·mole^{-1}·°K^{-1}.

plotted in Fig. 7 together with the results for the light hydrocarbons (see Table IV) as a function of the carbon number of the *n*-alkane.

Note that this plot is not linear. Therefore, the determination of the starting point of the chromatogram is not justified by linearization of the logarithms of the retention data of *n*-alkanes, as suggested repeatedly (for the same criticism, see also ref. 28).

In order to facilitate the conversion of retention indices, the recalculated specific retention volumes, obtained by using the regression coefficients, are given in Fig. 8.

The data summarized in Table VI give a rough comparison of hydrocarbon II with a methylsilicone and an alkane with a carbon number of C_{30} (*e.g.*, squalane). The relative retention of two consecutive *n*-alkanes is a measure of the separation efficiency of the phase for hydrocarbons. On two similar columns (with the same phase ratio and same number of theoretical plates but different stationary phases), the separation efficiency obviously decreases if the relative retentions are smaller.

TABLE VI

APPROXIMATE RELATIVE RETENTION OF TWO SUCCESSIVE *n*-ALKANES AT 120 °C AND THE SPECIFIC RETENTION VOLUME OF *n*-OCTANE AT 100 °C ON A FEW STATIONARY PHASES

Stationary phase	$r_{(z+1)/z}$ *at 120 °C*	V_g *(octane) (ml·g^{-1}) at 100 °C*
C_{30} hydrocarbon	1.979 (ref. 7), 1.95 (ref. 4)	230–250 (ref. 7)
Methylsilicone	1.77 (ref. 4)	≈100 (ref. 29)
Hydrocarbon II	1.95–1.90	157.7

T(°C)=	30	40	50	60	70	80	90	100	110	120	130	140	150
Z= 3	7.351	6.266	5.405	4.713	4.149	3.685	3.299	2.976	2.703	2.470	2.270	2.097	1.947
3.5	13.74	11.33	9.471	8.025	6.882	5.967	5.225	4.617	4.115	3.695	3.341	3.041	2.784
4	25.70	20.47	16.59	13.67	11.42	9.662	8.275	7.164	6.264	5.527	4.918	4.410	3.983
4.5	46.27	35.72	28.13	22.56	18.39	15.21	12.76	10.83	9.301	8.070	7.070	6.248	5.566
5	83.32	62.34	47.70	37.24	29.62	23.95	19.67	16.38	13.81	11.78	10.16	8.851	7.779
5.5	146.8	106.3	78.95	59.97	46.49	36.72	29.50	24.07	19.92	16.70	14.17	12.15	10.53
6	258.6	181.3	130.7	96.56	72.97	56.29	44.24	35.37	28.72	23.66	19.75	16.68	14.25
6.5	447.6	304.5	213.4	153.6	113.3	85.47	65.77	51.56	41.11	33.28	27.34	22.75	19.16
7	774.7	511.3	348.4	244.4	176.0	129.8	97.78	75.16	58.83	46.82	37.84	31.02	25.76
7.5	1315.	844.5	560.9	384.1	270.4	195.3	144.3	108.9	83.73	65.56	52.17	42.14	34.51
8	2233.	1395.	902.9	603.7	415.6	293.8	212.9	157.7	119.2	91.78	71.91	57.24	46.23
8.5	3852.	2332.	1467.	954.7	641.2	443.0	314.1	228.0	169.2	128.0	98.68	77.35	61.58
9	6645.	3899.	2383.	1510.	989.2	667.8	463.4	329.8	240.1	178.6	135.4	104.5	82.04
9.5	.1144E+05	6505.	3862.	2383.	1523.	1005.	682.5	476.0	340.2	248.6	185.5	141.0	109.1
10	.1968E+05	.1085E+05	6260.	3761.	2345.	1512.	1005.	687.2	482.0	346.2	254.1	190.2	145.1
10.5	.3379E+05	.1806E+05	.1012E+05	5923.	3602.	2270.	1477.	990.0	681.7	481.2	347.4	256.2	192.6
11	.5801E+05	.3006E+05	.1637E+05	9327.	5535.	3408.	2171.	1426.	964.1	668.7	475.1	345.0	255.7
11.5	.9937E+05	.4993E+05	.2642E+05	.1466E+05	8486.	5107.	3185.	2051.	1361.	927.7	648.5	463.9	339.0
12	.1702E+06	.8291E+05	.4264E+05	.2303E+05	.1301E+05	7654.	4672.	2950.	1921.	1287.	885.2	623.7	449.3
12.5	.2909E+06	.1374E+06	.6866E+05	.3612E+05	.1991E+05	.1145E+05	6840.	4234.	2707.	1782.	1206.	837.0	594.5
13	.4971E+06	.2276E+06	.1106E+06	.5664E+05	.3046E+05	.1712E+05	.1001E+05	6076.	3813.	2468.	1644.	1123.	786.7
13.5	.8475E+06	.3763E+06	.1776E+06	.8863E+05	.4651E+05	.2555E+05	.1463E+05	8705.	5363.	3412.	2236.	1505.	1039.
14	.1445E+07	.6220E+06	.2854E+06	.1387E+06	.7101E+05	.3813E+05	.2138E+05	.1247E+05	7542.	4716.	3041.	2017.	1373.
14.5	.2457E+07	.1026E+07	.4575E+06	.2166E+06	.1082E+06	.5679E+05	.3118E+05	.1783E+05	.1059E+05	6508.	4129.	2697.	1810.
15	.4180E+07	.1692E+07	.7335E+06	.3382E+06	.1649E+06	.8459E+05	.4546E+05	.2549E+05	.1486E+05	8979.	5606.	3608.	2387.
15.5	.7093E+07	.2785E+07	.1173E+07	.5269E+06	.2507E+06	.1257E+06	.6617E+05	.3638E+05	.2082E+05	.1237E+05	7599.	4817.	3143.
16	.1204E+08	.4583E+07	.1877E+07	.8210E+06	.3812E+06	.1869E+06	.9631E+05	.5192E+05	.2918E+05	.1703E+05	.1030E+05	6432.	4138.

T(°C)=	160	170	180	190	200	210	220	230	240	250	260	270	280
Z= 3	1.815	1.700	1.598	1.508	1.427	1.356	1.291	1.233	1.181	1.133	1.090	1.051	1.015
3.5	2.564	2.373	2.206	2.061	1.933	1.819	1.719	1.630	1.550	1.478	1.414	1.355	1.303
4	3.621	3.311	3.046	2.816	2.617	2.442	2.289	2.154	2.035	1.928	1.834	1.749	1.673
4.5	4.997	4.516	4.109	3.760	3.461	3.201	2.976	2.779	2.606	2.453	2.318	2.198	2.091
5	6.896	6.160	5.543	5.021	4.577	4.197	3.869	3.585	3.337	3.120	2.930	2.762	2.613
5.5	9.210	8.127	7.228	6.478	5.845	5.309	4.851	4.458	4.118	3.823	3.565	3.339	3.140
6	12.30	10.72	9.426	8.357	7.465	6.716	6.083	5.544	5.081	4.683	4.338	4.037	3.774
6.5	16.32	14.04	12.20	10.70	9.457	8.425	7.559	6.828	6.207	5.675	5.217	4.822	4.477
7	21.65	18.40	15.80	13.70	11.98	10.57	9.393	8.410	7.581	6.877	6.275	5.758	5.311
7.5	28.62	24.02	20.39	17.48	15.13	13.21	11.63	10.31	9.216	8.290	7.504	6.834	6.257
8	37.85	31.37	26.31	22.30	19.10	16.51	14.39	12.65	11.20	9.994	8.975	8.110	7.372
8.5	49.74	40.71	33.74	28.29	23.97	20.51	17.72	15.44	13.56	12.00	10.70	9.599	8.668
9	65.37	52.84	43.27	35.87	30.08	25.48	21.81	18.84	16.41	14.41	12.75	11.36	10.19
9.5	85.78	68.46	55.41	45.42	37.69	31.62	26.81	22.95	19.83	17.28	15.18	13.43	11.97
10	112.6	88.71	70.95	57.52	47.22	39.23	32.95	27.97	23.96	20.72	18.07	15.88	14.06
10.5	147.5	114.8	90.70	72.72	59.08	48.61	40.45	34.03	28.92	24.81	21.48	18.74	16.49
11	193.2	148.5	116.0	91.94	73.92	60.22	49.65	41.41	34.90	29.71	25.53	22.13	19.34
11.5	252.6	191.7	148.0	116.1	92.35	74.50	60.86	50.32	42.06	35.53	30.31	26.09	22.65
12	330.4	247.6	188.9	146.5	115.4	92.16	74.60	61.14	50.69	42.49	35.98	30.76	26.54
12.5	431.4	319.3	240.8	184.7	143.9	113.8	91.31	74.19	61.01	50.75	42.66	36.22	31.04
13	563.3	411.8	306.8	232.8	179.5	140.6	111.8	90.02	73.43	60.61	50.58	42.65	36.32
13.5	734.3	530.1	390.4	292.9	223.6	173.5	136.6	109.1	88.25	72.28	59.89	50.16	42.43
14	957.2	682.5	496.8	368.7	278.5	214.0	166.9	132.2	106.1	86.20	70.91	58.98	49.58
14.5	1246.	877.2	631.2	463.3	346.4	263.5	203.7	159.9	127.3	102.7	83.84	69.27	57.85
15	1621.	1128.	801.9	582.1	430.8	324.6	248.7	193.5	152.8	122.3	99.14	81.35	67.51
15.5	2106.	1447.	1017.	730.4	535.0	399.2	303.0	233.8	183.1	145.4	117.1	95.41	78.67
16	2737.	1857.	1290.	916.4	664.3	490.9	369.3	282.5	219.4	173.0	138.2	111.9	91.68

Fig. 8. Specific retention volumes of *n*-alkanes calculated with regression coefficients. Hypothetical *n*-alkanes with half carbon numbers are also listed in order to facilitate interpolation. Experimental values are limited to within the marked frames.

We observed that this number is about the same on hydrocarbon II and on the C_{30} alkane but it is smaller on methylsilicones.

Methylsilicones are often spoken of as "rapid" stationary phases, meaning that the chromatograms on them are shorter in comparison with, for instance, squalane. On the one example of the retention volume of *n*-octane at 100°C, we observed that hydrocarbon II resembles the methylsilicone more than squalane in this respect.

Retention data of selected compounds

The retention indices of about 150 compounds were measured between 50 and 250°C. Statistical analysis showed that there was no significant difference between columns A and B, and therefore all results were evaluated together. The variance of a single determination is of the order of 1–2 units, except for the pyridines. These substances had to be injected in larger amounts as small samples gave peaks with serious tailing and widely varying retention indices.

Examination of the results listed in Table VII would suggest that this stationary

TABLE VII

RETENTION INDICES OF SELECTED COMPOUNDS ON THE HYDROCARBON II

Under the heading *m* the number of determinations is given in the temperature range shown in the fourth column. *V* is the variance around the linear regression with $m - 2$ degrees of freedom. The constants of the linear regression, I_{130} and the temperature dependence for a 10 °C interval, $10(\partial I/\partial T)$, are listed in the last four columns. For convenience, the indices at 70 and 190 °C are also given. Experimental conditions: values on two columns A and B with 2.583 and 4.018 g of hydrocarbon; determination at intervals of 20 °C; injection of about 0.05 mg per component with the exception of pyridines, where larger amounts were applied (*ca.* 0.2 mg); flame-ionization detector.

Type of compounds	*Compounds*	*m*	*Temperature range (°C)*	*V*	*I*			*10(∂I/∂T)*
					70 °C	*130 °C*	*190 °C*	
Hydrocarbons	*Isoalkanes*							
	Neopentane*		30– 230		406.4	409.0	411.6	0.44
	2,2-Dimethylbutane	22	50–150	0.76	535.1	541.2		1.01
	2,3-Dimethylbutane	14	50–150	0.51	567.9	573.2		0.89
	2,2-Dimethylpentane	15	70–190	0.79	624.2	627.7	631.2	0.58
	2,3-Dimethylpentane	15	50–170	0.85	674.3	679.9	685.5	0.94
	2,4-Dimethylpentane	29	50–210	1.11	626.9	629.5	632.1	0.44
	2,2,3-Trimethylbutane	16	50–150	1.28	641.5	653.1	664.7	1.93
	2,2-Dimethylhexane	12	70–210	0.24	715.8	719.6	723.4	0.64
	2,3-Dimethylhexane	12	90–210	0.13	761.0	766.0	771.0	0.84
	2,4-Dimethylhexane	18	90–210	0.61	729.6	733.4	737.2	0.63
	3,4-Dimethylhexane	13	90–190	0.71	774.0	780.4	786.8	1.06
	2,3,4-Trimethylpentane	15	90–210	0.42	755.5	765.6	775.7	1.68
	2,2,4-Trimethylpentane	13	90–210	0.33	788.6	694.8	701.0	1.68
	2,2-Dimethylheptane	17	90–210	0.70	811.6	815.8	820.0	0.70
	2,2,4,6,6-Pentamethylheptane	11	130–250	2.10		990.5	1002.9	2.07
	Alkenes							
	1-Pentene	9	50–150	0.51	482.5	483.9		0.27
	1-Hexene	14	50–190	0.74	584.5	585.3	586.1	0.14
	1-Heptene	16	50–230	1.23	683.6	685.2	686.8	0.26
	1-Octene	19	110–250	1.92	783.7	784.7	785.9	0.19
	1-Nonene	21	110–250	1.52	883.4	885.0	886.6	0.26
	1-Decene	22	130–250	0.76		984.6	986.6	0.34
	1-Undecene	18	130–250	0.99		1084.3	1086.6	0.38
	1-Dodecene	14	170–250	0.53		1184.3	1186.6	0.38
	1-Tridecene	8	190–250	1.39		1284.4	1286.9	0.42

TABLE VII (*continued*)

Type of compounds	*Compounds*	*m*	*Temperature range (°C)*	*V*	*I*			*10 (∂I/∂T)*
					70 °C	*130 °C*	*190 °C*	
	Alkynes							
	1-Pentyne	13	50–130	1.02	484.5	484.9		−0.06
	1-Hexyne	14	50–190	0.95	587.3	587.6	587.9	0.05
	1-Heptyne	18	50–230	1.49	687.1	688.4	689.7	0.22
	1-Octyne	27	90–250	3.06	785.8	788.3	790.8	0.42
	1-Nonyne	18	110–250	1.78	885.3	888.0	890.7	0.45
	1-Decyne	16	130–250	1.97		986.7	990.6	0.65
	Monocyclic hydrocarbons							
	Cyclopentane	15	50–130	0.59	575.9	588.3		2.06
	Cyclohexane	22	50–210	0.99	675.6	694.5	713.4	3.15
	Cycloheptane	18	90–190	1.99	811.6	838.8	866.0	4.54
	Cyclooctane	16	130–230	0.50		966.9	999.2	5.38
	Cyclodecane	8	190–250	0.61		1180.0	1223.1	7.19
	Cyclododecane	8	190–250	0.40		1362.7	1412.6	8.32
	Bicyclic hydrocarbons							
	cis-Hydrindane	19	130–250	1.29		1034.9	1072.8	6.32
	trans-Hydrindane	11	130–250	2.11		1000.3	1035.3	5.83
	cis-Decalin	12	170–250	0.53		1153.9	1198.7	7.47
	trans-Decalin	12	170–250	0.47		1112.2	1153.4	6.86
	Alkylbenzenes							
	Benzene	24	50–230	2.47	659.2	678.8	698.4	3.27
	Toluene	25	70–250	2.22	766.8	786.5	806.2	3.29
	Ethylbenzene	24	90–250	1.57	855.2	875.9	896.6	3.45
	Propylbenzene	21	130–250	2.03	943.0	965.0	987.0	3.66
	Butylbenzene	18	150–250	0.78		1064.8	1087.0	3.70
	Pentylbenzene	16	170–250	2.85		1162.0	1183.9	3.65
	Hexylbenzene	13	190–250	1.35		1257.7	1281.2	3.91
	Others							
	Adamantane	14	170–250	0.38		1137.6	1189.5	8.65
	Tetrahydronaphthalene	11	190–250	1.25		1189.7	1231.1	6.90
	Naphthalene	12	190–250	0.93		1215.4	1264.8	8.23
	Azulene	6	190–250	0.04		1331.2	1388.9	9.62
Alkane derivatives	*1-Chloroalkanes*							
	1-Chloropropane	12	50–170	0.82	526.9	536.4	545.9	1.58
	1-Chlorobutane	19	50–190	1.51	630.4	641.4	652.4	1.84
	1-Chloropentane	19	90–230	0.89	732.2	743.3	754.4	1.85
	1-Chlorohexane	17	110–230	0.93	833.3	844.8	856.3	1.91
	1-Chloroheptane	14	130–230	1.28	934.5	946.3	958.1	1.97
	1-Chlorooctane	12	150–230	0.32		1047.4	1059.5	2.02
	1-Chlorononane	8	190–230	0.08		1146.3	1160.3	2.33
	1-Chlorodecane	7	190–230	0.10		1246.9	1260.9	2.34
	1-Bromoalkanes							
	Bromoethane	11	50–170	0.49	509.6	523.0		2.24
	1-Bromopropane	19	50–190	2.46	614.2	629.4	644.6	2.53
	1-Bromobutane	22	50–210	0.81	716.8	732.7	748.6	2.65
	1-Bromopentane	19	90–210	2.46	817.7	835.0	852.3	2.88
	1-Bromohexane	14	130–210	1.00	918.3	936.4	954.5	3.02
	1-Bromoheptane	14	130–250	1.13		1036.2	1056.8	3.43
	1-Bromooctane	14	130–250	0.88		1136.3	1157.6	3.55
	1-Bromononane	8	190–250	0.65		1235.2	1258.0	3.80
	1-Bromodecane	5	210–250	1.05		1334.5	1358.0	3.92

(Continued on p. 78)

TABLE VII (*continued*)

Type of compounds	*Compounds*	*m*	*Temperature range (°C)*	*V*	*I*			*10 (∂I/∂T)*
					70 °C	*130 °C*	*190 °C*	
	1-Iodoalkanes							
	Iodomethane	14	50–150	0.30	528.6	548.8	569.0	3.36
	Iodoethane	16	50–190	0.29	617.6	638.9	660.2	3.55
	1-Iodopropane	20	70–210	0.57	720.3	743.8	767.3	3.92
	1-Iodobutane	18	90–210	0.49	819.3	844.6	869.9	4.21
	1-Iodopentane	18	110–250	1.32	917.8	944.6	971.4	4.47
	1-Iodohexane	12	150–250	0.44		1045.1	1072.9	4.63
	1-Iodoheptane	10	170–250	0.52		1144.9	1173.6	4.79
	1-Iodooctane	6	190–250	0.41		1247.2	1275.2	4.67
	1-Cyanoalkanes							
	1-Cyanopropane	16	50–190	8.14	587 4	593.6	599.8	1.03
	1-Cyanobutane	19	70–210	0.97	689.1	697.4	705.7	1.39
	1-Cyanopentane	18	90–210	0.56	789.5	799.1	808.7	1.60
	1-Cyanohexane	16	110–230	0.62	888.2	899.7	911.2	1.91
	1-Cyanoheptane	7	130–230	1.08	990.3	1001.3	1012.3	1.84
	1-Cyanooctane	17	150–250	2.34		1102.9	1114.7	1.97
	1-Cyanononane	10	170–250	0.64		1202.9	1215.3	2.07
	1-Cyanodecane	7	190–250	0.15		1302.4	1315.6	2.20
	1-Nitroalkanes							
	Nitroethane	12	50–170	2.15	563.7	578.6		2.48
	1-Nitropropane	20	50–190	1.33	654.7	665.1	675.5	1.73
	1-Nitrobutane	15	90–230	0.68	754.6	767.2	779.8	2.10
	1-Nitropentane	14	110–230	0.90	855.1	868.8	882.5	2.29
	1-Nitrohexane	10	130–230	0.91		969.9	984.8	2.48
	1-Acetoxyalkanes							
	1-Acetoxyethane	11	50–170	2.35	548.6	544.0	539.4	−0.77
	1-Acetoxypropane	19	50–190	1.37	644.1	638.9	633.7	−0.87
	1-Acetoxybutane	17	90–230	2.01	743.7	740.9	738.1	−0.46
	1-Acetoxypentane	23	90–250	1.90	843.7	841.1	838.5	−0.44
	1-Acetoxyhexane	14	130–250	0.85	940.8	939.4	938.0	−0.24
	1-Acetoxyheptane	13	130–250	1.16		1039.9	1038.8	−0.19
	1-Acetoxyoctane	11	130–250	0.64		1138.2	1138.5	0.05
	1-Acetoxynonane	8	190–250	0.52		1237.7	1238.1	0.07
	1-Alkanols							
	1-Butanol	21	50–190	4.29	602.2	600.9	599.6	−0.22
	1-Pentanol	26	70–190	1.67	700.3	701.9	703.5	0.27
	1-Hexanol	25	90–230	0.57	798.0	803.6	809.2	0.94
	1-Heptanol	19	130–250	1.45	898.3	905.6	912.9	1.22
	1-Octanol	16	130–250	1.90		1006.6	1014.3	1.29
	1-Nonanol	8	190–250	2.80		1110.9	1117.5	1.10
	2-Alkanols							
	2-Propanol	7	70–110	2.21	446.0	442.0		−0.66
	2-Butanol	13	70–150	2.32	547.9	552.0		0.69
	2-Pentanol	18	70–230	1.74	643.6	648.2	652.8	0.77
	2-Hexanol	21	90–230	1.99	742.4	748.0	753.6	0.94
	2-Heptanol	22	110–230	0.87	841.8	848.0	854.2	1.04
	2-Octanol	16	130–230	0.95		948.3	855.1	1.13
	2-Methylalkan-2-ols							
	2-Methylpropanol-2	8	50–110	1.12	478.1	473.3		−0.80
	2-Methylbutanol-2	14	50–190	1.12	596.6	600.9	605.2	0.71
	2-Methylpentanol-2	19	50–230	3.11	688.8	693.8	698.8	0.83
	2-Methylhexanol-2	17	90–230	0.90	782.4	788.3	794.2	0.99
	2-Methylheptanol-2	15	110–230	0.98	879.9	885.8	891.7	0.99
	2-Methyloctanol-2	12	150–230	1.46		986.5	988.3	0.97

TABLE VII (*continued*)

Type of compounds	*Compounds*	*m*	*Temperature range (°C)*	*V*	*I*			*10 (∂I/∂T)*
					70 °C	*130 °C*	*190 °C*	
	2-Alkanones							
	2-Butanone	18	50–150	8.25	540.2	543.5		0.55
	2-Pentanone	21	50–190	1.71	629.6	632.2	634.8	0.43
	2-Hexanone	24	70–230	0.82	729.4	733.7	738.0	0.72
	2-Heptanone	17	90–250	0.63	828.8	833.4	838.0	0.76
	2-Octanone	12	150–250	0.68	927.9	933.2	938.5	0.88
	2-Nonanone	12	150–250	0.35		1033.4	1039.5	1.02
	2-Decanone	10	170–250	0.76		1134.4	1139.7	0.89
	2-Undecanone	8	190–250	0.45		1234.6	1240.4	0.96
	Ethers							
	Diethyl ether	11	70–130	0.98	482.6	470.7		−1.99
	Dipropyl ether	24	50–190	1.29	659.0	655.2	651.4	−0.64
	Dibutyl ether	20	110–210	1.20	858.0	855.1	852.2	−0.49
	Dipentyl ether	8	170–250	0.49		1053.0	1051.0	−0.34
	Halogenomethanes							
	Dichloromethane	13	50–170	0.94	497.9	509.1		1.86
	Trichloromethane	18	50–210	1.66	595.2	610.3	625.4	2.51
	Tetrachloromethane	22	70–210	1.22	663.1	681.8	700.5	3.12
	Dibromomethane	20	90–210	3.67	681.7	706.2	730.7	4.08
	Tribromomethane	14	130–210	1.10	873.1	912.9	952.7	6.44
Halogenobenzenes	Fluorobenzene	24	50–230	1.70	651.3	665.9	680.5	2.44
	Chlorobenzene	27	90–250	1.20	838.4	866.1	893.8	4.61
	Bromobenzene	26	110–250	0.94	925.8	961.1	996.4	5.89
	Iodobenzene	20	150–250	0.95		1081.1	1125.7	7.43
Alkylpyridines	Pyridine	18	90–230	3.42	705.9	728.3	750.7	3.73
	2-Picoline	20	90–230	3.41	786.6	805.4	824.8	3.23
	3-Picoline	11	110–190	2.24	826.8	848.0	869.2	3.54
	4-Picoline	16	90–230	2.51	823.2	846.7	870.2	3.91
	2-Ethylpyridine	10	110–210	0.66	871.8	890.2	908.6	3.06
	3-Ethylpyridine	17	130–230	2.30	918.0	941.7	965.4	3.95
	4-Ethylpyridine	10	150–210	2.72	921.4	945.9	970.4	4.08
	2,4-Lutidine	12	130–230	2.68	903.4	922.7	942.0	3.22
	2,5-Lutidine	15	130–230	1.71	903.2	922.3	941.4	3.18
	2,6-Lutidine	20	110–210	3.58	863.8	876.1	888.4	2.05
	3,4-Lutidine	9	150–210	5.78		992.3	1018.6	4.38
	3,5-Lutidine	13	130–230	2.67		967.7	991.6	3.99
	2-Propylpyridine	16	130–230	1.20		976.6	998.3	3.62
	4-Propylpyridine	16	130–230	3.71		1034.7	1061.1	4.40
	4-*tert.*-Butylpyridine	6	150–210	0.97		1073.3	1101.9	4.76
Miscellaneous	Tetrahydrofuran	16	50–170	1.92	602.6	612.9	623.2	1.71
	Dioxan	17	50–170	1.58	660.3	675.0	689.7	2.45
	Thiophen	17	50–190	3.23	664.6	685.3	706.0	3.45
	Tetramethylsilane*		30–230		429.4	427.1	424.8	−0.38

* See Table VI.

phase has a certain polarity if compared with squalane with Rohrschneider's empirical constants. However, it has been shown that the effect of increasing molecular weight of the stationary phase is to displace retention data in the same sense but not by the same amount as increasing polarity[7,15].

TABLE VIII

RETENTION INDICES OF NEOPENTANE AND TETRAMETHYLSILANE CALCULATED WITH SPECIFIC RETENTION VOLUMES RELATED TO THE REGRESSION COEFFICIENTS LISTED IN TABLE IV

Differences, δ, for 20 °C steps are given in italics.

Compound	*Temperature (°C)*										
	30	*50*	*70*	*90*	*110*	*130*	*150*	*170*	*190*	*210*	*230*
Neopentane	403.6	405.1	406.3	407.6	408.8	409.8	410.6	411.3	411.8	412.1	412.3
δ	*1.5*	*1.2*	*1.3*	*1.2*	*1.0*	*0.8*	*0.7*	*0.5*	*0.3*	*0.2*	
Tetramethylsilane	430.0	429.8	429.4	429.0	428.4	427.6	426.8	425.9	424.8	423.6	422.4
δ	*−0.2*	*−0.4*	*−0.4*	*−0.6*	*−0.8*	*−0.8*	*−0.9*	*−1.1*	*−1.2*	*−1.2*	

In Fig. 9, we have marked on the abscissa the retention index differences

$$\Delta^* I_{130} = I_{130}\,(\text{HC-}\infty) - I_{130}\,(\text{HC-30}) \qquad (11)$$

for compounds used by McReynolds to compare stationary phases[4]. In eqn. 11, I_{130} (HC-∞) is the retention index of the compound on a hypothetical branched alkane of infinite molecular weight at 130°C and I_{130} (HC-30) is that on a C_{30} hydrocarbon with the structure I, from ref. 15. By plotting ΔI values of the same substances, obtained as differences between indices on any two hydrocarbon phases, against the $\Delta^* I_{130}$ values as defined in eqn. 11, a linear relationship must be obtained.

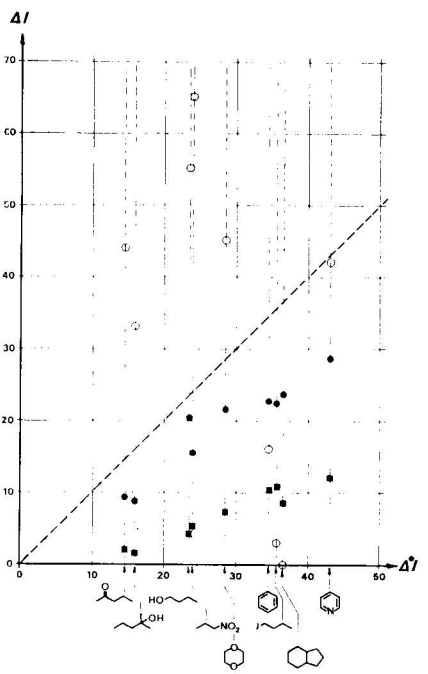


Fig. 9. ΔI values of selected substances on hydrocarbon stationary phases as a function of $\Delta^* I$ value of the same substances measured on a hypothetical hydrocarbon of infinite molecular weight referred to a hydrocarbon of carbon number C_{30} of structure I. For details, see text. ■, Average ΔI values on nujol, mineral oil and liquid paraffin referred to squalane from ref. 4; ●, ΔI values on hydrocarbon II referred to a C_{30} hydrocarbon of structure I; ○, average ΔI values on methylsilicones from ref. 4. ΔI values on a hypothetical alkane of structure I of infinite molecular weight referred to a C_{30} hydrocarbon should fall on the broken line.

Inspection of data on hexatriacontane, nujol, mineral oil and liquid paraffin listed in McReynolds' compilation show that ΔI values on these hydrocarbons (relative to squalane at 120°C) are very similar[4]. We therefore plotted their average value. The points are indeed aligned. Also, the ΔI values on hydrocarbon II relative to the C_{30} hydrocarbon of structure I (130°C from ref. 15) show a linear relationship. ΔI values of methylsilicones, on the contrary, show no correlation, which demonstrates clearly that this class of stationary phases has a different separating character.

As an example, it is interesting to calculate the retention indices of two sub-

stances by using the coefficients of the regression equations in terms of chemical potentials. In Table VIII, the retention indices of neopentane and tetramethylsilane are shown as a function of the temperature. It can be seen that, in fact, the temperature dependence of the retention index is hyperbolic but the error introduced by the linear approximation amounts only to ± 0.5 in a temperature range of 200°C. Probably, retention indices with higher temperature dependence will show a more pronounced curvature.

Finally, it should be noted that the results of an investigation of column packings prepared with hydrocarbon II in combination with different supports suggest that a good column performance can easily be obtained with this substance as stationary phase[30].

ACKNOWLEDGEMENTS

This paper reports part of a project supported by the Fonds National Suisse de la Recherche Scientifique, using some results of research supported by COST-Project 64b (European Cooperation in the Field of Scientific and Technical Research). We wish to thank Prof. G. Guiochon for valuable discussions.

REFERENCES

1 L. Rohrschneider, *Z. Anal. Chem.*, 170 (1959) 256.
2 A. Wehrli and E. sz. Kováts, *Helv. Chim. Acta*, 42 (1959) 2710.
3 L. Rohrschneider, *J. Chromatogr.*, 22 (1966) 6.
4 W. O. McReynolds, *J. Chromatogr. Sci.*, 8 (1970) 685.
5 G. J. Pierotti, C. H. Deal, E. L. Derr and P. E. Porter, *J. Amer. Chem. Soc.*, 78 (1956) 2989.
6 D. F. Fritz and E. sz. Kováts, *Anal. Chem.*, 45 (1973) 1175.
7 G. A. Huber and E. sz. Kováts, *Anal. Chem.*, 45 (1973) 1155.
8 D. E. Martire, *Anal. Chem.*, 46 (1974) 626.
9 D. H. Desty, E. Glueckauf, A. T. James, A. I. M. Keulemans, A. J. P. Martin and C. S. G. Phillips, in D. H. Desty and C. L. A. Harbourn (Editors), *Vapour Phase Chromatography*, Butter worths, London, 1957, p. xi.
10 P. Chovin and J. Lebbe, *Avant-Édition des Conférences aux Journées d'Étude de Séparation Immédiate*, Paris, 1961, p. 30.
11 J. J. Leary, J. B. Justice, S. Tsuge, S. R. Lowry and T. L. Isenhour, *J. Chromatogr. Sci.*, 11 (1973) 201.
12 S. Hawkes, D. Grossman, A. Hartkopf, T. Isenhour, J. Leary and J. Parcher, *J. Chromatogr. Sci.*, 13 (1975) 115.
13 L. Boksányi, O. Liardon and E. sz. Kováts, *Advan. Colloid Interface Sci.*, 6 (1976) 95.
14 H. Boer, P. Chovin, R. Delley, I. Halász, J. F. K. Huber, R. Kaiser, E. sz. Kováts, A. J. P. Martin, A. Prévôt, L. Rohrschneider, G. Schomburg and J. J. Walraven, in E. sz. Kováts (Editor), *Column Chromatography, 5th International Symposium on Separation Methods, Lausanne*, Sauerländer, Aarau, 1970, p. 9.
15 G. A. Huber, *Doctoral Thesis*, École Polytechnique Fédérale de Lausanne, 1973.
16 W. Heitz, Th. Wirth, R. Peters, G. Strobl and E. W. Fischer, *Makromol. Chem.*, 162 (1972) 63.
17 L. Boksányi, R. Peters, G. Tarján and E. sz. Kováts, to be published.
18 P. Tóth, E. Kugler and E. sz. Kováts, *Helv. Chim. Acta*, 42 (1959) 2519.
19 H. L. Clever, *J. Phys. Chem.*, 62 (1958) 375.
20 H. L. Clever, R. Battino, J. H. Saylor and P. M. Gross, *J. Phys. Chem*, 61 (1957) 1078.
21 J. E. Waters, G. A. Mortimer and H. E. Clements, *J. Chem. Eng. Data*, 15 (1970) 174.
22 M.-W. Cook, D. N. Hanson and B. J. Alder, *J. Chem. Phys.*, 26 (1957) 748.
23 E. S. Thompson and J. C. Gjaldbaek, *Acta Chem. Scand.*, 17 (1963) 127.

24 P. M. Cukor and J. M. Prausnitz, *J. Phys. Chem.*, 76 (1972) 598.
25 A. Lannung and J. G. Gjaldbaek, *Acta Chem. Scand.*, 14 (1960) 1124.
26 P. Flory, *J. Chem. Phys.*, 9 (1941) 660; 10 (1942) 51.
27 M. L. Huggins, *J. Phys. Chem.*, 9 (1941) 440.
28 L. Rohrschneider, *Chromatographia*, 2 (1969) 437.
29 W. O. McReynolds, *Gas Chromatographic Retention Data*, Preston Technical Abstracts Co., Evanston, Ill., 1966.
30 L. Boksányi and E. sz. Kováts, *J. Chromatogr.*, 126 (1976) 87.

THEORETICAL AND PRACTICAL ASPECTS OF GAS CHROMATOGRAPHY

Journal of Chromatography, 126 (1976) 87–95
© Elsevier Scientific Publishing Company, Amsterdam — Printed in The Netherlands

CHROM. 9426

A STUDY OF COLUMN PERFORMANCES IN GAS CHROMATOGRAPHY

A C_{87} HYDROCARBON ON CHEMICALLY MODIFIED SUPPORTS

LÁSZLÓ BOKSÁNYI and E. sz. KOVÁTS

Laboratoire de Chimie Technique de l'École Polytechnique Fédérale de Lausanne, Lausanne (Switzerland)

SUMMARY

The surfaces of quartz plates and Chromosorb W were made to react with trimethylsilanol, docosyl-1-dimethylsilanol and 4,7-dioxaoctyl-1-dimethylsilanol. The density of the chemically bonded monomolecular layer is assumed to be maximal. One sample of Chromosorb W and one quartz plate were treated only by heating to 1250°. The modified support materials were used to prepare chromatographic columns with a C_{87} hydrocarbon stationary phase. Van Deemter plots of three substances were measured at each of the temperatures 60, 150 and 240°. The mass transfer terms of the calculated Van Deemter equations could be qualitatively related to wetting angles of the stationary phase, which were measured on the surface-modified vitreous quartz plates. The results indicate a method by which the column performances for the stationary phase used can be improved by suitable surface modification.

INTRODUCTION

The constant C in the Van Deemter equation

$$H = A + B/\bar{u} + C\bar{u} \tag{1}$$

where $\bar{u}$ is the linear gas velocity, accounting for the resistance to mass transfer of the solute across the gas–liquid interface and in the liquid phase is largely influenced by the effective or apparent film thickness. For a uniform film on the surface of the support put forward in the model of Van Deemter *et al.*[1], the value of this constant has been given as

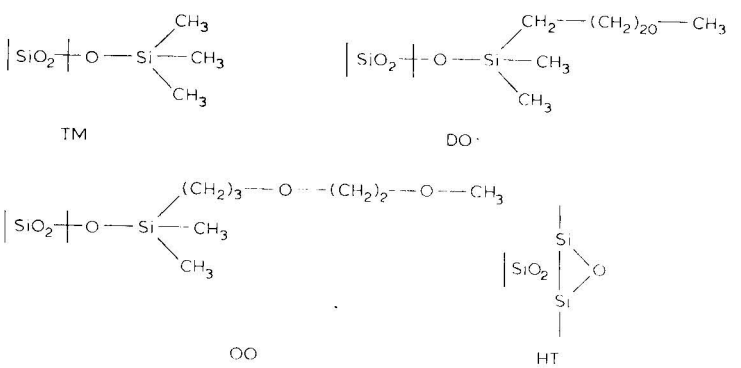
$$C = (2/\pi^2)\,[k'/(1 + k')^2]\,(d_f^2/D_f) \tag{2}$$

where k' is the net retention given in units of the dead volume of the column, d_f is the film thickness and D_f is the diffusion coefficient of the solute in the stationary phase. In packed columns, uniform films are rarely encountered in practice, especially on surface-modified supports.

Surface modifications of supports are carried out in order to transform the heterogeneous high-energy surface of silicon dioxide into a uniform low-energy surface. By anchoring organic reagents on the surface hydroxyl groups, "completely" covered surfaces should lose all activity as strong adsorbents. Therefore, in our laboratory, the question of the optimal coverage was put forward[2] and a method was developed for attaining the densest layers of alkyldimethylsiloxy groups by reaction of alkyldimethylsilanols with the surface hydroxyl groups of the hydrated fume silica Cab-O-Sil[3]. We have also obtained results which suggest that dense layers can be prepared by the same method on the surface of acid-leached glass and on silica gels[4,5]. Consequently, an acid-washed diatomaceous earth should behave in an analogous manner.

We also considered the wetting properties of such modified surfaces. Following from ideas put forward by Novotny and Zlatkis[6], a good support should have a low-energy surface to be inactive as an adsorbent but should be wettable by the stationary phase. The commonly used modification by dimethyldichlorosilane, trimethylchlorosilane and hexamethyldisilazane results in surfaces with a critical surface energy of about 20–24 erg·cm^{-2} (ref. 7). As the surface tension of most stationary phases exceeds this value, if complete wetting is achieved at all, it has to be attributed to surface roughness. Complete spreading would imply a thin uniform film with a low resistance to mass transfer, and the column packing would therefore be characterized by a small value of the constant C in the Van Deemter equation.

In this paper, we present preliminary results correlating the wettability of stationary phases and column performance, measured by the constant C in the Van Deemter equation. Three silanized supports were chosen as examples:



their surfaces being covered by trimethylsiloxy- (TM), docosyl-1-dimethylsiloxy (DO) and 4,7-dioxaoctyl-1-dimethylsiloxy (OO) groups; a fourth, thermally dehydrated, support (HT) was also included.

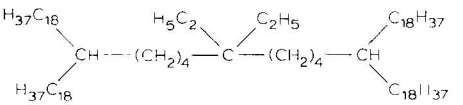
EXPERIMENTAL

An acid-washed diatomaceous support, Chromosorb WAW (Johns-Manville, Denver, Colo., U.S.A.; particle diameter 150–200 μm) was divided into four portions. One portion was heated at 1250° for 16 h: support HT (heat treated). Each of the other portions was made to react three times with an R-dimethylsilanol in an ampoule

at 100° in an ammonia atmosphere. The amount of silanol applied in the reaction was 10 μmol for every square metre of surface to be treated (specific surface area of Chromosorb WAW $\approx 2\ m^2 \cdot g^{-1}$). Between successive reactions, the support was extracted with diethyl ether and dried under argon. This series of reactions gave support TM with trimethylsilanol, support DO with docosyl-1-dimethylsilanol and support OO with 4,7-dioxaoctyl-1-dimethylsilanol. For the preparation of the silanols, see ref. 8.

Small quartz plates were immersed in concentrated hydrochloric acid for 2 days to ensure complete surface hydration. One plate was heated to 1250°, and in every ampoule one plate was silanized together with the support.

The stationary phase used was a hydrocarbon of structure I, prepared in our laboratory[9] (for the properties of hydrocarbon I, see ref. 10):



I

For the preparation of the column packing, the support was impregnated with a solution of hydrocarbon I in pentane (ratio of support to hydrocarbon I = 94:6, w/w), then the solvent was evaporated. The columns were Pyrex glass tubes of length 225 cm and I.D. 0.4 cm, all columns having about the same filling volume. The ready-to-use columns with the four supports had the following weights of packings: HT, 11.2; TM, 9.8; DO, 8.3; and OO, 8.5 g. The column filling HT had a higher packing density because of sintering on heat treatment.

The wetting angles were measured at 40, 50 and 60 °C. The quartz plates were placed in a thermostated aluminium block. By means of a syringe small, 1–2-μl droplets of hydrocarbon I were placed on each plate, then photographs taken after 30 min.

The chromatographic work was carried out on a Packard-Becker (Delft, The Netherlands) Model 419 instrument, equipped with flame-ionization detectors. Helium was used as the carrier gas. In order to determine the Van Deemter plots at 60, 150 and 240°, 0.1 μl of a mixture of two *n*-alkanes and a 1-chloroalkane was injected. The linear gas velocity was calculated from the retention time of methane.

The constants *A*, *B* and *C* in the Van Deemter equation were calculated by the program CARLIN from the library of the Centre de Calcul de l'École Polytechnique Fédérale de Lausanne. This program allows the use of the least-squares method for functions with linear parameters.

RESULTS AND DISCUSSION

It was shown in a detailed investigation[2] that by treating the surface of the fume silica Cab-O-Sil (Cabot Corp., Boston, Mass., U.S.A.) with alkyl- and oxa-alkyldimethylsilanols, a surface layer of maximum density can be attained in two or three consecutive treatments. The surface concentration of the chemically bonded layer was highest when the reaction was conducted at low temperature (100°) in the presence of ammonia as catalyst. This reaction gave, on the surface of Cab-O-Sil,

concentrations of 4.7 μmol·m^{-2} for trimethylsiloxy-, 4.1 μmol·m^{-2} for docosyl-1-dimethylsiloxy- and 3.5 μmol·m^{-2} for 4,7-dioxaoctyl-1-dimethylsiloxy groups. By applying the analogous treatment to acid-leached glass capillaries, a slight change of wettability was observed after the first and second consecutive treatment but further silanization did not have any effect[4]. We applied the same procedure to silanize the acid-washed Chromosorb W and the surface-hydrated vitreous quartz plates, assuming that the same surface concentrations were attained as on fume silica.

By heating fume silica to temperatures above 1100°, its surface is dehydrated completely with the formation of siloxane bridges[11,12]. After heat treatment, the surface is more or less deactivated as an adsorbent. We assume that the quartz plates and Chromosorb WAW were dehydrated in a similar manner by heating at 1250° for 16 h.

As described before, we assume that the surface concentration of organic substituents was the same on the quartz plates and on the silanized Chromosorb. Therefore, the wettability of the modified quartz plates is considered to be representative also for the surface-modified support. The results summarized in Table I show that the advancing wetting angle between the surface and hydrocarbon I is lowest on the plate treated with docosyl-1-dimethylsilanol. In the narrow experimental domain, the temperature had little or no effect on the wetting angle, variations being within the limit of experimental error (±2°). We therefore accepted the average to be characteristic of the wettability of the plates and the supports at lower temperatures.

TABLE I

WETTING ANGLES, θ, OF HYDROCARBON I ON SURFACE-MODIFIED VITREOUS QUARTZ

Averages of four measurements

Surface	θ (°)			$\bar{\theta}$ (°)
	40°	*50°*	*60°*	
Trimethylsiloxy (TM)	40	42	41	41
Docosyl-1-dimethylsiloxy (DO)	14	16	15	15
4,7-Dioxaoctyl-1-dimethylsiloxy (OO)	37	37	35	36
Siloxane bridges (heat treatment, HT)	29	30	28	29

In the Van Deemter equation, the constant A depends only on the geometry of the column and the column packing. The coefficient B shows a similar dependence, if the solute and temperature are kept constant. During column preparation, care was therefore taken to keep all geometrical factors and manipulations as similar as possible. The starting material used for preparation of the supports originated from the same batch, the temperature of the silanization was the same, all supports were prepared with the same relative amount of hydrocarbon I and on filling the columns care was taken to achieve about the same packing density. Of course, the heat-treated support showed slightly different packing properties.

Two *n*-alkanes and a chloroalkane were used to determine the Van Deemter plots at 60, 150 and 240°. The retention properties of the chosen substances are summarized in Table II.

For the evaluation of the results, we intended to use the least-squares method. Because of the strong heteroscedasticity in the experimental range, the value of A

TABLE II

RETENTION PROPERTIES OF THE SOLUTES USED FOR DETERMINATION OF VAN DEEMTER PLOTS

Retentions given as k values (= 1 + k', see eqn. 2). T_c, column temperature.

T_c (°C)	*Substance*	*Column*			
		TM	*DO*	*OO*	*HT*
60	*n*-Pentane	1.77	1.70	1.79	2.12
	1-Chlorobutane	3.70	3.40	3.65	4.35
	n-Heptane	6.16	5.65	6.18	7.30
150	*n*-Decane	4.14	3.82	4.12	5.05
	1-Chlorononane	8.50	7.68	8.30	10.30
	n-Dodecane	10.80	9.80	10.70	13.12
240	*n*-Hexadecane	5.83	5.20	5.76	7.16
	1-Chlorotetradecane	7.35	6.61	7.18	9.10
	n-Octadecane	11.07	9.75	10.70	13.60

showed wide variations. Therefore, different weighting functions were examined. Among them, the weighting of the experimental points by log $[\bar{u}/(\text{cm}\cdot\text{sec}^{-1})]$ values for A were obtained which agreed satisfactorily with values obtained by visual inspection of the plots. The average of all results was 0.018 cm, in good agreement with the

TABLE III

CONSTANTS OF THE VAN DEEMTER EQUATIONS WITH THE ASSUMPTIONS DESCRIBED IN THE TEXT

Constant	*Temperature (°C)*	*Column*	*Value of constant*			
A (cm)			0.018			
B (cm$^2\cdot$sec^{-1})	60		*Pentane*	*1-Chlorobutane*	*Heptane*	
			0.476	0.486	0.401	
	150		*Decane*	*1-Chlorononane*	*Dodecane*	
			0.478	0.443	0.382	
	240		*Hexadecane*	*1-Chlorotetradecane*	*Octadecane*	
			0.422	0.449	0.368	
$C\cdot10^4$ (sec)	60		*Pentane*	*1-Chlorobutane*	*Heptane*	*Average*
		TM	108.8	116.4	109.2	111.5
		DO	46.9	51.5	50.2	49.5
		OO	101.2	105.1	111.5	105.9
		HT	158.0	138.1	130.7	142.3
	150		*Decane*	*1-Chlorononane*	*Dodecane*	*Average*
		TM	38.8	38.2	44.3	40.4
		DO	8.1	9.2	9.1	8.8
		OO	54.7	49.4	50.3	51.5
		HT	63.2	61.8	68.5	64.5
	240		*Hexadecane*	*1-Chlorotetra-decane*	*Octadecane*	*Average*
		TM	30.7	25.9	33.6	30.1
		DO	8.0	4.0	7.5	6.5
		OO	51.3	45.3	49.0	48.5
		HT	63.7	57.2	70.1	63.7

value estimated from the particle diameter of the support with a form factor of 0.5 ($2\lambda d_p \approx 0.015$–$0.020$ cm). After the constant A had been fixed at 0.018 cm, the values of the constants B and C were calculated by assuming that B is the same for different columns if the same solute was used at the same temperature. The results are summarized in Table III.

As an example, Fig. 1 shows the experimental points and the regression function. Systematic deviations of the experimental points occurred in most instances, but they nevertheless represent the best function if the above-mentioned assumptions concerning the constants A and B are accepted.

The results show that the resistance to mass transfer is about the same for different substances at constant temperature. In Fig. 2, their average value is plotted as a function of temperature. The column packing DO, deactivated by docosyl-1-dimethylsiloxy groups, gives the best performance over the whole temperature range.

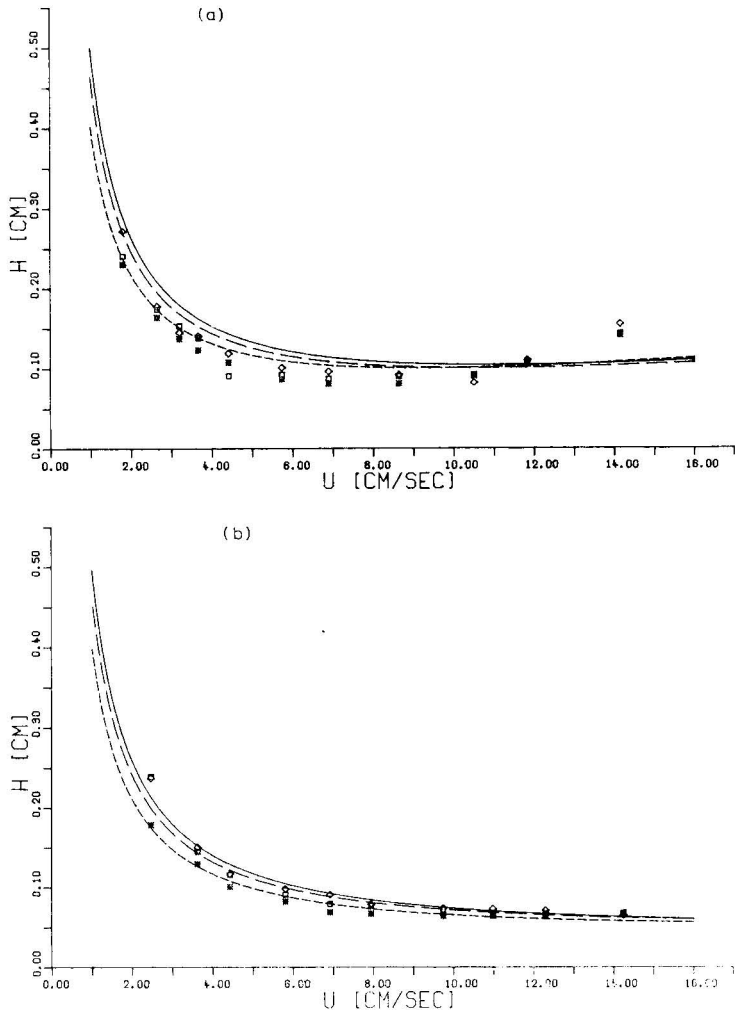


Fig. 1.

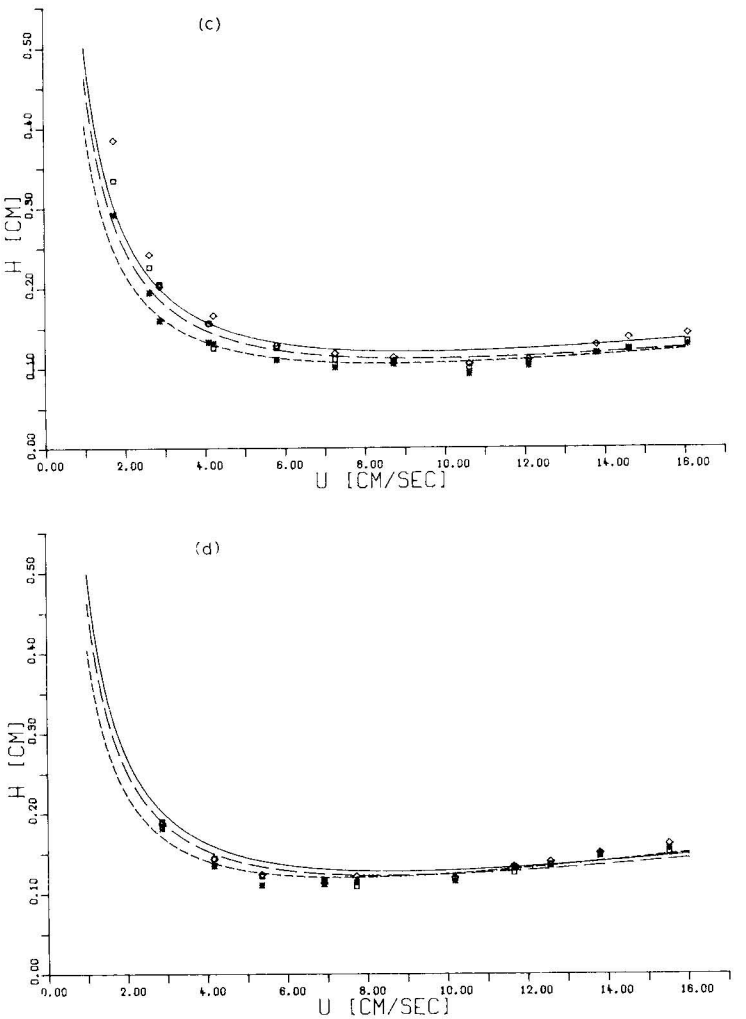


Fig. 1. Experimental values of theoretical plate height, H, on columns prepared with different surface-modified supports as a function of the linear gas velocity, u. Curves were calculated using the constants listed in Table III. Columns: (a) TM; (b) DO; (c) OO; (d) HT. Curves: ◇—◇, n-decane; □ - - □, 1-chlorononane; * - - - *, n-dodecane. All results at 150°.

It is interesting that the support covered with oxaalkyl chains shows a different temperature dependence compared with the other surfaces, having a relatively good performance at 60°, but resembles more the heat-treated surface at higher temperatures.

The wetting angles were measured at 40–60° and their average value is also shown in Fig. 2. For the results at 60° there is a linear relationship between the value of C and the wetting angle on the three silanized surfaces, but the support prepared by heat treatment is inferior, as would be expected from its wettability. In fact, we assumed that there is an analogy between the surface of quartz plates and that of the supports. However vitreous quartz is pure silicon dioxide and diatomaceous earth contains varying amounts of cations. Therefore, the thermally treated quartz and

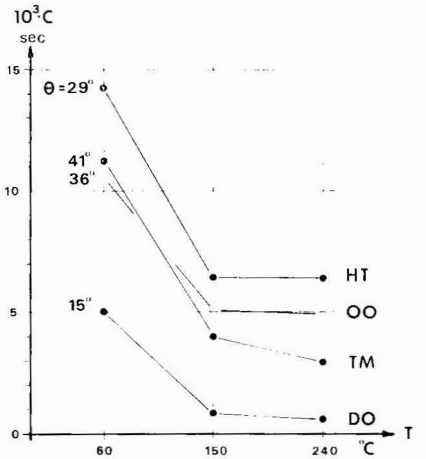


Fig. 2. Average values of the resistance to mass transfer expressed as the constant C as a function of the temperature on different columns.

Chromosorb must not have the same wettability. On the other hand, on surfaces covered by organic groups, the wettability is determined by the chemisorbed layer and so differences of the underlying surface will have little effect.

A small C value is not the only requirement of a support; it must also show a low activity on adsorption. Preliminary results[5] obtained on surface-modified silica gel have shown that for a maximally dense, chemically bonded monomolecular layer of R-dimethylsiloxy groups, the remaining surface activity depends upon the length and structure of the substituent. The activity decreases as a function of the substituent, R, as follows:

$$-CH_3 \gg -CH_2-(CH_2)_{20}-CH_3 > -CH_2(CH_2)_8-CH_3 \gg -CH_2-(CH_2)_3-O-CH_2-\\ -CH_2-O-CH_3$$

To show differences in adsorption, we injected primary alcohols onto the prepared columns capable of forming hydrogen bridges with surface hydroxyl groups. The chromatograms are shown in Fig. 3. Adsorption on the gas–liquid interface contributes to tailing, but differences must be the result of adsorbtion on the liquid–solid interface. The surface activity towards polar compounds is probably due to noncovered surface silanol groups. The alcohols are very strongly adsorbed on the chemically non-modified surface HT. Besides strong tailing, the appearance of ghost peaks on packing TM shows that the surface activity is higher than on packings DO and OO, where tailing is reduced on packing OO compared with packing DO. The ether groups of the deactivating agent 4,7-dioxaoctyl-1-dimethylsilyl groups on support OO can interact more strongly with the active sites of the surface than the longer alkyl chains bonded to the surface of support DO.

In conclusion, a better wettability of the support by the stationary phase will increase column efficiency. By extrapolation, the best results could be achieved if the contact angle of the pair stationary phase–support material is zero as a regular film thickness should result in the lowest minimal plate heights and the smallest increase

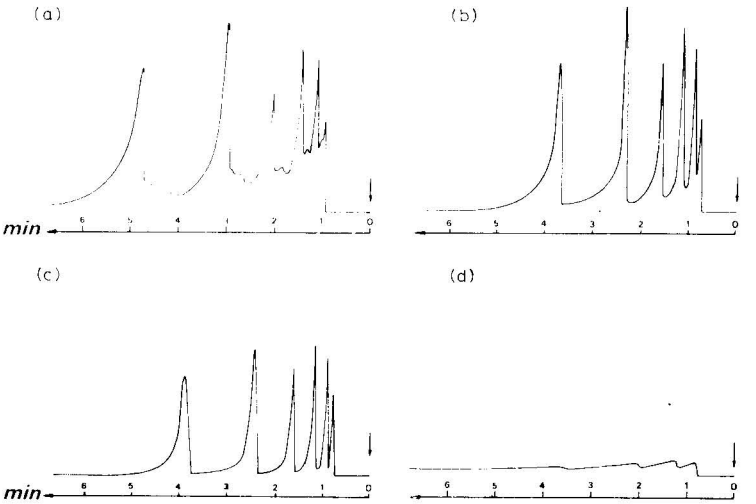


Fig. 3. Chromatograms showing separation of C_4–C_9 primary alcohols on different columns at 150°. Amount injected, 0.3 μl; different surface-treated supports with 6% of hydrocarbon I as stationary phase. Columns: (a) TM; (b) DO; (c) OO; (d) HT.

in the mass transfer term with gas velocity. The hydrocarbon stationary phase did not wet completely either of the supports, not even the surface modified by docosyl-1-dimethylsilanol. Further studies on wettability as well as adsorption characteristics are necessary in order to be able to choose the most appropriate treatment of the surface.

ACKNOWLEDGEMENTS

We thank F. Riedo for his advice and help in the execution of calculations. This work is part of a project supported by the Fonds National Suisse de la Recherche Scientifique.

REFERENCES

1 J. J. van Deemter, F. J. Zuiderweg and A. Klinkenberg, *Chem. Eng. Sci.*, 5 (1956) 271.
2 L. Boksányi, O. Liardon and E. sz. Kováts, *Advan. Colloid Interface Sci.*, 6 (1976) 95.
3 Booklet, Cabot Corp., Boston, Mass., U.S.A.
4 O. Liardon, *Doctoral Thesis*, École Polytechnique Fédérale de Lausanne, 1974.
5 L. Boksányi, *Doctoral Thesis*, École Polytechnique Fédérale de Lausanne, 1975.
6 M. Novotny and A. Zlatkis, *Chromatogr. Rev.*, 14 (1971) 1.
7 W. A. Zisman, *Ind. Eng. Chem.*, 55, No. 10 (1963) 19.
8 L. Boksányi, O. Liardon and E. sz. Kováts, *Helv. Chim. Acta*, 59 (1976) 717.
9 L. Boksányi, R. Peters, G. Tarján and E. sz. Kováts, to be published.
10 F. Riedo, D. Fritz, G. Tarján and E. sz. Kováts, *J. Chromatogr.*, 126 (1976) 63.
11 V. Ya. Davydov, A. V. Kiselev and L. T. Zhuravlev, *Trans. Faraday Soc.*, 60 (1964) 2254.
12 J. A. G. Taylor and J. A. Hockey, *J. Phys. Chem.*, 70 (1966) 2169.

Journal of Chromatography, 126 (1976) 97–111
© Elsevier Scientific Publishing Company, Amsterdam — Printed in The Netherlands

CHROM. 9449

N-ACYL DERIVATIVES OF CHIRAL AMINES AS NOVEL, READILY PREPARED PHASES FOR THE SEPARATION OF OPTICAL ISOMERS BY GAS CHROMATOGRAPHY

S. WEINSTEIN, B. FEIBUSH and E. GIL-AV

Department of Organic Chemistry, Weizmann Institute of Science, Rehovot (Israel)

SUMMARY

The results reported demonstrate that it suffices for a chiral stationary phase to contain an amide group and an asymmetric carbon atom, attached to the nitrogen atom [RCONHCH(CH_3)R'], in order to show selectivity in its interaction with the enantiomers of amides such as N-trifluoroacetylamines, N-trifluoroacetylamino acid esters and α-methyl- and α-phenylcarboxylic acid amides. The best efficiency is obtained when R' is aromatic, particularly α-naphthyl, as in N-lauroyl-*S*-α-(1-naphthyl)ethylamine.

The highest resolution factors were found for aromatic solutes, such as N-trifluoroacetyl-α-phenylethylamine and α-phenylbutyric acid amides, which could be resolved readily on packed columns.

The enantiomers of α-branched carboxylic acids were separated for the first time by gas chromatography.

Based on the packing arrangement in the crystalline form of the N-acetyl homologue of N-lauroyl-*S*-α-(1-naphthyl)ethylamine, a mechanism for the resolution is proposed. It is assumed that the mode of association found in the solid state is at least partially retained in the melt through a network of hydrogen bonds. The mechanism proposed is developed with particular reference to the aromatic solute–solvent systems. It is suggested that the solute is intercalated ("sandwiched") between two solvent molecules. Arguments, based on X-ray data, are given to explain the selectivity observed.

INTRODUCTION

The optically active phases used hitherto for the separation of enantiomers by gas chromatography were characterized by the following structural features: (1) one or two asymmetric carbon atoms each linked to the nitrogen atom of an amide group; and (2) one additional function, consisting of either an ester or an amide group. Examples are N-acyl-α-amino acid esters[1], N-acyldipeptide esters[2], diamides of the formula RCONHCH(*i*-Pr)CONHR'[3,4] and carbonylbis-(N-α-amino acid esters)[5,6].

It was the purpose of the present research to examine whether stationary phases still show selectivity when their structure is simplified to contain no more than one

amide group' (*i.e.*, compounds of type $RCONHCH(CH_3)R'$). We have already reported[5] that volatile amides of this type are resolved on carbonylbis-(N-L-valine isopropyl ester) (V). Furthermore, comparison[3,4] of diamide and dipeptide phases shows that selectivity is considerably increased when the polar part of the solvent molecule is reduced to the group –CONHCH(R)CONH–.

The substituents R and R' in the solvents studied were chosen as follows. In order to impart low volatility to the phases, the long lauroyl group ($RCO=C_{11}H_{23}CO$) was used throughout for acylation. The R' radicals were phenyl (I), cyclohexyl (II), α-naphthyl (III) and α-decahydronaphthyl (IV). The solutes examined included N-TFA* derivatives of aliphatic and cyclic amines, N-TFA esters of α-amino and α-methyl-α-amino acids, and amides of α-methyl- and α-phenylcarboxylic acids.

EXPERIMENTAL

Synthesis of amides

Equimolar ice-cold solutions of freshly distilled lauroyl chloride and the corresponding chiral amine in dry chloroform were slowly mixed. A 10% excess of triethylamine was added and the solution left overnight in the cold (5–10°). The solution was washed successively with water, saturated sodium hydrogen carbonate solution, 2% hydrochloric acid and water. After drying over magnesium sulphate and evaporation, the amides were crystallized several times from chloroform–*n*-hexane**.

Synthesis of hydroaromatic amides

These amides were prepared by catalytic hydrogenation of the corresponding aromatic amides with 5% rhodium–alumina in methanolic solution at a hydrogen pressure of 60 p.s.i. for 24 h. The catalyst was filtered off, the solution evaporated and the amides were purified by column chromatography with silica gel and light petroleum–dichloromethane as the eluent.

Synthesis of N-methylamides

N-Methylamides were prepared from the amides by treatment with methyl iodide in dimethylformamide in the presence of silver oxide for several days at room temperature[7].

Carbonylbis-(N-L-valine isopropyl ester) (V). This phase was purchased from Miles-Yeda, Rehovot, Israel.

The properties of the *S*-monoamide phases were as follows:

Phase	*M.p. (°C)*	$[\alpha]_D$	*(c in $CHCl_3$)*
I	62	−66.0	(1.5)
II	86	−10.0	(1.5)
III	96–97	−59.6	(1.5)
IV	76–80	+ 6.4	(2.0)

The structures of all of the phases were confirmed by NMR and IR spectroscopy and microanalysis.

* TFA = trifluoroacetyl.

** Phase III can be obtained from Yeda, Rehovot, Israel.

Synthesis of solutes

N-TFA amines[5] and N-TFA amino acid esters[8] were synthesized as described previously.

Aliphatic α-methylcarboxylic acids were prepared from α-methyl diethylmalonate[9] by the malonic ester synthesis[10] with the corresponding alkyl bromide.

α-Phenylbutyric acid and α-phenylpropionic acid were purchased from Norse Labs., Santa Barbara, Calif., U.S.A.

The acids were converted to the amides via the acyl chlorides by treatment with the corresponding amine in the presence of a 10% excess of triethylamine.

Application of Horeau's method[11] for the determination of the configuration to l-menthol

l-Menthol (1.6 mg; 10 μmole), 50 μl of a benzene solution of *d,l*-2-phenylbutyric anhydride (3.1 mg; 10 μmole) and 20 μl of dry pyridine were mixed in a small vial and left for 20 h at room temperature. Water (40 μl) was added and the mixture shaken occasionally for 2 h. After addition of diethyl ether, the heterogeneous mixture was washed twice with 2 ml of 1 *N* hydrochloric acid. The supernatant ether solution was dried over magnesium sulphate, evaporated to dryness and the residue dissolved in 40 μl of dry benezene and treated successively with 5 μl of *tert.*-butylamine and 5 μl of triethylamine. A few drops of ethyl acetate were added after 20 min, the solution was concentrated and a sample chromatographed on a packed column under the conditions given in Fig. 3. The first peak, corresponding to *S*-α-phenylbutyric acid, was markedly larger, as expected.

Gas chromatography

The experiments were carried out with a Varian Aerograph 1200 gas chromatograph equipped with a flame-ionization detector. The stainless-steel capillary columns (400 ft. × 0.02 in. or 150 ft. × 0.02 in.) were cleaned thoroughly[12] and then coated with a 5% solution of the stationary phase in chloroform at 10–15 p.s.i.

A description of the packed column used in some experiments is given in the legend of Fig. 2.

RESULTS AND DISCUSSION

The results are given in Tables I–III and Figs. 1–3.

N-TFA amines

As can be seen in Table I, the highest selectivity was found for phase III, which contains a naphthyl group in its molecule. This solvent is, in general, as efficient* as the carbonylbis-(N-L-valine isopropyl ester) (V)[5] and its homologues[13], which were previously the only phases known to resolve amine derivatives effectively. Solvent III is also much more convenient to prepare and has the further advantage of a lower melting point (96–97°) and higher upper operating temperature (at least 150°). An example of a chromatogram illustrating the excellent separation obtained for a N-TFA-2-amino-*n*-alkane is given in Fig. 1.

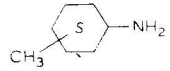
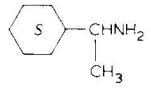
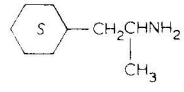
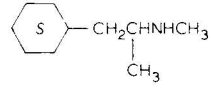
The influence of the aromatic system can clearly be seen when comparing

* Comparison with the behaviour on phase V and its homologues is made above the melting point of these solvents.

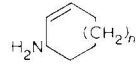
TABLE I

RESOLUTION OF CHIRAL N-TFA-AMINES

Compound	*Optically active stationary phase*											
	N-Lauroyl-S-α-phenylethylamine (I) **			*N-Lauroyl-S-α-(1-naphthyl)ethylamine (III)* *						*N-Lauroyl-S-α-(1-decahydronaphthyl)ethylamine (IV)* *		
	120°			*100°*			*130°*			*100°*		
	r(min) **	$r_{S/R}$ ***	R_s §	*r(min)* **	$r_{S/R}$ ***	R_s §	*r(min)* **	$r_{S/R}$ ****	R_s §	*r(min)* **	$r_{S/R}$ ***	R_s §
Aliphatic amines, $CH_3CH(NH_2)R$*:*												
$R =$												
C_2H_5				25.0 25.0	1.000	—				23.0 23.0	1.000	—
n-C_3H_7				60.0 60.0	1.000	—						
n-C_4H_9	*S* 31.6 *R* 31.0	1.020	0.5	*S* 115.0 *R* 108.8	1.057	0.95	*S* 29.8 *R* 28.8	1.036	0.8	*S* 83.0 *R* 81.6	1.016	0.5
n-C_5H_{11}	*S* 55.8 *R* 54.6	1.022	0.7	*S* 221.5 *R* 210.0	1.055	1.0	*S* 53.7 *R* 51.6	1.040	0.9	*S* 131.2 *R* 128.6	1.020	0.5
n-C_6H_{13}				*S* 432.0 *R* 408.0	1.059	1.0	*S* 96.3 *R* 92.4	1.042	1.0			
$CH_2C^*H(CH_3)CH_2CH_3$				160.3 150.7	1.064	1.0	26.6 25.5	1.041	0.8			
				166.0 160.3	1.035	0.85	27.5 26.6	1.034	0.6			
$CH_2CH_2CH(CH_3)_2$	176.8 173.2	1.020	0.5	172.5 161.6	1.068	1.5	45.3 43.2	1.048	0.8	95.1 92.7	1.025	0.5
$CH_2(CH_2)_2CH(CH_3)_2$	85.8 84.3	1.018	0.3	339.3 319.3	1.063	1.3	48.6 46.8	1.038	0.7			
$CH_2C(CH_3)_3$				115.5	1.050	0.95	20.7	1.030	0.2			

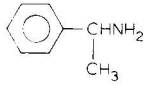
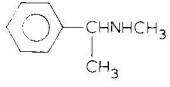
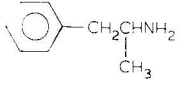
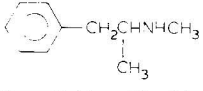
										
ortho *trans-*				167.8	1.021	0.3	37.0	sh[§§]		
ortho *cis-*				164.4			37.0			
trans-				423.0	1.028	0.8	77.8	1.019	0.6	
trans-				411.0			76.3			
meta *trans-*				209.0	1.022	0.5	49.3	1.012	0.2	
meta *cis-*				204.5			48.7			
cis-				400.0	1.029	0.9	81.7	1.019	0.6	
				388.0			80.0			
	*S* 52.3	1.020	0.7	*S* 649.0	1.067	2.5	*S* 89.2	1.047	0.9	
	R 51.3	(140°)		*R* 608.0			*R* 85.2			
							164.6	1.052	0.95	
							156.4			
							90.7	1.000	—	
							90.7			

Cyclic unsaturated amines

		$r_{II/I}$[§§§]				$r_{II/I}$[§§§]	
$n = 0$	27.0	1.011	0.3		42.3	1.024	0.5
	26.7				41.3		
$n = 1$	60.0	sh[§§]	—		96.0	1.022	0.8
	~ 60.0				94.0		
$n = 2$					(+) 228.7	1.037	1.0
					(−) 220.6		

(Continued on p. 102)

TABLE I *(continued)*

Compound	*Optically active stationary phase*											
	N-Lauroyl-S-α-phenylethylamine (I) *			*N-Lauroyl-S-α-(1-naphthyl)ethylamine (III)* *						*N-Lauroyl-S-α-(1-decahydronaphthyl)ethylamine (IV)* *		
	140°			*100°*			*130°*			*100°*		
	r(min) **	$r_{S/R}$ ***	R_s §	*r(min)* **	$r_{S/R}$ ***	R_s §	*r(min)* **	$r_{S/R}$ ***	R_s §	*r(min)* **	$r_{S/R}$ ***	R_s §
Aromatic amines												
	*S* 71.25 *R* 68.4	1.042	1.6	*S* 668.0 *R* 597.0	1.119	4.0	*S* 151.0 *R* 138.0	1.094	3.0			
				*S* 346.5 *R* 342.5	1.011							
							~ 150.0 150.0	sh §§	—			
							91.0 91.0	1.000	—			

* Chromatographed on stainless-steel columns of the following dimensions: (I) 400 ft. × 0.02 in. I.D.; (III) 400 ft. × 0.02 in. I.D.; (IV) 400 ft. × 0.02 in. I.D.

** r = corrected retention time.

*** Ratio of the corrected retention times of the *S*-enantiomer over that of the *R*-isomer. Assignment was made for a number of compounds by optically enriched mixtures (retention times marked *S* and *R*, respectively) and for the remainder by extrapolation.

§ Defined in the usual way by the expression $2d/(w_1 + w_2)$.

§§ sh = shoulder.

§§§ Ratio of the corrected retention time of the second peak over that of the first peak.

the data for III with those for its hydrogenated product IV. Thus, the $r_{S/R}$ values for the 2-amino-*n*-alkanes are, respectively, about 1.06 and 1.020. The selectivity is decreased to about the same extent for I, where R = phenyl. Finally, replacement of the benzene ring in I with a cyclohexyl group (II) results in complete loss of selectivity (*e.g.*, 2-amino-*n*-hexane, $r_{S/R} = 1.000$, not shown in Table I).

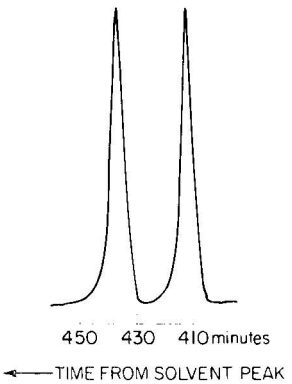


Fig. 1. Resolution of N-TFA-2-amino-*n*-octane. Phase: N-lauroyl-*S*-α-(1-naphthyl)ethylamine (III), coated on a capillary stainless-steel column, 400 ft. × 0.02 in. I.D.; temperature, 100°.

The order of emergence observed on all *S*-monoamide phases is *R*- before the *S*-solute, as on phase V. However, the effects of structural changes are very different for the two types of phases. For example, on V there is a gradual increase in the resolution coefficients ($r_{S/R}$) on lengthening the chain for the 2-amino-*n*-alkanes. In con-

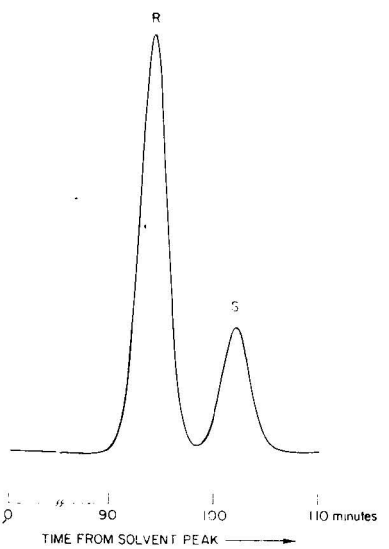


Fig. 2. Resolution of N-TFA-α-phenylethylamine. Phase: N-lauroyl-*S*-α-(1-naphthyl)ethylamine (III), 9% on Chromosorb W, HP. Column: 12 ft. × 1/8 in. I.D.; temperature, 140°.

tradistinction, on III the first two members of the series are not resolved, and for the higher homologues $r_{S/R}$ is about constant (*ca.* 1.06). The cycloolefinic amines are better separated on III than on V ($r_{S/R}$ values greater by about 0.01, although determined at a temperature higher by 10°). Perhaps the most interesting result is that N-TFA-α-phenylethylamine has a very high resolution factor ($r_{S/R}$ = 1.19 at 100°; resolved on packed columns, Fig. 2), and that insertion of a methylene group between the asymmetric carbon atom and the benzene ring (amphetamine) leads to almost complete loss of selectivity (shoulder, Table I). Similar observations were made for the carbonylbis-(N-L-α-amino acid esters)*.

As hydrogen bonding is an essential feature of the mechanism of resolution, it is not surprising that the introduction of a methyl group on the nitrogen atom leads to almost complete loss of resolution for N-methyl-N-TFA-α-phenylethylamine ($r_{S/R}$ = 1.011, 100°).

N-TFA-amino acid esters

The results obtained for N-TFA-amino acid esters on phase III are given in Table II. As for the amines, the solvent with the naphthyl group (III) shows a higher selectivity than the phenylic phase I (*e.g.*, $r_{L/D}$ for N-TFA-Ala-OMe = 1.025 (I), 1.053 (III); for N-TFA-Ala-O-*i*-Pr = 1.030 (I), 1.042 (III); for N-TFA-Val-OMe = 1.023 (I), 1.054 (III); all at 100°). No separation could be obtained on the hydrogenated phases II and IV for any N-TFA-amino acid ester.

The order of magnitude of the coefficients of resolution, and the fact that also α-methyl-α-amino acid esters are separated on III, illustrate the similarity to phase V[15]. However, as with the amines no systematic relationship between structure and resolution coefficient is apparent in homologous series. Also, branching of the chain of either the alcohol or the alkyl group attached to the asymmetric carbon atom shows irregular effects. Thus, isopropyl esters may have either higher or lower $r_{L/D}$ values compared with normal alcohol esters. The valine derivatives have virtually the same coefficients as those of alanine, whereas the esters of leucine are either badly resolved (O-*n*-Pr, 1.020) or not at all (OMe, OEt, O-*i*-Pr). The reversal of the order of emergence of the N-TFA-amino acid esters depending on the relative size of the alkyl group at the asymmetric carbon atom and the alcohol is a salient feature of the behaviour of phase V, but was not observed for III. Where resolution occurred, the order was always D-before the L-isomer on N-lauroyl-*S*-α-naphthylethylamine.

Proline is a difficult compound to resolve. As it contains a secondary amino function, no hydrogen is available for bonding after acylation, and hence its mechanism of resolution differs from that of amino acids with a primary amino group. On the dipeptide phases[8] and the diamides[3,4], proline is therefore one of the worst resolved amino acids. On phase III, however, the difference is much less pronounced, and the $r_{L/D}$ value of the methyl ester at 100° (1.039) is virtually the same as for the corresponding derivatives of *tert.*-leucine and α-aminobutyric acid.

On the whole, phase III is of little practical interest for the chromatography of α-amino acids, with perhaps the exception of proline. On the other hand, it could

* On a capillary column coated with V, only a shoulder was observed for amphetamine[14]; on packed columns, Lochmüller and Souter[13] did not notice any resolution with V or its homologues, either above or below the melting point of the phases.

be used with advantage for the separation of the enantiomers of α-methyl-α-amino acids, which cannot be resolved on the dipeptide and diamide phases.

α-Alkyl- and α-phenylcarboxylic acids

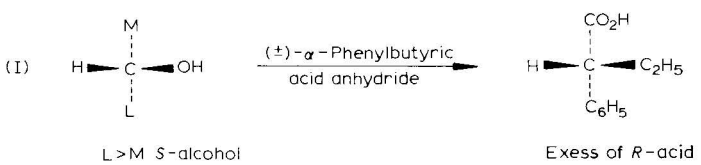
The α-alkyl- and α-phenylcarboxylic acid amides contain an asymmetric carbon atom linked to the carbonyl and not to the NH group as found in the two classes of solutes discussed above. It seemed likely that these compounds would also be separated on the monoamide phases, and we therefore examined derivatives of formula RCH(R')CONHR'', where R = methyl, ethyl or isopentyl, R' = methyl or phenyl and R'' = methyl, isopropyl or *tert.*-butyl.

The first experiments were carried out with phase V. As can be seen in Table III, resolution was obtained for α,δ-dimethylhexanoic acid, and the values for $r_{II/I}$ increased with the bulk of the alkyl group at the nitrogen atom. The *tert.*-butylamide is also the most volatile derivative.

Equally, phases I and III show the selectivity expected. The data available are as yet sparse, but it is noteworthy that α-methylbutyric acid amide is resolved on I but not on III, and that the derivatives of α,δ-dimethylhexanoic acid are best separated on III.

For the aromatic acids, III shows a relatively large selectivity, particularly for α-phenylbutyric acid *tert.*-butylamide ($r_{S/R}$ = 1.090, 130°), which can be separated on packed columns (Fig. 3). The order of emergence is the reverse of that found for the amines, namely *S*- before the *R*-isomer; this finding will be discussed in the following section*.

The ready resolution of the latter acid is of particular interest in connection with the analytical aspects of Horeau's method[11] for the determination of the configuration of secondary, optically active alcohols of structure I:



It has been found that esterification of these alcohols with an excess of racemic α-phenylbutyric acid anhydride leads to a relatively large optical enrichment of the unreacted reagent, with formation of an excess of the *R*-acid for the *S*-alcohol and *vice versa*.

The gas chromatographic determination of the enantiomeric composition of the excess of reagent will permit the Horeau method to be carried out on a microscale. A similar procedure was described by Gilbert and Brooks[16], who converted the excess of acid into a diastereomeric mixture by reaction with α-phenylethylamine. The direct resolution of enantiomers has, however, the advantage that chiral reagents (often of variable optical purity) are not required for derivatization. An example of the procedure as applied to *l*-menthol is given under Experimental.

* It is to be noted that the compounds discussed in this sub-section are the first enantiomers separated by gas chromatography that do not possess an NH group directly linked to the asymmetric carbon atom.

TABLE II

RESOLUTION OF N-TFA-AMINO ACID ESTERS ON N-LAUROYL-*S*-α-(1-NAPHTHYL)ETHY AMINE (III)*

α-Amino acid	t (°C)	Alcohol residue							
		Me			Et			n-Pr	
		r(min)**	$r_{L/D}$***	R_s§	r(min)**	$r_{L/D}$***	R_s§	r(min)**	$r_{L/D}$*
Ala	100	59.7 56.7	1.053	0.95	82.3 78.3	1.052	0.95	157.0 149.0	1.05
	120	28.8 27.6	1.043	0.9	37.5 36.0	1.042	0.9	78.4 75.0	1.04
Val	100	71.1 67.4	1.054	1.0					
	120	33.8 32.5	1.040	0.9					
Leu	100	200.0 ~ 200.0	sh§§	—	270.0 270.0	sh§§	—	549.0 538.0	1.02
	120	75.0 75.0	1.000	—	120.0 120.0	1.000	—		
tert.-Leu	100	59.1 56.5	1.044	0.9					
	130								
Pro	100	203.1 195.5	1.039	0.9					
	130	61.0 59.2	1.028	0.3					
Phenyl–Gly	130								
Phe	130	270.0 270.0	1.000	—					
α-Methyl α-amino acid									
α-Me-*tert.*-Leu	100	82.2 80.7	1.018	0.3					
α-Me-Val	100	72.9 72.3	1.008	—					
α-Me-Leu	100	60.0 60.0	1.000	—					
α-Me-Norleu	100	105.5 102.5	1.029	0.5					
α-Me-Norval	100	62.8 61.7	1.018	0.3					

* See Table I.

** See Table I.

*** Ratio of the corrected retention times of the L-enantiomer over that of the D-isomer. Assignment made with optically enriched mixtures, except for *tert.*-leucine for which the order of emergence was deduced extrapolation.

§ See Table I.

§§ sh = shoulder.

i-Pr			*n-Butyl*			*3-n-Pentyl*		
*r(min)***	$r_{L/D}$****	R_s§	*r(min)***	$r_{L/D}$****	R_s§	*r(min)***	$r_{L/D}$****	R_s§
85.6 82.2	1.042	0.9	303.5 288.5	1.052	1.5	86.8 83.0	1.046	1.0
39.2 37.8	1.037	0.9	126.4 120.9	1.045	1.5	37.5 36.0	1.042	1.0
104.3 98.8	1.055	0.9						
36.0 34.5	1.042	0.9						
320.0 320.0	1.000	—	1015.0 990.0	1.025	1.0			
95.0 95.0	1.000	—				80.0 80.0	1.000	—
58.2 56.1	1.034	0.3						
20.3 19.7	1.030	0.6						
170.0 166.0	1.024	0.5						
62.7 61.0	1.027	—						

TABLE III

RESOLUTION OF α-METHYL- AND α-PHENYLCARBOXYLIC ACID AMIDES

Compound	*Optically active stationary phase*							
	N-Lauroyl-S-α-phenylethylamine (I) *			*N-Lauroyl-S-α-(1-naphthyl)ethylamine (III)* *			*Carbonylbis-(N-L-valine isopropyl ester) (V)* *	
	r (min) **	$r_{III/I}$ ***	R_s §	*r (min)* **	$r_{III/I}$ ***	R_s §	*r (min)* **	$r_{III/I}$ ***
Aliphatic acids, $RCHCONHR'$ $\lvert$ CH_3								
$R=CH_3CH_2$ $R'=(CH_3)_3C$	45.0 45.0	1.000 (120°)	—	175.0 175.0	1.000 (100°)	—		
$R=(CH_3)_2CHCH_2CH_2$ $R'=(CH_3)_3C$	76.0 74.1	1.026 (140°)	0.7	119.6 115.3	1.037 (130°)	0.6	47.1 45.1	1.043 (120°)
				756.3 714.0	1.059 (100°)	2.0		
$R'=(CH_3)_2CH$ $R'=CH_3$	149.3 146.2	1.021 (140°)	0.4	230.5 222.7	1.035 (130°)	0.8	98.6 96.3	1.024 (120°)
							147.0 142.9	1.028 (120°)
Aromatic acids $RCHCONHC(CH_3)_3$ $\lvert$ C_6H_5								
$R=CH_3$	*R* 212.5 *S* 205.0	1.036 (130°)	1.5	*R* 352.5 *S* 335.5	1.051 (130°)	1.0		
$R=CH_3CH_2$				*R* 482.0 *S* 441.0	1.093 (130°)	3.0		

* Chromatographed on stainless-steel columns of the following dimensions: (I) 400 ft. × 0.02 in. I.D.; (III) 400 ft. × 0.02 in. I.D.; (V) 150 ft. × 0.02 in. I.D.

** See Table I.

*** Ratio of the corrected retention time of the second peak over that of the first peak.

§ See Table I.

Mechanism of resolution

In order to explain the selective association of enantiomers, such as the N-TFA-α- and -γ-amino acid esters with diamides, we have recently[3,4,17,18] proposed models based on the preferred conformations of the solvents (selectors*) and their

* In this section, "solvent" and "solute" will often be referred to by the equivalent terms "selector" and "selectand"; these are operational definitions first introduced by Mikeš *et al.* (see ref. 19 for a brief comment).

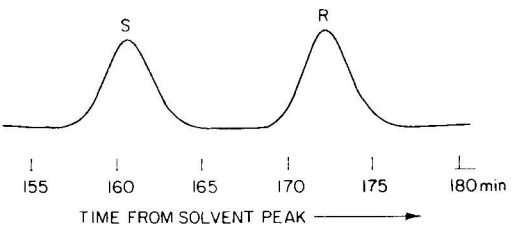


Fig. 3. Resolution of α-phenylbutyric acid *tert.*-butylamide. Chromatographic conditions as in Fig. 2; temperature, 150°.

modes of intermolecular hydrogen bonding. As a result of these considerations, the association between the solute and the solvent has been assumed to resemble the β-pleated sheet structure of peptides. An important aspect of the mechanism proposed is that the crystal structure is retained to a certain extent in the melt through intermolecular hydrogen bonding.

We have tried a similar approach to the interpretation of the present results, limiting ourselves to the strong selective effects observed for aromatic solutes and solvents.

For this purpose, the crystal structure of N-acetyl-α-(1-naphthyl)ethylamine

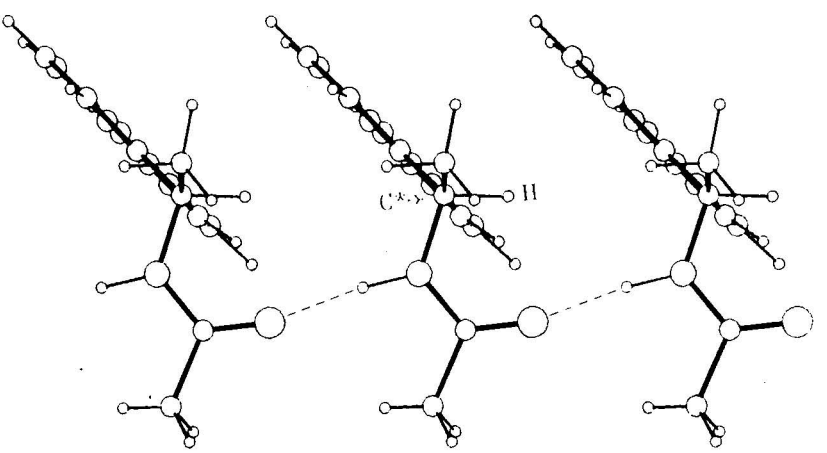
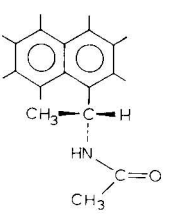


Fig. 4. Projection of hydrogen-bonded molecules of N-acetyl-*R*-α-(1-naphthyl)ethylamine, as arranged



in the crystal. The asymmetric carbon atom (C*) and the hydrogen (H) attached to it are labelled for the middle molecule of the stack.

(VI)* has been determined by X-ray crystallography[20]. Fig. 4 displays the experimentally determined packing arrangement of the molecules of (*R*)-VI along a short 4.9 Å translation axis with the hydrogen-bonded amide groups in the plane of the paper. A particularly relevant feature of the structure is that the hydrogen atom linked to the asymmetric carbon atom fits snugly between two naphthalene rings of the stack. The distance between this hydrogen atom and the nearest ring carbon atom is, in fact, only 2.6 Å, which is less than the sum of the corresponding Van der Waals radii.

A solute such as N-TFA-α-phenylethylamine, when introduced into an excess of solvent molecules, *i.e.*, under the conditions of the gas chromatographic column, will be able to implement fully its potential for hydrogen bond formation and associate with two selector molecules in a fashion similar to that shown in Fig. 4. The selectand could than readily assume a conformation analogous to that of VI in Fig. 4. If its configuration is the same as that of the selector, the chiral carbon atom with its attached hydrogen atom and methyl group, as well as the benzene ring, will replace the corresponding atoms and groups of the middle solvent molecule in the stack. This will lead to a good fit and close association.

The corresponding antipodic solute can also form hydrogen bonds with two selector molecules, but insertion into the stack of solvent molecules, in the same manner as above, will bring about inversion of the positions of the hydrogen atom and the methyl group attached to the asymmetric carbon atom. The placing of the methyl group between the aromatic rings makes stack formation impossible without considerable distortion. In fact, X-ray studies[20] of racemic crystals of VI showed that hydrogen bonding between *S*- and *R*- isomers leads to a looser structure around the hydrogen bond, which means less intermolecular contacts and a lower stability. It is thus understandable that the solute with the configuration opposite to that of the phase is less well retained.

The model of association through intercalation between two selector molecules also explains the reversal of order of emergence for the α-phenylaliphatic acid amides. In these molecules, the chiral atom –CH(R)Ph is attached to the carbonyl and not to the NH group. In order to form hydrogen bonds and, simultaneously, to maximize contacts by intercalation of the benzene between the naphthalene rings of the solvent, the amide groups of selectand and selector cannot be related by translation ("in parallel"), but have to be antiparallel. This arrangement will tend, by necessity, to place the methyl group linked to the chiral carbon between the aromatic rings in the stack, when the selectand and selector have the same configuration. On the other hand, for opposite configurations of solute and solvent, the smaller hydrogen atom will occupy this position. Thus the stability relationships discussed above for the α-phenylethylamine are reversed and, correspondingly, also the order of emergence.

The influence of the nature of the cyclic substitutent of both the selector and selectand molecules can be readily accounted for. The relatively large naphthalene ring system can form a more rigid (close fitting) stack than benzene (I), leading to higher selectivity for an intercalated solute molecule of the correct configuration. On the other hand, hydrogenation of the ring(s), as in II and IV, destroys the flat aromatic structure and makes close contacts more difficult; accordingly, these phases show little or no selectivity. Decrease in the resolution factor of α-cyclohexylethylamine,

* For III, crystals suitable for X-ray studies could not be obtained.

compared with that of α-phenylethylamine, on phase III can be interpreted in a similar manner by a reduction in the strength of the intercalation complex.

Amphetamine cannot form good contacts when inserted into the stack, and should be less well resolved than α-phenylethylamine according to the mechanism proposed. The complete loss of selectivity observed for this aromatic amine may be due to alternative non-selective associations involving the benzene ring of the solute.

The aliphatic amines $CH_3CH(NH_2)R$ show about the same $r_{S/R}$ values as α-cyclohexylethylamine. Here, too, "sandwich" associates of lesser selectivity could account for the resolution mechanism.

The importance of the intercalation-type of association is supported by the data for N-methyl-α-phenylethylamine. This compound can form only one hydrogen bond, and hence the resolution factor is very low. However, the $r_{S/R}$ value is not unity, and this result indicates that also a 1:1 complex with this type of solvent may show selectivity, which could possibly be increased by appropriate structural modifications.

For the amino acid derivatives, it must be remembered that they contain an ester group in addition to the amide function, and association with the selector could, therefore, proceed in a different fashion than for the other solutes studied.

The mechanism proposed should be considered as a working hypothesis only at this stage. The suggestive X-ray evidence must be corroborated by physical studies on association in the liquid state. However, it is gratifying to note that many of the experimental facts observed can be satisfactorily explained by the model used.

ACKNOWLEDGEMENT

The authors thank Mr. Lahmi for his invaluable assistance in carrying out the experimental work.

REFERENCES

1 E. Gil-Av, B. Feibush and R. Charles-Sigler, in A. B. Littlewood (Editor), *Gas Chromatography 1966*, Institute of Petroleum, London, 1967, p. 227.
2 B. Feibush and E. Gil-Av, *Tetrahedron*, 26 (1970) 1361.
3 R. Charles, U. Beitler, B. Feibush and E. Gil-Av, *J. Chromatogr.*, 112 (1975) 121.
4 U. Beitler and B. Feibush, *J. Chromatogr.*, 123 (1976) 149.
5 B. Feibush and E. Gil-Av, *J. Gas Chromatogr.*, 5 (1967) 257.
6 J. A. Corbin and L. B. Rogers, *Anal. Chem.*, 42 (1970) 974.
7 B. C. Das, S. D. Gero and E. Lederer, *Biochem. Biophys. Res. Commun.*, 29 (1967) 211.
8 S. Nakaparksin, P. Birrell, E. Gil-Av and J. Oró, *J. Chromatogr. Sci.*, 8 (1970) 177.
9 *Org. Syn.*, Collect Vol. II (1943) 272 and 279.
10 A. I. Vogel, *Practical Organic Chemistry*, Longmans, London, 3rd ed., 1955, p. 483.
11 A. Horeau, *Tetrahedron Lett.*, (1961) 506.
12 W. Parr, C. Yang, E. Bayer and E. Gil-Av, *J. Chromatogr. Sci.*, 8 (1970) 591.
13 C. Lochmüller and R. W. Souter, *J. Chromatogr.*, 88 (1974) 41.
14 T. Tamari, B. Feibush and E. Gil-Av, unpublished data.
15 N. Frydman, T. Tamari, B. Feibush and E. Gil-Av, *Proc. 42nd Meeting Israel Chem. Soc.*, Dec. 1972, p. 11.
16 J. D. Gilbert and C. J. W. Brooks, *Anal. Lett.*, 6 (1973) 639.
17 E. Gil-Av, *J. Mol. Evol.*, 6 (1975) 131.
18 E. Gil-Av and B. Feibush, in Y. Wolman (Editor), *Peptides 1974, 13th European Peptide Symp.*, Israel Universities Press, Jerusalem, 1975, p. 279.
19 F. Mikeš, G. Boshart and E. Gil-Av, *J. Chromatogr.*, 122 (1976) 205.
20 S. Weinstein and L. Leiserowitz, unpublished data.

Journal of Chromatography, 126 (1976) 113–116
© Elsevier Scientific Publishing Company, Amsterdam — Printed in The Netherlands

CHROM. 9409

"SELECTIVITY" OF HIGH-TEMPERATURE LIQUID PHASES FOR GAS CHROMATOGRAPHY

R. D. SCHWARTZ and R. G. MATHEWS
Pennzoil Company, Shreveport, La. (U.S.A.)

SUMMARY

Most of the high-temperature gas chromatographic columns, under their normal operating conditions, will not separate the test compounds usually employed to measure "selectivity". Therefore, we are proposing a new set of higher boiling test compounds to be utilized for measurement and comparison of the "selectivity" of high-temperature liquid phases.

INTRODUCTION

The liquid phase is an essential and very important part of every gas–liquid chromatography (GLC) column. Column efficiency, the elution order of sample components, peak shapes and background "noise" level depend upon the physical and chemical properties of the liquid phase.

Over the years, in order to improve chromatographic column performance, the number of liquid phases has increased from the few early compounds and polymers to several hundred which have been utilized and reported in the literature. As more difficult separations were attempted, and as operating temperatures were raised, chromatographers tried many new liquids, and, indeed, synthesized new polymers to achieve satisfactory results. This vast increase in the number of phases has created difficulty for suppliers, who have been requested to stock these many materials, and for theoreticians who have attempted to correlate and report the "selectivity" parameters of all these phases. There have been suggestions that the number of liquid phases be restricted, or limited, to a few materials which are widely used, and whose "selectivity" parameters are well known. The pros and cons, and the practical results of adopting this suggestion will be debated for some time. Although the authors have definite opinions on this topic, this suggestion will not be discussed here. Instead, we shall examine and discuss the systems of measuring liquid phase "selectivity." In particular, we shall propose a new set of test compounds to be employed in measuring the "selectivity" of liquid phases that are utilized at temperatures above 200°. We feel that this is a necessary extension of the systems of Kováts[1], Rohrschneider[2], and McReynolds[3].

Kováts index

Wehrli and Kováts[1] proposed a retention index system where the number for a normal paraffin is $n00$. (n = Number of carbon atoms in the compound.) Then, the retention time, or index, of other compounds is expressed relative to that of normal paraffins. If the relative retention of derivatives of saturated hydrocarbons containing unsaturation, halogen atoms, or oxygen atoms is measured, the retention index values may be used to characterize a given liquid phase.

Rohrschneider constants

Rohrschneider[2] developed a system for the measurement of "selectivity" and classification of liquid phases based upon the measurement of retention times for benzene, ethanol, methyl ethyl ketone, nitromethane, and pyridine.

McReynolds constants

In 1970, McReynolds[3] extended the work of Kováts and Rohrschneider by adding five additional compounds for "selectivity" measurement to those utilized by Rohrschneider. Further, he presented complete data for retention indices of about 200 liquid phases. These data were obtained at 120°.

High-temperature gas–liquid chromatography

During the past few years, a number of new liquid phases have been proposed for use at high-temperature (250–400°). Most of these are polymers prepared specially for these applications.

GLC separations at 250–400° are now used for separation, identification, and measurement of many organics including hydrocarbons, chlorinated compounds, lipid derivatives, pesticides, drugs, pollutants, etc.

In some cases, in order to achieve maximum thermal and chemical stability, it became necessary to employ polymers with relatively high melting points. For example, the polyphenyl ether sulfones melt at about 100° but do not yield efficient columns at 100°. Thus, their proper use is in the temperature range of about 175–400°. Obviously, in order to measure the "selectivity" of such phases, it is necessary to use a set of compounds which can be separated at these elevated temperatures.

If we were to extend the work of Rohrschneider or McReynolds by using higher-molecular-weight mono-substituted derivatives, we would be able to perform the separations at 175–400°. However, the "polarity" or "selectivity" of higher-molecular-weight mono-substituted compounds would be considerably less than that of the compounds proposed originally. Therefore, we decided to select compounds where the ratio of "polar" groups to hydrocarbon groups is similar to that of the compounds utilized by Rohrschneider and McReynolds.

In order to conform more closely to modern column technology, and to the newer high-temperature procedures, a few changes in column construction and operation were adopted for our measurements of "selectivity." First, a change was made to 1/8-in. columns packed with 100–120 mesh support. Then, the liquid phase loading was set at 10% rather than the 20% formerly employed. Many high-temperature preparations are performed with 2–5% loadings, and, it was felt that 10% would be adequate to overcome the adsorption effects of the support at these elevated temperatures. Further, it is often difficult to load 20% packings into 1/8-in. columns.

EXPERIMENTAL

Equipment

A Barber-Coleman Series 5000 gas chromatograph equipped with a hydrogen flame ionization detector was used in this study.

Reagents

The support material, 100–120 mesh Gas-Chrom Q, as well as the liquid phases (OV-275, Poly-S 179, and SE-30) were obtained from Applied Science Labs. (State College, Pa., U.S.A.).

Solvents used in preparing the column packings, *i.e.*, acetone and chloroform, were procured from Matheson, Coleman and Bell (East Rutherford, N.J., U.S.A.). Carbon disulfide used for dissolving the sample compounds was obtained from the same source.

Column preparation

The metal columns used in this study were prepared from Type 304 stainless steel, 0.125 in. O.D. × 0.062 in. I.D., from Handy and Harmon (Norristown, Pa., U.S.A.). All columns were 2 m in length.

SE-30 and Poly-S 179 were coated onto the support from chloroform solution. Acetone was used for the OV-275. All packings were prepared with a 10% loading of liquid phase. The columns were conditioned by programming from ambient temperature to 250° at 0.5°/min. The final temperature was held until the baselines had stabilized.

RESULTS

Retention times in mm, chart speed 12.7 mm/min, at 250°, corrected for the retention time of methane, were determined on SE-30, Poly-S 179, and OV-275 columns for the compounds we propose for high-temperature "selectivity" measurements. These results are presented in Table I.

As a further comparison, retention times for the first five compounds proposed by McReynolds were determined at 120° for the SE-30 and OV-275 columns. These results are presented in Table II. All columns were operated with helium at 20 p.s.i.

TABLE I

CORRECTED RETENTION TIMES (mm) AT 250°

Liquid phase	*n-Decane*	*Naphthalene*	*Dipyridyl*	*Benzil*
SE-30	3.5	9.0	15.5	37.5
Poly-S 179	1.5	16.5	44.5	139.0
OV-275	0	5.0	22.5	57.0

TABLE II

CORRECTED RETENTION TIMES (mm) AT 120°

Liquid phase	*n-Hexane*	*Benzene*	*Pyridine*	*2-Pentanone*	*n-Butanol*	*1-Nitropropane*
SE-30	2.0	4.0	7.0	4.5	4.0	7.0
Poly-S 179	Phase is not usable at 120°					
OV-275	1.0	4.5	17.5	6.5	9.5	25.0

At 250°, the retention times for dipyridyl and for benzil are appreciably greater on Poly-S and on OV-275. The hydrocarbons are eluted more rapidly on OV-275 than on SE-30, but naphthalene is retarded, most on Poly-S 179.

DISCUSSION

The systems of Kováts, Rohrschneider, and McReynolds are based upon measurement of retention times for the volatile organic compounds listed earlier. In order to extend these systems, so that they would be useful for liquid phases that are used at 200–400°, we looked for, and selected, certain compounds of higher molecular weight. In addition to those listed, namely, naphthalene, dipyridyl, and benzil, we attempted to utilize a dihydroxynaphthalene and a dinitronaphthalene. With our metal system, these compounds were not eluted in reasonable time. Further, we expect to use a diol compound (C_{10}), but this material was not available at the time this report had to be submitted.

REFERENCES

1 A. Wehrli and E. Kováts, *Helv. Chim. Acta*, 42 (1959) 2709.
2 L. Rohrschneider, *J. Chromatogr.*, 22 (1966) 6.
3 W. O. McReynolds, *J. Chromatogr. Sci.*, 8 (1970) 685.

Journal of Chromatography, 126 (1976) 117–132
© Elsevier Scientific Publishing Company, Amsterdam — Printed in The Netherlands

CHROM. 9445

PREPARATION OF GLASS CAPILLARY COLUMNS COATED WITH POLAR PHASE FOR HIGH-TEMPERATURE GAS CHROMATOGRAPHY

I. STUDY OF ROUGHENING OF THE GLASS SURFACE

J. J. FRANKEN, G. A. F. M. RUTTEN and J. A. RIJKS
Department of Instrumental Analysis, Eindhoven University of Technology, Eindhoven (The Netherlands)

SUMMARY

Some methods of surface roughening of glass capillary columns have been studied (*viz.*, HCl etching, controlled devitrification and deposition of fine particles).

The reaction of HCl with soda-lime glass proceeds easily, but is a self-limiting process. The resultant NaCl initially forms globules, which become cubic after prolonged heating. The presence of excess of HCl (as in flowing methods) or water reduces the crystallization rate markedly.

A method of surface crystallization based on controlled devitrification has been developed. Spiked surfaces are obtained, which can easily be deactivated by current methods.

The deposition of fine particles on the column wall offers another approach. A method is described for the preparation and application of (sub)micron NaCl particles, which results in a surface comparable with an HCl-etched surface.

Preliminary results are given for surface-roughened capillary columns at high temperatures coated with polar phases.

INTRODUCTION

At present, glass capillary columns offer the best prospects in the analysis of complex biochemical and environmental mixtures. High thermal stability and inertness of the column wall, in addition to a high separation efficiency, are essential for these columns.

During the last 10 years much progress has been made in the development of glass capillary columns[1,2].

It should be acknowledged, however, that current methods of column preparation are inadequate for high-temperature analysis (200–300°), notably for polar phases and trace analyses at the picogram level. The main problems with glass capillary columns in these fields are the catalytic and adsorptive properties (despite its relative inertness), and poor wettability of the glass wall.

The best means of overcoming these problems depend on the polarity of the

stationary phase, the sensitivity to be obtained, the column temperature, and the nature of the compounds to be analysed[3–5].

For polar stationary phases, the main problem is caused by poor wetting properties, which are a consequence of their high surface tensions. To promote spreading of these phases, the glass surface must be modified either by an interjacent layer or by roughening. Surface roughening is based on the deposition of a microlayer of fine particles or etching of the glass surface. It provides a convenient and universal approach to wetting promotion, which does not suffer from the limited stability of interjacent layers.

Roughening methods for glass capillary columns

Glass surfaces have been etched with ammonia solution[6,7], sodium hydroxide solution[8,9], hydrofluoric acid[10], and by successive treatments with these solutions[11]. Aqueous methods, however, deeply attack the glass surface[12], and produce strongly adsorbing columns that are useful only in gas–solid chromatography.

Gaseous etching methods are milder. Tesařík and Novotný[13,14] introduced hydrogen chloride and methyl trifluorochloroethyl ether, which splits off HF on heating. Ohline and Jojola[15] had earlier used HF to etch glass beads. The procedure followed by Zhdanov *et al.*[10] may be regarded as the forerunner of gas-phase etching.

Alexander and Rutten[16] prepared polar phase-coated columns for steroid analysis from HCl-etched soda-lime glass capillaries, and in a subsequent paper[17] they described studies on the wetting characteristics of etched glasses. It has been shown that HCl-etched columns can be coated with many statioqary phases[18–20] and can be applied in many different fields[21–23]. Etched columns are also useful in the preparation of thick-film capillaries[24] coated with non-polar phases. If coated with a polar phase, these columns show remarkable inertness, but for non-polar phases additional deactivation is necessary[18,20].

An interesting spiked glass surface was reported by Schieke *et al.*[25], who grew silica whiskers on the walls of Pyrex columns. The effect resulted from treatment with methyl trifluorochloroethyl ether at particular concentrations and temperature. The applicability of this type of column, however, is still in the development stage.

Etching not only roughens the glass surface, but also changes the composition of the upper glass layer. A change in surface composition of the glass affects its adsorptive and catalytic properties and may lead to improved inertness of the column wall. Desty[26] proposed the exchange of Na^+ with Li^+ ions, which results in a matt finish and excellent wettability of the glass. The suitability of these surfaces was not indicated.

Fine particles may also be applied directly to the glass wall. Blumer[27] used Silanox 101, a silanized fumed silica, which has been applied successfully in high-temperature analysis of biological samples[28–31]. The properties of Cab-O-Sil (a non-silanized silica) and some diatomaceous supports have been studied by Cramers *et al.*[32] and by Deelder and co-workers[33,34].

Scope of the present work

It has been our intention to prepare glass capillary columns with a high degree of separation, long durability and reproducible retention characteristics by relatively simple and standardized procedures.

Some years ago, our laboratory reported[16,17] the preparation of high-efficiency HCl-etched polar columns with excellent thermal stability (OV-225, SP 2401, FFAP, Dexsil). As we could not reproduce these results, they were considered to be fortuitous rather than the result from a knowledge of the processes involved. Uneven or incomplete etching has repeatedly been observed, as well as condensation of water on cooling after etching, which destroyed the microcrystals of sodium chloride. Imperfectly etched columns yielded poor performance and durability. Examination with scanning electron microscopy (SEM) revealed considerable differences in the distribution, shape and dimensions of the crystals[17,21,35].

To improve this situation we have concentrated on the various factors that influence the etching of soda-lime glass with gaseous hydrogen chloride, in order to establish a set of optimal conditions of pre-treatment, etching time and temperature.

As an alternative for the gaseous HCl etching (surface roughening by NaCl particles), a method was developed to deposite directly a layer of microparticles of NaCl onto the column wall. Within the framework of investigations to produce simple, rugged surface-roughening methods in our laboratory, we developed a method of surface roughening, based on controlled surface devitrification in the presence of a nucleation catalyst.

EXPERIMENTAL

Surface roughening

Gaseous HCl etching of the column wall. Gaseous HCl only attacks soft alkali glass. The composition of the glasses used in this study is given in Table I. The etching is accomplished either by stagnant (static etching) or flowing (dynamic etching), pure and dry HCl, taken from a cylinder (electronic grade, Matheson, Oevel, Belgium).

The set-up, shown schematically in Fig. 1, allows pre-conditioning of the columns at elevated temperatures as well as treatment with HCl at a constant or programmed temperature. To reduce the temperature gradient along the column during the

TABLE I

COMPOSITION OF THE ALKALI GLASSES

A.R. = A.R. glass, Scott-Ruhrglass, Wertheim, G.F.R.; Rö = Röntgen glass 06, Philips, Eindhoven, The Netherlands; B44 = Verre sodocalcique B44, Choisy-le-roi, France.

Component	*Glass*		
	A.R.	*Rö*	*B44*
SiO_2	67	70	70.2
Na_2O	15	17.8	12.6
CaO	7	8.8	6.0
ZnO	7	0.5	
Al_2O_3	2.5	2.3	4.2
Fe_2O_3			
B_2O_3			1.0
MgO			1.9
BaO			3.8
MnO		0.6	
Other elements		Traces	

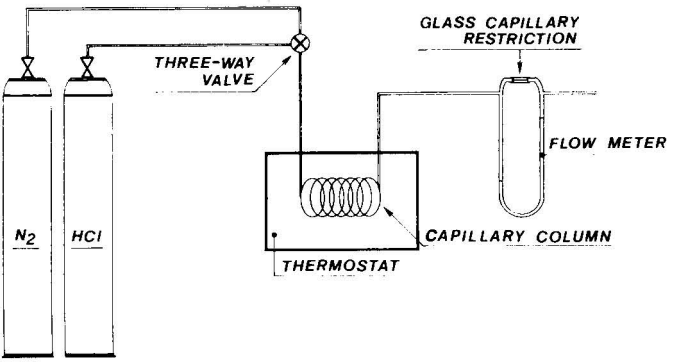


Fig. 1. Schematic set-up for the HCl etching of glass capillary columns.

etching procedure, the columns are wrapped in an aluminium foil in all of the experiments.

The flow is measured continuously with a capillary restriction flow meter, filled with *n*-hexane. Prior to etching all of the columns are dried rigorously by flushing with dry nitrogen at 400° for 16 h at the rate of 40 cm/sec.

After conditioning, the columns involved in the dynamic etching, are cooled to room temperature and the nitrogen flow is replaced with an HCl flow of 20 cm/sec. The column is kept at room temperature for at least 1 h and then heated to the required etching temperature. After etching, the column is flushed again with dry nitrogen, cooled to room temperature and sealed at both ends with a small flame.

For static etching, the columns are likewise pre-conditioned and filled with HCl at room temperature, and sealed at both ends when the HCl concentration exceeds 99.5%. To measure this concentration, a length of about 25 cm is melted off from the column. One end is crushed under water, which rises into the capillary by dissolution of HCl. The filled length is a direct measure of the HCl content in the column.

To study the influence of the etching time at different temperatures, the capillaries are divided in sealed parts of about 6 m, which are consecutively removed from the thermostat at different time intervals. After etching and cooling to room temperature, about 25 cm of each part is melted off to measure the HCl consumption. One end is opened under *n*-hexane which is sucked up into the capillary to an extent equivalent to the HCl consumption. This direct measurement can be used only in the case of static etching. Finally, one end of the remaining part is opened in a dry nitrogen atmosphere and the excess of HCl is forced out by dry nitrogen. Both ends are then sealed.

An indirect measurement of the etching rate, by analysis of the amount and nature of the reaction products, can be performed for both etching methods. The columns were rinsed with about ten times their volume of distilled water and the solutions obtained were analyzed for ionic species by isotachophoresis with an instrument developed by Everaerts *et al.*[36]. The presence of $SiO_2 \cdot nH_2O$ or silicates was assayed for separately by a colorimetric method[37], based on conversion to silicomolybdic acid.

Surface roughening by surface crystallization. A powdered and dried mixture

of 75 g of $LiNO_3$, 15 g of KNO_3, 10 g of $NaNO_3$ and 0.5 g of $AgNO_3$ (liquidus 217°) is melted at 240° in a heavy-walled Pyrex container, placed on the bottom of a tall thermostat (1452 D, Packard-Becker, Delft, The Netherlands). The alkali-glass tube (Rö 06, 40 cm × 13 mm O.D. × 6.8 mm I.D.) is placed in the molten salts through a hole in the top cover of the oven. The melt is sucked up gently into the tube until it solidifies in the cold part a few centimetres above the oven cover. The exchange of sodium ions with lithium and silver ions is allowed to take place for 2 h. After melting the plug of solid nitrates with a small flame, the melt runs back into the container. The tube is removed from the oven and, after cooling, is rinsed successively with water and methanol and dried. At this stage, the inner wall of the tube is white and non-transparent. The tube is enclosed in a wide-bore Pyrex tube, which is sealed at both ends after filling with hydrogen and heated at 200° for 20 min. This results in a conversion of Ag^+ ions into colloidal silver and the tube turns brownish yellow. From this tube, capillaries of 0.5 mm I.D. are drawn. The delivery speed was such that a residence time of 30 min in the oven of the glass-drawing machine (about 850°) was obtained.

Deposition of NaCl microparticles on the column wall. A saturated and filtered solution of NaCl in methanol is diluted with 10% of additional methanol. About 8 ml of 1,1,1-trichloroethane is spouted vigorously into 6 ml of this solution. After shaking, a further 8 ml of 1,1,1-trichloroethane are spouted into the sol. This stable and milky sol is then sucked through the column at the rate of 10 cm/sec. The column is provided with buffer columns at both ends in order to ensure a constant speed of the sol in the column. After the sol has left the column, the solvent is evaporated by continuing the suction. Next, the column is treated likewise four more times and then dried. At this stage the column has a faint white appearance. Finally, the NaCl conglomerates are recrystallized at 350° for 1 h.

Scanning electron microscopy

Within half an hour after roughening the capillaries are split open, immediately glued on specimen holders and coated with a gold–carbon layer, so as to avoid the influence of atmospheric water vapour. Kept over silica gel, the specimens were observed to remain unchanged for at least two weeks. Micrographs were taken using a "Stereoscan" (Cambridge Instruments, Cambridge, Great Britain).

RESULTS AND DISCUSSION

HCl etching

Analysis of the reaction products of the etching process showed that Na^+ and Cl^- ions were present in near to equimolar amounts. Ca^{2+} ions were present in trace amounts only, while silicates, $SiO_2 \cdot nH_2O$ and other cations were absent. The amount of NaCl formed in static experiments with a long etching time (26 h), was equivalent to 94% of the amount of HCl consumed. Therefore, this etching method can be described as a dealkalization process in which Na^+ ions in the glass are replaced with H^+ ions. Simultaneously, NaCl is deposited on to the surface as the main reaction product. The vitreous silica network remains intact.

The etching process will be treated as a multiple-step process involving:

(1) formation of NaCl nuclei;

(2) equilibration of the glass surface with gaseous HCl;

(3) diffusion of H^+ ions into the glass in exchange for Na^+ ions;

(4) migration of Na^+ ions across the surface towards NaCl nuclei and particles;

(5) location of Na^+ and Cl^- ions on their respective sites in the NaCl particles, *i.e.*, growth of randomly shaped NaCl particles;

(6) migration of Na^+ and Cl^- ions across the NaCl surface towards low index planes, *i.e.*, recrystallization of NaCl particles.

Under certain conditions, additional processes play a role: formation of extra nuclei during the etching, formation of conglomerates of NaCl particles and growth of large NaCl particles at the cost of smaller ones.

(Ad 1) Formation of NaCl nuclei. SEM pictures of freshly drawn and untreated columns showed a smooth surface carrying no or only a few impurities. SEM pictures of columns filled with HCl and kept at room temperature, revealed the presence of approximately spherical particles (diameter about 0.2 μm) which are uniformly distributed over the surface, *cf.* Fig. 2. Apparently nucleation even takes place at room temperature and is not a rate-determining step in the etching process. Because diffusion coefficients in the bulk of the glass are extremely small at room temperature, this observation can be explained only by the presence of free alkali on the inner wall of the column.

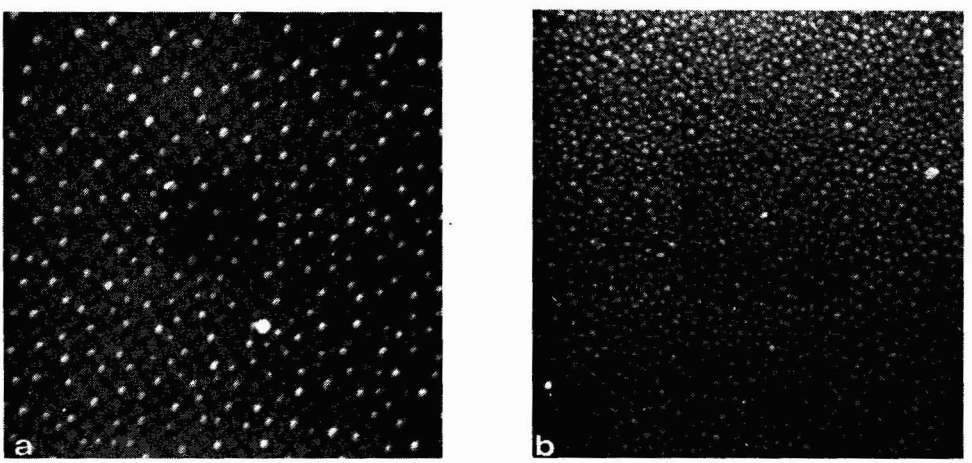


Fig. 2. SEM pictures (10 × 10 μm) of alkali-glass capillaries (A.R.) treated with HCl at room temperature. (a), 1 h; (b), 4 h.

Budd and Kirwan[38] reported surface free alkali on the inner wall of soda-lime silica glass vessels. They found that it was caused by evaporation of the relatively volatile Na_2O from the glass during forming. In glass capillary columns, the vapour-phase Na_2O cannot escape from the column, and on cooling it re-condenses, forming both an alkali-rich surface layer ("skin alkali") and surface free alkali. Nucleation is therefore a consequence of surface impurities rather than of a reaction between HCl and the glass.

(Ad 2–5) Kinetics of the HCl etching. When phase boundary reactions are

fast, the interdiffusion of Na^+ and H^+ in the bulk of the glass is the rate-determining factor. Assuming that the concentration of H^+ ions in the surface layer of the glass is small and proportional to the HCl concentration, the amount of NaCl (M_{NaCl}) formed per unit area in the dynamic etching procedure is given by[39]

$$M_{NaCl} = 2K\,[HCl] \cdot \sqrt{\frac{\tilde{D}t}{\pi}} \tag{1}$$

where

$$K = \frac{[H^+_{glass}]}{[HCl]}$$

The functional form of eqn. 1 is preserved even if the interdiffusion coefficient ($\tilde{D}$), describing this binary diffusion process, is a function of concentration[39]. Therefore, M is expected to be proportional to $\sqrt{t}$ no matter what the functional relation between $\tilde{D}$ and concentration may be.

Fig. 3, curve (a), gives the results of a dynamic etching experiment at 350°. The amount of NaCl rapidly approaches a maximum and then remains constant within the limits of experimental error (3%). Despite the continuous availability of HCl, the dynamic gaseous HCl etching apparently is a self-limiting process, not follow-

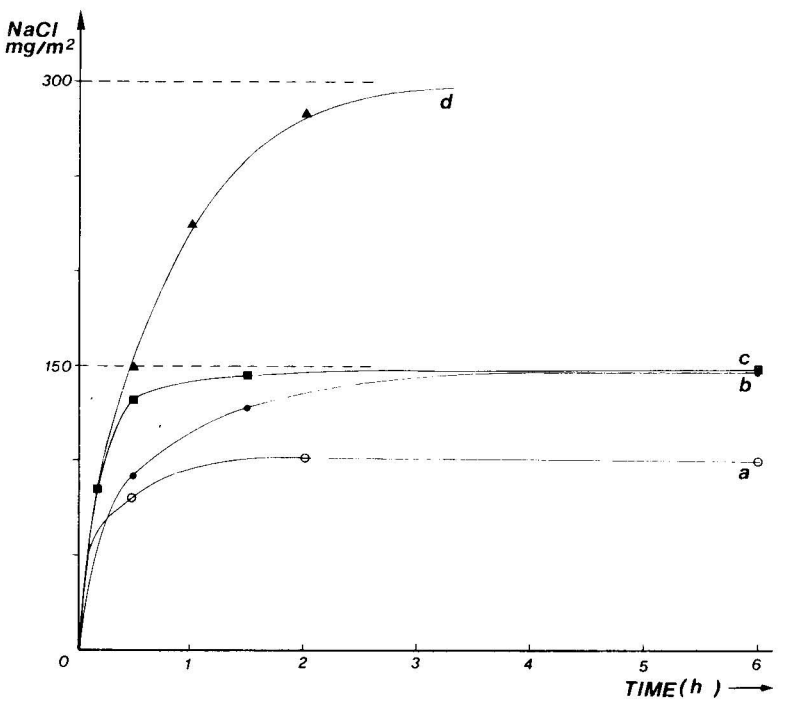


Fig. 3. HCl consumption, expressed as the amount of NaCl formed per square meter of glass surface, at 300° and 350°. Horizontal dashed lines indicate the maximum amount of NaCl that can be formed in 0.25 and 0.5-mm columns with static etching: (a), Dynamic, 350°, I.D. 0.25 mm; (b), static, 300°, I.D. 0.25 mm; (c), static, 350°, I.D. 0.25 mm; (d), static, 350°, I.D. 0.5 mm.

ing eqn. 1. Experiments were performed in which etched columns were rinsed to remove the NaCl and were etched again at 350°. Production of NaCl was observed but at an extremely low rate. Therefore, the limiting factor is connected with the surface layer of the etched glass itself and not with the layer of NaCl. In connection with the concept of skin alkali[38], a mechanism that might cause a sharp decrease in the expected rate of HCl uptake could be a decreasing concentration of alkali with depth into the glass. However, the amount of surface free alkali plus skin alkali, according to Budd and Kirwan, cannot account for the amount of NaCi actually found. This proves that this mechanism is only of marginal importance.

A more satisfactory explanation might be found in the work of Sendt[40] on the dealkalization of soda-lime glasses. He found that the exchange of Na^+ with H^+ is accompanied at and above 350° by a loss of water from the glass, according to the reactions



The glass surface layer loses non-bridging oxygen atoms and this loss is expected to reduce the values of both $\tilde{D}$ and K, so that eqn. 1 no longer holds. A surface layer deficient in non-bridging oxygen atoms is known to improve the chemical resistivity of the glass surface[40] and apparently also shields the glass from further attack by HCl.

Curves (b), (c) and (d) in Fig. 3 give the results of a series of static etching experiments at 300° and 350°. It is evident that in static etching of columns up to at least 0.5 mm the limiting factor is the amount of HCl available. For larger diameters shielding is again the limiting factor, as HCl was incompletely consumed in 0.7-mm columns. We reason that in static etching the rate of elimination of water from the glass is reduced by vapour-phase water. Contrary to the dynamic method, in the static method the eliminated water cannot escape from the sealed column. Hence, the development of a shielding layer is retarded, which results in a substantially increased amount of NaCl being formed. Ultimately, elimination of water does occur, which was confirmed experimentally by the condensation of water in colder parts of the columns on rapid cooling, after etching overnight at 350°.

(Ad 4–6) Growth and recrystallization of NaCl particles. The sequence of events occuring during the static etching procedure will be treated with reference to Figs. 2, 4 and 5. At the start of the etching process, exchange of Na^+ with H^+ is fast, partly due to the presence of skin alkali. The Na^+ ions move across the glass surface and randomly locate on the nearest Na^+ site, irrespective of the lattice energy of that particular site. Consequently, the NaCl particles formed tend to have a circular flattened convex shape, and are probably polycrystalline (Fig. 4a). The number of particles is considerably less than the number of nuclei originally present. The surface free energy of small particles is very high, and consequently the smaller nuclei have disappeared in favour of the larger growing particles.

In the course of time, the rate of NaCl formation decreases sharply. Particle growth and recrystallization become competitive effects and the particles tend to have rectangular shapes (Fig. 4b). Ultimately, the development of low index planes becomes predominant (Fig. 4c and d). If the heat treatment is continued for long periods, large NaCl crystals grow at the cost of smaller ones (Fig. 5).

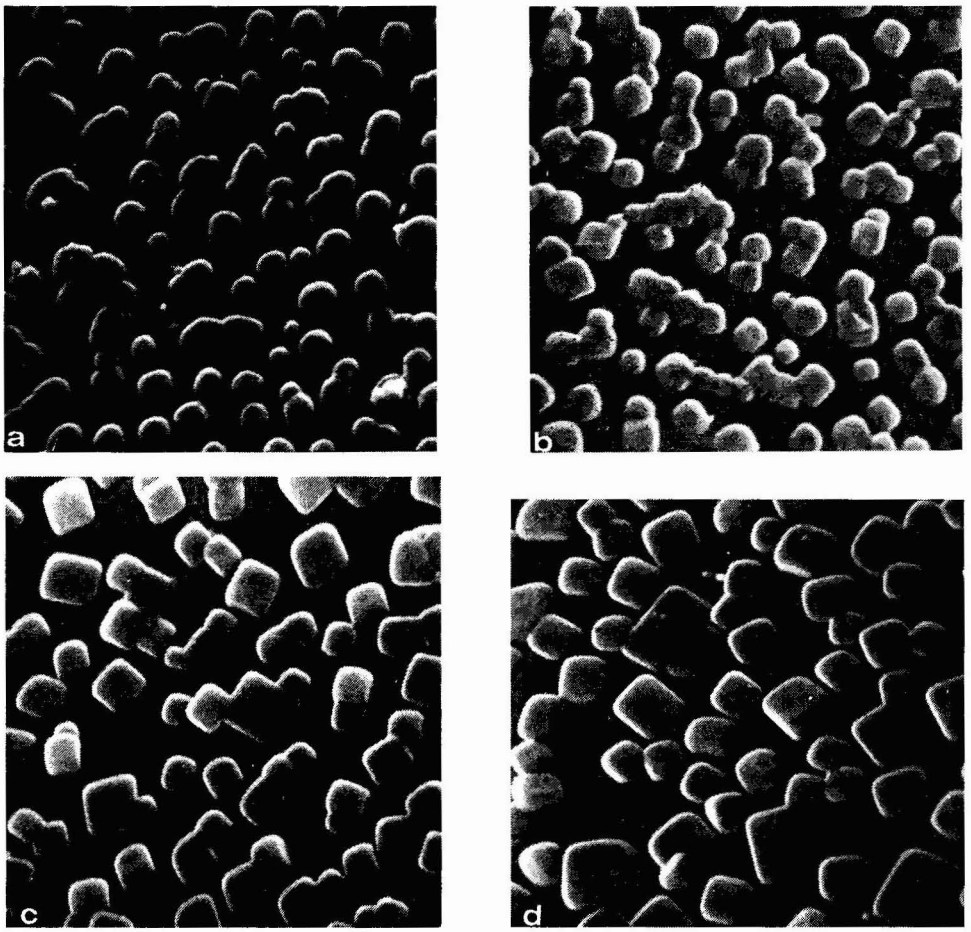


Fig. 4. NaCl particle growth in the course of time for the static procedure at 350°. SEM pictures (10 × 10 μm) of an alkali-glass (A.R.) capillary (I.D. 0.4 mm). (a), 30 min; (b), 60 min; (c), 120 min; (d), 240 min.

During the dynamic etching procedure, HCl is present in excess, which has a marked influence on the rate of particle growth and recrystallization (Fig. 6). The smaller nuclei disappear to a lesser extent than in the static etching. Hence, a large number of relatively small particles is observed. The excess of HCl even induces the formation of additional nuclei on bare parts of the surface (Fig. 6b). The result is that particles of dissimilar size and shape are present, even after 6 h of treatment. Recrystallization apparently is effectively inhibited by the excess of HCl. The number of rectangular particles after 6 h is still negligibly small.

Influence of the etching temperature. The description of the etching process given above relates to an etching temperature of 350°. At 300°, the sequence of events is essentially the same, but slower. At 400°, using A.R. glass, the results are variable. At the start of the etching in some parts of the column, the attack of the glass by HCl is confined to circular areas, randomly distributed over the surface. Consequently,

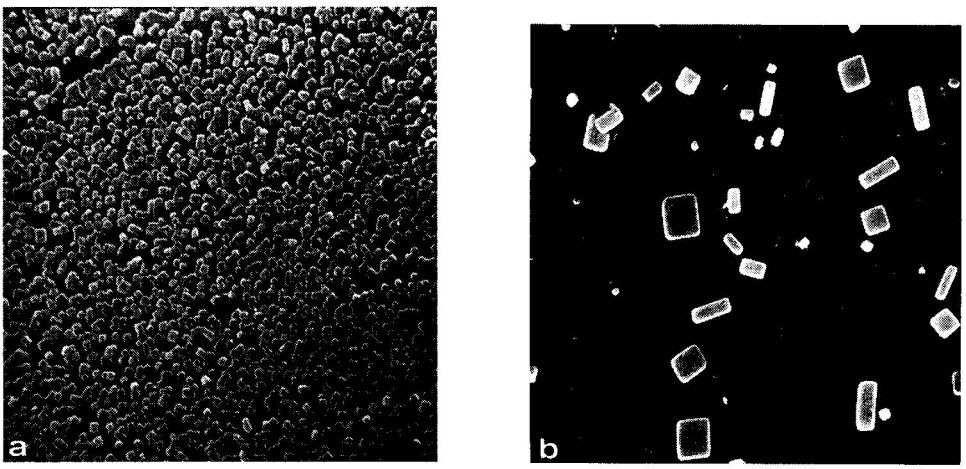


Fig. 5. NaCl particle growth in the course of time for the static procedure at 350°. SEM pictures (50 × 50 μm) of an alkali-glass (A.R.) capillary (*cf.* Fig. 4). (a), 2 h; (b), 22 h.

the distribution of NaCl is not uniform, nor is the rate of recrystallization. The final result is a column locally covered with particles of dissimilar size (up to more than 10 μm), which is far beyond those observed at 350°. This deviation of the "normal" process takes place over about 30% of the column area, the remaining 70% showing a distribution of NaCl as in Figs. 4–6. Therefore, we consider 350° to be the optimal etching temperature.

The rôle of the pre-conditioning. As described under Experimental, the freshly drawn columns are sealed at both ends immediately after drawing. Prior to etching, the columns are rigorously dried by flushing with dry nitrogen at 400°. The intention of these measures is to prevent the formation of a hydrated surface layer or to dehydrate such a layer. If these precautions are omitted, the surface free alkali deliquesces

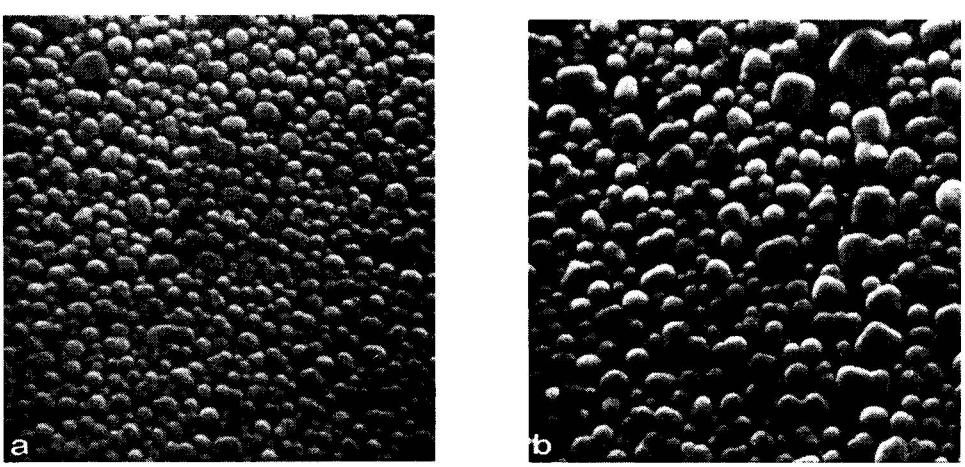


Fig. 6. NaCl particle growth in the course of time for the dynamic procedure. SEM pictures (10 × 10 μm) of an alkali-glass (B44) capillary at 350°. (a), 1 h; (b), 6 h.

during storage[38]. The alkaline water film thus formed attacks the vitreous silica network and the result is a loose layer of hydrated silicates. Attempts to etch such surfaces are bound to fail. As judged by the naked eye, NaCl is formed readily and the column turns opaque. SEM pictures, however, revealed that recrystallization did not occur in such columns or that it occurred to an unpredictable and non-uniform extent. Also, the formation of conglomerates of NaCl particles was frequently observed, which ultimately grew to particles of impractically large dimensions at the cost of smaller ones. The description of the normal etching process given above, holds fully only with pre-conditioned columns.

Surface roughening by controlled surface devitrification

Commercial soda-lime–silica glasses do not readily devitrify during heat treatment. The exchange of Na_2O for Li_2O promotes devitrification considerably, as near and above the softening point the mobility of Li^+ ions is large compared with that of the Na^+ ions[40,41]. The mere exchange of Na_2O with Li_2O, however, will not lead to an appreciable rate of crystallization during heat treatment, as the rate of homogeneous nucleation is very small. Stookey[42], in a study on controlled crystallization of lithium-rich glasses, used colloidal silver as a nucleation agent. Recently, Petzold and Kambor[43] described the introduction of silver in glass based on ion exchange between the glass and a mixture of molten nitrates, containing small amounts of $AgNO_3$. Ernsberger[44] reported that the exchange of Na^+ ions in glass with Li^+ ions from a mixture of $LiNO_3$, $NaNO_3$ and KNO_3 proceeds smoothly.

We chose to treat the glass with a mixture of molten nitrates, relatively rich in $LiNO_3$ and containing only small amounts of silver nitrate. Because of the considerably smaller size of the Li^+ ions (ratio of radii, $Li^+:Na^+ = 0.63$), replacement of Na^+ with Li^+ causes the glass surface layer to shrink. Under the experimental conditions used, micro-cracks form spontaneously. The melt penetrates into these cracks and the rate of penetration of Li^+ and Ag^+ into the glass is determined by the rate of propagation of the cracks, rather than by diffusion. The result is a cloudy surface layer of cracked ion-exchanged glass, the thickness of which is proportional to the time of ion exchange. Under the conditions used (see Experimental), the mean rate of propagation was 2.5 μm/min. The Ag^+ ions in the glass were readily reduced by treatment with hydrogen at elevated temperatures[43].

During drawing of the pre-treated tube, the following processes take place:

(1) growth of silver crystals to a minimum critical size for nucleation;

(2) nucleation of devitrification;

(3) growth of crystals in and on the surface;

(4) diffusion of Li^+ away from the surface in exchange for Na^+ from deeper layers;

(5) production of "new" surface as a consequence of the macroscopic surface increase during drawing;

(6) reduction of the "old" surface area as the cracks in the surface disappear at temperatures well above the softening point.

Maurer[45] studied the effect of catalyst size in heterogeneous nucleation and found that colloidal particles, smaller than 80 Å, were not effective as nuclei. Stookey[42] found that nucleation did not occur above a certain critical temperature. This temperature should not be attained before the Ag crystals reach the critical size for nuclea-



Fig. 7. SEM picture (50 × 50 μm) of an alkali glass (Rö 06) after controlled surface devitrification.

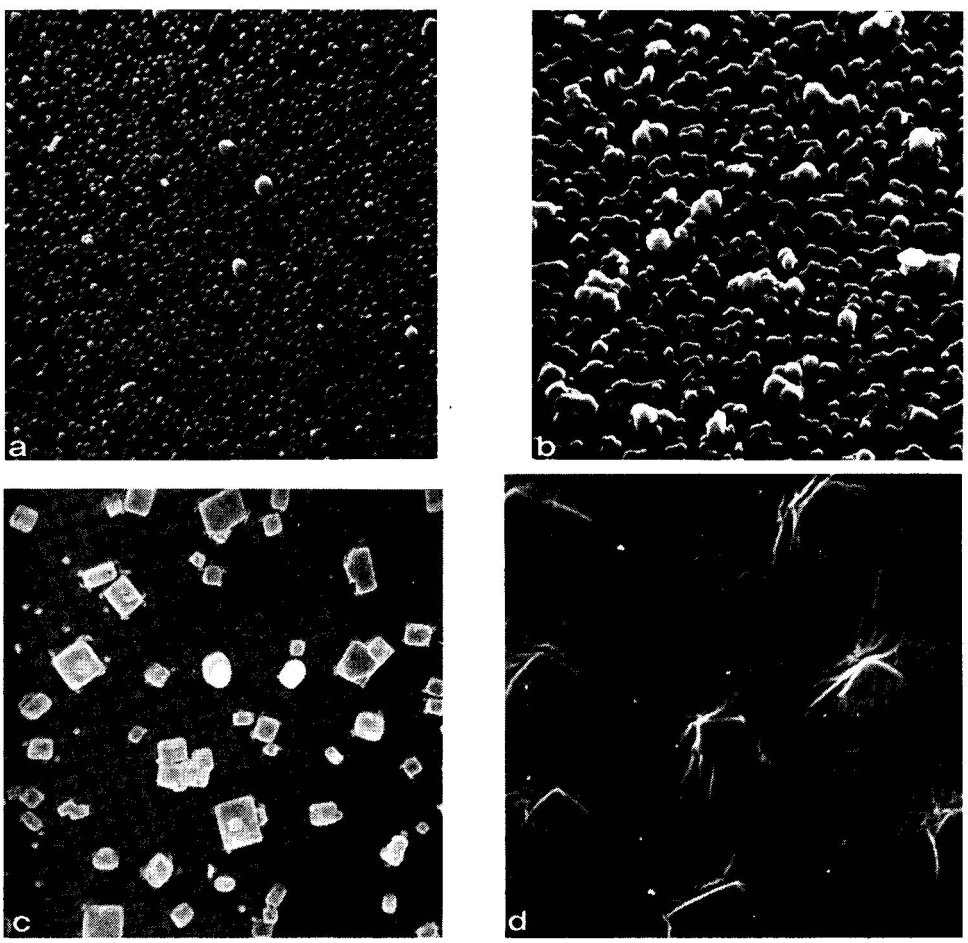


Fig. 8. SEM pictures (20 × 20 μm) of various stages in the preparation of an OV-225-coated NaCl SCOT column, I.D. 0.4 mm. (a), After one rinsing; (b), after 5 rinsings; (c), after recrystallization during 1 h; (d), after coating and use during 2 weeks at 225°.

tion, or crystallization of the glass will not occur. Therefore, the inner wall of the tube should not undergo too steep a temperature programme.

Although the nature of the crystals grown has not yet been established, the presence of lithium metasilicate or lithium disilicate is likely[41,42]. If Li^+ is incorporated in the crystal phase, steps 4 and 5 are competitive with step 3 and the net result depends on the coherence of the temperature programme that the tube undergoes, the temperature and time of pre-treatment and the elongation factor.

Under the particular set of conditions described (*cf.* Experimental), interesting "spiked" surfaces are obtained (Fig. 7). The dimensions of the spikes (diameter 0.3–0.5 μm, length 1–4 μm) compare reasonably well with stationary phase film thicknesses normally used. In a certain sense these surfaces can be compared with those reported by Schieke *et al.*[25]. In experiments in which the ion exchange was performed at 250° for 2 h instead of at 240°, the surface was uniformly covered with clusters of spikes, rather than with single spikes. The same experiments performed with A.R. glass instead of Rö glass did not yield predictable results.

As judged from the results of an intermediate test, according to Rutten and Luyten[46], these surfaces are well suited for gas chromatography. Current methods of deactivation proved fully satisfactory, which is in marked contrast to results obtained with columns that had merely undergone the ion exchange of Na^+ for Li^+ as was proposed by Desty[26]. These columns exhibited severe adsorption and catalytic activity, and could not be deactivated by current methods.

The final result of the surface devitrification depends on many parameters and the influence of each of these parameters is not yet fully understood. A better predictability of the length and closeness of the spikes will be the subject of further studies.

Deposition of NaCl particles on the column wall

Fig. 8 shows SEM pictures of coated and uncoated columns treated with an

TABLE II

COMPARISON OF THE PERFORMANCE OF OV-225-COATED COLUMNS AT 225° USING NITROGEN AS CARRIER GAS

SCOT = Support-coated open tubular.

Parameter	*Column No.*					
	1	*2*	*3*	*4*	*5*	*6*
Column type	SCOT*	SCOT*	SCOT*	HCl etched	HCl etched	SCOT
Support	Chromosorb R 6470-1	Cab-O-Sil	Cab-O-Sil	—	—	NaCl
Coating method	Dynamic	Dynamic	Dynamic	Static**	Static**	Static**
Length (m)	50	25	34	40	42	18.4
I.D. (mm)	0.4	0.4	0.4	0.25	0.25	0.35
Theoretical plates/m***	1780	1460	2340	2350	2480	2750
Coating efficiency (%)	63	52	82	52	56	86

* Prepared according to refs. 32 and 34.

** According to ref. 47.

*** Achieved at capacity ratios between 8 and 11.

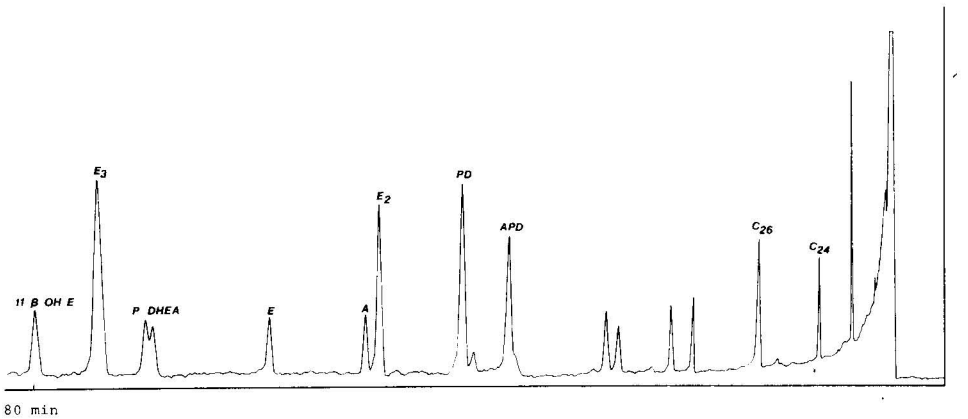


Fig. 9. Chromatogram of a mixture of trimethylsilyl derivatives of steroids on an HCl-etched glass (A.R.) capillary column (No. 5, Table II). APD = Allopregnanediol; PD = pregnanediol; E_2 = estradiol; A = androsterone; E = etiocholanolone; DHEA = dehydroepiandrosterone; P = pregnanolone, E_3 = estriol; 11-β-OH-E = 11β-hydroxyetiocholanolone.

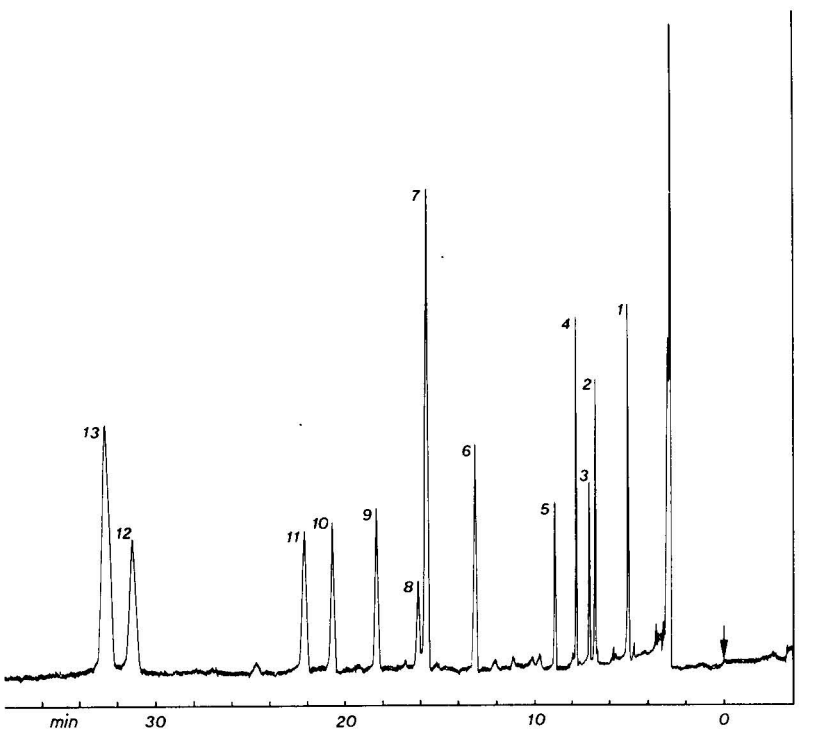


Fig. 10. Separation of a standard mixture of chlorinated pesticides on an NaCl SCOT column (No. 6, Table II). 1 = Hexachlorobenzene; 2 = 2,2′-dibromobiphenyl (internal standard); 3 = α-BHC; 4 = aldrin; 5 = γ-BHC; 6 = *o,p′*-DDE; 7 = *p,p′*-DDE; 8 = β-BHC; 9 = dieldrin; 10 = *o,p′*-DDT; 11 = *o,p′*-DDD; 12 = *p,p′*-DDT; 13 = *p,p′*-DDD.

NaCl sol. After one rinsing, the wall is uniformly covered with spherical particles, about 0.3 μm in diameter (Fig. 8a). Repeated rinsings increase the amount of NaCl and conglomerates of particles are seen (Fig. 8b), which, on heating, recrystallize within 1 h to cubic crystals of 0.5–2 μm (Fig. 8c). The rate of crystallization is considerably higher than for HCl-etched columns. This effect might be caused by minor impurities in the NaCl particles of the etched columns, possibly $CaCl_2$; isotachophoretic analysis revealed the presence of trace amounts of Ca^{2+}.

Performance of coated columns

Preliminary results of polar phase-coated columns, including some SCOT columns, are presented in Table II. Fig. 9 shows a chromatogram of a standard mixture of trimethylsilyl derivatives of steroids at the end of a period of 6 weeks at 225° (column 5). Fig. 10 shows a separation of chlorinated pesticides after 4 weeks of operation at 225° (column 6).

The stability of the columns 4–6 appears to be good. After decreasing about 10% during the first three weeks, the capacity ratio remained constant. Plate numbers and relative retentions remained constant within experimental error during the period studied (up to 6 weeks now). Adsorption effects and minimal sample quantity are well within the limits for reliable analysis, while bleeding and loading capacity enable coupling to the mass spectrometer.

CONCLUSION

The types of surface roughening reported here are in various stages of development.

For HCl-etched columns, we have shown that, under properly chosen conditions of pre-treatment, etching time and temperature, the size, shape and distribution of the particles can be predicted. This permits a systematic study of the relationship between these factors and column properties.

The preparation of NaCl SCOT columns is easy to carry out. The NaCl suspension will not clog narrow columns, which is an advantage over current supports. The direct deposition of NaCl particles yields a roughening of the column wall which is an attractive alternative for the HCl etching and is applicable to any type of glass.

The thermal stability of OV-225 columns appears to be very good.

The development of the method of surface devitrification is still continuing. We regard the results obtained so far an incentive for further work. The dimensions and shapes of the observed spikes and the easy deactivation of the column add to this optimism. In particular, the closeness and length of the spikes deserve further optimization.

ACKNOWLEDGEMENTS

The authors greatly appreciate the time and effort spent by Mrs. M.H.A. Blijlevens on taking a large number of SEM pictures. They are also indebted to Mr. M. L. Dingen for his care and patience in drawing many kilometres of glass capillary columns with a high degree of precision.

REFERENCES

1 M. Novotný and A. Zlatkis, *Chromatogr. Rev.*, 14 (1971) 1.
2 F. W. Karasek, *Res./Develop.*, Nov. (1975) 40.
3 J. J. Franken and G. A. F. M. Rutten, in S. G. Perry (Editor), *Chromatography 1972*, Applied Science Publ., Barking, 1973, pp. 75–88.
4 J. J. Franken and M. M. F. Trijbels, *J. Chromatogr.*, 91 (1974) 425.
5 G. A. F. M. Rutten, unpublished results.
6 M. Mohnke and W. Saffert, in M. van Swaay (Editor), *Gas Chromatography 1962*, Butterworths, London, 1962, p. 216.
7 W. Leibnitz and M. Mohnke, *Chem. Tech. (Berlin)*, 14 (1962) 753.
8 A. Liberti, G. P. Cartoni and F. A. Bruner, *J. Chromatogr.*, 12 (1963) 8.
9 F. A. Bruner and G. P. Cartoni, *Anal. Chem.*, 36 (1964) 1522.
10 S. P. Zhdanov, V. I. Kalmanovskii, A. V. Kiselev, M. M. Ficks and Y. I. Yashin, *Russ. J. Phys. Chem.*, 36 (1962) 595; *Zh. Fiz. Khim.*, 36 (1962) 1118.
11 E. L. Ilkova and E. A. Mistryukov, *Chromatographia*, 4 (1971) 77.
12 A. Liberti, in A. B. Littlewood (Editor), *Gas Chromatography 1966*, Elsevier, Amsterdam, 1967, p. 95.
13 K. Tesařík and M. Novotný, in H. G. Struppe (Editor), *Gas Chromatographie 1968*, Academie-Verlag, Berlin, 1968, p. 575.
14 K. Tesařík and M. Novotný, *Chromatographia*, 1 (1968) 332.
15 R. W. Ohline and R. A. Jojola, *Anal. Chem.*, 36 (1964) 1681.
16 G. Alexander and G. A. F. M. Rutten, *Chromatographia*, 6 (1973) 231.
17 G. Alexander and G. A. F. M. Rutten, *J. Chromatogr.*, 99 (1974) 81.
18 G. Schomburg, H. Husmann and F. Weeke, *J. Chromatogr.*, 99 (1974) 63.
19 G. Schomburg and H. Husmann, *Chromatographia*, 8 (1975) 517.
20 G. Alexander, G. Garzó and G. Pályi, *J. Chromatogr.*, 91 (1974) 25.
21 H. T. Badings, J. J. G. van der Pol and J. G. Wassink, *Chromatographia*, 8 (1975) 440.
22 F. Berthou, D. Picart, L. Bardou and H. H. Floch, *J. Chromatogr.*, 118 (1976) 135.
23 G. Schomburg, H. Husmann and F. Weeke, *J. Chromatogr.*, 112 (1975) 205.
24 M. Novotný and K. D. Bartle, *J. Chromatogr.*, 93 (1974) 405.
25 J. D. Schieke, N. R. Comins and V. Pretorius, *J. Chromatogr.*, 112 (1975) 97.
26 D. H. Desty, *Chromatographia*, 8 (1975) 452.
27 M. Blumer, *Anal. Chem.*, 45 (1973) 980.
28 A. L. German and E. C. Horning, *J. Chromatogr. Sci.*, 11 (1973) 76.
29 A. L. German, C. D. Pfaffenberger, J. P. Thenot, M. G. Horning, and E. C. Horning, *Anal. Chem.*, 45 (1973) 930.
30 P. van Hout, J. Szafranek, C. D. Pfaffenberger and E. C. Horning, *J. Chromatogr.*, 99 (1974) 103.
31 S.-N. Lin, C. D. Pfaffenberger and E. C. Horning, *J. Chromatogr.*, 104 (1975) 319.
32 C. A. Cramers, E. A. Vermeer, L. van Kuik, C. A. Meyers and J. A. Hulsman, *Clin. Chim. Acta*, submitted for publication.
33 R. S. Deelder, P. J. H. Hendricks and M. G. F. Kroll, *J. Chromatogr.*, 57 (1971) 67.
34 R. S. Deelder, J. J. M. Ramaekers, J. H. M. van den Berg and M. L. Wetzels, *J. Chromatogr.*, 119 (1976) 99.
35 J. D. Schieke, N. R. Comins and V. Pretorius, *J. Chromatogr.*, 115 (1975) 373.
36 F. M. Everaerts, J. L. Beckers and Th. P. E. M. Verheggen, *Isotachophoresis, Theory, Instrumentation and Applications*, Elsevier, Amsterdam, Oxford, New York, 1976.
37 J. Rodier, *L'Analyse Chimique et Physico-chimique de l'Eau*, Dunot, Paris, 2nd ed., 1960, p. 130.
38 S. M. Budd and J. J. Kirwan, in *Advances in Glass Technology*, Plenum Press, New York, 1962, pp. 527–540.
39 J. Crank, *The Mathematics of Diffusion*, Clarendon Press, Oxford, 1957.
40 A. Sendt, in *Advances in Glass Technology*, Plenum Press, New York, 1962, pp. 307–332.
41 P. W. McMillan, *Glass Ceramics*, Academic Press, London, 1964.
42 S. D. Stookey, *Ind. Eng. Chem.*, 45 (1953) 115.
43 A. Petzold and H.-U. Kambor, *Glastech. Ber.* 47 (1974) 226.
44 F. M. Ernsberger, *Proc. Roy. Soc., Ser. A*, 257 (1960) 213.
45 R. D. Maurer, *J. Chem. Phys.*, 31 (1959) 444.
46 G. A. F. M. Rutten and J. A. Luyten, *J. Chromatogr.*, 74 (1972) 177.
47 J. Bouche and M. Verzele, *J. Gas Chromatogr.*, 6 (1968) 501.

Journal of Chromatography, 126 (1976) 133–145
© Elsevier Scientific Publishing Company, Amsterdam — Printed in The Netherlands

CHROM. 9448

PREPARATION AND APPLICATION OF SURFACE-MODIFIED HIGH-RESOLUTION WALL-COATED OPEN TUBULAR COLUMNS

F. I. ONUSKA* and M. E. COMBA

Analytical Methods Research Section, Canada Centre for Inland Waters, P.O. Box 5050, 867 Lakeshore Road, Burlington, Ontario L7R 4A6 (Canada)

SUMMARY

Short wall-coated open tubular glass capillary columns were prepared from soft soda-lime and sodium borosilicate (Pyrex) glass. Whisker growth was affected by gaseous hydrogen fluoride at elevated temperatures. A substantial increase in total internal surface area was observed and documented by scanning electron microscopy. Examples of their application to mixtures of polychlorinated biphenyls, methyl esters of fatty acids, nonionic surfactants and polynuclear aromatic hydrocarbons are given.

INTRODUCTION

Adaptation of glass capillary wall-coated open tubular columns (WCOT) for routine applications in gas chromatography (GC) is slowly becoming a realization. Many of the problems previously encountered with capillary column systems have been dissipated by the commercial availability of instrumentation especially designed for these purposes. The original limitations of low partition ratios, small sample capacities and column quality have been substantially altered with considerable effort devoted to improvements in coating procedures, surface preparation, and instrumentation[1–20].

Propagation of whiskers on the inner surfaces of capillary walls has proven to be a significant advancement in the preparation of glass capillary columns. Tesařík and Novotný[19] successfully etched soft glass capillaries with hydrogen chloride, hydrogen fluoride, and 2-chloro-1,1,2-trifluoromethyl ethyl ether. The latter technique was extended by Schieke *et al.*[21–24] using more concentrated solutions which decompose at elevated temperatures to liberate hydrogen fluoride. During this process, formation of a carbon deposit was observed which can be very difficult and time consuming to remove[22]. Etching and surface modification techniques have also been described by Grob[11] and by Alexander and Rutten[14].

Treatment of glass surfaces with gaseous hydrogen fluoride has not been extensively used, although its corrosive aspects are well documented[19,25]. This is basically due to the safety precautions associated with hydrogen fluoride which detract from its suitability. In view of this, a simplified procedure was developed for forming whisker-

* Author to whom all correspondence should be addressed.

modified surfaces with gaseous hydrogen fluoride. Both Pyrex and soft glass were etched by this method to observe if any pronounced advantages in relation to other surface treatment techniques were obtained.

EXPERIMENTAL

Preparation of glass columns

Glass capillaries were prepared from soft soda-lime and sodium borosilicate (Pyrex) tubing according to the method outlined by Desty *et al.*[26] employing a Hewlett-Packard Model 1045 A drawing machine. A 40- and a 13-m column were drawn

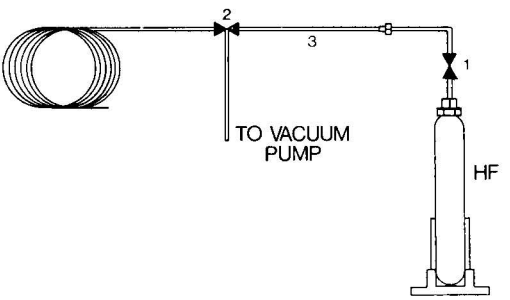


Fig. 1. Apparatus for hydrogen fluoride etching of glass capillary columns.

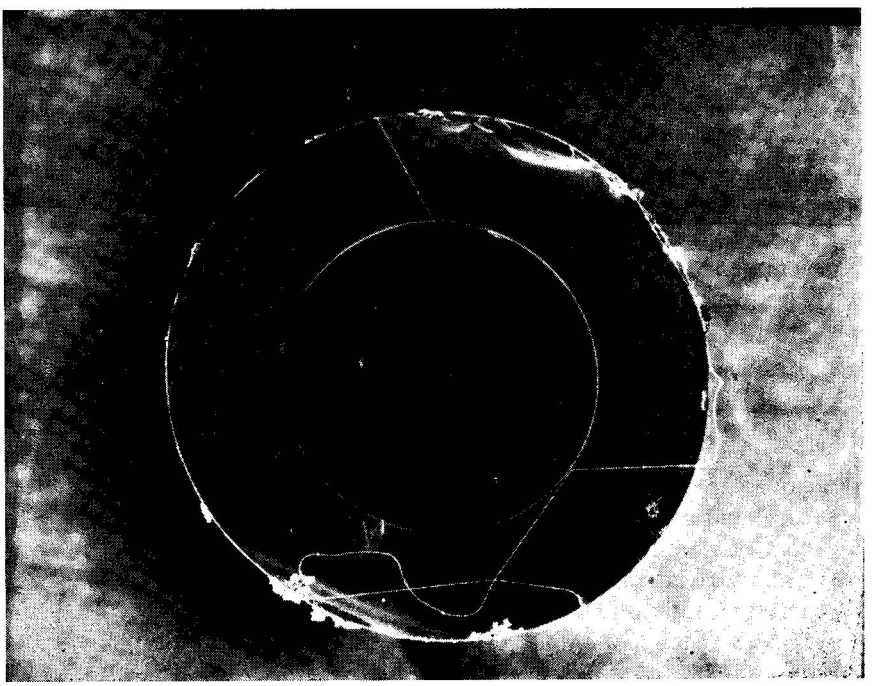


Fig. 2. Cross-section of column before treatment.



Fig. 3. Cross-section of etched soft glass capillary.

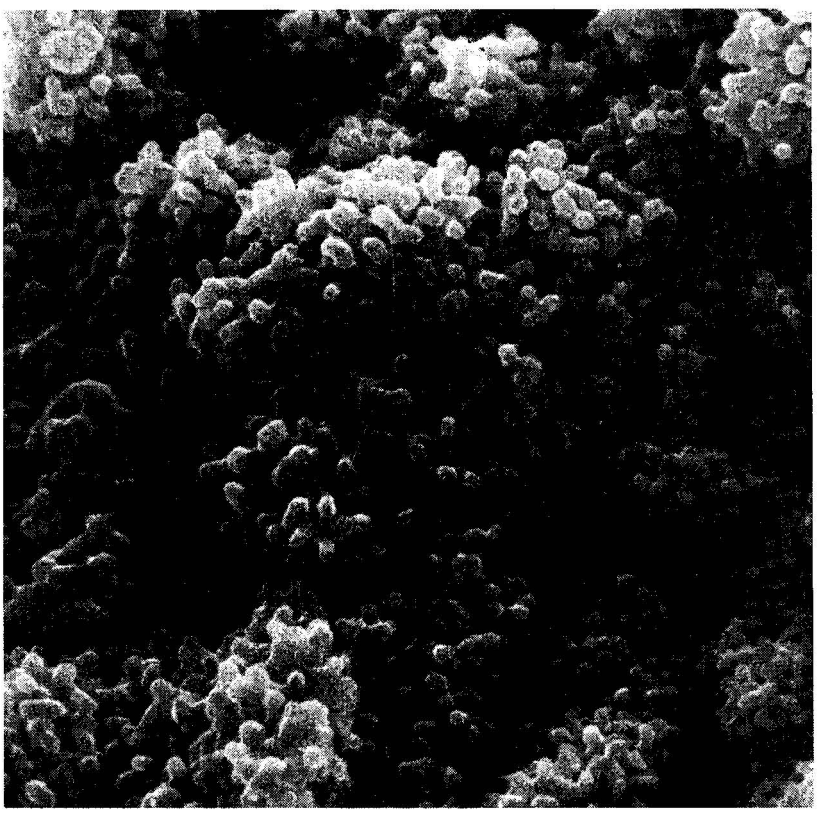


Fig. 4. Surface of etched soft glass capillary.

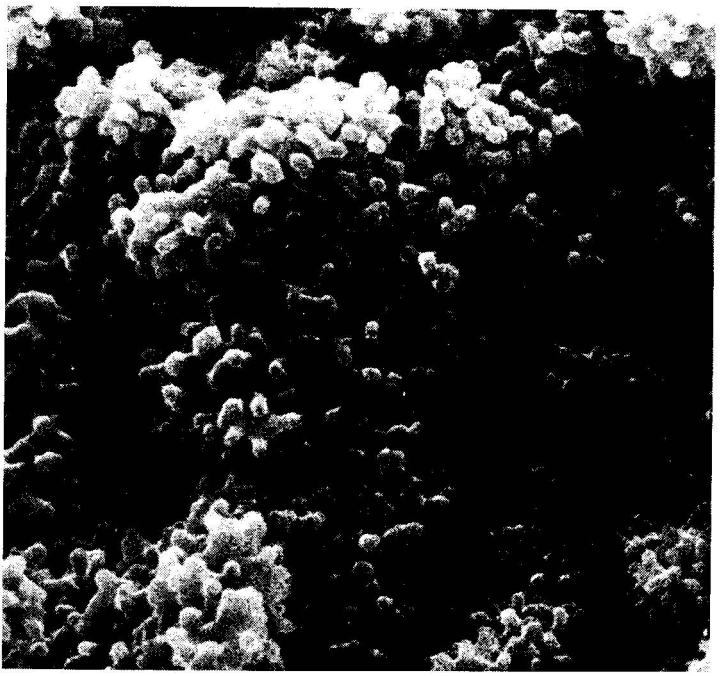


Fig. 5. Whisker formation on soft glass inner surface.

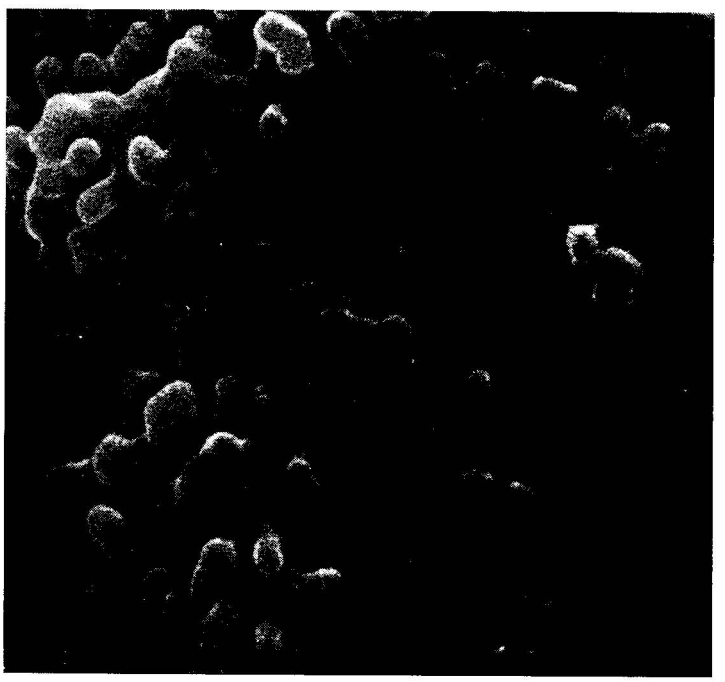


Fig. 6. Whisker formation on soft glass inner surface.

to 0.5 mm I.D. and 0.24 mm I.D. (tolerances of $\pm 0.5\%$ of I.D. were acceptable), respectively.

Surface modification

Since the whisker growth is affected in the vapor phase, it is essential to introduce the hydrogen fluoride in a uniform manner over the entire length of the column. This may be accomplished by using the apparatus described in Fig. 1. The system must be located in a well-ventilated fume hood and operated using rubber gloves, apron, and aspirator mask. The column was sealed at one end with the open end being connected to the three-way switching valve using shrinkable PTFE tubing. The column was evacuated to a least 10^{-1} mmHg using a small vacuum pump. Valve 2 was then switched to the hydrogen fluoride lecture bottle and hydrogen fluoride was released into the column by opening valve 1. The lecture bottle valve was closed and the column sealed off using a microflame torch. The seals on both ends of the column should be checked before removal by inserting each in a small beaker of water. The sealed column was then placed in a vented oven at ambient temperature. The oven was closed and the temperature raised to 400° for 12 h. After the hydrogen fluoride has

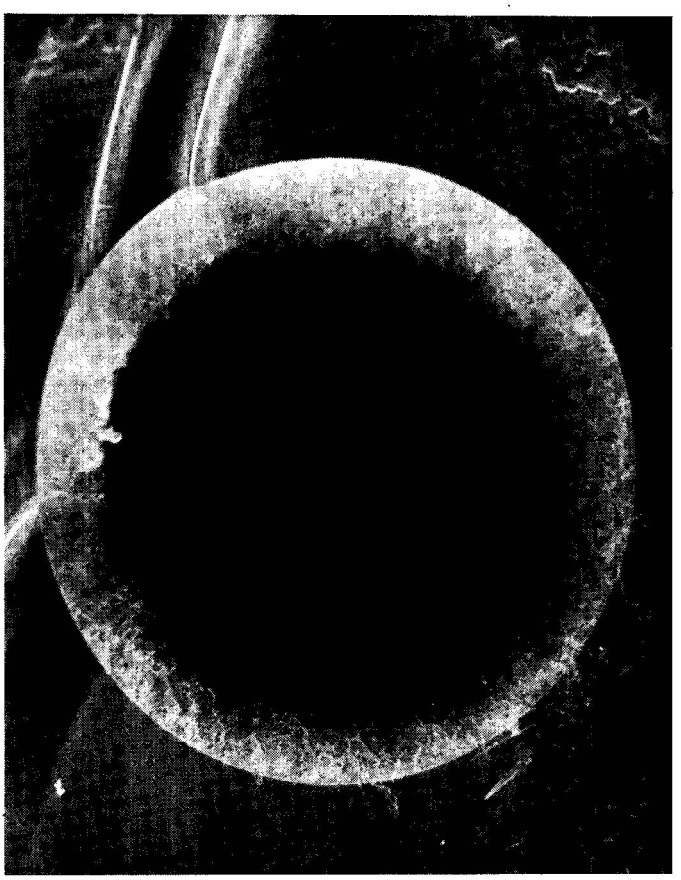


Fig. 7. Cross-section of etched Pyrex capillary.

been consumed the column has a translucent appearance. The column was then removed and flushed with helium for 80 min. The whisker growth was checked by breaking short lengths (10 mm) from both ends of the column. An AMR Model 1000 scanning electron microscope (SEM) with an EDAX attachment for X-ray electron dispersive analysis was used. Small portions of each length were taken and mounted vertically in a capillary holder. The etched surface was then treated with protamine sulfate and gold to eliminate charging effects.

Coating

Each column was tailored to a form suitable for connection to the gas chromatograph prior to coating. A liquid phase of 20% OV-17 (methyl phenyl silicone) in CH_2Cl_2 was then applied to the Pyrex column using a mercury plug method[17]. The column was filled with the coating solution by suction, followed by a 5-cm mercury plug. The vacuum was removed and the capillary plug was pushed through the capillary at a constant velocity (80 cm/min). The end of the capillary column was connected to a buffer column (10 m of shrinkable PTFE) to ensure a constant linear flow through

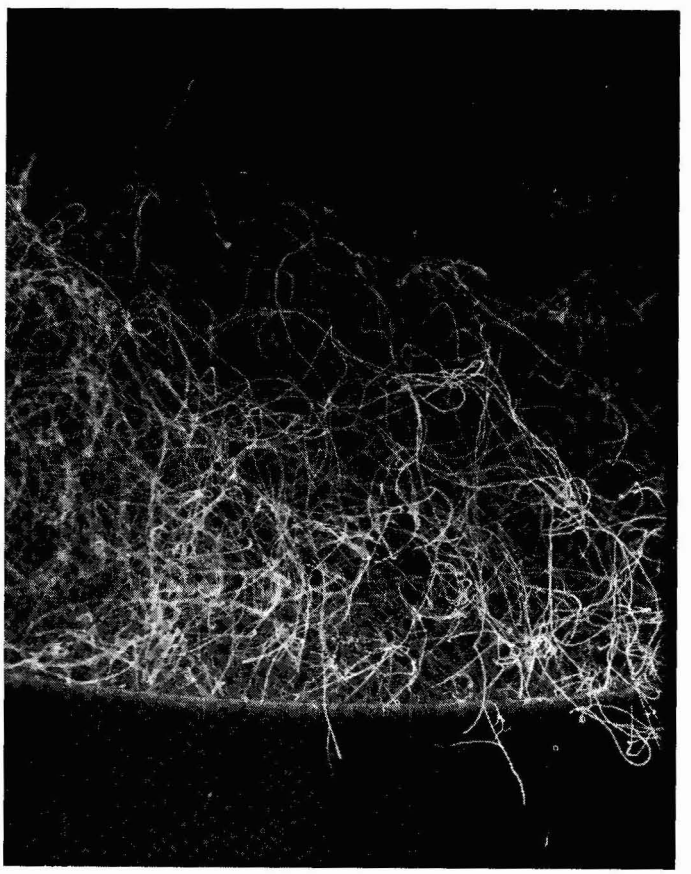


Fig. 8. End-view of whiskers formed on Pyrex capillary column.

the last part of the column. The quality of the column can be greatly reduced if degassed solvents are not used. Due to the enlarged surface area, air bubbles can be adsorbed on the surface and later may be entrained in the liquid phase. Excessive solvent was removed by passing helium through the column for approximately 80 min.

The soft (soda-lime) glass capillary was coated with a 4% solution of OV-3 in CH_2Cl_2 using a dynamic coating procedure[17] with a Shimadzu Model MC T-1A treating stand.

Gas chromatography

A Carlo Erba Model 2300 gas chromatograph equipped with a flame ionization detector was used. The instrument incorporates a splitless injector with a modified insert[27]. A pre-column containing an ultra-thin layer of non-extractable Apiezon L on a diatomaceous support, prepared according to Aue and Younker[28] was located directly in the injector to increase the sample capacity. The glass insert and column ends were deactivated with a low concentration of Carbowax 20M (20 mg/ml) prior to use. The column was conditioned at a slow programming rate overnight (60–260°).



Fig. 9. Surface of etched Pyrex capillary.

Film homogenity and column quality were evaluated using a polar mixture containing Reynolds mixture. Column inertness was checked according to Grob[11] using a mixture of *n*-undecane, dibutyl ketone, 2-*trans*-2-ethyl- and 2-*cis*-2-ethylcyclohexanol, and 2,6-dimethylaniline.

RESULTS AND DISCUSSION

In comparison to untreated surfaces (Fig. 2), ideal support media for the retention of the stationary phase were achieved by hydrogen fluoride etching. Whisker formations on the soft (soda-lime) glass were 2–3 μm in length, coral-like in nature, and relatively uniform, as shown in Figs. 3–6. Pyrex yielded finer whiskers, 3–5 μm in length, under the same conditions. Fairly dense, uniform silica fibres were observed (Figs. 7–10) resembling glass wool.

The prepared columns as described in Table I were applied to a number of complex mixtures. Figs. 11 and 12 show the separation of various distillation cuts of Aroclors, using the OV-17 capillary column. Although it is difficult to compare two

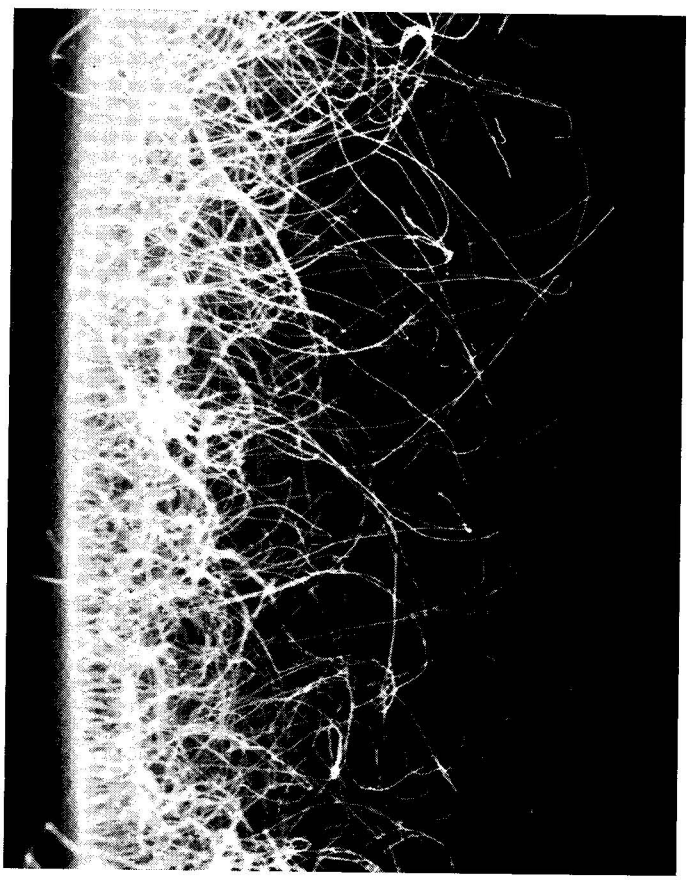


Fig. 10. End-view of etched Pyrex capillary.

TABLE I

PHYSICAL PARAMETERS OF WCOT COLUMNS

Parameter	*Unit*	*Column 1*	*Column 2*
Stationary phase	—	OV-17	OV-3
Flow-rate* (helium)	ml/min	4	1.4
Length	m	38	12
Internal diameter	mm	0.50	0.24
Total volume	ml	7.46	0.54
Number of theoretical plates** (N)	—	228,000	96,500
Number of theoretical plates per metre (N/m)	—	6000	8041
Height equivalent to a theoretical plate (HETP)	mm	0.166	0.125
Partition ratio (k)***	—	18	19
Separation number (TZ)	—	47	31

* Dial setting of 0.7–0.8 atm (at ambient temperature).
** Calculated for fluorene at 140°.
*** Calculated for fluorene.

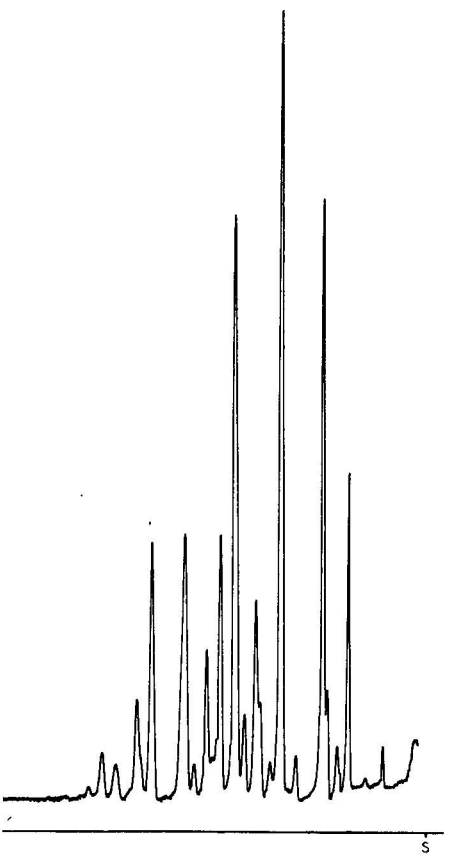


Fig. 11. Gas chromatogram of Aroclor 1016 on OV-17. Temperature programmed from 140–190° at 4°/min; 3 min hold. For other column conditions, see Table I.

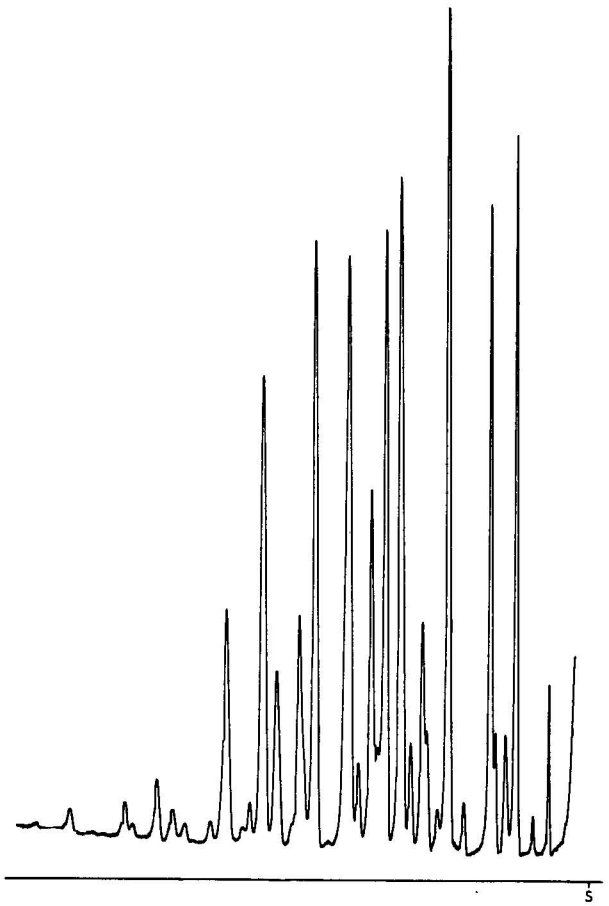


Fig. 12. Gas chromatogram of Aroclor 1242 on OV-17. Temperature programmed from 140–190° at 4°/min; 3 min hold. For other column conditions, see Table I.

different columns, the separation achieved on Aroclor 1016 was similar to that obtained by Schomburg *et al.*[13] on a 120-m Dexsil 300 column.

The separation of methyl esters of fatty acids using the same column is shown in Fig. 13. Although OV-17 is not a specific phase to effect proper separation, it is evident that reasonable results can be obtained for C_8–C_{22} esters using temperature programming, with reproducible retention data, symmetrical peaks, and short analysis time. Excellent separation was also achieved on a nonionic detergent formulation (Fig. 14) containing various amounts of ethoxy groups on a C_{14} alkoxy moiety.

The column prepared from soft glass and coated with OV-3 gave equivalent separation on a mixture of polynuclear aromatic hydrocarbons (Fig. 15), as previously experienced with a SE-52 column prepared by a static coating method.

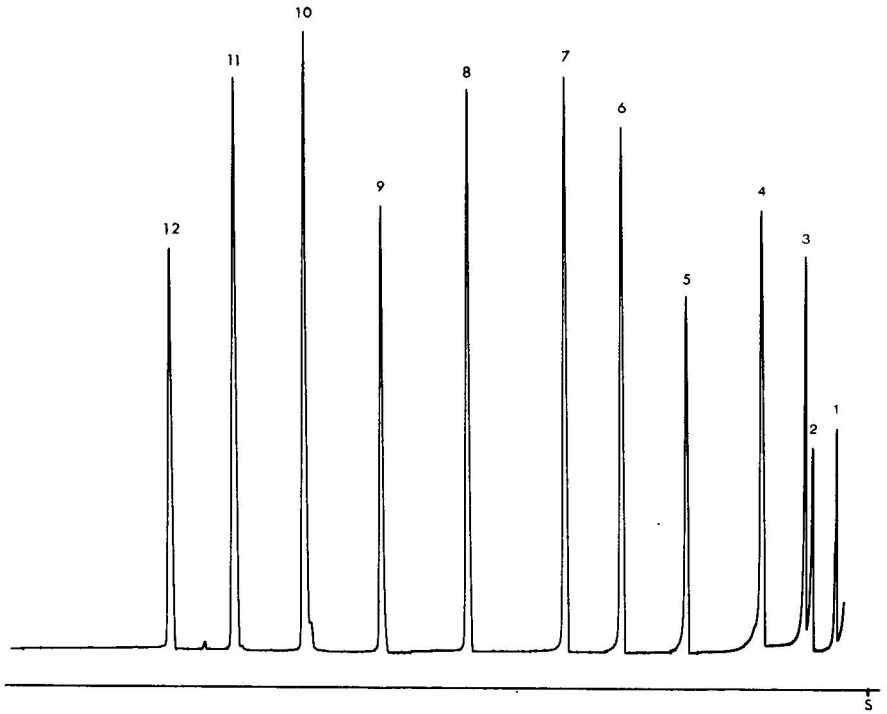


Fig. 13. Gas chromatogram of fatty acid methyl esters on OV-17. Temperature programmed from 70–210° at 4°/min; 3 min hold. For other column conditions ,see Table I. 1 = Hexanoic; 2 = heptanoic; 3 = octanoic; 4 = nonanoic; 5 = decanoic; 6 = hendecanoic; 7 = dodecanoic; 8 = tetradecanoic; 9 = hexadecanoic; 10 = octadecanoic; 11 = eicosanoic; 12 = docosanoic acids.

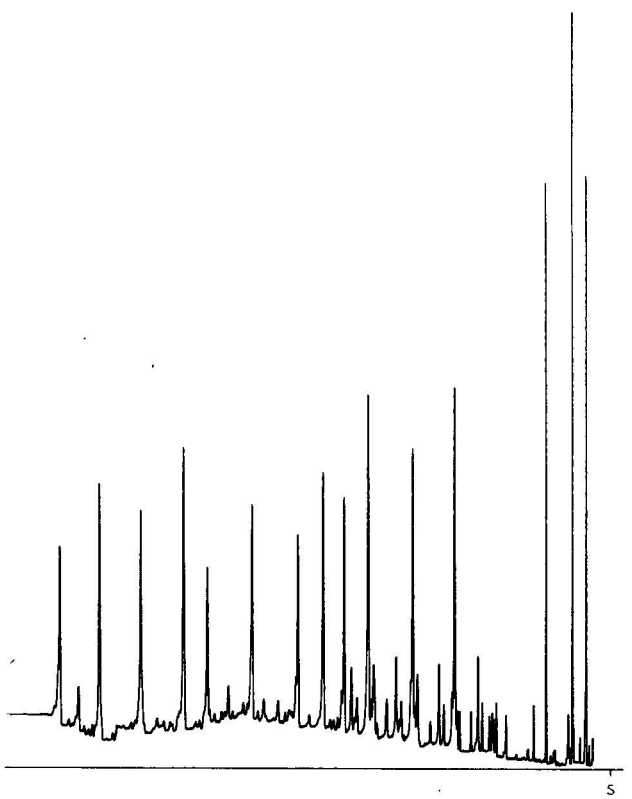


Fig. 14. Gas chromatogram of nonionic surfactant on OV-17. Temperature programmed from 90–250° at 4°/min; 3 min hold. For other column conditions, see Table I.

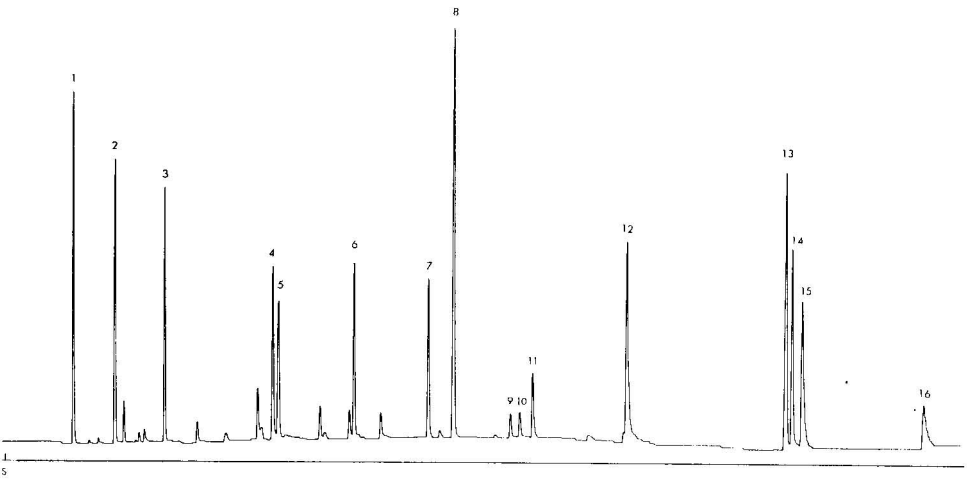


Fig. 15. Gas chromatogram of polynuclear aromatic hydrocarbons on OV-3. Temperature programmed from 60–230° at 2°/min; 3 min hold. For other column conditions, see Table I. 1 = Biphenyl; 2 = acenaphthene; 3 = fluorene; 4 = phenanthrene; 5 = anthracene; 6 = 9-methylphenanthrene; 7 = fluoranthrene; 8 = pyrene; 9 = benzo[*a*]fluorene; 10 = benzo[*b*]fluorene; 11 = 1-methylpyrene; 12 = triphenylene; 13 = benzo[*e*]pyrene; 14 = benzo[*a*]pyrene; 15 = perylene; 16 = dibenz[*a*,*c*]anthracene.

CONCLUSIONS

Surface modification of glass capillaries substantially contributes to the technology of column preparation and provides an excellent substrate for coating. It would be unreasonable to believe that only one general procedure can provide suitable results. We are confident, however, that etching with hydrogen fluoride will produce reliable columns and is competitive with other treatments.

ACKNOWLEDGEMENTS

We would like to thank Mr. T. Bistricki, AMRS, Canada Centre for Inland Waters, for developing the SEM technique and Dr. M. Novotný, Indiana University, Bloomington, Ind., for his friendly assistance.

REFERENCES

1 M. J. E. Golay, in U. J. Coates, H. J. Noebels and I. S. Fagerson (Editors), *Gas Chromatography*, Academic Press, New York, 1958, pp. 1–13.
2 M. J. E. Golay, in D. H. Desty (Editor), *Gas Chromatography 1958*, Butterworths, London, 1958, pp. 36–55.
3 L. S. Ettre, *Instr. News*, 13, No. 1 (1961) 1.
4 A. Zlatkis and J. Q. Walker, *J. Gas Chromatogr.*, 1 (5) (1963) 9.
5 K. Tesařík, K. Hana and M. Janiček, *Chem. Listy*, 55 (1961) 1467.
6 M. Novotný and A. Zlatkis, *Chromatogr. Rev.*, 14 (1971) 1.
7 K. Grob, *J. Gas Chromatogr.*, 3 (1965) 52.
8 A. V. Kiselev, in M. van Swaay (Editor), *Gas Chromatography 1962*, Butterworths, London, 1962, p. 3.
9 J. Merle d'Aubigne, C. Landault and G. Guiochon, *Chromatographia*, 4 (1971) 309.
10 M. Novotný, *Chromatographia*, 2 (1969) 350.
11 K. Grob, *Helv. Chim. Acta*, 51 (1968) 718.

12 K. Grob and G. Grob, *J, Chromatogr. Sci.*, 7 (1969) 584.
13 G. Schomburg, H. Husmann and F. Weeke, *J. Chromatogr.*, 99 (1974) 63.
14 G. Alexander and G. A. F. M. Rutten, *J. Chromatogr.*, 99 (1974) 81.
15 K. Grob, *Chromatographia*, 8 (1975) 423.
16 G. C. Goretti, A. Liberti and G. Nota, *Chromatographia*, 8 (1975) 486.
17 G. Schomburg and H. Husmann, *Chromatographia*, 8 (1975) 517.
18 J. Roeraade, *Chromatographia*, 8 (1975) 511.
19 K. Tesařík and M. Novotný, in H. S. Struppe (Editor), *Gas Chromatographia 1968*, Academie-Verlag, Berlin, 1968, p. 575.
20 M. Novotný and K. Tesařík, *Chromatographia*, 1 (1968) 332.
21 J. D. Schieke, N. R. Comins and V. Pretorius, *Chromatographia*, 8 (1975) 354.
22 J. D. Schieke, N. R. Comins and V. Pretorius, *J. Chromatogr.*, 112 (1975) 97.
23 J. D. Schieke, N. R. Comins and V. Pretorius, *J. Chromatogr.*, 114 (1975) 190.
24 J. D. Schieke, N. R. Comins and V. Pretorius, *J. Chromatogr.*, 115 (1975) 373.
25 A. V. Kiselev and Ya. I. Yashin, *Gazo-adsorbcionnaya Chromatografiya (Gas Adsorption Chromatography)*, Nauka, Moscow, 1967, p. 233.
26 D. H. Desty, J. N. Haresnape and B. H. Whyman, *Anal. Chem.*, 32 (1960) 302.
27 F. I. Onuska, M. E. Comba, M. Novotný and M. Lee, *Anal. Lett.*, (1976).
28 W. A. Aue and D. R. Younker, *J. Chromatogr.*, 88 (1974) 7.

Journal of Chromatography, 126 (1976) 147–160
© Elsevier Scientific Publishing Company, Amsterdam — Printed in The Netherlands

CHROM. 9509

EFFECT OF ETCHING WITH GASEOUS HYDROGEN CHLORIDE ON THE QUALITY OF GLASS CAPILLARY COLUMNS

J. KRUPČÍK, M. KRISTÍN, M. VALACHOVIČOVÁ and Š. JANIGA

Chemical Faculty, Department of Analytical Chemistry, Slovak Technical University, Bratislava 88037 (Czechoslovakia)

SUMMARY

The effect of etching with gaseous HCl on the quality of glass capillary columns made of soft soda-lime glass and coated with OV-101 and Carbowax 20M has been studied. The quality of the columns was evaluated in terms of the number of theoretical plates, coating efficiency and Kováts retention indices of polychlorinated biphenyls (PCBs). The retention indices depend, *inter alia*, on the time and temperature of etching of the inner walls of the capillary. Columns coated with a thin film of OV-101 show adsorption properties resulting in an increase in Kováts retention indices and are capable of separating pairs of PCBs which, when chromatographed on columns coated with a thicker film of stationary phase, remain unresolved.

It has been found that by coupling shorter columns together, extremely efficient columns or columns of required polarity can be prepared.

INTRODUCTION

The use of glass capillary columns in gas chromatography has been of increasing interest in recent years[1,2]. Glass capillary columns are often used for the separation of complex mixtures in environmental samples and in clinical, food and flavour chemistry[3]. Prior to coating, the inner surface of glass capillary columns is most often etched with hydrogen chloride[4,5] or methyl trifluorochloroethyl ether (CH_3OCF_2CHFCl)[6]. Good results have been obtained by coating the inner wall of the column with colloidal silicic acid[7,8] and graphitized carbon black[9].

It follows from published results that soft soda-lime glass is the most suitable column material when etching with gaseous HCl is to be applied[3–5]. The etching procedure considerably improves the wettability of the glass surface with polar stationary phases, because a layer of microcrystalline sodium chloride is formed[3,4]. This layer has been studied by scanning electron microscopy (SEM), analyzed by means of EDAX (energy dispersive X-ray analyzer) elemental analysis[10], and it has been proved that crystals on the etched surface consist mainly of sodium chloride. Obviously, sodium chloride on the glass surface is formed by the reaction



The liberated free SiOH groups, which are the source of adsorptive properties of the glass, with a negative effect on the properties of capillary columns coated with non-polar stationary phases, can be eliminated by silanization[11,12], by coating the active centres with surface-active agents[11], by addition of a polar stationary phase[11,12] or by increasing the film thickness of the layer of stationary phase[13].

When coating capillary columns, the best results were obtained with non-polar stationary phases. With these stationary phases, mainly polydimethylsiloxanes (OV-1, OV-101 and SE-30), columns with 2000–4000 theoretical plates per metre for capacity ratios greater than 2 could be prepared, which is a substantially better column efficiency than that usually achieved with metal capillary columns coated with the same phases[15]. Very good results could also be obtained when glass capillary columns were coated with some polar phases[2,5,8,9,12], and very efficient and thermally stable columns were found to be those coated with Carbowax 20M (ref. 14), the efficiency being almost as good as that of polydimethylsiloxane columns.

In the analysis of polychlorinated biphenyls (PCBs), we have previously tested glass and metal capillary columns coated with OV-101. It was found that glass columns were much more efficient and showed longer lifetimes at temperatures of about 470 °K than metal columns coated with the same stationary phase[15].

The aim of the present work was to study the effect of the most important variables (temperature and the etching time of the inner surface of the column with HCl) on the properties of capillary columns coated with OV-101 and Carbowax 20M in the analysis of PCBs.

EXPERIMENTAL

Capillary columns were drawn by a machine that was a modified version of the type proposed by Desty *et al.*[16]. The drawing machine was constructed at the Institute of Analytical Chemistry, Czechoslovak Academy of Science (Brno, Czechoslovakia). The capillaries were drawn from soda-lime soft glass (Unihost and PN glasses, Jablonec Glass Works, Czechoslovakia). Prior to drawing, the glass tubing was cleaned by rinsing it with chromic acid. The acid was washed out with water, then the tubes were washed with acetone and dried using a water pump. The composition of the glass material used is summarized in Table I.

TABLE I

CHEMICAL COMPOSITIONS (%) OF THE GLASSES USED

Component	*Type of glass*	
	Unihost	*PN*
SiO_2	68.6	67.0
B_2O_3	—	2.0
Al_2O_3	3.9	3.0
CaO	5.5	6.5
MgO	2.9	—
ZnO	—	8.0
Na_2O	17.8	13.5
K_2O	1.3	—

The tubes were 0.7–1.5 m long with 7–8 mm O.D. and 2–3 mm I.D. From these, capillaries up to 75 m long with 0.8–1.1 mm O.D. and 0.20–0.35 mm I.D. were drawn.

Glass capillary column I.D. measurements

With the aid of compressed nitrogen and a burette, the capillary was filled with dichloromethane. Using the equation $d = 2\sqrt{V/(\pi L)}$, where V is the known volume of dichloromethane and L is the length of the capillary, the mean inner diameter (d) was calculated with an accuracy of $\pm 2\%$.

Etching of glass capillaries with gaseous HCl

Gaseous HCl, generated from dry sodium chloride and sulphuric acid, was forced through the capillary. After the appearance of HCl at the end of tubing (indicated by wetted reagent paper), passage of HCl through the capillary was continued for a further 2 h and then the amount of air present in the tube was determined by the test of Alexander *et al.*[4]. Usually more than 90% of the capillary volume was filled with HCl. Both ends of the filled capillary were sealed using a micro-burner and the column was heated in a thermostat with a forced air circulation for 2–42 h at 523–653 °K.

Prior to the coating procedure, the capillaries were activated, while nitrogen was passed through them, with the temperature programmed from 323 to 433 °K at 5 °K/min. The etched surfaces were studied using SEM and an X-ray microanalyzer.

Dynamic coating procedure

The capillaries were coated dynamically using 0.15–3 ml of a 10–20% solution of the stationary phase in *n*-hexane or chloroform at a flow-rate 0.3–0.5 cm/sec[17]. Ultra-thin-film capillary columns were prepared by a modified dynamic procedure as proposed by Schomburg and Husmann[14]. The solution of stationary phase (0.15–0.30 ml of 10–20% solution) was sucked into the capillary followed by a plug of mercury (2–5 cm). The vacuum was discontinued and the mercury plug was pushed through the column by means of compressed nitrogen at a rate of 0.3–0.5 cm/sec.

Column conditioning and testing

The columns were conditioned at a nitrogen flow-rate of 0.5 ml/min with the temperature programmed from 323 to 533 °K at the rate of 4 °K/min and maintained isothermally at 533 °K for 60 min. The column efficiency was characterized by separating a mixture of PCBs at a carrier gas flow-rate 0.3–0.5 ml/min. The column efficiency was measured in terms of the number of theoretical plates. The coating efficiency was calculated according to Ettre[17].

Gas chromatography

The instrument used was an Erba Science (Carlo Erba, Milan, Italy) Fractovap Model 2300 gas chromatograph equipped with a flame-ionization detector and a stream splitter. Glass capillary columns were connected to the splitter and to the detector by means of shrinkable PTFE tubing. The retention times were measured with a stop-watch. The carrier gas flow-rate was calculated from the known column

volume, V, and the retention time of methane, t_M, using the equation $F_M = V/t_M$. For determinations of Kováts retention indices, methane and alkanes were injected together with the sample of PCBs. The characteristics of the capillary columns are given in Tables II and III.

TABLE II

CHARACTERISTICS OF COLUMNS COATED WITH OV-101

The columns used were as follows. No. 1: PN glass, length 28 m, I.D. 0.25 mm, etched 4 h at 623°K, coated dynamically with 0.3 ml of 10% OV-101 solution in *n*-hexane. No. 2: PN glass, length 29 m, I.D. 0.25 mm, etched 4 h at 623°K, coated dynamically with 3.0 ml of 10% OV-101 solution in *n*-hexane. No. 3: PN glass, length 29 m, I.D. 0.25 mm, etched 4 h at 623°K, coated dynamically with 3.0 ml of 10% OV-101 solution in *n*-hexane. No. 4: Unihost glass, length 74 m, I.D. 0.25 mm, inside volume 3.5 ml, etched 1 h at 373°K and 24 h at 573°K, coated dynamically with 0.15 ml of 20% OV-101 solution in chloroform using Hg plug at a rate 0.3 cm/sec. No .5: Unihost glass, length 70 m, I.D. 0.25 mm, inside volume 3.5 ml, etched 1 h at 373°K and 24 h at 573°K, coated dynamically with 0.15 ml of 20% OV-101 solution in chloroform using Hg plug at a rate 0.3 cm/sec. No. 6: Unihost glass, length 70 m, I.D. 0.25 mm, inside volume 3.53 ml, etched 1 h at 373°K and 24 h at 573°K, coated dynamically with 0.15 ml of 20% OV-101 solution in chloroform using Hg plug at a rate 0.3 cm/sec. No. 7: Unihost glass, length 66 m, I.D. 0.25 mm, inside volume 3.38 ml, etched 2 h at 623°K, coated dynamically with 0.3 ml of 10% OV-101 solution in *n*-hexane. k = capacity ratio; n = efficiency in theoretical plates; L = column length.

Column No.	*k*	*n*	*n/L*	*Coating efficiency (%)*
1	1.80	61,100	2260	—
	3 90	57,700	2140	
	5.98	56,900	2100	—
2	1.08	68,000	2340	
	2.24	70,300	2420	—
	4.05	63,900	2200	—
3	1.05	119,200	4770	—
	2.00	113,800	4550	—
	3.44	89,800	3590	—
4	2.53	255,200	3420	65.5
	5.08	241,300	3230	68.6
	8.53	196,300	2630	58.4
5	0.90	320,100	4560	68.4
	1.36	307,800	4385	73.8
	2.03	249,000	3547	65.5
6	1.46	204,800	2930	50.1
	2.61	176,000	2510	48.7
7	2.48	262,900	3980	76.4
	6.36	213,500	3230	72.4
	8.28	201,800	3060	68.5

Study of etched surfaces

For the studies of the glass capillaries after etching with gaseous HCl, a JEOL JXA-5A X-ray microanalyzer and a JEOL JSM-U3 scanning electron microscope (Jeol, Tokyo, Japan) were used. The SEM instrument (Dionýz Štúr Institute of Geology, Bratislava, Czechoslovakia) was used in cooperation with Dr. Švec.

TABLE III

CHARACTERISTICS OF COLUMNS COATED WITH CARBOWAX 20M

The columns used were as follows. No. 8: Unihost glass, length 54.6 m, I.D. 0.26 mm, inside volume 2.78 ml, etched 1 h at 373°K and 24 h at 573°K, coated dynamically with 0.15 ml of 10% Carbowax 20M solution in chloroform using Hg plug at a rate 0.36 cm/sec. No. 9: Unihost glass, length 51.8 m, I.D. 0.25 mm, inside volume 2.87 ml, etched 1 h at 373°K and 24 h at 573°K, coated dynamically with 0.15 ml of 10% Carbowax 20M solution in chloroform using Hg plug at a rate 0.33 cm/sec. No. 10: Unihost glass, length 53 m, I.D. 0.19 mm, inside volume 1.50 ml, etched 1 h at 373°K and 24 h at 573°K, coated dynamically with 0.15 ml of 10% Carbowax 20M solution in chloroform using Hg plug at a rate 0.33 cm/sec. No. 11: Unihost glass, length 67.5 m, I.D. 0.24 mm, inside volume 2.90 ml, etched 1 h at 373°K and 24 h at 573°K, coated dynamically with 0.15 ml of 10% Carbowax 20M solution in chloroform using Hg plug at a rate 0.28 cm/sec. No. 12: Unihost glass, length 70 m, I.D. 0.21 mm, inside volume 2.35 ml, etched 1 h at 373°K and 24 h at 573°K, coated dynamically with 0.15 ml of 10% Carbowax 20M solution in chloroform using Hg plug at a rate 0.40 cm/sec.

Column No.	*k*	*n*	*n/L*	*Coating efficiency (%)*
8	1.96	247,200	4530	84.7
	3.58	167,700	3070	63.9
9	1.68	238,500	4600	85.5
	4.84	181,500	3500	78.5
10	2.24	161,400	3045	43.6
	4.65	140,600	2600	43.0
11	1.59	230,000	3430	55.7
	2.92	200,000	2980	54.7
12	1.51	293,100	4200	59.3
	2.67	226,100	3230	51.7

RESULTS AND DISCUSSION

We have previously demonstrated that glass capillary columns coated with OV-101 stationary phase are suitable for the analysis of PCBs[15]. The columns used were prepared by etching their surface with methyl trifluorochloroethyl ether. As it is difficult to ensure the reproducibility of the filling and the etching of the column with the ether with this technique, we have made more extensive studies of glass capillary columns prepared from capillaries etched with HCl. The etched column surface was monitored by local electron microanalysis and scanning electron microscopy. The etched capillaries were coated dynamically. The reproducibility of column preparation and the effects of several variables on the quality of the columns prepared were tested by the separation of a mixture of PCBs (by the number of theoretical plates for peaks 9, 21 and 38 in Fig. 1) and by determining the Kováts retention indices of the PCBs.

It was found that some pairs of PCBs could not be separated on columns coated with OV-101, even though the columns used showed extremely good efficiencies. Therefore, the possibility of separating chlorinated biphenyls on capillary columns coated with polar stationary phases was also studied. Of the polar stationary phases tested in preliminary experiments, the best results were obtained with Carbowax 20M.

Columns with non-polar stationary phase (OV-101)

The separation of a mixture of PCBs (Aroclor 1242) together with C_{14}–C_{22} *n*-alkanes on a capillary column coated with OV-101 stationary phase is shown in Fig. 1 (column No. 7). This column was prepared using a capillary etched with HCl for 2 h

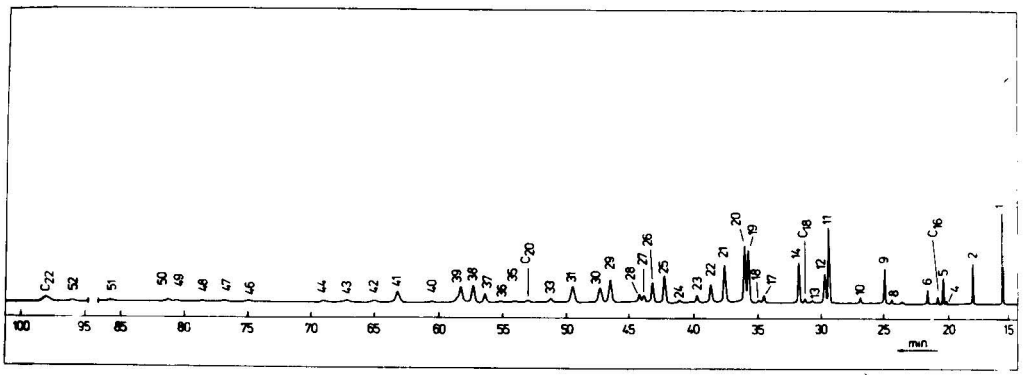


Fig. 1. Separation of components of Aroclor 1242 on a glass capillary column coated with OV-101 at 473°K (column No. 7). For peak numbering, see Table IV.

at 623 °K. It can be concluded, by comparing the results obtained by separating the same mixture of PCBs on a capillary column coated with OV-101 and having its surface etched with methyl trifluorochloroethyl ether[15] with those in Fig. 1, that the quality of the resolution of PCBs does not differ significantly.

In order to establish the effect of the variables on etching of the column surface with HCl and methyl trifluorochloroethyl ether, Kováts retention indices of PCBs on both columns were compared. Table IV gives the Kováts retention indices of PCBs found at 473 °K on column No. 7, together with published data[15]. The retention indices obtained for the column with its surface etched with gaseous HCl (column No. 7) were found to be lower than those for the column with the surface etched with methyl trifluorochloroethyl ether. It can be seen from the standard deviations (Table IV) that the fluctuations in the operating conditions during gas chromatography affects the variation of the results by less than ± 1 index unit.

Table V shows the Kováts retention indices of the main components of Aroclor 1242 found at 473 °K for columns coated with OV-101. The conditions of etching with HCl were identical. From the retention indices found for columns Nos. 1, 2 and 3 an average value $I = (I_1 + I_2 + I_3)/3$ and standard deviation (σ) were calculated. It follows from the results in Table V that the reproducibility of the preparation of the columns (expressed in terms of the retention indices of PCBs) after some standardization of the operating procedures can be better than ± 1 index unit. The last column in Table V gives the retention indices of PCBs obtained on a column made by coupling together columns Nos. 1, 2 and 3 (this coupling gave a 86-m long column having an efficiency of 261,200 theoretical plates for a capacity ratio $k = 2.19$, corresponding to about 3040 theoretical plates per metre). Moreover, the results show that by coupling individual columns together using shrinkable PTFE tubing, the retention indices were not affected significantly.

A comparison of the retention indices in Tables IV and V shows that they are also different when the process of etching the capillary surface with HCl was conducted at the same temperature but for a different period of time (the retention indices found for columns Nos. 1, 2 and 3, etched at 623 °K for 4 h, are higher than those found for column No. 7, etched at 623 °K for 2 h).

TABLE IV

KOVÁTS RETENTION INDICES (*I*) OF MAIN COMPONENTS OF AROCLOR 1242 MEASURED ON CAPILLARY COLUMNS COATED WITH OV-101 STATIONARY PHASE AT 473°K

Peak No.	*Structure*	*Column No. 7*		*I (ref. 15)*
		I	*Standard deviation (σ)*	
6	2,2′	1621.6	0.4	1625.8
8	2,3′	1686.0	0.7	1690.0
9	2,4′	1636.9	0.6	1700.9
10	2,2′,6	1731.8	0.4	1735.8
11	2,2′,5	1772.2	0.1	1776.2
12	4,4′ + 2,2′,3	1777.4	0.2	1781.8
14	2,2′,3	1805.8	0.6	1810.0
17	2,3′,5	1839.2	0.7	1843.6
18	2,3′,4	1844.2	0.7	1848.8
19	2,4′,5	1853.3	0.4	1858.1
20	2,4,4′	1856.7	0.6	1861.1
21	2′,3,4	1873.2	0.3	1878.1
22	—	1884.3	0.4	1890.2
23	—	1894.7	0.4	1899.7
24	—	1907.5	0.4	1912.5
25	2,2′,5,5′	1918.3	0.1	1922.7
26	2,2′,4,5′	1926.6	0.1	1931.3
27	2,2′,4,4′	1932.7	0.6	1937.1
28	—	1935.6	0.3	1939.1
29	2,2′,3,5′	1953.0	0.3	1958.1
30	2,2′,3,4′	1958.5	0.7	1965.2
31	—	1975.1	0.2	1980.1
33	2,2′,3,3′	1987.4	0.7	1992.7
37	—	2020.5	0.4	2025.7
38	2,3′,4′,5	2025.9	0.5	2031.3
39	—	2031.8	0.6	2037.4
41	—	2059.0	0.1	2065.3

As we have found that the reproducibility of the column preparation is significantly affected by the temperature at which the etching was performed, this process was carried out in a thermostat with a forced air circulation.

Table VI shows the Kováts retention indices of PCBs measured in three capillary columns coated with OV-101 at 473 °K. The conditions of etching with HCl were identical and the procedure applied was that used by Badings *et al.*[10]. It can be seen that the highest retention indices were found for column No. 5, which had the thinnest film of stationary phase ($k = 2.03$ for peak 37, Fig. 1), while the lowest retention indices were found for column No. 4, which had the thickest film ($k = 8.53$ for peak 37, Fig. 1). The data in Table VI also show that, when the surface of the glass column is etched with HCl using the procedure suggested by Badings *et al.*[10] and coated with a thin film of a non-polar stationary phase, the process of separation is governed, *inter alia*, also by the adsorption properties of the walls of the capillary columns.

TABLE V

KOVÁTS RETENTION INDICES (I) OF MAIN COMPONENTS OF AROCLOR 1242 MEASURED ON CAPILLARY COLUMNS COATED WITH OV-101 STATIONARY PHASE AT 473°K

Peak No.	*Column No.*			I	σ	A^*
	1	*2*	*3*			
6	1623.7	1624.2	1624.0	1624.0	0.5	1624.0
9	1698.3	1698.7	1699.0	1698.7	0.5	1698.9
10	1733.6	1734.2	1733.9	1733.9	0.4	1733.8
11	1774.0	1774.2	1774.2	1774.1	0.1	1774.4
12	1778.8	1778.9	1779.2	1779.0	0.3	1779.5
14	1807.1	1807.5	1807.5	1807.4	0.3	1807.5
17	1840.7	1841.3	1841.3	1841.1	0.4	1841.2
18	1845.7	1845.6	1845.4	1845.6	0.2	1846.3
19	1855.6	1855.7	1855.5	1855.6	0.1	1855.2
20	1858.5	1858.4	1859.0	1858.6	0.4	1858.7
21	1875.3	1875.3	1875.2	1875.3	0.2	1874.6
22	1886.4	1886.7	1886.0	1886.4	0.5	1887.0
23	1897.0	1897.4	1896.8	1897.1	0.3	1897.0
24	1909.7	1910.4	1909.9	1910.0	0.3	1909.6
25	1920.2	1920.3	1920.0	1920.2	0.2	1920.5
26	1928.5	1928.7	1928.2	1928.5	0.4	1928.8
27	1935.1	1934.8	1934.7	1934.9	0.4	1934.4
28	1937.3	1937.8	1937.0	1937.4	0.5	1937.6
29	1955.2	1955.2	1955.7	1955.5	0.1	1955.5
30	1961.4	1961.4	1961.3	1961.4	0.1	1961.5
31	1977.1	1977.3	1976.8	1977.1	0.3	1976.5
37	2022.4	2022.5	2022.1	2022.3	0.3	2022.6
38	2028.1	2028.6	2028.2	2028.3	0.4	2028.2
39	2034.2	2034.4	2034.1	2034.2	0.3	2033.9
41	2061.5	2061.8	2061.4	2061.6	0.3	2061.5

* Retention indices with columns Nos. 1, 2 and 3 coupled together (see text).

The separation of Aroclor 1242 on capillary column No. 4 coated with OV-101 at 473 °K is shown in Fig. 2.

It follows from a comparison of Figs. 1 and 2 that on the capillary column coated with a thin film (column No. 4) of OV-101 some of the peaks were split (peaks Nos. 12, 14 and 30). The splitting disappeared when the capillary was coated with a thicker film of the stationary phase. This observation agrees with the conclusions of Franken and Rutten[13], drawn from the separation of PCBs at extremely low substance concentrations on glass capillary columns coated with SE-30.

A comparison of the surface of the capillary etched with HCl at 573 °K for 4 h (Fig. 3) with that resulting from etching of the surface for 24 h (Fig. 4) shows some changes in the crystal structure as a function of the heating time.

By coupling together columns Nos. 4 and 6, a 144.4-m long column with an efficiency of 471,290 theoretical plates (for peak 37, with a capacity ratio $k = 4.12$) was obtained. When PCBs were separated on this capillary column, peaks 12, 14 and 30 (Fig. 5) remained unresolved.

TABLE VI

KOVÁTS RETENTION INDICES OF MAIN COMPONENTS OF AROCLOR 1242 MEASURED ON CAPILLARY COLUMNS COATED WITH OV-101 STATIONARY PHASE AT 473°K

Peak No.	*Column No.*		
	4	*5*	*6*
6	1620.7	1631.4	
9	1692.9	1698.3	1698.0
10	1726.5	1732.5	1731.4
11	1765.7	1773.6	1772.5
12	1770.5	1778.6	1777.5
14	1797.6	1806.5	1805.3
17	1832.5	1842.3	1840.2
18	1837.7	1848.6	1845.9
19	1847.3	1856.2	1854.5
20	1850.4	1859.8	1858.1
21	1868.0	1875.5	1873.9
22	1879.6	1887.0	1885.5
23	1890.3	1895.7	1894.9
24	1903.5	1908.7	1907.1
25	1915.0	1922.1	1917.8
26	1923.6	1929.8	1928.0
27	1929.6	1935.4	1933.5
28	1932.7	1936.8	1935.8
29	1951.1	1956.3	1954.5
30	1957.5	1961.8	1960.5
		1965.0	1963.5
31	1973.8	1976.5	1975.6
37	2020.4	2024.6	2022.5
38	2026.0	2030.1	2029.0
39	2031.8	2036.4	2034.7
41	2059.1	2063.2	2062.0

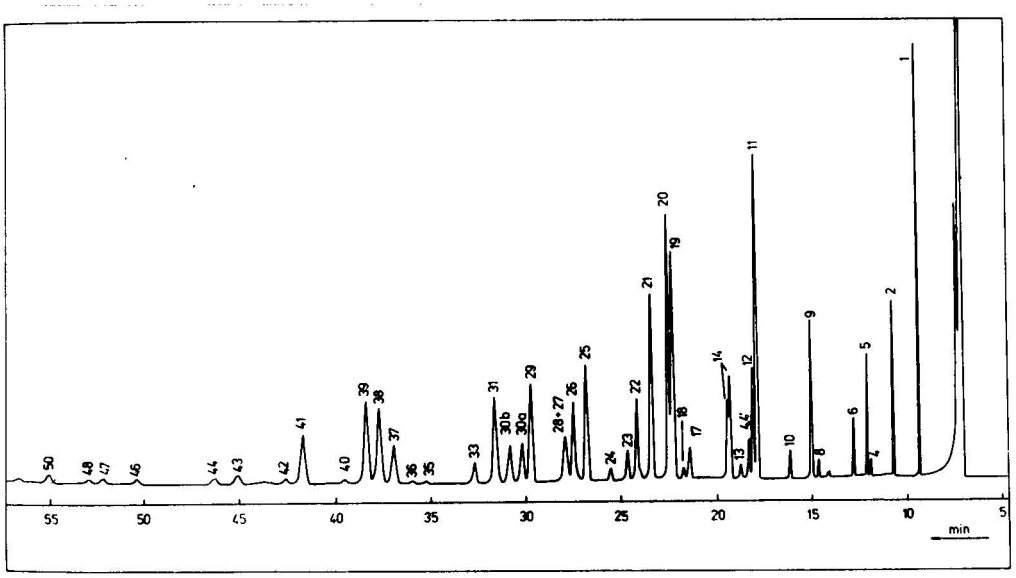


Fig. 2. Separation of components of Aroclor 1242 on a glass capillary column coated with OV-101 at 473°K (column No. 4).

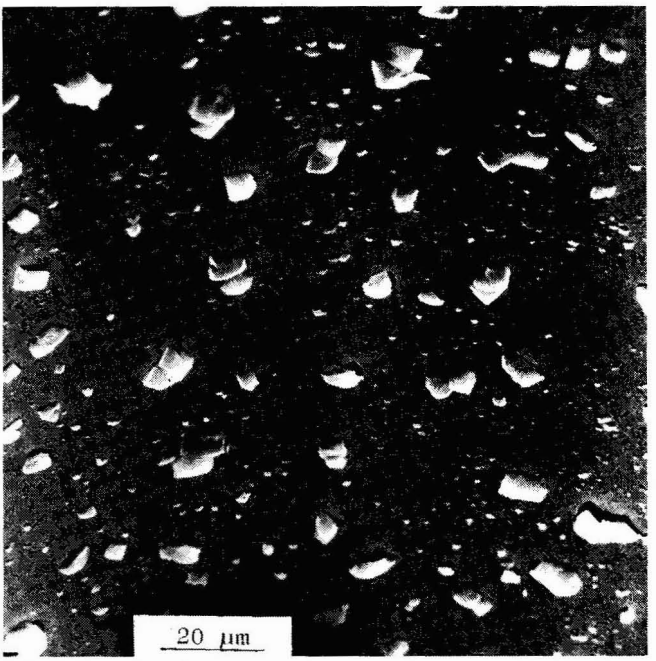


Fig. 3. Scanning electron micrograph of the inner wall of a glass capillary etched for 4 h at 573°K.

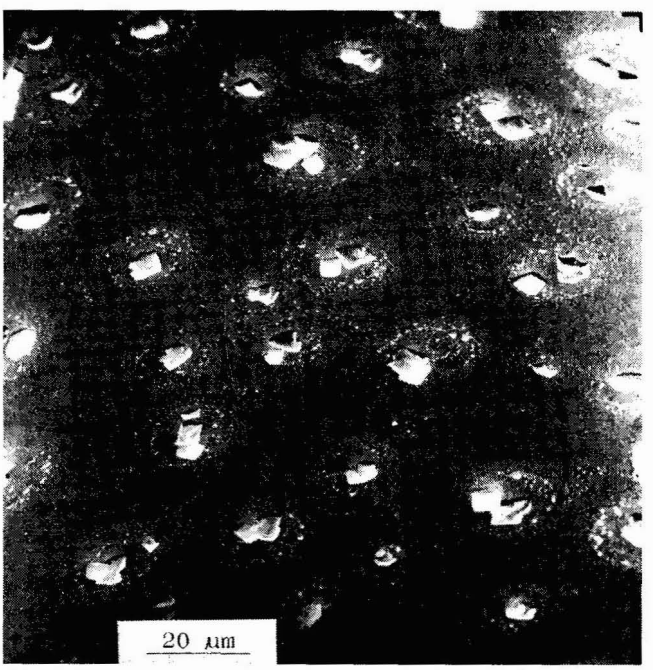


Fig. 4. Scanning electron micrograph of the inner wall of a glass capillary etched for 24 h at 573°K.

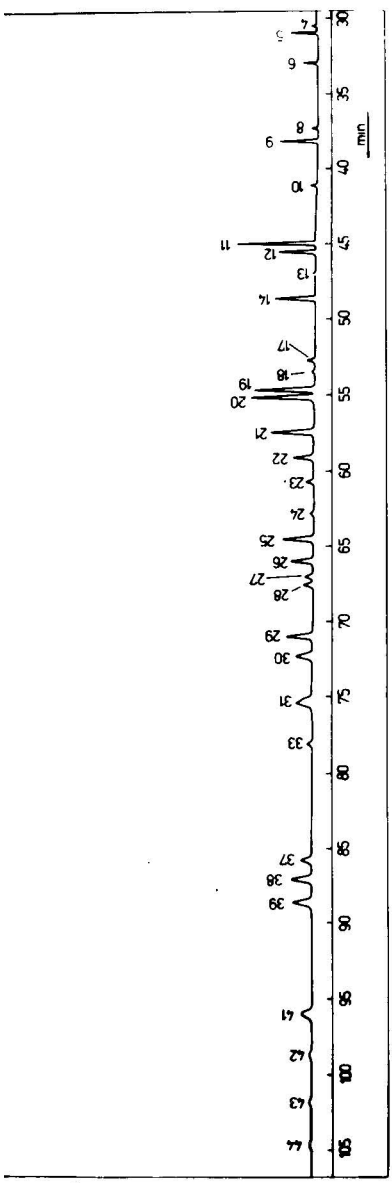


Fig. 5. Separation of components of Aroclor 1242 on a glass capillary column coated with OV-101 at 473°K (coupled columns Nos. 4 and 6).

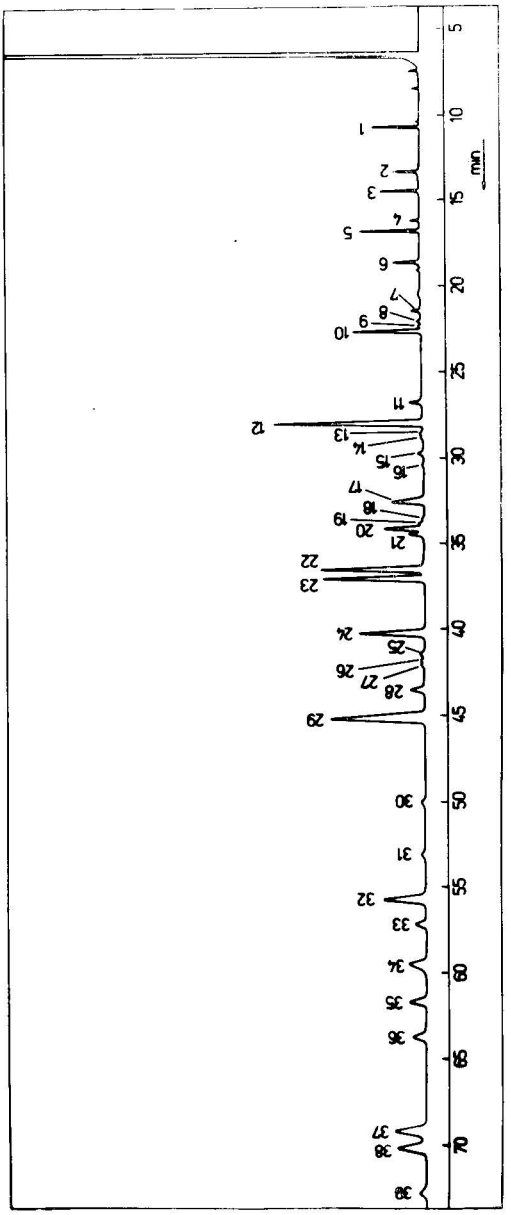


Fig. 6. Separation of components of Aroclor 1242 on a glass capillary column coated with Carbowax 20M at 473°K (column No. 8).

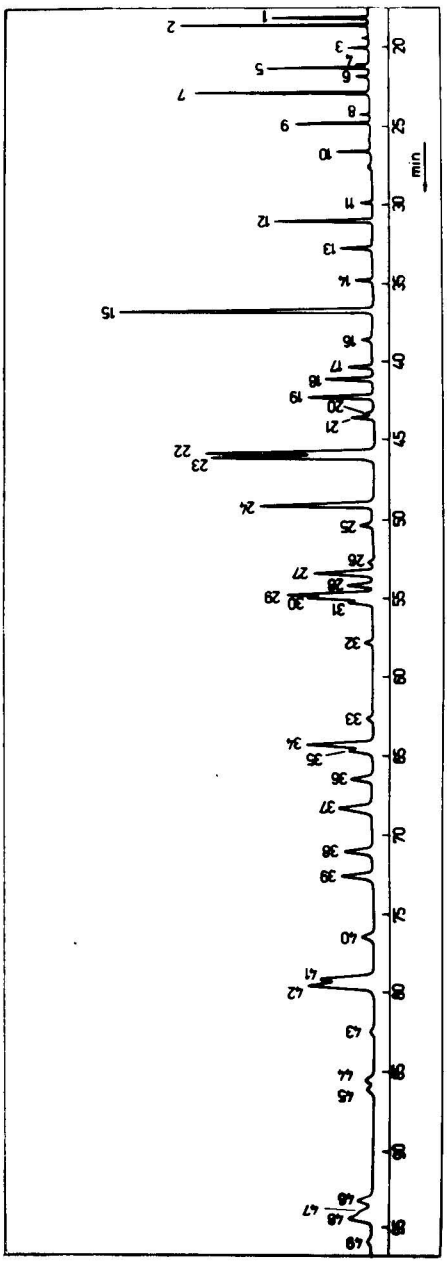


Fig. 7. Separation of components of Aroclor 1242 on a glass capillary column resulting from coupling column No. 7 (OV-101) with column No 11. (Carbowax 20M) at 473°K.

TABLE VII

KOVÁTS RETENTION INDICES OF SOME COMPONENTS OF AROCLOR 1242 MEASURED ON CAPILLARY COLUMNS COATED WITH CARBOWAX 20M STATIONARY PHASE AT 473°K

Peak No.	*Column No.*		
	8	*9*	*10*
1	2020.3	2019.3	2013.4
2	2158.7	2158.9	2152.0
3	2264.9	2255.9	2257.7
4	2282.9	2283.4	2275.7
5	2332.1	2332.5	2324.8
6	2418.6	2419.5	2411.2
7	2488.1	2489.1	2481.2
10	2529.4	2530.3	2509.9
12	2563.2	2565.4	2556.3
17	2611.3	2612.8	2604.5
20	2652.9	2653.6	2645.2
21	2658.0	2658.5	2650.1
22	2670.8	2672.1	2663.2
23	2682.4	2683.6	2674.4
24	2685.4	2686.8	2677.6
25	2720.5	2721.7	2712.4
26	2740.6	2741.6	2732.3
27	2757.0	2757.7	2748.4
28	2766.6	2767.2	2757.8
29	2780.0	2781.0	2771.3
30	2782.9	2783.7	2774.0
31	2792.7	2793.9	2783.5

Columns with polar stationary phase (Carbowax 20M)

The thermal stability of capillary columns coated with Carbowax 20M was studied by Schomburg and Husmann[14]. They found that on heating for 204 h at 473 °K, the capacity ratio of *n*-dodecane changed from the original value of $k = 1.87$ to 1.64 and the Kováts retention index of *n*-butanol at 353 °K changed from 1131 to 1116. It is thus obvious that the reproducibility of the preparation of the columns depends on the standardization of all operating procedures and that the properties of Carbowax 20M columns are also altered by ageing. In spite of this, separation of PCBs on a column coated with Carbowax 20M provides useful complementary information for the identification of PCBs in environmental analysis.

Fig. 6 shows the separation of Aroclor 1242 on a capillary column coated with Carbowax 20M at 473 °K (column No. 8). The peak numbering in Fig. 6 is different from that in Figs. 1–3.

A comparison of the data in Tables II and III shows that the efficiency of capillary columns coated with Carbowax 20M is comparable with that of columns coated with OV-101.

The Kováts retention indices found for PCBs (Table VII) differ significantly despite the fact that the etching procedure applied was identical and the film thickness of the phase does not differ significantly (the capacity ratio for peak 12 in Fig. 6 changes for the columns in Table VII from $k = 3.58$ to 4.65).

Column coupling provides a means for obtaining a column of required polarity. Fig. 7 shows the separation of Aroclor 1242 on a capillary column resulting from coupling column No. 7 (OV-101) with column No. 11 (Carbowax 20M). The column thus obtained showed for peak 15, with a capacity ratio $k = 2.14$, an efficiency of 487,000 theoretical plates.

The identification of PCBs present on chromatograms obtained using Carbowax 20M glass capillary columns is currently being studied and the results will be published later.

REFERENCES

1 M. Novotný and A. Zlatkis, *Chromatogr. Rev.*, 14 (1971) 1.
2 R. Kaiser (Editor), *Proceedings of the First International Symposium on Glass Capillary Chromatography Including Glass Micropacked Columns, May 4–7, 1975, Hindelang, G.F.R.*, Institut für Chromatographie, Bad Dürkheim, G.F.R., 1975.
3 K. Grob, *Chromatographia*, 8 (1975) 423.
4 G. Alexander, G. Garzó and G. Pályi, *J. Chromatogr.*, 91 (1974) 25.
5 G. Alexander and G. A. F. M. Rutten, *J. Chromatogr.*, 99 (1974) 81.
6 K. Tesařík and M. Novotný, in H. G. Struppe (Editor), *Gas-Chromatographie 1968*, Akademie-Verlag, Berlin, 1968, p. 755.
7 A. L. German and E. C. Horning, *J. Chromatogr. Sci.*, 11 (1973) 76.
8 S.-N. Lin, C. D. Pfaffenberger and E. C. Horning, *J. Chromatogr.*, 104 (1975) 319.
9 G. Nota, G. C. Goretti, M. Armenante and G. Marino, *J. Chromatogr.*, 95 (1974) 229.
10 H. T. Badings, J. J. G. van der Pol and J. G. Wassink, *Chromatographia*, 8 (1975) 440.
11 G. A. F. M. Rutten and J. A. Luyten, *J. Chromatogr.*, 74 (1972) 177.
12 G. Schomburg, H. Husmann and F. Weeke, *J. Chromatogr.*, 99 (1974) 63.
13 J. J. Franken and G. A. F. M. Rutten, in S. G. Perry (Editor), *Chromatography 1972*, Applied Science Publ., Barking, 1973, p. 75.
14 G. Schomburg and H. Husmann, *Chromatographia*, 8 (1975) 517.
15 J. Krupčík, P. A. Leclercq, A. Šímová, P. Suchánek, M. Čollák and J. Hrivňák, *J. Chromatogr.*, 119 (1976) 271.
16 D. H. Desty, J. N. Haresnape and B. H. F. Whyman, *Anal. Chem.*, 32 (1960) 302.
17 L. S. Ettre, *Open Tubular Columns in Gas Chromatography*, Plenum Press, New York, 1965.

Journal of Chromatography, 126 (1976) 161–169
© Elsevier Scientific Publishing Company, Amsterdam — Printed in The Netherlands

CHROM. 9452

NEW METHOD FOR THE PREPARATION OF HIGHLY STABLE POLYSILOXANE-COATED GLASS OPEN-TUBULAR CAPILLARY COLUMNS AND APPLICATION TO THE ANALYSIS OF HORMONAL STEROIDS

C. MADANI and E. M. CHAMBAZ
Laboratoire d'Hormonologie, C.H.U. de Grenoble, 38700 La Tronche (France)
and
M. RIGAUD, J. DURAND and P. CHEBROUX
Biochimie, C.H.U. Dupuytren, 87031 Limoges (France)

SUMMARY

A new approach to the preparation of methylsiloxane-coated glass open-tubular capillary columns is described. A siloxane polymeric mixture is first prepared by hydrolysis of dimethyldichlorosilane. The polymer is then coated on to the previously etched glass wall by a base-catalyzed reaction to yield a non-polar system of high stability and showing satisfactory chromatographic properties. This type of column has been used for the high-resolution separations of complex hormonal steroid mixtures. The flexibility of this method should permit the preparation of capillary systems with a wide range of polarity.

INTRODUCTION

During the last 10 years, considerable efforts have been devoted to the development of glass open-tubular columns suitable for high-resolution separations in biochemical analysis[1]. However, the lack of stability at high temperature of wall-coated open-tubular (WCOT) columns was an early recognized problem attributed to the tendency of the liquid film to break up into droplets[2]. Two main approaches have been followed in order to improve the spreading and stability of the stationary phase film. The first solution aims to achieve greater wettability of the column wall by chemical modification of the glass surface[3] or by adding a surfactant to the coated phase[4]. Using either dynamic or static coating procedures, this approach has been successful for the separation of hormonal steroid metabolites[5–7]. The second approach consists in retaining the stationary phase by coating it together with a finely powdered support material[8]. Both non-polar and polar columns obtained by following this principle have been successfully applied to the separation of biochemical mixtures, including steroids[9–11].

In this work, we followed another approach for the coating of the capillary glass wall, using a siloxane polymer obtained by prior hydrolysis of dimethyldichlorosilane (DMCS). The polymeric product was then made to react *in situ* under base-

catalyzed conditions to yield a coating with a high stability probably due to chemical bonding to the glass surface.

The capillary columns prepared by this procedure were evaluated for their chromatographic properties, especially with regard to their application in hormonal steroid analysis.

EXPERIMENTAL

Glass capillary tubes

Borosilicate glass tubing (Pyrex, Sovirel, Paris, France) of 6 mm O.D. and 4 mm I.D. was used after rinsing it successively with water, methanol and acetone. A coiled capillary tube (13 cm in diameter) was obtained using a Sedere (Paris, France) drawing machine, yielding a capillary of 0.20–0.25 mm I.D. The capillary tube was filled with gaseous hydrogen chloride according to the method of Alexander and Rutten[5], sealed at both ends and heated at 350° for 24 h. After this etching step, the tube was flushed with a stream of nitrogen and was then ready for coating.

Siloxane polymer

To an ice-chilled flask containing 40 ml of DMCS (Pierce, Rockford, Ill., U.S.A.) 60 ml of 12.5% ammonia solution were added dropwise with continuous agitation. The oily product that formed during the reaction was left overnight in the aqueous medium. The polymeric product was then thoroughly washed with distilled water until neutral and the remaining water was removed by centrifugation. The final clear fluid obtained was dissolved in methylene chloride (20%, v/v).

Coating of the column

A plug (about one quarter of the column length) of the polymer solution was pushed through the capillary tube under a slight nitrogen pressure (5–10 cm/sec). This step was carried out very easily owing to the fluidity of the polymeric preparation. The column was then dried with a nitrogen stream for 2 h and filled with ammonia generated in a connected flask by adding 25% ammonia solution to solid sodium hydroxide. After sealing at both ends, the column was heated in an oven at 320° for at least 24 h. Thereafter, the coated column was installed in the gas chromatograph and conditioned by programming the temperature from 150° to 200° at 2°/min. The column was then ready for use.

Gas chromatography

Gas chromatography was carried out with Carlo Erba Model 2400 T and 2200 instruments with a flame-ionization detector and hydrogen as the carrier gas at a flow-rate of 0.8–1.5 ml/min. The instruments were equipped with an all-glass solid injector system[12] and a temperature programmer accessory.

Infrared spectra

IR spectra were recorded with a Beckman IR-8 instrument, in methylene chloride as the solvent, at a 10% (v/v) concentration for the siloxane polymer and a 1% (v/v) concentration for the commercially available OV-1 phase (Supelco, Bellefonte, Pa., U.S.A.).

Biological samples

Steroids were purchased from Mann Labs. (New York, N.Y., U.S.A.). Methyloxime trimethylsilyl ethers (MO-TMS) were prepared according to Gardiner and Horning[13] and benzyloxime trimethylsilyl ethers (BO-TMS) as described by Devaux *et al.*[14]. Extraction and treatment of urinary steroid metabolites from human adult subjects or newborn infants were carried out as previously described[15,16].

RESULTS AND DISCUSSION

Chromatographic properties of the methylsiloxane-coated columns

Some fundamental chromatographic parameters were evaluated using straight-chain hydrocarbons and steroidal structures of biological interest as MO-TMS derivatives. The values obtained for different columns are listed in Table I. These parameters compared favourably with the data published for both WCOT and support-coated capillary systems[17], particularly with regard to their efficiency as reflected by the number of theoretical plates per metre. Although the capacity factors for the alkanes appeared satisfactory, further studies are needed in order to evaluate more precisely the amount of coated phase (*e.g.*, phase ratio) for the sake of comparison with established glass capillary systems[17].

TABLE I

CHARACTERISTICS OF METHYLSILOXANE-COATED OPEN-TUBULAR CAPILLARY COLUMNS

Property	*Column No.*		
	1	*2*	*3*
Length (m)	20	27	29
Internal diameter (mm)	0.20	0.20	0.20
Temperature (°C)	220	220	220
Capacity factor for:			
n-C_{24}	5.61	4.50	6.92
Androsterone	7.3	7.08	–
Etiocholanolone	7.7	7.46	–
Linear gas velocity (cm/sec)	23.8	23.48	24
Separation number (TZ), *n*-C_{24-26}	27.1	33.3	34.4
Plate height (mm)	0.41	0.28	0.31
Theoretical plates per metre for:			
n-C_{24}	2425	3524	3230
Androsterone	1620	3340	–
Etiocholanolone	1680	2712	–
Resolution: androsterone–etiocholanolone	6.46	13.09	–

The straightforward and easy procedure of preparation of these wall-coated columns yielded reproducible chromatographic characteristics and no failure due to practical difficulties such as clogging as in the preparation of support-coated material was encountered[17].

Nature of the coating

Various conditions have been described for obtaining a polymeric structure by

hydrolysis of DMCS[18]. Under our basic conditions (excess of ammonia solution) and in the absence of end-blocker[19], the reaction could be expected to yield both cyclic moieties of the type $(O\text{–}Si(CH_3)_2\text{–}O)_n$ (n being mostly 5–10) and linear chains bearing free terminal hydroxyl groups[18,19]. Infrared spectra of the prepared polymeric mixture and of a commercially available OV-1 phase were recorded and compared (Fig. 1). Similar general spectral features were obtained but an absorption band at 3600 cm^{-1} indicated that the siloxane mixture contained free hydroxyl groups whereas, as expected, the OV-1 did not.

After spreading of the siloxane polymeric mixture on to the column wall, the second step of the procedure involved heating of the preparation at 320° under alkaline conditions (gaseous ammonia generated from an aqueous medium). Under these conditions, one might expect rearrangements of the cyclic siloxane structures as well as hydrolysis of straight chains[18,19]. Under heating one might suppose that covalent bonding would occur between siloxane moieties and the glass surface. The

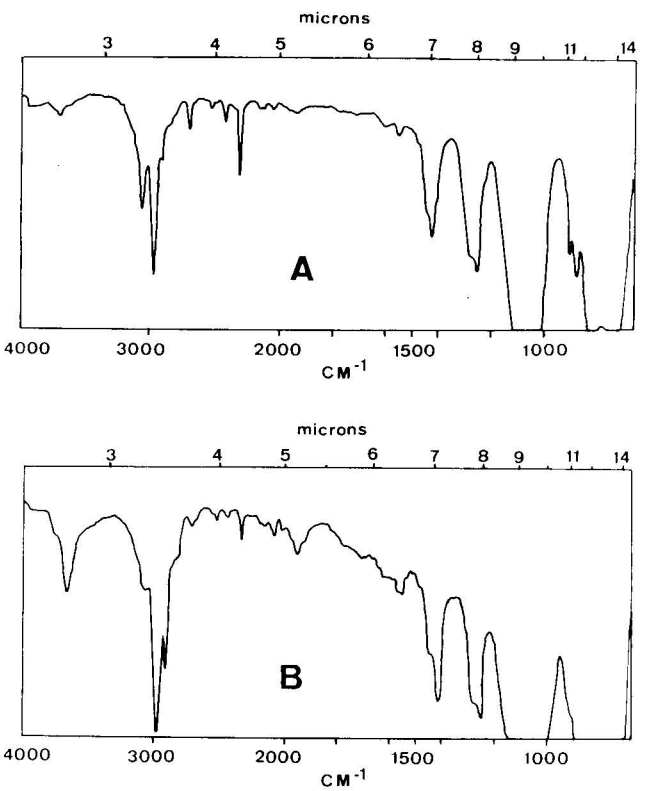


Fig. 1. Comparative infrared spectra (800–4000 cm^{-1}) of (A) commercially available methylpolysiloxane OV-101 in methylene chloride and (B) siloxane polymer, obtained by hydrolysis of DMCS, in methylene chloride.

latter had previously been etched and should present a large number of accessible free hydroxyl groups. Silica-bound siloxanes have been obtained under similar conditions by several research groups and attributed to dehydration reactions[20–22].

To check the extent of chemical bonding of the siloxane phase to the glass surface, a column was extracted overnight with dichloromethane. After elimination of the solvent, unchanged chromatographic properties were found for this extracted column. However, this result may not provide definite proof of chemical bonding as very stable ("non-extractable") association of a commercial polysiloxane phase with diatomaceous support has been reported[21]. In this instance, the association was explained by physical interactions favoured by a heating step at 350°[21]. However, under our conditions, chemical bonding with the participation of end-chain functional groups was further suggested by the fact that the presence of ammonia in the coating step was essential for satisfactory results. In addition, preliminary results showed that satisfactory capillary coating could be achieved by following the same procedure using phenyl-substituted silanes instead of DMCS as the starting monomer. This result suggested that chemical bonding is a major common mechanism leading to a stable phase film.

Separation of hormonal steroid metabolites

The retention parameters of several major human steroid metabolites as MO-TMS derivatives were determined on two different methylsiloxane-coated capillary columns. The values obtained could be compared with those given by a conventional 1% OV-1 packed column (Table II). The figures were mostly identical in all instances, showing that the capillary coating had very similar chromatographic properties compared with the widely used methylpolysiloxane OV-1, at least in the temperature range employed (190–280°).

TABLE II

RETENTION PARAMETERS OF STEROID METABOLITES AS MO-TMS (METHYLENE UNITS)

Compound	*Siloxane-coated capillary*		*1% OV-1 packed column (4 m)*
	27 m	*24 m*	
Androsterone	25.01	25.00	25.01
Etiocholanolone	25.20	25.21	25.22
Dehydroepiandrosterone	25.63	25.61	25.63
11-Ketoandrosterone	26.03	26.00	26.00
11-Ketoetiocholanolone	26.14	26.13	26.10
11-Hydroxyandrosterone	26.97	26.98	26.93
11-Hydroxyetiocholanolone	27.14	27.15	27.12
Pregnanediol	27.57	27.56	27.58
Pregnanetriol	27.89	27.89	28.00
Tetrahydrodesoxycortisol	28.63	28.71	28.61
Tetrahydrocortisone	29.60	29.69	29.60
Tetrahydrocortisol	30.21	30.29	30.23
allo-Tetrahydrocortisol	30.34	30.42	30.36
Cortolone	30.45	30.51	30.50
β-Cortolone	30.74	30.83	30.79

The separation of a model mixture of steroid metabolites as MO-TMS derivatives is shown in Fig. 2. The resolution was such as to yield a complete separation between metabolites that are usually difficult to resolve, *e.g.*, isomeric 11-oxoandrosterone and 11-oxoetiocholanolone. The very low bleeding level permitted the use of routine operating conditions using injection of 5 ng for each compound with the flame-ionization detector. In addition, very good response coefficients with regard to the internal standard were obtained, especially for the main corticosteroid metabolites. This indicated a limited adsorption level and satisfactory quantitative properties at the nanogram level.

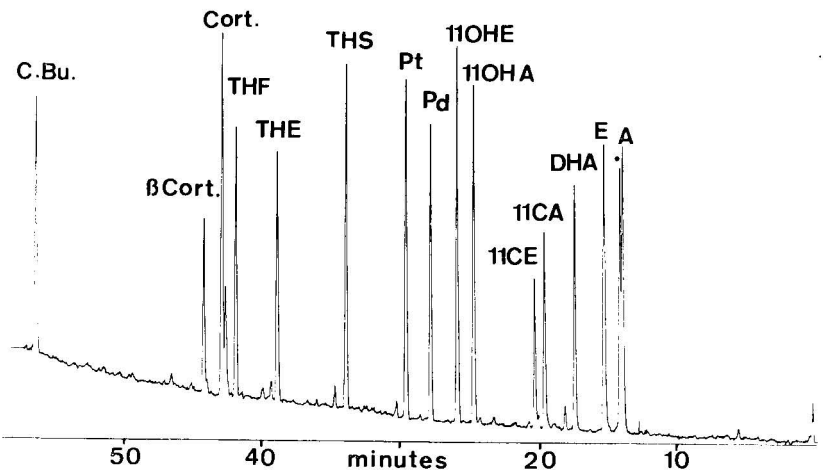


Fig. 2. GLC separation on a methylsiloxane-coated open-tubular column of a steroid mixture as MO-TMS derivatives. Temperature programming from 170° to 280° at 2°/min; 5 ng of each compound were injected. Peaks: A = androsterone; E = etiocholanolone; DHA = dehydroepiandrosterone; 11CA = 11-ketoandrosterone; 11CE = 11-ketoetiocholanolone; 11OHA = 11β-hydroxyandrosterone; 11OHE = 11β-hydroxyetiocholanolone; Pd = pregnanediol; Pt = pregnanetriol; THS = tetrahydro-11-deoxycortisol; THE = tetrahydrocortisone; THF = tetrahydrocortisol; Cort. = cortolone-20α; βCort. = cortolone-20β; C.Bu = cholesteryl butyrate (internal standard).

The chromatogram given by the neutral urinary steroid extract from a 2-year-old patient with a congenital adrenal cortex hyperplasia (21-hydroxylase defect) is given in Fig. 3. The isomeric pregnanetriols of clinical interest in such a case were completely resolved, as well as the related ketonic metabolites.

Fig. 4 illustrates the result obtained after administration of metyrapone in a normal adult subject. In such cases, conventional packed columns would give erroneously high values for the major metabolite of cortisone (THE), falsely suggesting a lack of effect of the drug on the adrenal hydroxylating capacity. The high resolution attained by the capillary column permitted the corresponding peak to be resolved into two components.

Fig. 5 shows the analysis of the urinary steroid metabolites extracted as sulpho-conjugates from a pool of 3-day-old normal human newborn urines. The use of BO-TMS derivatives is of great interest in this case for structural studies of unknown newborn steroid metabolites[14,23]. However, these bulky derivatives greatly increase

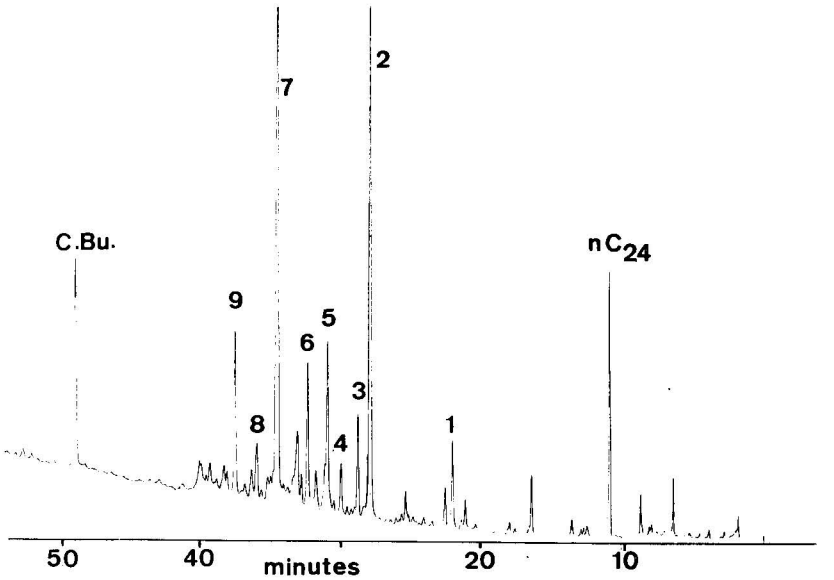


Fig. 3. GLC analysis of the neutral urinary steroid metabolites (MO-TMS) in a case of 21-hydroxylase defect. Analytical conditions as in Fig. 2. Peaks: 1 = androsterone; 2 = pregnanediolone; 3 = pregnanediolone; 4 = pregnanetriol; 5 = pregnanetriol; 6 = pregnanediolone; 7 = pregnanediol-dione; 8, 9 = unknown metabolites; C.Bu = cholesteryl butyrate (internal standard).

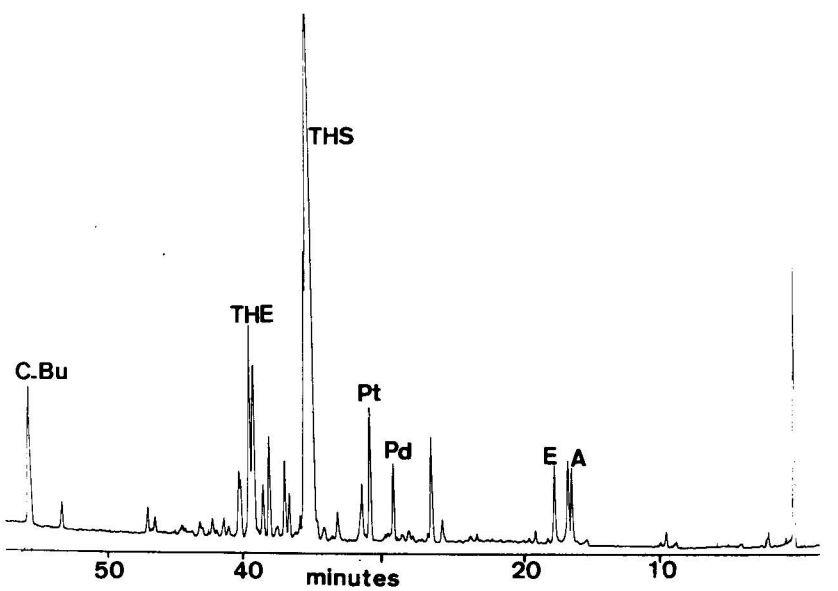


Fig. 4. Neutral urinary steroid extract (MO-TMS) from a normal subject after administration of metyrapone. Temperature programmed from 168° to 260° at 2°C/min. Abbreviations as in Fig. 2.

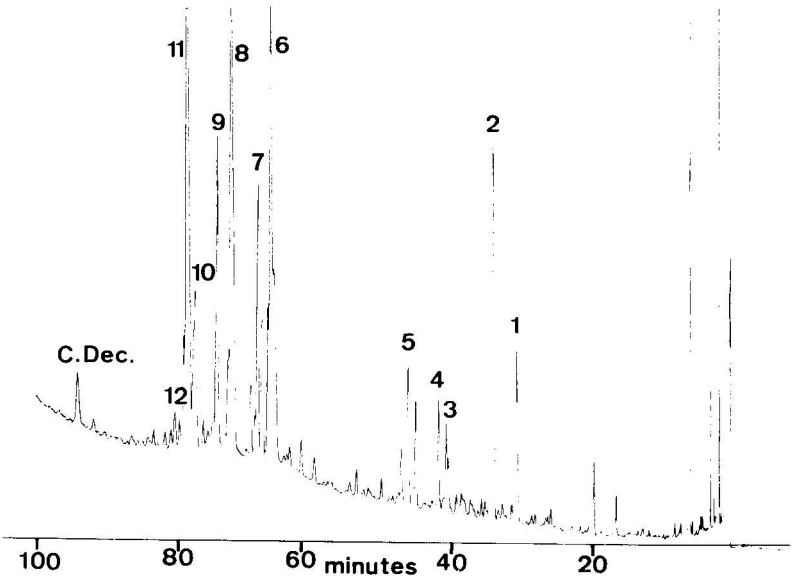


Fig. 5. Methylsiloxane-coated capillary column separation of the steroids excreted as sulphates in a urine pool from 3-day-old human newborns. BO-TMS derivatives; temperature programming from 190° to 310° at 2°/min. Peaks: 1 = androstenetriol; 2 = androst-5-ene-3β,16α,17β-triol; 3 = androstenetetrol; 4 = androstenetetrol; 5 = pregnanetriol; 6 = 3β,16α-dihydroxyandrost-5-ene-17-one; 7 = androstenetriolone; 8 = 3β,17β-dihydroxyandrost-5-ene-16-one + pregnanediolone; 9 = pregnenetriolone; 10 = androstenetriolone; 11 = 3β,16α-dihydroxypregn-5-ene-20-one; 12 = 3β,21-dihydroxypregn-5-ene-20-one; C.Dec. = cholesteryl decylate (internal standard).

the retention values and elution temperatures. The siloxane-coated capillary system appeared to remain very satisfactory both concerning its chromatographic properties and its stability under repeated routine temperature programming conditions up to 310°.

CONCLUSION

Although further studies are needed in order to characterize fully the molecular nature of the glass-coated siloxane material, our proposed procedure provides a new approach to the preparation of wall-coated glass open-tubular capillary columns. In addition to the simplicity of the procedure, which appeared devoid of practical pitfalls, preliminary evidence suggests that it may also be employed for the preparation of polar coatings. These columns have proved satisfactory for hormonal steroid analysis; their potential use for the separation of other types of biological mixtures, including prostaglandins, is currently being investigated.

REFERENCES

1 M. Novotný and A. Zlatkis, *Chromatogr. Rev.*, 14 (1971) 1.
2 J. Merle d'Aubigne, C. Landault and G. Guiochon, *Chromatographia*, 4 (1971) 309.
3 K. D. Bartle, *Anal. Chem.*, 45 (1973) 1831.

4 F. Farre-Rius, J. Henniker and G. Guiochon, *Nature (London)*, 196 (1962) 63.
5 G. Alexander and G. A. F. M. Rutten, *J. Chromatogr.*, 99 (1974) 81.
6 G. A. F. M. Rutten and J. A. Luyten, *J. Chromatogr.*, 74 (1972) 177.
7 J. A. Völlmin, *Chromatographia*, 3 (1970) 233.
8 J. G. Nikely, *Anal. Chem.*, 44 (1972) 625.
9 A. L. German, C. D. Pfaffenberger, J. P. Thenot, M. G. Horning and E. C. Horning, *Anal. Chem.*, 45 (1973) 930.
10 P. van Hout, J. Szafranek, C. D. Pfaffenberger and E. C. Horning, *J. Chromatogr.*, 99 (1974) 103.
11 S.-N. Lin, C. D. Pfaffenberger and E. C. Horning, *J. Chromatogr.*, 104 (1975) 319.
12 A. Ros, *J. Gas Chromatogr.*, 3 (1965) 252.
13 W. L. Gardiner and E. C. Horning, *Biochim. Biophys. Acta*, 115 (1968) 524.
14 P. G. Devaux, M. G. Horning, R. M. Hill and E. C. Horning, *Anal. Biochem.*, 41 (1971) 7.
15 E. M. Chambaz, C. Madani and A. J. Hadjian, in S. G. Perry (Editor), *Chromatography 1972*, Vol. 1, Bartholomew Press, Dorking, 1973, p. 89.
16 R. A. Anderson, E. M. Chambaz, G. Defaye, C. Madani, T. A. Baillie and C. J. W. Brooks, *J. Chromatogr. Sci.*, 12 (1974) 636.
17 R. S. Deelder, J. J. M. Ramaekers, J. H. M. van den Berg and M. L. Wetzels, *J. Chromatogr.*, 119 (1976) 99.
18 W. Patnode and D. F. Willock, *J. Amer. Chem. Soc.*, 68 (1946) 358.
19 C. R. Trash, *J. Chromatogr. Sci.*, 11 (1973) 196.
20 R. E. Majors and M. J. Hopper, *J. Chromatogr. Sci.*, 12 (1974) 767.
21 C. R. Hastings, J. M. Augl, S. Kapila and W. A. Aue, *J. Chromatogr.*, 87 (1973) 49.
22 J. J. Kirkland and J. J. De Stefano, *J. Chromatogr. Sci.*, 8 (1970) 309.
23 T. A. Baillie, C. Grass, C. J. W. Brooks, C. Madani and E. M. Chambaz, in A. Frigerio (Editor), *Mass Spectrometry in Biology and Medicine*, Raven Press, New York, 1974, p. 335.

Journal of Chromatography, 126 (1976) 171–189
© Elsevier Scientific Publishing Company, Amsterdam — Printed in The Netherlands

CHROM. 9444

NEW PERSPECTIVES IN THE PREDICTION OF KOVÁTS INDICES

JACQUES R. CHRÉTIEN and JACQUES-ÉMILE DUBOIS

Laboratoire de Chimie Organique Physique, Université de Paris VII, 1 Rue Guy-de-la-Brosse, 75005 Paris (France)

SUMMARY

Sets of Kováts indices corresponding to different chromatographic conditions and/or to different chemical families can be rendered coherent by the use of topology–information correlations established according to the principles of the DARC (Description, Acquisition, Retrieval and Conception) topological system. These correlations are based on the Kováts indices or on data derived from these indices (Kováts index increment, ΔI, and isotopology factor, τI). They serve to demonstrate the prediction potential, the minimization of the number of parameters and of the number of data, and the precision of our approach. Chromatographic retention data banks can be envisaged on the basis of this approach.

INTRODUCTION

In analytical organic chemistry, the methods used for the acquisition and automatic computer processing of mass and nuclear magnetic resonance (NMR) spectroscopic data are advancing rapidly. There are already operational data banks in mass spectroscopy[1], and ^{13}C NMR spectroscopic data banks are currently being set up[2,3]. "File search" or "library search" computer systems are being used successfully in the computer-aided interpretation of mass spectra[2,3]. Nevertheless, from the data processing point of view, the identification of new compounds that have no reference spectrum is still the most difficult problem[4]; thus, current research on the method of asking these banks a question is aimed at discovering resemblances between compound sub-structures[5], rather than determining the identities of the compounds themselves.

Together with the means required to develop and exploit these spectroscopic data processing methods, a preliminary and qualitative chromatographic analysis may be a simple and useful complementary means of identification, provided that there is a rapidly accessible data bank. We shall show how such a data bank can be set up, starting from an in-depth exploitation of a population of Kováts indices which, in gas–liquid chromatography, are recognized as being the most reproducible retention data.

Although very useful collections of chromatographic retention data already exist[6–8], they often appear in handbook form and their use is relatively restricted to establishing whether or not a particular compound has already been studied and, if

so, under what conditions. Thus, an organic chemist often encounters two types of problems:

(1) When synthesizing a new family of compounds there are often no chromatographic data available to identify these products; however, there might be some products already studied whose structures are comparable but whose substituents or chemical functions are different. If so, how can he extrapolate the behaviour of new compounds from already known compounds?

(2) For a known compound, there may be available retention data obtained under certain chromatographic conditions (stationary phase SP_1 and temperature T_1), but not under other chromatographic conditions (SP_2 and T_2). If so, how can he extrapolate the behaviour of a known compound under new conditions (SP_2 and T_2) from already known conditions (SP_1 and T_1)?

The same methodology can be used to solve both of these problems. Indeed, the functional group and each site of the molecular environment of compounds belonging to a same population contribute an additional value to the Kováts indices. The variations in these elementary contributions result either from a structural variation (functional group, environment) or from a variation of the chromatographic conditions (stationary phase, polarity and temperature). These contributions and their variations can be grasped by setting up topology–information correlations[9–11]. We shall show how, with these correlations, it is possible to analyze and extend the information content of already published populations of Kováts indices. We shall also stress the strategy required in choosing the minimum number of pertinent compounds to permit the characterization of a population of compounds.

METHOD AND RESULTS

There are already many works on the establishment of retention–structure relationships, notably for hydrocarbon analysis[12–14], which have been recently reviewed[15–18]. In referring to one of these methods. Souter repeated his opinion "that a method is required, based on a much smaller number of structural terms. These terms would be evaluated by solving an over-determined set of equations expressing retention data for a number of compounds; least-squares methods would probably be applied in this procedure"[19].

We shall give examples of how the DARC* topological system[20,21], which is based on the concept of an Environment which is Limited, Concentric and Ordered (ELCO) (*i.e.*, on a topological description of the molecular environment from an origin taken as a focus), meets these criteria. As the principles of the DARC system as well as its generalization to the processing of polyfunctional compounds, of those with no apparent functional group and the simultaneous processing of different populations, appear elsewhere with chromatographic applications[11], we shall not consider them here.

In order to show how an in-depth exploitation of the Kováts indices could be envisaged so as to extend the information content of already published populations of Kováts indices, we shall deal successively with four chromatographic problems:

(1) the interpolation and extrapolation of structural effects;

* Description, Acquisition, Retrieval and Conception.

(2) the prediction of indices to be determined on stationary phase SP_2 at temperature T_1 on the basis of indices already determined for the same compounds on SP_1 at the same temperature T_1;

(3) the prediction of indices to be determined on SP_2 at T_2 based on those already determined on SP_1 at T_1;

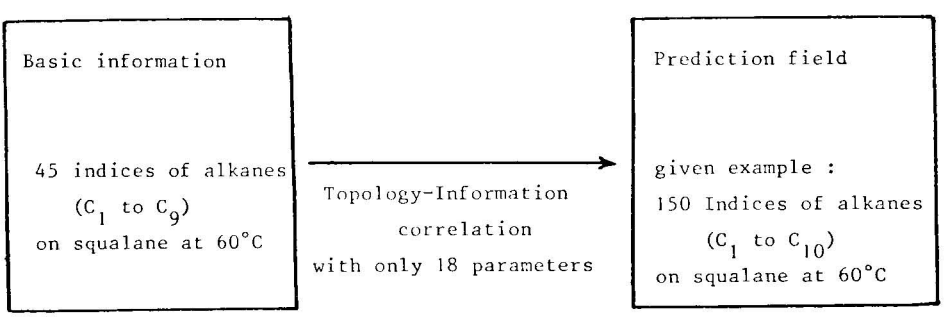
(4) the perturbations brought about by varying the functional group in different populations whose member compounds have comparable structures (*i.e.*, having the same ELCO).

Also, we shall consider the methodology problems raised by Souter: prediction potential, minimization of the number of parameters and of the number of data, and precision.

Prediction of structural effects: interpolation and extrapolation

Rijks[22,23] determined, on squalane at 50° and 70°, the Kováts indices of 45 alkanes having up to nine carbon atoms. We have re-calculated them at 60° and extended the population by including the first nine reference *n*-alkanes whose value is, by definition, already known. We have treated this population by a degree *n* topology–information correlation[13]. In the given example, we shall illustrate the flexibility in choosing a structural variable and the possibilities of minimizing the number of parameters. This will be done by re-grouping the topological sites located at the same distance from the focus, and having the same degree of ramification. We thus obtain a correlation having only 18 structural parameters. The correlation coefficient, R, is 0.9998 and the Exner ψ test is 0.026. For the 45 compounds analyzed by Rijks, the standard deviation is 3.9 I.U. and the average deviation between the experimental value and the value calculated on the basis of the correlation is 3.1 I.U., *i.e.*, the relative average deviation is $< 0.5\%$.

With this topology–information correlation, it is not only possible to make predictions for the alkanes with nine carbon atoms, but also those having more than nine carbon atoms. Insofar as the methodology is concerned, the extrapolations based on this correlation for alkanes having a greater number of carbon atoms than the alkanes used in establishing this correlation are justified by the degree *n* polyfocalization, thanks to the weight factors attributed to each of the topological sites[11]. As an example, in Table I we show the predictions for alkanes having up to ten carbon atoms, *i.e.*, 150 compounds of which only about 50 were used to establish the correlation (Scheme 1).



Scheme 1. Example of the prediction potential of a topology–information correlation.

TABLE I

PREDICTION OF KOVÁTS INDICES OF 150 C_1–C_{10} ALKANES ON SQUALANE AT 60° WITH A TOPOLOGY–INFORMATION CORRELATION LIMITED TO 18 PARAMETERS

With a 23-parameter correlation instead of a 17-parameter correlation, the maximum deviations are lowered by about half (*i.e.*, to *ca.* 1%).
The name of the main chain is indicated by the number of carbon atoms it contains (e.g., 6 = hexane, 11 = undecane). The main chain substituents are: M = methyl, DM = dimethyl, TM = trimethyl or tetramethyl, PM = pentamethyl, ET = ethyl, DET = diethyl, IPR = isopropyl.

Alkane	*Kováts indices on squalane at 60°*			*Difference*	
	Exptl. (Rijks) (a)	*Calc. (correlation) (b)*	*Exptl. (Matukuma) (c)*	$I_a - I_b$	$I_c - I_b$
1	100.0	100.0		0.0	
2	200.0	199.8		0.2	
3	300.0	297.9		2.1	
4	400.0	404.8		−4.8	
2-M3		360.3			
5	500.0	502.0		−2.0	
2-M4	475.4	478.4		−3.0	
2,2-DM3	412.6	407.1		5.5	
6	600.0	597.1		2.9	
2-M5	569.8	569.5		0.3	
3-M5	584.6	587.1		−2.5	
2,2-DM4	537.6	538.6		−1.0	
2,3-DM4	568.1	566.9		−1.2	
7	700.0	696.6		3.4	
2-M6	666.8	662.6		4.2	
3-M6	676.5	675.8		0.7	
3-ET5	686.6	686.1		0.5	
2,2-DM5	626.3	628.4		−2.1	
2,3-DM5	672.5	669.2		3.3	
2,4-DM5	630.1	633.9		−3.8	
3,3-DM5	660.2	660.4		−0.2	
2,2,3-DM4	641.1	643.6		−2.5	
8	800.0	797.8		2.2	
2-M7	765.0	761.2		3.8	
3-M7	772.6	773.4		−0.8	
4-M7	767.4	769.0		−1.6	
3-ET6		772.6			
2,2-DM6	719.9	715.6		4.3	
2,3-DM6	760.8	756.1		4.7	
2,4-DM6	732.4	738.3		−5.9	
2,5-DM6	728.7	726.7		2.0	
3,3-DM6	744.7	747.9		−3.2	
3,4-DM6	771.6	769.3		2.3	
2-M3-ET5	762.4	761.9		0.5	
3-M3-ET5	775.7	772.7		3.0	
2,2,3-TM5	738.6	744.8		−6.2	
2,2,4-TM5	690.9	694.9		−4.0	
2,3,3-TM5	761.4	759.2		2.2	
2,3,4-DM5	753.7	748.3		5.4	
9	900.0	899.0	900.0		1.0
2-M8		863.3	864.8		1.5

TABLE I (*continued*)

Alkane	*Kováts indices on squalane at 60°*			*Difference*	
	Exptl. (Rijks) (a)	*Calc. (correlation) (b)*	*Exptl. (Matukuma) (c)*	$I_a - I_b$	$I_c - I_b$
3-M8	870.4	873.7	870.8	−3.3	−2.9
4-M8		868.3	863.3		−5.0
3-ET7		874.6	867.4		−7.2
4-ET7		863.5	858.2		−5.3
2,2-DM7	815.9	815.6	816.5	0.3	0.9
2,3-DM7		852.7	855.5		2.8
2,4-DM7		830.6	821.2		−9.4
2,5-DM7		836.5	833.7		-2.8
2,6-DM7		819.6	827.5		7.9
3,3-DM7	836.9	839.6	837.3	−2.7	−2.3
3,4-DM7		860.5	858.0		−2.5
3,5-DM7		847.2	834.4		-12.8
4,4-DM7		839.9	828.6		-11.3
2M3-ET6		846.5	844.7		−1.8
2M4-ET6		833.2	824.9		−8.3
3M3-ET6		858.0	856.0		−2.0
3M4-ET6		859.7	855.6		−4.1
2,2,3-TM6	822.9	825.7	823.3	−2.8	−2.4
2,2,4-TM6	790.4	793.4	790.7	−3.6	−2.7
2,2,5-TM6	776.9	774.1	777.3	2.8	3.2
2,3,3-TM6		844.9	841.7		3.2
2,3,4-TM6	850.5	846.5	849.7	4.0	3.2
2,3,5-TM6	812.8	817.1	813.2	−4.3	−3.9
2,4,4-TM6	809.2	812.6	809.7	−3.4	−2.9
3,3,4-TM6		858.1	855.1		−3.0
3,3-DET5	879.8	875.3	880.2	4.5	4.9
2,2-DM-3-ET5	824.2	836.3	824.4	−12.1	−11.9
2,3-DM-3-ET5		865.2	875.0		9.8
2,4-DM-3-ET5	838.2	834.7	838.4	3.5	3.7
2,2,3,3-TM5	854.8	853.4	855.8	1.4	2.4
2,2,3,4-TM5	822.2	826.0	821.9	−3.8	−4.1
2,2,4,4-TM5	774.5	763.2	774.6	11.3	11.4
2,3,3,4-TM5	860.6	855.0	861.1	5.6	6.1
10		1000.2	1000.0		−0.2
2-M9		964.5	963.9		−0.6
3-M9		975.8	969.6		−6.2
4-M9		968.6	960.0		−8.6
5-M9		967.6	957.4		−10.2
3-ET8		976.6	964.0		−12.6
4-ET8		967.2	951.5		−15.7
2,2-DM8		918.6	914.9		−3.7
2,3-DM8		954.0	952.1		−1.9
2,4-DM8		930.8	915.8		−15.0
2,5-DM8		932.3	921.8		−10.5
2,6-DM8		933.0	931.5		−1.5
2,7-DM8		928.8	928.5		−0.3
3,3-DM8		941.4	932.0		−11.2
3,4-DM8		949.0	936.0		−13.0

(Continued on p. 176)

TABLE I (*continued*)

Alkane	*Kováts indices on squalane at 60°*			*Difference*	
	Exptl. (Rijks) (a)	*Calc. (correlation) (b)*	*Exptl. (Matukuma) (c)*	$I_a - I_b$	$I_c - I_b$
3,5-DM8		941.2	921.8*		−19.4
3,6-DM8		948.1	929.0*		−19.1
4,4-DM8		933.3	918.0		−15.3
4,5-DM8		953.9	943.1*		−10.8
4-IPR7		935.5	925.0		−10.5
2-M-3-ET7		947.6	941.0		−6.6
2-M-4-ET7		923.2	907.4		−15.8
2-M-5-ET7		936.8	924.8		−12.0
3-M-3-ET7		954.0	953.0		−1.0
3-M-4-ET7		948.7	935.7*		−13.0
4-M-3-ET7		955.3	940.5		−14.8
4-M-4-ET7		947.7	937.6		−10.1
2,2,3-TM7		923.8	914.4		−9.4
2,2,4-TM7		887.2	875.7		−11.5
2,2,5-TM7		885.4	878.1		−7.3
2,2,6-TM7		870.2	873.0		2.8
2,3,3-TM7		935.6	931.7		−3.9
2,3,4-TM7		936.9	933.4*		−3.5
2,3,5-TM7		925.1	912.9*		−12.2
2,3,6-TM7		909.7	919.0		+8.9
2,4,4-TM7		903.7	889.4		−14.3
2,4,5-TM7		920.6	906.7		−13.9
2,4,6-TM7		886.0	870.1		−15.9
2,5,5-TM7		897.2	891.7		−5.5
3,3,4-TM7		943.4	936.6		−6.8
3,3,5-TM7		915.6	907.7		−7.9
3,4,4-TM7		948.2	932.2		−16.0
3,4,5-TM7		949.0	945.0*		−4.0
2-M-3-IPR6		917.4	915.5		−1.9
3,3-DET6		958.3	954.1		−4.2
3,4-DET6		947.8	945.8		−2.0
2,2-DM-3-ET6		914.9	902.1		−12.8
2,2-DM-4-ET6		882.3	881.3		−1.0
2,3-DM-3-ET6		948.5	949.4		0.9
2,3-DM-4-ET6		935.0	930.6		−4.4
2,4-DM-3-ET6		930.6	929.8*		−0.8
2,4-DM-4-ET6		920.7	920.7		0.0
2,5-DM-3-ET6		905.6	891.4		14.2
3,3-DM-4-ET6		947.3	937.8		−9.5
3,4-DM-3-ET6		961.8	964.6		3.0
2,2,3,3-TM6		933.1	928.8		−4.3
2,2,3,4-TM6		918.2	908.8*		−9.4
2,2,3,5-TM6		881.1	873.3		−7.8
2,2,4,4-TM6		875.0	888.6		13.6
2,2,4,5-TM6		866.6	872.1		5.5
2,2,5,5-TM6		811.9	820.2		8.3
2,3,3,4-TM6		952.0	949.1		−2.9
2,3,3,5-TM6		908.0	903.3		−4.7

TABLE I (*continued*)

Alkane	*Kováts indices on squalane at 60°*			*Difference*	
	Exptl. (Rijks) (a)	*Calc. (correlation) (b)*	*Exptl. (Matukuma) (c)*	$I_c - I_b$	$I_c - I_b$
2,3,4,4-TM6		937.4	935.0		−2.4
2,3,4,5-TM6		922.2	923.1*		0.9
3,3,4,4-TM6		965.5	983.7		18.2
2,4-DM-3-IPR5		904.6	915.1		10.5
2,2,3-TM-3-ET5		958.2	965.7		7.5
2,2,4-TM-3-ET5		911.3	903.9		−7.4
2,3,4-TM-3-ET5		954.6	969.4		14.8
2,2,3,3,4-PM5		951.3	953.4		2.1
2,2,3,4,4-PM5		911.0	921.7		10.7
11		1101.4	1100.0		−1.4

* An average value is given for the two diastereoisomeric compounds analyzed by Matukuma.

The predictions based on the correlation are compared to Matukuma's experimental values[24] on squalane at 60° for alkanes with nine or ten carbon atoms. For the set of compounds having nine and ten carbon atoms the average deviation between the experimental and the calculated values is 7.0 I.U., *i.e. ca.* 0.8%. The maximum deviations are less than 2%.

The above example shows that, contrary to other methods requiring a *ca.* ten-fold larger number of structural parameters[14], the behaviour of any alkane can be predicted with a limited number of parameters. The number of parameters can be modulated either by re-grouping, or by not re-grouping, fairly equivalent topological sites. By using a 23-parameter correlation (obtained by not re-grouping topological sites in the first environment, E_B^1) instead of an 18-parameter correlation, the structural variable better reflects the molecular behaviour. The precision is also greater. The average deviation between Rijks' experimental value and the calculated value decreases to 2.7 I.U. and the standard deviation decreases to 3.3 I.U. For the particularly hindered 2,2-dimethyl-3-ethylpentane, the absolute deviation decreases from 12 to 6 I.U., *i.e.*, the relative deviation decreases from 1.5 to 0.7%. However, when establishing the retention–structure correlation, one should seek an optimum between the number of parameters, related to a minimal number of necessary data, and the desired precision in the predictions.

Prediction of the influence of stationary phase variation

Rijks also determined the Kováts indices of about 70 alkenes on squalane (SQ) and acetyltributyl citrate (CIT) at 50°. We shall show that these data can be used to predict the influence of a variation in the stationary phase on the behaviour of a population of compounds, and that these same data verify our predictions, thereby stressing the precision of our approach.

This population of alkenes covers a structural field characterized by the dummy target compound associated to the population (Fig. 1). This dummy target compound is obtained by superposing the characteristic graph of each alkene in the population. In order to characterize the behaviour of a population of compounds while

minimizing the number of experimental data required, it suffices to choose wisely the compounds and introduce progressively each topological site into the ELCO according to the notion of a key population in the DARC/PELCO (Peturbation of an ELCO) strategy[25].

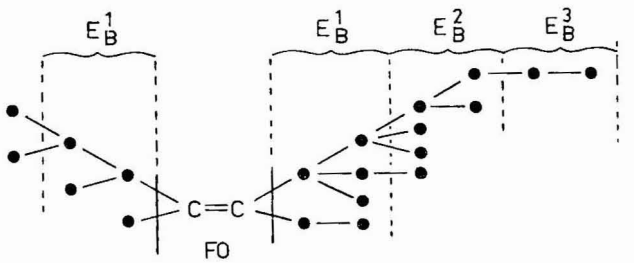
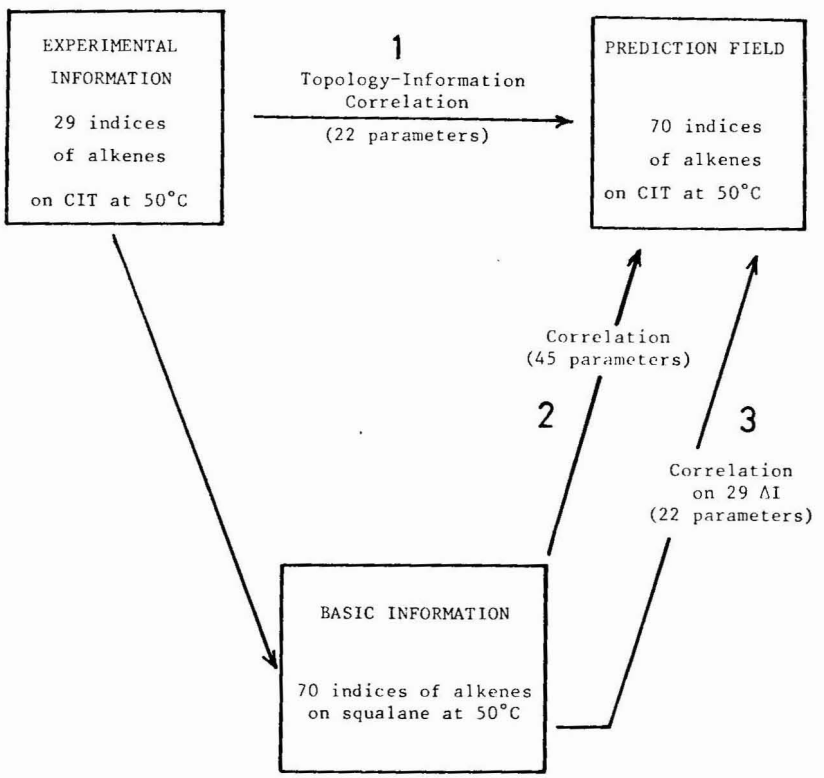


Fig. 1. The dummy target compound associated to the alkene population analyzed by Rijks. This trace is compounded from the sum of the environments (ELCO) of the condensed graph of every alkene.

Thus, from the 29 indices of alkenes on CIT at 50° shown in Table II, we have established a 22-parameter topology–information correlation according to pathway (1) in Scheme 2. This correlation allows us to predict the behaviour of about 70 alkenes



Scheme 2. Possible pathways for predicting the behaviour of at least 70 alkenes on acetyltributyl citrate (CIT) with a minimum of experimental values (29). Pathway (3) offers the greatest precision.

TABLE II

PREDICTION OF KOVÁTS INDICES OF ALKENES AT 50° ON ACETYLTRIBUTYL CITRATE (CIT) (b) BY USING A LARGE AMOUNT OF BASIC INFORMATION ON SQUALANE* AND A MINIMUM OF EXPERIMENTAL INFORMATION ON CIT (a)

Examples of names of alkenes: 1.6 = 1-hexene; c-3,4,4-TM-2.5 = *cis*-3,4,4-trimethyl-2-pentene; t-3-M-3.6 = *trans*-3-methyl-3-hexene.
Average deviation = 0.9 I.U., *i.e.*, *ca.* 0.1%.
Standard deviation = 2.4 I.U.

Alkene	*Kováts indices on acetyltributyl citrate at 50°*			*Difference (c) − (b)*
	Used (a)	*Calc. (b)*	*Exptl. (c)*	
c-2.4		454.2	454.5	0.3
t-2.4		441.5	440.9	−0.6
1.5	515.5	516.2	515.5	−0.7
c-2.5	542.2	541.9	542.2	0.3
t-2.5	535.1	534.6	535.1	0.5
3-M-1.4				
2-M-1.4	525.2	525.3	525.2	−0.1
2-M-2.4		551.7	551.5	−0.2
1.6	616.9	616.5	616.9	0.4
c-2.6		640.2	640.1	−0.1
t-2.6		631.1	630.4	−0.7
c-3.6		627.9	627.2	−0.7
t-3.6	625.0	625.0	625.0	0.0
2-M-1.5		617.0	616.7	−0.3
3-M-1.5		583.3	582.1	−1.2
4-M-1.5	581.4	581.4	581.7	0.3
2-M-2.5		633.5	634.5	1.0
c-3-M-2.5		642.2	640.0	−2.2
t-3-M-2.5		649.8	649.4	−0.4
c-4-M-2.5		590.7	589.1	−1.6
t-4-M-2.5		594.0	593.5	−0.5
2-ET-1.4	628.0	627 8	628.0	0.2
2,3-DM-1.4	593.7	593.6	593.7	0.1
2,3-DM-2.4	663.4	663.8	663.4	−0.4
3,3-DM-1.4	536.7	537.4	536.7	−0.7
1.7	717.2	716.7	717.2	0.5
t-2.7		732.4	732.1	−0.3
c-3.7		725.2	724.7	−0.5
t-3.7		720.0	719.3	−0.7
2-M-1.6		714.8	715.3	0.5
3-M-1.6		676.5	675.6	−0.9
4-M-1.6		690.1	691.2	1.1
5-M-1.6	685.1	685.1	685.1	0.0
2-M-2.6		725.4	727.2	1.8
c-4-M-2.6		689.1	686.5	2.5
t-4-M-2.6		688.4	684.2	4.2
t-5-M-2.6		691.6		
t-2-M-3.6		677.5	676.8	−0.7
c-3-M-3.6		722.3	726.4	4.1
t-3-M-3.6		726.6	720.7	−5.9

(Continued on p. 180)

TABLE II (*continued*)

Alkene	*Kováts indices on acetyltributyl citrate at 50°*			*Difference (c) − (b)*
	Used (a)	*Calc. (b)*	*Exptl. (c)*	
2-ET-1.5		717.2	716.7	−0.6
3-ET-1.5	676.0	675.8	676.0	0.2
3-ET-2.5		732.8	733.4	0.6
2,3-DM-1.5		684.8	684.2	−0.6
2,4-DM-1.5		672.5	671.9	−0.6
3,4-DM-1.5	667.1	666.8	667.1	0.3
2,3-DM-2.5		741.8	741.4	−0.4
2,4-DM-2.5		671.3	674.8	3.5
c-3,4-DM-2.5		707.6	713.0	5.4
t-3,4-DM-2.5		712.9	712.9	0.0
2-ET-3-M-1.4	692.3	692.5	692.3	−0.2
3,3-DM-1.5		656.4	656.0	−0.4
4,4-DM-1.5	634.8	634.3	634.8	0.5
c-4,4-DM-2.5		668.2	668.0	−0.2
t-2,2-DM-3.6		721.5	720.7	−0.7
c-3-M-2.6		732.3	729.4	−2.9
t-2,5-DM-3.6	720.6	720.6	720.6	0.0
2,4,4-TM-1.5	736.0	736.5	736.0	−0.5
2,4,4-TM-2.5		746.0	749.7	3.5
c-2,2-DM-3.6		747.8	746.9	−0.9
2,3,3-TM-1.5	768.3	767.3	768.3	1.0
2-M-3-ET-1.5	766.2	766.4	766.2	−0.2
2,3-DM-1.6	773.2	773.6	773.2	−0.4
t-2-M-3.7	769.4	770.1	769.4	0.3
c-3,4,4-TM-2.5	782.0	782.3	782.0	−0.3
2,5-DM-2.6	783.8	783.8	783.8	0.0
2,3,4-TM-2.5	802.2	801.8	802.2	0.4
1.8	816.8	816.8	816.8	0.0
t-4.8	814.3	814.6	814.3	−0.3
2,3-DM-2.6		826.8	825.9	−0.9
t-2.8	831.9	832.4	831.9	−0.5

* These alkene indices on squalane at 50° (from Rijks) are given in Table III.

on CIT at 50°. For the compounds used to establish this correlation, the following values apply: correlation coefficient $R = 0.999$; Exner's ψ test = 0.06; standard deviation = 4.8 I.U.; average deviation = 3.6 I.U. For the entire set of estimated compounds, the average deviation = 8.8 I.U., *i.e. ca.* 1.4%.

In order to increase the precision of the predictions while using the same number of experimental data on CIT, we can exploit the basic information (Scheme 2) corresponding to the behaviour of the same alkene population on squalane. This can be done through pathway (2) or (3).

Pathway (2) entails a 45-parameter topology–information correlation regrouping the basic and the experimental information used. However, the results obtained in this manner are not much better than those obtained through pathway (1). Indeed, the stationary phase variation characterized by the Kováts index increments ΔI [I(CIT, 50°) − I(SQ, 50°)] represents only 5% of the basic information. Thus, in

comparison to the virtually ideal behaviour of alkenes on squalane, this variation is only a second-order one.

So that the errors introduced by the computer processing of the basic information when establishing the topology–information correlation do not partially shadow the structural influence on ΔI, we have envisaged pathway (3). This pathway represents the establishment of a 22-parameter correlation ($R = 0.99$, $\psi = 0.2$, average deviation = 0.3 I.U., standard deviation = 0.4 I.U.) of the Kováts index increments for the 29 key population alkenes. The ΔI estimated on the basis of this correlation are automatically added to the already available "basic information" obtained on squalane and give the calculated values of the Kováts indices for the "prediction field", *i.e.*, for alkenes on CIT at 50°. The results are given in Table II. The average deviation for the set of Kováts indices is 0.9 I.U., *i.e.*, *ca.* 0.1%; the relative maximum deviation is $< 1\%$ and the standard deviation = 2.4 I.U.

Although pathways (1) and (3) have the same number of correlation parameters and use the same number of data on CIT at 50°, the prediction of the results obtained with pathway (3) is about 10 times greater than with pathway (1). This stresses the interest that lies in using to the utmost advantage already known data for a structural population before trying to predict new data.

Prediction of the influence of variations in the stationary phase and temperature

The same population of about 70 alkenes studied by Rijks at 50° on squalane and acetyltributyl citrate was also studied by him at 70°. We shall show how the behaviour of these same alkenes on CIT at 70° can be predicted on the basis of their known behaviour on SQ at 50° (Scheme 3).

If, in accordance with their size, we qualify the Kováts index increments, ΔI, as second-order variations, then the variations of the indices with temperature, $\delta I/\delta T$, are third-order variations. The latter data can also be used in establishing topology–information correlations, despite statistical criteria of average quality.

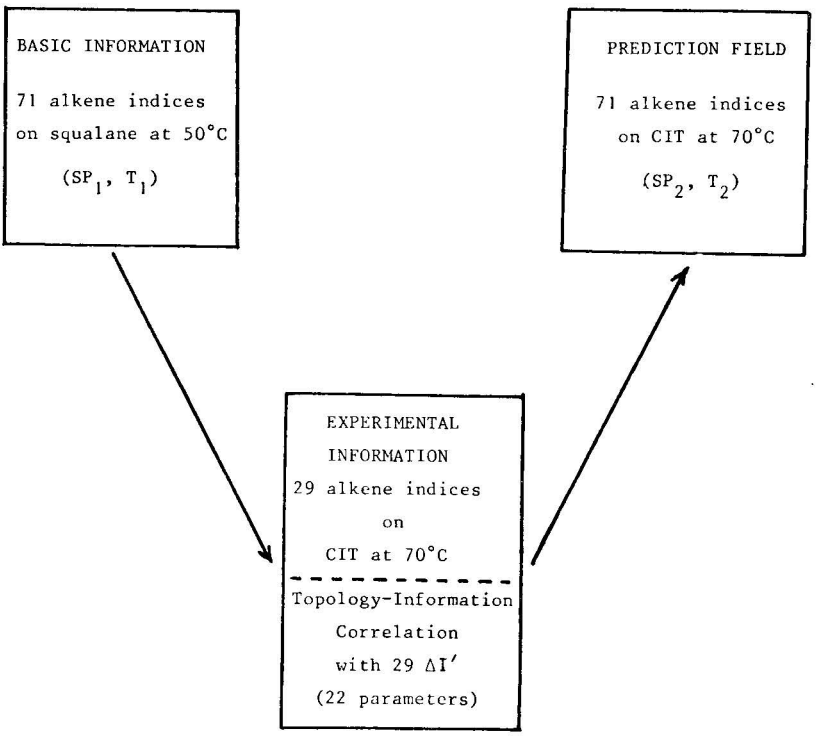
A topology–information correlation is established with the Kováts index increments, $\triangle I'$, corresponding to the difference between new chromatographic conditions (SP_2 and T_2) and already known chromatographic conditions (SP_1 and T_1) for the 29 compounds shown in Table III. Thus:

$$\begin{aligned} \Delta I' &= I(SP_2, T_2) - I(SP_1, T_1) \\ &= I(CIT, 70°) - I(SQ, 50°) \\ &= \Delta I + 20\,\delta I/\delta T \end{aligned}$$

Then the $\Delta I'$ are estimated for all of the compounds in Table III and added to the corresponding Kováts indices obtained on squalane at 50°, thus yielding the Kováts indices on CIT at 70°. When these calculated values are compared with Rijks' experimental values [I(CIT, 70°)], the average deviation for this set of compounds is 1.1 I.U., *i.e.*, *ca.* 0.15%, the maximum deviation is $< 0.8\%$ and the standard deviation = 3.0 I.U.

Prediction of the influence of the functional group: exploitation of the isotopology factor

The preceding three paragraphs deal with the interpolation and extrapolation of data pertaining to the behaviour of compounds with the same structural popula-



Scheme 3. Prediction of the behaviour of alkenes under new chromatographic conditions (SP_2 and T_2) from already known conditions (SP_1 and T_1).

tion. We shall now demonstrate how complementary data between structurally different populations can be exploited for more general problems such as how the chromatographic behaviour of alkanes can be used in predicting the behaviour of alkenes, and how the chromatographic behaviour of alkenes can be used in predicting the behaviour of dibromoalkanes.

We have used the isotopology factor, τI, which is a generalization of Schomburg's homomorphism factor[26]:

$$\tau I = I_{\text{substance}} - I_{\text{isotopologous compound}}$$

The substance and the isotopologous compound have the same ELCO. The only difference lies either in the nature of the focus (FO) or in the chromaticity of certain topological sites.

In both of the above-mentioned cases the procedure for treating the isotopological factors is the same. A 22-parameter correlation is established on the basis of the τI factors corresponding to each of the compounds: the alkenes in Table IV and the dibromoalkanes in Table V. Then the values of τI are estimated from this correlation and added to the Kováts indices of their corresponding isotopologous compounds.

In the first case, both the alkenes and the alkanes were studied on squalane

TABLE III

PREDICTION OF 71 KOVÁTS INDICES OF ALKENES ON ACETYLTRIBUTYL CITRATE (CIT) AT 70°

Basic information on squalane (SQ) at 50° and a minimum of experimental information on CIT at 70° were used, with the aid of a correlation of topology–information established on $\Delta I' = [I(\text{CIT}, 70°) - I(\text{SQ}, 50°)]$.
Average deviation = 1.1 I.U., *i.e. ca.* 0.15%. Standard deviation = 3.0 I.U.

Alkene	*Kováts indices*				$I_{exptl.} - I_{calc.}$
	SQ, 50°	*CIT, 70°*			
		Used	*Calc.*	*Exptl.*	
c-2.4	416.9		453.7	454.3	0.6
t-2.4	406.6		440.6	440.3	−0.3
1.5	481.8	515.6	517.3	515.6	−1.7
c-2.5	504.9	542.0	541.4	542.0	0.6
t-2.5	500.0	534.3	533.7	534.3	0.6
3-M-1.4	450.3		483.0		
2-M-1.4	488.0	524.9	525.1	524.9	−0.2
2-M-2.4	514.3		551.2	551.2	0.0
1.6	582.3	617.1	616.7	617.1	0.4
c-2.6	603.6		641.2	640.2	−1.0
t-2.6	596.9		631.8	629.8	−2.0
c-3.6	592.6		627.2	627.4	0.2
t-3.6	592.1	624.0	624.0	624.0	0.0
2-M-1.5	580.1		618.4	616.7	−1.7
3-M-1.5	551.4		585.2	583.4	−1.8
4-M-1.5	549.4	582.0	582.7	582.0	−0.7
2-M-2.5	597.8		632.9	633.7	0.8
c-3-M-2.5	602.8		642.0	640.1	−1.9
t-3-M-2.5	612.7		649.2	649.2	0.0
c-4-M-2.5	556.2		591.0	589.1	−1.9
t-4-M-2.5	561.9		593.9	592.7	−1.2
2-ET-1.4	592.0	627.9	627.6	627.9	0.3
2,3-DM-1.4	558.8	594.3	594.3	594.3	0.0
2,3-DM-2.4	625.1	663.4	663.4	663.4	0.0
3,3-DM-1.4	506.8	537.4	538.4	537.4	−1.0
1.7	681.8	717.3	716.7	717.3	0.6
t-2.7	698.4		732.2	731.7	−0.5
c-3.7	690.4		726.2	724.9	−1.3
t-3.7	687.5		720.5	718.6	−1.9
2-M-1.6	678.1		715.3	715.3	0.0
3-M-1.6	644.7		677.4	676.6	−0.8
4-M-1.6	657.9		690.1	692.2	2.1
5-M-1.6	650.0	685.5	685.5	685.5	0.0
2-M-2.6	691.2		723.7	726.7	3.0
c-4-M-2.6	654.9		690.8	687.4	−3.4
t-4-M-2.6	656.7		689.9	687.1	−2.8
t-5-M-2.6	659.5		692.2		
t-2-M-3.6	647.1		677.3	675.7	1.6
c-3-M-3.6	684.6		722.1	725.7	3.6
t-3-M-3.6	691.2		725.9	720.5	−5.4
2-ET-1.5	681.8		718.5	716.7	−1.8

(Continued on p. 184)

TABLE III (*continued*)

Alkene	*Kováts indices*				$I_{exptl.} - I_{calc.}$
	SQ, 50°	*CIT, 70°*			
		Used	*Calc.*	*Exptl.*	
3-ET-1.5	646.9	677.8	677.7	677.8	0.1
3-ET-2.5	697.2		732.1	733.4	1.2
2,3-DM-1.5	650.4		687.0	685.7	−1.3
2,4-DM-1.5	637.7		673.8		
3,4-DM-1.5	636.9	669.2	668.5	669.2	0.7
2,3-DM-2.5	703.4		741.4	741.8	0.4
2,4-DM-2.5	640.6		669.8	673.5	−3.7
c-3,4-DM-2.5	670.6		708.3	713.0	4.7
t-3,4-DM-2.5	678.3		713.2	712.9	−0.3
2-ET-3-M-1.4	659.1	692.7	693.0	692.7	−0.3
3,3-DM-1.5	626.2		659.0	658.1	−0.9
4,4-DM-1.5	604.6	636.4	636.1	636.4	−0.3
c-4,4-DM-2.5	635.5		669.3	669.7	0.4
t-2,2-DM-3.6	692.8		722.0	719.5	−2.5
c-3-M-2.6	693.3		733.7	729.8	−3.9
t-2,5-DM-3.6	695.1	719.5	719.5	719.5	0.0
2,4,4-TM-1.5	704.3	738.3	738.6	738.3	−0.3
2,4,4-TM-2.5	715.4		744.6	749.9	5.3
c-2,2-DM-3.6	716.8		748.8	748.6	−0.2
2,3,3-TM-1.5	734.6	772.0	770.3	772.0	1.7
2-M-3-ET-1.5	735.0	768.5	768.6	768.5	−0.1
2,3-DM-1.6	739.3	774.5	774.9	774.5	−0.4
t-2-M-3.7	741.1	768.8	768.8	768.8	0.0
c-3,4,4-TM-2.5	747.1	783.1	783.7	783.1	−0.6
2,5-DM-2.6	749.9	783.7	783.7	783.7	0.0
2,3,4-TM-2.5	765.9	802.2	802.2	802.2	0.0
1.8	781.2	817.0	817.0	817.0	0.0
t-4.8	783.6	814.1	814.1	814.1	0.0
2,3-DM-2.6	788.8		827.9	826.4	−1.5
t-2.8	797.7	831.4	832.0	831.4	−0.6

at 50°. The isotopology factors of the Kováts indices are determined from the Kováts indices of 28 isotopologous alkanes. The Kováts index must be measured experimentally for 23 of them, as those of the remaining 5 reference *n*-alkanes are, by definition, already known. When the calculated values are compared with the experimental values obtained by Rijks (Table IV), the average deviation = 3.1 I.U., *i.e.*, *ca.* 0.5%, and the standard deviation = 4.0 I.U.

We wish to stress the prediction potential and the precision afforded by such an approach. The number of τI data can be minimized to, let us say, the 29 compounds of the key population of alkenes in order to establish a topology–information correlation, labelled A. From correlation A, we are able to predict the behaviour of > 70 alkenes. For the purpose of comparison we can establish another correlation, labelled B, by a direct exploitation of the Kováts indices for the same 29 key-population alkene compounds without resorting to the complementary information contributed by the isotopologous alkanes, *i.e.*, by the same procedure indicated in pathway (1) in Scheme 2. The precision of our predictions is clearly better when using correlation A

TABLE IV

CALCULATION OF KOVÁTS INDICES FOR ALKENES FROM INDICES OF ISO-TOPOLOGICAL ALKANES ON SQUALANE AT 50°

A topology–information correlation on τI was used ($\tau I = I_{alkene} - I_{isotopologous\ alkane}$). Average deviation = 3.1 I.U., i.e. *ca.* 0.5%. Standard deviation = 4.0 I.U.

Alkene	τI	*I (SQ, 50°)*		*Difference, Exptl. — calc.*
		Calc.	*Exptl.*	
c-2.4	16.9	415.3	416.9	1.6
t-2.4	6.6	415.9	406.6	−9.3
1.5	−18.2	484.9	481.8	−3.1
c-2.5	4.9	502.4	504.9	2.5
t-2.5	0.0	503.1	500.0	−3.1
3-M-1.4	−25.0	447.2	450.3	3.1
2-M-1.4	12.7	485.7	488.0	2.3
2-M-2.4	39.0	516.5	514.3	2.2
1.6	−17.7	580.5	582.3	−1.8
c-2.6	3.6	597.8	603.6	5.8
t-2.6	−3.1	598.4	596.9	−1.5
c-3.6	−7.4	592.6	592.6	0.0
t-3.6	−7.9	593.3	592.1	−1.2
2-M-1.5	10.4	575.4	580.1	4.7
3-M-1.5	−32.8	551.4	551.4	0.0
4-M-1.5	−20.3	552.0	549.4	−2.6
2-M-2.5	28.1	596.6	597.8	1.2
c-3-M-2.5	18.6	607.3	602.8	−4.5
t-3-M-2.5	28.5	608.1	612.7	4.6
c-4-M-2.5	−13.5	554.5	556.2	1.7
t-4-M-2.5	−7.8	555.1	561.9	6.8
2-ET-1.4	7.8	587.3	592.0	4.7
2,3-DM-1.4	−8.5	559.9	558.8	−1.1
2,3-DM-2.4	57.8	613.3	625.1	11.8
3,3-DM-1.4	−30.0	508.7	506.8	−1.9
1.7	−18.2	683.0	681.8	−1.2
t-2.7	−1.6	697.6	698.4	0.8
c-3.7	−9.6	687.9	690.4	2.5
t-3.7	−12.5	688.5	687.5	−1.0
2-M-1.6	11.5	671.5	678.1	6.6
3-M-1.6	−31.5	642.6	644.7	2.1
4-M-1.6	−18.3	657.8	657.9	0.1
5-M-1.6	−16.6	650.0	650.0	0.0
2-M-2.6	24.6	691.3	691.2	−0.1
c-4-M-2.6	−21.3	656.2	654.9	−1.3
t-4-M-2.6	−19.5	656.9	656.7	0.2
t-5-M-2.6	−7.1	662.4	659.5	−2.9
t-2-M-3.6	−19.5	642.2	647.1	4.9
c-3-M-3.6	8.4	689.5	684.6	−4.9
t-3-M-3.6	15.0	690.3	691.2	0.9
2-ET-1.5	5.6	674.6	681.8	7.2
3-ET-1.5	−39.1	642.9	646.9	4.0
3-ET-2.5	11.2	702.5	697.2	−5.3
2,3-DM-1.5	−21.3	659.6	650.4	−9.2

(Continued on p. 186)

TABLE IV (*continued*)

Alkene	τI	*I (SQ, 50°)*		*Difference, Exptl. − calc.*
		Calc.	*Exptl.*	
2,4-DM-1.5	7.9	632.9	637.7	4.8
3,4-DM-1.5	−34.8	636.3	636.9	0.6
2,3-DM-2.5	31.7	704.8	703.4	−1.4
2,4-DM-2.5	10.8	644.2	640.6	−3.6
c-3,4-DM-2.5	−1.1	677.1	670.6	−6.5
t-3,4-DM-2.5	6.6	677.9	678.3	0.4
2-ET-3-M-1.4	−12.6	657.0	659.1	2.1
3,3-DM-1.5	−32.7	626.2	626.2	0.0
4,4-DM-1.5	−21.0	611.9	604.6	−7.3
t-4,4-DM-2.5	−10.9	611.1	614.7	3.6
2,3,3-TM-1.4	−11.2	632.4	628.5	−3.9
t-2,2-DM-3.6	−26.6	695.0	692.8	−2.2
c-3-M-2.6	17.1	694.6	693.3	−1.3
t-2,5-DM-3.6	−33.3	691.5	695.1	3.6
2,4,4-TM-1.5	14.4	697.0	704.3	7.3
2,4,4-TM-2.5	25.5	715.4	715.4	0.0
2-M-3-ET-1.5	−26.4	739.0	735.0	−4.0
2,3-DM-1.6	−20.8	747.2	739.3	−7.9
t-2-M-3.7	−23.8	738.3	741.1	2.8
c-3,4,4-TM-2.5	10.0	742.6	747.1	4.5
2,5-DM-2.6	21.5	749.9	749.9	0.0
2,3,4-TM-2.5	13.5	767.8	765.9	−1.9
2-M-3-ET-2.5	17.0	787.1	778.4	−8.7
1.8	−18.8	781.2	781.2	0.0
t-4.8	−16.4	786.3	783.6	−2.7
2,3-DM-2.6	28.7	788.5	788.8	0.3
t-2.8	−2.3	796.5	797.7	1.2

than when using correlation B: with A, the average deviation is about half of that obtained with B (4.9 compared with 8.8 I.U.) and the standard deviation with A is one third of that obtained with B.

However, practical reasons might dictate the choice of the isotopologous series (*e.g.*, filiation in organic synthesis). This can lead to molecules having very different "polarities", as shown in Table V. The behaviour of isomeric and diastereoisomeric dibromoalkanes is calculated from the behaviour of the alkenes that were brominated. The alkene indices, *I*, were determined on squalane at 50° [22,23] and ultimately completed by other values[24]. The dibromoalkane indices, *J*, were determined on squalane at 100° with the bromoalkanes serving as the reference series[27]. Although index *J* is about 316 I.U. less than index *I*, we shall use these unstandardized data in order to demonstrate that the same methodology is still valid. The correlation coefficient $R = 0.99$ and $\psi = 0.15$ with the correlation established on the basis of the isotopology factors considered in this example. The average deviation between the calculated and experimental values of *J* is 2.6 I.U., and the standard deviation = 3.6 I.U.

The interest in exploiting the isotopology factor lies not only in the fact that the precision of the predictions is better, but also that there are numerous extrapolation possibilities. Indeed, the isotopologous compound accounts for a large part of the

TABLE V

CALCULATION OF KOVÁTS INDICES OF DIBROMOALKANES AT 100° FROM KOVÁTS INDICES OF ALKENES AT 50°

Stationary phase, squalane. $\tau I = J_{DB,\ SQ,\ 100°} - I_{alkene,\ SQ,\ 50°}$.
Average deviation = 2.6 I.U. Standard deviation = 3.6 I.U.

Isotopologous alkene	*Dibromoalkane**	τI	I_{DB}		*Difference, exptl. − calc.*
			Calc.	*Exptl.*	
1.2	1,2-DB2	299.0	473.7	473.7	0.0
1.3	1,2-DB3	238.0	527.2	527.0	−0.2
1.4	1,2-DB4	234.0	631.3	627.1	−4.2
1.5	1,2-DB5	231.2	708.2	712.6	4.4
1.6	1,2-DB6	224.7	801.8	807.5	5.7
1.7	1,2-DB7	220.2	897.9	902.4	4.5
3-M-1.4	1,2-DB-3M4	251.7	703.1	702.2	−9.0
3-ET-1.5	1,2-DB-3ET5	222.1	869.0	869.0	0.0
3,3-DM-1.4	1,2-DB-3,3DM4	276.2	791.8	782.8	−0.9
4-M-1.5	1,2-DB-4M5	211.6	761.5	761.5	0.0
4,4-DM-1.5	1,2-DB-4,4-DM5	214.4	819.3	819.3	0.0
2-M-1.3	1,2-DB-2M3	190.0	577.3	572.5	−4.8
2-M-1.4	1,2-DB-2M4	191.0	682.8	679.1	−3.7
2-ET-1.4	1,2-DB-2ET4	192.0	783.5	783.5	0.0
2,3-DM-1.4	1,2-DB-2,3DM4	210.2	768.3	769.3	1.0
2,3,3-TM-1.4	1,2-DB-2,3,3TM4	249.5	870.6	877.6	7.7
c-2.4	(T) 2,3-DB4	193.1	607.7	610.4	2.7
t-2.4	(E) 2,3-DB4	189.4	593.7	596.2	2.5
c-3.6	(T) 3,4-DB6	191.4	781.2	783.7	1.6
t-3.6	(E) 3,4-DB6	187.9	778.8	780.4	1.6
c-4.8	(T) 4,5-DB8	161.8	948.8	948.3	−0.5
t-4.8	(E) 4,5-DB8	159.4	942.2	942.8	0.6
c-2,5-DM-3.6	(T) 3,4-DB-2,5DM6	218.0	911.9	919.1	7.2
t-2,5-DM-3.6	(E) 3,4-DB-2,5DM6	200.0	903.2	896.0	−7.2
c-2.5	(T) 2,3-DB5	192.1	695.5	697.2	1.7
t-2.5	(E) 2,3-DB5	190.0	686.7	689.8	3.1
c-2.6	(T) 2,3-DB6	177.4	782.3	780.7	−1.6
t-2.6	(E) 2,3-DB6	176.1	772.0	772.6	0.6
c-2.7	(T) 2,3-DB7	165.6	878.1	872.5	−5.6
t-2.7	(E) 2,3-DB7	167.6	866.4	866.3	−0.1
c-2.8	(T) 2,3-DB8	165.5	970.7	968.3	−2.4
t-2.8	(E) 2,3-DB8	162.3	962.4	960.4	−2.0
c-3.7	(T) 3,4-DB7	175.6	868.8	866.0	−2.8
t-3.7	(E) 3,4-DB7	174.5	862.3	861.9	−0.4
t-4-M-2.5	(E) 2,3-DB-4M5	193.1	763.3	755.2	−8.1
t-4,4-DM-2.5	(E) 2,3-DB-4,4-DM5	235.3	848.5	849.9	1.4

* DB = dibromo; diastereoisomers, (E) = *erythro* and (T) = *threo*.

data. The further away we move from the focus, the weaker the influence of the isotopology factor, and the weaker its contribution as we move beyond the first layer sites of the second environment (*i.e.*, beyond layer A of E_B^2).

CONCLUSION

We have shown through a series of examples that different sets of Kováts indices, whether obtained for the same population of compounds by a variation in chromatographic conditions, or obtained for different populations of compounds under the same chromatographic conditions, or obtained for different populations of compounds under different chromatographic conditions, can be rendered coherent by using the methodology of the DARC topological system.

The overlapping of sets of Kováts indices of different origins increases the information content of each set and facilitates the interpolation and extrapolation possibilities. Thus, for example, the large amount of data on hydrocarbon analysis can be exploited in order to increase the prediction potential of experimental data relative to populations of alkyl-substituted compounds.

The interest in experimentally determining a new set of Kováts indices does not lie in the number of compounds studied, but rather in the nature and extent of the structural pattern covered by the compound population. The topology–information correlations established according to the principles of the DARC/PELCO strategy show the interest that lies in experimentally determining further sets of Kováts indices on the basis of a minimum number of compounds. This strategy avoids the introduction of redundant data and the presence of gaps in a structural space which would normally arise from the experimental study of lists of commercial compounds.

Rohrschneider[28,29] and McReynolds[30], as well as the resulting recent exploitations of Kováts indices by factorial analysis[31,32] or numerical taxonomy[33,34], chiefly stress stationary phase behaviour. This topological analysis, however, stresses solute behaviour. By thermodynamically exploiting the values attributed to the parameters of the topology–information correlations, established on the basis of the Kováts indices or from their derived data (ΔI and τI), the behaviour of the solutes can be analyzed virtually at the level of each molecular atom[35,36].

Our prediction and physico-chemical studies are currently aimed at the processing of retention data in gas and liquid chromatography. It should be stressed that these two aims are complementary, and that establishing a prediction system without a physico-chemical support is not to be recommended.

REFERENCES

1 S. R. Heller, D. C. Maxwell and A. McCormick, *Advan. Mass Spectrom.*, 6 (1974) 1037.
2 R. Schwarzenbach, J. Meili, H. Könitzer and J. T. Clerc, *Org. Magn. Resonance*, 8 (1976) 11.
3 B. A. Jezl and D. L. Dalrymple, *Anal. Chem.*, 47 (1975) 203.
4 F. W. McLafferty, R. Venkataraghavan, K. S. Kwok and G. Pesyna, *Advan. Mass Spectrom.*, 6 (1974) 999.
5 W. Bremser, M. Klier and E. Meyer, *Org. Magn. Resonance*, 7 (1975) 97.
6 O. E. Schupp and J. L. Lewis, *Gas Chromatographic Data Compilation*, AMD 25 A, A.S.T.M., Philadelphia, Pa., 1967; AMD 25 A-S1, A.S.T.M., Philadelphia, Pa., 1971.
7 W. O. McReynolds, *Gas Chromatographic Retention Data*, Preston Technical Abstracts Co., Niles, Ill., 1966.
8 G. Zweig and J. Sherma, *Handbook of Chromatography*, CRC Press, Cleveland, Ohio, 1972.
9 M. Chastrette, G. Lenfant and J. E. Dubois, *C. R. Acad. Sci., Ser. C*, 265 (1967) 602.
10 G. Lenfant, M. Chastrette and J. E. Dubois, *J. Chromatogr. Sci.*, 91 (1971) 220.
11 J. E. Dubois and J. R. Chrétien, *J. Chromatogr. Sci.*, 12 (1974) 811, and references cited therein.
12 G. Schomburg and G. Dielmann, *J. Chromatogr. Sci.*, 11 (1973) 151.

13 G. Castello, M. Lunardelli and M. Berg, *J. Chromatogr.*, 76 (1973) 31.
14 J. M. Takács, *J. Chromatogr. Sci.*, 11 (1973) 210.
15 J. K. Haken, *J. Chromatogr. Sci.*, 11 (1973) 144.
16 L. S. Ettre, *Chromatographia*, 6 (1973) 489.
17 L. S. Ettre, *Chromatographia*, 7 (1974) 39.
18 L. S. Ettre, *Chromatographia*, 7 (1974) 261.
19 P. Souter, *J. Chromatogr. Sci.*, 12 (1974) 418 and 424.
20 J. E. Dubois, in W. T. Wipkey, S. R. Heller R. J. Feldmann and E. Hyde (Editors), *Computer Representation and Manipulation of Chemical Information*, Wiley, New York, 1974, p. 239.
21 J. E. Dubois, *Isr. J. Chem.*, 14 (1975) 17.
22 J. A. Rijks, *Thesis*, Eindhoven, 1973.
23 J. A. Rijks and C. A. Cramers, *Chromatographia*, 7 (1974) 99.
24 A. Matukuma, in C. L. Harbourn (Editor), *Gas Chromatography 1968*, Institute of Petroleum, London, 1969, p. 55.
25 J. E. Dubois, D. Laurent and A. Aranda, *J. Chim. Phys.*, 70 (1973) 1608 and 1616.
26 G. Schomburg, *Advan. Chromatogr.*, 6 (1968) 211.
27 J. R. Chrétien, M. Lafosse and M. H. Durand, *Bull. Soc. Chim. Fr.*, (1975) 1013.
28 L. Rohrschneider, *J. Chromatogr.*, 22 (1966) 6.
29 L. Rohrschneider, *J. Chromatogr. Sci.*, 11 (1973) 160.
30 W. O. McReynolds, *J. Chromatogr. Sci.*, 8 (1970) 685.
31 P. H. Weiner and J. F. Parcher, *Anal. Chem.*, 45 (1973) 302.
32 R. B. Selzer and D. G. Howery, *J. Chromatogr.*, 115 (1975) 139.
33 D. L. Massart, M. Lauwereys and P. Lenders, *J. Chromatogr. Sci.*, 12 (1974) 617.
34 A. Eskes, F. Dupuis, A. Dijkstra, H. de Clercq and D. L. Massart, *Anal. Chem.*, 47 (1975) 2168.
35 J. R. Chrétien, *C.R. Acad. Sci., Ser. C*, 281 (1975) 151.
36 J. E. Dubois and J. R. Chrétien, to be published.

Journal of Chromatography, 126 (1976) 191–204
© Elsevier Scientific Publishing Company, Amsterdam — Printed in The Netherlands

CHROM. 9471

CHROMATOGRAPHIC SOLUTE IDENTIFICATION USING PEAK SHAPE ANALYSIS

SANDRA D. MOTT and ELI GRUSHKA

Department of Chemistry, State University of New York at Buffalo, Buffalo, N.Y. 14214 (U.S.A.)

SUMMARY

Solute identification by retention data alone does not yield a positive identification for two or more solutes with approximately the same retention times. In such cases, two columns with two different stationary phases are needed for solute verification. For this reason, the concentration profiles of gas chromatographic peaks have been studied using the empirically derived eight-parameter model of Chesler and Cram. A non-linear least squares fit of the data to this model has made it possible to derive parameters which allow homologous class recognition and specific solute identification. Two methods for determining the initial estimates are presented. In one method the initial estimates were calculated from the data in a purely empirical manner, while the other is based mathematically on the model. The fitted values of the parameters from the two methods are compared for the purpose of illustrating the dependence of the fit on the choice of initial estimates. Some of the parameters are believed to have physical significance. For example, an almost linear relationship between one of the fitted parameters, C_2, and the diffusion coefficient, D_{AB}, of the solute in the carrier gas was found. Similar results were found for C_7 *versus* D_{AB}, the capacity ratio k' and C_2, and $k'/(1 + k')^2$ and C_2.

INTRODUCTION

The qualitative analysis of gas chromatographic peaks can be obtained from retention data. Such data are reported in terms of the Kováts indices[1], the Rohrschneider constants[2], etc. This approach works quite well[3] provided that there is enough of a difference between the retention data of the standards. If there can be no positive identification made for the specified column conditions from which the retention data are obtained, the stationary phase or temperature must be changed and the analyses re-evaluated[4].

Various port and pre-column devices have been utilized for solute identification (*cf.* ref. 3). While these devices are extremely useful, it is of basic interest to examine the relationship between the eluted peak shape and its nature, since this might also lead to a better understanding of column processes.

One approach to the identification procedure involves the use of moments and their derived parameters, skew and excess[5–10]. The correlation between skew and ex-

cess for various homologous families does not yield a positive identification of a solute according to its family, since there is a pronounced overlap for certain families[5]. Since moment analysis is very sensitive to noise, the use of the higher moments (*e.g.*, skew and excess) amplifies this noise[8] and the accuracy of this technique diminishes.

Slope analysis[5,7] may be employed by the use of second derivative plots as in the case of double peak recognition. This method is tedious as far as the mathematics are concerned but much simpler than moment analysis.

Curve fitting of the data to some predetermined model is still another alternative. For the application of this method, a mathematical model must be assumed. Throughout the literature various functions have been used such as the Poisson distribution[11], Bessel function[11], Gaussian[12,13], bi-Gaussian[12], exponentially modified Gaussian[5], a linear combination of the Cauchy function with a Gaussian[13], quadratic at the data closest to the maximum of the peak[14], Edgeworth series[12], Gram-Charlier series[9], a Gaussian with a triangular joining function to an exponentially weighted tail[8,10], and a Gaussian convoluted with a hyperbolic tangent joining function to an exponential decay[15]. The last function proposed is very similar in structure to the empirical equation developed by Gutknecht and Perone[16] for their work in polarography.

The models used for the description of chromatographic profiles have generally been based on phenomena associated with the chromatographic interactions of the solute[10,11]. Many of these functions assume a Gaussian leading edge from which valuable chromatographic data are readily obtainable. The shape of the tail of the peak presents the major problem that arises in the selection of a model for curve fitting analysis.

Sternberg[10] discusses the various parameters that affect the shape of the peak. These include the input function (sample injection), detector delay, and peak spreading in the connectors and tubing, as well as adsorption–desorption kinetics and diffusion in the carrier gas[11]. He proposes an approximation of the actual peak shape by Gaussian, triangular, and exponential portions. The "mirroring" of the front half of the peak to the back and compensating for the difference with his joining function is in close resemblance to the model suggested by Chesler and Cram[15]. In the latter instance, the hyperbolic tangent function joins smoothly with the Gaussian and decay portions.

Macnaughton *et al.*[17] monitored the shape of high-precision gas chromatographic peaks during principle component analysis of a homologous series, whereby changes in the chromatographic system were detectable along with sample composition. Anderson *et al.*[18] used computer analysis for resolving non-Gaussian peaks using a curve fitting procedure. They emphasize that it is known that the shape of the peak is a function of its position in the chromatogram, and sometimes due to its molecular structure if there is adsorption. As will be discussed in this work, it is the molecular structure that plays the more important role of the two, and the curve fitting procedure employed is feasible for qualitative analysis.

It was the aim of this study to determine the feasibility of classifying graphic peaks using the parameters of the function of Chesler and Cram[15] for three homologous families. It was thought that some of the parameters in the equation are characteristic of the solutes. Also, it is of interest to examine and see if functions such as suggested by Chesler and Cram can have physical significance. That is, if the parameters of the equation are a reflection of the column processes.

EXPERIMENTAL

Apparatus

The apparatus used for this work was similar to that used by Grushka and Maynard[19] and Grushka and Schnipelsky[20]. The column used was 200 cm in length and 0.64 cm O.D. The column packing consisted of Carbowax 1540 on Chromosorb W-AW-DMCS 80–100 mesh. The data were collected on paper tape, as described by Grushka and Schnipelsky[20], and converted to cards. All programs were run on a CDC 6400 computer.

Procedure

Three solutes from each of three homologous series were introduced individually to the chromatograph via a Seiscor Model VIII injection valve (Seiscor, Tulsa, Okla., U.S.A.). The oven temperature was maintained at 60°, except for one study, where the temperature was 80°. The carrier velocity was kept at 10 cm/sec.

All of the solutes were obtained from various vendors and were of reagent grade.

THEORY

The function used in the curve fitting procedure is the eight-parameter function suggested by Chesler and Cram[15]. This model can be expressed as follows:

$$Y(t) = C_1 \left\{ \exp \frac{-(t - C_4)^2}{2C_5} + \left[1 - 0.5\,(1 - \tanh[C_2(t - C_3)])\right] \cdot C_6 \exp\left[-0.5\,C_7\,(|t - C_8| + t - C_8)\right] \right\} \quad (1)$$

where

$Y(t)$ = value of the function at time t
C_1 = maximum of the peak
C_2 = slope of the hyperbolic tangent
C_3 = midpoint of the hyperbolic tangent
C_4 = position of the peak maximum
C_5 = variance of the peak at 0.61 of C_1
C_6 = ratio of the height of the exponential decay to C_1 at $t = C_8$
C_7 = rate of decay of the exponential
C_8 = position where the decay function originates.

The first term in the equation is the Gaussian which defines the front part of the peak. The remaining two terms are the hyperbolic tangent joining and exponential decay functions. As an approximating fucntion, more flexibility is allowed, due to the increased number of parameters that control the shape of the peak as opposed to other models, for example, the exponentially modified Gaussian[7,21]. Also these parameters, or a combination of such, may contain other chromatographic information.

The leading edge of the peak is assumed to be Gaussian from which estimates of C_1, C_4, and C_5 can be obtained directly from the digitized data. For the remaining parameters, C_2, C_3, C_6, C_7, and C_8, it is imperative that these values be estimated systematically from peak to peak to avoid any fluctuations in the fitted values. The al-

gorithm used for evaluating the initial estimates from the digitized data is straightforward and can be done within the computer program. It was found that the estimates for C_2, C_3, and C_8 are all directly related to τ, defined as the skewness factor by Roberts *et al.*[21]. This constant τ is evaluated by the difference between the width of the peak at 1/4 C_1 on the tailing edge and the width of the peak at 1/2 C_1 on the leading edge. Estimates for C_2 can be obtained from $(\tau)^{-\frac{1}{2}}$, but for cases where τ is small (less than 1.0) the estimate for C_2 is determined as $(\tau)^{-1}$. C_2 indicates the broadness or asymmetry of the peak; thus as τ increases, the estimate for C_2 decreases with increasing asymmetry. Estimated values for C_3 and C_8 are evaluated as $C_4 + \tau$ and $C_4 + 2\tau$, respectively. In this case, as τ increases C_3 and C_8 occur further from the peak maximum than for a peak with a small value of τ. The height ratio of the exponential decay C_6 is determined by the value of the data at approximately C_8 divided by the peak height. Likewise for C_7, the slope of the curve is calculated between C_8 and the next data point, divided by the peak height, since the decay function is assumed predominant at this point.

An alternative method was derived for the evaluation of the initial estimates. In this case the front half of the peak was subtracted from the back half. The remaining data resembled another peak which will be referred to as the difference peak. From this difference peak C_2, C_3, C_6, C_7, and C_8 are estimated.

The midpoint of the hyperbolic tangent function, *i.e.*, C_3, is taken as the position of greatest slope of the increasing portion on the difference peak, while C_2 is this slope divided by the original peak height, C_1. Assuming that $C_8 \geqslant C_3$, C_6 is estimated as

$$C_6 \approx 2\, Y_d/C_1 \tag{2}$$

where Y_d is the value of the difference peak at the estimated value of C_3. The rate of the exponential decay C_7 is estimated by selecting two points along the tail of the difference peak such that the joining function would be approximately unity and the only function with significant influence would be the decay function. Thus, C_7 is calculated as

$$C_7 \approx \frac{\ln \dfrac{Y_{d1}}{Y_{d2}}}{t_2 - t_1} \tag{3}$$

where Y_{d1} and Y_{d2} are taken from the tail of the difference peak with t_1 and t_2 as their corresponding time values. The starting position of the exponential can be estimated by calculating C_8 at some point on the tail of either the difference peak or the main peak, far removed from C_3 such that the hyperbolic tangent is unity. Thus,

$$C_8 \approx t + \frac{1}{C_7} \ln \left(\frac{Y}{C_1 C_6} \right) \tag{4}$$

where t is the corresponding time of the data point Y.

It is interesting to note that the product of the joining function and exponential decay passes through a maximum which is not necessarily at $t = C_8$ as previously re-

ported[15]. Assuming that the maximum occurs at $t \geqslant C_8$, after differentiation of the remaining terms in eqn. 1, the position of the maximum can be evaluated at

$$t = C_3 + \frac{1}{2C_2} \ln \left[\frac{C_2}{C_7} + \sqrt{\left(\frac{C_2^2}{C_7^2} + 1 \right)} \right] \tag{5}$$

Since C_2 and C_7 are always greater than zero, the argument of the natural logarithm function is positive, thus only real values will exist for the position of the maximum. If the value of C_2 was to tend to infinity, *i.e.*, for a very symmetrical peak, the second term would diminish to zero and the maximum would be very close to C_3, if C_3 were to exist at all.

Applying a mathematical model to a physical system necessitates the implementation of constraints in the curve fitting program. One of the most crucial constraints is that none of the parameters are allowed to become negative. If they do, then the physical significance of the model will be lost. To alleviate this problem eqn. 1 was modified and supplied to the program in the following manner[22]

$$Y(t) = C_1^2 \left\{ \exp \left[\frac{[(t - C_{4*}^2)]^2}{2C_{5*}^2} \right] + \left[1 - 0.5 \left(1 - \tanh \left[C_{2*}^2 (t - C_{3*}^2) \right] \right) \right] \cdot C_{6*}^2 \exp \left[-0.5 C_{7*}^2 \left(|t - C_{8*}^2| + t - C_{8*}^2 \right) \right] \right\} \tag{6}$$

where C_{1*}, C_{2*}, C_{3*}, C_{4*}, C_{5*}, C_{6*}, C_{7*}, and C_{8*} correspond to the square root of their respective parameters in the original equation. This revision of the equation allows the parameters to become negative during the iterative processes, but when substituted in the equation itself they are squared, thus resulting in positive values. It should also be noted that the modified form of the equation does not require any special software for checking the values of the parameters between iterations. Another constraint is that for the method to be internally consistent within a given set of experimental data, the same method of initial estimates must be utilized throughout, as well as the manner in which it is fitted.

By the application of the aforementioned modifications, it is possible to fit experimental data to the given model with the chances of false convergence being minimized. The method by which the data are supplied to the curve fitting program is entirely up to the user. The data can be fitted in two parts. The front part of the peak up to the peak maximum is fitted to the Gaussian portion of the equation, while the remaining part is fitted to the entire model, using the values of C_1, C_4, and C_5 from the first fitting and keeping them constant. Another alternative is to follow the above method and then proceed by fitting the entire set of data to the complete model using the values from the previous fits as initial estimates. Finally, one can follow the method used by Chesler and Cram[15], where the entire set of data is fit to the model holding C_1, C_4, and C_5 constant while the other parameters are being fitted. The choice of the method to fit the data should be consistent for a particular analysis.

The program for the non-linear least squares curve fitting used in this study, NLIN2, was written at E. I. du Pont de Nemours Company and modified by the computing center at this university[22]. The algorithm this routine was written from was developed by Marquardt[23]. It combines the Taylor series method with the method of steepest descent to interpolate the estimates of the parameters for a non-linear function.

RESULTS AND DISCUSSION

Qualitative analysis

The study of peak shapes via the non-linear least squares curve fitting technique was first investigated by visually estimating the parameters C_2, C_3, C_6, C_7, and C_8. This technique was not satisfactory because the parameters for different runs of the same solute did not converge consistently. With this problem a systematic method of initial estimates had to be followed for the duration of the study. The simplest method to implement was the empirical, τ based estimates. All of the data yielded parameters that were consistent, with the exception of hexane, as will be discussed shortly.

To test the validity of the model for symmetric profiles, a Gaussian peak was simulated by the computer, and was fitted to eqn. 6 by estimating the parameters according to the τ method. The values used for generating the Gaussian peak were: $C_1 = 100$, $C_4 = 1.50$, and $C_5 = 2.25$. Estimates for the eight parameters and their final fitted values are given in Table I. The least square fit was excellent: the "goodness" of the fit, Φ (sum of the squares of the residuals), was 7.2×10^{-18} for the front of the peak and 5.9×10^{-18} for the fitting of the back half to the entire equation.

As illustrated by Table I, the most significant parameter that caused such a good fit of the data is C_6. If C_6 is zero, the product of the joining function and exponential decay is also zero, resulting in a pure Gaussian peak. It was expected that C_2, since it controls the broadening of the peak, would tend to infinity, while C_3 and C_8 would approach C_4 for the Gaussian profile. As seen in Table I this did not occur. A possible explanation might lie in the nature of the model and in the fact that it has adjustable parameters. Nevertheless, it will be shown that useful information can be obtained from the procedure used.

TABLE I

LEAST SQUARES FIT OF A GAUSSIAN PEAK TO THE PROPOSED EQUATION BY CHESLER AND CRAM

Parameter	*Initial estimate*	*Fitted value*
C_1	100.0	100.0
C_2	1.11	0.973
C_3	5.40	9.88
C_4	4.50	4.50
C_5	1.82	2.25
C_6	0.430	3.93×10^{-8}
C_7	0.362	1.77
C_8	6.30	5.02

If one is to study carefully the model proposed by Chesler and Cram, the parameters that control the shape of the tail, C_2, C_3, C_6, C_7, and C_8, must be fully understood. Supposing a peak has a characteristically long tail, it should be intuitive that this implies a small value (<0.5) of C_2, a large value of C_6 (>0.5), a small value of C_7 (≈ 0.1), and that C_3 and C_8 have values that are far removed from the actual peak maximum. C_2 is extremely important, since it controls the broadness of the peak. Defining two new parameters, C_3' and C_8' as the distance C_3 and C_8 occur from C_4, respectively, the broadness of any peak may be studied in more detail. It is on the ratio

of these differences, C_3'/C_8', as well as on C_2 and C_7 that the identification process will be based.

The data given in Table II show the results of fitting chromatographic peaks to eqn. 6 for three homologous families. The values of the parameters show consistency within a given family. All of the peaks were fitted in exactly the same manner, *i.e.*, using the τ method of initial estimates and fitting first the front half of the peak to a Gaussian, then the remaining data to the entire equation using the values of C_1, C_4, and C_5 from the first fit. The precision of the data is quite good for most of the parameters. Hexane presented a special case. For a sample of over ten hexane peaks, fluctuations of the fitted parameters were very predominant. This was most noticeable for C_2. An explanation for this is the fact that the τ estimates varied between 0.40, 0.45, and 0.50 sec. Due to the 0.05 recorder digitization rate, and a very limited amount of data available for the narrow hexane peaks, this variation in τ was shown to be highly significant. Values of C_2 for hexane could be grouped into three categories: 4.31 (τ = 0.50 and 0.45), 2.72 (τ = 0.40), and 2.17 (τ = 0.40). The value of C_2 = 4.31 was eliminated by the use of eqn. 5 and locating the position of the maximum of the difference peak. Because of the experimental error involved in digitized data, the remaining values of C_2 were averaged and used for the identification analysis.

TABLE II

VALUES OF THE FITTED PARAMETERS FOR THREE HOMOLOGOUS FAMILIES PLUS STANDARD DEVIATIONS

Solute	C_2	C_3	C_4	C_5	C_6	C_7	C_8
n-Hexane	2.40	27.35	26.73	0.203	0.649	2.16	27.29
	± 0.30	± 0.06	± 0.01	± 0.0004	± 0.271	± 0.11	± 0.15
n-Heptane	1.68	33.32	32.14	0.537	0.425	1.18	32.81
	± 0.06	± 0.05	± 0.05	± 0.001	± 0.019	± 0.04	± 0.04
n-Octane	1.11	51.52	49.84	1.314	0.410	0.698	50.73
	± 0.01	± 0.02	± 0.03	± 0.003	± 0.001	± 0.012	± 0.02
Benzene	0.434	129.95	125.10	7.725	0.391	0.348	127.49
	± 0.007	± 0.10	± 0.89	± 0.022	± 0.007	± 0.001	± 0.09
p-Xylene	0.168	400.99	388.88	52.99	0.364	0.137	394.35
	± 0.002	± 0.46	± 0.16	± 0.14	± 0.013	± 0.004	± 0.33
Mesitylene	0.0892	729.45	770.40	171.66	0.376	0.0818	780.56
	± 0.0029	± 1.38	± 0.45	± 1.34	± 0.090	± 0.0104	± 0.49
Ethanol	0.739	134.43	132.65	5.480	0.334	0.209	137.20
	± 0.003	± 0.08	± 0.05	± 0.043	± 0.007	± 0.003	± 0.10
n-Propanol	0.391	256.00	252.50	21.75	0.194	0.0779	260.49
	± 0.002	± 0.18	± 0.08	± 0.16	± 0.004	± 0.0019	± 0.09
n-Butanol	0.196	515.55	508.24	75.34	0.227	0.039	524.66
	± 0.004	± 0.20	± 0.14	± 0.64	± 0.004	± 0.0005	± 0.25

For the identification procedure it was assumed that C_2 and C_3'/C_8' would be most beneficial. Fig. 1 shows the relationship between C_3'/C_8' and C_2. The three families studied here are grouped together in different regions on the plot. If one had two peaks of approximately the same retention time (C_4) (consider ethanol and benzene), normally the column conditions must be changed (stationary phase, temperature, etc.) to distinguish between these two solutes. With the use of the C_3'/C_8'

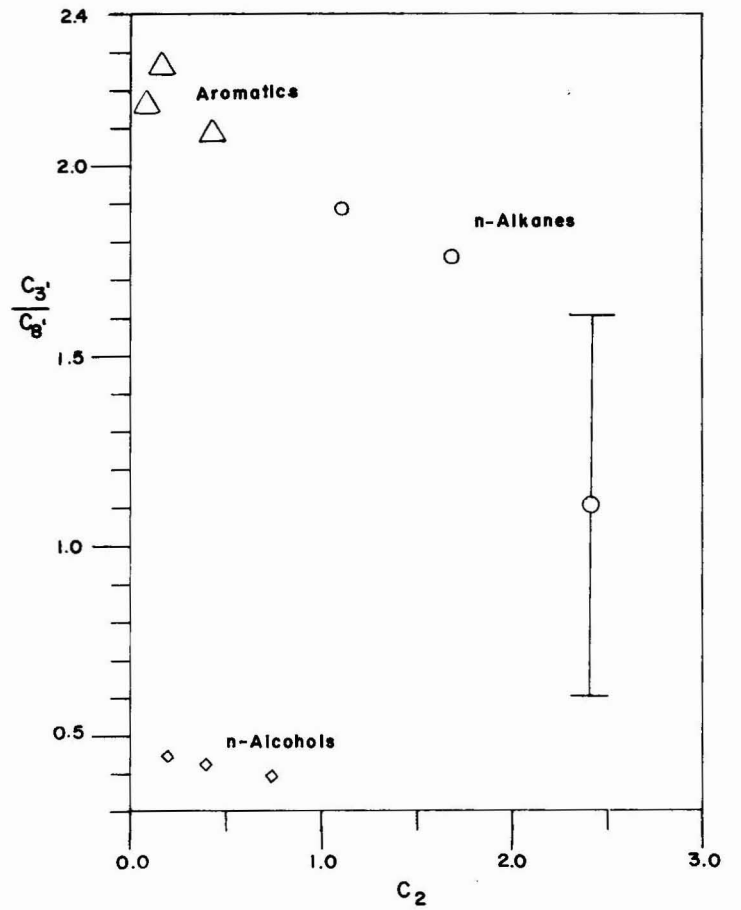


Fig. 1. C_3'/C_8' *versus* C_2 for three homologous families. Column temperature, 60°; carrier velocity, 10 cm/sec. The vertical bar represents the extremely large deviation for hexane in C_3'/C_8'. All other deviations are included.

versus C_2 plot, one can readily distinguish between different solutes. Conversely, if two solutes have either the same C_3'/C_8' or C_2 value their retention times, most likely, would be different. Thus using the parameters in Fig. 1 and C_4 qualitative identification can be made. Similar results can be seen in Fig. 2. In this plot of C_3'/C_8' *versus* C_7 the solutes are grouped into families in a comparable fashion to Fig. 1. This can be taken to imply that even though the value of C_4 increases within a given family, the characteristics of the shape of the peak exhibited by the tail are consistent within that family.

The second method of initial estimates was used as the next step to study the dependence of initial estimates on convergence. It was found that this method breaks down for symmetrical peaks and for profiles due to overloaded columns. The reason for this is that the difference peak calculated is very sensitive to noise and is negative for the most part, therefore making initial estimation virtually impossible. This was

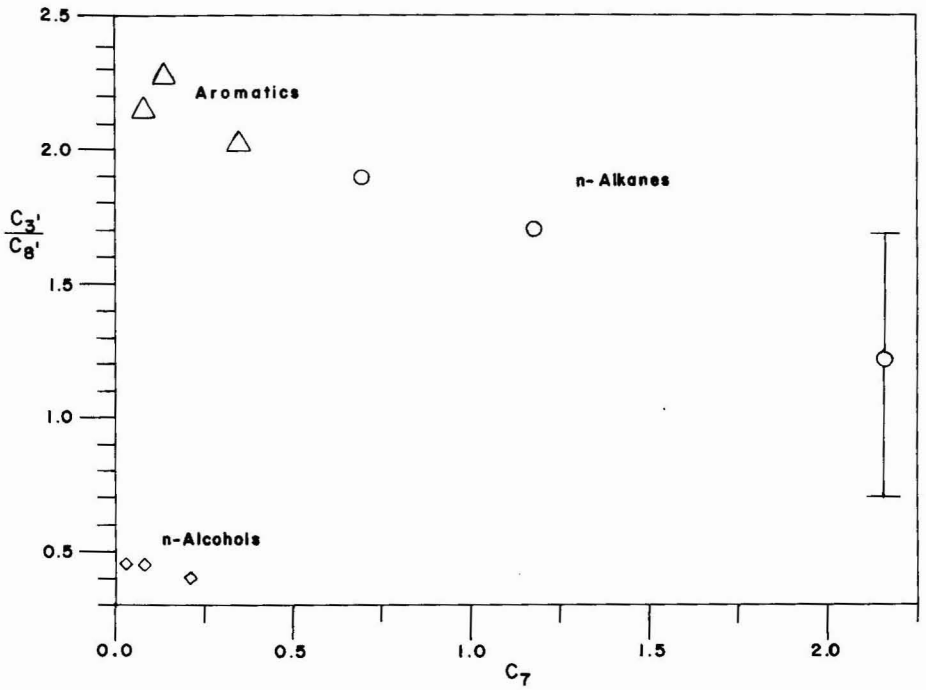


Fig. 2. C_3'/C_8' *versus* C_7 for three homologous families. Column temperature, 60°; carrier velocity, 10 cm/sec. The vertical bar presents the extremely large deviation in C_3'/C_8' for hexane.

the case for some of the solutes analyzed. Various conditions of column overloading are presently being studied in more detail. As an added note of interest, the τ method of estimates is not as sensitive to column overloading, and this may be the more versatile of the two methods of estimation.

Preliminary studies at 80° seem to indicate that the present method of solute identification is still valid. The dependence of the method on various operating conditions is now being studied.

It should be emphasized that the present study was done with individual solutes. In reality, the chromatogram can be quite complex and complete resolution of the various solute might not be complete. In such cases, the identification procedure is not as clear cut. However, for process control purposes, this method in conjunction with calibration curves, can be quite useful. While ancillary equipment such as a mass spectrometer is extremely beneficial, the peak shape allows solute identification with relative ease.

Relation of parameters to chromatographic data

The parameter C_2, as discussed previously, controls the broadness of the back portion of the peak which may contain valuable chromatographic information. Similarly, the parameters C_3'/C_8' and C_7, also used for the qualitative analysis study, were thought to contain such data. By examination of the processes that occur within the column and correlating them with various parameters of the equation of Chesler and Cram, much more information may be readily obtainable by the chromatographer.

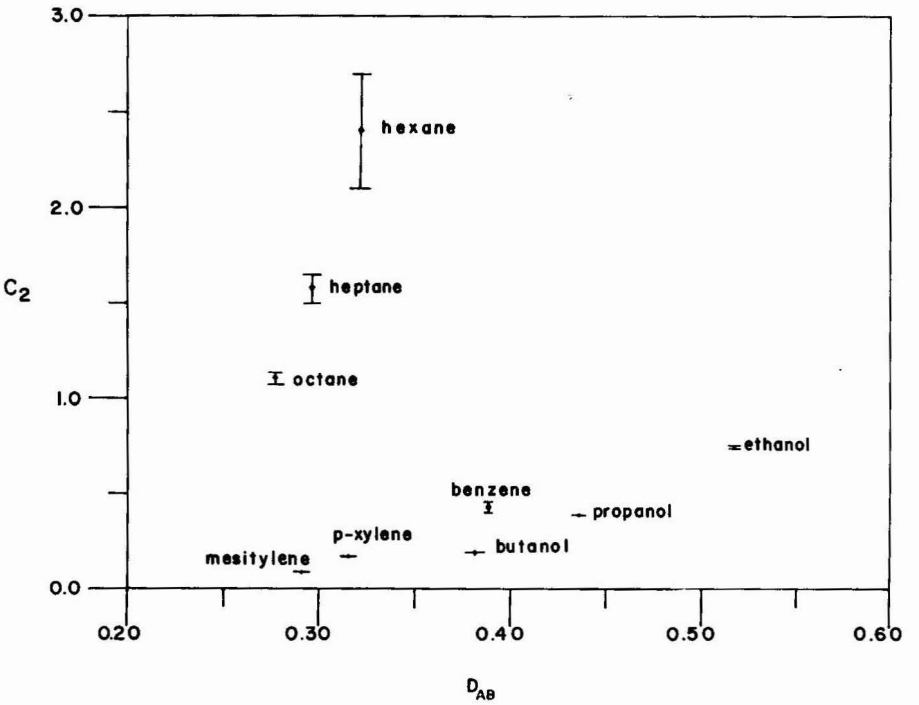


Fig. 3. Relationship between C_i and the diffusion coefficients of the solutes in helium. The vertical bars indicate the standard deviation in C_2. The horizontal bars indicate that the errors involved were so small that they could not be shown on this scale.

The first process investigated was the diffusion of the solute in the mobile phase. If diffusion was to play an important role in the shape of the profile, it should be reflected in the various parameters. Fig. 3 shows a plot of C_2 *versus* D_{AB}, the diffusion coefficient of the solute in helium at 60°, calculated from the equation of Fuller *et al.*[24]. All of the solutes seem to be reflecting the same behavior according to their family, namely, an almost linear dependence of C_2 on the diffusion coefficient D_{AB} exists. If indeed this is the case, such graphs could be used to estimate diffusion coefficients with relative ease. This is an exciting extension of the fitting procedure. The trend that occurs when plotting C_7 *versus* D_{AB} (Fig. 4) is not as linear, but again a reasonable estimate of D_{AB} may still be possible to obtain. It is interesting to note that for the C_3'/C_8'–D_{AB} coordinate system (Fig. 5) the aromatics retained the configuration that they had exhibited in the C_3'/C_8'–C_2 coordinate system. Figs. 3–5 seem to imply that the diffusion in the mobile phase plays a singificant role in the shape of the profile. A more extensive study into the dependence of C_2, C_7, C_8, and C_3 on D_{AB} is now being carried out in this laboratory.

The next chromatographic parameter that was examined was the capacity ratio k'. Since this parameter reflects the amount of the solute in the stationary and mobile phases, it is characteristic of the solute for a given combination of stationary

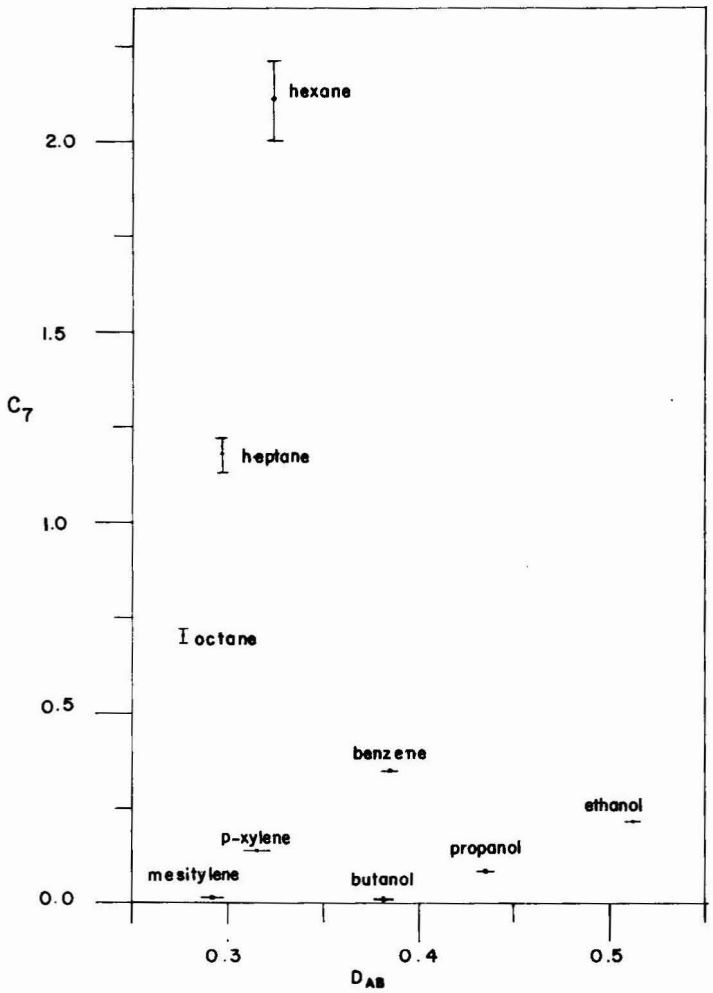


Fig. 4. Relationship between C_7 and D_{AB} of the solutes in helium. The vertical bars indicate the standard deviation in C_7. The horizontal bars denote small errors that could not be shown to scale.

and mobile phases. In Fig. 6, a plot of k' *versus* C_2 illustrates the relationship between these two parameters. As the size of the molecule increases within a given family, its capacity ratio increases as C_2 decreases. This was found to be the case for the three families studied. It was this relationship that prompted the correlation of C_2 to the resistance to mass transfer in the stationary phase.

The dependence of the resistance to mass transfer in the stationary phase on the capacity ratio is via the term $k'/(1 + k')^2$ (ref. 11). By plotting C_2 against this term (Fig. 7), it is shown that, again, nearly a linear relationship exists for a specific family. It is of interest to note that while the aromatics and alcohols correlate with a positive slope, the alkanes follow a negative slope. This can be explained by virtue of the fact that the capacity ratios for the alkanes range from 0.3–1.5 while the remaining families have k' values with a minimum of 5.2. It is well known that the resistance to mass

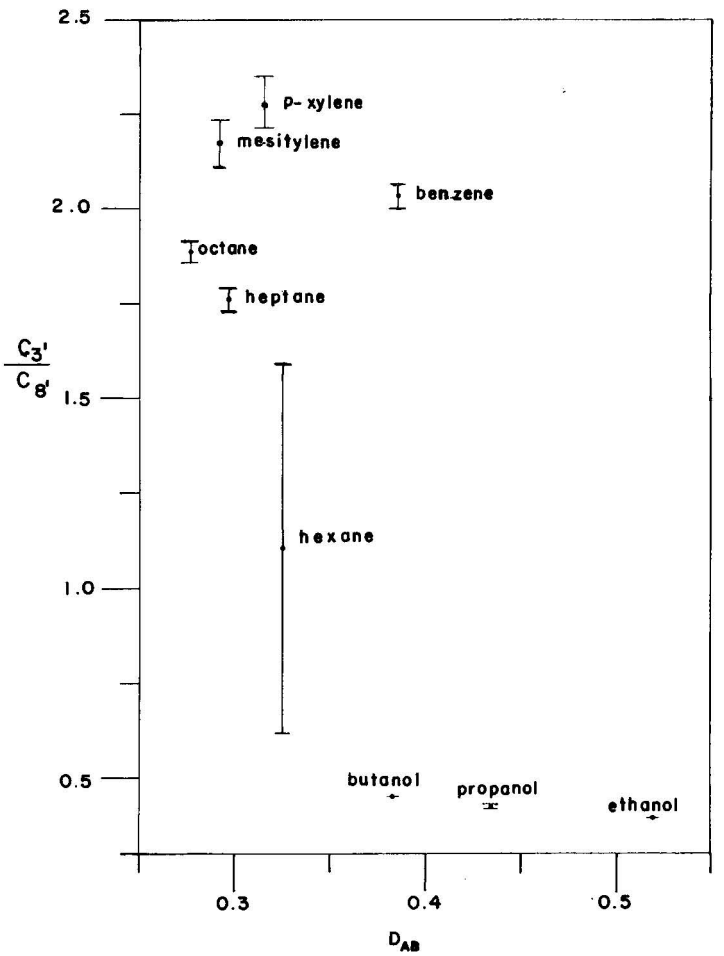


Fig. 5. Relationship between C_3'/C_8' and D_{AB} of the solutes. The vertical bars indicate the standard deviation in C_3'/C_8'. The errors denoted by the horizontal bars were too small to be drawn on this scale.

transfer in the stationary phase shows a maximum at $k' = 1$. Thus it is possible that C_2 is related to the plate height. Further work is being done to test the validity of the correlation of C_2 to the resistance to mass transfer term. If a definite correlation can be established, then rates of adsorption–desorption, diffusivity of the solute in the stationary phase, and the thicknes sof the film of stationary phase on the solid support may become easily evaluated via C_2 and other parameters of the equation of Chesler and Cram. Similarly, surface activity coefficients and other related thermodynamic data[25] may be correlated to these parameters.

In summary, the use of the mathematical model proposed by Chesler and Cram for non-linear least squares curve fitting can allow the identification of two solutes with approximately the same retention times without alteration of the column conditions. Also, the relation of these fitted parameters to the physical processes associ-

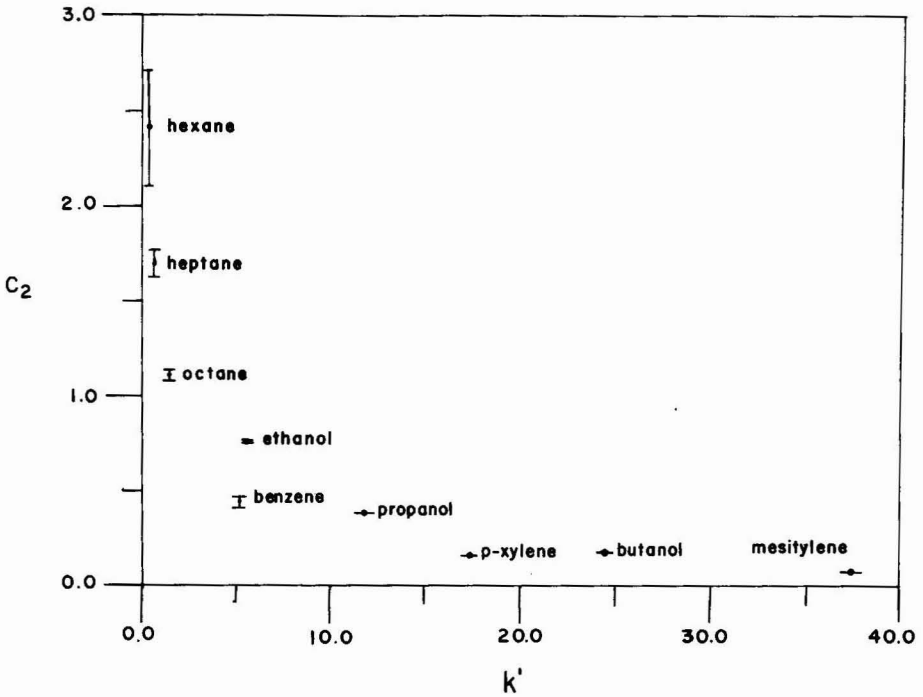


Fig. 6. Relationship between C_2 and the capacity ratio, k', of the solutes. The vertical bars indicate that the errors involved could not be shown on this scale.

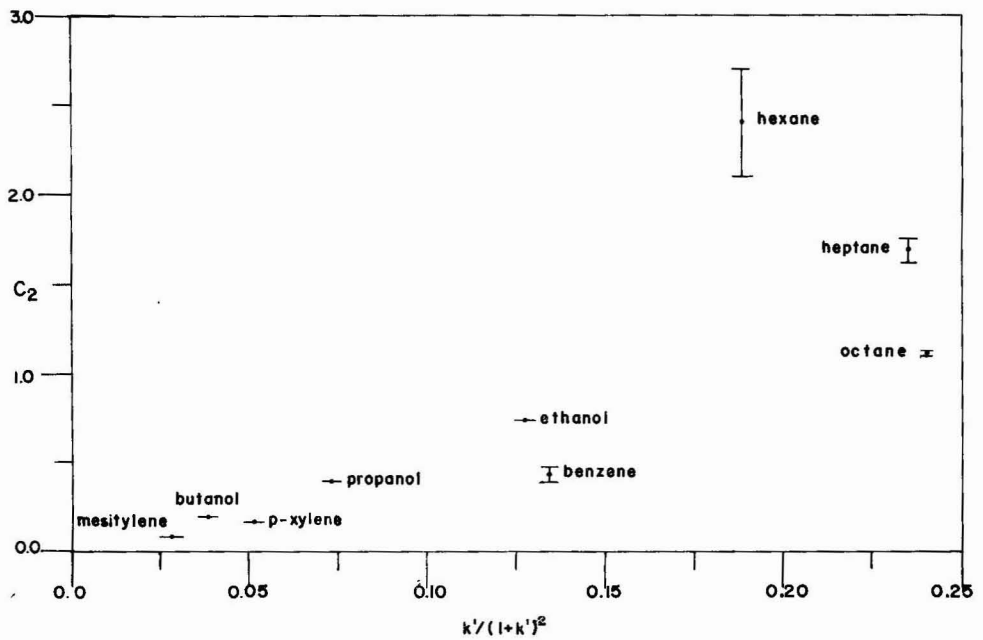


Fig. 7. Relationship between C_2 and $k'/(1 + k')^2$ for the various solutes. The vertical bars indicate the standard deviation in C_2. All horizontal bars indicate an error too small to be shown on this scale.

ated with the chromatographic analysis may produce a deeper insight into column processes. For both qualitative analysis and relating the parameters to chromatographic data, this method is much simpler and easier to use than the previous method of moment analysis. By expanding this study to various other families and column conditions, it is the goal of the authors to provide sufficient physical data for the support of the empirical model employed in this work.

ACKNOWLEDGEMENT

The authors wish to thank Paul Schnipelsky for the collection of data used for this study.

REFERENCES

1 E. Kováts, in J. C. Giddings and R. A. Keller (Editors), *Advances in Chromatography*, Marcel Dekker, New York, 1965, p. 22.
2 L. Rohrschneider, *Anal. Chem.*, 45 (1973) 1241.
3 D. A. Leathard and B. C. Shurlock, *Identification Techniques in Gas Chromatography*, Wiley-Interscience, New York, 1970, pp. 41–63.
4 J. Tranchant (Editor), *Practical Manual of Gas Chromatography*, Elsevier, Amsterdam, 1972, pp. 245–250.
5 E. Grushka, in N. Catsimpoolas (Editor), *Methods of Protein Separation*, Vol. 1, Plenum Press, New York, 1975, pp. 161–192.
6 E. Grushka, M. N. Meyers, P. D. Schettler and J. C. Giddings, *Anal. Chem.*, 41 (1969) 889.
7 E. Grushka, *Anal. Chem.*, 44 (1972) 1733.
8 S. N. Chesler and S. P. Cram, *Anal. Chem.*, 43 (1971) 1922.
9 O. Grubner, *Anal. Chem.*, 43 (1971) 1934.
10 J. C. Sternberg, in J. C. Giddings and R. A. Keller (Editors), *Advances in Chromatography*, Vol. 2, Marcel Dekker, New York, 1966, pp. 205–270.
11 J. C. Giddings, *Dynamics of Chromatography, Part 1, Principles and Theory*, Marcel Dekker, New York, 1965.
12 M. H. J. van Rijswick, *Chromatographia*, 7 (1974) 491.
13 R. D. B. Fraser and E. Suzuki, *Anal. Chem.*, 41 (1969) 37.
14 R. S. Swingle and L. B. Rogers, *Anal. Chem.*, 44 (1972) 1415.
15 S. N. Chesler and S. P. Cram, *Anal. Chem.*, 45 (1973) 1354.
16 W. F. Gutknecht and S. P. Perone, *Anal. Chem*, 43 (1971) 883.
17 D. Macnaughton, Jr., L. B. Rogers and G. Wernimont, *Anal. Chem.*, 44 (1972) 1421.
18 A. Anderson, T. C. Gibb and A. B. Littlewood, *Anal. Chem.*, 42 (1970) 434.
19 E. Grushka and V. R. Maynard, *J. Phys. Chem.*, 77 (1973) 1437.
20 E. Grushka and P. Schnipelsky, *J. Phys. Chem.*, 78 (1974) 1428.
21 S. M. Roberts, D. H. Wilkinson and L. R. Walker, *Anal. Chem.*, 42 (1971) 886.
22 "*S/RNLI*", State University of New York at Buffalo Computing Center, Buffalo, N.Y.
23 D. W. Marquardt, *J. Soc. Ind. Appl. Math.*, XI (1963) 431.
24 E. N. Fuller, P. D. Schettler and J. C. Giddings, *Ind. Eng. Chem.*, 58 (1966) 19.
25 E. Eon and G. Guiochon, *J. Colloid Interface Sci.*, 45 (1973) 521.

Journal of Chromatography, 126 (1976) 205–211
© Elsevier Scientific Publishing Company, Amsterdam — Printed in The Netherlands

CHROM. 9429

APPLICATION OF GAS CHROMATOGRAPHIC HEADSPACE ANALYSIS TO THE CHARACTERIZATION OF CHEMICAL EQUILIBRIA IN SOLUTIONS

A. G. VITENBERG, B. V. IOFFE, Z. ST. DIMITROVA and T. P. STRUKOVA
Chemistry Department, Leningrad State University, 199164 Leningrad (U.S.S.R.)

SUMMARY

The possibility is considered of using headspace analysis in studies of chemical equilibria in solutions of volatile organic compounds. The main theoretical relationships for the determination of the constants of $X + Y \rightleftarrows XY$ type equilibria by the gas chromatographic analysis of equilibrated vapour above a solution are derived. New methods are proposed and have been checked experimentally for the measurement of the ionization constants of volatile organic compounds, and of the stability constants of metal complexes with unsaturated and aromatic hydrocarbons.

INTRODUCTION

Because of their wide use and obvious advantages, gas chromatographic methods for the characterization of liquids and solids based on the analysis of the equilibrated vapour phase, the so-called headspace analysis (HSA), are important not only to analytical chemists working with industrial and agricultural products and biochemical and medical personnel[1], but also to chemical research workers engaged in the determination of various physico-chemical parameters. Indeed, the possibility of employing HSA for the characterization of non-ideal solutions has recently been pointed out[2]. Binary systems exhibiting positive and negative deviations from Raoult's law have been used to illustrate the possibility of determining activity coefficients and some thermodynamic functions. In this paper, we wish to draw attention to an interesting and promising application of HSA to the determination of the constants of chemical equilibria in solutions with volatile organic compounds.

THEORETICAL

Consider the simplest case of a chemical equilibrium which is the reversible interaction of equimolecular amounts of components X and Y involving the formation of an adduct XY:

$$X + Y \rightleftarrows XY$$

only one of the reagents (X) being volatile and thus present in the vapour above the solution.

To determine the equilibrium constant

$$K = \frac{[X]\,[Y]}{[XY]} \tag{1}$$

it is sufficient in this instance to measure the equilibrium concentration of the volatile reagent X in the vapour above two solutions with different concentrations of the non-volatile reagent Y. Indeed, if the total amount of the volatile reagent in a heterogeneous vapour–liquid system is maintained constant while varying the concentration of the non-volatile reagent from [Y] to [Y′], then the balancing equation can be written in the form

$$C_x v_g + [X]v_l + \frac{[X]\,[Y]v_l}{K} = C_x' v_g + [X']v_l + \frac{[X']\,[Y']v_l}{K} \tag{2}$$

where C_x and C_x' are the equilibrium concentrations of component X in the gas phase of the corresponding solutions, and v_g and v_l are the gas and liquid phase volumes, respectively. Assuming the partition coefficient, K_p, of component X to be constant, one can take write that

$$K_p = \frac{[X]}{C_x} = \frac{[X']}{C_x'}$$

after which eqn. 2 reduced to

$$K = \frac{(C_x\,[Y] - C_x'\,[Y'])\,K_p v_l}{(C_x' - C_x)\,(v_g + K_p v_l)} \tag{3}$$

Vapour sample collection for a gas chromatographic determination of the concentrations C_x and C_x' without violating the equilibrium in the system can be performed by the technique making use of variable-volume vessels representing essentially thermostated glass hypodermic syringes developed in our laboratory[3]. The same technique can be employed in the determination of the partition coefficients, K_p (ref. 4).

Depending on the actual numerical values of the constants K and K_p, and on the methods of selecting (or determining) the concentrations [Y] and [Y′], the general relationship expressed in eqn. 3 can be simplified and modified to fit the study of specific chemical equilibria in solutions, *e.g.*, dissociation of volatile organic bases or complexing with volatile ligands. This will be discussed below, after giving the basic experimental data.

EXPERIMENTAL

Commercial preparations of hydrocarbons, amines and pyridine were used. The amines and pyridine were additionally purified by distillation in a rectification column.

The samples were analyzed on a Tsvet-102 chromatograph with a flame-ionization detector under the conditions specified in Table I.

The initial ligand concentration in solution when studying the complex stability

TABLE I

CONDITIONS OF GAS CHROMATOGRAPHIC ANALYSIS

Chromatographic parameters	*Compounds to be analyzed*				
	Olefins	*Aromatic hydrocarbons*	*Amines*		
			Trimethylamine and pyridine	*Diisopropylamine*	*Aromatic*
Stationary phase	Triethylene glycol butyrate	Polyethylene glycol adipate	Polyethylene Polyox-100 + Na_3PO_4	Pennwalt 223 + KOH	Polyethylene Polyox-100 + Na_3PO_4
Amount of stationary phase (%)	30	20	10/1	28/4	10/1
Support, particle diameter (mm)	Spherochrome-1, 0.25–0.375	Spherochrome-1, 0.20–0.25	Chromosorb W, 0.20–0.25	Gas-Chrom R, 0.16–0.20	Chromosorb W, 0.20–0.25
Column length (m)	6	2	2	2	2
Column temperature (°C)	30	90	100	100	135
Carrier gas	Argon	Argon	Nitrogen	Nitrogen	Helium
Carrier gas flow-rate (ml/min)	55	60	60	60	60
Gas sample valve temperature (°C)	40	100	130	130	130
Sample volume (ml)	1	1	1.5	1.5	1.5

constants was 10^{2}–10^{-3}%. Such concentrations of gaseous hydrocarbons in solution were prepared by introducing 0.3–0.8 ml of the compound of interest into the reaction vessel with the known gas-to-liquid volume ratio ($V_g/V_l = 0.5$–2). The values of the liquid–gas partition coefficients required to calculate the stability constant and the pre-set olefin concentration in solution were determined by the method based on measuring the change in the concentration of a compound in the gas phase with the equilibrated gas replaced with pure gas[3]. Liquid substances were introduced into the reaction vessel in the form of a solution, its concentration being adjusted to the required level by diluting a saturated aqueous solution of the corresponding hydrocarbon.

To determine the stability constants of weak complexes, the reaction vessel, after introducing the ligand, was thermostated to within ± 0.1°C for 30–40 min under continuous stirring. Next, the gas phase was injected into the chromatograph (5–10 samples) and the peak area corresponding to C_g° was determined.

The complexing agent was introduced into the reaction vessel in the form of a solution of known concentration by means of a hypodermic syringe. The amount of the solution introduced was determined by weighing it to ± 0.3%. After the injection of the complexing agent, the system was shaken periodically for 1–1.5 h. Next, the gas phase was chromatographed and the peak area corresponding to C_g' measured.

The value of pK was determined in the following way. Some of a buffer solution containing the compounds under study at concentrations of 0.07–0.5% was introduced into the reaction vessel[3] thermostated at 25 ± 0.1°. The system was shaken periodically for 30 min to establish equilibrium, after which the equilibrated gas was injected into the chromatographic column by means of a thermostated gas

sample valve[4]. The peak areas were measured with a Takeda-Riken TR-2213 digital integrator.

It should be pointed out that in order to exclude errors associated with the strong sorption of amines, the tubes admitting the gas under study to the chromatograph were saturated, prior to the analysis of the equilibrated gas phase, with an auxiliary gas sample containing the amines of interest in concentrations close to those encountered in the gas to be analyzed.

STUDY OF SPECIFIC CHEMICAL EQUILIBRIA IN SOLUTIONS

Determination of ionization constants of volatile organic compounds by the HSA method

The basicity of a volatile compound B can be characterized by the dissociation constant of the conjugated acid BH^+:

$$K_{BH^+} = \frac{[B]\,[H^+]}{[BH^+]} \tag{4}$$

As eqn. 4 is only a special case of eqn. 1 at X = B, Y = H^+ and XY = BH^+, one can use eqn. 3 to calculate K_{BH^+}. The partition coefficient of volatile organic bases between water and air is usually sufficiently high so that $K_p \gg v_g/v_l$. If the magnitude of K_p is unknown, the constancy of [B] with the equilibrium gas being replaced with a pure gas may serve as a criterion for meeting this condition. In this case, neglecting the possibility of ionization of the base in the gas phase, eqn. 3 reduces to a simpler equation:

$$K_{BH^+} = \frac{\frac{C_B}{C'_B}[H^+] - [(H^+)']}{1 - \frac{C_B}{C'_B}} \tag{5}$$

If equal volumes of the vapour samples are injected into a gas chromatograph at different pH values of the solutions, the concentration ratio of the free base in the vapours, C_B/C'_B, can be replaced with the ratio of the areas of the corresponding peaks in the chromatograms, S_B and S'_B, or simply by the ratio of the integrator readings:

$$K_{BH^+} = \frac{\frac{S_B}{S'_B}[H^+] - [(H^+)']}{1 - \frac{S_B}{S'_B}} \tag{6}$$

The proposed method of determining the basicity constants of volatile organic compounds thus reduces to measuring the peak area ratio for the free bases in the vapour chromatograms of solutions with different hydrogen ion concentrations. The latter can be measured directly with a hydrogen electrode or can simply be fixed by employing buffer solutions with accurately known values of pH. In this simplest version, the proposed method of the basicity constant determination consists in injecting equal amounts of the base-containing compound of interest into a predetermined volume of buffer solutions with different values of pH, chromatographing the equilibrated vapours of these solutions and calculating K_{BH^+} with eqn. 6.

It should be stressed that such a determination of the basicity constants can be

carried out in complex mixtures of compounds of different nature and different volatility, even if the total quantitative and qualitative compositions of these mixtures remain unknown. However, in order to obtain sufficiently accurate results, it is essential to select the pH value of the solutions under study such that the peak areas S_B and S'_B are determined with the maximum accuracy possible and that the operating pH range lies in the region of maximum sensitivity of the areas S_B to the change in pH. The quantity pK_{BH^+} corresponds to the centre of this region, and therefore solutions with pH $\approx pK_{BH^+} \pm 1$ will be optimal for the measurement of K_{BH^+}. The magnitudes of pK_{BH^+} for most volatile organic bases (amines, hydrazines, nitrogen heterocyclic compounds) lie from 4 to 11, and all of this range can be covered by four or five buffer solutions with pH 3–12. It is these four or five solutions that should be used in determining the basicity constants by the proposed version of the gas chromatographic method.

The results of these determinations, listed in Table II, indicate that the accuracy of pK_{BH^+} of the order of ± 0.2 pK units reached is sufficient for the purposes of qualitative analysis and classification. The method proposed can also be used when known techniques of determining the basicity constants cannot be employed (*e.g.*, the characterization of complex mixtures of unknown composition) and represent an additional useful tool.

TABLE II

DETERMINATION OF BASICITY CONSTANTS BY THE GAS CHROMATOGRAPHIC HSA METHOD

Base	*pH and pH′*	*Base peak area ($\bar{S}$) on vapour chromatogram (integrator reading)*	*Values of pK_{BH^+}*		*Error, I–II*
			By eqn. 6 (I)	*Literature data (II)*	
Diisopropylamine	11.27	175,657	11.30	11.05[5]	+ 0.25
	11.58	238,234			
Trimethylamine	8.82	22,241	9.65	9.80[6]	− 0.15
	10.10	127,709			
Aniline	4.45	68,063	4.65	4.61[6]	+ 0.04
	6.15	169,726			
Diethylamine	5.42	7117	6.66	6.56[6]	+ 0.10
	6.80	75,910			
Pyridine	4.45	20,541	5.51	5.25[5]	+ 0.26
	6.80	242,494			

Determination of stability constants of complexes with volatile ligands

If we introduce into a heterogeneous gas–liquid system containing a volatile ligand X without a complexing agent ([Y] = 0), a non-volatile complexing agent in an amount corresponding to its concentration in the liquid phase [M], the ligand concentration in the vapour will decrease from the original value C_x to C'_x. For low stability constants $K_{st} = 1/K$ (<100) and low ligand concentrations in solution (10^{-3}–10^{-4}%), one can assume [Y′] to be approximately equal to [M], so that eqn. 3 will become

$$K_{st} = \left(\frac{C_x}{C'_x} - 1\right) \cdot \frac{v_g + K_p v_l}{K_p v_l [M]} \qquad (7)$$

or, replacing the ligand concentration ratio by the ratio of the peak areas on chromatograms obtained from equal samples of vapour over the solution,

$$K_{st} = \left(\frac{S_x}{S'_x} - 1\right) \cdot \frac{v_g + K_p v_l}{K_p v_l [M]} \quad (8)$$

Thus, as for the basicity constants, the problem of determining the stability constants of complexes reduces to the measurement of the peak area ratio on the vapour chromatograms of two solutions, one of which does not contain the complexing agent while the other contains it at a concentration [M].

The applicability of the proposed method and of eqn. 8 was checked on well studied cases of complexing of silver salts with olefins and aromatic hydrocarbons in aqueous solutions.

Table III presents a comparison of the stability constants obtained by this method for silver complexes of four simple olefins and two aromatic hydrocarbons with the data available in the literature. The comparison shows a fairly good agreement with the results obtained by both static and dynamic methods. A larger disagreement with the results obtained by the dynamic method for α- and *cis*-butenes can be attributed to the poor accuracy inherent in the dynamic determination of small partition coefficients of olefins in volatile solvents ($K_p < 0.1$).

TABLE III

STABILITY CONSTANTS OF SILVER AND THALLIUM NITRATE COMPLEXES WITH HYDROCARBONS IN AQUEOUS SOLUTION AT 25°

Ligand	*Silver nitrate*			*Thallium nitrate*
	Obtained by injection of complexing agent into system	*Literature data*		*Obtained by injection of complexing agent into system*
		Static method	*Dynamic method*	
Ethylene	88.9 ± 4.0	85.3[9]	85[8]	7.6 ± 3.1
Propylene	70.8 ± 4.2	87.2[9]	79[8]	5.1 ± 2.3
α-Butene	121.8 ± 8.7	119.4[9]	110[8]	7.7 ± 3.0
cis-Butene	65.9 ± 2.8	62.3[9]	83[8]	4.7 ± 1.4
Benzene	2.67 ± 0.13	2.41[7]	1.58*[8]	0.65 ± 0.04
Toluene	3.19 ± 0.16	2.95[7]	1.19[8]	0.93 ± 0.04

* Data for calculation obtained at 23.2°.

The application of the proposed method in the study of weak interactions ($K_{st} < 10$) is illustrated by the data on the silver nitrate complexes with benzene and toluene, which agree well with the results of the static method based on spectrographic analysis[7] while differing considerably from the constants obtained by the dynamic method[8]. Good agreement between the results obtained by static methods based on different principles permits one to consider the values of the constants of weak complexes obtained under static conditions to be more reliable and accurate. Such weak interactions apparently do not permit one to use the dynamic gas chromatographic method successfully in this cace.

The possibilities offered by the proposed method in the determination of the K_{st} values of weak complexes are also illustrated by the results of a study of thallium

nitrate complexes with hydrocarbons. The data listed in Table III show that even for fairly weak complexes with aromatic hydrocarbons a good agreement is obtained, relative variations in the value of the constant not exceeding 5%. The relative error of K_{st} depends, however, essentially on the values of K_p, so that for olefin complexes it reaches a few tens percent despite the considerably larger absolute value of K_{st}.

REFERENCES

1 A. G. Vitenberg, B. V. Ioffe and V. N. Borisov, *Chromatographia*, 7 (1974) 610.
2 B. Kolb, *J. Chromatogr.*, 112 (1975) 287.
3 A. G. Vitenberg, I. L. Butaeva and Z. St. Dimitrova, *Chromatographia*, 8 (1975) 693.
4 A. G. Vitenberg, B. V. Ioffe, Z. St. Dimitrova and I. L. Butaeva, *J. Chromatogr.*, 112 (1975) 319.
5 J. A. Riddick and W. B. Bunder, *Organic Solvents, Physical Properties and Methods of Purification*, 3rd ed., 1970, p. 2.
6 *Metodi organicheskoi Khimii (Methods of Organic Chemistry)*, Vol. 1, Khimia, Moscow, 1967.
7 L. A. Andrews and R. M. Keefer, *J. Amer. Chem. Soc.*, 71 (1949) 3644.
8 S. P. Wasik and W. Tsang, *J. Phys. Chem.*, 74 (1970) 2970.
9 K. N. Trueblood and H. J. Lucas, *J. Amer. Chem. Soc.*, 74 (1952) 1333.

Journal of Chromatography, 126 (1976) 213–224
© Elsevier Scientific Publishing Company, Amsterdam — Printed in The Netherlands

CHROM. 9506

CHARACTERIZATION OF COAL-DERIVED FLUIDS BY CAPILLARY COLUMN GAS CHROMATOGRAPHY–MASS SPECTROMETRY

W. BERTSCH and E. ANDERSON
Department of Chemistry, University of Alabama, University, Ala. 35486 (U.S.A.)
and
GUENTHER HOLZER
Department of Biophysics, University of Houston, Houston, Texas 77004 (U.S.A.)

SUMMARY

A coal-derived fluid has been analyzed by high-resolution gas chromatography–mass spectrometry with glass capillary columns, both before and after liquid chromatography on silica gel. The bulk of the sample consists of only a few types of compounds. Alkyl-substituted indanes and tetralins account for most of the constituents at the high-molecular-weight end of the mixture and cycloalkanes are the predominant substance type in the high-volatility range. Substituted aromatic hydrocarbons and alkanes, in particular *n*-alkanes, are distributed over the entire boiling point range. Oxygen- and nitrogen-containing substances are present in only small concentrations and cannot be analyzed directly without enrichment. A new method for the concentration of eluents resulting from liquid chromatography is introduced.

INTRODUCTION

The need for more and more energy with a concurrent decline in petroleum supplies has focused interests to fuels derived from coal, shale and tar sands. It can be expected that fuels derived from such sources will play a significant role in the future. Coal is the most abundant source of energy in the U.S.A. Many different technical approaches to convert coal into liquefied fuels have been experimented with, dating back to World War II. Within limits, some variables in the liquefaction process can be adjusted for a maximum yield of the desired products. Depending on the composition of the coal, varying proportions of undesirable byproducts also have to be dealt with. The composition of liquefied coal must be known in some detail to determine the reaction mechanisms underlying the conversion process. The necessary steps can then be undertaken to obtain the best product distribution.

Coal-derived fluids differ from petroleum products mainly in respect to the heterocyclic fraction. Nitrogen-containing compounds and oxygenated substances are relatively abundant in such fluids. In the U.S.A., there are presently only a few pilot plants in operation. Most technical operations are supported by the United States Energy Research and Development Administration and some of its agencies.

Many of the analytical procedures have been worked out at the Bartlesville Energy Research Center, and samples of coal fluids are available from this source for experimental purposes.

Chemical characterization of coal liquids have been performed only on a limited number of samples. Such analyses have usually been limited to relatively narrow boiling-point fractions, due to the complexity of the material. Some analytical data are also available on full-boiling-range liquids, but these are less detailed.

Coal fluids represent mixtures of extreme complexity and several analytical methods have been applied towards their characterization. In most cases, samples have been divided into several fractions by distillation. Adsorption chromatography, gel permeation chromatography or a combination of both has been extensively used for group type separations[1–7]. Acid/base extraction or ion-exchange techniques often preceeded chromatography and removal of certain groups of compounds by complexation or selective destruction has also been described[8,9]. In most cases, several chromatographic steps had to be applied, making sample preparation rather time consuming. Spectroscopic methods, in particular NMR, have generally been applied to describe the overall compound distribution[10]. Mass spectroscopy[11–16] (MS) occupies a special position in the analytical scheme. Both low-resolution and high-resolution MS have been extensively applied, using matrices with sophisticated computer programs. This approach is especially useful for routine analysis, but has also been applied for the fraction containing heterocyclic and oxygenated compounds which are sometimes difficult to handle by chromatographic techniques. The cost of mass spectral instrumentation, however, is considerable.

Some of the first and most impressive applications of high-resolution gas chromatography (GC) with capillary columns have been in the field of petroleum chemistry where the technique is still extensively used. GC, however, has a limited scope in the overall characterization of coal-derived fluids. One of its major uses is for simulated boiling-point distributions[17,18]. Short capillary columns are especially useful in that respect, since they easily cover a boiling-point range of several hundred degrees in a very short time with good accuracy and at minimal expenditure.

Capillary column GC can provide a detailed picture of individual components in a complex sample. In some cases, it may be desirable to identify such trace compounds for investigation of toxicological properties and to establish data which are related to health aspects. Although coal fluids have been fairly well characterized in respect to the chemical groups present, no detailed analysis of individual compounds by GC–MS has been done to this date. One purpose of this study was to obtain a picture of the distribution of major individual hydrocarbons. It was also of interest to determine to what extent the technique could serve as supplement or replacement for the mass spectral procedures in present use.

EXPERIMENTAL

Two Hewlett-Packard gas chromatographs, Models 5830 and 5720, with single flame ionization detector were used. Both instruments were modified to accept glass capillary columns. To protect the capillary columns from heavy materials, a short plug of approximately 10 mg of Tenax GC (Applied Science, State College, Pa., U.S.A.) held between two glass wool plugs, was inserted into the injector port glass

liner. The septum was partially insulated from the heat of the injector body by a disc of polyimide.

Thick-wall soft-glass tubing 1500 × 10 mm O.D. × 4 mm I.D. (Kimble Glass Co., Article No. 46475) was rinsed with several solvents, including detergents. The tubes were then carefully rinsed with water and dried in a flame. A Shimadzu glass drawing machine was slightly modified to accept this extra heavy tubing.

OV-101 and Dexsil 300 GC (Applied Science) served as stationary phases. The glass capillaries underwent different types of pretreatment before the final coating. Some columns were silanized in the gas phase[19] followed by the deposition of a layer of Silanox 101[20] (Cabot Corp., Boston, Mass., U.S.A.). Others were coated with a thin layer of Carbowax 20M, heated to 275° overnight and then extracted with methylenechloride[21]. The columns were coated by either the mercury plug method[22] or a modified static evaporation technique[23] in which the column is screwed into a hot oven. All these techniques yielded columns of approximately equal performance. We do not have a preference for any particular procedure for these nonpolar columns.

Group separations were performed on activated silica gel. Columns 300 × 10 mm O.D. were slurry packed with hexane Hexane and benzene (Burdick and Jackson Labs., Muskegon, Mich., U.S.A.) were used without further purification. A 50-μl aliquot of the coal fluid (Syncrude from Western Kentucky Coal, obtained from Dr. J. E. Dooley) was transferred onto the head of the column with a syringe. 30-ml fractions were collected for each of these solvents. Further concentration was done by one of two methods: Blowing a gentle stream of purified nitrogen (charcoal cold trap) over the surface of the liquids, or by a modified microdistillation technique. In the latter, a 50-ml flask with a graduated tip at the bottom was used with a Snyder column. After the solvent had been reduced to 500 μl an appropriate aliquot, usually between 10 and 50 μl, was withdrawn and injected into a small tube, 80 × 4 mm O.D., filled with 20 mg of conditioned Tenax. The bulk of the solvent was blown off at ambient temperature for a few minutes with nitrogen, at a flow-rate of 40 ml/min. The adsorbent tube was placed directly into the injector port of the gas chromatograph for thermal elution of the trapped substances onto the glass capillary column. A small U trap at the beginning of the capillary, immersed in liquid nitrogen, provided the necessary sharp injection.

Identifications were performed on a LKB 9000 gas chromatograph–mass spectrometer combination. The glass capillary column was connected to the instrument via Vespel ferrules (Alltech, Arlington Heights, Ill., U.S.A.). The glass capillary 45 m × 0.35 mm I.D. was flow controlled at a rate of 3 ml/min. A single jet, held at 250°, served as interface. Spectra were taken at an ionization voltage of 70 eV and a trap current of 80 μA. Scan time was 2 sec per decade. Spectra were largely deducted from standard tables[24]. The boiling point distribution was determined by coinjection of a standard of *n*-alkanes.

RESULTS AND DISCUSSION

Several coal-derived fluids of various boiling-point ranges were run by GC with glass capillary columns coated with a nonselective high-temperature phase. A fluid, derived from Kentucky coal and prepared by the Char-Oil-Energy-Development

(COED) process, was chosen for our studies. The brownish viscous liquid was centrifuged, but failed to produce a noticeable amount of sediment.

Both acidic and basic substances are known to be present in the total fluid, and care has to be taken to select a glass capillary column with the proper acid/base behavior or to simultaneously employ two columns, one with a slightly acidic and the other with a slightly basic surface. Glass capillaries were tested for their behavior towards acidic and basic compounds. An acidic standard was prepared consisting of phenol, cresol isomers and *p*-ethylphenol. Another standard contained the basic compounds pyridine, aniline and N,N-dimethylaniline. Approximately 10 ng of each of these compounds, in a suitable solvent, were introduced into the column and all substances eluted, although some tailing was observed, especially with the phenols. Since both types of substances passed through the column at trace levels, it was decided not to prepare columns with basic or acid surfaces. Such surfaces are difficult to prepare reproducibly.

Proper surface deactivation for glass capillary columns is of prime importance for the analysis of mixtures as heterogeneous as coal fluids. Such samples contain large amounts of relatively nonvolatile substances. These heavy ends cause a deterioration of column performance with extensive use. It is therefore important to protect the column from such materials. The application of a short precolumn is a possibility. Passage of the desired substances onto the analytical column, however, must be verified, and the adsorbent also must be highly inert.

Two adsorbents, Carbopack BHT and Tenax GC, were tested for their suitability to serve as packing material for the precolumn. Plugs of approximately 1 cm length were introduced into the glass injector port lines. A standard consisting of *n*-alkanes in the range of C_5–C_{40} was used to determine the boiling-point range for which the method is applicable at a given injector port temperature. The data are summarized in Table I. It can be seen that Carbopack BHT is rather active, whereas Tenax GC is more suitable for the purpose. Substances having boiling-points as high as pentacosane (b.p. 410°) can be desorbed at 320° without difficulty.

For MS applications, capillary columns must meet additional requirements.

TABLE I

COMPARISON OF CARBOPACK BHT AND TENAX GC AS PRECOLUMN ADSORBENTS AT INJECTOR PORT TEMPERATURE OF 320°

n-Alkane	*Recovery from precolumn (%)*	
	Tenax GC	*Carbopack BHT*
C_8	100	100
C_{10}	100	100
C_{16}	100	100
C_{18}	100	94
C_{19}	100	87
C_{22}	78	15
C_{24}	28	<5
C_{28}	≈ 0	0
C_{32}	0	0
C_{36}	0	0
C_{38}	0	0

Low bleeding at elevated temperature is of particular importance if the analysis of high-boiling substances is contemplated. A number of high-temperature stationary phases are commercially available. In some respect polar substrates such as the cyanosilicones are preferable since column deactivation becomes less critical. Resolutions are also often improved, since the elution of substances within a given boiling-point range is extended. Nonpolar phases, however, usually offer a wider temperature range and produce less bleeding at high temperature. We prefer OV-101 as stationary phase for high-temperature applications for these reasons. The phase can be used well beyond 200° at a very low background in the MS. Substances having boiling-points of above 350° can be eluted with ease.

Separation schemes for coal derived fluids are complex, and generally involve acid/base extraction and various combinations of liquid chromatography. It was planned to cut down on these sample preparation steps and take advantage of the extraordinary resolving power of an efficient glass capillary column. The selection of an essentially nonpolar stationary phase results in a separation according to the boiling-points of the sample components. Fig. 1 shows the total ion current monitor chromatogram of the coal fluid under study. Substances eluting after *n*-heneicosane have been omitted from the chart. Obviously, a considerable proportion of the components remains unresolved, especially at trace levels. About 280 mass spectral scans were taken during the run, but many substances eluted too fast to obtain adequate spectral scans. Overlap was still extensive in spite of the good separation power of the capillary. Investigation of the mass spectra revealed that most peaks were composed of several components.

Table II summarizes the identification of major components in the sample and gives an overview of the general nature of the most common substance types in the fluid. As expected, hydrocarbons, in particular homologues of substituted naphthenes, aromatics, indanes and naphthalenes make up the bulk of the sample. The mass spectra clearly indicate the substance type, but in cases where more than two hydrogen atoms have been substituted by alkyl groups, a large number of different patterns is possible. Since the mass spectra for such isomers are quite similar, GC retention data should be used if the identity of an individual compound needs to be established unequivocally.

There was no need for such detailed analysis, since the properties of interest of such homologues in a coal fluid are similar. Substitution patterns were only established in a few cases where standards are readily available. On well deactivated nonpolar columns, elution generally follows the boiling-points of the substances. Sometimes slight irregularities from this rule have been observed[18]. Caution must therefore be exercised if the order of elution is used as the basis for structural correlations.

Direct injection resulted in a very complicated chromatogram, and a way was sought to simplify the picture. A simple separation scheme involving silica gel column chromatography was applied to reduce some of the interferences. The sample was divided into polar and nonpolar fractions. Considerable overlap was observed, but the distribution ratio of a particular component in the fractions provided additional clues to its identity. Fig. 2 shows a total ion monitor chromatogram of a hexane fraction. The sample was prepared by successive injection of several charges of preconcentrated hexane eluent into an adsorbent tube containing Tenax, followed by frontal development of the solvent. The method is simple, fast and easily applicable

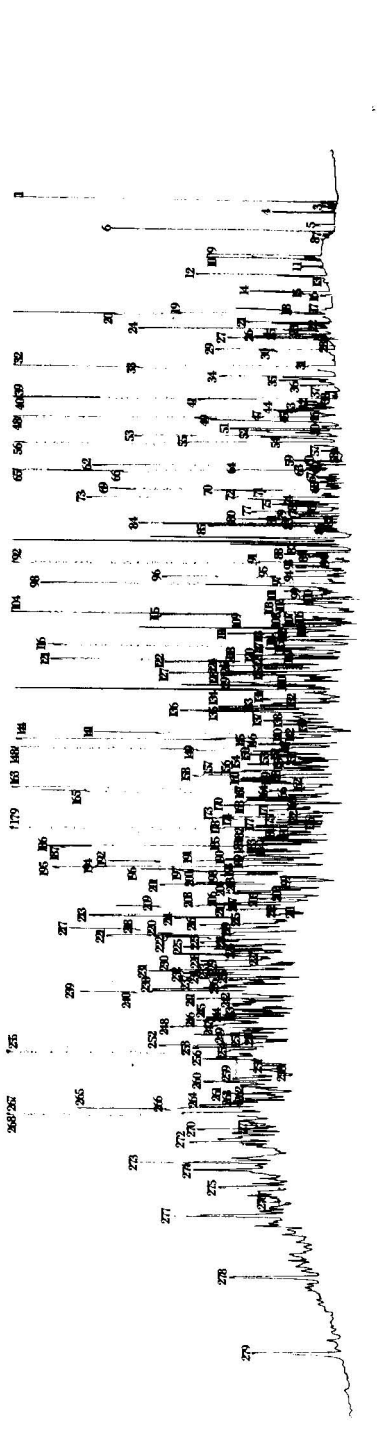


Fig. 1. Total ion current monitor chromatogram of a coal fluid derived from Western Kentucky coal. Conditions: glass capillary column, 45 m × 0.35 mm I.D. coated with OV-101; carrier gas (helium) flow-rate: 3.0 ml/min; temperature program: 0° (10 min), 0–220° at 2°/min. For identification of peaks see Table II.

TABLE II

IDENTIFICATION OF MAJOR COMPOUNDS IN A COAL-DERIVED FLUID

Peak No.	*Compound*	*Peak No.*	*Compound*
1	Ethane	80	*o*-Xylene
3	Chloromethane	82	C_9H_{18}
4	C_4H_{10}	84, 85	Methylethylcyclohexane
6	Pentane	87	Isopropylbenzene
7	Dichloromethane	88	Propylcyclohexane
9	2-Pentene	90, 91	Methylethylcyclohexane
10	2-Methylpentane	92, 93	Propylcyclohexane
11	3-Methylpentane	95, 96	*n*-Propylbenzene
12	*n*-Hexane	97	1-Methyl-3-ethylbenzene
14	Methylcyclopentane	98	1-Methyl-4-ethylbenzene + *trans*-hexahydroindan
15	C_7H_{14}		
17	C_7H_{14}	99	1,3,5-Trimethylbenzene + methylnonane
18	Benzene		
19, 20	Cyclohexane	100	1-Methyl-2-ethylbenzene
21	Dimethylpentane	101	1-Methyl-2-ethylbenzene
23	Cyclohexene	102	$C_{10}H_{20}$ + C_4-alkylcyclohexane
24	C_7H_{16}	103	1,2,4-Trimethylbenzene
25	C_7H_{14}	104	*cis*-Hexahydroindan
27	Dimethylcyclopentane	105	C_4-Alkylcyclohexane
28	C_5H_{16}	106	$C_{10}H_{22}$
29	C_7H_{16}	107	C_3-Alkylcyclohexane
31	Dimethylpentane	108, 109	$C_{10}H_{22}$ + C_4-alkylcyclohexane
32	Dimethylpentene	110	$C_{10}H_{20}$
34	3-Ethyl-1-pentene	111	$C_{10}H_{18}$
35	3-Ethyl-2-pentene	112	1,2,3-Trimethylbenzene + $C_{10}H_{18}$
36	C_2-Alkylcyclopentane	113	$C_{10}H_{18}$ + C_4-alkylbenzene
37	C_8H_{18}	115	Indan
38	Methylhexadiene + C_8H_{18}	117	*sec.*-Butylcyclohexane
39–41	Toluene	118	*n*-Butylcyclohexane
43	Methylhexadiene	119	C_4-Alkylcyclohexane
44	2,5-Dimethylhexane	120	$C_{10}H_{18}$
45	C_8H_{18}	121	C_4-Alkylbenzene
46	C_8H_{18}	122	C_4-Alkylbenzene
48–50	Dimethylcyclohexane	124, 125	C_4-Alkylbenzene
51, 52	Methylethylcyclopentene	126	C_4-Alkylcyclohexene + $C_{10}H_{18}$
53	Dimetyhlcyclohexane	127	*trans*-Decahydronaphthalene
54	Dimethylcyclohexane	128	C_4-Alkylbenzene + $C_{10}H_{18}$
56	Dimethylcyclohexane	129	*cis*-Decahydronaphthalene
59	Methylethylcyclopentane	130	C_4-Alkylbenzene
60	Dimethylcyclohexene	131	$C_{11}H_{24}$
64–66	C_3-Alkylcyclopentane	134	C_5-Alkylbenzene
67	C_8H_{16}	135	$C_{10}H_{18}$ + $C_{11}H_{22}$
68	C_3-Alkylcyclopentane	136	Methyldecane + nor-undecane
69	Ethylbenzene	137	Methyldecahydronaphthalene
71	Trimethylcyclohexane	138	Dimethylindan
72	*p*-Xylene	140	Ethylstyrene + C_5-alkylbenzene + 5-methylindan
73	*m*-Xylene		
74	C_8H_{14}	141	Methyldecahydronaphthalene
75	Ethylcyclohexene	142	C_2-Alkylindan + C_5-alkylbenzene
77	Methyloctene	143	C_5-Alkylbenzene
78, 79	Trimethylcyclohexane	144	5-Methylindan

(Continued on p. 220)

TABLE II *(continued)*

Peak No.	*Compound*	*Peak No.*	*Compound*
145	4-Methylindan	200	C_2-Alkyltetrahydronaphthalene + methylcyclohexylhexane
147	C_5-Alkylbenzene		
148	Tetrahydronaphthalene	201	C_2-Alkyltetrahydronaphthalene
150	C_5-Alkylbenzene + methyldecahydronaphthalene	204	C_2-Alkyltetrahydronaphthalene
		205	C_2-Alkyltetrahydronaphthalene
151	C_5-Alkylbenzene	206	C_2-Tetrahydronaphthalene
153	C_5-Alkylbenzene	208	$C_{13}H_{18}$
154	Naphthalene	210	$C_{13}H_{18}$
155, 156	C_2-Alkylindan	212	$C_{13}H_{18}$
157	C_2-Alkylindan	213	C_2-Alkylnaphthalene + C_3-alkylindan + $C_{13}H_{28}$
158	C_2-Alkylindan		
159	C_2-Alkylindan	214	C_3-Alkylindan
160	C_2-Alkylindan	215	C_2-Alkylnaphthalene + $C_{13}H_{18}$
161	4,1-Dimethylindan	216, 217	C_2-Alkylnaphthalene + $C_{13}H_{18}$
162	C_5-Alkylbenzene	218	$C_{13}H_{18}$
163	*n*-Dodecane	219	C_2-Alkylnaphthalene
164, 165	Methyltetrahydronaphthalene	220	C_2-Alkylnaphthalene
166	C_3-Alkylindan	221	C_2-Alkylnaphthalene + $C_{13}H_{18}$
167	C_5-Alkylbenzene	222	$C_{13}H_{18}$
168	C_6-Alkylbenzene + $C_{13}H_{28}$	223	$C_{13}H_{18}$
169	Methyltetrahydronaphthalene	224	$C_{13}H_{18}$
170, 171	C_3-Alkylindan	225	C_3-Alkylnaphthalene
172	C_3-Alkylindan	226	$C_{13}H_{18}$
173	C_2-Alkylindan	229	C_3-Alkyl-1,2-dihydronaphthalene
174, 175	C_6-Alkylbenzene	230	$C_{14}H_{20}$ + $C_{15}H_{32}$
177	C_3-Alkylindan	231	Diphenylmethane
178, 179	Methyltetrahydronaphthalene + $C_{17}H_{24}$	232	$C_{13}H_{18}$
		235	$C_{14}H_{20}$
181	C_3-Alkylindan	237	C_3-Alkylnaphthalene
182	C_3-Alkylindan	238	*n*-Pentadecane
183	C_3-Alkylindan	240	$C_{14}H_{20}$
184	$C_{13}H_{28}$	241	$C_{14}H_{20}$
185	C_3-Alkylindan	243	C_3-Alkylnaphthalene
186	Methyltetrahydronaphthalene + C_3-alkylindan	247	C_3-Alkylnaphthalene
		249	Fluorene
187	2-Methylnaphthalene	255	Hexadecane
188	C_3-Alkylindan	260	$C_{17}H_{36}$
189	C_2-Alkyltetrahydronaphthalene	262	Octahydrophenanthrene
190	1-Methylnaphthalene	263, 264	Methylfluorene
191	*n*-Tridecane	265	*n*-Heptadecane
193	Cyclohexylcyclohexane	268	$C_{18}H_{38}$
194, 195	Dimethyltetrahydronaphthalene	269	Methoxyfluorene
196	Ethyltetrahydronaphthalene + C_7-alkylbenzene	273	*n*-Octadecane
		274	Dimethylfluorene
197	C_3-Alkylindan	277	*n*-Nonadecane
198	C_3-Alkylindan	278	*n*-Eicosane
199	C_3-Alkylindan	279	*n*-Heneicosane

for any dilute sample which requires additional concentration by solvent removal. The procedure is especially useful for the concentration of relatively small sample volumes (*i.e.*, between 10–100 μl).

Fig. 3 shows a chromatogram of a sample which was concentrated by con-

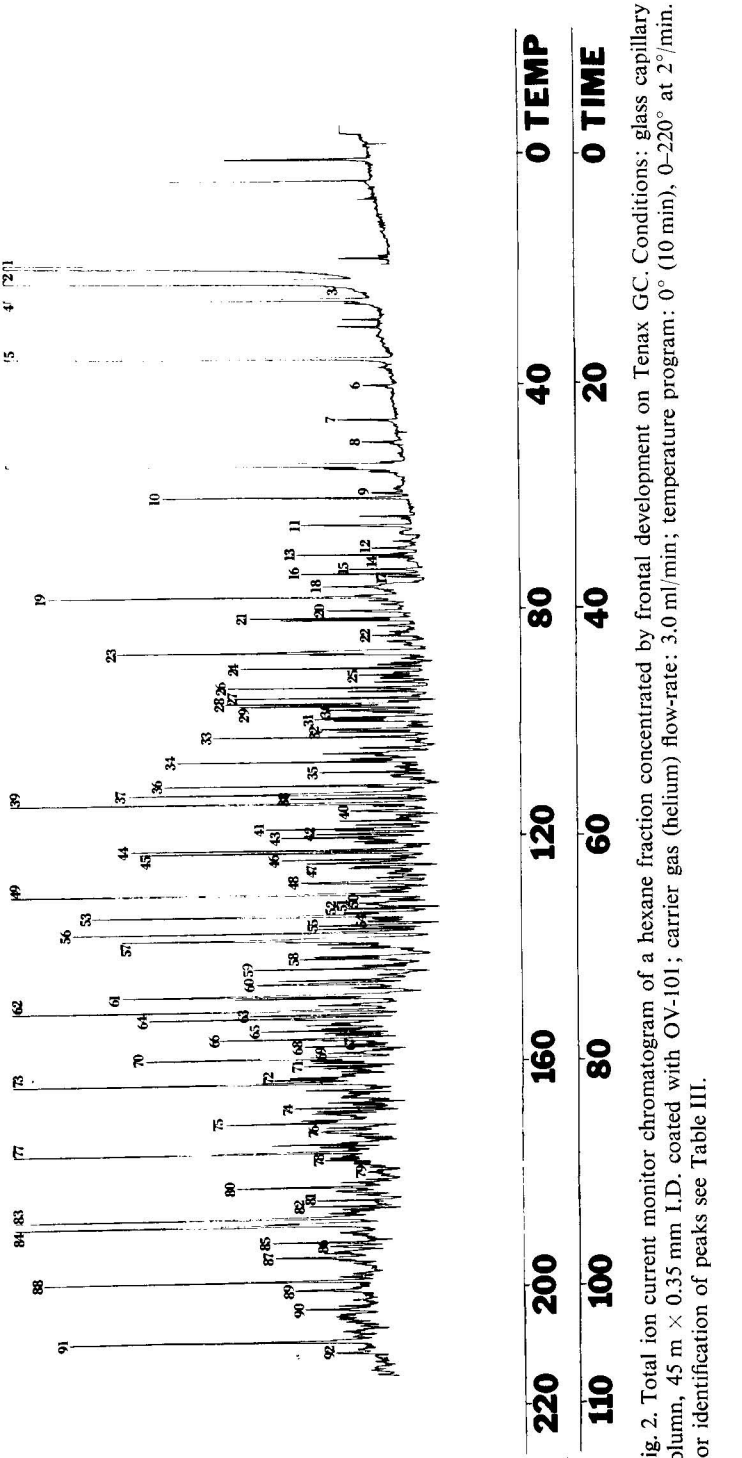


Fig. 2. Total ion current monitor chromatogram of a hexane fraction concentrated by frontal development on Tenax GC. Conditions: glass capillary column, 45 m × 0.35 mm I.D. coated with OV-101; carrier gas (helium) flow-rate: 3.0 ml/min; temperature program: 0° (10 min), 0–220° at 2°/min. For identification of peaks see Table III.

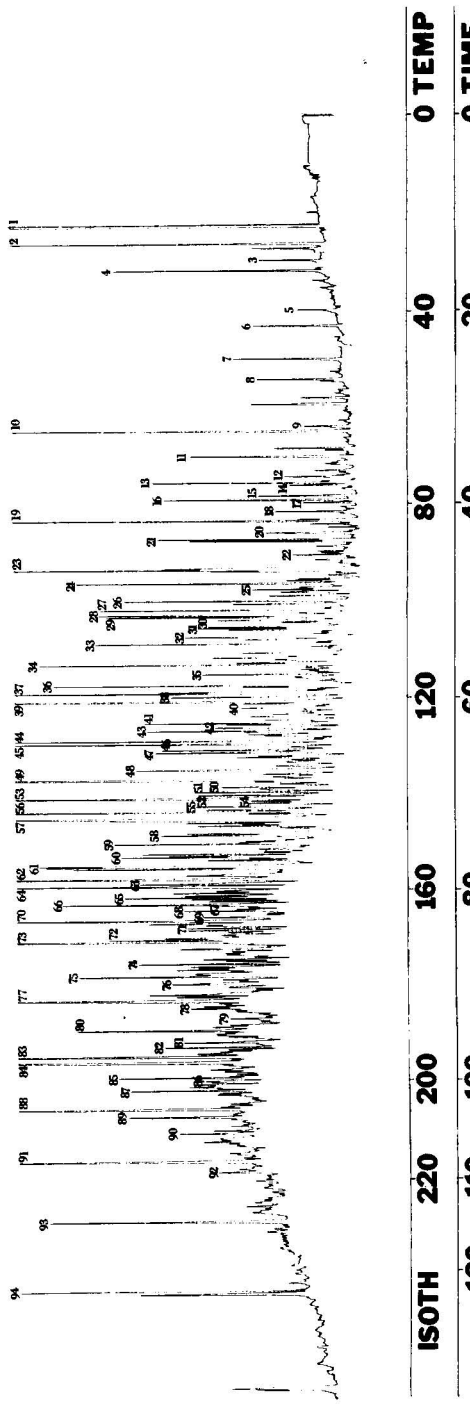


Fig. 3. Total ion current monitor chromatogram of a hexane fraction, concentrated by sweeping the solvent surface with nitrogen at room temperature. Conditions as in Fig. 2.

ventional methods. The surface of the hexane eluent was swept at room temperature with a stream of purified nitrogen. Both chromatograms also indicate good reproducibility between the two methods. Table III lists substances identified in this fraction.

Analysis was also performed on polar fractions. A multitude of substituted

TABLE III

IDENTIFICATION OF MAJOR COMPOUNDS IN THE HEXANE FRACTION

Peak No.	*Compound*	*Peak No.*	*Compound*
1	C_6H_{14}	43	4,7-Dimethylindan
2	*n*-Hexane	44	*n*-Dodecane
3	Benzene	45	Methyltetrahydronaphthalene
4	Cyclohexane	46	C_5-Alkylbenzene + C_3-alkylindan
5	C_7H_{16}	47	C_6-Alkylbenzene + $C_{13}H_{28}$
6	2,3-Dimethylpentane	48	C_2-Alkylindan
7	Toluene	49	C_3-Alkylindan + $C_{17}H_{24}$
8	C_2-Alkylcyclohexane	50	C_3-Alkylindan
9	Methylcyclohexane	51	C_3-Alkylindan
10	C_3-Alkylcyclopentane	52	$C_{13}H_{28}$
11	*m*-Xylene + *p*-xylene	53	2-Methylnaphthalene + C_3-alkylindan
12	*o*-Xylene		
13	C_9H_{16}	54	C_3-Alkylindan
14	1-Methyl-1-ethylcyclohexane	55	C_2-Alkyltetrahydronaphthalene
15	Dimethylheptane	56	$C_{14}H_{30}$
16	C_9H_{18}	57	C_2-Alkyltetrahydronaphthalene
17	Isopropylbenzene	58	C_2-Alkyltetrahydronaphthalene
18	C_3-Alkylcyclohexane	59	C_2-Alkyltetrahydronaphthalene
19	Propylcyclohexane	60	C_3-Alkyltetrahydronaphthalene
20	*n*-Propylbenzene	61	C_2-Alkylindan
21	1,4-Ethylbenzene	62	C_2-Alkylnaphthalene + $C_{13}H_{18}$
22	1-Methyl-2-ethylbenzene	63	C_2-Alkylnaphthalene
23	C_4-Alkylcyclohexane	64	$C_{13}H_{18}$
24	$C_{10}H_{22}$ + $C_{10}H_{20}$	65	$C_{13}H_{18}$
25	$C_{10}H_{18}$	66	C_3-Alkyltetrahydronaphthalene
26	$C_{10}H_{20}$	67	$C_{14}H_{20}$
27	Butylcyclohexane	68	$C_{13}H_{18}$
28	C_4-Alkylbenzene	69	C_3-Alkyldihydronaphthalene
29	C_4-Alkylbenzene	70	Diphenylmethane
30	Decyne + C_4-alkylcyclohexene	71	$C_{14}H_{20}$
31	C_4-Alkylbenzene	72	*n*-Pentadecane
32	Decahydronaphthalene	73	$C_{14}H_{20}$
33	$C_{11}H_{22}$	74	C_3-Alkylnaphthalene
34	Methyldecahydronaphthalene	75	$C_{17}H_{36}$
35	Methyldecahydronaphthalene	76	Fluorene
36	Methyldecahydronaphthalene + $C_{11}H_{24}$	77	*n*-Hexadecane
		80	$C_{17}H_{36}$
37	5-Methylindan	84	$C_{18}H_{38}$
38	4-Methylindan	88	*n*-Octadecane
39	Tetralin	89	Dimethylfluorene
40	C_5-Alkylbenzene + methyldecahydronaphthalene	91	*n*-Heptadecane
		93	*n*-Octadecane
41	C_2-Alkylindan	94	*n*-Nonadecane
42	C_2-Alkylindan		

phenols ranging up to C_5 were observed. Only traces of nitrogen-containing compounds were detected. The analysis of the polar fraction will be the subject of a separate communication.

Several coal fluids from different sources were compared by GC. As expected, large differences exist and the correlation among samples from different sources is very poor. High-resolution GC does provide a good picture of the general composition of such fluids and is a valuable aid in their characterization. The complexity of the samples, however, is beyond the present level of instrumental capability. Group separations by liquid chromatography, although time consuming, do provide the necessary simplification which makes a detailed analysis much easier.

ACKNOWLEDGEMENTS

We would like to thank G. Merijanian and H. Mayfield for experimental assistance. Financial assistance from RGC, University of Alabama (Project No. 828) is acknowledged. Samples of coal-derived fluids, obtained from Dr. J. E. Dooley, Bartlesville Energy Research Center, Bartlesville, Oklahoma are also greatly appreciated.

REFERENCES

1 J. E. Dooley, G. P. Sturm, Jr., P. W. Woodward, J. W. Vogh and C. J. Thompson, *Technical Publication BERC/RI-75/7*, U.S. Energy Research Development Administration 1975.
2 G. P. Sturm, Jr., P. W. Woodward, J. W. Vogh, S. A. Holmes and J. E. Dooley, *Technical Publication BERC/RI-75/12*, U.S. Energy Research and Development Administration, 1975.
3 P. W. Woodward, G. P. Sturm, Jr., J. W. Vogh, S. A. Holmes and J. E. Dooley, *Technical Publication BERC/RI-76/2*, U.S. Energy Research and Development Administration 1975.
4 H. M. Tenney and F. E. Sturgis, *Anal. Chem.*, 26 (1954) 946.
5 H. R. Coleman, C. J. Thompson, R. L. Hopkins and H. T. Rall, *J. Chromatogr.*, 20 (1965) 240.
6 D. E. Hirsch, R. L. Hopkins, H. J. Coleman, F. O. Cotton and C. J. Thompson, *Anal. Chem.*, 44 (1972) 915.
7 C. D. Thompson, J. E. Dooley, J. W. Vogh and D. E. Hirsch, *Hydrocarbon Process.*, 53 (1974) 93.
8 H. J. Coleman, J. E. Dooley, D. E. Hirsch and C. J. Thomson, *Anal. Chem.*, 45 (1973) 1724.
9 L. P. Jackson, C. S. Allbright and H. B. Jensen, *Anal. Chem.*, 46 (1974) 604.
10 D. R. Clutter, L. Petrakis, R. L. Stenger and R. K. Jensen, *Anal. Chem.*, 44 (1972) 1395.
11 J. T. Swansinger, F. E. Dickson and H. T. Best, *Anal. Chem.*, 46 (1973) 730.
12 H. Pichler and A. Herlan, *Erdoel Kohle, Erdgas, Petrochem. Brennst.-Chem.*, 26 (1973) 401.
13 J. L. Schulz, T. Kessler, R. A. Friedel and A. G. Sharkey, *Fuel*, 51 (1972) 242.
14 T. Aczel, D. E. Allan, J. H. Harding and E. A. Knipp, *Anal. Chem.*, 42 (1970) 341.
15 A. W. Peters and J. G. Bendoraitis, *Anal. Chem.*, 48 (1976) 968.
16 J. T. Swansinger, F. E. Dickson and H. T. Best, *Anal. Chem.*, 46 (1974) 730.
17 T. H. Gow, I. M. Whittenmore and R. E. Jentoff, *Anal. Chem.*, 42 (1960) 1394.
18 B. W. Jackson, R. W. Judges and J. L. Powell, *J. Chromatogr. Sci.*, 14 (1976) 49.
19 M. Novotný and K. D. Bartle, *Chromatographia*, 3 (1970) 272.
20 A. L. German, C. D. Pfaffenberger, J. P. Thenot, M. G. Horning and E. C. Horning, *Anal. Chem.*, 45 (1973) 930.
21 L. Blomberg, *J. Chromatogr.*, 115 (1975) 365.
22 G. Schomburg, H. Husmann and F. Weeke, *J. Chromatogr.*, 99 (1974) 63.
23 E. L. Ilkova and E. A. Mistryukov, *J. Chromatogr. Sci.*, 9 (1971) 569.
24 *Eight Peak Index of Mass Spectral Data*, Mass Spectrometry Data Centre, Aldermaston, 2nd ed., 1970.

Journal of Chromatography, 126 (1976) 225–237
© Elsevier Scientific Publishing Company, Amsterdam — Printed in The Netherlands

CHROM. 9421

COMPREHENSIVE INTERFACED PYROLYSIS GAS CHROMATOGRAPHIC PEAK IDENTIFICATION SYSTEM

PETER C. UDEN, DAVID E. HENDERSON and ROBERT J. LLOYD
Department of Chemistry, University of Massachusetts, Amherst, Mass. 01002 (U.S.A.)

SUMMARY

A versatile interfaced pyrolysis gas chromatographic peak identification system has been set up. It incorporates instrumentation for thermal degradation under slow or ultra-rapid temperature rise conditions. Evolved volatiles are transferred to a master trap manifold where precolumn procedures may be applied prior to gas chromatographic separation. Identification and analysis of individual peaks is then performed on-the-fly by vapor phase infrared spectrophotometry, mass (molecular weight) chromatography, elemental analysis, and functional group fingerprint fragmentation. An interfaced laboratory computer system provides for data acquisition, reduction and control.

INTRODUCTION

Gas chromatography (GC) has established a primary role as an analytical separation technique during a period of more than two decades, being amenable to any chemical species which maintains its integrity in the vapor phase. While separation and resolution with associated qualitative and quantitative analysis have always been paramount, it has always been clear that GC alone can provide absolute identification of species only indirectly or by inference. The use of retention data frequently provides adequate identification of unknowns whose probable molecular class or structure is already known or suspected, but is seldom sufficient in other circumstances. Two alternative approaches are available to provide unequivocal proof of identity of eluted species; the component peak may be collected in sufficient quantity to enable it to be subjected to subsequent identification procedures using any appropriate methodology; alternatively, eluate together with or without mobile phase may be passed directly into some identification device. The general applicability of such ancillary techniques has been well covered in the text by Ettre and McFadden[1], and it is clear that virtually any physical or chemical identification method may be used in conjunction with GC.

The power of mass spectrometry (MS) has been effectively exploited with regard to the directly interfaced GC identification mode[2]. Normal criteria of mass spectral identification naturally apply and while confirmation of known species is often straightforward, problems inherent in the GC–MS interface or in the ionization

of the molecule itself may often preclude definitive conclusions. The simultaneous achievement of qualitative and quantitative data for multicomponent mixtures or labile species is often impossible. While such techniques as chemical ionization (CI) mass spectrometry and programmed multiple-ion-current monitoring are useful, they also add to the already considerable expense and complexity of the technique. Alternative on-the-fly measurements on eluates in GC have been much less explored[1], but a number offer substantial advantages notably when used in combination; additional facility for on-the-fly chemical reaction to be included may also be most helpful in elucidation of the data produced.

An area of particular importance where eluate identity is concerned is that of pyrolysis gas chromatography (PGC) or more generally evolved gas analysis (EGA), the latter having been primarily considered as the counterpart to thermal gravimetric analysis (TGA). PGC has been much applied in the elucidation of polymer degradation products[3,4], but the general application of the technique to gaseous, liquid, or solid samples can give valuable information on structure from observed fragmentation patterns[5,6]. A major problem, in common with most thermal analysis has been one of reproducibility, both qualitative and quantitative. Instrumentation for slow programmed thermal degradation is now available[7]. This method has been shown to produce minimal secondary fragmentation products. The alternative approach of using ultra-rapid rise-time temperature profiles can now give a high degree of reproducibility in pyrogram profiles[4].

The present paper describes the conception, implementation and some initial applications of a novel GC peak identification system. Volatile samples may be introduced directly, may be evolved by thermal degradation under slow temperature gradient conditions, or may be produced by pyrolysis with temperature rise rates of up to 20,000°/sec, in any desired atmosphere. Volatiles are transferred to a master trap manifold operable to 300° which provides for the selection of the course of the analytical sequence to be followed. On-line chemical reactions may be performed, components separated chromatographically, and the nature of individual peaks determined by means of the following valve selectable interfaced procedures:

(i) rapid scan vapor phase IR spectrophotometry
(ii) elemental analysis for carbon, hydrogen, oxygen, nitrogen, sulfur, etc.
(iii) functional group fingerprinting by vapor phase thermal cracking
(iv) molecular weight determination by differential gas density measurement.

Any or all of these techniques may be applied in series or in parallel for identification of a component peak. An interfaced laboratory computer system is available for data acquisition, reduction, and control. Central to the concept is the selectability of analytical configuration as most relevant to the problem in hand, based on information obtained during the course of the analysis. The analyst may choose the next identification step on the basis of data from the previous step. In addition, multiple flow paths also enable several routine analyses to be carried out simultaneously.

INSTRUMENTATION AND SYSTEM DESIGN

An overall system diagram is shown in Fig. 1. Samples may be introduced at several points; injection may be made into the MP-3, the CDS 820, the CDS 1200, the MC-2, or through an injection port in the trap manifold connected directly to the

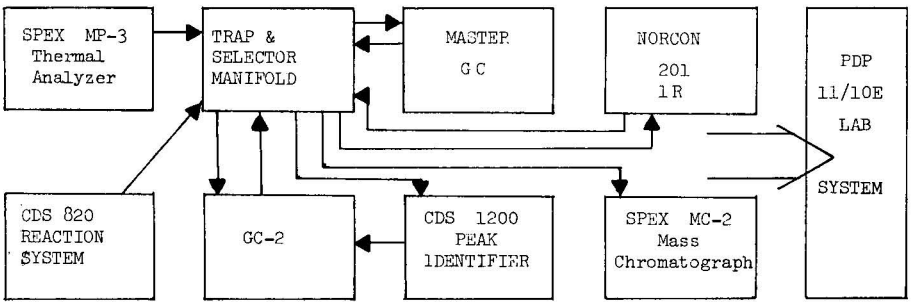


Fig. 1. System block diagram of the interfaced peak identification system.

master GC. Samples may be pyrolyzed in the MP-3, in the CDS 820 pyroprobe system, or in the trap manifold injection port. The MP-3 incorporates an internal gas chromatograph allowing stand-alone evolved GC, while the CDS 820 can utilize GC-2 for stand-alone operation. All samples enter the identification system through the trap manifold, where the course of the analysis is selected. The manifold also allows valve selection of several precolumn reactors and trapping sequences specific for individual problems. After GC separation, the peaks may first be characterized by vapor phase IR spectrophotometry, then return to the trap manifold, where either vapor phase pyrolysis (catalytic for elemental analysis or "thermal" for structural determination) in the CDS 1200, or molecular weight determination in the MC-2 may be carried out.

In order to make clear the operation of the system, a detailed discussion of individual instruments and system design follows. As noted above, the system comprises seven instruments, some appropriately modified. They comprise the following.

MP-3 multipurpose thermal analyzer (thermal chromatograph)

The MP-3 (Spex Industries), designed to produce evolved volatiles profiles with temperature increase followed by GC analysis of the profiles, was modified by the addition of two laminar flow controllers (HGC 187; Analabs) which provide controlled atmospheres in addition to helium as desired for thermal degradations. The three streams are all divertable for measurement of flow and meet at a mixing cross prior to the pyrolysis chamber. The three rear vents were removed and all streams pass to the trap manifold through standard transfer lines.

CDS 820 reaction system (incorporating CDS pyroprobe 100)

The CDS 820 (Chemical Data Systems) provides the controlled atmosphere for the Pyroprobe pyrolysis system. The standard heated interface for the pyroprobe was replaced by a Perkin-Elmer 900 series GC injection port which was installed in place of the reactor inlet of the CDS 820, allowing direct insertion of the probe. This solved leakage problems and allowed better control of pyroprobe temperature before pyrolysis. In addition, a water-cooled aluminum block can be placed over the exposed portion of the port to allow low probe temperatures to be maintained before pyrolysis. Further details of this cooled port design and operation will be reported elsewhere.

Master gas chromatograph

A Varian 2760 instrument with thermal conductivity and flame ionization detection was chosen for the large oven space and the ease with which major modifications could be made to the injector and detector systems. Injection ports were removed and two valves mounted to provide column switching and stop-flow capability, as shown in Fig. 2. The eight-port column switch and ten-port stop-flow valve are Valco Instruments HT series valves, heated by 50-W cartridge heaters controlled by the original Varian injection port heaters. Thermal safety switches were adjusted to prevent valve overheating. Swagelok bulkhead unions were mounted on an aluminum plate inside the oven to provide connections for two columns. Internal transfer lines were 0.016 in. O.D. stainless-steel (SS) tubing inside 1/8 in. O.D. copper tubing to ensure even heat transfer, bundled and heated with nichrome wire. The aluminum column bulkhead was heated by a 50-W cartridge heater to maintain efficiency for high-boiling species. The entire injection area was insulated with Johns Manville glass micro fibers. The detectors were arranged to provide three configurations, TC only, FID only, and TC split to FID, selected by the appropriate connection of the sample and reference streams from the ten-port valve to the detector fittings. Input and output are through the standard heated transfer lines.

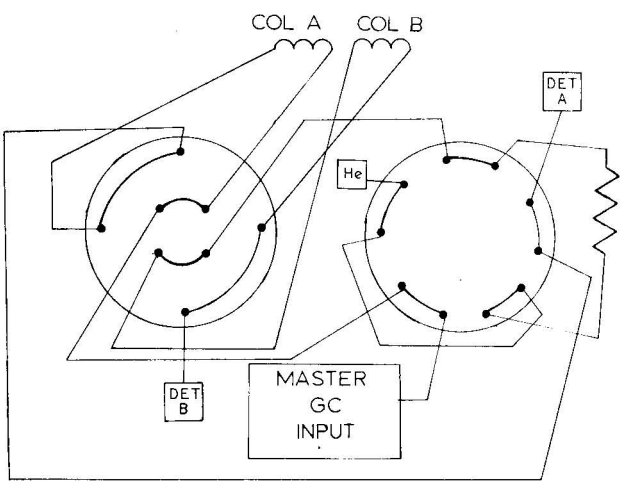


Fig. 2. Flow system of the master gas chromatograph stop-flow and column switching valve.

GC-2

The second gas chromatograph (a Varian 2760) has a detector arrangement identical to that of the master GC. It serves for analysis of samples from two sources, pyrolysis products from the CDS 820, and from the structural determination function of the CDS 1200. The former enter through a transfer line from the trap manifold and pass through the detector oven to a bulkhead fitting at the rear of the column oven. The latter pass through a transfer line from the CDS 1200 to a bulkhead fitting at the front of the column oven, the injection ports being moved to the right to accommodate this line in the usual column A position.

CDS 1200, functional group and elemental analyzer

The CDS 1200 (Chemical Data Systems) is present in the system with no modification. The instrumental transfer line is used for sample input, and a minimum length transfer line to GC-2 was made in the standard fashion.

MC-2 mass chromatograph

The MC-2 (Spex Industries) has been modified only by the addition of a 1/16 in. "tee" in the sample injection line for the transfer line input. The Spex transfer line enters through the detector section at the rear of the instrument. A helium purge flow is maintained through this transfer line and this interface does not interfere with the normal syringe injection of samples into the instrument.

Norcon 201, vapor phase IR spectrophotometer

The 201 (Norcon Instruments) has been modified to adapt it to the system. The output stream from the sample cell is returned to the trap manifold for further analysis. The original transfer lines were replaced with 3 1/16 in. SS lines in a single 3/8 in. heated copper tube to provide sample and reference flow and sample return. The return line is 0.043 in. I.D. to minimize back pressure, and all transfer lines are connected as close as possible to the "sample hold" valve in the 201. The computer data output and synchronizing signals provided were found not to be optimal for direct interfacing to the PDP-11/10e computer. An interface board was added, consisting of a voltage divider for the synch (VALID) signal and an adjustable gain amplifier (AD536J, Analog Devices), to invert the signal output and adjust it to make maximum use of the A/D converter sensitivity. This also facilitated auto gaining of data such that the switch to higher gains would occur near 100% T rather than near 0% T.

Transfer lines

These were constructed of 1/16 in. O.D. by 0.016 in. I.D. stainless steel where band broadening was a factor to be minimised, and of 1/16 in. O.D. by 0.043 in. I.D. stainless steel where samples were only to be trapped or where back pressure was a factor. Grade 304 stainless steel was used (Microweld) and welded 1/8 in. to 1/16 in. terminations (Microweld) were used for connections to 1/8 in. fittings in instruments. The 1/16 in. lines were passed through larger copper tubing to facilitate uniform heating. 1/8 in., 1/4 in., or 3/8 in. O.D. tubing was used to carry one, two or three, and more than three lines, respectively. The copper tubing was wrapped with glass electrical tape (Scotch No. 69, 3M Company) for electrical insulation, and a type J or K thermocouple (Omega Engineering) was installed in the line and insulated with tape. Heat was provided by 26 gauge glass insulated nichrome wire (Bergquist) wrapped tightly with one wire separation. Another layer of electrical tape was added and the line inserted into a silicone rubber sleeve for thermal insulation (Spex Industries).

Transfer line heating is controlled by Powerstat variable-voltage transformers mounted on aluminum chassis boxes. All lines are fused and the thermocouples are read on auxiliary positions on the various instruments; lines are normally maintained at approximately 300°. On lines longer than a few feet, the heating wire was divided at even intervals which were then connected in parallel to the powerstat. The hot lead

from the transformer was connected to the center of the lines and the common lead to the ends.

Trap manifold

This contains the valve oven where all sample switching is done. It also houses ports for ten traps and four precolumns and contains three sample loops. The six valves in the valve oven are Valco HT valves. The valve oven was constructed from a $21\frac{1}{2} \times 15 \times 13$ in. steel chassis box, and the valves mounted on aluminum bars insulated from the exterior of the cabinet by ceramic insulators. An aluminum plate mounted similarly provides support for the $28^1/_8$ in. SS bulkhead Swagelok unions to which traps and precolumns are attached. Transfer lines enter through the back and sides and the oven is insulated with glass microfibres held in place where necessary by $\frac{1}{2}$ in. galvanized wire cloth. An approximately 1 in. thickness of this insulation was found adequate to keep the exterior of the manifold cool. The oven is heated by a 700-W heater with an associated blower and temperature is controlled by a CDS 200 temperature controller employing a platinum resistance sensor (Omega Engineering). Temperature control for the traps and precolumns is provided by a trap monitor constructed in a separate chassis, containing a switching pyrometer (Assembly Products) to turn off trap heat at a set limit and a 12 position switch for selection of any of the traps or precolumns for readout. The switch also connects the output of a powerstat to the selected trap. A second powerstat provides heat for the precolumns but is not switched by the pyrometer, thus allowing continuous heating of the precolumns. A voltage meter is provided for resetting trap and precolumn voltages. A 28-V d.c. power supply in the monitor provides power for the necessary relays and indicators.

Traps and precolumns

The traps and precolumns used on the trap manifold were constructed of $^1/_8$ in. O.D. stainless steel, the construction paralleling that of the transfer lines except that no insulation was added over the nichrome wire, to allow more rapid heating and cooling. Traps have been packed with standard chromatographic column materials, 10% SE-30 on Chromosorb W, Porapak Q, glass microbeads, and a combination trap was constructed with 10% SE-30 followed by Porapak Q in the same trap. The latter has been found useful as a general purpose trap for most volatiles except light hydrocarbons and permanent gases at room temperature, even methane being retained for a short period.

PDP 11 data system

This consists of a PDP 11/10e laboratory computer system with the LPS data acquisition system. The LPS contains sixteen channels of multiplexed 12-bit A/D with the BA 408 switched gain multiplex system (Digital Equipment). Other peripherals include a single RK05 disk, a TU60 cassette, and a LA36 terminal. A Hewlett-Packard 130B oscilloscope is used for data display from the D/A converter of the LPS and analog output is also directed to an Omniscribe recorder (Houston Instruments) for hard copy. Input data are obtained from the computer outputs of the Varian 2760 gas chromatographs and from the previously described interface to the Norcon 201. The remaining instruments do not have direct computer output terminals and

data are presently obtained by connection across the detector attenuators. This approach will be modified as the data buffering requirements are determined.

System software includes the RT 11 foreground/background operating system, FORTRAN, and Lab Applications Program Library VO3. The latter includes SPARTA and THRU programs for preliminary data acquisition and modules for tailoring data acquisition to the needs of the system. These are being used to generate a program to acquire all data under one program in the foreground and perform peak integration and other data reduction functions. A new data acquisition program, IRFLAV, provides for IR data acquisition in the foreground with digital filtering. Another routine, IRSOUT, performs background subtraction and normalization, and prints out the spectrum to the recorder. This program may be operated under the RT 11 BATCH system for output of large accumulations of data. A FORTRAN program used for data reduction from the MC-2 mass chromatograph is discussed elsewhere[8].

System design

The design of the overall system grew from an in depth study of the application requirements of the seven component instruments. The trap manifold was designed to optimize flexibility and throughput of the instruments, consideration being given to the need for several users to work with different instruments with a minimal degree of interference and with no degradation of individual instrumental performance. The flow schematic of the valves in the trap manifold is shown in Figs. 3 and 4. The six valves have been divided for clarity between the two diagrams. Fig. 3 shows the input of samples into the system via the INPUT valve and the selection of samples for identification by means of the two remaining valves.

An important consideration in design of this type of interfaced system is the destination of all flowing streams in all switch positions. It is important that no flows to thermal conductivity detectors be stopped lest filaments be damaged, thus makeup flow must be provided and streams not selected for identification must be vented at

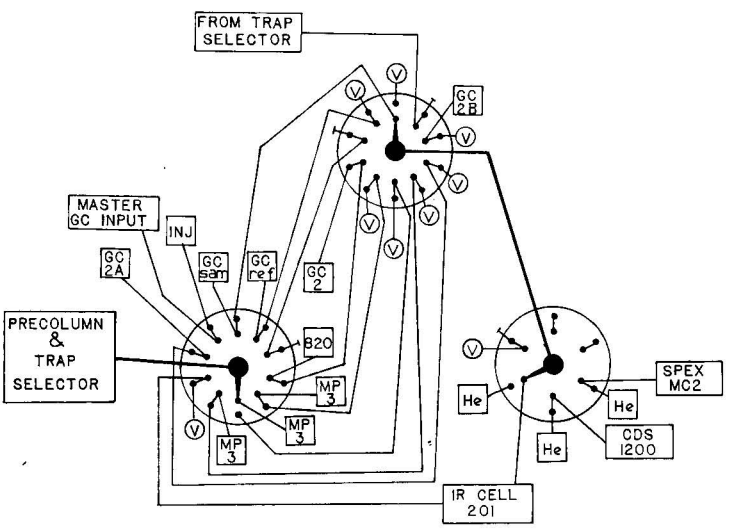


Fig. 3. Flow system of the input and identification selection valves of the trap manifold.

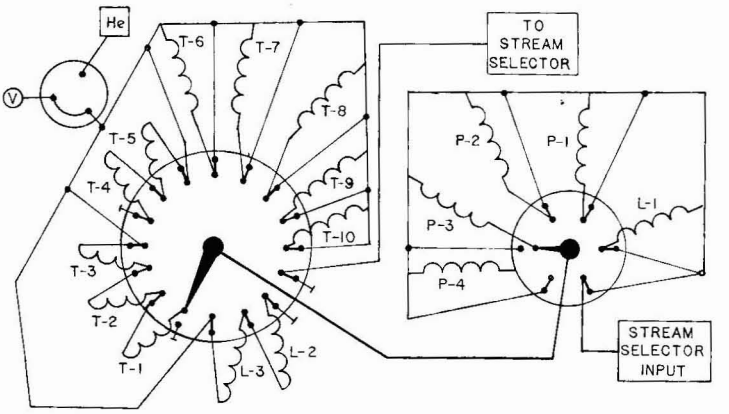


Fig. 4. Flow system of the precolumn and trap selection valves of the trap manifold.

all times. Samples entering the INPUT valve may either be selected for trapping or passed into the identification selection section. This arrangement allows effluent from the gas chromatographs to be trapped as well as identified, this being particularly useful with the precolumn reactions. It is also possible to pass an entire evolved gas envelope to any of the identification instruments without prior separation and trapping. Thus two valves are used first to select the stream for analysis and then the instrument for analysis. All streams not selected in this section pass to vents which are centrally located for convenient flow measurement. Two exceptions are the reference flow to the Norcon 201 which vents at the end of the reference cell, and the effluent from the CDS 820. Since the latter does not contain GC capability and does not therefore stand alone, its exit line leaves the selection system and passes to GC-2. These thus act together as a PGC system while the MP-3 is at the same time providing samples for identification to the remainder of the system.

The trapping and precolumn valving system shown in Fig. 4 was designed to provide maximum flexibility of analysis in complicated identification problems. The use of precolumns as subtractors or reactors has been demonstrated as valuable in complex analyses[1]; thus a switch selection of four precolumns is provided. In the bypass position these are completely isolated. A sample loop within the oven is also provided as part of this valving to allow 30-ml volumes of effluent to be held without trapping. Samples may be subjected to precolumn reactions either on the trap cycle or the backflush cycle or both. In addition, the bypass line from the trap valve to the selector valve allows samples to be passed through the precolumns and then directly to the identification function.

The selector valve for the traps allows any of the ten traps or two sample loops to be selected. Five of these traps are "single user" traps designed to allow various facilities for specific research areas; this aids in minimizing memory effects and carry over from one sample type to the next. The other five traps are general use system traps providing for various process chromatographic applications. Traps 6 and 7 and also traps 8, 9 and 10 are designed for series trapping followed by parallel backflush. In this mode a preliminary separation by either volatility or column affinity may be done at the trapping stage and then the appropriate column may be selected for anal-

ysis of the various fractions using the column selector valve. By determining the retention times of species on the traps, it is also possible to perform operations such as heart cutting using this valve system.

EVALUATION AND DISCUSSION

The quality of the chromatographic separations obtained in the interfaced system shows little or no deterioration from that obtained on the MP-3 alone or by the CDS 820 interfaced to the Varian 2760 gas chromatograph (GC-2). Preliminary evaluations were carried out using a mixture of normal hydrocarbons in the range C_7–C_{24}. This mixture was chromatographed in the master GC on a 6 ft. × $^1/_8$ in. O.D. column of 1.5% OV-101 on Chromosorb G, with a constant helium flow-rate of 20 ml/min and a 20°/min temperature program from 50–300°. Column efficiency was closely similar for the C_8 and the C_{24} alkanes and there was no evidence of band broadening or sample holdup in the transfer line from the MP-3 or in the trap manifold on the basis of plate number measurements, as compared with efficiency in the internal MP-3 gas chromatograph. The problem of hot spots in transfer lines due to excess insulation or passage through a bulkhead has not yet been addressed specifically using compounds known to be thermally unstable; however, the copper heat transfer tubes should minimize this problem as they do for the cold spots. In fact, only a single serious cold spot was found in the initial set up stage, at the aluminum column bulkhead of the master GC; this was satisfactorily corrected by incorporation of a 50-W cartridge heater at this point.

Further analysis of the *n*-alkane mixture injected into the MP-3 and initially trapped and separated in the master GC was carried out on the MC-2. The sample was transfered a second time through the trap manifold to the MC-2 traps and analyzed in the standard manner[8–10]. CO_2 and Freon 115 carrier gases were employed at flow-rates of 10 ml/min on matched 6 ft. × $^1/_8$ in. O.D. 8% Dexsil 300 GC columns on Chromosorb W-HP, using a program rate of 10°/min from 50–325°. The C_{12}–C_{24} portion of this chromatogram is shown in Fig. 5. Molecular weights calculated using the expression

$$M_x = \frac{(A_1/A_2)\,K \cdot M_{CG1} - M_{CG2}}{(A_1/A_2)\,K - 1}$$

where A_1/A_2 is the peak height response ratio of the compound in the two detectors, 1 and 2, M_{CG1} and M_{CG2} are the molecular weights of carrier gases 1 and 2, and K is the instrument calibration factor obtained by measuring responses for known compounds, and using the expression

$$K = (A_1/A_2)\left(\frac{MW_{\text{Standard}} - M_{CG1}}{MW_{\text{Standard}} - M_{CG2}}\right)$$

gave comparable precision for molecular weights to those obtained from direct injection of the hydrocarbon mixture into the MC-2 in the conventional way. The relative precision of the order of 2% so obtained may be improved by up to a factor of ten by using an iterative computer curve fitting technique to account for the variation of the instrumental K factor with molecular weight[8]. It is noteworthy that the

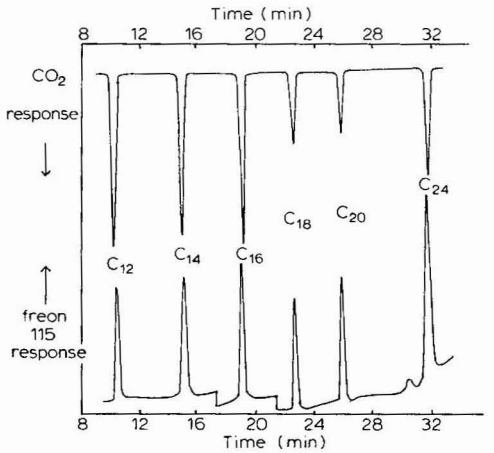


Fig. 5. Mass chromatogram of C_{12}–C_{24} *n*-alkanes initially injected into the MP-3 and transferred to the MC-2 as described in the text. Carrier gases, CO_2 and Freon 115; other chromatographic conditions, as given in the text.

flow and transfer path employed for the *n*-alkane sample in this particular example is as lengthy as is possible in the system, involving as it does transfer between three instruments, each involving passage through the trap manifold.

Several advantages have become immediately apparent in using this system. Firstly, the sample throughput for the MP-3 is virtually doubled by introducing the external trapping and gas chromatograph, since one sample may be pyrolyzed while another is chromatographed. Second is the advantage in the ability to rechromatograph the same sample several times by trapping the GC sample output. This allows analysis of a single sample before and after the use of a pre-column. It also allows the same sample to be sequentially analyzed on more than one GC column. This makes more efficient use of sample preparation time and helps eliminate problems of reproducing sampling and pyrolysis parameters.

An evaluation of the trapping and precolumn system was carried out using a sample of Green River oil shale which was pyrolysed separately in the MP-3 and in the CDS 820 and evolved volatiles passed through the various flow paths. The identical column was used (1.5% OV-101) as noted above with a carrier gas flow-rate and a temperature program of 12°/min from 30–300°. Fig. 6 shows the programmed temperature chromatogram obtained for the pyrolysis products produced from the thermal degradation of the oil shale in the MP-3 under helium with the 2-mg sample heated to 550° at 40°/min. Chromatogram A shows the separation of the original decomposition products, which consists of the typical unresolved component envelope upon which are superimposed a number of resolved and partially resolved components, considered to be primarily aliphatic, aromatic and unsaturated hydrocarbons[11]. The unresolved envelope is considered to comprise the non-hydrocarbon portion of the shale oil volatiles, including nitrogen, oxygen, and sulfur containing species. Chromatogram B is that of the eluent from A after passage through a Molecular sieve 5A 9 in. × $^1/_8$ in. O.D. SS precolumn at 275°. A large proportion of components in A are reproducibly removed; this type of precolumn has been shown to

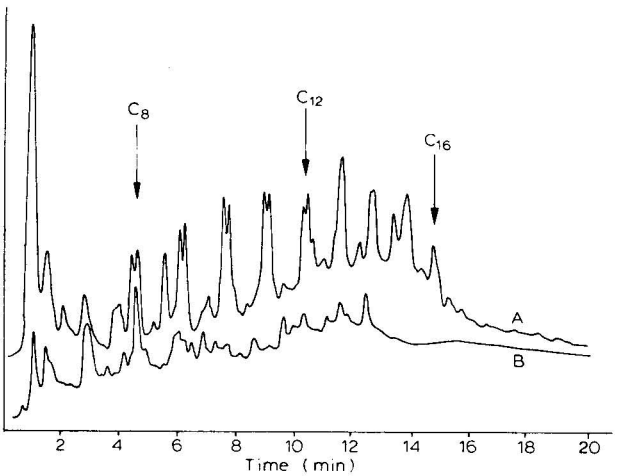


Fig. 6. Chromatograms of Green River oil shale pyrolyzates from the MP-3. (A) Volatiles transferred through the trap manifold and separated on the master GC. (B) Residual volatiles after passage of eluent from A through molecular sieve 5A trap. Chromatographic and pyrolysis conditions are given in the text.

remove preferentially normal and terminally branched molecules[12]. A variety of other specific precolumns have been used in this oil shale analysis[11,13] and are proving of great utility in the selective simplification of this exceedingly complex pyrolysis product mixture.

Preliminary data for the application of the Norcon 201 to the identification of unknowns is encouraging, very clean spectra of extracted material from shale oil having been obtained and presented elsewhere[11]. Data for methyl salicylate was obtained from a chromatographed peak of a 1% solution in acetone separated on the 1.5% OV-101 column at 130° with a 30 ml/min helium flow-rate of carrier gas. After determination of the delay time for transfer to the Norcon 201, scans were taken of the IR spectrum using the 6-sec scan mode and 3× scale expansion. Data were collected both on the Norcon 201 recorder and using the assembly language program IRFLAV. Spectra are presented in Fig. 7, the upper three traces showing output from the recorder directly while the lower trace shows the computer generated spectrum using IRFLAV and IRSOUT programs. This well defined spectrum corresponds to 5 μg of sample injected, and further optimization of the interface and of the Norcon 201 optical system should extend this limit to below the microgram level.

For the present the CDS 1200 unit has not been extensively utilized in the fully interfaced mode. Its operation and application have, however, been described by Liebman *et al.*[14], and we consider that the data obtained in the present configuration should be entirely equivalent to those reported by these authors.

CONCLUSIONS

The present paper is primarily devoted to discussion of the rationale behind the design and development of an interfaced vapor phase thermal analysis and GC peak identification system; the advantages of this type of approach to real laboratory

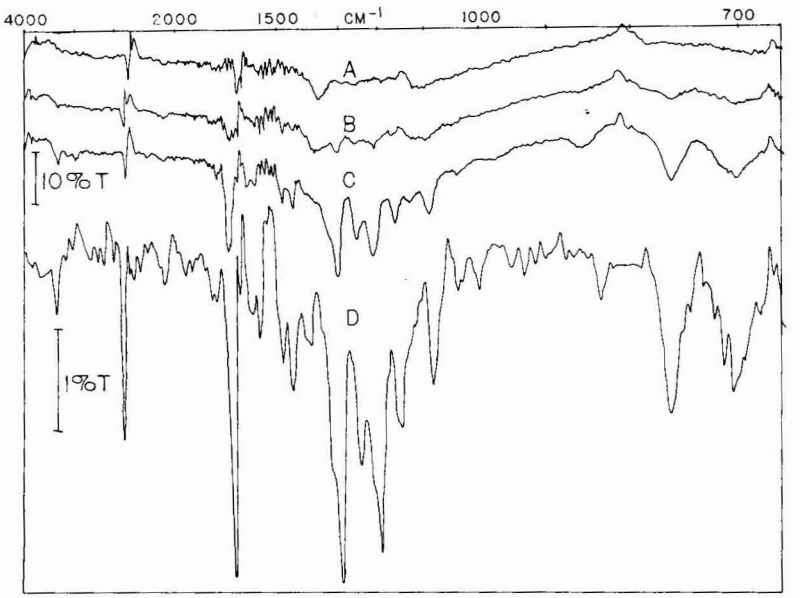


Fig. 7. Vapor phase IR spectra of eluted methyl salicylate peaks. Scan time on the Norton 201, 6 sec; range, 3×; other conditions, as given in the text. A = Background; B = 5 μg; C = 20 μg; D = computer printout of spectrum B after digital filtering, background subtraction, and normalization (from computer routines IRFLAV and IRSOUT).

problems are readily apparent. While a principal spur to the development of the system has been the interest in applications requiring pyrolysis or thermal degradation followed by evolved gas analysis by GC, a parallel involvement has been in the implementation of versatile on-the-fly peak identification procedures presently available but little developed or exploited in the interfaced mode.

Many interfaced systems utilize single identification instruments, but while this approach is sometimes adequate, it may lack sufficient versatility to provide adequate characterization of many unknowns particularly when present in poorly resolved multicomponent mixtures. The development of the interfaced system incorporating multiple identification capabilities is a logical advance, and when used in combination with on-line chemical precolumns and selective trapping devices it promises to be a very powerful and widely applicable system.

Thus far, development has concentrated primarily on the instrumental interfacing and the valving and peak transfer and reaction design. Some of the capabilities of the system have been assessed. Development is continuing and will be reported in future publications, as will present applications, particularly in the areas of oil shale analysis, polymer degradation, applications to fire retardant studies, and investigations of thermal properties of metal complexes and organometallics.

ACKNOWLEDGEMENTS

We wish to acknowledge the support of the National Science Foundation through Research Instrument Grant GP 42542 to the University of Massachusetts

which supported the development of the laboratory. Partial support from NSF Grant MPS74 15244 is also acknowledged. We are also grateful for valuable discussion on system design with Dr. E. J. Levy (Chemical Data Systems), Mr. M. Boyle (Norcon Instruments), Dr. R. Reed and Mr. L. Levase (Spex Industries), and Mr. J. Brooker (Valco Instrument).

REFERENCES

1 L. S. Ettre and W. H. McFadden, *Ancillary Techniques of Gas Chromatography*, John Wiley, New York, 1969.
2 W. H. McFadden, *Techniques of Combined Gas Chromatography–Mass Spectrometry, Applications in Organic Chemistry*, John Wiley, New York, 1973.
3 R. L. Levy, *Chromatogr. Rev.*, 8 (1966) 49.
4 N. Iglauer and F. F. Bentley, *J. Chromatogr. Sci.*, 12 (1974) 23.
5 H. Groenendyk, E. J. Levy and S. F. Sarner, *J. Chromatogr. Sci.*, 8 (1970) 599.
6 S. F. Sarner, *J. Chromatogr. Sci.*, 10 (1972) 65.
7 "*Thermal Chromatography*", "*The Spex Speaker*", Spex Industries, Metuchen, N.J., Vol. XVIII, No. 2, June 1973.
8 R. J. Lloyd, D. E. Henderson and P. C. Uden, *Anal. Chem.*, 48, No. 9 (1976) in press.
9 A. C. Lanser, J. O. Ernst, W. F. Kwolek and H. J. Dutton, *Anal. Chem.*, 45 (1973) 2344.
10 E. Kiran and J. K. Gillham, *Anal. Chem.*, 47 (1975) 983.
11 P. C. Uden and S. Siggia, *Amer. Chem. Soc. Nat. Meet., 171st, New York, April, 1976.*
12 C. K. Hersh, *Molecular Sieves*, Reinhold, New York, 1961.
13 P. C. Uden, S. Siggia, H. Hackett, F. DiSanzo and D. E. Henderson, to be published.
14 S. A. Liebman, D. H. Ahlstrom, C. D. Nauman, R. Averitt, J. L. Walker and E. J. Levy, *Anal. Chem.*, 45 (1973) 1360.

Journal of Chromatography, 126 (1976) 239–247
© Elsevier Scientific Publishing Company, Amsterdam — Printed in The Netherlands

CHROM. 9379

QUANTITATIVE PYROLYSIS STUDIES OF STYRENE, ACRYLATE ESTER SYSTEMS, AND THEIR α-METHYL-SUBSTITUTED HOMOLOGS

J. K. HAKEN* and D. K. M. HO

Department of Polymer Science, University of New South Wales, P.O. Box 1, Kensington, N.S.W. 2033 (Australia)

SUMMARY

The pyrolytic degradation of copolymers and homopolymer mixtures of styrene, methyl acrylate, α-methylstyrene, and methyl methacrylate has been examined using a Curie Point pyrolysis system. The pyrolysis behaviour at several temperatures allows copolymers and mixtures to be distinguished. The essentially individual behaviour of homopolymers is observed and the concept of fragmentation indices as proposed for acrylic systems is considered.

INTRODUCTION

Pyrolysis gas chromatography of polymers has been the subject of many reports and has been described in a number of reviews[1–3]. Much of the work has been of a qualitative nature and in many cases was conducted before the effects of the experimental and instrumental parameters had been evaluated. Large samples, *i.e.*, 2–15 mg, were frequently employed and with poor heat transfer and a preponderance of competing side reactions attempts at quantitation were of limited success.

The degradation mechanism of *n*-alkyl methacrylates with depropagation and depolymerisation with little accompanying transfer reaction is well established. The degradation of the *n*-alkyl acrylates is demonstrated by studies with polymethyl acrylate. Cameron and Kane[4,5] proposed random initiation and a propagation step involving mainly transfer reactions with little depropagation. Subsequent analysis of the reaction products has substantiated these proposals[6].

The early quantitative pyrolysis gas chromatographic studies of polyacrylic esters have been considered by McCormick[7], who confirmed the observations of Strassburger *et al.*[8] and of Gatrell and Mao[9] that the yield of an acrylate monomer is substantially increased when pyrolysis of a copolymer containing a polymethacrylate is carried out as compared to pyrolysis of a homopolymer or of mixtures containing polyacrylate homopolymer. The ability of distinguishing between a copolymer and a mixture of homopolymers was demonstrated and the possibility of determining

* Temporary address until February 1977: Chemistry Department, Kent State University, Kent, Ohio 44242, U.S.A.

polymer composition suggested. Pyrolysis employed a helical filament with single shot or stepwise degradation with five polymer systems, *i.e.*, ethyl acrylate–methyl methacrylate, ethyl acrylate–*n*-butyl methacrylate, 2-ethylhexyl acrylate–methyl methacrylate, *n*-butyl acrylate–methyl methacrylate, and *n*-butyl methacrylate–methyl methacrylate.

The difficulties of calculating the pyrolysis yields with stepwise degradation at increasing temperatures were eliminated by the use of a radio frequency pyrolyser with several samples on elements of different Curie temperatures[10]. Copolymers and homopolymer mixtures of methyl to *n*-hexyl acrylate and methacrylate were studied. A constant fractional recovery of methacrylate monomer was achieved with homopolymers, copolymers, or a mixture containing polyalkyl methacrylates, while with polyacrylates the monomer yields were dependent on the presence of the esters in copolymers or homopolymers and in addition in a copolymer the yield of monomer decreased slightly as the percentage of acrylate was increased. The variations at the temperature used were relatively minor and the use of monomer yield allowed constants described as Homopolymer Fragmentation Indices (HFI) or Copolymer Fragmentation Indices (CFI) to be established and the composition of unknown copolymers or mixtures of homopolymers to be determined from pyrolysis data. The variation of the CFI values of the polyacrylates introduced only minor errors in the calculation of copolymer composition, the effect being most significant with copolymers of very high or very low acrylate content.

The present work examines the utility of these indices with several other polymers, namely, styrene, where thermal degradation occurs by a complex series of reactions which produce both monomer and transfer reaction products[11,12], and with α-methylstyrene, where depolymerisation predominates with high yields of monomer[13–15]. In this work copolymers and homopolymer mixtures of these monomers have been considered together and in combination with methyl acrylate and methyl methacrylate.

EXPERIMENTAL

Gas chromatography

Gas chromatography was conducted on a modified F & M Model 810/29 dual-column research chromatograph with flame ionization detection and fitted with an improved flow control system and on a Hewlett-Packard Model 5750 instrument. Two 12 ft. × 1/4-in. O.D. aluminium columns packed with 10% OV-1 on 60–80 mesh Chromosorb W were programmed between 100 and 220° at 10°/min with the top temperature held for 5 min before automatic recycling occurred. Helium was used as the carrier gas at 40 ml/min. The amplifier sensitivity used generally was 16×10^2 A.f.s.d. and 2×10^2 A.f.s.d. for minor components.

Radiofrequency pyrolysis

A Philips Curie Point pyrolyzer was used. The ferromagnetic sample probes were prepared by forming a flat surface with light hammering for lengths of 1 cm at the end of the wires and then folding back these prepared tips to form a closed loop.

Solutions of the polymers were prepared and $0.50 \pm 0.2\,\mu$l of solution was deposited on wires with Curie Points of 510, 610, 770, and 980°. The amount of poly-

methyl methacrylate deposited was $10 \pm 0.4\ \mu g$ and the approximate film thickness was calculated to be $0.5\ \mu m$.

The coated wires were stored for 24 h to allow evaporation of solvent and the residual material was removed by allowing several minutes to elapse after mounting in the pyrolysis head prior to firing.

Polymer and copolymer preparation

Five sets of copolymers were prepared by free radical polymerisation using styrene–α-methylstyrene, styrene–methyl methacrylate, styrene–methyl acrylate, α-methylstyrene–methyl acrylate, and α-methylstyrene–methyl methacrylate. With each series five ratios were prepared, homopolymer mixtures of the same compositions were prepared from polymers free radical initiated, with the exception of α-methylstyrene, which employed an ionic initiator (concentrated sulphuric acid) at a low temperature (−50°).

RESULTS AND DISCUSSION

Pyrolyses of the homopolymers have been carried out at four temperatures, namely 510, 610, 770, and 980° and the monomer yields are shown in Table I.

TABLE I

MONOMER YIELDS FROM HOMOPOLYMERS WITH CURIE POINT PYROLYSIS

Compound	*510°*	*610°*	*770°*	*980°*
Methyl acrylate	2.1	8.0	8.8	9.5
Polystyrene	5.0	71.6	74.8	75.3
Polymethyl methacrylate	76.3	98.6	97.4	96.6
Poly(α-methylstyrene)	91.0	98.0	98.0	98.0

Polymethyl acrylate and polymethyl methacrylate have previously been considered at the first three temperatures[10], and while the monomer yields with polymethyl acrylate are somewhat lower than previously reported[10], the temperatures of the maximum yield are the same for both polymers, as in the earlier report.

Pyrolysis of homopolymer mixtures (6:4) of styrene and α-methylstyrene exhibited pyrolysis patterns of the individual homopolymers which were similar to those of a copolymer of the same composition, which however showed a distinctly larger styrene monomer peak. Quantitative recoveries of monomer are shown in Table II for the series styrene–α-methylstyrene.

The homopolymers in the mixtures exerted little influence on each other and behaved independently although the presence of α-methylstyrene in the copolymers increased the proportionate yield of styrene. As the α-methylstyrene content increased, the relative yield of styrene showed a continued minor increase. The presence of styrene, however, did not influence the essentially quantitative yield of α-methylstyrene at 610, 770, and 980°. At 510° the presence of styrene had a marked influence on the α-methylstyrene yield, which decreased with increasing styrene content.

The proportionate monomer recoveries at 770° are shown in Figs. 1a and b for styrene and α-methylstyrene, respectively. Plots of the molar ratio of polymer and of

TABLE II

PYROLYSIS YIELDS AT 510°, 610°, 770°, AND 980° FOR COPOLYMERS AND HOMOPOLYMER MIXTURES

Relative ratios		*Percentage yield at 510°*				*Percentage yield at 610°*				*Percentage yield at 770°*				*Percentage yield at 980°*			
M_1	M_2	*Copolymer*		*Homopolymer*		*Copolymer*		*Homopolymer*		*Copolymer*		*Homopolymer*		*Copolymer*		*Homopolymer*	
		M_1	M_2	M_1	M_2	M_1	M_2	M_1	M_2	M_1	M_2	M_1	M_2	M_1	M_2	M_1	M_2
Styrene	α-Methyl styrene																
9	1	12.0	21.2	4.2	90.7	76.5	94.1	63.2	96.8	77.4	95.9	75.9	96.9	75.8	94.8	95.3	96.8
7	3	38.0	99.6	4.5	91.7	86.8	94.3	63.3	97.5	88.0	96.3	76.0	97.5	85.0	94.5	74.6	97.5
6	4	61.7	67.6	4.7	92.1	90.3	95.8	63.5	97.8	91.8	97.1	75.5	97.5	88.8	95.2	75.6	97.5
4	6	74.8	74.3	5.0	92.5	96.6	96.0	63.2	98.7	97.0	98.0	75.9	98.5	98.1	95.4	75.1	98.7
3	7	75.8	80.5	9.8	92.7	96.7	98.6	63.0	98.7	97.0	98.8	76.1	98.5	96.2	98.0	76.0	98.8
Styrene	Methyl methacrylate																
9	1	6.8	24.6	5.0	76.3	77.1	78.7	64.9	96.6	79.0	88.6	73.8	94.1	78.4	84.4	72.5	93.6
7	3	10.1	33.4	5.2	73.4	82.4	84.3	66.2	95.6	89.4	91.0	73.8	94.7	87.8	87.7	72.8	93.8
5	5	31.6	40.2	10.8	75.9	87.8	89.3	64.9	95.6	93.8	93.8	73.8	95.1	92.3	91.0	72.8	94.0
3	7	58.5	60.2	5.7	73.4	93.5	93.7	65.3	96.6	94.4	94.5	73.8	95.5	93.6	93.0	72.9	95.0
1	9	74.0	71.6	8.0	76.0	94.4	94.1	65.8	96.8	95.0	95.0	73.8	95.8	94.5	93.2	72.8	95.1
Styrene	Methyl acrylate																
9	1	6.7	2.3	6.7	2.2	61.0	38.6	65.1	8.1	69.3	47.3	75.5	8.8	69.7	48.2	75.3	9.5
7	3	4.9	2.0	5.0	2.4	44.1	33.3	65.2	8.2	59.4	40.2	75.0	8.7	60.5	41.0	75.3	9.5
5	5	5.0	2.8	5.0	2.2	42.9	28.9	63.8	8.0	49.0	34.1	75.2	8.8	51.2	35.3	75.3	9.4
3	7	5.0	2.0	6.0	2.1	31.6	14.0	63.9	7.9	38.6	17.3	75.2	8.7	40.4	17.7	75.3	9.4
1	9	4.9	2.0	6.0	2.1	29.1	9.8	63.5	7.3	31.5	11.5	75.3	8.8	32.8	12.1	75.3	9.4
α-Methyl styrene	Methyl methacrylate																
7	3	92.3	79.4	91.6	78.2	98.5	96.2	98.3	98.6	98.5	97.0	98.3	97.4	98.5	98.7	98.3	97.0
6	4	91.7	80.2	91.2	78.8	98.5	95.3	98.0	98.5	98.5	96.2	98.0	97.6	98.6	98.0	98.0	97.1
4	6	92.0	81.0	91.0	78.5	98.4	96.8	98.2	98.6	98.4	97.2	98.2	97.2	98.6	98.4	98.2	96.9
3	7	92.0	78.8	91.1	78.5	98.2	97.1	98.0	98.5	98.4	97.6	98.0	97.8	98.4	98.2	98.0	97.0
1	9	91.5	80.1	91.4	78.7	98.0	97.2	98.2	98.2	98.1	97.8	98.2	97.3	98.4	98.3	98.2	96.8
α-Methyl styrene	Methyl acrylate																
9	1	79.8	36.6	90.6	2.1	96.3	48.8	98.2	7.4	98.0	50.1	98.2	8.8	97.4	49.1	98.2	9.5
1	1	75.8	30.1	92.0	2.0	96.5	45.3	98.0	7.2	98.2	48.7	98.0	8.5	97.5	45.6	98.0	9.2
4	6	73.4	28.0	71.0	2.1	97.3	43.4	98.0	7.4	98.0	46.2	98.0	8.7	98.0	44.2	98.0	9.5
3	7	92.2	5.8	91.4	2.2	95.8	16.4	98.0	7.2	98.0	17.2	98.0	8.6	98.0	17.0	98.0	9.3
1	9	24.0	3.4	71.3	2.3	96.0	10.0	97.8	7.5	98.0	10.9	98.0	8.8	98.0	10.9	98.0	9.5

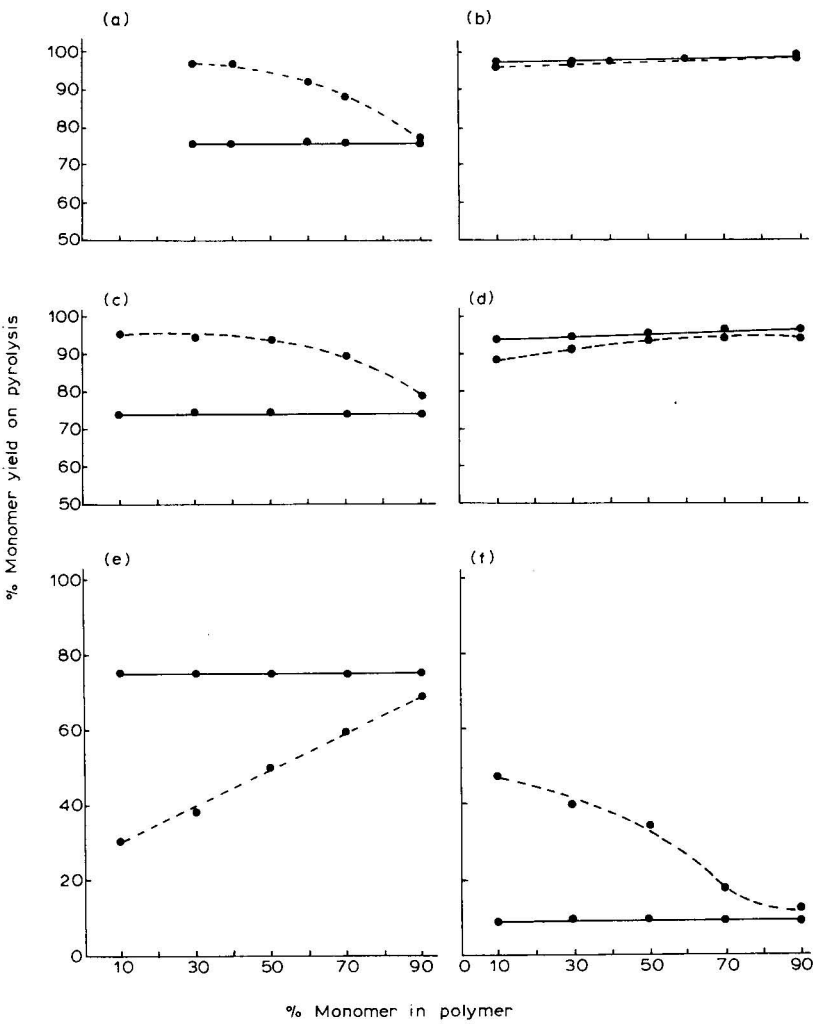


Fig. 1. Plots showing proportionate monomer recoveries for copolymer and homopolymer mixtures of: (a) styrene, (b) α-methylstyrene, (c) styrene, (d) methyl methacrylate, (e) styrene, and (f) methyl acrylate. – – –, Copolymer; ———, polymer mixture.

pyrolysis products are shown in Fig. 2a, where it is apparent that essentially linear relationships exist, the copolymer plot being uppermost due to the greater styrene yields and the higher styrene/α-methylstyrene ratio.

By considering pyrolysis at various temperatures, it was possible to differentiate between copolymers and polymer mixtures. With mixtures α-methylstyrene showed maximum recoveries at 610°, 770°, and 980°, while styrene showed maxima at 770° and 980°. In copolymers, both monomers showed the greatest yields at 770°. The effects with systems of 6:4 monomer ratios arre shown in Fig. 3.

CFI and HFI values were determined for all samples at 770° and are shown in Table III. It is apparent that the CFI and HFI values for α-methylstyrene show

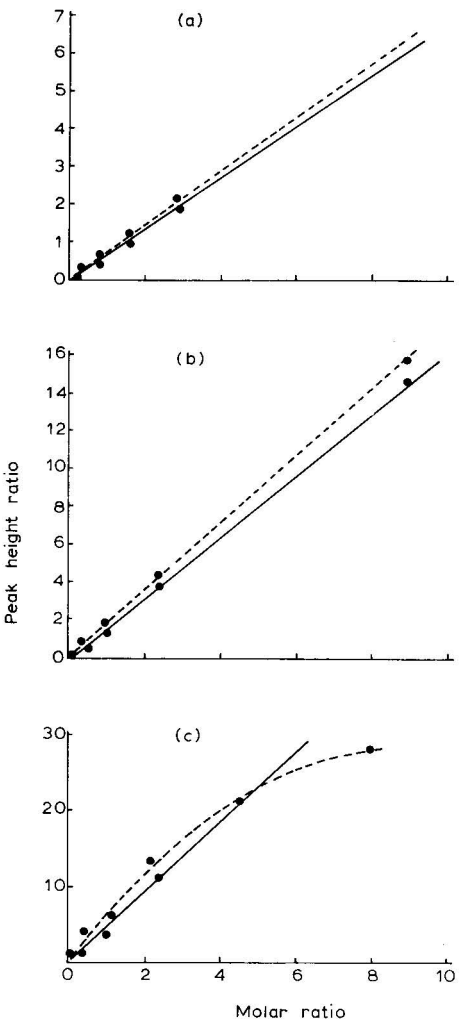


Fig. 2. Plots of percentage composition (peak height ratios) of polymers and of pyrolysis products for: (a) styrene–α-methylstyrene, (b) styrene–methyl methacrylate, and (c) styrene–methyl acrylate. – – –, Copolymer; ———, polymer mixture.

respective constancies, while with styrene the HFI values are constant but the CFI values show a variation according to the composition of the copolymer.

Quantitative yields of monomer from copolymers and homopolymers of styrene and methyl methacrylate are shown in Table II, the individual performance of the homopolymers in admixture being again evident while in the copolymers both styrene and methyl methacrylate yields were influenced by the presence of each other. In general, the styrene yield was increased with increased contents of methyl methacrylate while the methyl methacrylate yield showed a gradual decrease as the styrene concentration in the copolymer increased (Figs. 1c and d).

Maximum styrene monomer recovery was achieved at 770° for both copolymers

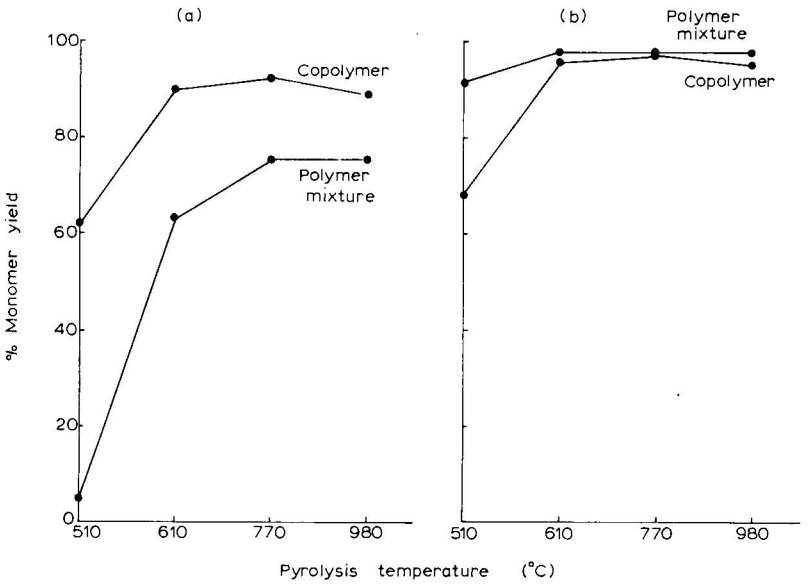


Fig. 3. Influence of pyrolysis temperature on monomer yields of: (a) styrene and (b) α-methylstyrene from copolymer and polymer mixtures.

and mixtures. By the use of the recovery of methyl methacrylate the sample could be identified as a mixture. With homopolymers the maximum ester yield was at 610° and in copolymers at 770°.

Molar ratio plots, *i.e.*, peak height ratios of pyrolysis products *vs.* molar ratios of polymers, for both copolymers and homopolymer mixtures exhibited linear relationships, as shown in Fig. 2b. The CFI and HFI values are shown in Table III and with both monomers the HFI values were constant while the CFI values again varied, slightly depending on the composition of the copolymer.

Both copolymers and homopolymer mixtures of styrene and methyl acrylate yielded complex pyrograms characteristic of those of the individual homopolymers.

Quantitative yields of monomer from copolymers and homopolymer blends are shown in Table II. The individual behaviour of the two monomers in homopolymer mixtures was again evident, however, with copolymers both styrene and methyl acrylate affected each other in monomer yields. When the styrene molar ratio was increased, the percentage recovery of both styrene and methyl acrylate increased accordingly, and when the molar ratio of methyl acrylate was increased, the percentage recovery of both monomers decreased. The effect is shown in Figs. 1e and f and again in Fig. 3c, where the considerable variation in the molar ratios of the polymer and the pyrolysis products is evident from the lack of linearity of the copolymer plot. The HFI values for both monomers are constant and the CFI values greatly variant, as shown in Table III.

Yields of monomer from the series α-methylstyrene and methyl methacrylate are shown in Table II, while fragmentation indices are shown in Table III, where it is evident that both these monomers, which degrade by depolymerisation, are virtually unaffected by the presence of the comonomer.

TABLE III

COPOLYMER AND HOMOPOLYMER FRAGMENTATION INDICES AT 770°

	Styrene		*α-Methylstyrene*		*α-Methylstyrene*		*Methyl methacrylate*	
	CFI	*HFI*	*CFI*	*HFI*	*CFI*	*HFI*	*CFI*	*HFI*
1	1.29	1.32	1.03	1.03	1.02	1.02	1.03	1.03
2	1.14	1.32	1.04	1.03	1.02	1.02	1.04	1.02
3	1.09	1.32	1.02	1.02	1.02	1.02	1.03	1.03
4	1.03	1.32	1.06	1.01	1.02	1.02	1.02	1.02
5	1.03	1.32	1.01	1.02	1.02	1.02	1.02	1.03
Av.	1.12	1.32	1.03	1.03	1.02	1.02	1.03	1.03

	Styrene		*Methyl methacrylate*		*α-Methylstyrene*		*Methyl acrylate*	
	CFI	*HFI*	*CFI*	*HFI*	*CFI*	*HFI*	*CFI*	*HFI*
1	1.27	1.35	1.13	1.06	1.02	1.04	2.00	11.40
2	1.12	1.32	1.10	1.06	1.02	1.02	2.06	11.59
3	1.06	1.32	1.07	1.05	1.02	1.02	2.16	11.39
4	1.05	1.33	1.06	1.06	1.02	1.02	5.79	11.62
5	1.04	1.32	1.05	1.05	1.03	1.02	9.20	11.38
Av.	1.11	1.33	1.08	1.06	1.02	1.02	4.24	11.48

	Styrene		*Methyl acrylate*	
	CFI	*HFI*	*CFI*	*HFI*
1	1.44	1.32	2.12	11.40
2	1.65	1.33	2.49	11.55
3	2.02	1.31	2.94	11.26
4	2.47	1.32	5.77	11.34
5	3.19	1.32	8.67	11.32
Av.	2.15	1.32	4.40	11.37

When methyl acrylate is replaced by methyl methacrylate the monomer yields are significantly altered (Table II), as shown by plots of peak height ratios and composition.

The CFI and HFI values for α-methylstyrene are essentially identical, although with methyl acrylate the values are widely variant, higher yields of methyl acrylate from copolymers being evident by the lower CFI values, as shown in Table III.

From Table III it is apparent that the average values of the fragmentation indices for a particular monomer are very similar when in combination with any of the three comonomers, the exception being with styrene when copolymerised with methyl acrylate, where increased methyl acrylate in the copolymers leads to decreased styrene recovery.

The linearity of the plots of the molar ratio of the pyrolysis products and the copolymer composition for styrene with α-methylstyrene and with methyl methacrylate is in agreement with the work of Strassburger *et al.*[8] and that of Ferlanto *et al.*[16], who considered copolymers of methyl methacrylate with methyl and ethyl

acrylate, respectively. In all of these examples one of the monomers is substantially depolymerised while the other is subjected to significant degradation. In this work the system styrene–methyl acrylate is anomalous as both of the monomers are subject to substantial degradation. The individual behaviour of homopolymers in mixtures is in agreement with earlier works[8,9], with the exception that Ferlanto *et al.*[16] reported a concentration dependence. In the absence of data, it is not possible to consider the degree of this dependence. From the systems studied it is evident that homopolymer mixtures are of limited value for use as compositional models for pyrolysis studies of copolymer systems.

The acrylate–methacrylate system has been discussed[10,16] and while random polymerisation is involved, the product is considered analogous to a block copolymer. The number of acrylate–methacrylate bonds tend to remain constant once the limiting number of these bonds are formed and these rather than the size of the acrylate block determine the pyrolysis yield of acrylate monomer. To further investigate this hypothesis Ferlanto *et al.* employed the sequence distribution of Harwood *et al.*[17] to determine the number of acrylate–methacrylate bonds. Some support was obtained with low-conversion copolymers but with high-conversion copolymers considerable discrepancies were evident. The variation between calculations with high- and low-conversion copolymers is not unexpected due to the limitations of the copolymer composition equation with increasing conversion.

REFERENCES

1 M. P. Stevens, *Characterization and Analysis of Polymers by Gas Chromatography*, Marcel Dekker, New York, 1969.
2 G. M. Brauer, in P. E. Slade, Jr. and L. T. Jenkins (Editors), *Thermal Characterization Techniques*, Marcel Dekker, New York, 1970.
3 J. K. Haken, *Gas Chromatography of Coating Materials*, Marcel Dekker, New York, 1974.
4 G. G. Cameron and D. R. Kane, *Makromol. Chem.*, 109 (1967) 194.
5 G. G. Cameron and D. R. Kane, *J. Polym. Sci., Part B*, 2 (1964) 693.
6 J. K. Haken and D. K. M. Ho, *J. Polym. Sci., Polym. Chem. Ed.*, 12 (1974) 1163.
7 H. McCormick, *J. Chromatogr.*, 40 (1969) 1.
8 J. Strassburger, G. M. Brauer, M. Tyron and A. F. Forziati, *Anal. Chem.*, 32 (1960) 454.
9 R. L. Gatrell and T. J. Mao, *Anal. Chem.*, 37 (1965) 1294.
10 J. K. Haken and T. R. McKay, *Anal. Chem.*, 45 (1973) 1251.
11 S. L. Madorsky and S. Straus, *J. Res. Nat. Bur. Stand.*, 40 (1948) 417.
12 P. Bradt, V. H. Dibeler and F. L. Mohler, *J. Res. Nat. Bur. Stand.*, 50 (1953) 201.
13 W. S. Reid, *J. Soc. Chem. Ind.*, 68 (1949) 244.
14 S. Straus and S. L. Madorsky, *J. Res. Nat. Bur. Stand.*, 50 (1953) 165.
15 S. Straus and S. L. Madorsky, *J. Res. Nat. Bur. Stand., Sect. A*, 66 (1962) 401.
16 E. C. Ferlanto, M. K. Lindemann, C. A. Lucchesi and D. R. Gaskell, *J. Appl. Polym. Sci.*, 15 (1971) 445.
17 J. H. Harwood, N. W. Johnston and H. Piotrowski, *Polym. Prepr., Amer. Chem. Soc., Div. Polym. Chem.*, 8 (1967) 199.

Journal of Chromatography, 126 (1976) 249–256
© Elsevier Scientific Publishing Company, Amsterdam — Printed in The Netherlands

CHROM. 9378

ANALYSIS OF PYROLYSIS GAS CHROMATOGRAMS USING PATTERN RECOGNITION TECHNIQUES

E. KÜLLIK, M. KALJURAND and M. KOEL
Institute of Chemistry, Academy of Sciences of the Estonian SSR, Tallinn (U.S.S.R.)

SUMMARY

A set of 120 polymers was analyzed by using pattern recognition methods such as the cluster analysis, *K*-nearest neighbour and linear learning machine methods. A two-dimensional display of multivariate data is used to illustrate the results.

INTRODUCTION

The use of pyrolysis gas chromatography as a powerful analytical technique has been demonstrated many times[1–3]. However, its possibilities have not been exhausted and its wider application as an analytical method is complicated for several reasons. As an empirical method, the disadvantage of pyrolysis gas chromatography is that for the identification of unknown substances a compilation of pyrograms must be available. Depending on the conditions of pyrolysis and gas chromatographic analysis, different results may be obtained by different laboratories.

A possible means of analyzing empirical results is to apply the pattern recognition technique, which seems to be very useful for handling pyrolysis gas chromatographic data. Firstly, the pattern recognition method enables one to obtain information about a substance of interest when no reference chromatograms are available, and secondly, it can tolerate the existence of deviations in the initial data. It also enables one to overcome the problem of deviations in the retention times of corresponding pyrolysis products from different polymers. The second characteristic provides the possibility of reconciling differences in results obtained by different laboratories.

In a previous study[4], we described one of the pattern recognition methods (the linear learning machine method) used to identify different molecular groups in fibres. The task in the present work was to continue studies on the application of this method. The theory of pattern recognition is not given here because sufficient information is available elsewhere[5,6].

EXPERIMENTAL

Unfortunately, the pyrolysis gas chromatograms presented in many scientific papers were obtained under different conditions, and it was difficult to find suitable

chromatograms. We therefore used chromatograms produced in our laboratory. The set of 120 polymers selected consists mainly of several natural and synthetic fibres. All fibres were pyrolyzed by using a Curie-point Pye Unicam pyrolyzer at 980°. A Perkin-Elmer Model 900 gas chromatograph was used for the analysis of the thermal degradation products.

The other operating conditions were: dual flame-ionization detector; Inerton AW-DMCS/Carbowax 20M column, length 2 m, I.D. 2 mm; initial column temperature 70°, programmed at 6.5°/min to a final temperature of 190°, which was maintained for 10 min.

For data processing, an off-line computer system was used. The gas chromatographic output signal was handled by using a Hewlett-Packard 3370A integrator and a Videoton 1010B computer. The retention time and peak area of every peak were punched on to paper tape.

PRESENTATION OF PYROGRAMS TO THE COMPUTER

The most precise method for the presentation of pyrolysis gas chromatograms to the computer is to give the name (retention time) and intensity (peak area) of each individual thermal degradation product for all pyrograms available. The best means of solving this problem is to identify all individual components in the pyrogram. For the calculation, each pyrogram is presented as a sequence of numbers, every peak being characterized by numbers that are in accordance with the peak intensity. If there is no peak, the intensity is zero. Such a presentation is commonly used for plotting gas chromatograms in tabular form. Unfortunately such a method of coding is limited by the set of substances used and needs a large computer memory.

In our study, peaks were coded as in infrared or mass spectroscopy. Each pyrogram was divided into zones of equal width and the most intense peak was taken into account. All chromatograms were presented to the computer as a normalized and logarithmic sequence of intensities of selected peaks. For the calculation, the integer part of the logarithmic value was taken.

Pyrolysis gas chromatograms were divided correspondingly into 20 and 40 zones, giving two sets of data (Fig. 1). Such "low" and "high" data sets permit one to estimate the loss of information by coding.

An essential parameter is the ratio between the number of objects presented and the number of measurements that characterize a particular object. Let us denote this ratio by s. From the literature[6] it is known that $s \geqslant 3$ is needed. In our work, the conditions $s_{20} = 6$, $s_{40} = 3$ were followed. According to the general geometric concept, coded programs in pattern recognition are treated as a set of points in either 20- or 40-dimensional hyperspace.

CLUSTER ANALYSES OF PYROGRAMS

It is interesting to elucidate groups of similar pyrolysis gas chromatograms in the given set of data, *i.e.*, to make a classification of polymers on the basis of their pyrolysis chromatograms. In a geometric sense, one looks for a set of points (clusters) in the hyperspace. We used the Euclidean distance between two points for as a measure of similarity; for finding clusters, two algorithms were used.

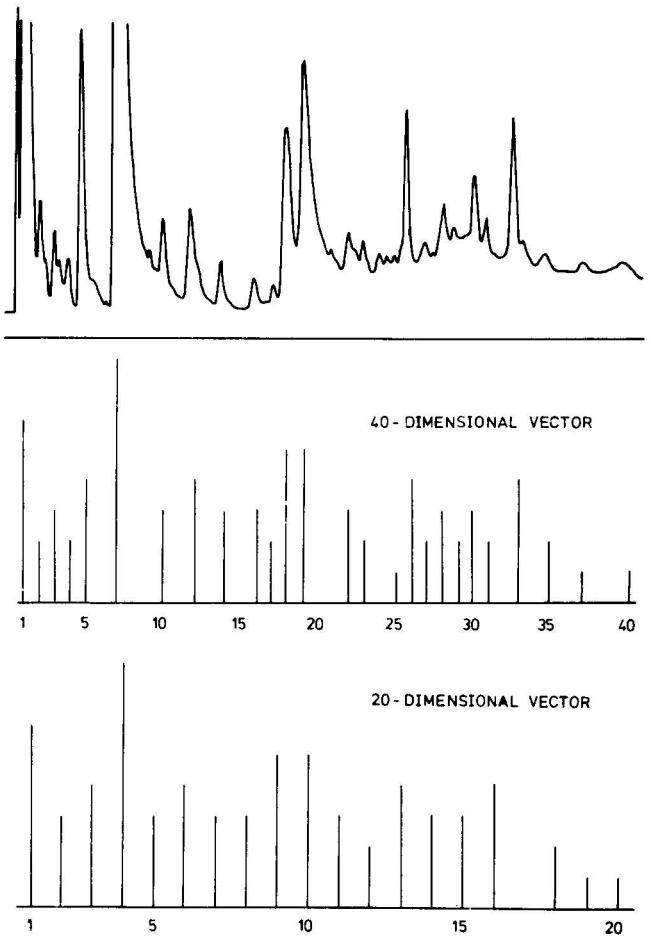


Fig. 1. Coding a pyrogram in the 40- and 20-dimensional cases.

In the first algorithm[7], the number of clusters is not fixed and a parameter R is assigned to determine the number of clusters; the points that are in one hypersphere, of radius R, form a cluster. The centre of the hypersphere is located at the maximum density of the points. If the number of clusters is constant for different R values, then there are well separated and compact clusters in the hyperspace.

Another algorithm may start from an arbitrary point. All points that are nearer to that point than the value of the threshold, r, are included in a cluster. According to the measure of similarity, r new points are included with these points in a cluster. The procedure is repeated until there are no points to add to this cluster, then a new point that does not belong to the cluster so formed is taken and the above procedure repeated. In this way, one can connect all of the existing objects to the clusters.

These two techniques gave virtually identical results for both the 40- and 20-dimensional cases. Three large clusters are formed; one consists of rubbers and the second of polyacrylonitrile fibres. The third cluster consists of $-CH_2-CHR$-type fibres,

where R is an alcoholic hydroxyl acetate radical or chlorine group. The other fibres (polyamides, polyurethanes, polyesters) have no tendency to form clusters, *i.e.*, they are homogeneously distributed in the hyperspace.

If the radius R or the similarity measure r was increased, then all three clusters converged into one large cluster, but the separately located points remained beyond the cluster as before. The parameters R and r must, of course, be changed within the appropriate limits, otherwise one obtains only one cluster or as many clusters as there are objects.

The results of the cluster analysis demonstrate that there is a cluster with a large number of members (about half of the inspected polymers), which can be divided into three smaller clusters, and a number of separately located substances.

CORRELATION STUDIES BETWEEN PYROLYSIS GAS CHROMATOGRAMS AND THE STRUCTURES OF SUBSTANCES

It is convenient to use pattern recognition techniques to establish whether or not a certain property of the object appears in the pyrolysis gas chromatogram. For classification purposes we used two methods, the K-nearest neighbour[8] and the linear learning machine methods[9]. If the K-nearest neighbour method is used, the substance is classified according to its K-nearest neighbours; in this work $K = 1$ and 3. Using the linear learning machine method, one calculates the dot product between the object vector and an appropriately derived weight vector, the object being classified according to the sign of the dot product. Geometrically, this means that the object is classified according to the side of the classifying hyperplane on which it lies.

The results are presented in Table I. We have a binary classification for each property, *i.e.*, the object may or may not have a particular property. Table I gives the percentage of the prediction that characterizes the probability of classification

TABLE I

PERCENTAGES OF PREDICTION

Property	*Positive class number*	*K-nearest neighbour method*				*Linear learning machine method*	
		$K = 1$		$K = 3$			
		20-dimensional	*40-dimensional*	*20-dimensional*	*40-dimensional*	*20-dimensional*	*40-dimensional*
Nitrogen	57	73	77	72	72	55	59
–CN	25	92	91	93	90	74	74
NH–CO	31	76	81	74	79	67	51
Benzene ring	20	86	83	90	83	61	75
Oxygen	61	73	83	72	75	58	55
O, N and benzene ring in main chain	50	72	82	67	77	59	48
–C=O	49	68	75	66	70	43	51
–O–C=O	26	77	74	77	77	81	74
–Cl	19	85	89	84	85	59	69
Polyolefin	14	92	87	85	84	84	84

correctness[10]. The column "positive class number" shows the number of polymers that have a particular property. The greater the prediction, the clearer the structural element of a polymer is expressed in the pyrogram.

Fukunaga and Olsen[11] described an interesting technique for the two-dimensional display of multivariate data, namely the so-called *d*-displays, and we used it to illustrate our results. The method displays the points on a two-dimensional display, the coordinates of which are the squared Euclidean distances from two particular points in the *n*-dimensional space. These two points are the geometric centres of two classes. The method preserves some geometric structure while placing a heavy weight on class separability. A straight line on the *d*-display corresponds to some decision boundary in the *n*-dimensional object space that is reduced to a hyperplane for the line with an angle of 45° with respect to the d_1 axis. Fig. 2 shows the *d*-display for five classes. The overlapping of the $-C\equiv N$, $.=N-$ and –Cl classes is considerably less than for the "hetero-atom in the main chain" class. Partial overlapping of two classes in the display does not mean that the two classes are not separated at all but that other method must be used to find the decision boundary, such as *e.g.*, the linear learning machine method or the data must be normalized appropriately[11].

DISCUSSION

Bearing in mind the specific features of pyrolysis gas chromatography, the results of the cluster analyses of the pyrolysis products of the polymers can be summarized as follows. Polyacrylonitrile, polyvinyl and rubber polymers give characteristic pyrograms that enable one to differentiate them from the others. However, it is difficult to differentiate the above polymers inside a given class. On the other hand, individual polyamide, polyether and polyurethane pyrograms are very characteristic and are easily differentiated from each other.

It is evident that our results depend on the experimental conditions used. Using another liquid phase with a polarity different from that of Carbowax 20M, one can obtain different results. As a practical consequence, we have a method for estimating the suitability of a particular liquid phase for the analysis of a particular class of polymers. In this work it seems to be valid for polyamide, polyester and polyurethane polymers. However, if the constituents of the polymers are very similar, the polarity change might have no effect. All this is also valid for the pyrolysis conditions.

The results in Table I show that there are several functional groups the existence of which can be established with reasonable probability (–CN, –Cl and benzene ring). There are some functional groups, however, for which the prediction is on the random guessing level (–CO, –O–). In the linear learning machine method, the random guessing level is 50%. If the use of the pattern recognition technique fails for some property, the two main reasons are that either the presentation (or method used) does not express the expected property, or the presentation is coarse.

As can be seen from Table I, the prediction for $K = 1$ (40-dimensional) is better than for $K = 1$ (20-dimensional) and $K = 3$ (40- and 20-dimensional). $K = 1$ (20-dimensional) and $K = 3$ (40- and 20-dimensional) give virtually identical results. Therefore, we can conclude that improving the resolution (as well as K) does not have a significant effect on the improvement of prediction. The percentage of prediction

obtained characterizes the ability of the pyrograms to express the tested property. It can be seen from Fig. 2 that most of the classes overlap considerably and on increasing the dimension of the hyperspace the overlapping of the classes decreases. It seems that they did not form the linearly separated set of points (as in our previous work[4]), which is why the results of the *K*-nearest neighbour method are better than those of the linear learning machine method. On the other hand, it is evident that the results obtained with pattern recognition techniques depend on the pre-processing method, *i.e.*, the way in which the pyrograms are presented to the computer. In this work, we did not attempt to obtain a good separation for a particular class. There are effective pre-processing and feature selection methods in pattern recognition for improving inter-class resolution[5] and one can obtain considerably better results than those in Table I for a particular problem of interest. Our presentation (logarithmic intensities), which places a heavy weight on the smaller peaks, may emphasize unimportant features for a particular class. It is clear from the above discussion that pre-processing methods for pyrograms need further investigation.

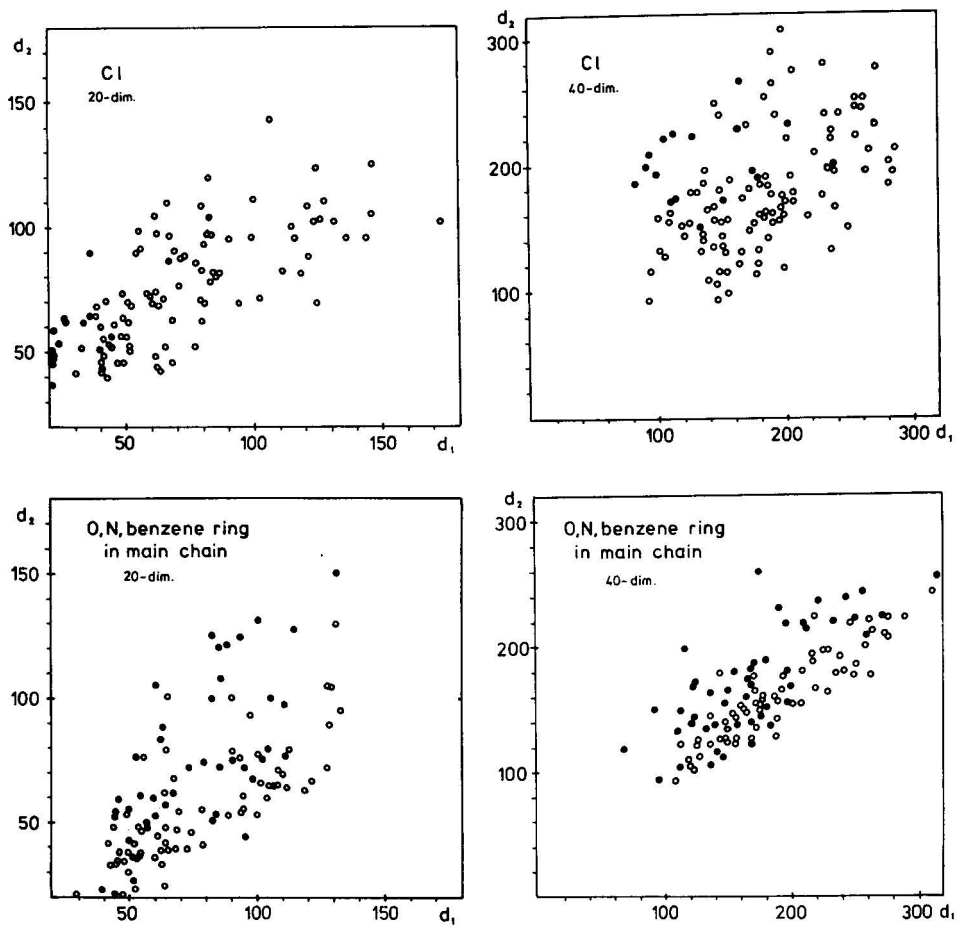


Fig. 2.

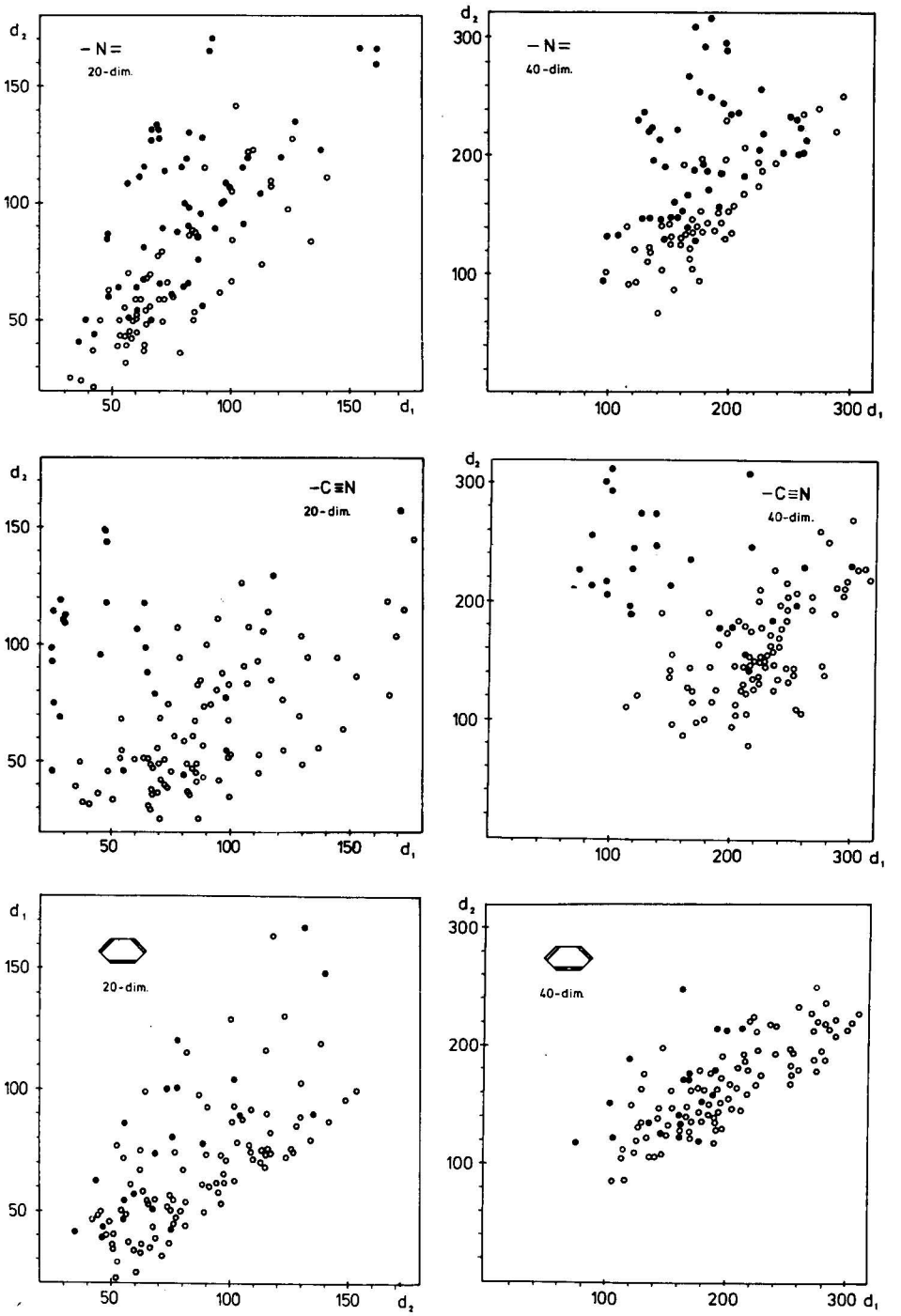


Fig. 2. *d*-Displays for some tested properties. d_1- and d_2-squared distances from the geometric centres of the positive and negative classes. ●, Positive class members; ○, negative class members.

The interpretation of spectral data with pattern recognition is a completely empirical method, and therefore only practical results will show which chemical structures are classified well.

REFERENCES

1 P. G. Simmonds, G. P. Shulman and C. H. Stembridge, *J. Chromatogr. Sci.*, 7 (1969) 36.
2 J. Janák, *Collect. Czech. Chem. Commun.*, 25 (1960) 1780.
3 L. S. Ettre, *J. Chromatogr.*, 112 (1975) 1.
4 E. Küllik, M. Kaljurand and M. Koel, *J. Chromatogr.*, 112 (1975) 297.
5 J. M. Mendel and K. S. Fu (Editors), *Adaptive, Learning and Pattern Recognition Systems*, Academic Press, New York, 1970.
6 B. R. Kowalski and C. F. Bender, *J. Amer. Chem. Soc.*, 94 (1972) 5632.
7 V. N. Elkina and N. G. Zagoruiko, *Vychislitel. Sist.*, 22 (1966).
8 T. M. Cover and P. E. Hart, *IEEE Trans. Inf. Theory*, IT-13 (1967) 21.
9 N. J. Nilsson, *Learning Machines*, McGraw-Hill, New York, 1965.
10 T. L. Isenbour and P. C. Jurs, *Anal. Chem.*, 43 (1971) 20A.
11 K. Fukunaga and D. R. Olsen, *IEEE Trans. Comput.*, C-20 (1971) 917.

Journal of Chromatography, 126 (1976) 257–261
© Elsevier Scientific Publishing Company, Amsterdam — Printed in The Netherlands

CHROM. 9443

POSSIBILITY OF INCREASING THE SELECTIVITY OF CHROMATOGRAPHIC SEPARATION UNDER THE ACTION OF LASER RADIATION

K. I. SAKODYNSKI, R. I. SOKOLOVSKI, N. N. TUNITZKI and S. A. VOLKOV
Karpov Institute of Physical Chemistry, Moscow (U.S.S.R.)

SUMMARY

The possibility of increasing the selectivity of chromatographic separation when carried out in a field of laser radiation has been considered. This increase is the result of the selective excitation of one of the types of the molecules to be separated, the sorption of which decreases owing to the excitation. It has been shown that as a result of this effect, the rate of movement of the excited type of molecules along the column under favourable conditions may be nearly twice that of the non-excited variety. The method can be used in a capillary along which the laser beam is propagated and employed, for example, to resolve isotope mixtures.

In the laser chromatographic separation of different varieties of molecules, for instance isotopes, the chromatography is carried out in a field of laser radiation. In such a field, provided there is a corresponding frequency of excitation, some varieties of molecules are excited, while others remain non-excited. It is assumed that upon colliding with the surface of the adsorbent the excited molecules are either not adsorbed or are sorbed with a lower probability than the non-excited molecules[1–4]. The non-adsorbed molecules lose their excitation and return to the gas phase, where they are excited again. As a result of this process, the selectivity of separation (α) must be significantly increased.

Let the partition coefficient of a substance, K, be equal to b/a (in the absence of laser radiation), where b and a are the concentrations of the substance in the gas and the liquid phase, respectively. As a result of the action of radiation, the concentration of particles in the gas phase will increase by a value b^*, and the partition coefficient will be equal to $(b + b^*)/(a - [b^* \kappa]/[\kappa_1])$, where κ and κ_1 are fractions of the column volume occupied by the gas and the liquid phase, respectively. As laser chromatography is more conveniently effected on short columns at low temperatures, it can be assumed that $(a/b) \gg (\kappa/\kappa_1)$; then the partition coefficient, under conditions of laser radiation, will be $(b + b^*)/a$. As it is known that the velocity of movement of the band, V, is related to the carrier gas flow-rate, U, by

$$V(0) = \frac{U}{1 + \kappa_1/K\kappa}$$

or, taking into account the above inequality,

$$V(0) \approx \kappa UK/\kappa_1$$

then accordingly, under conditions of laser radiation with an intensity I

$$V(I) = \frac{U(b + b^*)\kappa}{a\,\kappa_1}$$

The ratio $V(I)/V(0)$ is equal to $\dfrac{b + b^*}{b}$.

As can be seen from the above equation, the acceleration of the band movement under the action of excitation depends on b^*. If it is assumed that the excited molecules upon collision with the surface are not sorbed, the ratio $(b + b^*)/b$ will increase with an increase in the laser radiation intensity.

We shall obtain the following relationship, by considering an one-dimensional problem:

$$D\frac{\partial^2 b}{\partial y^2} = \sigma I(b - b^*) \tag{1a}$$

$$D\frac{\partial^2 b^*}{\partial y^2} = -\sigma I(b - b^*) \tag{1b}$$

with the boundary conditions

$$y = 0\colon b = Ka,\ D\frac{\partial b^*}{\partial y} = b^*\bar{U}/\sigma \tag{2}$$

$$y = d\colon \frac{\partial b}{\partial y} = 0,\ \frac{\partial b^*}{\partial y} = 0 \tag{3}$$

where y is the distance from the point considered to the phase interface, D the diffusion coefficient of the substance to be resolved, I the intensity of laser radiation, σ the cross-section of radiation transition, $\bar{U}$ the heat velocity of the molecules and d the half-thickness of the gas phase layer.

Eqns. 1a and 1b describe the diffusion of the non-excited and the excited particles, their formation and decay under the action of laser radiation being taken into account. The first of the boundary conditions shows that on the phase interface the usual condition of sorption equilibrium for non-excited molecules is maintained. The boundary condition in eqn. 2 expresses that any excited particle that finds its way to the wall loses its excitation and diffuses to the gas phase without being sorbed. The stream of excited particles $b^*\bar{U}$ must be equal to the stream of deactivated particles on the surface. Finally, the boundary condition in eqn. 3 expresses the symmetry of the problem and shows that the concentration of the excited particles is at a maximum in the middle of the column, while that of the non-excited ones is at a minimum.

In eqns. 1a and 1b, the terms describing spontaneous transitions are omitted, which is justified only when the time of diffusion to the wall, $\tau^* = d^2/D$, is much less than the time of spontaneous transition.

Strictly speaking, the condition in eqn. 2, expressing the equality of the diffusion stream to the gas kinetic stream, should be put at a distance from the boundary Λ equal to the length of the free path of the molecule, with $\Lambda \ll d$, is practically satisfied with $y = 0$.

On solving eqns. 1–3, we obtain

$$\frac{V(I)}{V(0)} = \mathrm{F}(I) = \frac{1 + (6D/\bar{U}d)\sqrt{2\sigma I\tau^*}\ \mathrm{tg}\ \sqrt{2\sigma I\tau^*}}{1 + (3D/\bar{U}d)\sqrt{2\sigma I\tau^*}\ \mathrm{tg}\ \sqrt{2\sigma I\tau^*}} \tag{4}$$

If we reject the assumption of deactivation of any molecule that reaches the phase interface and assume that the probability of its sorption is β ($0 \leqslant \beta \leqslant 1$), then instead of eqn. 4 the following is obtained:

$$\mathrm{F}(I) = \frac{1 + (6D/\bar{U}d)\sqrt{2\sigma I\tau^*}\ \mathrm{tg}\ \sqrt{2\sigma I\tau^*}}{1 + (1+\beta)(3D/\bar{U}d)\sqrt{2\sigma I\tau^*}\ \mathrm{tg}\ \sqrt{2\sigma I\tau^*}} \tag{5}$$

If $\beta < 1$, the velocity of movement of the chromatographic band changes, reaching a value of $2V(0)/(1+\beta)$ with $\sigma I\tau^* \gg 1$.

Plots of the function F (I) with $\beta = 0$ and different values of the dimensionless parameter $3D/\bar{U}d \approx \Lambda/d$, where Λ is the length of the free path of the molecules, are given in Fig. 1. It can be seen that the intensity of light required to increase the velocity of movement of the chromatographic band by 10% rapidly increases with an increase in the value of the ratio d/Λ, tending (with $d/\Lambda \geqslant 100$) to a value independent of d, which can be found from the equation $\sigma I\Lambda/\bar{U} \approx 2 \cdot 10^{-3}$.

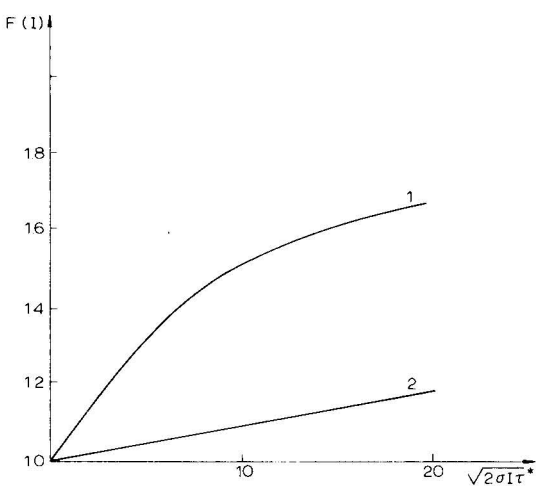


Fig. 1. Plot of function F (I) for different values of the parameter $3\,D/Ud$: (1) 0.1; (2) 0.01.

The life of the oscillatory excitement of molecules may reach values of the order of 10^{-5} sec. The average time of diffusion to the wall has the same order of magnitude

for capillaries of radius 10^{-2} cm at atmospheric pressure. From the estimates given by Gochelashvili *et al.*[1], it follows that in this instance the powers of gaseous CO_2 lasers are sufficient for a marked increase in the rate of movement of a chromatographic band. Thus, the use of lasers for the selective excitation of molecules makes possible the separation of substances that have similar sorption coefficients but different optical properties, even at atmospheric pressure.

The theory presented above is based on a number of assumptions, playing different roles in laser chromatography. For example, taking into account factors such as degeneration of the combining levels, the Poiseuille distribution according to velocities and diffusion of molecules in a liquid film, one merely obtains a more precise form of eqn. 5, without changing the basic deduction of the theory as to the influence of laser radiation upon the velocity of movement of a chromatographic band. The process considered is found to be critical to only one phenomenon, namely weaker sorption of the optically excited molecules.

Laser chromatography could be a sufficiently universal means of separating substances if lasers with a rearranged frequency of sufficient power are used. To demonstrate this possibility, CO_2 lasers are suitable for the chromatographic separation of boron isotopes in BCl_3. To demonstrate the effect of changing the velocity of movement of a chromatographic band, SF_6 could be used if a suitable liquid phase is selected.

In practice, laser chromatography can be carried out in a capillary the inner walls of which are coated with a liquid film, the laser ray being propagated along the capillary. Measures should be undertaken to prevent the evaporation of the liquid phase film under the action of laser radiation. For this purpose, the capillary must be well cooled and the thickness of the liquid phase film must not exceed a few microns.

Let us attempt to evaluate the parameters of the capillary required for detecting the effect discussed.

From purely optical considerations, let us assume that the diameter of the capillary is 1 mm and its length is 20 cm. For such a capillary, the thickness of the stationary phase film being about 2 μm, $\kappa \approx 1$ and $\kappa_1 = 10^{-2}$, and the retention time, t_R, is equal to $20/U\,(1 + 0.01/K)$. To ensure reliable measurement, it is necessary that the retention time of SF_6 should be at least twice that of the non-sorbed component; to ensure this requirement, it is necessary to have $0.01/K \approx 1$, *i.e.*, $K \approx 0.01$. Under this condition, with a rate $U \approx 1$ cm/sec, $t_R \approx 40$ sec. According to the estimates given above, even on such a short capillary the retention time of SF_6 after irradiation must decrease by 5–7 sec, which can easily be recorded. Unfortunately, very little information is available on the retention of SF_6 on liquid phases. If some literature data[5,6] are used, the value of K for this compound on Kel-F 3 can be estimated at room temperature. This value is about 1, which is obviously insufficient for our purpose. On decreasing the temperature, however, K decreases rapidly. At temperatures below 0°, using fluorinated hydrocarbons as the stationary phase, it will be possible to attain the required values of $K \leqslant 0.01$.

In conclusion, it can be expected that laser radiation will help to increase the selectivity of chromatography in the multi-stage separation of mixtures that are difficult to resolve, such as mixtures of isotopes.

REFERENCES

1 K. S. Gochelashvili, N. V. Karlov, A. N. Orlov, R. P. Petrov, Yu. N. Petrov and A. M. Prokhorov, *Zh. Eksp. Teor. Fiz.*, 21 (1975) 640.
2 H. G. Basov, E. M. Belenov, C. A. Isaakov, Yu. S. Leonov, E. P. Markin, A. I. Oraevski, V. I. Romanenko and N. B. Feropontov, *Zh. Eksp. Teor. Fiz.*, 22 (1975) 221.
3 Yu. V. Brzhazovski, Yu. S. Kusner, A. K. Rebrov, B. I. Proshin and V. P. Chebotarev, *Zh. Eksp. Teor. Fiz.*, 23 (1976) 288.
4 K. S. Gochelashvili, N. V. Karlov, A. S. Obchenkov, A. N. Orlov, R. P. Petrov, Yu. N. Petrov and A. M. Prokhorov, *Zh. Eksp. Teor. Fiz.*, 70 (1976) 531.
5 R. N. Cambell and B. I. Gudzinowicz, *Anal. Chem.*, 33 (1961) 842.
6 I. Lysyi and P. Newton, *Anal. Chem.*, 35 (1963) 90.

Journal of Chromatography, 126 (1976) 263–269
© Elsevier Scientific Publishing Company, Amsterdam — Printed in The Netherlands

CHROM. 9431

A SEMI-SPECIFIC FLAME-IONIZATION DETECTION SYSTEM

J. ŠEVČÍK, R. E. KAISER and R. RIEDER
Institute of Chromatography, P.O. Box 1308, D-6702 Bad Duerkheim-1 (G.F.R.)

SUMMARY

A modification of the flame-ionization detector (FID) has been designed, based on the change in the detection mechanism due to a pre-reaction zone containing a heated hydrogen path and the simultaneous handling of the signal by parallel combination with a normal-mode FID. Owing to the reactions in the pre-flame zone, organic substances are cracked and the reactions lead to higher yields of radicals, in addition to hydrogenation reactions.

The simultaneous use of a normal FID together with this modified FID, which is called an EFID (thermally and chemically energized) permits the identification of organic substances by means of numerical factors related to the structure and particular behaviour of the EFID. These numerical factors are, within the linear dynamic range of the detectors, highly reproducible, because of the exclusion of all chromatographic errors and sampling problems.

The parallel use of the EFID/FID system is demonstrated with examples and some results are reported.

This simultaneous EFID/FID is especially useful for the analysis of compounds of similar structure and gives more information about one sample than highly specific detectors of the element-sensing type such as the NID, SID and PID, halogen detectors and the oxygen-sensing FID.

INTRODUCTION

The flame-ionization detector (FID) is widely used in gas chromatography (GC) and its underlying mechanism is the subject of continuous research. The normal FID uses a diffusion flame, the eluate and hydrogen being mixed after the GC column. It has been found that only this arrangement gives a constant response related to the CH_2 groups of organic substances[1]. It has also been shown that temperature has an important effect on the magnitude of the FID signal.

On the basis of our earlier results[2], we can state that the ionization efficiency of FID increases rapidly with the number of CH_3 functional groups present in organic molecules and that the proportion of $CH_3\cdot$ radicals is correlated with the resulting FID ion current.

The mechanism of the FID is based on two steps:

(1) radical formation, requiring the absence of oxygen;

(2) chemical ionization of radicals formed by excited atomic or molecular oxygen states.

It is possible to change the resulting ion current due to reactions that decrease the yield of the recombiantion reaction. By changing the radical formation in step 1, we can obtain a higher yield of $CH_3\cdot$ radicals and, as the $CH_3\cdot$ radical has at least a 10 times higher ionization efficiency than the $CH\cdot$ radical, the magnitude of the FID signal is increased[2].

The equations involved in step 1 are:

$$C\text{–}C\text{–}C\text{–}C\text{–}OH \rightarrow 1\ CH_3\cdot + 3\ CH_2\cdot + OH\cdot$$
$$C\text{–}C\text{–}C\text{–}C\text{–}OH + H \rightarrow 4\ CH_3\cdot + OH\cdot$$
$$C_6H_6 \rightarrow 6\ CH\cdot$$
$$C_6H_6 + 12\ H \rightarrow 6\ CH_3\cdot$$

The equations involved in step 2 are

$$CH_3\cdot + O^* \rightarrow CH_2O\cdot + H$$
$$CH_3\cdot + O_2^* \rightarrow CH_2O + OH$$
$$CH_2O\cdot + O^* \rightarrow CHO^+ + OH^-$$
$$CH_2\cdot + O^* \rightarrow CHO^+ + OH^-$$

In an atmosphere of water vapour, the primary CHO^+ ions formed react rapidly and a hydrated proton is formed[3,4]:

$$CHO^+ + H_2O \rightarrow H_3O^+ + CO$$

and the probability of recombination increases.

EXPERIMENTAL

The measurements were carried out on the apparatus shown schematically in Fig. 1. The eluate from the column was split into two streams, to one of which hydrogen at a flow-rate of about 50–100 cm^3/min was added before the EFID inlet. The materials used were stainless steel, nickel and nickel in platinum–iridium alloy tubes.

The tubing of the EFID was heated by an external heating coil to 200–550°. The whole arrangement was mounted within a Model F 22 gas chromatograph (Perkin-Elmer Bodenseewerh), allowing both the EFID and FID signals to be measured simultaneously and independently. Separations were carried out on various micropacked glass columns in separation cassettes (IfC), 2–3 m in length and 0.8 mm I.D., packed with 80–100-mesh synthetic carrier material (Merck, Darmstadt, G.F.R.) and OV-101, UCON 50 HB 5100 and OV-225 as liquid phases.

The signal was handled off-line by measuring the peak height data from the recorded chromatogram as well as integrated areas from a Spectra Physics System 1 integrator and a Spectra Physics Minigrator for the double-channel signals. Direct conversion of simultaneous signal to peak ratios by a multi-integration system such as the Spectra Physics 4000 would be the best solution to the problem, but this is not yet possible.

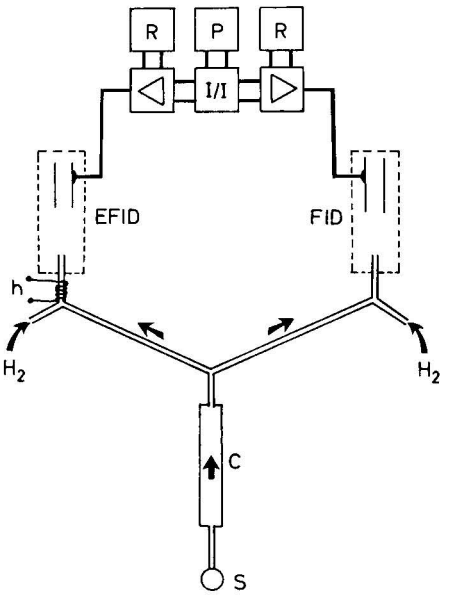


Fig. 1. Schematic diagram of EFID–FID combination. S = sample inlet; C = column; h = heating device; R = recorder; I/I = double-channel integrator with signal relation capability for channel one/channel two; P = printer for relative adjusted retention time data $k' = (t_{ms} - t_m)/t_m$, area correction and quantitation from FID channel and together with the k' data s_X number presentation.

RESULTS AND DISCUSSION

The changes in ionization efficiencies are based on cracking reactions in front of the flame, termed the pre-reaction zone. It was assumed that the radical formation changes owing to the change in temperature. At low temperatures, the formation of $CH_3\cdot$ radicals does not occur and therefore there is no difference in the signals in the normal FID and the EFID modes. If electronegative groups or atoms are present, the EFID signal must be smaller than the FID signal owing to an increased probability of electron recombination.

With increasing temperature, the yield of $CH_3\cdot$ radicals is increased and, owing to its higher ionization efficiency, the EFID signal must be higher than that of FID.

The signal of a compound X in an FID can be written as S_X^{FID} and we can write

$$S_X^{FID} = q_X^{FID} \cdot \frac{c}{n}$$

where q_X^{FID} is the ionization efficiency of substance X in the FID mode, c is the concentration in the effective detector volume or flow-rate in grams per second and n is the number of carbon atoms in one molecule of X. The resulting signal of the same compound X in the EFID can be written as

$$S_X^{EFID} = q_X^{EFID} \cdot \frac{c}{n}$$

A simultaneous but not identical flow of X into both detectors will remain constant, when the pressure, temperature, flow-rate, etc. remain constant.

If we use methane as a normalizing compound, the relationship of the CH_4 signal (FID) to the CH_4 signal (EFID) will remain constant and acts as an equalization factor, as

$$q_{CH_4}^{FID} = q_{CH_4}^{EFID}$$

Therefore

$$\frac{S_{CH4}^{FID}}{S_{CH4}^{EFID}} \cdot \frac{S_X^{EFID}}{S_X^{EFID}} = \frac{q_X^{EFID}}{q_X^{FID}} = s_X \qquad (1)$$

s_X is a numerical factor, that corresponds to the structure of a compound under given conditions of the EFID–FID detection system.

s_X is independent of the concentration or flow-rate of X, provided that both detectors remain in their linear dynamic range. Therefore, s_X is a function only of the different ionization efficiencies in the simultaneously operating detectors and is an identification number, independent of all possible errors of sampling, vaporization, separation, column polarity and disproportionation at the inlet splitter, if present. Of course, for s_X to offer precise information for identification purposes, a complete separation into individual compounds is necessary.

It has long been known that relative response factors can be useful in making qualitative identifications. However, they cannot act as identification numbers, for instance in hydrocarbon class identifications, nor are highly specific detectors, used simultaneously with non-specific detectors, a real help in identifications, for instance in the trace level range, as the differences in the q factors are often too large. It is the semi- or moderate specifity of the EFID together with a normal FID that can help analysts to solve qualitative analysis problems in GC. There are many possibilities for changing the specifity of the EFID, but only slight changes are of interest in order to help positively with identification. For instance, temperature effects change the q to q relationship (see eqn. 1).

Temperature effects

Temperature effects were studied in the range 20–750°. Between 20° and 200°, s_X changes significantly for substances that contain electronegative atoms in their molecules. At 500°, most of the structure-dependent quantitative reactions are stabilized to constant values. Above 500°, futher effects become dominant and the materials of tubes tend to have a greater influence.

Fig. 2 illustrates as an example the effect of temperature at the EFID inlet, and Table I gives further data.

Effect of material used for the reaction tube

Stainless steel, nickel and nickel in platinum–iridium alloy (75:25%, w/w) were examined and the results are given in Table II. The lifetime of nickel tubes does not permit their use without an inert environment.

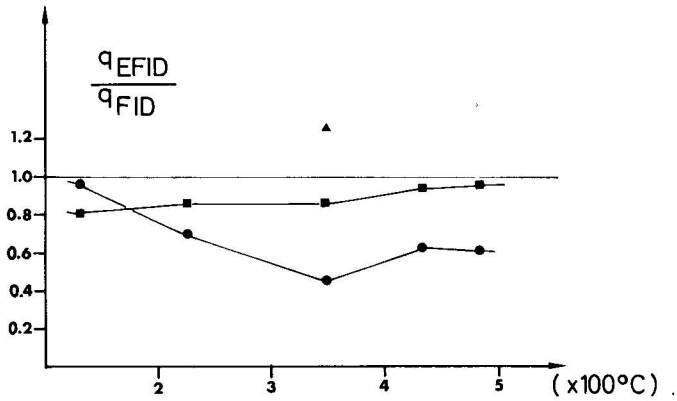


Fig. 2. Dependence of ionization efficiency ratio (q_{EFID}/q_{FID}) on the temperature applied to the EFID inlet. ▲, 1-propene; ●, methyl chloride; ■, 2-methyl-1-propene.

TABLE I

EFFECT OF EFID TEMPERATURE ON THE STRUCTURE FACTOR (s_X)
Conditions: stainless-steel tube, 140-mm heated zone, 0.8 mm I.D.

Compound	s_x			
	100°	*200°*	*400°*	*500°*
n-Heptane	1.00	1.00	1.00	
Benzene	1.01	0.98	0.91	
Methyl propyl ketone	1.00	0.33	0.28	
n-Nonane	1.00		0.99	
n-butanol	1.01	0.286	0.29	
n-Decane	1.01	0.83?	0.98	
Pyridine	1.01		0.42	
	Coefficient of variation: ± 0.3%			
Ethanol				0.467
2-Propanol				0.885
1-Propanol				0.676
2-Methyl-1-butanol				0.833

TABLE II

EFFECT OF TUBE MATERIAL ON s_X

Tubing material	s_X *at 400°*			
	n-Butane	*2-Methyl-1-propene*	*1-Butene*	*Methyl chloride*
Stainless steel	0.625 ± 0.008	0.763 ± 0.011	0.774 ± 0.008	0.683 ± 0.007
Nickel	1.186 ± 0.011	1.030 ± 0.046	1.279 ± 0.025	0.600 ± 0.008

We consider that metallic traces on the inner surface of the tubes are of importance, and a precisely known surface quality is essential.

TABLE III

PARAMETERS OF EFID AND FID

Mode	*Compound*	*Linearity*	*Linear dynamic range*	*Lowest detectable amount (g)*
EFID	CH_4	0.588	6	2.8×10^{-11}
	CH_2Cl_2	8	8	6.3×10^{-12}
FID	CH_4	0.629	4.7	1.6×10^{-11}
	CH_2Cl_2	0.503	5	8.6×10^{-11}

Linearity, linear dynamic range, detection limit (lowest detectable amount, LDA)

The logarithmic dilution flask method was used. Measurements were carried out with methane and methylene chloride and the results are given in Table III.

The calculation of the detector parameters is based on eqns. 1–4 below[5]. For measurements of the linearity (l) of detectors, eqn. 1 holds:

$$l = \frac{\log n \cdot S^{\mathrm{EFID}} - \log q_X^{\mathrm{EFID}}}{\log w} \tag{1}$$

where n = number of carbon atoms: S = signal for X in amperes; q_X is the ionization efficiency of X in ampere·seconds per gram; and w is the amount of compound X in grams per second.

For the linear dynamic range ($\alpha_2 - \alpha_1$) of detectors, eqn. 2 holds:

$$\alpha_2 - \alpha_1 = \log S_{\alpha_1}^{\mathrm{EFID}} - \log S_{\alpha_2}^{\mathrm{EFID}} \tag{2}$$

when the amount of substance is changed in the interval from $10^{-\alpha_2}$ to $10^{-\alpha_1}$ and in which the linearity (l) is constant.

For the lowest detectable amount, (w_{LDA}) eqn. 3 holds:

$$\log w_{\mathrm{LDA}} = \frac{\log \Delta S^{\mathrm{EFID}} - \log q_X^{\mathrm{EFID}}}{l} \tag{3}$$

where $\Delta S^{\mathrm{EFID}} = 2K(S_{\mathrm{noise}})$ (4)

and K is the chosen probability constant[5], which is as follows:

n	*K for 95% probability*	*K for 99% probability*
3	5.2	12.04
5	2.04	3.36
10	1	1.32

where n is the time range for noise measurements and n = 3.40 times the peak width at half-height for substance X.

On the basis of the results obtained, the hydrogenation of eluted substances plays an important but not the only role. The magnitude of the EFID signal depends on temperature and the material used, which has an important catalytic effect.

In the mechanism of EFID, two phenomena are dominant: cracking leads to radical formation, and in the presence of electronegative groups or atoms there is a higher probability of recombination. This phenomenon is demonstrated with alcohols. Isoalcohols generally produce a higher signal than *n*-alcohols, as they have more CH_3 groups per molecule. When the substances do not carry electronegative atoms, the EFID signal is determined by the yield of $CH_3\cdot$ radicals. If hydrogenation of unsaturated hydrocarbons was the only reaction in the EFID mechanism, the resulting signal could not be higher than that of saturated hydrocarbons. The experimental results, however, show higher signals for unsaturated hydrocarbons, and $CH_3\cdot$ formation is therefore probable.

The repeatibility of the data for s_X is high, as demonstrated by the value of estimated standard deviations. Values of s_X are generally lower for substances with electronegative atoms, but the EFID tested showed a broader linear dynamic range and a smaller lowest detectable amount when compared with the normal FID (same type electronics, geometry, manufacturer, materials, etc.).

These preliminary results should serve as a basis on which further development will continue.

REFERENCES

1 A. T. Blades, *J. Chromatogr. Sci.*, 11 (1973) 251.
2 J. Ševčík and M. Klima, *Chromatographia*, 9 (1976) 69.
3 F. W. Karasek and D. M. Kane, *J. Chromatogr. Sci.*, 10 (1972) 673.
4 F. W. Karasek and D. M. Kane, *Anal. Chem.*, 45 (1973) 576.
5 J. Ševčík, *Detectors in Gas Chromatography*, Elsevier, Amsterdam, Oxford, New York, 1976, p. 30.

Journal of Chromatography, 126 (1976) 271–277
© Elsevier Scientific Publishing Company, Amsterdam — Printed in The Netherlands

CHROM. 9418

CONTINUOUS STIRRED REACTOR MODEL AS BASIS FOR OPTIMISATION OF ELECTRON CAPTURE DETECTOR OPERATION IN COULOMETRIC AND CONSTANT CURRENT MODES

EMIL BROŚ* and F. M. PAGE

Chemistry Department, The University of Aston in Birmingham, Gosta Green, Birmingham B4 7ET (Great Britain)

SUMMARY

The paper analyses the theoretical reasons for the empirical observations that the operational conditions in the constant current mode are contradictory to those in the coulometric mode. On the basis of the continuous stirred reactor model the necessary conditions for the two different modes are formulated.

INTRODUCTION

During the last few years considerable progress has been made in understanding the mechanism of the electron capture detector (ECD) and in improving the detector parameters. The main effort has been concentrated on improving the limits of detection and increasing the linear range. It was shown that the coulometric detector[1] is better with regard to the detection limit but the detector working with constant current[2] is better as far as the linear range is concerned. However, the decision which of these two parameters is more important must be taken before the detector is going to be built, because simultaneous optimisation of both of them is impossible. In this paper it is shown how the contradictory demands concerning conditions of operation of the ECD in the coulometric and constant current modes stem from the chemical stirred reactor model of the detector. This model, sometimes called Lovelock's model[1], describes the mechanism of the ECD by two differential equations derived from the conservation of number for the relevant species, assuming uniform concentration (good mixing) within the cell.

$$\frac{dn_e}{dt} = A/V - n_e (k_1 n_a + k_d) \quad (1)$$

$$\frac{dn_a}{dt} = B/V - n_a (k_1 n_e + k_x + u/V) \quad (2)$$

* IAEA Fellow on leave of absence from Institute of Nuclear Physics, Krakow, Poland.

where

n_e, n_a = number of electrons and sample molecules per unit volume inside the detector cell, respectively

A, B = rates of injection of electrons and sample molecules, respectively

k_1 = rate constant for removal of sample molecules in electron capture process

k_d = pseudo-recombination rate constant

V = detector volume

u = flow-rate of carrier gas

k_x = rate of destruction of sample molecules by other processes (this constant will be neglected in the further consideration)

Eqns. 1 and 2 may be treated as linear differential equations of the first order.

$$\frac{dx}{dt} = a - \lambda x \tag{3}$$

with the solution

$$x = a/\lambda\,(1 - e^{-\lambda t}) \tag{4}$$

The system may be regarded as having reached a steady state after times greater than $3 \times$ time constant $(1/\lambda)$, that is, for pulse intervals (t_p) given by

$$t_p \geqslant 3\,\frac{1}{k_d + k_1\,n_a} \tag{5}$$

The concentration of the electrons reaches the value

$$n_e = \frac{A/V}{k_d + k_1\,n_a} \tag{6}$$

and the ionization current, provided that every pulse removes all electrons from the cell, becomes

$$I_e = \frac{Vn_e}{t_p} = \frac{A}{(k_d + k_1\,n_a)t_p} \tag{7}$$

Under the assumption that B is constant or changes slowly, the concentration of sample molecules in the detector cell is given by

$$n_a = \frac{B/V}{k_1\,n_e + u/V} \tag{8}$$

or, replacing B/V by $n_{cg} \cdot u/V$ (9)

(where n_{cg} is the concentration of sample molecules in the carrier gas entering the detector cell)

$$n_a = n_{cg}\,\frac{u/V}{k_1\,n_e + u/V} \tag{10}$$

The concentration of sample molecules inside the detector is a holomorphic function of the ventilation rate constant u/V, which is, of course, the reciprocal of the residence time.

CONSTANT CURRENT MODE

In order to increase the linear range of the ECD, Maggs *et al.*[2] suggested the constant current mode, in which the ionization current is kept constant by varying the pulse frequency. As the electric current is given by

$$I_e = A\ 1/\varepsilon\ (1 - e^{-\varepsilon}) \tag{11}$$

where

$$\varepsilon = t_p\ (k_d + k_1\ n_a) \tag{12}$$

constant current is guaranteed by constancy of the argument ε

$$t_p\ (k_d + k_1\ n_a) = \text{const.} = \varepsilon_0 \tag{13}$$

For the pure carrier gas

$$n_a = 0$$

and

$$t_p\ (k_d + k_1\ n_a) = k_d\ t_{p0} \tag{14}$$

where t_{p0} is the initial time interval.

If ventilation is the main process in the depopulation of the sample molecules in the ECD which occurs for

$$u/V \gg k_1\ n_e \tag{15}$$

eqn. 10 can be simplified to

$$n_a = n_{cg} \tag{16}$$

which results in

$$t_p\ (k_d + k_1\ n_{cg}) = t_{p0}\ k_d \tag{17}$$

or

$$\frac{\nu - \nu_0}{\nu_0} = \frac{k_1}{k_d} \cdot n_{cg} \tag{18}$$

where frequency $\nu = 1/t_p$ and $\nu_0 = 1/t_{p0}$, and also in

$$\Delta\nu = \varepsilon_0^{-1}\ k_1\ n_{cg} \tag{19}$$

Eqn. 19 implies that for good sensitivity $\varepsilon_0 = k_d\, t_{p0}$ should be chosen as small as possible. However, sensitivity is not the only factor considered in selecting ε_0 in practice and others like the linear range and the magnitude of an error must be taken into account.

The span of frequency is limited by the initial frequency ν_0, which is of our choice and the final frequency ν_c, which is determined by the pulse width (provided that input time constant of the detector electric system is negligible). The pulse width (t_w) must be of a sufficient length to enable collection of nearly all electrons, and may be roughly estimated by the relation

$$t_w = \frac{d}{v_d} \tag{20}$$

where d is the distance between the electrodes and v_d is the electron drift velocity. It is usually of the order of magnitude of 1 μsec.

From eqn. 19 the relation for the maximum analysed concentration can be obtained as

$$n_{cg\ \max.} = \frac{\nu_c - \nu_0}{k_1}\,\varepsilon_0 \tag{21}$$

which implies that ε_0 should be rather large if higher concentrations are to be analysed.

The last but not least factor which should be taken into account is an error introduced by inaccuracy in keeping the current I_e constant, which causes the fluctuations of ε_0. Because the current is the function of ε, those fluctuations are given by

$$\delta I = \mathrm{f}'(\varepsilon)\,\delta\varepsilon \tag{22}$$

where $\mathrm{f}'(\varepsilon)$ is the derivative of the function $I = \mathrm{f}(\varepsilon)$ given by eqn. 11. From eqn. 19 it is evident that the relative error of an assessed sample concentration is at least equal to the relative error of ε_0, which can be derived from eqn. 22 as

$$\frac{\delta\varepsilon}{\varepsilon} = \frac{1}{\varepsilon \mathrm{f}'(\varepsilon)} \cdot \delta I \tag{23}$$

For a given fluctuation δI, the relative error of ε_0 is the least for the ε_0 for which $\varepsilon \cdot \mathrm{f}'(\varepsilon)$ reaches maximum. This occurs for $\varepsilon_0 \approx 1$ and means that both very small and very large values of ε_0 should be avoided because for both of them $\varepsilon \cdot \mathrm{f}'(\varepsilon)$ is nearly nil.

As the result of all these considerations $\varepsilon_0 \approx 1$ may be recommended, which means

$$t_{p0} \cdot k_d \approx 1 \tag{24}$$

It is interesting to see that if condition 15 is to be satisfied for every concentration n_{cg}, *i.e.*

$$\frac{u}{V} \gg k_1 \frac{A/V}{k_d + k_1\, n_{cg}} \tag{25}$$

it is enough to have

$$\frac{u}{V} \gg \frac{k_1}{k_d} \cdot \frac{A}{V} \tag{26}$$

or

$$u \gg A\, k_1/k_d \tag{27}$$

Conditions 24 and 27 are satisfactory for long linear range and accuracy in constant current mode.

COULOMETRIC MODE

The signal of an ordinary ECD depends not only on the concentration but also on the kind of a sample. For quantitative analyses it is necessary to calibrate the detector separately for every analysed compound. The calibration, even if performed with the exponential dilution flask, is tedious and time consuming. Then an attempt was made[1,3] at constructing the detector whose signal is not dependent on the analysed species. Theoretically it can be easily achieved by making the electron attachment the dominating process over the ventilation

$$k_1 n_e \gg u/V \tag{28}$$

because, after that, it follows from eqn. 8 that

$$n_a = \frac{B/V}{k_1 u_e} \tag{29}$$

and from eqn. 1 that

$$n_e = \frac{A - B}{k_d V}(1 - e^{-t_p k_d}) \tag{30}$$

and

$$I_e = \frac{A - B}{t_p k_d}(1 - \mathrm{e}^{-t_p k_d}) \tag{31}$$

As for pure carrier gas

$$I_{e0} = \frac{A}{t_p k_d}(1 - \mathrm{e}^{-t_p k_d}) \tag{32}$$

then the detector signal is given by

$$\Delta I = \frac{B}{t_p k_d}(1 - \mathrm{e}^{-t_p k_d}) \tag{33}$$

In the case of the ECD, coulometry means that

$$\frac{\text{Number of electrons not collected}}{\text{Time}} = \frac{\text{Number of molecules coming into the detector}}{\text{Time}} \tag{34}$$

To obtain coulometric response, an additional condition must be satisfied, *viz.*

$$t_p k_d \ll 1 \tag{35}$$

because it results in

$$\Delta I = B \tag{36a}$$

or

$$\Delta I = u n_{cg} \tag{36b}$$

For very small t_p

$$n_e = A/V \cdot t_p \tag{37}$$

what allows to rewrite condition 28 as

$$A \cdot k_1 t_p \gg u \tag{38}$$

It is not very difficult to satisfy these two conditions 35 and 38 if the rate constant for electron attachment is large as for SF_6, but it is hardly possible for species for which the rate constant is small. The chance to increase k_1 by proper choice of carrier gas and pressure in the detector seems to be little. Another way out is to maximise the ratio A/k_d which determines the current and the electron density by the selection of a strong ionization source and a carrier gas for which the recombination coefficient is small and the ionization cross-section high. It is interesting to notice that the two conditions do not explicitly include any volume term, but it should not be forgotten that the fundamental assumption about the ideal mixing in the detector cell is true only for small volumes.

CONCLUSIONS

The continuous stirred reactor model can be very useful in the determination of the operational conditions for the ECD in the constant current mode. It gives an

TABLE I

CONDITIONS OF THE ECD OPERATION

Constant current mode of ECD	*Coulometric mode of ECD*
$t_{p0} k_d \approx 1$	$t_p k_d \ll 1$
$k_1 n_e \ll u/V$	$k_1 n_e \gg u/V$
$A \frac{k_1}{k_d} \ll u$	$A k_1 t_p \gg u$
k_d large	k_d small
k_1 small	k_1 large
A small	A large

explanation of the fact that the operational conditions in these two modes are contradictory, what was known much earlier empirically from a comparison of the performance of commercial detectors.

The summary of the contradictory conditions which must be satisfied in these two modes of operation is given in Table I.

The last three conditions in Table I for the constant current mode are in obvious contradiction to the demand of the best detectivity. However, this disadvantage must be accepted in return for longer linear range.

REFERENCES

1 J. E. Lovelock, *J. Chromatogr.*, 99 (1974) 3.
2 R. J. Maggs, P. L. Joynes, A. J. Davies and J. E. Lovelock, *Anal. Chem.*, 43 (1971) 1966.
3 J. E. Lovelock, R. J. Maggs and E. R. Adlard, *Anal. Chem.*, 43 (1971) 1962.

Journal of Chromatography, 126 (1976) 279–300
© Elsevier Scientific Publishing Company, Amsterdam — Printed in The Netherlands

CHROM. 9468

EFFECTS OF DIGITAL FILTERS ON CHROMATOGRAPHIC SIGNALS

STUART P. CRAM*
Varian Instrument Division, 2700 Mitchell Drive, Walnut Creek, Calif. 94598 (U.S.A.)
STEPHEN N. CHESLER**
Department of Chemistry, University of Florida, Gainesville, Fla. 32601 (U.S.A.)
and
ARTHUR C. BROWN, III
Varian Instrument Division, 2700 Mitchell Drive, Walnut Creek, Calif. 94598 (U.S.A.)

SUMMARY

Digital filters are quantitatively evaluated for their effects on chromatographic digital data. Changes in peak-shape parameters for Gaussian and asymmetrical chromatographic peaks are described by the error levels introduced. Reductions in baseline noise are discussed in terms of reducing the amplitude and the frequency response. An example of the practical considerations and trade-offs in implementing digital filters in a microprocessor-based data system is presented, so as to minimize peak distortion, and enhance peak detection and signal-to-noise ratio.

INTRODUCTION

Numerical data-handling techniques are extensively applied in chromatographic data systems today to enhance effectively the information content, signal-to-noise ratio (S/N), accuracy, and precision of analytical signals. Many of these advanced techniques have been reviewed by Annino[1] and Hieftje[2,3]. However, minimal attention has been given to the quantitative aspects of digital filters since the publication of the landmark paper in the analytical literature by Savitzky and Golay[4] in 1964. Their paper treated numerical smoothing and differentiation by least-squares procedures and presented tables of convoluting integers and their normalizing factors. These tables were later corrected[5], but the effects of the filters and interpretation for their application to chromatographic systems has not been reported. Digital filters are usually applied as part of the signal-processing algorithms of incoming signals to digital data systems and are therefore critical in terms of subsequent data processing and interpretation programs. They are rarely an operator-controlled param-

* To whom correspondence should be addressed.
** Present address: Analytical Chemistry Division, National Bureau of Standards, Washington, D.C. 20234, U.S.A.

eter in chromatography data systems and therefore it is even more important that their effects, potential power, and limitations be understood.

Noise in its various forms is a random error that directly affects the precision and useable range of analytical measurements. Thus it is desirable to remove as much noise as possible without distortion of the signal beyond acceptable limits. Several analog and digital filtering techniques are available.

Passive analog filters (LRC types) have the advantage of low cost and simplicity of design and construction. However, they are (1) limited in most cases to real-time signals, (2) cannot produce derivatives of the input signal (although other analog techniques are available for doing so), (3) must be voltage and impedance matched to the signal source, (4) show variations from one unit to the next owing to component tolerances, and (5) do not lend themselves to systems requiring dynamic changes in filtering characteristics. Active analog filters have the same basic characteristics as passive filters, except that the filtering characteristics can be varied over limited ranges and lower frequencies are more easily filtered. These filters can add amplifier noise to the signal and are complex and expensive to implement. These types of filters are commercially available today for chromatography systems.

Digital filters are numerical counterparts to analog filters. Hard-wired digital filters (1) can implement sophisticated algorithms, such as Fast Fourier Transforms, (2) are very fast, (3) can operate on either real-time or data stored in memory, and (4) can produce derivatives of the input signal. These types of filters are costly, may be complex to design into a system, have limited adaptability, and require accurate digitization.

Software-based digital filters take advantage of the logical and arithmetic capabilities of digital computers and may be adaptive. They (1) are the most versatile in that very sophisticated filters and numerical techniques can be designed, (2) may be changed in real-time and optimized for the S/N and frequency response desired, (3) are simple to implement and use, and (4) allow the versatibility of post analysis recalculations. Hard-wired analog and digital filters must be replicated for each input channel to be filtered, whereas any number of different software filters (from 1 to n) can be applied to m channels of incoming signals.

It should be pointed out that, in addition to analog and digital filters, other techniques may also be used for noise reduction or S/N enhancement. These techniques include integration (analog and numerical), modulation, digitization, data bunching, correlation, synchronous detection, multiple pass filters, and averaging. In all cases, these techniques should be characterized in terms of their gain in S/N, frequency response, and effects on precision, resolution, and accuracy (*i.e.*, reduction in systematic error). As an example, it is imperative that the data-bunching rate in chromatography data systems and integrators be set or selectable in terms of the frequency of response (peak width) rather than by the number of data points. The effects of chromatographic noise have been treated in terms of their effect on the precision and accuracy of statistical moments[6], digitization errors[7,8], retention time measurements[9], detection limits[10], and the design of chromatography data systems to handle sensitive peak detection and spike trapping[11].

This paper follows directly from the one by Savitzky and Golay[4], which is recommended as an introduction to the subject. Therefore, we will treat only moving average (MA) and polynomial smoothing functions as digital filters here in detail.

CHARACTERIZATION OF DIGITAL FILTERS

Digital filters basically serve to attenuate random noise and/or to differentiate the signal. The filters discussed are of the symmetric, non-recursive, linear type which operate only on the input signal. One requirement of these filters is that the digitized data must be in fixed time increments in order to be smoothed with the Savitzky–Golay convolutes[4]. Secondly, data to be filtered will be assumed to be a continuous function such as chromatographic peaks, as either resolved or unresolved elution profiles. High-frequency spikes are "trapped" by such filters and are thus reduced in amplitude. Repetitive spiking at high frequencies may introduce a systematic error in the data, but this is assumed to be a minimal effect in stable, clean chromatographic systems and therefore is not considered in this work. Thirdly, polynomial smoothing requires that an odd number of data points be fit.

Polynomial smoothing functions will be given by

$$Y_p^{(n)} = \sum_{i=-m}^{+m} w_{pi}^{(n)} y_i \tag{1}$$

where

$Y_p^{(n)}$ = amplitude of the smoothed value

p = position of smoothed value within convolution interval. $p = 0$ (midpoint) for symmetrical filters

n = order of the smoothing formula

$2m + 1$ = number of data points in the smooth

$w_{pi}^{(n)}$ = convolute coefficient of the ith data point for smoothing operations

y_i = amplitude of the ith data point before smoothing

such that

$$\sum_{i=-m}^{+m} w_{pi}^{(n)} = 1 \tag{2}$$

and

$$w_{pi}^{(n)} = w_{(-p)(-i)}^{(n)} \tag{3}$$

It should be noted for later reference that if n is even, *e.g.*, $n = 2q$, then

$$w_{pi}^{(2q)} = w_{pi}^{(2q+1)} \tag{4}$$

which says that the formula obtained for finding the smoothed value at the midpoint of the interval ($p = 0$) by using an even-degree polynomial is the same as that obtained with the next higher odd-degree polynomial.

For the special case where $n = 1$, as for linear smoothing formulas,

$$w_{0i}^{(1)} = \frac{1}{2m + 1} \tag{5}$$

it can be seen that

$$Y_p^{(1)} = \sum_{i=-m}^{+m} \frac{y_i}{(2m + 1)} \tag{6}$$

which is the MA digital filter.

Effects of smoothing

In chromatography, the error signal or noise may be considered as random at high frequencies whereas the errors at low frequency are more systematic as they approach the bandwidth of the elution profile. Therefore, it would be desirable to design a lowpass filter for error signals at frequencies higher than that of the signal to be observed. From eqn. 1 it may be shown that the results of a polynomial smoothing function may be expressed as a function of the frequency, ω, in terms of a filter function, given by

$$\mathrm{f}(j\omega) = w_0 + 2 \sum_{i=1}^{m} w_i \cdot \cos i\,\omega \Delta t \tag{7}$$

where

$$\bar{y}(j\omega) = \mathrm{f}(j\omega) \cdot y(j\omega) \tag{8}$$

and $\bar{y}(j\omega)$ and $y(j\omega)$ are the Laplace transforms of $\bar{Y}(t)$ and $Y(t)$, respectively.

This may be illustrated by considering a 7-point linear smooth which is given by eqn. 5 as

$$w_{0i}^{(1)} = \frac{1}{7} \tag{9}$$

so that the filter function will be

$$\mathrm{f}(j\omega) = \frac{1}{7}(1 + 2\cos\omega\Delta t + 2\cos 2\,\omega\Delta t + 2\cos 3\,\omega\Delta t) \tag{10}$$

which is illustrated in Fig. 1a. It can be seen that for the frequencies where $\mathrm{f}(j\omega) = 1$, the original data will be passed by the smoothing function without change. For frequencies where $\mathrm{f}(j\omega) < +1$, the original data will be attenuated by the smoothing function. In the case of $\mathrm{f}(j\omega) < 0$, the filter function is given by $|\,\mathrm{f}(j\omega)\,|$. The negative values relate only to phase shifts in the data.

When data points are sampled at data rate intervals of Δt, data components and noise with frequencies of greater than $1/\Delta t$ will not be completely filtered in the smoothed data. This effect can be predicted from Fig. 1 by the cyclic nature of the filter function, as well as the attenuation factor as a function of frequency. Although this smoothing function is a good lowpass filter, different filter functions may be applied as shown in Fig. 1. The 7-point second-order smooth will follow the true peak shape more closely than a linear smooth and therefore distort the peak shape parameters less. However, it can be seen from Fig. 1b that a second-order filter function will be less effective for high frequencies than one of a lower order when $(2m+1)$ is a constant.

When it is desired to remove the higher-frequency noise components in order to enhance the analytical signal information content, or to develop a filter with a lower bandpass, or one with less cyclic character, a number of alternatives are available; all of which may be predicted from their filter function: (1) The data may be prefiltered with notched analog cutoff filters, as previously discussed. (2) The sampling time interval, Δt, may be increased so that higher frequencies fall in the region where

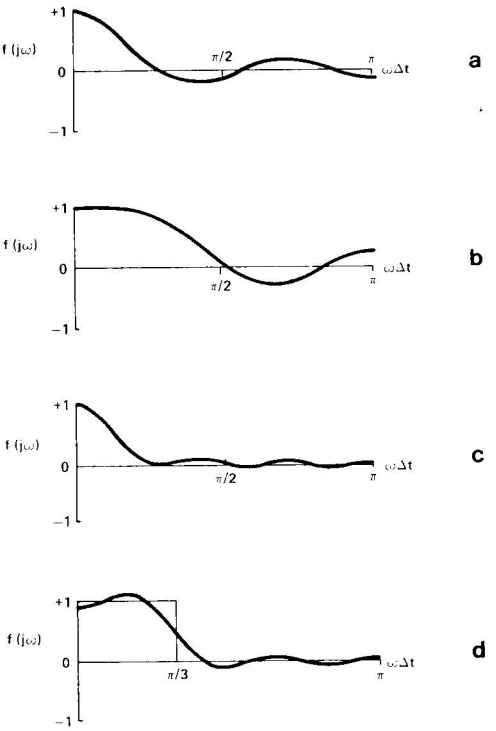


Fig. 1. Filter functions as a function of frequency for (a) a 7-point linear smooth, (b) a 7-point second-order smooth, (c) two passes with a 7-point linear smooth, and (d) a truncated Fourier series.

$\omega\Delta t > \frac{1}{2}\pi$ so that they will be cut off by the analog-to-digital converter (ADC) and further at tenuated by thedigital filter. (3) Increase m so as to lower the bandpass of the polynomial filter function. (4) Use a multipass filter as shown in Fig. 7c, where the filter function of k smooths is $[f(j\omega)]^k$. (5) Use operators other than polynomials, as shown in Fig. 7d for a Fourier series. Such functions may be tailored to the functionality of the response curve when it is well defined. All of these filters are extremely versatile, precise, and are well defined when implemented in software. Further it is then possible to update the weighting coefficients on the basis of the incoming signal if it is time dependent, as in the case of chromatography. The results and discussion presented in this work will treat the effects of sampling times, order of the polynomial, and multipass filters (Nos. 2–4 above). Only polynomial and moving average filters will be discussed because they are easier to implement in small data systems and will be shown to be more than adequate for most chromatographic applications when properly applied.

Optimization of the filter band width

Van Rijswick[12] has shown that optimum detection of a Gaussian peak for a filter band width that maximizes the signal-to-noise ratio after filtering, $(S/N)_f$, is given by

$$\left(\frac{S}{N}\right)_f = \frac{0.87A}{\sigma_y w_p} \cdot \left(\frac{w_p}{\Delta t}\right)^{\frac{1}{2}} \left[\frac{K^5}{(1+K^2)^3}\right]^{\frac{1}{2}} \tag{11}$$

where A is the peak area, σ_y the mean amplitude of the normal random noise before filtering, w_p is the Gaussian peak width, Δt is the sampling interval, (note that $w_p/\Delta t$ is the sampling density), and $K = w_f/w_p$ or the ratio of the filter width to the Gaussian peak width. It should be noted that filtering will increase the peak width to $(w_p^2 + w_f^2)^{\frac{1}{2}}$ or $(1 + K^2)^{\frac{1}{2}}$. K will thus reach an optimum at $K = 2.24$ so that for optimum peak detection, the width of the matched filter should be proportional to the width of the chromatographic peak. Although detection limits are not discussed in the results section of this paper, it is important to point out that digital filters may enhance or reduce the detection limits of any chromatographic detector, affect the area recovery and peak width, and must be applied in relationship to the sampling frequency.

EXPERIMENTAL

All of the computer programs for calculations and simulation were run on a PDP-8/L laboratory computer system with 8 K of core (Digital Equipment Corp.). The system includes the following peripheral devices: four-tape magnetic tape cartridge system (Model 4096, Tri-Data Corp.), high-speed paper tape reader (Mark V, Datascan), 15-in. display oscilloscope (Model 1735D, I.T.T.), ASR-33 Teletype (Teletype Corp.), Type 547 laboratory oscilloscope (Tektronix), 10-bit ADC and digital-to-analog converter (Models A811/A618, Digital Equipment Corp.), sample and hold amplifier (A400, Digital Equipment Corp.), multiplexers, a programmable clock, and programmable gain amplifier.

RESULTS AND DISCUSSION

From eqn. 6 it can be seen that the MA filter smooths by taking a running average over $2m + 1$ data points as the convoluting interval. Further, all data points in the smoothing interval are equally weighted and therefore the MA does not track sharp changes in slope. Thus, the most pronounced effect will be seen as a decrease in the peak height, especially for sharp narrow peaks. It should be noted that this means that peak shape parameters will always be distorted by some degree, regardless of the peak shape or symmetry. On the other hand, all symmetrical digital filters treat data points both ahead and behind the data point of interest ($p = 0$), whereas analog filters treat only the current and past data points ($p \leq 0$) and therefore introduce a undirectional symmetric distortion and error into the results.

Least-squares fits of polynomial filters are more versatile because both the order of the polynomial and the number of data points in the convolute may be varied. Consequently, these functions are better fits for continuous form functions such as chromatographic peaks and introduce less peak distortion than a MA with the same size convolution interval. In terms of high-frequency filtering, the converse is true, as was shown in Fig. 1. If very fast data acquisition rates and small convoluting intervals are used, the polynomial filter will follow the experimental peak profile without significant deviation and effectively filter the noise which is much greater than the bandwidth of the chromatographic peak. Lower-frequency noise will not be filtered as effectively and larger convoluting integrals and/or lower order polynomials will be required.

These effects can be qualitatively predicted by examining the trends in the

normalized convolution coefficients in Fig. 2 for quadratic–cubic polynomial smooths and for quartic–quintic smooths in Fig. 3. These plots show that the coefficients are symmetrical about $p = 0$, and that the greater the number of points in the smooth, the greater the filtering effect will be on both the peak and the noise for a given sampling density. Thus a 7-point smooth will track a changing signal with greater fidelity than will a 19-point smooth. However, the larger smooth will reduce the noise level and frequency more. In compliance with the optimum filter bandwidth criterion, larger smooths require a higher data point density (points per peak width at half-height) to maintain a fixed ratio of filter width to peak width than do smaller smooths. In practice this ratio should be about 1.1 (points in smooth/data point density) for a quadratic–cubic smooth, and about 0.5 for a linear smooth. In the limiting case where the entire peak profile is included within the convolution interval, peak distortion becomes too severe for chromatographic use even with quartic–quintic smooths.

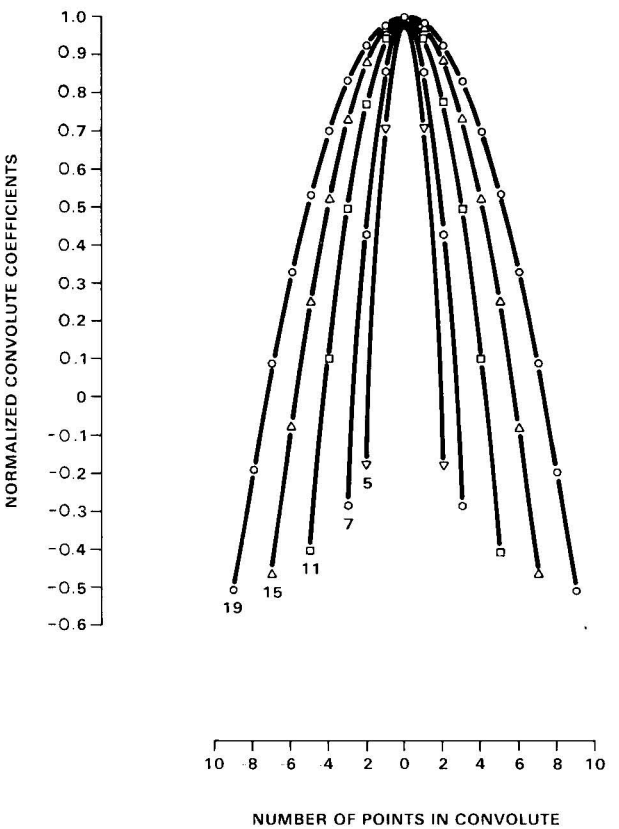


Fig. 2. Convolute coefficients for symmetrical quadratic–cubic smoothing filters plotted about $p = 0$ as a function of p for 5–19-point convolution intervals.

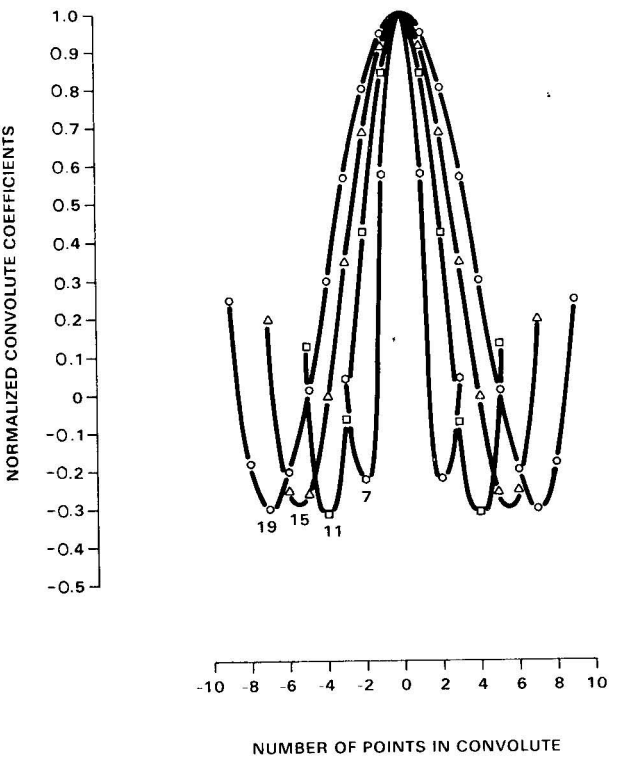


Fig. 3. Convolute coefficients for symmetrical quartic–quintic smoothing filters plotted about $p = 0$ as a function of p for 7–19-point convolution intervals.

Effects on peak shape

Earlier publications described and defined Gaussian and asymmetrical (Type I, II) chromatographic peaks[6,7]. These peak shapes will be used to illustrate the effects of the digital filters. It should also be noted that a large number of data points were used to represent all peak profiles in order that the accuracy of the peak parameter measurements not be limited by the number of data points per peak[6]. All of the studies reported here were made by computer simulation in order to measure accurately the changes in peak parameters, *i.e.*, the *true* value of all of the peak parameters must be known *before* the errors can be measured.

Peak height was chosen as the simplest peak parameter to illustrate the difference between polynomial and MA smoothing. The relative decrease in the peak height for Gaussian and Type II curves is shown in Fig. 4 for single-pass quartic–quintic polynomial and MA smooths. The asymmetrical peak shows a larger decrease in the peak height than the Gaussian peaks in all cases. The 9-point quartic–quintic smooth decreases the Gaussian peak height by less than 1 part in 10^4 and by 0.38% for the Type II peak so that the peak height ratio is 1.004. In comparison, the 9-point MA smooth decreases the Gaussian peak height by 1.0% and the Type II peak by 5.94% to give a peak height ratio of 1.05. Therefore, as predicted from the discussion earlier in the paper, the MA smooth will always be more detrimental to retaining the

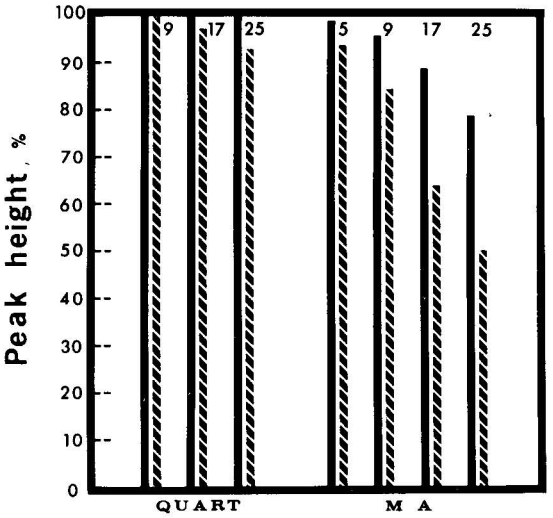


Fig. 4. Plot of the percent of original peak height after filtering with a single smooth as a function of the number of points in the convolute interval for quartic–quintic (QUART) and moving average (MA) smooths. Solid and broken lines represent Gaussian ($\geqslant$75 data points/peak) and Type II ($\geqslant$150 data points/peak) peaks, respectively.

integrity of the peak height because of the sharp change in slope. Further, it may be seen that large convolutes are not justifiable for doing good quantitative computer-based chromatography because the peak height ratio (Gaussian/Type II) decreases from 1.004 to 1.073 in going from a 9- to a 25-point quartic–quintic smooth and from 1.05 to 1.62 over the range of a 5- to a 25-point MA smooth. Since true Gaussian peaks are rarely obtained in GC or liquid chromatographic practice, it is particularly important to realize that, as the peak asymmetry increases, the peak height losses will increase and small convolutes with higher-order polynomial filters become the only method of choice. Type I peaks are not shown as they represent an intermediate case between the Gaussian and Type II peaks.

Because the Type II peak shape is more realistic in experimental work, the effects of the type of filter, number of points in the convolute, and the sampling density ($w_p/\Delta t$) are shown in Fig. 5. It is readily apparent that any digital filter applied to a peak where the sampling density is too low has disasterous effects. A minimum of 3.3 data points/σ is required for accurate Gaussian peak area characterization according to the criteria of Chesler and Cram[6]. By comparing 9-point convolutes for the higher sampling density it is seen that the quartic–quintic smooth (97.4%) is more accurate (in terms of peak height recovery) than the quadratic–cubic (94.5%) which is more accurate than the MA (79.3%). However, when the same peaks, filters, and convolutes are compared in the frequency domain, the MA is more effective than the quadratic–cubic which is more effective than the quartic–quintic in reducing the peak-to-peak amplitude of normal random noise. Fig. 5 also shows that to recover $\geqslant$90% of the peak height at a sampling density of 3.3 points/σ the following filters could be used for a Type II peak: 7–19-point quartic–quintic, 5–13-point quadratic–cubic, or a 3–5-point MA.

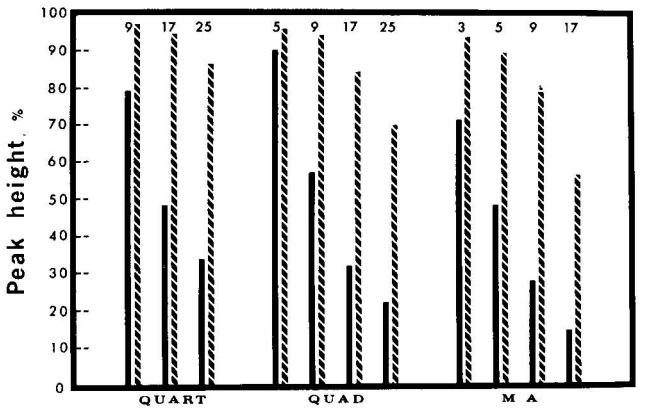


Fig. 5. Plot of the percent of original peak height of a Type II peak after filtering with a single smooth as a function of the number of points in the convolute interval for quartic–quintic (QUART), quadratic–cubic (QUAD), and moving average (MA) smooths. Solid lines represent a sampling density of 1 data point/σ and broken lines are 3.3 points/σ.

Fig. 6 is a summary of the trends of the data in Table I. The error in the filtered data for the zeroth moment (u_0, area) of the Type II peak is consistently larger than for a Gaussian by approximately an order of magnitude, regardless of the type of smooth or the size of the convolute interval. In terms of peak area recovery, it may be seen that only the $\geqslant$ 25-point filters will introduce significant errors in the peak area. This is because of the relative weighting of the peak symmetry and the use of

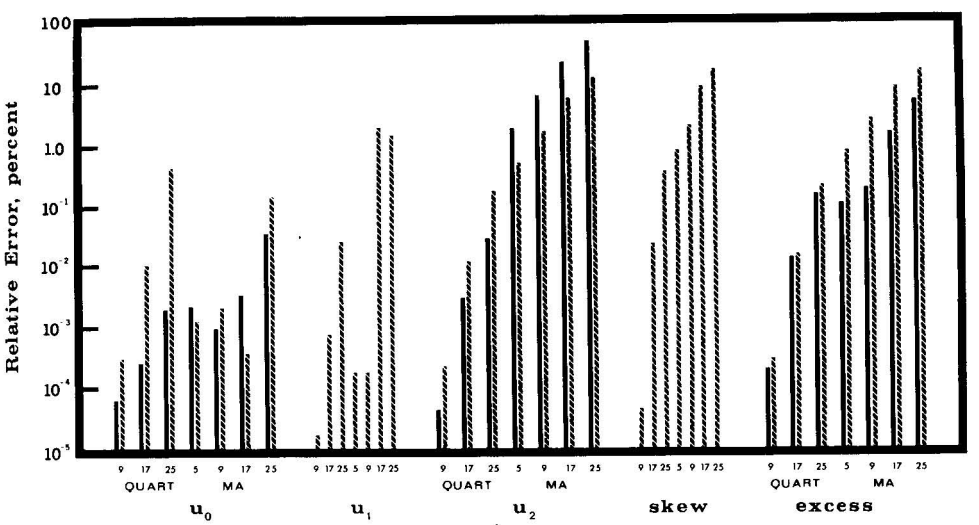


Fig. 6. Plot of the relative error after a single smooth in the zeroth moment (u_0, peak area), first moment (u_1, retention time), second moment (u_2, peak width), skew, and excess for Gaussian (solid lines) and Type II (broken lines) peaks after applying quadratic–cubic (QUAD) and moving average (MA) smooths. The peak integration limits are $\pm$ 0.1% for sampling densities of $\geqslant$75 points/peak for the Gaussian and $\geqslant$150 points/peak for the Type II peak.

TABLE I

RELATIVE ERRORS IN CHROMATOGRAPHIC PEAK SHAPE PARAMETERS AS A FUNCTION OF PEAK SYMMETRY AND FILTER FUNCTION

	u_0	u_1	u_2	u_3	u_4	*Skew*	*Excess*
(I) Gaussian peaks (⩾75 data points/peak)							
(a) No smooth value	1.00	0.00	1.00	0.00	3.00	0.00	3.00
(b) Relative error, %							
9-pt. quadratic–cubic	$6\cdot10^{-5}$	—	$4\cdot10^{-5}$	—	$3\cdot10^{-4}$	—	$2\cdot10^{-4}$
17-pt. quadratic–cubic	$3\cdot10^{-4}$	—	$3\cdot10^{-3}$	—	$2\cdot10^{-2}$	—	$1\cdot10^{-2}$
25-pt. quadratic–cubic	$2\cdot10^{-3}$	—	$3\cdot10^{-2}$	—	$2\cdot10^{-1}$	—	$2\cdot10^{-1}$
5-pt. MA	$2\cdot10^{-3}$	—	2.0	—	3.9	—	$1\cdot10^{-1}$
9-pt. MA	$1\cdot10^{-3}$	—	6.7	—	14	—	$2\cdot10^{-1}$
17-pt. MA	$4\cdot10^{-3}$	—	24	—	51	—	1.6
25-pt. MA	$4\cdot10^{-2}$	—	51	—	117	—	5.4
(II) Type II peaks (⩾150 data points/peak)							
(a) No smooth value	1.58	2.54	23.3	273	$5.51\cdot10^{3}$	2.42	10.1
(b) Relative error, %							
9-pt. quadratic–cubic	$3\cdot10^{-4}$	$2\cdot10^{-5}$	$2\cdot10^{-4}$	$1\cdot10^{-4}$	$2\cdot10^{-4}$	$5\cdot10^{-2}$	$3\cdot10^{-4}$
17-pt. quadratic–cubic	$1\cdot10^{-2}$	$8\cdot10^{-4}$	$1\cdot10^{-2}$	$5\cdot10^{-3}$	$9\cdot10^{-3}$	$2\cdot10^{-2}$	$2\cdot10^{-2}$
25-pt. quadratic–cubic	$5\cdot10^{-1}$	$3\cdot10^{-2}$	$2\cdot10^{-1}$	$9\cdot10^{-2}$	$1\cdot10^{-1}$	$4\cdot10^{-1}$	$2\cdot10^{-1}$
5-pt. MA	$1\cdot10^{-3}$	$2\cdot10^{-4}$	$5\cdot10^{-1}$	$4\cdot10^{-2}$	$2\cdot10^{-1}$	$8\cdot10^{-1}$	$8\cdot10^{-1}$
9-pt. MA	$2\cdot10^{-3}$	$2\cdot10^{-4}$	1.7	$1\cdot10^{-1}$	$8\cdot10^{-1}$	2.7	2.6
17-pt. MA	$4\cdot10^{-4}$	2.0	6.2	$5\cdot10^{-1}$	2.9	9.2	8.8
25-pt. MA	$2\cdot10^{-1}$	1.5	13	$4\cdot10^{-1}$	7.4	18	17

symmetrical filter functions. For all filters with smaller convolutes, the accuracy of peak area recovery will be limited by the errors associated with sensing peak start and end rather than by the filter. Therefore peak area will always be the least sensitive peak parameter to distortion by digital filters. In all cases, the error in measuring a filtered peak area will increase as the peak asymmetry increases.

The effect of quadratic–cubic and MA smooths on the first moment (u_1, center of gravity) are negligible for a Gaussian peak. The errors in u_1 increase markedly as the convoluting integral is made larger for a fixed data set. However, even a 25-point quadratic–cubic smooth will only shift the retention time by 0.5 sec for a peak eluting in 30 min while the same peak at the same retention time will increase by 36 sec if a 25-point MA smooth is used.

The error in the second moment (u_2, variance) was discussed earlier in the paper for Gaussian peaks and the resultant is that the Type II peak will give smaller errors than the Gaussian for an MA smooth. The magnitude of the peak width error for the Gaussian may be derived from eqn. 11. The errors in u_2 in a Type II peak are larger than those for a Gaussian peak using a polynomial smoothing function, although most reasonably sized filters will have a negligible effect. This is important in that the resolution and efficiency of the column are not degraded by the filter function. However, a 9-point MA filter could result in an apparent decrease in column resolution from 1.0 to 0.94 for a Gaussian peak.

The relative error introduced in skew of a Gaussian peak is negligible because the skew is zero by definition. Therefore only the results for the Type II peak are shown in Fig. 6. Skew (and excess) are seen to be particularly sensitive to digital filtering. This is caused by the weighting of the tail of the peak in the calculation of u_3 and the high sensitivity to even minor changes in the profile of the tail. Thus the results are predictable: polynomial smooths will always introduce smaller errors than a MA, and the higher the order of the polynomial and the smaller the convoluting interval, the smaller the peak symmetry distortion.

There is no effect of peak symmetry after smoothing with a polynomial on the excess, which indicates that the relative error introduced in the peak flatness and the increase in peak variance are of the same magnitude. This is not true for a MA smooth because of the effect of equally weighting data points ahead and behind the data point of interest ($p = 0$) with asymmetric peaks. Therefore the effect is to flatten the peak more than to broaden it. In other words, the fourth moment (u_4) is extremely sensitive to shifts in the distribution of the peak area away from the center of gravity. The large errors for the skew and excess, shown in Fig. 6, indicate that meaningful measurements will only be made for these parameters by using low-noise chromatographic systems and peaks with a large signal-to-noise ratio.

The effects of multiple smooths were described earlier as increasing the filter function by the kth power for k consecutive smooths, and decreasing the frequency bandwidth. The effects of ten consecutive smooths are shown in Fig. 7 to show the accuracy of polynomial smooths for all reasonable chromatographic peak shapes and another reason for avoiding MA smoothing. The compounded errors in the Gaussian peak heights are: 0.37% for the quadratic–cubic, $< 10^{-2}$% for the quartic–quintic,

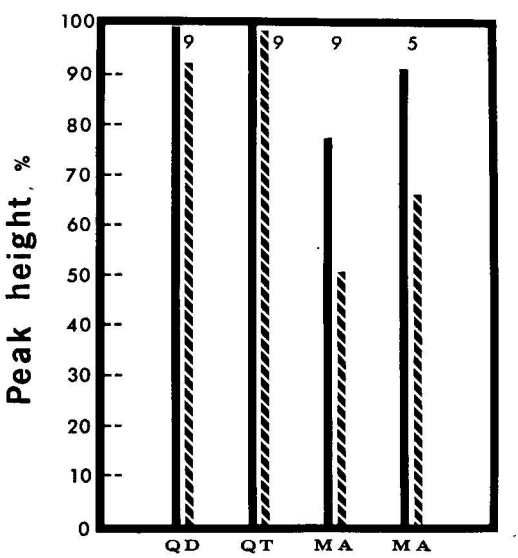


Fig. 7. Plot of the percent of original peak height after ten consecutive smooths as a function of the number of points in the convolute interval for quadratic–cubic (QD), quintic–quartic (QT), and moving average (MA) smooths. Solid and broken lines represent Gaussian ($\geqslant$85 data points/peak) and Type II ($\geqslant$210 data points/peak) peaks, respectively.

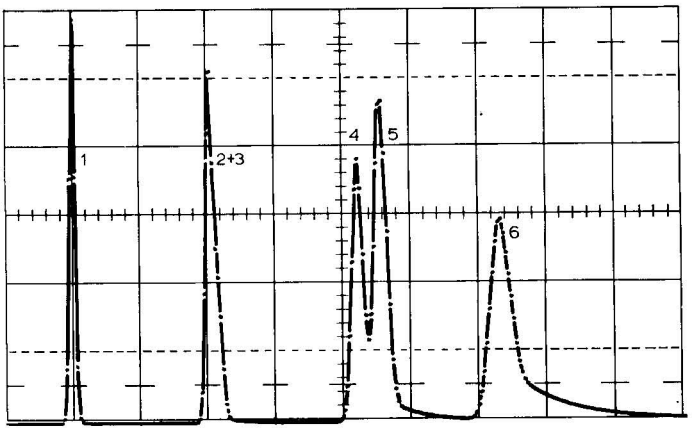


Fig. 8. Simulated 6-component chromatogram shown without smoothing. Peak No. 1 is normalized to 100% of full scale. Peak sampling densities are given in Table II.

22.7% for the 9-point MA, and 8.75% for the 5-point MA. The corresponding errors for the Type II peak are: 7.76, 1.25, 49.6, and 29.0%, respectively.

Figs. 8–14 are simulated chromatograms to show graphically the effects of applying different digital filters. The 6-component chromatograms are simulated to illustrate the effects on a sharp narrow peak (No. 1), a sharp peak with an unresolved shoulder (Nos. 2 and 3), a pair of overlapping peaks (Nos. 4 and 5), and a broad, skewed peak (No. 6). Fig. 8 shows the original, unsmoothed chromatogram, normalized to the peak height of peak No. 1. Table II describes the sampling density for the

TABLE II

PEAK HEIGHTS OF THE SIMULATED CHROMATOGRAM (FIG. 8) MEASURED AFTER DIGITAL FILTERING*

	Peak height (%)	
	Peak No. 1	*Peak No. 6*
No smoothing	100	100
3-pt. MA	72	94
5-pt. MA	48	90
9-pt. MA	28	79
17-pt. MA	15	56
5-pt. quadratic–cubic	86	96
9-pt. quadratic–cubic	57	94
17-pt. quadratic–cubic	32	84
25-pt. quadratic–cubic	22	70
9-pt. quartic–quintic	80	97
17-pt. quartic–quintic	48	95
25-pt. quartic–quintic	34	86

* Sampling density for the simulated chromatogram (data points/σ): Peak No. 1 = 1.0; No. 2 = 1.25; No. 3 = 1.43; No. 4 = 2.0; No. 5 = 2.22; No. 6 = 3.33.

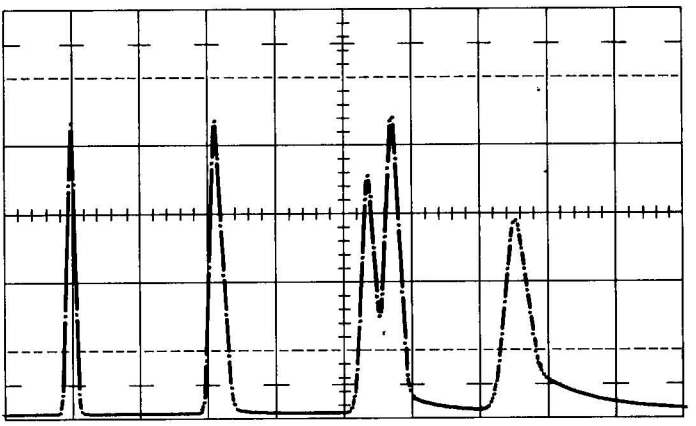


Fig. 9. Simulated 6-component chromatogram after smoothing with a 3-point MA. Scaling factors same as in Fig. 8.

peaks and the attenuation factors for the sharp narrow peak with a typical but insufficient sampling density (No. 1) and the broad peak with an acceptable sampling density (No. 6). Note that in the chromatogram in Fig. 8, the shoulder on peak No. 2 is not discernable in that no peak broadening is apparent, and that the valley between peaks Nos. 4 and 5 is about 25% of the peak height of peak No. 5.

Using the same scaling factors for display as in Fig. 8, the results of 3- and 9-point MA smooths are shown in Figs. 9 and 10. The peak height recoveries, normalized to those in Fig. 8, are reported in Table II. More importantly,note that the 3-point MA has not seriously perturbed the peak shape, resolution, peak tail, or baseline compared with Fig. 8, even though the sampling density is too low on all of the peaks. However, Fig. 10 shows the striking contrast between a 3- and 9-point MA, where the differences are accentuated by the low sampling density. In Fig. 10, peak No. 3 serves to broaden and skew peak No. 2 and peaks Nos. 4 and 5 have been fused by

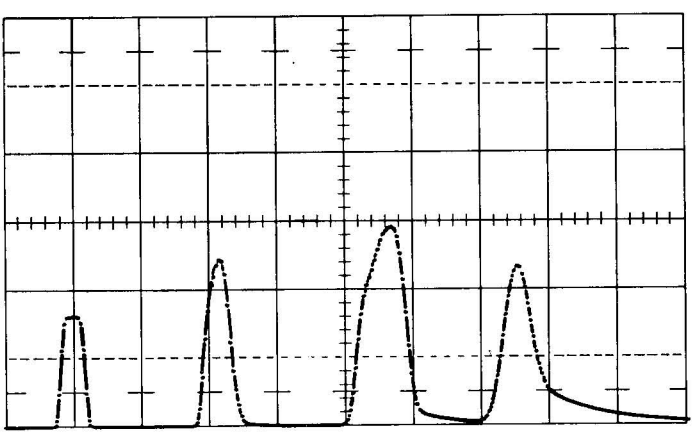


Fig. 10. Simulated 6-component chromatogram after smoothing with a 9-point MA. Scaling factors same as in Fig. 8.

the filter. Similar comparisons may be made between Figs. 11 and 12 for the 9- and 17-point quadratic–cubic and Figs. 13 and 14 for the quartic–quintic smooth of the same convolute intervals. The striking distinction between the 17-point polynomial smooths in Figs. 12 and 14 is the resolution between peaks Nos. 3 and 4 which illustrates the power of the higher-order polynomials as previously discussed. The "ringing" on the leading and tailing edges of the peaks is a consequence of the convoluting coefficients for higher-order polynomials where the sampling density is too low. The extreme case is where the convoluting interval is larger than the number of data points in the peak. In this case "ringing" and peak area "amplification" will result as shown in Fig. 12.

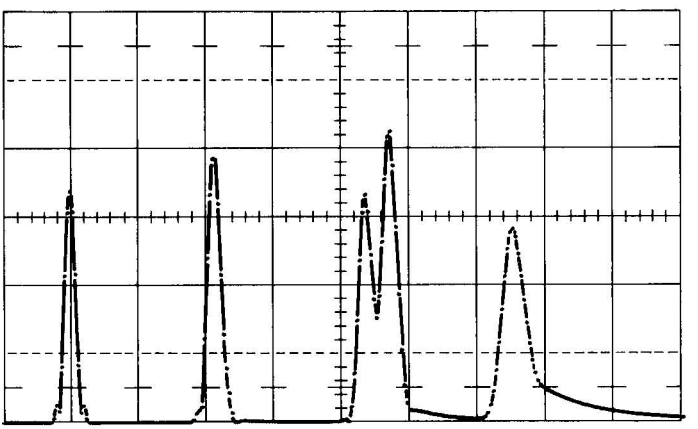


Fig. 11. Simulated 6-component chromatogram after smoothing with a 9-point quadratic–cubic. Scaling factors same as in Fig. 8.

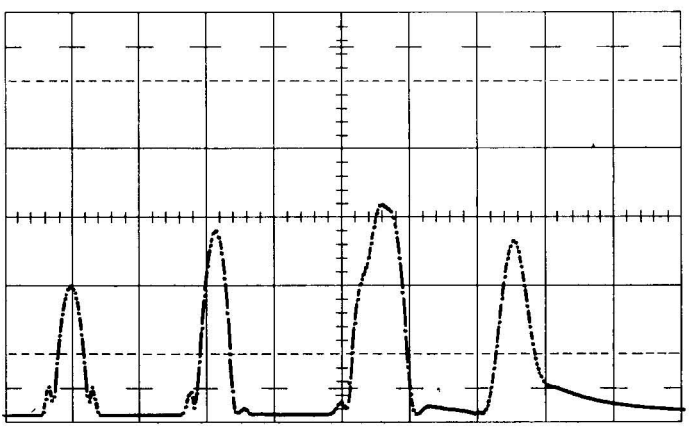


Fig. 12. Simulated 6-component chromatogram after smoothing with a 17-point quadratic–cubic. Scaling factors same as in Fig. 8.

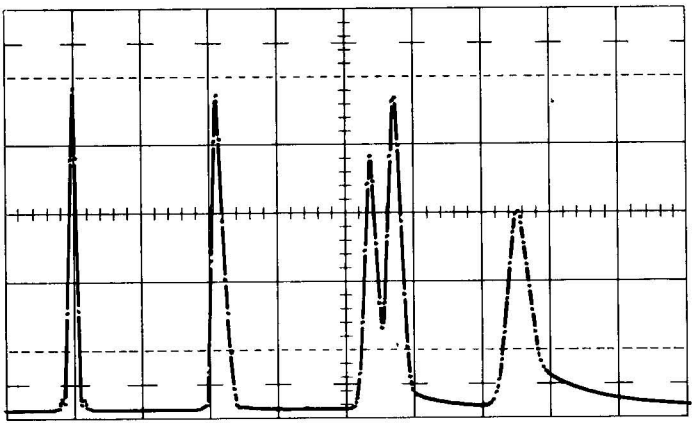


Fig. 13. Simulated 6-component chromatogram after smoothing with a 9-point quartic–quintic. Scaling factors same as in Fig. 8.

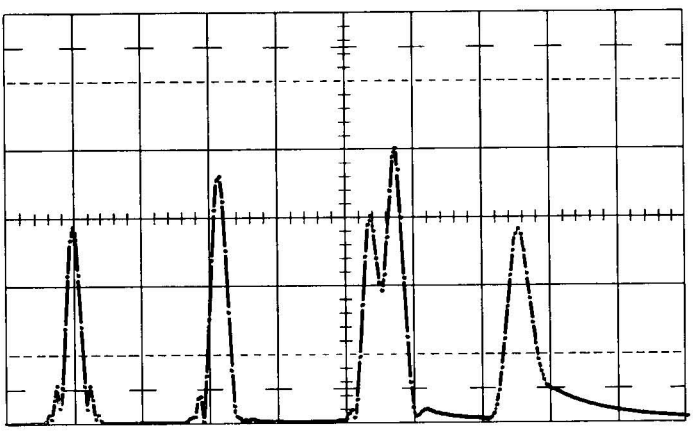


Fig. 14. Simulated 6-component chromatogram after smoothing with a 17-point quartic–quintic. Scaling factors same as in Fig. 8.

Effects on noise

The objective of this paper is to treat the effects of digital filters on chromatographic peaks and peak shape parameters. In addition to peak or signal considerations, we will briefly illustrate the effects on noise, although these effects are well known and have been treated comprehensively elsewhere[13,14]. To quantitate the noise attenuation, we have defined a "filter factor", Φ, by

$$\Phi = \frac{\sigma_n - \sigma_s}{\sigma_n} \tag{12}$$

where σ_n is the standard deviation of the normal random noise and σ_s is the standard deviation of the noise after smoothing. Thus for $\Phi = 0$ there is no smoothing effect because $\sigma_n = \sigma_s$, and $\Phi = 1$ represents complete smoothing such that the noise is below the detection limit ($\sigma_s = 0$). Figs. 15–17 illustrate the reduction of the normal random baseline noise before and after filtering for the 9-point MA, quadratic–cubic,

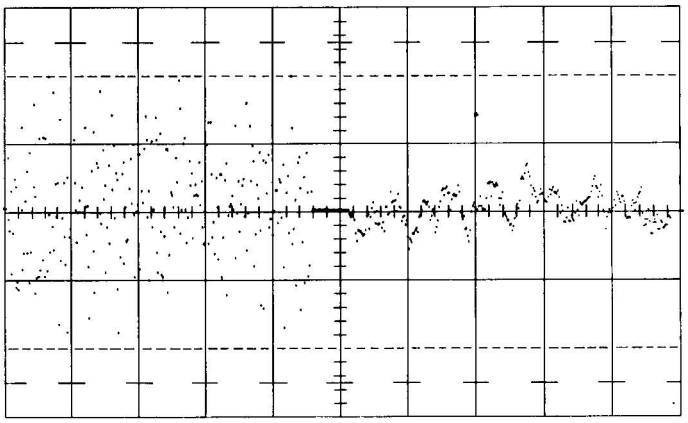


Fig. 15. Simulated normal random noise on a chromatographic baseline. Left-hand side is original noise trace normalized to 2/3 of full scale. Right-hand side is the same trace, displayed after smoothing with a 9-point MA.

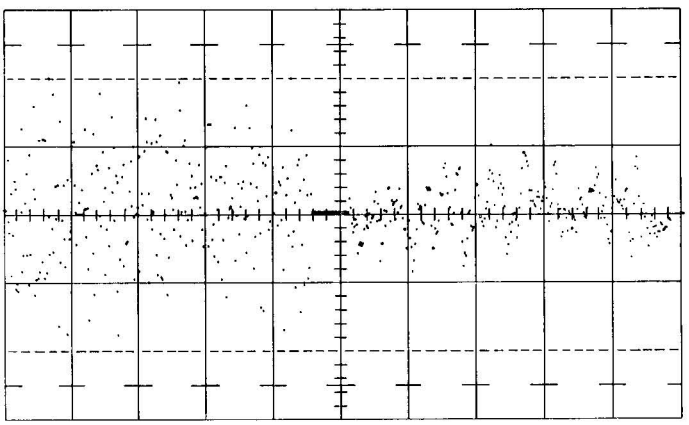


Fig. 16. Simulated normal random noise on a chromatographic baseline. Left-hand side is original noise trace normalized to 2/3 of full scale. Right-hand side is the same trace, displayed after smoothing with 9-point quadratic–cubic.

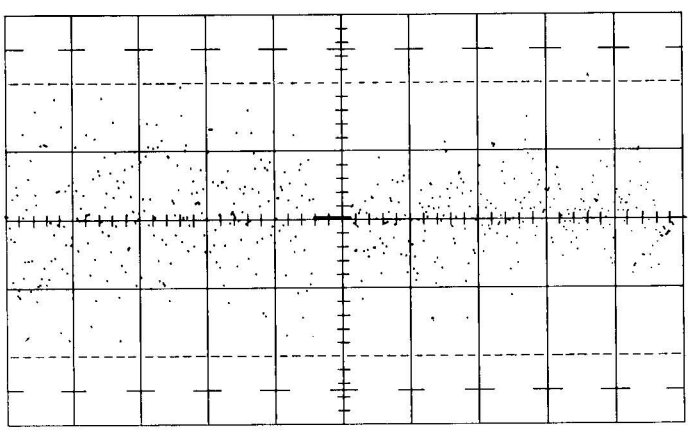


Fig. 17. Simulated normal random noise on a chromatographic baseline. Left-hand side is original noise trace normalized to 2/3 of full scale. Right-hand side is the same trace, displayed after smoothing with a 9-point quartic–quintic.

and quartic–quintic smooths, respectively. The left-hand side of the baseline segment is the unfiltered noise display, normalized to two-thirds of full scale for display, and the right-hand side of the trace is the same baseline segment after filtering. The filter factors are given in Table III. Where the filter factor is large, the lower-frequency noise components may be observed (*e.g.*, Fig. 15) which is often referred to as "wander" in the chromatographic literature.

TABLE III

ATTENUATION OF NORMAL RANDOM NOISE

Filter function	*Filter factor*
9-pt. MA	0.702
9-pt. quadratic–cubic	0.553
9-pt. quartic–quintic	0.387
25-pt. MA	0.825
25-pt. quadratic–cubic	0.733
25-pt. quartic–quintic	0.667

Fig. 18 compares the MA and polynomial filters treated in this paper in terms of the filter factor for each type as a function of the number of points in the convolute. Thus, a 5-point MA filter will reduce normal random noise with the same filter factor as an 11-point quadratic–cubic and a 17-point quartic–quintic smooth. As the number of points in the convolute increases, the filter factor becomes less affected by the type or order of the smooth. For the smaller, more commonly used convolute intervals, Fig. 18 shows that the filter factor may range from 0.25 for a 7-point quartic–quintic filter to 0.65 for a 7-point MA. Note that the filter factor changes fastest in this range of convolutes.

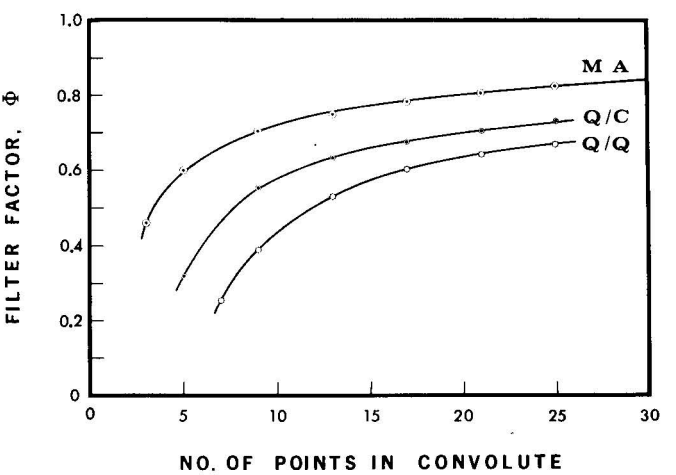


Fig. 18. Response of the filter factor for normal random noise as a function of the number of points in a convolute interval for moving average (MA), quadratic–cubic (Q/C), and quartic–quintic (Q/Q) smoothing functions.

Fig. 19 shows the cutoff filter frequencies for 5-, 17-, and 19-point quadratic–cubic filters in terms of their effectiveness (Φ). The smaller the convolute interval, the higher the bandpass of the filter for a given polynomial order and this is in agreement with the theory. For the range shown in Fig. 19, the midpoint of the frequency cutoff ranges from 20 to 70 Hz which is *not* a large range. Therefore principal consideration should be given to choosing a filter on the basis of the peak parameter to be measured and the amplitude of the noise. This is the experimental verification analogous to the theoretical curves shown in Fig. 1, which emphasizes the fact that a digital filter may be "tuned" to a cutoff frequency by design if the noise has been characterized and the filter factor is known as a function of the frequency, the number of points in the convolute interval, and the order of the polynomial.

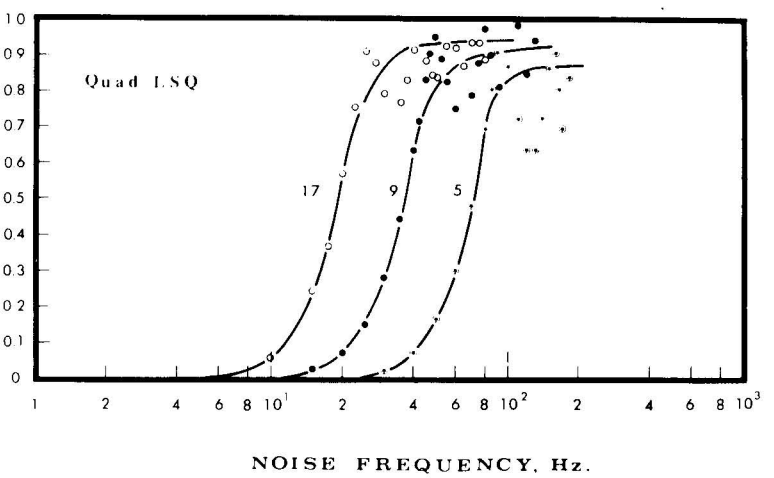


Fig. 19. Frequency response of 5-, 9- and 17-point quadratic–cubic digital filters for normal random noise as measured by the filter factor.

From Figs. 8–15 it can be seen that S/N may be significantly improved to decrease detection limits. At the same time, it is pointed out that peak area, retention time, resolution, and all other peak parameters for real chromatographic peaks are not conserved. It has been shown that all kinds of digital filters may be used to enhance S/N and that the error level is dependent upon: (1) number of data points/σ; (2) band width of the peak; (3) amplitude of the noise; (4) frequency distribution of the noise; (5) peak shape parameter to be measured; (6) S/N; and (7) accuracy desired.

IMPLEMENTATION IN PRACTICE

The Varian CDS-111 and CDS-101 (Varian Instrument Division) are new, dedicated, small chromatography data systems which serve as examples of the practical considerations and trade-offs in designing and implementing digital filters. The following basic objectives governed the design of the filter algorithm in order to make the system as generally applicable, accurate, precise, and reliable as possible within the constraints of a microprocessor-based system. The filter must:

(1) Reduce medium- and low-frequency noise from the column and detector. This noise is close to the frequency of the peak: $F_{noise} \geqslant 3\ F_{peak}$. High-frequency noise is attenuated by a two-pole analog filter and an integrating ADC (attenuation of 50- or 60-Hz power line noise and harmonics).

(2) Conserve peak area, and limit the distortion of peak height and width. The peak area measurements must not be adversely affected by the digital filter (*i.e.*, no side lobes or generation of false peaks, no distortion of peak shapes to affect area measurement on fused peaks).

(3) Calculate the first derivative of the detector signal (slope) for use in peak detection (peak–baseline discrimination). Reduce the slope noise due to the "frequency gain" characteristic of the differentiation process. The slope values must be reliable (accurate, precise, and continuous over the full domain of values) so that the peak detection programs do not have to contain the more complex noise–peak–baseline discrimination routines. Slope values for narrow peaks must cover a wide range while slope values for wide peaks must have high resolution.

(4) Operate with an existing ADC producing 20 conversions per second, with a resolution of 1 μV at the most sensitive range, and autoranging to 4, 32 and 256 μV at higher voltage levels. Total dynamic range is 10^6. The ADC translates a smoothly changing signal into a stair-step progression of digital values. With slowly changing signals (*i.e.*, baseline), the ADC values remain constant until the signal moves into the next digital value. This produces a spike or pulse in the first derivative, which should be suppressed to the extent of not affecting the peak detection programs. This effect is not present when the noise level of the signal equals or exceeds the resolution of the ADC.

(5) Be self-adapting to changes in peak frequency, specifically to self-update filtering when peak widths increase. Also to adjust simultaneously the peak detection threshold level (the slope) to take advantage of the reduction of noise due to the filtering increase. Fixed-frequency filters are not suitable to isothermal or isocratic chromatographic separations owing to the increase in peak widths. The filter should not self-adjust when peak widths remain constant as in temperature or gradient programmed separations. The operator should be able to change the filter for different peak widths at will.

(6) Be implemented in an 8-bit, binary microcomputer having an average instruction execution time of 30 μsec, and operate at the ADC speed (20 data points per second).

The digital filter includes four software elements: a variable pre-integration step to provide the variable frequency response characteristic (also known as data bunching); a 4-point symmetrical MA to suppress momentary signal curvature due to noise, but not suppress the trend of the slope caused by a real peak; a 5-point quadratic least-squares estimate of the first derivative; and an algorithm for the self-adjusting portion of the filter.

The pre-integration step is disabled at the minimum peak width setting, leaving only the MA and first derivative calculation in operation. At wider peak widths, data points are summed in groups of 2, 4, 8... up to 256. This causes two effects: first, the time interval between the 4 data points in the MA and the 5 data points in the slope calculation is increased. The time interval changes from 1/20 sec with no pre-integration to 1/10 sec with 2 points summed, and so on. This spreading effect

produces a reduction in noise by $\sqrt{2}$ for each doubling of the number of data points summed. The second effect is the reduction of noise produced by the integration process itself. This also produces noise reduction of $\sqrt{2}$, and thus the combined noise reduction is $(\sqrt{2})^2$ or 2. The dynamic range of the filter frequency is 256:1 using this technique.

The MA smooth was selected because of its high efficiency in suppressing curvature (change in slope) of the data points contained within the MA. Because of its potential for severe shape distortion, a small MA was selected. This allows efficient piece-wise smoothing of the peak profile while still maintaining the peak shape. A 4-point average was selected instead of the more usual 3- or 5-point averages because of an area integration consideration. The 4-point average only includes 20% of the peak width at half-height at any time (20 data points per peak width at half-height are used, or 8 data points/σ), which minimizes the peak shape distortion. The 4-point average produces a smoothed value at the midpoint of the average where in fact no data point exists. This $\frac{1}{2}$-data point offset is used by the area integration routine to help compensate for the fact that valley points are located $\frac{1}{2}$ data point late on the average. This improves the accuracy of peak area measurement on fused peaks if the results of replicate analyses are averaged.

The 5-point slope calculation uses the convolution technique. Here the least-squares estimate is calculated based on the data points after going through pre-integration and the MA. One effect of pre-integration is scaling of the first derivative values. As the number of points in the pre-integration step increases, the slope values increase as the square of the increase. This is due in part to the design of the filtering program because all normalization factors are grouped together at one operation. However, the scaling of the slope is reduced to a linear relationship of the number of points in the pre-integration step, and this produces the exact increase in peak detection sensitivity that can be made owing to the decrease in noise produced by the change in the number of points used in the pre-integration step.

Finally the filter is self-adapting by responding to the peak width of the currently eluting chromatographic peaks. When a peak is 50% wider than the expected peak width, the filter doubles the number of points in the pre-integration step. The change takes place only at valley points or on the baseline following the peak. To reduce the effect of peak tailing the time from peak start to the peak maximum is used as the measure of peak width. The filter can also accept changes specified by the operator to occur at specific points in the chromatogram.

The overall performance of this digital filter produced no measurable change in peak area measurements, and only depressed a Gaussian peak amplitude by 0.4%. It adjusts itself for variable-width peaks and simultaneously increases the peak detection sensitivity. The noise characteristics of the ADC are easily handled by the filter. The filter algorithm has an execution speed of about 20 msec per slope calculation in the microcomputer system, which allows enough time for execution of the real time peak detection program.

REFERENCES

1 R. Annino, *Advan. Chromatogr.*, in press.
2 G. M. Hieftje, *Anal. Chem.*, 44 (1972) 81A.
3 G. M. Hieftje, *Anal. Chem.*, 44 (1972) 69A.

4 A. Savitzky and M. J. E. Golay, *Anal. Chem.*, 36 (1964) 1627.
5 J. Steiner, Y. Termonia and J. Deltour, *Anal. Chem.*, 44 (1972) 1906.
6 S. N. Chesler and S. P. Cram, *Anal. Chem.*, 43 (1971) 1922.
7 S. N. Chesler and S. P. Cram, *Anal. Chem.*, 44 (1972) 2240.
8 M. Goedert and G. Guiochon, *Chromatographia*, 6 (1973) 76.
9 M. Goedert and G. Guiochon, *Chromatographia*, 6 (1973) 39.
10 H. C. Smit and H. L. Walg, *Chromatographia*, 8 (1975) 311.
11 A. C. Brown, D. L. Wallace and S. Kung, *Pitts. Conf. Anal. Chem. Appl. Spectr., Cleveland, Ohio, March 1–5, 1976*, Abstr. No. 336.
12 M. H. J. van Rijswick, *Philips Res. Rep., Suppl.*, No. 7 (1974) 32.
13 R. B. Blackman, *Linear Data-Smoothing and Prediction in Theory and Practice*, Addison-Wesley, Reading, Mass., 1965.
14 S. D. Stearns, *Digital Signal Analysis*, Hayden, Rochelle Park, N.J., 1975.

Journal of Chromatography, 126 (1976) 301–314
© Elsevier Scientific Publishing Company, Amsterdam — Printed in The Netherlands

CHROM. 9406

TOTALLY PNEUMATIC GAS CHROMATOGRAPHIC PROCESS STREAM ANALYZER

RAYMOND ANNINO

Canisius College, Buffalo, N.Y. (U.S.A.)

and

JOHN CURREN, Jr., RICHARD KALINOWISKI, EDWIN KARAS, ROY LINDQUIST and ROBERT PRESCOTT

The Foxboro Company, Foxboro, Mass. (U.S.A.)

SUMMARY

A nonelectric pneumatic based process stream gas chromatographic analyzer is described. The unit automatically and repetitively analyzes a process stream for one or two preselected components and transmits a 3–15 p.s.i. signal which is proportional to their concentration in the process stream.

INTRODUCTION

A closed-loop process control chromatograph operates continuously, on-line, analyzing a process stream in a cyclic and repetitive manner. It transmits the information to a controller which then takes corrective action so as to maintain the process at the desired set point.

The factors, therefore, which determine the design criteria for this type of analyzer are quite different from those which influence the design of laboratory units[1]. For instance, the requirement for long-term stability and minimum down time over extended periods of unattended operation puts a premium on simplicity of design, ruggedness, and dependability of all components. The fact that the unit will usually be located in areas where hazardous concentrations of inflammable gases are present further complicates the design problem. On the other hand, many common process applications do not require low detection limits and thus the more exotic but trouble-plagued chromatographic detectors need not be used. In addition, programming the analysis cycle is simplified since control of the process can normally be achieved by monitoring only one or two components of the process stream.

Pneumatic process control instrumentation has a long history of proven reliability, serviceability, and safety, which is difficult to match. It was felt, therefore, that the development of a totally pneumatic chromatograph would be an excellent way to achieve the above stated objectives.

The purpose of this paper is to describe the development of a viable pneumatic detector, an appropriate thermostated steam heated enclosure, and a unique pro-

gramming philosophy which allowed the automation of the unit using standard pneumatic components.

ORIFICE DETECTOR

Theory

The chromatographic detector which is to be described utilizes a jeweled orifice nominally 0.002 in. in diameter. This element responds to the density of the flowing gas by accelerating the gas to a higher velocity. The force required to produce this acceleration is measured as a pressure drop across the orifice and this constitutes the chromatographic signal. The theoretical pressure drop across the detector orifice is given by:

$$P_b = \frac{8\,F^2}{K^2\,\pi^2\,d^4}\,\varrho \tag{1}$$

where

F = volumetric flow-rate
ϱ = density of gas within the detector
d = orifice diameter
K = orifice contraction coefficient (usually 0.62).

In actual practice the exponent of F may vary depending on the ratio of internal length of the orifice to orifice diameter.

Eqn. 1 can be used to calculate the orifice pressure due to carrier gas flowing at a specified rate and at a given temperature. For example, using an orifice of 0.0022 in. diameter and helium carrier gas at a flow-rate of 50 ml/min, orifice pressure is calculated to be 3.4 p.s.i., which is in good agreement with that obtained by experiment.

The chromatographic signal may be visualized as appearing on top of this steady state signal. When helium is used as the carrier gas, the sample components eluting from the column are usually more dense than helium and ϱ increases, causing a proportionate increase in P_b.

The total mass, m, of a sample component is assumed to be added to the carrier gas stream as a Gaussian distribution of concentration with time. It may be more conveniently viewed as a mass of sample distributed in a volume of carrier gas such that the increased density is a Gaussian distribution. The maximum increase in density can be shown[2] to be

$$\Delta\varrho_{\max.} = \frac{m\sqrt{N}}{\sqrt{2\pi}\,V_r} \tag{2}$$

where N is the number of theoretical plates and V_r is retention volume. Since m is the product of (sample volume, V_s, concentration in the sample, C_c, and density of pure component, ϱ_s), at sampling pressure and temperature, then

$$\Delta\varrho_{\max.} = \frac{V_s\,C_c\,\varrho_s\,\sqrt{N}}{\sqrt{2\pi}\,V_r} \tag{3}$$

Substituting for ϱ in eqn. 1 yields a pressure change in response to the density change of the eluting peak

$$\text{Peak height} = \Delta P_{\text{max.}} = \frac{8F^2 \Delta \varrho_{\text{max.}}}{K^2 \pi^2 d^4} \tag{4}$$

which becomes

$$\text{Peak height} = \Delta P_{\text{max.}} = \frac{8F^2 V_s C_c \varrho_s \sqrt{N}}{K^2 \pi^2 d^4 \sqrt{2\pi} V_r} \tag{5}$$

As can be seen in the equation the pressure drop is critically dependent on orifice diameter. It was decided early in the research that a sensitivity specification which would indicate a full-scale response for a 1-ml sample volume containing 1 % methane was a reasonable goal. In view of the limited gain of pneumatic amplifiers this specification required a 0.08 p.s.i. orifice pressure change at the methane peak maximum. Again the 0.002-in. orifice operated between 50–60 ml/min satisfies this requirement.

Flow sensitivity

The use of an orifice or capillary restrictor as a detector was first suggested by Griffiths *et al.*[3]. The main disadvantage of this detector for laboratory applications is its high sensitivity to flow variations.

The flow sensitivity of the orifice detector can be easily verified with eqn. 1. The baseline offset which results from slow changes in flow due to overall changes in system components such as regulators, etc., can be easily offset by splitting the carrier gas stream ahead of the column, passing this stream through a balancing restrictor and thence to another orifice, and taking the chromatographic signal as the difference in the two orifice signals. This is similar in philosophy to the thermal conductivity measurement system, and is the basis of a recent patent[4]. Unfortunately, no report is available in the open literature as to its performance. In any case it is doubtful whether this arrangement will compensate for the flow variations which occur due to viscosity changes in the flowing medium when it is mixed in the column with sample*. This effect and its implications for quantitative analysis have been discussed in detail by Dyson and Littlewood[6] and need not be elaborated here.

Fig. 1 is an amplified orifice detector signal obtained using the split stream design discussed above. The large offset in the baseline is due to the viscosity-modified flow which occurs while the sample is in the column; the baseline returns to its original value when the last peak elutes.

Flow compensation

The pressure drop across a capillary restriction is given by

$$\Delta P_{\text{cap}} = \frac{K F L \eta}{r^4} \tag{6}$$

* For a review of the various flow and pressure effects which accompany the elution of solutes, see ref. 5.

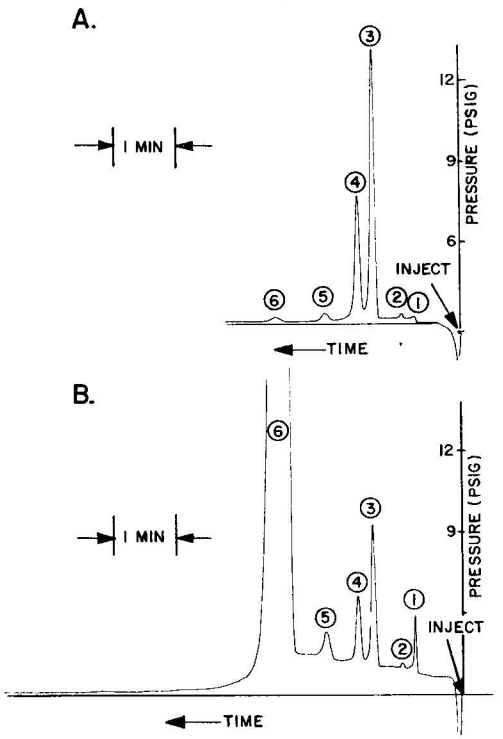


Fig. 1. Chromatographic signals obtained as the difference between reference and sensing orifices. (A) Hydrocarbon sample diluted with helium. (B) Pure hydrocarbon sample containing 90% butane. Column, 6 ft. × 0.085 in. I.D., 20% w/w bis(2-ethoxyethyl)sebacate on 80–100 mesh Chromosorb P; ambient temperature; flow-rate, 50 ml/min. 1 = Methane; 2 = ethane; 3 = propane; 4 = propylene; 5 = isobutane; 6 = butane.

where

r = radius of the capillary
L = length of the capillary
η = viscosity of the fluid in the capillary
F = volume flow-rate
K = constant.

Since the capillary does not respond directly to density changes it can be used to sense flow variations in a gas stream of constant viscosity. The capillary compensation can be used in parallel with the orifice (bridge network) or in series. We elected to try the latter approach. The final design is shown schematically in Fig. 2.

The flapper nozzle unit, amplifier relay and feedback bellows shown in Fig. 2 are arranged in a force balance system. Any difference between orifice and capillary pressure is sensed by movement of the flapper from its equilibrium position at the nozzle. This in turn is reflected in a change in the output signal of the relay which is also fed to the feedback bellows. The magnitude of this feedback signal is sufficient to keep the flapper at its equilibrium position and thus is proportional to the initial disturbing force. Gain is achieved through the area relationships and positions of the

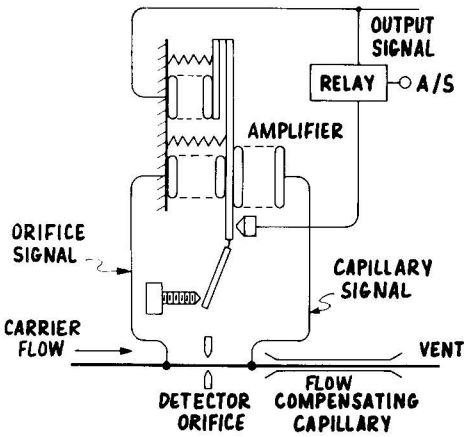
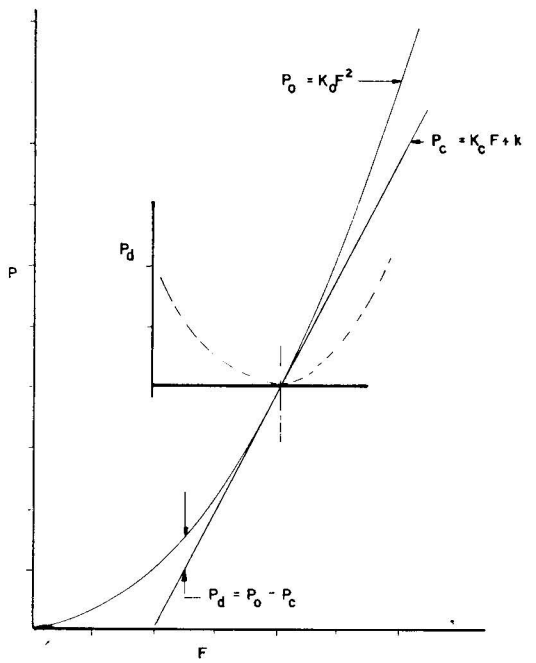


Fig. 2. Orifice-capillary detector and amplifier.

bellows with respect to the pivot point of the lever arm. The output range of the relay is usually 3–15 p.s.i.

In practice it was convenient to obtain compensation at the desired flow by changing the capillary restriction with the appropriate length of 0.008-in. wire. Since the orifice pressure varies as the square of the flow and the capillary pressure varies linearly with flow, compensation could not be precisely achieved at all flows (see



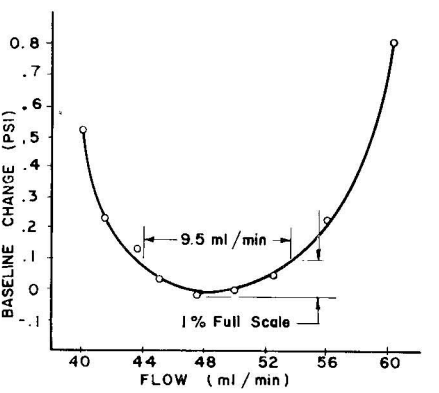


Fig. 3. Flow dependence of orifice and capillary signals, and the origin of the final detector signal. P_o = Orifice pressure; P_c = capillary pressure; P_d = detector signal; F = flow-rate.

Fig. 4. Variation in detector baseline as a function of flow.

Fig. 3). However, as can be seen from Fig. 4, flow changes of 10 ml/min lead at the most to 1% changes in the baseline position. This was deemed sufficient stability for all but the catastrophic problems. In terms of temperature, a $\pm 5°$ change about a mean temperature of 60° produced a flow change of 1.4 ml/min and a consequent change in baseline of 0.25% when the system was adjusted to the compensation minimum at 60° and 49 ml/min.

The ability of this detector to compensate for the flow perturbations caused by sample in the column is illustrated in Fig. 5. Note that the large baseline offset which is present in the uncompensated chromatogram shown in Fig. 1 has been eliminated.

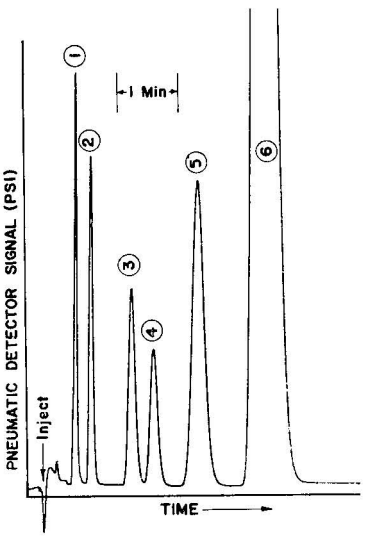


Fig. 5. Orifice-capillary signal for a pure hydrocarbon sample containing 90% butane.

Detector response —linearity

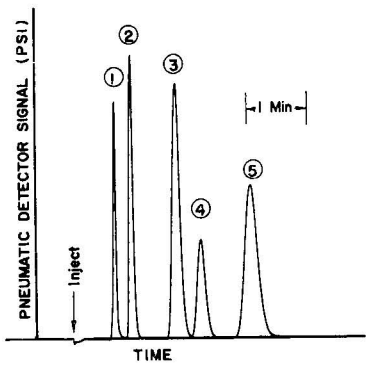
Since the flow compensator senses gas viscosity in addition to flow, and is an integral part of the detector, the total detector response can be written as

$$\Delta P = A_o K_o F^2 \Delta\varrho - A_c K_c F \Delta\eta + k \tag{7}$$

where

ΔP = detector signal above baseline
K_o, K_c = lumped orifice and capillary constants
F = volumetric flow-rate
$\Delta\varrho$ = change in density due to sample component
$\Delta\eta$ = change in viscosity due to sample component
A_o, A_c = orifice and capillary gain factors
k = additional force necessary to achieve displacement of capillary flow curve from the origin.

For the analysis of hydrocarbons with helium as carrier gas, $\Delta\eta$ is negative and $\Delta\varrho$ is positive. Thus the signal is the summation of both terms in eqn. 7.



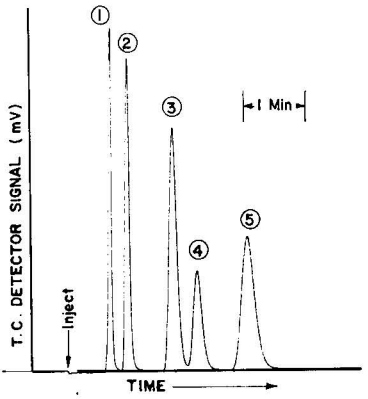


Fig. 6. Orifice-capillary signal for the same hydrocarbon sample shown in Fig. 7.

Fig. 7. Thermal conductivity detector signal for a hydrocarbon sample. 1 = Methane; 2 = ethane; 3 = propane; 4 = propylene; 5 = isobutane.

Chromatograms of identical samples obtained with this detector and a small-volume thermal conductivity (TC) detector are compared in Figs. 6 and 7.

Results for chromatographic analysis of various standard samples are shown in Fig. 8. Linearity was defined as the maximum deviation from a 45° calibration curve secured by setting the gain so that the most concentrated sample in the series registered at 100% of range. For 1-ml samples containing less than 10% of the particular component, detector response was linear to within 1%. The nonlinearities noted at high concentrations were apparently due to a chromatographic problem. The 1-ml sample volume used for all samples resulted in a column overload and distorted peaks at the higher sample concentrations. Similar nonlinearities were obtained when the same column was fitted into an HP-3750 chromatograph equipped with a flame ionisation detector and 1-ml sample loop.

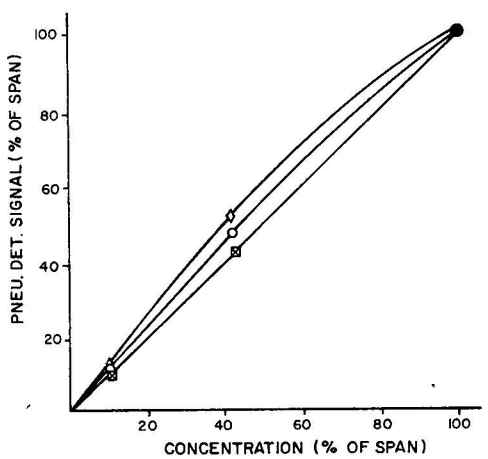


Fig. 8. Linearity studies with the orifice-capillary detector. ×, 0–1% C_3H_8 range; □, 0–10% C_3H_8 range; ○, 0–22% C_3H_8 range; ◇, 0–47% C_3H_8 range.

The gain of the amplifier was changed by varying the pivot position of the lever arm (screwdriver adjustment) and was not amenable to auto-ranging. Thus large dynamic ranges were not automatically attainable. However, for process control, large changes in process stream composition are not usually encountered and thus lack of auto-ranging was not expected to be a disadvantage.

As mentioned previously, it was decided that a minimum change of signal of 0.08 p.s.i. should register as a 12 p.s.i. change in pressure at the output. This requires an amplification of 150 and is a considerable fraction of the open loop gain available to most pneumatic amplifiers. However, since a second peak height amplifier is available in the peak processor portion of the final system, it is not necessary to take all of the 150 gain on one amplifier. Current operating practice uses a gain of 20–30 on the detector amplifier and a gain of 5 on the peak height amplifier.

Temperature sensitivity

It is well known that column flow changes with temperature in a manner that compensates for changes in retention volume due to temperature variation in the partition function. However, this compensation is fairly small. Because of the large flow sensitivity of the pneumatic detector response, there was reason to suspect that the peak heights would be less sensitive to temperature with this detector than with a thermal conductivity device.

From the known relationship between retention volume and temperature it can be shown that[2,7]

$$\frac{\mathrm{d}V_r}{V_r} = \frac{-k'}{(1+k')}\frac{\Delta H}{RT_c}\frac{\mathrm{d}T_c}{T_c} \tag{8}$$

where

R = universal gas constant
k' = the capacity factor
V_r = retention volume
ΔH = heat of solution
T_c = column temperature

also for Gaussian peaks

$$\mathrm{d}V_r/V_r = -\mathrm{d}h/h$$

where h = peak height.

The flow dependence of the response of a detector (D) can be written as

$$D \propto h \propto F^{\varphi}$$

Then

$$\mathrm{d}D/D = \mathrm{d}h/h = \varphi\, \mathrm{d}F/F$$

Since flow is inversely proportional to viscosity, which in turn varies with temperature, as $T_c^{0.8}$

$$\mathrm{d}h/h = -0.8\,\varphi\, \mathrm{d}T_c/T_c$$

Thus the total variation in peak height due to the temperature sensitivity of flow and retention volume is

$$\frac{\mathrm{d}h}{h} = \frac{k'}{(1+k')}\frac{\Delta H}{RT_c}\frac{\mathrm{d}T_c}{T_c} - 0.8\,\varphi\,\frac{\mathrm{d}T_c}{T_c} \tag{9}$$

For TC cells φ is usually negative and thus the flow dependence aggravates the problem. For the pneumatic detector φ is approximately 2.

The results of a set of experiments comparing the temperature sensitivity of the pneumatic detector with a TC detector shown in Fig. 9 are consistent with the above prediction.

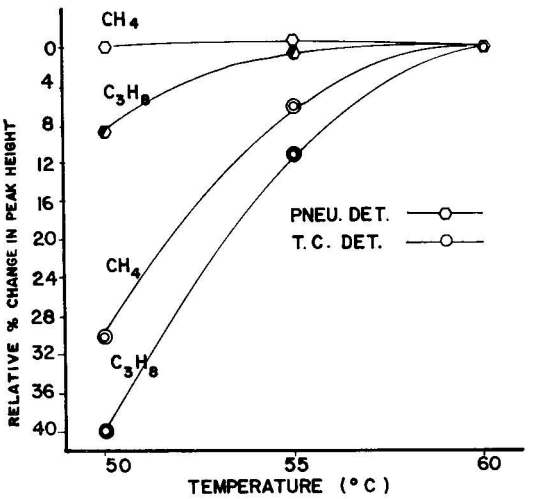


Fig. 9. Comparison of the temperature sensitivity of the orifice-capillary and thermal conductivity detectors.

OVEN AND TEMPERATURE CONTROL

The small temperature coefficient for the detector, coupled with the use of the yet-to-be-described self-adjusting programmer, simplified the oven design since it reduced the temperature specifications on the oven and control system from the $\pm 0.2^\circ$ of electronic models to $\pm 1^\circ$ for the pneumatic system.

A detailed discussion of the oven and controller system will be published elsewhere. It is schematically illustrated in Fig. 10. Energy was supplied from 30 p.s.i. steam through the heat exchanger. Control was achieved with a no-moving-parts pneumatic fan through a controlling element which consisted of a flapper (A) made of temperature-sensitive bimetal and a nozzle (B). The force on the nozzle was generated by the spring constant of the flapper. Below the set-point temperature the nozzle was blocked causing full 20 p.s.i. output at the relay which in turn fed a nozzle situated at the entrance to the heat exchanger.

The high-velocity air molecules emerging from this nozzle momentum interchanged with other low velocity molecules, thus creating a large volume movement of air through the exchanger into the oven. As temperature approached the set point, the flapper began to move away from the nozzle, thereby decreasing the relay output and consequently decreasing the exchanger throughput. At set point this system operated in a proportional mode giving sufficient air movement through the exchanger

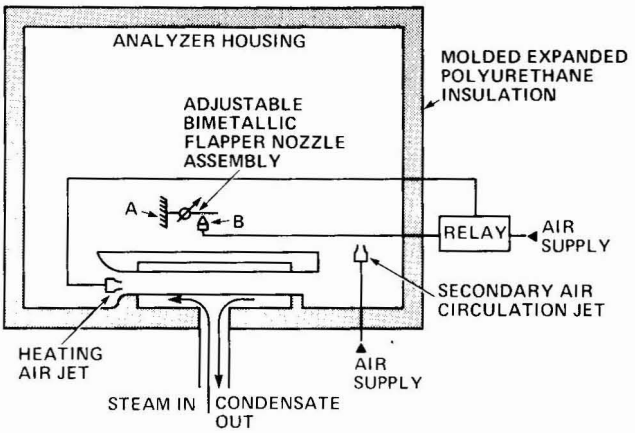


Fig. 10. Pneumatically controlled steam heated enclosure.

to maintain the desired temperature. Oven temperatures were easily varied by changing the spring force on the flapper.

With the oven thermostat set at 75°, average column temperatures were found to be stable to 1.5° over ambient temperature swings of 97° (−32–65°). Chromatographic peak heights under these conditions varied by less than the 1% measurement error.

SAMPLE VALVE

The sample valve was a pneumatically actuated two-position, ten-port slider type. The slides were manufactured of fired Al_2O_3 and lapped to optical flatness. This material is extremely hard and eliminated the problems of scratching and consequent leakage experienced with PTFE-faced sliders. One valve performed the function of both sample inject and back-flush valves. The two common configurations are shown in Fig. 11. The valve was found to be extremely reliable —the only significant observation after one million cycles being that the two faces had lapped each other to a greater degree of flatness.

AUTOMATION

A process gas chromatograph must be operated automatically. In this mode it must make a sample injection, switch the valve to the back-flush position at the appropriate time, select the correct peak or peaks, and measure the peak height, update the trend signal with the new information and then repeat the cycle with a new sample. These objectives are summarized in the system diagram shown in Fig. 12.

In order to implement these ideas it was necessary to develop a pneumatic clock, a programmer, and a peak processor. It is not the purpose of this section to discuss in detail the mechanics of the system elements. They were constructed using standard pneumatic hardware although obviously a comparable electronic system is possible. Rather it is the manner in which they were used to yield a more reliable and trouble-free system that is of interest here.

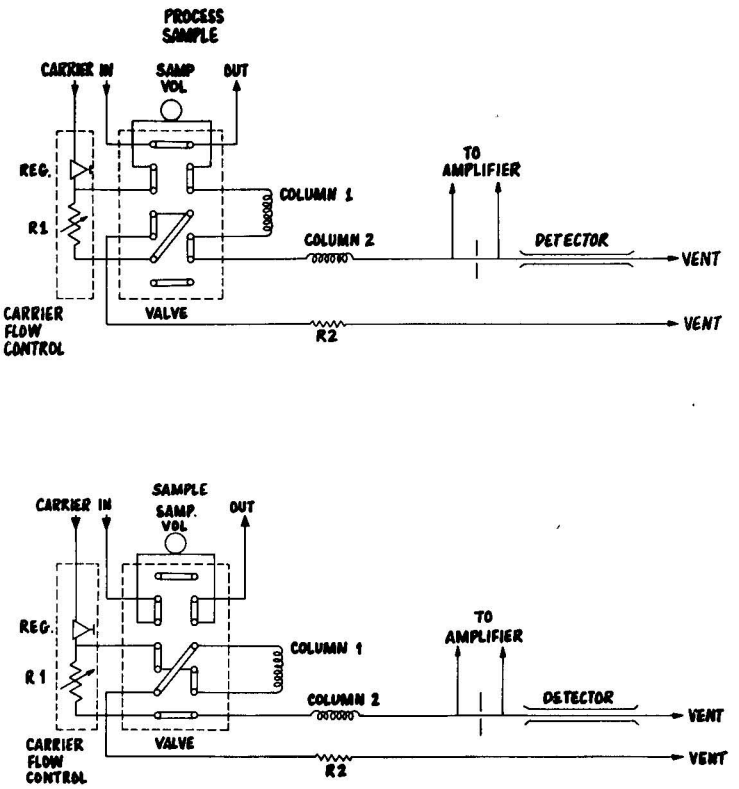


Fig. 11. Schematic representation of the sample fill and sample inject positions of the sample valve.

PNEUMATIC CLOCK

A linear time-dependent pressure signal was obtained with a simple constant input flow integrator. Since the gas flow and consequent ramp rate are quite temperature-sensitive, it appeared that the clock would also have to be thermostated. However, as will be shown in the succeeding discussion, this became unnecessary with the programming procedure which was developed during this research.

PROGRAMMER

Except in the case described by one previous report from this laboratory[8], process gas chromatograph programmers are usually designed around an absolute time base. An accurate clock is used to time a sequence of events such as column switching, auto-zero, peak selection, etc.

The problem with this approach is that peak retention times are not constant. They vary with changes in column load (aging), flow, or temperature. Since it would be disastrous to start controlling the process on the wrong information, this necessitates periodic manual reprogramming of the unit.

Some attempt has been made to provide continuous adjustment of the program

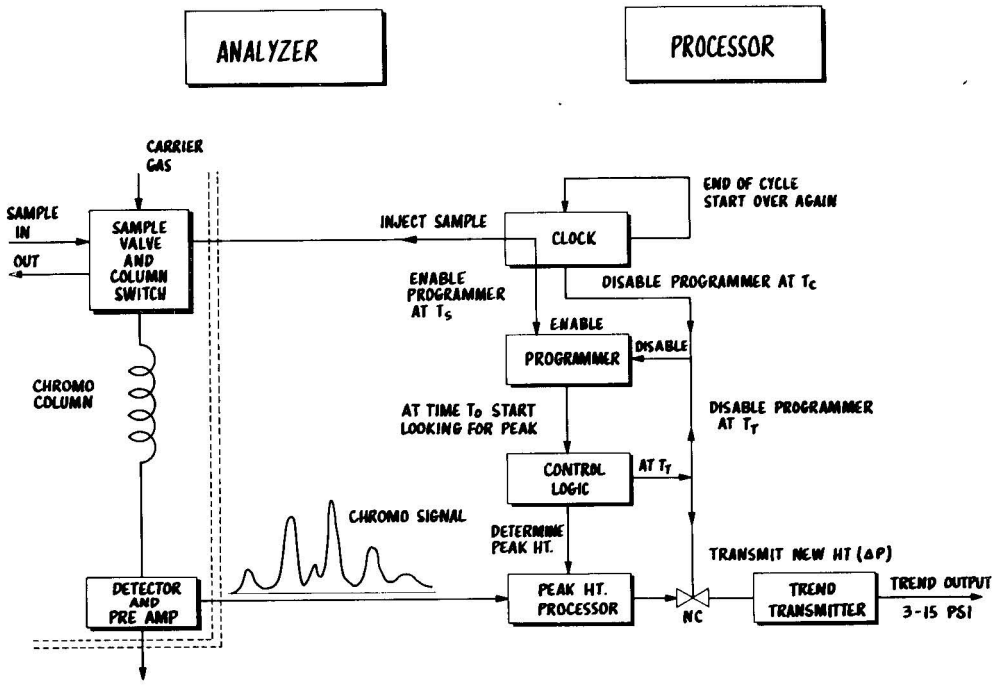


Fig. 12. Schematic representation of the system operation.

by automatically changing temperature or flow in order to maintain the peak position at the same absolute time[9].

We have adopted a somewhat different philosophy and that is to automatically change the programmer event time in response to peak movement. This allows faster adaption to changing conditions and is somewhat simpler to implement.

In one embodiment of this approach the peak window is opened at a time based on the appearance of a reference peak[8]. Since relative retention times are fairly constant over large ranges of temperature, flow and column load, this assures reliable peak selection under a variety of conditions.

The present work utilizes the peak of interest as its own reference point and that of the second component. The time (clock pressure) at which this peak appears is memorized and used to create a reference pressure (time) for opening the window to analyze the same peak in the next cycle. Thus, the reference time is one cycle out of date. It is certainly sufficiently current to insure accurate programming except under the most catastrophic conditions.

The relationship of events to the appearance of the chromatographic peak is summarized in Fig. 13. Sample is injected at the beginning of the analysis cycle. Not shown in the diagram is the return of the sample to its "sample fill back flush" position at some selected time in the program. At time T_0, which is usually 90% of the retention time, T_t, of the desired sample component, the control logic activates the differential peak height analyzer. T_0 is adjusted to be anywhere between the top of the preceding peak and the beginning of the selected peak. The differential peak height analyzer tracks the signal and finds the difference between the lowest point and the next high

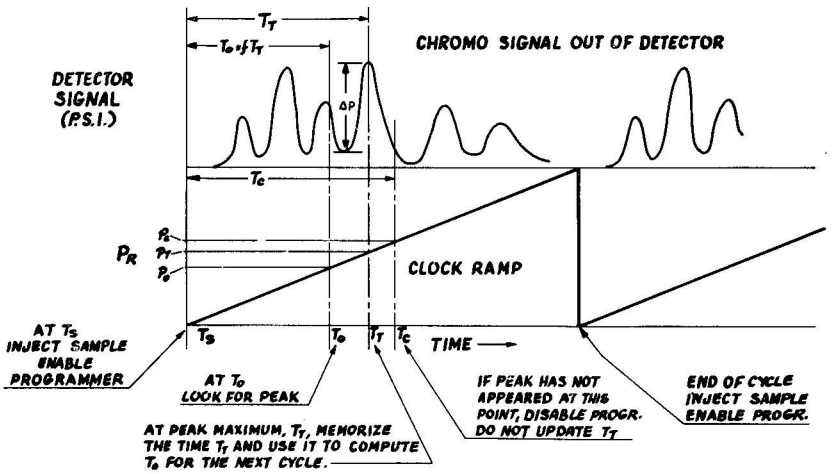


Fig. 13. Relationship of events to the appearance of chromatographic peaks.

point. This differential peak height is then memorized and transmitted as an updated trend signal. In addition, the retention time of the peak is memorized and used to calculate a new T_0 for the next cycle. Thus the peak window is constantly being automatically adjusted for small movements in peak position due to changes in temperature, flow, column load, etc. The auto-zero also "floats" since it is the lowest point after the differential peak height analyzer is enabled. The program is protected by disabling the programmer if a detectable peak has not appeared by time T_c. It is also protected against air failure by using a mechanical memory to store T_t.

Large, abrupt changes in retention time cannot be accommodated if the shift is so large as to have T_0 appear earlier than the previous peak maximum or on the leading edge of the selected peak. The only system variable that could possibly change fast enough to accomplish this would be flow.

The advantage to the above approach is that the system not only adjusts itself for chromatographic retention time shifts but also for shifts in performance of the mechanical components of the system due to varying temperature, changing restrictor resistances, etc. In terms of design, it meant that the pneumatic clock, programmer and processor units did not need to be thermostated. The ambient temperature tests (−32–65°) referred to under the section on oven design were conducted on a completed system containing the clock programmer, and peak processor in a separate non-thermostated package. Although clock ramps varied by more than 10% over this temperature range, programming accuracy was not affected.

FINAL DESIGN AND PERFORMANCE

As the result of the research described herein, a commercial pneumatic process stream composition transmitter has become available. A recent report discusses the mechanics in a little more detail than presented here, and the results of field trial evaluation of six production units are also given[10].

CONCLUSIONS

In summary, a new look at implementing design criteria for process chromatographs has resulted in the synthesis of a new and unique system which should have a significant impact in the field of process control.

The development of a rugged and accurate pneumatic detector, the use of standard pneumatic control technology and the introduction of a novel chromatographic programming philosophy lead to a compact design of improved reliability while at the same time offering the advantages of easy maintainability, safety, immunity to electrical interference, and economy.

REFERENCES

1 R. Villabos, *Anal. Chem.*, 47 (1975) 983A.
2 M. Goedert and G. Guiochon, *J. Chromatogr. Sci.*, 7 (1969) 323.
3 J. H. Griffiths, D. James and C. S. G. Phillips, *Analyst (London)*, 77 (1952) 901.
4 J. Novák and J. Janák, *U.S. Pat.*, 3,354,696 (Nov. 28, 1976).
5 P. C. Haarhoff and H. J. van der Linde, *Anal. Chem.*, 37 (1965) 1742.
6 N. Dyson and A. B. Littlewood, *Anal. Chem.*, 39 (1967) 638.
7 M. Goedert and G. Guiochon, *Anal. Chem.*, 42 (1970) 962.
8 R. Annino, *J. Chromatogr. Sci.*, 8 (1970) 288.
9 F. D. Martin, *Instrum. Tech.*, June No. (1972) 46.
10 A. W. Waters, R. Annino, R. C. Prescott and E. L. Karas, *Proc. IMEKO Congr., 7th, London, May 1976.*

THEORETICAL AND PRACTICAL ASPECTS OF LIQUID COLUMN CHROMATOGRAPHY

Journal of Chromatography, 126 (1976) 317–325
© Elsevier Scientific Publishing Company, Amsterdam — Printed in The Netherlands

CHROM. 9450

FLUORESCENCE ENHANCEMENT

NEW SELECTIVE DETECTION PRINCIPLE FOR LIQUID CHROMATOGRAPHY

PAUL A. ASMUS, JAMES W. JORGENSON and MILOS NOVOTNÝ*
Department of Chemistry, Indiana University, Bloomington, Ind. 47401 (U.S.A.)

SUMMARY

A new detection principle for liquid chromatography based on the continuous measurement of the fluorescence emission intensity of a fluorescent dye, and its enhancement in the presence of solute, is described. The selective detection of polar lipids using 1-anilinonaphthalene-8-sulfonic acid as the fluorescent dye was demonstrated. Detector sensitivity, linearity, and several response-affecting factors were studied for this type of detection.

INTRODUCTION

The lack of sensitive detection in modern liquid chromatography (LC) is a frequent hindrance to many potential applications of this powerful analytical method. Whereas the development of a universal, highly sensitive detector for LC would be the most welcomed solution to the sensitivity problems, many useful applications can be covered by one of the available high-sensitivity selective detectors, such as small-volume spectrophotometric, spectrofluorometric, or electrochemical flow cells. In addition, many classes of compounds that do not possess selectively detectable features in their molecules can be derivatized to introduce them.

Among the available detection principles for LC, fluorescence surpasses most, if not all, other measurement methods in terms of sensitivity. Unfortunately, only the compounds which fluoresce or those easily convertible to fluorescent derivatives can be detected. Perhaps the best example of the potential of highly sensitive detection in LC is the detection of fluorescent derivatives[1,2].

It has been observed in numerous instances that the fluorescence of certain compounds can be influenced by a physical interaction with other (non-fluorescent) solution components. These can either quench or enhance the fluorescence intensity. Whereas such phenomena may actually contribute to errors in analytical measure-

* To whom all correspondence should be directed.

ments in mixtures, they could be potentially utilized, under controlled conditions, to one's advantage. The present publication describes some preliminary results obtained on the application of such phenomena to improved detection in LC.

Lipids are just one of the classes of compounds of biologic interest that have been limited in terms of sensitive detection[3]. Unless derivatizations are carried out[4-6] that are presently feasible in a few cases, only the refractive index monitor or transport-type detectors[3,7] are feasible for continuous detection. Therefore, our primary interest in exploring the above-mentioned detection principle has been focussed on chromatography of lipids.

Diverse chemicals have been used as fluorescent probes to provide information on the microenvironments of biopolymers and micellar systems as well as for labelling of membranes[8-11]. Among them, 1-anilinonaphthalene-8-sulfonic acid (ANS) appears most popular. Also, hydrophobic bonding with other molecules is responsible for the increased fluorescence of dansyl (a term used for 1-dimethylaminonaphthalene-5-sulfonyl) amino acids in organic solvents[12].

Whereas systematic searches leading to the utilization of fluorescence enhancement and quenching phenomena in LC detection are underway in this laboratory, this communication pertains to the utilization of ANS (as an example of fluorescent dye) in connection with improved detection of certain polar lipids. Firstly, the magnitude and nature of the fluorescence enhancement phenomena were investigated by means of a scanning spectrofluorometer. Subsequently, selected conditions were applied to monitoring the output of an LC column used for separating polar lipids. Sensitivity, selectivity, and the linearity of response were studied, and several response-affecting variables were also briefly investigated.

EXPERIMENTAL AND RESULTS

Spectrofluorometric measurements

In order to estimate detectability of selected lipids in an LC fluorometric detector and find optimum detection conditions, fluorescence spectra of ANS were recorded under a variety of conditions of pH and solvent composition in the absence and presence of small amounts of lipid. All measurements were carried out with a Farrand Optical Co. Model 104243 single-beam scanning spectrofluorometer. The light source was a high-pressure xenon/mercury arc lamp. The spectra obtained were not corrected for spectral characteristics of the source or detector.

The fluorescence enhancement effect of lecithin on ANS is shown in Figs. 1 and 2. Fig. 1 is the excitation spectrum of ANS (5×10^{-4} *M* concentration) in a 0.1 *F* phosphate buffer (pH 6.8), with enhancement obtained by the addition of egg-yolk lecithin (50 μg/ml). Excitation occurs between 300 and 450 nm, with enhancement seen as a general increase in intensity at all wavelengths. The region around the 405 nm mercury line exhibits the strongest enhancement.

Fig. 2 shows the characteristically broad emission spectrum of ANS. Whereas unenhanced emission is centered around 520 nm, enhancement by phospholipid induces a shift in the emission maximum to shorter wavelengths. The degree of shift appears to be somewhat a function of the lipid concentration. The choice of excitation wavelength used does not qualitatively affect the emission spectrum, permitting selection of an excitation wavelength based primarily on maximizing the enhancement sig-

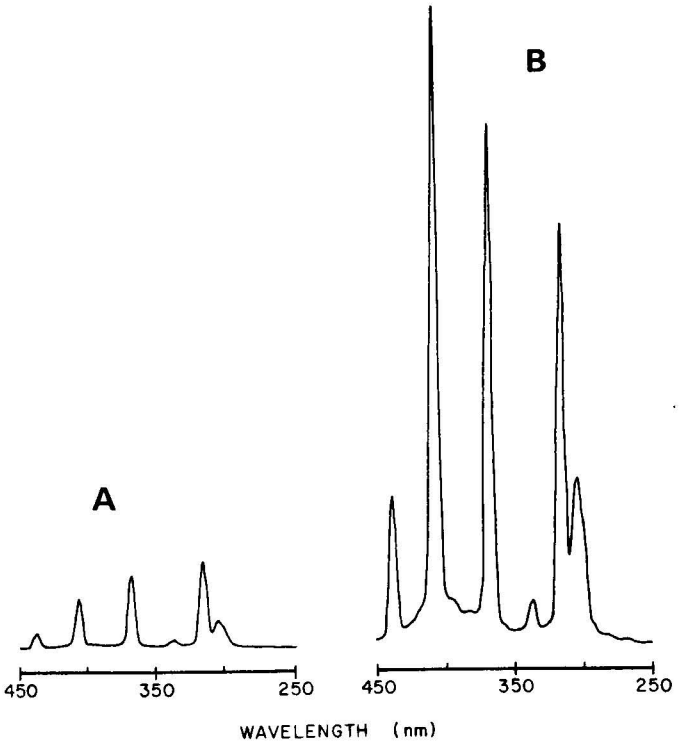


Fig. 1. Excitation spectra of ANS (5×10^{-4} *M*) in 0.1 *F* phosphate buffer (pH 6.8) in the absence of lecithin (A), and with lecithin (50 μg/ml) added (B). Emission monitored at 485 nm.

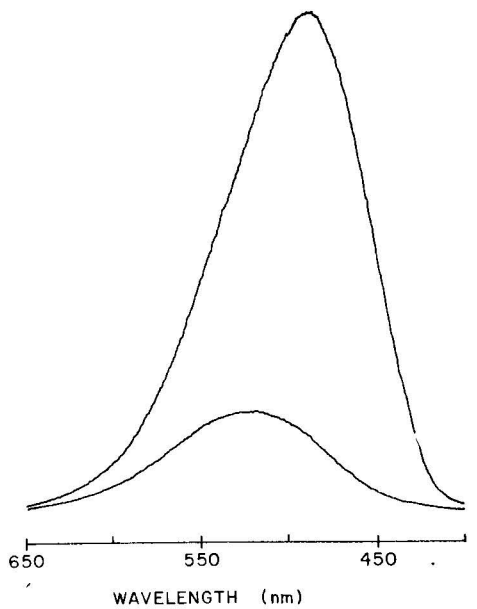


Fig. 2. Emission spectra of ANS (5×10^{-4} *M*) in 0.1 *F* phosphate buffer (pH 6.8) in the absence of lecithin (lower curve), and with lecithin (50 μg/ml) added (upper curve). The excitation wavelength used was 365 nm.

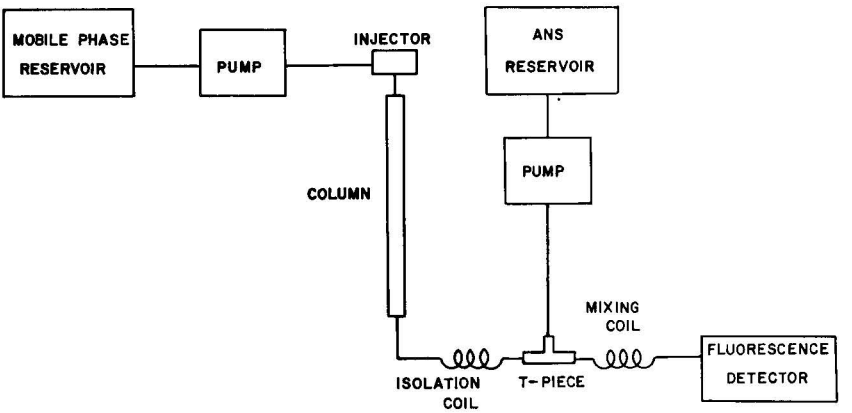


Fig. 3. Schematic diagram of chromatographic system.

nal. With a mercury lamp source, the 365 or 405 nm excitation lines should result in the most sensitive detection.

Buffer pH was found to have only a minor influence on the recorded spectra. Addition of organic solvents reduces the magnitude of the lipid enhancement phenomenon by raising the level of fluorescence in the non-enhanced solution. A methanol concentration of around 40% (v/v) is the maximum amount which will still allow a useful enhancement effect to be observed.

Detector system

An aqueous solution is necessary for the fluorescence enhancement of ANS in the presence of polar lipids, while chromatography of these compounds appears best accomplished in organic mobile phases[13]. For this reason, chromatography was carried out with methanol as the mobile phase, with subsequent addition of aqueous ANS to the column effluent for detection.

The experimental set-up which accomplishes this goal is shown in Fig. 3. The mobile phase is delivered by a syringe pump (Series 4100; Varian Aerograph, Walnut Creek, Calif., U.S.A.) to the chromatographic column. The column consists of ammonium hydroxide-treated Corasil II (Waters Assoc., Milford, Mass., U.S.A.)[14] packed into a 90 cm × 2.1 mm I.D. seamless, stainless-steel tube terminated with a stainless-steel frit of 5-μm average porosity (Crawford, Cleveland, Ohio, U.S.A.). A high-pressure reciprocating piston pump (M 6000; Waters Assoc.) was employed to deliver a phosphate buffer solution of the fluorescent dye to the T-piece and mixing coil. An isolation coil was used to separate the chromatographic column from the T-piece. This was found necessary to prevent the ANS solution from backing up into the column during injection of samples.

Presumably, micelles are formed upon the elution of lipids from the column into the aqueous solution. ANS, which partitions into the nonpolar interior of the micelle, exhibits enhanced fluorescence and is detected by the fluorescence detector (Model 1209; Laboratory Data Control, Riviera Beach, Fla., U.S.A.). The excitation source of this detector is an UV lamp with broad emission from 300–400 nm peaking at 365 nm. A sharp UV cut-off filter allows transmission of the ANS fluorescence to the

photodetector while blocking excitation light. The broadband nature of the detector response minimizes effects of wavelength shifts in fluorescence emission.

Chromatographic measurements

Several detector variables were investigated by performing chromatography of standard polar lipids. Pure standards of phosphatidylcholine dipalmitoyl, cardiolipin, and sphingomyelin were obtained from Sigma (St. Louis, Mo., U.S.A.), and gangliosides were purchased from Analabs (North Haven, Conn., U.S.A.). A mobile phase of 1% ammonium hydroxide in methanol was used to minimize tailing of these very polar compounds. The mobile phase flow-rate of 0.33 ml/min was chosen as a reasonable compromise between chromatographic efficiency and analysis time. A flow-rate of 3.0 ml/min for the buffered ANS solution was found to be sufficient in diluting the mobile phase, while still allowing a high concentration of lipid for detection.

Physical interactions between the fluorescent dye and a lipid micelle are likely to depend on the conditions of the experiment such as temperature, pH, presence of various ions, other compounds, etc. Fig. 4 demonstrates the dependence of the detector response (peak heights) for standard lipids upon pH. While there is no great pH dependence, a switch from the ANS solution in phosphate buffer to pure water resulted in a substantially smaller response. No studies of the effects of temperature or various ions were performed.

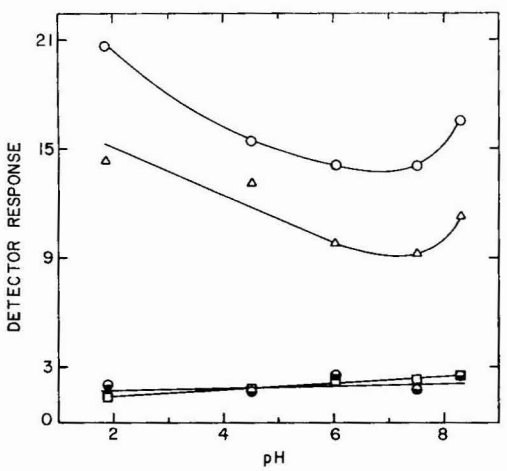


Fig. 4. Dependence of detector response on pH. Conditions: 1×10^{-3} *M* ANS in 0.1 *F* phosphate buffer; flow-rate, 3.0 ml/min. Data reflect the pH of solution actually entering the fluorescence detector. Detector responses were measured as relative peak heights of the solutes chromatographed (approximately 30 μg each). ○, Phosphatidylcholine; △, sphingomyelin; □, cardiolipin; ◒, gangliosides.

The effect of ANS concentration on the detector response was also investigated. Fig. 5 illustrates the corresponding dependence using phosphatidylcholine as the standard solute. The optimum concentration of the fluorescent agent for maximum sensitivity under these conditions was 5×10^{-4} *M*. A possible explanation for the decreased response at high ANS concentration may be normal fluorescent self-quenching effects, or a disruption of the micelle by ANS.

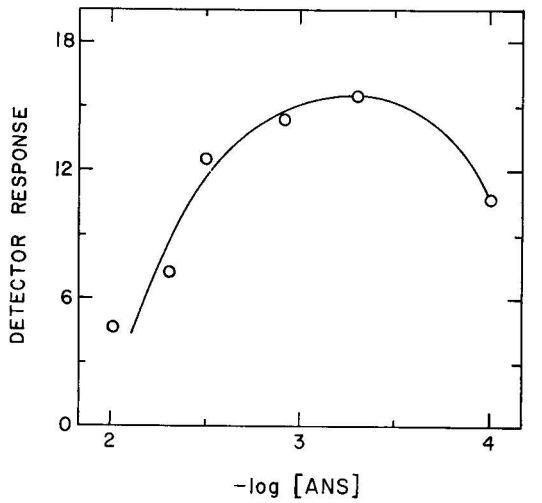


Fig. 5. Dependence of detector response on the concentration of ANS added through T-piece. Conditions: solute, 32 μg phosphatidylcholine; ANS was dissolved in 0.1 F ammonium phosphate buffer, pH 4.55.

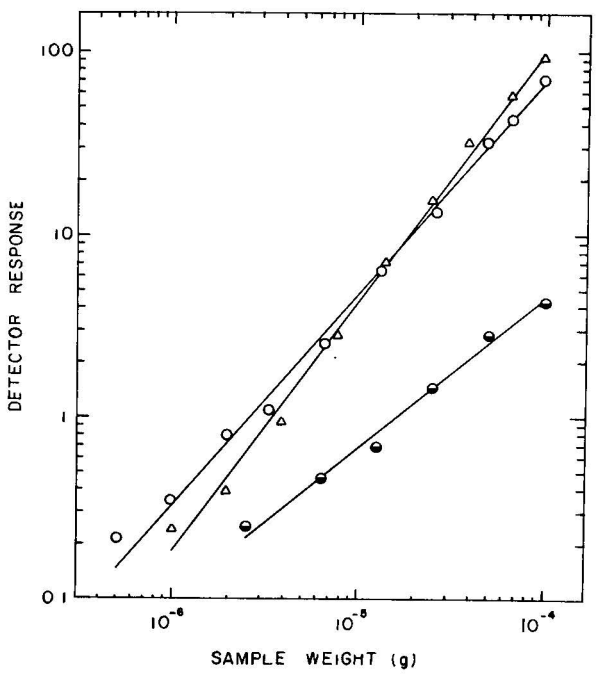
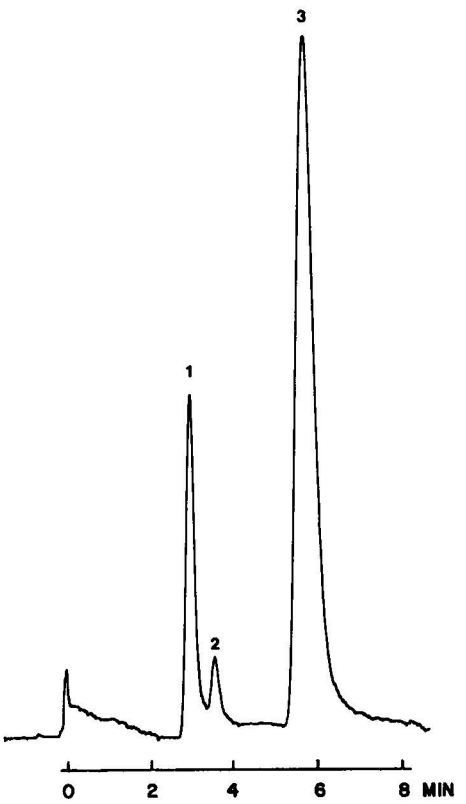


Fig. 6. Linearity of detector response for various standard solutes. Conditions: 5×10^{-4} M ANS dissolved in 9.4×10^{-2} F H_3PO_4 (pH 7.00). ○, Phosphatidylcholine; △, sphingomyelin; ◒, gangliosides.

Fig. 6 demonstrates that different lipids yield different responses, but the relationship between peak height (detector response) and sample weight injected is essentially linear. The relation of response to solute structure has not been extensively studied as yet. However, the compounds which respond all have very polar head groups, and would be expected to form micelles easily.

A typical chromatogram of a mixture of standard phospholipids is shown in Fig. 7. It demonstrates that even with non-standard chromatographic conditions a useful separation is possible with the present system. A chromatogram of the polar lipids in a 1-ml Folch extract of human blood plasma[15] is shown in Fig. 8. No identification of the constituents of the plasma sample was carried out.



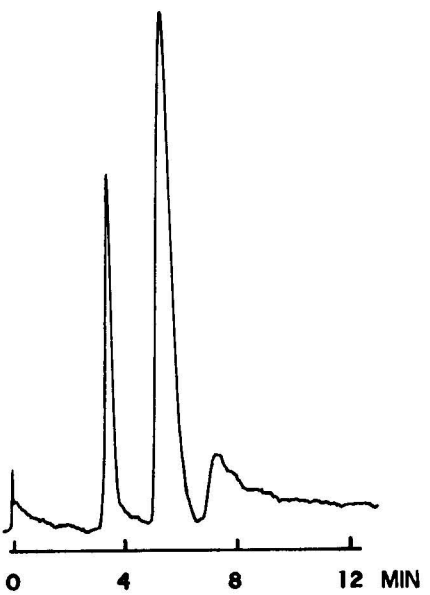


Fig. 7. Chromatogram of standard phospholipids. Conditions: mobile phase, 1% ammonium hydroxide in methanol; flow-rate, 0.33 ml/min; ANS solution, same as for Fig. 6. 1 = Cardiolipin (84 μg); 2 = solvent impurity; 3 = phosphatidylcholine (29 μg).

Fig. 8. Chromatogram of polar lipids of human plasma. Conditions, same as in Fig. 7.

DISCUSSION

The inherent sensitivity of fluorescence measurements will undoubtedly cause a wider use of LC fluorescence monitors in the near future for detection of both naturally fluorescent and selectively derivatized compounds. The detection principle described

in this work can serve as a valuable addition to high-sensitivity detection. Although it has thus far been demonstrated for specific cases, more systematic studies of fluorescent dyes and their properties should lead to further applications of this and related principles in the detection of other classes of compounds.

This work demonstrates that even at relatively non-optimized detection conditions, fluorescence enhancement detection has led to a significant improvement in sensitivity for polar lipids compared to hitherto available continuous detection systems. Whereas different lipids studied as model solutes in this work possess different (and yet, comparable) response factors, a linear relationship between detector response and solute concentration was maintained. A practical sensitivity limit for the system as constructed was approximately 500 ng of phosphatidylcholine. This amount corresponds to a detection limit of 17 ng/sec for a peak of 29-sec width at half-height.

As previously indicated, the present system is a compromise between chromatography and successful detection. This situation might be improved through the use of mobile phases containing tetrahydrofuran and dioxane which are less polar than methanol but are still water-miscible. Such solvents would ideally show minimal interference with the fluorescence enhancement effect while expanding the range of useful chromatographic separations. Another approach would be the use of a system analogous to the reversed-phase system described by Arvidson[16] for the separation of egg-yolk lecithins on alkylated Sephadex with a methanol–water mobile phase. This arrangement might change the chromatographic separation as well as the necessary amount of ANS buffer solution added at the end of the column. The large dilution (10:1) of column effluent currently necessary is one unfortunate sensitivity-reducing factor in the system, which might be improved by such a scheme. However, no mechanically stable analog of alkylated Sephadex suitable for high-pressure LC is available at present.

In future efforts to improve sensitivity it will be necessary to concentrate primarily on reducing the low-frequency baseline noise, which is the major limitation of the currently existing system. The main contributors to such noise are instabilities in solvent delivery by the pumps (pulses) and non-instantaneous mixing of the two solvent streams in the T-piece. Further refinement in design of the system should reduce such problems, and thus allow more significant utilization of the available sensitivity of this detection principle.

Another, but perhaps less attractive alternative to alleviating the problems of incompatibility of the mobile phase composition with detection conditions could be the design of a transport detection system, similar to that described by Werthessen *et al.*[17].

Finally, it should be emphasized that the fluorescence enhancement effect that forms the basis of detection shown in this work should be looked upon as an example of the many fluorescence-related phenomena[18] that can be potentially utilized in LC detection of non-fluorescent compounds.

ACKNOWLEDGEMENT

This work was supported by the research grant No. GM-20671-02 from the National Institute of General Medical Sciences, U.S. Public Health Service.

REFERENCES

1 S. Udenfriend, S. Stein, P. Böhlen, W. Dairmann, W. Leimgruber and M. Weigele, *Science*, 178 (1972) 871.
2 W. Voelter and K. Zech, *J. Chromatogr.*, 112 (1975) 643.
3 K. Aitzetmüller, *J. Chromatogr.*, 113 (1975) 231.
4 J. E. Evans and R. H. McCluer, *Biochim. Biophys. Acta*, 270 (1972) 565.
5 H. D. Durst, M. Milano, E. J. Kikta, Jr., S. A. Connelly and E. Grushka, *Anal. Chem.*, 47 (1975) 1797.
6 F. B. Jungalwala, R. J. Turel, J. E. Evans and R. H. McCluer, *Biochem. J.*, 145 (1975) 517.
7 A. Stolyhwo, O. S. Privett and W. L. Erdahl, *J. Chromatogr. Sci.*, 11 (1973) 263.
8 I. Tasaki, A. Watanabe, R. Sandlin and L. Carnay, *Proc. Nat. Acad. Sci. U.S.*, 61 (1968) 883.
9 D. F. H. Wallach, E. Ferber, D. Selin, E. Weidekamm and H. Fischer, *Biochim. Biophys. Acta*, 203 (1970) 67.
10 N. E. Schore and N. J. Turro, *J. Amer. Chem. Soc.*, 97 (1975) 2488.
11 B. Bhattacharyya and J. Wolf, *Arch. Biochem. Biophys.*, 167 (1975) 264.
12 R. F. Chen, *Arch. Biochem. Biophys.*, 120 (1967) 609.
13 W. W. Christie, *Lipid Analysis*, Pergamon, Oxford, p. 176.
14 A. Stolyhwo and O. S. Privett, *J. Chromatogr. Sci.*, 11 (1973) 20.
15 J. Folch, M. Lees and G. H. Sloane-Stanley, *J. Biol. Chem.*, 226 (1957) 497.
16 G. A. E. Arvidson, *J. Chromatogr.*, 103 (1975) 201.
17 N. T. Werthessen, J. R. Beall and A. T. James, *J. Chromatogr.*, 46 (1970) 149.
18 C. M. O'Donnell and T. N. Solie, *Anal. Chem.*, 48 (1976) 175R.

Journal of Chromatography, 126 (1976) 327–345
© Elsevier Scientific Publishing Company, Amsterdam — Printed in The Netherlands

CHROM. 9453

VARIABLES AFFECTING PRECISION AND ACCURACY IN HIGH-PERFORMANCE LIQUID CHROMATOGRAPHY

STEPHEN R. BAKALYAR and RICHARD A. HENRY
Spectra-Physics Inc., 2905 Stender Way, Santa Clara, Calif. 95051 (U.S.A.)

SUMMARY

Quantitative analysis by peak height or peak area measurement using a UV photometric detector can be performed with a high degree of precision, by both isocratic and gradient methods, if variables such as mobile phase composition and flow-rate are carefully controlled.

If flow control is poor but composition can be maintained precisely, peak height measurement yields better quantitative results because height is relatively independent of flow-rate. This may be a common condition with older liquid chromatography pumping systems. If flow control is good but solvent composition cannot be maintained precisely, peak area measurement is better because area is relatively independent of composition. This may be a common condition in adsorption chromatography where trace water and polar contaminants in the mobile phase are difficult to control, and in any type of affinity chromatography where mobile phases comprise volatile solvents.

Retention time is strongly affected by both composition and flow-rate, but retention time precision can be inherently better in gradient elution than in isocratic analysis.

INTRODUCTION

Analytical precision and accuracy in high-performance liquid chromatography (HPLC) depend on the reproducibility of peak retention time, peak height, and peak area. This peak behavior is a function of many chromatographic variables, including sample size, mobile phase composition, mobile phase flow-rate, and column temperature.

In this study, mobile phase composition and flow-rate were systematically varied in both isocratic and gradient analysis, while sample size and column temperature were held constant. The resulting peak behavior was observed and compared with theory. General guidelines were developed for quantitation techniques, depending on the equipment available.

Theory suggests that the composition and flow dependence of peak behavior will be different for peaks with different capacity factors (k') and for packings with

different chemical functionality. Therefore, the experiments attempted to define relationships for peaks of widely varying k' values on the most commonly used new packing, hydrocarbon reversed phase.

EXPERIMENTAL

Columns, solvents, and samples

250 × 3.1 mm I.D. Type 316 stainless-steel columns (Li-Chroma I.D.™ tubing; Handy and Harman, Norristown, Pa., U.S.A.) were packed by a partial balanced density slurry technique[1]. The packing used was 10-μm Spherisorb™ ODS, a totally porous spherical material with covalently bonded octadecyl functionality (Spectra-Physics, Santa Clara, Calif., U.S.A.).

Mobile phases were prepared from distilled-in-glass solvents (Burdick and Jackson Labs., Muskegon, Mich., U.S.A.). No drying or adjustment of water content was undertaken. Water was glass distilled. Trace organics in the water were not removed. All solvents were degassed prior to use.

Multicomponent samples were prepared by adding enough of each pure component to a 1:1 mixture of water and methanol to produce approximately equal peak areas. The approximate concentration was 0.1 mg/ml for each component.

Control of flow, composition, temperature, and sample volume

A Spectra-Physics Model 3500B gradient liquid chromatograph was used. It employs a continuous-flow, reciprocating-piston pump for Solvent A and an identical but independent one for Solvent B. Each pump has its own electronic flow feedback system for precise flow control. The two pump outlets are mixed at high pressure in a dynamically stirred chamber. The mobile phase composition and the flow-rate through the column are determined, respectively, by the ratio and the sum of the A and B pump flow-rates. This two-pump architecture has become the most common type in HPLC.

The flow feedback restrictors were placed in a 3-l insulated container of water to eliminate minor flow changes caused by any large ambient temperature fluctuations in the laboratory. Under these conditions, the flow-rate can be maintained to $\pm$ 0.2% or better. The temperature dependence of flow-rate produced by the pump due to the feedback system is typically 1% change in flow per °C change due to a combination of viscosity, pressure, and compressibility effects in the flow restrictor and the chromatographic column. The flow-rate was volumetrically measured at each setting to confirm accuracy.

The Model 3500B forced-air oven controlled column temperature at 40.0 $\pm$ 0.1°. No attempt was made to compensate for changes in the internal temperature of the column due to mobile phase composition and flow-rate changes[2].

The sample injector employed was of the 10-μl external loop type. The loop was filled slowly, taking care not to form microbubbles inside the loop. Volumetric precision was determined independently to be about 0.05% relative standard deviation.

The detector was a Spectra-Physics Model SP 8200 multiple-wavelength UV photometer operated at 254 nm.

Measurement of peak retention time, height, and area

Peak behavior was measured by computing integrators —the Minigrator® and the SP 4000™ Chromatography Data System (Spectra-Physics)—which are capable of retention time, peak height, and peak area determination with a precision of better than 0.1 %[3]. The SP 4000 built-in program for calculating relative standard deviations of peak areas from several runs was also used.

Selection of chromatographic conditions

Fig. 1 shows the chromatogram and operating conditions of the isocratic analysis on the Spherisorb ODS column. The conditions were chosen to be representative of current practice. For example, although the 7,000 p.s.i. (478 bar) capability of the chromatograph would permit a faster flow-rate and faster analysis, most workers continue to operate in the 1–2 ml/min range. Sample components and solvent composition were chosen to provide a range of k' from 0–8 in order to provide data on the peak behavior for this variable.

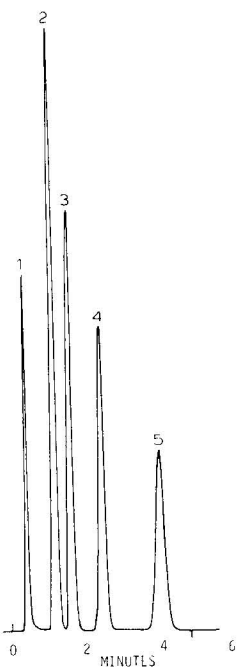


Fig. 1. Isocratic analysis. Column, 250 × 3.1 mm I.D.; packing, 10-μm Spherisorb ODS; solvent, water–methanol (1:1); flow-rate, 2.00 ml/min; pressure, 1840 p.s.i.; temperature, 40°; detector, Model SP 8200 multiple-wavelength UV photometer operated at 254 nm; sample size, 10 μl. 1 = Tartrazine; 2 = methyl *p*-hydroxybenzoate; 3 = ethyl *p*-hydroxybenzoate; 4 = propyl *p*-hydroxybenzoate; 5 = butyl *p*-hydroxybenzoate.

Fig. 2 shows the chromatogram of the gradient analysis on Spherisorb ODS. Again, conditions are representative of current practice. The speed of the analysis can be improved by starting the run at 30 %B. However, the intention here was to provide large k' values. An extra component, benzyl alcohol, was added to the test

TABLE I

EFFECT OF FLOW-RATE VARIATIONS ON RETENTION TIME, PEAK AREA AND PEAK HEIGHT IN ISOCRATIC ANALYSIS

Compound	*k'*	*Retention time (sec)*				*Peak area (integrator counts*)*				*Peak height (scale divisions)*			
		Flow-rate (ml/min)				*Flow-rate (ml/min)*				*Flow-rate (ml/min)*			
		2.00	*1.92*	*1.84*	*1.76*	*2.00*	*1.92*	*1.84*	*1.76*	*2.00*	*1.92*	*1.84*	*1.76*
Tartrazine	0	26	27	28	30	782	815	864	903	1245	1260	1299	1323
Methyl *p*-hydroxybenzoate	1.8	73	76	80	85	1800	1865	1974	2061	2057	2058	2097	2127
Ethyl *p*-hydroxybenzoate	2.8	98	103	109	115	1686	1749	1845	1932	1553	1549	1572	1588
Propyl *p*-hydroxybenzoate	4.7	147	154	164	174	1655	1714	1811	1901	1090	1080	1093	1099
Butyl *p*-hydroxybenzoate	8.3	242	254	271	289	1491	1546	1632	1710	620	615	620	620

* 1 integrator count = 0.2 mV sec.

TABLE II

EFFECT OF COMPOSITION VARIATIONS ON RETENTION TIME, PEAK AREA AND PEAK HEIGHT IN ISOCRATIC ANALYSIS

Compound	*k'*	*Retention time (sec)*					*Peak area (integrator counts)*					*Peak height (scale divisions)*				
		Composition (%B)					*Composition (%B)*					*Composition (%B)*				
		50	*49*	*48*	*47*	*46*	*50*	*49*	*48*	*47*	*46*	*50*	*49*	*48*	*47*	*46*
Tartrazine	0	26	26	26	26	26	799	779	789	782	793	1259	1255	1277	1279	1250
Methyl *p*-hydroxybenzoate	1.8	74	76	79	82	86	1788	1795	1796	1810	1820	2028	2000	1978	1935	1857
Ethyl *p*-hydroxybenzoate	2.8	100	103	110	117	124	1675	1680	1682	1687	1698	1520	1480	1438	1372	1303
Propyl *p*-hydroxybenzoate	4.8	151	159	171	186	203	1644	1648	1649	1654	1665	1055	1012	959	890	825
Butyl *p*-hydroxybenzoate	8.6	250	268	294	327	363	1479	1482	1485	1489	1494	602	557	515	468	420

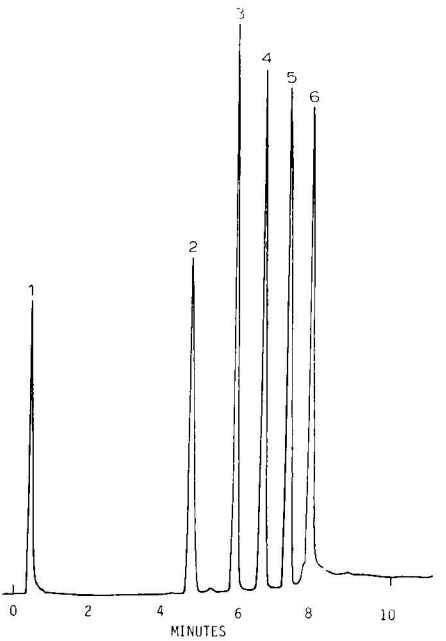


Fig. 2. Gradient analysis. Column conditions, same as for Fig. 1, except: Solvent A, water; Solvent B, methanol; gradient profile, 0 → 99%B in 10 min. 1 = Tartrazine; 2 = benzyl alcohol; 3 = methyl *p*-hydroxybenzoate; 4 = ethyl *p*-hydroxybenzoate; 5 = propyl *p*-hydroxybenzoate; 6 = butyl *p*-hydroxybenzoate.

sample for this analysis. The small peak at 5.3 min and the small peaks which interfere with the last major peak are impurities in the water which are concentrated at the top of the column and subsequently eluted by the gradient. These impurities can be removed, but were intentionally allowed in order to study their effect on the precision of observed peak behavior.

RESULTS

Isocratic analysis: Effects of flow-rate variations

Table I shows the effect of flow-rate variations on retention time, peak area, and peak height, respectively. The 2.00 ml/min is the reference flow-rate, the other three representing successively 4, 8, and 12% reductions from the reference.

Fig. 3 presents the following data for one compound, propyl *p*-hydroxybenzoate: per cent change in retention time, peak area, and peak height *versus* per cent change in flow-rate. The other compounds with different k' values exhibited similar behavior.

Results show that retention time and peak area are inversely proportional to flow-rate, while peak height is relatively independent of flow-rate.

Isocratic analysis: Effects of composition variations

Table II shows the effect of composition variations on retention time, peak area, and peak height, respectively. The 50.0%B is reference composition, the other

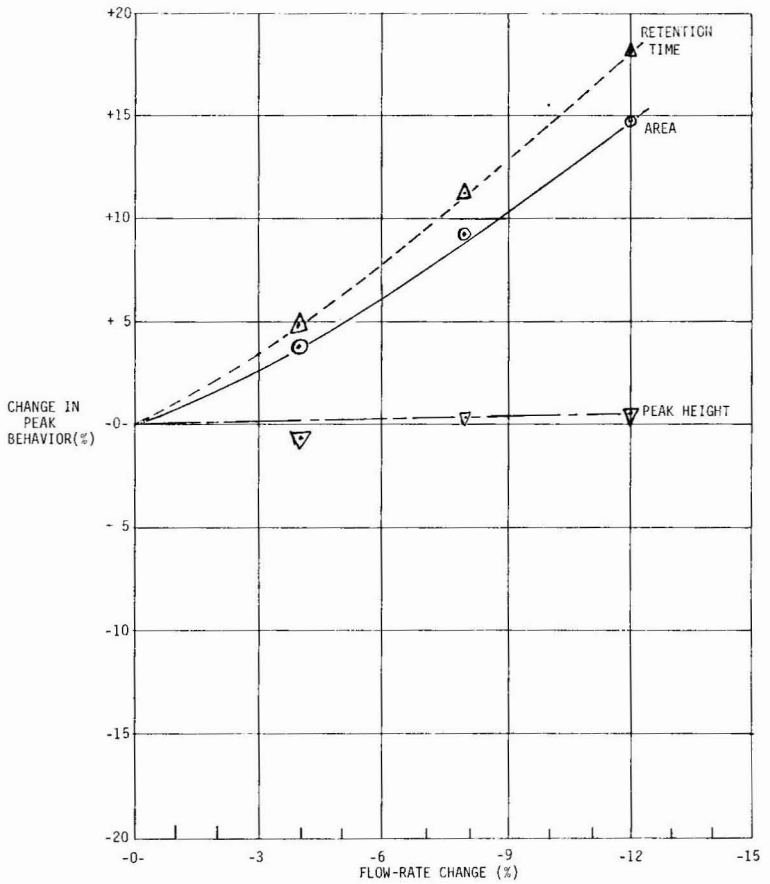


Fig. 3. Retention time, peak area, and peak height *versus* flow-rate in isocratic analysis.

four representing successively 2, 4, 6, and 8 rel. % reductions from the reference. Since the absolute value of composition itself is expressed in per cent, the following nomenclature clarification is made: 2% relative reduction from 50%B means 2% of 50% = 1% absolute reduction, or a drop from 50 to 49%B.

Fig. 4 presents peak area data for propyl *p*-hydroxybenzoate as a graph of per cent change in composition; other compounds with different k' values behaved the same. Fig. 4 also presents the retention time and peak height data for the other four compounds.

Results show that retention time is inversely proportional to composition. However, the dependence increases with increasing k'. Peak height is directly proportional to composition. However, the dependence increases with increasing k'. Peak area is independent of composition for all k' values.

Gradient analysis: Effects of flow-rate variations

Table III shows the effect of flow-rate variations on retention time, peak area, and peak height, respectively. The 2.00 ml/min is the reference flow-rate, the other four representing successively 2, 4, 6, and 8% reductions from the reference.

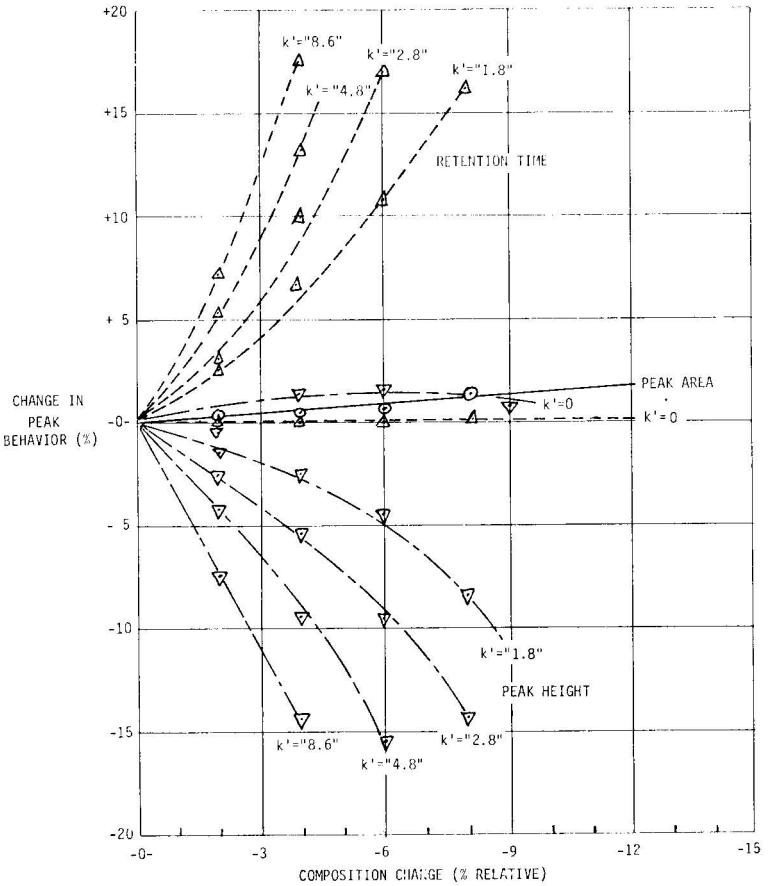


Fig. 4. Retention time, peak area, and peak height *versus* composition in isocratic analysis.

Fig. 5 presents peak area and peak height data for propyl *p*-hydroxybenzoate as a graph of per cent change in retention time, peak area, and peak height *versus* per cent change in flow-rate; it also presents retention time data for several other components. The peak height data are only for the adjusted 1.84 ml/min conditions as noted in Table III.

Results show that retention time is inversely proportional to flow-rate. However, the dependence decreases with increasing k'. Peak area is inversely proportional to flow-rate and peak height is relatively independent of flow-rate, for all k' values.

Gradient analysis: Effects of composition variations

Table IV shows the effect of composition variations on retention time, peak area, and peak height, respectively. The %B composition of 49.5, 5 min after the start of the gradient run from 0–99 %B in 10 min, is the reference composition, the other three representing successively 3, 6, and 9 rel. % reductions from the reference. All compositions are expressed as %B 5 min after the start of the run.

TABLE III

EFFECT OF FLOW-RATE VARIATIONS ON RETENTION TIME, PEAK AREA AND PEAK HEIGHT IN GRADIENT ANALYSIS

Compound	*k'*	*Retention time (sec)*						*Peak area (integrator counts)*						*Peak height (scale divisions)*					
		Flow-rate (ml/min)						*Flow-rate (ml/min)*						*Flow-rate (ml/min)*					
		2.00	*1.96*	*1.92*	*1.88*	*1.84*	*1.84**	*2.00*	*1.96*	*1.92*	*1.88*	*1.84*	*1.84**	*2.00*	*1.96*	*1.92*	*1.88*	*1.84*	*1.84**
Tartrazine	0	27	28	29	29	30	30	755	770	789	810	830	820	999	990	989	993	997	985
Benzyl alcohol	9.5	283	287	293	297	302	314	1252	1275	1301	1330	1356	1356	1150	1167	1190	1213	1239	1163
Methyl *p*-hydroxybenzoate	12.2	355	359	365	368	373	393	1690?	1717	1746	1786	1824	1835	1935	1979	2019	2059	2095	1995
Ethyl *p*-hydroxybenzoate	13.8	400	404	409	412	417	442	1514	1535	1565	1601	1633	1642	1770	1813	1850	1885	1915	1827
Propyl *p*-hydroxybenzoate	15.3	440	444	448	452	456	486	1581	1594	1606	1641	1695	1690	1705	1747	1785	1817	1840	1759
Butyl *p*-hydroxybenzoate	16.6	475	478	483	486	490	524	1811	1841	1875	1915	1955	1998	1630	1669	1700	1730	1753	1673

* Conditions adjusted to provide a gradient program, in volumetric terms, equal to the reference run at 2.00 ml/min. The adjusted conditions are 0–99%B in 11 min, compared to the reference conditions of 0–99%B in 10 min.

TABLE IV

EFFECT OF COMPOSITION VARIATIONS ON RETENTION TIME, PEAK AREA AND PEAK HEIGHT IN GRADIENT ANALYSIS

Compound	*k'*	*Retention time (sec)*				*Peak area (integrator counts)*				*Peak height (scale divisions)*			
		Composition (%B) at 5 min				*Composition (%B) at 5 min*				*Composition (%B) at 5 min*			
		49.5	*48.0*	*46.5*	*45.0*	*49.5*	*48.0*	*46.5*	*45.0*	*49.5*	*48.0*	*46.5*	*45.0*
Tartrazine	0	27	28	27	27	756	757	748	754	993	1008	1008	1010
Benzyl alcohol	9.3	279	286	287	293	1247	1252	1244	1255	1163	1150	1108	1105
Methyl *p*-hydroxybenzoate	12.0	350	359	363	371	1673	1680	1672	1694	1951	1989	1887	1873
Ethyl *p*-hydroxybenzoate	13.6	395	405	411	420	1495	1504	1500	1514	1780	1765	1723	1707
Propyl *p*-hydroxybenzoate	15.2	436	446	454	465	1550	1562	1562	1574	1713	1707	1667	1640
Butyl *p*-hydroxybenzoate	16.4	471	482	492	503	1789	1805	1733	1760	1633	1623	1577	1558

Fig. 6 presents data for propyl *p*-hydroxybenzoate as a graph of the per cent change in retention time, peak area, and peak height *versus* the relative per cent change in composition. The other compounds with different k' values exhibit similar behavior.

Results show that retention time is inversely proportional to composition, peak height is directly proportional to composition, and peak area is independent of composition.

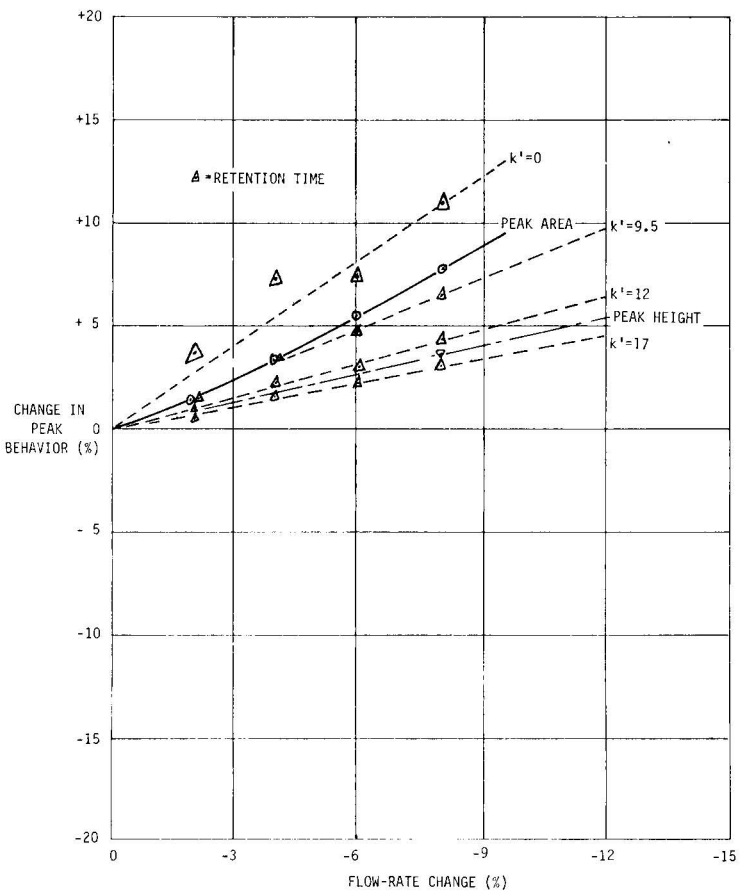


Fig. 5. Retention time, peak area, and peak height *versus* flow-rate in gradient analysis.

Precision of gradient analyses

The inherent precision of the flow-rate and the composition of the experimental system was measured by a series of gradient runs, as shown in Table V. Data show that the precision of the experiments was sufficient to validate the data obtained in the previous tables.

TABLE V

PRECISION OF RETENTION TIME AND PEAK AREA IN GRADIENT ANALYSIS

Compound	*Retention time (sec)*						*% RSD*	*Peak area (integrator counts)*						*% RSD*
	Run No.							*Run No.*						
	1	*2*	*3*	*4*	*5*	*6*		*1*	*2*	*3*	*4*	*5*	*6*	
Tartrazine	28	27	27	27	27	27	1.50	761	756	756	754	753	756	0.36
Benzyl alcohol	285	279	279	281	282	283	0.83	1249	1247	1247	1248	1251	1252	0.17
Methyl *p*-hydroxybenzoate	354	350	350	352	354	355	0.62	1677	1673	1673	1680	1684	1690	0.40
Ethyl *p*-hydroxybenzoate	398	395	395	397	399	400	0.52	1502	1495	1497	1503	1509	1514	0.48
Propyl *p*-hydroxybenzoate	438	436	435	437	439	440	0.43	1554	1550	1556	1568	1555	1581	0.75
Butyl *p*-hydroxybenzoate	472	471	470	472	474	475	0.39	1792	1789	1780	1793	1814	1811	0.74

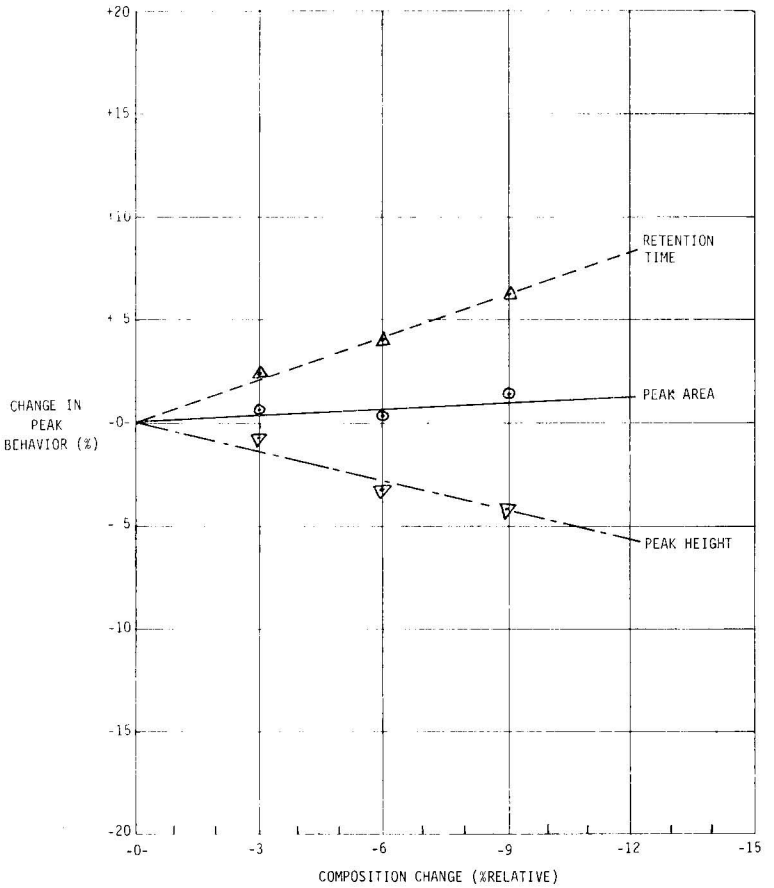


Fig. 6. Retention time, peak area, and peak height *versus* composition in gradient analysis.

DISCUSSION

Isocratic analysis

It is possible to explain the results observed in terms and equations that are familiar to the chromatographer. In the case of flow-rate dependence, peak behavior can be defined generally as follows

$$\text{Peak behavior} = f(F)$$

where F is the mobile phase flow-rate in ml/min. In the case of composition dependence, peak behavior can be defined as follows

$$\text{Peak behavior} = f(S)$$

where S is a mobile phase composition parameter intended to be directly related to

the %B of a binary solvent mixture. Since here the B solvent is always considered the stronger of the two, S may be thought of as a solvent strength parameter.

Of the different types of peak behavior studied, retention time is the easiest to understand, and is explained below.

Retention time versus flow-rate. Retention time can be expressed by the fundamental chromatography equation[4]

$$t_R = \frac{L}{u}(1 + k') \tag{1}$$

where L is column length in cm, u is mobile phase linear velocity in cm/sec, and k' is the capacity factor. u depends on the flow-rate F in ml or cm^3/sec and on the average cross-sectional area of voids between packing particles A_{xs} in cm^2

$$u = \frac{F}{A_{xs}} \tag{2}$$

A_{xs} and L are constants for a given column and k' is constant for a given sample component and mobile phase composition. Substituting eqn. 2 into eqn. 1 and grouping constants into a new constant K

$$t_R = \frac{K}{F} \tag{3}$$

For small changes, a per cent change in flow-rate causes a per cent change in retention time of the same numerical value but of opposite sign. This is consistent with the data in Fig. 3.

Retention time versus composition. Referring to eqn. 1, retention time is seen to depend on k', which is a function of mobile phase composition. The relationship of k' to composition is complex and not well understood; therefore, a nonrigorous statement will suffice as follows

$$k' = \frac{K}{S} \tag{4}$$

Substituting eqn. 4 into eqn. 1, considering L and u constant for a given column and flow-rate, and grouping constants

$$t_R = K_1 + \frac{K_2}{S} \approx \frac{K}{S} \tag{5}$$

A per cent change in composition (%B) causes a change in retention time of opposite sign. The magnitude of the change can be small or large, depending on the nature of the mobile and stationary phases, and depending on the k' of the peak. The experimental results of Fig. 4 agree with the description. The reason for the k' dependence is related to the dependence of resolution on k'[5].

Peak area versus flow-rate. In order to understand the effect of variables on peak area, it is useful to refer to the concentration profile of a component zone, independent of detector considerations, as illustrated in Fig. 7. In this concentration-

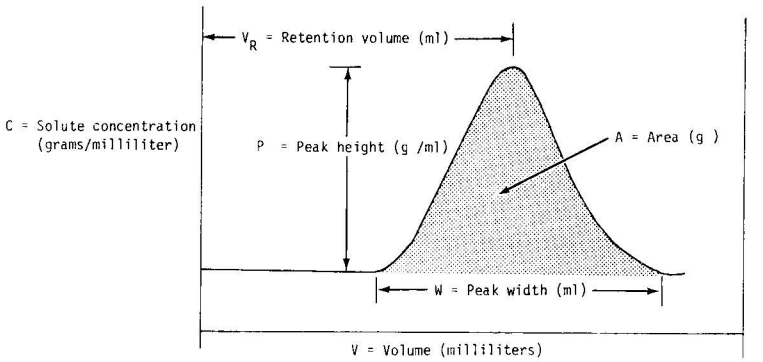


Fig. 7. Volumetric peak behavior.

volumetric type of description, the area of the peak can be expressed as the integral of concentration C with respect to volume, from the volume V_1 at peak onset to the volume V_2 at peak end

$$A_V = \int_{V_1}^{V_2} C \, dV \tag{6}$$

The concentration profile may change shape due to any number of causes, but the total weight of sample component remains constant, and thus the peak area remains constant. For example, the peak may become taller and narrower due to a decreased k' caused by a stronger mobile phase. Or it may become shorter and wider due to a decrease in efficiency caused by increased flow-rate. But the area, expressed in terms of (g/ml) (ml) = g, remains unchanged for a given column and is independent of both flow-rate and composition

$$A_V = K \tag{7}$$

Because we must depend upon a detector to monitor the compounds as they emerge from the column, Fig. 8 defines a peak in terms of detector signal and time as opposed to the terms of concentration and volume in Fig. 7. The detected area of the peak is

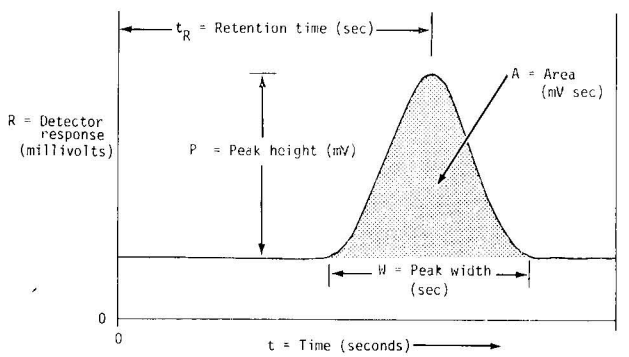


Fig. 8. Detected peak behavior.

expressed as the integral of detector signal R with respect to time, from the time t_1 at peak onset to the time t_2 at peak end

$$A = \int_{t_1}^{t_2} R \, dt \tag{8}$$

The photometric detector instantaneous signal R in mV is directly proportional to the instantaneous solute concentration C. Since there is a one-to-one correspondence between R and C, detected peak area will behave the same as actual peak area insofar as detector response is concerned; however, eqn. 3 shows that retention time is inversely proportional to flow-rate. This applies to all retention times, including peak onset and end. Thus, the time $t_2 - t_1$ over which area integration takes place expands or contracts inversely with flow-rate changes. As a consequence, eqn. 7, expressing the volumetric area dependence on flow-rate, must be modified to convert it to an expression for detected area dependence on flow-rate. The modification simply takes into account the inverse dependence of retention time on flow-rate

$$A = \frac{K}{F} \tag{9}$$

For small changes, a per cent change in flow-rate causes a per cent change in peak area of the same numerical value but of opposite sign. The experimental results of Fig. 3 agree. It is obvious that this conclusion would be different for a detector whose signal is proportional to mass rate instead of concentration.

Peak area versus composition. When mobile phase composition is changed to a weaker eluting strength, peaks elute slower and occupy more volume. At constant flow-rate, a direct translation can be made from C to R and from dV to dt in eqns. 6 and 8. As a consequence, eqn. 7, which expresses the dependence of volumetric area on composition, also applies to detected area

$$A = K \tag{10}$$

Peak area is independent of mobile phase composition. This was experimentally observed in Fig. 4.

Peak height versus flow-rate. Fig. 7 shows that the peak height is the maximum concentration of the peak, and Fig. 8 shows it as the maximum instantaneous detector response

$$P_V = C_{max} \tag{11}$$

$$P = R_{max} \tag{12}$$

R_{max} is independent of how fast the peak goes through the detector, except for time constant considerations discussed later. However, C_{max} has a small flow dependency related to column efficiency factors. By approximating the peak as a triangle of height P, width W, and area A

$$P_V = \frac{2A}{W} \tag{13}$$

Per eqn. 7 the volumetric area is constant, so we can express eqn. 13 as

$$P_V = \frac{K}{W} \tag{14}$$

Peak width W is related to efficiency by the definition of plate height H, the degree of zone spreading per unit length of column[6]

$$H = \frac{\sigma^2}{L}, \quad \sigma = (LH)^{0.5} \tag{15}$$

Since one σ is approximately $W/4$, we can substitute into eqn. 15 and group constants

$$W = KH^{0.5} \tag{16}$$

Most columns have a plate height dependence on flow-rate which is approximated by the empirical expression

$$H = Du^n \tag{17}$$

where D and n are constants for a given column and mobile phase[7]. Normally $0.3 < n < 0.6$. Substituting eqn. 17 into eqn. 16, grouping constants, and using the 0.6 value for n since it represents the worst case of flow dependence

$$W = Ku^{0.3} \tag{18}$$

Substituting eqn. 18 into eqn. 14, using the relationship between linear velocity and flow-rate expressed in eqn. 2, and grouping constants

$$P_V = \frac{K}{F^{0.3}} \tag{19}$$

This expresses the relationship between flow-rate and peak height when the latter is in concentration terms as in eqn. 11. Since there is a one-to-one correspondence between R and C, the relationship also applies in detector response terms

$$P = \frac{K}{F^{0.3}} \tag{20}$$

A per cent change in flow-rate causes a much smaller change in observed peak height of opposite sign. For example, a 10% reduction in flow-rate causes a 3% increase in peak height. This is consistent with the experimental results in Fig. 3, which shows a 1% peak height increase for a 10% flow reduction.

Peak height versus composition. It is well known that peak height, peak width, and retention time change dramatically with composition. Eqn. 14 states that the height in concentration is inversely proportional to the width in volume. This relationship is also true for detector signal and time, at constant flow-rate

$$P = \frac{K}{W} \tag{21}$$

The well known zone-spreading equation implies a direct relationship between width and retention time[8], since N is constant for all retention times.

$$N = 16\left(\frac{t_R}{W}\right)^2 \tag{22}$$

$$W = Kt_R \tag{23}$$

Substituting eqn. 23 into eqn. 21

$$P = \frac{K}{t_R} \tag{24}$$

Eqn. 5 expressed t_R in terms of S

$$t_R = \frac{K}{S} \tag{5}$$

Substituting eqn. 5 into eqn. 24

$$P = KS \tag{25}$$

A per cent change in composition causes a corresponding change in peak height. This was experimentally observed in Fig. 4. As with retention time as a function of composition, a family of curves is produced.

Gradient analysis

The previously derived isocratic relationships can be easily modified to describe peak behavior in gradient analysis.

Retention time versus flow-rate. As in isocratic analysis, a reduction in flow-rate during gradient elution causes an increase in retention time. The isocratic expression

$$t_R = \frac{K}{F} \tag{3}$$

must be modified, however, for gradient analysis because there are some important differences. In gradient analysis, composition is not constant and the instantaneous k' for each peak decreases during the run. As an oversimplified but instructive model, consider that a peak eluting with $t_R = 10$ min is not migrating at all during the first 9 min of the run. During this time, flow changes have no effect on t_R. Only during the last minute, when the peak is migrating, do flow changes affect t_R. A 10% flow-rate change causes only a 1% retention time change. This behavior is roughly approximated by the empirical expression

$$t_R = \frac{K}{F/(1 + k')} \tag{26}$$

At $k' = 0$ the numerical value of the retention time change equals that of the flow-rate change, and eqn. 26 reduces to eqn. 3. At large k' values there is less flow de-

pendence of retention time. This relationship was experimentally observed in Fig. 5 and has often been seen in published data[9] without explanation.

Retention time versus composition. The purpose of gradient elution is to reduce retention time by increasing solvent strength during the run. Eqn. 5, which expressed the inverse dependence of retention time on composition for isocratic analysis, also applies to gradient operation

$$t_R = \frac{K}{S} \tag{5}$$

A percent change in composition causes a change in retention time of opposite sign. The magnitude of the change can be small or large, but for a given column and set of conditions it is relatively constant for any compound. This was observed in Fig. 6. This k' independence is in contrast to the relationships in Fig. 4. Gradient operation has a leveling effect, which makes all compounds behave as though they had the same k' value.

Peak area versus flow-rate. Eqn. 9 expressed the inverse dependence of peak area on flow-rate in isocratic analysis. Eqn. 10 showed that area is independent of composition. The fact that composition changes throughout the run does not change the above relationships, so eqn. 9 is valid

$$A = \frac{K}{F} \tag{9}$$

For small changes, a per cent change in flow-rate causes a per cent change in peak area of the same numerical value but of opposite sign. This was experimentally observed in Fig. 5.

Peak area versus composition. Eqn. 10 expressed the peak area independence of mobile phase composition in isocratic operation. All of the arguments used to deduce this relationship also apply to the gradient mode.

$$A = K \tag{10}$$

Peak area is independent of mobile phase composition. This was experimentally observed in Fig. 6.

Peak height versus flow-rate. Eqn. 20 describes for isocratic analysis the small dependence of peak height on flow-rate which is due to efficiency phenomena. The fact that the composition is changing during the run should not influence efficiency significantly, so this same expression applies

$$P = \frac{K}{F^{0.3}} \tag{20}$$

A per cent change in flow-rate causes a much smaller change in peak height of opposite sign. This was experimentally observed in Fig. 5. We should note, however, that peak height data for Fig. 5 were taken only from the adjusted values in Table III. The adjusted %B *versus* time gradient program was changed in proportion to flow-rate in order to hold the %B *versus* volume gradient program equal to the reference program. Without this adjustment, reducing the flow-rate causes an increase in the

slope of the composition *versus* volume program, consequently, causing peaks to elute earlier, narrower, and taller. Since, in practice, chromatographs do not make such adjustments when flow-rate changes, there is usually a higher peak height dependence on flow-rate than is indicated in Fig. 5 and by eqn. 20.

Peak height versus composition. The reasoning employed in developing the isocratic relationship also applies to gradient conditions

$$P = KS \tag{25}$$

A per cent change in composition causes a corresponding change in peak height. This is consistent with the experimental results of Fig. 6. Again, as with gradient retention time behavior, there is a leveling effect. All sample components exhibit the same dependence.

CONCLUSIONS

We have demonstrated that high-precision quantitative analysis is achievable with HPLC using a photometric detector for both isocratic and gradient operation. During gradient analysis, the flow precision of the system is indicated by the early eluting peaks, while the composition precision is indicated by the late eluting peaks.

With photometric detectors, as with all detectors responding to concentration, it is important to control flow-rate when area is used for quantitation, and to control composition when height is used for quantitation. Stated differently, peak height should be used for quantitation if flow-rate cannot be carefully controlled, and peak area should be used if composition cannot be carefully controlled.

For detectors responding to mass rate, such as the flame ionization detector, other relationships apply. However, the peak behavior dependence described herein should apply to gas chromatography as well as liquid chromatography, when the differences between detectors are taken into account.

Preliminary experimental work, not reported here, has indicated that the retention time, peak area, and peak height dependence on flow-rate can be significantly affected by the detector time constant. The semiquantitative expressions for flow dependence presented here apply only when the rate of change of peak profile is small compared to the detector time constant.

ACKNOWLEDGEMENT

The skillful technical assistance of Mr. Ronald Honganen is gratefully acknowledged.

REFERENCES

1 S. R. Bakalyar, J. Yuen and R. A. Henry, *How to Pack Liquid Chromatography Columns*, Technical Bulletin 114-74, Spectra-Physics, Santa Clara, Calif., 1976.
2 I. Halász, R. Endele and J. Asshauer, *J. Chromatogr.*, 112 (1975) 37.
3 J. Hettinger, *Lab Automation News*, Vol. 1, Spectra-Physics, Santa Clara, Calif., 1973, p. 5.
4 B. L. Karger, in J. J. Kirkland (Editor), *Modern Practice of Liquid Chromatography*, Wiley-Interscience, New York, 1971, Ch. 1, p. 11.

5 L. R. Snyder and J. J. Kirkland, *Introduction to Modern Liquid Chromatography*, Wiley, New York, 1974, Ch. 3, p. 68.
6 B. L. Karger, in J. J. Kirkland (Editor), *Modern Practice of Liquid Chromatography*, Wiley-Interscience, New York, 1971, Ch. 1, p. 20.
7 L. R. Snyder and J. J. Kirkland, *Introduction to Modern Liquid Chromatography*, Wiley, New York, 1974, Ch. 2, p. 32.
8 L. R. Snyder and J. J. Kirkland, *Introduction to Modern Liquid Chromatography*, Wiley, New York, 1974, Ch. 2, p. 29.
9 D. Colby, *Model 3500B Liquid Chromatograph Gradient Reproducibility*, Chromatography Application Brief No. 141-75, Spectra-Physics, Santa Clara, Calif., 1975.

Journal of Chromatography, 126 (1976) 347–368
© Elsevier Scientific Publishing Company, Amsterdam — Printed in The Netherlands

CHROM. 9361

NEW MINI-COMPUTER AUTOMATED LINEAR PHOTODIODE ARRAY SPECTROMETER SYSTEM FOR HIGH-RESOLUTION LIQUID CHROMATOGRAPHY

R. E. DESSY

Department of Chemistry, Virginia Polytechnic Institute and State University, Blacksburg, Va. 24061 (U.S.A.)

W. D. REYNOLDS*

Food and Drug Administration, National Center for Toxicological Research, Jefferson, Ark. 72079 (U.S.A.)

W. G. NUNN and C. A. TITUS

Department of Chemistry, Virginia Polytechnic Institute and State University, Blacksburg, Va. 24061 (U.S.A.)

and

G. F. MOLER

Food and Drug Administration, National Center for Toxicological Research, Jefferson, Ark. 72079 (U.S.A.)

SUMMARY

A third generation multi-wavelength array spectrometer was developed as a detector for the high-resolution liquid chromatographic characterization of metabolites. The design features include a PDP-8/e mini-computer, a matched pair of linear photodiode (256 element) arrays (Reticon), holographically ruled gratings, fiber optics, flow cells, and a high-intensity xenon light source. The wavelength range is 256 nm differential with 1 nm resolution and can be independently adjusted in the spectral range of 200–800 nm. Correction for the quantum efficiency curve is made on both of the cooled (−30°) photodiode arrays by an assembly language subroutine. The system is capable of 20 spectra/sec (200–456 nm) in a dual-beam mode. The dynamic range and linearity of the photodiode arrays are approximately 4000:1. Special features include mini-computer driven signal enhancement via integration as a function of signal strength. The display output includes presentation of the total absorption chromatogram *vs.* elution time in both real and post-run time as well as selectable single absorption band (*e.g.*, 280 nm) *vs.* elution time (post-run time). Application of this dedicated mini-computer automated liquid chromatography–UV spectrometry system for the separation and characterization of the metabolites of a carcinogen, 4-ethylsulfonyl-1-naphthalenesulfonamide, will be discussed.

* Author to whom reprint requests should be addressed.

INTRODUCTION

Over the past few years, considerable effort has been expended on developing and improving UV detectors for high-speed liquid chromatographic (LC) separations of biochemically important components[1–14]. Generally, the UV detectors can be divided into two classes which are identified with their end-use, *i.e.*, monitoring *vs.* identification[4]. For general monitoring purposes, most liquid chromatographs successfully utilize a single-wavelength (element) detector at 254 or 280 nm[12]. Other discrete element monitoring has been utilized depending upon the specific sought-for component[8]. For qualitative identification needs, full UV scanning on each component in the LC effluent yields additional spectroscopic information.

Although many varieties of rapid scanning spectrometer systems are available, the *first* generation units relied on moving mechanical parts to scan the spectrum[12,14]. The *second* generation instruments utilized the Vidicon tubes, which eliminated the construction and maintenance problems associated with rotating mirrors or vibrating galvanometers[15,16]. But, the Vidicons suffer from substantial coherent pattern noise, limited integration time due to high dark current as well as memory effects[17,18]. The recent availability of inexpensive solid-state linear photodiode arrays (Reticons) as simultaneous wavelength detectors has enabled the development of *third* generation spectrometers for use in LC[19].

The attainment of rapid-scan UV spectra generates several advantages beyond simple component identification. These advantages occur in several ways, including both time and spectral domains[12–21]. The time–domain advantage accrues in a straightforward manner from the simultaneous detection of the total UV spectra[20,21]. The simultaneous detection of all dispersed radiation (N spectral or spatial resolved elements) reduces the observation time by a factor of N in the case of signal-to-noise ratio (SNR) limited measurements and improves the SNR by a factor of $\sqrt{N}$ for a fixed observation time as in the case of finite LC peak widths. However, further improvements in spectral data (SNR) based on the Hadamard or Fourier methods are limited, at best, for UV spectroscopy, in which the noise is statistical and source dependent[17,20].

In the rapid-scan spectral domain, an improvement in detection level is gained by virtue of the total UV spectrum. By summing the output intensity over all discrete 1-nm channels from 200–350 nm as a single output intensity, an advantage is gained over select single-channel (254 nm) detectability[19]. This increase in detectability (F) varies from component to component but is dependent on the ratio of the integrated area under the spectral curve (200–350 nm) to that at the selected single channel (250 nm). Thus

$$F = \frac{\int_{200}^{350} A\,d\lambda}{\int_{250}^{251} A\,d\lambda}$$

In most cases, this can account for an increase in factors of 5–500 in detectability. For high-speed LC biochemical separations with limited sample size or trace-level components (hormones) in complex physiological mixtures (urine), this improvement would be a decided advantage[22].

Along with the expanding use and development of pesticides, herbicides, food additives, plasticizers, and other environmental chemicals, there has been a growing concern for possible untoward effects of these chemicals in man. Long-term, low-dose feeding effects and related mechanism studies of a few of these agents and model compounds are under study at this Center. Complete studies including identification and monitoring of these agents and their metabolites can be highly informative regarding the activity of the agent, the toxicity and the mechanism of action. High-resolution anion-exchange LC is an excellent analytical tool for studies of this kind because both unconjugated and conjugated metabolites can be separated for structural determination in a single sample without the need for hydrolysis or extensive sample pretreatment. A number of investigators have utilized the anion-exchange column for good separation of diphenylhydantoin and its metabolites, of the glucuronide and sulfate conjugates of *p*-nitrophenol, and of *p*-hydroxyacetanilide metabolites as well as of acetaminophen and its metabolites in human urine[23–25]. Two recent books summarize the application of ion-exchange LC methods to problems in biochemistry and biology[26,27].

This report outlines the development of a minicomputerized linear photodiode array spectrometer system for use as a detector for high-resolution ion-exchange LC. Application of this automated LC–UV system to the separation and characterization of conjugates of 4-ethylsulfonyl-1-naphthalenesulfonamide (ENS) in the urine of BALB/C mice is demonstrated.

INSTRUMENT

General

A proto-type system consisting of a Reticon detector, a light source, optics and a micro-processor was previously constructed by this group[19]. It was determined from this earlier version that certain improvements in system configuration would need to be made in order to develop a system for the high-resolution anion exchange LC separation, UV characterization and identification of metabolic products in urine. Even with maximum external hardware support, the micro-processor limitations in math (data handling, transfer, reduction) and plotting (formatting, I/O) would have to be overcome; and, the spectrometer hardware would also need to be revised for the new design objective. Specifically, the requirements for this type of dedicated mini-computer automated LC–UV system are as follows:

(1) The LC detector system would need to include dual-beam spectrometer operation to accommodate gradient elution.

(2) The system must be capable of taking about 25 spectra/sec to accommodate ensemble averaging (if required).

(3) The spectrum must be in the 200–450 nm range.

(4) Because of the need to quantify the results, the system must be capable of operation in the absorption mode.

(5) The UV source and the electronics must be stable over long periods since a typical LC run utilizing an ion-exchange column would involve a maximum of 80 h and produce nearly 250 peaks.

(6) Due to the large expected volume of data (2.5 million bits/run), all meaningful RAW spectral data must be stored on disk for limited post-run appraisal and then

transferred to industry compatible tape for storage or transfer to the central computing facility. There it would be subjected to various in-depth data reduction programs.

(7) The output format should include total integrated absorption at all measured wavelengths *vs.* elution time (real-time LC) and selectable single-band wavelengths *vs.* elution time as well as individual spectra.

(8) For data handling and reduction, a mini-computer with 12K core and a teletype, a disk, a scope, a magnetic tape and plotter I/O devices will be required.

Although it was fully expected that the ultimate use of such a system might see these stringent requirements relax against long-term needs, the exploration stage would involve a period when it was not known which wavelengths (200–450 nm) were of most importance to the metabolite characterization research. It might be necessary to rescreen previous runs many times to finally focus on the observations which would be used in component identification or for routine monitoring.

The present automated LC–UV system consists of several major units including the high-resolution liquid chromatograph with associated electro-mechanical and electronic controls, a 12-bit computer unit based around a PDP-8/e CPU with 12K of memory and with four interactive storage and display devices, and a spectrometer unit consisting of a xenon light source, fiber optics, and a pair of holographically ruled gratings along with two cooled (−30°) photodiode arrays. Each major unit is discussed in the following sections.

Liquid chromatograph

A high-resolution liquid chromatographic unit utilizing the 150–200 cm ion-exchange columns similar to that developed by Scott was fabricated with some additions and changes[28]. Figs. 1 and 2 are photos of the completed unit. A pH gradient section was added which develops a descending hyperbolic pH gradient (8 → 4.40) during the first 5 h of the 60-h LC run. The system is gradient programmable in five separate inter-dependent functions. The five functions control the two separate gradient development cycles and a final wash cycle as well as start and stand-by modes. The pH buffer gradients are developed from two source solution reservoirs, an initial mixing vessel solution and wash reservoir. The mixing vessel starting solution contains 0.1 *M* buffer (ammonium acetate–acetic acid) adjusted to pH 8 while the other two source reservoirs contain "acid solution" (pH 4.0; 3 *M* buffer) and "buffer solution" (pH 4.40; 6 *M*), respectively. The mixing vessel (stirred) is fed from the three reservoirs through three separate solenoid valves and a mixing vessel feeder pump (two pre-set speeds). A sequence of mixing steps is pre-determined by the operation of the timers and pump speed control. Any combination of curve/linear gradients can be set by this operation. For example, a descending pH gradient can be overlayed on a slow rising linear buffer gradient. A typical operation of the timer sequence is as follows:

(1) The counter/timers are automatically reset upon injection with movement of the injection lever from load to inject (Waters UK6, 6000 p.s.i. injector).

(2) The counter/timers start to count down from their various pre-set points at the rate of one count each minute.

(3) The first counter/timer reaches 0000, which determines the end of the first function and a solenoid valve is switched.

(4) Each successive counter/time in turn continues to count down to 0000 from its individual pre-set point for each designated function.

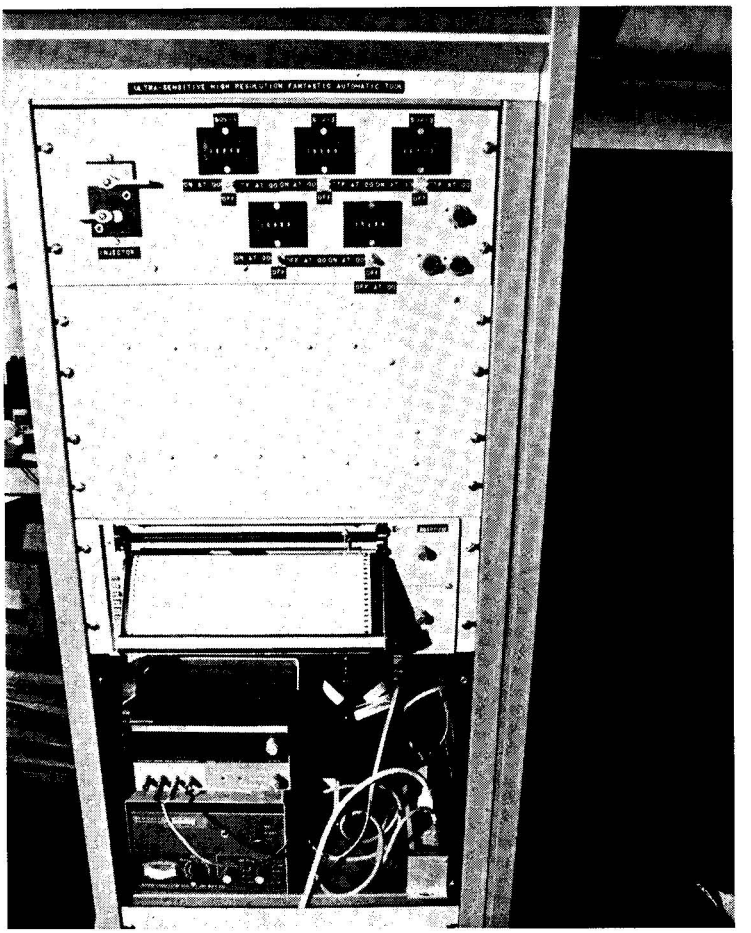


Fig. 1. High-resolution liquid chromatograph utilizing a 150-cm anion-exchange column. Front view.

(5) As the last counter/timer reaches 0000, END OF PROGRAM, the feed pump comes on and pumps the initial solution into the mixing vessel until the level-sensor shuts off the feed pump —END OF RUN (column purged). The column has now been cycled to start the gradient again for another sample.

All materials of construction contacting the sample and eluent are 316 stainless steel, glass or PTFE.

Several different columns (75, 100, 150 cm $\times$ 1/8 in. O.D. have) been utilized for the determination of the optimum separation of components in the urine of BALB/C mice. Various anion-exchange resins and particle sizes from several manufacturers have been utilized. Aminex A-27, average particle diameter 13.5 μm (BioRad Labs., Richmond, Calif., U.S.A.), was used with fair resolution but with high ΔP (5000 p.s.i. for 8 M buffer). Another Aminex resin (1-X8L: 9160) of smaller size (6.5 $\pm$ 1.5 μm measured) was used in the 75-cm column with excellent resolution but the ΔP was excessive ($\approx$6200 p.s.i.) at 0.07 ml/min. However, the Aminex A-27 (13.5 μm, 150-cm column; see also Application) appeared to be the best compromise

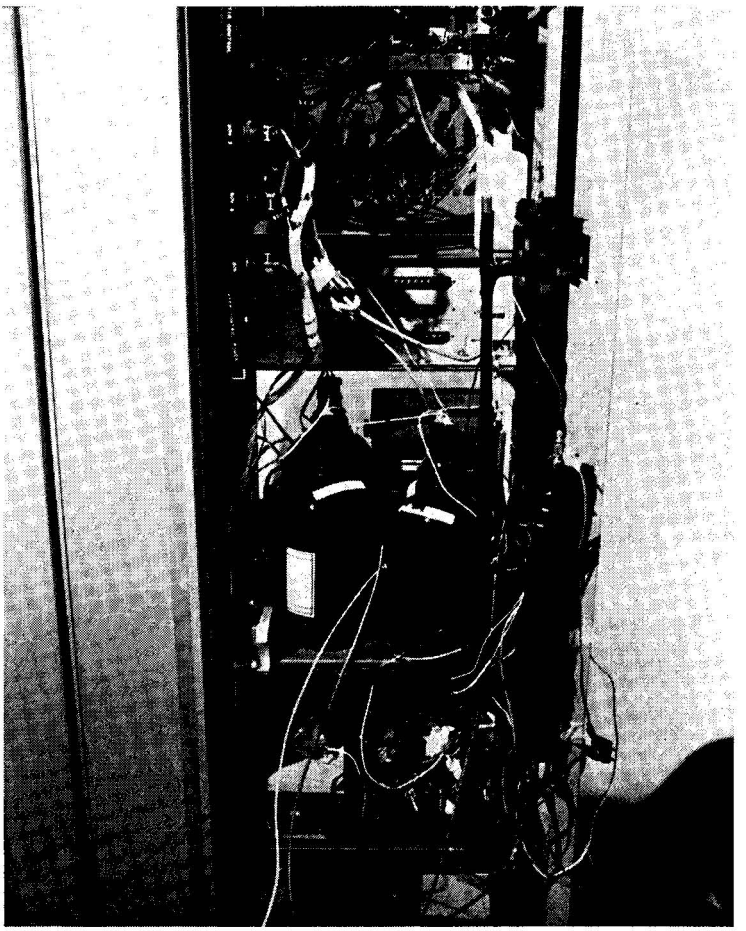


Fig. 2. High-resolution liquid chromatograph utilizing 150-cm anion-exchange column. Rear view.

between flow-rate (elution time), pressure drop, and resolution of the large numbers of urinary components from the conjugates of the model compound, ENS. An example of the separation of both the conjugates of ^{14}C-labeled ENS and urinary components is shown in Fig. 3.

Reticon spectrometer

Light source. A high-intensity 150 W xenon arc lamp and housing with regulated power supply was utilized for the UV source (Model 7301, Oriel Corp.). A fairly smooth continuum output develops from 190–750 nm, as seen in the typical spectral output curve (Fig. 4). The source size is 0.5 × 2.2 mm while the image size at the focal point (76 mm from housing) is 0.9 × 4.0 mm.

Flow-cell. The micro flow-cells, one each for the reference and sample beams, were fabricated in the standard "Z" pattern. The dimensions chosen were dependent both on the size of the available light beam from the fiber optics and the optimum

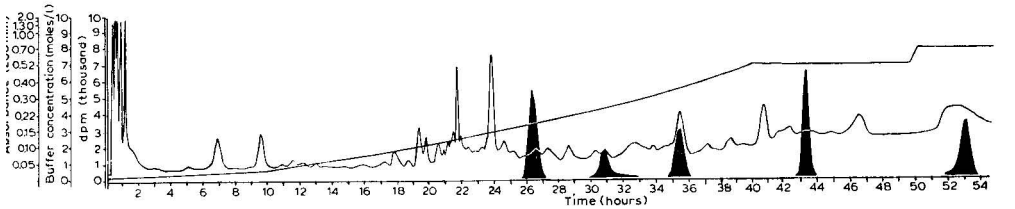


Fig. 3. High-resolution liquid chromatogram of the urine of BALB/C mice (100 μl) containing ^{14}C-labeled ENS metabolites (cross-hatch) and UV urinary components (260 nm).

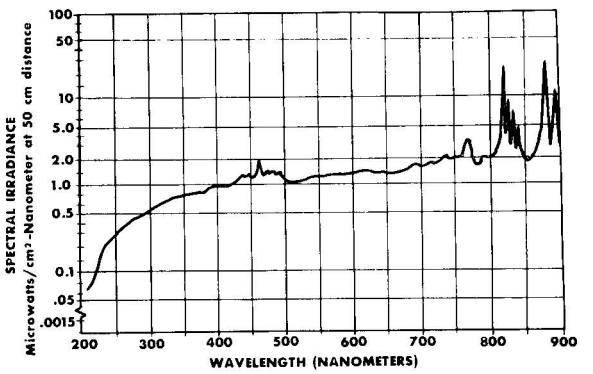


Fig. 4. Spectral irradiance curve *vs.* wavelength of 150 W xenon source.

absorption path-to-volume ratio (1 cm/31 μl) for chromatographic band-width. These flow cells were made from stainless steel with quartz windows and PTFE gaskets.

Grating. The necessity of attaining sub-nanogram sensitivity required a system with best available optics. A high-quality holographically ruled concave grating (600 lines/mm) was used (Model 3B, Jobin-Yvon Optical Systems). This minimized spherical aberration problems as well as keeping reflection and transmission losses to a minimum[15].

Optical path and sensitivity. A metal housing with flat black interior that was also light-tight and purgeable (nitrogen) was fabricated for the optics system. All external entrances and exits were made to minimize light leakage. An optical configuration based on a Rowland circle (F/3.0, 200 mm) as shown in Fig. 5 was placed inside this housing. Use of the grating and fiber-optic bundles reduced the component count over that of other systems, *e.g.*, Czerny–Turner, and hence transmission and reflection losses. The fiber-optics bundle further reduced the alignment problem, so that

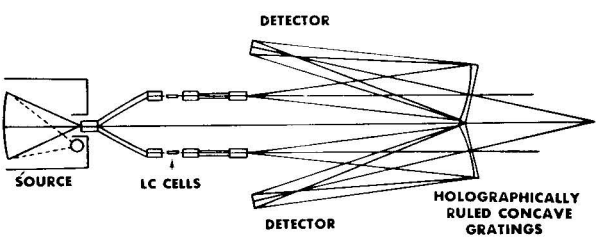


Fig. 5. Optical path including LC flow cells for photodiode array spectrometer.

the system could run for long time periods without recalibration. The overall system involved an F/3.0 rather than the earlier proto-type of F/4.5[19].

Design and optimized performance calculations were completed on the optical system from the light source to signal read-out. These are summarized in Appendices I, II and III. The maximum dynamic range of the linear array (average pixel) was calculated to be 4×10^4:1 (Appendix I). Theoretical design calculations of source strength and sensitivity indicated that with an LC effluent sample containing guanosine ($\varepsilon_{250} = 11{,}050$) and an estimated peak width of 3 min (31 μl cell volume), 1 ng could be detected (Appendices I and II).

Reticon detector. The silicon photodiode linear array detector utilizes a reverse biased p–n junction diode as the photosensitive element. These linear arrays are available in several pixel*/array sizes and pixel areas. Currently, arrays can be obtained with 128–1024 pixels/array with pixel areas of either 1×25 μm or 1×425 μm. These linear arrays are sensitive from below 200 to above 900 nm. They are most efficient in the 600–820 nm region as seen in the typical photon efficiency curve (Fig. 6). Correction for the quantum efficiency curve to a maximum value of 1.0 is made via an assembly language sub-routine before data storage.

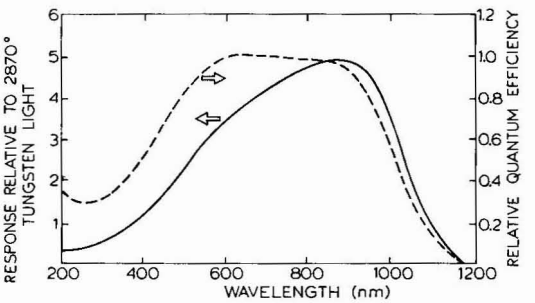


Fig. 6. Quantum efficiency response *vs.* wavelength of the photodiode array (Reticon).

Since the wavelength region of interest for the present instrument was 200–400 nm, a 256-linear array was selected which would enable 1 nm resolution (25 μm centers) with a 256 nm range (200–456 nm). However, this range could be adjusted to any 256 nm band in the 200–900 nm region. Two matched arrays which are individually housed with Pelletier cooling plates (−30°) were selected based on their identical energy response (Model RL256 EC/17, Reticon). Cooling to a −30° aids in the reduction of noise since the noise is reduced by a factor of 2 for each 10° lowering of temperature[17]. A 256-linear array Reticon with a printed circuit background is illustrated in Fig. 7. A schematic of the linear array is shown in Fig. 8. The operation of the photodiode array occurs as follows:

(1) As light strikes the surface of the detector, hole pairs are created and migration occurs toward the capacitor element (Fig. 8).

(2) As the light continues to strike the detector surface this action leads to a gradual discharge of the capacitor.

* A pixel is a simple photodiode and, in the present design, it receives the light from a single wavelength band.

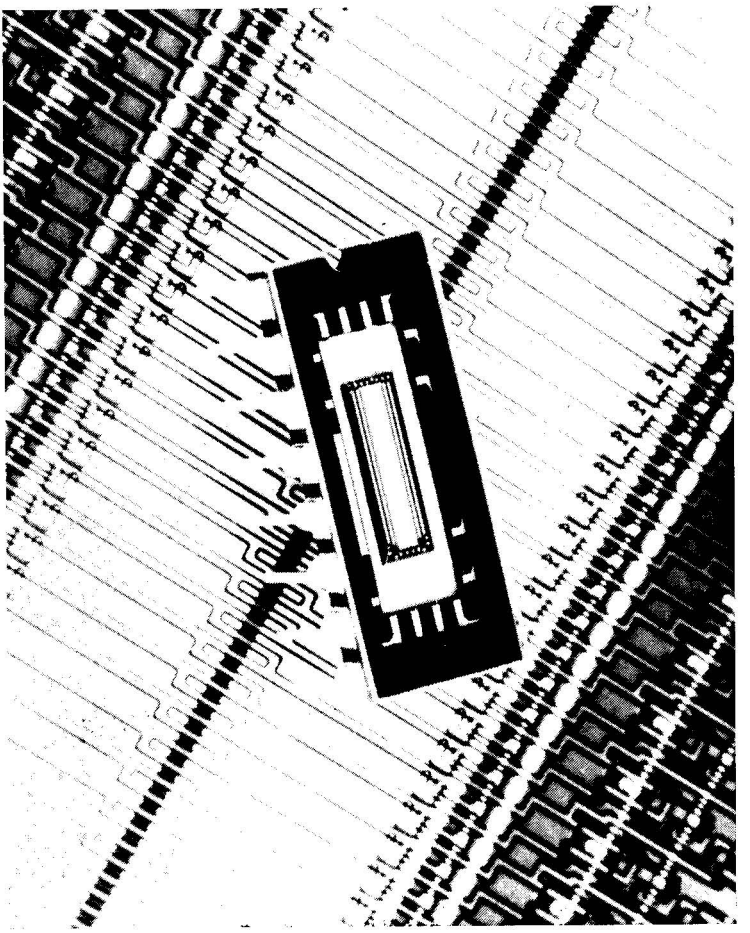


Fig. 7. Photodiode linear array (256 pixel) with printed circuit background.

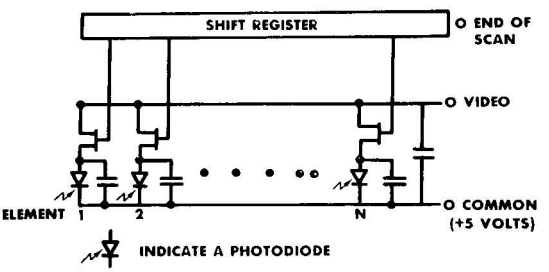


Fig. 8. Schematic of photodiode linear array. Operational view.

(3) Over the integration time (light impact time), the charge on the capacitor drops an amount equivalent to the amount of integrated light following on the detector.

(4) When the pixel is "read", a multiplexer attaches the detector to a voltage source which charges the capacitor back up to a standard potential.

(5) A signal, corresponding to the current-flow necessary to recharge the voltage source, is sent down a wire (video-line).

(6) The multiplexer then causes the voltage source to be switched to the next pixel in the detector, and the process is repeated.

Reticon "read-out". In the fast scanning environment of high-resolution LC operation, continuous monitoring of the photodiode array is unnecessary. 1000 spectra/sec provides more data than can be either stored or handled by a dedicated computer. In practice, it is normal to initiate data collection only periodically. The concepts involved are as follows: During a dead period, when the detector is not being used, the light striking the surface of the detector rapidly leads to saturation of all elements. (See Appendix I for "saturation exposure".) In order to prepare for gathering of spectral information, the array must be "dummy read". This is accomplished by applying a read pulse which starts the drive electronics, and all elements in the array are recharged back to their starting charge points. The jth element in the array is read-out at a different time than the zth element. However, the time interval between the reading out of the jth element in successive scans (integrate or "dwell time") is the same for successively read zth elements. Since the "rippling" through elements is fast compared to the LC effluent concentration changes being observed, a truly simultaneous multi-wavelength detector is involved. Consequently, each individual element is continually "on" except for a very short "blink" out of each cycle which can yield a duty time as high as 95%.

If one views the single vidio-line output of the device, a series of pulses appear, each corresponding to the amount of light striking the element of the array that the pulse represents (Fig. 9). These arrays operate with the multiplexer switching between elements at a clock rate of 1 KHz to slightly above 1 MHz. A complete reading of the array (256 pixels) can be as fast as 12 msec to a slower speed of 0.25 sec. The integrate time can be altered between the limits of the Reticon "shift out" rate (20 KHz) and that time when the dark current noise becomes a serious problem. This places a upper limit of 80 spectra/sec to a lower unit of 1 spectra/1000 sec (4 sec/pixel) for the cooled (−30°) array. For optimum integration time, a rate of 20 spectra/sec was chosen.

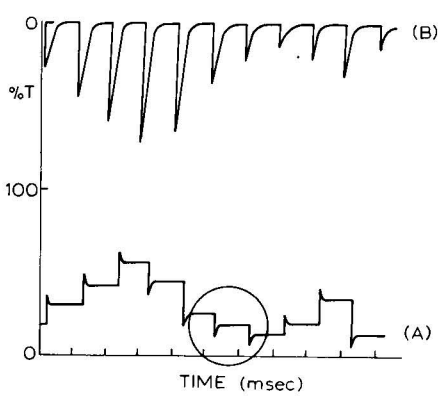


Fig. 9. (A) Time base response of a single pixel to varying light intensity. (B) Video line pulse signal to the single pixel capacitor.

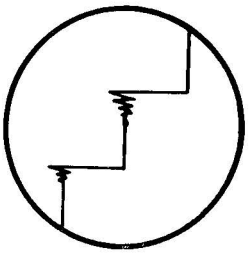


Fig. 10. Typical switching transients developed during a single pixel read-out.

In order to properly condition the serial pulse train exiting from the common video-line of the detector for input to a computer system, it is normal to run it through an amplifier, integrate, sample/hold system with high rejection of periodic noise. The majority of the noise in the detector arises from switching transients induced at times shown in Figs. 9 and 10. This noise can be decreased by careful amplifier design and separation of the clock drive circuitry from the detector itself. Each pulse is integrated over a major fraction of its width, which leads to a reduction in noise by the analog integration operation. A schematic of the detector and amplifiers for both "real time" recording output (integrator) and mini-computer data acquisition (absorbance, transmittance) is shown in Fig. 11. The integrator sums the absorbance signal over all measured wavelengths (200–450 nm) for a given set of "scans".

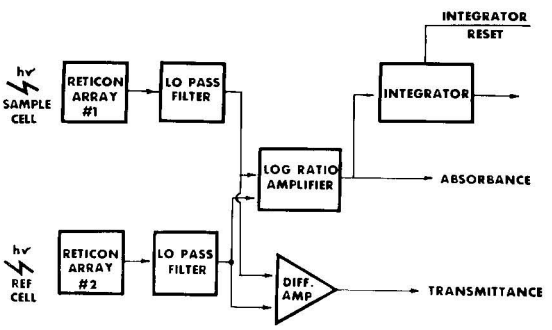


Fig. 11. Schematic of Reticon array detectors (sample, reference) and analog "front-end" for computer input.

Computer

General. The basic computer configuration used to acquire, process, and display the formatted spectral data is based around a 12-bit mini-computer, PDP 8/e (Digital Equipment Corp.) with 12K words of core memory. Additional bus-bar hardware components include a 10-bit A/D convertor (AD8A; D.E. Corp.), a real time clock (DK8E-P; D. E. Corp.), a 10 Hz dayclock, a D/A convertor (VC-8E point plot; D.E. Corp.), and a hardware multiply/divide processor (KE8E; D.E. Corp.). The storage devices include two 3.2 million word disk and controller units (RK8E; D. E. Corp.) and a 9-track magnetic tape (TU-10; D. E. Corp.). The I/O devices include a multi-speed alpha/numeric terminal (LA-36; D.E. Corp.), an incremental plotter

(Cal-Comp No. 565; Cal-Comp Corp.) with interface (XY8E; D.E. Corp.) and display oscilloscope (No. 5051; Tektronix Corp.). A configuration diagram of the computer system is shown in Fig. 12.

Operation. The CPU uses a 10-bit A/D convertor to change the incoming analog signal from the detector to digital which is stored in a 4K word input buffer in the CPU. The data input rate is controlled by two separate clocks. The first real time clock is used to control the integration or exposure time of the Reticon array. The second clock is used as a day clock which is started when an LC run is initiated. This clock is read each time a spectrum is taken, which allows data to be taken only when there is a signal above the baseline. If the response in the reference beam falls below a certain level, the integrate time is increased in binary progression. This is an operation corresponding to slit opening on a regular spectrometer, but without loss in resolution. The integrate time (a 2-bit number) and the output of the A/D (a 10-bit number) are ANDED to provide a 12-bit data point for each pixel in the array, yielding a dynamic range of 1000:1.

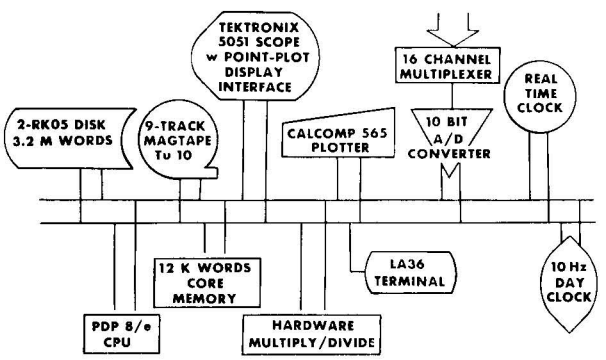


Fig. 12. Mini-computer configuration with I/O devices.

The three data modes (absorbance, transmittance or integral) are carried by the analog multiplexer, which acts as a front-end to the A/D convertor. The data are collected in ping pong double buffers. As each buffer is filled, it is transferred to the disks using assembler drivers that are interrupt oriented. By using this type of rotating buffer for data storage, the possibility of missing incoming data is small. The data are stored on disk in single-word binary formatted files.

The analog amplifiers (front-end) performed all the correction functions except the one for responsivity of the Reticon array (see Fig. 6). This calibration function is accomplished in the computer by ADDING the appropriate correction factor stored in memory for each wavelength as a LOG. The addition function is much faster than other math operations since data through-put is at a premium for ensemble averaging.

Software. A series of software routines were written in various levels of computer languages (assembler, Basic and Fortran) to acquire data, transfer to mag-tape as well as to format, and display the data. After the LC run is over, USER SERVICE ROUTINES and assembly coding is used to rewrite the directory area of the OPERATING SYSTEM (OS-8), so that access to the data may be had by using conventional keyboard or USR assembler calls. An overview schematic of the soft-

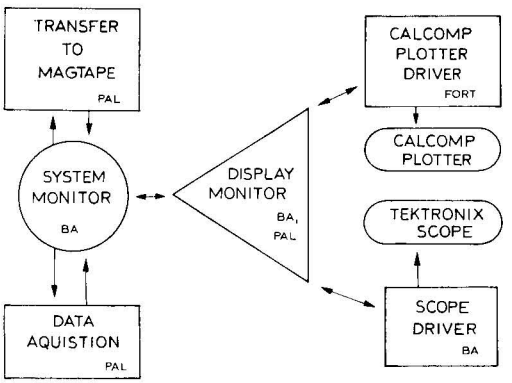


Fig. 13. Overview of computer system data flow and display.

ware support is shown in Fig. 13. A flow-chart for the shortest of the ten software programs is shown in Fig. 14.

I/O Display. During the 60-h LC run, a large amount of data (approximately 2.5 M words) is acquired that requires display in standard spectral and chromatographic format. During an LC run, the total absorbance chromatogram (TAC) is plotted out on a *Y/t* plotter associated with the system. This is the normal LC plot of response *vs.* time that is typical of single-wavelength monitors. The post-run operations include the following:

(1) Plotting of the absorbance at any single wavelength, or continuous band of wavelengths, or a selected group of wavelengths *vs.* time. A digital incremental plotter is used to provide the resolution and labeling required for documentation purposes. (absorbance band chromatogram, ABC)

(2) Listing of absorption peaks and times on the system terminal so that the technician can determine the elution time of a component for preparative purposes.

(3) Present an oscilliscope display of any given spectrum.

(4) Dumping of the data to industry compatible tape for storage, or transfer to a larger computer for full spectral display purposes or library search and matching of catalogued spectra.

APPLICATION

Pathological effects (mice)

ENS has several effects on the mouse bladder epithelium (C57 female, 12 weeks). A single oral dose (5–160 mg/kg) induces epithelial hyperplasia of the bladder in mice, whereas prolonged dietary administration (0.01 %, 8 weeks) of ENS produces a greater degree of epithelial hyperplasia and, frequently, bladder tumors at 30 weeks[29–31]. ENS, initially, causes a violent proliferative epithelial response which later settles into a chronic phase, in which cell tumor varies from animal to animal and site to site within the same bladder.

The sulfonamide group appears to be essential to the activity of the molecule due to the results of recent studies on sulfonyl and sulfonamide groups[30]. Maximum activity was found when the sulfonamide group was attached to an aromatic system

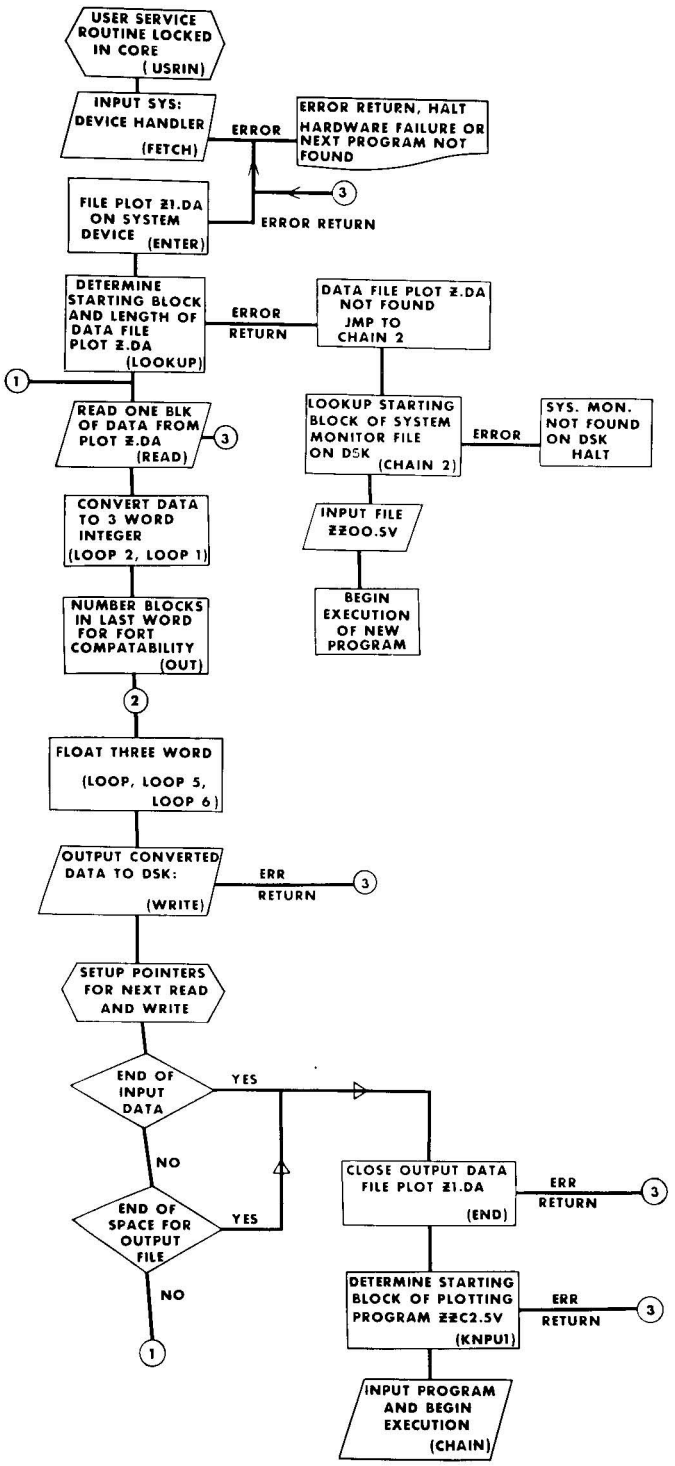


Fig. 14. Software program for binary to 3-word floating point convertor.

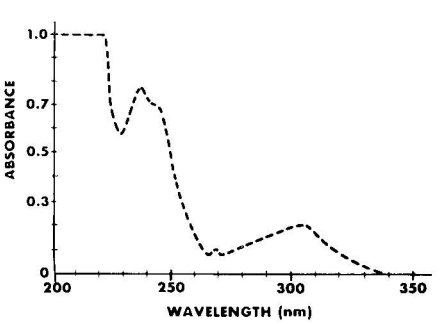
(benzene or naphthalene) containing an alkylsulfonyl or sulfonamide group. These implications of a structure–activity relationship have a bearing on the non-nutritive artificial sweeteners[29].

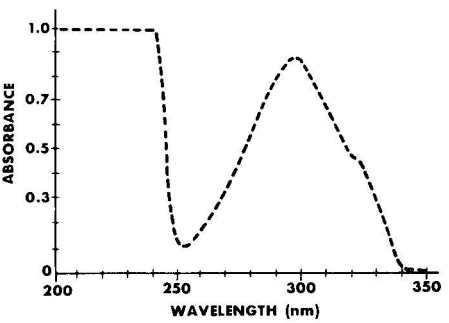
^{14}C-Labeled ENS metabolites

Presently, the metabolism of ENS in mice strains has not been fully determined. In the current series of studies, female BALB/C mice (20 weeks) were each fed 1.05 μCi of ^{14}C-labeled ENS (sp. act. 11 μCi/μmole). The urine was collected over a 24-h period in special metabolism cages. The pooled urine was filtered through a Millipore filter (0.2 μm) before chromatography. One hundred microliters of filtered urine were injected onto the 150 cm × 1/8 in. O.D. Aminex A-27 anion-exchange column and eluted with buffer gradient during the 55-h period. The separation was conducted under the following conditions: 0.1 ml/min flow-rate, 50° (isothermal), hyperbolic descending pH (8 → 4.40) over the first 5 h, ascending buffer gradients 0.1–6 *M* ammonium acetate–acetic acid over a 0–40 h period, holding 6 *M* buffer constant during a 40–55 h period. Fractions were taken every 10 min during the 50-h elution period. Individual ^{14}C-containing fractions were counted by a Nuclear-Chicago Mark II liquid scintillation instrument equipped with a Model PDS/3 data reduction system. The 1-ml fractions were added to a vial containing 12 ml of PCS solubilizer (Amersham-Searle, Arlington Heights, Ill., U.S.A.) and counted for 2 min. A plot of the count-rate data (dpm) *vs.* retention time for each 10-min fraction having significant dpm (>50) is shown in Fig. 3 (cross-hatch). The individual metabolites are shown at retention times of 26.5, 31.0, 35.5, 43.3, and 53.0 h. These accounted for 96% of the total measured radioactivity in the 100-μl urine sample.

LC–UV display

Work is continuing on improving the computer-driven Cal-Comp plotter display of both the total absorbance chromatogram and the absorbance band chromatogram. A recent example of the spectral output for both ENS (t_R = 31.0 h) and a suspected sulfonate conjugate (t_R = 43.3 h) is shown in Figs. 15 and 16, respectively.





Fig, 15. Illustration of UV spectra (200–350 nm) of ENS from the Reticon spectrometer.

Fig. 16. Illustration of UV spectra (200–350 nm) of ENS metabolite from the Reticon spectrometer.

DISCUSSION

Our interest in the computerized LC–UV system is two-fold. First, the generation of a UV-spectral data base of urinary components (human and selected animal) associated with normal and pathological states with subsequent computer retrieval and matching is required for profiling of various in-born errors of metabolism. The acquisition of this data bank would aid immensely in the selection of UV spectral "windows" or binary descriptors for utilization in urinary profile development of specific human pathological states via computer pattern recognition techniques. The second purpose is the general utilization of the system for rapid UV data characterization of toxic chemical agents and their metabolites in urine. As shown by the current system, computer data manipulation can certainly enhance both the detection levels of components as well as aid in the chromatographic resolution of compounds.

LC has been hindered by the lack of a universal detector, and, consequently, no equivalent for the GC–MS system has yet been described. In the present work, we have begun to demonstrate the utility of a computerized LC–UV system for the rapid UV data acquisition and identification of various toxic chemical agents and their metabolites. Computer retrieval and display of selected UV spectra upon completion of an LC run saves many hours of tedious collection of many hundreds of fractions and transfer to a UV spectrometer. The added advantage of the capability to re-run the entire LC at a wavelength specific for the chemical toxicant or its metabolites under study enables its rapid location in the chromatogram for further spectroscopic study.

At this stage in the development, we have not "fine tuned" the system for maximum detectability. However, the spectrometer system has demonstrated increased sensitivity over single band monitoring by virtue of its computerized signal integration routine. Enhanced sensitivity will enable several improvements in LC column technology. Although the capacities of conventional resins are several hundredfold greater than those of pellicular resins, the improved sensitivity will enable lower sample loadings along with increased resolution with the concomitant use of pellicular resins for urinary metabolite identification and screening.

Future data manipulations for enhanced spectral presentation will include: (a) the use of ratios at two selected wavelengths for determination of peak homogeneity, (b) spectral base-line or background subtraction technique via computer routine, (c) peak de-convolution for improved resolution, and (d) on-line quantitative analysis.

ACKNOWLEDGEMENTS

The mini-computerized spectrometer unit was developed by the Instrumentation and Computer Interfacing Group, Department of Chemistry, Virginia Polytechnic Institute and State University and the National Center for Toxicological Research under Contract No. 222-75-2047(c). The mouse urine containing the ^{14}C-labeled ENS and metabolites was kindly supplied by Dr. James Stanley, Molecular Biology Division, National Center for Toxicological Research.

APPENDIX I —CALCULATION OF PHOTON RATE, REFERENCE BEAM RATE, SATURATION EXPOSURE, DYNAMIC RANGE, AND SAMPLE BEAM DETECTABILITY

Light source

From the spectral irradiance curve given in Fig. 4, $S_1 = 0.28\ \mu W/cm^2 \cdot nm$, and extrapolating to a 40.3 cm^2 mirror at 12.44 cm from the source, the total energy striking source mirror, E_m, is

$$E_m = \left(\frac{50}{12.44}\right)^2 (0.28)\,(10^{-6})\,(250)\,(40.3) = 0.114\ \text{W (250 nm)}$$

and

$$E_2 - E_1 = h\nu = 8 \times 10^{-12}\ \text{ergs/photon}$$

where the number of photons/W·sec is given by

$$\frac{1}{8 \times 10^{-12}}\,\frac{1}{10^{-7}} = 1.25 \times 10^{18}\ \text{photons/W}\cdot\text{sec (at 250 nm)}$$

or

N = total photon flux at mirror (at 250 nm)

$$N = (0.114)\,(1.25 \times 10^{18}) = 1.42 \times 10^{17}\ \text{photons/sec (at 250 nm)}$$

The photon loss to entrance of fiber optics is approximated by the area ratios of image to fiber end

$$\frac{0.9 \times 1.5}{0.9 \times 4.0} = 0.38$$

The total number of photons/sec entering the fiber optics, assuming no scattering loss upon entrance,

$$N_1 = 0.38 \times 1.42 \times 10^{17}$$
$$= 5.39 \times 10^{16}\ \text{photons/sec}$$

The fiber optics are split into two beams, or

$$N_2 = 2.70 \times 10^{16}\ \text{photons/sec}$$

Assume a 50% loss through the fiber optics

$$N_3 = 1.35 \times 10^{16}\ \text{photons/sec}$$

These are the number of photons/sec at 250 nm presented to each of the reference and sample beams.

Reference beam

Assume 0.6 M acetic acid–acetate buffer (pH 4.4) and at 250 nm, the measured

absorbance is 0.015 (1 cm path length). The number of photons/sec which exit from the flow cell are

$$\frac{1}{2.3} \ln \frac{I_0}{I} = A, \text{ where } I_0 = N_3 = 1.4 \times 10^{16}$$

Solving for I

$$I = 1.3533 \times 10^{16} \text{ photons/sec}$$

Assume 50% loss through exit fiber optics to grating, or

$$I = 6.72 \times 10^{15} \text{ photons/sec at 250 nm}$$

Assume 50% energy transfer through grating and divergence loss proportional to area ratios [(pixel area)/(light beam area) = 0.0274]

$$I = (0.0137)\,(6.72 \times 15^{15})$$
$$= 9.135 \times 10^{13} \text{ photons/sec}$$

Saturation exposure (SE)

Given as 0.27 μW·sec/cm^2 (ref. 32) but the area of a single pixel is

$$A = 2.11 \times 10^{-4} \text{ cm}^2$$

or

$$SE_{CH} = 5.67 \times 10^{-5} \mu\text{W} \cdot \text{sec}$$
$$= 5.67 \times 10^{-5} \times 1.25 \times 10^{18} \times 10^{-6}$$
$$= 7.09 \times 10^{7} \text{ photons (at 250 nm)}$$

Noise per channel (NE)[32]

Given as 6.9×10^{-6} μW·sec/cm^2 at 30° then

$$NE_{CH} = 6.9 \times 10^{-6} \times 2.1 \times 10^{-4}$$
$$= 1.45 \times 10^{-9} \times 1.25 \times 10^{18} \times 10^{-6}$$
$$= 1.8 \times 10^{3} \text{ photons}$$

Dynamic range

Defined as maximum signal at saturation to the noise signal both measured at a fixed pixel

$$DR = \frac{SE_{CH}}{NE_{CH}}$$

$$= \frac{7.09 \times 10^{7}}{1.8 \times 10^{3}}$$

$$\approx 4 \times 10^{4} \text{ at } 30^\circ$$

(By cooling to −30°, the DR may improve by a factor of 10.)

Sample beam

From previous calculation, $I_0 = 1.40 \times 10^{16}$ photons/sec at 250 nm, assume a guanosine concentration of 10^{-9} g/25 μl mouse urine (BALB/C); for guanosine

$$\varepsilon_{250} = 11{,}050 \text{ l/mole}\cdot\text{cm (mol. wt.} = 283)$$

LC peak width = 3 min (estimated for 10^{-9} g); flow-rate = 0.1 ml/min; $V_R = 0.3$ ml; assume a true Gaussian peak shape, where $W = 10^{-9}$ g solution of

$$C(V) = \frac{W}{\sqrt{2\pi\sigma}} \int_{V_1}^{V_2} e^{\frac{-(V-V_0)^2}{2\sigma^2}} dv \qquad \text{(see Appendix II)}$$

Yields

$W_1 = 2.40 \times 10^{-10}$ g, or, the concentration in the light beam, $C_1 = 2.68 \times 10^{-8}$ moles/l.
Then

$$\text{Total absorption} = A_{\text{buffer}} + A_{\text{guan.}} \text{ (at 250 nm)}$$

or

$$\frac{1}{2.3} \ln \frac{I_0}{I} = 0.015 + a\cdot b\cdot c$$

where

$$I = 1.40 \times 10^{16},\ a = 1 \text{ cm},\ b = 11{,}050, \text{ and } c = 2.68 \times 10^{-8}.$$

Substituting gives

$$37.1778 - \ln I = 0.0352$$
$$I = 1.36 \times 10^{16} \text{ photons/sec}$$

Correcting for loss through exit fiber-optics and grating divergence loss (0.0068): $I = 9.192 \times 10^{13}$ photons/sec. The differential signal developed between the reference and sample detectors will be the net photons/sec times the photodiode sensitivity

$$dI_{\text{det.}} = (9.192 - 9.135)\ 10^{13} \text{ photons/sec}$$
$$= 5.7 \times 10^{11} \text{ photons/sec}$$

or

$$S_{\text{det.}} = \frac{(5.7 \times 10^{11})\,(8 \times 10^{-12})\,(10^{-7})\,(10^{6})\,(12 \times 10^{-12})}{2.2 \times 10^{-4}} = 5.2 \times 10^{-9} \text{ A}$$

APPENDIX II —SOLUTION OF GAUSSIAN CURVE FOR CONCENTRATION OF GUANOSINE IN 0.030-ml DETECTOR CELL

See Fig. 17 for details and peak measurements. V_0 = Retention volume of guanosine; $V_b - V_a = 0.030$ ml; $V_2 - V_1 = 0.3$ ml; $W = 10^{-9}$ g guanosine. The curve is of the general form

$$C(V) = \frac{W}{\sqrt{2\pi}\sigma} \exp \frac{-(V - V_0)^2}{2\sigma^2}$$

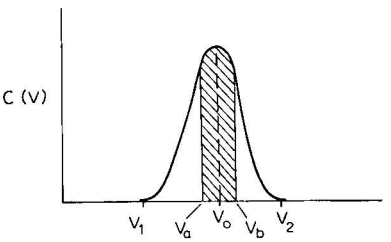


Fig. 17. LC Gaussian peak shape for guanosine

Let $V_a = V_0 - \bigtriangledown$ and $V_b = V_0 + \bigtriangledown$ for the area

$$A_T = \int_{V_a}^{V_b} C(V)\mathrm{d}v$$

Because the area in the cross-hatched region is symmetrical about V_0, we simplify

$$A_1 = 2 \int_{V_a}^{V_b} C(V)\mathrm{d}v$$

The function, F(x) is a cumulative probability function of a uniform normal distribution and has been extensively tabulated, or

$$\mathrm{F}(x) = \frac{1}{\sqrt{2\pi}} \int_{-\infty}^{x} \mathrm{e}^{\frac{-t^2}{2}} \mathrm{d}t$$

By making the transformation, $t = (V - V_0)/\sigma$, then $t = \mathrm{d}V/\sigma$.
So

$$\int_{-\infty}^{V'} C(V)\mathrm{d}v = WF(x')$$

then

$$A = 2 \int_{V_0}^{V_b} C(V)\mathrm{d}v = 2 \left[\int_{-\infty}^{V_b} C(V)\mathrm{d}v - \int_{-\infty}^{V_0} C(V)\mathrm{d}v \right]$$

$$= 2 [W\mathrm{F}(X_b) - W\mathrm{F}(0)]$$
$$= 2 W [\mathrm{F}(X_b) - 0.5]$$

For the LC curve, σ can be approximated as follows:

$$\sigma = \frac{V_2 - V_1}{6} = 0.5 \text{ ml}$$

then $x_b = 6\nabla/(V_2 - V_1)$
where $\nabla = 0.015$ and W and $V_2 - V_1$ have been given previously.
Thus

$$A = 2 \times 10^{-9}\left[\frac{F(6 \times 0.015)}{0.3} - 0.5\right]$$

$$= 2 \times 10^{-9}\,[F(0.3) - 0.5]$$
$$= 2 \times 10^{-9}\,(0.6179 - 0.5)$$
$$= 2.36 \times 10^{-10}\text{ g}$$

APPENDIX III —COMPARISON OF THE LINEAR PHOTODIODE ARRAY (512 PIXELS) UTILIZING SINGLE PIXEL TO THE PHOTOMULTIPLIER[33,34]

For the Reticon

$$\left(\frac{S}{N}\right)_{CH} = \frac{N_p\, Q_v\, T_e}{N_n\, N_f}$$

where

N_p = input photons/sec (= 10^4)
Q_v = quantum efficiency at specified wavelength (0.32 at 250 nm)
T_e = integration or dwell time per channel (1 sec)
N_n = noise (electrons/frame) (= 770)
N_f = number of frames (= 1)

$$\left(\frac{S}{N}\right)_{CH} = \frac{(10^4)\,(0.32)\,(1)}{(770)\,(1)} = \frac{32}{7.7} = 4.1{:}1$$

For photomultiplier, single-wavelength sensing for grating (250 nm, 1 nm bandwidth)

$$\left(\frac{S}{N}\right)_{CH} = \frac{N_p\, Q_p\, GK}{N_{PM}}$$

where

N_p = input photons/sec (= 10^4)
Q_p = quantum efficiency (0.1 at 250 nm)
G = gain ($\approx 10^6$)
K = C/electro-static units (= 1.6×10^{-19})
N_{PM} = photomultiplier dark current noise ($\approx 6 \times 10^{-12}$ A)

$$\left(\frac{S}{N}\right)_{PM} = \frac{(10^4)\,(0.1)\,(10^6)\,(1.6 \times 10^{-19})}{6 \times 10^{-12}} = \frac{16}{6} = 26{:}1$$

REFERENCES

1 K. Callmer and O. Nilsson, *Chromatographia*, 6 (1973) 517.
2 C. J. O. R. Morris, *Lab. Pract.*, 23 (1974) 513.
3 H. Veening, *J. Chem. Educ.*, 50 (1973) A481.
4 M. Krejci, *Chem. Listy*, 57 (1973) 843.
5 E. S. Watson, *Ger. Offen. Pat.*, 2,258,208, 7 June (1973).
6 E. D. Pellizzari and C. M. Sparacino, *Anal. Chem.*, 45 (1973) 378.
7 D. R. Baker, R. C. Williams and J. C. Steichen, *J. Chromatogr. Sci.*, 12 (1974) 499.
8 A. Sonnenschein, *Anal. Instrum.*, 12 (1974) 123.
9 J. Koszewski, A. Bylina, D. Sybilska and Z. R. Gravowski, *Brit. Pat.*, 1,339,475, 5 December, 1973.
10 J. C. Steichen, *J. Chromatogr.*, 104 (1975) 39.
11 N. P. Dimov, *Dokl. Bolg. Akad. Nauk*, 27 (1974) 1407.
12 M. S. Denton, T. P. DeAngelis, A. M. Yacynych, W. R. Heineman and T. W. Gilbert, *Anal. Chem.*, 48 (1976) 20.
13 B. Sauer, *GIT Fachz. Lab.*, 17 (1973) 1152.
14 A. Bylina, D. Sybilska, Z. R. Grabowski and J. Koszewski, *J. Chromatogr.*, 83 (1973) 357.
15 M. J. Milano and H. L. Pardue, *Anal. Chem.*, 47 (1975) 25.
16 H. L. Pardue, A. E. McDowell, D. M. Fast and M. J. Milano, *Clin. Chem.*, 21 (1975) 1192.
17 Y. Talmi, *Anal. Chem.*, 47 (1975) 659A.
18 Y. Talmi, *Anal. Chem.*, 47 (1975) 687A.
19 R. Dessy, W. G. Nunn, W. D. Reynolds and C. A. Titus, *Pittsburgh Conf. Anal. Chem. Appl. Spectrosc., 27th, March 1976*, paper No. 375.
20 A. G. Marshall and M. B. Comisarow, *Anal. Chem.*, 47 (1975) 491A.
21 F. W. Plankey, T. H. Glenn, L. P. Hart and J. D. Winefordner, *Anal. Chem.*, 46 (1974) 1000.
22 B. L. Karger, M. Martin and G. Guiochon, *Anal. Chem.*, 46 (1974) 1640.
23 M. W. Anders and J. P. Latorre, *Anal. Chem.*, 42 (1970) 1430.
24 M. W. Anders and J. P. Latorre, *J. Chromatogr.*, 55 (1971) 409.
25 J. E. Mrochek, S. Katz, W. H. Cristie and S. R. Dinsmore, *Clin. Chem.*, 20 (1974) 1086.
26 J. X. Khym, *Analytical Ion-Exchange Procedures in Chemistry and Biology*, Prentice-Hall, Englewood Cliffs, N.J., 1974.
27 P. R. Brown, *High-Pressure Liquid Chromatography; Biochemical and Biomedical Applications*, Academic Press, New York, 1973.
28 C. D. Scott, *Sep. Purif. Methods*, 3 (1974) 263.
29 A. Flaks, J. M. Hamilton and D. B. Clayson, *J. Nat. Cancer Inst.*, 51 (1973) 2007.
30 D. B. Clayson, A. J. Bedford and R. Turner, *Chem.-Biol. Interactions*, 6 (1973) 107.
31 P. E. Levi, J. C. Knowles, D. M. Cowen, M. Wood and E. H. Cooper, *J. Nat. Cancer Inst.*, 46 (1971) 337.
32 R. R. Buss (Reticon Corp., 910 Benicia Avenue, Sunnyvale, Calif.), personal communication.
33 Y. Talmi, R. Crosmum and N. M. Larson, *Anal. Chem.*, 48 (1976) 326.
34 G. G. Olson, *Amer. Lab.*, February (1972) 69.

Journal of Chromatography, 126 (1976) 369–380
© Elsevier Scientific Publishing Company, Amsterdam — Printed in The Netherlands

CHROM. 9423

A FLOW CONTROLLER FOR HIGH-PERFORMANCE LIQUID CHROMATOGRAPHY AND ITS APPLICATIONS

KEI ASAI, YOH-ICHI KANNO, AKIRA NAKAMOTO and TASUKU HARA
Scientific and Industrial Instrument Division, Shimadzu Seisakusho Ltd., Kyoto 604 (Japan)

SUMMARY

A new flow control system has been developed for high-performance liquid chromatography, which consists of a flow sensor (a bubble flow tube) connected to the detector outlet, an electro-pneumatic controller and a pressure control valve for a pneumatic amplifier pump.

The flow sensor measures the volumetric flow-rate of the carrier from the column with no influence of viscosity changes. The system keeps the flow-rate of the carrier constant within an accuracy of $\pm$ 0.3%.

A high-performance liquid chromatograph equipped with this flow controller provides various advantages:

(1) The repeatability of the retention time and peak area is better than $\pm$ 0.5%, even in gradient elution analysis.

(2) The flow-rate is set digitally with no calibration factor for any type of carrier.

(3) The real flow-rate is indicated every few seconds on a recorder or a meter.

(4) Calibration procedures involved in gradient rate changes can be eliminated.

INTRODUCTION

High-performance liquid chromatography (HPLC) has become a very important technique in analytical chemistry, and the repeatability and the accuracy of the results obtained are becoming increasingly important.

One of the important parameters that affects the analytical accuracy is the flow-rate of the carrier. The causes of changes in this flow-rate in liquid chromatographic systems have been suggested[1,2] to be leakage at the piston seal or check valve in a reciprocating piston pump, liquid compressibility under high pressure in a constant displacement pump, and carrier viscosity changes owing to changes in temperature and/or composition in a pneumatic amplifier pump. In addition to these factors, the column permeability, which is influenced by the settling and swelling of the packing in the column, and clogging in a line filter are also causes of changes in flow-rate. Further, in gradient elution chromatography, the composition of the carrier changes with time, which is accompanied by changes in viscosity and liquid volume. All of these factors adversely affect the analytical results.

Jackson and Henry introduced a feed-back flow controller in order to overcome these problems[3]. They employed a pressure transducer as a flow-sensing element, which monitors the pressure drop (Δp) across a calibrated flow restrictor. Therefore, their flow controller could not compensate for flow changes due to changes in viscosity and temperature.

In this study, the volumetric flow-rate of the carrier was measured at the outlet of the analytical column and this flow-rate was kept constant by using new electro-pneumatic flow controller. The design, characteristics and some applications of this flow controller in HPLC are described.

EXPERIMENTAL

Flow meter design

In order to eliminate viscosity-dependent characteristics involved in the method which monitors Δp across a flow restrictor, we employed a bubble flow tube, which is capable of measuring the volumetric flow-rate directly.

The flow meter is illustrated in Fig. 1. A very small air stream, for instance 40 μl/min, is introduced into the carrier flow through a small nozzle, and bubbles are formed periodically. The air line consists of a very narrow restrictor tube, a 60-m stainless-steel pipe of 0.08 mm I.D. and a pressure regulator that supplies a constant pressure of about 5–6 atm to this narrow restrictor tube so that the air flow-rate is kept constant, independent of changes in the carrier flow-rate and/or viscosity. With an aqueous carrier, bubbles are formed about every 20 sec and with methanol about every 5 sec.

The bubbles flow successively into a transparent flow tube (glass, 1 mm I.D.) and the time of travel between two points a definite distance apart on the flow tube (32 mm) is measured photoelectrically.

The inlet-side photo-transistor detects the entry of an air bubble into this flow tube by the change in intensity of the light from a light-emission diode, and starts the

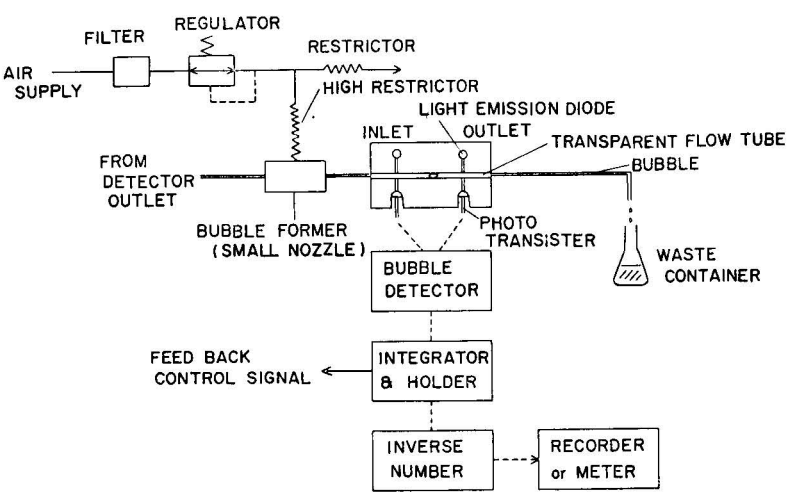


Fig. 1. The flow meter.

integrator circuit integrating a certain constant voltage with respect to time. The outlet-side photo-transistor detects the exit of the bubble and stops the integration. Thus, the integrator output voltage is proportional to the time of travel of the bubble and is inversely proportional to the sum of the bubble and carrier flow-rates.

The integrated voltage is held until the next bubble is measured and is used as the feed-back control signal. For direct reading purposes, this integrated voltage is converted into an inverse number. Then the air flow-rate, which has been measured independently, is subtracted from this inverted value to give the carrier flow-rate on a strip-chart recorder or a meter.

Flow control system

A pneumatic amplifier pump (Haskel, Burbank, Calif., U.S.A.) was used as the pumping system. In this constant-pressure system the carrier flow-rate changes slowly owing to a change in the column back-pressure (*i.e.*, caused by settling of the packing, or by swelling, etc.), or changes in the viscosity due to temperature or when solvent gradients are used. The time lag from the change in pressure of the air supply to the resulting carrier flow-rate change at the column outlet is relatively large. In view of these system characteristics and the fact that the flow-rate measurement is discontinuous, we employed a control system in which a control signal is fed back to re-set the setting of a precision pressure controller (booster relay) for the pneumatic amplifier pump. The control system is illustrated in Fig. 2 and a block diagram of the electronic control circuits is shown in Fig. 3.

As shown in Fig. 3, the flow-rate is set by using a digital switch in the voltage that is inversely proportional to the total flow-rate of the carrier and air. The integrator output voltage is compared with this pre-set voltage and the deviation is amplified in the differential amplifier circuit. This amplified deviation is fed to a motor drive circuit via a linearizer, which converts the deviation into a value proportional to the actual flow-rate deviation, and the motor is driven during the time proportional

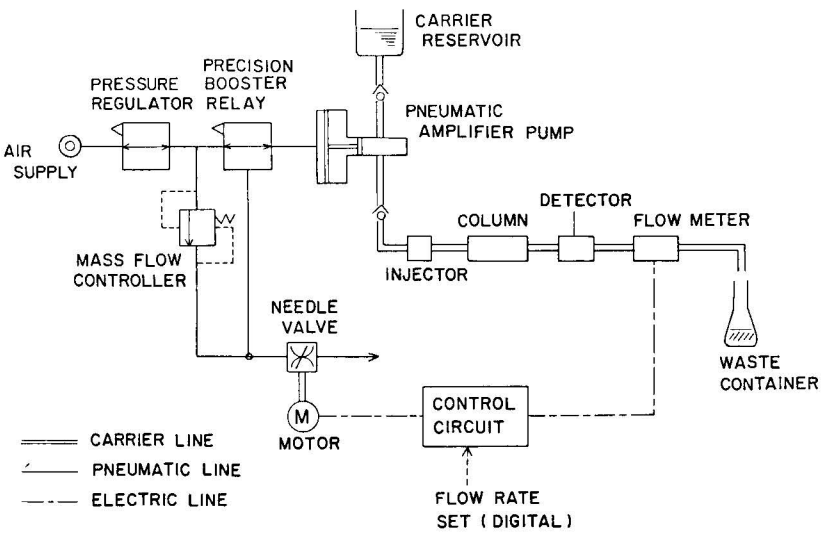


Fig. 2. Flow diagram of DuPont 830 liquid chromatograph with flow controller.

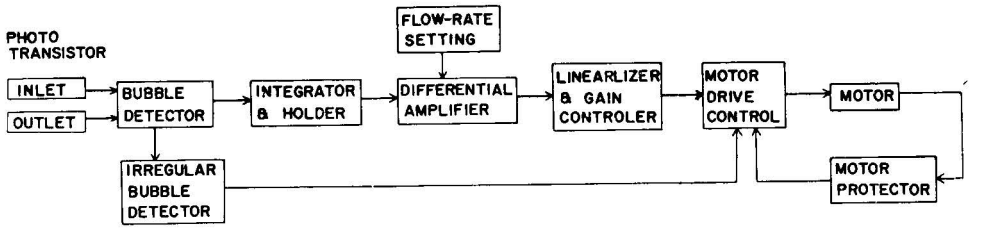


Fig. 3. Block diagram of electrical circuit for flow controller.

to the flow-rate deviation to rotate the needle valve shaft. The driving time can be adjusted by a gain controller.

As shown in Fig. 2, the needle valve is in the pneumatic control line. The pneumatic control line has a mass flow controller, a needle valve and a precision booster relay, and provides the following functions.

The mass flow controller always maintains a flow velocity of about 2 l/min, independent of the flow resistance of the needle valve. Hence the resistance change of the needle valve according to the shaft rotation by the motor causes a change in the inlet pressure of the needle valve. This pressure is supplied to the setting side of the precision booster relay to control the air pressure to the pneumatic amplifier pump so that the column inlet pressure is regulated so as to maintain the carrier flow-rate constant.

As described above, there is some time delay in the control loop and the measurement of the flow-rate is discontinuous. Therefore, the amount of feed-back must be suppressed so as to follow the set flow-rate gradually. The relationships between the kind of carrier and the amount of feed-back were carefully examined.

Liquid chromatograph

The liquid chromatograph used was a DuPont Model 830 instrument equipped with gradient elution accessories. A photograph of the combined Model 830 instrument and the flow controller (on the left) is shown in Fig. 4.

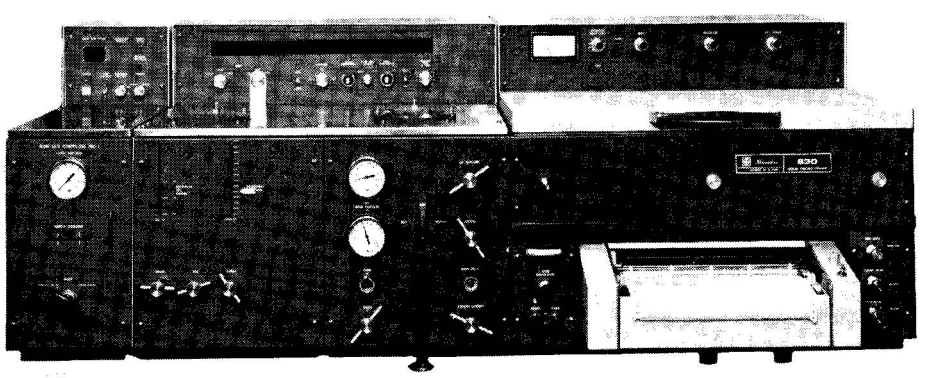


Fig. 4. Liquid chromatograph with flow controller (left-hand module).

The liquid chromatographic column (1 m × 2.1 mm I.D.) was packed with Permaphase ODS (DuPont, Wilmington, Del., U.S.A.). The carriers were distilled water and reagent-grade methanol. The samples were fused-ring aromatic hydrocarbon standards such as naphthalene, biphenyl, anthracene, pyrene, chrysene and benzo[*a*]pyrene. Sample injections were made with a high-pressure sampling valve. The sample volume was 12 μl.

Other equipment

A Model ITG-4A and Chromatopac-1A (Shimadzu Seisakusho Ltd., Kyoto, Japan) digital integrator was used. In addition to a DuPont gradient programmer, a Model GRE-1 multi-linear gradient programmer (Shimadzu Seisakusho Ltd.) was also used.

RESULTS AND DISCUSSION

Flow-rate measurement and control

In the flow meter, if the back-pressure at the air-bubble former (nozzle) is changed, the air flow-rate is also changed and this change causes an error in the measurement of the carrier flow-rate. In order to avoid this erroneous measurement, it is necessary to keep the back-pressure as low as possible and to take precautions so that the influence of the change in back-pressure is as small as possible. In this study, the back-pressure was kept as low as 0.01 kg/cm^2, and the air pressure supply was as high as 5 kg/cm^2. Hence the air flow-rate was maintained constant.

It was observed that in the measurement of flow-rate, the resistance change in the narrow restrictor tube and the change in the length of the flow tube by fluctuations in the ambient temperature were negligibly small.

The relationship between the set flow-rate and the real flow-rate controlled by the flow controller is shown in Table I. The real flow-rate was measured by the gravimetric method using water as carrier. The linearity is better than approximately 1% in the range from 1.0 to 4.5 ml/min in water. As a result, the controller is capable of covering a range from 0.3 to 4.9 ml/min.

TABLE I

RELATION BETWEEN SET FLOW-RATE AND REAL FLOW-RATE

Carrier, water; bubble interval, about 20 sec.

Set flow-rate (ml/min)	*Real flow-rate (ml/min)*	*Deviation (%)*
1.0	0.995	0.5
2.0	2.020	1.0
3.0	3.024	0.8
4.5	4.524	0.5

Fig. 5 shows an example of actual control functions. It shows the recorder trace of 0.8 ml/min of water with the full scale of recorder set to 1 ml/min. The results indicate that the flow-rate is controlled to within ± 0.2–0.3% of the set flow-rate.

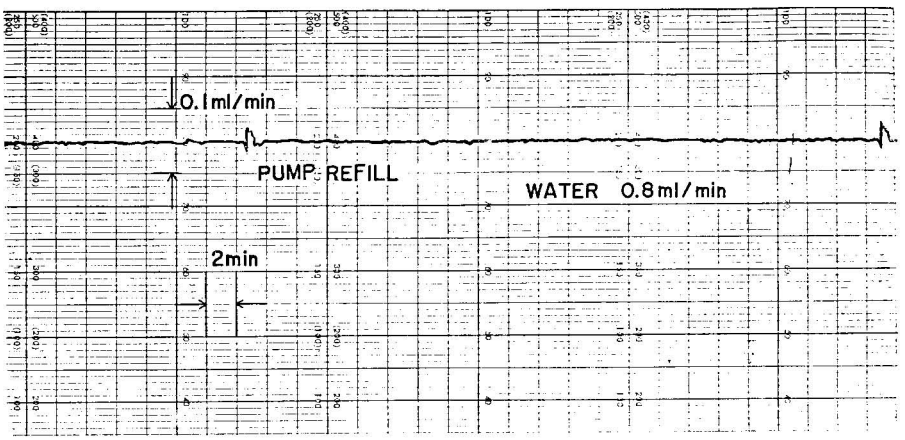


Fig. 5. Example of flow-rate record. One division corresponds to 0.01 ml/min.

Application in isocratic elution chromatography

Fig. 6 is an example of a high-performance liquid chromatogram of fused-ring aromatic hydrocarbon standards obtained by using a Model 830 liquid chromatograph equipped with the flow controller. The flow-rate was also recorded simultaneously. Five peaks were recorded in the order solvent, unknown, biphenyl, an-

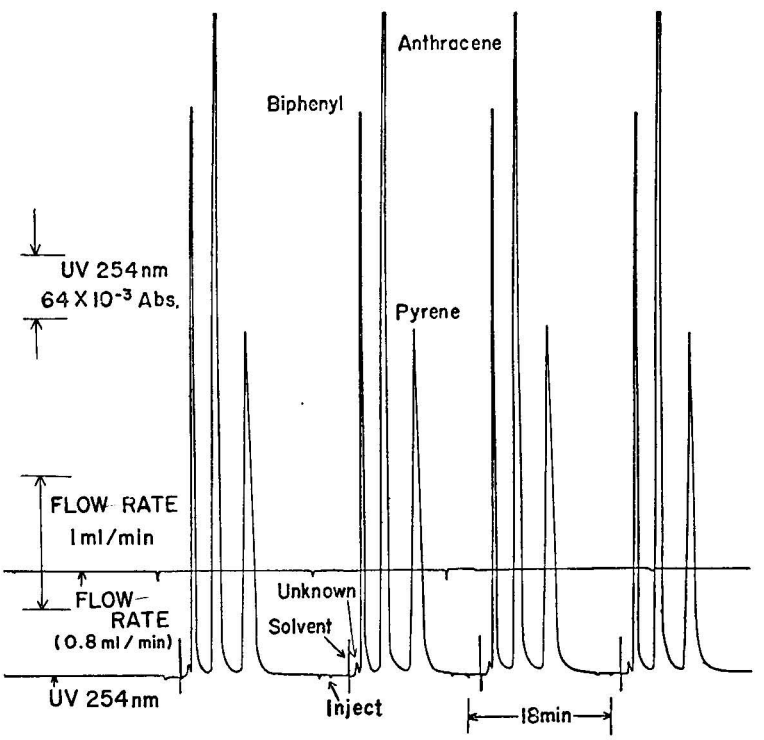


Fig. 6. Chromatogram for reproducibility check. Operating conditions: column, Permaphase ODS, 1 m × 2.1 mm I.D.; temperature, 50°; carrier, methanol–water (3:2); flow-rate, 0.8 ml/min; detector, UV photometer (254 nm) at $64 \cdot 10^{-2}$ a.u.f.s.

TABLE II

REPRODUCIBILITY OF RETENTION TIME IN ISOCRATIC ELUTION

Column, Permaphase ODS, 1 m × 2.1 mm I.D.; temperature, 50°; carrier, methanol–water (3:2); flow-rate, 0.8 ml/min; detector, UV photometer at 254 nm.

Run No.	*Retention time (min)*				
	Solvent	*Unknown*	*Biphenyl*	*Anthracene*	*Pyrene*
1	1.63	2.80	3.54	6.51	10.64
2	1.64	2.81	3.55	6.52	10.64
3	1.64	2.81	3.55	6.50	10.61
4	1.64	2.81	3.55	6.50	10.61
5	1.65	2.81	3.55	6.50	10.62
6	1.65	2.82	3.55	6.51	10.63
7	1.65	2.81	3.55	6.51	10.62
8	1.65	2.81	3.55	6.51	10.62
9	1.64	2.81	3.54	6.51	10.62
10	1.65	2.81	3.55	6.51	10.63
11	1.65	2.82	3.56	6.52	10.66
12	1.64	2.81	3.55	6.52	10.65
Average	1.6442	2.8108	3.5492	6.52	10.629
σ	0.0064	0.00493	0.00493	0.00707	0.01439
Coefficient of variation	0.39%	0.175%	0.139%	0.109%	0.141%

thracene and pyrene. The carrier was 60% methanol in water. A UV 254 absorption detector was used at the full-scale range of $64 \cdot 10^{-2}$ absorbance unit. The flow-rate was 0.8 ml/min. Under such conditions, the reproducibilities of the retention time and peak area were determined and the results are shown in Tables II and III.

TABLE III

REPRODUCIBILITY OF PEAK AREA IN ISOCRATIC ELUTION

Operating conditions as in Table II.

Run No.	*Peak area ratio*	
	Biphenyl/anthracene	*Pyrene/anthracene*
1	0.4228	0.6751
2	0.4206	0.6747
3	0.4204	0.6864
4	0.4176	0.6738
5	0.4179	0.6740
6	0.4194	0.6773
7	0.4187	0.6753
8	0.4161	0.6703
9	0.4168	0.6717
10	0.4172	0.6745
11	0.4199	0.6758
12	0.4159	0.6710
Average	0.4186	0.6750
σ	0.00197	0.00395
Coefficient of variation	0.472%	0.585%

It can be seen from Table II that the reproducibility of the retention time was excellent. The coefficients of variation were 0.39% for the solvent peak, 0.175% for the unknown peak, 0.139% for biphenyl, 0.109% for anthracene and 0.141% for pyrene.

The reproducibility of the peak area measured by a digital integrator (Shimadzu ITG-4A) is shown in Table III. The reproducibilities of the peak area ratio of biphenyl to anthracene and pyrene to anthracene are 0.472 and 0.585% (coefficients of variation), respectively.

Application in gradient elution chromatography

The change in flow-rate in gradient elution chromatography using the flow controller is shown in Fig. 7. In this instance the carrier was varied from 100% water to 100% methanol at a gradient rate of 5%/min. As can be seen from Fig. 7, the flow-rate is kept constant even in the gradient elution operation. Thus, the gradient elution chromatography is carried out with no effect from changes in flow-rate, and the separation is expected to be governed only by the characteristics of the solvent.

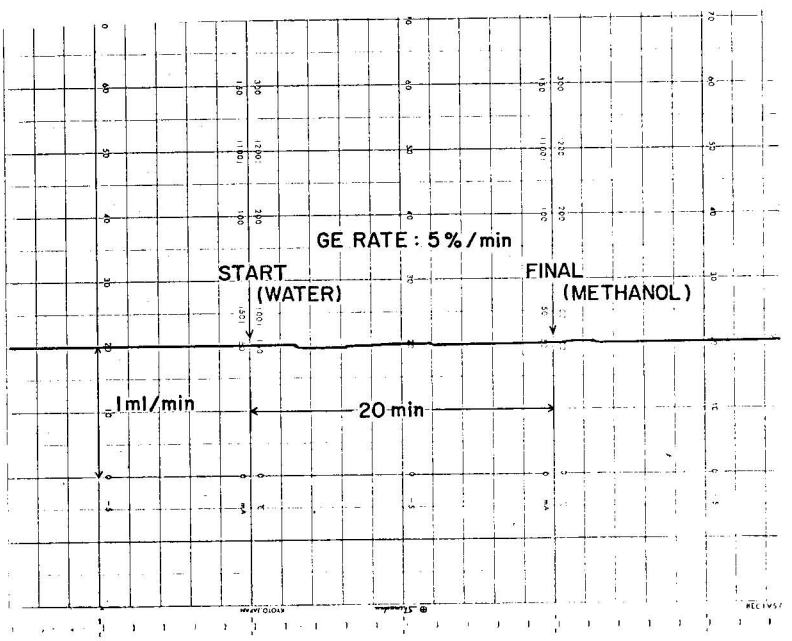


Fig. 7. Flow-rate during gradient elution using flow controller. Operating conditions: column, Permaphase ODS, 1 m × 2.1 mm I.D.; temperature, 50°, carrier, from 100% water to 100% methanol at the rate of 5%/min.

Table IV illustrates the reproducibility of the retention times in gradient elution chromatography. This analysis was carried out in 2 days and the results demonstrate that a reproducibility of better than 0.3% is obtained for all peaks.

Constant flow operations in gradient elution chromatography have a great advantage in quantitative analysis. The effects of the gradient rate on peak retention

TABLE IV

REPRODUCIBILITY OF RETENTION TIME IN GRADIENT ELUTION

Column, Permaphase ODS, 1 m × 2.1 mm I.D.; temperature, 50°; carrier, from 100% water to 100% methanol at the rate of 4%/min; flow-rate, 1.0 ml/min; detector, UV (254 nm) at $64 \cdot 10^{-2}$ a.u.f.s.

Run No.	*Retention time (min)*						
	Naphthalene	*Biphenyl*	*Anthracene*	*Pyrene*	*Chrysene*	*Benzo[e]-pyrene*	*Benzo[a]-pyrene*
1	12.38	16.08	19.22	21.72	23.69	25.53	25.91
2	12.33	16.09	19.25	21.74	23.69	25.50	25.92
3	12.47	16.23	19.35	21.82	23.75	25.54	25.94
4	12.42	16.17	19.28	21.79	23.70	25.50	25.90
5	12.38	16.19	19.28	21.78	23.72	25.52	25.91
6	12.39	16.18	19.31	21.77	23.71	25.50	25.89
7	12.37	16.14	19.26	21.76	23.66	25.44	25.86
8	12.35	16.12	19.25	21.72	23.17	21.41	25.83
9	12.35	16.12	19.23	21.75	23.69	25.47	25.88
10	12.38	16.13	19.22	21.69	23.69	25.43	25.85
Average	12.383	16.145	19.265	21.753	23.687	25.484	25.889
σ	0.038	0.045	0.039	0.037	0.036	0.042	0.032
Coefficient of variation	0.307%	0.276%	0.204%	0.172%	0.168%	0.166%	0.125%

time and area are shown in Tables V, VI and VII. The gradient rate examined is also shown in Fig. 8. For the purpose of comparison, the effects of carrier composition on retention time and area in isocratic elution chromatography are shown in Table VIII and the chromatogram is shown in Fig. 9.

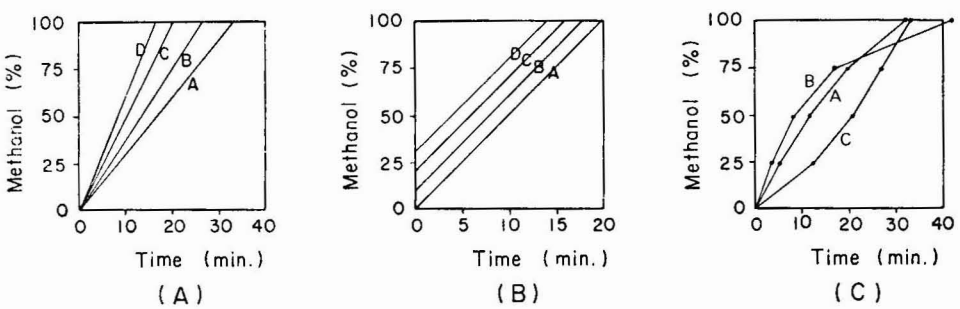


Fig. 8. Gradient function.

It was observed clearly that the effect of changes in the carrier composition on the peak area is fairly small. Therefore, when the concentration-sensitive detector (*e.g.*, a UV absorption detector) is used, the re-calibration procedures associated with gradient rate change can be expected to be eliminated.

TABLE V

EFFECTS OF GRADIENT RATE ON RETENTION TIME AND PEAK AREA

Column, Permaphase ODS, 1 m × 2.1 mm I.D.; temperature, 55°; detector, UV (254 nm); carrier, methanol added to water (from 0 to 100%); flow-rate, 0.8 ml/min. Gradient rate: A, 3%/min; B, 4%/min; C, 5%/min; D, 6%/min (as shown in Fig. 8A).

Gradient function	*Naphthalene*		*Biphenyl*		*Anthracene*		*Pyrene*		*Chrysene*		*Benzo[a]pyrene*	
	t_R*	*Area***	t_R*	*Area***	t_R*	*Area***	t_R*	*Area***	t_R*	*Area***	t_R*	*Area***
A	1496	11158	1836	10324	2131	68230	2311	9278	2478	18466	2685	10798
B	1317	10806	1563	10701	1778	66682	1915	9710	2038	18906	2195	10755
C	1165	10876	1352	10330	1517	63698	1622	9143	1717	17930	1839	10116
D	1079	15740	1229	10301	1372	64549	1464	9433	1542	18415	1645	10263
Average		10947		10414		65790		9396		18429		10483
σ		152		166		1779		142		345		298
Coefficient of variation		1.39%		1.59%		2.70%		2.21%		1.87%		2.84%

* t_R = retention time; 1/100 min.

** Area = area counts measured with Chromatopac 1A.

TABLE VI

EFFECTS OF INITIAL CONCENTRATION ON RETENTION TIME AND PEAK AREA

Operating conditions are as in Table V except for the initial concentration and gradient rate. Gradient rate, 5%/min. Gradient: A, 0–100%; B, 10–100%; C, 20–100%; D, 30–100% (as shown in Fig. 8B).

Gradient function	*Naphthalene*		*Biphenyl*		*Anthracene*		*Pyrene*		*Chrysene*		*Benzo[a]pyrene*	
	t_R*	*Area***	t_R*	*Area***	t_R*	*Area***	t_R*	*Area***	t_R*	*Area***	t_R*	*Area***
A	1165	10876	1352	10330	1517	63698	1622	9143	1717	17930	1839	10116
B	971	10887	1155	10284	1331	66915	1443	9174	1541	18213	1665	10558
C	794	11360	975	10135	1145	64380	1254	9027	1345	17985	1475	10425
D	587	11379	760	10106	932	64430	1042	8917	1140	18607	1270	10807
Average		11125.5		10213.8		14855.8		9065.3		18183.8		10476.5
σ		244		95		280		101		266		249
Coefficient of variation		2.194%		0.932%		1.887%		1.121%		1.465%		2.379%

* t_R = retention time; 1/100 min.

** Area = area counts measured with Chromatopac 1A.

TABLE VII

EFFECTS OF GRADIENT RATE ON RETENTION TIME AND PEAK AREA

Operating conditions as in Table V except for the gradient function: A, 0–25% at 5%/min; 25–50% at 4%/min, 50–75% at 3%/min, 75–100% at 2%/min; B, 0–25% at 7%/min, 25–50% at 5%/min, 50–75% at 3%/min, 75–100% at 1%/min; C, 0–25% at 2%/min, 25–50% at 3%/min, 50–100% at 4%/min (as shown in Fig. 8C).

Gradient function	*Naphthalene*		*Biphenyl*		*Anthracene*		*Pyrene*		*Chrysene*		*Benzo[a]pyrene*	
	t_R*	*Area***	t_R*	*Area***	t_R*	*Area***	t_R*	*Area***	t_R*	*Area***	t_R*	*Area***
A	1201	10771	1426	10097	1646	63658	1805	9134	1961	16758	2166	10885
B	1061	10392	1233	10037	1433	65231	1583	8785	1731	16326	1924	10340
C	1823	10623	2228	9908	2535	64191	2702	9289	2845	18498	3015	10324
Average		10595		10014		64360		9069		17194		10522
σ		156		78.9		653		210		938		280
Coefficient of variation		1.47%		0.78%		1.01%		2.32%		5.45%		2.66%

* t_R = retention time; 1/100 min.

** Area = area counts measured with Chromatopac 1A.

TABLE VIII

EFFECTS OF METHANOL CONCENTRATION ON RETENTION TIME AND PEAK AREA

Column, Permaphase ODS, 1 m × 2.1 mm I.D.; temperature, 55°; detector, UV (254 nm); carrier, methanol added to water.

Methanol (%)	*Naphthalene*		*Biphenyl*		*Anthracene*		*Pyrene*		*Chrysene*		*Benzo[a]pyrene*	
	t_R*	*Area***	t_R*	*Area***	t_R*	*Area***	t_R*	*Area***	t_R*	*Area***	t_R*	*Area***
40	374	10779	613	10231	1253	69962	2239	8571	4453	16625	10506	9752
45	304	11033	447	10256	822	69995	1372	8804	2479	17176	5306	9685
50	255	10674	339	9934	559	69231	869	8829	1445	17363	2905	10337
55	218	—***	268	—***	396	67884	569	8975	862	17261	1619	10389
60	196	—***	226	—***	305	—***	411	8498	574	18271	999	10547
Average		10804		10064		69035		8799		17344		10282
σ		137		182		890		214		484		306
Coefficient of variation		1.271%		1.819%		1.298%		2.430%		2.797%		2.989%

* t_R = retention time; 1/100 min.

** Area = area counts measured with Chromatopac 1A.

*** These peaks were not separated from neighbouring peaks.

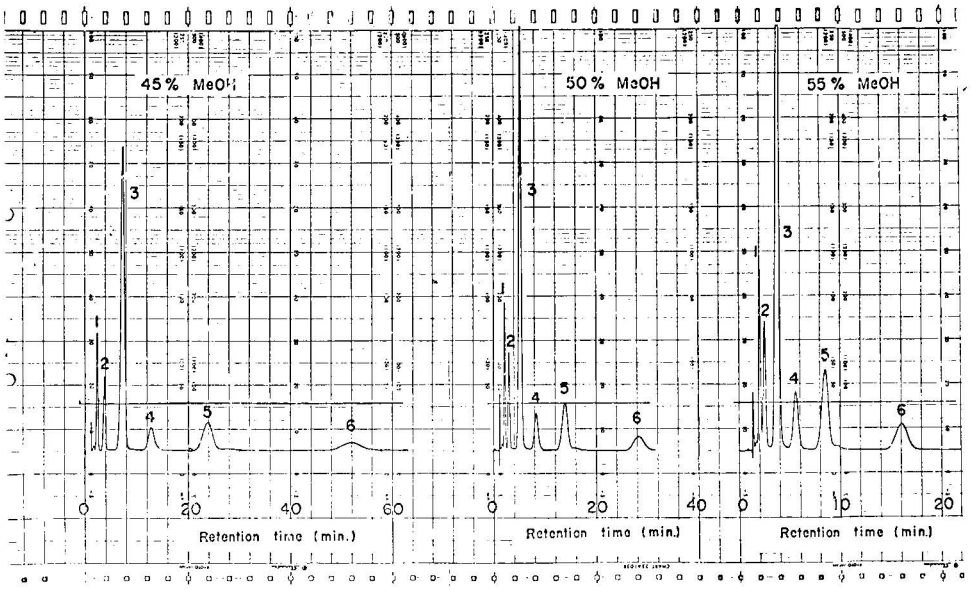


Fig. 9. Influence of carrier composition on peak retention time and area. Operating conditions: column, Permaphase ODS, 1 m × 2.1 mm I.D.; temperature, 55°; mobile phase, methanol–water (0.8 ml/min); detector, UV 254. Peaks: 1, naphthalene; 2, biphenyl; 3, anthracene; 4, pyrene; 5, chrysene; 6, benzo[*a*]pyrene.

ACKNOWLEDGEMENTS

The authors are grateful to Dr. T. Haruki for his helpful advice on this work, and to Dr. K. Okamoto for technical assistance.

REFERENCES

1 L. Berry and B. L. Karger, *Anal. Chem.*, 45 (1973) 819A.
2 M. Martin, G. Blu, C. Eon and G. Guiochon, *J. Chromatogr.*, 112 (1975) 399.
3 M. T. Jackson and R. A. Henry, *Int. Lab.*, Nov./Dec. (1974) 57.

Journal of Chromatography, 126 (1976) 381–400
© Elsevier Scientific Publishing Company, Amsterdam — Printed in The Netherlands

CHROM. 9417

PRESSURIZED, ANNULAR CHROMATOGRAPH FOR CONTINUOUS SEPARATIONS

CHARLES D. SCOTT, ROGER D. SPENCE and WARREN G. SISSON
Oak Ridge National Laboratory, Oak Ridge, Tenn. 37830 (U.S.A.)*

SUMMARY

The concept for a continuous chromatograph utilizing a rotating annulus was presented over 25 years ago. Such a system with a stationary feed point and stationary effluent ports can accept a continuous feed stream and separate it into a series of constituent streams that appear as separate helical bands in the annulus. A theoretical plate concept can be used to mathematically describe the system. Recent developments for continuous liquid chromatography include the addition of gas overpressure for higher pressure operation and the use of segmenting spacers at the feed entry to allow gradient elution. Molecular sieves and ion-exchange systems are being investigated for utility in several specific separations.

INTRODUCTION

Preparative, large-scale chromatographic separations are usually achieved by increasing the diameter of the analytical-scale sorption column. This expanded size allows larger amounts of feed material to be introduced in a batch mode without seriously overloading the column. Unfortunately, the increase in the dimension normal to the eluent flow contributes to a loss of resolution due to radial flow variations and other mixing effects. As a result, the scale-up of conventional columns beyond about 2.5 cm diameter leads to a measurable loss of resolution.

Much consideration has been given to the technique of continuous liquid chromatography and to various systems designed to take advantage of its capabilities. One system would contain provisions for the solid sorbent phase to move countercurrent to the eluent stream and have intermediate takeoff points for the various different solutes; however, the design problems associated with such a scheme would be quite difficult. A variation of the technique developed by Arehart *et al.*[1], which is the closest approach to this concept, would still not be adequate since it contributes to extensive backmixing. In any case, the bulk sorbent phase must have the capability of moving past the feed entry point and various product takeoff points in order for the chromatograph to be truly continuous.

* Research sponsored by the Energy Research and Development Administration under contract with Union Carbide Corporation.

An annular chromatograph rotating with respect to a feed stream and eluate collection points was proposed by Martin[2] over 25 years ago. Later, it was considered on a theoretical basis by Giddings[3]. Several other workers have developed and evaluated various versions of this concept during the past 20 years, but apparently were not able to circumvent the operational problems. For example, Svensson *et al.*[4] utilized an annular array of individual columns while Fox *et al.*[5] used a rotating annulus. On the other hand, Dunnill and Lilly[6] carried out experiments to determine the effectiveness of a stationary annulus with rotating feed nozzle and fraction collector. In these cases, the designs of the various systems resulted in relatively simple biochemical separations; however, such systems used only gravity or low-pressure flow, making it difficult to take advantage of high-resolution separations and the designs of the systems were not compatible with gradient elution techniques.

We are now considering an extension of this concept in which a rotating annulus will be used with stationary feed and elution streams as well as stationary eluate collection ports. Further, the feed and eluent streams will be introduced through appropriate seals to permit pressurized operation with an overpressure of gas, and segmenting vanes will be included at the top of the annular bed to reduce feed backmixing and to allow gradient elution.

A more complete theoretical analysis of the system utilizing a theoretical plate concept has also been completed, and a photometric monitor has been developed for measuring elution position and band spreading.

THEORETICAL CONSIDERATIONS*

Principle of operation

In our approach, operation of the continuous, annular chromatograph involves moving an annular bed of sorbent past a stationary feed entry point and stationary effluent recovery ports (Fig. 1). As the annulus rotates, it is subjected to a short feed introduction time followed by a relatively long period of elution from a series of eluent nozzles. During this operational sequence, the initial entry point completes a revolution.

As elution proceeds, the eluted substances progress down the annulus, giving the appearance of helices as the annulus rotates. The more strongly sorbed species exit from the rotating annulus at a greater distance from the feed point, thus providing a continuous separation of species with differing sorption characteristics.

Mathematical description

The annular chromatograph can be described mathematically by a theoretical plate approach similar to that developed by Martin and Synge[7] and amplified by Said[8] for stationary columns. The mathematical description should result in algebraic expressions for the elution position (as measured from the feed point) of each solute and for the bandwidth as a function of elution position or other system parameters.

General considerations. The following simplifying assumptions are made: (1) The annulus consists of a series of equally sized segments arranged circumferentially. (2) Each of these annular segments is made up of a series of theoretical plates,

* See also List of symbols at the end of the article.

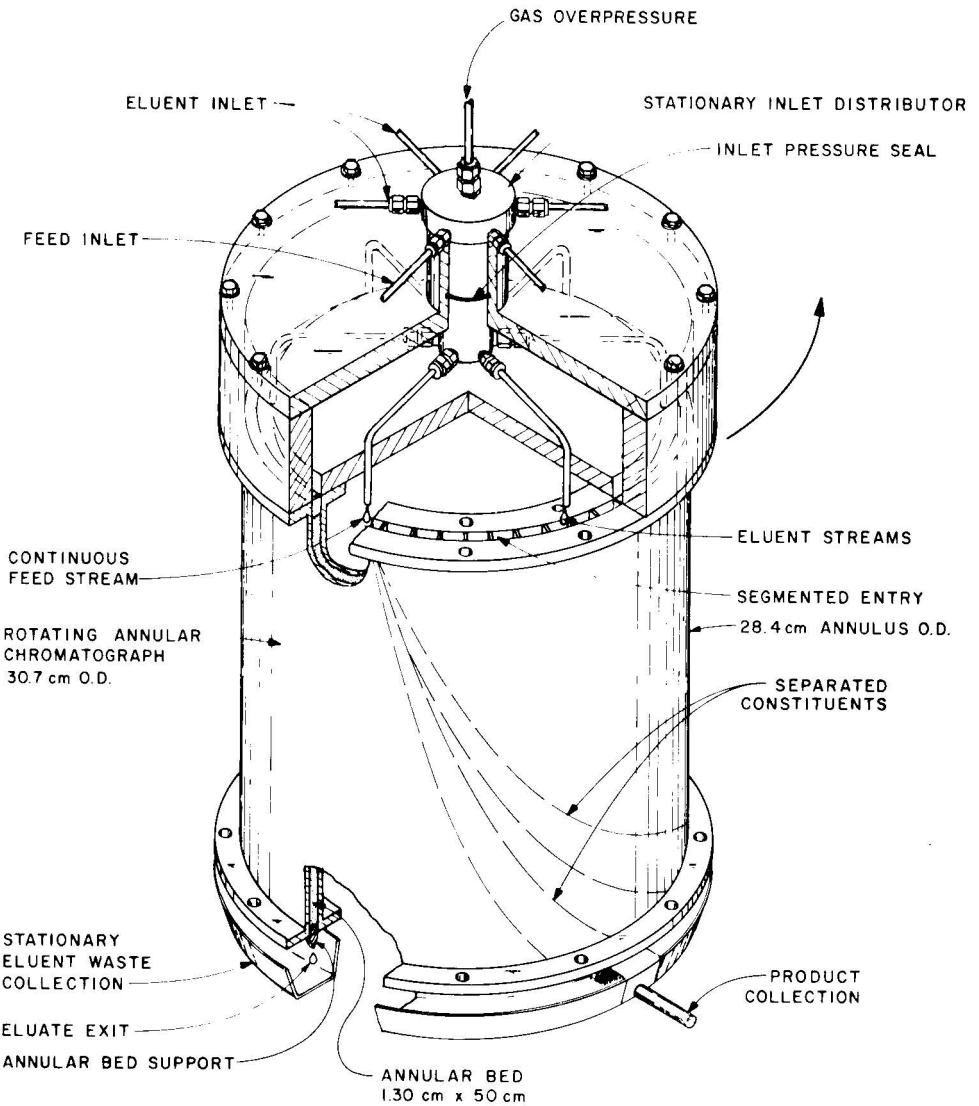


Fig. 1. Pressurized, continuous annular chromatograph.

progressing from the top to the bottom, that have identical fixed heights. (3) The concentration of a solute as it leaves the theoretical plate is at equilibrium with the average concentration of the solute sorbed in the stationary phase. (4) There is no lateral mass transport of the solute or solvent to adjoining annular segments. (5) No radial variation exists in either the fluid or the sorbent phase. (6) The superficial velocity of the eluent is constant throughout the annulus.

One of the problems encountered in mathematically describing the annular chromatograph is the establishment of a usable point of reference. This is somewhat difficult since the feed and eluate recovery points are stationary while the annular

sorbent phase is in motion. In fact, it is convenient to use two references, *viz.* the stationary feed point and a specific point in the rotating annulus (*e.g.*, the top). For the sake of simplicity, the following additional assumptions were made in an attempt to circumvent this problem: (1) A single annular segment as it rotates will be one reference point for the mathematical treatment and the feed point will be the other. (2) All of the solute is assumed to be in the first theoretical plate at the end of the feed introduction period.

The actual chromatographic process begins at $t = 0$, when the reference annular segment just leaves the feed zone. Thereafter, the elution sequence occurs and the annular position of the reference segment, in terms of the stationary feed point, is dependent on the time and angular speed of the annulus. The steady-state chromatographic patterns can be established by following the chromatographic process in a single columnar segment as it makes a complete circuit.

The mathematical description of the process with the above assumptions can be generated by considering a series of material balances of the solute around each of the theoretical plates of the reference segment. For example, at plate 1, after the feed stage during the time lapse of Δt (or an eluent flow through the segment of Δv and an angular displacement of $\Delta\Theta$ from the feed point), the material balance would be (Fig. 2)

$$\text{solute in} - \text{solute out} = \text{change in solute inventory} \tag{1}$$

If Δt, Δv, and $\Delta\Theta$ become vanishingly small, the differential form of the material balance becomes

$$0 - c_1\,\mathrm{d}v = \mathrm{d}\left[\frac{V}{N}\varepsilon c_1 + \frac{V}{N}(1-\varepsilon)\,Kc_1\right] \tag{2}$$

where

c_1 = concentration of solute in the fluid phase leaving the first theoretical plate, moles/cm^3

v = total eluent flow through an annular segment during time t and displacement Θ, cm^3

V = total volume of an annular segment, cm^3

N = total number of theoretical equilibrium plates in the annular segment

$$K = \text{distribution coefficient, } \frac{\text{moles solute/cm}^3\text{ sorbent phase}}{\text{moles solute/cm}^3\text{ fluid phase}}$$

$$\varepsilon = \text{void fraction in chromatograph, } \frac{\text{cm}^3\text{ fluid phase}}{\text{cm}^3\text{ annular volume}}$$

Rearrangement yields

$$\frac{\mathrm{d}c_1}{c_1} = -B\,\mathrm{d}v \tag{3}$$

where

$$B = \frac{N}{V}\left[\frac{1}{\varepsilon + (1-\varepsilon)\,K}\right]$$

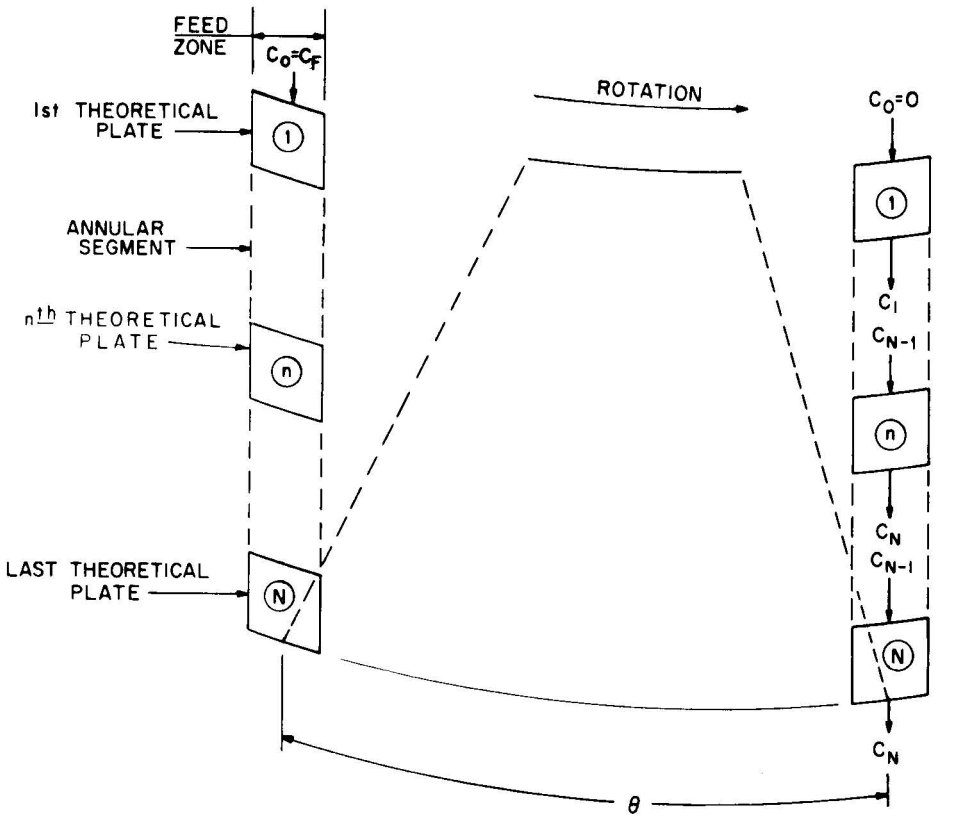


Fig. 2. Movement of an annular segment in the continuous annular chromatograph.

Here the boundary conditions are

$$v = 0,\ t = 0,\ c_1 = c_f$$

where c_f = solute concentration in the feed, moles/cm^3. The solution of eqn. 3 results in the fluid phase solute concentration in plate 1 of the annular segment after the flow of a volume, v, of the eluent

$$c = c_f e^{-Bv} \tag{4}$$

During the time required for the flow of v through the annular segment, the segment has rotated away from the feed point by an angle of

$$\Theta = \omega t = \frac{\omega v}{uA} \tag{5}$$

where

A = cross-sectional area of the annular segment, cm^2

t = time for the reference annular segment to be displaced by an angle of Θ from the feed point, sec

u = eluent superficial velocity, cm/sec

ω = angular velocity, rad/sec

Therefore, the concentration of the solute as it leaves the first theoretical plate at a position Θ from the feed point is given by eqn. 4.

Similarly, the mobile phase concentration can be represented at any theoretical plate, n, in the annular segment at any point around the annulus by

$$\frac{c_n}{c_f} = e^{-Bv} \frac{(Bv)^{n-1}}{(n-1)!} = e^{-B'\theta} \frac{(B'\Theta)^{n-1}}{(n-1)!} \tag{6}$$

where

$$B' = \frac{Nu}{\omega L} \left[\frac{1}{\varepsilon + (1-\varepsilon) K}\right]$$

L = vertical distance from feed point to exit, cm. In the case of the system exit, this equation becomes

$$\frac{c_N}{c_f} = \frac{e^{-B'\theta} (B'\Theta)^{N-1}}{(N-1)!} \tag{7}$$

This is a Poisson distribution, which can be approximated by a Gaussian distribution for large values of $B'\Theta$ (ref. 9)

$$\frac{c_N}{c_f} = \frac{1}{\sqrt{2\pi B'\Theta}} \exp - \left\{\frac{[B'\Theta - (N-1)]^2}{2B'\Theta}\right\} \tag{8}$$

Elution position. The maximum value of solute concentration at the exit will occur at a specific angular location, $\bar{\theta}$, and can be determined by allowing the differential of eqn. 7 with respect to Θ to approach zero:

$$\left[\frac{e^{-B'\Theta} (B'\Theta)^{N-2}}{(N-2)!}\right] \left(1 - \frac{B'\Theta}{N-1}\right) = 0 \tag{9}$$

Eqn. 9 indicates that the first derivative is zero at

$$B'\Theta = N-1, \quad B'\Theta = 0, \quad B'\Theta = \infty$$

or at

$$\Theta = \frac{N-1}{B'}, \Theta = 0, \Theta = \infty$$

The maximum exit concentration or "elution position", $\bar{\Theta}$, of the solute must then be at the point where

$$\bar{\Theta} = \frac{N-1}{B'} \tag{10}$$

or, for large values of N

$$\bar{\Theta} = \frac{N}{B'} \tag{11}$$

Minimum values will be found at

$$\Theta = 0 \text{ and } \Theta = \infty$$

From eqns. 8 and 11 the maximum concentration will then be

$$\left(\frac{c_N}{c_f}\right)_{\text{max.}} = \frac{1}{\sqrt{2\pi B'\overline{\Theta}}} = \frac{1}{\sqrt{2\pi\,(N-1)}} \approx \frac{1}{\sqrt{2\pi N}} \tag{12}$$

If we introduce the expression for B' into eqn. 11, the elution position is defined by

$$\overline{\Theta} = \frac{\omega L}{u}\,[\varepsilon + (1-\varepsilon)\,K] \tag{13}$$

Thus, eqn. 13 should predict the radial exit location of the maximum concentration of a solute (elution position) as a function of system length (L), angular velocity or rotational speed (ω), superficial velocity (u), void fraction (ε), and the distribution coefficient (K).

Bandwidth. In order to establish conditions for separating two or more solutes, both the elution position and the width of solute bands must be predictable. The solute band is defined as the solute concentration in the circumferential or horizontal direction. Disregarding circumferential diffusional effects and mixing, there are two major contributions to the width of the helical bands as they exit the chromatograph: the initial width of the feed stream and longitudinal diffusional and mixing effects. The first of these is easily measured and thus predictable at the feed introduction point, while the second can be estimated with the assumptions inherent in the theoretical plate theory.

As indicated by the mathematical treatment of Van Deemter *et al.*[10], the various band spreading phenomena in combination can be represented by a simple addition of the variances of each of the mechanisms. Thus, the total variance, σ_t^2, would be a linear combination of the two effects noted above

$$\sigma_t^2 = \sigma_f^2 + \sigma_l^2 \tag{14}$$

or

$$\sigma_t = \sqrt{\sigma_f^2 + \sigma_l^2} \tag{15}$$

where the subscripts t, f, and l represent total, feed, and longitudinal, respectively.

It is most convenient to express band spreading by angular displacement since this fits in with the angular elution position. In this case, the standard deviation of band spreading, σ, will be expressed as the angle of displacement from the midpoint of the band.

The contribution of the feed bandwidth is rather straightforward sincd it is defined by the distance between spacers at the top of the chromatograph. On the other hand, band spreading in the longitudinal direction, σ_l, can be approximated by modifying the expression developed for the concentration profile given by eqn. 6. As

previously mentioned, this expression for large values of $B'\Theta$ can be approximated by a Gaussian distribution which, when put in the standard form, could be used to determine the standard deviation.

As before, we have considered a reference segment of the annulus rotating sequentially through the feed zone and the elution zone. The total quantity of solute, Q, leaving the segment during the course of the elution would be

$$Q = \int_{-\infty}^{\infty} c_N \, dv \text{ or } Q = \frac{uA}{\omega} \int_{-\infty}^{\infty} c_N \, d\Theta \tag{16}$$

(Note: Because all of the material is eluted in a single revolution after which feed is again introduced, the limits of integration, $-\infty$ and ∞, are actually "dummy" limits, relating only to a single sample input pulse.)

The total quantity of feed introduced to the first plate was:

$$Q = c_f \frac{AL}{N} [\varepsilon + (1 - \varepsilon) K] \tag{17}$$

Normalizing eqn. 16 by dividing by eqn. 17 results in

$$\int_{-\infty}^{\infty} B' \frac{c_N}{c_f} \, d\Theta = 1 \tag{18}$$

which is a necessary criterion for a standard Gaussian distribution of the function

$$\left(B' \frac{c_N}{c_f}\right)$$

From eqn. 12 it can be seen that

$$\left(\frac{B' c_N}{c_f}\right)_{\text{max.}} = \frac{B'}{\sqrt{2\pi N}} \tag{19}$$

But, for a standard Gaussian distribution, the maximum value will also be

$$\left(\frac{B' c_N}{c_f}\right)_{\text{max.}} = \frac{1}{\sigma_l \sqrt{2\pi}} \tag{20}$$

Combining eqns. 19 and 20 and substituting eqn. 11 results in

$$\sigma_l = \frac{\overline{\Theta}}{\sqrt{N}} \tag{21}$$

The total bandwidth at the exit of the chromatograph can then be approximated by

$$\sigma_t = \sqrt{\sigma_f^2 + \frac{\overline{\Theta}^2}{N}} \tag{22}$$

EXPERIMENTAL EQUIPMENT

An annular chromatograph and a photometric monitoring device were developed and fabricated for this study.

Annular chromatograph

The annular chromatograph (Fig. 1) was fabricated from Plexiglas®. The annulus was formed from two concentric open cylinders and appropriately sealed at the top and the bottom by flanges. The annulus was 1.30 cm wide and 50 cm long, with an outside diameter of 28.4 cm. The top of the cylinder forming the inner annulus wall was also sealed. The enclosed head space above the annulus was created by bolting another open cylinder with sealed top to the flange on the outside annulus wall. A Teflon® flow distributor fit into a special port provided in the top of the chromatograph with a double O-ring seal. Inlet holes drilled through this distributor allowed access of the feed line and six eluent lines, while an air line provided constant overpressure. The head space in the top of the chromatograph provided a gas blanket over the annulus which could be pressurized to a maximum of 25 p.s.i.g., while the O-ring seal allowed the distributor to remain stationary during rotation of the annulus.

Forty-eight spacers were placed across the annulus at regular intervals at the top and the bottom of the annulus. These spacers not only served to maintain a constant annulus width, but also segmented the top of the column into different regions for gradient elution.

The sorbent bed was held in place by a plastic fabric over a wire mesh, which was clamped in place between two plastic gaskets, and the entire chromatograph was bolted onto a support plate. The eluate stream tended to contact solid surfaces at the system exit which could result in flow over the surfaces, extensive mixing, and separation into a few, discrete eluate streams. To circumvent this problem, a series of 1/8-in.-thick spacers was also placed in the annular exit just below the stationary phase support. Each spacer extended across the annulus exit, and had a triangular cross section whose apex extended below the chromatograph. This arrangement, which resulted in channeling of the eluate stream onto each spacer, with eluate dripping from each apex, prevented gross backmixing. The spacers were placed at 2-cm intervals around the annulus exit.

A slow-speed drive system allowed the support plate (and the annular chromatograph) to rotate at speeds of approximately 0.1 to 20 rph. Metering pumps were available to introduce the feed and eluent streams through the stationary distributor; for nongradient elution, an electrical feedback level control was available to maintain a constant eluent level above the surface of the sorbent.

Monitoring device

A device for monitoring the concentration of solute in the helical bands was developed. It included a light source that imposed light through the outer chromatograph wall into the eluting band and a photo detector that measured reflected light. These were enclosed in an aluminum body (see Fig. 3). Light from the source was focused with a lens into the sorbent phase, and the reflected light was then focused onto a photovoltaic silicon detector. The signal from the silicon detector was amplified and subsequently recorded on a strip-chart recorder.

Operation

For gradient elution, the top of the sorbent bed was just above the lower edge of the top spacers. This separated the top of the annulus into a series of "segments" with a small amount of contained headspace above each. During operation, the feed

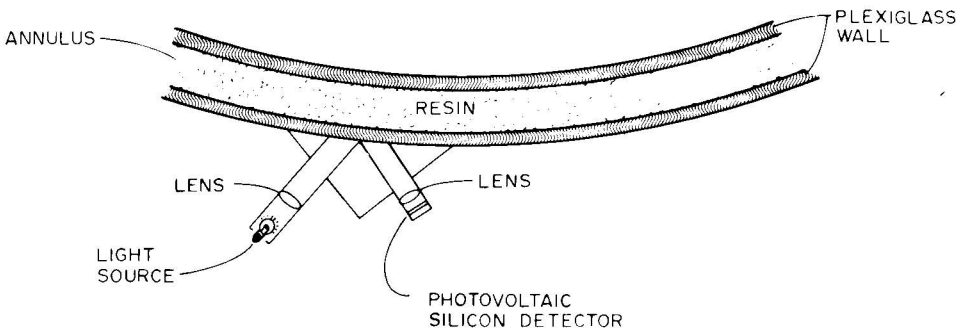


Fig. 3. Schematic of solute monitoring device.

stream was introduced sequentially into each segment as the annulus rotated past the feed nozzle. The separation process was actually begun before the solute had progressed below the bottom of the spacer. The feed rate was controlled so that the head space in each segment was not exceeded during the time that the feed point was above the segment. With this mode of operation, the eluent streams were introduced into each segment as it passed sequentially under the individual eluent nozzles. The eluent flowrates were also adjusted so that the segment head space was not exceeded. The spacing of the eluent nozzles was such that the eluent in the segment head space was exhausted just as the segment progressed to the next nozzle.

For isocratic elution, the sorbent level was maintained above the top of the spacers and the feed nozzle tip was adjusted so that it was below the surface of the sorbent bed. This resulted in the feed nozzle plowing through the top portion of the bed. In most cases, the packed sorbent material had enough fluidity to prevent any permanent trace from the feed nozzle; however, an overlay of a nonadsorbing gel could be used to circumvent this problem. With such an approach, feed convective mixing was retarded and the initial feed bandwidth was about half that when the segments were used. A constant head of eluent fluid was maintained above the entire bed by a simple liquid-level feedback controller and the gas overpressure forced the eluent through the sorbent.

Solute monitor. Band eluting position was simply determined visually as the midpoint of the exiting solute band. However, the concentration across the solute band was determined by the monitoring device. Since the helical band appeared to be stationary while the annulus rotated, band monitoring was achieved by attaching the monitoring device to the outer surface of the chromatograph and allowing it to scan across the band with the motion of the annulus (Figs. 4 and 5).

EXPERIMENTAL RESULTS

Two different types of separation were studied: (1) a system using cross-linked dextran gels for separation by molecular size, and (2) a system using ion-exchange resins. The former would be typically applied to biochemical separations, while the latter would normally be used for separation of inorganic solutes. The primary experimental parameters measured were the elution position and the bandwidth as a function of bed depth. These data were correlated by the expressions developed

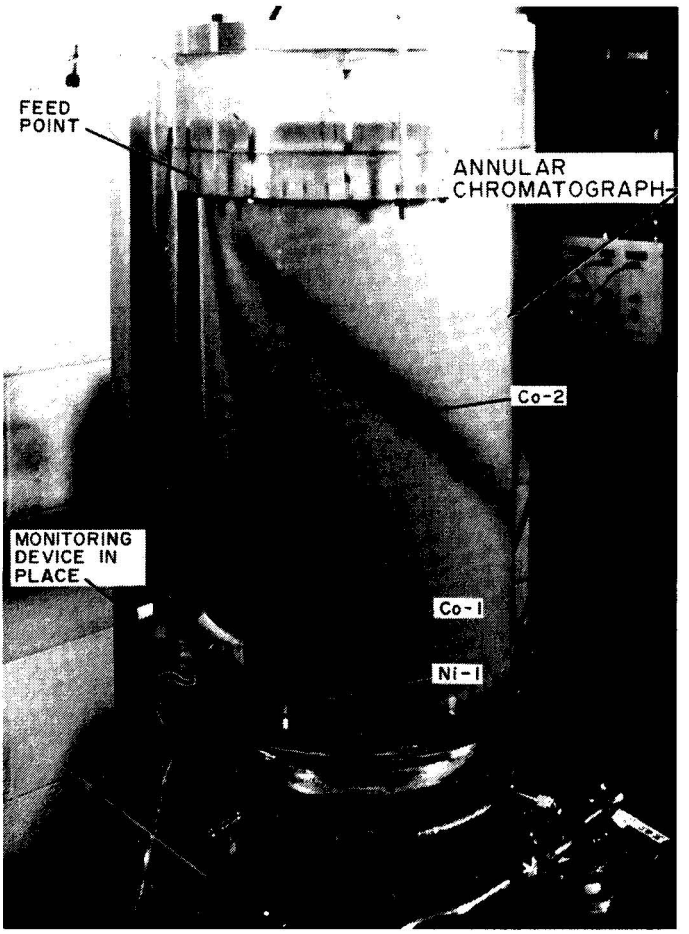


Fig. 4. Separation of a nickel and two cobalt complex ions in a simulated ammonia process liquor by the continuous annular chromatograph.

by the mathematical model, and the resulting correlations were used to verify the validity of that mathematical interpolation.

Molecular sieve separations

Cross-linked dextran gels can be used to separate mixtures of biological macromolecules by difference in molecular size. This molecular sieving operation is one of the most important separation tools used in biochemical research.

In order to evaluate the continuous annular chromatograph for such applications and, at the same time, to verify the mathematical model, a series of tests was made with various Sephadex* gels as the stationary phase. Typicall, Sephadex G-25 in the size range of 100–300 μm was used with a test feed stream containing Blue Dextran 2000* (a high-molecular-weight, soluble dextran) either as a single solute or in

* Trademark of Pharmacia Fine Chemicals, Uppsala, Sweden.

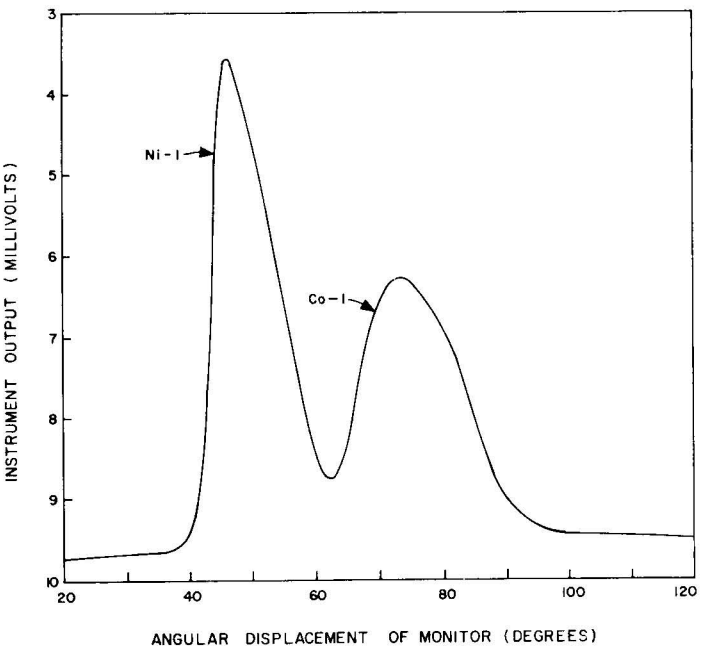


Fig. 5. Typical output of monitoring device as it scans across the elution bands in the ion-exchange separation of nickel and cobalt complex ions. Scanning wavelength, 620 mm; scanning speed, 49°/h.

combination with $CoCl_2$. In the latter case, the significant difference in the molecular size of the two solutes (the Blue Dextran molecule was much too large to penetrate the gel matrix) gave a clear indication of the molecular sieving action. Since both solutes were highly colored materials, they were easily detected and quantified in the experimental apparatus. Distilled water was used as the eluent.

Ion-exchange separation

The separation of nickel and cobalt from a synthetic process liquor was investigated as an ion-exchange separation of potential utility. In the preferred process for nickel recovery from oxide ores[11], an ammonia-rich process liquor is produced that contains a nickel complex ion and as many as three cobalt complex ions. Hurst[12] recently identified these complexes as $[Ni(NH_3)_{6-x}(H_2O)_x]^{2+}$, $[Co(NH_3)_4CO_3]^+$, $[Co(NH_3)_5CO_3]^+$, and $[Co(NH_3)_6]^{3+}$, referred to hereafter as Ni-1, Co-1, Co-2, and Co-3 and he proposed that a high-resolution ion-exchange separation could be used for the final purification step in this process with recovery of both nickel and cobalt. In such a process, a continuous chromatograph would be most useful.

Dowex 50W-X8 ion-exchange resin (50–60 μm) was used to separate the components in a synthetic feed liquor containing Ni-1, Co-1, and Co-2. The third cobalt species was not included since it represents a relatively simple separation. The eluent was 1 *M* $(NH_4)_2CO_3$ buffered to a pH of 7.8, and the elution sequence was Ni-1 followed by Co-1 and Co-2 (Fig. 4). Since all three solutes are colored substances with useful light absorption properties, the separation could be easily followed by the monitor.

Calibration of the solute monitor

In order to measure the bandwidths of the eluting solutes, it was necessary to measure the concentration profile across the eluting band. Thus, the output of the solute monitoring device had to be related to solute concentration. In this context, the measurement of actual concentration was not as important as determining the relative concentration across the band.

Calibration of this device was accomplished by fabrication of a stationary section of the chromatographic annulus divided into segments, which allowed the stationary phase to be introduced with several different solute concentrations. Each segment could then be scanned by the monitor and the instrument reading compared to actual solute concentration.

This procedure was followed for several solutes in various sorbents in a variety of concentration ranges. The solute concentration was found to be related to the instrument output by an inverse log relationship similar to that expected for the dependence of absorbance on transmittance measurements:

$$c = C \ln \frac{1}{R} \tag{23}$$

where

R = ratio of the instrumental reading at a solute concentration of c to the instrument reading for zero solute

C = calibration constant

A typical plot of such data for Blue Dextran in the Sephadex G-25 is shown in Fig. 6. Such a relationship was used in subsequent tests to determine the bandwidth at half the maximum band concentration.

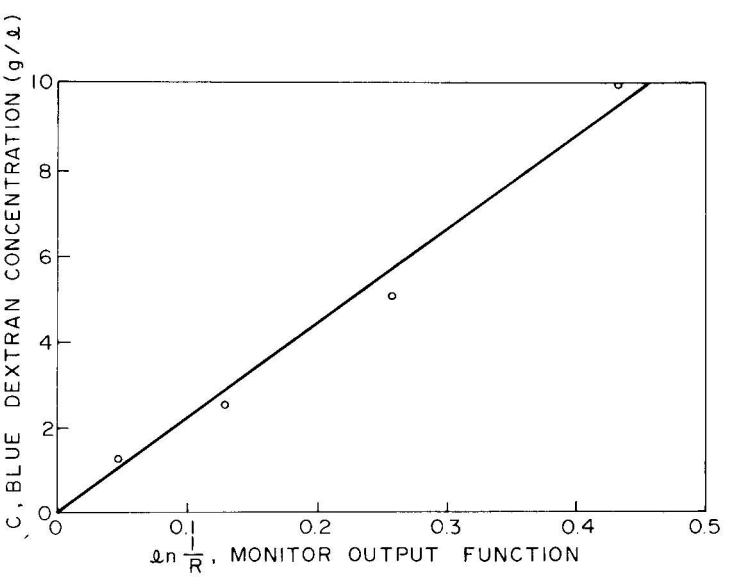


Fig. 6. Relationship between Blue Dextran concentration in a bed of Sephadex G-25 and the output from the solute monitor. Measurement at 620 nm.

Void fraction

The elution position of a specific solute, measured as the angular displacement of the band from the feed point, should be dependent on the length of the chromatograph, speed of rotation, superficial velocity, void fraction, and distribution coefficient, as indicated in eqn. 13. Blue Dextran 2000 has such a large molecular weight that it should not penetrate the pores of Sephadex gels, and minimal surface sorption phenomena are expected. Thus, it could be used to measure the efficiency of the chromatographic system.

Since no interaction of the solute with the stationary phase is expected, the distribution coefficient should be zero and the mathematical expression for elution position should be

$$\bar{\Theta} = \frac{\omega L \varepsilon}{u} \tag{24}$$

Since ε should be relatively constant at a given elution rate (where u is constant), we would expect a plot of $\bar{\Theta}$ *vs.* L to produce a straight line at a given rotational speed. This was found to be true at rotational speeds of 0.0013–0.0044 rad/sec, where the band displacement was measured vertically down the annulus (Fig. 7).

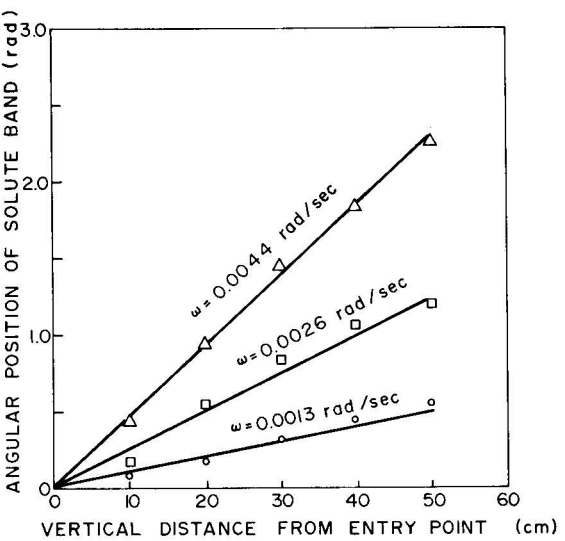


Fig. 7. Effect of vertical distance and rotational speed on elution position of the Blue Dextran band eluting through Sephadex G-25 (100–300 μm) in the continuous annular chromatograph. Eluent, distilled water; feed, 20 g/l Blue Dextran at 1 ml/min.

Further, it would be expected that, upon measurement of the elution position of Blue Dextran at specific operating conditions, eqn. 24 after rearrangement could be used to establish the void fraction, ε. If this value was found to be relatively constant over a range of operating conditions, the mathematical interpretations of the system would prove to be useful. Using this approach, the void fraction was found to be essentially constant for all runs, that is, it was independent of flow-rate (Table I).

TABLE I

VOID FRACTION AND DISTRIBUTION COEFFICIENTS CALCULATED FROM ELUTION POSITIONS FOR SEPARATION OF BLUE DEXTRAN AND $CoCl_2$ IN A CONTINUOUS ANNULAR CHROMATOGRAPH USING SEPHADEX G-25 AS THE SORBENT PHASE

Operating conditions: temperature, 25 ± 2°; gas overpressure, 5–7 p.s.i.; eluent, distilled water; sorbent phase, Sephadex G-25; particle size, 100–300 μm.

Annular velocity, ω (rad/sec × 10³)	*Superficial velocity, u (cm/sec × 10²)*	*Elution position, $\bar{\Theta}$* (rad)*		*Calculated value of ε** for Blue Dextran*	*Calculated value of K** for $CoCl_2$*
		Blue Dextran	*$CoCl_2$*		
1.05	1.37	1.38	2.21	0.36	0.34
1.05	1.63	1.11	1.77	0.34	0.32
1.01	1.95	0.94	1.58	0.36	0.39
1.02	1.93	0.97	1.60	0.37	0.37
1.03	1.92	0.93	1.58	0.35	0.37
1.05	2.15	0.93	1.54	0.38	0.40
1.03	2.41	0.69	1.16	0.32	0.33
1.05	2.68	0.74	1.19	0.38	0.37
1.05	3.40	0.58	0.92	0.38	0.35
1.11	2.10	1.01	1.64	0.38	0.39
2.60	1.89	2.41	3.98	0.35	0.35
		Mean (standard deviation)		0.36 (0.02)	0.36 (0.026)

* Measured at 50 cm below the feed point.
** Calculated using eqn. 13.

Distribution coefficient

After the void fraction is known, eqn. 13 can also be used to determine the distribution coefficient for eluting substances which have an affinity for sorption. In the molecular sieve separation, $CoCl_2$ does penetrate the gel pores, where it undergoes a weak ionic interaction with the stationary phase. This causes the solute to elute after Blue Dextran. The elution position can be used to establish a distribution coefficient. As shown in Table I, this distribution coefficient was reasonably constant over the range of operating conditions, thus further showing the utility of the mathematical interpretation. As expected, the Blue Dextran and $CoCl_2$ were well separated in all tests.

All of the measured ionic constituents in the ion-exchange separation were sorbed more strongly by the solid phase than was $CoCl_2$ by the Sephadex G-25. Using an externally measured void fraction ($\varepsilon = 0.40$) and the elution positions of the three constituents, distribution coefficients were again determined. The calculated distribution coefficients were relatively constant over a minimal range of operating conditions (Table II), but were up to 25% less than those measured by stationary analytical columns. The distribution coefficients were quite dependent on pH and it is expected that variations in pH within the annular chromatograph caused the difference.

Theoretical plates

In a few of the runs, the solute monitoring device was used to measure the width of the $CoCl_2$ band just prior to the elution exit (at 45 cm from the feed point) in the molecular sieve separation and the width of the Ni-1 band in the ion-exchange

TABLE II

SEPARATION OF NICKEL AND COBALT COMPLEX IONS BY CATION-EXCHANGE RESIN IN THE CONTINUOUS ANNULAR CHROMATOGRAPH

Operating conditions: temperature, 25 ± 2°; gas overpressure, 9–10 p.s.i.; eluent, 1 *M* $(NH_4)_2CO_3$ buffered to pH 7.8; sorbent phase, Dowex 50-X8; particle size, 50–60 μm.

Annular velocity, ω (rad/sec × 10^4)	*Superficial velocity, u (cm/sec × 10^2)*	*Bed length of measurement, L (cm)*	*Initial bandwidth for Ni-1, W_0 (rad)*	*Final bandwidth for Ni-1, W^* (rad)*	*Elution position, $\bar{\Theta}^*$ (rad)*			*Distribution coefficient, K^{**}*			*Number of theoretical plates, N^{***}*
					Ni-1	*Co-1*	*Co-2*	*Ni*	*Co-1*	*Co-2*	
2.43	2.52	44.5	0.119	0.162	0.942	1.38		2.98	4.69		403
2.35	2.43	43.8	0.131	0.164	0.838	1.24	2.51	2.63	4.21	9.20	393
2.11	2.25	43.8	0.035	0.110	0.942	1.45	3.63	3.15	5.20	14.03	451
							Mean	2.92	4.70	11.62	416
							Measured on analytical column	3.98	5.57	14.80	

* Measured at bed length, L.
** Calculated using eqn. 13.
*** Calculated from bandwidth data using eqn. 28.

separation. These data, coupled with the feed bandwidth and elution position, will allow determination of the number of theoretical plates.

Band spreading due to longitudinal dispersion should be approximated by eqn. 21. That expression rearranged for determining the number of theoretical plates, N, will be

$$N = (\bar{\Theta}/\sigma_t)^2 \tag{25}$$

From the relationship for total band spreading, eqn. 15, it can be shown that

$$\sigma_t = \sqrt{\sigma_t^2 - \sigma_f^2} \tag{26}$$

The width of the band at half the maximum concentration, W, is much easier to measure than the standard deviation. This parameter can be related to the standard deviation by

$$\sigma^2 = W^2/8 \ln 2 \tag{27}$$

Recognizing the contribution of the initial feed bandwidth, W_0, to total band spreading and incorporating eqns. 26 and 27 into eqn. 25 result in

$$N = \frac{8 \ln 2 \, \bar{\Theta}^2}{W^2 - W_0^2} \tag{28}$$

This relationship was used to determine the number of theoretical plates in the vertical section of the annular chromatograph from elution and bandwidths data.

The number of theoretical plates in the annular chromatograph using the molecular sieve separation was calculated from $CoCl_2$ bandwidths to be 646, with a standard deviation of 109, over four different tests (Table III). The Ni-1 bandwidth was used to determine the number of theoretical plates in the ion-exchange separation. The results of three tests gave a mean value of 416, with a standard deviation of

TABLE III

NUMBER OF THEORETICAL PLATES FOR $CoCl_2$ ELUTION IN THE CONTINUOUS CHROMATOGRAPH

Operating conditions: temperature, 25 ± 2°; gas overpressure, 5–7 p.s.i.; eluent, distilled water; sorbent phase, Sephadex G-25; particle size, 100–300 μm.

Angular velocity, ω (rad/sec × 10³)	*Superficial velocity, u (cm/sec × 10²)*	*Initial bandwidth, W_0 (rad × 10²)*	*Bandwidth at 45 cm, W^* (rad × 10²)*	*Elution position $\bar{\Theta}^*$ (rad)*	*Number of theoretical plates, N^{**}*
1.05	1.37	0.7	17.6	1.90	645
1.01	1.95	3.8	13.3	1.41	687
1.02	1.93	6.8	16.8	1.45	497
2.60	1.89	7.9	31.1	3.51	755
				Mean (standard deviation)	646 (109)

* Measured at 45 cm below the feed point.

** Calculated with eqn. 28.

31 (Table II). Neither of these systems constitutes a high-resolution system; however, the number of theoretical plates are probably in the expected range for the type of solid phase used.

Effect of feed rate on bandwidth

The feed rate was 3 ml/min in each of the tests with ion-exchange resin. This represented a superficial velocity of 0.024 cm/sec, about equal to the average elution rate around the chromatograph. Obviously, as the feed rate was increased, additional mixing and band spreading would be expected. Indeed, it was found that the bandwidth increased at feed rates which resulted in a superficial velocity greater than twice the average eluting superficial velocity (Table IV). This effect will have to be taken into account when studying or designing for a specific separation.

TABLE IV

EFFECT OF FEED RATE ON Ni-1 BANDWIDTH

Operating conditions: temperature, 25 ± 2°; gas overpressure, 5 and 10 p.s.i.; eluent, 1 M $(NH_4)_2CO_3$ buffered to pH 7.8; sorbent phase, Dowex 50-X8; particle size, 50–60 μm.

Eluent superficial velocity (cm/sec)	*Feed superficial velocity (cm/sec)*	*Bandwidth, W* (rad)*
0.24	0.24	0.11
0.24	0.53	0.12
0.24	0.78	0.20
0.24		0.23
0.12	0.78	0.30

* Bandwidth measured at 40 cm below the feed point.

CONCLUSIONS

The rotating annular chromatograph has been shown to represent a potentially useful concept for continuous chromatography. The use of gas overpressure allows pressurized operation, which is usually required in modern chromatography, and the use of segmenting spacers at the chromatograph top allows gradient elution. A monitoring device, measuring reflected light, can be used to detect band positions and bandwidth when a transparent annulus is used.

The system can be mathematically described by a modified theoretical plate model, and the resulting correlations can be used for design purposes. Future experiments will be required to completely define the effects of feed stream concentration and flow-rate.

LIST OF SYMBOLS

A = cross-sectional area of the annular segment, cm^2

$$B = \frac{N}{V}\left[\frac{1}{\varepsilon + (1 - \varepsilon)\,K}\right]$$

$$B' = \frac{Nu}{\omega L}\left[\frac{1}{\varepsilon + (1 - \varepsilon)\,K}\right]$$

c = concentration of solute in the fluid phase, moles/cm^3
C = calibration constant
K = distribution coefficient, $\frac{\text{moles solute/cm}^3\text{ sorbent phase}}{\text{moles solute/cm}^3\text{ fluid phase}}$
L = vertical distance from feed point to exit, cm
n = general designation for theoretical plate number
N = total number of theoretical equilibrium plates in the annular segment
Q = total quantity of solute introduced to an annular segment, mole.
R = ratio of solute monitor reading at a solute concentration of c to the instrument reading for zero solute
t = time for the reference annular segment to be displaced an angle of Θ from the feedpoint, sec
u = eluent superficial velocity, cm/sec
v = total eluent flow through an annular segment during time t and displacement Θ, cm^3
V = total volume of an annular segment, cm^3
W = width of solute band at half the maximum solute concentration, rad
ε = void fraction in chromatograph, $\frac{\text{cm}^3\text{ fluid phase}}{\text{cm}^3\text{ annular volume}}$
ω = angular velocity or rotational speed, rad/sec
σ = standard deviation of the solute concentration across a solute band, rad
Θ = angular displacement of the solute band measured from the feed point, rad
$\bar{\Theta}$ = angular displacement of the maximum solute concentration at the chromatograph exit, rad

Subscripts
1 = first theoretical plate
f = feed point
l = longitudinal
n = nth theoretical plate
N = Nth theoretical plate
0 = initial
t = total

ACKNOWLEDGEMENTS

The outstanding technical support of F. H. Wilson is gratefully acknowledged. This research is supported by the Division of Physical Research, Energy Research and Development Administration, under contract with Union Carbide Corporation.

REFERENCES

1 T. A. Arehart, J. C. Bresee, C. W. Hancher and S. H. Jury, *Chem. Eng. Progr.*, 52 (1956) 353.
2 A. V. P. Martin, *Disc. Faraday Soc.*, 7 (1949) 332.
3 V. C. Giddings, *Anal. Chem.*, 34 (1962) 37.

4 H. Svensson, C. Agrell, S. Dehlén and L. Hadgahl, *Sci. Tools*, 2 (1955) 17.
5 J. B. Fox, R. C. Calhoun and W. J. Eglinton, *J. Chromatogr.*, 43 (1969) 48.
6 P. Dunnill and M. D. Lilly, in E. L. Gaden (Editor), *Biotechnology and Bioengineering Symposium No. 3*, John Wiley, New York, 1972, pp. 97–113.
7 A. V. P. Martin and R. L. M. Synge, *Biochem. J.*, 35 (1941) 1358.
8 A. S. Said, *AIChE J.*, 3 (1956) 477.
9 F. S. Merritt, *Mathematics Manual*, McGraw-Hill, New York, 1962, p. 354.
10 J. J. van Deemter, F. J. Zuiderweg and A. Klinkenberg, *Chem. Eng. Sci.*, 5 (1956) 271.
11 M. H. Caron, *Trans. Amer. Mining. Met. Eng.*, 188 (1950) 67.
12 F. J. Hurst, *Hydrometallurgy*, in press.

Journal of Chromatography, 126 (1976) 401–420
© Elsevier Scientific Publishing Company, Amsterdam — Printed in The Netherlands

CHROM. 9460

MOVEMENT AND BAND SPREADING OF UNSORBED SOLUTES IN LIQUID CHROMATOGRAPHY

CSABA HORVATH and HUNG-JYE LIN

Chemical Engineering Group, Department of Engineering and Applied Science, Yale University, New Haven, Conn. 06520 (U.S.A.)

SUMMARY

The different mobile phase velocities which can be measured in liquid chromatography have been described in order to facilitate an unambiguous specification of the velocity frame and the mobile phase hold-up volumes required to relate experimental data to the theory. The interplay of convective and diffusional mixing, which is responsible for band spreading in the mobile phase, has been treated by using the interstitial stagnant fluid model. Plate height equations have been derived for unsorbed tracers, which are totally excluded from the column material, as well as for unsorbed solutes, which permeate the stagnant mobile phase inside the particles. Band spreading was measured over a wide range of the reduced velocity with a single column packed with glass beads. The results show that the equation derived from the interstitial stagnant fluid model describes the velocity dependence of plate height more accurately than those found in the literature. It is suggested that the packing structure of a column be characterized by three dimensionless parameters.

INTRODUCTION

Recent advances in liquid chromatography (LC) with precision instruments allow us to obtain chromatographic data of greater accuracy than before. The interpretation of data, however, requires a knowledge of the thermodynamic, kinetic, and transport phenomena underlying the chromatographic process in order to exploit the full potential of the technique for more efficient separation of complex mixtures as well as for physico-chemical measurements. Whereas the theory of gas chromatography, which has mainly been established in the past twenty years, can greatly facilitate our understanding of LC, there are certain differences between the two techniques. In LC, the viscosity of the mobile phase is higher, the diffusivity of the solutes is lower, and the sample components can be partially or completely excluded from the interior of the porous column material.

In this study, we first examine the different types of fluid velocities which can be measured in chromatographic experiments. We feel that this subject requires clarification because a correct interpretation of band spreading and solute retention is impossible without an unambiguous specification of the fluid velocity or the pertinent

mobile phase hold-up volume[1]. In addition, the measurement of the flow velocity with different tracers can be very useful to evaluate important column parameters. The main part of the present study deals with the band spreading of an unsorbed solute in packed columns which is caused by convective and molecular diffusion. A great deal of study has been conducted both by chemical engineers[2,3] and chromatographers[4,5] to shed light on factors affecting axial dispersion. The classical eddy diffusion theory[6,7] has been refuted by Giddings[8,9], whose coupling theory is the result of a thorough analysis of the interplay of flow and diffusion in packed beds. Yet, the simple coupling theory does not agree well with the experimental data, whereas the more elaborate version of the coupling theory escapes experimental verification according to the extensive study of mobile phase band spreading by Knox[5]. In dealing with the factors determining axial dispersion of retarded peaks, Huber and Hulsman[10] and Huber[11,12] also introduced a term to account for the interplay of convective and diffusional mixing in the mobile phase. His expression, however, has not been related to any model or verified experimentally.

Consequently, there is a need for a relatively simple theory which involves measurable parameters only and can be used to characterize columns with respect to band spreading in the mobile phase. In our approach, we modified the classical eddy diffusion concept, assuming that there is a stagnant fluid space in the interstices of the column packing. The plate height expression derived from this model is not unlike the simple coupling term introduced by Giddings or the term of Huber, but it shows better agreement with experimental data. Our model has also been extended to express band spreading due to the stagnant mobile phase inside the porous packing material.

FLOW VELOCITIES AND HOLD-UP VOLUMES OF UNSORBED SOLUTES IN LIQUID–SOLID CHROMATOGRAPHY

Superficial or empty tube velocity

Superficial or empty tube velocity, u_s, is used most commonly in the chemical engineering literature. It can be evaluated without tracer experiments and is not subject to interpretation as the hold-up volume is arbitrarily but unambiguously defined as the empty tube volume. The superficial velocity is given by

$$u_s = \frac{1}{O}\frac{\mathrm{d}V}{\mathrm{d}t} \tag{1}$$

where O is the cross-section of the empty column and $\mathrm{d}V/\mathrm{d}t$ is the volumetric flow-rate. At constant flow, $\mathrm{d}V/\mathrm{d}t = F$, and $u_s = F/O$. As shown below, u_s is related to the other flow velocities by important column parameters. Therefore, it is highly desirable that in chromatographic experiments aimed toward physico-chemical studies the volumetric flow-rate is accurately measured and reported together with the column inner diameter.

Interstitial velocity

Interstitial velocity, u_e, is probably the most significant linear flow velocity in LC. It is defined by

$$u_e = \frac{u_s}{\varepsilon_e} \tag{2a}$$

where ε_e is the interparticulate porosity, which is given by

$$\varepsilon_e = \frac{V_e}{V} \tag{2b}$$

where V_e and V are the interstitial fluid volume in the column and the empty column volume, respectively. The interstitial velocity can be measured from the hold-up time of an unsorbed tracer, t_e, which cannot penetrate the particles in the packing, *i.e.*, is completely excluded. In exclusion chromatography, u_e is routinely measured with a solute of sufficiently high molecular weight in order to evaluate the interstitial volume, which equals the hold-up volume of the excluded tracer. The following relationships are of interest

$$u_e = \frac{L}{t_e} \tag{2c}$$

where L is the length of the column, and at constant flow

$$V_e = Ft_e \tag{2d}$$

Thus, the interparticulate porosity is readily obtained by one of the following expressions

$$\varepsilon_e = \frac{u_s}{u_e} = \frac{V_e}{V} = \frac{Ft_e}{V} \tag{2e}$$

Chromatographic velocity

Chromatographic velocity, u, is measured by the hold-up time of an unsorbed solute that can explore not only the interstitial but also the total intraparticulate fluid space in the column. It is given by

$$u = \frac{u_s}{\varepsilon_T} \tag{3a}$$

where ε_T is the total porosity defined by

$$\varepsilon_T = \frac{V_e + V_i}{V} = \varepsilon_e + \varepsilon_i (1 - \varepsilon_e) \tag{3b}$$

V_i is the intraparticulate pore volume in the column packing, which is filled with the eluent, and ε_i is the corresponding intraparticulate porosity of the packing material given by $V_i/(V - V_e)$. The chromatographic velocity can be measured with a tracer which has the same molecular dimensions as the solvent. The corresponding hold-up time, t_0, and hold-up volume, V_0, is expressed by

$$t_0 = \frac{L}{u} \tag{3c}$$

and

$$V_0 = V_e + V_i = Ft_0 \tag{3d}$$

The relationship between the chromatographic and interstitial velocities is given by

$$u_e = u\left[1 + \frac{\varepsilon_i(1 - \varepsilon_e)}{\varepsilon_e}\right] \tag{3e}$$

In chromatographic practice, u is measured most commonly and the "unretained" solute is usually a small molecule which explores the intraparticular fluid space. With pellicular packings the ratio $\varepsilon_i(1 - \varepsilon_e)/\varepsilon_e$ is usually small so that the chromatographic velocity is about the same as the interstitial velocity.

Velocity of the unsorbed solute

Velocity of the unsorbed solute, u_M, is the velocity of a given solute when it is eluted without being sorbed by the stationary phase, *i.e.*, at very high eluent strength. As the molecular dimensions of the solute can be between those of the solvent and a totally excluded solute, it does not necessarily explore the total intraparticulate fluid space. If a φ fraction of this space is accessible to the solute, we obtain that

$$u_M = \frac{u_s}{\varepsilon_e + \varphi\varepsilon_i(1 - \varepsilon_e)} = \frac{u_e\varepsilon_e}{\varepsilon_e + \varphi\varepsilon_i(1 - \varepsilon_e)} = u\frac{\varepsilon_e + \varepsilon_i(1 - \varepsilon_e)}{\varepsilon_e + \varphi\varepsilon_i(1 - \varepsilon_e)} \tag{4a}$$

and the intraparticulate fluid volume explored by the solute is φV_i. The value of φ depends on the size of the solute molecule and the pore size distribution of the porous column material. Usually φ decreases with increasing molecular weight of the solute and becomes zero for completely excluded solutes.

The hold-up time of the unsorbed solute, t_M, and the corresponding hold-up volume, V_M, are given by

$$t_M = \frac{L}{u_M} \tag{4b}$$

and

$$V_M = V_e + \varphi V_i \tag{4c}$$

It is seen that the hold-up volume of an intermediate-size solute under elution conditions when it is not sorbed is between the hold-up volume of the excluded tracer and the eluent. With a sufficiently large and a sufficiently small solute, the unsorbed solute velocities become u_e and u, respectively.

Fig. 1 illustrates the hold-up times and volumes which characterize the movement of unsorbed solutes in LC columns. The limiting values V_e and V_i have been of great interest in exclusion chromatography. Only very recently Scott[13] demonstrated that siliceous column materials commonly used in adsorption chromatography have also exclusion properties and that the mobile phase hold-up volume of solutes of relatively small molecular weight lies between the two limits at sufficiently high eluent strength where no sorption occurs. Rigid porous materials are widely used in high-pressure LC. It is expected that their pore structure and the interparticulate porosity of the column are unchanged under a wide range of elution conditions. Then the fluid velocities listed above are proportional to each other and subject to a precise definition. In order to extract physico-chemical data from chromatographic measure-

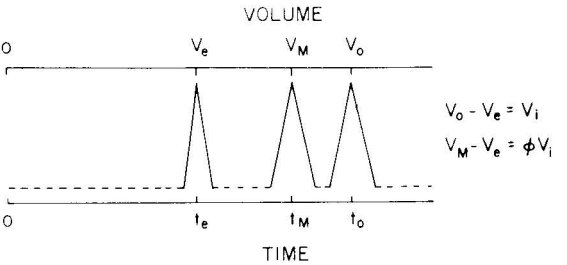


Fig. 1. Illustration of the three different mobile phase hold-up times and the corresponding hold-up volumes which can be measured with unsorbed tracers of different sizes in chromatographic experiments.

ment the appropriate flow velocity or hold-up volume have to be employed and clearly specified.

In liquid–liquid chromatography, the situation is more complicated because a tracer which is not totally excluded can explore the intraparticulate volume occupied by the liquid stationary phase. Under such conditions, the above definitions of the velocity of the unsorbed solute and the chromatographic velocity do not apply and more detailed approach such as given by Huber[11] is needed to relate the flow velocity and hold-up volume obtained from chromatographic measurements to the theory.

On the other hand, the situation is greatly simplified for columns packed with glass beads which have often been used to study mobile phase band spreading. In this case, the column material is impervious to the solute so that $\varepsilon_T = \varepsilon_e$. Then

$$u_e = u = u_M = \frac{u_s}{\varepsilon_e} \tag{5a}$$

$$t_e = t_0 = t_M \tag{5b}$$

$$V_e = V_0 = V_M = V\varepsilon_e \tag{5c}$$

Reduced velocity

Reduced velocity, ν, has frequently been used in chromatographic science. In order to avoid ambiguities, it is most appropriate to define ν with the interstitial velocity, so that the reduced velocity is given by

$$\nu = \frac{u_e d_p}{D_e} \tag{6}$$

where d_p is the effective particle diameter of the column material and D_e is the molecular diffusivity of the solute in the eluent.

It is noted that all velocities defined above represent the mean value of the corresponding local velocities in the packed column.

INTERSTITIAL STAGNANT FLUID MODEL

This model postulates that when a liquid flows through a packed bed at low Reynolds numbers an appreciable fraction of the interstitial fluid is essentially stag-

nant with respect to the actual stream in the center region of the interparticulate channels, as shown in Fig. 2. Whereas in reality the fluid velocity in the channels changes continuously from its maximum value to zero at the surface, the assumption of a fluid space which is stagnant with respect to the free fluid stream has certain physical justification. First of all, the hydrodynamic boundary layer at the surface of the particles can be relatively thick under conditions employed in LC[14,15]. In addition, as seen in Fig. 2, around the points of contact of the particles, the passages available for flow are very narrow and vanish at the points of contact. It is obvious then that the flow in these cusp regions will be considerably smaller than the mean flow through the voids. Hence, a significant fraction of the fluid will be, in fact, essentially stagnant as compared to the mean flow of the fluid streaming through the voids.

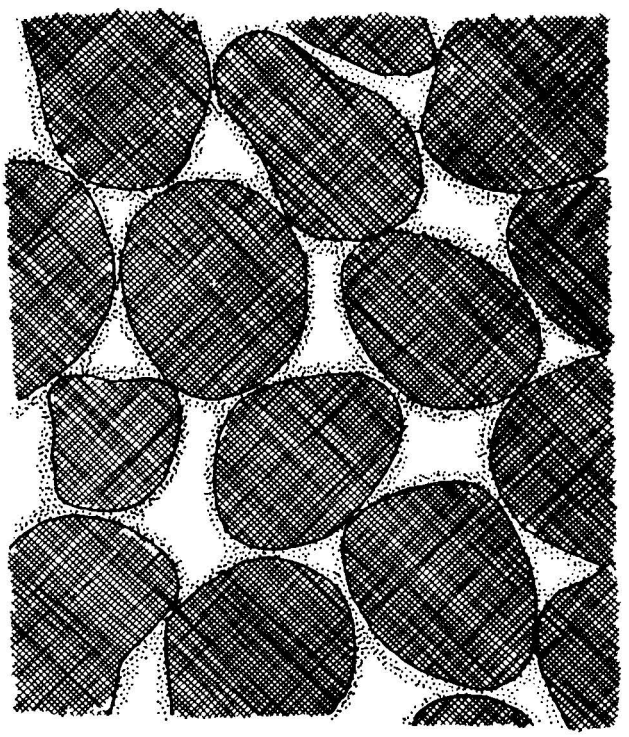


Fig. 2. Illustration of a cross-sectional area in a packed column. The fluid stream in the middle of the interstitial channels is normal to the cross-sectional plane. The particles are surrounded by quasi-stagnant fluid.

Our goal is to express the axial dispersion of an unsorbed solute in the mobile phase by using the interstitial stagnant fluid model. As shown schematically in Fig. 3, the fluid space in the column is considered to consist of three domains: the free streaming fluid space, the stagnant interstitial fluid space, and the intraparticulate fluid space, which is assumed to be also stagnant in LC.

In order to evaluate the relative magnitude of the stagnant interstitial fluid volume, we employ the theory of Pfeffer[16], who described steady-state mass transfer

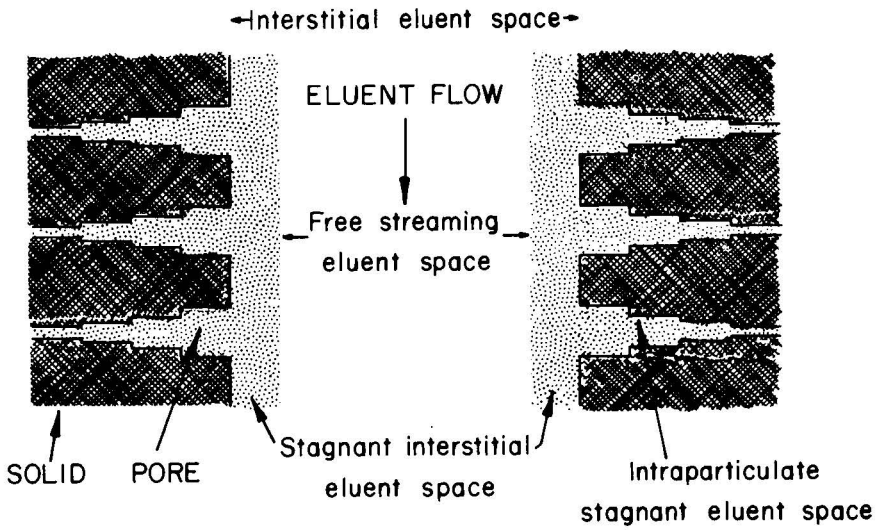


Fig. 3. Schematic illustration of the fluid spaces in a column packed with porous particles.

in packed beds at low Reynolds numbers by using the "free surface" model[17]. The mass transfer coefficient, k_e, derived by Pfeffer is given by

$$k_e = \frac{\Omega D_e \nu^{1/3}}{d_p} \tag{7}$$

The value of Ω is a function of the interparticulate porosity only and changes from 3.6–3.2 when ε_e varies from 0.36–0.42. The data calculated from eqn. 7 showed very close agreement with experimental data in the domain of $Re < 70$ and $\nu < 450{,}000$, which is of most interest in LC.

We assume that the stagnant liquid is a thin film surrounding spherical particles and the film thickness, δ, can be evaluated from eqn. 7 by the following relationship

$$\delta = \frac{D_e}{k_e} = \frac{d_p}{\Omega \nu^{1/3}} \tag{8}$$

When the stagnant fluid occupies the fraction η of the interstitial space the corresponding streaming fluid space can be evaluated from δ as follows

$$1 - \eta = \frac{1}{1 + \omega \nu^{-1/3}} \tag{9a}$$

where ω is related to Ω by

$$\omega = \frac{6(1 - \varepsilon_e)}{\varepsilon_e \Omega} \tag{9b}$$

and is a function of the porosity only. The theoretical value of ω varies from 2.9–2.6 in the range of ε_e from 0.36–0.42. It is noted that eqn. 9a is applicable also when η becomes large, *i.e.*, the thin film assumption does not hold at low values of ν.

The expression of ω in eqn. 9b has been derived for steady-state conditions from the "free surface" model, which is based on certain idealizations. Therefore, the ω values stated probably represent the lower limit for this parameter. It is expected that the departure from steady state also manifests itself in an increased value for ω. In fact, ω has to be a measure of the quality of the packing with respect to band spreading in the mobile phase and the value of ω is expected to decrease with increasing interstitial porosity.

BAND SPREADING OF A COMPLETELY EXCLUDED NONSORBED SOLUTE

In columns packed with fluid impervious particles such as glass beads, any unsorbed solute moves with the interstitial velocity, u_e. In columns packed with porous particles, solutes that are completely excluded from the interior of the particles also move with u_e.

The band spreading which independently occurs due to longitudinal molecular diffusion in the mobile phase[9] is expressed by the plate height contribution, H_L, given by

$$H_L = \frac{2\gamma D_e}{u_e} \tag{10a}$$

where γ is the obstruction factor. It is more convenient to use the reduced value of H_L which is given by

$$h_L = \frac{H_L}{d_p} = \frac{2\gamma}{v} \tag{10b}$$

The band spreading caused by non-uniform flow and anastomosis in packed beds has been originally related[6] to an eddy diffusion coefficient, E, which has the dimension of diffusivity and is given by

$$E = \lambda d_p u_e \tag{11}$$

where λ is a measure of the flow inequality in the bed. The eddy diffusion process independently contributes to band spreading with respect to the longitudinal diffusion discussed above. Giddings[18] suggested and experimental data with unsorbed solutes showed[5] that the plate height contribution derived from E is not independent of the flow velocity as had been thought originally[6].

Our interstitial stagnant fluid model postulates that flow occurs only in the free stream space. Consequently, eddy diffusion can only take place in this space and the solute is subject to eddy diffusion only during the time t^* that it spends in the free eluent stream. This time is readily evaluated from the relationship

$$t^* = \frac{L(1-\eta)}{u_e} \tag{12a}$$

as $u_e/(1-\eta)$ is the free stream velocity.

We assume that the expression for E in eqn. 11 is correct and can evaluate the peak variance, σ_E^2, caused by eddy diffusion as

$$\sigma_E^2 = 2Et^* \tag{12b}$$

Substituting E from eqn. 11 we obtain that the plate height contribution from eddy diffusion, H_E, is given by

$$H_E = \frac{\sigma_E^2}{L} = 2\lambda d_p(1 - \eta) \tag{13a}$$

Substituting the expression for $1 - \eta$ from eqn. 9a into eqn. 13a we obtain that

$$H_E = \frac{2\lambda d_p}{1 + \frac{\omega}{\nu^{1/3}}} \tag{13b}$$

and the corresponding reduced plate height increment, h_E, is given by

$$h_E = \frac{H_E}{d_p} = \frac{2\lambda}{1 + \frac{\omega}{\nu^{1/3}}} = \frac{1}{\frac{1}{2\lambda} + \frac{\omega}{2\lambda\nu^{1/3}}} \tag{13c}$$

By combining eqns. 10b and 13c we obtain for the reduced plate height of a nonsorbed solute, which cannot permeate the interior of the packing material, the following expression

$$h = \frac{2\gamma}{\nu} + \frac{2\lambda}{1 + \omega\nu^{-1/3}} \tag{14}$$

Eqn. 14 has also been derived from the interstitial stagnant fluid model by solving the pertinent mass balance equation. When $\nu^{\frac{1}{3}} \ll \omega$, *i.e.*, $\nu \ll \omega^3$, eqn. 14 can be simplified to

$$h = \frac{2\gamma}{\nu} + \frac{2\lambda}{\omega}\nu^{1/3} \tag{15a}$$

On the other hand, at sufficiently high reduced velocities the effect of longitudinal diffusion vanishes and h_E approaches a constant value of 2λ so that

$$h = 2\lambda \tag{15b}$$

From eqn. 14 the optimum value of the reduced velocity, ν_{opt}, where the h *vs.* ν plot goes through a minimum, h_{min}, has been evaluated analytically. The values of ν_{opt} and h_{min} are solely determined by γ/λ and ω. As the mathematical expression is rather complex, the relation is graphically illustrated in Figs. 4 and 5. The value of γ was fixed at 0.6, which has been frequently found experimentally[19].

BAND SPREADING IN A BED PACKED WITH PARTICLES PERMEABLE BY THE NON-SORBED SOLUTE

As shown schematically for a single porous particle in Fig. 6, the solute molecules diffuse from the free stream across the diffusional boundary layer first to the surface, then into the stagnant fluid inside the particle. The solute concentration in the free stream space, C_e, is assumed to be uniform. In our model, we use the mass

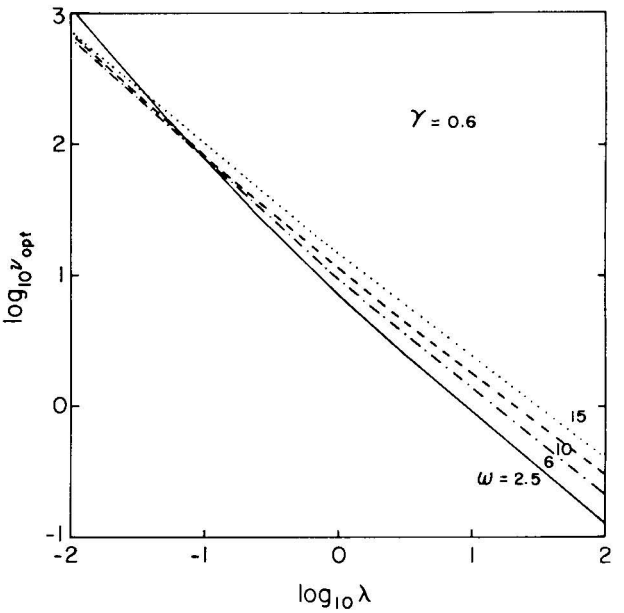


Fig. 4. Plot of the optimum reduced velocity for unsorbed solutes which do not permeate the packing material, as a function of λ with ω as the parameter. The value of the obstruction factor is arbitrarily chosen as $\gamma = 0.6$.

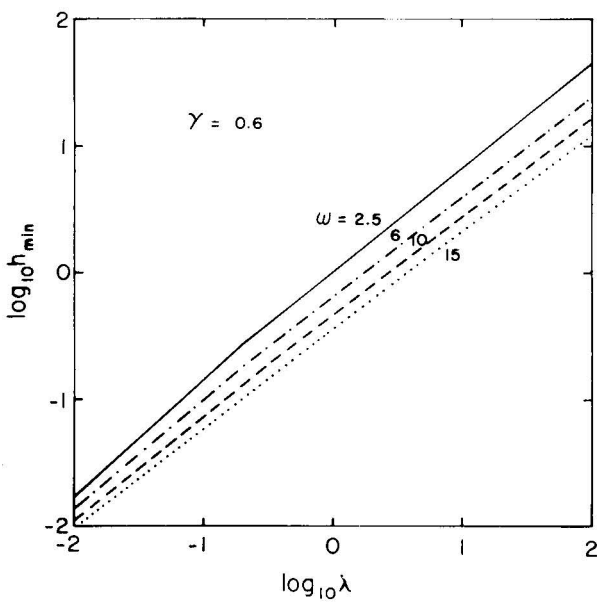


Fig. 5. Plot of the minimum reduced plate height for unsorbed solutes which do not permeate the packing material, as a function of λ with ω as the parameter for $\gamma = 0.6$.

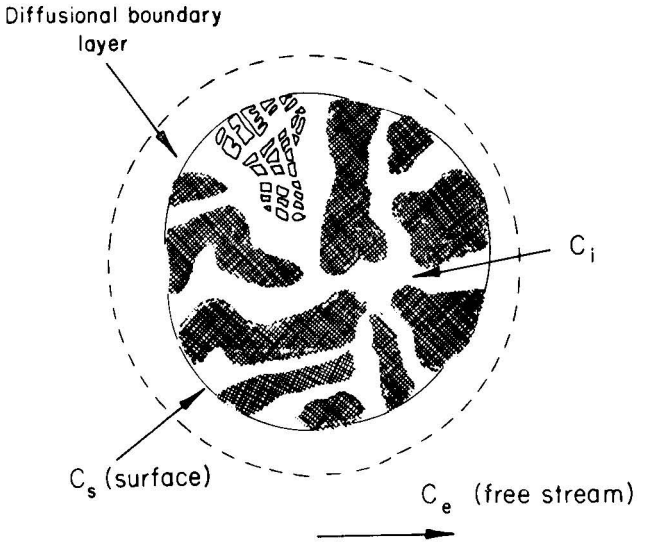


Fig. 6. Illustration of the instantaneous solute concentrations inside and outside a porous particle.

transfer coefficient, k_e, given in eqn. 7 to calculate the solute concentration at the surface, C_s, for any value of C_e in the Laplace domain. The transient penetration of the solute into and out of the accessible interparticulate stagnant space is characterized by the transfer function, $H(s)$, which is given by

$$H(s) = \frac{\bar{C}_i}{\bar{C}_s} \tag{16a}$$

where s is the parameter of the Laplace transform, $\bar{C}_i$ is the Laplace transform of the average instantaneous solute concentration inside the particle, C_i, and $\bar{C}_s$ is the Laplace transform of C_s.

In order to express the overall band spreading in terms of the plate height, we first evaluated $\bar{C}_i$ from the pertinent mass balance equation and derived the relationship between C_i and C_e by using the method described by Villermaux[20]. Thereafter, the diffusion equation has been solved with the axial dispersion coefficient, $\mathscr{D}$, by using Laplace transform to evaluate the overall band spreading due to mobile phase effects both in the interstitial and intraparticulate space. The axial dispersion coefficient which expresses band spreading due to longitudinal molecular diffusion and eddy diffusion was obtained from eqns. 10a and 13b as

$$\mathscr{D} = \gamma D_e + \frac{\lambda d_p u_e}{1 + \omega \nu^{-1/3}} \tag{16b}$$

After going through the elaborate mathematical procedures, we obtained the following relationship for the reduced plate height of a nonsorbed solute

$$h = \frac{2\gamma}{\nu} + \frac{2\lambda}{1 + \omega \nu^{-1/3}} + \frac{\omega \varphi \varepsilon_i \varepsilon_e k_0}{18(1 - \varepsilon_e)(1 + k_0)^2} \nu^{2/3} + \frac{k_0}{30\tau(1 + k_0)^2} \nu \tag{17}$$

where k_0 is defined as $\varphi V_i/V_e$, *i.e.*, the ratio of the intraparticulate void space accessible to the solute and the interstitial space in the column. τ is the tortuosity factor which relates the effective solute diffusivity inside the particles, D_i, to D_e by $D_i = \tau D_e$. Eqn. 17 yields for the plate height proper the following expression

$$H = \frac{A}{u_e} + \frac{B}{1 + Cu_e^{-1/3}} + Du_e^{2/3} + Eu_e \tag{18a}$$

with the parameters

$$A = 2\gamma D_e \tag{18b}$$

$$B = 2\lambda d_p \tag{18c}$$

$$C = \frac{\omega D_e^{1/3}}{d_p^{1/3}} \tag{18d}$$

$$D = \frac{\varphi \varepsilon_i \varepsilon_e \omega}{18(1 - \varepsilon_e)} \frac{k_0}{(1 + k_0)^2} \frac{d_p^{5/3}}{D_e^{2/3}} \tag{18e}$$

$$E = \frac{1}{30} \frac{k_0}{(1 + k_0)^2} \frac{d_p^2}{\tau D_e} \tag{18f}$$

At low reduced velocities eqn. 18a can be simplified to give

$$H = \frac{A}{u_e} + B'u_e^{1/3} + C'u_e^{2/3} + D'u_e \tag{19a}$$

where

$$B' = \frac{2\lambda d_p^{4/3}}{\omega D_e^{1/3}} \tag{19b}$$

$$C' = D \text{ and } D' = E \tag{19c}$$

At sufficiently high reduced velocities, when $\nu \gg \omega^3$, the second term of eqn. 18a becomes constant, so that we have

$$H = \frac{A}{u_e} + B + C'u_e^{2/3} + D'u_e \tag{20a}$$

It is noted that the mobile phase velocity in eqns. 18a, 19a, and 20a is expressed by the interstitial velocity. As frequently the chromatographic velocity is measured experimentally, both the inter- and intraparticulate porosity have to be evaluated independently in order to calculate u_e from eqn. 3e.

EXPERIMENTAL

The chromatograph used in the measurement of band spreading was assembled from the following moduli: Altex Model 100 reciprocating pump, Rheodyne Model 7010 sample injector with a 20-μl loop, Perkin-Elmer Model LC-55 detector, and

Perkin-Elmer Model FGA-1 recorder. The variable-wavelength detector was set to 240 nm. The dead volume between the sampling valve and the column inlet as well as between the column outlet and the flow cell was minimized by using the shortest possible lengths of 0.25 mm I.D. connector tubing. The column was prepared from a 98.3 cm × $^1/_4$ ft. O.D. × 0.467 cm I.D. stainless-steel tubing which was packed dry with Code 0202 glass beads (Corning Glass Works) having an average particle diameter of 48.5 μm. The inner wall of the stainless-steel tube was not polished. Whatman low dead volume fittings were used at both ends of the column, which was straight and kept in vertical position.

Experiments were carried out with three solvent–solute systems at 25°. In one series of experiments *n*-hexane containing 0.3% (v/v) methanol was used as the mobile phase and a 1% (v/v) acetone solution in *n*-hexane was injected. In another series, the same eluent was used but a 1% (v/v) benzene solution in *n*-hexane was injected. The third set of experiments was carried out with a 1% (w/v) benzoic acid solution in ethylene glycol as the sample. The flow-rate was varied between 0.02 and 9.99 ml/min. The sensitivity of the detector–recorder system was adjusted so that the peak height was at least half of the full scale length of the chart paper.

The peaks obtained with hexane as the mobile phase were symmetrical, but those obtained with ethylene glycol as the eluent showed slight fronting. Plate heights were calculated from half-height widths and baseline intercepts[21] and average values were taken. In each run, the flow-rate was measured by using a buret and stopwatch. The linear flow velocity, u_e, was calculated from the elution time of the peak center as measured from the chromatogram, and the column length.

The porosity of the bed was evaluated by using eqn. 2e and the average value was found to be 0.38. The reduced velocities were obtained by using the following values for solute diffusivity calculated by the Wilke–Chang equation[22]: acetone in hexane, $D_e = 4.6 \times 10^{-5}$ cm^2/sec, and benzene in hexane, $D_e = 5.8 \times 10^{-5}$ cm^2/sec. For benzoic acid in ethylene glycol, $D_e = 4.3 \times 10^{-7}$ cm^2/sec was taken from the literature[23].

RESULTS AND DISCUSSION

In the chromatographic literature, several simple equations have been proposed to express the plate height of a non-permeating and unsorbed solute as a function of the flow velocity. These equations, together with eqn. 14, are listed in Table I. The simple coupling equation of Giddings is shown because his more complex coupling theory does not yield an expression which can be verified experimentally.

It is seen that the essential difference between eqn. 14 and those put forward by Giddings and by Huber is the exponent of the flow velocity. The equation of Done and Knox[24] is identical with eqn. 14 at sufficiently low values of the reduced velocity, as has been shown in eqn. 15a. None of the equations accounts for the effect of turbulence which may occur at high Reynolds numbers in packed beds[5], but in usual chromatographic practice, the Reynolds number is sufficiently low so that turbulence does not play a role.

In order to test the dependence of the reduced plate height on the reduced velocity experimentally, a wide range of ν has to be covered. In addition, we have to consider the following points. Measurements have to be carried out with the same

TABLE I

EQUATIONS DESCRIBING THE PLATE HEIGHT OF AN UNSORBED AND NONPERMEATING SOLUTE AS A FUNCTION OF THE FLOW VELOCITY

For the sake of comparison the equations are presented in dimensionless form and the same symbols are used for the three column parameters.

Giddings[18]	$h = \frac{2\gamma}{\nu} + \frac{2\lambda}{1 + \omega\nu^{-1}}$
Huber[11]	$h = \frac{2\gamma}{\nu} + \frac{2\lambda}{1 + \omega\nu^{-1/2}}$
Done and Knox[24]	$h = \frac{2\gamma}{\nu} + \frac{2\lambda}{\omega}\nu^{1/3}$
Eqn. 14	$h = \frac{2\gamma}{\nu} + \frac{2\lambda}{1 + \omega\nu^{-1/3}}$

column because columns which have particles of different size, shape or size distribution or different tube to particle diameter or aspect ratios are expected to have different λ and ω values. In fact, the large body of literature data available[25] is not adequate for testing the equations because the experiments have been performed with different columns and plate height values have been obtained with each in a relatively narrow reduced velocity range only. It is also important that the experimental conditions are such that the effect of turbulence is negligible even at very high reduced velocities. In addition, great care has to be taken to avoid entrance effects as well as extra column band spreading.

In accordance with these considerations, we selected a relatively long column packed with intermediate size fluid impervious particles so that high values of u_e could be obtained at the available inlet pressure and the extra column dead space was negligibly small. By varying both the eluent and the solutes, we covered a wide range of u_e at the available flow-rate range and the maximum Reynolds number was less than 1 with hexane at $\nu = 250$ and less than 5×10^{-3} with ethylene glycol, even at a reduced velocity of 10,000.

The results are illustrated in Fig. 7, which shows the experimental data and the curves obtained by fitting the data to the various equations given in Table I, except the equation of Knox, which has not been claimed to be valid at high reduced velocities. The curve fitting was performed by the least squares method on a PDP-11 minicomputer. We assumed $\gamma = 0.6$ in each case and the parameters calculated with the different equations are listed in Table II. The average absolute error was 28% for the simple coupling equation of Giddings, 12% for the equation of Huber, and 9% for eqn. 14. It is seen that with this set of data both the Huber equation and eqn. 14 agree reasonably well with the experimental results. Nevertheless, the fit of the data to the latter equation is better than that to Huber's equation as the average error is a poor measure of the fit.

There is other support for the superiority of eqn. 14. This equation is derived from a theoretical model which showed excellent agreement with data measured for steady state mass transfer in packed beds. In addition, at low reduced velocities eqn.

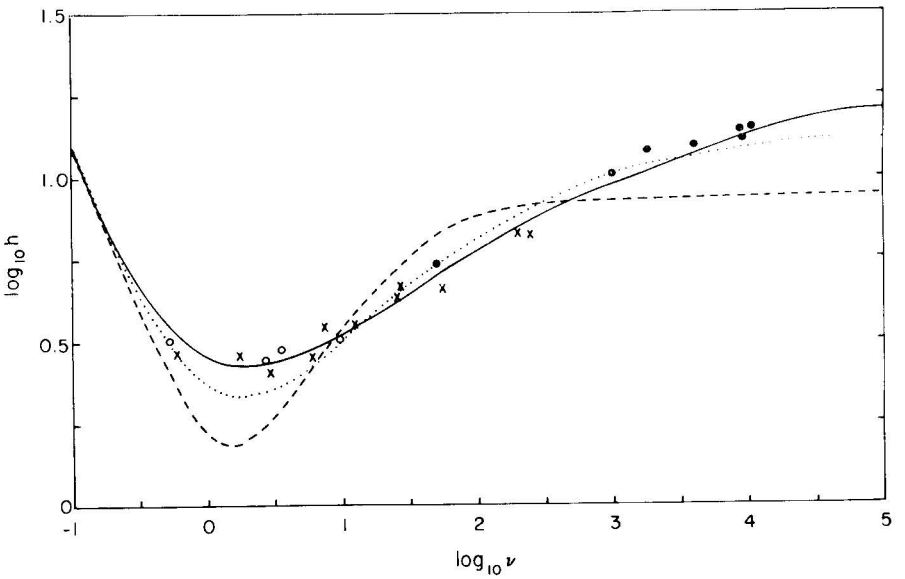


Fig. 7. Plots of the reduced plate height against the reduced velocity. The data points were obtained with a single glass bead column by using acetone in *n*-hexane (×), benzene in *n*-hexane (○), and benzoic acid in ethylene glycol (●). The curves represent the equations given in Table I with the parameters which gave the best fit to the experimental data which are listed in Table II. – – –, Giddings' equation; ·····, Huber's equation; ———, eqn. 14.

TABLE II

VALUES OF THE PARAMETERS OBTAINED FOR THE EQUATIONS GIVEN IN TABLE I WHICH REPRESENT THE VARIOUS CURVES IN FIG. 7

Equation	γ	λ	ω
Giddings	0.6	4.35	16.1
Huber	0.6	6.85	11.1
Eqn. 14	0.6	10.47	11.2

14 reduces to the equation given by Knox on the basis of extensive investigations of band spreading in glass bead columns. Consequently, the empirical equation of Done and Knox is a limiting form of eqn. 14.

In order to express the interplay of flow and diffusion in the anfractuous interstitial space of packed columns, we arrived at eqn. 14 by applying the mixing concept of eddy diffusion to the movement of the solute in the free streaming fluid only. Whereas the coupling theory of Giddings considers the relaxation of convective axial mixing by the transverse diffusion of the solute between fixed stream channels, our model postulates the attenuation of the classical eddy diffusion by a velocity-dependent quasi-stagnant fluid fraction in the interstices. Although the calculation of this fluid fraction proper entails several approximations, eqn. 14 appears to represent the band spreading of a nonpermeating solute in packed beds adequately.

It has been mentioned previously that λ is a measure of the velocity inequality of the streaming fluid flowing through the column and ω is related to the stagnant

fraction of the interstitial fluid in the bed. Together with the obstruction factor γ they represent the parameters of the column packing in view of eqn. 14. The value of γ, however, does not vary significantly from column to column and is assumed to be 0.6–0.7 (ref. 4). Consequently the quality of a given column packing can be quantified by the overall values of λ and ω. Eqn. 14 allows us to evaluate for any given column the two parameters from experimental data obtained with a totally excluded tracer, provided there are sufficient data points relating h to ν at least over the domain from $\nu = \nu_{opt}$ to $\nu = 10^3 \nu_{opt}$.

The effect of ω on the dependence of h on ν has been calculated from eqn. 14 for a nonpermeating solute and is illustrated in Fig. 8. It can be seen that at a fixed λ the minimum of the h *vs.* ν curve shifts to higher values of ν with increasing values of ω, in agreement with the results shown in Figs. 4 and 5. Generally, when λ is the same, a higher ω appears to represent a "better" column packing because it yields a given reduced plate height at a higher reduced velocity with a totally excluded tracer. The value of ω is dependent on the interstitial porosity but the relationship is likely to be more complicated than suggested by eqn. 9b. When ν is not much higher than the minimum, the column packing can be characterized by λ/ω according to eqn. 15a. On the other hand, λ is a packing characteristic which represents the limiting value of h for a nonpermeating solute at high reduced velocities in the absence of turbulence. Both λ and ω are determined not only by the materials used to make a column but

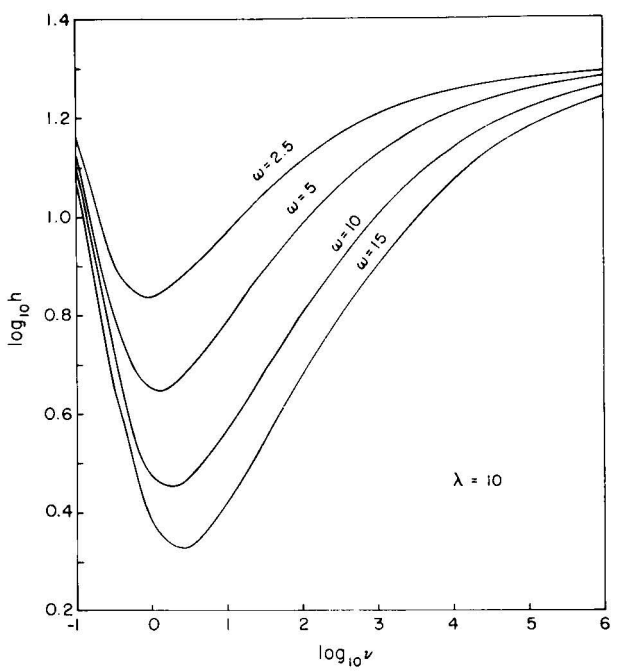


Fig. 8. Graph illustrating the effect of ω on band spreading of a totally excluded unsorbed solute. The reduced plate height is plotted against the reduced velocity according to eqn. 14 with the fixed parameters $\lambda = 10$, $\gamma = 0.6$, and $\varepsilon_e = 0.4$, and with the ω values shown on the graph.

also by the packing procedure itself. Thus, for a given type of column the comparison of the corresponding λ and ω values can shed light on the efficacy of the various packing procedures employed.

The experimentally obtained column parameters are overall values, *i.e.*, the averages of numerous local λ and ω values, because no column packing can be considered completely uniform. Thus, the overall λ and ω values account for, among others, the five velocity inequalities discussed by Giddings[9]. With columns of low aspect ratio, entrance and exit effects could be related to the corresponding local λ and ω values but these phenomena still require further study. On the other hand, the so-called wall effect, *i.e.*, perturbances in the packing at the wall region, has been extensively investigated[26]. It is intriguing to view the wall effect as the result of significant differences between the average local λ and ω values in the wall and the center regions of the packing. The disturbances caused by the wall in the packing can result in an annulus of relatively high interstitial porosity. According to our model, the local ω values in this annulus, which may extend over many particle diameters, could be significantly lower than in the center region. Consequently, the local band spreading of a nonpermeating solute would be much greater in this annulus even if the local average interstitial velocity would be close to that in the center part of the packing. Of course the locally greater "persistence-of-velocity-span"[9] in the wall region would also result in an increase in the average local value of λ with respect to that in the center region.

Whereas the study of the detailed structure of a packed bed by measuring local values of the column parameters is of great interest, in our view a separation of the packing and the tube wall as two different entities with respect to axial dispersion is not justifiable to a chromatographer who is interested in the overall effect. As soon as the solute molecules explore the wall region, the tube wall becomes a part of the packing as far as band spreading is concerned and it is a quodlibetical proposition that dispersion due to wall effect should not be considered "true" dispersion since it is not a function solely of the packed bed[27]. Furthermore, the wall effect is only one of several factors which can give rise to local λ and γ values significantly different from the overall parameters obtained with the whole column.

When the unsorbed solute can diffuse into the intraparticulate void space of the packing, the plate height equation becomes more complicated than that for the excluded solute, because two additional terms have to be added, as shown in eqn. 17. One of these terms accounts for the mass transfer resistance in the diffusional boundary layer surrounding the particles, the other for the mass transfer resistance in the intraparticular stagnant fluid. In essence, this stagnant fluid acts as an "apparent" stationary phase that is associated with a hold-up volume, φV_i, as shown in Fig. 1. This hold-up volume results in an "apparent" capacity factor, k_0, when the interstitial volume of the column is used as the reference volume for the mobile phase.

Once the axial dispersion coefficient is evaluated by eqn. 16b, a straightforward and rigorous mathematical procedure clearly yields eqns. 17 and/or 18a. These equations can be used to assess the significance of the effect of the intraparticulate stagnant mobile phase on the band spreading of a permeating unsorbed solute. In Fig. 9 this effect is exemplified by h *vs.* ν plots calculated from eqns. 14 and 17. In both cases, the column parameters except ε_i are the same, so that the relatively higher h values shown by the upper curve are solely caused by the last two terms of eqn. 17. It is noted that

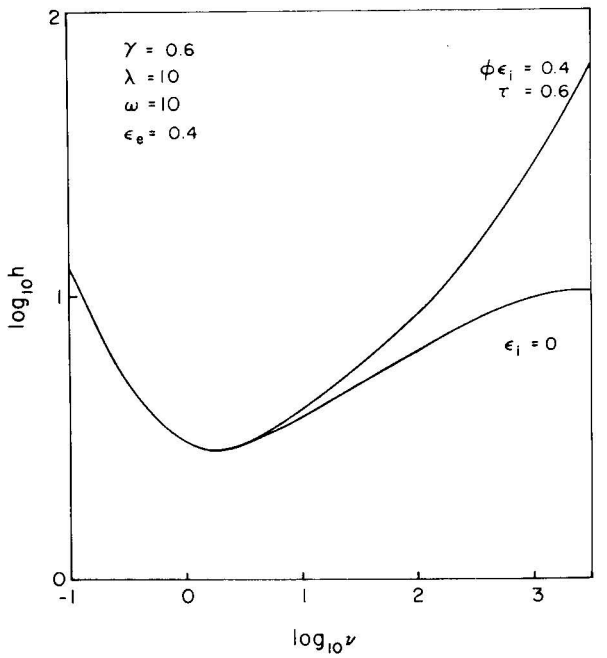


Fig. 9. Graph illustrating the effect of the mass transfer resistance arising from solute diffusion into the intraparticulate space on the reduced plate height as a function of the reduced velocity. The lower curve refers to a completely excluded solute ($\varepsilon_i = 0$), the upper curve to a solute which explores the intraparticulate void ($\varphi\varepsilon_i = 0.4$). The other column parameters in both cases are as shown on the graph.

with porous particles, when τ is greater than 0.3 and ω is about 10, the ratio of D/E is of the order of unity. Then the last term in eqn. 17, which is linear in velocity, would dominate band spreading only at reduced velocities as high as 10^6. Consequently, under practical conditions the plate height does not depend linearly on the flow velocity, except with microreticular resinous stationary phases when τ can be very small, as long as ω is sufficiently large.

We should note that ω appears in the denominator of the second term and in the numerator of the third term in eqns. 17 and 18a. Accordingly, the stagnant fluid in the interstices not only attenuates convective band spreading but can also augment zone dispersion at relatively high flow velocities when the solute diffuses into the particles. In the latter case, which reflects the usual chromatographic situation, the stagnant fluid represents a mass transfer resistance and the relationship between ω and the quality of the packing with respect to column efficiency becomes obscured. More precisely the effect of ω on band spreading depends on the properties of the solute, the flow velocity and other features of the column packing as well. An interesting conclusion from this is that for various types of chromatographic systems in the practical flow velocity range different overall ω values, *i.e.*, different packing structure in the column could yield optimum efficiency, whereas in columns packed with fluid impervious particles axial dispersion invariably decreases with increasing ω.

Eqn. 19a allows us to make a rough estimate of the flow dependence of the

plate height at low reduced velocities and with columns of practical interest. With pellicular packings the ratio $\varphi\varepsilon_i/\varepsilon_e$ is relatively small and the band spreading of an unsorbed solute is dominated by the second term in eqn. 19a. As a result, the plate height is expected to depend largely upon $u_e^{\frac{1}{3}}$ under practical conditions. On the other hand, with totally porous particles the third term of eqn. 19a may dominate and then the plate height would depend roughly on $u_e^{2/3}$. According to Snyder[28], in the two cases experimental data indicate a flow dependence of the plate height with approximately $u_e^{0.4}$ and $u_e^{0.6}$, respectively. In view of the foregoing discussion and eqn. 18a these exponents can readily be explained. The increase in the apparent exponent from the expected value of 0.33–0.4 with pellicular packings can be caused by the influence of the last two terms in eqn. 19a which have a stronger velocity dependence than the second term. With totally porous particles the observed exponent is smaller than the expected value of 0.67 and this is indicative of the influence of the second term in eqn. 18a, which has a weaker velocity dependence than the third and fourth terms.

In the present study, we examined the effect of the mobile phase on the band spreading of unsorbed solutes in LC and derived plate height equations for solutes which can or cannot permeate the packing material. Our approach is also applicable to describe band spreading of sorbed solutes, the treatment of which is the subject of a subsequent investigation.

NOTE ADDED IN PROOF

Professor J. Villermaux brought to our attention that mass exchange between the streaming and stagnant interstitial fluid also has to be included in our model. This generates an additional term in eqn. 14 which is correctly given by

$$h = \frac{2\gamma}{\nu} + \frac{2\lambda}{1 + \omega\nu^{-1/3}} + \frac{2\omega/\Omega^2}{1 + \omega\nu^{-1/3}}$$

Nevertheless, the form of eqn. 14 remains unchanged when λ is replaced by the term $\lambda + (\omega/\Omega^2)$. We expect that under practical conditions $\lambda \gg \omega/\Omega^2$.

Professor Villermaux also pointed out that the effective interparticulate diffusivity is calculated by $D_i = \varepsilon_i D_e/\theta$ with θ as the tortuosity factor[29]. Accordingly, $\tau = \varepsilon_i/\theta$ in this paper.

ACKNOWLEDGEMENTS

This work was supported by a research grant GM 20993 from NIH and by grant number CA 17245, awarded by the National Cancer Institute, DHEW.

REFERENCES

1 S. J. Hawkes, *J. Chromatogr.*, 68 (1972) 1.
2 J. J. Carberry and R. H. Bretton, *AIChE J.*, 4 (1958) 367.
3 M. F. Edwards and J. F. Richardson, *Chem. Eng. Sci.*, 23 (1968) 109.
4 D. S. Horne, J. H. Knox and L. McLaren, *Sep. Sci.*, 1 (1966) 531.

5 J. H. Knox, *Anal. Chem.*, 38 (1966) 255.
6 J. J. van Deemter, F. J. Zuiderweg and A. Klinkenberg, *Chem. Eng. Sci.*, 5 (1956) 271.
7 A. Klinkenberg, *Anal. Chem.*, 38 (1966) 489 and 491.
8 J. C. Giddings, *Anal. Chem.*, 38 (1966) 490.
9 J. C. Giddings, *Dynamics of Chromatography*, Marcel Dekker, New York, 1965, pp. 39–65.
10 J. F. K. Huber and J. A. R. J. Hulsman, *Anal. Chim. Acta*, 38 (1967) 305.
11 J. F. K. Huber, *J. Chromatogr. Sci.*, 7 (1969) 85.
12 J. F. K. Huber, *Ber. Bunsenges.*, 77 (1973) 179.
13 R. P. W. Scott and P. Kucera, *J. Chromatogr.*, 125 (1976) in press.
14 J B. Rosen, *Ind. Eng. Chem.*, 46 (1964) 1590.
15 C. N. Satterfield, *Mass Transfer in Heterogeneous Catalysis*, MIT Press, Cambridge, Mass., 1970, p. 79.
16 R. Pfeffer, *Ind. Eng. Chem. Fundam.*, 3 (1964) 380.
17 R. Pfeffer and J. Happel, *AIChE J.*, 10 (1964) 605.
18 J. C. Giddings, *J. Chromatogr.*, 5 (1961) 61.
19 J. H. Knox and L. McLaren, *Anal. Chem.*, 35 (1963) 449.
20 J. Villermaux, *J. Chromatogr. Sci.*, 12 (1974) 822.
21 C. Horvath, *Methods Biochem. Anal.*, 21 (1973) 82.
22 C. R. Wilke and P. Chang, *AIChE J.*, 1 (1955) 264.
23 P. Chang and C. R. Wilke, *J. Phys. Chem.*, 59 (1955) 592.
24 J. N. Done and J. H. Knox, *J. Chromatogr. Sci.*, 10 (1972) 606.
25 J. R. Cluff and S. J. Hawkes, *J. Chromatogr. Sci.*, 14 (1976) 248.
26 J. W. Hiby, in P. A. Rottenburg (Editor), *Proc. Symp. Interaction between Fluids and Particles*, London, June 20–22, 1962, Institution of Chemical Engineers, London, p. 312.
27 E. J. Cairns and J. M. Prausnitz, *Chem. Eng. Sci.*, 12 (1960) 20.
28 L. R. Snyder, private communication.
29 J. Villermaux, *Can. J. Chem. Eng.*, 51 (1973) 638.

Journal of Chromatography, 126 (1975) 421–437
© Elsevier Scientific Publishing Company, Amsterdam — Printed in The Netherlands

CHROM. 9442

CHROMATOGRAPHIC REPRODUCIBILITY IN HIGH-PERFORMANCE LIQUID CHROMATOGRAPHIC GRADIENT ELUTION

SETH R. ABBOTT, JOHN R. BERG, PIERRE ACHENER and ROBERT L. STEVENSON
Varian Instrument Division, 2700 Mitchell Drive, Walnut Creek, Calif. 94598 (U.S.A.)

SUMMARY

Normal bonded phase chromatography in a syringe pump gradient system satisfies a basic requirement for high-performance liquid chromatography of retention time reproducibility within half a peak width. Reversed bonded phase chromatography is characterized by a retention time variance in excess of this goal in certain cases. The source of the variance was traced to fluid compressibility effects and ambient thermal fluctuations.

Fluid compressibility effects, due to the change in system backpressure with changing mobile phase viscosity, generated a retention time variation of the order of a peak width for solutes eluting in the 20–50% B portion of a 0–100% acetonitrile (B) in water (A) gradient. However, the retention of solutes eluting beyond 50% acetonitrile was not significantly affected by fluid compressibility. Thermal effects, due to ambient temperature variation, generated retention time variations of the order of a peak width for solutes eluting throughout the gradient program.

A constant backpressure valve was developed which successfully eliminated fluid compressibility effects during gradient elution. Thermal effects were eliminated by use of a water-jacketed column and circulating constant-temperature bath. The dual syringe pump gradient system operating with these modifications reproduced retention times to better than 6 sec out of 1200 sec (σ_{rel} values below 0.5%).

INTRODUCTION

Gradient elution is the most effective technique available for solution of the general elution problem in liquid chromatography. It allows rapid separation of mixtures of solutes having widely different chromatographic behavior and yields symmetric, narrow peaks throughout the chromatogram.

Chromatographic quantitation requires the assignment of response factors to individual peaks. Peak identity is based on elution order and/or retention time. Retention time reproducibility is necessary to avoid erroneous peak identity–response factor assignments. Automated data processing in which peak identities are based on pre-set retention time windows has tightened the requirements on chromatographic reproducibility.

A minimum resolution of 0.5 is required to distinguish two solute maxima separated by a minimum. Differentiation of such peaks on the basis of retention time requires a 95% confidence interval of one half a peak width ($0.5w$). The development of highly efficient microparticle columns yielding small peak widths has thus placed stringent reproducibility requirements on chromatographic instrumentation. For the case in which a systematic variation occurs with successive runs, the confidence interval should be based on the range in retention over a typical sample population rather than on the variance of a series of runs.

Gradient retention time reproducibility has often been considered insufficient for quantitative work. Due to this problem, coupled to the need to reequilibrate the column after each gradient program, many chromatographers have confined their use of gradient elution to a sample scouting technique for defining optimum conditions for isocratic elution.

The development of bonded phase high-performance liquid chromatography (HPLC) columns has significantly reduced column equilibration time between gradients and improved the control of column activity. Gradient reproducibility with bonded phase columns has thus approached that obtained in isocratic elution for many chromatographic systems.

Chromatographers have still observed excessive run-to-run variance in retention time for certain column–mobile phase–solute systems. In some cases, systematic trends in retention time have been observed. A study of the parameters involved in gradient elution was thus conducted in order to improve the reproducibility of the technique. A theoretical description of solute migration in a gradient was developed to aid in studying the effects of gradient parameters on retention time.

EXPERIMENTAL

Gradient elution data were obtained on a dual, constant displacement rate syringe pump liquid chromatograph (Varian 8520 LC). The volume between the mixer and the column was about 500 μl. Injections were made by a six-port high-pressure valve injector (Valco) controlled by an Autosampler™ (Varian 8050). Retention data were collected and stored by a chromatography data system (Varian CDS 101). The syringe pumps were filled (250 ml each) prior to each series of gradient runs. The initial gradient run was always a blank where no sample was injected.

The syringe pump chromatograph was operated with and without a constant backpressure valve (CPV) in the system. The CPV is a low dead volume (100 μl) valve designed to avoid fluid compressibility effects in the pump reservoirs due to a change in column backpressure as mobile phase viscosity changes during the gradient run. The valve operates as a variable resistor, compensating for changes in column backpressure by making a complementary change in its own backpressure. The backpressure on the pump reservoirs is thus maintained constant ($dP/dt = 0$) during gradient elution.

The CPV maintains system pressure to within ± 2 atm out of 400 atm for a wide range of mobile phases and flow-rates. A complete description of the theory, design, and construction of the CPV will be reported elsewhere[1].

System pressure was monitored during gradient runs with a strain gauge pressure transducer located between the A pump outlet and the mixer. The transducer

output was amplified and then displayed on a strip chart recorder. The transducer had been calibrated at pressures of 1 and 540 atm with a reference gauge.

Normal-phase gradient elution studies were run with a microparticulate, polar bonded phase column (Varian MicroPak™ CN-10). Reversed-phase gradient elution studies were run on a microparticulate octadecyl–silica bonded phase column (MicroPak™ CH-10). The octadecyl stationary phase was polymeric, thus exhibiting higher selectivity towards aromatic hydrocarbons than a comparable monomeric stationary phase. The permeability of the polymeric octadecyl column is about 60% of that of a monomeric column, tending to increase compressibility effects.

Both normal- and reversed-phase columns had dimensions of 25 cm × 0.21 cm I.D. and had approximately 500-μl void volumes. Reversed-phase column temperature was either controlled at 35° with a water jacket connected to a circulating constant-temperature bath (Haake F423) or left uncontrolled at ambient temperature. The normal-phase column was run at ambient temperature.

RESULTS AND DISCUSSION

I. Solute migration in gradient elution — Constant flow, constant temperature conditions

Reproducibility of gradient retention time requires precise control of mobile phase composition, column activity, flow-rate, and temperature. A theoretical treatment of solute migration in gradient elution is a prerequisite to understanding the effects of variations in the above parameters on solute retention time.

Consider a gradient program in which the mobile phase composition (C_i) is programmed in increments of 1% B (A, B are the solvents used to form the gradient). The rate at which these steps occur and the gradient limits are set on a programmer. Assume that flow velocity (u) and temperature (T) are constant throughout the runs.

Solute migration can be described in terms of the parameter F_i, the fractional column length traversed during the time interval τ spent at each 1% B step in mobile phase composition C_i. The simplest case to treat is a linear gradient for which τ will be a constant. The more complex case of an exponential gradient is treated in the Appendix.

$$R = \frac{dC_i}{dt}$$

$$\tau = \frac{0.01}{R}$$

where R = gradient rate, sec^{-1}

F_i can be described as

$$F_i = \frac{u_{bi}\,\tau}{L} \tag{1}$$

where

$$u_{bi} = \frac{u}{1 + K_i} = \text{solute band velocity}$$

L = column length
u = mobile phase velocity
K_i = solute capacity factor

and

$$F_i = \frac{u}{(1 + K_i)} \cdot \left(\frac{\tau}{L}\right) = \frac{u}{(1 + K_i)} \cdot \left(\frac{0.01}{RL}\right) \tag{2}$$

K_i is typically a log-linear function of C_i and thus

$$F_i = \frac{0.01u}{RL} \cdot \left(\frac{1}{1 + Ae^{mC_i}}\right) \tag{3}$$

where the constants A and m are the y-intercept and slope, respectively, of the linear plot of ln K_i *versus* C_i. Fig. 1 shows an experimental plot of ln K_i *versus* C_i for a series of polynuclear aromatic hydrocarbon solutes eluted from a reversed-phase column with water–acetonitrile mobile phases.

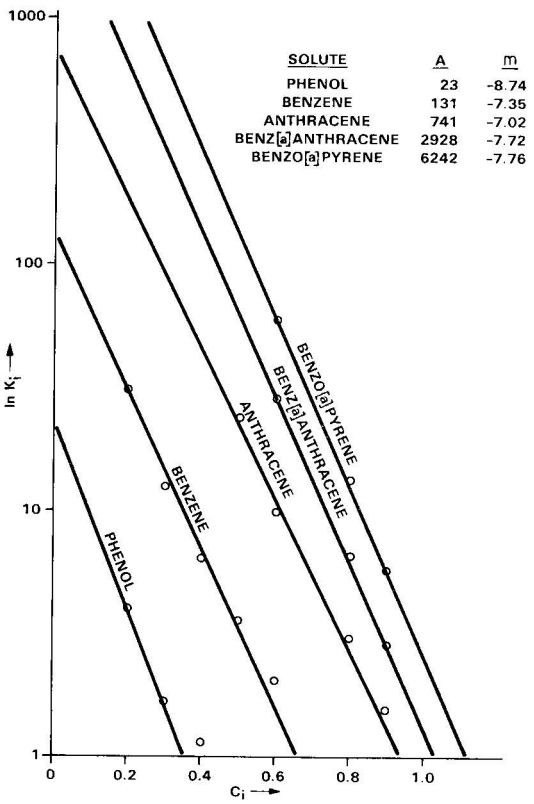


Fig. 1. Plot of ln K_i *versus* C_i for polynuclear aromatic hydrocarbons eluted from a 25 cm × 0.21 cm I.D. MicroPak CH-10 column with water–acetonitrile mobile phases at a temperature of 35°.

The mobile phase composition delivered to the mixer at any time t is

$$C_i^M = C_i^0 + Rt \tag{4}$$

where

C_i^M = mobile phase composition delivered to mixer
C_i^0 = initial gradient composition

The mobile phase composition at the head of the column, C_i^C, will "lag" that in the mixer due to the mobile phase transit time from the mixer to the column.

$$C_i^C = C_i^M - R\tau_{MC} \tag{5}$$

where

τ_{MC} = transit time from mixer to column

From eqns. 4 and 5 it follows that

$$C_i^C = C_i^0 + R(t - \tau_{MC})$$

The mobile phase composition at the solute band, C_i, will "lag" that at the column head as the band migrates further down the column. Thus

$$C_i = C_i^0 + R(t - \tau_{MC} - F_{i-1}\tau_C) \tag{6}$$

where F_{i-1} is the running total of the previous F_i steps and τ_C is the mobile phase transit time through the column.

The lag times τ_{MC} and τ_C can be related to flow terms

$$\tau_{MC} = \frac{V_{MC}}{Q} \tag{7}$$

where

V_{MC} = volume between mixer and column
Q = flow-rate

and

$$\tau_C = \frac{L}{u} \tag{8}$$

To determine the fractional column length traversed in a given time period, one can sum F_i between the period limits t_1 and t_2. For $t_1 = 0$, one obtains the expression

$$F = \frac{0.01u}{RL} \sum_0^t \frac{1}{1 + Ae^{m[C_i^0 + R(t - \tau_{MC} - F_{i-1}\tau_C)]}} \tag{9}$$

F can be determined by numerical evaluation of each F_i value followed by summation. Elution of the solute corresponds to $F = 1.00$. $F(t)$ was evaluated for several polynuclear aromatic hydrocarbon solutes by computer* solution of eqn. 9 with experi-

* Computer programs, written in BASIC, are available upon request for the solution of the equations for solute migration in both linear and exponential gradients.

mentally determined values of A and m and the gradient parameters: A = water; B = acetonitrile; $R = 0.000833\ \text{sec}^{-1}$ (5% B/min) from 0 → 100% B; $u = 0.833$ cm/sec (1 ml/min) through a 25 cm × 0.21 cm I.D. MicroPak CH-10 column. The resultant $F(t)$ curves are shown in Fig. 2.

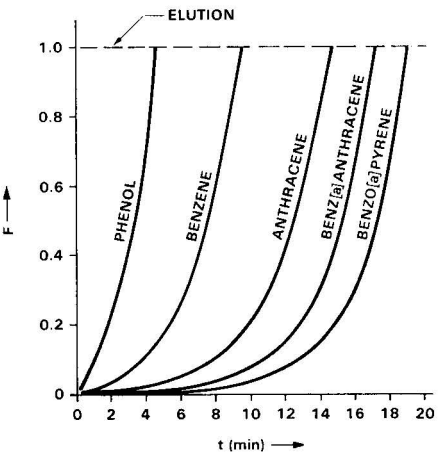


Fig. 2. Theoretical $F(t)$ migration of solutes of polynuclear aromatic hydrocarbons in reversed-phase gradient elution. Column, 25 cm × 0.21 cm I.D., MicroPak CH-10. A = water; B = acetonitrile; gradient, 0 → 100% B at 5% B/min; u = 60 ml/h (0.833 cm/sec). $F(t)$ is calculated from eqn. 9, based on experimentally determined values of A and m for each solute (see Fig. 1).

TABLE I

REPRODUCIBILITY DATA —POLAR BONDED PHASE GRADIENT ELUTION OF STEROIDS

Conditions: Column, 25 cm × 0.21 cm I.D., MicroPak CN-10; 120 ml/h (1.67 cm/sec linear velocity); 25°; 15 → 42% B concave gradient in 6 min; A = *n*-hexane; B = 33% isopropanol in dichloromethane. Pressure varies from 1400–1900 p.s.i. during the run. 254 nm absorbance, 1.0 a.u.f.s. Peak identities: 1 = progesterone; 2 = testosterone; 3 = Reichstein S; 4 = prednisolone acetate; 5 = unknown; 6 = dexamethasone; 7 = prednisolone.

Run	*Pump volume (ml)*		*Peak retention time (sec)*						
	V_A	V_B	*1*	*2*	*3*	*4*	*5*	*6*	*7*
1	170	228	53.0	87.0	183.0	220.2	270.0	329.4	370.2
2			53.0	86.0	181.2	218.4	268.8	328.2	367.2
3			53.0	87.0	181.2	219.0	269.4	327.6	368.4
4			53.4	88.2	184.2	220.2	270.6	329.4	370.2
5			53.4	88.8	186.0	222.6	272.4	330.6	371.4
6			52.2	87.0	183.6	220.2	270.6	330.0	371.4
7			52.2	87.0	184.2	220.8	271.2	329.4	370.2
8			53.0	87.6	185.4	222.6	273.0	331.8	371.4
9	7	175	54.0	89.4	187.8	224.4	274.8	333.6	373.2
$\overline{t_R}$, sec			53.0	87.6	184.1	220.9	271.2	330.0	370.4
σ			0.6	1.1	2.2	1.9	1.9	1.8	1.8
σ_{rel}, %			1.1	1.3	1.1	0.9	0.7	0.5	0.5
95% confidence interval, sec			1.0	1.8	3.0	3.0	3.2	2.6	3.0

II. Gradient reproducibility studies

Chromatographers are often uncertain as to the cause(s) of variation in the reproducibility achievable by gradient elution with different column/mobile phase systems. For example, consider the experimental data of Tables I and II.

Table I demonstrates the reproducibility of nine consecutive gradient separations of a mixture of steroids on a polar bonded phase column (MicroPak CN-10). A dual syringe pump chromatograph (Varian 8520 LC) with hexane in the A pump and a solution of 33% isopropanol in dichloromethane in the B pump was used. A 6-min concave gradient between 15 and 42% B was run at 2 ml/min. Column equilibration after each run was effected by use of a −8% B/min reverse gradient followed by 2 min at 15% B.

The efficient microparticulate column produced 15–30 sec peak widths throughout the chromatogram (Fig. 3). The retention time variations appeared random. The 95% confidence interval for retention time of the seven steroids varied from 1–3 sec and was well within the goal of half a peak width. The data of Table I are representative of those observed for gradient elution with polar bonded-phase microparticulate columns.

The data in Table II demonstrate the reproducibility of nine successive reversed-phase gradient separations of a mixture of polynuclear aromatic hydrocarbons on a MicroPak CH-10 column. The dual syringe pump chromatograph contained water in the A pump and acetonitrile in the B pump. A 20-min linear gradient

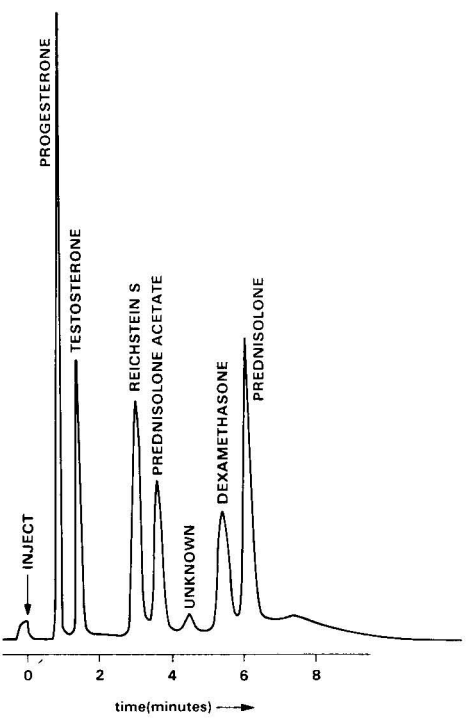


Fig. 3. Normal-phase gradient elution of steroids. For column conditions, see Table I.

TABLE II

REPRODUCIBILITY DATA —C_{18} REVERSED-PHASE GRADIENT ELUTION OF POLYNUCLEAR AROMATIC HYDROCARBONS

Conditions: Column, 25 cm × 0.21 cm I.D., MicroPak CH-10; 60 ml/h; 35°; 0 → 100% B in 20 min at +5% B/min; A = water; B = acetonitrile. Pressure varies between a minimum of ~2000 p.s.i. (at 100% B) and a maximum of ~3200 p.s.i. (at ~45% B) during the gradient run. 254 nm absorbance, 0.32 a.u.f.s. Peak identities: 1 = phenol; 2 = benzene; 3 = anthracene; 4 = benz[*a*]-anthracene; 5 = benzo[*a*]pyrene.

Run	*Pump volume (ml)*		*Peak retention time (sec)*				
	V_A	V_B	*1*	*2*	*3*	*4*	*5*
1	218	218	319.8	642.6	886.8	1015.8	1124.4
2	195	195	295.8	644.4	883.8	1014.0	1123.8
3	173	173	291.0	638.4	882.6	1013.4	1123.2
4	150	150	293.4	633.6	880.2	1012.2	1122.6
5	128	128	297.6	629.4	877.2	1011.0	1121.4
6	105	105	297.6	627.6	877.8	1012.2	1122.0
7	83	83	296.4	624.0	874.8	1011.0	1122.0
8	60	60	295.8	616.8	873.6	1012.2	1122.6
9	38	38	295.8	610.8	873.0	1014.0	1124.4
t_R, sec			297.9	629.7	878.9	1012.9	1122.9
Range, sec			27.0	31.8	13.8	4.8	3.0
σ			7.8	11.4	4.9	1.6	1.1
σ_{rel}, %			2.6	1.8	0.55	0.16	0.10
95% confidence interval, sec			13.1	range	range	2.7	1.8

between 0 and 100% B was run at 1 ml/min to obtain the separation. The column was water-jacketed and the temperature was maintained at 35°. Column equilibration after each run was achieved by use of a negative 10% B/min reverse gradient followed by 7 min at 0% B.

Peak widths were about 25 sec throughout the chromatogram (Fig. 4). A systematic trend toward decreasing retention time with successive runs was observed for peak 2 (benzene). The retention time range for benzene was about 32 sec or 1.3w, which is in excess of the half-peak-width goal. A similar trend was observed for anthracene, although the retention range was relatively small, at about half a peak width.

A systematic trend in retention time was not observed for peaks 1, 4, or 5 (phenol, benz[*a*]anthracene, and benzo[*a*]pyrene). The 95% confidence intervals for these peaks were equivalent to 0.52, 0.11, and 0.07 peak widths, respectively.

Re-filling the syringe pumps and repeating the series of runs produced similar data in terms of absolute and relative retention times on successive runs. A systematic change in temperature or column activity was thus ruled out as the cause of the trend in retention time of the benzene and anthracene peaks. The latter retention trends did correlate to the gradual decrease in syringe pump volumes with successive runs.

This observation suggests that the retention time trend reflects the effect of fluid compressibility (χ) on the gradient flow-rate and mobile phase composition. Theoretical treatments of compressibility effects in isocratic elution[2,3] and a descrip-

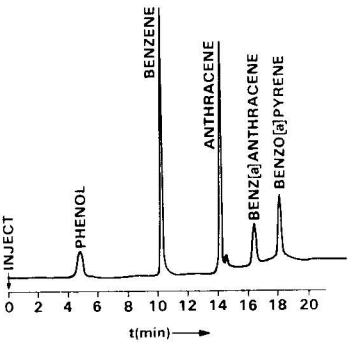


Fig. 4. Reversed-phase gradient elution of polynuclear aromatic hydrocarbons. For column conditions, see Table II.

tion of a commercial syringe pump design[3] which avoids such effects have recently been published. However, neither study extended its treatment to the more complex case of compressibility effects in gradient elution.

III. Effect of fluid compressibility on gradient elution parameters

Consider the operation of a gradient system based on dual, constant displacement syringe pumps. The piston flow-rate of each pump is programmed so as to vary the mobile phase composition delivered to the mixer according to a pre-set schedule, while the total piston flow-rate is kept constant

$$Q_O = Q_{OA} + Q_{OB} = \text{constant} \tag{10}$$

$$C_i^M(t) = \frac{Q_{OB}(t)}{Q_O} \tag{11}$$

where

Q_{OA} = A pump piston flow-rate
Q_{OB} = B pump piston flow-rate
Q_O = total piston flow-rate
$C_i^M(t)$ = mobile phase composition delivered to mixer

During the gradient program, the mobile phase viscosity, η, varies continuously as its composition changes. Since the column backpressure is proportional to mobile phase viscosity, a pressure differential in time, dP/dt is produced. The instantaneous pressure change causes a slight compression or expansion of the solvent into or out of each pump. The fractional change in fluid volume with pressure is the fluid compressibility, χ

$$\chi = \frac{dV}{V dP} \tag{12}$$

The instantaneous flow-rate out of each pump will thus deviate from the programmed piston flow-rate by the quantity $\chi V dP/dt$.

$$Q_A = Q_{OA} - \chi_A V_A \frac{dP}{dt} \tag{13a}$$

$$Q_B = Q_{OB} - \chi_B V_B \frac{dP}{dt} \tag{13b}$$

where

Q_A, Q_B = fluid flow-rates

The total flow-rate at any time t is then

$$Q(t) = Q_A + Q_B = Q_O - (\chi_A V_A + \chi_B V_B) \frac{dP}{dt} \tag{14}$$

The mobile phase composition C_i^M delivered to the mixer at time t is then

$$C_i^M(t) = \frac{Q_B}{Q} = \frac{Q_{OB} - \chi_B V_B \frac{dP}{dt}}{Q_O - (\chi_A V_A + \chi_B V_B) \frac{dP}{dt}} \tag{15}$$

Eqns. 14 and 15 predict that the effect of fluid compressibility on gradient parameters will be greatest for fast gradient rates in systems operating at relatively high pressure (low column permeability, high flow-rates, viscous solvents) in which the mobile phase viscosity varies widely with composition.

Reversed-phase HPLC utilizes relatively viscous aqueous–organic mobile phases which are "associating" mixtures, leading to a wide range in η with composi-

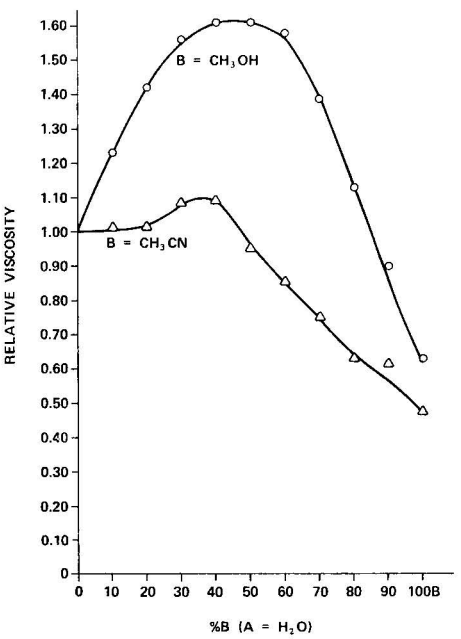


Fig. 5. Mobile phase relative viscosity as a function of composition for water–methanol and water–acetonitrile mixtures at a temperature of 25°. η (water) = 0.89 cP at 25°.

tion[4], as shown in Fig. 5. Thus, eqns. 14 and 15 predict greater compressibility effects in reversed-phase relative to normal-phase chromatography, in agreement with the data of Tables I and II.

Compressibility-generated flow deviations will diminish with successive chromatographic runs, as the pump volumes decrease. To evaluate the resultant deviations in solute retention for successive runs, one must calculate $Q(t)$ and $C_i^M(t)$ as functions of V_A and V_B and then substitute these terms into a form of the equation for solute migration (eqn. 9) derived in Section I. Since the flow velocity, u, is no longer a constant, the equation for solute migration becomes

$$F_i = \frac{0.01}{RL} \sum_0^t \frac{u_i}{1 + Ae^{m[C_i^M - R\,(V_{MC}/Q_i + F_{i-1}L/u_i)]}} \tag{16}$$

Eqns. 14 and 15 express $Q(t)$ and $C_i^M(t)$ in terms of the program settings $Q_O(t)$ and $Q_{OB}(t)$; pump volumes V_A, V_B; fluid compressibilities χ_A and χ_B; and the pressure differential in time dP/dt. dP/dt can be measured experimentally through use of a strain gauge pressure transducer. Thus, eqn. 16 can be solved to predict the effect of compressibility on gradient retention times.

IV. Effect of fluid compressibility on gradient retention times

Pressure was monitored during the gradient runs beginning with 218 ml and with 38 ml in each syringe pump (runs 1 and 9 of Table II). A plot of dP/dt during each gradient is presented in Fig. 6. The shape of the dP/dt curve follows the general

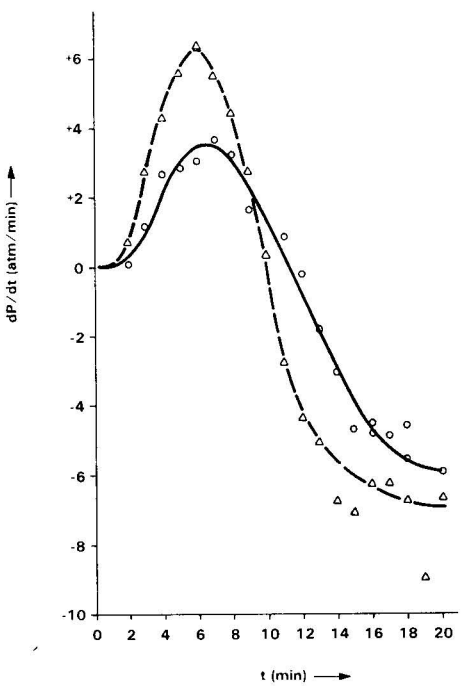
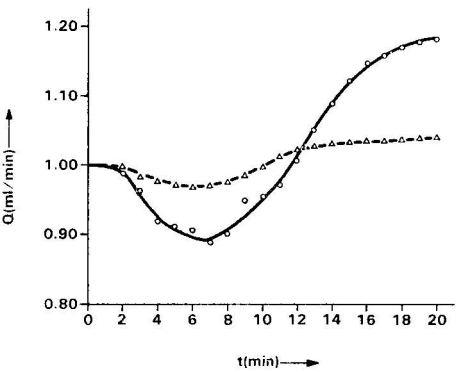


Fig. 6. Experimental values of dP/dt during reversed-phase gradient of Fig. 4, for syringe pumps initially at 218 ml (near full) (———) and at 38 ml (near empty) (– – –).

shape of the mobile phase viscosity curve of Fig. 5. The flow-rate and mobile phase composition delivered to the mixer were evaluated through use of eqns. 14 and 15. Fluid compressibilities for water and acetonitrile of 4.5×10^{-5} atm^{-1} and 9.6×10^{-5} atm^{-1}, respectively, were used[3]. Although fluid compressibility is a function of pressure, it is relatively constant in the pressure range of the gradient studied. $Q(t)$ and $C_i^M(t)$ are plotted in Figs. 7 and 8.



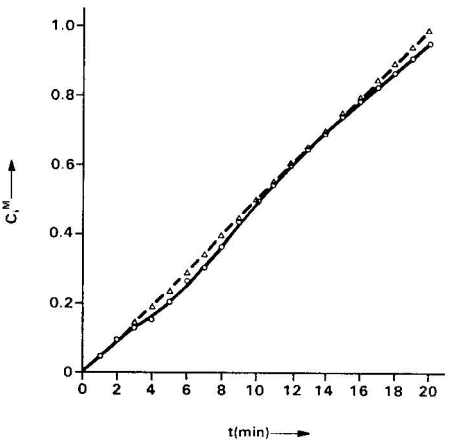


Fig. 7. Flow-rate Q, during reversed-phase gradient of Fig. 4, for syringe pumps initially at 218 ml (near full) (———) and at 38 ml (near empty) (– – –).

Fig. 8. Mobile phase composition, C_i^M, during reversed-phase gradient of Fig. 4, for syringe pumps at 218 ml (nearly full) (———) and at 38 ml (nearly empty) (– – –).

Inspection of Figs. 7 and 8 provides an intuitive grasp of the effects of compressibility on gradient retention time. Fig. 8 predicts the maximum compressibility-related variance in mobile phase composition to occur in the 20–50% and 80–100% B regions. The B concentration will be low for the 218-ml relative to the 38-ml case in both regions. However, whereas the compressibility-related flow deviation compounds the composition variance in the 20–50% B region, it counteracts it in the 80–100% B region (Fig. 7). Thus one would expect the compressibility-related retention variance to be greatest for phenol and benzene and significantly smaller for anthracene, benz[*a*]anthracene and benzo[*a*]pyrene (see Fig. 2).

The $Q(t)$ and $C_i^M(t)$ data were substituted into eqn. 16 along with experimentally determined values of A and m of several polynuclear aromatic hydrocarbons. Predicted values of retention time in the presence and absence of compressibility effects are compared to experimental data in Table III. An $F(t)$ plot for benzene in the presence and absence of compressibility effects is presented in Fig. 9.

The theoretical prediction of a systematic decrease in benzene retention time was confirmed by the experimental data. The observed range of 31.8 sec between the pumps near full at 218 ml and near empty at 38 ml agrees with the calculated value of 31.0 sec.

The theoretical prediction of only a slight effect of compressibility on the retention time of anthracene, benz[*a*]anthracene, and benzo[*a*]pyrene was also confirmed

TABLE III

COMPARISON OF THEORETICAL AND EXPERIMENTAL GRADIENT RETENTION TIMES OF POLYNUCLEAR AROMATIC HYDROCARBONS

Solute	*Peak retention time (sec)*							
	No χ effects		*χ effects operant*					
	*Theor.**	*Exp.***	*Theoretical*			*Experimental*		
			$V_A = V_B =$ *218 ml*	$V_A - V_B =$ *38 ml*	*Range*	$V_A = V_B =$ *218 ml*	$V_A - V_B =$ *38 ml*	*Range*
Phenol	273.7	266.7	314.8	294.2	20.6	319.8	295.8	24.0
Benzene	566.2	578.7	608.7	577.7	31.0	642.6	610.8	31.8
Anthracene	873.7	866.7	876.7	871.6	5.1	886.8	873.0	13.8
Benz[*a*]anthracene	1028.2	1021.2	1021.5	1023.7	−2.2	1015.8	1014.0	1.8
Benzo[*a*]pyrene	1141.3	1134.3	1139.7	1138.6	1.1	1124.4	1124.4	0

* Eqn. 16.

** Data obtained through the use of a constant-pressure valve in a dual syringe pump system. The observed retention time is corrected for a 7-sec delay due to transit through the valve volume.

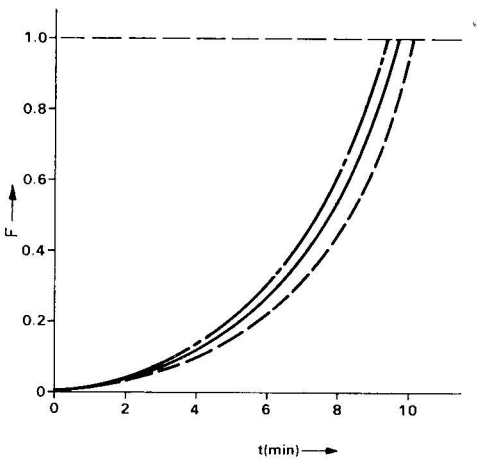


Fig. 9. Solute migration, $F(t)$, of benzene in the absence and presence of compressibility effects for reversed-phase gradient conditions of Fig. 4. – –, No χ effects; ———, χ effects operant, $V_A - V_B = 38$ ml; – – –, χ operative, $V_A - V_B$ 218 ml.

by the experimental data. A systematic trend was not observed for benz[*a*]anthracene and benzo[*a*]pyrene. This observation is due to the fact that non-compressibility-related retention variances are similar to or exceed the slight (1–2 sec) variations predicted due to compressibility for these late eluting peaks.

The theoretical prediction of a 25-sec range in phenol retention time was also confirmed by the experimental data. However, intermediate runs did not show a clear trend in retention time. This observation suggests a confounding effect on retention. Phenol elutes early in the gradient (see Fig. 2), and thus the retention time may also be more sensitive to variations in column equilibration. This hypothesis is consistent with observations described in a later section of this paper.

V. Elimination of compressibility effects through use of a constant backpressure valve

The compressibility-generated variance in retention time can be eliminated through use of a "constant backpressure valve" (CPV) in the dual syringe pump chromatograph. An automatic valve installed at the outlet of the mixer maintains the system at a constant pressure set in excess of that developed by the column during the gradient. The valve operates so as to maintain $dP/dt = 0$. Compressibility effects on the gradient parameters are thus eliminated.

Retention time data obtained with such a system are presented in Table IV. The systematic trends previously observed for the retention times of benzene and anthracene were eliminated, confirming the hypothesis that these trends (Table II) had been compressibility-generated. The phenol (peak 1) retention time shows a variance similar to that observed for the system operated without a CPV. This may be due to still uncontrolled variations in column equilibration which should be more important for the early eluting phenol peak.

The confidence intervals for polynuclear aromatic hydrocarbons (PNA) gradient retention times were all within the goal of half a peak width with the CPV system. Confidence intervals for the latter system are compared to those for the system without the valve in Table V. Note the marked improvement in benzene and anthracene reproducibility.

The observed retention times in the CPV system agree within about 3% or better with the times predicted by eqn. 9 when the experimentally determined A and m values of each PNA compound are used.

TABLE IV

RETENTION TIME REPRODUCIBILITY IN REVERSED-PHASE GRADIENT ELUTION WITH COMPRESSIBILITY EFFECTS AVOIDED THROUGH THE USE OF A CONSTANT-PRESSURE VALVE

Conditions: Column, 25 cm × 0.21 cm I.D. MicroPak CH-10; 60 ml/h; 35°; 0 → 100% B in 20 min at +5% B/min; A = water; B = acetonitrile. Pressure constant at 5000 p.s.i. during run due to the use of a constant pressure valve in the system.

Run	*Pump volume (ml)*		*Peak retention time (sec)*				
	V_A	V_B	*1*	*2*	*3*	*4*	*5*
1	218	218	281.4	583.8	889.2	1033.2	1140.6
2	195	195	276.0	588.6	889.2	1033.2	1138.8
3	173	173	274.2	588.0	888.6	1032.6	1139.4
4	150	150	280.2	585.6	890.4	1033.8	1139.4
5	128	128	285.0	588.0	892.8	1034.4	1138.8
6	105	105	264.6	582.6	890.4	1034.4	1140.0
7	83	83	273.6	585.0	891.6	1035.6	1141.8
8	60	60	264.0	585.6	891.6	1036.8	1143.0
9	38	38	264.0	583.8	892.2	1036.2	1143.6
$\bar{t}_R$, sec			273.7	585.7	890.7	1034.5	1140.6
Range, sec			17.4	6.0	3.6	4.2	4.8
σ			8.0	2.1	1.5	1.3	1.8
σ_{rel}, %			2.92	0.36	0.17	0.13	0.16
95% confidence interval, sec			13.4	3.6	2.6	2.2	3.0

TABLE V

EFFECT OF COMPRESSIBILITY AND TEMPERATURE ON GRADIENT RETENTION TIMES

Solute	*Retention time confidence interval (sec)*		
	Compressibility effects avoided; T constant at 35°	*Compressibility operative; T constant at 35°*	*Compressibility effects avoided; ambient T varies ~25 → 31° during experiment*
Phenol	13.4	13.1	36.6 (R)
Benzene	3.6	31.8 (R)*	9.0 (R)
Anthracene	2.6	13.8 (R)	11.4 (R)
Benz[*a*]anthracene	2.2	2.7	21.0 (R)
Benzo[*a*]pyrene	3.0	1.8	25.2 (R)

* (R) = Confidence interval taken as the range since the variation in retention time was systematic. All other data shown are 95% confidence intervals based on the retention time variance.

TABLE VI

REPRODUCIBILITY DATA —C_{18} REVERSED-PHASE GRADIENT ELUTION OF POLYNUCLEAR AROMATIC HYDROCARBONS

Compressibility effects are avoided by the use of constant-pressure valve. Ambient temperature increased from ~25–31° during the course of the experiment. Further conditions, same as in Table IV.

Run	*Pump volume (ml)*		*Peak retention time (sec)*				
	V_A	V_B	*1*	*2*	*3*	*4*	*5*
1	218	218	309.0	593.4	907.2	1065.0	1185.6
2	195	195	293.4	591.0	908.4	1068.0	1185.6
3	173	173	297.6	594.0	907.2	1062.0	1180.2
4	150	150	299.4	592.2	904.8	1060.2	1178.4
5	128	128	295.8	589.2	903.0	1057.2	1173.6
6	105	105	288.0	589.2	899.4	1051.2	1166.4
7	83	83	288.0	586.8	897.6	1048.8	1161.6
8	60	60	272.4	585.0	897.6	1048.2	1161.0
9	38	38	277.2	589.2	897.0	1047.0	1160.4
$\bar{t}_R$, sec			291.2	590.0	902.5	1056.4	1172.5
Range, sec			36.6	9.0	11.4	21.0	25.2

VI. Effect of temperature on gradient retention time

The previous reversed-phase gradient data had been obtained under controlled column temperature conditions* so as to allow the study of compressibility effects. Through the use of the constant pressure valve one can now eliminate compressibility effects, allowing the study of thermal effects on retention time variation.

A series of gradient runs was executed at ambient temperature throughout the course of an extremely hot day. The ambient temperature rose from 25° to 31° over

* Although the column temperature was controlled at 35°, the temperatures of the pump reservoir and the constant pressure valve were not controlled. However, thermal effects on retention time due to ambient temperature variation (25–31°) of these components should be significantly less than those due to column temperature variation.

the course of the runs. A systematic decrease in retention time on successive runs was observed for all five PNA peaks, as seen in Table VI. The temperature effect can be as significant as the compressibility effect on retention variance, as seen in Table V.

CONCLUSION

A dual syringe pump HPLC system incorporating a constant backpressure valve and column temperature control provide gradient retention time reproducibility to ≤ 6 sec out of retention times of up to 1200 sec. This reproducibility is comparable to that achievable in well-controlled isocratic elution[3] and is adequate for use of retention time for peak assignment in automated HPLC systems.

APPENDIX

In an exponential solvent gradient, the gradient rate can be described by

$$R = \frac{dC_i}{dt} = R_0 e^{at} \tag{A-1}$$

where a is a constant and R_0 is the initial gradient rate. The time τ spent at each 1 % B step in mobile phase composition is then

$$\tau = \frac{0.01}{R_0 e^{at}} \tag{A-2}$$

The mobile phase composition delivered to the mixer at time t is then

$$C_i^M(t) = C_i^0 + \int_0^t dC_i = C_i^0 + \frac{R_0}{a}(e^{at} - 1) \tag{A-3}$$

Substitution of eqn. A-3 into eqn. 9 yields the expression for solute migration in exponential gradient elution

$$F = \frac{0.01u}{L} \sum_0^t \frac{1}{R_0 e^{at}\left(1 + Ae^{m[C_i + R_0/a\,(e^{at}-1) - R_0 e^{at}(\tau MC + F_{i-1}\tau C)]}\right)} \tag{A-4}$$

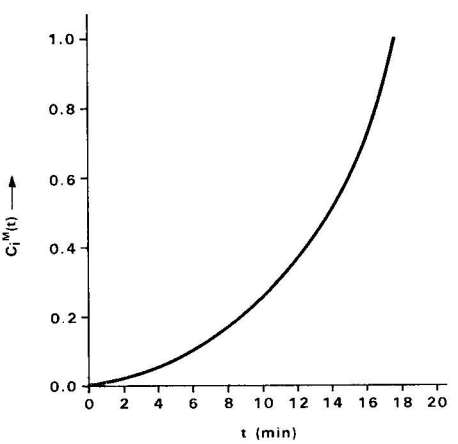


Fig. 10. $C_i^M(t)$ for typical exponential gradient: $R = R_0 e^{at}$, $a = 0.00268$.

A plot of $C_i^M(t)$ for a typical exponential gradient is presented in Fig. 10. A plot of $F(t)$ for polynuclear aromatic hydrocarbons, based on eqn. A-4 for the exponential gradient of Fig. 10, is presented in Fig. 11.

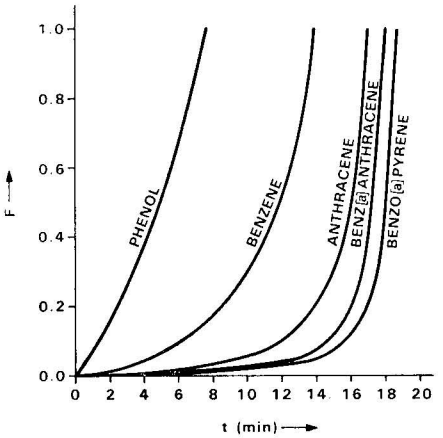


Fig. 11. Theoretical $F(t)$ migration of polynuclear aromatic hydrocarbons solutes in reversed-phase gradient elution. Column, mobile phase, and flow-rate, same as in Fig. 2. Exponential gradient profile of Fig. 10.

ACKNOWLEDGEMENTS

The authors acknowledge Pierre Achener, John Helmer, Miner Munk, and Detlef Boehme for the design and construction of the CPV valve. We also thank John Helmer for his illuminating discussions of fluid compressibility, Art Brown for his aid in computer programming, and Heiner Kern for experimental work in normal bonded phase chromatography.

REFERENCES

1 P. Achener, D. R. Boehme and J. Helmer, to be published.
2 M. Martin, G. Blu, C. Eon and G. Guiochon, *J. Chromatogr.*, 112 (1975) 399.
3 P. Achener, S. R. Abbott and R. L. Stevenson, *J. Chromatogr.*, to be published.
4 A. K. Covington and T. Dickinson (Editors), *Physical Chemistry of Organic Solvent Systems*. Plenum Press, New York. 1973.

Journal of Chromatography, 126 (1976) 439–445
© Elsevier Scientific Publishing Company, Amsterdam — Printed in The Netherlands

CHROM. 9427

PREPARATIVE LIQUID CHROMATOGRAPHY USING RADIALLY COMPRESSED COLUMNS

JAMES N. LITTLE, RICHARD L. COTTER, JAMES A. PRENDERGAST and PATRICK D. McDONALD

Waters Associates Inc., Maple Street, Milford, Mass. 01757 (U.S.A.)

SUMMARY

This study describes a new preparative liquid chromatography system, based on the principles of high-speed liquid chromatography, which is capable of separating multigram quantities of materials in minutes. To demonstrate the capabilities of the system, examples were chosen of difficult separations ($\alpha = 1.1$), previously accomplished only by analytical high-pressure liquid chromatography, and of less difficult separations ($\alpha > 1.3$), where multigram quantities were previously obtained by time-consuming column chromatography or preparative thin-layer chromatography.

INTRODUCTION

There has been a great need in natural products isolation and organic synthesis chemistry to increase the resolution and speed of separating multigram (5–30 g) mixtures. The most useful methods up to now have been column chromatography and/or multi-development preparative thin-layer chromatography (TLC). Within the last few years, analytical high-pressure liquid chromatography (HPLC) has been perfected and gained wide utilization in many laboratories.

This study was undertaken to determine what present principles of HPLC could be applied to preparative-scale chromatography. Using higher pressure and thus flow-rate as well as continuous detection of effluent were obvious principles of HPLC which were used to increase the speed of preparative separations. Column design in HPLC did not seem compatible with preparative separations.

In HPLC, rigid-walled (stainless-steel), small-volume (3–5 ml) columns are carefully packed and used repetitively. In preparative chromatography one uses large-volume columns (100–1000 ml) and analyzes very complex mixtures in which all components may not elute from the column. If great expense is put into these columns, they must be used repetitively and thus be purged with large volumes (up to 100 l) of solvent, which adds to the expense. In this report, flexibly-walled cartridges are used which are compressed quickly and consistently into high-efficiency preparative columns. This concept allows high performance and economy in preparative separations.

EXPERIMENTAL

All solvents were "distilled in glass" grade (Burdick & Jackson Labs., Muskegon, Mich., U.S.A.) and were used without further purification. Chromatograms were obtained from a Waters Assoc. Prep LC/System 500 preparative liquid chromatography system (Waters Assoc., Milford, Mass., U.S.A.). This instrument includes a high-speed pumping system delivering solvent at flow-rates up to 500 ml/min at 500 p.s.i. back pressure, dual solvent inlets, on-column injection with unlimited sample size, and a multi-function valve which diverts the column effluent to waste, recycles the sample, or directs the flow to a pair of switchable ports for collection of fractions of any size in any convenient vessel. When not in use, each collect line is purged with air so as to minimize contamination of the current fraction by the previous one. The separation is monitored by a differential refractometer with a relative response range of 1000×. Approximately 1% of the column effluent is diverted into the 10-μl cell of the refractometer, and the detector output signal is monitored on an integral servo recorder using 100-mm scale width Z-fold chart paper.

PrepPak-500 cartridges, 30 × 5.7 cm containing chromatographic-quality silica gel, average particle diameter approx. 75 μm, are automatically sealed in a column chamber and compressed radially with nitrogen gas at 500 p.s.i.g. A series of electronic monitors and circuits protect the column from operation under improper compression conditions. A differential pressure of at least 200 p.s.i.g. above system back pressure is maintained on the external column wall. The entire process of inserting a PrepPak cartridge into the chamber, and converting it into a chromatographic column ready for use takes less than 1 min.

Analytical LC was done on a Waters Assoc. Model 244 liquid chromatograph equipped with a μPorasil column, 30 cm × 4.2 mm I.D.

RESULTS AND DISCUSSION

In Fig. 1 is shown an analytical LC separation of an 80:20 synthetic mixture of 1- and 4-hydroxy-1,2,3,4-tetrahydrophenanthrenes, respectively. This sample typically would be purified by column chromatography or fractional crystallization. On a thin-layer microplate (chloroform–1% ethanol) these compounds had corresponding R_F values of 0.18 and 0.24, indicating an α value of only 1.43. This degree of separation was improved considerably to 2.18 by using an LC system with 5% ethyl acetate in methylene chloride, thus allowing a larger load to be used in the preparative separation. At the same time, the degree of retention was significantly decreased ($k' = 1.38$ and 0.63, respectively), which not only allows heavier loading but also decreased solvent consumption since less solvent is needed to elute the compounds from the column bed. A semipreparative separation of a 54-mg sample load using the analytical LC system is shown in Fig. 2, while in Fig. 3 is shown the scale-up to a 10-g sample load on a 30-cm preparative LC column using the same solvent system in the preparative instrument. The purity of the 4-hydroxy isomer (1.7 g) recovered from Fraction 2 and that of the 1-hydroxy isomer from Fractions 4 and 5 (total 6.3 g) was better than 99.9% by analytical LC, as shown in Figs. 4 and 5, respectively.

A separation ($\alpha = 1.3$) which would be difficult by TLC is shown in Figs. 6a,

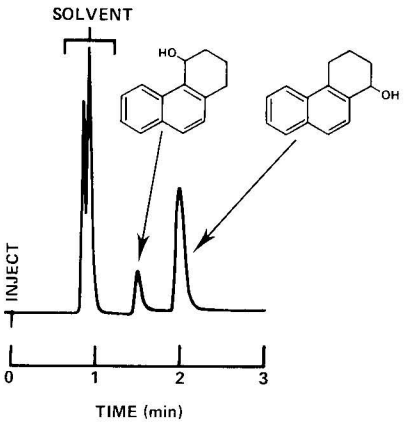


Fig. 1. Analytical separation of 1- and 4-hydroxy-1,2,3,4-tetrahydrophenanthrene (80:20 synthetic mixture). The chromatograph was operated isocratically at 4.0 ml/min. Column, 30 cm × 4.2 mm I.D. μPorasil; solvent, methylene chloride–ethyl acetate (95:5); detector, RI, 16×; sample, 100 μg in 10 μl.

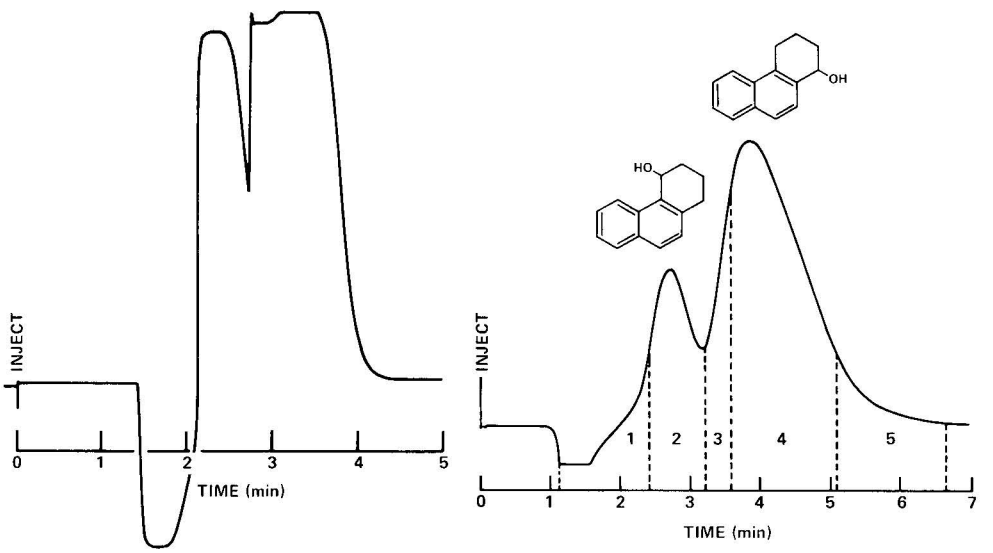
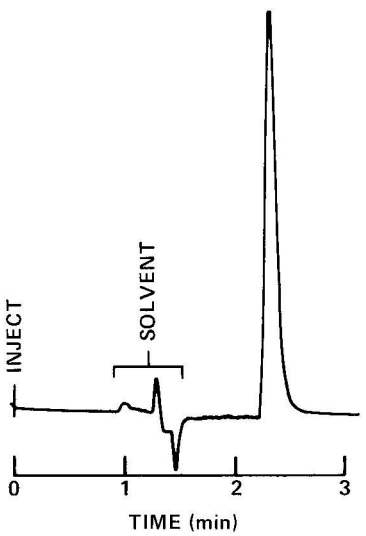


Fig. 2. Small-scale preparative separation of tetrahydrophenanthrene mixture. Solvent and column, *cf.* Fig. 1; flow-rate, 2.5 ml/min; detector, RI, 128×; sample, 54 mg in 1.75 ml.

Fig. 3. Preparative separation of tetrahydrophenanthrene mixture. Column, 30 cm × 5.7 cm PrepPak-500; solvent, *cf.* Fig. 1; flow-rate, 300 ml/min; detector, RI, relative response 1; sample, 10 g in 45 ml.

b, c, and d. A mixture of butyl acetate and ethyl acetate (each 10% w/v) and hexane (1% w/v) in methylene chloride was prepared to demonstrate the relationship between column length, sample load, and resolution. As can be seen, resolution of a 200-mg load is improved from about 0.8 (Fig. 6a) to 1.3 (Fig. 6b) by using a second PrepPak in series. This is a result of increased efficiency due to a longer bed and larger sample



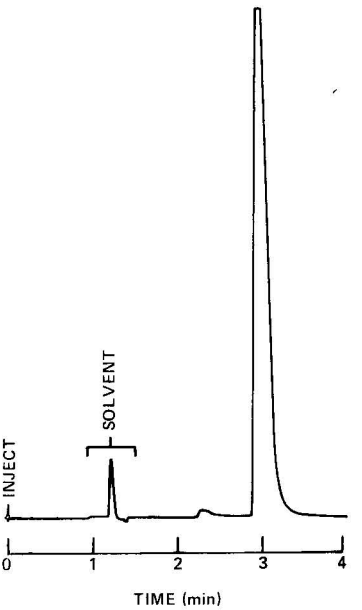


Fig. 4. Analysis of Fraction 2 from preparative separation in Fig. 3. Solvent and column, *cf.* Fig. 1; flow-rate, 2.5 ml/min; detector, RI, 8×; sample, 20 μl of Fraction 2; purity, >99.9%.

Fig. 5. Analysis of Fraction 4 from preparative separation in Fig. 3. Solvent, column, flow-rate, and detector, *cf.* Fig. 4; sample, 20 μl of Fraction 4; purity, >99.9%.

capacity. A tenfold increase in load with only a twofold increase in column length (four PrepPaks in series) gives a resolution of about 1.2 (Fig. 6c), demonstrating the benefits to be gained by extending column length. An alternate method of increasing effective column length while reducing solvent consumption is shown in Fig. 6d. Here again a single column was used with a sample identical to that in Fig. 6c. However, the sample was recycled three times. The resolution on the third pass can be seen to correspond nearly to that obtained on 4 ft. of column in a single pass (Fig. 6c). This clearly demonstrates the advantages of recycle in reducing column costs and solvent consumption, while increasing sample capacity and separation efficiency.

A difficult separation ($\alpha = 1.1$) which can only be accomplished chromatographically by analytical LC is shown in Fig. 7. Here an equal mixture of ethyl acetate and isopropyl acetate (10% w/v) and hexane (2% w/v) was separated on only 60 cm of preparative column using the technique of recycle. By the fourth pass, a resolution of 0.7 was obtained and by the seventh pass the resolution was better than 1.0.

The technique of recycle, as previously discussed, becomes of extreme importance when high purity with minimal loss of a desired component or components is required. The following example emphasizes the utility of preparative recycle for maximization of yield and purity of a given component with minimal loss of the component of interest. Minimal loss with maximum throughput is accomplished by combining and then repurifying those collected fractions which have been insufficiently

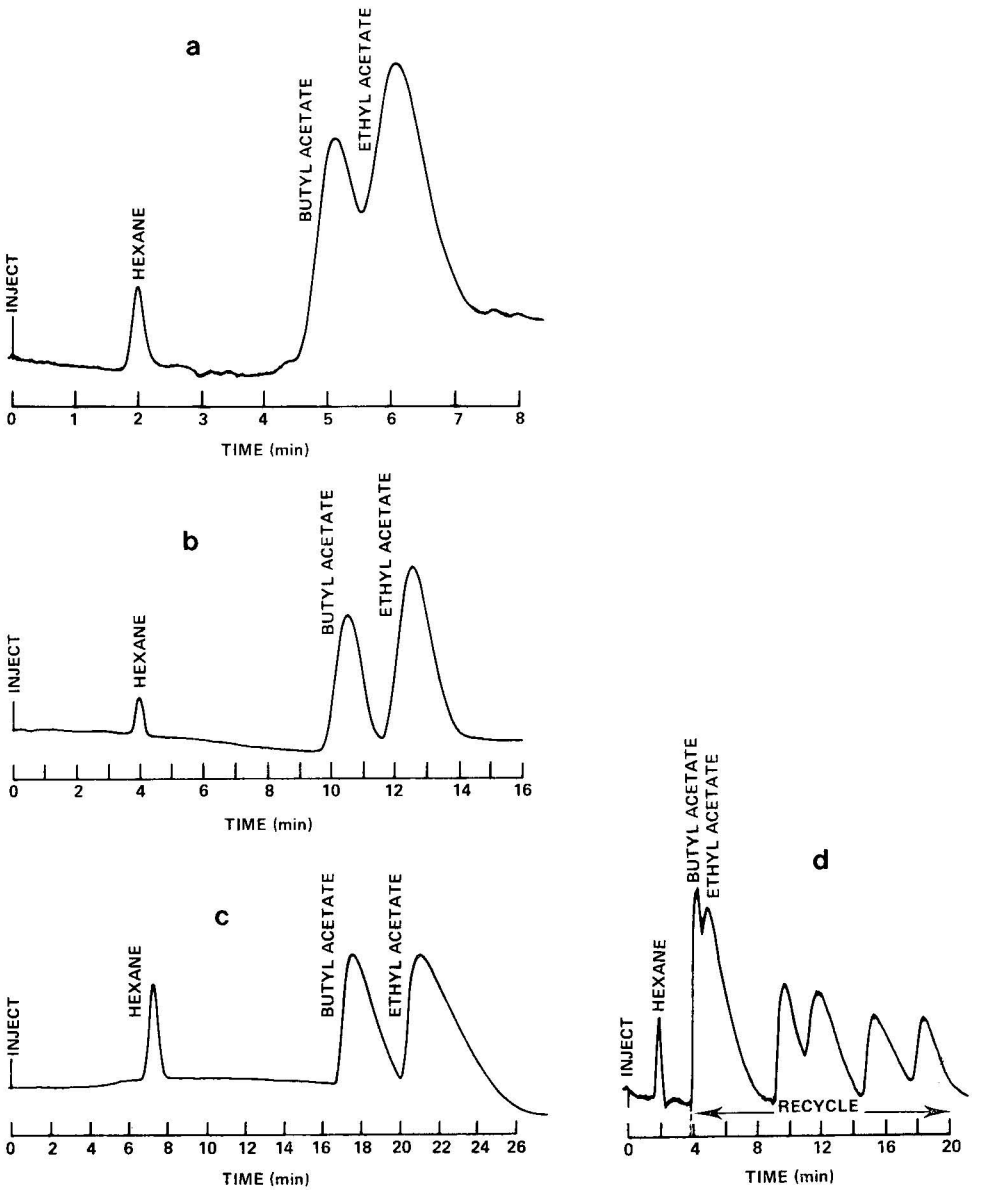


Fig. 6. Relationship between column length, sample load, and resolution. The sample in each case was a standard mixture of butyl acetate and ethyl acetate (each 10% w/v), $\alpha = 1.3$, and hexane (1% w/v, unretained) in methylene chloride. Solvent, methylene chloride. (a) Column, 30 cm × 5.7 cm PrepPak-500; flow-rate, 250 ml/min; detector, RI, relative response 200; sample, 10 ml (100 mg each of butyl acetate and ethyl acetate. 10 mg hexane). (b) Column, two 30 cm × 5.7 cm PrepPak-500 columns in series; flow-rate, 250 ml/min; detector, RI, relative response 200; sample, 10 ml. (c) Column, four 30 cm × 5.7 cm PrepPak-500 columns in series; flow-rate, 300 ml/min; detector, RI, relative response 100; sample, 100 ml (1 g of each retained component, 100 mg hexane). (d) Column, 30 cm × 5.7 cm PrepPak-500; flow-rate, 300 ml/min; detector, RI, relative response 50; sample, 100 ml. Retained components were recycled through the column twice, extending the effective column length to 90 cm.

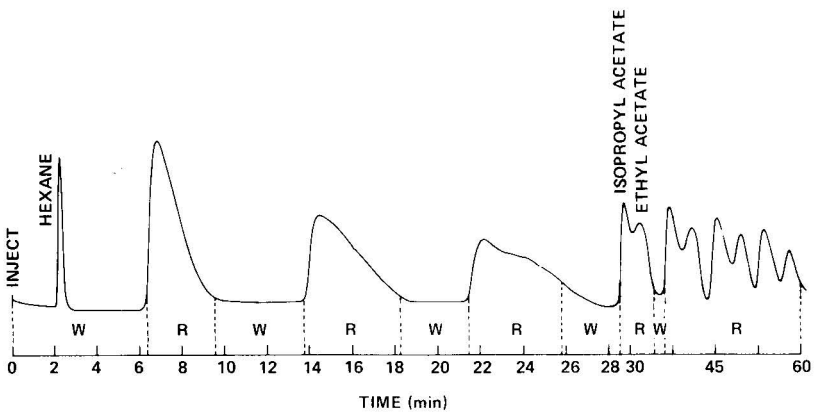


Fig. 7. A difficult (α = 1.1) preparative separation accomplished by recycle. Column, two 30 cm × 5.7 cm PrepPak-500 columns in series; solvent, methylene chloride; flow-rate, 450 ml/min; detector, RI, relative response 50, then 100 after third pass; sample, 0.5 g isopropyl acetate, 0.5 g ethyl acetate and 0.1 g hexane in methylene chloride, total volume 5 ml. Retained components were recycled through the column six times, extending the effective column length to 4.2 m. (Abbreviations used: R = recycle; W = waste.)

enriched in the component of interest. The determination of fraction purity is made by use of analytical HPLC.

The sample chosen to demonstrate the above principles was a reaction product, predominantly a mixture of *cis* and *trans* isomers of a simple unsaturated amide. The compound of primary interest was the *cis* amide. Conditions for the preparative run were conveniently determined by use of a μPorasil analytical column. The analysis of the reaction mixture using ethyl acetate as the mobile phase at a flow-rate of 3 ml/min is shown in Fig. 8A. The analytical system remained operative during the preparative run to check the purity of the collected fractions (Fig. 8C–L). The preparative separation (2 g load) was performed on two PrepPak-500 cartridges at a flow-rate of 200 ml/min. The sample was recycled three times with fractions collected as shown in Fig. 8B. The first two fractions (Fig. 8C and D) were collected to remove the early eluting impurities. Fraction 3 (Fig. 8E) was shaved from the front of the major peak to remove the remaining minor impurities and obtain relatively pure *cis* amide which could be pooled with subsequent fractions of comparable purity from this and later runs and rechromatographed, Fraction 4 was shaved from the major peak to remove some of the *trans* component (Fig. 8F). This makes each subsequent recycle more effective in resolving the two components present du toe the total reduction in mass being recycled. To check the purity of the components now being recycled a narrow band was shaved from the front edge of the eluting components on the first recycle. From Fig. 8G it can be seen that Fraction 5 contains pure *cis* amide. Again the back edge of the now partially resolved second peak was shaved to reduce the amount of *trans* amide in the remaining mixture. Fraction 6 (Fig. 8H), which is predominantly *trans* amide, could be pooled with Fraction 4 (Fig. 8F) for subsequent purification. On the second recycle pure *cis* amide was again recovered in Fraction 7, as shown in Fig. 8I. Also on this pass, Fraction 8 was collected to remove most of the remaining *trans* amide (Fig. 8J). On the third recycle the remainder of the sample was collected

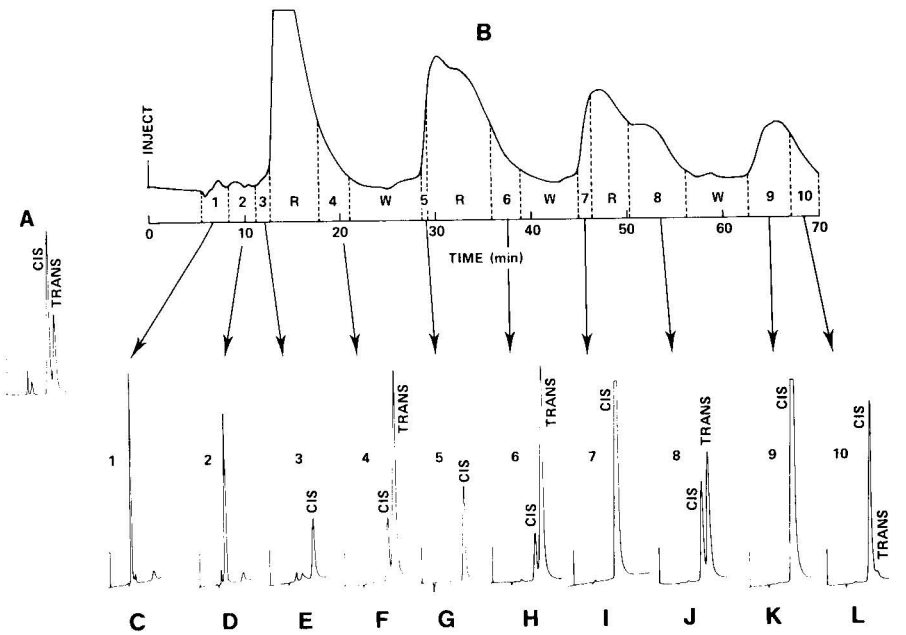


Fig. 8. Isolation of *cis* R_1R_2:R_1CONH_2 from a *cis–trans* reaction product mixture ($\alpha = 1.2$). A, Analytical separation of reaction product. Column, 30 cm × 4.2 mm I.D. μPorasil; solvent, ethyl acetate; flow-rate, 3.0 ml/min; detector, UV at 254 nm, 0.5 a.u.f.s.; sample size, 5 μg. B, Preparative separation of reaction product. Column, two 30 cm × 5.7 cm PrepPak-500 columns in series; solvent, ethyl acetate; flow-rate, 250 ml/min; detector, RI, relative response 10; sample size, 2.0 g. C–L, Analytical separations of collected fractions from preparative separation. Conditions, same as in Fig. 8A.

in two fractions. Fraction 9 is pure *cis* amide (Fig. 8K), and Fraction 10 is greater than 90% *cis* isomer, as shown in Fig. 8L.

Once the analyses of the fractions have been completed, the appropriate fractions can be combined. The fractions containing pure *cis* amide (5, 7 and 9) should be pooled, concentrated and used for further research. Fractions 3 and 10 should be saved until other runs are made, then combined with fractions of comparable purity and further purified. If desired, the *trans* isomer can be recovered from Fractions 4, 6, and 8 at a later time.

Thus, the complementary use of high-efficiency analytical LC enables the chromatographer to establish rapidly the conditions for the preparative separation, monitor the composition of each fraction immediately after its collection, and thereby maximize the yield and purity of the compound or compounds of interest. The examples used in this study demonstrate the ability of radially compressed preparative LC columns to separate easy ($\alpha > 2$) to difficult ($\alpha = 1.1$) mixtures with minimum investment in time, solvent, and column length.

ACKNOWLEDGEMENT

The authors wish to thank Dr. Donald Jerina of the National Institutes of Health, Bethesda, Maryland, U.S.A., for the sample of tetrahydrophenanthrenes used in a portion of this study.

HIGH-PERFORMANCE THIN-LAYER CHROMATOGRAPHY

Journal of Chromatography, 126 (1976) 449–456
© Elsevier Scientific Publishing Company, Amsterdam — Printed in The Netherlands

CHROM. 9472

COMPUTER-CONTROLLED EVALUATION IN THIN-LAYER CHROMATOGRAPHY

RESULTS AND POSSIBILITIES

S. EBEL and J. HOCKE

Department of Pharmaceutical Chemistry, University of Marburg, 3550 Marburg (G.F.R.)

SUMMARY

The results of quantitative optical *in situ* scanning with a computer-controlled double-beam densitometer for thin-layer chromatography are given. Each spot is positioned in an optimum way with respect to the light beam so that deviations in sample application and in the chromatographic process no longer cause errors. The measurement of peak height in connection with the internal standard method gives very good results. As there is no time-consuming step in the quantitation, this system is suitable for routine analysis in pharmaceutical quality control (content uniformity test). Furthermore, peak areas can be determined by digital integration or by a special peak approximation. The detection limit is lowered, as signal averaging or integrating analogue to digital conversion gives better signal-to-noise ratios than in the usual scanning methods.

INTRODUCTION

Quantitative determinations of different classes of substances on thin-layer plates by optical scanning have been carried out for about 15 years. During the past 10 years, chromatogram photometers for reflectance, transmission and fluorescence measurements have been commercially available. There are highly sophisticated instruments for avoiding errors due to the irregularities of the sorbents, solvents and the chromatographic process itself, which operate in a double-beam or double-wavelength mode or by simultaneous measurement of the reflectance and transmission. Quantitative *in situ* thin-layer chromatography (TLC) is a very flexible analytical method and the separations of different compounds from each other and from the interfering matrix are effected in a single procedure directly followed by the quantitation.

EXPERIMENTAL

TLC-photometer

A Schoeffel SD 3000 was used with a modified stage, driven by stepper motors controlled by a Hewlett-Packard 9830 or 9810 desk calculator (*cf.*, Fig. 3).

Reference substances

Reference substances were of pharmaceutical quality, reagent grade.

Solvents

Solvents were reagent grade materials obtained from E. Merck (Darmstadt, G.F.R.).

TLC and high-performance TLC-plates

Pre-coated Kieselgel 60 plates were obtained from Merck.

Sample application

Microcaps (0.5 μl) were used (Drummond, Broomall, Pa., U.S.A.).

AUTOMATIC SCANNING UNITS

The time-consuming step in the quantitation of the separated spots is the positioning of each track in the centre of the light beam. The commonly used TLC densitometers are sensitive to mispositioning and the resulting errors can easily exceed 1–2%. We have described two methods for constructing electronically controlled automatic scanning units for TLC: one system with precision analogue time bases[1] and the other with digital electronics[2]. Small errors in spotting and deviations in developing the chromatogram can cause large errors. Therefore, another system has been developed commercially (Zeiss, Zürich, Switzerland) that avoids this error by a special scanning mode, as shown in Fig. 1. Each track of the plate can be scanned,

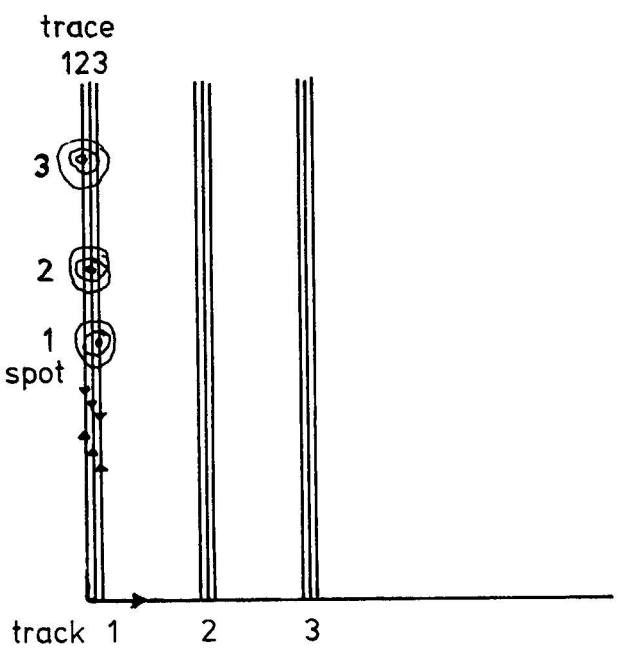


Fig. 1. Principle of the automatic scanning unit for TLC (Zeiss, Zürich, Switzerland).

examining close traces different distances apart (0.1, 0.2, ... mm). Scanning with and against the direction of development with averaging of the two integration counts for each peak leads to better results and to a higher reproducibility[3]. The system is coupled to a computer and from each scan all peak areas are compared to give the most probable value for the estimation of the content of the spots to be determined (Fig. 2).

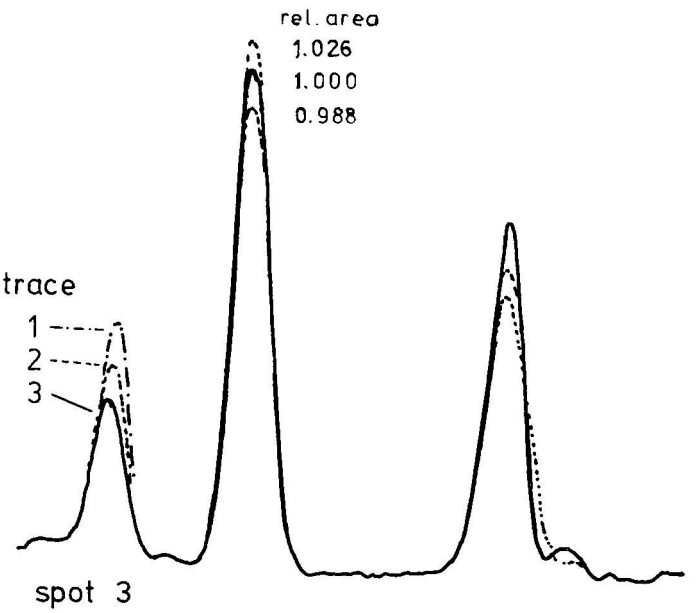


Fig. 2. Chromatogram recorded using the method of scanning shown in Fig. 1 with the results of the electronic integration.

COMPUTER-CONTROLLED TLC DENSITOMETER

We recently described a computer-controlled TLC densitometer[4–6]. In this system, the signal of the densitometer is fed by an analogue–digital converter or by a

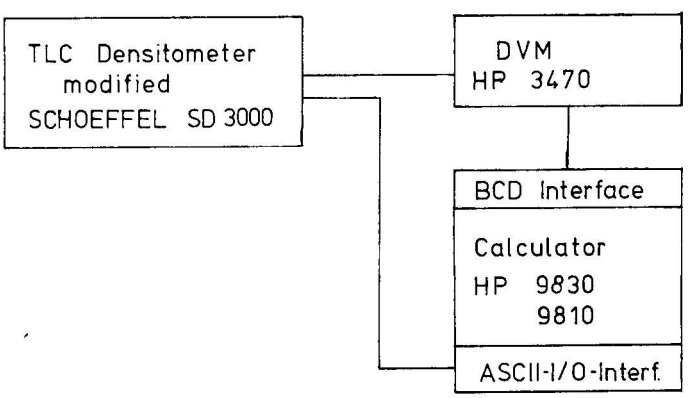


Fig. 3. Schematic diagram of the computer-controlled TLC densitometer.

digital voltmeter with BCD output via an interface to a programmable desk calculator (Fig. 3). The calculator works like a process computer and is able to control the stage of the TLC densitometer. Therefore, a Schoeffel SD 3000 double-beam instrument was equipped with stepper motors for the x- and y-directions of the stage. This system allows the position of each spot to be controlled by the computer optimally with respect to the light beam, as shown in Fig. 4. The stage is moved in discrete steps in the y-direction (the direction of development) until the first peak is found by four successive pieces of increasing data. With a lower resolution defined by the software, the maximum peak height is searched first in the y- and then in the x-direction. In order to avoid errors due to irregular spots, this procedure is repeated a second time using backscan for a defined distance. The resolutions A_y, a_y, a_x and the distance of the backscan, D_y can be changed, in order to give optimal values for different problems or in order to scan the commonly used TLC plates as well as the new high-performance TLC plates. The resolution is related to the stepper motors and the gear, and it is possible to position any spot to within 0.05–0.1 mm. This permits a reproducibility (expressed as relative standard deviation), measured on 20 spots using 25 scans of the same plate, of less then 0.4%.

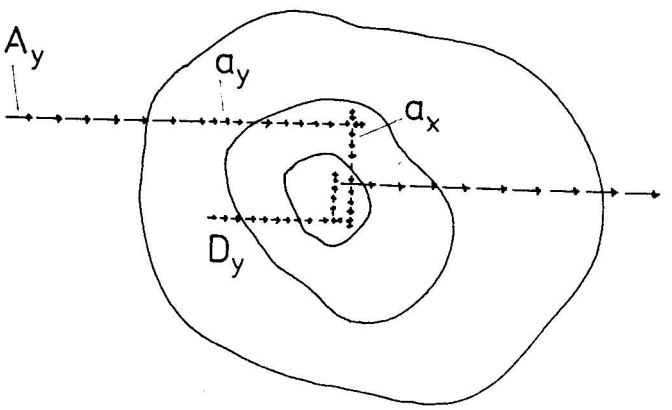


Fig. 4. Method of positioning the spot in the light beam of the TLC densitometer. A_y and a_y, resolution in direction of development; a_x, resolution at right-angles to solvent flow; D_y, backscan before the second positioning.

EVALUATION USING PEAK HEIGHT AND INTERNAL STANDARD

In a recent paper, we compared the estimation of the same spots by the integration and peak height methods[7]. In routine pharmaceutical analysis, the peak height method gives very good results only if there is a limited range of concentration[8] or at low concentrations[9,10]. Using the internal standard method[11–13], the error caused by spotting the solution on the plate can be eliminated and a larger number of analyses can be carried out on the same plate. Using a double-beam densitometer, many effects of the sorbents (gradients in thickness or particle size) and the solvents (UV absorption near the front) have smaller influence on the results in comparison with single-beam instruments. A large number of routine analyses have been carried out with this computer-controlled TLC densitometer in the past 2 years and some results

are given in Tables I–III. All of these results are based on peak height measurements with an internal standard. The time that is needed to scan one plate depends on the numbers of tracks, spots and the distance from the first to the last spot. A mixture of three components plus an internal standard, with 8 tracks (32 singular spots), is processed in about 25 min using the equipment shown in Fig. 3 or in about 18 min using a fast analog-to-digital converter instead of the digital voltmeter. The method described can be used, for instance, in the content uniformity test.

TABLE I

DETERMINATION OF DIMETHINDEN IN VIBROCIL WITH PHENAZON AS INTERNAL STANDARD[14]

Dimethinden: 100% ≈ 1.88 μg per spot ≈ 2.5 mg per 10 ml. Solvent: acetonitrile–ethanol–25% NH_3 (30:5:3). λ = 254 nm; slit width ≈ 7 × 0.5 mm.

Stock No.	*Results*			
	Mean (%)	*Standard deviation (%)*	*Number of results*	*Mode**
2240	97.6	1.12	20	a
2250	98.5	1.74	20	
2200	102.9	1.53	16	
2240	98.8	1.09	30	b
2250	98.0	2.43	29	
2200	102.5	2.51	16	

* a, 4 analyses/4 references/plate; b, 6 analyses/2 references/plate.

TABLE II

DETERMINATION OF CAFFEINE AND ASPIRIN IN CAFASPIN TABLETS (CONTENT UNIFORMITY TEST) WITH ACETOPHENETIDIN AS INTERNAL STANDARD[14]

Caffeine: 100% ≈ 0.25 μg per spot ≈ 50 mg per tablet. Aspirin: 100% ≈ 2.5 μg per spot ≈ 500 mg per tablet. Solvent: *n*-hexane–dioxan–formic acid (45:40:2). λ = 275 nm; slit width ≈ 6 × 0.3 mm.

Substance	*Results*		
	Mean (%)	*Standard deviation (%)*	*Number of results*
Caffeine	100.5	1.16	29
Aspirin	99.4	1.64	29

TABLE III

DETERMINATION OF AN ANALGESIC MIXTURE IN DRAGEES (CONTENT UNIFORMITY TEST) WITH CORNECAIN AS INTERNAL STANDARD[14]

Dichloralphenazon: 100% ≈ 10 μg per spot ≈ 100.0 mg per dragée. Caffeine: 100% ≈ 2 μg per spot ≈ 20.0 mg per dragée. Papaverin: 100% ≈ 2 μg per spot ≈ 20.0 mg per dragée. Solvent: acetonitrile–25% NH_3 (50:4). λ = 280 nm; slit width ≈ 6 × 0.5 mm.

Substance	*Results*		
	Mean (%)	*Standard deviation (%)*	*Number of results*
Dichloralphenazon	98.2	2.69	24
Caffeine	101.0	3.42	24
Papaverin	99.1	3.39	24

QUANTITATION OF HIGH-PERFORMANCE TLC PLATES

As mentioned above, all steps in the x- and y-directions are controlled by the software and can easily be changed. Using the HP 9830 desk calculator, a dialogue is possible between the user of the system and the computer. Therefore, there is no limitation to the estimation of spots on high-performance TLC plates. A typical result is given in Table IV. Some lipophilic dyestuffs used by Ripphahn and Halpaap[15] for controlling the separation properties of the thin layer were also quantified by peak height measurement and the internal standard method. Only a measurement at one wavelength (ca. 420 nm with a relative large bandwidth) was made, and therefore some peaks are very small and others very large. In some instances the ratios of the peak heights exceed 1:10, as shown in Fig. 5.

TABLE IV

DETERMINATION OF 30 ng OF DYESTUFFS (*cf.*, FIG. 5) ON HIGH-PERFORMANCE TLC PLATES WITH COMPOUND 4 AS INTERNAL STANDARD[14]

Mode: alternating tracks with reference and analysis.

No.	*Substance*	*Results*		
		Mean (ng)	*Standard deviation (%)*	*Number of results*
1	Ceresviolett BRN	29.8	0.49	8
2	Ceresschwarz G	29.8*	1.68	8
3	Accompanying substance with 2	29.9*	2.81	8
4	Fettgelb (internal standard)	—	—	—
5	Bleu VI F Organrot	29.7	4.69	8
6	Ceresrot G	29.3	2.57	8
7	Ceresbraun BRN	30.1	3.19	8

* Relative results.

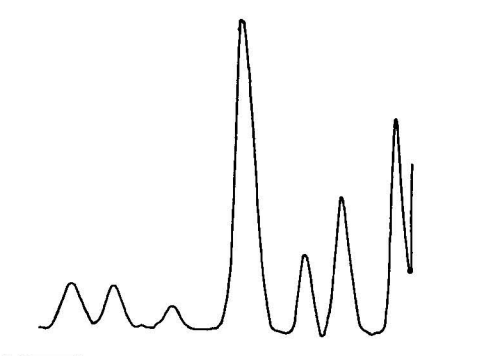


Fig. 5. Mixture of seven lipophilic dyestuffs[15] measured at about 420 nm and relatively large monochromator exit slit.

PEAK AREA DETERMINATION

In some instances, the determination of only the peak height is erroneous. For instance, in the examination of biological fluids or tissue extracts, there are many interferences by the matrix in the analysis. Therefore, the determination of the integral peak area is more useful. After positioning the spot in the centre of the light beam, the stage is re-scanned for a defined length and the peak area is found by scanning and numerical integration. The method of determining peak areas by numerical integration is used in many commercial data systems (Hewlett-Packard, Siemens, IBM, etc.), and some special problems with regard to TLC have been described in the literature[15,16]. Another method is the determination of peak areas by a modified Gauss approximation[17].

DETECTION LIMIT

In some fields (biochemistry, clinical chemistry, naturally occurring compounds), it is of interest to detect substances at very low concentrations. In quantitative *in situ* determinations in TLC, Sudanred is often used to determine the detection limit[18,19]. The detection limit is directly related to the signal-to-noise ratio but also depends on a number of parameters of the chromatographic process[10]. The noise that arises during the recording of a chromatogram arises from the lamp (especially xenon lamps), photomultiplier, amplifier and, to a large extent, small irregularities in the sorbent layer. With a computer-controlled TLC-photometer, the signal-to-noise ratio can be decreased by signal averaging. After having carried out a defined number of

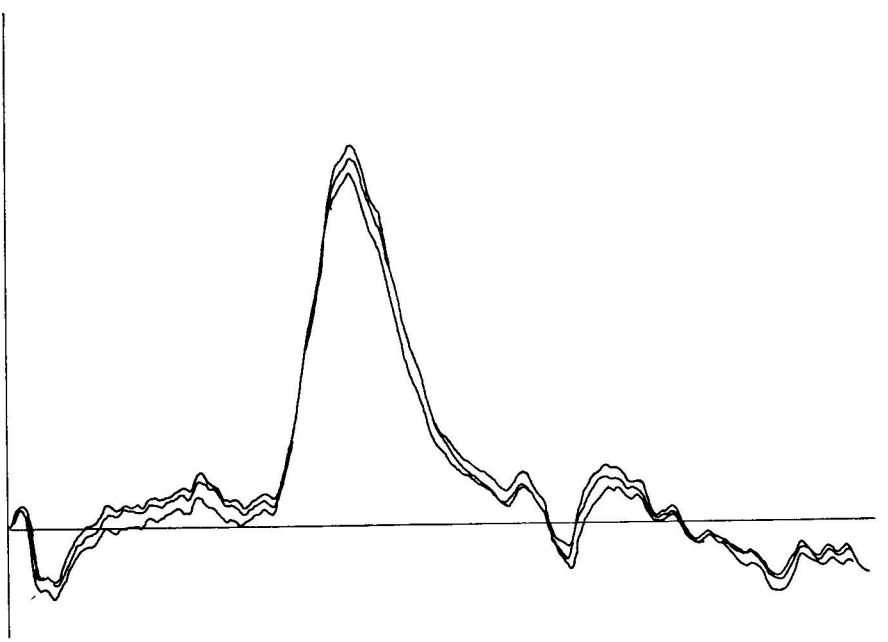


Fig. 6. Computer-controlled repeated scan of the same spot. The reproducibility of optical scanning is evident. Caffeine, 5 ng per 0.5 μl per spot. $\lambda = 275$ nm; slit width $\approx 5 \times 0.3$ mm.

steps in any direction, the stage is stopped and a discrete number of data can be summed and averaged. For instance, a spot containing 10 ng of caffeine (sample application 0.5 μl, spot migration about 5 cm) is detectable with a signal-to-noise ratio of about 4. The detection limit of the computer-controlled system without signal averaging but with integrating analogue–digital conversion defined by the sampling rate of the digital voltmeter (100 ms) is less than 5 ng. Signal averaging, digital smoothing and pseudo-Gaussian approximation[17] can further decrease this detection limit. The real boundary is given by the irregularities of the plate. Fig. 6 shows the computer-controlled scan of the same spot; it can be seen that the deviations in the baseline are not due to statistical noise by the lamp, photomultiplier and amplifier but are real effects from the plate.

ACKNOWLEDGEMENTS

We thank the Deutsche Forschungsgemeinschaft and the Fonds der Chemischen Industrie for financial support, Frau E. Koch for her assistance in this work, and Frau H. Herbert (Merck, Darmstadt, G.F.R.) for preparing the high-performance TLC plates.

REFERENCES

1 S. Ebel and J. Hocke, *Chromatographia*, 8 (1975) 573.
2 S. Ebel and J. Hocke, *Chromatographia*, 9 (1976) 76.
3 S. Ebel and G. Herold, *Z. Anal. Chem.*, 266 (1973) 281.
4 S. Ebel and J. Hocke, *Workshop on Quantitative TLC, Darmstadt, 1975 and 1976.*
5 S. Ebel and J. Hocke, *Achema Symposium 1976, Frankfurt/Main.*
6 S. Ebel and J. Hocke, *Chromatographia*, in press.
7 S. Ebel and J. Hocke, *Chromatographia*, in press.
8 E. A. MacMullen and J. E. Heveran, in J. C. Touchstone (Editor), *Quantitative Thin-Layer Chromatography*, Wiley, New York, 1973.
9 H. Bethke and R. W. Frei, *J. Chromatogr.*, 91 (1974) 433.
10 S. Ebel, G. Herold and J. Hocke, *Instrument und Forschung*, (1976) 42.
11 R. Klaus, *J. Chromatogr.*, 62 (1971) 99.
12 S. Ebel and G. Herold, *Chromatographia*, 8 (1975) 37.
13 S. Ebel and G. Herold, *Arch. Pharm. (Weinheim)*, 308 (1975) 839.
14 J. Hocke, *Thesis*, University of Marburg, Marburg, in preparation.
15 J. Ripphahn and H. Halpaap, in R. E. Kaiser (Editor), *Einführung in die HPDC*, Institut für Chromatographie, Bad Dürkheim, 1976, p. 82.
16 S. Ebel and H. Kussmaul, *Z. Anal. Chem.*, 268 (1974) 268.
17 S. Ebel, E. Glaser and M. Kaal, in preparation.
18 H. Jork, *J. Chromatogr.*, 82 (1973) 85.
19 K. Hezel, *Angew. Chem.*, 85 (1973) 334.

Journal of Chromatography, 126 (1976) 457–462
© Elsevier Scientific Publishing Company, Amsterdam — Printed in The Netherlands

CHROM. 9477

USE OF A GASEOUS ELECTRICAL DISCHARGE TO INDUCE FLUORESCENCE IN ORGANIC COMPOUNDS SEPARATED BY THIN-LAYER CHROMATOGRAPHY

H. SHANFIELD, F. HSU and A. J. P. MARTIN
University of Houston, Chemistry Department, Houston, Texas 77004 (U.S.A.)

SUMMARY

It has been found that a simple gaseous electrical discharge can induce visible fluorescence in a variety of organic compounds separated on silica gel thin-layer chromatoplates. Exposure times ranging from 5 sec to 5 min are ample to detect submicrogram quantities with the unaided eye. The method is simple and convenient, and appears to have broad applicability to a wide variety of organic compounds. It is anticipated that this procedure will lend itself to sensitive quantitation by the use of spectrofluorimetric instrumentation.

INTRODUCTION

Segura and Gotto[1] were able to induce fluorescence in a number of organic compounds on silica gel thin-layer chromatograms, by exposing them to the vapors from ammonium hydrogen carbonate. After a 2–12 h exposure of the plates to a temperature between 110 and 150° in a pressure cooker, blue fluorescent spots were visible when irradiated with a wavelength of 365 nm. There was a substantial similarity for both the exciting and emitted wavelengths of the radiation, irrespective of the organic substances used.

The variety of substances which gave fluorescence was remarkable. Carbohydrates, lipids, steroids, amino acids, heterocyclic compounds and alkaloids all gave similar results. The presence of an inorganic adsorbent was essential. Silica and alumina were of similar effectiveness. Good quantitative measurements were possible with a spectrofluorimeter. Segura and Gotto suggest that a chromophoric system of the type RN=CH–CH=CH–NH–R could explain the fluorescence, and suggest a mechanism similar to the production of malonaldehyde and Schiff bases therefrom during the irradiation of various compounds by γ-rays.

It appeared to us as probable that Segura and Gotto's[1] conditions must be producing free radicals and that these yielded essentially the same compounds from all the starting substances. We considered a variety of means of accomplishing this to see whether it was possible to produce the fluorescent substances. X-Rays, UV and gaseous electrical discharges seemed the most obvious ways of approaching the subject.

The electrical discharge was convenient in producing UV, electrons, positive ions, and excited molecules, atoms and free radicals. A variety of simple electric discharge tubes were constructed and did indeed induce fluorescence in various substances on thin-layer plates after a brief exposure, and the conditions were not at all critical. It was found that all the classes of substances used by Segura and Gotto would fluoresce under our conditions, especially when nitrogen was present in the system.

After exposure in the discharge tube, heating for a brief period was desirable, often greatly increasing the intensity of the fluorescence. In the presence of oxygen, the fluorescence at first increased and later decreased, although if the fluorescence had been brought to maximum intensity by heating, it appeared to be relatively stable on further exposure to the discharge.

The vapors from ammonium hydrogen carbonate, air, oxygen, argon or nitrogen may all be used as a gas in the tube. Nitrogen, however, may be most effective in the gas or when it is contained in the substance irradiated.

Later it was found that using a nitrogen-containing substance in the gas, better results were obtained if the sample were not exposed directly to the radiation or the ions. The sample was enclosed in a bent aluminum foil container which permitted flow of gas through it, but screened off radiation and which could be relied upon to pick up any ions. Under these conditions stronger fluorescence was produced and no destruction appeared to take place even after prolonged exposure.

EXPERIMENTAL

Compounds and reagents

More than 30 compounds have been examined so far, in amounts ranging from 1 μg to 1 ng. These were obtained from various commercial and laboratory sources.

All solvents used to dissolve these compounds and subsequently spot the thin-layer plates were of analytical or spectroquality grades. Control experiments were done regularly with solvents alone to avoid artifacts due to solvent impurities or fluorescent impurities in the plates.

Ammonium hydrogen carbonate, when employed, was obtained from Fisher Scientific (Pittsburgh, Pa., U.S.A.). Nitrogen, hydrogen, oxygen and argon were obtained from IWECO (Houston, Texas, U.S.A.).

Thin-layer chromatoplates

The majority of the experiments were conducted with the so-called permanent-surface "Permakote" thin-layer plates (Applied Science Labs., State College, Pa., U.S.A.). In these plates, the silica gel is permanently bonded to the glass surface, and contains no organic binder. The layer thickness was 0.23 mm. They can be reused by treatment with "chromic acid" without noticeable change in their properties. These plates made it possible to achieve an absolute minimum of fluorescent background, while other commercial plates appeared to contain an organic binder which developed fluorescence. The adsorption activity of the silica gel is rated as "moderate" by the company. A few experiments were done with other plates, notably the high-performance plates from Merck (silica gel 60, catalog No. 5631-9H, E. Merck, Darmstadt, G.F.R.) which give exceptionally compact spots during chromatography.

Test procedure

Normally, solutions were made of 1 μg of substance per μl of solvent and 1 μl of solution was spotted on the plate. The solvent was evaporated with gentle heat. Solvents were tested, if necessary side by side with solution, to make sure that no residue remained, which might produce a fluorescent artifact.

The small piece of plate was then placed in the discharge tube, which was evacuated to approximately 0.2 torr, and the discharge run for a period of 5 sec to 5 min. After removal from the tube the plate was placed on a hot plate at about 130°. The development of fluorescence was watched under a 365-nm UV lamp (Ultraviolet Products, San Gabriel, Calif., U.S.A.) until it appeared to reach a maximum value. This usually occurred in 1–2 min. Sometimes the intensity of fluorescence increased on cooling to room temperature. The fluorescence was rated by eye on a 1 to 10 scale of intensity (1 = weak, 10 = strong).

Electrical discharge chamber

A schematic diagram of the electrical discharge chamber ("plasma" chamber) is shown in Fig. 1. The plasma discharge was produced by a Tesla coil-type high-frequency generator rated at a maximum of 20,000 V, 0.5 MHz. These coils are used routinely to detect leaks in glass vacuum systems (Model BD-40, Electro-Technic Products, Chicago, Ill., U.S.A.). The high-frequency output was coupled to the plasma chamber by simply wrapping aluminum foil externally around one section of a glass tube, to which the electrode tip was connected (capacitive coupling). A second steel rod electrode was inserted in the tube as shown, and connected to ground (resistively coupled). When operating, an intense glow filled the tube from within the foil covered region to the steel electrode. Thin-layer plate test specimens were placed inside the evacuated tube between the electrodes.

The plasma chamber was provided with a side chamber into which a solid like ammonium hydrogen carbonate could be placed. In addition, provision was made

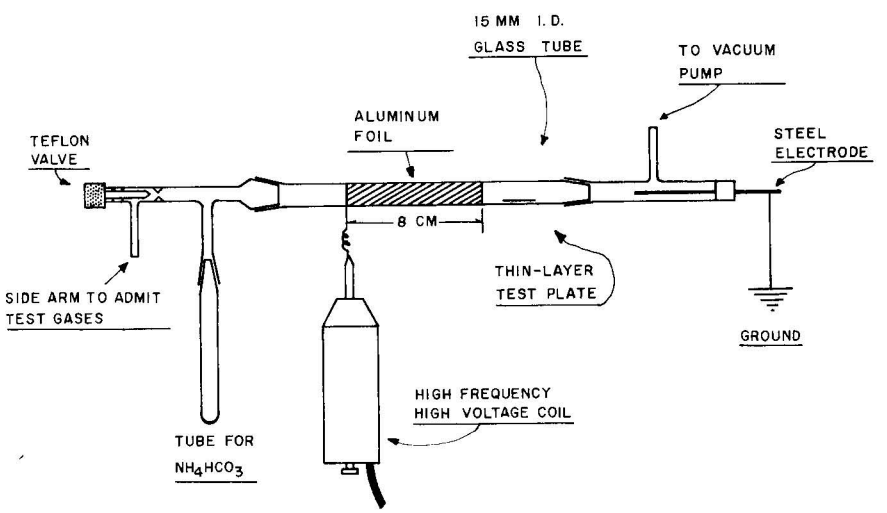


Fig. 1. Schematic diagram of electrical discharge chamber for inducing fluorescence in organic compounds spotted or separated on silica gel thin-layer chromatoplates.

to allow any chosen gas to be admitted to the chamber. The system was evacuated to a pressure of about 0.2 torr.

RESULTS

General observations

All the organic compounds tested in the atmosphere resulting from ammonium hydrogen carbonate at room temperature gave readily observable fluorescence at the 1-μg level, although the maximum intensity varied. Compounds with simple structures and relatively low molecular weight (*e.g.* glycerol, glucose, simple amino acids) appear to reach their peak intensity after only a few seconds of exposure, and thereafter tended to diminish in intensity. This is presumably due to decomposition by the active particles in the electrical discharge. Compounds with ring structures, conjugated or otherwise, tend to give very strong fluorescence, and can be subjected to as much as 5 min exposure with continuing enhancement of fluorescent intensity. Higher molecular weight compounds also tend to give strong fluorescence in 1–3 min of exposure.

When the gaseous environment is nitrogen, or hydrogen, the fluorescence produced is approximately equivalent to ammonium hydrogen carbonate, as judged by the unaided eye. With oxygen however, fluorescence is decisively lower, though not altogether absent for compounds containing ring structures. Possibly this is due to simple destructive oxidation of the organic compounds. Air alone gives intermediate results. Vapors from an ammonia solution also induce fluorescence. Argon gives discernible, but somewhat weaker fluorescence. It is interesting to note that organic vapors such as pyridine, isopropylbenzene and phenol produce intense fluorescent derivatives covering the entire thin-layer plate. Clearly active fragments from such compounds are able to combine in some way on the silica gel surface to give fluorescent compounds. These compounds were found to be substantially elutable by water or ethanol with an R_F value approaching unity.

It should be noted that silica gel or alumina appears to be essential to the formation of fluorescent derivatives. There was no evidence of visible fluorescence when compounds were spotted on a bare glass plate, or a ground glass surface, and later subjected to the electrical discharge, even though these same compounds were extremely fluorescent on the silica gel. We found a number of compounds which would fluoresce faintly on silica gel after mild heating (130° for 1 min), but not in the absence of silica gel. Mixing silica gel powder with the compounds and later subjecting this to the electrical plasma produced the usual strong fluorescence. The effect of heat alone has been reported by Segura and Gotto[1].

Many compounds come out of the plasma chamber fluorescing strongly at room temperature. Most compounds however, showed a distinct enhancement of fluorescence when the plate was heated at 130° for 1–2 min. It is assumed that such heating results in rearrangement of active substances on the silica gel surface to produce the fluorophores. In some rare instances, fluorescence diminished with heating, but was fully restored at room temperature. Once formed, the fluorescent spots appear to be fully stable for at least several months.

The adsorbent alumina was tried briefly and found to give similar results, but further work has been deferred for the present.

Summary of compounds examined ("Permakote" plates)

Table I lists a number of compounds which have been examined by this technique. One microliter spots were placed on the thin-layer plates representing 1-μg amounts in most cases (except where indicated). Following exposure in the plasma chamber, the spots were examined by the unaided eye and rated as to intensity. Spot sizes were typically 3–4 mm in diameter.

TABLE I

FLUORESCENCE INDUCED BY GASEOUS ELECTRICAL DISCHARGE IN VARIOUS ORGANIC COMPOUNDS (NITROGEN ENVIRONMENT)

Intensity of fluorescence is indicated qualitatively by a scale rating from 1 = weak, to 10 = strong, using the unaided eye, with little dark adaption.

Compound	*Amount*	*Estimated fluorescent intensity*	*Exposure time (sec)*
Cholesterol	1 μg	10	60
	1 ng	3	60
Cholesteryl pelargonate	1 μg	8	60
Progesterone	1 μg	10	60
Testosterone	1 μg	10	60
Lindane	1 μg	3	60
Dieldrin	1 μg	6	60
Glucose	1 μg	3	5
Glycerol	1 μg	3	5
Glycine	1 μg	2	5
Serine	1 μg	3	10
Arginine	1 μg	3	10
Phenylalanine	1 μg	3	5
Methionine	1 μg	2	5
Morphine	1 μg	9	180
Codeine	1 μg	9	180
Cocaine	1 μg	8	180
Demerol	1 μg	8	180
Phenobarbitol	1 μg	8	180
Chloropromazine	1 μg	10	180
	1 ng	3	30
Prochlorperazine dimaleate	1 μg	10	180
d-Amphetamine sulfate	1 μg	8	180
Methadone	1 μg	10	180
	1 ng	4	30
Tetrahydrocannabinol	1 μg	10	60
Lauryl alcohol	1 μg	7	180
n-$C_{22}H_{46}$	1 μg	8	180
Phenol	1 μg	6	180
Oleic acid	1 μg	7	180
Inositol	1 μg	9	60

Results on chromatograms

A few experiments were conducted on thin-layer plates where a group of spotted compounds were separated chromatographically. Cocaine, morphine and methadone were spotted on a "Permakote" plate, and eluted with ethyl acetate–dioxane–benzene–ammonium hydroxide (5:40:50:5). The plate was dried, placed in the discharge chamber with ammonium hydrogen carbonate for three minutes and examined for separation and fluorescence. The spots were clearly visible under the 365-nm UV

lamp, with a rating of 8 or better.

A similar experiment was carried out using a Merck silica gel 60 high-performance plate and the spots were clearly discernible at a rating of about 9–10, in spite of obvious background fluorescence induced in the organic binder employed in their manufacture. As is characteristic of these plates, the spots were very compact, resulting in a smaller area of high fluorescent intensity.

DISCUSSION

The detection procedure described combines rapidity, simplicity and sensitivity. Within a few minutes, plates can be uniformly exposed to an electrical discharge in a "plasma" chamber, and be ready for UV scanning. It seems plausible that sensitivities, for some compounds at least, can reach the picogram range if, for example, one uses the cylindrical support technique for thin-layer chromatography described by Gietz *et al.*[2], coupled with spectrofluorimetric instrumentation. The other attractive aspect of this detection technique is its very broad applicability to organic compounds of many classes. It appears to be especially sensitive to compounds whose analysis in biological fluids is commonly being sought (*e.g.* drugs, steroids).

The mechanisms involved in producing fluorophores must indeed be complex. It is conceivable that the resulting fluorophores may be much simpler as a class, and this is an area worthy of further investigation. The gaseous environment on which the electrical discharge acts is an important determinant in the production of fluorophores, and the sensitivity achieved. Nitrogen and ammonium hydrogen carbonate vapors appear to be about equivalent in producing intense fluorescence. Argon, on the other hand, produces less intense fluorescence, yet clearly makes no direct chemical contribution to fluorophore production. Based on the results obtained thus far, it appears that the electrical discharge can promote the formation of fluorescence by both chemical species produced (ions, free radicals) and energy transfer to the thin-layer spot by such active species as electrons, ions or excited molecules. We can also see the potential destructive effects of the electrical discharge, particularly on simple organic compounds, where fluorescence reaches a peak after a few seconds of exposure, and then diminishes. This leaves open the question of not only the gaseous environment, but the power introduced into the discharge. These and many other factors remain to be investigated.

It should be noted that Boshoff *et al.*[3] have recently completed work in which thin-layer chromatography has been interfaced efficiently with high-performance liquid chromatography. They applied the technique of Segura and Gotto to detect the thin-layer spots, with satisfactory results.

ACKNOWLEDGEMENTS

The authors wish to thank the Robert A. Welch Foundation for their support of this work. We are also grateful to Dr. David Fenimore of the Texas Research Institute of Mental Sciences for his valuable suggestions and for providing test substances, and to Dr. Albert Zlatkis for his assistance.

REFERENCES

1 R. Segura and A. M. Gotto, Jr., *J. Chromatogr.*, 99 (1974) 643.
2 W. Gietz, A. A. Boulton and V. Pollak, *J. Chromatogr.*, 107 (1975) 81.
3 P. R. Boshoff, B. J. Hopkins and V. Pretorius, *J. Chromatogr.*, 126 (1976) 35.

BIOMEDICAL APPLICATIONS OF GAS AND LIQUID CHROMATOGRAPHY

Journal of Chromatography, 126 (1976) 465–474
© Elsevier Scientific Publishing Company, Amsterdam — Printed in The Netherlands

CHROM. 9407

RAPID QUANTITATIVE MICROANALYSIS OF KETONES IN URINE BY GAS CHROMATOGRAPHY–MASS FRAGMENTOGRAPHY

H. M. LIEBICH and G. HUESGEN

Medizinische Universitätsklinik, Abteilung IV, Otfried-Müller-Strasse, 74 Tübingen (G.F.R.)

SUMMARY

A quantitative method is described for determination of 4-heptanone and its precursor in urine. The method involves a single-step extraction of urine with cyclohexane and the analysis of 1 μl of the extract by gas chromatography–mass fragmentography. The detection limit is $8 \cdot 10^{-12}$ g, corresponding to 2 μg per 1000 ml of urine. The method is linear in the concentration range of $7.6 \cdot 10^{-9}$–$1.5 \cdot 10^{-5}$ g/ml and the relative standard deviations for the individual values are between 1.2 and 10%. Approximately 40 samples can be analyzed per day or 1 sample in 7–8 min. By varying the experimental conditions, the method is applicable to other ketones.

INTRODUCTION

In the past 5 years a number of workers[1–4] have shown that low-molecular-weight and gas chromatographically volatile metabolites are excreted in urine, especially ketones, alcohols, furans, pyrroles and sulphur compounds. The analyses of the profiles of these substances were qualitative. Under strictly standardized conditions for the sampling procedure and the gas chromatographic or mass fragmentographic analysis, semi-quantitative results were obtained. Under such conditions abnormal and pathological profiles can be recognized.

Detailed results have been described on pathologically increased concentrations of ethanol, *n*-propanol, *n*-butanol, isobutanol and isopentanol in the urinary profiles of patients with diabetes mellitus[5–8]. It has also been established that the concentrations of the ketones, especially 4-heptanone, correlate with metabolic disorders related to diabetes[6,8].

We postulate that, analogous to acetone, the higher ketones are formed from β-keto acids by decarboxylation. We could show that the concentrations of the ketones and of their precursors in the urine of patients with diabetes mellitus depend on several factors. The levels of 4-heptanone and the corresponding precursor are influenced by the blood glucose level, the glucose concentration in urine, the insulin activity and probably by the type of diabetes. 4-Heptanone can be considered to be a very sensitive indicator for metabolic changes.

To test the behaviour of this ketone, to establish the correlations between 4-heptanone and the other clinical-chemical parameters and to investigate its clinical

relevance, we had to develop a precise and rapid quantitative method that can be used as a routine procedure and enables one to analyze a large number of urines in a reasonable time.

The method involves a simple single-step extraction and analysis by gas chromatography–mass fragmentography. In this paper, transformation of the precursor, extraction yield, sensitivity, linearity, precision, interferences and practicability of the method for the determination of 4-heptanone are described. By varying the experimental parameters, the method can be used for other ketones and also other low-molecular-weight constituents in urine.

EXPERIMENTAL

Apparatus

A combination of a Model 2700 gas chromatograph and a CH 5 mass spectrometer (Varian-MAT, Bremen, G.F.R.) was used. The gas chromatograph and the mass spectrometer were directly interfaced over a 30 cm × 0.1 mm I.D. platinum capillary. The total effluent from the gas chromatographic column entered the ion source of the mass spectrometer.

Reagents

The following chemicals were used: GC-grade 2-heptanone (Ega-Chemie 12,336-6; Ega-Chemie, Steinheim, G.F.R.), 3-heptanone (Ega-Chemie H 315-1), 4-heptanone (Ega-Chemie 10,174-5), cyclohexanone (Merck 9664, Merck, Darmstadt, G.F.R.) and cyclohexane (Merck 9666); and Triton X-100 (Serva 37238, Serva Feinbiochemica, Heidelberg, G.F.R.). A Triton solution was prepared containing 0.1 % of Triton X-100 in double-distilled water.

Standard solutions

Stock solutions. Three standard stock solutions were prepared from 2-heptanone, 3-heptanone and 4-heptanone, by dissolving 80 mg of the ketone in 100 ml of Triton solution, resulting in a concentration of $8.0 \cdot 10^{-4}$ g/ml.

Internal standard working solution. A 0.1-ml volume of the 3-heptanone stock solution was diluted to 25 ml with Triton solution ($3.2 \cdot 10^{-6}$ g/ml).

Standard working solutions. Fourteen standards were prepared by pipetting equal aliquots of the 2-heptanone and the 4-heptanone stock solutions (0.005–10.0 ml) and 0.1 ml of the 3-heptanone stock solution into Triton solution up to a final volume of 25 ml. All 14 standards had the same concentration of 3-heptanone as the internal standard working solution. When stored at 4°, the solutions were stable for at least 6 weeks.

Extraction procedure

To 4 ml of urine, 0.2 ml of the internal standard working solution was added and this mixture was extracted with 1 ml of cyclohexane by shaking for 1 min. After the extraction, the sample was centrifuged for 5 min at 1500 *g* in order to separate the two phases.

To determine the calibration graphs for 2-heptanone and 4-heptanone, 14

aqueous samples prepared by dissolving 0.2 ml of the standard working solutions in 4.0 ml of double-distilled water (concentrations $7.6 \cdot 10^{-9}$–$1.5 \cdot 10^{-5}$ g/ml) were extracted with cyclohexane in the same manner as the urine samples.

Determination of the extraction yield of 4-heptanone

Two standards containing 4-heptanone in Triton solution ($1.5 \cdot 10^{-7}$ and $1.5 \cdot 10^{-6}$ g/ml) were extracted with cyclohexane using five different extraction ratios: 1, 2, 4, 5 and 10 ml of standard with 1 ml of cyclohexane. To 0.5 ml of each extract, 25 μl of a solution of the internal standard 3-heptanone in cyclohexane ($3.2 \cdot 10^{-6}$ g/ml) were added, resulting in a 3-heptanone concentration of $1.5 \cdot 10^{-7}$ g/ml in the extract.

Each of the standards was extracted a second time using half of the aqueous portion for extraction with 0.5 ml of cyclohexane. To 0.25 ml of the second extracts, 12.5 μl of the internal standard solution were added.

The extraction yields were determined on the basis of a calibration graph obtained by directly injecting several concentrations of 4-heptanone in cyclohexane (internal standard 3-heptanone, $1.5 \cdot 10^{-7}$ g/ml).

Transformation of the precursors into ketones

By heating the urine samples (4 ml) in PTFE-lined screw-capped vials for 60–90 min in a water-bath at 90°, the ketones were formed from their precursors. Approximately 20 urine samples were processed simultaneously.

Gas chromatographic and mass fragmentographic procedure

The gas chromatographic separation was performed on a 100 m × 0.5 mm I.D. stainless-steel column, coated with Emulphor ON-870, at an oven temperature of 80° and an injector temperature of 150°. Helium was used as the carrier gas at a flow-rate of 5 ml/min. The mass spectrometric conditions were as follows: electron energy of the ion source, 70 eV; emission current, 300 μA; accelerating voltage, 3 kV; multiplier voltage, 3.1 kV; ion source temperature, 220°; interface temperature, 200°; resolution, 400; and operating pressure, $4 \cdot 10^{-5}$ torr. For the determination of 4-heptanone and 2-heptanone, the mass spectrometer was focused on the molecular ion *m/e* 114. The sample size was 1 μl of the extract. A 30-cm pre-column was used to protect the separating column from higher boiling substances.

RESULTS AND DISCUSSION

Formation of 4-heptanone from its precursor

4-Heptanone as such is excreted in urine in only small amounts, ranging in normal urines between 10 and 30 μg per 24 h. By heating the urine, its concentration is increased 5- to 15-fold. The same behaviour was observed for 2-heptanone. Figs. 1 and 2 show the formation of the two ketones in a normal urine and a diabetic urine, respectively. The amounts of 4-heptanone in the urines after heat treatment were 184 μg per 24 h in the normal urine and 900 μg per 24 h in the diabetic urine. For 2-heptanone, we determined approximately 27 μg per 24 h in the normal urine and 62 μg per 24 h in the diabetic urine.

We propose that the increase in concentration of the ketones is caused by the

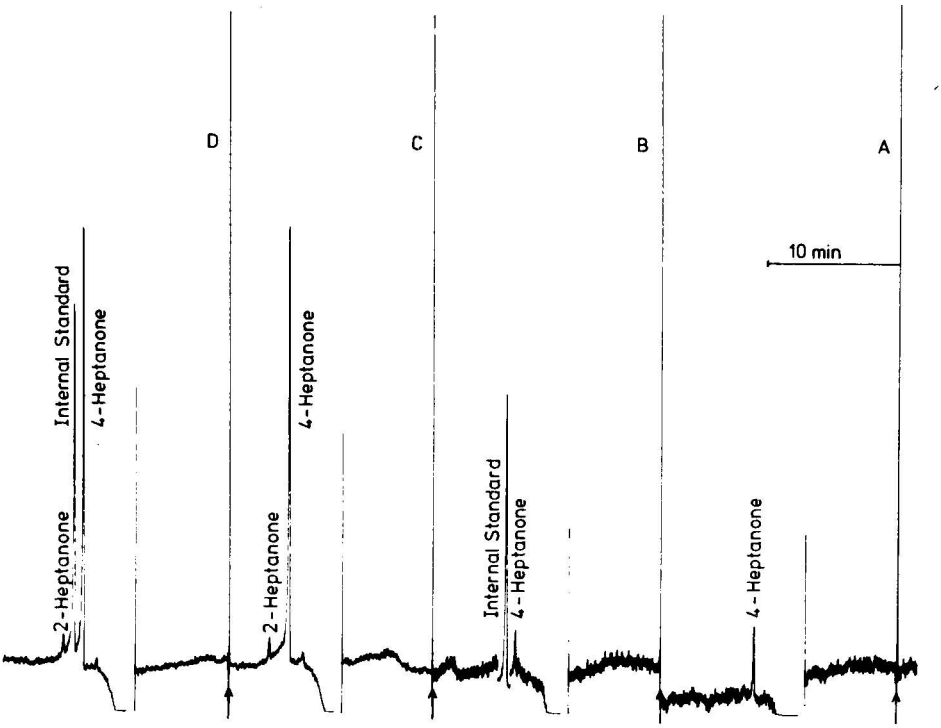


Fig. 1. Mass fragmentograms of a normal urine, *m/e* 114. A, urine not heated, full-scale recorder signal 5 mV; B, urine not heated, addition of internal standard, recorder 5 mV, internal standard with 10 mV; C, urine heated at 90° for 90 min, recorder 10 mV; D, urine heated at 90° for 90 min, addition of internal standard, recorder 10 mV. The arrows below the baseline indicate the starting points of the analyses. The drops in the baseline are caused by the pressure change by the solvent.

transformation of a precursor into the ketone. By analogy with the formation of acetone from acetoacetic acid, β-ketocarboxylic acids can be postulated as precursors of the other ketones. This postulation is supported by the observation that the concentration of 4-heptanone is only slightly increased by heating the sample when the urine is alkalinized with potassium hydroxide prior to heat treatment.

The correlation between concentration of 4-heptanone and reaction time was studied at 70°, 90° and 99° (Fig. 3). We conclude that the precursor can be quantitatively transformed. At 90° and 99°, the transformation was virtually complete after 90 min. By the method described in this paper, the actual amount of 4-heptanone in fresh urine and the total amount of 4-heptanone and its precursor can be determined. In our routine analyses of normal urines and of urines of diabetic patients, we determine the total 4-heptanone after heating the urine sample at 90° for 90 min.

Extraction yield

The non-polar solvent cyclohexane is suitable for the mass fragmentographic determination of the C_7 ketones because of its very low background at mass *m/e* 114. No interfering peaks are observed. The extraction yield was determined for 4-hepta-

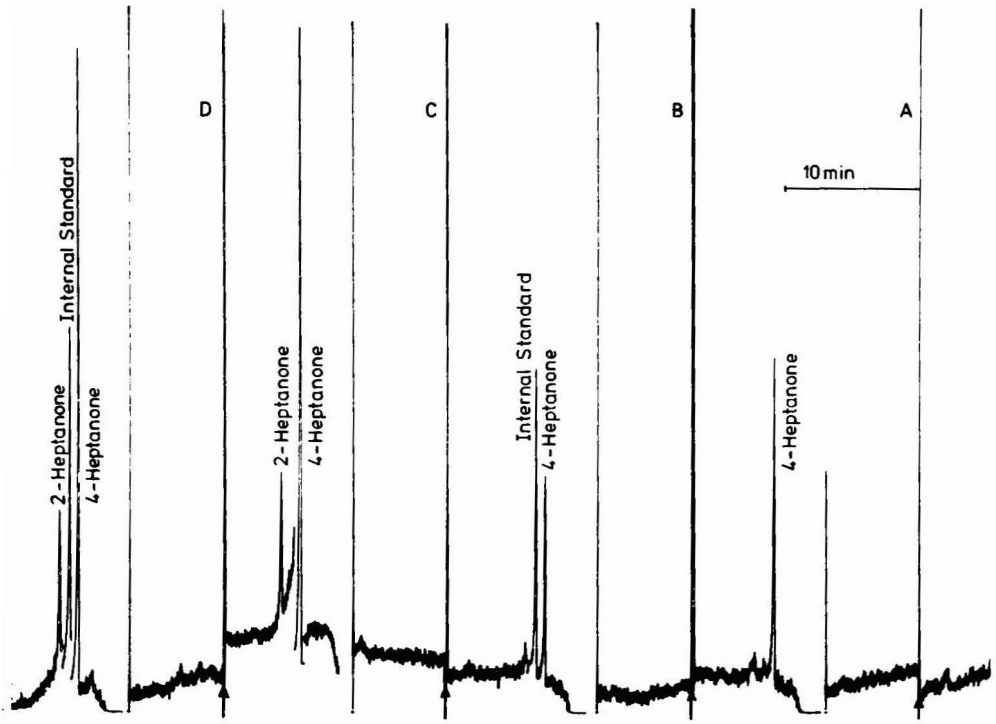


Fig. 2. Mass fragmentograms of urine of a diabetic patient, *m/e* 114. A, urine not heated, recorder 5 mV; B, urine not heated, addition of internal standard, recorder 5 mV, internal standard with 10 mV; C, urine heated at 90° for 90 min, recorder 5 mV, 4-heptanone with 50 mV; D, urine heated at 90° for 90 min, addition of internal standard, recorder 5 mV, 4-heptanone with 50 mV and internal standard with 10 mV. The arrows below the baseline indicate the starting points of the analyses. The drops in the baseline are caused by the pressure change by the solvent.

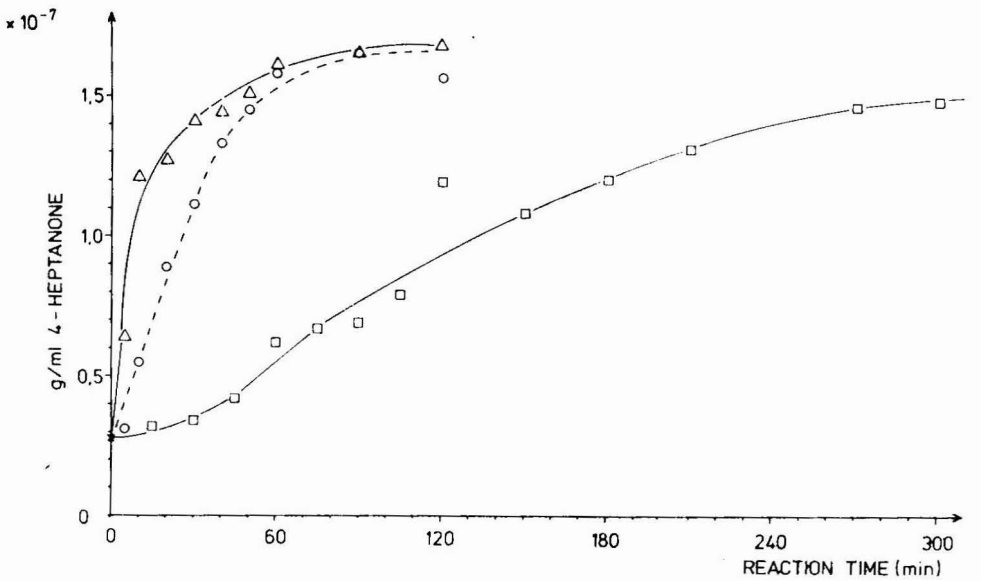


Fig. 3. Concentration of 4-heptanone *versus* reaction time. □, 70°; ○, 90°; △, 99°.

none and found to be satisfactory. At an extraction ratio of 1 ml of urine and 1 ml of cyclohexane, the extraction yield for one extraction step is 97–100% (Fig. 4). To increase the sensitivity of the method, in routine analyses we use an extraction ratio of 4 ml of urine and 1 ml of cyclohexane, resulting in an extraction yield of 95%.

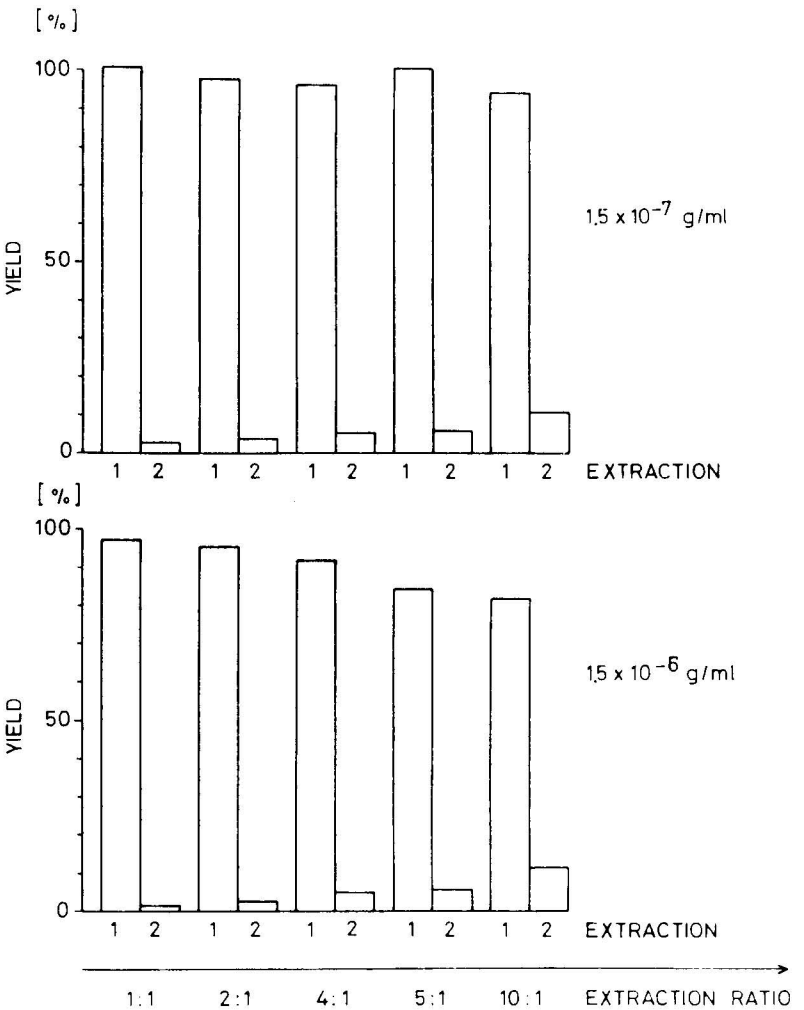


Fig. 4. Extraction yields of 1 and 2 extractions of 4-heptanone *versus* extraction ratios. Extraction ratios, *X* ml urine:*Y* ml cyclohexane: 1:1; 2:1; 4:1; 5:1; and 10:1.

Sensitivity of the method

Because of the high sensitivity of mass fragmentographic detection, the extract can be analyzed directly without any concentration. Therefore, no irreproducible losses, which are difficult to avoid when a sample has to be concentrated, can occur. The detection limit for 4-heptanone under the described conditions was determined to be $8 \cdot 10^{-12}$ g, corresponding to a concentration of 2 μg per 1000 ml of urine. This

sensitivity of the method enables us to use it as a microanalytical procedure, in which only 1 μl of the non-concentrated extract is required.

Linearity of the method and calculation of the concentrations

From 14 standard working solutions in the concentration range $7.6 \cdot 10^{-9}$–$1.5 \cdot 10^{-5}$ g/ml, the calibration graph for 4-heptanone was determined. Fig. 5 shows that with a concentration range of more than three orders of magnitude the method has a very broad range of linearity. The calibration graph for 4-heptanone was plotted on double-logarithmic paper. The same range of linearity was found for 2-heptanone.

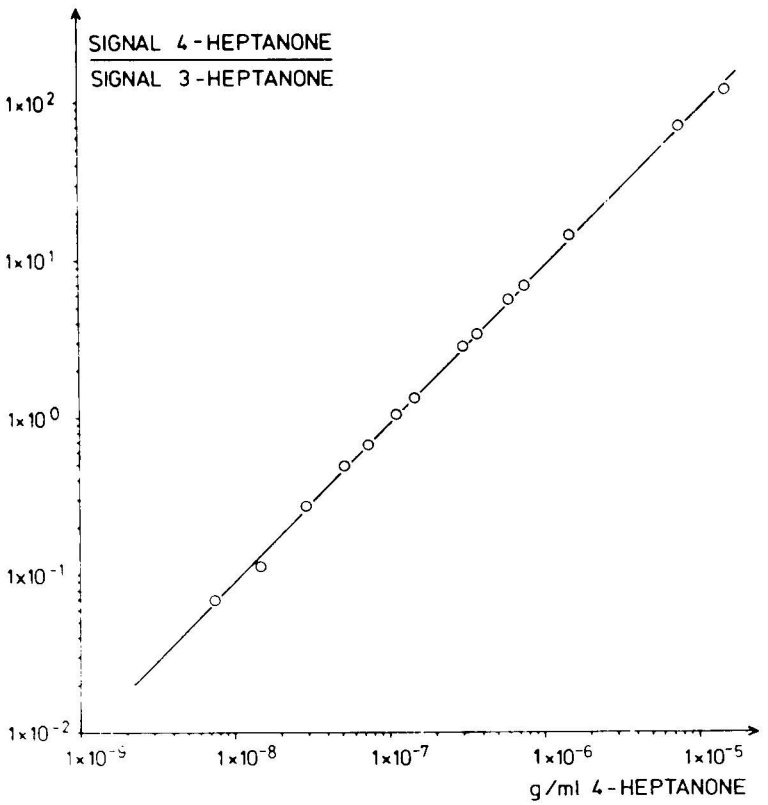


Fig. 5. Calibration graph for determination of 4-heptanone.

The calculation of the 4-heptanone concentration is based on the ratio of the peak heights of 4-heptanone and the internal standard 3-heptanone. By this procedure, the effect of errors during the extraction and uncontrolled variations of the instrumental conditions is eliminated. Controls have shown that a calibration graph can be used for at least 1 month. For routine determinations of 4-heptanone, we use the following equation, which was derived from the calibration graph:

$$X = 1.13 \cdot 10^{-7} Y$$

where X (g/ml) is the concentration of 4-heptanone and Y is the 4-heptanone:3-heptanone signal ratio.

Precision

The values used for plotting the calibration graph for 4-heptanone are mean values of double determinations, three of them being mean values of five-fold determinations. For the five-fold determinations we calculated the absolute standard deviation (S) and the relative standard deviation (S_{rel}) and the results are given in Table I. With S_{rel} values of 1.2 and 1.7% in the normal range of concentration the precision of the method is very good. At the higher concentration, the ratio of 4-heptanone to 3-heptanone is less favourable, resulting in $S_{rel} = 8.3\%$. In this range of concentration of 4-heptanone, S_{rel} can be improved significantly by using a higher concentration of internal standard.

TABLE I

PRECISION OF THE METHOD

Mean value, X (g/ml)	*Absolute standard deviation, S (g/ml)*	*Relative standard deviation, S_{rel} (%)*
$7.6 \cdot 10^{-8}$	$1 \cdot 10^{-9}$	1.2
$3.0 \cdot 10^{-7}$	$1 \cdot 10^{-8}$	1.7
$7.6 \cdot 10^{-7}$	$7 \cdot 10^{-8}$	8.3

The precision discussed here was determined with the standard working solutions, which were not heated. Using urine samples subject to the heating process the precision is somewhat worse (S_{rel} 8–10%), which can be explained by irreproducible losses of ketones when the urine samples are heated. Methodical improvements are possible.

Interferences

No interfering substances were found except in one instance. In urine from a patient with porphyria, 3-heptanone was present and interfered with the internal standard. In all other urines from normal individuals and from patients with diabetes mellitus and other diseases, no interference from 3-heptanone was found.

Practicability of the method

The procedure described for determining the concentration of 4-heptanone is suitable for use in routine analyses. Fig. 6 shows two examples of double determinations of total 4-heptanone after heating the urines. The analysis time was 13 min, but we reduced the time to 7–8 min by using an overlapping injection procedure. In this way we can analyze approximately 40 samples in a normal working day, including the extraction of the samples. In closed vials and at 4°, the cyclohexane extracts are stable for 1 day.

Substances that are extracted from the urine together with the ketones do not interfere in the analysis. After several hundred injections of urine extracts, no increased column bleeding and no deterioration of the column were observed. The

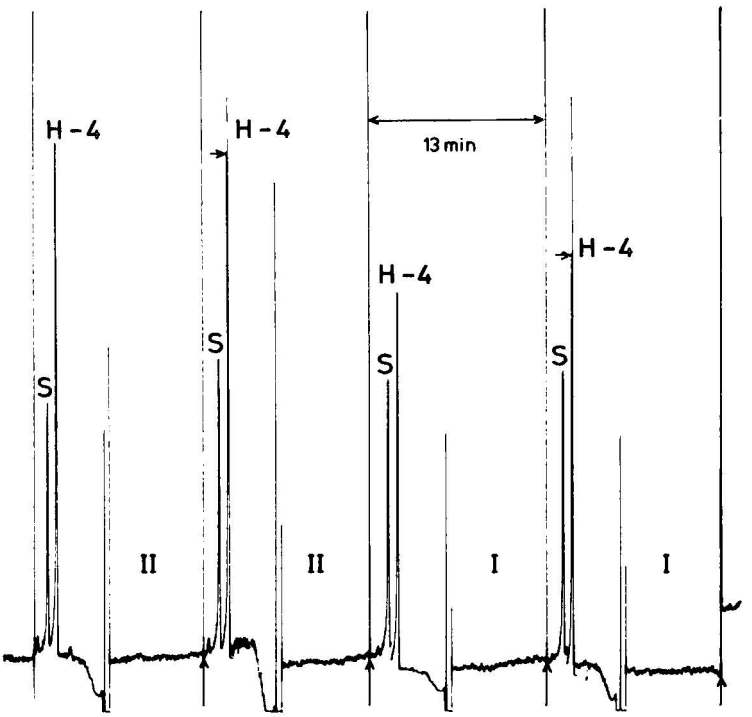


Fig. 6. Double determinations of 4-heptanone in urines I and II. H-4, 4-heptanone; S, internal standard. Urine I, full-scale recorder signal 10 mV, 4-heptanone with 20 mV; urine II, recorder signal 10 mV. The arrows on the peaks indicate sensitivity changes. The arrows below the baseline indicate the starting points of the analyses. The drops in the baseline are caused by the pressure change by the solvent.

glass insert of the injector block is cleaned after every 100 samples and the protecting pre-column is washed after every 200–300 samples.

2-Heptanone can be determined simultaneously with 4-heptanone. By focusing the mass spectrometer on *m/e* 86 or 98, the method can be applied to the determination of 2-pentanone and cyclohexanone, respectively.

Because of the broad range of linearity, samples of pathologically high concentrations of 4-heptanone do not have to be diluted. In our study of normal and diabetic urines we determined concentrations between 7 and 4000 μg per 24 h. The high sample capacity makes the method suitable for correlating the concentration of 4-heptanone and its precursor with other clinical–chemical parameters on a statistical basis.

ACKNOWLEDGEMENT

We gratefully acknowledge the support of this work by the Deutsche Forschungsgemeinschaft.

REFERENCES

1 A. Zlatkis and H. M. Liebich, *Clin. Chem.*, 17 (1971) 592.
2 K. E. Matsumoto, D. H. Partridge, A. B. Robinson, L. Pauling, R. A. Flath, T. R. Mon and R. Teranishi, *J. Chromatogr.*, 85 (1973) 31.
3 A. Zlatkis, W. Bertsch, H. A. Lichtenstein, A. Tishbee, F. Shunbo, H. M. Liebich, A. B. Coscia and N. Fleischer, *Anal. Chem.*, 45 (1973) 763.
4 M. Novotny, M. L. McConnell, M. L. Lee and R. Farlow, *Clin. Chem.*, 20 (1974) 1105.
5 H. M. Liebich, O. Al-Babbili, A. Zlatkis and K. Kim, *Clin. Chem.*, 21 (1975) 1294.
6 H. M. Liebich and O. Al-Babbili, *J. Chromatogr.*, 112 (1975) 539.
7 H. M. Liebich, *J. Chromatogr.*, 112 (1975) 551.
8 H. M. Liebich, O. Al-Babbili, G. Huesgen and J. Wöll, *Z. Anal. Chem.*, 279 (1976) 148.

Journal of Chromatography, 126 (1976) 475–485
© Elsevier Scientific Publishing Company, Amsterdam — Printed in The Netherlands

CHROM. 9436

COLUMN ELUTION AND CONCENTRATION OF VOLATILE COMPOUNDS IN BIOLOGICAL FLUIDS

ALBERT ZLATKIS and KYOUNG KIM
Chemistry Department, University of Houston, Houston, Texas 77004 (U.S.A.)

SUMMARY

A new solvent elution method is described for the isolation and concentration of volatile metabolites in biological fluids. The procedure involves elution of the sample with a solvent through a micro-column of an adsorbent into glass-wool and evaporation of the excess solvent in a stream of helium at room temperature. The volatiles are recovered by subsequent heat desorption into a chromatographic system. Both elution and evaporation are made in a single step using a novel sampling device. Since the technique is based on liquid–solid adsorption chromatography, the adsorbent–solvent system which gives the maximum yield of volatile constituents was studied. The method is simple, highly efficient and reproducible, requiring only small volumes of biological fluids (less than 100 μl).

INTRODUCTION

Within the last few years, the profile studies of volatile metabolites in biological fluids have been the subject of considerable investigation. A primary goal of these studies has been to correlate characteristic chromatographic profiles to human normal and disease states. This area of research was pioneered by Zlatkis and Liebich[1]. Prior to gas chromatographic separation utilizing high-resolution columns, volatile components require isolation from their substrates, with subsequent concentration of these substances. Four techniques for isolation of volatile substances from dilute aqueous solutions are in common use: solvent extraction, steam distillation, vacuum distillation, and headspace analyses.

Solvent extraction[1,2], although relatively simple, introduces problems due to solvent impurities, selective extraction and loss of low-boiling compounds. On the other hand, headspace techniques frequently overemphasize the importance of the more volatile components. However, due to its good reproducibility, rapidity and simplicity, the headspace method has been a preferred technique. This technique has already been established and refined in detail in order to be more amenable for research and routine analyses in the laboratory[3,4].

The headspace method fails to provide a desirable sampling method in situations where only very small volumes of samples are available. For these circumstances,

a micro extraction procedure has been recently developed in our laboratory[5]. This sampling method involves single diethyl ether extraction of the sample saturated with ammonium carbonate, followed by concentration on a glass-wool trap by stripping off the excess diethyl ether. Since this simple method, like ordinary solvent extraction, requires vortex mixing, centrifuging and then transferring of the extract, the loss of some volatiles during these procedures is unavoidable. In order to isolate total volatiles from the micro sample without any loss and contamination, the sampling procedure should involve as few steps as possible.

As a continuation of the study on the total volatile metabolites in biological fluids, a more efficient, reliable, and rapid sampling method has been investigated. This paper describes the column solvent elution method for the sampling of volatiles present in serum in the order of 100 μl. The procedure utilizes the principle of extraction column chromatography developed on a macro scale[6].

EXPERIMENTAL

Reagents

Isopropyl chloride (Eastman-Kodak, Rochester, N.Y., U.S.A.) and methylene chloride, reagent grade (Mallinckrodt, St. Louis, Mo., U.S.A.) were distilled from phosphorus pentoxide, Baker Analyzed Reagent (J. T. Baker, Phillipsburg, N.J., U.S.A.), respectively.

Diethyl ether, anhydrous (Fisher Scientific, Pittsburgh, Pa., U.S.A.) was distilled from lithium aluminum hydride (Alfa Products, Danvers, Mass., U.S.A.).

Adsorbents

Porasil E, 80–100 mesh, and Anachrom 545A, 90–100 mesh, were obtained from Analabs (North Haven, Conn., U.S.A.); hydroxyapatite, spheroidal, from Gallard-Schlesinger (Long Island, N.Y., U.S.A.); Chromosorb P, regular, 80–100 mesh, from Varian-Aerograph (Walnut Creek, Calif., U.S.A.); Carbopack B-HT-100 from Supelco (Bellefonte, Pa., U.S.A.); and aluminium oxide, active, neutral (activity I) from EM Labs. (Elmsford, N.Y., U.S.A.).

Apparatus

The elution column was a glass tube (9.3 cm × 5 mm O.D. × 3 mm I.D.) containing an adequate amount of an adsorbent with a plug of glass-wool at both ends, shown in Fig. 1. Prior to packing, the adsorbents were conditioned at 380° by purging with nitrogen at 20 ml/min for 3 h. The glass-wool trap, serving as a concentrating column, was a glass tube (11 cm × 10 mm O.D. × 8 mm I.D.), tightly packed with glass-wool (Pyrex brand; Corning Glass Works, Corning, N.Y., U.S.A.). It was conditioned in the same manner as above. The elution apparatus consisted basically of a custom-made "transevaporator" and a conical-tip centrifuge tube with a glass stopper (Ⓢ 10/18), as shown in Fig. 1.

Sampling procedure

The volatile constituents in serum were isolated and concentrated in the following manner. The inlet of a "transevaporator" was connected to helium carrier and an elution column was attached to one end of the "transevaporator". A glass-wool

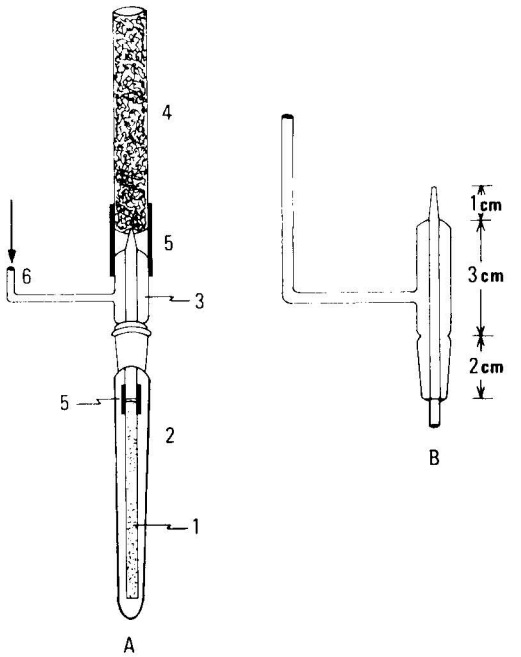


Fig. 1. (A), Elution sampling apparatus. 1 = Elution column; 2 = conical-tip centrifuge tube; 3 = "transevaporator"; 4 = glass-wool trap; 5 = heat-shrinkable PTFE sleeve; 6 = helium inlet. (B), Transevaporator.

trap was secured to the other end. A conical-tip centrifuge tube was fitted to the transevaporator. Gas-tight connections between glass and glass were made via shrinkable PTFE sleeves. The purified helium (cold trap) was allowed to flow through the elution column to the glass-wool trap and the needle valve was adjusted to give a 10 ml/min flow-rate at the trap. Once the flow had been controlled, the conical tube was disconnected from the transevaporator and a 100-μl serum sample was transferred into it with a syringe. The tube was connected back to the transevaporator and the serum was allowed to wet the elution column homogeneously for about 1 min with the aid of helium. After adsorption on the column, 1 ml of solvent, such as isopropyl chloride, diethyl ether or methylene chloride, was introduced to the tube, thereby starting the solvent-elution process.

High-molecular-weight substances, solids and water were retained by the column adsorbent. Only the volatile and soluble constituents were eluted from the column together with solvent and flowed to the glass-wool trap, from which excess solvent was stripped. Sample blanks were prepared by the above procedure, except for the addition of serum to the sampling tube. After the evaporation step, the trap was disconnected from the transevaporator, and inserted into a modified injector port[4], maintained at 280–300°, the outlet of which was connected to a pre-column cooled at liquid nitrogen temperature. The concentrated volatiles were thermally desorbed from the trap by purging with helium at 6 ml/min for 20 min and condensed in the form of a plug in the pre-column (stainless steel, 50 cm × 1 mm I.D., coated with the same phase as the separating column).

Gas chromatographic separation

A Hewlett-Packard Model 5830A gas chromatograph with flame ionization detector and a Type 18850A GC Terminal (Hewlett-Packard, Avondale, Pa., U.S.A.) was used in this study. A separating column (stainless steel, 100 m × 0.5 mm I.D.) was coated with 10% Witconal LA-23 (Witco, Houston, Texas, U.S.A.) in methylene chloride. After desorption, the pre-column was connected to a separating column and the gas chromatographic run was started at a flow-rate of 6 ml helium/min at 25°, according to the preset operating parameters: isothermally at 60° for 5 min, programming 2°/min to 160°, and held for 100 min.

RESULTS AND DISCUSSION

Solvents

Diethyl ether is the most widely used solvent for the extraction of the volatile components from biological fluids[1,2]. However, it has some disadvantages such as low stability and high contamination, and also purification by distillation requires the utmost care. Therefore, it was decided to search for another solvent which could serve the same purpose.

The best candidate should have: (1) high volatility, (2) high solvent power with low water solubility, and (3) high stability. With these requirements in mind, a thorough solvent survey was made. The two solvents isopropyl chloride and methylene chloride were the most promising from the standpoint of physical properties, as shown in Table I.

TABLE I

COMPARISON OF PHYSICAL PROPERTIES OF SOLVENTS

Physical properties	*Diethyl ether*	*Isopropyl chloride*	*Methylene chloride*
Boiling point (°C)	34.55	35.74	39.75
Density	0.71	0.86	1.33
Dielectric constant	4.33	9.82	8.93
Dipole moment	1.15	2.02	1.14
Water solubility (%)	6.04	1.30	0.34

A micro extraction technique[5] was employed for testing the solvent power. Isopropyl chloride was found to be comparable to diethyl ether, as illustrated by Fig. 2. Because of its higher density, methylene chloride was not applicable to the extraction method, but was satisfactory for the elution method. As expected, methylene chloride has a high solvent power. Its boiling point, however, is relatively high compared with those of diethyl ether and isopropyl chloride, thus requiring about 10 min more to strip off the excess methylene chloride. Isopropyl chloride was therefore the solvent of choice. It gave a considerably high yield of volatiles and the chromatograms did not reveal any artifacts.

Adsorbents

The elution column behaves as a selective filter for fractionating out the volatile components from the non-volatile matrix. Therefore, the proper adsorbent

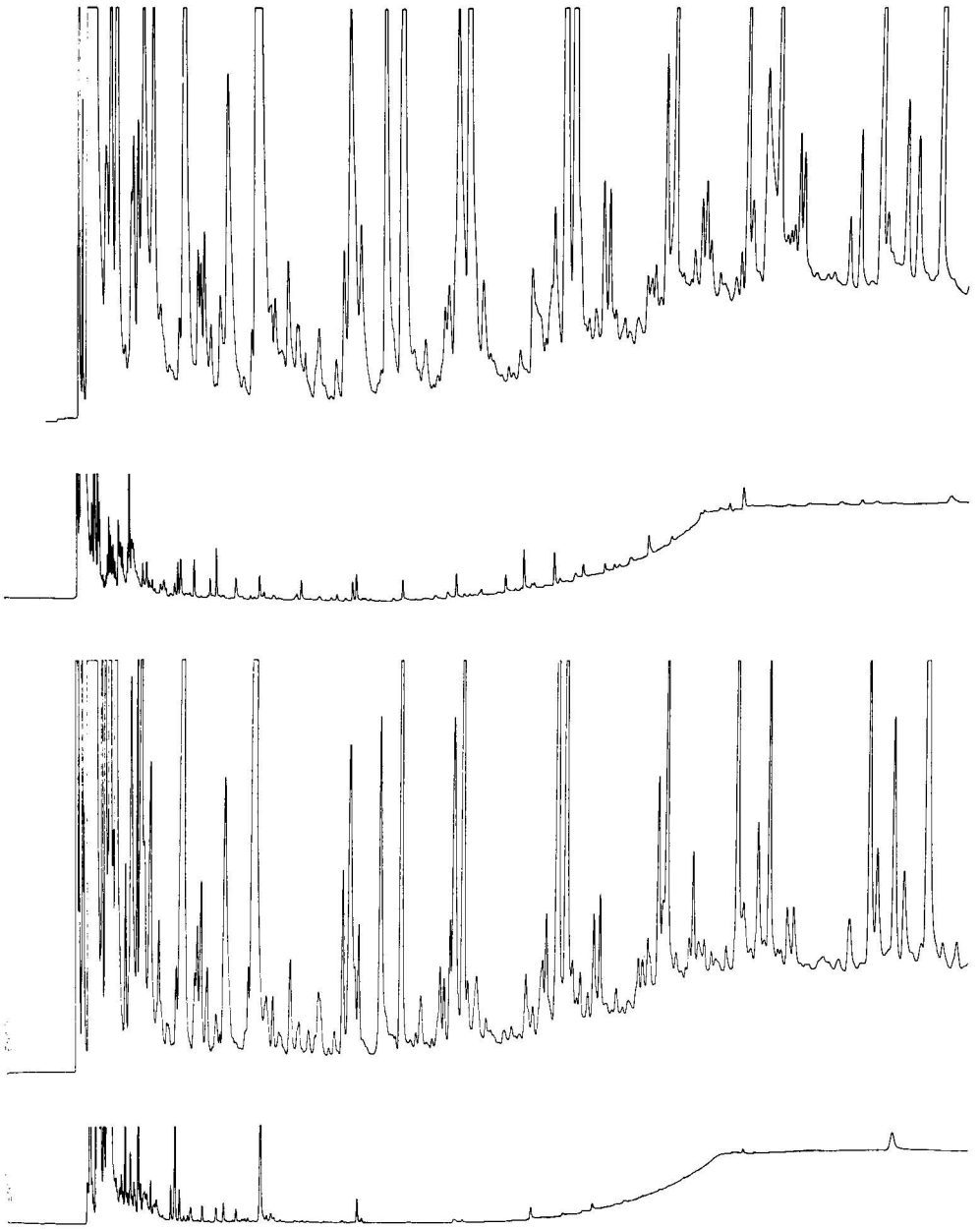


Fig. 2. Partial chromatogram of volatile compounds in 150 μl of serum extracted with 1 ml of solvent. Top: diethyl ether extract; bottom: isopropyl chloride extract. For sampling and operating conditions, see text.

of the elution column should be moderately hydrophilic, in order to hold the water component preferentially, and non-extractable with a given solvent. From these considerations, porous polymers are not applicable, and only the inorganic adsor-

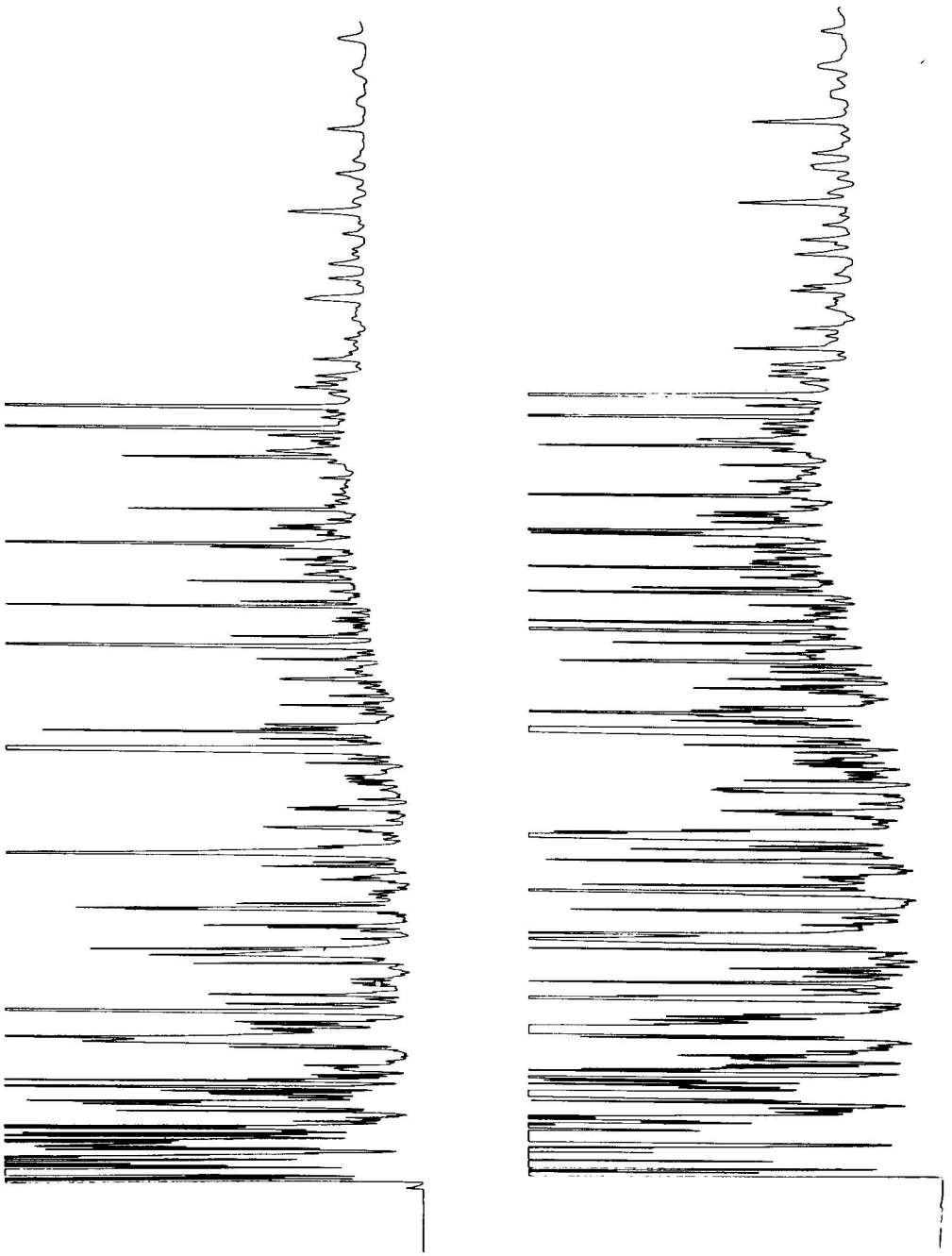


Fig. 3. Chromatogram of volatile compounds in 100 μl of serum eluted with 1 ml of isopropyl chloride through an elution column. Top:

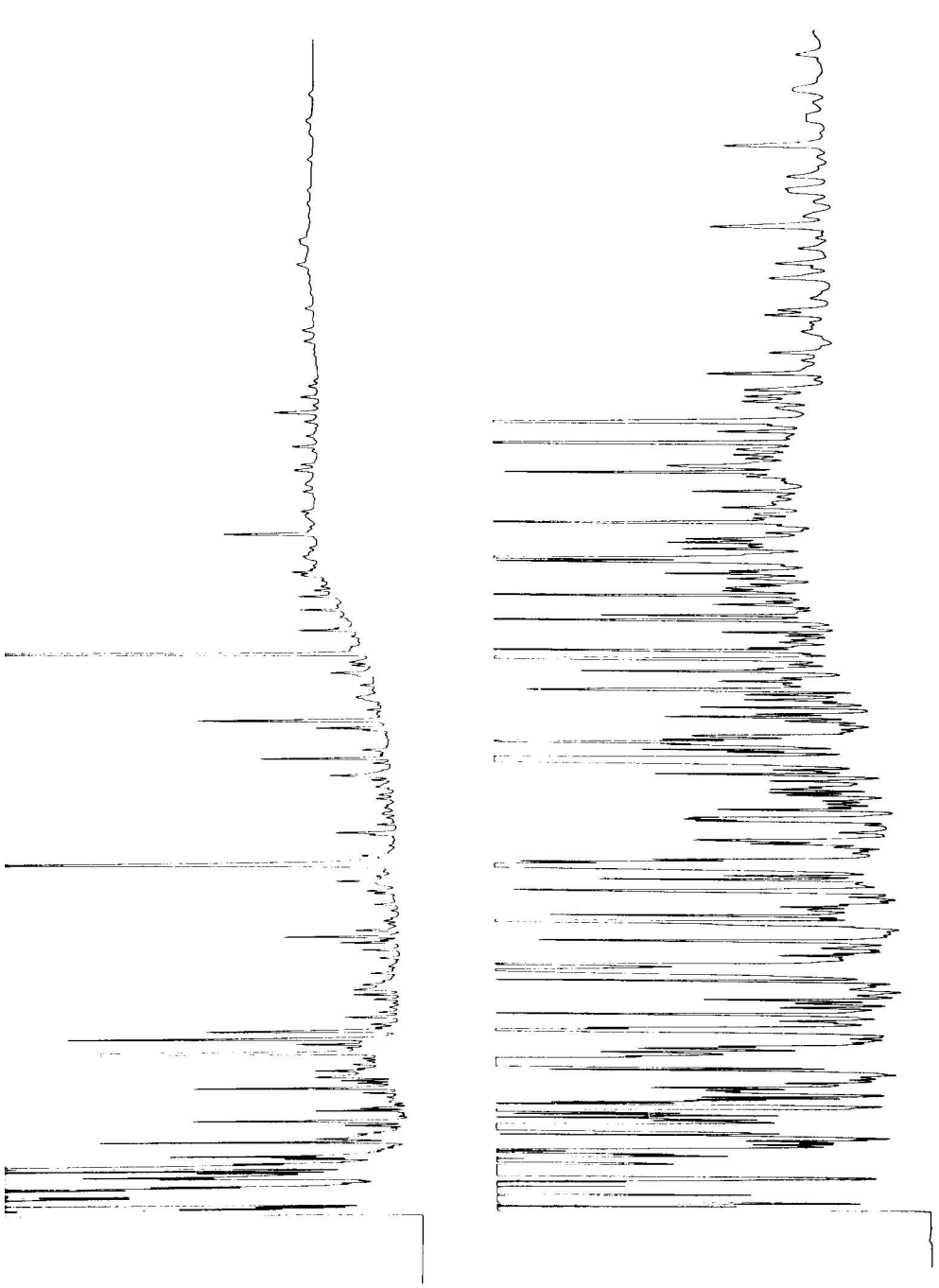


Fig. 4. Chromatogram of volatile compounds in 100 μl of serum obtained with elution method. Top: 1 ml of isopropyl chloride through alumina; bottom: 1 ml of isopropyl chloride through Porasil E. For sampling and operating conditions, see text.

bents are to be preferred. The adsorbent should be in the form of porous, mechanically stable and spherical particles, so that the particles can be packed into the micro column rapidly and uniformly, giving stable and incompressible columns with reproducible flow-rates.

With isopropyl chloride as the eluting agent, experimental selection of the proper adsorbent which would give the maximum yield has been made. All other conditions were kept constant except the amount of each adsorbent. Due to the varying adsorptivities, the optimum size of adsorbent for a given amount of sample differed for each of the adsorbents. Table II shows a list of properties of the adsorbents which have been examined. It was obvious that the sampling efficiency depends on the amount of a given adsorbent, as demonstrated by Fig. 3. The optimum result was obtained with a Porasil E column and the least desirable with that of alumina. Fig. 4 shows the profiles obtained from the two adsorbents. The other adsorbents gave about the same profiles as that with Porasil E in qualitation, but not in quantitation. Interestingly, in the case of diethyl ether as the eluting agent, both Porasil E and alumina gave good results.

TABLE II

PHYSICOCHEMICAL CHARACTERISTICS OF ADSORBENTS

Adsorbent	*Type of material*	*Polarity*	*Specific surface area (m^2/g)*	*Mesh*	*Relative adsorptivity**
Porasil E	Porous silica beads	polar	25	80–100	0.33
Chromosorb P	C-22 firebrick	polar	4	80–100	0.25
Alumina	Active aluminum oxide	polar	100–200	—	0.25
Hydroxyapatite	Porous, spheroidal hydroxy-apatite of calcium phosphate	polar	—	—	0.2
Anachrom 545A	Flux-calcined diatomaceous earth	polar	1	90–100	0.17
Carbopack B	Graphitized carbon black	non-polar	100	—	<0.15

* Adsorptivity was calculated according to the following formula: amount of serum used/amount of adsorbent needed.

Porasil E is in the form of perfectly spherical beads of porous silica. According to Cadogan and Sawyer[7], upon heating from 200–500°, silica loses all hydrogen-bonded water and most of the coordinated water molecules from its surface, and surface free hydroxyls are converted to reactive hydrogen-bonded hydroxyls serving as the site of adsorption.

Since Porasil E was conditioned at 380° prior to use, it might become more polar. Water in serum was retained by Porasil E after elution, thus eliminating the water as a problem. The optimum amount of Porasil E for 100 μl of serum was in the order of 0.3 ml and the sampling time including both elution and evaporation was about 27 min.

Sampling procedure

The main purpose of this work was to develop a better sampling procedure in terms of efficiency, sampling time, and simplicity. Fig. 5 compares the efficiency of

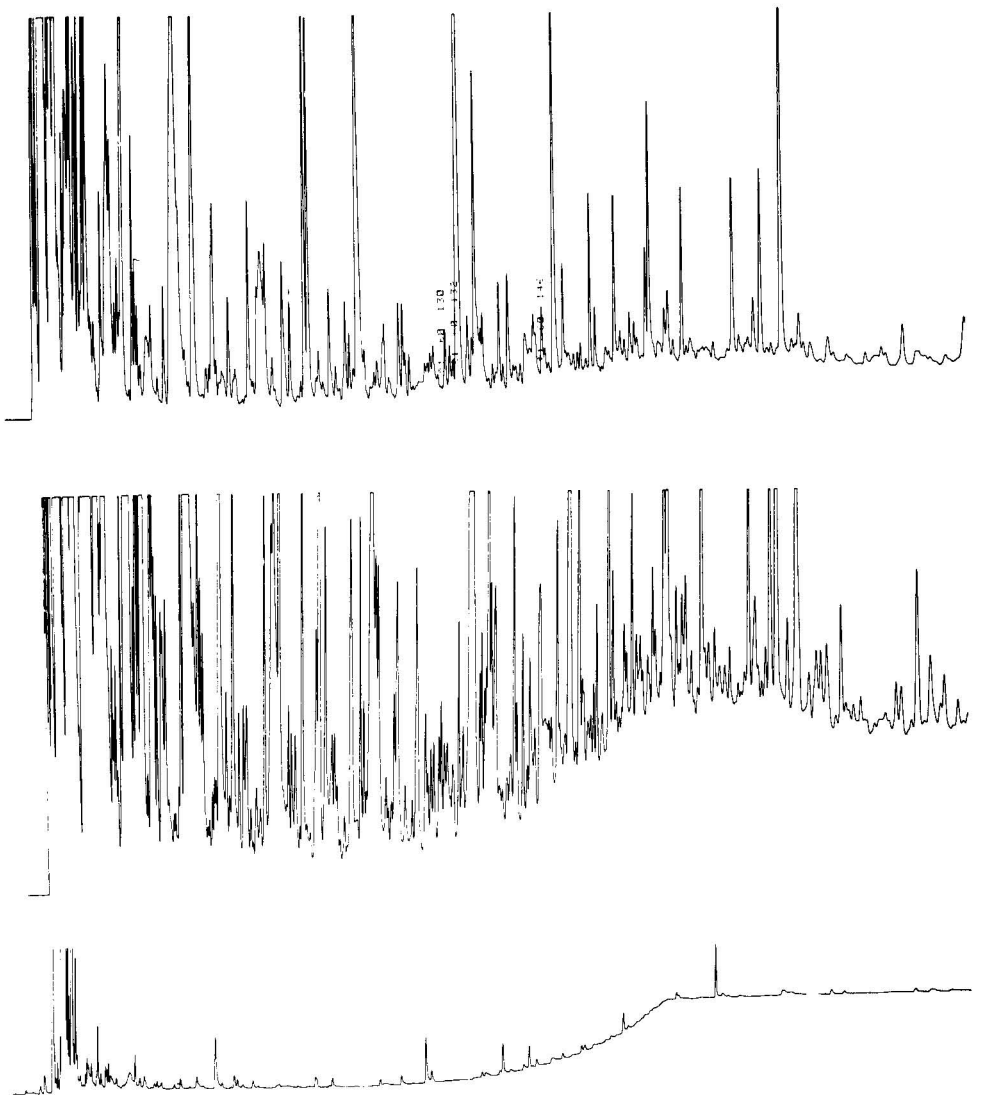


Fig. 5. Chromatogram of volatile compounds in 100 μl of serum. Top: extraction with 1 ml of isopropyl chloride; middle: elution with 1 ml of isopropyl chloride through a Porasil E column; bottom: blank. For sampling and operating conditions, see text.

extraction and elution (through Porasil E) methods for the same amount of the same serum sample. Qualitatively, the two profiles are comparable, but quantitatively, the elution profile is about three times better than the extraction profile. The sampling time needed for the elution method was less than 30 min, but more than 40 min for the extraction method. The elution apparatus provided both efficient elution and evaporation in a single step. In regular intervals, blanks were run to control the total sampling and gas chromatographic procedure for contaminants. This was particularly important for the sample of micro size. A 25-μl sample of serum was eluted through a col-

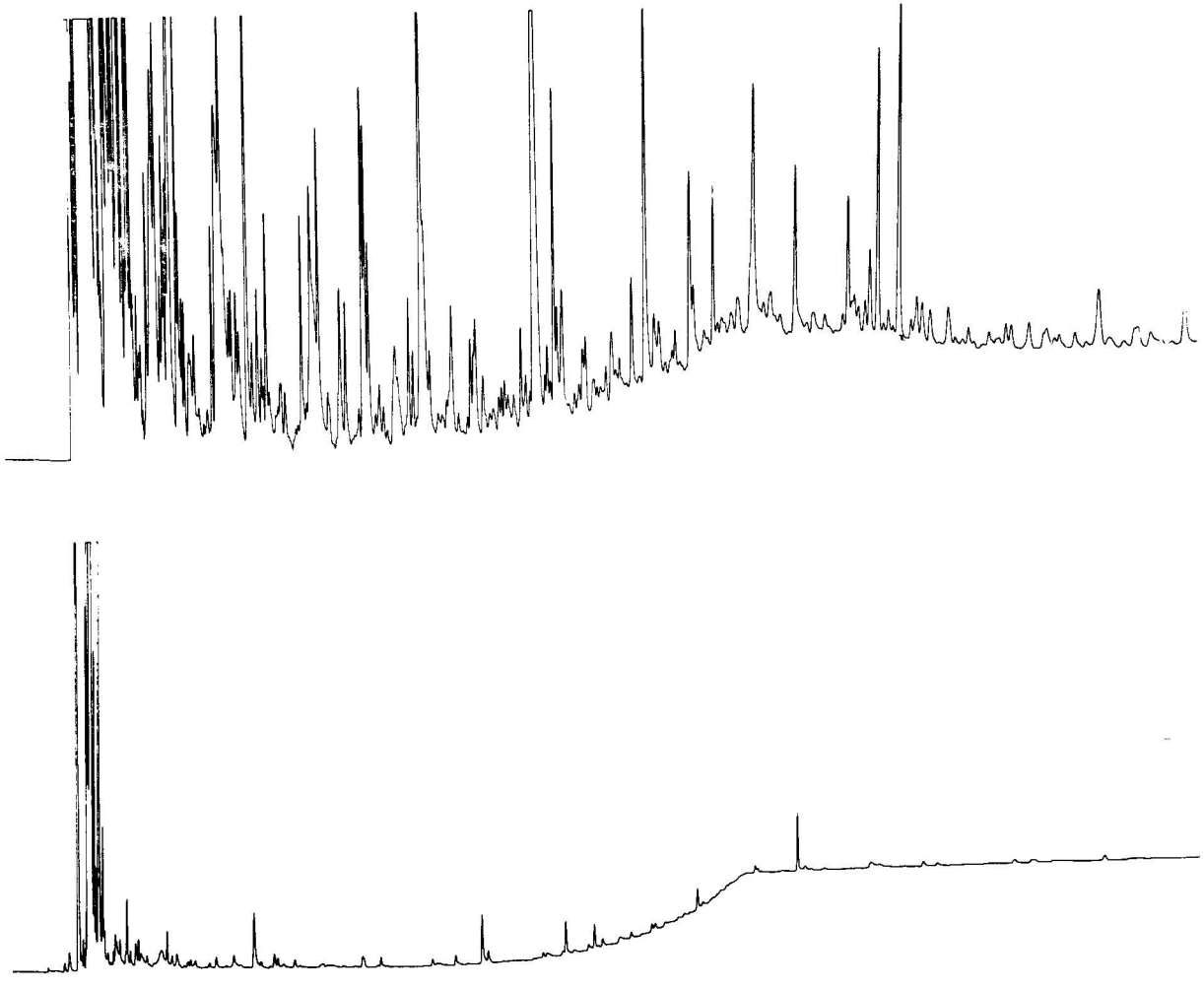


Fig. 6. Chromatogram of volatile compounds in 25 μl of serum eluted with 1 ml of isopropyl chloride through a column containing 0.1 ml of Porasil E. Bottom: blank. For sampling and operating conditions, see text.

umn (3 mm O.D., 2 mm I.D.) containing 0.1 ml of Porasil E with 1 ml of isopropyl chloride. Fig. 6 shows that such a sample was sufficient for a gas chromatographic profile.

The sampling procedure developed should prove useful for a wide range of materials other than blood specimens in determining trace amounts of volatiles in an aqueous medium such as urine, cerebrospinal fluid, saliva, flavors, and contaminated water. Identification of the compounds shown on the profiles is presently being made by mass spectrometry and will be reported subsequently.

ACKNOWLEDGEMENT

The authors gratefully acknowledge the support of the National Aeronautics and Space Administration, Life Sciences Directorate, Johnson Space Center, Houston, Texas (Contract NAS 9-13457).

REFERENCES

1 A. Zlatkis and H. M. Liebich, *Clin. Chem.*, 17 (1971) 592.
2 E. Stormer, D. Cowburn and L. C. Craig, *Anal. Chem.*, 44 (1975) 344.
3 A. Zlatkis, H. A. Lichtenstein and A. Tishbee, *Chromatographia*, 6 (1973) 67.
4 A. Zlatkis, H. A. Lichtenstein, A. Tishbee, W. Bertsch, F. Shunbo and H. M. Liebich, *J. Chromatogr. Sci.*, 11 (1973) 299.
5 A. Zlatkis and F. Andrawes, *J. Chromatogr.*, 112 (1975) 533.
6 A. D. Cooper and S. R. Missan, private communication.
7 D. F. Cadogan and D. T. Sawyer, *Anal. Chem.*, 42 (1970) 190.

Journal of Chromatography, 126 (1976) 487–493
© Elsevier Scientific Publishing Company, Amsterdam — Printed in The Netherlands

CHROM. 9416

APPLICATION OF GLASS CAPILLARY-COLUMN GAS CHROMATOGRAPHY–MASS SPECTROMETRY TO THE STUDIES OF HUMAN DISEASES

E. JELLUM*, P. STØRSETH, J. ALEXANDER**, P. HELLAND, O. STOKKE and E. TEIG
Institute of Clinical Biochemistry and Department of Otolaryngology, Rikshospitalet, University of Oslo, Oslo 1 (Norway)

SUMMARY

Open-tubular glass capillary columns have been used in gas chromatography in combination with mass spectrometry (GC–MS) and computer methods to study human diseases. Patients with maple syrup urine disease excrete not only α-keto and α-hydroxy acids but also six other metabolites which hitherto have been overlooked. The GC–MS methods demonstrated that a group of patients suffering from hereditary progressive loss of hearing have an impaired metabolism of leucine, leading to the accumulation of 3-hydroxyisovaleric acid and 3-methylcrotonylglycine. GC using the capillary columns proved suitable for mapping of the carbohydrate profile of human seminal fluid and for the analyses of organic compounds accumulating in human adipose tissue. The high resolving power and long life of the glass capillary columns suggest that they will be valuable in the diagnosis and studies of human disorders.

INTRODUCTION

The value of gas chromatography (GC) and mass spectrometry (MS) in the diagnosis of and studies on human diseases is now well recognized. Blood and urine samples from "problem cases", for instance, are routinely examined by GC–MS methods in several hospital laboratories throughout the world (*e.g.*, refs. 1–3). The analytical procedures nearly always involve the use of packed GC columns, although it has been realized for a long time that many components of the highly complex biological fluids are not resolved on these columns.

The high resolving power of capillary columns have been known for nearly 20 years[4], but only during the last few years has it been possible to prepare thermostable glass open-tubular capillary columns that have proved suitable for separation of biological specimens (*e.g.*, refs. 5–10). Columns of this type have recently become commercially available and have now been incorporated in our GC–MS–computer system[11,12], which is used for investigations of human diseases.

* To whom reprint requests should be addressed.
** Research Fellow of the Norwegian Cancer Society.

We report here some of the results obtained using capillary column GC–MS for the multicomponent analysis of body fluids and tissues in normal and diseased states.

EXPERIMENTAL

Apparatus

The combined GC–MS–computer instrument consisted of a Varian 1400 gas chromatograph, a Varian 112 double-focusing mass spectrometer and a Spectrosystem 100 MS computing system (Varian-MAT, Bremen, G.F.R.). The gas chromatograph was fitted with a variable split injection system and a 25-m glass capillary column (LKB, Stockholm, Sweden), coated with either SE-30 or SP-1000. The number of theoretical plates on these columns was in the range 80,000–90,000. The mass spectrometer was fitted with dual turbomolecular pumps, allowing direct inlet of the effluent from the capillary column into the ion source, which was operated at 70 eV. The computing system included automatic computer evaluation of the chromatographic profiles (CASAC, first version[13]) and search programs for matching of unknown mass spectra against a library containing 77,120 entries[12].

Sample work-up and gas chromatography

Details of our routine analytical procedures, which involve several extractions (with diethyl ether) and derivatization methods (with diazomethane and trifluoroacetic anhydride), have been published earlier[11]. Additional methods were developed for the analyses of keto acids, in which use was made of oxime-TMS derivatives[14]. Analyses of carbohydrates in seminal fluid involved the use of a filtration technique for deproteinization and ion exchange for removal of charged compounds before derivatization with methoxylamine and with BSTFA silylating reagent (see legend to Fig. 4). Analyses of human adipose tissue included saponification with ethanolic sodium hydroxide and with aqueous sodium hydroxide and subsequent removal of the neutral, unsaponified material from the soap by extraction with diethyl ether.

The gas chromatographic conditions were, unless otherwise stated, the following: splitting ratio, 1:60; temperature of injection port, 245°; column temperature programmed from 50° to 270° at a rate of 6°/min; flow-rate of carrier gas (helium), 1.0 ml/min. Uptakes of mass spectra were normally effected in the repetitive scan mode, with a total scan time of about 2 sec for every spectrum (mass range 20–500) including the fly-back time.

RESULTS AND DISCUSSION

Organic acids in the urine

A number of metabolic disorders are characterized by increased excretion in the urine of one or more organic acids. The systematic search for carboxylic compounds in the urine from patients has consequently become of considerable importance, and packed-column gas chromatography (and mass spectrometry) has so far led to the discovery of more than 15 new diseases. Fig. 1 shows the separation of urinary organic acids from a patient with ketoacidosis on a packed column and on a capillary column. Comparison of the two chromatograms demonstrates that every

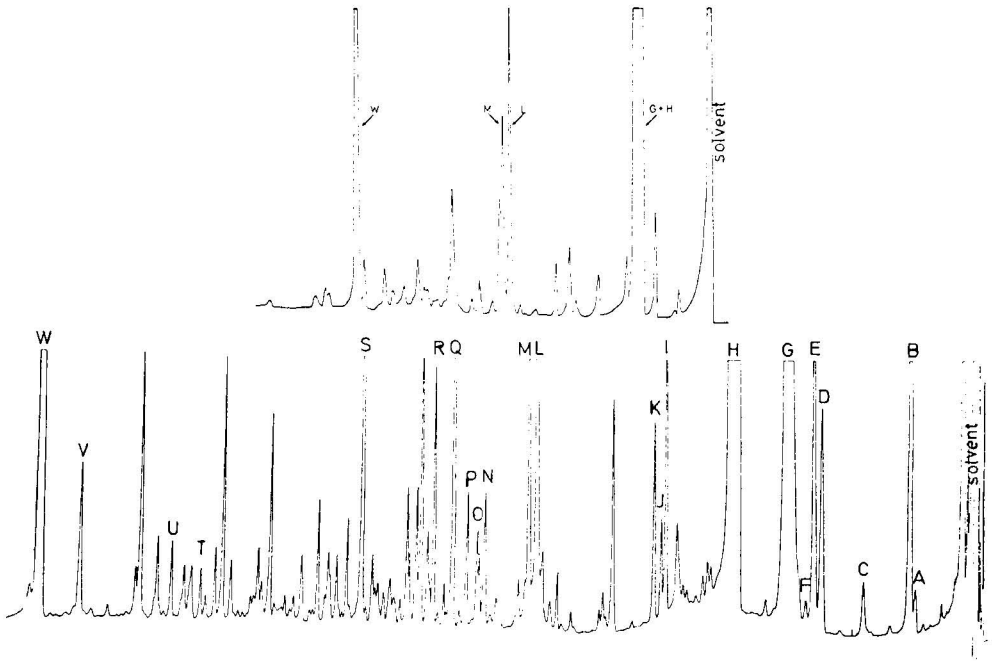


Fig. 1. Organic acids in the urine of a ketoacidotic patient. Top chromatogram: separation on a packed GC column (6 ft. × 1/4 in., 10% OV-17 on Gas-Chrom Q, temperature programmed from 80° to 300° at a rate of 8°/min). Bottom chromatogram: separation on a 25-m SP-1000 glass capillary column (GC conditions as described in text). The organic acids were extracted with diethyl ether and converted into methyl esters with diazomethane prior to GC. The top chromatogram was recorded with an FID and the bottom chromatogram with the mass spectrometer as detector, explaining the difference in response. Peaks: A = 2-hydroxyisobutyric acid; B = artifact from 3-hydroxybutyric acid; C = lactic acid; D = 3-hydroxyisovaleric acid; E = 2-hydroxybutyric acid; F = 2-hydroxyisovaleric acid; G = acetoacetic acid; H = 3-hydroxybutyric acid; I = 3-hydroxyisobutyric acid; J = succinic acid; K = benzoic acid; L = adipic acid; M = 3-methyladipic acid; N = pimelic acid; O = 3-methylpimelic acid; P = cyclopropaneadipic acid; Q = eicosane (internal standard); R = suberic acid; S = thymol (added preservative); T = diphenylamine (from the diethyl ether); U = homovanilic acid; V = *p*-hydroxyphenylacetic acid; W = hippuric acid.

peak from the packed column must consist of a mixture of several components. It is obvious that valuable information may be hidden underneath these composite peaks, and that metabolites of importance for a particular disease may easily be overlooked.

With this in mind, we undertook a re-investigation of certain metabolic disorders, using capillary-column GC–MS. The first disease to be considered was maple syrup urine disease (MSUD), which arises as a result of a defect in the degradation of the branched-chain amino acids leucine, isoleucine and valine. It has previously been shown by a variety of methods, including packed-column GC, that urine from these patients contains three branched-chain α-keto acids, their corresponding hydroxy acids and usually also lactic acid and β-hydroxybutyric acid. GC using capillary columns (Fig. 2) demonstrates that the urine from these patients contains in addition six other pathological metabolites which hitherto have been overlooked. As the cause of the clinical symptoms in MSUD still remains unclear, it may be that some

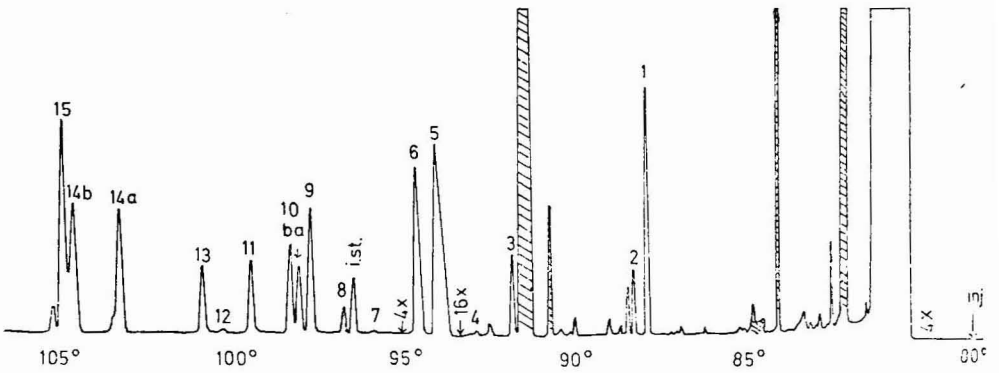


Fig. 2. Metabolites in the urine of an untreated patient with maple syrup urine disease. An acidified aliquot of the urine was extracted with ethyl acetate and the extract was derivatized with hydroxylamine in pyridine followed by BSTFA treatment. Gas chromatographic conditions: injection temperature, 250°; splitting ratio, 1:12; capillary column (25-m SE-30) programmed from 80° to 110° at a rate 0.5°/min. The hatched peaks belong to solvent and reagents. Peaks: 1 = lactic acid; 2 = 2-hydroxyisobutyric acid; 3 = 2-hydroxybutyric acid; 4 = pyruvic acid; 5 = 3-hydroxybutyric acid; 6 = 2-hydroxyisovaleric acid; 7 = 2-ketobutyric acid; 8 = 2-methyl-3-hydroxyisobutyric acid; 9 = 3-hydroxyisovaleric acid; 10a and 10b = 2-ketoisovaleric acid; 11 = acetoacetic acid; 12 = 2-hydroxyisocaproic acid; 13 = 2-hydroxy-3-methylvaleric acid; 14a = L-2-keto-3-methylvaleric acid; 14b = D-2-keto-3-methylvaleric acid; 15 = 2-ketoisocaproic acid. Peaks 2, 3, 7, 8, 9 and 14b have not previously been associated with MSUD. Internal standard = malonic acid (i.st.).

of the metabolites revealed in Fig. 2 may contribute to the symptoms of the disease. (A full account of this investigation will be published separately[14].)

Recently, we undertook a systematic examination of the organic acids in the urine from a group of patients suffering from a hereditary, progressive loss of hearing. A large family in Norway with over 80 members suffers from this unusual disorder, which results in deafness at the age of about 30–40 years[15]. No other clinical symptoms have been found. Capillary-column GC–MS demonstrated that the urine samples from these patients contain two abnormal metabolites, identified as 3-hydroxyisovaleric acid and 3-methylcrotonylglycine. These metabolites are intermediates in the metabolism of leucine, and are likely to accumulate if the enzyme 3-methylcrotonyl-CoA carboxylase is partially defective. The disorder is now under thorough investigation, using a variety of biochemical methods, enzyme determinations in fibroblast cells from the patients, oto-toxicity studies and loading experiments with leucine. Fig. 3 shows the effect of a peroral intake of 20 g of leucine on the pattern of carboxylic acid in the urine. The bottom capillary gas chromatogram is from a normal person and the top chromatogram is from one of the deaf patients. Large amounts of 3-methylcrotonylglycine and 3-hydroxyisovaleric acid have accumulated in the patient, suggesting impaired activity of the above-mentioned enzyme.

Our preliminary studies clearly show that the deaf patients have a partial block in the degradation of leucine. It remains to be proved, however, that this enzyme defect is the cause of the deafness.

Carbohydrates in seminal plasma

The causes of male infertility are frequently very difficult to establish. Although

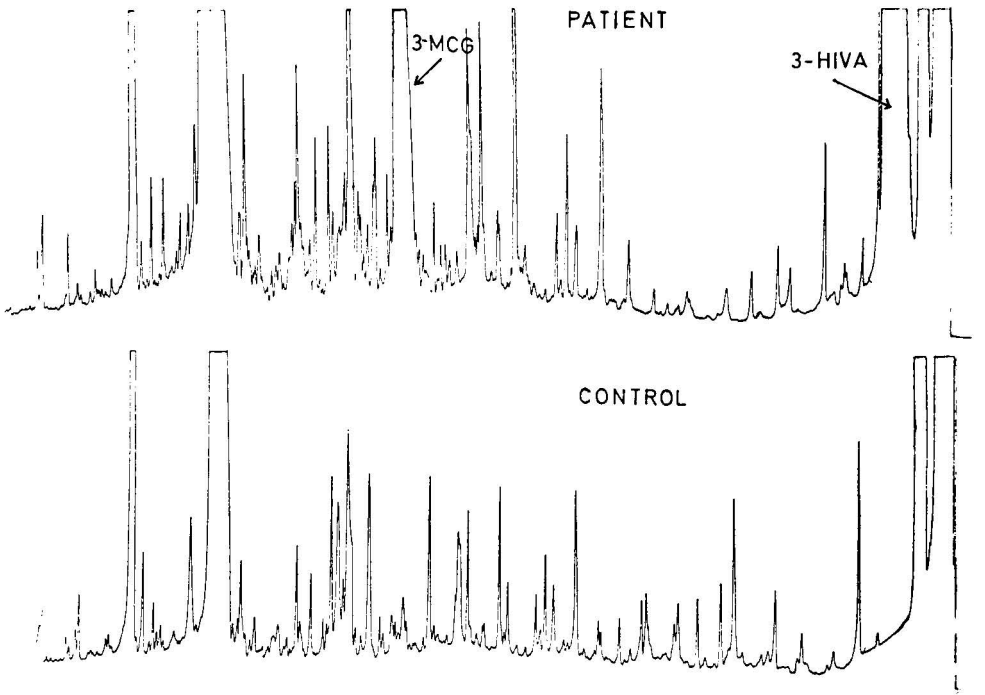


Fig. 3. Organic acids in normal urine and in the urine of a patient with hereditary progressive deafness. The normal subject and the patient were given 20 g of leucine *per os*, and urine was collected during the subsequent 3 h. Aliquots were analyzed on a 25-m SE-30 glass capillary column as described in the text. Extractions and derivatization as in Fig. 1. 3-HIVA = 3-hydroxyisovaleric acid; 3-MCG = 3-methylcrotonylglycine.

morphological methods and clinical chemical methods (*e.g.*, determination of zinc, magnesium, γ-glutamyltranspeptidase and fructose) are in use, the clinical significances of these determinations are uncertain. The latter methods also often fail to differentiate between various types of infertility. There is consequently a great need for more specific diagnostic methods. It is possible that the determination of carbohydrate profiles of seminal fluid might be such a supplementary method. This is based on the general assumption that the carbohydrate metabolism provides an important source of the energy required by the spermatozoa. Disturbances in the metabolism of sugars may therefore be a contributory factor to infertility. In this context, it should be mentioned that an example ascribing infertility (in three brothers) to a defect in carbohydrate metabolism has recently appeared[16].

The complete separation of complex carbohydrate mixtures, like that of seminal fluid, is difficult to achieve on packed GC columns. Greatly improved separation is, however, found on glass capillary columns, as demonstrated in Fig. 4, which shows the carbohydrate pattern of a normal seminal fluid. Two hitherto unrecognized components of semen were found (glycerol and erythritol), but several other components still remain unidentified. The role of variations in the carbohydrate profile in seminal fluid in healthy and diseased states are under investigation in our laboratory.

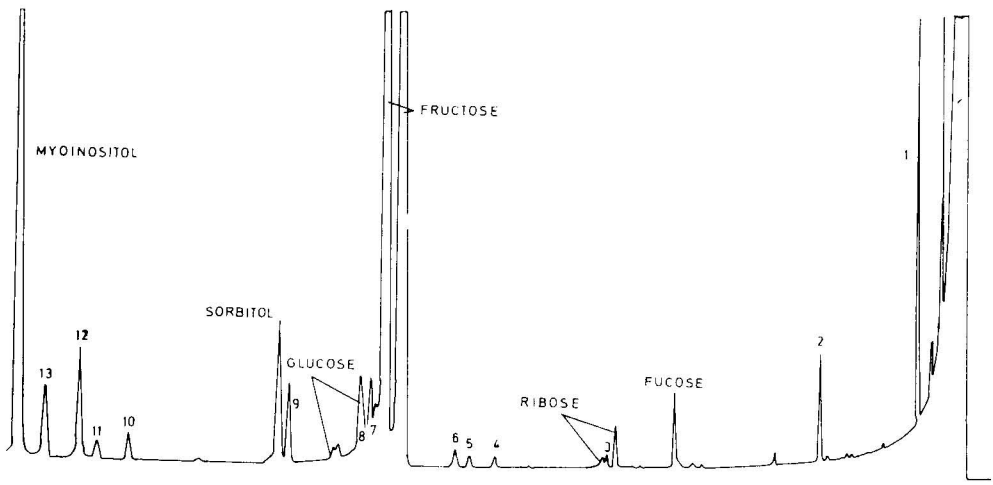


Fig. 4. Carbohydrate pattern in normal seminal fluid. Seminal fluid (0.5 ml) was filtered through a Millipore PSAC membrane and the filtrate was passed through a mixed-bed ion-exchange resin [Dowex 1 (CO_3^{2-}), Dowex 50 (H^+)]. The eluate was evaporated to dryness and derivatized with methoxylamine and BSTFA in pyridine[17]. The GC column was a 25-m SE-30 glass capillary column and the GC conditions were as described in the text. The named peaks represent previously described carbohydrates of semen. Peak 1 and 2 were identified as glycerol and erythritol. Peaks 3–13 are unknown.

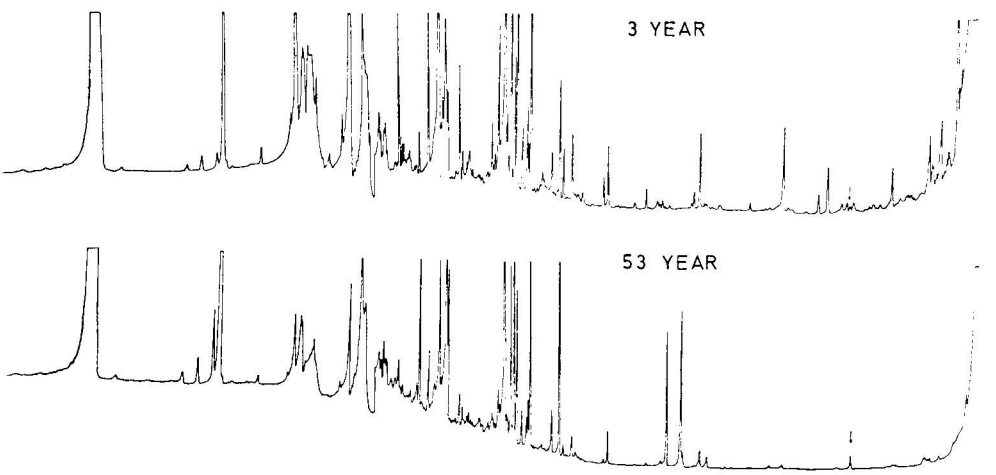


Fig. 5. Metabolic profile of unsaponifiable components of human adipose tissue. Top chromatogram is from a 3-year-old boy, bottom chromatogram from a 53-year-old man. Fat (4 g) was refluxed with sodium hydroxide (40 ml of 2 *N* NaOH in aqueous ethanol) and extracted with re-distilled diethyl ether after dilution with 60 ml of water. The ether extract was washed five times with dilute NaOH and evaporated to dryness at room temperature. The residue was re-hydrolyzed with 2 *N* NaOH (30 min at 100°) and re-extracted with diethyl ether. The extract was concentrated and injected into the capillary column (25-m, SE-30). Splitless injections were used, and the column temperature was programmed from 80° to 280° at a rate of 6°/min. Reagent blanks were run as controls.

Multicomponent analyses of human fat biopsies

During life, man is continuously exposed to a variety of chemicals, many of which may be of a hazardous, *e.g.* carcinogenic, nature. Because of the high solubility of many organic compounds in lipid material, it is likely that many environmental contaminants may accumulate in the fat deposits in the body. Thus, it is well known that pesticides, chlorinated hydrocarbons, etc.[18–20] have a great tendency to accumulate in adipose tissue. Capillary-column GC–MS–computer methods offer the possibility of investigating in detail the chemical contaminants in human fat biopsies and to estimate variations in the chemical content with age, smoking habits, occupational exposure, etc. Fig. 5 shows two capillary-column chromatograms of the non-saponifiable, alkali-stable and diethyl ether-soluble fraction of fat biopsies. The top chromatogram is from a 3-year-old child and the bottom chromatogram is from the fat deposits of a 53-year-old man. The peaks represent hydrocarbons (including polynuclear aromatics), alcohols, steroids and other substances that withstand the chemical pre-treatment described in the legend. It is striking that over 100 compounds of this chemical nature are present in human fat. There are also marked quantitative and qualitative differences between "young" and "old" adipose tissue. Further investigations are now in progress to clarify the significance of these variations.

REFERENCES

1 O. A. Mamer, W. J. Mitchell and C. R. Scriver (Editors), *Application of Gas Chromatography and Mass Spectrometry to the Investigation of Human Disease*, Montreal Children's Hospital Publication, McGill University, Montreal, 1974.
2 E. Jellum, in B. J. Mitruka (Editor), *Application of Gas Chromatography in Microbiology and Medicine*, Wiley, New York, 1975, p. 447.
3 A. M. Lawson, *Clin. Chem.*, 21 (1975) 803.
4 M. J. E. Golay, in D. H. Desty (Editor), *Gas Chromatography 1958*, Butterworths, London, 1958, p. 36.
5 K. Grob, *Helv. Chim. Acta*, 48 (1965) 1362.
6 M. Novotny and A. Zlatkis, *J. Chromatogr. Sci.*, 8 (1970) 346.
7 A. L. German, C. D. Pfaffenberger, J. P. Thenot, M. G. Horning and E. C. Horning, *Anal. Chem.*, 45 (1973) 930.
8 A. Zlatkis, W. Bertsch, H. A. Lichtenstein, A. Tishbee, F. Shunbo, H. M. Liebich, A. B. Coscia and N. Fleischer, *Anal. Chem.*, 45 (1973) 763.
9 K. E. Matsumoto, D. H. Partridge, A. B. Robinson, L. Pauling, R. A. Flath, T. R. Mon and R. Teranishi, *J. Chromatogr.*, 85 (1973) 31.
10 J. Eyem and J. Sjøquist, *Anal. Biochem.*, 52 (1973) 255.
11 E. Jellum, O. Stokke and L. Eldjarn, *Clin. Chem.*, 18 (1972) 800.
12 E. Jellum, O. Stokke and L. Eldjarn, *Anal. Chem.*, 45 (1973) 1099.
13 E. Jellum, P. Helland, L. Eldjarn, U. Markwardt and J. Marhöfer, *J. Chromatogr.*, 112 (1975) 573.
14 C. Jakobs, E. Solem, J. Ek, K. Halvorsen and E. Jellum, *J. Chromatogr.*, 143 (1977) in press.
15 E. Teig, *Acta Otolaryng.*, 65 (1968) 365.
16 C. J. G. van der Horst and J. J. Bol, *Andrologia*, 7 (1975) 15.
17 R. A. Laine and C. C. Sweeley, *Carbohyd. Res.*, 27 (1973) 199.
18 E. O. Oswald, P. W. Albro and J. D. McKinney, *J. Chromatogr.*, 98 (1974) 363.
19 J. Bios, A. C. Walker and A. Medbery, *Bull. Environ. Contam. Toxicol.*, 5 (1970) 317.
20 M. Doguchi, S. Fukano and F. Ushio, *Bull. Environ. Contam. Toxicol.*, 11 (1974) 3.

Journal of Chromatography, 126 (1976) 495–502
© Elsevier Scientific Publishing Company, Amsterdam — Printed in The Netherlands

CHROM. 9476

PROFILES OF VOLATILE METABOLITES IN BODY FLUIDS

M. STAFFORD and M. G. HORNING
Institute for Lipid Research, Baylor College of Medicine, Houston, Texas 77030 (U.S.A.)
and
A. ZLATKIS
Department of Chemistry, University of Houston, Houston, Texas 77004 (U.S.A.)

SUMMARY

A method for the analysis of volatile metabolites present in plasma, urine, breast milk and amniotic fluid collected from mother–infant pairs has been developed which requires only 100 μl of plasma, 3 ml of urine, 20 μl of breast milk and 500 μl of amniotic fluid. After extraction with diethyl ether, the volatile compounds were adsorbed on glass wool in a special concentration tube and subsequently desorbed and transferred to a 100-m nickel capillary column for analysis by gas chromatography and gas chromatography–mass spectrometry. The separations, carried out by temperature programming, were complete in 90 min.

INTRODUCTION

Methods for the analysis of the volatile compounds in human urine were developed by Zlatkis and co-workers[1–3] and by Matsumoto *et al.*[4]. Ketones, aldehydes, alcohols, furans, pyrroles and sulfides with molecular weights between 40 and 160 were separated and tentatively identified by capillary gas chromatography (GC) and mass spectrometry (MS). The volume of urine employed varied from 50 to 450 ml. The procedure has been employed in a study of the low-molecular-weight aliphatic alcohols excreted in the urines of hospitalized patients with diabetes mellitus[3].

A procedure for the analysis of volatile components in plasma based on liquid–liquid extraction followed by capillary GC was developed by Stoner *et al.*[5]; 15 ml of plasma was used. Subsequently, Zlatkis and Andrawes[6] developed a semi-micro-extraction procedure based on the use of ammonium carbonate–diethyl ether as a salt–solvent pair[7]. The volatiles extracted from 100 μl of plasma were concentrated by adsorption on glass wool, and then desorbed and transferred to the capillary column for GC analysis.

The results of Zlatkis and Andrawes[6] suggested that a method could be developed for the analysis of volatiles in biological fluids which involved considerably smaller volumes than had been employed in earlier studies. This paper describes a general method for the analysis of volatile compounds in plasma, urine, breast milk

and amniotic fluid. The size of the biological samples varied from 20 μl (breast milk) to 3 ml (urine).

EXPERIMENTAL

The biological samples analyzed in this study were obtained from mother–infant pairs. Maternal urine, plasma and amniotic fluid were obtained at the time of delivery; breast milk was obtained from the mother after delivery. Neonatal urine and plasma were collected during the first 48 h after birth. All of the samples were stored at $-14°$ until analyzed.

The volatile compounds were extracted by the use of ammonium carbonate–diethyl ether as a salt–solvent pair. The sample (100 μl plasma, 3 ml urine, 500 μl amniotic fluid, or 20 μl breast milk) was transferred to a 12-ml centrifuge tube fitted with a PTFE-lined screw cap. After saturation of the aqueous phase with anhydrous ammonium carbonate, the volatiles were extracted with glass-distilled diethyl ether that had been refluxed over lithium aluminum hydride prior to distillation. The volume of diethyl ether used was 500 μl, 1 ml, 750 μl and 100 μl for plasma, urine, amniotic fluid and breast milk, respectively. The contents of the tube were mixed thoroughly on a Vortex mixer and the layers were separated by centrifugation. After chilling the tube in an ice-bath, the diethyl ether layer was transferred to a 2.5-ml glass stoppered centrifuge tube and stored at $-14°$ until analyzed.

For analysis by GC, the diethyl ether extract was transferred with a 1.0-ml syringe equipped with a 5-inch 22-gauge needle to a small concentration tube packed with 0.5 g Pyrex glass wool[6]. The volatile compounds were desorbed and transferred from the concentration tube to a stainless-steel precolumn (12 in. $\times$ 1/16 in.), cooled in liquid nitrogen. The transfer was carried out by raising the temperature of the concentration tube to 240° while sweeping with helium (30 ml/min). After a 15-min trapping period, the liquid nitrogen reservoir was removed from the precolumn, and the temperature of the GC column was raised to 70° and held for 15 min. The separations were carried out by temperature programming from 70 to 150° at 2°/min and then isothermally at 150° for 50 min.

A Tracor 550 gas chromatograph equipped with a modified injection port and flame ionization detector was employed. The 100 m $\times$ 0.5 mm I.D. nickel column coated with Emulphor ON-870 was prepared according to the procedure of Bertsch *et al.*[8]. The flow-rate of helium, the carrier gas, was 30 ml/min. The flow-rates of the detector gases were: hydrogen, 37 ml/min; air, 100 ml/min; and nitrogen make-up gas, 10 ml/min.

The MS analyses were carried out with an LKB Model 9000 gas chromatograph–mass spectrometer; the separator was kept at 150° and the source temperature was 190°. For analysis by GC–MS, a heating block and concentration tube were placed in series with a 12 in. $\times$ 1/16 in. O.D. stainless-steel precolumn and the GC column. A PTFE micro-needle valve was placed between the precolumn and the GC column so that the precolumn and flash heater could be opened for insertion of the concentration tube while the GC column and the separator of the mass spectrometer were maintained under vacuum[9]. The separations were carried out by temperature programming from 70 to 150° as described above.

RESULTS

Plasma

Profiles of the volatile compounds present in maternal and neonatal plasma are shown in Figs. 1 and 2. The samples were obtained from a mother–infant pair

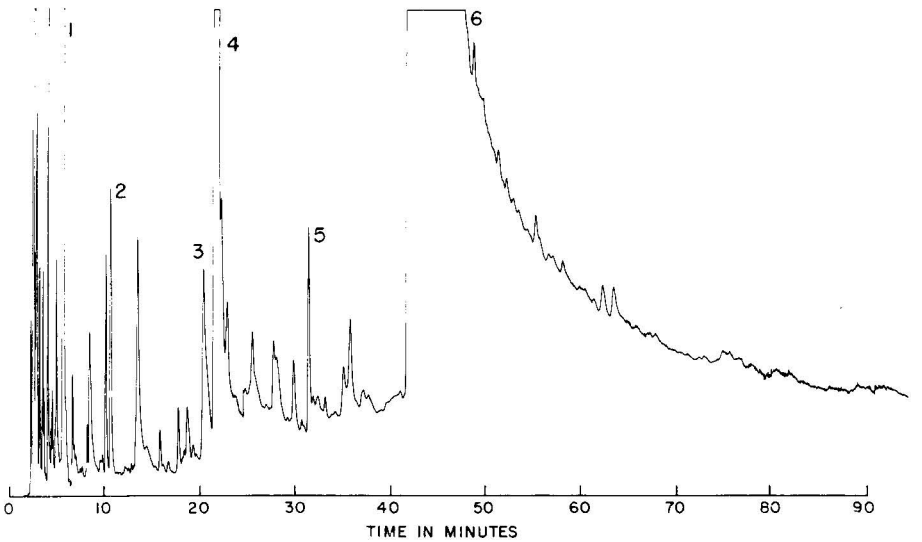


Fig. 1. GC analysis of the volatiles extracted from 100 μl of plasma obtained from a newborn infant. The compounds tentatively identified by GC–MS were: (1) 5-acetonyl-2-methylfuran; (2) ethylcyclopentanone; (3) ethylcyclohexanone; (4) benzaldehyde; (5) 1-cyclohexan-2-buten-4-ol; and, (6) benzyl alcohol. The GC conditions employed for all the analyses are described in the text.

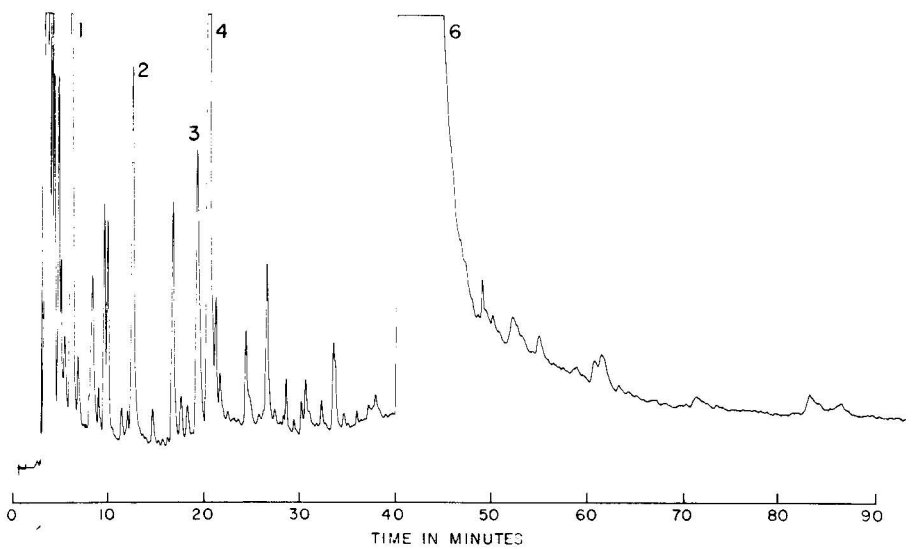


Fig. 2. GC analysis of the volatiles extracted from 100 μl of plasma obtained at the time of delivery from the mother of the newborn infant (Fig. 1). The compounds tentatively identified were the same as those listed in Fig. 1.

and the profiles were strikingly similar. The maternal plasma profile differed from the profiles of normal adults described by Zlatkis and Andrawes[6] in that a very large peak with a retention time (t_R) of 40–48 min was observed in the maternal plasma profile obtained at delivery. For comparison plasma samples were obtained from young adult females who were not pregnant and were not taking any medication. When the latter samples were analyzed for volatile components by the same procedure, it was found that the large peak with a t_R of 40–48 min was absent from the chromatograms. Fig. 3 shows a typical profile of the volatiles isolated from the plasma of a non-pregnant female, 27 years of age.

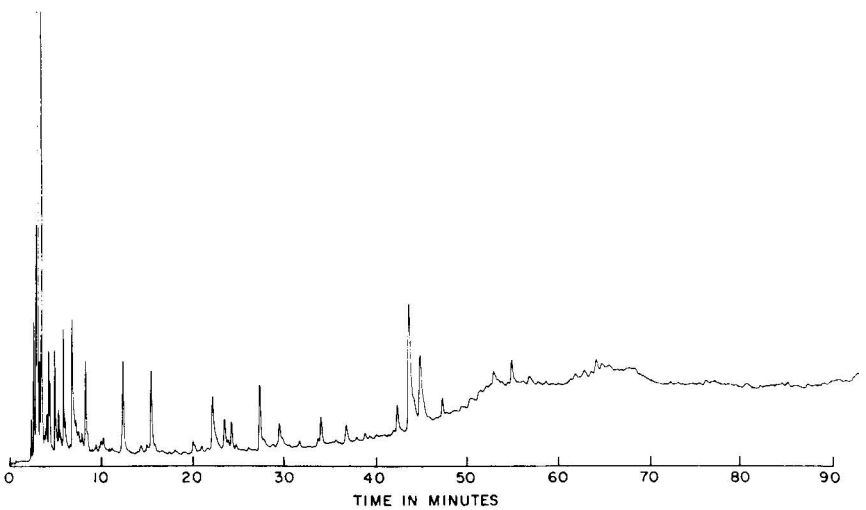


Fig. 3. GC analysis of the volatile components extracted from 3-ml aliquot of a urine sample obtained from a young adult non-pregnant female.

When the samples were analyzed by GC–MS, it was possible to tentatively identify several of the plasma volatiles (Fig. 1). The mass spectrum of the major component (t_R = 40–48 min) exhibited a molecular ion at m/e 108 and the spectrum was identical with the published spectrum[10] of benzyl alcohol (MW = 108).

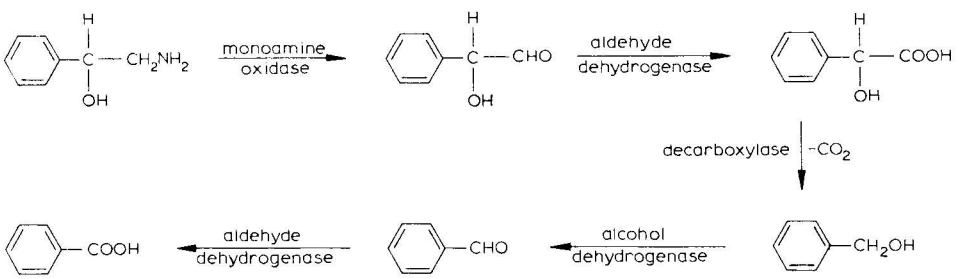
In order to confirm the identity of this component, a larger sample (300 μl) of maternal plasma was extracted with diethyl ether as described. After removal of the diethyl ether with a nitrogen stream, the residue was dissolved in 100 μl of pyridine and acetylated with 50 μl of acetic anhydride by heating at 60° for 15 min. When the derivatized sample was analyzed by GC–MS, the molecular ion of the major peak in the chromatogram had shifted by 42 a.m.u. from m/e 108 to m/e 150. The mass spectrum of the acetylated derivative in the biological sample was identical with the mass spectrum of benzyl acetate prepared by acetylation of benzyl alcohol.

A second characteristic peak present in the plasma profile had a t_R of 21–23 min. MS analysis of this peak indicated that the molecular ion occurred at m/e 106. The occurrence of a component with a molecular weight 2 a.m.u. less than benzyl alcohol suggested that this compound might be benzaldehyde. The t_R and mass

spectrum of this plasma component and the t_R and mass spectrum of a benzaldehyde standard were identical.

At the present time, the origin of the two volatiles, benzaldehyde and benzyl alcohol, is not known. Medication administered to the mother during labor and delivery, which included oxytocin, pethidine, promethazine and diazepam, did not appear to be the source. The two compounds were not artifacts introduced during the isolation procedure. Neither compound was present in the chromatogram when reagent blanks were analyzed; in the blanks, water was substituted for blood in a heparinized tube and the extractions were carried out as described.

If the benzyl alcohol and benzaldehyde found in maternal and neonatal plasma were of endogenous origin, they may have been formed from phenylethanolamine by a minor pathway of metabolism which has been described for phenylethylamine moieties[11]. In this pathway the side-chain is shortened and this conversion is most likely to occur with amines having a β-hydroxyl group. For example, 3,4-dihydroxybenzoic acid and 4-hydroxy-3-methoxybenzoic acid were identified as metabolites of noradrenaline in the rat. The corresponding alcohols were not found in rat urine[11]. However, the alcohols formed by decarboxylation of vanilmandelic acid and dihydroxymandelic acid were presumably intermediates in the metabolic conversion to the benzoic acid derivatives. It is possible that a related enzyme system which converts phenylethanolamine to benzyl alcohol, benzaldehyde and benzoic acid is operative in humans:



Urine

A typical profile of the volatile compounds present in maternal and neonatal urine is shown in Figs. 4 and 5. The compounds identified by MS analysis were acetonylfuran, acetophenone, 2-methyl-4-hexene, ethylcyclohexane, hexanol, acetic acid, and benzyl alcohol.

Two large off-scale peaks were usually present in the chromatograms of extracts of neonatal urine. The peak with a t_R of 23 min was identified by GC–MS as a mixture of 2-methyl-4-hexene and ethylcyclohexane. The identity of the peak with a t_R of 47 min is under investigation.

Breast milk

A chromatogram of the volatile components in a sample of human breast milk collected 30 days after delivery is shown in Fig. 6; only 20 μl of breast milk was used in the extraction. Characteristic peaks eluting at 5 min (hexanal), 19–20 min

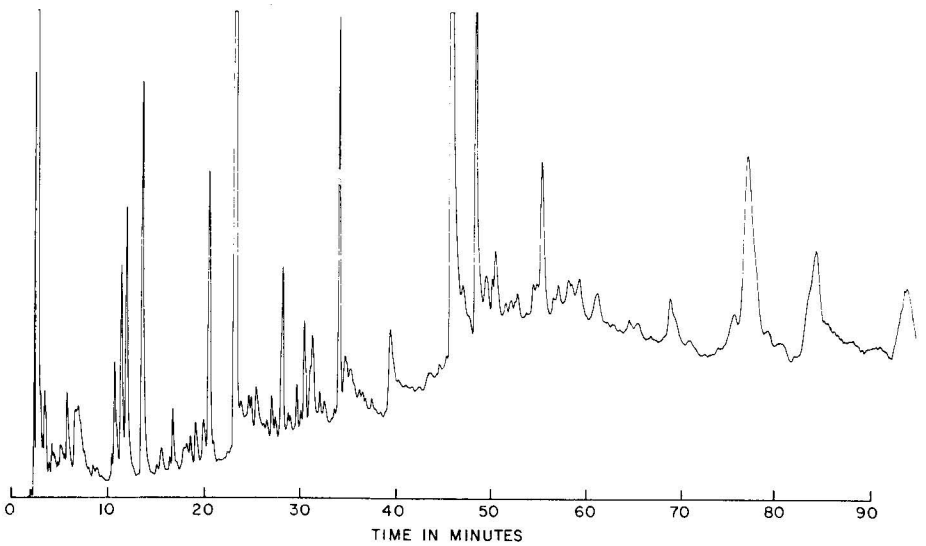


Fig. 4. GC analysis of the volatile compounds extracted from neonatal urine (3 ml).

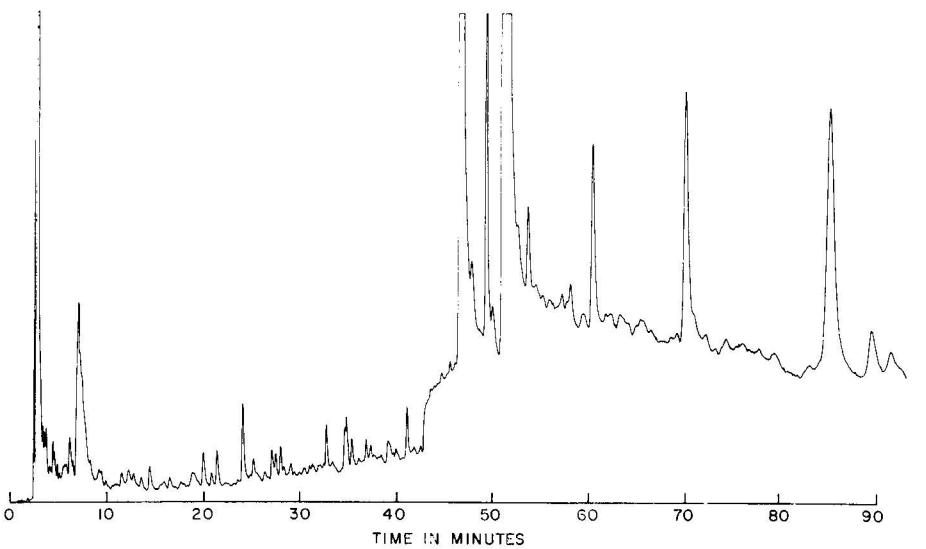


Fig. 5. GC analysis of the volatile compounds extracted from maternal urine (3 ml).

(ethylcyclohexenone andethylcyclohexanone), and a triplet of peaks at 38–42 min (pentenylcyclohexene, and aminopentanylfuran and its isomer) were tentatively identified by GC–MS. Profiles obtained from three different individuals were very similar; although there were quantitative differences, there were no significant qualitative differences in the profiles. The volatile compounds in breast milk that have been characterized by GC–MS are listed in Table I.

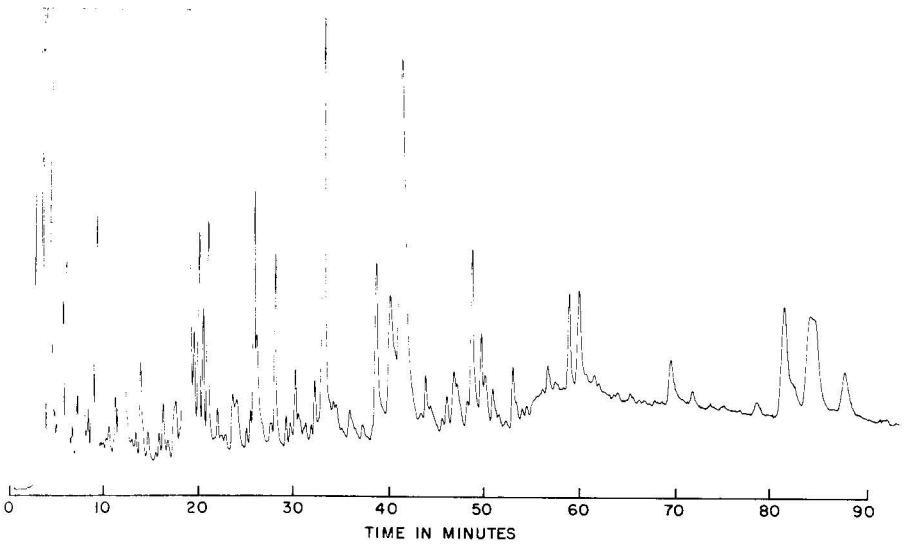


Fig. 6. GC analysis of the volatile compounds extracted from human breast milk (20 μl).

TABLE I

VOLATILE COMPONENTS OF HUMAN BREAST MILK

Tentative identification based on GC–MS analysis.

Compound	*Compound*
hexanal	methylhexanal
heptanal	2-methyl-4-hexene
6-methyl-2-heptanone	2-methylamylnitrile
2-pentylfuran	hexanol
ethylcyclopentanone	4-methyl-1-pentene
acetonylfuran	pentenylcyclohexene
ethylcyclohexanone	aminopentanylfuran
ethylcyclohexenone	

Amniotic fluid

A typical analysis of the volatiles present in amniotic fluid is shown in Fig. 7; the sample was collected 4 h prior to delivery. Two large peaks with retention times of 17 and 81–82 min were usually observed. Because of the small amount of fluid available and the low concentration of the volatiles in amniotic fluid, it was not possible to carry out MS analyses. It is of interest that the doublet eluted between 58–62 min was also present in breast milk.

From the examples cited, it is evident that characteristic profiles of the volatile components of body fluids can be obtained with quite small samples. The overall procedure including isolation and GC analysis requires 2–3 h. A number of components have been tentatively characterized by GC–MS. The excretion of relatively large amounts of benzyl alcohol is of particular interest if this compound is found to be of endogenous origin.

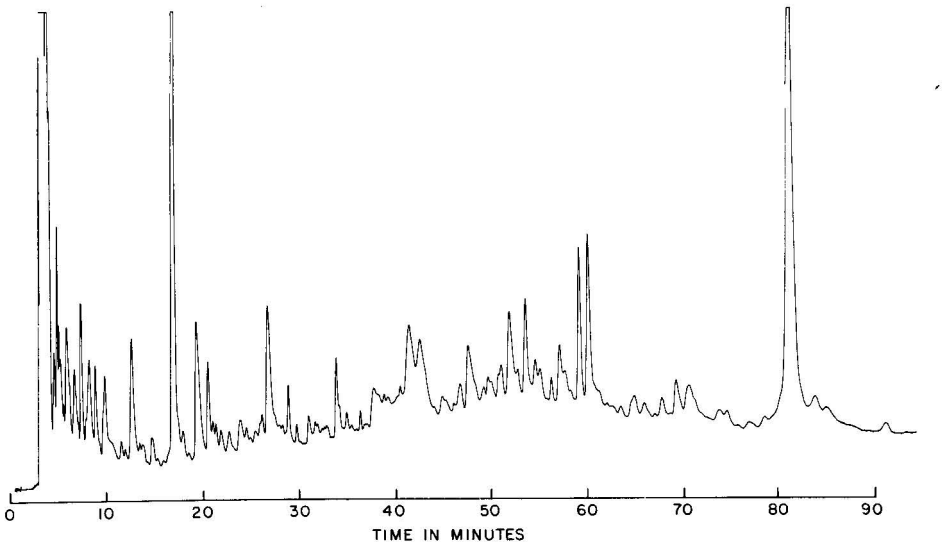


Fig. 7. GC analysis of the volatile compounds extracted from human amniotic fluid (500 μl).

ACKNOWLEDGEMENT

The authors gratefully acknowledge the support of the National Aeronautics and Space Administration, Life Sciences Directorate, Johnson Space Center, Houston, Texas (Contract NAS 9-13457).

REFERENCES

1 A. Zlatkis and H. M. Liebich, *Clin. Chem.*, 17 (1971) 592.
2 A. Zlatkis, W. Bertsch, H. A. Lichtenstein, A. Tishbee and F. Shunbo, *Anal. Chem.*, 45 (1973) 763.
3 H. M. Liebich, O. Al-Babbili, A. Zlatkis and K. Kim, *Clin. Chem.*, 21 (1975) 1294.
4 K. E. Matsumoto, D. H. Partridge, A. B. Robinson, L. Pauling, R. A. Flath, T. R. Mon and R. Teranishi, *J. Chromatogr.*, 85 (1973) 31.
5 E. Stoner, D. Cowburn and C. C. Lyman, *Anal. Chem.*, 47 (1975) 344.
6 A. Zlatkis and F. Andrawes, *J. Chromatogr.*, 112 (1975) 533.
7 M. G. Horning, P. Gregory, J. Nowlin, M. Stafford, K. Lertratanangkoon, C. Butler, W. G. Stillwell and R. M. Hill, *Clin. Chem.*, 20 (1974) 282.
8 W. Bertsch, F. Shunbo, R. C. Chang and A. Zlatkis, *Chromatographia*, 7 (1974) 128.
9 A. Zlatkis, H. A. Lichtenstein and A. Tishbee, *Chromatographia*, 6 (1973) 67.
10 G. G. Grasselli (Editor), *CRC Atlas of Spectral Data and Physical Constants for Organic Compounds*, CRC Press, Division Chemical Rubber Co., Cleveland, Ohio, 1973.
11 B. Peskar, G. Hellmann and G. Hertting, *J. Pharm. Pharmacol.*, 23 (1971) 270.

Journal of Chromatography, 126 (1976) 503–516
© Elsevier Scientific Publishing Company, Amsterdam — Printed in The Netherlands

CHROM. 9457

PICOGRAM ANALYSIS OF FREE TRIIODOTHYRONINE AND FREE THYROXINE HORMONES IN SERUM BY EQUILIBRIUM DIALYSIS AND ELECTRON CAPTURE GAS CHROMATOGRAPHY

BRUCE A. PETERSEN, ROBERT N. HANSON, ROGER W. GIESE and BARRY L. KARGER*

Institute of Chemical Analysis and Department of Chemistry, Northeastern University, Boston, Mass. 02115 (U.S.A.)

SUMMARY

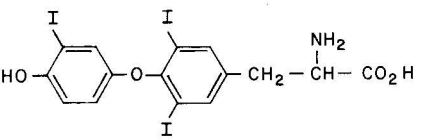
A methodology involving equilibrium dialysis and gas chromatography has been developed to measure concurrently the concentration of the dialyzable (*i.e.*, free) fractions of thyroxine and 3,5,3′-triiodothyronine in serum. The electron capture response of the N,O-diheptafluorobutyryl methyl ester derivatives of these hormones allows their detection and quantitation in the picogram range (detection limit approx. 0.2 pg). Purification of the dialysate is achieved using a cation-exchange column which is pretreated with diiodothyronine. Adsorption problems on the glassware are eliminated by silanization. The methodology also resolves 3,3′,5′-triiodothyronine (reverse T_3).

INTRODUCTION

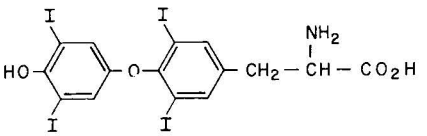
At present, two active thyroid hormones have been found in significant quantities in human serum, thyroxine (T_4) and 3,5,3′-triiodothyronine (T_3). A related substance which has attracted recent interest because of its different serum levels in various normal and diseased states is 3,3′,5′-triiodothyronine or reverse T_3 (RT_3). The major fractions (more than 99%) of each of these substances in serum are reversibly bound to proteins such as thyroxine-binding globulin, albumin, and thyroxine-binding prealbumin. However, it is the free (unbound) forms of T_3 and T_4 (FT_3 and FT_4), present only in trace amounts (generally 1–50 pg/ml), which provide the most indicative index of thyroid function[1].

The analysis of the trace levels of the free thyroid hormones in serum presents a major analytical challenge. Not only is the serum sample itself extremely complex and limited in supply, but the free hormones are engaged in a facile equilibrium with a vastly greater amount of bound hormones. Even a minor perturbation of this equilibrium causes the reported levels of FT_3 and FT_4 to change. Further, the large molecular weights of these hormones (near 1000), the lability of their iodine atoms,

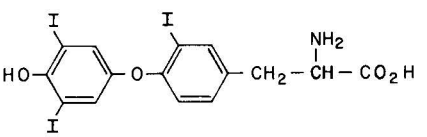
* To whom reprint requests should be addressed.



T_3



T_4



REVERSE T_3

their tendency to adsorb onto solid surfaces, and their presence and availability in only trace amounts in serum (in the free form) impose additional constraints.

The problem of isolating free from protein-bound hormone without significantly perturbing the equilibrium involved has been approached most effectively by means of equilibrium dialysis[2], in spite of certain shortcomings, which have been summarized[3]. Ultrafiltration and brief exposure to a binding agent, such as Sephadex, have also been used[3,4].

Due to the trace levels of the free hormones in serum, a variety of methods based on radiochemical techniques have been selected for estimating and monitoring FT_3 and FT_4 (refs. 2–4). While these techniques are currently employed, they suffer certain disadvantages, among which may be the need for accompanying assays of the total amounts of T_3 and T_4, the necessity to work with radioactive materials and their degradation products, the requirement for short half-lived radioisotopes such as ^{125}I because of the need for high specific activities, and the extra work and reagents involved in assaying for both FT_3 and FT_4.

Gas chromatographic (GC) analysis with electron capture detection (GC–ECD) of volatile derivatives of the thyroid hormones has been reported; however, the detection limits to date have only permitted the analysis of the total amounts of T_3 and T_4 in 1 ml of serum[5–12]. Nevertheless, the structure of the hormones, including at least three iodine atoms, would lead one to expect that with the appropriate derivatives and detector noise levels GC–ECD ought to achieve the required detection limits for the analysis of free forms.

This paper reports the successful concurrent analysis of the free thyroid hormones in 1 ml of serum using the GC separation of the N,O-diheptafluorobutyryl methyl ester derivatives with ECD at the required low noise level. Detection limits of 0.2 pg have been achieved. The method utilizes equilibrium dialysis to remove the free thyroid hormone fraction from serum, cation-exchange clean-up of the dialysate, derivatization, and GC–ECD.

EXPERIMENTAL

Apparatus

A Hewlett-Packard Model 5730A gas chromatograph (Avondale, Pa., U.S.A.) equipped with a variable frequency, constant current mode ECD was used. The radioactive source was 15 mCi ^{63}Ni plated directly on the interior of the cell. A 6 ft. $\times$ 4 mm I.D. glass column packed with 3% SE-30 on 80–100 mesh Supelcoport (Supelco, Bellefonte, Pa., U.S.A.) was used throughout. The injector and column were maintained at 250° and the detector at 300°, at which the response to the thyroid hormones was found to be optimized. A carrier gas of 5% methane and 95% argon was maintained at 60 ml/min.

Mass spectra of the thyroid hormone derivatives were obtained using a Nuclide 12-90-G single focusing magnetic deflection mass spectrometer (Nuclide, State College, Pa., U.S.A.). The accelerating potential was 3 kV, the electron energy was 70 eV, and the temperature of the ion source was maintained at 250°.

Reactivials (0.3, 1.0, 3.0, and 5.0 ml) from Pierce (Rockford, Ill., U.S.A.) were used to form the derivatives and perform the dialyses. Hamilton microliter syringes (10, 50, and 100 μl) (Reno, Nev., U.S.A.) were employed for all microtransfers and additions. A Cahn 4100 electrobalance (Ventron, Paramount, Calif., U.S.A.) was employed to weigh microgram quantities of the derivative standards.

An IN-V-TRON 2000 (Nuclear Systems, Chicago, Ill., U.S.A.) gamma counter was used to count radioactive T_4 in the experiment dealing with adsorption losses.

The dialysis membranes were Visking precision Nojax cellulose casing (Union Carbide, Chicago, Ill., U.S.A.). Minienert caps equipped with septum injection ports (Supelco) were used to seal the vials which contained solutions to be injected into the gas chromatograph. Polyethylene chromatographic columns (10 cm $\times$ 1 cm I.D.) were purchased from Eastman-Kodak (Rochester, N.Y., U.S.A.).

Reagents and chemicals

The esterifying reagent was 25% (w/w) gaseous HCl (Matheson, Gloucester, Mass., U.S.A.) in methanol (Burdick and Jackson, Muskegon, Mich., U.S.A.). The methanol was redistilled and dried over molecular sieve Type 5A. The acetylating agent agent was heptafluorobutyric anhydride (K & K, Plainview, N.Y., U.S.A.) in acetonitrile (Burdick and Jackson). Upon arrival, the heptafluorobutyric anhydride was stored over anhydrous calcium sulfate in a desiccator at $-4°$ and subsequently used without further purification. Acetonitrile was redistilled and dried over molecular sieve Type 5A. Diiodothyronine (T_2), T_3, and T_4 were obtained as the free acids from Sigma (St. Louis, Mo., U.S.A.) and stored in a desiccator at $-4°$. RT_3 was kindly given to us by Dr. R. I. Meltzer of Warner-Lambert Research Laboratories.

Cation-exchange resin Bio-Rad AG 50W-X2 (H^+), 100–200 mesh, was ob-

tained from Bio-Rad Labs. (Richmond, Calif., U.S.A.). [^{125}I]T_4 was obtained from Abbott Labs. (Chicago, Ill., U.S.A.). The silanizing agent, trimethylchlorosilane, was purchased from Supelco.

Silanization of glassware

Glassware was first cleaned by boiling in concentrated nitric acid for 1 h and rinsing to neutrality with distilled water. The glassware was then boiled in distilled water for 1 h and dried in an oven (140°) overnight. Silanization was conducted using a 4% (v/v) solution of trimethylchlorosilane in dry toluene for 10 min at room temperature. The glassware was returned to the 140° oven for 4 h, and was subsequently allowed to cool in a desiccator. When at room temperature, the vials were sealed with PTFE-coated septa. The silanization procedure was used throughout the entire experiment on all glassware, including reaction vials, volumetric flasks, and pipets, that were to come in contact with the thyroid hormones.

Preparation of 25% (saturated) HCl–methanol (w/w)

A 10-ml volume of dry methanol was pipeted into a dry 25-ml centrifuge tube and weighed. The tube was then placed in a dry ice–methanol bath and a stream of nitrogen was maintained above the solution while a stream of HCl gas was bubbled through the solution for approximately 15 min. After this time, the HCl and nitrogen streams were removed, and the tube was withdrawn, dried, and quickly weighed. This procedure was continued until a 25% increase in weight ($\pm$0.1 g) was observed. Once the proper percentage had been obtained (usually after 15 min), the solution was transferred to the esterification samples (*e.g.*, 0.5 ml/serum sample) by decantation. The HCl–methanol solution was always prepared for immediate use.

Derivatization of T_2, T_3, RT_3, and T_4 standards

T_2, T_3, or T_4 (25.0 mg) was placed in a 40-ml centrifuge tube and 25 ml of 25% HCl in methanol were added for esterification. The tube was sealed immediately with a septum and agitated for 3 min on a vortex. Esterification was allowed to continue for 1 h at 60°; subsequently the solution was evaporated to dryness under a stream of dry nitrogen. A freshly prepared solution of 1.5 ml of heptafluorobutyric anhydride in 6 ml of acetonitrile was then added. The tube was kept at 60° for 1 h, cooled to room temperature, and the solution was blown to dryness with dry nitrogen. The resulting solids were recrystallized from acetonitrile.

Since we had only a small quantity of RT_3, 1.00 mg was used to form the derivative. This was done in a 1-ml reaction vial using similar conditions to those mentioned above except that 0.5 ml of HCl–methanol solution and 100 μl of heptafluorobutyric anhydride in 400 μl of acetonitrile were employed. Recrystallization again was from acetonitrile.

In order to determine the percentage yield, the derivatization scheme was conducted on microgram quantities of material, using the appropriate volumes of the esterification and acetylating solutions. After completion of the reaction, the residue was redissolved in acetonitrile and injected into the gas chromatograph. Comparison of the ECD responses with those of standard solutions made from the pure material revealed a 99% yield in each case.

Elemental analyses and melting points of the derivatized thyroid hormone standards were as follows:

Derivatized T_2 — Found: 30.69% C; 1.29% H; 28.45% F; 27.24% I; 1.52% N; 10.81% O; m.p. 103–105°
Calc. for $C_{24}H_{13}F_{14}I_2NO_6$: 30.94% C; 1.41% H; 28.57% F; 27.27% I; 1.50% N; 10.31% O

Derivatized T_3 — Found: 27.18% C; 1.08% H; 25.10% F; 36.01% I; 1.33% N; 1.30% O; m.p. 118–119°
Calc. for $C_{24}H_{12}F_{14}I_3NO_6$: 27.25% C; 1.14% H; 25.17% F; 36.03% I; 1.32% N; 9.05% O

Derivatized T_4 — Found: 24.15% C; 0.86% H; 22.39% F; 42.88% I; 1.20% N; 8.52% O; m.p. 148–150°
Calc. for $C_{24}H_{11}F_{14}I_4NO_6$: 24.35% C; 0.94% H; 22.49% F; 42.92% I; 1.18% N; 8.11% O

Molecular-weight determination was also verified by mass spectrometry. Each of the compounds exhibited easily recognizable molecular ion peaks (M^+) of high relative intensity. The base peak in each spectrum appeared at *m/e* values corresponding to $(M - 213)^+$. Significant peaks in the spectrum for each compound having relative intensities greater than 40% occurred at *m/e* values of $(M - 284)^+$, $(M - 410)^+$ and $(M - 538)^+$. Mechanisms of the fragmentation patterns of these molecules are currently being studied by isotopic labeling and high-resolution techniques.

The thyroid hormone derivatives have proven to possess remarkable stability both in solid form and in solution. Although ECD calibrations of the standards were made immediately after derivatization, solutions stored up to four months revealed no decomposition. The only precaution taken was to store the derivatives in the dark at −4°.

Phosphate buffer

The 0.15 *M* phosphate buffer was composed of 19.70 g dipotassium hydrogen phosphate and 4.92 g potassium dihydrogen phosphate in 1 l of distilled water. Phosphoric acid or sodium hydroxide solutions were used to adjust the pH to 7.40. The solution was stored at 4° in the dark. Before use, the buffer solution was allowed to reach room temperature, and the pH was checked.

Equilibrium dialysis of sera

Dialysis membranes were prepared using the method of Sterling[13], in which membranes were soaked in 0.1 *M* HNO_3 for 24 h and in 0.01 *M* HNO_3 for three days, followed by storage in distilled water at 4°. Before use, the dialysis bags were washed repeatedly with distilled water. During handling of the membranes, plastic disposable surgical gloves were worn. Using forceps, the moist membrane was doubly knotted at one end, filled with 1 ml of phosphate buffer, and inspected visually for pin holes. If satisfactory, the buffer was removed and the bag was rinsed again with distilled water. The pH of the serum was measured and adjusted to 7.40, if necessary. Serum (1.00 ml) was introduced into the bag with a pipet, and the end of the membrane was doubly knotted. The membrane was folded in a "V" and placed in a 5-ml silanized microreaction vial. This vial also contained a triangular stirring bar to provide a gentle stirring of the solution. A 1.50-ml aliquot of phosphate buffer was pipetted into

the vial. The vial was sealed with a PTFE septum, wrapped with aluminum foil (in order to minimize photooxidation) and placed in a water-bath maintained at 37 ± 0.5°. Dialysis with stirring was assumed to be complete after 18 h[14], at which time the vials were removed and allowed to reach room temperature.

Cation-exchange chromatography

The cation-exchange resin (Bio-Rad AG 50W-X2 (H^+), 100–200 mesh) was washed four times in distilled water and the fines were decanted. An aqueous slurry of the resin was poured into a 10 cm × 1 cm I.D. polyethylene column, which contained a silanized glass wool plug, and settled to a packed height of 5 cm with 15 ml of distilled water. The column was then activated with 5 ml of 2 *N* HCl and washed with 5 ml of distilled water. A solution of 15 pg of T_2 in 1.0 ml of phosphate buffer (determined by GC) was injected onto the column, and the column was washed with 15 ml of 0.15 *M* ammonium acetate (pH 8.5), 2 ml of methanol, and 4 ml of methanol–12 *N* ammonium hydroxide (97:3, v/v). The column was treated successively as before with 3 ml of water, 5 ml of 2 *N* HCl, and 5 ml of water. The serum dialysate was pipeted onto the top of the column, and the dialysis vial was rinsed four times onto the column with 0.5-ml volumes of phosphate buffer. The intact dialysis bag was placed over the column and washed with 1 ml of phosphate buffer. Again, the ion-exchange column was washed with 15 ml of 0.15 *M* ammonium acetate (pH 8.5) and then 2 ml of methanol. The thyroid hormone fraction was subsequently eluted from the column with a 4-ml volume of methanol–12 *N* ammonium hydroxide solution (97:3, v/v). This wash procedure followed essentially that used by Tajuddin and Elfbaum[15]. The eluate was then collected in a 5-ml microreaction vial and evaporated to dryness at 40° under a stream of nitrogen.

Derivatization of the free thyroid hormones

The eluent from the cation-exchange column containing the thyroid hormones was dried under a stream of nitrogen at 40° for 20 min. To the residue was added 0.5 ml of the 25% (w/w) HCl–methanol solution, the vial was sealed with a PTFE septum and heated to 60° for 1 h in order to esterify the acids. After this time, the reaction mixture was allowed to reach room temperature before removing the septum. The esterifying solution was evaporated to dryness at 40° with a stream of nitrogen for 15 min. Acetylation was accomplished by adding separately 50 μl of heptafluorobutyric anhydride and 200 μl of acetonitrile to the residue, mixing on a vortex for 3 min and heating to 60° for 30 min. After removing the acetylating solution under a stream of nitrogen at 40°, the reaction vial was sealed with a Minienert cap. This cap was used so that aliquots could be added or removed without exposure of the sample to the atmosphere.

The residue in the vial was taken up in 20 μl of acetonitrile and mixed on a vortex for 5 min. Injections into the gas chromatograph were made by removal of aliquots from the sclution via the septum port valve on the Minienert cap. Injection volumes were 5 μl.

RESULTS AND DISCUSSION

As we have already noted, the goal of this research was to develop an

analytical methodology that would permit the simultaneous analysis of the dialyzable (*i.e.*, free) thyroid hormones in sera. The expected amount of the dialyzable hormones in 1 ml of undiluted sera was at the 1–50 pg level[1]. This level places severe demands on detection, and it was clear that beyond incorporation of radioactive species, one of the only possible means of detection was GC–ECD. With such a procedure, severe demands are also placed on the sample clean-up and derivatization steps in order that sample losses are minimized.

For purposes of reference, the overall analytical scheme is shown in Fig. 1. As noted, equilibrium dialysis has been shown to be a valid method for isolating a quantity of unbound thyroid hormone that correlates with disease state[1,13,15–21]. We have simply followed a standard procedure in this step. Originally, derivatization was conducted on a lyophilized serum dialysate. This approach failed to yield a satisfactory sample for GC analysis, and so an additional clean-up step was necessary. A modified cation-exchange procedure proved to be adequate. Derivatization of the eluted fraction, GC separation, and ECD completed the analysis of the thyroid hormones at the picogram level.

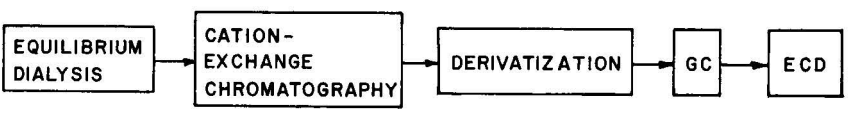


Fig. 1. Block diagram of the procedure for the analysis of free thyroid hormones.

Elimination of adsorption on glassware

Other workers have noted that the thyroid hormones tend to adsorb to glassware[14,22]. At the picogram level this could represent a significant problem in terms of both the accuracy and reproducibility of the analysis. We have found that a satisfactory method for eliminating adsorption on glassware is via silanization with trimethylchlorosilane.

An experiment was performed using $[^{125}I]T_4$ to illustrate the effective elimination of adsorption. Four test tubes each from six sources were selected for study. Two of each set were cleaned and silanized by the previously outlined procedure, and the remaining two were used as received. In each of the test tubes was placed 1.5 ml of phosphate buffer (see Experimental) containing 25,000 cpm of $[^{125}I]T_4$. The tubes were sealed with PTFE tape and placed in a shaker bath at 37° for 18 h (corresponding to the conditions for dialysis). After this time period, the solutions were withdrawn by pipet and each tube rinsed four times with 0.5 ml of phosphate buffer. The tubes were then dried under a stream of nitrogen, resealed and placed in the gamma counter for analysis of the $[^{125}I]T_4$ that adhered to the sides of the tubes. Each tube was counted three times and averaged.

The results of this experiment are shown in Table I. Each value of counts per minute is the average of the two tubes treated identically. (Deviations were generally less than 5%.) As the background cpm is roughly 200, it can be seen that silanization does completely eliminate the adsorption problem. Note that treatment with silicone (tube F) does not reduce adsorption at the low levels of this experiment. In order to standardize the analytical procedure, cleaning and silanization were conducted on all glassware that was used in the work.

TABLE I

COUNTS PER MINUTE (cpm) OF *T_4 ADSORBED ONTO GLASS TUBES

Average background = 203 cpm. Tubes: (A) 16 mm × 150 mm, Rochester Scientific No. 7045; (B) 16 mm × 100 mm, Fisher Scientific No. 14-957-16B; (C) 12 mm × 75 mm, Becton-Dickinson No. 7813; (D) 20 mm × 150 mm, Van-Lab No. 60825-389 (Pyrex); (E) 16 mm × 100 mm, Curtin-Matheson No. 339-309; (F) 16 mm × 100 mm, Venaject No. L-30 (silicone treated). *T_4 = [^{125}I] T_4 (25,000 cpm).

Tube	*No treatment*	*Silanized*
A	1568	207
B	2704	212
C	1338	211
D	1588	198
E	1335	204
F	1382	209

Thyroid hormone standards —separation and calibration

While N,O-dipivalyl methyl esters and other derivatives of the thyroid hormones have been successfully chromatographed, the reported detection limits were not sufficient for our purposes. One of the reasons for the poor detection limits was in part due to detector limitations. With the ECD used in this work, we were routinely able to work at very low noise levels (1×10^{-12} A). In addition, we employed fluorinated derivatives of the thyroid hormones for enhanced volatility and possibly improved detection limits. For this purpose, we selected the N,O-diheptafluorobutyryl methyl ester derivatives of the thyroid hormones.

After successful derivatization of the standards, a GC separation at 250° was developed, as shown in Fig. 2. We have included in this separation reverse T_3, which recently has been evaluated in a variety of normal and diseased states[23]. Note that roughly 10 pg of each standard has been injected.

Calibration plots (peak heights) were found to be identical for each of the three standards, and this calibration is shown in Fig. 2. The standard error in peak height using the data from all three standards was found to be ±1%. Although the plots were found to have a linear dynamic range of 10^5 with correlation coefficients of greater than 0.99, the required linear dynamic range for physiological concentrations in 1 ml of serum is only 10^3. The detection limits for each of these derivatives were found to be 0.2 pg. Accepting the values of free T_3 and T_4 from equilibrium dialysis by Sterling[13], our detection limits indicate that we should be readily able to detect the dialyzable hormones in 1 ml of serum even from hypothyroid individuals (reduced T_3 and T_4 levels), if no losses in sample handling occur. We shall discuss reverse T_3 later in the paper.

Cation-exchange clean-up of dialysate

As mentioned previously, it was found necessary to clean-up the dialysate prior to derivatization. We employed the established method of cation-exchange chromatography[5,6,16,24,25], but in agreement with others[2,5] found recoveries were not quantitative.

In order to assess recoveries at the picogram level, a standard solution of 9 pg/ml T_3 and 30 pg/ml of T_4 in phosphate buffer was prepared. The concentrations

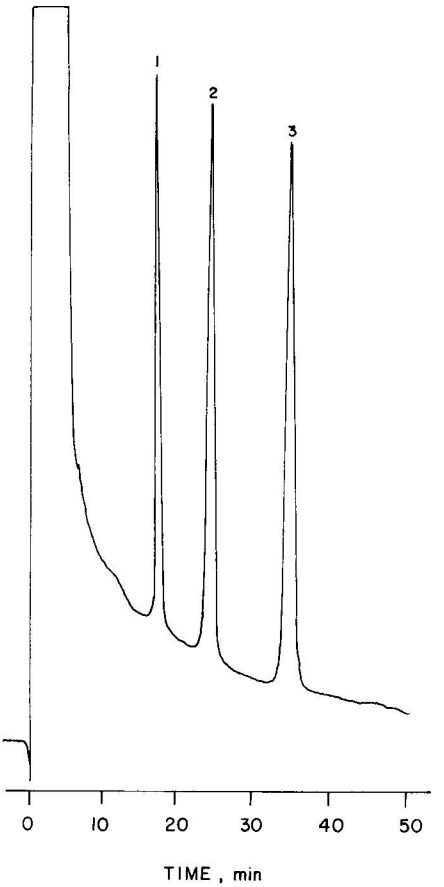


Fig. 2. GC–ECD of the N,O-diheptafluorobutyryl methyl ester derivatives of thyroid hormones. Column, 6 ft. × 4 mm I.D. glass coil packed with 3% SE-30 on 80–100 mesh Supelcoport; temperature, 250°; carrier, methane–argon (5:95); flow-rate, 60 ml/min; injector temperature, 250°; detector temperature, 300°; injection volume, 5 μl; attenuation, ×1.1 = T_3; 2 = reverse T_3; 3 = T_4; 10 pg each.

of the thyroid hormones were ascertained by derivatization and GC analysis. One milliliter of this standard solution was pipetted on top of the cation-exchange column and the column was washed with 0.15 *M* ammonium acetate and then methanol, as outlined in Experimental. The hormones were then collected in an eluent of methanol–12 *N* ammonium hydroxide (97:3), derivatized, and injected into the gas chromatograph. As seen in Table II, recovery of the hormones was found to be only 54% for T_3 and 65% for T_4.

It was assumed that the losses were due in part to adsorption on the polyethylene column, based on observations made by Lee and Pileggi[14]. Following on their work, it was believed that the column might be "deactivated" by the addition of a reagent to the column prior to sample loading. The deactivating agent selected was diiodothyronine (T_2) as its properties of adsorption might be expected to be related to those of T_3 and T_4. Moreover, any T_2 eluting from the resin column with

TABLE II

RECOVERY OF T_3 AND T_4 FROM CATION-EXCHANGE COLUMNS PRETREATED WITH DIIODOTHYRONINE (T_2)

Solution, 9 pg/ml T_3 and 30 pg/ml T_4.

T_2 added (pg)	*T_3 recovered (pg)*	*T_4 recovered (pg)*	*Recovery T_3 (%)*	*Recovery T_4 (%)*
0	5	20	55	55
5	5	24	55	80
8	6	25	67	83
10	6	27	67	90
12	8	29	89	97
15	9	30	100	100
20	9	30	100	100
25	9	30	100	100

the T_3 and T_4 fraction ought to be readily derivatized under the conditions for derivatization of the active hormones. Finally, the T_2 derivative would elute much earlier than the T_3 derivative so that no chromatographic interference would be expected.

Known amounts of T_2 in 1 ml of phosphate buffer were added to the cation-exchange column. Each amount of T_2 was separately determined by derivatization and GC–ECD, using a small-range (1–50 pg) calibration plot for T_2. The column was washed in the same manner as described above, including elution with methanol-ammonium hydroxide. After this elution, the column was washed with 3 ml of distilled water and reactivated with 5 ml of 2 *N* HCl. The column was next loaded with 1 ml of standard solution (9 pg T_3/30 pg T_4), washed, and the fraction containing T_3 and T_4 collected. The thyroid hormones were derivatized and detected by GC–ECD.

The results of this experiment are shown in Table II. As the quantity of T_2 added to the column is increased, the recovered amounts of T_3 and T_4 also increase. It is found that after the addition of 15 pg T_2 in the manner described above, the

TABLE III

REPEATED ANALYSIS OF FREE T_3 AND FREE T_4 IN SERUM

Sample No.	*FT_3 (pg/ml)*	*FT_4 (pg/ml)*
1	6	32
2	4	30
3	6	31
4	6	31
5	6	29
6	5	29
7	6	31
8	5	30
9	7	29
10	6	30
Average	5.7 ± 0.8	30.3 ± 1.9

recovery of T_3 and T_4 is maximized. For all subsequent experiments, the resin columns were first prepared by the addition of approx. 15 pg of T_2, washed, and reactivated before loading of the dialysate.

Serum dialysate analysis

Our next study dealt with the question of losses in the analysis of the dialysate from an actual serum sample. As described in Experimental, 1 ml of serum was dialyzed against 1.50 ml of phosphate buffer, and two 0.50-ml aliquots of dialysate were withdrawn. One aliquot was untreated while to the other was added a 25-μl solution of 15 pg of T_3 and 70 pg of T_4 (as determined from the calibration plot of Fig. 3). Both aliquots were chromatographed by cation exchange, derivatized, and analyzed by GC–ECD.

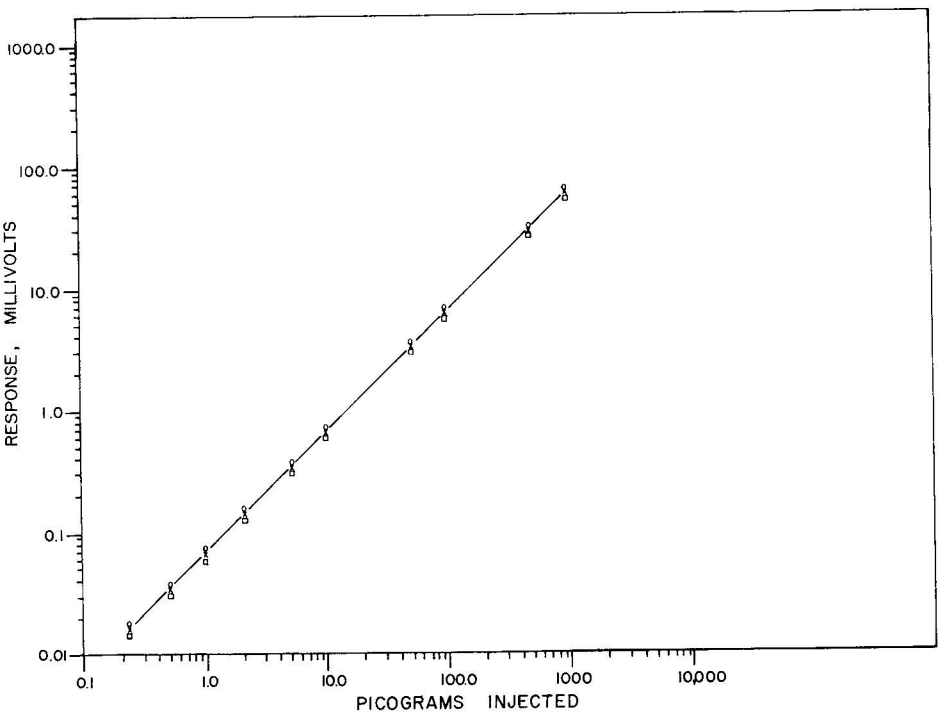


Fig. 3. Calibration plot of the thyroid hormone derivatives. Chromatographic conditions, same as in Fig. 2. ○, T_4; ×, RT_3; □, T_3.

For the untreated dialysate fraction, chromatographic results with 5-μl sample injections indicated 0.5 pg of T_3 and 2.5 pg of T_4. Since the sample had been taken from a total of 20 μl, the amounts of dialyzed hormones were 2 pg of T_3 and 10 pg of T_4. In the same manner the amounts of hormones found in the aliquot containing the added standards were 17 pg of T_3 and 80 pg of T_4. Thus, within the limits of the analytical procedure, no losses after the serum dialysate were observed, indicating quantitative recovery from the dialysate.

In order to determine the overall reproducibility of the method (*i.e.*, dialysis

and analysis) 12 ml of sera were pooled and ten 1-ml samples from this pool were separately dialyzed against 1.5 ml of buffer. Each dialysate was cleaned up by the previously outlined procedure and analyzed by GC–ECD.

The results for each milliliter of serum are shown in Table III. The percentage standard deviations for FT_3 and FT_4 are $\pm 14\%$ and $\pm 7\%$, respectively. Considering the various steps in the procedure and the very low amounts of the thyroid hormones present, the repeatability is good.

An improvement in the reliability of the method can be achieved by the addition of a suitable internal standard to the serum dialysate before cation-exchange chromatography in order to monitor losses and variations. We have tested 5′-chloro-3,5,3′-triiodothyronine (Cl-T_3) as a potential internal standard, as it elutes between T_3 and T_4 in the GC separation of the derivatives and ought to possess similar physical and chemical properties as the hormones. Addition of this compound to the dialysate and subjection to the same analytical steps as described previously for T_3 and T_4 revealed a repeatability of $\pm 1\%$ for FT_3 and FT_4 for the ten sera samples shown in Table III. However, the retention time of the internal standard was found to be identical with that of reverse T_3. We are therefore currently investigating the synthesis of other possible internal standards that maintain the same properties as the thyroid hormones but can be resolved from T_3, T_4, and RT_3.

In Fig. 4 we show a chromatogram of (free) thyroid hormones from the serum of a presumably normal individual. The results correspond to 5 pg of T_3 and 32 pg of T_4 in 1 ml of serum. (Note that only 1/4 of the final sample volume was injected into the gas chromatograph to achieve the chromatogram shown.) Comparable results were obtained on a serum from a second normal person. These values are within the range of concentrations expected for normal FT_3 and FT_4 as reported by Sterling[13] using equilibrium dialysis. As discussed by Lee and Pileggi[14], the dialyzed quantities of T_3 and T_4 are dependent on the conditions of dialysis, *e.g.*, temperature, degree of dilution of serum with buffer prior to dialysis, and relative solution volumes inside and outside the dialysis bag.

Preliminary analyses of pathological sera show the method to be completely applicable without any further modification to such samples. While we have analyzed only a limited number of abnormal samples up to this point, the FT_3 and FT_4 levels were as much as four-fold above and below the levels observed for the two normal sera in our study. Reverse T_3 was also seen in some of these abnormal samples. This was expected, since reverse T_3 is known to be elevated in a number of disease states[23]. We did not observe a peak for reverse T_3 in the two normal sera which we analyzed, however, perhaps because we dialyzed only 1 ml of serum and injected only 1/4 of the final sample volume in each case. A peak for free reverse T_3 might have been seen if the procedure had been scaled up. Chopra *et al.*[23] report a level of free reverse T_3 in euthyroid serum by dialysis–radioimmunoassay to be 1 pg/ml. Work with pathological samples is continuing and will be reported in detail in a future paper.

CONCLUSION

A method has been developed for the analysis of the concentrations of free (*i.e.*, unbound) thyroid hormones in 1 ml of serum. After equilibrium dialysis, a standard procedure, the dialysate is cleaned-up by cation-exchange chromatography,

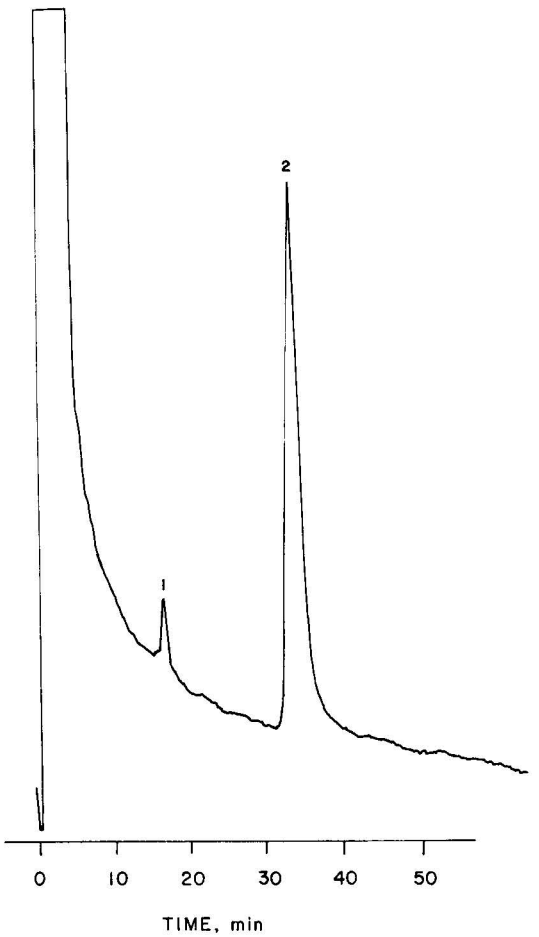


Fig. 4. GC–ECD of the N,O-diheptafluorobutyryl methyl ester derivatives of the dialyzed thyroid hormones. Chromatographic conditions, same as in Fig. 2. 1 = approx. 1 pg T_3; 2 = approx. 8 pg T_4; injection volume, 5 μl; attenuation, $\times 1$.

derivatized to the N,O-diheptafluorobutyryl methyl esters, and subjected to GC–ECD. Detection limits of 0.2 pg are achieved. Reasonable values for FT_3 and FT_4 are obtained from two normal sera, and preliminary work shows free RT_3 in some of the pathological sera examined. Although the repeatability of the method is good and the recovery after dialysis is essentially quantitative, it is expected that introduction of a suitable internal standard will enhance the routine reliability of the procedure based on results with a trial internal standard.

ACKNOWLEDGEMENTS

The authors wish to thank Dr. Michael A. Davis, Children's Hospital, Boston, Mass., for use of the gamma counter in the labeled adsorption studies, Clin. Chem. Laboratory, Boston, Mass., and Dr. P. Reed Larsen, Head, Thyroid Unit, Depart-

ment of Medicine, Peter Bent Brigham Hospital, Boston, Mass., for providing us with some abnormal sera, and Dr. Robert I. Meltzer, Warner-Lambert Research Institute, Morris Plains, N.J., for giving us the RT_3. The authors also wish to acknowledge NIH for support of this work under grant GM-15847-07. Contribution number 14 from the Institute of Chemical Analysis, Applications and Forensic Science.

REFERENCES

1 P. R. Larsen, *Med. Clin. N. Amer.*, 59 (1975) 1063.
2 K. A. Sterling and A. Hegedus, *J. Clin. Invest.*, 41 (1962) 1031.
3 S. S. Levinson and S. V. Rieder, *Clin. Chem.*, 20 (1974) 1568.
4 J. S. Annino and R. W. Giese, *Clinical Chemistry*, Little, Brown and Co., Boston, Mass., 1976, p. 306.
5 M. Tajuddin and S. G. Elfbaum, *Clin. Chem.*, 19 (1973) 109.
6 N. N. Nihei, M. C. Gershengorn, T. Mitsuma, L. R. Strigham, A. Cordy, B. Kuchmy and C. S. Hollander, *Anal. Biochem.*, 43 (1971) 433.
7 P. I. Jaakonmäki and J. E. Stouffer, *J. Gas Chromatogr.*, 5 (1967) 303.
8 J. E. Stouffer, P. I. Jaakonmäki and T. J. Wenger, *Biochim. Biophys. Acta*, 127 (1966) 261.
9 A. H. Richards and W. B. Mason, *Anal. Chem.*, 38 (1966) 1751.
10 N. M. Alexander and R. Scheig, *Anal. Biochem.*, 22 (1968) 187.
11 F. Shahrokhi and C. W. Gehrke, *Anal. Biochem.*, 24 (1968) 280.
12 K. Funakoshi and H. J. Cahnman, *Anal. Biochem.*, 27 (1969) 150.
13 K. A. Sterling, in H. Breuer, D. Hamel and H. L. Krüskemper (Editors), *Methods of Hormone Analysis*, Wiley, New York, 1976, p. 156.
14 N. D. Lee and V. J. Pileggi, *Clin. Chem.*, 17 (1971) 166.
15 K. A. Sterling and M. A. Brenner, *J. Clin. Invest.*, 45 (1966) 153.
16 K. Sterling, D. Bellabarba, E. S. Newman and M. A. Brenner, *J. Clin. Invest.*, 48 (1969) 1150.
17 C. W. Burke and C. J. Eastman, *Brit. Med. Bull.*, 30 (1974) 93.
18 D. Plaut, *Amer. J. Med. Technol.*, 40 (1974) 434.
19 B. G. Anderson, *J. Amer. Med. Ass.*, 203 (1968) 135.
20 U. S. Fang and H. A. Selenkow, *Clin. Chem.*, 16 (1970) 185.
21 J. Herrman and H. L. Krüskemper, in H. Breuer, D. Hamel and H. L. Krüskemper (Editors), *Methods of Hormone Analysis*, Wiley, New York, 1976, p. 126.
22 S. H. Ingbar, L. E. Braverman, N. A. Dawber and G. Y. Lee, *J. Clin. Invest.*, 44 (1965) 1679.
23 I. J. Chopra, U. Chopra, S. R. Smith, M. Reza and D. H. Solomon, *J. Clin. Endocrinol. Metab.*, 41 (1975) 1043.
24 E. T. Backer, T. J. Postnies and J. P. Wiener, *Clin. Chim. Acta*, 15 (1967) 77.
25 C. G. Lewallen, in F. W. Sunderman and F. W. Sunderman, Sr. (Editors), *Evaluation of Thyroid and Parathyroid Functions*, Lippincott, Philadelphia, Pa., 1963, p. 37.

Journal of Chromatography, 126 (1976) 517–534
© Elsevier Scientific Publishing Company, Amsterdam — Printed in The Netherlands

CHROM. 9459

DETERMINATION OF HYDRALAZINE AND ITS METABOLITES BY GAS CHROMATOGRAPHY–MASS SPECTROMETRY

KLAUS D. HAEGELE*, HAROLD B. SKRDLANT, NORMAN W. ROBIE, DAVID LALKA and JOHN L. McNAY, Jr.

Clinical Pharmacology Program, University of Texas Health Science Center, Departments of Pharmacology and Pathology and the Audie Murphy Veterans Administration Hospital, San Antonio, Texas 78284 (U.S.A.)

SUMMARY

Metabolism of the vasodilator hydralazine was investigated by *in vivo* and *in vitro* studies. Standards to identify metabolic products were synthesized. Determination and quantification of hydralazine and its metabolites were accomplished by gas chromatography–mass spectrometry. A deuterium-labeled internal standard was used for quantification. ^{14}C-labeled internal standards were synthesized and used to demonstrate recoveries from the biological samples.

INTRODUCTION

Hydralazine (1-hydrazinophthalazine) is a widely used vasodilator antihypertensive drug[1–17] its administration in combination with propranolol[2] represents one of the most efficacious antihypertensive regimens currently in use.

Despite the importance of hydralazine as a drug, many aspects of its metabolic fate remain unsolved. The instability of hydralazine at physiologic pH[3] has been one of the main adversities of its analysis. So far, lack of both specificity and sensitivity characterized the methods employed to: (1) measure hydralazine levels in blood or urine and (2) distinguish definitely between the parent drug and its metabolites[4–7]. Recently, the first unambiguous analytical method to measure the parent drug concentration in plasma was reported[8].

N-Acetylation was found to be one of the major metabolic pathways in rat, rabbit, and man[6,9–11,14]. This so called N-acetyl-hydralazine[12] was subsequently found to be the hydrate of 3-methyl-*s*-triazolo[3,4-*a*]phthalazine[13–15]. The time course of plasma levels and urinary and fecal excretion was determined[4,6,11,16]. It was found that more than 70% of an administered dose was excreted within 24 h in the urine (as measured with ^{14}C-hydralazine)[11]. Feces accounted for up to 10% of administered dose excreted within several days[11]. The same authors also showed that hydralazine and some of its metabolites are highly bound to human albumin and plasma.

* To whom correspondence should be addressed.

Our objective was to develop a gas chromatographic–mass spectrometric (GC–MS) method to unequivocally determine hydralazine and its metabolites in biological samples. In order to do so, we synthesized most of the metabolites as well as a deuterium-labeled internal standard to quantify these compounds. ^{14}C-Labeled metabolites were synthesized as well and their recovery from biological samples was determined.

EXPERIMENTAL

Reagents

All solvents were obtained from Burdick and Jackson Labs. (Muskegon, Mich., U.S.A.). The hydralazine administered to rats was Apresoline. The silylating reagent Regisil TMCS (trimethylchlorosilane), was obtained from Regis (Chicago, Ill., U.S.A.).

Other derivatizing agents were purchased from Fisher Scientific (Houston, Texas, U.S.A.), except for d_6-acetic anhydride, which was obtained from Merck (St. Louis, Mo., U.S.A.). [^{14}C]Hydralazine was obtained from California Bionuclear (Sun Valley, Calif., U.S.A.).

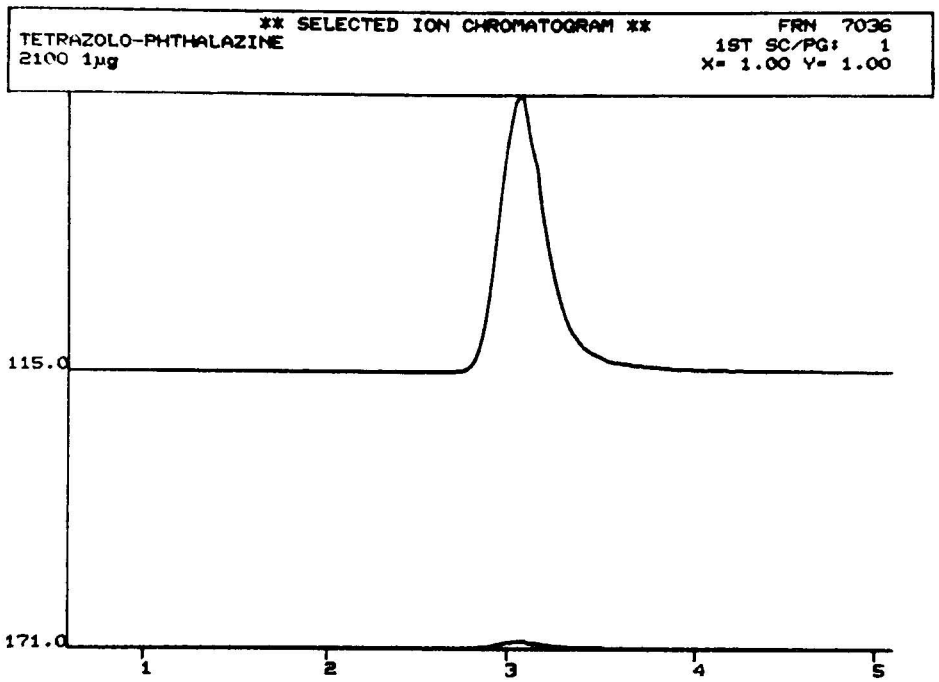
Synthesis

(1) Tetrazolo[1,5-α]phthalazine (tetrazolo-P)[18]. 1-Hydrazinophthalazine-HCl (495 nm; 2.4 mmoles) was dissolved in 2 ml of 4 *N* acetic acid. Upon addition of an excess of a concentrated solution of sodium nitrite in water, the reaction mixture was allowed to stand for 1 h at room temperature. The crystalline product was collected and dried. Yield: 390 mg or 90% of theory. Its mass spectrum showed a molecular ion at *m/e* 171. The base peak is observed at *m/e* 115. Since the molecular ion was of low abundance under the instrumental parameters used, the ion at *m/e* 115 was chosen for single ion monitoring (SIM)

(2) 3-Methyl-s-triazolo[3,4-α]phthalazine (MTP)[18]. 1-Hydrazinophthalazine-HCl (395 nm; 2 mmoles) was heated to reflux with 2 ml of acetic anhydride for 2 h. The solvent was evaporated to dryness and the residue dissolved in hot water. Upon cooling, MTP crystallized. The crystals were collected and dried over P_2O_5. Yield: 280 mg or 75% of theory. The mass spectrum gave the molecular ion at *m/e* 184 as the base peak; a prominent fragment ion was observed at *m/e* 115. Both ions were chosen for SIM (Fig. 2a).

(3) s-Triazolo[3,4-α]phthalazine (TP)[18]. 1-Hydrazinophthalazine-HCl (395 mg; 2 mmoles) was refluxed with 2 ml of 85% formic acid. After evaporation of the solvent, the residue was dried over P_2O_5. Yield: 335 mg or 98% of theory. The mass spectrum gave the molecular ion at *m/e* 170 as the base peak; the second most abundant ion was observed at *m/e* 115. Both ions were chosen for SIM (Fig. 3).

(4) 1-Hydrazinophthalazine acetone hydrazone (acetonide). 1-Hydrazinophthalazine-HCl (395 mg; 2 mmoles) was dissolved in 2.5 ml of acetone and allowed to react for 1 h with one drop of acetic acid added to the mixture. The solvent was evaporated and the slightly yellow material was dried *in vacuo*. Yield: 411 mg or 99% of theory. The pass spectrum showed the moleculiar ion at *m/e* 200, with the base peak being observed at *m/e* 185. A prominent ion was alse observed at *m/e* 115. Both *m/e* 185 and *m/e* 115 were chosen for SIM (Fig. 4).



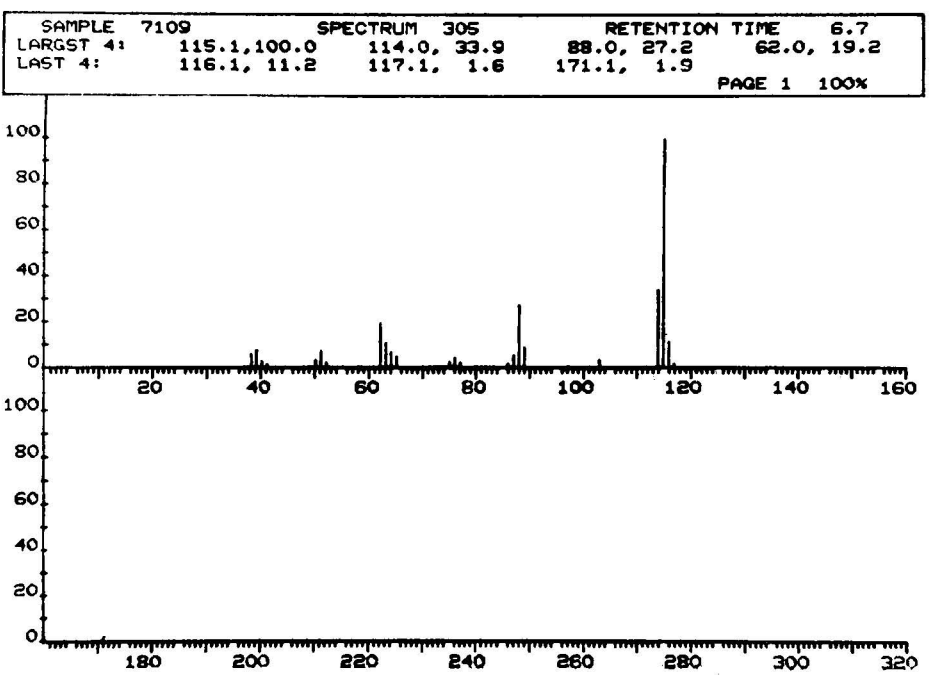


Fig. 1. Mass spectrum of tetrazolo-P.

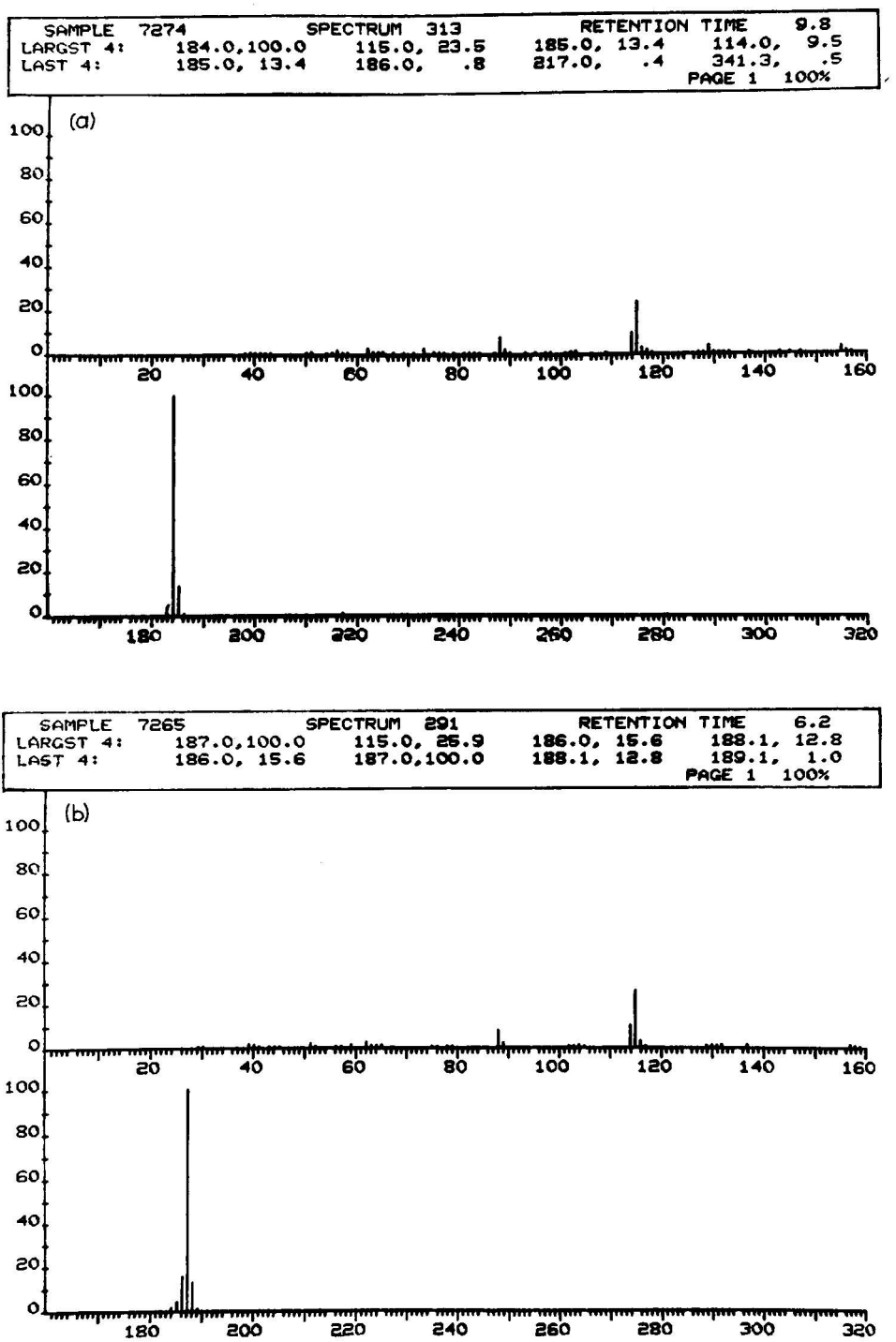
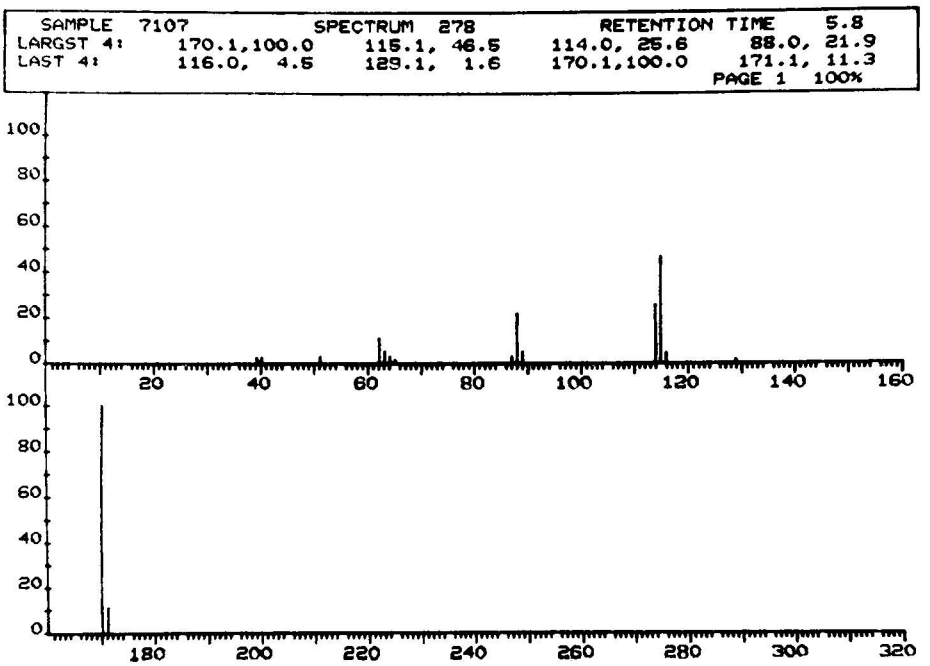


Fig. 2. (a) Mass spectrum of MTP; (b) Mass spectrum of d_3-MTP.



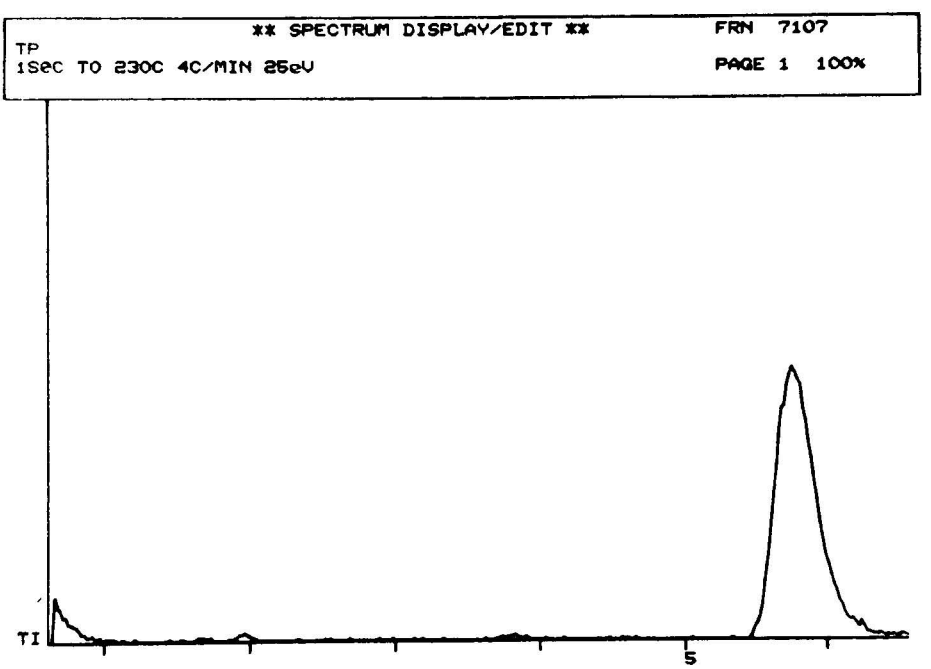


Fig. 3. Mass spectrum of TP.

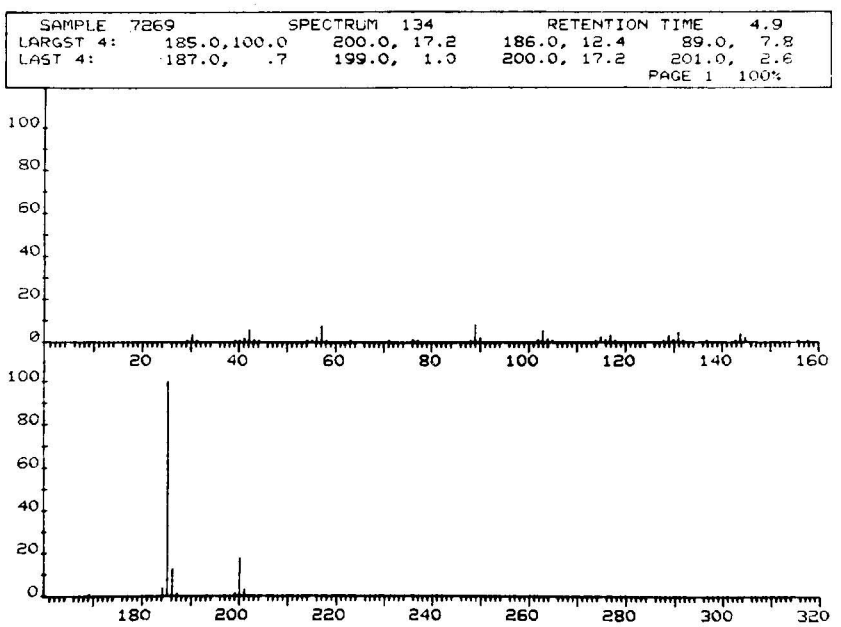


Fig. 4. Mass spectrum of acetonide.

(5) 1-Hydrazinophthalazine pyruvic acid hydrazone (pyruvate)[18]. 1-Hydrazinophthalazine-HCl (395 mg; 2 mmoles) and 1 ml pyruvic acid were refluxed in 5 ml of methanol. The methanol was evaporated. After addition of 1 ml of water, the sample was extracted with isopropanol–chloroform (1:3). The extracts were first dried over sodium sulfate and the solvent was subsequently evaporated. Yield: 70 mg or 15% of theory. The compound was esterified with trimethylsilylating reagent and injected onto the gas chromatograph for identification. No molecular ion was observed. The base peak of the spectrum was represented by the ion at *m/e* 212 (M − TMS-OH). Other ions of significance were *m/e* 184 (212 − CO) and *m/e* 115. Methylating the compound with Methelute (Pierce, Rockford, Ill., U.S.A.) yielded the N,O-dimethylated derivative with the molecular ion at *m/e* 258. Loss of $\cdot COOCH_3$ from the molecular ion forms *m/e* 199, the base peak of the spectrum. These mass spectra therefore showed the compound to be indeed pyruvate. The ions at *m/e* 212 and *m/e* 115 were selected for SIM (Figs. 5 and 6).

(6) Phthalazine (P). Treatment of 1-hydrazinophthalazine-HCl (395 mg; 2 mmoles) with 5 ml of 1 *N* sodium hydroxide and extraction with chloroform–isopropanol (3:1) yielded 215 mg of P (82% of theory). The mass spectrum of P gave the molecular ion at *m/e* 130 as the base peak. Elimination of HCN froms *m/e* 103, loss of another HCN moiety forms *m/e* 76. The ions at *m/e* 130 and *m/e* 103 were chosen for SIM (Fig. 7).

(7) d_3-3-Methyl-s-triazolo[3,4-a]phthalazine (d_3-MTP). Synthesis of d_3-labeled MTP was accomplished analogously as described in Section 2 but with d_6-acetic anhydride. Yield after recrystallization from ethanol–water: 72 mg or 19% of theory. MS yielded the molecular ion at *m/e* 187 as the base peak, *m/e* 115 is the most abundant fragment ion found. These two ions were utilized for SIM of the compound (Fig. 2b).

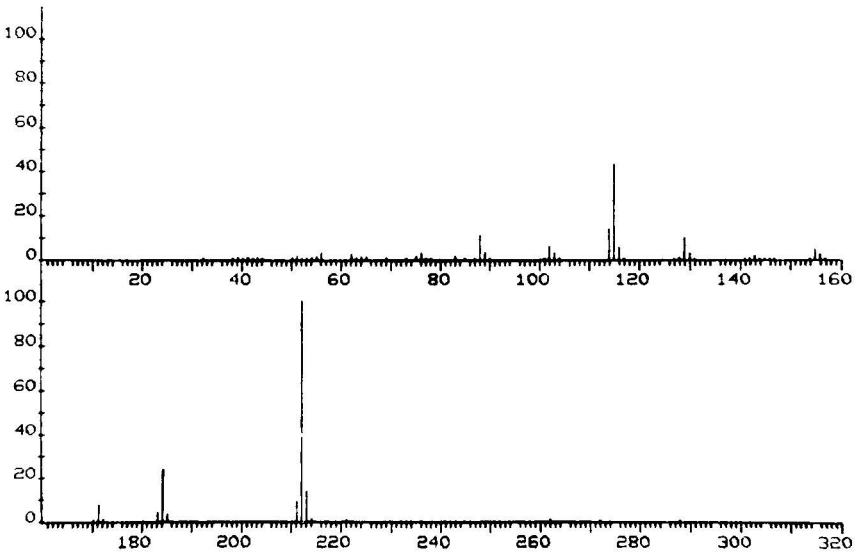


Fig. 5. Mass spectrum of pyruvate, TMS ester.

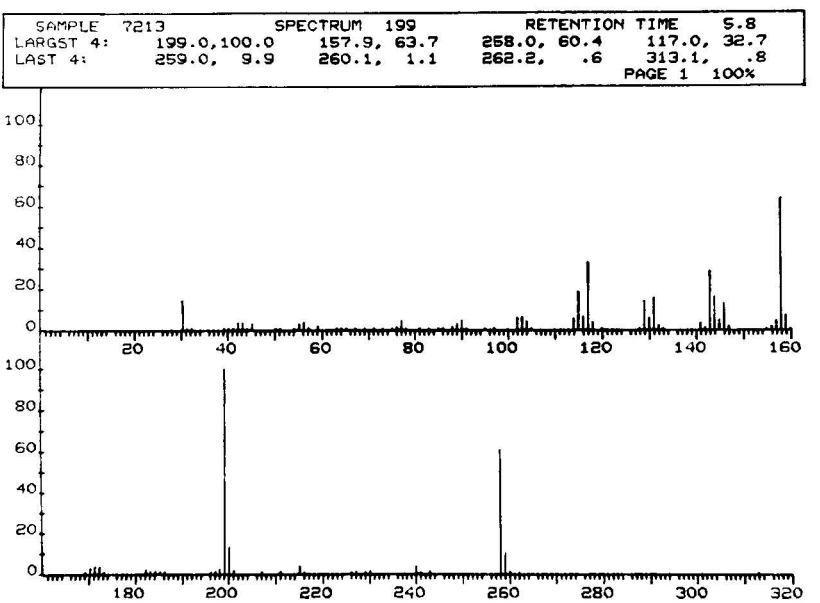


Fig. 6. Mass spectrum of pyruvate, N,O-dimethylated.

Gas chromatography–mass spectrometry

MS analysis was carried out on a combined gas chromatograph–mass spectrometer–computer system (Hewlett-Packard Models 5110A, 5980A, and 5933A). The column was a 3 ft. × 4 mm I.D. glass coil packed with 3% OV-17 on Chromosorb W (80–100 mesh). Helium carrier gas was kept at a flow-rate of 40 ml/min. The column

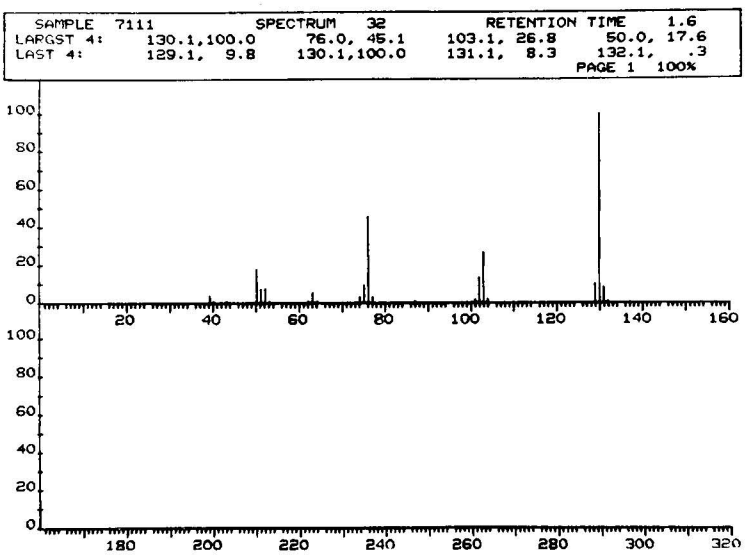


Fig. 7. Mass spectrum of P.

temperature was programmed from 170–240° at a rate of 4°/min. The injector temperature was 250°. The gas chromatograph was interfaced via a membrane separator (Hewlett-Packard) to the mass spectrometer. The ion source temperature was 210°, ionization energy 25 eV (electron impact). The mass spectrometer was interfaced to a Hewlett-Packard Model 5933A computer system which controlled the scan of the mass spectrometer, and processed and displayed mass spectral data.

Metabolic studies

(1) In vitro —Hydralazine metabolism as studied by rat liver homogenate. Rats weighing 450–600 g were fasted for a minimum of 12 h prior to decapitation. The liver was immediately removed and placed into 0° buffer (0.05 *M* potassium phosphate, pH 7.4). The liver was minced and then homogenized in 40 ml of buffer using a standard glass and PTFE tissue grinder (A. H. Thomas, Philadelphia, Pa., U.S.A.). The homogenate was centrifuged at 3000 × *g* (max.) and the supernatant decanted. For the incubations, 4.0 ml of this supernatant was added to 1.0 ml of buffer containing hydralazine (and cofactors when used). This mixture was incubated with shaking for 90 min at 37° in room atmosphere.

Immediately prior to extraction, the samples were adjusted to pH 2 and derivatized by reacting with 50% aqueous $NaNO_2$ to a final concentration of 3% (w/v) for 15 min at room temperature. This converts unmetabolized hydralazine to tetrazolo-P, which, unlike hydralazine, can be extracted from aqueous solution with organic solvents[8].

After derivatization with HONO, the samples were extracted first at the acidic pH and then again at pH 10–11. The extraction procedure involved transferring the aqueous sample to a conical centrifuge tube with 25 ml of chloroform–isopropanol (3:1). The contents were shaken for a minimum of 1 min on a vortex mixer and centrifuged. The organic (bottom) phase was removed and filtered into a round-

bottom flask. The aqueous phase was extracted two more times with 10 ml of chloroform–isopropanol and the organic phases combined and evaporated to dryness under vacuum at a maximum temperature of 35°. The aqueous phase was then adjusted to pH 10–11 and extracted again as described. Further processing of the sample for GC–MS was carried out as described for the *in vivo* experiments.

(2) In vivo —Hydralazine metabolites in rat urine. Male Sprague-Dawley rats weighing 450–600 g were anesthetized with 40 mg/kg pentobarbital sodium intraperitoneally (i.p.). Supplemental doses were administered i.p. as needed. The bladder was exposed via a small midline abdominal incision. A short segment of PE 50 tubing was inserted into the bladder and urine collected into an ice-cooled graduated cylinder. As soon as urine flow had been established, 1 mg/kg hydralazine (Apresoline) was administered i.p. in a volume of 0.5 ml. Care was taken that there was no effluent from the area of incision. The hydralazine solution contained a total of 8×10^5 cpm of ^{14}C-labeled hydralazine (specific activity 6.77 mCi/mmole). Urine was collected for 4–5 h. Upon termination of the procedure, the urine was either analyzed directly or frozen immediately for subsequent analysis within 24 h. Before acidification of the urine (2–3 ml), 1 mg of EDTA was added. This was followed by 1 ml of 2 *N* HCl and 0.2 ml of a 50% $NaNO_2$ solution. The reaction mixture was allowed to stand for 15 min. Estraction was carried out with three 10-ml portions of chloroform–isopropanol (3:1). The urine was then adjusted to pH 10 with 4 *N* NaOH solution and re-extracted with three portions chloroform–isopropanol. The extracts were combined and dried over Na_2SO_4.

Aliquots of this solution were transferred to Reactivials (Pierce, Rockford, Ill., U.S.A.) and evaporated to dryness. The sample was redissolved in 50 μl acetonitrile. Then 50 μl of Regisil-TMCS were added and the sample heated at 100° for 15 min. After addition of the deuterium-labeled internal standard (d_3-MTP), aliquots were injected onto the GC column for analysis by GC–MS.

RESULTS AND DISCUSSION

Mass spectrometric fragmentation pathway

It is interesting to note that, except for P itself, all the tricyclic derivatives of hydralazine as well as acetonide and pyruvate yield an abundant fragment ion at *m/e* 115. Little or no contribution from background impurities of the biological sample was observed for this ion. Therefore *m/e* 115 served as a characteristic feature to recognize hydralazine metabolites in the sample by MS even when no standard was available. The formation of this ion is rationalized in the fragmentation pathway for the TMS ester of pyruvate given in Fig. 8.

Elimination of TMS-OH from the unobserved molecular ion leads to *m/e* 212. Expulsion of a CO moiety from *m/e* 212 yields MTP at *m/e* 184. Further losses of CH_3CN and nitrogen lead to *m/e* 115. This explains why *m/e* 115 occurs in MTP as well as in d_3-MTP, TP, tetrazolo-P, and in the hydrazone derivatives. Expulsion of HCN from this ion leads further to *m/e* 88, a fragment ion also found in most of the hydralazine derivatives, but due to background contribution, this ion is less suitable for SIM.

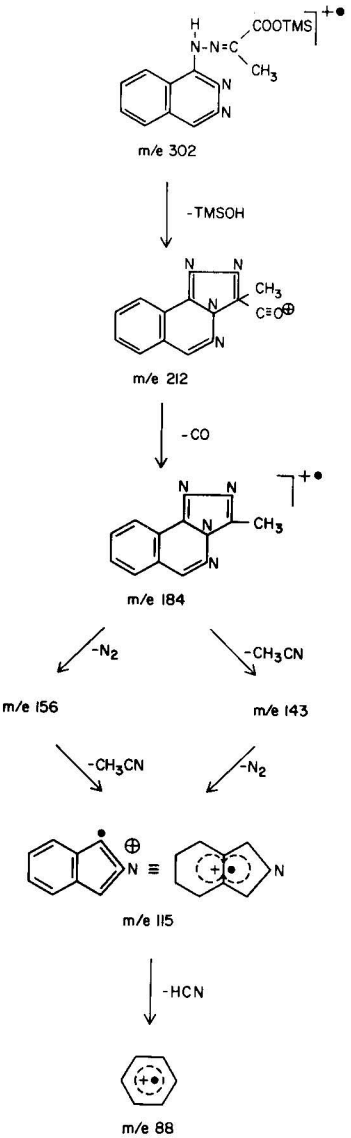


Fig. 8. Fragmentation pathway of pyruvate, TMS ester.

Recovery studies

^{14}C-Labeled internal standards were synthesized analogously to the syntheses for corresponding nonradioactive standards. ^{14}C-Hydralazine was directly added to urine and converted to tetrazolo-P as already described. Extraction was carried out in the same manner as described for the nonradioactive compounds. Radioactivity was measured with a Packard 3375 liquid scintillation spectrometer. Table I shows the recoveries obtained.

When ^{14}C-hydralazine was administered to rats and their urine collected for

TABLE I

RECOVERIES OF STANDARDS FROM BIOLOGICAL SAMPLES

Compound	*Recovery (%)*
MTP	98
TP	99
Tetrazolo-P	95
Pyruvate	76

5 h following a single i.p. dose, recovery was 79.4%. When this urine was incubated with Glusulase (Endo Labs., Garden City, N.J., U.S.A.) for 24 h at 37°, recovery increased as follows: recovery of radioactivity previously unrecovered, 45.6%; total recovery, 88.7%. The additional recovery of 9.3% radioactivity indicates that this amount was originally present in the urine as glucuronides or sulfates.

GC–MS analysis

Table II list the ions chosen for SIM.

TABLE II

GC–MS ANALYSIS OF STANDARDS

Compound	*Retention time (min)*	*Ions for SIM (m/e)*	*Base peak of mass spectrum (25 eV)*
P	1.7	103; 130	130
Phthalazinone	2.3	117; 146	146
Acetonide	4.9	115; 185; 200	185
TP	8.0	115; 170	170
Tetrazolo-P	8.9	115	115
MTP	9.6	115; 184	184
d_3-MTP	9.6	115; 187	187
Pyruvate, TMS ester	17.0	115; 184; 212	212

Figs. 9 and 10 show the SIM curves for the standards: P, acetonide, TP, tetrazolo-P, MTP, d_3-MTP, and pyruvate, TMS ester.

Up to four ions can be monitored at once with the Hewlett-Packard GC–MS–computer system, but up to four groups of ions can be followed during a GC run. Fig. 11 shows a SIM chromatogram of a rat urinary extract. The group chosen monitors, MTP, d_3-MTP, TP, and tetrazolo-P, represented by the ions at *m/e* 184, 187, 170, and 115. The first three *m/e* values represent the molecular weights and base peaks in the mass spectra of these compounds, respectively; *m/e* 115 is the characteristic fragment ion common to all four of these compounds.

All of the compounds listed in Table III were found to be present in the sample. The occurence of P[11,18], phthalazinone[19], MTP[13–15], TP[19,20], and pyruvate[9] has been reported in the literature previously. The findings that acetonide is also a metabolite of hydralazine is therefore not surprising. It was suggested[11,20] that TP was formed by oxidative demethylation of MTP and 3-hydroxymethyl-TP was indeed identified in human urine[20]. Since no standard was available for this compound,

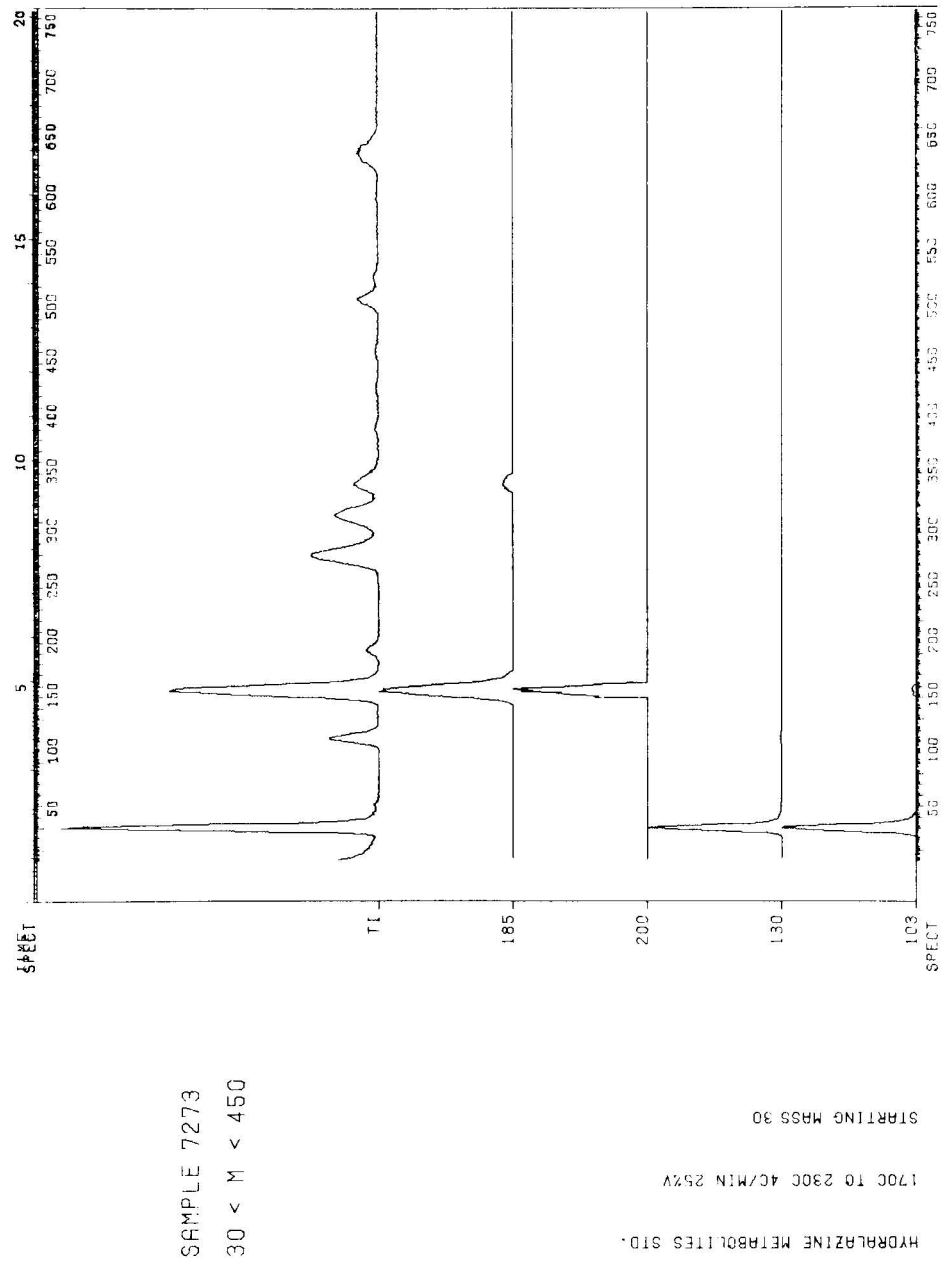


Fig. 9. SIM for standards: *m/e* 200 and 185 for acetonide; *m/e* 130 and 103 for P.

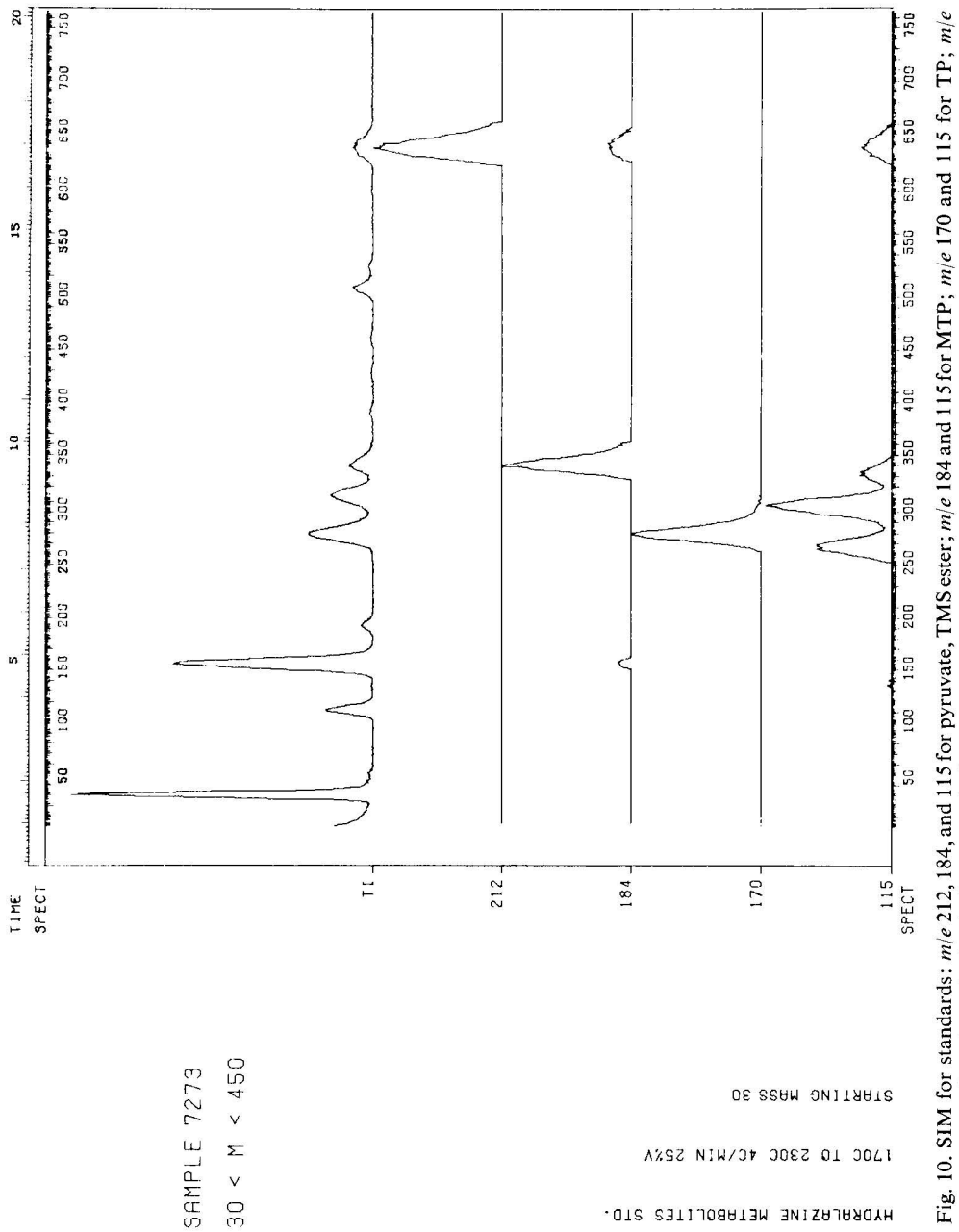


Fig. 10. SIM for standards: *m/e* 212, 184, and 115 for pyruvate, TMS ester; *m/e* 184 and 115 for MTP; *m/e* 170 and 115 for TP; *m/e* 115 at a retention time of 8.9 min for tetrazolo-P.

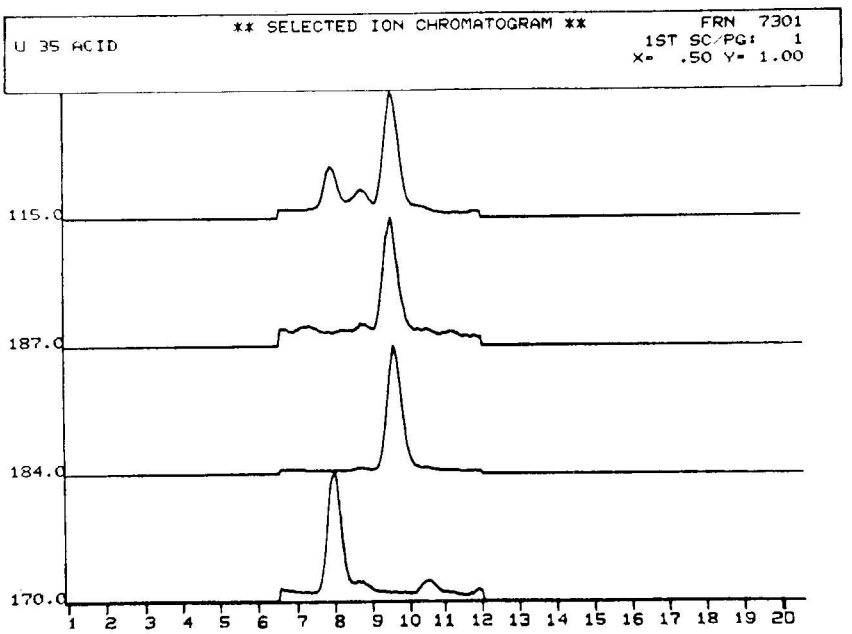


Fig. 11. SIM for rat urinary extract; *m/e* 115 for tetrazolo-P; *m/e* 187 and 115 for d_3-MTP; *m/e* 184 and 115 for MTP; *m/e* 170 and 115 for TP.

likely occurring ions due to this compound were monitored: $M^{+\cdot}$ at *m/e* 272; M – CH_3^+ at *m/e* 257; M – TMS-O^+ at *m/e* 183 and *m/e* 115. Indeed, positive responses were found at two retention times: 14.8 and 18.8 min. The full-scan mass spectrum

TABLE III

QUANTITATIVE ANALYSIS OF LIVER HOMOGENATE SAMPLES

(a) No cofactors added; (b) with cofactors added (glucose-6-phosphate, NADPH, NADH).

Compound	*Recovered (%)*	
	a	*b*
P*	0.2	1.6
Phthalazinone*	7.0	4.5
Parent drug*	0.4	0.2
MTP*	69.5	70.8
TP-CH_2OH	12.2	9.5
TP-COOH	0.1	0.6
TP*	6.8	5.1
"Ring-OH-MTP"	3.1	8.0
Acetonide*	0.8	0.6
Pyruvate*	0.1	0.1
	100.2	100.0

* For these compounds standards were synthesized and their retention times on GC and their mass spectra matched these standards.

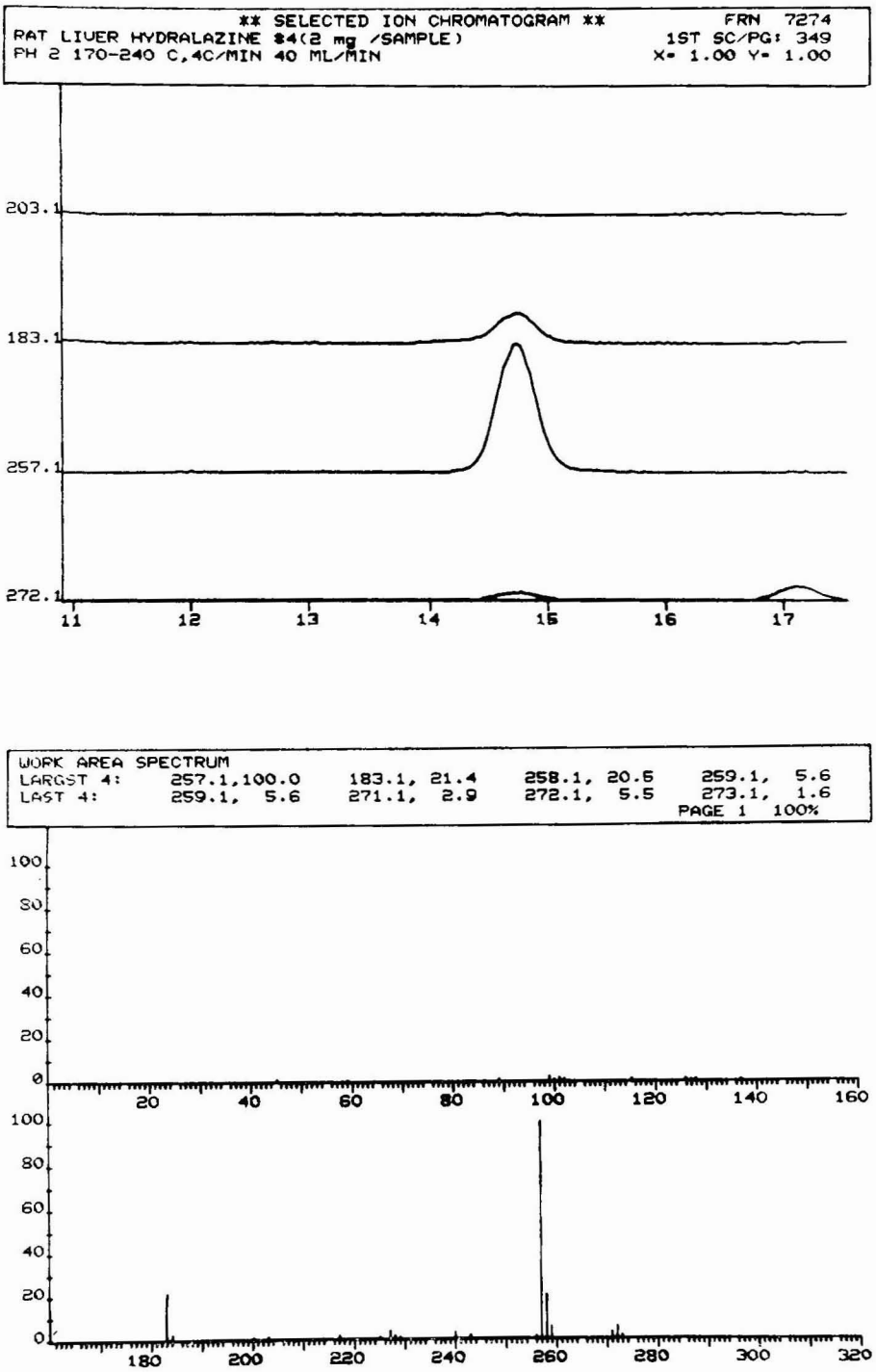


Fig. 12. Mass spectrum of the compound with retention time 14.8 min tentatively identified as 3-hydroxymethyl-TP, TM ester.

TABLE IV

QUANTITATIVE ANALYSIS OF URINARY EXTRACT

Compound	*%*
P*	6.9
Phthalazinone*	3.4
Parent drug*	2.0
MTP*	31.8
TP-CH_2OH	4.3
TP-COOH	0.2
TP*	20.5
"Ring-OH-MTP"	29.5
Acetonide*	0.8
Pyruvate*	0.6
	100.0

* For these compounds standards were synthesized and their retention times on GC and their mass spectra matched these standards.

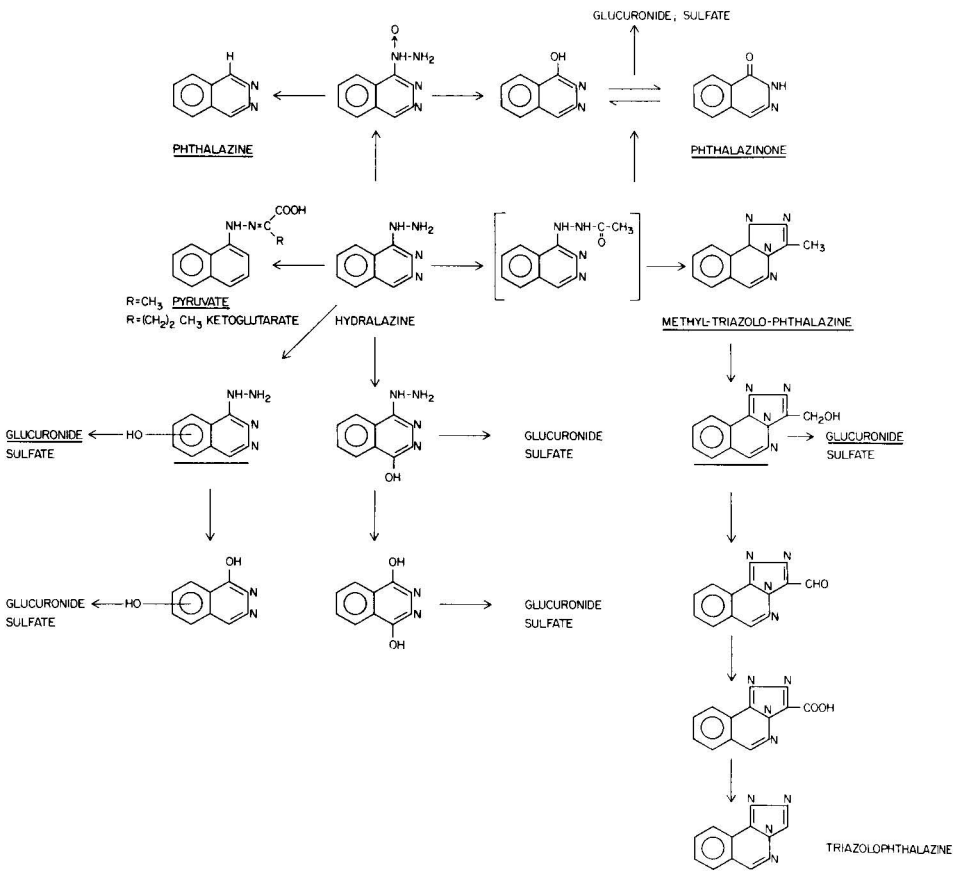


Fig. 13. Metabolic scheme of hydralazine. Underlined compounds have been reported in the literature previously.

of the GC peak at 14.8 min is shown in Fig. 12. The peak at 18.8 min gives a similar mass spectrum, but *m/e* 272 is the base peak of the spectrum. We assume therefore that the first peak represents 3-hydroxymethyl-TP, whereas the second one may represent a ring-hydroxylated MTP. However, further investigation is still needed, especially synthesis of the appropriate standard will be necessary.

Table III shows a quantitative analysis of a liver homogenate sample. MTP was found to be the major metabolite. Extensive further metabolism of this product is observed, as indicated by the oxidation products TP-CH_2OH, TP-COOH, and the decarboxylation product of TP-COOH, TP. In addition, significant amounts of "ring-hydroxylated MTP" were found. M-Carboxyl-TP was tentatively identified by the occurrence of ions *m/e* 286 ($M^{+\cdot}$), *m/e* 271 ($M - CH_3^+$), and *m/e* 197 (M — TMS-O^+), however, no *m/e* 115 was observed for this compound. Synthesis of the appropriate standard will therefore be necessary to clearly identify this product.

Analysis of a single rat urine sample is shown in Table IV. The most striking difference observed, as compared to the rat liver homogenate, is the lower ratio of MTP *versus* TP-CH_2OH and "ring-hydroxylated MTP". The higher percentage of P is most likely due to decomposition of excreted parent drug and/or the hydrazones with pyruvic acid and acetone. The decomposition takes place spontaneously at the pH of distilled water[21] (usually about 5.8–6.4) and is even more pronounced at more basic pH values[3].

Fig. 13 represents the metabolic scheme for hydralazine which takes into account fall the metabolic products reported in the literature, those described in this report, and those expected but not yet identified. (Underlined compounds represent those reported in the literature.)

ACKNOWLEDGEMENTS

This work was supported by NIH 5T32 GM07014 and the Veterans Administration, MRIS 5628. The technical assistance of Mr. Marion S. Dyches, Jr. is gratefully appreciated.

REFERENCES

1 D. Alrcon-Segovia, K. G. Wakimn, J. W. Worthington and L. E. Ward, *Medicine*, 46 (1967) 1.
2 R. Zacest, E. Gilmore and J. Koch-Weser, *N. Engl. J. Med.*, 286 (1972) 617.
3 A. R. Schulert, *Arch. Int. Pharmacol. Ther.*, 131 (1961) 1.
4 H. M. Perry, H. A. Schroeder and J. W. Morrow, *Amer. J. Med. Sci.*, 228 (1954) 405.
5 R. Zacest and J. Koch-Weser, *Clin. Pharmacol. Ther.*, 13 (1972) 420.
6 M. Reidenberg, D. Drayer, J. Martin, A. L. de Marco and C. T. Bello, *Clin. Pharmacol. Ther.*, 14 (1974) 971.
7 S. B. Zak, M. F. Bartlett, W. E. Wagner, T. G. Gilleran and G. Lukas, *J. Pharm. Sci.*, 63 (1974) 225.
8 D. B. Jack, S. Brechbühler, P. H. Degen, P. Zbinden and W. Riess, *J. Chromatogr.*, 115 (1975) 87.
9 W. M. McIsaac and M. Kanda, *J. Pharmacol. Exp. Ther.*, 143 (1964) 7.
10 D. E. Drayer, J. M. Strong, B. Jones, A. Sandler and M. M. Reidenberg, *Drug Metab. Disp.*, 2 (1974) 499.
11 J. M. Lesser, Z. H. Israili, D. C. Davis and P. G. Dayton, *Drug Metab. Disp.*, 2 (1974) 351.
12 C. D. Douglass and R. Hogan, *Proc. Soc. Exp. Biol. Med.*, 100 (1959) 446.
13 S. Edwards and F. H. Marquardt, *Hoppe-Seyler's Z. Physiol. Chem.*, 350 (1969) 85.

14 H. Zimmer, J. McManus, T. Novinson, E. V. Hess, and A. H. Litwin, *Arzneim.-Forsch.*, 20 (1970) 1386.
15 H. Zimmer, J. Kokosa and D. A. Garteiz, *Arzneim.-Forsch.*, 23 (1973) 1028.
16 H. M. Perry and H. A. Schroeder, *Amer. J. Med. Sci.*, 228 (1954) 396.
17 M. Velasco, C. A. Gilbert, C. O. Rutledge and J. L. McNay, *Clin. Pharmacol. Ther.*, 18 (1975) 145.
18 J. Druey and B. H. Ringer, *Helv. Chim. Acta*, 34 (1951) 195.
19 S. B. Zak, T. G. Gilleran, J. Karliner and G. Lukas, *J. Med. Chem.*, 17 (1974) 381.
20 H. Zimmer, R. Glaser, J. Kokosa, E. V Hess and A. Litwin, *J. Med. Chem.*, 18 (1975) 1031.
21 K. D. Haegele, H. B. Skrdlant and J. L. McNay, unpublished results.

Journal of Chromatography, 126 (1976) 535–545
© Elsevier Scientific Publishing Company, Amsterdam — Printed in The Netherlands

CHROM. 9402

GAS CHROMATOGRAPHIC STUDY OF FREE POLYOLS AND ALDOSES IN CATARACTOUS HUMAN LENS TISSUE

C. D. PFAFFENBERGER, J. SZAFRANEK and E. C. HORNING
Institute for Lipid Research, Baylor College of Medicine, Houston, Texas 77030 (U.S.A.)

SUMMARY

An analytical procedure for the qualitative and quantitative analysis of human lens tissue for polyol and aldose content is described. Profile samples are obtained by direct derivatization of lyophilized lenses. The components are analyzed as per-O-acetylpolyols (from the polyols) and per-O-acetylaldononitriles (from the aldoses). This procedure converts each component into a single derivative and terminal dissymmetry for each aldose is retained. The derivatives form in quantitative yield, give good chromatographic peaks, are thermally stable and readily volatilized. They are not subject to adsorption on gas chromatographic columns and are suitable for both qualitative and quantitative analytical studies.

Six non-cataractous lenses and fourteen lenses from patients with senile cataract (in seven instances complicated by diabetic pathology) were analyzed. Thermostable borosilicate glass open-tubular capillary columns, coated with the non-polar phase SE-30, and containing dispersed particles of silanized silicic acid, were used for the gas chromatographic separations.

The results are discussed in relation to what is known from earlier studies of human and animal cataracts.

A gas chromatographic method for determining the polyol and aldose excretion levels of controlled diabetics is also reported along with a typical metabolic profile.

INTRODUCTION

Cataract formation results in a loss of transparency of the lens of the eye. No cure or means of preventing senile cataract, the most common form of the disorder, is known. Most investigations of this circumstance have indicated that cataract formation, both in man[1–4] and in experimental animals[5–13], involves the accumulation of one of several polyols within the tissue of the lens. A diabetic is about five times more likely to have an initial cataract operation than is a nondiabetic of the same age and sex[14]; the polyol in these instances is believed to be glucitol.

It has recently become possible to separate complex mixtures of polyols and aldoses completely and rapidly by gas chromatography (GC)[15]. The recommended GC procedure, based on the classical Wohl degradation of aldoses, includes the use

of high-resolution glass open-tubular capillary columns which possess high theoretical plate efficiencies (125,000–150,000). In this method each sample component forms a single derivative with retention of terminal dissymmetry for each aldose. Polyols are analyzed as per-O-acetylpolyols and aldoses as per-O-acetylaldononitriles. The procedure has been successfully used[16] to determine normal excretion ranges and average excretion values for seventeen polyols and aldoses usually found in the urine of human neonates, juveniles, and adults.

This study includes the results of GC analyses of six human non-cataractous lenses (obtained at autopsy) and fourteen lenses from patients having senile cataract, with seven cases complicated by diabetic pathology. Values are reported in μg of free polyol or aldose per mg of lyophilized lens. Also included are excretion values (mg/g creatinine) for eleven polyols and aldoses found in the urine of five of the subjects whose lenses were analyzed. Urinary analyses of two closely controlled diabetics are included in this group.

EXPERIMENTAL

Reference compounds

Reference aldoses, alditols, *myo*-inositol and glyceryl-1-decyl ether were purchased from Supelco (Bellefonte, Pa., U.S.A.).

Preparation of analytical sample from lens tissue

Adherent tissue (zonular ligament, ciliary muscle) was removed from surgically extracted human lenses. The intact lens was quickly weighed and frozen under an atmosphere of nitrogen. Lyophilization was effected over a 48-h period at 0.5 Torr using a Virtis Model 10-300CF lyophilizer. The dry lens was weighed (Table I), pulverized to a homogeneous powder using a glass rod, and stored under nitrogen, under deep-freeze conditions, until analyzed.

Analytical samples were prepared by adding to 10 mg of powdered lens, 10 mg of hydroxylamine hydrochloride, 0.0315 mg of glyceryl-1-decyl ether (internal reference compound, from a solution of 6.30 mg per 10.0 ml of methanol) dissolved in 50 μl of methanol, 23 mg of sodium acetate, and 1 ml of methanol. The mixture was heated at 60° for 2 h, evaporated to dryness using a nitrogen stream, and treated with 1 ml of acetic anhydride. After this mixture had been heated for 2 h at 110°, it was allowed to stand overnight in a desiccator for complete conversion of the carbohydrates, which react more slowly in tissue preparations than they do as pure reference compounds[17]. Precipitated protein was removed by centrifugation. GC samples were removed from the clear supernatant solution and co-injected with *n*-alkanes when methylene unit (*MU*)[18,19] values were being determined (Tables I and II).

Preparation of analytical sample from urine

Urine samples from patients were collected over a 24-h period just prior to cataract extraction. No preservative was used, but the sample was kept at 4° during the collection period and stored under deep-freeze conditions as soon as possible after the volume had been determined. The pH of a 20-ml aliquot of urine was adjusted to 4.5 using 10% aqueous acetic acid. This sample was poured onto a packing of DEAE-Sephadex A-25 Medium (Pharmacia, Uppsala, Sweden) contained in a

10 × 1.3 cm I.D. glass column. Basic and neutral compounds were eluted by washing the packing with 100 ml of deionized water which had been glass-distilled from potassium permanganate. The eluate was collected in a 250-ml round-bottomed flask and lyophilized to constant weight. The dry residue was dissolved in 10 ml of methanol. A 1-ml aliquot of the methanolic solution was heated with 5 mg of hydroxylamine hydrochloride and 12.5 mg of sodium acetate at 60° for 30 min in a PTFE-lined screw-cap vial. The product was dried at 40° using a nitrogen stream, and derivatized in 1 h using 300 μl of acetic anhydride at 100°. When an internal reference compound was required, 200 μl of a solution of glyceryl-1-decyl ether (6.30 mg/10.0 ml of methanol) were added prior to heating with hydroxylamine hydrochloride. Also, in these instances 100 μl of pyridine was substituted for the sodium acetate catalyst, and the dry residue from these reactions was treated with 300 μl of acetic anhydride and 50 μl of pyridine at 100° for 1 h.

Gas chromatography

Column preparation. Sixty-meter borosilicate glass capillaries (1.0 mm O.D., 0.3 mm I.D.) were drawn from 1.25-m tubes (7.8 mm O.D., 3.8 mm I.D.) using a Hupe-Busch glass drawing and coiling apparatus (now available from Hewlett-Packard). Novotný and Zlatkis[20] have described the general procedure. Pyrex tubes to be drawn were successively rinsed with acetone, methylene chloride, 1% aqueous potassium hydroxide, and methanol, and dried under vacuum. The diameter of the capillary coil was 12 cm.

Using the method of German and Horning[21], glass capillaries silanized with dimethyldichlorosilane (DMCS) and coated with SE-30 containing Silanox 101 (Cabot, Boston, Mass., U.S.A.) were prepared. These were conditioned under carrier gas (nitrogen) flow by temperature programming at 1°/min from 25–280°, holding at 280° for 2 h, lowering to 200°, programming at 1°/min to 300°, and holding at 300° for 1 h. The theoretical plate efficiencies of the resulting columns (for *n*-tetracosane at 250°) ranged from 125,000–150,000.

Instrumental conditions. Separation of both the lens and the urinary polyols and aldoses as per-O-acetylpolyols and per-O-acetylaldononitriles was carried out with a Hewlett-Packard Model 5710A gas chromatograph which had been modified to include a previously described[22] glass inlet system and to accept 60-m glass capillary columns. A Fisher Recordall Series 5000 recorder was used and the flame ionization detector was modified (see next section) for use with glass capillary columns. Temperature programming was employed at 1°/min from 150°. Other GC conditions included: sample volume, 2 μl; split ratio, 5:1; precolumn-inlet splitter temperature, 250°; detector block temperature, 300°; column inlet pressure, 18 p.s.i., resulting in a carrier gas (helium) linear velocity of 16–18 cm/sec (200°); hydrogen flow-rate, 30 ml/min; air flow-rate, 240 ml/min; nitrogen make-up gas to the detector, 20 ml/min.

Detector modification. The HP Model 18765A flame ionization detector (standard equipment on the Hewlett-Packard Model 2710A gas chromatograph) is a highly satisfactory detector for packed columns. The suggested carrier gas flow-rate through a 2 m × 6.4 mm O.D. conventionally packed column is 30 ml/min, and the recommended burner flow-rates are 30 ml/min hydrogen and 240 ml/min air.

Carrier gas (helium) flow-rate through an open-tubular glass capillary column rarely exceeds 2 ml/min. It was therefore necessary to modify the standard flame noz-

zle of the detector as indicated in Fig. 1. (Extensive modification of another type of flame ionization detector has been reported previously[23].)

The modification consisted of drilling the bottom end of the original flame nozzle stem (1) to a diameter which could accept a concentric 1/8 in. length of stainless-steel hypodermic tubing (1/32 in. O.D., 0.020 in. I.D.). When this tube (A) was to be joined to the end of the modified flame nozzle, it was first inserted all the way into the newly drilled portion of the nozzle, then withdrawn 1/32 in., and positioned there until the nut which anchors the two-piece ferrule union (2) to the base of the detector was tightened. This arrangement made it possible to introduce sufficient make-up gas (nitrogen) into the flame so that the original ion collector of the detector could be utilized.

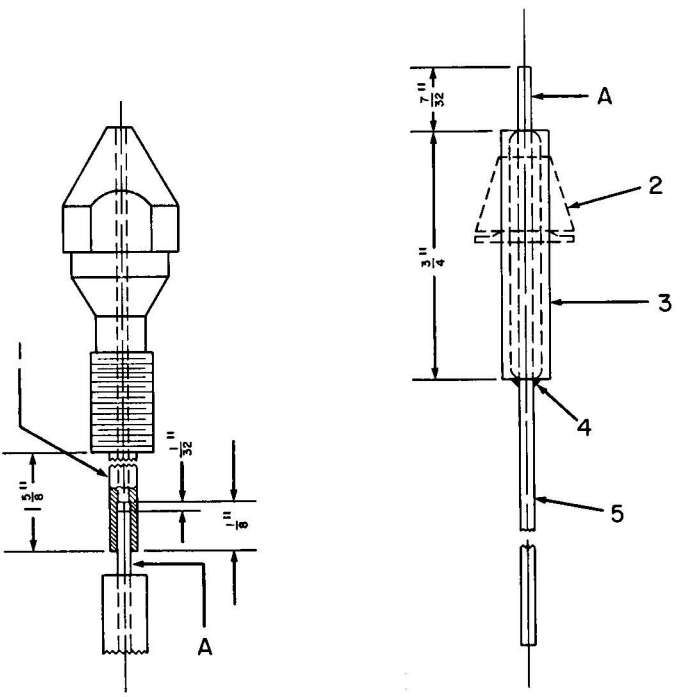


Fig. 1. Flame nozzle assembly for modified flame ionization detector: (1) original flame nozzle stem; the bottom end was drilled to accept a concentric 1/8 in. length of hypodermic tubing, (2) stainless-steel two-piece Swagelok union ferrule by which assembly A is attached to the base of the detector, (3) stainless-steel tubing (1/8 in. O.D.; 0.020 in. wall thickness) with both ends rolled closed, and then drilled to accept 1/32 in. tubing, (4) silver-soldered joint, (5) stainless-steel hypodermic tubing (1/32 in. O.D.; 0.020 in. I.D.; 2 1/2 in. long).

Quantitative analysis. Calculations were made by hand; area measurements were made by multiplying the height of the peak by the width at half height. The chart speed and pen line width are variables that affect the results; in our work the height was measured to the outside of the pen line, but the width at half height was measured to the inside of the pen line. A magnifying scale was used for the width measurement. Usually a chart speed of 1.25 cm/min was used for quantitative calculation

charts and 0.5 cm/min for illustrations. The precision of this method is about 2% (standard deviation).

The quantitative calculations were based on previously reported molar response factors (MRF), calculated in relation to the detector response observed for the di-acetyl derivative of glyceryl-1-decyl ether[16].

Mass spectrometry

Mass spectra were obtained using an LKB 9000 gas chromatograph–mass spectrometer (LKB Produkter, Stockholm, Sweden) fitted with a 3 m × 4 mm I.D. glass column packed with 2% SE-30 on Gas-Chrom P (100–120 mesh, acid-washed, DMCS-treated); column temperature, 180°; flash heater temperature, 230°; molecular separator temperature, 260°; ion source temperature, 250°; electron energy, 70 eV.

RESULTS AND DISCUSSION

Glass open-tubular capillary column separations

Analyses of six non-cataractous lenses and fourteen lenses from patients having senile cataract (seven of the cases complicated by diabetic pathology) are reported in Table I. The age range in both the non-patient and the patient group was from 52–81 years. A typical gas chromatogram is given in Fig. 2 for lens 5. Polyol and aldose contents of the lyophilized lenses were determined according to a slightly modified version of the method of Pfaffenberger *et al.*[16]. GC separations were made using thermostable borosilicate glass open-tubular capillary columns, coated with the non-polar phase SE-30, and containing dispersed particles of silanized silicic acid. Identities were confirmed by retention behavior and by mass spectral data obtained using an LKB 9000 gas chromatograph–mass spectrometer. Fig. 3 shows the mass spectra of *myo*-inositol from lens 12, and of an authentic reference sample (both analyzed as the corresponding per-O-acetylpolyol).

Free polyols and aldoses in human lenses

By far the largest free polyol component of human lens tissue is *myo*-inositol. This is evident in Fig. 2. Amounts of this component ranged (in μg/mg lyophilized lens) from 2–19 for non-cataractous lenses, 3–23 for uncomplicated senile cataractous lenses, and 7–29 for senile cataractous lenses from patients with diabetes.

All lenses contained a trace (>0.1 but <1.0 μg/mg lyophilized lens) of glucose. One non-cataractous lens, obtained at autopsy from an individual 81 years of age, contained a trace of glucitol, two of the uncomplicated senile cataractous lenses contained a trace of glucitol, and all but two of the senile cataractous lenses from patients with diabetes contained at least a trace of glucitol. Lenses 2 and 4 contained 2 and 1 μg glucitol per mg lyophilized lens, respectively.

All except two lenses (non-cataractous) contained a trace of an unidentified compound with $MU = 19.79$, and all except four lenses contained an unidentified compound with $MU = 20.95$. The first unknown was not one of the simple aldohexoses which elute within an MU range[16] of 19.02–19.56 under the analytical conditions employed here. The second unknown was not mannitol[15], galactitol[16], *scyllo*-inositol[24], or 1,5-anhydroglucitol[25]. (Study of the two unidentified compounds is continuing.)

TABLE I

POLYOLS AND ALDOSES* DETECTED IN HUMAN LENS TISSUE

	Cataractous lenses														*Non-cataractous lenses*					
	Diabetic source							*Non-diabetic source*												
Lens number	1	2	3	4	9	11	13	5	6	7	8	10	12	14	15	16	17	18	19	20
Age (years)	52	69	71	58	74	77	58	67	73	54	64	81	72	65	58	74	81	63	52	70
Dry weight (mg)**	67	58	88	65	80	59	68	69	67	55	72	51	81	61	70	86	86	73	54	64
Glucose ($MU = 19.12 \pm 0.01$)***	T§	T	T	T	T	T	T	T	T	T	T	T	T	T	T	T	T	T	T	T
Unknown 1 ($MU = 19.79$)	T	T	T	T	T	T	T	T	T	T	T	T	T	T	T	X§§	T	T	T	T
myo-Inositol ($MU = 20.50 \pm 0.03$)	15	16	12	7	29	14	21	11	3	3	19	4	23	8	2	16	19	12	2	15
Glucitol ($MU = 20.68 \pm 0.01$)	X	2	T	1	T	X	T	T	X	X	X	X	T	X	X	X	T	X	X	X
Unknown 2 ($MU = 20.95 \pm 0.01$)	T	T	T	T	T	T	T	T	T	X	T	X	T	T	X	T	T	T	X	T

* Values are in μg/mg lyophilized lens.

** Each lens was lyophilized 48 h.

*** All methylene unit (*MU*) values are for the corresponding per-O-acetylaldononitriles (from aldoses) and the per-O-acetylpolyols (from polyols) as determined on an SE-30 open-tubular glass capillary column temperature programmed at 1°/min from 150°.

§ "T" signifies $<1.0\,\mu$g/mg but $>0.1\,\mu$g/mg lyophilized lens.

§§ "X" signifies that this compound was not present above $0.1\,\mu$g/mg lyophilized lens.

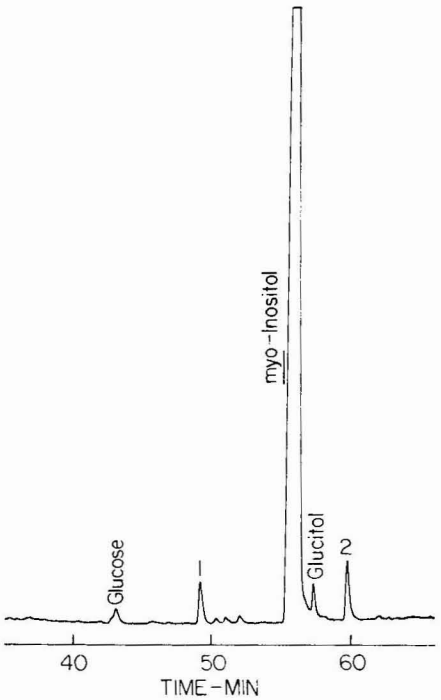


Fig. 2. Profile of the free aldoses and polyols found in human cataractous lens tissue (lens 5 of Table I). Separation of the components as per-O-acetylaldononitriles ("Wohl" derivatives from aldoses) and per-O-acetylpolyols (from polyols) was carried out on a 60-m SE-30 open-tubular glass capillary column temperature programmed 1°/min from 150°. For further conditions see text.

Structure of the human lens

The lens is an isolated organ; fibers of the zonule attach it radially to the ciliary body. The lens contains no internal blood vessels or nervous tissue. Its cells depend on the circulating aqueous humor both for needed compounds and for the removal of the products of catabolism. Trauma, various forms of radiation[26], and metabolic changes within the lens can damage it directly. Changes in the composition of the aqueous humor can upset lens metabolism and damage it indirectly[3].

Osmotic balance of the lens

A single layer of cells encases the lens and forms a capsule which permits diffusion of small molecules such as glucose, amino acids, salts, vitamins, and other substances from the aqueous humor. Amino acids are mainly responsible for maintaining osmotic balance of the lens[10]. An excess of potassium ions and a deficit of sodium ions is maintained within the tissue; potassium and chloride ions make osmotic contributions[3]. Free polyols and aldoses also affect the osmotic balance. Polyols are believed to modify the usual osmotic balance[10] of the lens and to initiate loss of its transparency.

Mechanisms initiating cataract formation

Kinoshita and coworkers have demonstrated that lens swelling can be caused

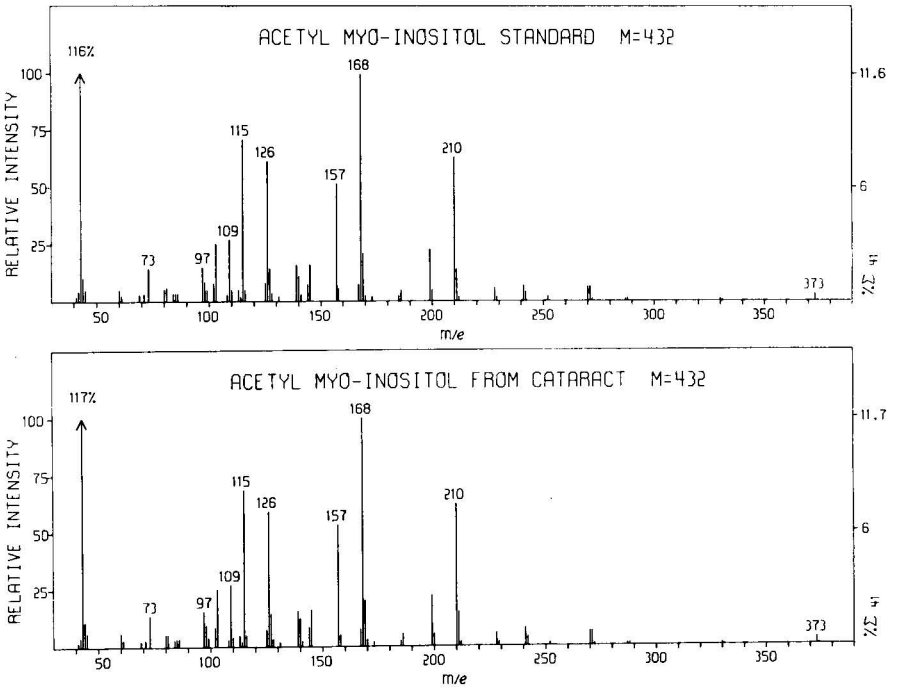


Fig. 3. Mass spectra of authentic *myo*-inositol and *myo*-inositol found in cataractous lens 12 (both samples analyzed as the corresponding per-O-acetylpolyol). The most abundant ion fragment at *m/e* 43 (CH_3CO^+) is not taken as the base peak; the ion fragment at 168 is used. Instrumental conditions are given in Experimental.

by any of the three cataractogenic sugars: glucose[9], galactose[8], and xylose[12]. If the lens is exposed to one of these aldoses, the sugar is converted into the corresponding sugar alcohol by the enzyme aldose reductase (EC 1.1.1.21), which requires for its activity the reduced coenzyme nicotinamide-adenine dinucleotide phosphate (NADPH). With this system, glucose is converted into glucitol, galactose into galactitol, and xylose into xylitol.

The sugar alcohol, because it is not further metabolized effectively and is not able to penetrate readily the lens capsule, accumulates in higher than normal amounts[5]. The hypertonicity this creates is corrected by an influx of water[3]. The osmotic changes which occur initially from polyol accumulation do not seriously alter the state of viability of the lens, and in the early stages of sugar cataract formation the process is reversible. If normal osmotic balance is not restored, lens opacity develops. At this stage there is a gradual breakdown of the permeability barrier and the electrolytes and polyols, including *myo*-inositol[27,28], become freely permeable and only the larger proteins are retained. After this stage becomes fully established, quantities of free sugar alcohol found in the cataract are insignificant and free *myo*-inositol levels are significantly altered from normal. This agrees with the wide range of values obtained experimentally in this study for *myo*-inositol.

Senile cataract accompanied by diabetic pathology

It is accepted that blood sugar fluctuates in diabetics and that the control

achieved by therapy may vary over both short and long periods. Caird *et al.*[29] showed that control of diabetes was below average in effectiveness in diabetics who required cataract extraction. He and his coworkers[30] later demonstrated a direct relationship between degree of control of diabetes and frequency of lens opacity in men of middle age.

The low concentration of glucitol observed in the cataractous lens has been explained[1] by the facts that diabetes is usually well controlled before an operation and the cataractous lens (advanced) is abnormally permeable and has lost glucitol to the aqueous humor by diffusion[3].

Excretion values for urinary polyols and aldoses

Table II contains excretion values (in mg/g creatinine) for eleven polyols and aldoses found in the urine of five of the subjects whose lenses were analyzed. (The peak-numbering system used in Table II and Figs. 4 and 5 is the same one employed in previous[15,16] publications.) The excretion values of samples LU5, LU14 and LU15 are typical of the adult human over 50 years of age[16]. No obvious difference can be seen between the non-cataractous subject (LU15) and the two patients having senile cataracts (LU5 and LU14).

TABLE II

EXCRETION VALUES* FOR URINARY POLYOLS AND ALDOSES

*Peak No.***	*Assignment****	*MU value (±0.01)*	*LU1*§	*LU5*	*LU11*	*LU14*	*LU15*
1	Erythritol	15.73	42	65	44	50	46
2	Threitol	15.91	10	11	10	14	10
7	Ribitol	18.22	T§§	12	8	18	6
9	Arabinitol	18.30	12	48	27	54	33
10	Xylitol	18.47	12	11	10	58	7
12	Glucose	19.13	56	5	32	14	6
13	Galactose	19.41	T	T	T	X§§§	T
14	*myo*-Inositol	20.50	6	25	8	7	16
15	Mannitol	20.60	X	12	92	X	T
16	Glucitol	20.68	4	9	10	X	4
17	Galactitol	20.76	X	4	6	6	9

* Values are in mg/g creatinine.

** The peak numbering system is identical to the one used in ref. 16.

*** Based on methylene unit (*MU*) values; *myo*-inositol was confirmed by gas chromatography–mass spectrometry using an LKB 9000.

§ LU1 is the urinary sample which corresponds to lens 1 etc.

§§ "T" signifies a trace component (<4 mg/g creatinine).

§§§ "X" signifies that this compound is not present in the chromatogram.

Fig. 4 is a metabolic profile of the urinary polyols and aldoses excreted by the patient from whom non-cataractous lens 15 was obtained at autopsy. Excretion values for glucose, *myo*-inositol and glucitol in this sample were 6, 16, and 4 mg/g creatinine, respectively.

Fig. 5 is a urinary metabolic profile for a diabetic patient with senile cataract.

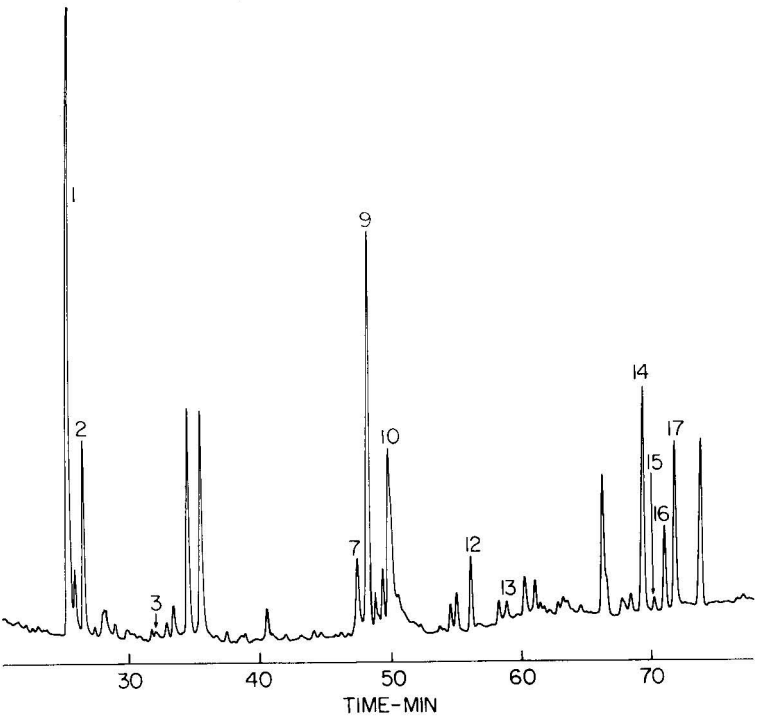


Fig. 4. Metabolic profile of urinary polyols and aldoses excreted by a patient with non-cataractous lens (LU15). Separation was carried out on a 60-m SE-30 open-tubular glass capillary column temperature programmed 1°/min from 150°. For further conditions see text. 1 = Erythritol; 2 = threitol; 3 = ribose; 7 = ribitol; 9 = arabinitol; 10 = xylitol; 12 = glucose; 13 = galactose; 14 = *myo*-inositol; 15 = mannitol; 16 = glucitol; 17 = galactitol.

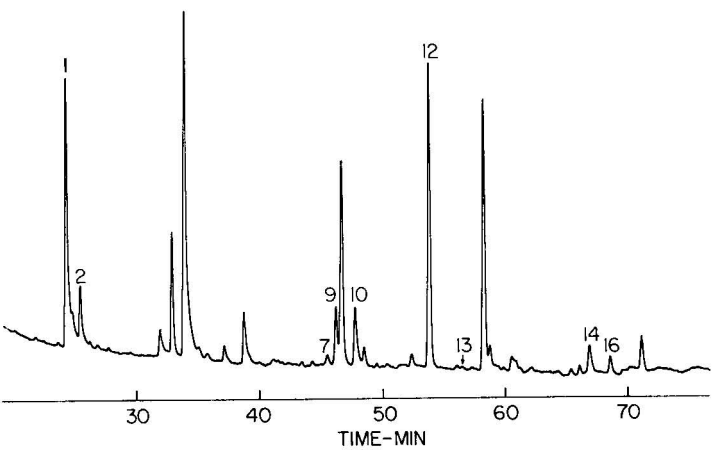


Fig. 5. Metabolic profile of the urinary polyols and aldoses excreted by a controlled diabetic patient from whom senile cataractous lens 1 was obtained. Separation was carried out on a 60-m SE-30 open-tubular glass capillary column temperature programmed 1°/min from 150°. For further conditions see text. 1 = Erythritol; 2 = threitol; 7 = ribitol; 9 = arabinitol; 10 = xylitol; 12 = glucose; 13 = galactose; 14 = *myo*-inositol; 16 = glucitol.

Excretion values for glucose, *myo*-inositol and glucitol in this sample were 56, 6, and 4 mg/g creatinine, respectively. The excretion values for sample LU11, also from a controlled diabetic with senile cataract, are similar except for elevated mannitol excretion.

ACKNOWLEDGEMENTS

This work was aided by Grant GM-13901 and Contract NIH 69-2161 of the National Institute of General Medical Sciences, Grant HL-17269 of the National Heart and Lung Institute, and Grant Q-125 of the Robert A. Welch Foundation.

We are indebted to our colleague, J. W. Boys-Smith, M.D., Department of Ophthalmology, for the lenses used in this study. We also thank Mr. A. G. Grill for his aid in the modification of the flame ionization detector, and for the drawing used in Fig. 1.

REFERENCES

1 A. Pirie and R. van Heyningen, *Exp. Eye Res.*, 3 (1964) 124.
2 R. Gitzelmann, H.-C. Curtius and I. Schneller, *Exp. Eye Res.*, 6 (1967) 1.
3 J. H. Kinoshita, *Invest. Ophthalmol.*, 4 (1974) 713.
4 D. J. Heaf and D. J. Galton, *Clin. Chim. Acta*, 63 (1975) 41.
5 R. van Heyningen, *Nature (London)*, 184 (1959) 194.
6 E. Cotlier, *Invest. Ophthalmol.*, 7 (1968) 118.
7 J. H. Kinoshita, D. Dvornik, M. Kraml and K. H. Gabbay, *Biochim. Biophys. Acta*, 158 (1968) 472.
8 J. H. Kinoshita, L. O. Merola and B. Tung, *Exp. Eye Res.*, 7 (1968) 80.
9 L. T. Chylack and J. H. Kinoshita, *Invest. Ophthalmol.*, 8 (1969) 401.
10 J. H. Kinoshita, W. G. Barber, L. O. Merola and B. Tung, *Invest. Ophthalmol.*, 8 (1969) 625.
11 D. Dvornik, N. Simard-Duquesne and M. Kraml, *Science*, 182 (1973) 1146.
12 H. Obazawa, L. O. Merola and J. H. Kinoshita, *Invest. Ophthalmol.*, 13 (1974) 204.
13 S. D. Varma and J. H. Kinoshita, *Biochim. Biophys. Acta*, 338 (1974) 632.
14 A. Pirie, *Invest. Ophthalmol.*, 4 (1965) 629.
15 J. Szafranek, C. D. Pfaffenberger and E. C. Horning, *Anal. Lett.*, 6 (1973) 479.
16 C. D. Pfaffenberger, J. Szafranek, M. G. Horning and E. C. Horning, *Anal. Biochem.*, 63 (1975) 501.
17 W. R. Sherman, M. A. Stewart, M. M. Kurien and S. L. Goodwin, *Biochim. Biophys. Acta*, 158 (1968) 197.
18 W. J. A. VandenHeuvel, W. L. Gardiner and E. C. Horning, *J. Chromatogr.*, 19 (1965) 263.
19 E. C. Horning, M. G. Horning, N. Ikekawa, E. Chambaz, P. I. Jaakonmaki and C. J. W. Brooks, *J. Gas Chromatogr.*, 5 (1967) 283.
20 M. Novotný and A. Zlatkis, *Chromatogr. Rev.*, 14 (1971) 1.
21 A. L. German and E. C. Horning, *J. Chromatogr. Sci.*, 11 (1973) 76.
22 A. L. German and E. C. Horning, *Anal. Lett.*, 5 (1972) 619.
23 P. van Hout, J. Szafranek, C. D. Pfaffenberger and E. C. Horning, *J. Chromatogr.*, 99 (1974) 103.
24 W. R. Sherman, M. A. Stewart, P. C. Simpson and S. L. Goodwin, *Biochemistry*, 7 (1968) 819.
25 E. Pitkänen, *Clin. Chim. Acta*, 48 (1973) 159.
26 J. H. Kinoshita, L. O. Merola and E. Dikmak, *Doc. Ophthalmol.*, 20 (1966) 91.
27 R. M. Broekhuyse, *Biochim. Biophys. Acta*, 163 (1968) 269.
28 M. A. Stewart, M. M. Kurien, W. R. Sherman and E. V. Cotlier, *J. Neurochem.*, 15 (1968) 941.
29 F. I. Caird, M. Hutchinson and A. Pirie, *Brit. Med. J.*, 2 (1964) 665.
30 F. I. Caird, A. F. Burditt and G. J. Draper, *Diabetes*, 17 (1968) 121.

Journal of Chromatography, 126 (1976) 547–557
© Elsevier Scientific Publishing Company, Amsterdam — Printed in The Netherlands

CHROM. 9475

GAS CHROMATOGRAPHIC–MASS SPECTROMETRIC–COMPUTER METHODS IN THE STUDY OF DRUG METABOLISM

R. N. STILLWELL and W. G. STILLWELL
Institute for Lipid Research, Baylor College of Medicine, Houston, Texas 77030 (U.S.A.)

SUMMARY

The computer-assisted interpretation of repetitively scanned mass spectra can be of great value in the analysis of a complex mixture even in the absence of a library of reference spectra. We have written a set of interpretation programs for a PDP11/45 laboratory computer. A file structure is used that combines economy of storage with ease of creation and retrieval. User interaction is by a simple command language implemented by an interpreter. The program structure is such that additional functions can be added easily.

INTRODUCTION

The study of the metabolic fate of exogenous compounds, including drugs, is of importance in obtaining information about both the activity and the actual or potential toxicity of these compounds. Of particular interest to us and to others is the obtaining of evidence for the metabolism of unsaturated and aromatic compounds via epoxide intermediates. Epoxidation has been shown to be a common pathway of metabolism, and whereas many epoxides appear to be harmless (at least on limited exposure), some have been implicated in mutagenesis, carcinogenesis, teratogenesis, and cytotoxicity[1,2].

Methods have been developed in our laboratory for the isolation, derivatization and gas chromatographic (GC)–mass spectrometric (MS)–computer analysis of metabolites including dihydrodiols, which are produced by the action of epoxide hydrase enzymes on epoxides and are the normal excretory products of compounds metabolized by the epoxide pathway. These methods have enabled us to detect a great number of dihydrodiols and hydroxylated dihydrodiols from a variety of compounds[3–8]. In this paper we report the computer-assisted analysis program used in this work[9,10].

Mini-computers dedicated to MS data acquisition and display are available in many laboratories. Many of these systems provide a great variety of output options such as library searching, reconstruction of mass chromatograms, etc. In general, however, they permit only one function at a time, so that new samples cannot be run while old data are being reviewed. Effective analysis of data obtained by rapid

repetitive scanning of the mass spectrometer requires an interactive system so that the experimenter can combine his knowledge of chemistry and MS, much of which is "intuitive" in that he cannot state it in algorithmic form, with the number-processing capacity of the computer. Such an interactive system requires the passing of large amounts of information in graphic form to the experimenter's terminal at high data rates. The high data rates and large amounts of processing time required make the use of a university or commercial time-sharing system economically infeasible. The decline in cost of computer components, particularly of processors and memory, has, however, made it possible for many laboratories to install central laboratory computers of sufficient capacity to support one or more users running such interactive programs. Our laboratory uses a PDP11/45 computer (Digital Equipment Corp.) for this purpose.

EXPERIMENTAL

Apparatus

Mass spectra were obtained on an LKB Model 9000 gas chromatograph–mass spectrometer interfaced to a PDP12 computer. The interface and programs were those developed by Holmes *et al.*[11]. A 9 ft. × 2 mm 1% SE-30 column was used. The computer was fitted with the TC12F option, which allows conversion from the LINCtape format normally used on the PDP12 to DECtape format; the standard conversion program supplied by DEC was modified to copy PDP12 LINCtape to PDP11-format DECtape. Since the basic DECtape word length is 18 bits, of which the PDP11 controller ignores two, one 12-bit LINCtape word is copied into one DECtape word; hence $1\frac{1}{2}$ DECtapes are required for one LINCtape.

The data analysis was performed with a PDP11/45 computer equipped with 64 K words of core memory, memory management, three 1.2 M-word disks, and DECtape. This computer runs under the RSX-11D operating system. The programs used for the analysis are described below. The user's terminal is an Imlac PDS-1 graphic display terminal; it is programmed to simulate a Tektronix 4010 storage scope terminal with a few additional features; the analysis programs do not use these features and hence would run without modification on a Tektronix. A Houston Instruments DP-1 incremental plotter is the hard-copy device; it is interfaced to the PDP11 by the standard DEC XY11 interface and is driven by a handler task that also simulates a Tektronix terminal with the addition of third-order X and Y coordinate control bytes, extending its "display" field to $2^{15} \times 2^{15}$ increments. This allows the data analysis program to use the same code to produce the hard copy as the original display. The plotter output is spooled to disk.

Sample extraction and derivatization

The urine sample was collected from a hospitalized patient 4 days after ingestion of an overdose of methaqualone. The drug and its metabolites were isolated from 20 ml of urine using an ammonium carbonate–ethyl acetate procedure previously described[8]. The ethyl acetate extract was evaporated to dryness under a nitrogen stream, and the residue was dissolved in pyridine and converted to the trimethylsilyl derivatives for analysis by GC and GC–MS–computer.

Data acquisition

After injection of the derivatized sample on to the GC column, the oven temperature was programmed from 150° at 2°/min. Shortly before the first peak of interest (unchanged methaqualone) was due to come off, the switch on the computer was set to start acquiring data automatically. The mass range from *m/e* 10 to 550 was scanned at a speed setting of 7 (5 sec/scan) at a scan interval of 8 sec. The mass error display was monitored on the scope to guard against mass marker drift. After 260 spectra had been obtained and stored, the tape was copied to two PDP11-format DECtapes.

Analysis programs

Analysis of the repetitive scan data is carried out in two stages. The first is to read the tapes and store the data on disk in a specially constructed file format; this is done by a program called SAVE. The second is the analysis proper, which is carried out by LEXER.

SAVE. This program when loaded queries the user for the input and output file names, etc., then reads the tape directory to find the input file. Reading spectra from the tape is for the most part straightforward decoding of the bitmap and intensity format in which they are stored. An attempt is made, however, to follow the trend of the mass marker in order to correct the integral mass in cases where the sum of the mass marker error and the mass defect exceed 0.5 a.m.u.

Block-inverted file format. SAVE creates in a single pass a file that allows for rapid retrieval of either a given mass spectrum or a given mass chromatogram (Fig. 1). Although the structure of the file is optimized for the PDP11 disk, it is created and read using FORTRAN direct-access READ and WRITE statements of the type that is an almost universal enhancement to ANSI FORTRAN. The file is a direct access file of 256-word blocks, numbered from 0 to N. Block 0 is the index block. Blocks 1 through N are treated as arrays of 16 mass numbers of 16 spectrum numbers; each word contains in its low-order 13 bits the intensity associated with the corresponding mass number and spectrum number. For purposes of exposition, the arrays are described here as if they were numbered from (0,0) to (15,15). In the actual program, subscripts start at (1,1), according to the FORTRAN convention. Mass numbers 0 through 5 are reserved for the total ion current, etc., while mass number 6 corresponds to the least mass stored in the file (usually 40); this number (LOMASS) is placed in the index block along with the total number of blocks (TBLKS) and the total number of spectra (TSPEC) in the file. The file is also considered to be organized into groups of blocks, each group (except for the last) containing 16 spectra. Since spectra vary in length throughout the run, space is saved by terminating each group after all 16 of its spectra are complete. This requires that the index block also contain a pointer to the first block of each group (Fig. 1). Of course, this requires one extra disk access per spectrum or mass chromatogram, or else that the index block be retained in memory during the analysis. In order to access a given mass number or spectrum number, the given number is divided by 16, the quotient being either the starting block number less 1 (for mass chromatograms) or the index into the pointer array (for spectra). The remainder is the row or column, respectively. Fig. 1 illustrates the method of addressing. In practice, of course, since both FORTRAN and users number things starting from 1, not 0, the given number is decremented by 1 before the division, and the quotient and remainder are incremented by 1 afterwards.

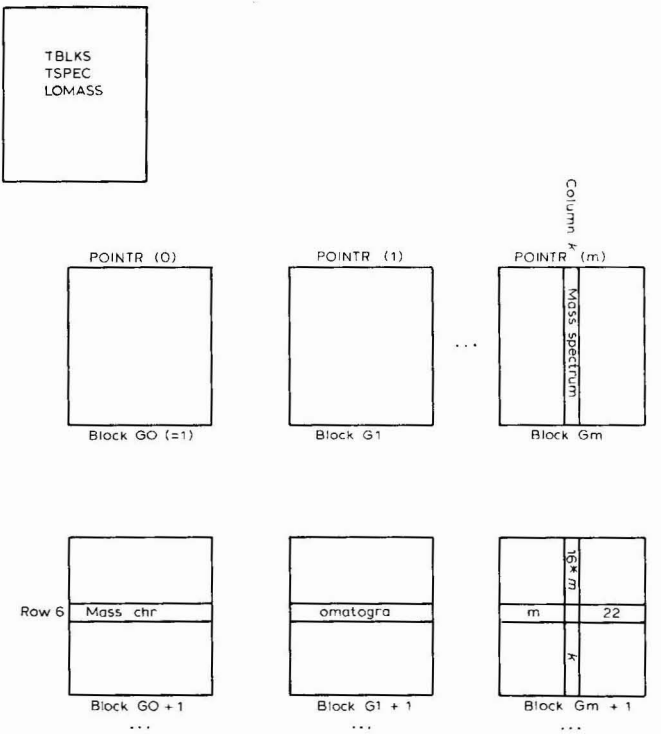


Fig. 1. Block-inverted file format used by LEXER. Each row is a mass chromatogram; each column is a mass spectrum. Block 0, the index block, contains pointers to the beginning of each spectrum group.

Reading a spectrum or a mass chromatogram with a range of 500 mass or spectrum numbers takes about 2 sec with a single user on the system.

A file of this type, with the addition of another file containing compound names, etc., is also in use as a spectrum library. Performing a mass search on this file is equivalent to reading a mass chromatogram from a repetitive scan data file. The library file was not used in the work described here.

LEXER. This program, the interactive analysis program proper, derives its name from the way in which it handles user input. Instead of going through a question-and-answer procedure for each operation, which is all very well for the novice user but soon gets tiresome, the program incorporates an interpreter for a simple command language. Commands are typed in response to the prompt "ENTER COMMAND". A user command consists in its complete form of a keyword (*e.g.* "DISPLAY") followed by one or more PL/I-like assignment statements (*e.g.* "*spectrum* = 147;"). In this article, keyword names are in capitals and parameter names are in italics. Both, of course, are typed in capitals on the keyboard. Parameters which are not to be changed need not be re-entered. Each user's parameters are stored in a file under his account number and hence are available for successive runs of the program. Parameter types include integers, floating point numbers, strings ("*mode* = normal; *file* = 'DK1:RUNB';"), and arrays ("*mass* = 147, 191, 207;"). In general, keywords correspond to program overlays; new functions can be easily added to LEXER. The

principal functions used for interactive data analysis are MAXIMA, DRGC, and DISPLAY.

MAXIMA scans the data file by groups of 16 mass chromatograms and flags local maxima by setting the high-order bit[9,10]. A similar program has been reported by Biller and Biemann[12]. A maximum is defined by the parameters *halfwidth*, *threshold*, and *factor*. A point satisfies the criteria for a local maximum if its intensity exceeds *threshold*, is greater than or equal to that of the preceding spectrum number (at the same mass) and greater than that of the succeeding spectrum number, and is greater than *factor* times the intensity of at least one point within *halfwidth* spectra on either side. In addition, MAXIMA accumulates a total intensity of flagged peaks for each spectrum number; these are stored in one of the reserved mass number rows.

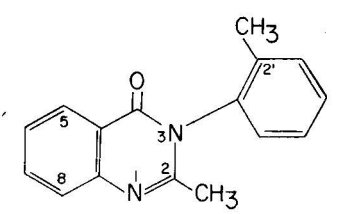
DRGC (for "display reconstructed gas chromatogram") displays on the CRT screen one or more superimposed mass chromatograms. The parameter *mass* determines which mass chromatograms are to be displayed: for example, "DRGC *file* = RUN22; *mass* = 191, *tic*, *tmax*;" causes the display of the mass chromatogram for *m/e* 191 together with the total ion current trace and the total of the maxima for the file named RUN22. *Tic* and *tmax* are parameters permanently equated to 0 and 1, respectively, and are simply mnemonic acids. Other parameters control the size of the plot and the vertical spacing between traces.

Once a mass chromatogram or spectrum has been requested, the first frame (about 200 masses or spectrum numbers) is shown on the screen. The prompt "#" then invites the user to request a hard copy or to modify the display. Hard copy is requested by typing COPY; the whole spectrum or chromatogram (not merely the current frame) is spooled to disk for later output on the incremental plotter. Other display requests are R: next frame; L: previous frame; U: vertical expansion (×2); D: vertical contraction; >: horizontal expansion; <: horizontal contraction; X: exit to "ENTER COMMAND". Requests can be ganged: RRRRRUU displays the last (or at least the 6th) frame of the display, expanded vertically by a factor of 4.

DISPLAY causes the display of a single spectrum. *Spectrum* specifies the spectrum number; *mode* ("normal" or "maxima") specifies whether all peaks or only those flagged are to be displayed; *norm* specifies the peak to which the spectrum is to be normalized ("*norm* = 147;"), or peaks which are not to be used as the base peak ("*norm* = −73, −75;"). Requests to modify the display or produce hard copy are the same as for DRGC.

RESULTS AND DISCUSSION

The techniques described above were applied to a study of the metabolism of methaqualone in the human. Urine was obtained from a patient who had been hospitalized with an overdose of methaqualone. The drug and its metabolites were



Methaqualone.

extracted and derivatized as described previously[8]. Mass spectra were obtained at 8-sec intervals during the relevant portion of the temperature-programmed GC separation. The spectra on tape were converted into a block-inverted file on the PDP11/45 disk as described above, and the maxima were flagged using the program default values for the relevant parameters (the command was "MAXIMA *file* = 'DK1:M66C';"; the defaulted parameters were equivalent to "*halfwidth* = 4; *threshold* = 5; *factor* = 1.4;"). The total ion current and the total of the maxima were then displayed by giving in turn the commands "DRGC *mass* = *tic*;" and "DRGC *mass* = *tmax*;". As each display appeared on the screen, the display request "COPY" was given. This caused a plot file to be created and spooled to disk. On termination of LEXER, the plotter was made ready and plotting was initiated; the results are shown in Figs. 2 and 3. The *tmax* plot provides a chromatographic trace of considerably enhanced resolution. One might expect an effect of infinite resolution; *i.e.* a bar graph with each component represented by a single vertical line, since all the ions due to a component should reach a maximum intensity at the same time. That this is not observed is partly because spectra are not taken instantaneously but scanned over a period of time, and hence are biased, and partly due to noise (especially ion statistical noise) in the system, which displaces the maxima of certain ions, particularly the weaker ones.

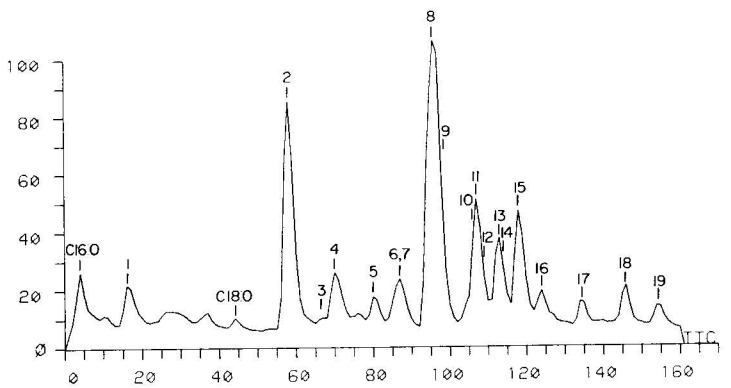


Fig. 2. Total ion current. Numbers above the trace indicate the position of elution of methaqualone and its metabolites, as listed in Table I. C16:0 and C18:0 are trimethylsilyl palmitate and trimethylsilyl stearate, respectively.

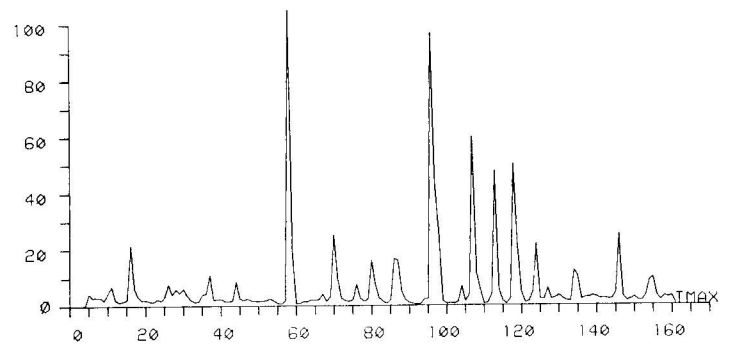


Fig. 3. Total of flagged peaks. The effect is that of a chromatogram of markedly enhanced resolution.

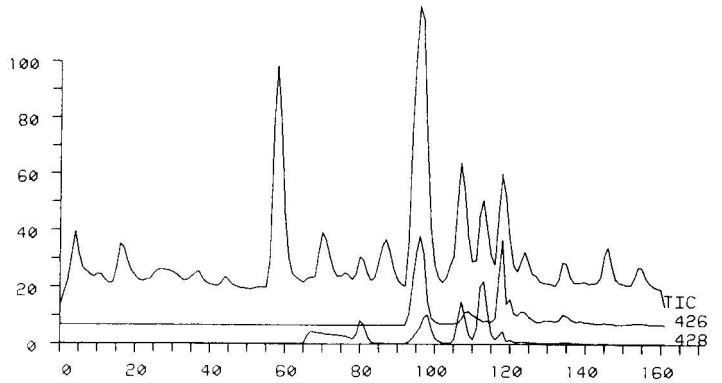


Fig. 4. Mass chromatograms for *m/e* 426 and 428 and total ion current. The peaks at spectrum numbers 97 and 107 contain unresolved mixtures. The peak at *m/e* 426 corresponds to M^+ for di-OTMS derivatives of methaqualone, *m/e* 428 to M^+ for dihydro-di-OTMS derivatives.

Fig. 4 shows the reconstructed mass chromatograms for *m/e* 426 and 428, which are the molecular weights of trimethylsilyl (TMS) derivatives of diol and dihydrodiol metabolites, respectively. A peak in the mass chromatogram is not, of course, proof of the presence of the compound of corresponding molecular weight, as the ion may be a fragment ion (inspection of spectrum 135 showed that *m/e* 426 at that point was due to trimethylsilanol elimination from a hydroxydihydrodiol derivative, for example) or an isotope peak (the peak at *m/e* 428 at spectrum 117 is simply due to the second isotope peak of *m/e* 426). In most cases, inspection of the spectrum is sufficient to confirm or refute the assignment. Where the chromatographic peaks overlap, however, the evidence of maxima for other ions must be used. Fig. 5 shows that *m/e* 191 has maxima corresponding to the four principal peaks for *m/e* 428. The peak at *m/e* 191 corresponds to the well known ion of structure $TMSO–CH=\overset{+}{O}TMS$, which is diagnostic for trimethylsilyloxy groups on vicinal saturated carbon atoms. More complete information, and in many instances virtually

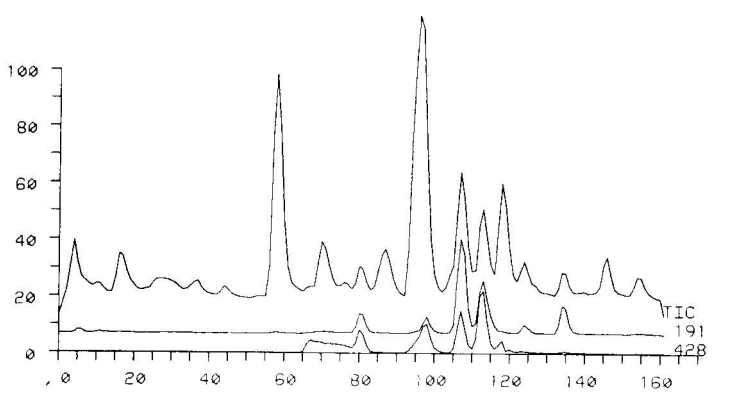


Fig. 5. Mass chromatograms for *m/e* 191 and 428 and total ion current. The peak at *m/e* 191 confirms the presence of a vicinal diol TMS structure in each of the four major compounds possessing a peak at *m/e* 428.

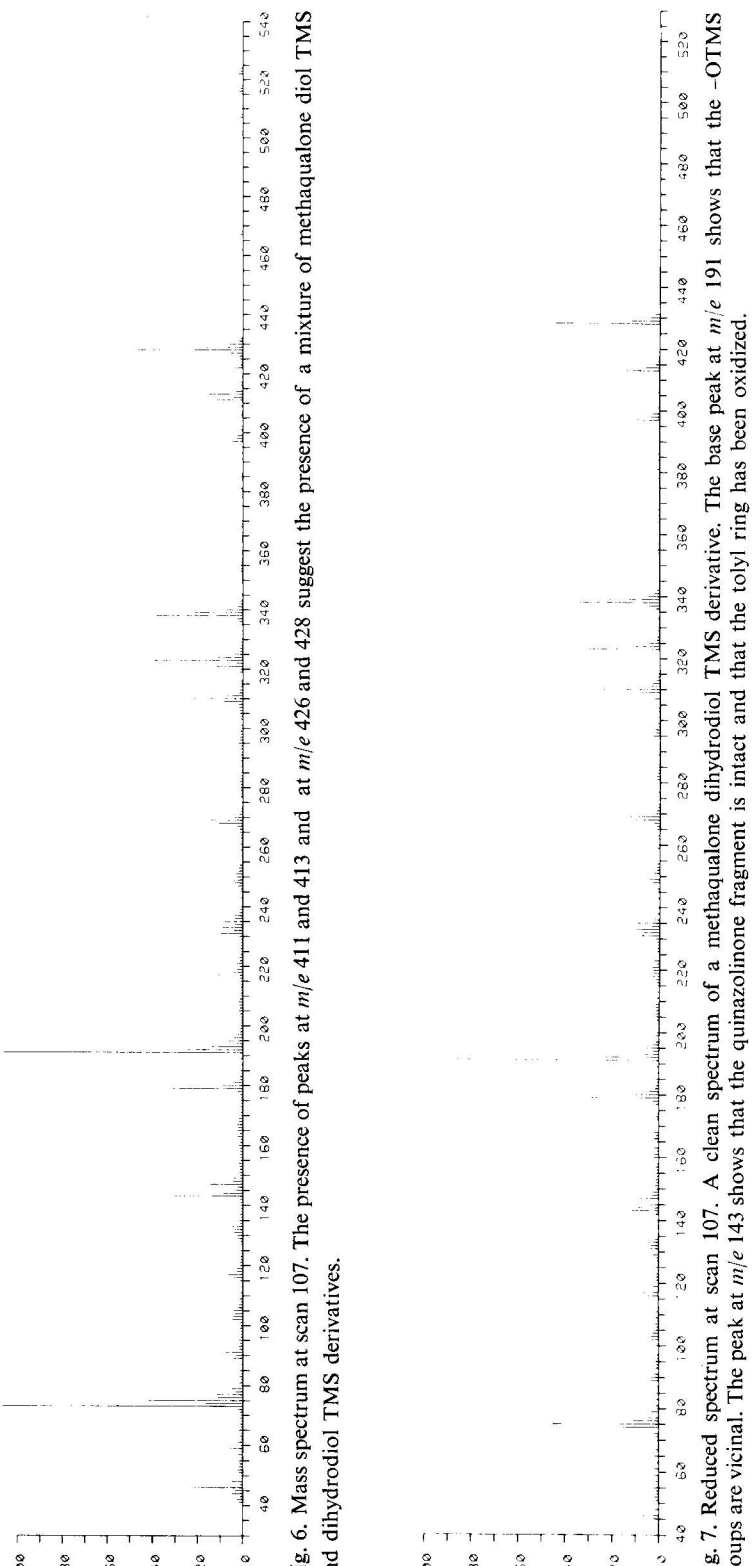


Fig. 6. Mass spectrum at scan 107. The presence of peaks at *m/e* 411 and 413 and at *m/e* 426 and 428 suggest the presence of a mixture of methaqualone diol TMS and dihydrodiol TMS derivatives.

Fig. 7. Reduced spectrum at scan 107. A clean spectrum of a methaqualone dihydrodiol TMS derivative. The base peak at *m/e* 191 shows that the -OTMS groups are vicinal. The peak at *m/e* 143 shows that the quinazolinone fragment is intact and that the tolyl ring has been oxidized.

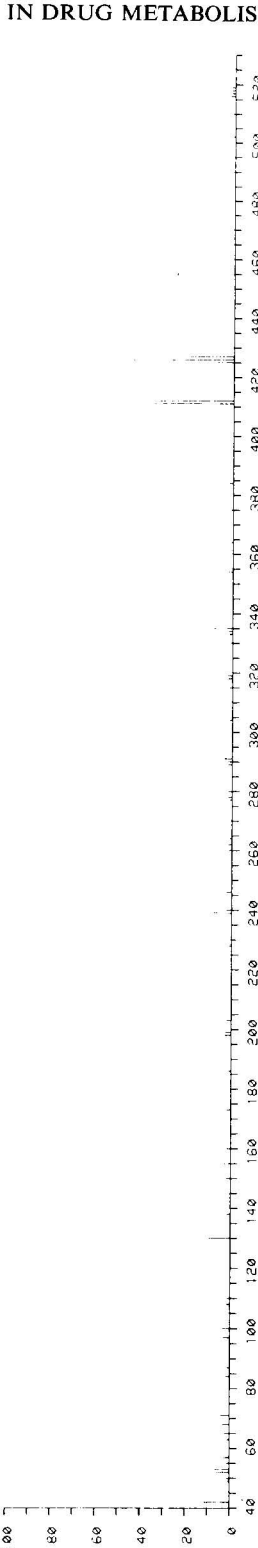


Fig. 8. Reduced spectrum at scan 109. The molecular ion shows up at *m/e* 516, indicating that the compound is the TMS derivative of a hydroxydihydrodiol metabolite of methaqualone. The peaks at *m/e* 426 and 411 represent loss of trimethylsilanol and loss of trimethylsilanol and methyl, respectively, from the molecular ion. This compound has not previously been reported.

complete separation of the spectra of overlapping compounds, may be obtained by plotting the spectra of only the flagged masses. Fig. 6 is the normal spectrum number 107, corresponding to the top of the peak in the total ion current chromatogram; clearly it contains more than one compound. It was obtained from LEXER by the command "DISPLAY *spectrum* = 107;". The reduced spectrum at that point was obtained by typing "DISPLAY *mode* = maxima;". The parameter *spectrum* was unchanged and so did not need to be repeated; the word "maxima" was not a legal parameter (although it is a keyword), and therefore was accepted by the program simply as a character string. The resulting spectrum is shown in Fig. 7. It is essentially the spectrum of the pure dihydrodiol TMS derivative. The command "DISPLAY *spectrum* = 109;" produced the reduced spectrum of the diol TMS derivative (Fig. 8). Since this is the minor component of the mixture, many fragments that it has in common with the major component disappear since they peak at the elution time of the major component. However, the spectrum is clearly that of the TMS derivative of a hydroxydihydrodiol metabolite of methaqualone. It should, in theory, be possible to reconstruct each spectrum completely by deconvoluting each mass chromatographic peak, perhaps using an ion unique to each component to determine the peak shape. In biological work, however, where the sample size is small and the scan time must be kept fairly long relative to the peak width in order not to lose sensitivity, it would be difficult to gain much additional information with any reliability.

The components which could be identified in this mixture are indicated by numbers in Fig. 2 and listed in Table I. With the exception of compounds 10 and 12 all of the metabolites in the table have been previously reported[8,13,14].

TABLE I

METHYLENE UNIT (MU) VALUES AND MOLECULAR WEIGHTS (TMS DERIVATIVES) OF METHAQUALONE AND ITS METABOLITES

Numbers refer to the peaks in Fig. 2. Hydroxyl groups labeled as 2 and 2′ are on the methyl groups at those positions. Q and T refer to positions on the quinazolinone and tolyl nuclei, respectively.

No.	*Compound*	*MU 5% SE-30*	*MW*
1	Methaqualone	21.1	250
2	2′-Hydroxy	23.3	338
3	Q-Dihydrodiol	23.8	428
4	8-Hydroxy	23.9	338
5	T-Dihydrodiol	24.5	428
6	3′-Hydroxy	24.7	338
7	4′-Hydroxy	24.7	338
8	2,T-Diol	25.1	426
9	Q-Dihydrodiol	25.1	428
10	Hydroxydihydrodiol	25.6	516
11	T-Dihydrodiol	25.6	428
12	Hydroxydihydrodiol	25.7	516
13	T-Dihydrodiol	25.9	428
14	T-hydroxy-T-methoxy	25.9	368
15	2′,T-Diol	26.1	426
16	2′-Hydroxy-T-dihydrodiol	26.5	516
17	2′-Hydroxy-T-dihydrodiol	26.9	516
18	Mixed triols	27.5	514
19	2,T,T-Triol	28.0	514

ACKNOWLEDGEMENTS

This work was supported by Grant GM-16216 from the National Institutes of Health. We thank Stephen S. Bates for programming assistance and Carol S. Myron for running the mass spectrometer.

REFERENCES

1 D. M. Jerina and J. W. Daly, *Science*, 185 (1974) 573, and references therein.
2 P. G. Wislocki, A. W. Wood, R. L. Chang, W. Levin, H. Yagi, O. Hernandez, D. M. Jerina and A. H. Conney, *Biochem. Biophys. Res. Commun.*, 68 (1976) 1006.
3 M. G. Horning, C. Stratton, A. Wilson, E. C. Horning and R. M. Hill, *Anal. Lett.*, 14 (1971) 537.
4 D. J. Harvey, L. Glazener, C. Stratton, D. B. Johnson, R. M. Hill, E. C. Horning and M. G. Horning, *Res. Commun. Chem. Pathol. Pharmacol.*, 4 (1972) 247.
5 D. J. Harvey, L. Glazener, C. Stratton, J. Nowlin, R. M. Hill and M. G. Horning, *Res. Commun. Chem. Pathol. Pharmacol.*, 3 (1972) 557.
6 W. G. Stillwell, M. Stafford and M. G. Horning, *Res. Commun. Chem. Pathol. Pharmacol.*, 6 (1973) 579.
7 W. G. Stillwell, *Res. Commun. Chem. Pathol. Pharmacol.*, 12 (1975) 25.
8 W. G. Stillwell, P. A. Gregory and M. G. Horning, *Drug Metab. Dispos.*, 3 (1975) 287.
9 R. N. Stillwell, *22nd Annual Conference on Mass Spectrometry and Allied Topics, Philadelphia, Pa., 1974*, paper V-11.
10 W. G. Stillwell, P. A. Gregory and R. N. Stillwell, *23rd Annual Conference on Mass Spectrometry and Allied Topics, Houston, Texas, 1974*, paper J-4.
11 W. F. Holmes, W. H. Holland and J. A. Parker, *Anal. Chem.*, 43 (1971) 1806.
12 J. E. Biller and K. Biemann, *Anal. Lett.*, 7 (1974) 515.
13 R. Bonnichsen, C.-G. Fri, C. Negoita and R. Ryhage, *Clin. Chim. Acta*, 40 (1972) 309.
14 R. Bonnichsen, Y. Marde and R. Ryhage, *Clin. Chem.*, 20 (1974) 230.

Journal of Chromatography, 126 (1976) 559–568
© Elsevier Scientific Publishing Company, Amsterdam — Printed in The Netherlands

CHROM. 9473

ANALYSIS OF THE ACIDIC FRACTION OF MARIJUANA SMOKE CONDENSATE BY CAPILLARY GAS CHROMATOGRAPHY–MASS SPECTROMETRY

MICHAEL P. MASKARINEC, GABOR ALEXANDER* and MILOS NOVOTNÝ**
Department of Chemistry, Indiana University, Bloomington, Ind. 47401 (U.S.A.)

SUMMARY

A method for the analysis of organic acids and phenols isolated from marijuana smoke condensate has been developed. Comparative analyses of standard tobacco, Mexican, and Turkish marijuana smoke condensates carried out by means of capillary gas chromatography indicated both qualitative and quantitative changes in the constituents of chromatographic profiles. Samples were converted to volatile derivatives by methylation and trimethylsilylation; whereupon, 49 aliphatic acids, aromatic acids, and phenolic compounds were identified by means of capillary gas chromatography–mass spectrometry.

INTRODUCTION

It is widely suspected that many fundamental problems associated with limited understanding of the pharmacological and toxicological effects of marijuana may have their origin in the insufficient chemical characterization. Although much progress has been made in the recent years[1], marijuana smoke still remains a poorly defined conglomerate of chemicals. Whereas much attention has been given to the many effects of a major marijuana constituent, Δ^9-tetrahydrocannabinol, this substance and marijuana are not always pharmacologically and toxicologically synonymous. Thus, activity can sometimes be located in fractions of the plant extract that contain no Δ^9-tetrahydrocannabinol or other related substances (*e.g.*, refs. 2 and 3).

Detailed knowledge of the composition of marijuana smoke will be urgently needed for future studies of its physiological effects. This paper is an extension of the characterization of marijuana plant and smoke materials performed in this laboratory[4–6].

Smoke fractionation is accomplished by a modified procedure of Schmeltz *et al.*[7] that has been used for isolation of polynuclear aromatic hydrocarbons from

* On leave from the Hungarian Academy of Sciences, Laboratory for Inorganic Chemistry, Budapest, Hungary.
** To whom correspondence should be addressed.

marijuana and tobacco smoke[6]. The acidic fraction yielded as a result of the fractionation scheme has now been chemically characterized in this study. Phenolic substances and aromatic and aliphatic acids that can be volatilized for gas chromatographic (GC) investigations through derivatization have been of primary interest.

General interest in acidic components stems from the fact that both phenols and acids contained in tobacco smoke were found to be a contributory factor in tumor formation and to possess a cilia-inhibiting activity[8,9]. Whereas positive identification of all constituents of marijuana smoke acidic fraction, biological testing and physiological interpretation of such studies remain a long-term goal, a method for selective screening for unusual compounds is of utmost importance in the beginning stages of such investigations. One approach that can facilitate orientation in any complex fraction of marijuana smoke is using tobacco smoke as a "baseline material" for comparison and screening the available samples for obvious qualitative and quantitative differences.

The methodology for analysis of the acidic fraction of marijuana smoke described in this paper consists of solvent partitioning, purification and selective fraction enrichment by gel chromatography, followed by conversion of sample components to volatile derivatives for GC. Efficient glass capillary columns further provide a degree of resolution required for the mass spectrometric (MS) investigation of the sample components. High-resolution GC profiles of the fractions obtained from Mexican and Turkish marijuana and standard tobacco smoke condensates have been compared. Also, numerous components of the acidic fraction from Mexican marijuana have been identified in this work.

EXPERIMENTAL AND RESULTS

Sample preparation

One hundred cigarettes each of Mexican and Turkish marijuana (National Institute of Drug Abuse, Rockville, Md., U.S.A.) and standard tobacco (Tobacco–Health Research Institute, University of Kentucky, Lexington, Ky., U.S.A.) prepared from equal weights, were smoked with a standard smoking machine[10] at approximately 35-ml puff volume for a duration of 2 sec at a frequency of 1 min. The content of Δ^9-tetrahydrocannabinol was 2.8%, for Mexican, and 0.3% for Turkish marijuana, respectively. The smoke condensates were separately collected in acetone-filled traps cooled with dry ice–acetone.

Some of the acetone was removed *in vacuo* at 40° and the brown oily residue redissolved in 250 ml of methylene chloride. The extract was partitioned three times with 250 ml of 1 *N* sodium hydroxide solution, and the aqueous layer was washed twice with 300 ml of methylene chloride. The aqueous extract was subsequently adjusted with hydrochloric acid to pH 1.0, and the organics of acidic nature were re-extracted with two 450-ml volumes of methylene chloride. The extracts were dried over magnesium sulfate and filtered. The solvent was finally removed *in vacuo*.

The acidic residues from Mexican marijuana and standard tobacco were weighted, yielding 6.25 and 2.05 mg/cigarette, respectively. Whereas much of this material is obviously non-volatile, the primary objective of this study has been to recognize differences in the constituents of marijuana and tobacco smoke that are either volatile or can be volatilized through derivatization. Addition of an internal

standard to the total acid fractions revealed that they contain only about 20% of elutable material.

Selection of analytical column for high-resolution gas–liquid chromatography

It has been well established that both acid and phenolic compounds are more easily chromatographed in the gas phase when converted to less polar derivatives[11–14]. When acidic stationary phases are coated on the wall of a capillary column, highly volatile acids and phenols can also be chromatographed without derivatization. Such cases were demonstrated by Averill[15] and Zoccolillo *et al.*[16]. More recently, Hrivňák *et al.*[17] have also demonstrated an efficient separation of C_2–C_6 fatty acids with steel capillary columns coated with Ucon LB-550-X, with the addition of phosphoric acid.

It has been our experience in this work that adequate glass capillary columns can be prepared by coating the etched glass-surface[18] with both FFAP ("free fatty acid phase"; Supelco, Bellafonte, Pa., U.S.A.) and Trimer Acid (Applied Science Labs., State College, Pa., U.S.A.) with addition of phosphoric acid. Whereas such columns perform well when freshly prepared, the resolution of free fatty acids diminishes rapidly with time. This phenomenon is illustrated in Fig. 1. Because the long-term column stability is maintained for hydrocarbons, the loss of resolution for

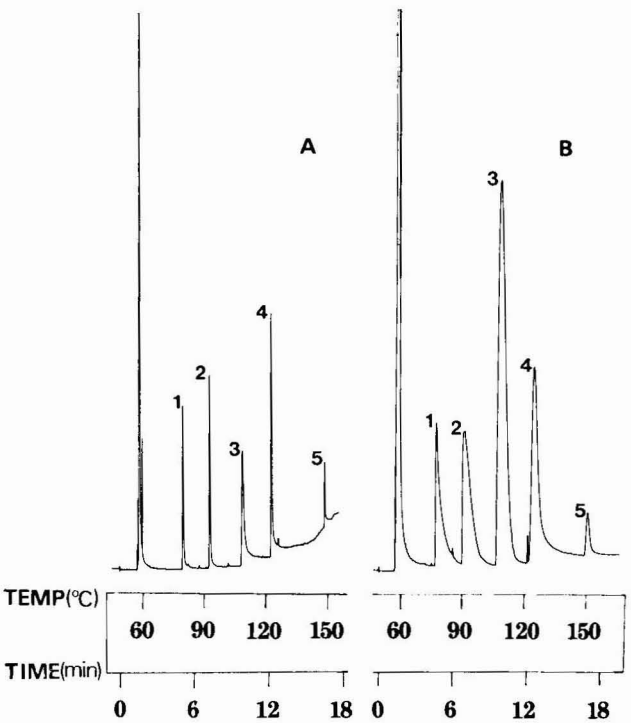


Fig. 1. Chromatograms of a standard mixture of free fatty acids. (A) Chromatogram obtained with a freshly prepared column and short conditioning at 180°. (B) Chromatogram obtained after 20 h conditioning at 180°. 1 = Propionic acid; 2 = butyric acid; 3 = valeric acid; 4 = hexanoic acid; 5 = octanoic acid. Conditions: 2? m × 0.25 mm I.D., glass capillary column coated with Trimer Acid + 30% phosphoric acid; injector temperature, ?20°; detector temperature, 210°; splitting ratio, 1:50.

free fatty acids can be attributed to a loss of surface acidity and/or deactivation that is most likely due to an easy migration of alkali ions within the silica framework[19]. Perhaps, this problem could be overcome by a more permanent surface modification.

Owing to its good temperature stability and selective properties, FFAP was chosen as the stationary phase for separations of derivatized acids and phenols. The glass capillary column (20 m × 0.25 mm I.D.) was prepared by etching with dry hydrogen chloride[18,20] and was coated dynamically with a 15% solution of FFAP in methylene chloride by the mercury-plug method recommended by Schomburg *et al.*[21]. A Varian Model 1400 gas chromatograph with a modified splitting injector, linear temperature programmer and flame ionization detector was used for all GC separations.

Comparison of chromatographic profiles

In order to obtain volatile derivatives, a methylation technique reported by Middleditch and Desiderio[13] was applied to aliquots of the acidic fractions of marijuana and tobacco smoke condensates. Fifty to one hundred μl of the extract were evaporated to dryness in a micro-vial, and the residue was dissolved in 25 μl of the 0.2 *M* solution of trimethylanilinium hydroxide (Methelute; Pierce, Rockford, Ill., U.S.A.), and 2.5 μl of the solution were immediately injected in to the gas chromatograph (splitting ratio, 1:50).

The comparative analyses of the three investigated total acidic fractions after methylation are shown in Fig. 2, demonstrated both qualitative and quantitative differences in all fractions. Since MS data acquired on the resolved peaks showed that these chromatograms were primarily dominated by fatty acids, and that the derivatization of the total extract resulted in incomplete reaction of certain aromatic constituents, further selective fractionation by liquid column chromatography was found necessary. Two mg of the dry total acidic fraction dissolved in 0.5 ml of methanol were placed on a 25 × 0.8 cm I.D. DEAE-Sephadex A-25 (Cl^-) (weak anion exchanger) column and eluted with methanol as the mobile phase, taking advantage of the well-known phenomenon of reversible adsorption of aromatics by Sephadex gels. Whereas most non-volatile material was unretained and aliphatic acids were eluted in one column volume, phenolic substances and aromatic acids required a double amount of methanol for elution.

The fraction from all materials containing phenols and aromatic acids were evaporated to dryness and their equal aliquots methylated and analyzed on the same capillary column. Fig. 3 compares all chromatographic profiles of this aromatic fraction.

Gas chromatography–mass spectrometry

The FFAP glass capillary column was connected to the ion source of a Hewlett-Packard Model 5980A dodecapole mass spectrometer through an all-glass jet molecule separator (Scientific Glass Engineering). Electron-impact ionization spectra were obtained with an electron energy of 20 or 70 eV. Chromatographic peaks were scanned at the rate of 100 a.m.u./sec and mass spectra were recorded on oscillograph paper.

Many major acidic components of Mexican marijuana smoke were tentatively identified from mass spectra of their methylated derivatives. Since the methylation

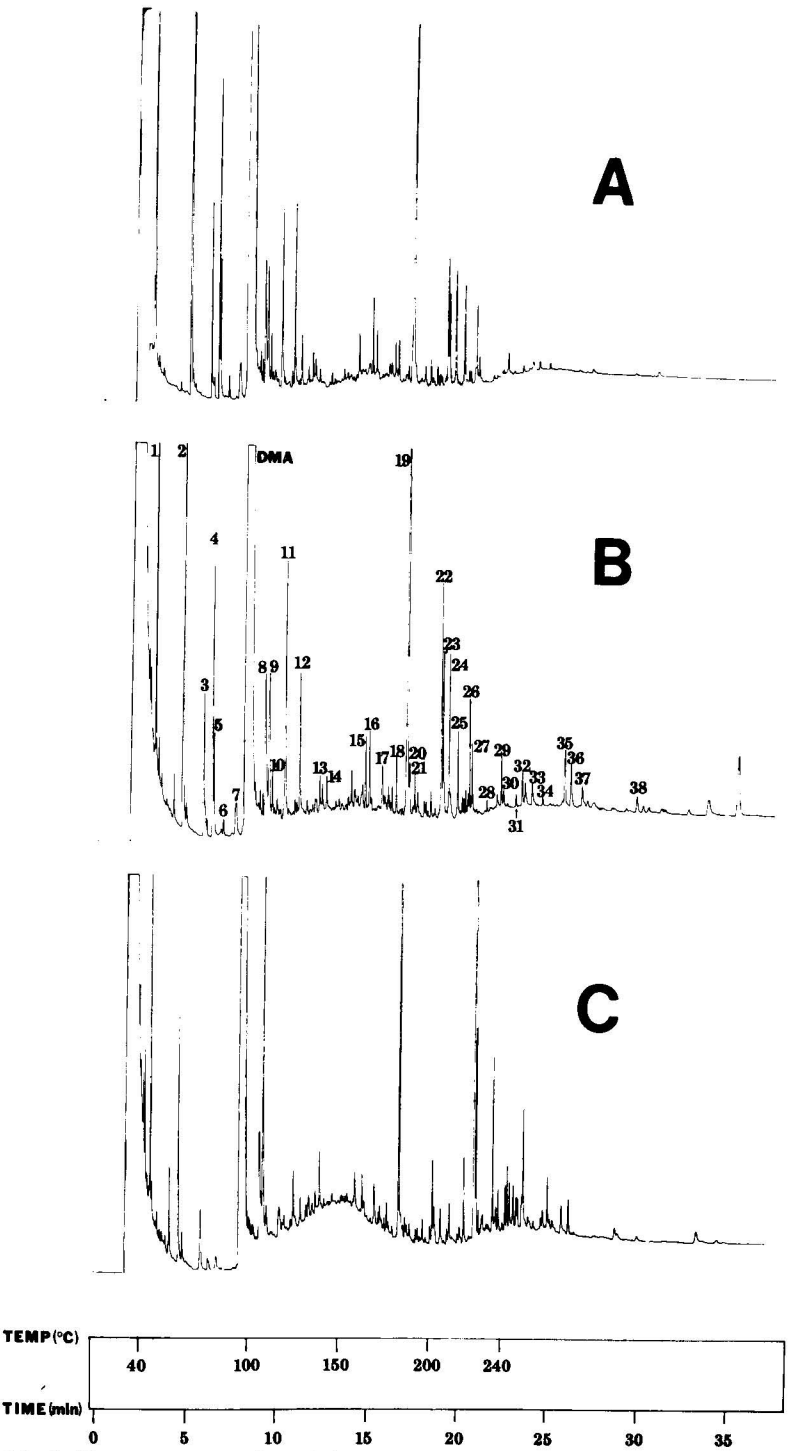


Fig. 2. Chromatograms of methylated total acidic extracts of cigarette smoke condensates. (A) Standard tobacco; (B) Mexican marijuana; and (C) Turkish marijuana. Conditions: 20 m × 0.25 mm I.D., glass capillary column coated with FFAP; injector temperature, 260°; detector temperature, 210°. Injected amount was approximately 60 μg of extract; splitting ratio, 1:50. For peak identification, see Table I; DMA = dimethylaniline.

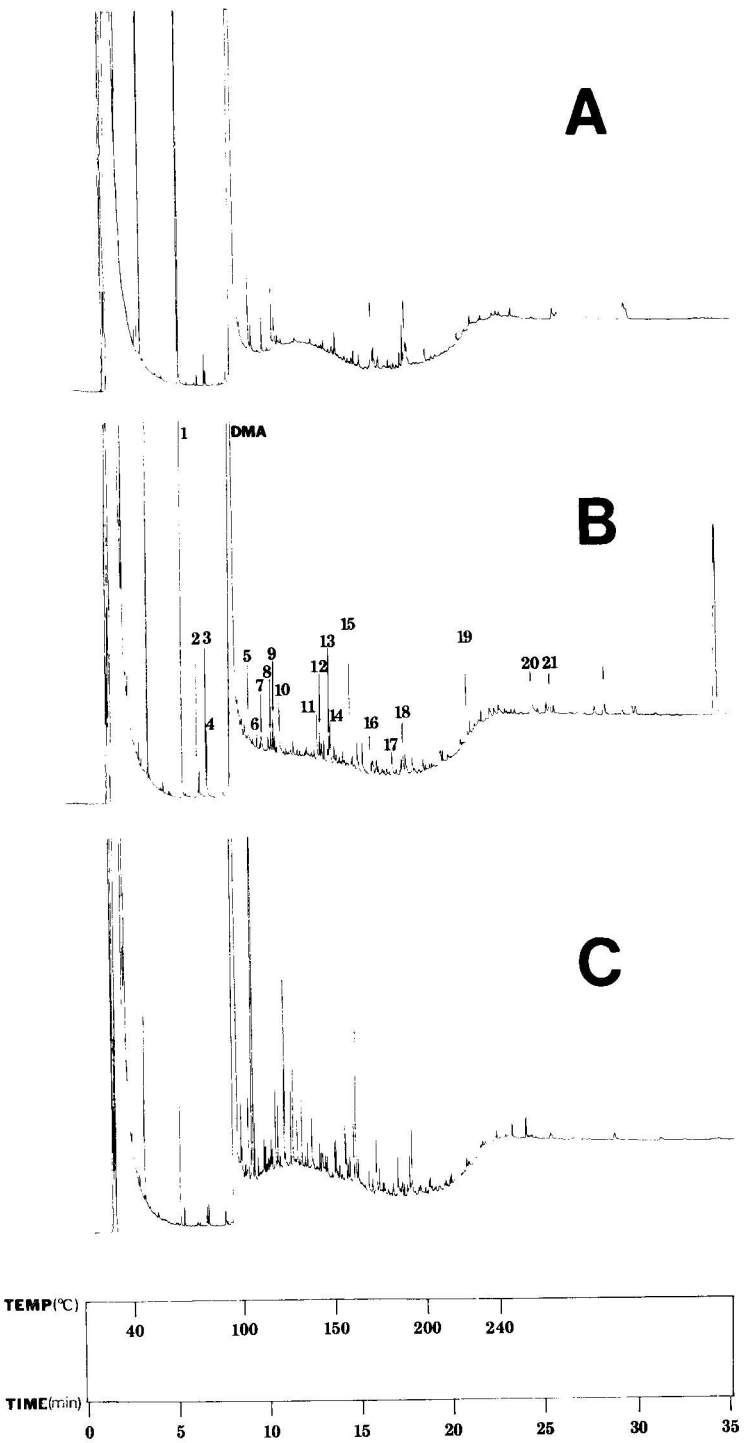


Fig. 3. Chromatograms of the methylated aromatic fraction obtained through DEAE-Sephadex liquid chromatography. (A) Standard Tobacco; (B) Mexican marijuana; and (C) Turkish marijuana. Conditions: same as in Fig. 2. For peak identification, see Table I.

procedure masks the possible presence of naturally occurring methoxy compounds within the aromatic fraction, silylation with N-methyl-N-trimethylsilyltrifluoroacetamide (Pierce), was carried out at 80° for 2 h to provide additional information. Chromatogram of the silylated fraction of Mexican marijuana aromatics is shown in Fig. 4.

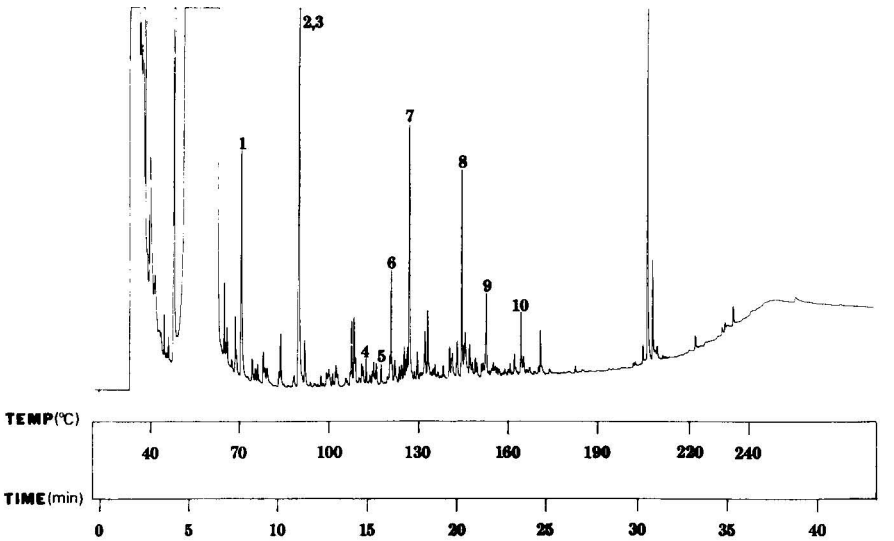


Fig. 4. Chromatogram of a silylated aromatic fraction (after liquid chromatography). Conditions: same as in Fig. 2. For peak identification, see Table I.

The results of the MS identifications of components of the total acidic fraction (Fig. 2) and methylated and silylated aromatic fractions (Figs. 3 and 4) are listed in Table I. In total, 49 components have been identified.

DISCUSSION

Whereas a limited number of acidic components have been reported in cannabis plant material[1] and also, more recently, in marijuana smoke condensate[22], this study illustrates for the first time the real complexity of such mixtures and provides an efficient methodology for identification of the elutable acidic components. It also points out that much further work will be necessary to identify the many trace components, some of which might bear physiological significance.

A significantly higher total acidic content of marijuana smoke compared with tobacco smoke could be important in view of the possible implication of such substances in co-carcinogenic and ciliostatic activities[8,9]. A role of various acidic compounds in this direction must first be substantiated by detailed analytical data on both volatile and heavy constituents and, most importantly, biological experiments.

The comparisons of both the total and the aromatic fractions of acidic constituents, as shown in Figs. 2 and 3, indicate a higher complexity and total amounts for marijuana as compared with tobacco. Also, both qualitative and quantitative dif-

TABLE I

COMPOUNDS IDENTIFIED IN ACIDIC FRACTION OF MEXICAN MARIJUANA

Compound	*Peak Number*		
	Fig. 2	*Fig. 3*	*Fig. 4*
Hexanoic acid	1	—	
Phenol*,**	2	1	
o-Cresol*	3	2	
p-Cresol*	4	3	
m-Cresol*	5	4	
Furoic acid*	6		—
Nonanoic acid	7	—	
Decanoic acid	8	—	—
Benzoic acid*	9	5	—
o,p-Divinylphenol	10	6	2, 3
Catechol*	—	7	1
Glutaric acid	11	—	—
Phenylacetic acid*	—	8	—
o-Isopropenylphenol	—	9	6
m-Hydroxy-*p*-methoxystyrene	12	10	1
Dodecanoic acid	13		—
2,4-Dihydroxy anisole	14	11	8
o-Hydroxybenzaldehyde*		12	4
Phenylpropionic acid		13	
Phenylisopropionic acid		14	
o-Hydroxyacetophenone	15	15	5
Tetradecanoic acid*	16	—	
Olivetol	17	16	10
3-Isopropyl-5-hydroxybenzaldehyde		17	
2,4-Dihydroxybenzaldehyde	18	18	9
p-Hydroxybenzyl 2-butenyl ketone		19	
Palmitic acid*	19		—
Palmitoleic acid*	20		—
Palmitolenic acid	21		
Stearic acid*	22		
Oleic acid*	23	—	
Linoleic acid*	24		
Linolenic acid*	25		—
Arachidic acid*	26	—	
Eicosenoic acid	27		
Eicosadienoic acid	28		
Behenic acid	29		
Erucic acid	30		—
Tricosanoic acid	31		
2-Ethyl-3-hydroxy-5-pentylbenzoic acid	32	20	
2-Vinyl-3-hydroxy-5-pentylbenzoic acid	33	21	
Lignoceric acid	34		
Tetracosatetraenoic acid	35	—	
Hexacosanoic acid	36		
Hexacosadienoic acid	37		
Octacosanoic acid	38		

Also identified under the solvent peak:
2-Methylbutanoic acid
3-Methylbutanoic acid
4-Pentenoic acid

* Denotes compounds compared with standards.

** Since anisol was recently found[26] to originate from the thermal decomposition of trimethylanilinium hydroxide, phenol cannot be quantitated from the present chromatograms.

ferences between Mexican and Turkish marijuana profiles are noteworthy. Although probably without any physiological meaning, it is interesting to observe that the ratio of fatty acids in Turkish marijuana is strikingly different from Mexican marijuana and standard tobacco, which are of somewhat similar composition.

Whereas the complete identification of all mixture components was not within the scope of this study owing to a lack of both standard compounds and additional structural information, many potentially interesting compounds were found in the smoke condensate of Mexican marijuana. Just as with the hypothesis that many simple phenolic compounds present in tobacco smoke condensate have their origin in the carbohydrate content of tobacco leaf[23], the same is likely to be true for marijuana. However, it can be easily speculated that certain cannabinoids could give rise to various substituted phenols upon pyrolysis. In fact, recent studies of Küppers *et al.*[24] on the model pyrolysis of cannabidiol appear to substantiate this idea.

Evidence presented by Burstein *et al.*[2,25] that certain substituted phenols present in the extracts of *Cannabis sativa* are strong inhibitors of prostaglandin biosynthesis indicates that some of the phenolic constituents found in this work may bear pharmacological significance. We have found one of the substances with proven physiological activity[25], olivetol, to be present in the acidic fraction of Mexican marijuana smoke in appreciable quantity.

Finally, it should be pointed out that, whereas the present methodology has been developed specifically for fractionation, analytical separation, and identification of the elutable acidic components of marijuana smoke condensate, its wider applicability to any analysis of acidic compounds present in mixtures of comparable complexity is likely.

ACKNOWLEDGEMENTS

We thank Dr. John Benner and Miss Carolyn Keene of the Tobacco–Health Research Institute, University of Kentucky for their help with smoking experiments. This work was supported by Grant No. R01-DA-00507-02 from the National Institute of Drug Abuse, U.S. Public Health Service.

REFERENCES

1 R. Mechoulam, N. K. McCallum and S. Burstein, *Chem. Rev.*, 76 (1976) 75.
2 S. Burstein, C. Varanelli and L. T. Slade, *Biochem. Pharmacol.*, 24 (1975) 1053.
3 A. B. Segelman, R. D. Sofia, F. P. Segelman, J. J. Harakal and L. C. Knolboch, *J. Pharm. Sci.*, 63 (1974) 962.
4 M. Novotný, M. L. Lee, C.-E. Low and A. Raymond, *Anal. Chem.*, 48 (1976) 24.
5 M. Novotný, M. L. Lee, C.-E. Low and M. P. Maskarinec, *Steroids*, 27 (1976) 665.
6 M. L. Lee, M. Novotný and K. D. Bartle, *Anal. Chem.*, 48 (1976) 405.
7 I. Schmeltz, C. J. Dooley, R. L. Stedman and W. J. Chamberlain, *Phytochemistry* 6 (1967) 33.
8 E. L. Wynder and D. Hoffmann, *Advan. Cancer Res.*, 8 (1964) 249.
9 E. L. Wynder and D. Hoffmann, *Tobacco and Tobacco Smoke*, Academic Press, New York, 1967, p. 396.
10 F. Seehofer and J. E. Miller, *Beitr. Tabakforsch.*, 3 (1965) 75.
11 D. W. Grant and G. A. Vaughan, in M. van Swaay (Editor), *Gas Chromatography 1962*, Butterworths, London, 1962, p. 305.
12 A. E. Pierce, *Silylation of Organic Compounds*, Pierce, Rockford, Ill., 1968.
13 B. S. Middleditch and D. M. Desiderio, *Anal. Lett.*, 5 (1972) 605.

14 I. Gan, J. Korth and B. Halpern, *J. Chromatogr.*, 92 (1974) 435.
15 W. Averill, *J. Gas Chromatogr.*, 1 (1963) 22.
16 L. Zoccolillo, A. Liberti and G. C. Goretti, *J. Chromatogr.*, 43 (1969) 497.
17 J. Hrivňák, L. Soják, E. Beška and J. Janák, *J. Chromatogr.*, 68 (1972) 55.
18 K. Tesařík and M. Novotný, in H. G. Struppe (Editor), *Gas-Chromatographie 1968*, Akademie-Verlag, Berlin, 1968, p. 575.
19 G. Koranyi, *Surface Properties of Silicate Glasses*, Akademiai Kiado, Budapest, Hungary, 1963 (English edition), p. 80.
20 G. Alexander, G. Garzó and G. Pályi, *J. Chromatogr.*, 91 (1974) 25.
21 G. Schomburg, H. Husmann and F. Weeke, *J. Chromatogr.*, 99 (1974) 63.
22 A. F. Fentiman, Jr., R. L. Foltz and G. W. Kinzer, *Anal. Chem.*, 45 (1973) 580.
23 J. H. Bell, A. O. Saunders and A. W. Apears, *Tobacco Sci.*, 10 (1966) 138.
24 F. J. E. M. Küppers, C. A. L. Bercht, C. A. Salemink, R. J. J. Ch. Lousberg, J. K. Terlouw and W. Heerma, *J. Chromatogr.*, 108 (1975) 375.
25 S. Burstein, E. Levin and C. Varanelli, *Biochem. Pharmacol.*, 22 (1973) 2905.
26 K. M. Williams and B. Halpern, *J. Chromatogr.*, 97 (1974) 267.

Journal of Chromatography, 126 (1976) 569–580
© Elsevier Scientific Publishing Company, Amsterdam — Printed in The Netherlands

CHROM. 9408

STUDY OF THE INTESTINAL TYROSINE METABOLISM USING STABLE ISOTOPES AND GAS CHROMATOGRAPHY–MASS SPECTROMETRY

H. Ch. CURTIUS and M. METTLER

Division of Clinical Chemistry, Department of Pediatrics, University of Zürich, Steinwiesstrasse 75, 8032 Zürich (Switzerland)

and

L. ETTLINGER

Department of Microbiology, Swiss Federal Institute of Technology, 8006 Zürich (Switzerland)

SUMMARY

Deuterated tyrosine, 4-hydroxyphenyllactic acid, 4-hydroxyphenylpropionic acid, 4-hydroxyphenylacetic acid and 4-hydroxybenzoic acid were incubated under anaerobic conditions with human faecal specimens for the *in vitro* study of their respective metabolisms. After 1 week, aromatic acids and phenols were extracted and analyzed by gas chromatography–mass spectrometry.

[3′,5′-$^2H_2$]Tyrosine produced 4-hydroxyphenyllactic acid, 4-hydroxyphenylpropionic acid and 4-hydroxyphenylacetic acid; [3′,5′-$^2H_2$]-4′-hydroxyphenyllactic acid produced 4-hydroxyphenylpropionic acid, 3-hydroxyphenylpropionic acid, 4-hydroxyphenylacetic acid and phenylpropionic acid; [3′,5′-$^2H_2$]-4′-hydroxyphenylpropionic acid produced 3-hydroxyphenylpropionic acid and phenylpropionic acid; [3′,5′,2,2-$^2H_4$]-4′-hydroxyphenylacetic acid produced *p*-cresol; and [3′,5′-$^2H_2$]-4′-hydroxybenzoic acid produced phenol.

Thus the intestinal flora showed activities for decarboxylation leading to phenol and *p*-cresol, dehydroxylation leading to phenylpropionic acid and rearrangement leading to 3-hydroxyphenylpropionic acid. Retention of both deuterium labels was observed in the rearrangement reaction.

INTRODUCTION

Deuterated amino acids and steroids have been used for *in vivo* studies of their respective metabolisms in man. These labelled compounds have been given orally to healthy subjects as well as to patients, and the metabolites and their isotope content have been analyzed in urine using combined gas chromatography–mass spectrometry (GC–MS). This technique elucidated the metabolic pathways *in vivo* without risk to the subjects. We previously reported our results from patients with irregularities in the tyrosine degradation pathway, one patient with phenylketonuria, one with hyperphenylalanineamia and the third with oligophrenia of unknown genesis[1]. The patients were dosed orally with 150 mg/kg of deuterated L-tyrosine. GC–MS investigations of

the urine revealed that the same metabolites were deuterated as in normal controls, but in addition deuterated benzoic acid, hippuric acid, 3-hydroxyhippuric acid and 3-hydroxyphenylhydracrylic acid were found deuterated and excreted in increased concentrations. When neomycin was given during 3 days for partial sterilization of the intestine before the dosing, tyrosine was no longer converted into the four additional compounds mentioned above. No excretion of the ordinary urinary metabolites *p*-cresol and phenol was found after admission of neomycin.

Bakke[2] reported similar results after treating rats orally with neomycin. When experimenting with rats, the level of urinary phenols was reduced to almost zero.

It must be concluded that benzoic acid, hippuric acid, 3-hydroxyhippuric acid, 3-hydroxyphenylhydracrylic acid, phenol and *p*-cresol should be derived from the degradation of tyrosine or tyrosine metabolites by the intestinal flora. We were interested, therefore, to study the metabolic activity of the human intestinal flora with tyrosine and its metabolites. Drasar and Hill[3] described the production of phenolic acids and phenols from tyrosine. Bacteria desaminate tyrosine by reduction to 4-hydroxyphenylpropionic acid, which is decarboxylated to 4-ethylphenol or oxidized to 4-hydroxyphenylacetic acid. These compounds are either decarboxylated to *p*-cresol or oxidized to *p*-hydroxybenzoic acid. The latter is further decarboxylated to phenol. Bakke[2] demonstrated the decarboxylation of 4-hydroxyphenylacetic acid and *p*-hydroxybenzoic acid by rat caecal content. When tyrosine was incubated with rat caecal content, he found 4-hydroxyphenylacetic acid, *p*-cresol and phenol. Scott *et al.*[4] demonstrated that 4-hydroxyphenylpropionic acid was dehydroxylated to phenylpropionic acid by sheep rumen content. Studies of bacterial metabolism were often carried out with radioactive test substances in connection with thin-layer chromatography, high-voltage electrophoresis or GC[5]. *In vitro* studies of the tyrosine metabolism using gut bacteria are handicapped by the bacteriostatic action of some aromatic acids. Hence, only small amounts of labelled substances could be used for incubation with human faecal content.

For *in vitro* studies with labelled precursors, the stable isotope GC–MS technique seems to be very advantageous. Apart from physiological safety, there are analytical advantages in using stable isotopes. The components can be separated by GC and their isotope content can be directly analyzed by mass spectrometry. The GC–MS combination is superior in its separating capacity to conventional methods of determining radioactive isotopes, where the components are usually separated by paper, thin-layer or column chromatography and then measured off-line with a liquid scintillation counter.

For these reasons and in analogy with our previously published *in vivo* experiments, we used deuterated compounds for incubation.

EXPERIMENTAL

Collection of samples

Two normal persons were dosed with 150 mg/kg of deuterated tyrosine and 500 mg of carmine red, the latter serving as a coloured marker, which could be easily re-found in the faeces. A 50-g amount of the first red-coloured faeces was suspended in 100 ml of a sterile phosphate buffer of pH 7 which was flushed with nitrogen. The urine of these persons was also collected from the time of the dosing until 2 days after-

wards. Another faecal specimen of 50 g suspended in 100 ml of phosphate buffer was delivered by a patient with phenylketonuria. The patient had been dosed with phenylalanine $2\frac{1}{2}$ days before collection of the sample.

Materials

The following chemicals were used: 4-coumaric acid (Fluka 28190; Fluka, Buchs, Switzerland), 3-coumaric acid (Fluka 28180), 3-(4-hydroxy)phenylpropionic acid (Fluka 56190), *p*-cresol (Fluka 61030), 4-ethylphenol (Merck 821290; Merck, Darmstadt, G.F.R.), phenol (Merck 822296), hydrochloric acid-d_1, 20% in D_2O (Merck 2900), phenylpropionic acid (Fluka 56670), deuterium oxide (Ciba-Geigy 10690; Ciba-Geigy, Basel, Switzerland), bis(trimethylsilyl)trifluoroacetamide (BSTFA) (Regis 270112; Regis, Morton Grove, Ill., U.S.A.), 3% XE-60 liquid phase on 80–100-mesh Gas-Chrom Q (Supelco, Bellefonte, Pa., U.S.A.), DL-4-hydroxyphenyllactic acid (Sigma H-3253; Sigma, St. Louis, Mo., U.S.A.) and DL-4-hydroxymandelic acid (Sigma H-0502). 3-Hydroxyphenylpropionic acid was synthesized from 3-coumaric acid by catalytic hydrogenation with platinum in glacial acetic acid. All other reagents and solvents were of analytical-reagent grade.

Deuterated compounds

3,5-Dideutero-L-tyrosine and 3,5-dideuterobenzoic acid were synthesized by A. Wessiak and P. Hemmerich, Department of Biology, University of Konstanz, G.F.R.

By analogy with the method of Jacobsen[6], 4-hydroxyphenylacetic acid and 4-hydroxyphenylpropionic acid were deuterated with hydrochloric acid-d_1 and deuterium oxide. The aromatic acid (0.5 g) was suspended in 0.5 ml of 20% deuterohydrochloric acid and 1 ml of deuterium oxide. The test-tube containing the reaction mixture was sealed under atmospheric pressure. After incubation at 120° for 24 h, the mixture was evaporated to dryness. The deuteration was controlled by nuclear magnetic resonance (NMR) spectroscopy and GC–MS.

For the NMR spectroscopy, 30 mg of substance were dissolved in 0.5 ml of acetone-d_6. As the internal standard we used tetramethylsilane. The NMR spectrum was obtained with a Hitachi Perkin-Elmer R-24 high-resolution NMR spectrometer. For the MS, a few milligrams of substance were dissolved in 0.5 ml of ethyl acetate and the derivatization was carried out as described below. 4-Hydroxyphenylpropionic acid was deuterated twice in the aromatic ring. 4-Hydroxyphenylacetic acid had two deuterium atoms in the aromatic ring and two in the side-chain in the α-position to the carboxyl group. 4-Hydroxyphenyllactic acid and coumaric acid were completely destroyed under the same conditions.

4-Hydroxyphenyllactic acid could be deuterated by a modified deuteration procedure. The test-tube, containing the same amounts of aromatic acid, deuterohydrochloric acid and deuterium oxide as above, was sealed under high vacuum and incubated at 100° for 24 h. The slightly red-coloured reaction mixture was extracted three times with ethyl acetate and evaporated to dryness. NMR spectroscopy and GC–MS were carried out as above. 4-Hydroxyphenyllactic acid was deuterated twice in the aromatic ring. Coumaric acid was again destroyed under these incubation conditions.

METHODS

Incubation of faecal specimens with deuterated aromatic acids

Clostridial medium (12.7 g) was dissolved in 300 ml of water. The test substances tyrosine, 4-hydroxyphenyllactic acid, 4-hydroxyphenylpropionic acid, 4-hydroxyphenylacetic acid and 4-hydroxybenzoic acid were dissolved in water to give a concentration of 10 μmole/ml and 10.8 ml of clostridial medium and 1.2 ml of the test substances were placed in test-tubes with screw-caps. The test-tubes were heated in a boiling water-bath for 15 min and cooled under nitrogen–carbon dioxide (1:1). After sterilization (20 min at 120°), the ten tubes (two of each test substance) were inoculated with faeces in a glove bag under nitrogen–carbon dioxide (1:1). The test-tubes were placed in serum bottles which were closed under nitrogen–carbon dioxide (1:1). After incubation at 37° for 1 week, all of the test-tubes were closed with screw-caps and stored at −4°. In order to control the anaerobic conditions an oxygen indicator according to Willis[7] accompanied the test-tubes through the whole process.

Extraction of urine, faeces and cultures of faecal specimens

The well established extraction method for aromatic acids in urine described by Völlmin *et al.*[8] was also applied to faecal suspensions and cultures of faecal specimens.

A 10-ml volume of urine, faecal suspension or culture of faecal specimens was acidified with 6 *N* hydrochloric acid to pH 1 saturated with sodium chloride and extracted three times with 20 ml of ethyl acetate. The organic phase was then brought to pH 1 with 6 *N* hydrochloric acid, saturated with sodium chloride and again extracted three times with 20 ml of ethyl acetate. The organic phase was dried with sodium sulphate and the solvent evaporated to 0.1 ml in a vacuum rotary evaporator. This extract was used for GC–MS analysis.

The phenols were extracted from 10 ml of urine, faeces or cultures of faecal specimens. The samples were acidified with 2 ml of 6 *N* hydrochloric acid and steam distillation by use of a Kjeldahl apparatus was performed. This procedure resulted in acid hydrolysis of the phenolic sulphate esters and in extraction of the free phenols. The pH of the solution of phenols in water was adjusted to 7.5 with 0.1 *N* sodium hydroxide solution. The solution was saturated with sodium chloride and extracted three times with 20 ml of diethyl ether. The combined extracts were dried with sodium sulphate, cooled in an ice-bath for 10 min and evaporated to 0.5 ml at room temperature using a vacuum rotary evaporator. The sample was then transferred to a test-tube. After addition of 1 μmole of 4-ethylphenol in 0.5 ml of ethyl acetate as an internal standard, the sample was evaporated to 0.2 ml.

Derivatization

The methyl esters were formed by adding an excess of diazomethane in diethyl ether. After reducing the volume to 0.2 ml under a stream of nitrogen, 0.1 ml of BSTFA was added for silylation. Undecylenic acid methyl ester (1 μmole in 0.1 ml of ethyl acetate) was added as an internal standard. For the GC–MS analysis of the phenols, no derivatization was carried out.

Gas–liquid chromatography with flame-ionization detection

The quantitative determination of aromatic acids and phenols in urine, faeces and faecal cultures was carried out with a Hewlett-Packard Model 7620A gas chromatograph with a dual flame-ionization detector. The glass column (3.3 m × 2 mm I.D.) was packed with 3% XE-60 on Gas-Chrom Q (80–100 mesh). The flow-rate of the carrier gas (nitrogen) was 30 ml/min, and the temperature of the injector block and the detector was 250°.

For the chromatography of the aromatic acids, we used the following temperature programme: 10 min isothermal at 80°, then heating to 220° at the rate of 2°/min. The chromatography of the phenols started isothermally at 70° during 10 min, followed by heating to 130° at the rate of 2°/min. The oven was heated to 170° and kept isothermal for 10 min before starting a new programme. Volumes of 1–2 μl of the samples were injected.

Gas–liquid chromatography–mass spectrometry

A combination of a Carlo Erba Fractovap 2101 gas chromatograph coupled to a vacuum generator mass spectrometer (Micromass 16F) and a vacuum generator data system (Type 2000) was used.

The GC column (2 m × 3 mm I.D.) was filled with 3% XE-60 on 80–100-mesh Gas-Chrom Q. The flow-rate of the carrier gas (helium) was 30 ml/min and the flash heater temperature was 250°. The chromatography of phenol and *p*-cresol was carried out with an oven temperature of 105°, increased to 150° at the rate of 4°/min; for the aromatic acids the initial temperature of 90° was maintained for 3 min and then increased to 200° at the rate of 2.5°/min. The temperature of the single jet separator and the ion source was 230°. The accelerating voltage was 4 kV, the electron multiplier voltage 3 kV and the trap current 20 μA. The mass spectra were obtained at 20 eV.

RESULTS

In vivo studies

From the two normal persons who had been orally dosed with deuterated L-tyrosine, we determined the aromatic acids and phenols in urine and some faecal specimens. In faeces we did not find any aromatic acids or phenols up to 72 h after the dosing test. After these dosing tests we found the following deuterated urinary tyrosine metabolites: 4-hydroxyphenylacetic acid, 4-hydroxybenzoic acid, 4-hydroxymandelic acid, homovanillic acid, 4-hydroxyphenyllactic acid, vanillylmandelic acid, 4-hydroxyhippuric acid, phenol and *p*-cresol.

In vitro studies

*Incubation with dideutero-*L*-tyrosine.* The incubation of faecal specimens from the two normal controls with dideutero-L-tyrosine showed the following deuterated aromatic acids, which contained two deuterium atoms: 4-hydroxyphenylacetic acid, 4-hydroxyphenylpropionic acid and 4-hydroxyphenyllactic acid. Fig. 1 shows the gas chromatogram of the faecal aromatic acids after incubation with tyrosine.

Only very small amounts of 4-hydroxyphenylpropionic acid and 4-hydroxyphenylacetic acid could be detected after incubation of the faecal specimen from the

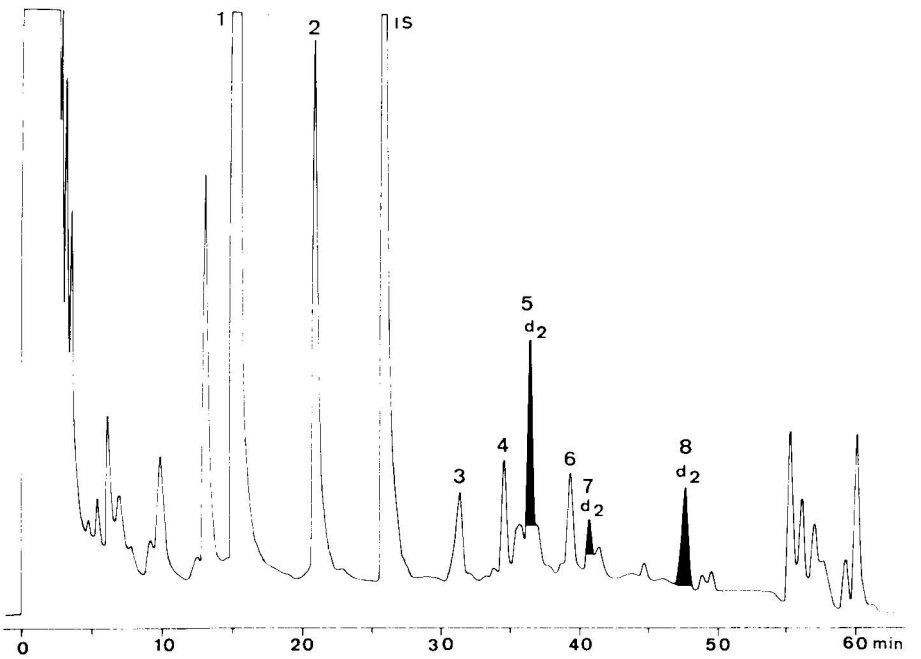


Fig. 1. Gas chromatogram of the aromatic acids extracted from incubation of tyrosine with a faecal specimen from a normal person. The peaks marked in black signify deuterated aromatic acids. Peaks: 1 = phenylacetic acid; 2 = phenylpropionic acid; 3 = phenyllactic acid; 4 = 3-hydroxyphenylacetic acid; 5 = 4-hydroxyphenylacetic acid; 6 = 3-hydroxyphenylpropionic acid; 7 = 4-hydroxyphenylpropionic acid; 8 = 4-hydroxyphenyllactic acid; IS = internal standard.

phenylketonuric patient with tyrosine. Phenols were not found in any of faecal cultures with tyrosine as a test substance.

Incubation with dideutero-4-hydroxyphenyllactic acid. Different kinds of deuterated aromatic acids were detected after incubation of the faecal specimens from the three subjects with 4-hydroxyphenyllactic acid. Phenylpropionic acid was found in the highest concentration, followed by 4-hydroxyphenylpropionic acid and 3-hydroxyphenylpropionic acid and 4-hydroxyphenylacetic acid in smaller amounts. All compounds still contained two deuterium atoms, also 3-hydroxyphenylpropionic acid.

Fig. 2 shows the gas chromatogram of the faecal aromatic acids after incubation with deuterated 4-hydroxyphenyllactic acid. 3-Hydroxyphenylpropionic acid was identified by its retention time and mass spectrum using a reference compound synthesized from 3-coumaric acid (see *Materials*). The mass spectra of the deuterated and non-deuterated 3-hydroxyphenylpropionic acid are shown in Figs. 3 and 4.

Incubation with dideutero-4-hydroxyphenylpropionic acid. After incubation of 4-hydroxyphenylpropionic acid with faeces from one of the normal controls, deuterated phenylpropionic acid was found in large amounts. After incubation of faeces from the second normal subject we detected smaller amounts of deuterated phenylpropionic acid and, in addition, dideutero-3-hydroxyphenylpropionic acid. The faecal specimen from the phenylketonuric patient showed the presence of phenyl-

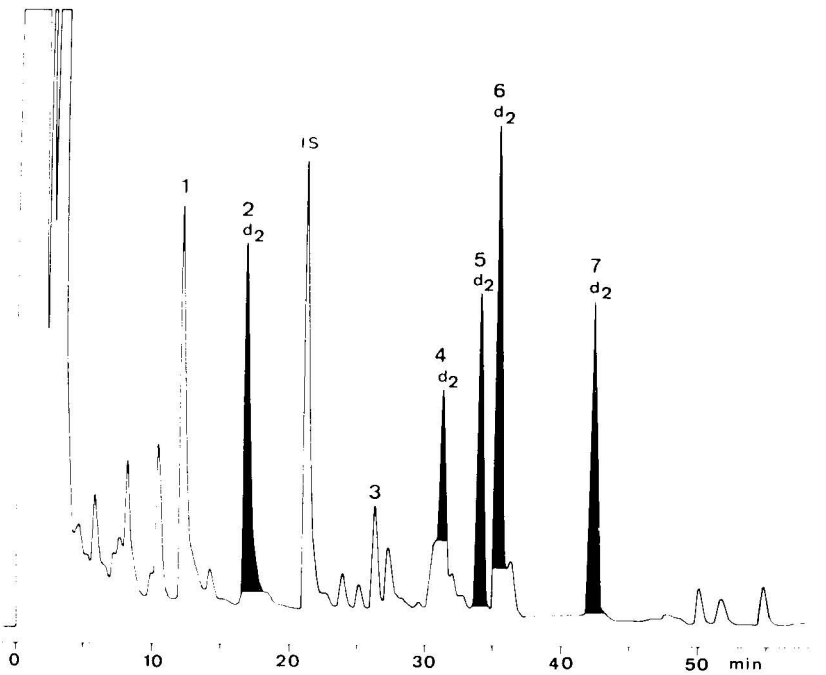


Fig. 2. Gas chromatogram of the aromatic acids extracted from incubation of 4-hydroxyphenyllactic acid with a faecal specimen from a normal person. The peaks marked in black signify deuterated aromatic acids. Peaks: 1 = phenylacetic acid; 2 = phenylpropionic acid; 3 = phenyllactic acid; 4 = 4-hydroxyphenylacetic acid; 5 = 3-hydroxyphenylpropionic acid; 6 = 4-hydroxyphenylpropionic acid; 7 = 4-hydroxyphenyllactic acid.

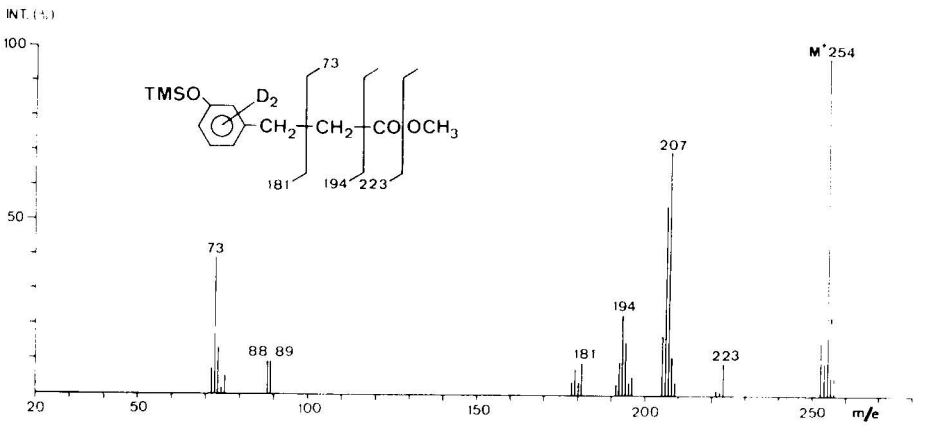


Fig. 3. Mass spectrum of partly dideuterated 3-hydroxyphenylpropionic acid obtained after incubation of a faecal specimen with [3′,5′-$^2H_2$]-4′-hydroxyphenyllactic acid.

propionic acid, 3-hydroxyphenylpropionic acid and 4-hydroxyphenyllactic acid. Deuterated phenols were not detected in any incubation with faecal specimens.

Incubation with dideuterophenylacetic acid and dideutero-4-hydroxybenzoic acid. Further incubations with faeces from the three different test persons with deuterated

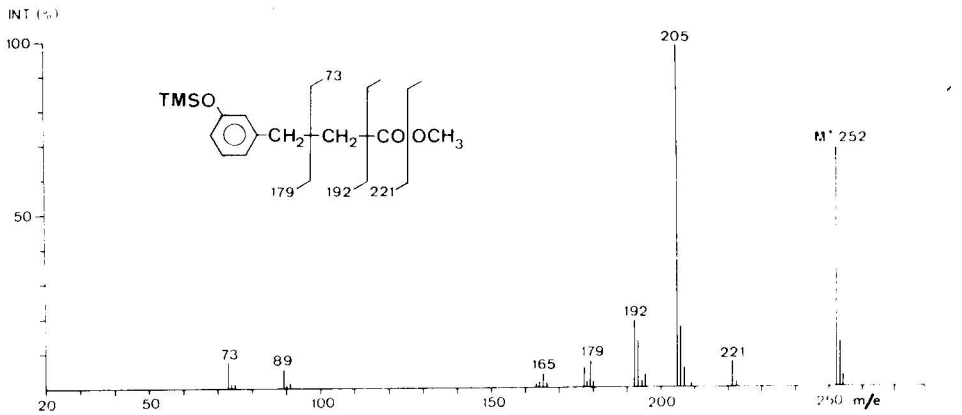


Fig. 4. Mass spectrum of non-deuterated 3-hydroxyphenylpropionic acid.

4-hydroxyphenylacetic acid yielded large amounts of *p*-cresol, and incubations with 4-hydroxybenzoic acid showed large amounts of phenol.

The mass spectrum of *p*-cresol, which was obtained after incubation with tetradeutero-4-hydroxyphenylacetic acid, is shown in Fig. 5. In comparison, Fig. 6 shows the mass spectrum of non-deuterated *p*-cresol.

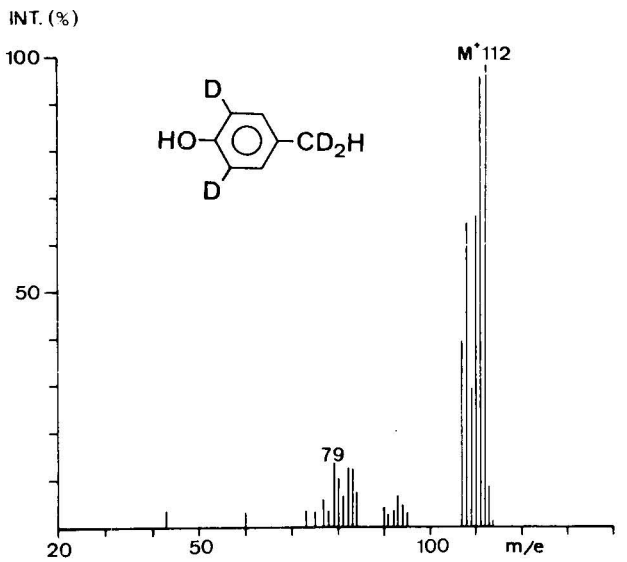


Fig. 5. Mass spectrum of partly tetradeuterated *p*-cresol, a metabolic product of [3′,5′,2,2-$^2H_2$]-4′-hydroxyphenylacetic acid.

Fig. 7 shows the metabolic pathways of the tyrosine metabolism, referring only to the monohydroxylated and non-hydroxylated aromatic acids and to the phenols.

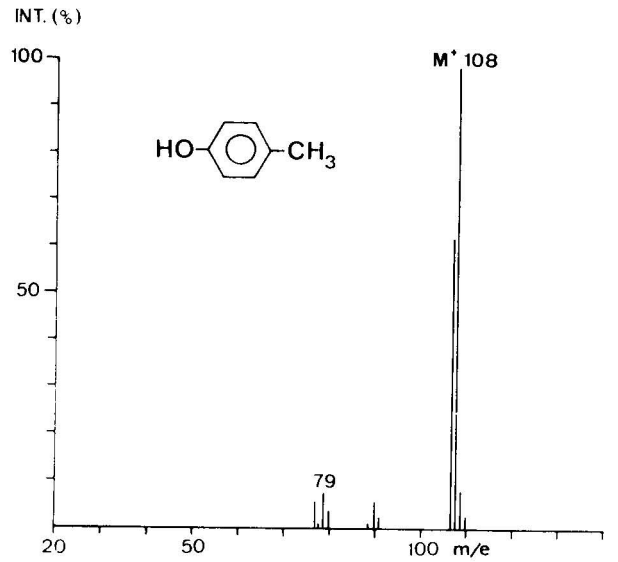


Fig. 6. Mass spectrum of non-deuterated *p*-cresol.

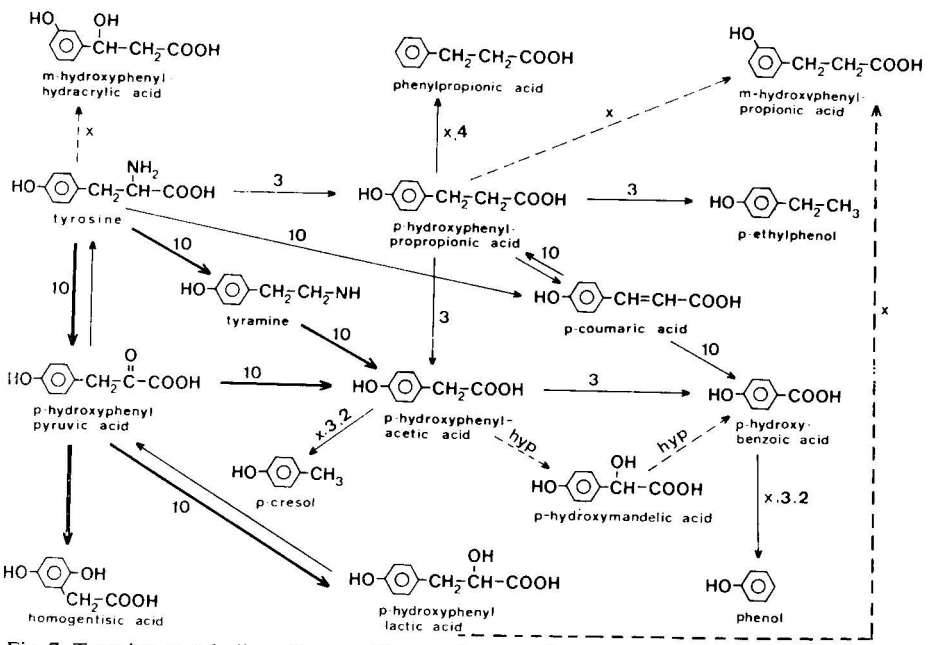


Fig. 7. Tyrosine metabolic pathways. The numbers on the arrows refer to the references; × refers to our results obtained by incubation of faecal specimens with tyrosine metabolites; hyp is a hypothetical route for 4-hydroxybenzoic acid.

DISCUSSION

Our studies of the correlation of human endogenous metabolism and intestinal bacterial flora showed that stable isotope techniques combined with GC–MS are

suitable for the investigation of metabolism both *in vivo* and *in vitro*. In order to obtain comparable results, we applied incubation methods similar to those reported by Drasar and Hill[3] and Bakke[2] for intestinal flora. The isolation of the aromatic acids from faecal specimens and urine was performed according to our earlier method[8]. Further purification of the extract, including high-voltage electrophoresis, active charcoal and chromatography on Kieselguhr, resulted in the loss of some of the aromatic acids.

In normal human urine, there is usually a relatively large amount of conjugated phenol and *p*-cresol which makes it difficult to determine small amounts of the deuterated compounds. The same difficulties occurred in faecal incubations, where sometimes large amounts of free phenol and *p*-cresol were detected. In a few instances it was difficult to differentiate the labelled isotope from natural isotope content.

To the faecal suspension we added 10% of glycerol in order to avoid bursting of the bacteria and stored the suspension in a deep-freeze.

After dosing two normal persons with dideuterotyrosine, we found decarboxylated products, *viz.*, phenol and *p*-cresol, in their urine. In earlier dosing tests with three patients having irregularities in their tyrosine metabolism we were able to find a dehydroxylation activity leading to benzoic and hippuric acid as well as to a rearrangement activity leading to 3-hydroxyphenylhydracrylic acid and 3-hydroxyhippuric acid[1]. These products were absent after disinfection of the intestine with neomycin. The result is in agreement with the statement of Drasar and Hill[3] that the dehydroxylation activity is destroyed by neomycin.

Dehydroxylation reactions

In the *in vitro* studies with human faecal specimens, we found dehydroxylation products only after incubation with two test substances. The incubation with 4-hydroxyphenylpropionic acid resulted in large amounts of phenylpropionic acid; 4-hydroxyphenyllactic acid yielded 4-hydroxyphenylpropionic acid and, in smaller amounts, phenylpropionic acid. The influence of neomycin on these incubations will be studied later.

None of the test substances used in the incubations with faecal specimens resulted in benzoic acid or hippuric acid, which we have found in large amounts in the urine of several persons after dosing tests with tyrosine.

Decarboxylation reactions

With respect to decarboxylation reactions, the faecal incubation with deuterated 4-hydroxyphenylacetic acid and 4-hydroxybenzoic acid showed large amounts of phenols. On the other hand, the incubation of faeces with 4-hydroxyphenylpropionic acid never resulted in 4-ethylphenol. In the urine of all of the test persons we found, after dosing with dideuterated tyrosine, large amounts of phenol and *p*-cresol, except after medication with neomycin. In contrast to Drasar and Hill[3], we never detected 4-ethylphenol.

It is possible that urinary phenols play a role in human cancer, and this aspect was discussed by Drasar and Hill[3].

Rearrangement reactions

We previously reported on three patients with the abnormal urinary tyrosine metabolites 3-hydroxyphenylhydracrylic and 3-hydroxyhippuric acid[1]. Either migra-

tion of the side-chain or of the hydroxyl group might be caused by the intestinal flora. We cannot exclude the possibility that neomycin interferes with the enzyme which is responsible for the migration.

The *in vitro* incubation studies with deuterated tyrosine metabolites showed analogous results. While using 4-hydroxyphenyllactic acid or 4-hydroxyphenylpropionic acid for incubation, we obtained 3-hydroxyphenylpropionic acid which was still dideuterated.

There are three possibilities for the rearrangement reaction.

(1) One possibility is a rearrangement of the hydroxyl group. We cannot describe any pathway for such a reaction because *m*-hydroxylphenylpropionic acid still contains two deuterium atoms to a large extent and therefore one deuterium atom must have shifted with the hydroxyl group (Fig. 8).

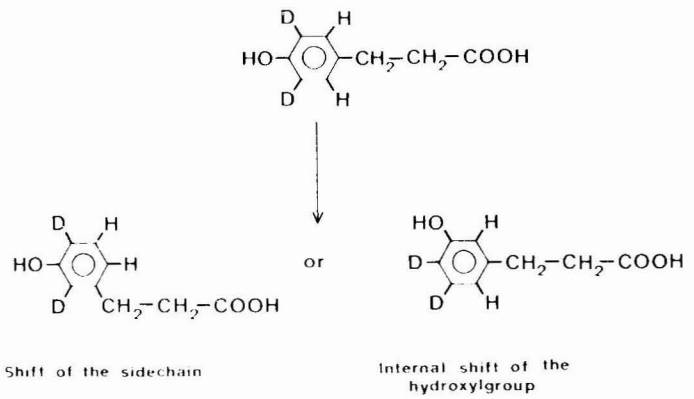


Fig. 8. The incubation of faecal specimens with 4-hydroxyphenylpropionic acid or with 4-hydroxyphenyllactic acid resulted in 3-hydroxyphenylpropionic acid; either the side-chain or the hydroxyl group may have been shifted, as shown.

(2) A second possibility is a shift of the side-chain without introduction of a further hydroxyl group (Fig. 8), as known in the case of the formation of homogentisinic acid.

(3) The third possibility is a *meta*-hydroxylation by tyrosine 3-hydroxylase followed by a *para*-dehydroxylation. This reaction is improbable because 3-hydroxyphenylpropionic acid is still dideuterated after incubation with 4-hydroxyphenylpropionic acid and an NIH shift is not possible in phenols, as described by Massey and Hemmerich[9]. Further, we performed our incubation studies under anaerobic conditions, excluding hydroxylation by tyrosine 3-hydroxylase, which requires molecular oxygen for its activity.

We intend to carry out further studies on the reaction mechanism of the above-mentioned rearrangements.

The induction of bacterial enzymes is a very important source of artefacts, which we cannot eliminate and which we have to consider by faecal incubation and loading tests. The test substances can induce the bacterial enzyme system, resulting in a much higher bacterial activity compared with the non-induced normal gut flora. We chose the long incubation time of 1 week in order to obtain enough metabolic

products for a qualitative analysis. For further experiments, we should assimilate our incubations to physiological conditions by reducing the incubation time. In order to minimize induction, we plan to reduce the amount of the test substances used to a minimum.

ACKNOWLEDGEMENT

This study was supported by the Schweizerischer Nationalfonds zur Förderung der wissenschaftlichen Forschung (Grant No. 3.3050.74).

REFERENCES

1 H. Ch. Curtius, U. Redweik, B. Steinman, W. Leimbacher annd R. Wegmann, *Second International Conference on Stable Isotopes, Chicago, October 20–23, 1975*, in press.
2 O. M. Bakke, *Scand. J. Gastroenterol.*, 4 (1969) 603.
3 B. S. Drasar and M. J. Hill, *Human Intestinal Flora*, Academic Press, New York, 1974.
4 T. W. Scott, P. F. V. Ward and R. M. C. Dawson, *Biochem. J.*, 90 (1964) 12.
5 O. M. Bakke, *Acta Pharmacol. Toxicol.*, 30 (1971) 115.
6 R. J. Jacobsen, *Spectrochim. Acta*, 21 (1965) 433.
7 A. T. Willis, *Anaerobic Bacteriology in Clinical Medicine*, Butterworths, London, 1960.
8 J. A. Völlmin, H. R. Bosshard, M. Müller, S. Rampini and H. Ch. Curtius, *Z. Klin. Chem. Klin. Biochem.*, 9 (1971) 402.
9 V. Massey and P. Hemmerich, in P. D. Boyer (Editor), *The Enzymes*, Vol. 12, Part B, Academic Press, New York, 3rd ed., 1975, p. 220.
10 C. van der Heiden, S. K. Wadman, D. Ketting and P. K. de Bree, *Clin. Chim. Acta*, 31 (1971) 133.

Journal of Chromatography, 126 (1976) 581–589
© Elsevier Scientific Publishing Company, Amsterdam — Printed in The Netherlands

CHROM. 9474

ALDEHYDE CONDENSATION PRODUCTS AS DERIVATIVES FOR THE VAPOR PHASE ANALYSIS OF BIOGENIC AMINES

BRIAN S. MIDDLEDITCH

Department of Biophysical Sciences, University of Houston, Houston, Texas 77004 (U.S.A.)

SUMMARY

The mass spectra of six tetrahydroisoquinolines and five tryptolines are surveyed. It is concluded that tryptolines are suitable for analysis of tryptamines, after condensation with aldehydes.

INTRODUCTION

Combined gas chromatography–mass spectrometry (GC–MS) is the method of choice for the sub-microgram analysis of most organic compounds with molecular weights lower than about 1000[1–4]. The technique of selective ion monitoring (SIM) is particularly useful when a high degree of selectivity and/or sensitivity is required[5]. If the instrument is equipped with a suitable data handling system, it is convenient to acquire complete mass spectra during a chromatogram and to reconstruct "single ion" chromatograms later. However, greater sensitivity is attainable if the "single ion" chromatogram is recorded directly[6]. The ultimate sensitivity of the technique may be limited by one or more of several factors. If the sample is not absorbed or destroyed on the gas chromatographic column[7] and if the sample affords sufficient ions to be detected by the mass spectrometer, the most troublesome aspect of selective ion monitoring is background interference. This may derive from the gas chromatograph (O-rings, septa, stationary phases, etc.) or from contaminants in the mass spectrometer (pump oil, previous samples, etc.). These may be distinguished readily if the instrument is equipped with a valve between the gas chromatograph and the mass spectrometer[5]. A background spectrum recorded at maximum amplification at a normal scan speed will indicate the *m/e* values at which major background ions appear. If the sensitivity is increased by widening the focusing slits in the mass spectrometer and increasing the filtering capacity[5], many more minor background ions can be measured. Under such conditions, complete mass spectra cannot be scanned dynamically, but abundances of individual ions may be determined by slowly adjusting the magnet current[5].

In general, maximum sensitivity during SIM is attained under conditions of low background. One approach to the solution of this problem is to use derivatives which render the samples more volatile, thus permitting the use of lower column temperatures. This, in turn, reduces the amount of bleed from the stationary phase,

septum, and O-rings. An alternative approach, the feasibility of which is explored here, is to use derivatives which increase the molecular weight of the sample so that it affords ions of *m/e* values higher than the majority of the background ions. This concept is examined by surveying the utility of mass spectra of aldehyde condensation products of various biogenic amines[8]. The results are also of intrinsic interest since the resulting tetrahydroisoquinolines and tryptolines are of biochemical and clinical significance, yet few of their mass spectra have been examined in detail.

EXPERIMENTAL

Tetrahydroisoquinolines and tryptolines were obtained from commercial sources (Aldrich, Milwaukee, Wisc., U.S.A.; Alfred Bader Chemicals, Milwaukee, Wisc., U.S.A.; K & K Rare and Fine Chemicals, Plainview, N.Y., U.S.A.) or were synthesized as previously described[8] by condensation of the appropriate amine and aldehyde.

Trimethylsilyl (TMS) derivatives were prepared using trimethylsilylimidazole, to produce TMS ethers and esters, or bis(trimethylsilyl)acetamide, which also derivatizes the amino groups.

Low-resolution mass spectra were obtained using the direct insertion probe inlets of LKB 9000 and DuPont 21-490 instruments at 22.5 eV. High-resolution mass spectra were recorded using a CEC 21-110B instrument under similar conditions.

RESULTS AND DISCUSSION

Low-resolution spectra of compounds I–XI are represented in Figs. 1–11. All interpretations are compatible with the high-resolution data.

Tetrahydroisoquinoline (I)

The mass spectrum (Fig. 1) of this compound contains a relatively abundant molecular ion (*m/e* 133) but the base peak (*m/e* 104) is formed by a retro-Diels–Alder rearrangement. Abundant fragment ions are formed also by elimination of up to four

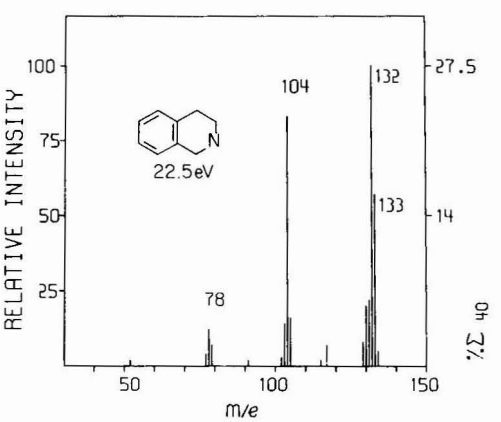


Fig. 1. Mass spectrum (22.5 eV) of tetrahydroisoquinoline (I).

hydrogen atoms from the molecular ion. It should be noted, in particular, that the hydrogen atom at C-1 is readily lost since it is β to both the nitrogen atom and the aromatic ring.

1-Benzyltetrahydroisoquinoline (II)

The mass spectrum (Fig. 2) of this compound further illustrates the propensity for eliminating the substituent at C-1: this fragmentation mode leads to the formation of the base peak of *m/e* 132. The molecular ion (*m/e* 223) is very weak, but a relatively abundant ion of *m/e* 220 is formed by loss of hydrogen atoms from C-1, C-3, and C-4. The $[M - 5]^+$ ion (*m/e* 218) is apparently formed by condensation of the two aromatic nuclei. There is no ion of *m/e* 194 formed by a retro-Diels–Alder rearrangement.

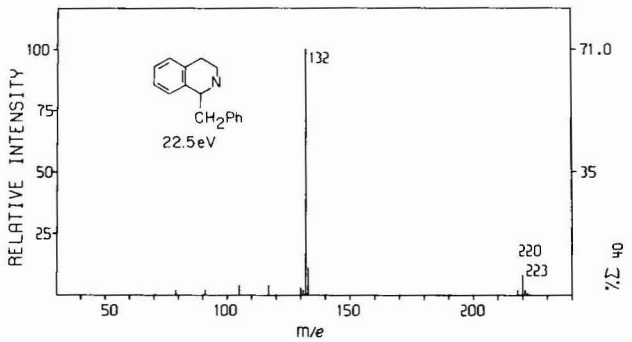


Fig. 2. Mass spectrum (22.5 eV) of 1-benzyltetrahydroisoquinoline (II).

1-Phenyltetrahydroisoquinoline (III)

The cleavage of bonds adjacent to an aromatic nucleus is not commonly observed but, in this compound (see Fig. 3), the substituent at C-1 is sufficiently labile for the ion of *m/e* 132 to become the base peak. This compound also gives rise to an $[M - 5]^+$ ion. The product of a retro-Diels–Alder rearrangement appears at *m/e* 180.0899 ($C_{14}H_{12}$ requires 180.0939). High-resolution data show that all of the other ions in the range *m/e* 151–179 are also formed by cleavage of the heterocyclic ring and elimination of the nitrogen atom. These fragmentations are apparently mediated by the formation of tricyclic products.

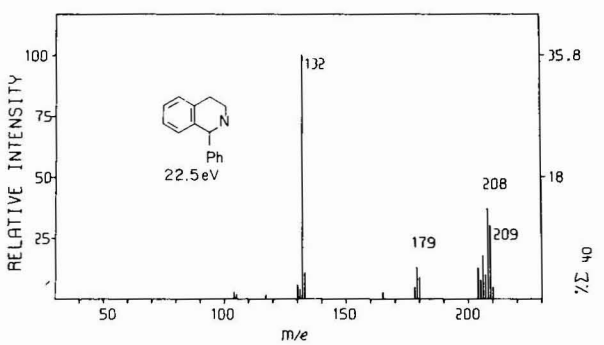


Fig. 3. Mass spectrum (22.5 eV) of 1-phenyltetrahydroisoquinoline (III).

Salsolidine (IV)

All three methyl substituents in this compound are in labile environments, and the spectrum (Fig. 4) is dominated by an $[M - 15]^+$ ion (*m/e* 192). There is a weak ion of *m/e* 178 formed by a retro-Diels–Alder rearrangement. The relatively intense peak of *m/e* 176 is a doublet comprised of $C_{10}H_{10}NO_2$ (calc. 176.0712, obs. 176.0703) and $C_{11}H_{14}NO$ (calc. 176.1076, obs. 176.1051) in the ratio 6:1. The major component is apparently formed by loss of a methoxyl methyl group and methane from the heterocyclic ring of the molecular ion. Both components of this doublet eliminate a molecule of hydrogen to give ions at *m/e* 174 of type $C_{10}H_8NO_2$ (calc. 174.0555, obs. 174.0543) and $C_{11}H_{12}NO$ (calc. 174.0919, obs. 174.0911), respectively, in a ratio of 2:1.

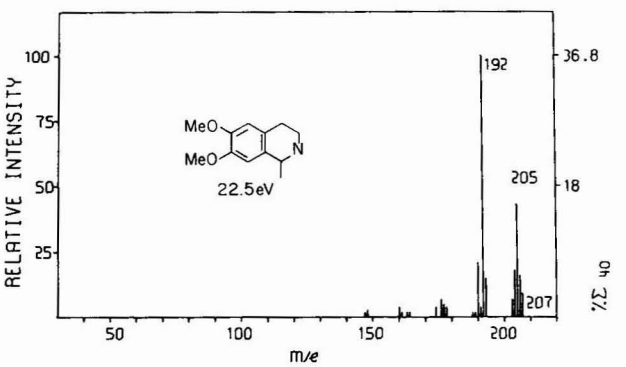


Fig. 4. Mass spectrum (22.5 eV) of salsolidine (IV).

Salsoline (V)

The spectrum (Fig. 5) of this compound exhibits many features of the spectrum of salsolidine. The base peak is of type $[M - 15]^+$ (*m/e* 178), but there is an ion of *m/e* 163 formed by loss of a second methyl group. The accompanying ion of *m/e* 164, formed by a retro-Diels–Alder rearrangement, is less significant. There is,

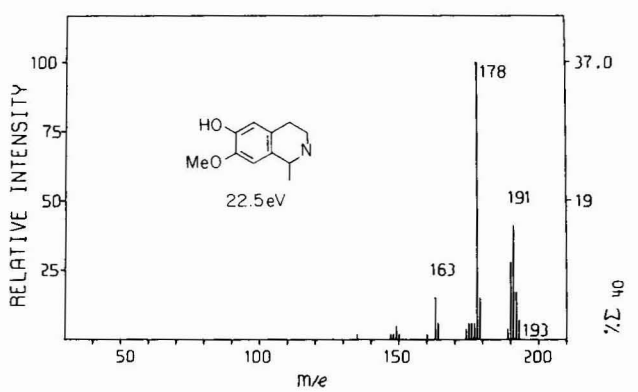


Fig. 5. Mass spectrum (22.5 eV) of salsoline (V).

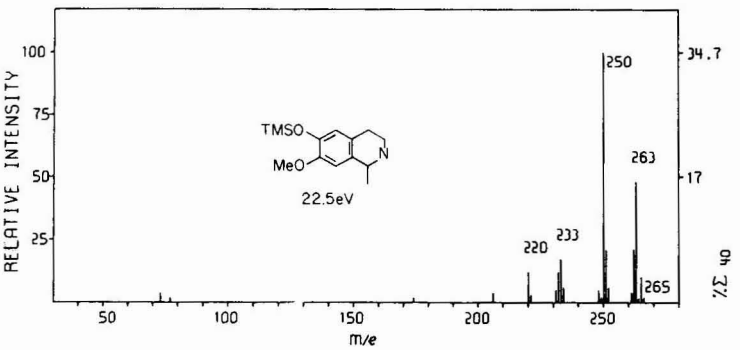


Fig. 6. Mass spectrum (22.5 eV) of salsoline mono-TMS (VI).

however, an ion of *m/e* 149 which may be formed by a retro-Diels–Alder rearrangement of an $[M - 15]^+$ ion, in which a methoxyl methyl group is lost from the molecular ion. Moreover, there is a corresponding ion at *m/e* 220 in the spectrum of the O-trimethylsilyl derivative of salsoline (VI, Fig. 6).

1-Methyltryptoline (VII)

In contrast to the tetrahydroisoquinolines, the molecular ion in the spectrum (Fig. 7) of this and the other tryptolines is more abundant than the accompanying ions formed by loss of one or more hydrogen atoms. As expected, the $[M - 15]^+$ ion (*m/e* 171) is very abundant. The ion of *m/e* 157 is formed by a retro-Diels–Alder rearrangement.

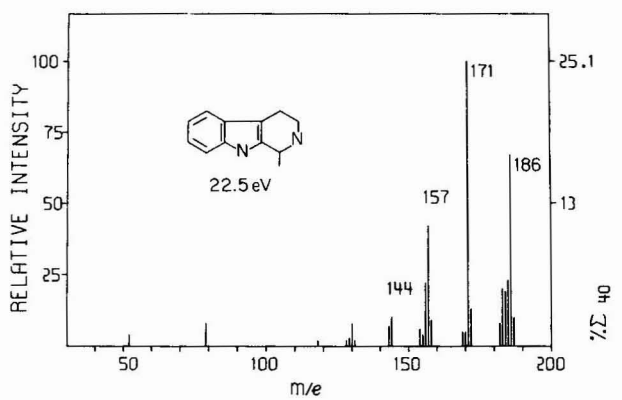


Fig. 7. Mass spectrum (22.5 eV) of 1-methyltryptoline (VII).

Tryptoline-3-carboxylic acid mono-TMS (VIII)

The spectrum (Fig. 8) of this compound contains an abundant molecular ion and only two major fragment ions. Loss of the carboxy-TMS group affords the ion of *m/e* 171, while a retro-Diels–Alder rearrangement yields the ion of *m/e* 143.

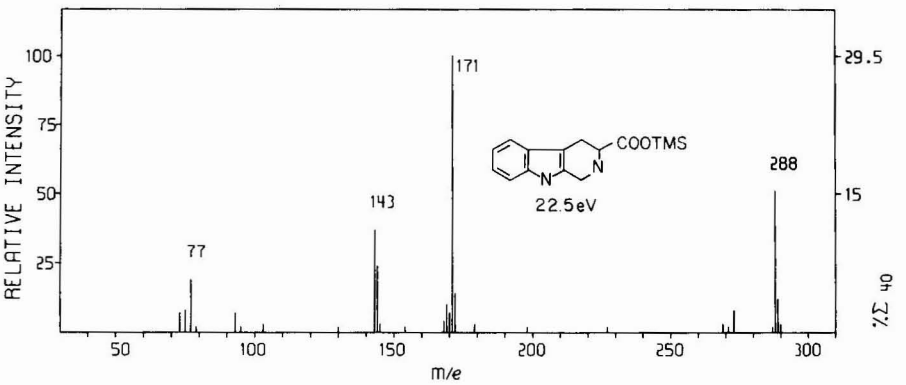


Fig. 8. Mass spectrum (22.5 eV) of tryptoline-3-carboxylic acid mono-TMS (VIII).

Tryptoline-3-carboxylic acid tri-TMS (IX)

In this spectrum (Fig. 9) also, the major ions are the molecular ion (*m/e* 432) and fragment ions due to loss of carboxy-TMS (*m/e* 315) or a retro-Diels–Alder rearrangement (*m/e* 216).

1-(Diethylmethyl)tryptoline-3-carboxylic acid mono-TMS (X)

The alkyl substituent at C-1 is readily lost, so the spectrum (Fig. 10) of this compound is dominated by the ion of *m/e* 287 ($M - C_5H_{11}$). The molecular ion and other fragment ions are relatively weak.

1-Phenyltryptoline-3-carboxylic acid mono-TMS (XI)

There is only a weak ion (*m/e* 287) formed by loss of phenyl group from the molecular ion. Moreover, the product of a retro-Diels–Alder rearrangement (*m/e* 219) is also of very low abundance. The major ions in the spectrum (Fig. 11) are the molecular ion (*m/e* 364) and that formed by loss of carboxy-TMS (*m/e* 247).

Some general observations can be made on the spectra of tetrahydroisoquinolines. In the absence of a substituent at C-1, the molecular ion is relatively abundant and also undergoes a retro-Diels–Alder rearrangement. This type of rearrangement does not afford abundant fragment ions in the spectra of compounds with substituents at C-1. Instead, the molecular ion is generally of low abundance and the substituent at C-1 is readily eliminated. In the case of the 1-phenyl compound, the molecular ion is relatively abundant but the phenyl group is lost, even though this requires a cleavage between a phenyl group and the adjacent carbon atom. The sequential elimination of hydrogen atoms, culminating in the formation of highly conjugated unsaturated polycyclic species is a notable tendency in each of the spectra.

The spectra of the tryptolines, on the other hand, are much simpler. With no substituent at C-1, abundant molecular ions and fragment ions due to loss of the substituent at C-3 and retro-Diels–Alder rearrangements are observed. This rearrangement is suppressed by the presence of a phenyl group at C-1. If an alkyl group is present at C-1 it is readily lost from the molecular ion.

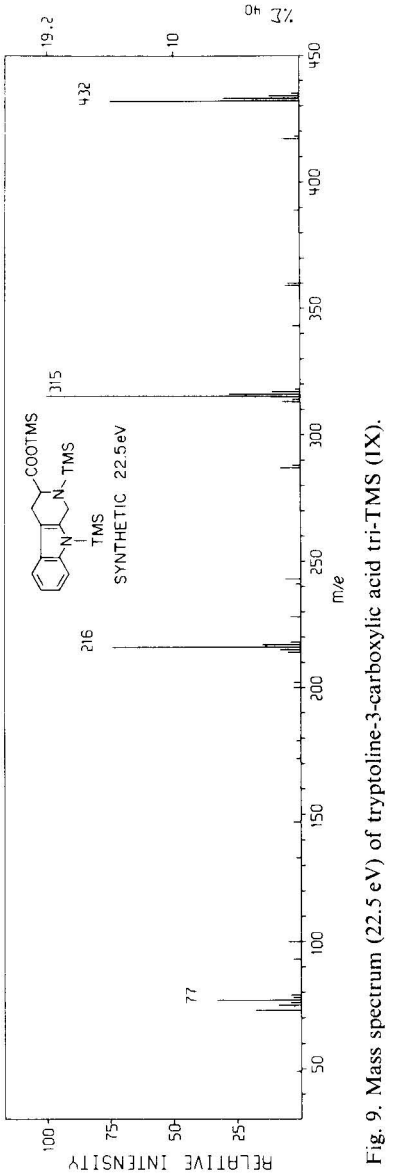


Fig. 9. Mass spectrum (22.5 eV) of tryptoline-3-carboxylic acid tri-TMS (IX).

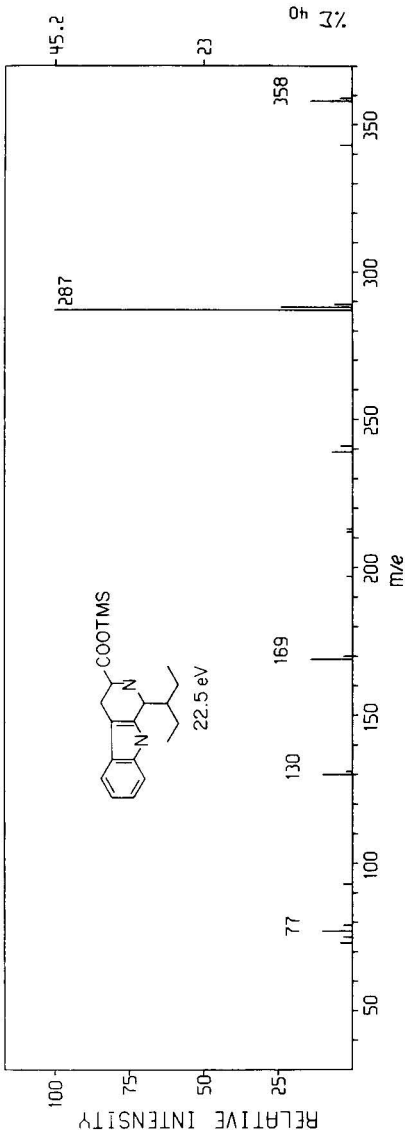


Fig. 10. Mass spectrum (22.5 eV) of 1-(diethylmethyl)tryptoline-3-carboxylic acid mono-TMS (X).

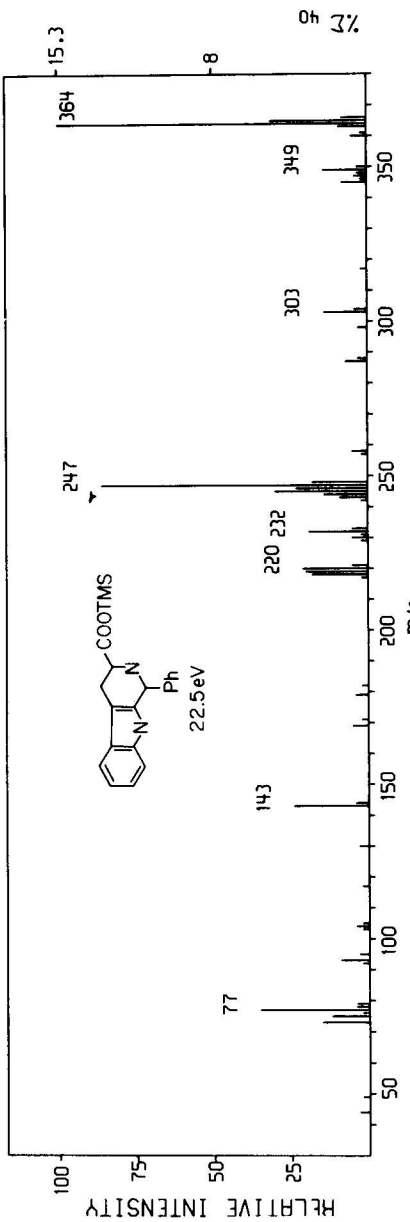


Fig. 11. Mass spectrum (22.5 eV) of 1-phenyltryptoline-3-carboxylic acid mono-TMS (XI).

CONCLUSIONS

The tetrahydroisoquinolines are somewhat disappointing in terms of their potential use as derivatives of β-phenylethylamines for SIM since their molecular ions are usually of low relative abundance. However, ions formed by loss of one or more hydrogen atoms are clearly visible, accounting for 15–20% Σ for IV–VI. In comparison, other derivatives of β-phenylethylamines rarely afford strong molecular ions or related ions formed by loss of hydrogen atoms since the side-chain is so readily cleaved.

In contrast, the tryptolines are more suitable for SIM. With the exception of X, the molecular ions of the compounds studied account for about 15% Σ, and there are only a few (well defined) fragment ions.

The derivatization procedure could be used with a variety of aldehydes, including fluorinated or deuterated compounds, to yield products at almost any *m/e* value, thus avoiding background ions which limit the sensitivity of SIM. Another practical aspect of these compounds is that they may be detected in amine-containing tissues which have been preserved in aldehydes.

ACKNOWLEDGEMENTS

Part of this work was performed at Baylor College of Medicine, where it was partially supported by the National Institutes of Health (GM-13901) and the Robert A. Welch Foundation (Q-125). The work is now being continued with support from the University of Houston. The high-resolution data were kindly supplied by P. Crain.

REFERENCES

1 C. J. W. Brooks, in D. H. Williams (Senior Reporter), *Specialist Periodical Report: Mass Spectrometry*, Vol. 1, Chemical Society, London, 1971.
2 C. J. W. Brooks and B. S. Middleditch, in D. H. Williams (Senior Reporter), *Specialist Periodical Report: Mass Spectrometry*, Vol. 2, Chemical Society, London, 1973.
3 C. J. W. Brooks and B. S. Middleditch, in R. A. W. Johnstone (Senior Reporter), *Specialist Periodical Report: Mass Spectrometry*, Vol. 3, Chemical Society, London, 1975.
4 C. J. W. Brooks and B. S. Middleditch, in R. A. W. Johnstone (Senior Reporter), *Specialist Periodical Report: Mass Spectrometry*, Vol. 4, Chemical Society, London, 1977.
5 C. J. W. Brooks and B. S. Middleditch, *Clin. Chim. Acta*, 34 (1971) 145.
6 B. S. Middleditch and D. M. Desiderio, *Anal. Chem.*, 45 (1973) 806.
7 T. A. Baillie, C. J. W. Brooks and B. S. Middleditch, *Anal. Chem.*, 44 (1972) 30.
8 B. S. Middleditch, *Anal. Lett.*, 8 (1975) 397.

Journal of Chromatography, 126 (1976) 591–599
© Elsevier Scientific Publishing Company, Amsterdam — Printed in The Netherlands

CHROM. 9412

APPLICATIONS OF BORONATE DERIVATIVES IN THE STUDY OF CERAMIDES BY GAS–LIQUID CHROMATOGRAPHY–MASS SPECTROMETRY

SIMON J. GASKELL, CHARLES G. EDMONDS and CHARLES J. W. BROOKS
Department of Chemistry, University of Glasgow, Glasgow G12 8QQ (Great Britain)

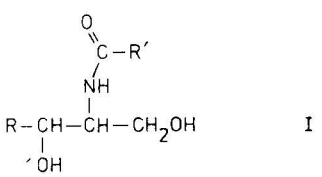
SUMMARY

Methaneboronate derivatives of ceramides possess excellent gas–liquid chromatographic properties and give informative mass spectra. Molecular ions, present at high abundance where an unsaturated acyl substituent is present, are accompanied in the electron impact mass spectra by fragment ions which denote the acyl group and long-chain base. In the gas–liquid chromatographic–mass spectrometric analyses of natural ceramides, as methaneboronate derivatives, the properties of open-tubular columns are exploited to give good separations in moderate analysis times. An application is made to the analysis of ceramides derived from sphingomyelin of human arterial tissue.

INTRODUCTION

Ceramides (N-acyl sphingosines, I) are important components of natural lipid mixtures, both in the free form and as structural constituents of sphingomyelin, cerebrosides, gangliosides, etc. Analyses of ceramides are usually reported in terms of the constituent fatty acids and long-chain bases (sphingosines); less commonly, molecular species are analysed by gas–liquid chromatography (GLC) and combined gas–liquid chromatography–mass spectrometry (GLC–MS)[1–7]. For the purposes of GLC and GLC–MS, ceramides have generally been converted to the bis-O-trimethylsilyl (TMS) ethers; the mass spectra of the derivatives have been extensively studied and major features satisfactorily explained[2,3,5,7]. MS studies have also been reported of ceramides in the free form[8,9], and as acetylated[8] or methylated[9] derivatives.

The 2-amido-1,3-diol structure of ceramides is amenable to the preparation of



I

R,R′=alkyl or alkenyl or hydroxyalkyl

cyclic boronate esters. Since their introduction in 1967 as derivatives for GLC and GLC–MS[10,11], boronates have found wide application in the analysis of diols and amino alcohols. Methaneboronates[12,13] are particularly useful by virtue of the low mass increment accompanying derivative formation, and consequently short GLC retention times. We recently reported[14,15] an evaluation of boronates and related derivatives for the GLC–MS of sphingosines; satisfactory GLC and MS properties were observed for the derivatives, which in certain respects, such as the intensity of molecular ions in electron impact mass spectra, possessed advantages over the corresponding TMS compounds. In a preliminary communication[14], we have also described the preparation and GLC–MS properties of a synthetic ceramide boronate, but these derivatives have not been previously applied in the GLC and GLC–MS analyses of ceramide mixtures. (Complexing of the 1,3-diol function with borate ions has, however, been utilised in the separation of ceramides on columns and thin layers of borate-impregnated silica[16].) In the present paper we report GLC and MS data for synthetic ceramide boronates and describe the application of boronate derivatives to the analysis of natural ceramide mixtures.

GLC and GLC–MS analyses of ceramide mixtures, as TMS derivatives, have hitherto relied on the use of conventional short packed columns of limited separation efficiency (*e.g.*, refs. 1–5). Moreover, the high temperatures required for the elution of high-molecular-weight ceramide derivatives have resulted in high column "bleed", impairing the interpretation of mass spectra of minor components recorded during GLC–MS[17]. Accordingly, in the analyses of ceramide boronate mixtures reported here, we have exploited the ability of open-tubular columns to provide good separation efficiency combined with relatively short analysis times[18]. Furthermore, the use of comparatively wide-bore (*ca.* 0.55 mm) columns has enabled a greater sample loading with a consequent increase in the range of concentrations of sample components over which useful spectra may be obtained during GLC–MS.

EXPERIMENTAL

Materials

N-Palmitoyl sphinganine and N-stearoyl sphinganine were obtained from Miles-Seravac (Slough, Great Britain); other ceramides were prepared from the methaneboronates of sphinganine (Miles-Seravac) or 4-sphingenine (Supelco, Bellefonte, Pa., U.S.A.) and the appropriate acyl chloride (Nu-Chek-Prep, Elysian, Minn., U.S.A.) by a method to be described elsewhere[19]. A mixture of ceramides from bovine brain was obtained from Sigma (Kingston-upon-Thames, Great Britain).

Preparation of methaneboronates

Methaneboronates of sphingosines and ceramides were prepared in pyridine solution by the addition of 1.1 molar proportions of methaneboronic acid (Alfa Inorganics, Ventron-Hicol, Rotterdam, The Netherlands)[13]. For ceramides derived from 2-hydroxyacids, 2.2 molar proportions of reagent were used.

Isolation of ceramides from sphingomyelin of human arterial tissue

Human arterial tissue, obtained within 24 h *post mortem*, was washed with saline solution and broadly classified according to the severity of the atherosclerotic

lesions. Total lipids were obtained by chloroform–methanol (2:1) extraction, and phospholipids were separated from neutral components on a silica gel column. The crude phospholipid mixture was subjected to phospholipase C hydrolysis[20]; ceramides were separated from other products (mainly diglycerides) by preparative thin-layer chromatography (TLC) on Anasil B (Analabs, North Haven, Conn., U.S.A.) using chloroform–ethyl acetate (3:1) as the mobile phase.

Gas–liquid chromatography

Open-tubular glass spirals were drawn from 6-mm light-walled Pyrex glass tubing, in a device constructed according to the design of Desty *et al.*[21], to an internal diameter of *ca.* 0.55 mm. Column blanks (30–80 m) were deactivated by a gas phase silanization method[22] and by passage of a solution of dimethyldichlorosilane in toluene. Column coating with 6–10 μm Silanox (Cabot, Billericia, Mass., U.S.A.) and OV-1 liquid phase was performed essentially according to the method of German and Horning[23].

Columns were installed in a Pye 104 gas chromatograph equipped with a "falling needle" type dry injector device[24]. The column inlet was inserted directly into the flash heater zone and was connected to the flame ionisation detector via a short length of glass-lined stainless-steel tubing (Scientific Glass Engineering, London, Great Britain). Helium was used as carrier gas at a flow-rate of 15 ml/min. Analyses were performed at 300°.

Gas–liquid chromatography–mass spectrometry

GLC–MS, employing an open-tubular column (40 m) of the type described, was carried out using an LKB9000 instrument, fitted with a dry-injection device. Helium was added to the effluent of the column to afford optimum flow-rate (30 ml/min) to the two-stage jet separator. Spectra were recorded at 70 eV, with a separator temperature of 280° and an ion source temperature of 270°. Reference electron impact mass spectra of synthetic ceramide methaneboronates were obtained by analyses on short glass columns (1 m × 3.5 mm I.D.) packed with 1% SE-30 on 100–120 mesh Gas-Chrom Q, installed in the LKB9000 or a DuPont 21-490F instrument. In the latter instance, the ion source temperature was 240°.

RESULTS

Methaneboronate derivatives of ceramides were readily formed by addition of 1.1 molar proportions of methaneboronic acid in pyridine solution. Quantitative conversion to the cyclic boronates, as judged by TLC, occurred within 10 min. With chloroform–ethyl acetate (3:1) as the mobile phase, the derivatives migrated as well defined spots. The derivatives were stable to storage under refrigeration in ethyl acetate solution for a period of several weeks.

Ceramide methaneboronates were found to possess excellent GLC properties. Figs. 1a and b illustrate the analyses, carried out on an open-tubular Silanox-type glass column coated with OV-1 liquid phase, of a mixture of synthetic N-palmitoleoyl and N-palmitoyl sphinganine methaneboronates, and a mixture of synthetic N-palmitoleoyl sphinganine and N-palmitoleoyl 4-sphingenine methaneboronates,

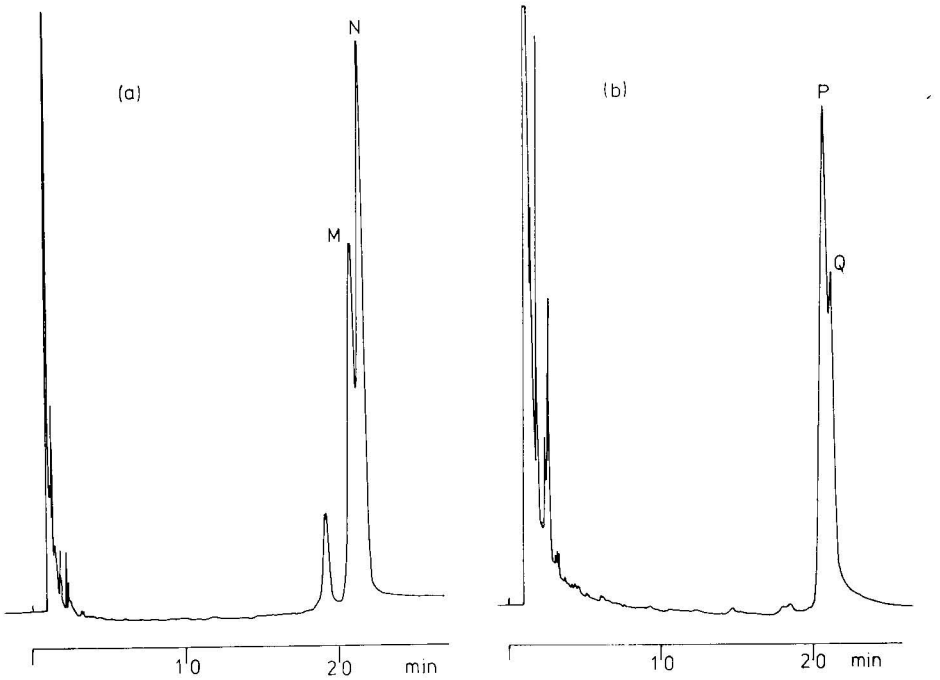


Fig. 1. Open-tubular gas–liquid chromatograms of methaneboronates of synthetic ceramides. Column 40 m × 0.55 mm I.D., coated with OV-1 on Silanox; carrier gas (helium) flow-rate, 15 ml/min; temperature, 300°. (a) Derivatives of N-palmitoleoyl sphinganine (M) and N-palmitoyl sphinganine (N). The minor peak of lower retention time is associated with peak N which was derived from a commercial sample. (b) Derivatives of N-palmitoleoyl sphinganine (P) and N-palmitoleoyl 4-sphingenine (Q). Retention index values are cited in Table I.

TABLE I

GLC RETENTION DATA, USING OV-1 AS THE LIQUID PHASE, FOR SYNTHETIC CERAMIDE METHANEBORONATES

Retention indices were determined on an open-tubular column (40 m × 0.55 mm I.D.) coated with OV-1 on Silanox, at 300°, with a carrier gas (helium) flow-rate of 15 ml/min. Ceramide methaneboronates were co-injected with n-C_{38} and n-C_{42} alkanes.

Ceramide	*Abbreviation**	*Retention index (I)*
N-Myristoyl sphinganine	(LCB 18:0; 14:0)	3702
N-Palmitoyl sphinganine	(LCB 18:0; 16:0)	3896
N-Palmitoleoyl sphinganine	(LCB 18:0; 16:1)	3886
N-Stearoyl sphinganine	(LCB 18:0; 18:0)	4097
N-Oleoyl sphinganine	(LCB 18:0; 18:1)	4073
N-Linoleoyl sphinganine	(LCB 18:0; 18:2)	4074
N-Palmitoyl 4-sphingenine	(LCB 18:1; 16:0)	3912
N-Palmitoleoyl 4-sphingenine	(LCB 18:1; 16:1)	3898

* Abbreviated ceramide names indicate carbon number and degree of unsaturation of the long-chain base (LCB) followed by the carbon number and degree of unsaturation of the N-acyl substituent.

TABLE II

MS DATA FOR SYNTHETIC CERAMIDE METHANEBORONATES

*Ceramide**		*EI mass spectrum (70 eV)***					
LCB	*acyl*	$M^+\cdot$	$[M-15]^+$	*a*	*b*	*c*	*d*
18:0	14:0	535 (4)	520 (27)	228 (100)	295 (18)	324 (9)	308 (3)
18:0	16:0	563 (1)	548 (13)	256 (100)	323 (9)	352 (7)	308 (1)
18:0	16:1	561 (74)	546 (28)	254 (50)	321 (5)	350 (5)	308 (4)
18:0	18:0	591 (2)	576 (30)	284 (100)	351 (5)	380 (4)	–
18:0	18:1	589 (98)	574 (34)	282 (62)	349 (4)	378 (4)	308 (5)
18:0	18:2	587 (100)	572 (10)	280 (9)	347 (2)	376 (1)	308 (3)
18:1	16:0	561 (3)	546 (8)	256 (100)	323 (37)	–	306 (46)
18:1	16:1	559 (30)	544 (6)	254 (88)	321 (42)	350 (1)	306 (44)

* For nomenclature, see Table I.

** Characteristic fragment ions (Fig. 2) specified as *m/e* (relative intensity); the base peak refers to ions above *m/e* 50, and was *m/e* 55 except as specified above.

respectively. Table I records Kováts' retention indices for a number of synthetic ceramide methaneboronates.

Salient features of the electron impact (EI) mass spectra of synthetic methaneboronates are recorded in Table II. Molecular ions were observed in all spectra, though relative abundances were low for ceramide methaneboronates containing a saturated N-acyl substituent. The high relative intensity of molecular ions in the spectra of ceramide boronates containing an unsaturated N-acyl substituent is noteworthy. N-Acyl groups are characterised by fragment ions a and b (Fig. 2). Mass spectra of ceramide methaneboronates incorporating sphinganine and 4-sphingenine are distinguished by the presence in the former of ions c and in the latter of ions d (Fig. 2). A full discussion of the MS characterisation of ceramide methaneboronates will be presented elsewhere[19].

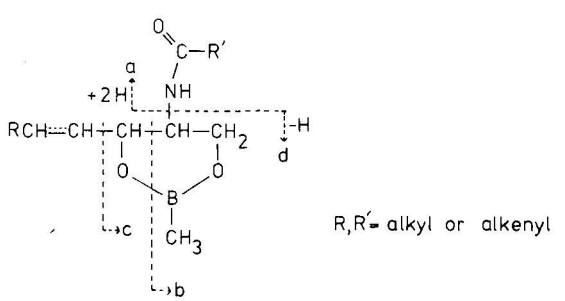


Fig. 2. Principal fragmentation modes of ceramide methaneboronates under electron impact.

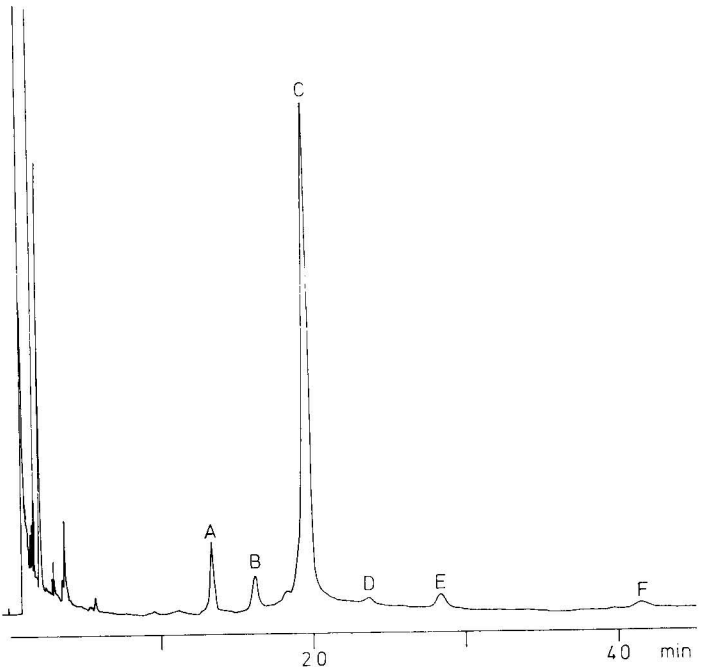


Fig. 3. Open-tubular gas–liquid chromatogram of methaneboronates of ceramides derived from sphingomyelin of human arterial tissue. Conditions, as for Fig. 1. Proposed structural assignments are given in Table III.

Analysis of ceramide mixtures

The application of methaneboronate derivatives to the analysis of natural ceramide mixtures is illustrated by the separation, shown in Fig. 3, of ceramides derived from sphingomyelin of human arterial tissue. The tissue, containing raised fibrous plaques, formed part of a severely atherosclerotic artery. Structural assignments to the components of the ceramide mixture are given in Table III. The low background "bleed" level from the open-tubular column during GLC–MS enabled the recording and interpretation of mass spectra of components of low concentration. The abundances of fragment ions of type d (Fig. 2) in each of the spectra indicated Δ^4-unsaturated long-chain bases; fragmentation of the 2,3-bond is promoted by the presence of the allylic double bond. Spectra recorded during the emergence of peak A (Fig. 3) indicated the presence of two unresolved compounds, assigned the structures N-palmitoyl hexadeca-4-sphingenine methaneboronate and N-myristoyl 4-sphingenine methaneboronate. The mass spectrum of component B, N-palmitoyl heptadeca-4-sphingenine methaneboronate, is shown in Fig. 4. The low concentration in the arterial mixture of ceramides containing very long-chain ($>C_{20}$) acyl substituents is surprising, although an increase in the relative proportions of shorter-chain acyl constituents with increasing severity of atherosclerosis has been reported[25].

Fig. 5 shows the GLC analysis of the methaneboronate derivatives of a mixture of ceramides derived from bovine brain. The separation efficiency is modest by the standards of open-tubular column GLC but analyses of very-high-molecular-weight

TABLE III

CONSTITUENTS OF A MIXTURE OF CERAMIDES DERIVED FROM HUMAN ARTERIAL SPHINGOMYELIN, ANALYSED AS THE METHANEBORONATES

*Constituent**	*Retention index***	*EI mass spectrum****						*Assignment*	
		$M^+\cdot$	$[M-15]^+$	*a*	*b*	*c*	*d*	*LCB*	*acyl*
A_1	3710	533 (6)	518 (10)	256 (100)	323 (33)		278 (34)	16:1	16:0
A_2				228 (64)	295 (22)	324 (6)	306 (29)	18:1	14:0
B	3815	547 (2)	532 (5)	256 (100)	323 (32)	352 (1)	292 (29)	17:1	16:0
C	3913	561 (2)	547 (7)	256 (100)	323 (34)	–	306 (35)	18:1	16:0
D	4012	575 (2)	560 (5)	270 (100)	337 (31)	366 (4)	306 (30)	18:1	17:0
E	4109	589 (3)	574 (3)	284 (100)	351 (29)	380 (2)	306 (44)	18:1	18:0
F§	4307	615 (2)	600 (5)	312 (100)	379 (35)	408 (1)	304 (25)	18:2	20:0

* See Fig. 3.

** Recorded on a glass open-tubular column (40 m × 0.55 mm I.D.), coated with OV-1 on Silanox, at 300°, with a carrier gas (helium) flow-rate of 15 ml/min.

*** For nomenclature of fragmentation, see Fig. 2. Fragment ions given as *m/e* (relative intensity).

§ Tentative assignment; low-intensity mass spectrum.

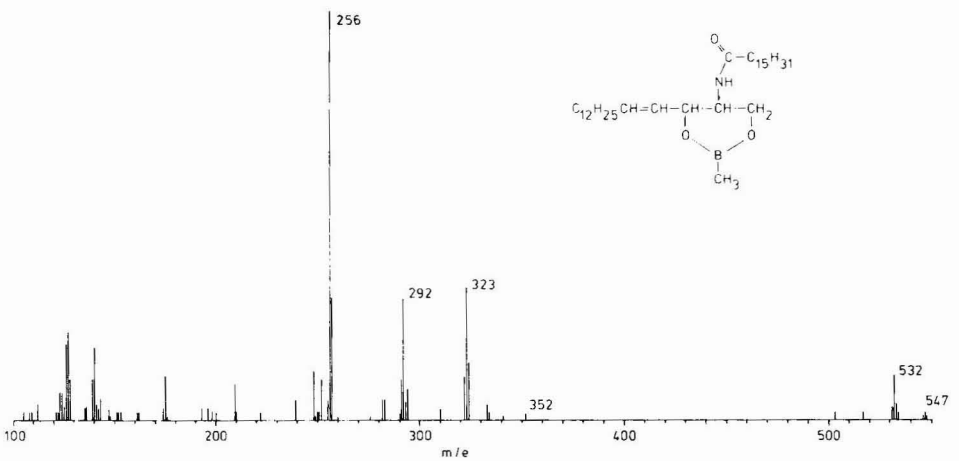


Fig. 4. Electron impact (70 eV) mass spectrum of component B (I = 3815) in the gas chromatogram (Fig. 3) of methaneboronates of ceramides derived from human arterial sphingomyelin. The proposed structural assignment is indicated.

components are achieved in relatively short times at moderate temperatures. The mass spectrum of component X is shown in Fig. 6 together with a tentative assignment of structure as the bis(methaneboronate) of N-2-hydroxystearoyl 4-sphingenine. Prominent ions are attributable to fragmentations analogous to those observed for the methaneboronates of ceramides containing unsubstituted acyl groups.

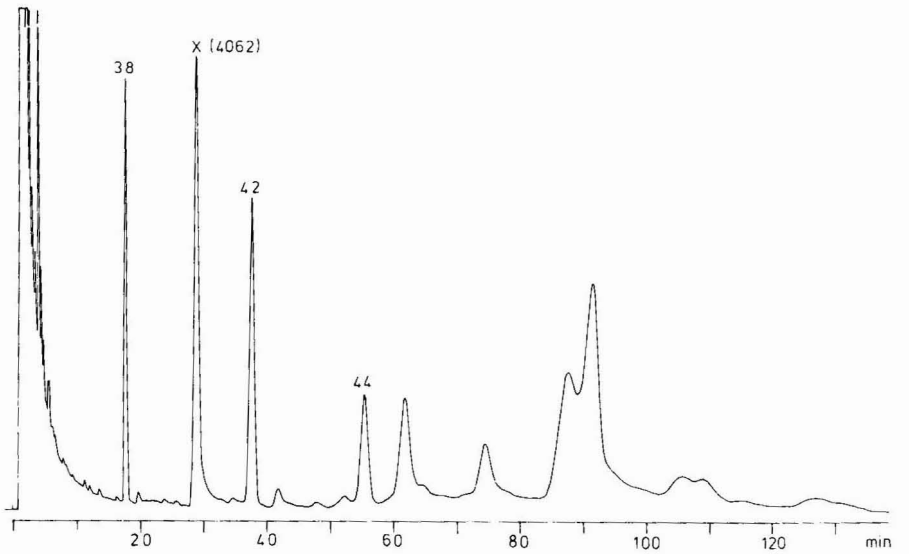


Fig. 5. Open-tubular gas–liquid chromatogram of methaneboronates of ceramides derived by enzymic hydrolysis of sphingolipids of bovine brain. Conditions, as for Fig. 1. Co-injected *n*-alkanes are labelled with the appropriate carbon number. The mass spectrum of component X is shown in Fig. 6.

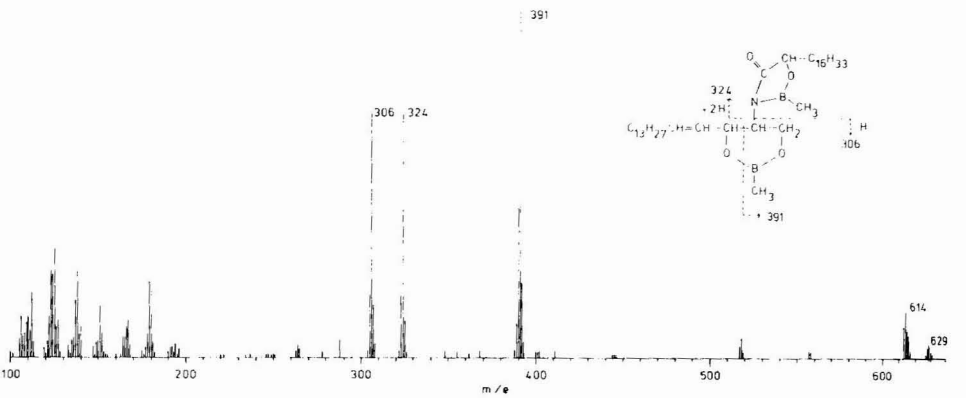


Fig. 6. Electron impact (70 eV) mass spectrum of component X (I = 4062) in the gas chromatogram (Fig. 5) of methaneboronates of ceramides from bovine brain. A tentative structural assignment is indicated.

ACKNOWLEDGEMENTS

We thank Dr. I. Maclean (The Distillers Co., Ltd.) for glass column-drawing facilities. This work was supported by the Medical Research Council through a project grant to Dr. C. J. W. Brooks and Professor W. A. Harland. The LKB9000 gas–liquid chromatograph–mass spectrometer was provided by Science Research Council grant B/SR/2398, and the DuPont 21-490F instrument by Medical Research Council grant G973/346/C.

REFERENCES

1 B. Samuelsson and K. Samuelsson, *Biochim. Biophys. Acta*, 164 (1968) 421.
2 B. Samuelsson and K. Samuelsson, *J. Lipid Res.*, 10 (1969) 41.
3 S. Hammarström, B. Samuelsson and K. Samuelsson, *J. Lipid Res.*, 11 (1970) 150.
4 K. Samuelsson and B. Samuelsson, *Chem. Phys. Lipids*, 5 (1970) 44.
5 S. Hammarström. *J. Lipid Res.*, 11 (1970) 175.
6 R. T. C. Huang, *Hoppe-Seyler's Z. Physiol. Chem.*, 352 (1971) 1306.
7 C. V. Viswanathan, *J. Chromatogr.*, 98 (1974) 105.
8 S. P. Markey and D. A. Wenger, *Chem. Phys. Lipids*, 12 (1974) 182.
9 G. Aranda, H. E. Audier and M. Fetizon, *C.R. Acad. Sci., Ser. C*, 280 (1975) 1505.
10 C. J. W. Brooks and J. Watson, *Chem. Commun.*, (1967) 952.
11 C. J. W. Brooks and J. Watson, in C. L. A. Harbourn (Editor), *Gas Chromatography 1968 (Proc. Int. Symp., 7th, Copenhagen)*, Institute of Petroleum, London, 1969, p. 129.
12 C. J. W. Brooks and D. J. Harvey, *Biochem. J.*, 114 (1969) 15P.
13 C. J. W. Brooks and D. J. Harvey, *J. Chromatogr.*, 54 (1971) 193.
14 S. J. Gaskell, C. G. Edmonds and C. J. W. Brooks, *Anal. Lett.*, 9 (1976) 325.
15 S. J. Gaskell and C. J. W. Brooks, *J. Chromatogr.*, 122 (1976) 415.
16 K.-A. Karlsson and I. Pascher, *J. Lipid Res.*, 12 (1971) 466.
17 M. E. Breimer, *J. Lipid Res.*, 16 (1975) 189.
18 L. S. Ettre, *Open Tubular Columns in Gas Chromatography*, Plenum Press, New York, 1965.
19 S. J. Gaskell and C. J. W. Brooks, in preparation.
20 K.-A. Karlsson, *Acta Chem. Scand.*, 22 (1968) 3050.
21 D. H. Desty, J. N. Haresnape and B. H. F. Whyman, *Anal. Chem.*, 32 (1960) 302.
22 M. Novotný, L. Blomberg and K. D. Bartle, *J. Chromatogr. Sci.*, 8 (1970) 390.
23 A. L. German and E. C. Horning, *J. Chromatogr. Sci.*, 11 (1973) 76.
24 P. M. J. van den Berg and T. P. H. Cox, *Chromatographia*, 5 (1972) 301.
25 J. C. Dousset, G. Soula, A. M. Fourcade, L. Douste-Blazy, M. Jullian, M. T. Pieraggi and H. Bouisson, *Paroi Artérielle*, 2 (1974) 123.

Journal of Chromatography 126 (1976) 601–613
© Elsevier Scientific Publishing Company, Amsterdam — Printed in The Netherlands

CHROM. 9469

ELECTRON CAPTURE AND MULTIPLE ION DETECTION OF BENZODIAZEPINE ESTERS IN PHARMACOKINETIC STUDIES

M. C. SÁNCHEZ and J. COLOMÉ

Centro de Investigación de Ferrer Internacional S.A., Av. C. López Varela 106, Barcelona (Spain)

and

E. GELPÍ

Instituto de Biologia Fundamental, Universidad Autonoma, Av. S. Antonio Ma. Claret 171, Barcelona (Spain)

SUMMARY

A sensitive and highly specific gas–liquid chromatographic method is described for the determination of benzodiazepine esters. The method involves the extraction of pivoxazepam and 2′-chloropivoxazepam from blood and urine samples and the hydrolysis of both drugs with strong acid to the corresponding 2-amino-5-chlorobenzophenone (ACB) and 2-amino-5,2′-dichlorobenzophenone (ACDB). Recoveries of 97–98% have been obtained and the trifluoroacetic (TFA) derivatives of both benzophenones (ACB-TFA and ACDB-TFA) can be chromatographed on OV-17, in a short time, with good electron-capture detector (ECD) responses. The mass spectra of these derivatives provide abundant molecular ions suitable for mass spectrometric detection by multiple ion detection (MID), with a considerable improvement in specificity compared with the ECD responses. The detection limits in blood specimens have been established at 5–10 ng/ml by ECD and 0.5–0.8 ng/ml by MID. The method has been applied to the study of blood levels attained after i.v. and oral doses in rats and in man.

INTRODUCTION

1,4-Benzodiazepines are widely used as psychotropic drugs[1] and constitute a relatively new class of compounds that includes various chemically related derivatives, such as diazepam, oxazepam, chlordiazepoxide and flurazepam. A recent addition to this series, 7-chloro-1,3-dihydro-5-phenyl-1H-2-oxo-3-pivalyloxy-1,4-benzodiazepine[2] or pivoxazepam[3], exerts an anxiolytic activity that prevails over other pharmacological effects. In relation to its parent drug, oxazepam, the former drug has weaker sedation, hypnosis and muscle relaxation effects, which suggest that it may be a "pro-drug" with good potential for clinical applications[4]. The main metabolic pathway of pivoxazepam proceeds according to the scheme[5] given in Fig. 1.

The pharmacokinetic study of this drug requires an analytical method suitable for the quantitative determination of the intact drug at nanogram levels, and at the same time specific enough to differentiate the drug from its own metabolites and/or

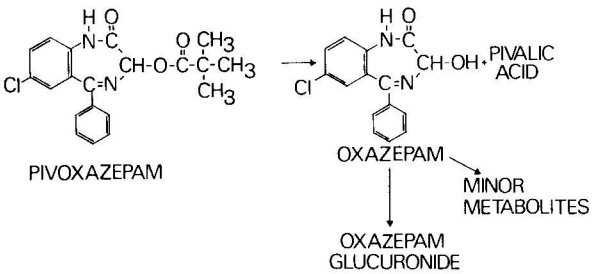


Fig. 1. Metabolic pathway of pivoxazepam.

other interfering components in physiological fluids. In this sense, the experiments carried out have shown that the necessary sensivity levels can be attained by gas–liquid chromatography (GLC) with electron capture detection (ECD), as also described by other workers[6,7].

However, in our experience, the ECD does not provide sufficient specificity of response to cope with the usual complexity of biological extracts, a fact also verified in the course of this work. For this reason, seeking higher sensitivities and greater specificity, we investigated selected ion monitoring techniques[8], designing and building our own alternating voltage accelerating unit for multiple ion detection (MID) purposes[9], a brief account of which is also included here.

To our knowledge, GLC–MID has not been used previously for the biological assay of benzodiazepines, which is surprising in view of the lower limit of detection obtained for pivoxazepam (500–800 pg/ml in plasma compared with 5–10 ng/ml with the ECD) and the high level of specificity observed.

The method developed involves the detection of pivoxazepam as the corresponding trifluoroacetylated benzophenone using a chlorinated analogue as the internal standard. The method has been applied to the assay of human and rat plasma levels and also to studies related to the urinary elimination of the drug in rats. It has also been shown that the method described can be applied to other benzodiazepine pivalates, presently under study in our laboratories.

EXPERIMENTAL

Chemicals and reagents

The chemicals used for calibration and testing purposes were 2-amino-5-chlorobenzophenone (ACB), pivoxazepam, lorazepam pivalate (2′-chloropivoxazepam) and 2-amino-5,2′-dichlorobenzophenone (ADCB) (Synthesis Department, Ferrer Internacional, Barcelona, Spain).

The reagents used were trifluoroacetic anhydride (TFAA) (Merck, Darmstadt, G.F.R.) and hexamethyldisilazane (HMDS) (Pierce Eurochemie, Rotterdam, The Netherlands). The solvents used were pyridine, 0.05 *M* in benzene; 99% *n*-hexane (Merck), washed with concentrated sulphuric acid; diethyl ether (Carlo Erba, Milan, Italy), RP grade, free of peroxides; benzene (Merck); and acetone (Carlo Erba), RP grade, kept over anhydrous sodium sulphate. The solvents were redistilled before use. The buffers and neutralizing solutions used were 1 *M* phosphate buffer (pH 7.4), 1 *M*

acetate buffer (pH 4.5), 6 *N* sodium hydroxide solution and 6 *N* hydrochloric acid. The water used in extractions and the preparation of buffer solutions was thrice-distilled.

Extraction procedure for pivoxazepam

A 3-ml volume of heparinized plasma is extracted with 9 ml of benzene containing an appropriate amount of 2′-chloropivoxazepam (internal standard). A portion of the benzene phase (4 ml) is then extracted three times with 5 ml of 1 *N* hydrochloric acid, 3.5 ml of the benzene phase remaining after the extractions are taken to dryness and the residue is redissolved in 40 μl of absolute ethanol, adding 5 ml of 6 *N* hydrochloric acid and keeping the solution at 100° for 1 h. This acidified solution is neutralized with sodium hydroxide solution, using 40 μl of a 1% solution of bromothymol blue as indicator.

The solution containing the benzophenone thus formed is adjusted to pH 7.4 with 1 ml of phosphate buffer and extracted twice with 10-ml volumes of diethyl ether, subsequently adding the necessary amount of solvent to give a final volume of 25 ml.

Derivatization

The ether extracts (20 ml) are taken to dryness and the residue is then treated with 10 μl of TFAA and 25 μl of a 0.05% solution of pyridine in benzene, maintaining the mixture at 60° in a tightly closed vial for 10 min. After careful elimination of the solvent and reagent, the residue is redissolved in 100 μl of *n*-hexane–acetone (1:1), injecting 2 μl of the solution obtained into the gas chromatograph.

Note that before attempting to derivatize the sample it is necessary for it to be free of any traces of water. For this purpose, the ether extracts are concentrated to 1 ml in a rotary film evaporator and centrifuged. If any appreciable amount of water remains, it is removed with a clean syringe and the ether is evaporated under a stream of purified nitrogen. After keeping the residue in a desiccator for 1 h, it is ready for derivatization as indicated above.

Gas chromatography

The separations were carried out on a Perkin-Elmer Model 900 gas chromatograph equipped with a nickel-63 ECD. The glass columns (2 m × 2 mm I.D.) were treated with a 10% solution of HMDS in *n*-hexane, dried and packed with 3% OV-17 on Gas-Chrom Q, 100–120 mesh (Applied Science Labs., State College, Pa., U.S.A.).

The columns were conditioned for 16 h at 300° with nitrogen at a flow-rate of 30 ml/min. Argon–methane (95:5) was used as the carrier gas, adjusting the flow through the ECD to a total of 160 ml/min by means of the auxiliary carrier gas accesory. The detector was operated for maximum sensitivity at a 50 μsec pulse interval, and the column temperature was set at 220°.

Gas chromatography–mass spectrometry (GC–MS)

The mass spectra of the various compounds and derivatives were obtained with a single-focusing Hitachi RMU-6H mass spectrometer, coupled through a new type of single-stage jet interface to a Perkin-Elmer Model 3920 gas chromatograph. The operating conditions of the mass spectrometer were as follows: electron energy,

70 eV; emission current, 80 μA; accelerating voltage, 2400 V; ion chamber temperature, 200°; separator temperature, 220–240°.

A novel feature of the GC–MS interface is that all of the transfer lines from the column exit leading to the jet unit and from there on to the mass spectrometer inlet are made of 1/16-in. O.D. stainless-steel tubing containing an inner gold capillary. The unit is manufactured for Hitachi by Perkin-Elmer (Norwalk, Conn., U.S.A.).

Multiple ion detection

As the Hitachi mass spectrometer is not equipped with the necessary alternating voltage facilities for single ion detection or MID of selected components in a gas chromatographic profile[10,11], we undertook the design and construction of a four-channel MID unit suitable to our specifications. The design and operation of this unit, which will be reported in detail elsewhere[9], can be briefly summarized as follows. The system consists of six main components: (A) a programmed 0–1100 V voltage source; (B) a digital programmer; (C) a variable ramp generator; (D) a signal distributor; (E) four holding amplifiers; and (F) an oscilloscopic monitor.

In this system, a regulated voltage increment given as a function of time, $\Delta V(t)$, is added to the nominal accelerating voltage (V) in each of the four channels. This $\Delta V(t)$ is the sum of a fixed ΔV supplied by the programmed voltage source (A) and a variable voltage sawtooth wave which is supplied by the ramp generator (C), thus obtaining a "miniscan" around each of the selected masses. The addition of the four different $\Delta V(t)$ values and their synchronization with the horizontal scan of the oscilloscopic monitor (F) is driven by the digital programmer (B). The regulated voltage (ΔV) can be changed continuously from 0 to 1100 V, which allows the operator to cover a maximum mass range of 30% of the lowest range mass at $V = 3600$ V and of about 90% at $V = 1200$ V.

The four signals are collected separately by means of a signal distributor (D), which is also synchronized with the voltage source (A) and the horizontal scan of the monitor (F). These signals are amplified through four holding amplifiers (peak detector and S/H amplifier). The oscilloscopic monitor is used for the initial search and focusing operations, which are based on the background reference peaks, owing to the lack of a mass marker, and provides likewise a real time control for the correct focusing of each peak. These features contribute to the minimization of the errors due to defocusing effects[12], allowing the addition of ΔV's as high as those described. The miniscan time is continuously adjustable between 0.5 and 12 sec and the switching time between two adjacent channels is 50 msec. These relatively high scan times permit the use of high time constant filters, with the consequent decrease in noise and therefore increase in sensitivity, expressed as signal-to-noise ratio.

Pharmacokinetic studies

Experimental animals. This work was carried out using male SPFF rats weighing on average 236.8 g. The animals were subjected to i.v. (2.58 mg/kg) and oral (30 mg/kg) doses of pivoxazepam, equivalent to 2 and 23.2 mg, respectively, of free oxazepam per kilogram of body weight.

Blood extractions after i.v. injections were performed at 5, 10, 20, 30 and 40 min and 1, 2, 3 and $5\frac{1}{2}$ h. The first two points of the dose–response curves were ob-

tained with ten animals and the remainder with five. The responses to oral administrations from 0 to 24 h were followed, drawing blood samples at each hour. For the assay of 24-h urine samples, the subjects received doses of 50 mg per kilogram of body weight.

Humans. Four healthy volunteers each received one capsule containing 25.86 mg of pivoxazepam, equivalent to 20 mg of free oxazepam. Blood samples were drawn before the first administration and after 1, 2, 4, 6, 8, 12 and 24 h.

RESULTS AND DISCUSSION

Gas chromatographic separations

The initial attempts to chromatograph pivoxazepam on OV-17 were unsuccessful, as it apparently undergoes an extensive pyrolytic breakdown, either on the injection port or on the column itself, as indicated by the complexity of the 2-h GLC multiple peak pattern obtained. However, silanization of both pivoxazepam and the internal standard, 2′-chloropivoxazepam, with a BSA–1 % TMCS mixture in acetonitrile gave sharp symmetrical peaks with retention times of the order of 8 and 10 min, respectively, at 270°. Nevertheless, the quantitative response of the ECD to the TMS derivatives did not meet our specifications in terms of the necessary sensitivity levels required for biological applications ($<$50 ng/ml in urine or plasma).

This aspect is reflected in Fig. 2A, which shows the GLC profile obtained by extraction of a urine sample according to the procedure outlined, which included the acid hydrolysis of pivoxazepam to yield the corresponding 2-amino-5-chlorobenzophenone (ACB). The retention time of ACB is of the order of 20 min and the peak tails considerably. In contrast, the TFA derivative of ACB produced a sharp peak (Fig. 2B) with a retention time of about 6 min, much like the TMS derivatives of pivoxazepam but with a significantly higher response on the ECD.

Under these conditions, the profile of the urine extract (Fig. 2B) appears cleaner and the peak presumably corresponding by retention time to the acylated ACB of pivoxazepam is more amenable to the quantitative determination of low dose–response curves in comparison with the corresponding ACB peak in the upper trace of Fig. 2A.

Hydrolysis and extraction of pivoxazepam

In concentrated acid, the molecule of pivoxazepam breaks down, yielding the same aminochlorobenzophenone as that obtained from oxazepam[13]. On the other had, the possibility of transforming pivoxazepam into oxazepam by basic hydrolysis has been proved unfeasible because the molecule decomposes to various by-products without forming the expected benzodiazepin.

The determination of pivoxazepam as 2-amino-5-chlorobenzophenone, which, as stated, could also be derived from oxazepam, obviously requires the separation of both compounds, precursor and metabolite, prior to the hydrolysis in concentrated hydrochloric acid.

Pivoxazepam and its free metabolites, as well as the internal standard used for its determination (2′-chloropivoxazepam), can be efficiently extracted with benzene, as described for diazepam[14]. On the other hand, the separation of the unconjugated metabolites of pivoxazepam, including oxazepam, can be accomplished quantitatively

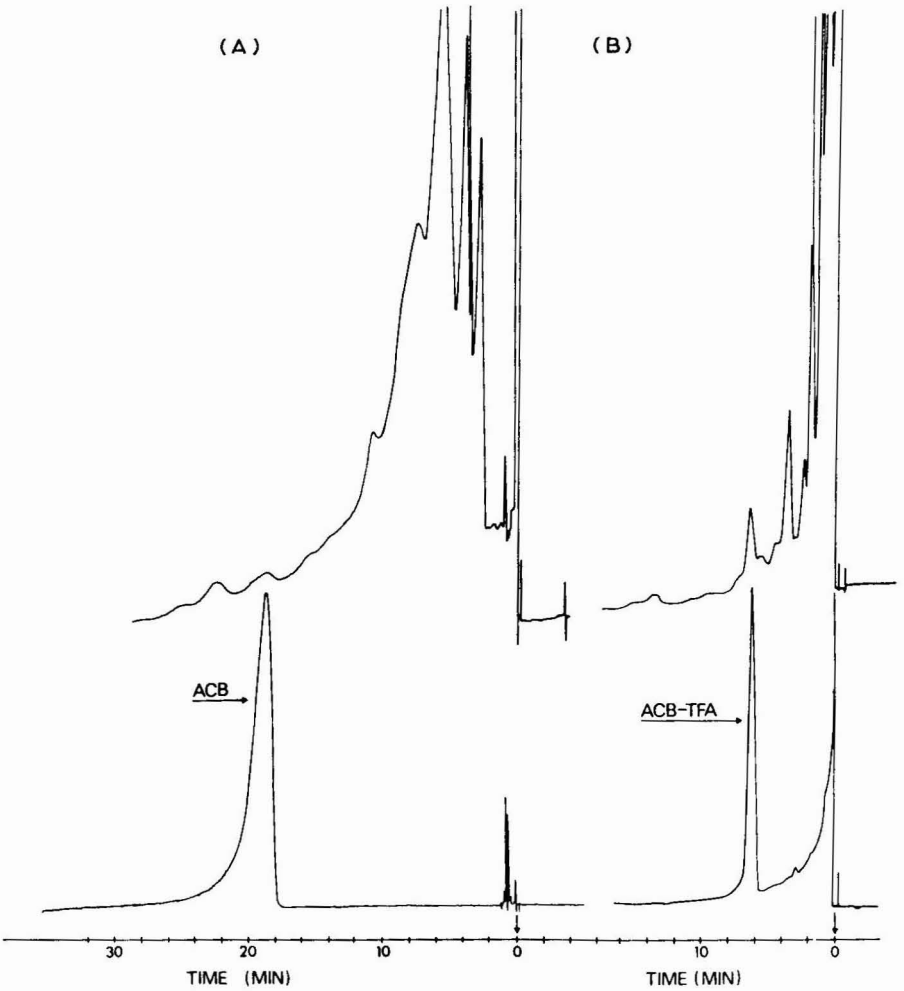


Fig. 2. (A) Gas chromatogram of the free 2-amino-5-chlorobenzophenone (lower trace) and chromatographic profile obtained after the acid hydrolysis of an extract of a urine pool from various rats administered an oral dose of 50 mg/kg of pivoxazepam (upper trace). (B) Same samples after derivatization of both with TFAA. Chromatographic conditions for (A) and (B): 2 m × 2 mm I.D. glass column packed with 3% OV-17 on Gas-Chrom Q, 100–120 mesh; oven temperature, 200; injector and detector blocks, 270°; carrier gas, Ar–CH_4 at a flow-rate of 30 ml/min.

by extraction of the benzene phase with 1 *N* hydrochloric acid, which prevents the possible premature degradation of pivoxazepam before its hydrolysis to the benzophenone with 6 *N* hydrochloric acid.

From the point of view of the extraction procedure, the method described is highly specific in the sense that the partition coefficient of pivoxazepam (K = [organic phase]/[aqueous phase]) favours the organic phase, with over 99% of pivoxazepam remaining in the benzene phase. A K value of 0.45 has been reported for the extraction of oxazepam from a diethyl ether phase with 1 *N* hydrochloric

acid[15], while the corresponding value in 1 *N* hydrochloric acid in benzene is 0.17, and even in 6 *N* hydrochloric acid the value is only 0.35.

Thus, the separation of the intact drug and its metabolites can be easily accomplished by re-extraction of the initial benzene phase with dilute hydrochloric acid owing to the low partition coefficient of oxazepam in this system.

Recoveries

The calibration graph obtained by adding various amounts of pivoxazepam and 2′-chloropivoxazepam, extracting and analyzing in the manner described, indicates that the recoveries change depending on the weight ratio of sample to internal standard. A maximum recovery of 97.7% for a series of five replicate determinations was obtained when the weight ratio of pivoxazepam to 2′-chloropivoxazepam was 0.65 (the respective peak heights corresponding to this weight ratio give a ratio close to unity.

Concurrently with the analysis of biological specimens, it is advisable to prepare a calibration graph by adding known amounts of pivoxazepam plus internal standard to equivalent volumes of blank specimens. The amounts added must be in the same range as that expected for the sample. This is needed in order to determine, from each weight ratio given by the calibration graph, the recovery factor that must be applied to obtain the initial amount of pivoxazepam present in the sample.

GLC calibration and quantitative responses

Although none of the reports related to the analysis of benzodiazepines mentions the determination of their benzophenone by-products as acyl derivatives, we have verified their considerable advantages with regard to (1) their lower retention times (Fig. 2B), which allow the use of lower oven temperatures, (2) less peak tailing and (3) higher sensitivity with the ECD.

For equivalent amounts of both compounds, the response of the TFA derivatives of ACB is about 20 times higher than that of the free ACB. The upper trace in Fig. 3 shows the response curve for ACB-TFA using ADCB-TFA as the internal standard. The linear regression coefficient for the data shown has been estimated as 0.983, with a standard deviation varying between ± 1.2 and 2.5% in an R_A range of 0.5–1.5 (where R_A is defined as the area ratio of the peak due to ACB-TFA to that of ADCB-TFA). For this reason, the internal standard is always added in an amount adjusted so that the value of R_A falls within this range. The linearity of response is limited to a power of ten range (linear between 0 and 0.1 ng and between 0.1 and 1 ng), which requires the adjustment of calibration graphs to the concentration range of the sample. The minimum absolute amount of ACB-TFA detected is lower than 25 pg at an attenuation of 40.

However, in plasma extracts, the limit of detection of ACB-TFA has been established as 2–4 ng/ml (corresponding to 5–10 ng/ml of pivoxazepam). These values were determined with a confidence limit of $\pm 10\%$ (defined as the value of the standard error times the estimated Student t value) for ten replicate runs, assuming an optimal weight ratio (R_w in Fig. 3). The results are statistically significant at the 95% confidence level ($P < 0.05$). The magnitude of the variations in the limit of detection observed as the method is applied to physiological fluids seem to be strongly dependent on the presence and relative levels of interfering substances, as shown by the blank

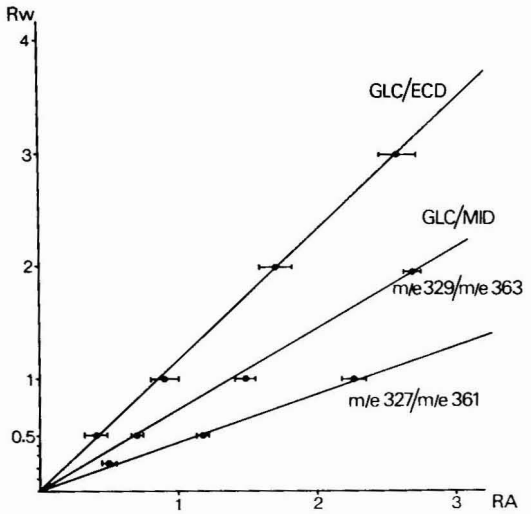


Fig. 3. GLC–ECD and GLC–MID quantitative response curves. ECD curve: Rw is defined as the value of the ACB-TFA:ADCB-TFA weight ratio. RA defines the corresponding area ratios obtained from the chromatograms. MID curves: Rw is the same weight ratio. RA gives the values of the peak height ratios of the ion current profiles of the peaks at *m/e* 329/363 and 327/361.

controls. This problem is considerably reduced by the use of selected ion monitoring techniques for multiple ion detection, as described below.

Multiple ion detection

In view of the good results recently obtained in the laboratory by single ion monitoring[10,11] or multiple ion detection (MID)[16], we decided to apply the latter technique to these benzodiazepine esters as a means of achieving greater specificity and, if possible, a lower limit of detection.

The first step consisted in the evaluation of the mass spectra of these substances, which are shown in Fig. 4. The mass spectrum of the free benzophenone shows a major ion at $M - 1$ (*m/e* 230), which in principle would be suitable for MID[17]. However, in biological determinations in general it is more useful to focus on higher mass values, in order to avoid the larger relative contribution of stationary phase bleeding and/or interfering components to the lower end of the mass spectral region. In this sense, the TFA derivative adds to its inherent GLC advantages a relatively high abundance molecular ion at *m/e* 327 (70%). Likewise, the internal standard also shows a relatively high peak at *m/e* 361 (85%). These ions plus their corresponding ^{37}Cl isotope peaks at *m/e* 329 and 363, respectively, where the peaks selected for MID. Their ion current profiles, obtained with the four-channel monitoring system, are also shown on the right-hand side of Fig. 4. Once these ions are selected and the mass spectrometer operating parameters are properly adjusted for their detection, a response is obtained only when a compound giving rise to any of these four ions is eluted from the chromatograph.

As seen in these profiles, the peaks obtained at about 7 and 9 min are in accordance with the expected retention times of the TFA derivatives of ACB and

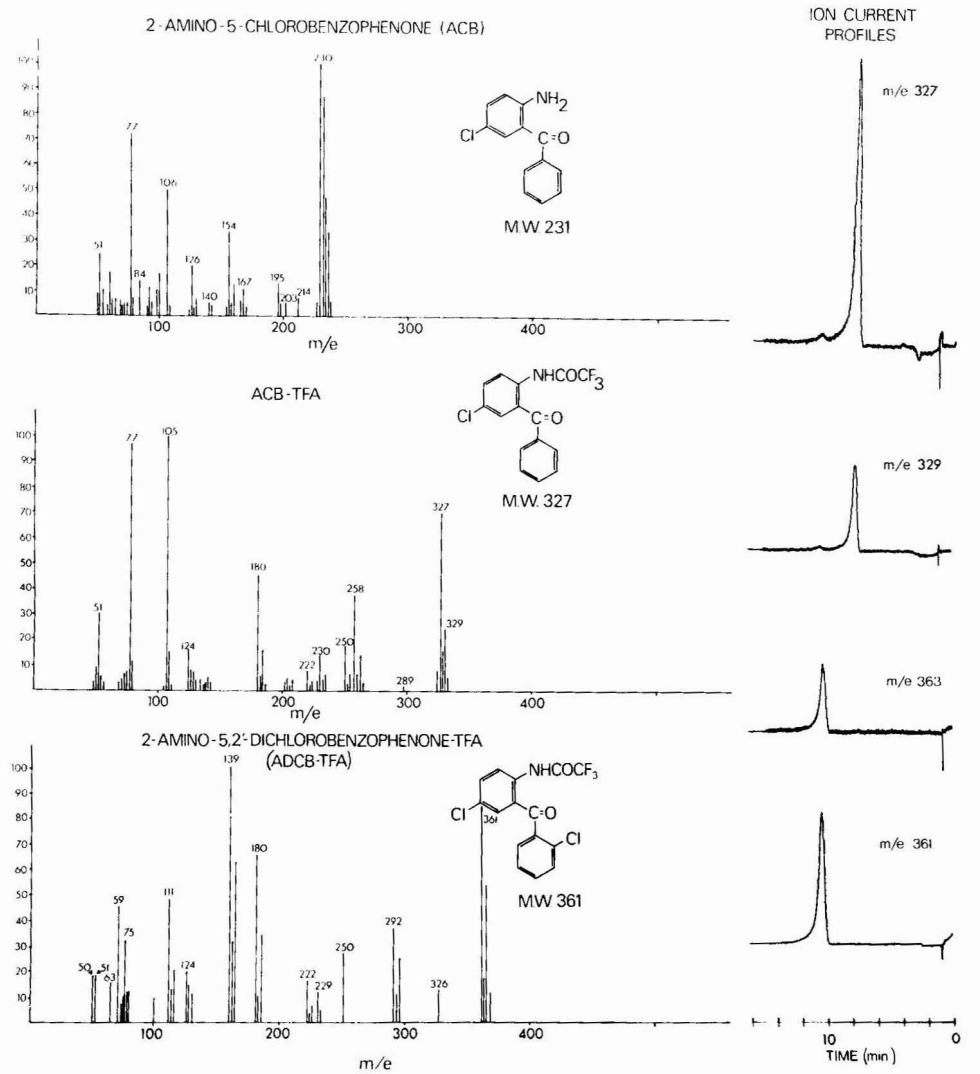


Fig. 4. Mass spectra of the free benzophenone and TFA derivatives of ACB and ADCB. The ion current profiles shown on the right illustrate the responses obtained by focusing the four recording channels of the MID on ions *m/e* 327 and 329 for ACB and *m/e* 361 and 363 for ADCB. These profiles were obtained under the following conditions: ionization energy, 70 eV; emission current, 80 μA; nominal acceleration voltage, 2400 V for *m/e* 363 + the corresponding ΔV values required to focus on the other three ions at a constant magnet current of 260 mA; source temperature, 200°; interface, 250°. Chromatographic conditions as indicated for Fig. 2, except for the column temperature, which was set at 220°.

ADCB. Note that these ion pairs have also been selected because of their characteristic abundance ratios. The *m/e* 327:329 ratio is *ca.* 3 for the monochlorinated benzophenone and *ca.* 1.5 for the dichlorinated analogue (ratio *m/e* 361:363). This is a very specific feature that carries significant weight with regard to the unequivocal identification of these substances in biological extracts. The considerable specificity of

detection thus achieved is reflected in the practical example in Fig. 5, which compares the results obtained with the ECD and those obtained by MID. The left-hand traces depict the GLC profile of an extract of human plasma obtained 2 h after ingestion of an oral dose of pivoxazepam. It is obvious that the ECD response of the ACB-TFA and ADCB-TFA peaks may be affected by the levels of other interfering components that are either co-eluted exactly with them or are eluted with a similar retention time. The retention times of the two benzophenone derivatives are indicated by the arrows on the GLC pattern of a plasma blank. On the right-hand side are shown the ion current profiles of the two ion pairs selected. The specificity is absolute in this instance. The peak of the ACB-TFA is unequivocally identified by (1) its responses at *m/e* 327 and 329, (2) their relative abundance ratio and (3) the retention time. The same reasoning applies to the ADCB-TFA.

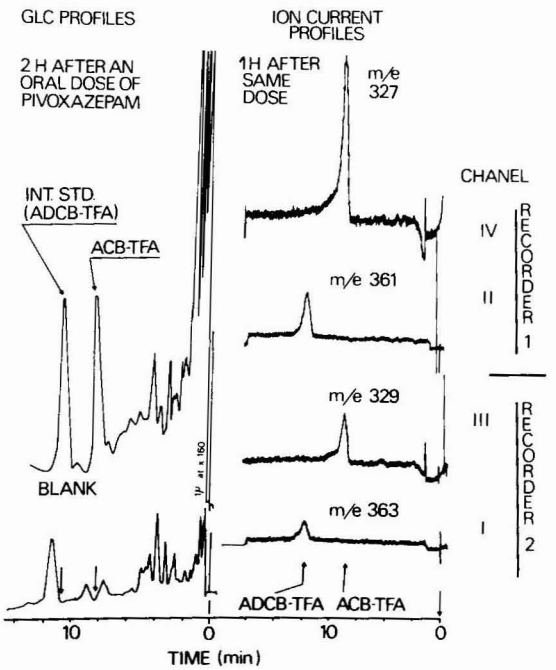


Fig. 5. Gas chromatographic profiles of an extract of human blood drawn 2 h after an oral dose of pivoxazepam. The blank shown below corresponds to the extract of a blood sample taken before the administration of the drug. On the right are shown the ion profiles of the masses selected for identification of the two derivatives. One of the pen recorders registers the two molecular ions *m/e* 327 and 361 (see Fig. 4) focused on the MID channels IV and II, respectively, while the corresponding $M + 2$ ions on channels III and I are registered on a second recorder. The peak height ratios thus obtained are used to construct the calibration graphs (Fig. 3).

It is worth noting that the results far exceeded our expectations with regard to the extreme degree of specificity achieved as it would not have been unreasonable to see the appearance of some extra peaks derived from other components of the plasma extract that could possibly also contribute to these mass values. However, when extra peaks appear they do so at different retention times and their relative abundances do not agree with the calculated ratios[11].

MID response curves

Fig. 3 also shows the GLC–MID calibration graphs compared with the ECD response in the same range of area and weight ratios. To obtain these graphs, the four signals coming from the signal distributor of the MID unit were fed to two dual-pen recorders so that one of the recorders received the ion currents generated by the molecular ions of the two benzophenones (*m/e* 327 and 361) and the other recorder received the signals generated by their respective isotope $M + 2$ peaks (*m/e* 329 and 363). For instance, this arrangement is indicated in Fig. 5.

Although not shown in Fig. 3, the response is linear for values of R_A in the range 0–8, equivalent to R_w values of 0–4, and the dispersions observed for replicate measurements are 40–50% lower than by GLC–ECD.

The absolute lower limit of detection by MID has been established at 300 pg for ACB-TFA, and for biological assays the limit is 500–800 pg/ml.

The heptafluoroacylated derivatives of ACB and ADCB were also tried initially but, although their ECD response was twice that of the TFA derivatives and their GLC behaviour was as good, their mass spectral pattern did not provide sufficiently abundant high-mass ions for MID. For instance, there are no peaks higher than 30% past the base peak at *m/e* 105 (the ion at *m/e* 258 shows a relative abundance of 30% while the molecular ion at *m/e* 427 represents only 12% of the base peak). However, the *m/e* 427 and 429 ions could still prove useful in the event that any interference appearing at the masses selected for the TFA derivatives would make it necessary to focus on higher masses in order to improve specificity.

Pharmacokinetic studies

Fig. 6 shows the blood fall-off curve of pivoxazepam in rats after an i.v. dose (2.58 mg/kg). The various points were obtained taking serial blood samples at the times indicated (0–5½ h). Details and statistical data are given in Table I. Control

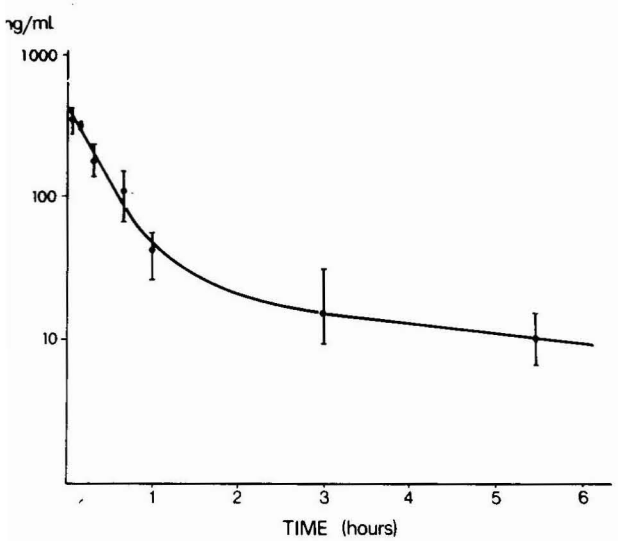


Fig. 6. Blood level fall-off curve after intravenous administration of a pivoxazepam dose (2.58 mg/kg) in rat.

TABLE I

BLOOD PLASMA CONCENTRATIONS (ng/ml) OF PIVOXAZEPAM IN TWO SERIES OF 5 AND 10 RATS FOLLOWING ADMINISTRATION OF 2.58-mg/kg DOSES

Values at 5 and 10 min were obtained with 10 rats; the remainder of the entries apply to 5 rats. S.D. = standard deviation; S.E. $\times$ t = confidence interval. As the size of the populations sampled differs, these values are only comparable within each of the two populations; S.D./$\bar{x}$ represents the corresponding coefficient of variation that allows a direct comparison among the values obtained at various times.

Time (min)	*Rat No.* 1	2	3	4	5	6	7	8	9	10	*Mean* ($\bar{x}$)	*S.D.*	*S.E.* $\times$ t (%)	*S.D.*/$\bar{x}$
5	311.7	234.9	437.7	312.1	507.2	248.8	263.0	490.5	604.4	220.4	363.0	60	± 23.6	0.165
10	350.1	339.8	316.0	294.6	—	341.2	382.2	333.0	333.0	305.3	332.8	12	± 5.9	0.036
20	131.5	147.8	165.8	233.3	206.2	—	—	—	—	—	176.9	19	± 29.5	0.107
40	138.6	130.2	138.6	76.9	79.3	—	—	—	—	—	112.7	14	± 34.9	0.124
60	17.7	82.9	34.2	43.7	29.4	—	—	—	—	—	41.6	11	± 74.2	0.264
180	—	37.3	21.3	63.4	13.3	—	—	—	—	—	15.6	10	±103.7	0.641
330	16.5	8.0	13.3	5.8	6.1	—	—	—	—	—	9.9	2.2	± 59.0	0.222

specimens were drawn before the administration of the first dose. The drug is detected at its maximum concentration at 5 min, declining progressively with time.

The relatively high blood levels of the intact drug attained after an i.v. dose facilitate the study of its elimination pattern by GLC–ECD. However, the lower levels detected after oral doses underline the relative importance of the presence of any ECD interfering substances in the control blanks (Fig. 5), which is a contributory factor to the sample variations observed. These are the type of samples where the GLC–MID method has proved most useful for its specificity.

Fig. 7 shows the blood levels observed in rats in response to an oral dose of pivoxazepam (30 mg/kg) throughout a 24-h period. The points corresponding to the upper trace were determined by GLC–ECD while the lower trace was obtained by MID. These curves are representative of the type of results that we have consistently obtained with both methods.

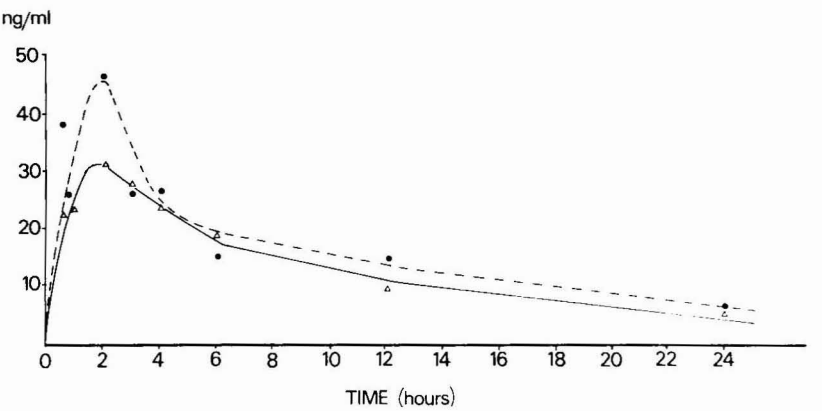


Fig. 7. Blood level fall-off curves following the oral administration of a dose of pivoxazepam in rat (30 mg/kg). ●, Curve obtained by GLC–ECD analysis of the extracts; △, curve obtained by GLC–MID analysis of the same samples.

Likewise, as the internal standard itself shows interesting pharmacological properties, its own elimination profile has been studied in a similar way, using pivoxazepam as the internal standard. The data obtained prove the feasibility of the GLC–MID method described for the determination of other benzodiazepine ester analogues.

ACKNOWLEDGEMENTS

M. C. Sánchez thanks J. L. Vélez for his contributions to the development of the GLC method. Thanks are also due to J. E. Beneyto for his encouragement. E. Gelpí acknowledges the Comisión Asesora de Investigación Científica y Técnica for support received.

REFERENCES

1 G. Zbinden and L. O. Randall, *Advan. Pharmacol.*, 5 (1967) 213.
2 *Span. Patent* 425842, Ferrer Internacional S. A., Barcelona, Spain.
3 W.H.O. list 3429,9, Suppl. 1975.
4 M. E. Tornos, S. S. Chatterjee and J. Colomé, *Sixth International Congress on Pharmacology, Helsinki, Finland, July 1975.*
5 Ferrer Internacional, unpublished data.
6 F. Marcucci, in S. Garattini, E. Mussini and L. O. Randall (Editors), *The Benzodiazepines*, Raven Press, New York, 1973, p. 75.
7 J. A. F. de Silva, I. Bekersky, C. V. Puglisi, M. A. Brooks and R. E. Weinfeld, *Anal. Chem.*, 48 (1976) 10.
8 F. C. Falker, B. J. Sweetman and J. T. Watson, *Appl. Spectrosc. Rev.*, 10 (1975) 51.
9 F. Artigas, M. Prudencio, J. A. Alonso, J. Baillart and E. Gelpí, *7th Int. Mass Spectrom. Conf Florence, August 30–September 3, 1976.*
10 E. Peralta and E. Gelpí, *Clin. Chim. Acta*, 73 (1976) in press.
11 J. Segura, F. Artigas, E. Martínez and E. Gelpí, *Biomed. Mass Spectrom.*, 3 (1976) 91.
12 C. C. Sweeley, J. F. Holland, N. D. Young and R. B. Blaiser, *22nd Annual Conference on Mass Spectrometry and Allied Topics, Philadelphia, Pa., May 19–24, 1974.*
13 J. A. F. de Silva, M. A. Schwartz, V. Stefanovic, J. Kaplan and L. d'Arconte, *Anal. Chem.*, 36 (1964) 2099.
14 E. Arnold, *Acta Pharmacol. Toxicol.*, 36 (1975) 335.
15 J. Vessman, G. Freij and S. Strömberg, *Acta Pharm. Suec.*, 9 (1972) 447.
16 J. Roselló, J. Tusell and E. Gelpí, *J. Chromatogr.*, in press.
17 S. Rendić, L. Klasinc, V. Šunjić, F. Kajfež, V. Kramer and P. Mildner, *Biomed. Mass Spectrom.*, 2 (1975) 97.

Journal of Chromatography, 126 (1976) 615–623
© Elsevier Scientific Publishing Company, Amsterdam — Printed in The Netherlands

CHROM. 9490

CHEMICAL IONIZATION MASS SPECTROMETRY FOR RAPID ASSAY OF DRUGS IN SERUM

MICHAEL LEHRER and ARTHUR KARMEN

Department of Laboratory Medicine, Albert Einstein College of Medicine of Yeshiva University, 1300 Morris Park Avenue, Bronx, N.Y. 10461 (U.S.A.)

SUMMARY

A rapid procedure has been devised for analyzing anti-epileptic drugs in serum by chemical ionization mass spectrometry. An internal standard, 5-(*p*-methylphenyl)-5-phenylhydantoin (MPPH), is added to serum diluted in buffer at pH 12. The mixture is washed with diethyl ether to remove neutral lipids, acidified, extracted with chloroform and the chloroform extract evaporated to dryness. The residue is then dissolved in methanol and an aliquot, corresponding to approximately 2% of the original mixture, is deposited in the glass capillary sample cup of the solid probe inlet of the mass spectrometer. The sample is then volatilized by heat into the ion source of the mass spectrometer, where it reacts with ionized methane reagent gas.

As the temperature of the probe is increased, quasimolecular ion peaks of the protonated anticonvulsants appear, rise and fall on the oscilloscope tracing, indicating similar but not identical rates of volatilization. We recorded these peaks photographically by opening the shutter of the oscilloscope camera for the entire heating cycle. The concentrations of the anticonvulsants were estimated from the ratio of the height of the peaks of the drug to that of the internal standard on the photograph. The peak-height ratios were proportional to concentration within, above and below the therapeutic range. Other drugs, including barbiturates, carbamazepine, nicotine and caffeine, were readily identified when present. With one solid probe inlet, an assay could be performed every 2 min.

INTRODUCTION

Compared with the complex fragmentation patterns that result from electron impact ionization, the mass spectra produced by chemical ionization (CI) contain very few peaks. For each compound there is generally a characteristic "quasi-molecular" ion peak, corresponding to the molecular weight of the compound plus one, which predominates, and a lower yield of a few fragment ions. Identification of compounds by their molecular weight is thus simplified, although the high specificity of the identification given by electron impact fragmentation patterns is not available. Compounds that have different molecular weights generally yield spectra with minimal overlap. CI thus makes more feasible the analysis of mixtures that contain only

a few compounds, or only a few compounds that are present in appreciably higher concentration than other compounds, by introducing all of the compounds in the mixture into the mass spectrometer at one time.

The detection of sedative drugs in blood serum is this kind of analytical problem. Milne *et al.*[1] demonstrated the use of CI for identifying drugs in the serum of patients who had attempted suicide. Their report prompted the study described here, in which we devised a similar technique for the quantitative assay of anticonvulsant drugs in serum. Knowledge of the concentrations of these drugs is considered helpful in the management of patients with epilepsy. These analyses have become popular applications of gas–liquid chromatography (GLC) in the clinical laboratory, but the time required for each assay often limits the rapidity with which data can be reported and, therefore, the clinical utility of the information. Our objective was to devise a means for assaying several of these drugs simultaneously with a rapidity comparable to that with which other, more simple, clinical assays are now available.

EXPERIMENTAL

The mass spectrometer used was a Finnigan Model 3200 F GC–MS (Finnigan Corp., Sunnyvale, Calif., U.S.A.) operating in the chemical ionization mode at 1.0 torr with methane as the reagent gas.

Stock solutions of 5,5-diphenylhydantoin (DPH) (Aldrich, Milwaukee, Wisc., U.S.A.), 5-(*p*-methylphenyl)-5-phenylhydantoin (MPPH) (Aldrich), primidone (Pr) (Ayerst Labs., New York, N.Y., U.S.A.) and phenobarbital (PB) (Mallinckrodt, St. Louis, Mo., U.S.A.) in methanol were prepared to contain 200 μg/ml in each instance.

Standard solutions containing 0.5 μg/ml, also in methanol, for calibrating the response of the spectrometer, were prepared by dilution.

Procedure

Diphenylhydantoin, phenobarbital and primidone were extracted from blood by a modification of the methods described by Chang and Glazko[2] and Evenson *et al.*[3]. To 1.0 ml of serum were added 65 μl of methanol containing 26 μg of the internal standard, MPPH. The solution was made basic with 0.3 ml of 0.1 *M* phosphate buffer (pH 12) and was then washed with 2-ml aliquots of diethyl ether to remove neutral lipids; the combined ethereal washings were back-extracted with 3 ml of 0.1 *M* phosphate buffer (pH 12). The basic aqueous fractions were then combined, acidified with 1 ml of 10% hydrochloric acid and extracted with two 5-ml aliquots of chloroform. The chloroform extracts were then evaporated to dryness and the residue was taken up in 65 μl of methanol. A 1-μl volume of the methanolic solution was transferred into a glass capillary cup contained in the heater coil of the solid probe inlet of the mass spectrometer. The sample was volatilized into the ion source of the mass spectrometer by applying a sufficient voltage to the heater coil of the inlet to increase the temperature of the capillary from 40° to 200° in approximately 40 sec. The spectrometer was set to scan continuously from 155 to 340 a.m.u. To record the evolution of the compounds, the shutter of the oscilloscope camera was opened for the entire heating period, producing peaks comparable in anayltical value to the

peak heights on GLC records without the corresponding peak-width measure of the time rate of rise and fall of the peaks. The concentrations of the anticonvulsants were then estimated from the heights of the peaks of the drug and the internal standard on the photograph with the aid of a calibration graph.

The mass spectrometer was set to scan the mass range 155–340 a.m.u. The sensitivity was set at 10^{-7} A/V and the scope sensitivity was set at 2–5 V per division, depending on the concentration of a particular sample.

RESULTS

Washing the solution in serum–basic buffer with diethyl ether prior to extraction removed most of the fatty acids and their esters, thus reducing the interfering background.

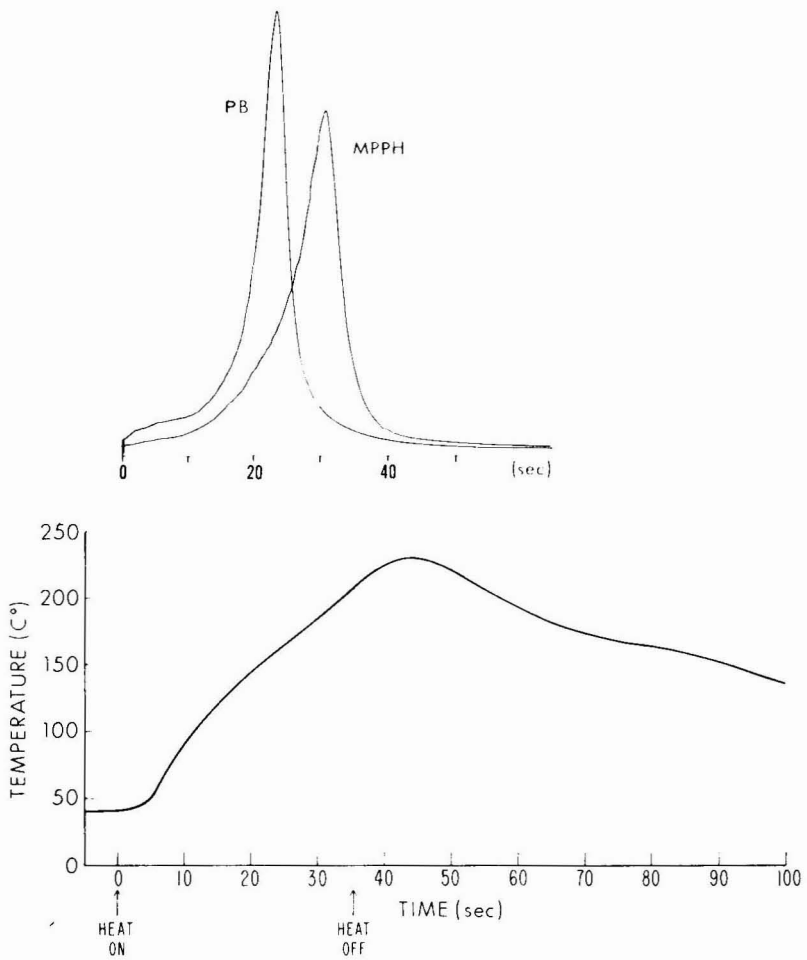


Fig. 1. Evaporation profiles (total ion current) of phenobarbital (PB) and 5-(*p*-methylphenyl)-5-phenylhydantoin (MPPH) as heat is applied to the sample capillary cup of the solid probe.

Diphenylhydantoin and phenobarbital added to human plasma were quantitatively recovered. This result had previously been confirmed by conventional GLC assays of these extracts. Only 60% of the primidone was recovered, possibly because of its poor solubility and its extremely weak acidic character[4].

The voltage applied to the heating coil increased the temperature from 40° to 200° in 40 sec. Compounds volatilize at different rates, but the volatilization of phenobarbital, the lowest boiling compound, and MPPH were both complete at the end of this period (Fig. 1).

The quasimolecular ion peaks corresponding to the molecular weight of the protonated drugs $(MH)^+$ appear at *m/e* 219 (primidone), *m/e* 233 (phenobarbital), *m/e* 253 (diphenylhydantoin) and *m/e* 267 (MPPH) (Fig. 2). The quasimolecular ion for each of the drugs is the base peak and accounts for more than 50% of the total ion current (Fig. 3).

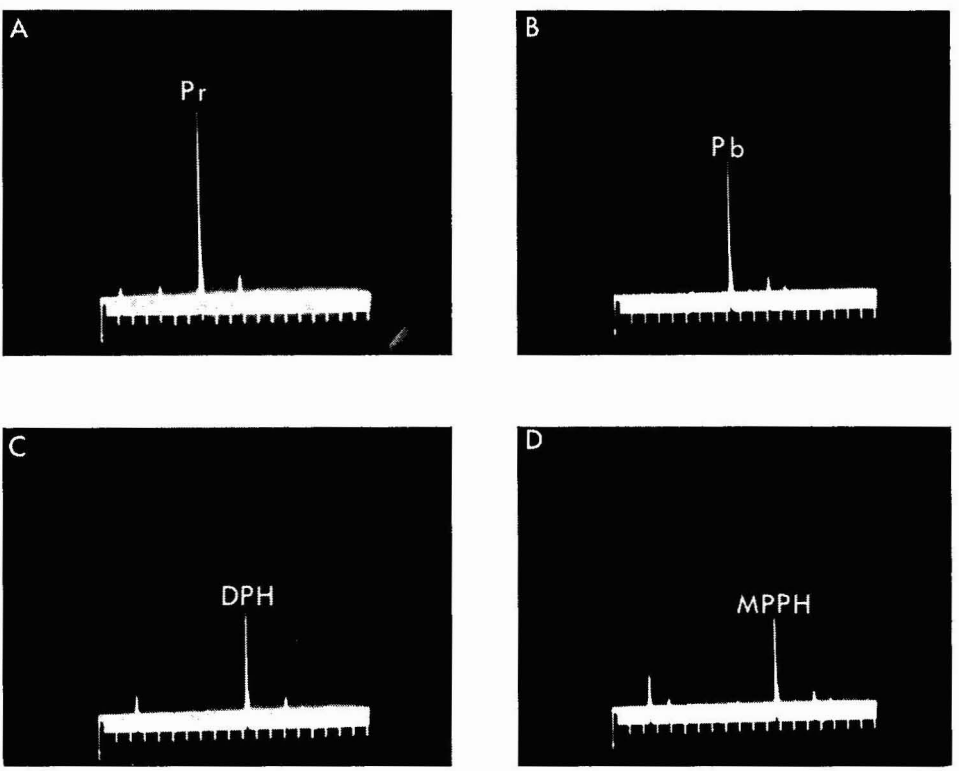


Fig. 2. Chemical ionization mass spectra of (A) primidone, (B) phenobarbital, (C) diphenylhydantoin and (D) the internal standard. The scanning range shown is 155–340 a.m.u.

In addition to those listed, fragment ions characteristic of the methane reagent gas appear at M + 15 $(MCH_3)^+$, M + 29 $(MC_2H_5)^+$ and M + 41 $(MC_3H_5)^+$.

When all four compounds are introduced into the mass spectrometer simultaneously, the four quasimolecular ions corresponding to the molecular weight of

CI FRAGMENTATION PATTERNS

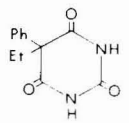
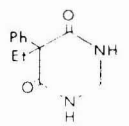
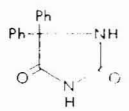
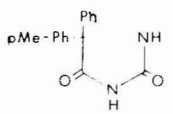
COMPOUND	m/e	RELATIVE INTENSITIES (%)	
a) Phenobarbital, MW 232	233	100	(MH^+)
	204	< 2	(Loss of Et)
b) Primidone, MW 218	219	100	(MH^+)
	190	8	(Loss of Et)
	163	10	(Loss of Et, CH_2NH)
c) Diphenylhydantoin, MW 252	253	100	(MH^+)
	225	3	(Loss of CO)
	175	15	(Loss of Ph)
d) MPPH, MW 266	267	100	(MH^+)
	189	2	(Loss of Ph)
	175	15	(Loss of CH_2Ph)

Fig. 3. Relative abundance of ions in the CI spectra of the anticonvulsants and the internal standard.

the protonated compounds are easily distinguished. None of the secondary ion-fragments interferes (Fig. 4).

The ratios of the peak heights of DPH, PB and Pr to that of the internal standard were directly proportional to the concentration of drugs added in the therapeutic range of interest (3–30 μg/ml in plasma) (Fig. 5).

Other acidic compounds present in the sample could be identified (Figs. 6–9). We noted no interference by any of these compounds with the quantification of the anticonvulsants.

Sensitivity

The sensitivity was such that $5 \cdot 10^{-9}$ g of diphenylhydantoin and phenobarbital produced peaks 3× and 5× the noise level respectively; $1 \cdot 10^{-9}$ g of primidone gave a signal-to-noise ratio of 4.

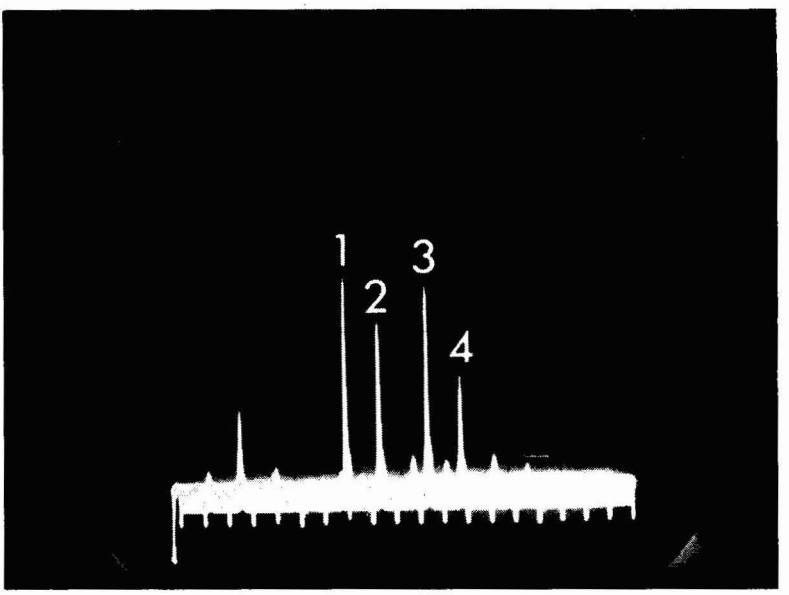


Fig. 4. Chemical ionization spectra obtained when all four compounds are introduced together. Quasimolecular ion peaks: (1) primidone, *m/e* 219; (2) phenobarbital, *m/e* 233; (3) DPH, *m/e* 253; (4) MPPH, *m/e* 267.

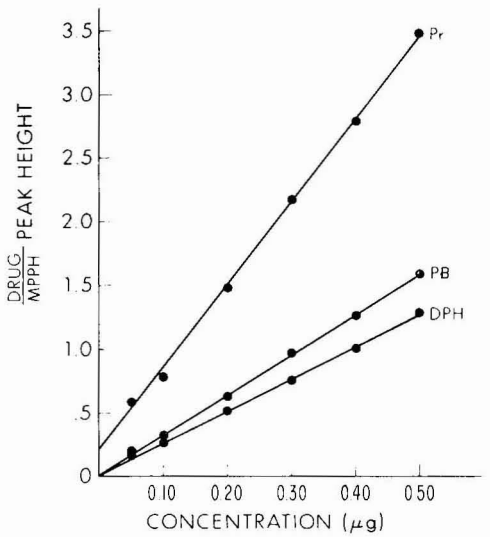


Fig. 5. Proportionality between the ratios of the heights of the quasimolecular peaks and the concentrations of each drug to that of the internal standard.

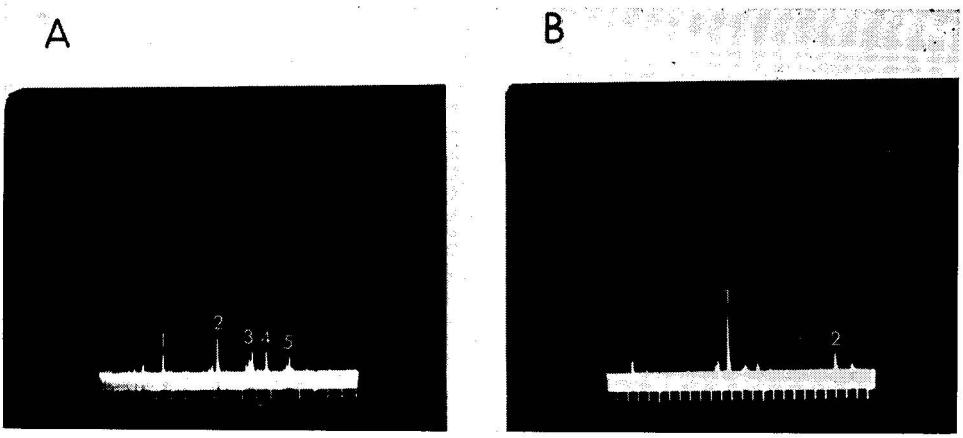


Fig. 6. Chemical ionization mass spectra of extracts of two sera submitted to the clinical laboratory for assay for diphenylhydantoin. Quasimolecular peaks identified: (A), (1) caffeine; (2) phenobarbital; (3) palmitic acid; (4) MPPH; (5) stearic acid. (B), (1) MPPH; (2) cholesterol.

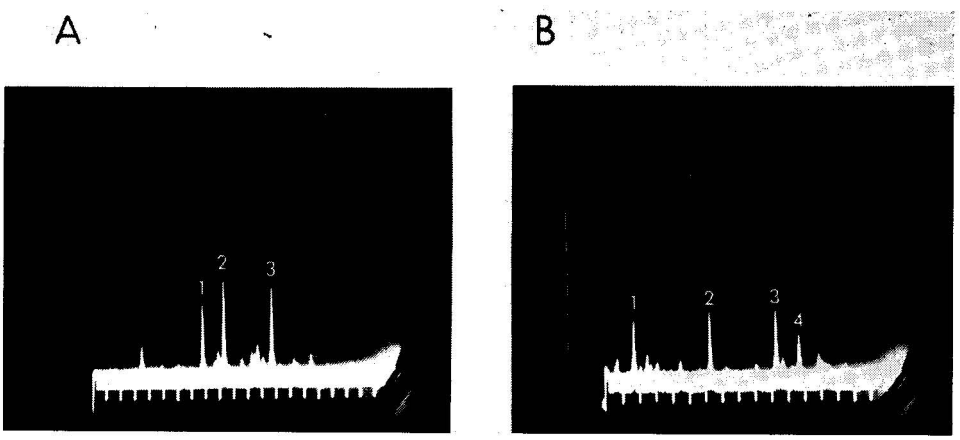


Fig. 7. Chemical ionization mass spectra of extracts of two sera submitted to the clinical laboratory for assay for diphenylhydantoin. Quasimolecular peaks identified: (A), (1) glutethimide; (2) phenobarbital; (3) MPPH. (B), (1) phthalate plasticizer; (2) butabarbital; (3) DPH; (4) MPPH.

DISCUSSION

Chemical ionization offers the possiblity of assaying simple mixtures without the preliminary separation by GLC that is so helpful in GC–MS with electron impact ionization. Milne *et al.*[1] suggested its use for detecting and identifying drugs taken in overdose amounts, in which the concentration of the compound of interest is generally appreciably greater than those of other compounds which might otherwise interfere.

The technique offers very rapid, simultaneous analysis with less than the ultimate in positive identification. We have not noted any significant interferences by compounds other than those we were attempting to assay.

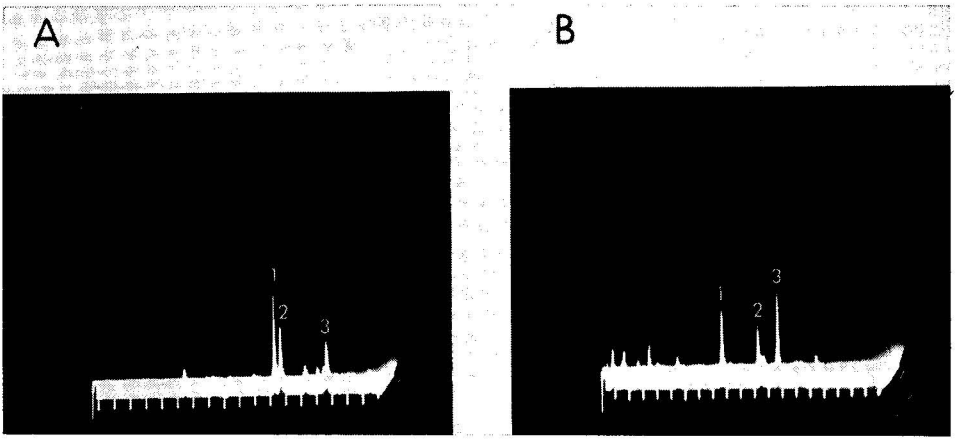


Fig. 8. Chemical ionization mass spectra of extracts of two sera submitted to the clinical laboratory for assay for diphenylhydantoin. Quasimolecular peaks identified: (A), (1) phenobarbital; (2) carbamazepine; (3) MPPH. (B) (1) amobarbital; (2) DPH; (3) MPPH.

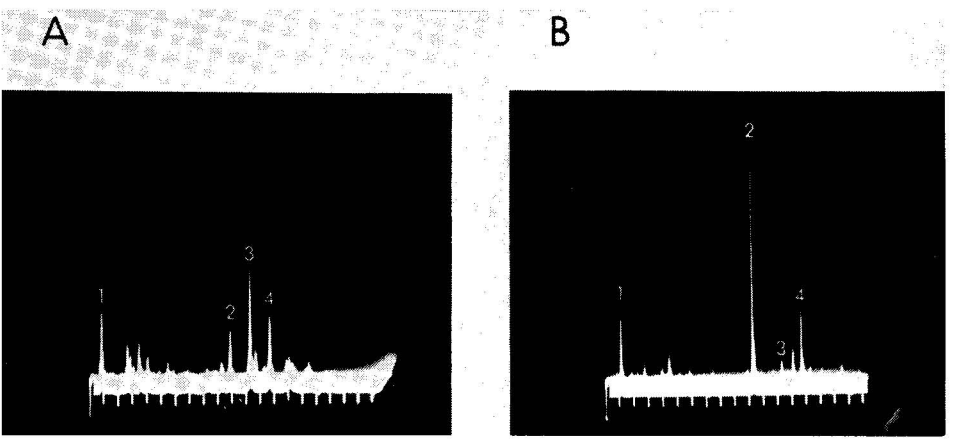


Fig. 9. Chemical ionization mass spectra of extracts of two sera submitted to the clinical laboratory for assay for diphenylhydantoin. Quasimolecular peaks identified: (1) (A), phthalate plasticizer; (2) secobarbital; (3) DPH; (4) MPPH. (B) (1) ethosuximide; (2) phenobarbital; (3) DPH; (4) MPPH.

Recording the spectra can be accomplished in several ways: (a) continuous sweep and recording of the complete mass spectrum in a computer memory; (b) photographic recording of the images displayed on the oscilloscope; and (c) multiple ion detection, *i.e.*, time sharing the detector among the expected quasimolecular ion peaks. Although the first two approaches offer less sensitivity than the third, they permit the detection of unexpected compounds. We chose photography only to study the feasibility of the approach we describe. We were surprised that the quantification was so good. The use of a computer should offer significant advantages.

Other acidic compounds present in the serum could be identified and quantified provided that a suitable calibration graph is obtained. The assay time of 2 min per sample could be shortened by the use of more than one solid probe inlet.

ACKNOWLEDGEMENT

This work was supported by N.I.H. Grant GM 19478.

REFERENCES

1 G. W. A. Milne, H. M. Fales and T. Axenrod, *Anal. Chem.*, 43 (1971) 1815.
2 T. Chang and A. J. Glazko, *J. Lab. Clin. Med.*, 75 (1970) 145.
3 M. A. Evenson, P. Jones and B. Darcey, *Clin. Chem.*, 16 (1970) 107.
4 H. J. Kupferberg, *Clin. Chim. Acta*, 29 (1970) 283.

Journal of Chromatography, 126 (1976) 625–639
© Elsevier Scientific Publishing Company, Amsterdam — Printed in The Netherlands

CHROM. 9413

SOLUBILITY FACTORS IN GAS–LIQUID CHROMATOGRAPHY

COMPARISON BETWEEN TWO APPROACHES AND APPLICATION TO SOME BIOLOGICAL STUDIES

PAUL LAFFORT and FRANÇOIS PATTE
Groupe de Laboratoires du C.N.R.S., 91190 Gif-sur-Yvette (France)

SUMMARY

Solubility factors in gas–liquid chromatography have mainly been determined by the work of two groups of workers: Snyder, Karger and Eon through an expanded version of the Hildebrand solubility parameter, and Laffort, Patte and Etcheto through a computer program related to factor analysis. An experimental comparison between these two approaches has been made, giving a mutual improvement (approximately 80% of mutual agreement). Some applications in biology are considered, especially in olfaction.

INTRODUCTION

Several workers have attempted to characterize the cohesion of solutions from factors of solutes and of solvents. In the more restricted field of gas–liquid chromatography (GLC), Rohrschneider proposed in 1965[1] a linear equation to calculate the Kováts retention indices:

$$I = I_0 + ax + by + cz \quad (1)$$

where I_0 is the retention index for squalane, a, b and c are the solute factors and x, y, z the solvent factors. Rohrschneider himself extended this equation to six terms in 1966[2] and McReynolds proposed one of eight terms in 1970[3].

The general purpose of these approaches was to classify stationary phases simply, without attempting to obtain factors mutually independent or "orthogonal".

Weiner and Howery, in 1972[4,5], obtained from the experimental data of Rohrschneider and McReynolds eight abstract orthogonal factors by using factor analysis. They then tried to superimpose a physico-chemical space on the mathematical space defined. They had some success: in their two papers, three of the eight factors were identified. In one, the molar polarizability, the square of dipole moment and the heat of vaporization were identified, and in the other the "gas imperfection term using the Van der Waals equation of state", an "alcohol-like character" and an "electron donor ability" were given. There is, of course, a large overlap between these

two groups of properties, and there remain five factors to be identified in both instances.

Also in 1972, Dravnieks and Laffort[6] proposed to characterize this space by a linear equation of only four terms, in which the solute factors were identified as: α, the molecular volume (or apolar factor); ϱ, the receptor of proton ability; π, the proton donor ability; and ε, an index of local volume polarizability (or electron factor). Numerical data for 31 substances were obtained, and highly significant correlations between these physico-chemical properties and a biological property (olfactory) were found.

In 1974, Laffort, Patte and Etcheto[7] improved the method. They derived these molecular properties with good accuracy from only 4 stationary phases instead of 25 and gave numerical data for 85 substances.

Let us consider the different numbers of factors involved according to the several workers quoted*. The number of factors to be taken in account depends on their orthogonality, on the sample of substances and phases, and on the mean accuracy of the calculated retention indices. This accuracy has to be comparable to the mean experimental accuracy, which most of the workers estimate to be within 6 and 9 Kováts index units. An accuracy of 3 index units found by Weiner and Howery with 8 orthogonal factors must be considered as illusory.

In a parallel direction to this empirical progress from 1965 to 1974, there is a semi-theoretical approach, elaborated by Snyder in 1971[9] and further developed in 1975 by Snyder and co-workers[10,11]. They expanded the "solubility parameter" of Hildebrand and Scott's theory[12,13] to five partial parameters, which they called parameters of dispersion (δ_d), orientation (δ_o), induction (δ_{in}), basicity (δ_b) and acidity (δ_a). They developed from this a general theory of retention, valid for the several kinds of chromatography: by partition or adsorption, in the gaseous phase or in a liquid, which takes into account the partial solubility parameters of the solutes, solvents and adsorbents, and the molar volume of the solutes. An equation with five terms was proposed for GLC.

The purpose of the present work is to compare this semi-theoretical approach and the empirical approach of Laffort *et al.*[7], in order to try to realize the suggestion made by Keller in 1973[14]: "It seems clear that factor analysis needs to be applied to test the value of extended solubility parameters once a more complete set becomes available".

Note

We mention the topological approach only as a reminder, because it implies that a limited number of physico-chemical factors cannot explain the solutions and the adsorptions. To our knowledge, this approach has been fruitful only in pharmacology, when families of very similar substances are involved. For GLC, Lenfant *et al.*[15] in 1971, by using the DARC system, proposed an equation of seven terms to predict the retention times of saturated ketones, which is not valid, of course, for substances with other functional groups. It is to be hoped, however, than in the future a comparison between topology and thermodynamics will be made, similar to

* Dupuis and Dijkstra[8] studied the classification of phases and estimated that 10 factors are necessary.

the physico-chemical comparison between theoretical and empirical approaches that we are analyzing in this paper.

MATERIALS AND METHODS

The methods used were the same as those used by Dravnieks and Laffort[6] and Laffort *et al.*[7], with the numerical partial solubility parameters given by Snyder[9] in addition.

Kováts retention indices

Kováts retention indices were measured by McReynolds in 1970[16] for the interaction of 68 substances on 25 phases at 120°. We added seven *n*-alkanes in order to make the computations easier.

Computer program

The program used was established by Robin and Laffort in 1971[17]. It is related to the programs of factor analysis, but it requires an initiation by values that approximate to the real solution. Fig. 1 shows how it works.

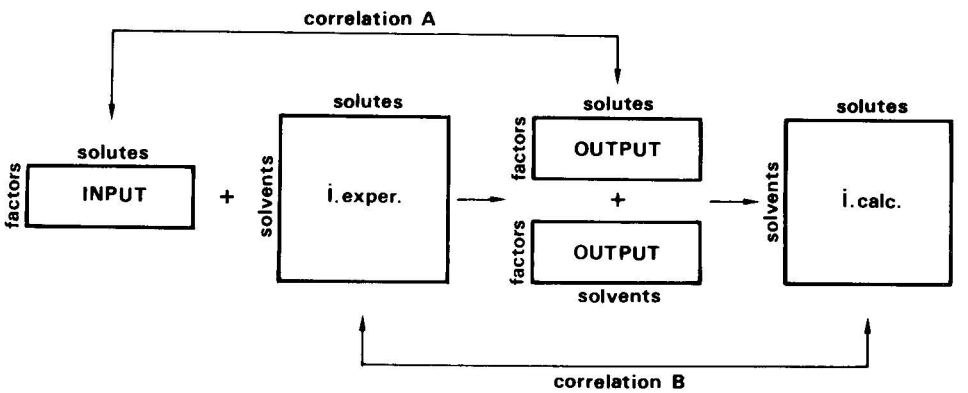


Fig. 1. Representation of the Robin–Laffort computer program[17]. Correlation B depends only on the number of factors, whereas correlation A depends on the INPUT solutes factors matrix for a given number of factors (see text).

The correlation A depends, for a given number of factors, on the initiation of solute factors; if the matrix INPUT is made with randomized digits, the correlation will be bad. If, on the other hand, it is made with molecular factors involved in the phenomenon, the correlation will be good. The correlation B between experimental and calculated Kováts indices depends only on the number of factors chosen. It will be unity if the number of factors is the same as the number of solvents (25 in our case). Fig. 2 shows how Dravnieks and Laffort[6] estimated, in 1972, that the number of factors involved is four. Instead of a correlation coefficient, they calculated the "standard error" between the calculated and experimental retention indices using eqn. 2,

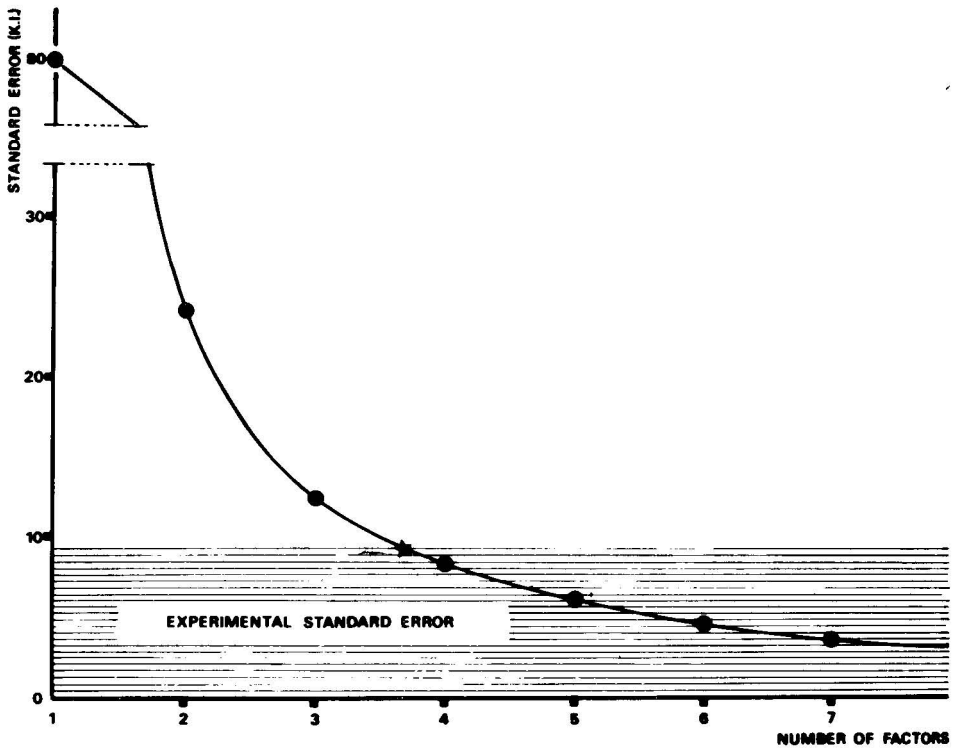


Fig. 2. Comparison between the "standard error" of calculated retention indices in GLC and the "experimental standard error". The latter, being found to be equal to 9 index units, seems to indicate that four factors are sufficient to explain the phenomenon. Index range, 200–1600; mean, 900. (From Dravnieks and Laffort[6], modified.)

which they compared to the value of the "experimental standard error" given by eqn. 3.

$$\text{Standard error} = \sqrt{\Sigma (I_{\text{calc.}} - I_{\text{exp.}})^2/(n-1)} \tag{2}$$

$$\text{Experimental standard error} = \sqrt{\Sigma (I_{\text{exp.}} - I_{\text{exp.}})^2/(n-1)} \tag{3}$$

The experimental standard error, on the basis of numerical experimental data, was evaluated as 9 Kováts' index units. The consequence was the assumption that four factors were involved. A hypothesis of an experimental standard error of six index units would have implied five factors, etc.*.

Partial solubility parameters

Let us consider briefly how Snyder *et al.*[10] define the components of the Hildebrand solubility parameter (δ):

$$\Delta E^v = V_{20}\,\delta^2 = V_{20}\,(\delta_d^2 + \delta_o^2 + 2\delta_{in}\,\delta_d + 2\delta_a\,\delta_b) \tag{4}$$

* The method of Rohrschneider (six non-orthogonal factors) for a matrix of 20 solutes by 25 solvents gives also, by using eqn. 2 on McReynolds data, a standard error of 9 Kováts index units.

where ΔE^v is the free enthalpy of vaporization.

The calculation of the free enthalpy of solubility of a binary mixture gives, according to these workers, in the particular case of GLC, the following equation, in which i is related to the solute and j to the stationary phase:

$$I = -[100\ V_i/(\Delta E_{me})_j]\ [2\delta_d^i\,\delta_d^j + 2\delta_o^i\,\delta_o^j + 2\delta_{in}^j\,\delta_d^i + 2\delta_{in}^i\,\delta_d^j + 2\delta_a^j\,\delta_b^i + 2\delta_a^i\,\delta_b^j] \tag{5}$$

If we take into account in a first stage only the solute factors as variables, the solvents factors can be gathered in arbitrary constants. Under these conditions

$$I = V_i\,(A\delta_d^i + B\delta_o^i + C\delta_{in}^i + D\delta_a^i + D\delta_b^i) \tag{6}$$

Therefore, the experiments we made were essentially an initiation of the Robin–Laffort program by $V_{20}\,\delta_d$, $V_{20}\,\delta_o$, $V_{20}\,\delta_{in}$, $V_{20}\,\delta_a$ and $V_{20}\,\delta_b$, on the basis of retention indices established by McReynolds.

RESULTS AND DISCUSSION

First stage

The 25 substances for which both Kováts indices on 25 phases and partial solubility parameters were available are given in Table I. Also reported are the partial solubility parameters, the products $V_{20}\,\delta$ and $(V_{20}/V_b)\,\delta_d$ (V_b being the molar volume at the boiling point)*.

Preliminary examination of Table I suggests that the products $V_{20}\,\delta_o$, $V_{20}\,\delta_a$ and $V_{20}\,\delta_b$ are relatively constant for a given functional group and environment. This will be confirmed later by the values found for substances included in larger homologous series. It is also evident that the product $(V_{20}/V_b)\,\delta_d$ is constant for a given functional group. This can be explained easily. From Snyder *et al.*[10], we have the approximate relationship

$$\delta_d = 30.7\left(\frac{n^2 - 1}{n^2 + 2}\right) \tag{7}$$

that is

$$\delta_d = 30.7\,\frac{R_m}{V_{20}}$$

from which

$$\delta_d\,\frac{V_{20}}{V_b} = 30.7\left(\frac{R_m}{V_{20}}\cdot\frac{V_{20}}{V_b}\right) = 30.7\,\frac{R_m}{V_b}$$

Because R_m and V_b are both additive properties, the ratio will be virtually

* δ_d, δ_o, δ_a and δ_b were given by Snyder[9]; δ_{in} was calculated from eqn. 4; the global value of δ was also given by Snyder[9].

TABLE I

PARTIAL SOLUBILITY PARAMETERS ACCORDING TO SNYDER[9], AND DERIVED TERMS USED TO INITIATE THE COMPUTER PROGRAM, FOR 25 SUBSTANCES (SEE TEXT)

Compound	δ_d	δ_o	δ_b	δ_a	δ_{in}	V_{20}	V_b	$\frac{V_{20}}{100}\delta_d$	$\frac{V_{20}}{100}\delta_o$	$\frac{V_{20}}{100}\delta_b$	$\frac{V_{20}}{100}\delta_a$	$\frac{V_{20}}{100}\delta_{in}$	$\frac{V_{20}}{V_b}\delta_d$
Methanol	6.2	5.0	7.5	7.5	−0.8	41	42	2.5	2.0	3.0	3.0	−0.3	6.0
Ethanol	6.8	4.0	5.0	5.0	1.0	58	62	4.0	2.3	2.9	2.9	0.6	6.4
1-Propanol	7.2	2.5	4.0	4.0	1.0	77	81	5.6	1.9	3.1	3.1	0.8	6.8
Acetone	6.8	5.0	2.5	0.0	1.3	73	77	5.0	3.7	1.8	0.0	0.9	6.4
2-Butanone	7.1	3.7	2.0	0.0	1.4	90	100	6.4	3.3	1.8	0.0	1.3	6.3
Chloroform	8.1	3.0	0.5	3.0	0.3	81	85	6.6	2.4	0.4	2.4	0.3	7.7
Carbon tetrachloride	8.6	0.0	0.5	0.0	0.0	97	102	8.3	0.0	0.5	0.0	0.0	8.1
Ethyl bromide	7.8	3.0	0.0	0.0	0.5	75	77	5.8	2.2	0.0	0.0	0.4	7.5
Methyl iodide	9.3	2.0	0.5	0.0	0.4	62	65	5.8	1.3	0.3	0.0	0.3	8.9
Nitromethane	7.3	8.0	1.0	0.0	0.3	54	63	3.9	4.3	0.5	0.0	0.1	6.2
Acetonitrile	6.5	8.0	2.5	0.0	2.5	52	58	3.4	4.2	1.3	0.0	1.3	5.9
Pyridine	9.0	4.0	5.0	0.0	0.6	81	93	7.3	3.2	4.0	0.0	0.5	7.8
Benzene	9.2	0.0	0.5	0.0	0.0	89	98	8.2	0.0	0.4	0.0	0.0	8.4
Toluene	8.9	0.0	0.5	0.0	0.0	106	118	9.5	0.0	0.5	0.0	0.0	8.0
2,4-Dimethylpentane	7.1	0.0	0.0	0.0	0.0	149	159	10.6	0.0	0.0	0.0	0.0	6.6
2-Methylheptane	7.4	0.0	0.0	0.0	0.0	164	180	12.1	0.0	0.0	0.0	0.0	6.7
3-Methylheptane	7.4	0.0	0.0	0.0	0.0	162	180	12.0	0.0	0.0	0.0	0.0	6.6
2,2,5-Trimethylhexane	7.4	0.0	0.0	0.0	0.0	182	201	13.4	0.0	0.0	0.0	0.0	6.7
1,4-Dioxane	7.8	4.0	3.0	0.0	1.2	85	89	6.6	3.4	2.6	0.0	1.1	7.5
Anisole	9.1	2.5	2.0	0.0	0.3	109	126	9.9	2.7	2.2	0.0	0.3	7.9
Cyclohexane	8.2	0.0	0.0	0.0	0.0	108	117	8.9	0.0	0.0	0.0	0.0	7.6
Hydrindane	8.5	0.0	0.0	0.0	0.0	144	161	12.2	0.0	0.0	0.0	0.0	7.6
Decalin	8.7	0.0	0.0	0.0	0.0	154	178	13.4	0.0	0.0	0.0	0.0	7.5
1-Octane	7.4	0.0	0.0	0.0	0.0	163	187	12.0	0.0	0.0	0.0	0.0	6.4
Tetradecane	7.9	0.0	0.0	0.0	0.0	260	319	20.6	0.0	0.0	0.0	0.0	6.4

constant for a given homologous series. For example, for C_4–C_{18} *n*-alkanes the δ_d values lie in the range 6.4–8.1, but the product δ_d (V_{20}/V_b) is always 6.4.

Table II indicates the method used by Kopp (quoted by Partington[18], pp. 17–28) to calculate V_b. The original list of increments was expanded by Laffort in 1969[19] and Laffort and Dravnieks in 1973[20,*].

TABLE II

LIST OF INCREMENTS FOR EVALUATING MOLAR VOLUMES AT BOILING POINT, V_b, ACCORDING TO KOPP, LOSSEN, SCHIFF AND ZANDER AND LE BAS (ALL QUOTED BY PARTINGTON[18])

The balance between authors and additional increments are from Laffort[19] and Laffort and Dravnieks[20].

Group	*Increment (ml)*	*Group*	*Increment (ml)*
H—	5.5	—O—	7.8
—C—	11.0	O=	10.2
C=	13.0	—S—	22.6
=C= and —C≡	15.0	S=	28.6
N (in CN and NO_2)	15.6	F—	12.6
Ring of 6 atoms	15.0	Cl—	22.8
Ring of 5 atoms	11.5	Br—	27.8
Ring of 4 atoms	8.5	I—	37.5
Ring of 3 atoms	−6.5	P(III) and P(V)	25.4

Second stage

The Robin–Laffort computer program was initiated by three sets of random numbers for the substances in Table I. The correlation coefficients between the INPUT and OUTPUT solute factors are reported at the top of Table III. According to this table, it seems that an initiation has to generate correlations close to 0.9 in order to be valid.

The same program was then initiated by $V_{20}\,\delta_d$, $V_{20}\,\delta_o$, $V_{20}\,\delta_{in}$, $V_{20}\,\delta_a$ and $V_{20}\,\delta_b$ according to Snyder *et al.*[10]. All of the initiations, as seen from Table III, seems to be accurate except for $V_{20}\,\delta_{in}$.

If the product $(V_{20}/V_b)\,\delta_d$ takes the place of $V_{20}\,\delta_{in}$, all initiations are good (see also the results in Table III). Useful conclusions can be drawn from these results: on the one hand, it appears that five factors have to be taken into account, instead of four as Laffort *et al.* believed; on the other hand, Snyder *et al.*'s theory, in its application to GLC is verified at 80% (4 out of 5 initiation terms) and becomes easy to verify at 100% with a slight adjustment. The degree of overlapping between these results and the factors proposed by Laffort *et al.* in 1974[7] will be seen later.

* In the particular case of *n*-alkanes, V_b can be calculated by the very simple equation

$$V_b\,(\text{ml}) = 22n + 11 \qquad (8)$$

in which n is the number of carbon atoms.

TABLE III

CORRELATIONS BETWEEN THE INPUT AND OUTPUT SOLUTE FACTORS FOR 25 SUBSTANCES

See explanation in text.

	1st factor	*2nd factor*	*3rd factor*	*4th factor*	*5th factor*
Random numbers	0.22	0.04	0.56	0.15	0.10
	0.19	0.05	0.00	0.15	0.12
	0.38	0.29	0.39	0.39	0.05
Strict Snyder *et al.* theory	$V_{20}\,\delta_d$	$V_{20}\,\delta_a$	$V_{20}\,\delta_{in}$	$V_{20}\,\delta_a$	$V_{20}\,\delta_b$
	0.99	0.93	0.56	0.87	0.92
Adapted Snyder *et al.* theory	$V_{20}\,\delta_d$	$V_{20}\,\delta_a$	$(V_{20}/V_b)\,\delta_d$	$V_{20}\,\delta_a$	$V_{20}\,\delta_b$
	0.98	0.93	0.89	0.93	0.94

Third stage

As can be seen in Fig. 1, the program also generates solvent factors matrix. With the matrix obtained in the last case of the second stage, we found easily (by regression analysis the solute factors for the 75 substances, the retention indices of which were available on 25 phases.

Fourth stage

At this stage, we selected the five stationary phases reproducing with accuracy the results of the third step. As in 1974, according to Laffort *et al.*[7], no set including an apolar phase was acceptable. The five phases selected were Zonyl E7 (DuPont, Wilmington, Del., U.S.A.), Carbowax 1000, tricyanoethoxypropane, polyphenyl ether (6 rings) and diethylene glycol succinate (Applied Science Labs., State College, Pa., U.S.A.). The first four are the same as those previously selected.

Fifth stage

The solute factors obtained at this stage were compared with an "index of cohesive energy" (ICE) defined by eqns. 9 and 9a.

$$\mathrm{ICE}_{25} = -(\text{log vapour pressure at } 25^\circ \text{ in atm}) \quad \text{if } t_b \geqslant 25^\circ \tag{9}$$

$$\mathrm{ICE}_{25} = \left[\frac{T_b}{402.8} + 0.6168\right]^3 - 2.45 \qquad \text{if } t_b < 25^\circ \tag{9a}$$

The comparison was made with a polynomial regression program. Eqns. 10 reproduce the definition of the primary factors in GLC in this "1976 version", as we have proposed.

$$\left.\begin{aligned}
\alpha &= 0.503\,Z - 0.119\,C + 0.016\,T + 1.602\,P - 1.514\,D \\
\omega &= 0.286\,Z + 0.433\,C - 0.220\,T - 0.041\,P - 0.458\,D \\
\varepsilon &= -0.737\,Z + 0.651\,C + 0.905\,T - 0.654\,P - 0.165\,D \\
\pi &= -0.031\,Z - 0.127\,C - 0.283\,T + 0.567\,P - 0.126\,D \\
\beta &= 0.273\,Z - 0.816\,C - 0.596\,T - 0.008\,P + 1.147\,D
\end{aligned}\right\} \tag{10}$$

in which

$Z = (I - 100)/100$ on Zonyl E7;
$C = (I - 100)/100$ on Carbowax 1000;
$T = (I - 100)/100$ on tricyanoethoxypropane;
$P = (I - 100)/100$ on polyphenyl ether (6 rings);
$D = (I - 100)/100$ on diethylene glycol succinate.

According to this definition, each factor has the same weight in its contribution to the "index of cohesive energy", as shown in eqn. 11:

$$ICE_{25}(X) - ICE_{25}(CH_4) = \alpha + \omega + \varepsilon + \pi + \beta - 1.2\,\varepsilon\pi \quad (r = 0.99). \qquad (11)$$

The ICE_{25} value for methane is -1.74. The values of α, ω, ε, π and β in the 1976 version for the 75 substances studied are reported in Table IV.

Our approach suggests two comments about the global solubility parameter as defined by Hildebrand and Scott[12,13]. The first comment was implicit in the first stage of the present work: why is V_{20} instead of V_b used as an approach to the actual molar volume? The second comment concerns the choice of the free enthalpy of vaporization, ΔE^v, rather than the saturated vapour pressure as a criterion of "cohesion energy". Several forces of cohesion are not necessarily implied in the same proportions at different temperatures, because of molecular motion. The following experiment confirmed this hypothesis.

The saturated vapour pressure at 120° for the same 75 substances was treated by a polynomial regression program. We obtained ($r = 0.99$):

$$-(\log \text{vapour pressure at } 120° \text{ in atm}) = 0.62\,\alpha + 0.55\,\omega + 0.66\,\varepsilon + 0.27\,\pi + 0.62\,\beta - 0.44\,\varepsilon\pi - 5.0 \qquad (12)$$

To simplify, we can say that the factor π (proton donor) is proportionally half as involved, in comparison with the other factors, at 120° as at 25° (coefficient of proportionality is 0.3 instead of 0.6). Therefore, it seemed to us more precise to choose an index of cohesion, determined at a given temperature. However, for the substances too near their critical temperature, we preferred to derive this index of cohesion from boiling points rather than saturated vapour pressures. We estimated that this was the case for all substances in the gaseous state at 25°.

Sixth stage

We believe that solute factors are expressed in an easier form in terms of α, ω, ε, π and β rather than δ, because four out of five factors characterize only the functional group and its environment, whereas only the last one characterizes the molar volume. On the other hand, eqn. 11, relating the "index of cohesive energy" to these factors, is simple, with no squared terms and only one cross-product. However, while waiting to see more clearly which kind of expression will be the most useful, we established eqns. 13 in order to pass easily from one expression to another:

TABLE IV

SOLUTE FACTORS IN GLC DERIVED FROM FIVE PHASES, EXPRESSED IN TERMS OF α, ω, ε, π, AND β (1976 VERSION) ACCORDING TO EQNS. 10 AND IN TERMS OF V_{20}, δ_d, δ_o, δ_a AND δ_b ACCORDING TO EQNS. 13 FOR 75 SUBSTANCES

No.	*Compound*	α	ω	ε	π	β	V_{20}	δ_d	δ_o	δ_a	δ_b
1	Methanol	0.26	0.78	−0.14	0.64	0.97	45	6.01	5.76	7.73	5.86
2	Ethanol	0.53	0.69	0.02	0.55	0.88	55	6.71	4.01	5.22	4.18
3	Propanol	1.09	0.67	0.0	0.56	0.88	73	7.15	2.69	3.69	2.90
4	Isopropanol	0.89	0.72	−0.14	0.45	0.86	69	6.42	3.25	3.33	3.18
5	Butanol	1.64	0.67	−0.02	0.57	0.90	92	7.40	2.07	2.88	2.28
6	*tert.*-Butanol	1.08	0.75	−0.27	0.30	0.85	77	6.03	3.03	1.99	2.81
7	1-Hexanol	2.80	0.63	−0.18	0.62	1.02	131	7.21	1.31	2.11	1.73
8	2-Hexanol	2.40	0.67	−0.17	0.42	0.91	119	7.04	1.57	1.61	1.74
9	3-Hexanol	2.32	0.64	−0.02	0.37	0.79	117	7.47	1.54	1.45	1.55
10	Allyl alcohol	0.79	0.68	0.12	0.70	1.00	61	7.60	3.27	5.51	3.94
11	2-Methyl-2-pentanol	2.12	0.73	−0.22	0.27	0.82	112	6.70	1.88	1.14	1.72
12	3-Methyl-3-pentanol	2.01	0.69	−0.04	0.21	0.78	108	7.22	1.84	0.92	1.71
13	2-Methyl-2-heptanol	3.12	0.67	−0.32	0.29	0.92	146	6.63	1.28	0.90	1.43
14	3-Methyl-3-heptanol	3.03	0.66	−0.15	0.23	0.83	142	7.16	1.29	0.73	1.32
15	Cyclopentanol	1.79	0.55	0.34	0.50	0.97	95	8.70	1.60	2.38	2.31
16	Acetone	0.78	1.41	−0.11	−0.15	0.39	64	6.48	6.83	−1.19	1.55
17	2-Butanone	1.29	1.35	0.05	−0.19	0.26	81	7.31	4.89	−1.13	0.77
18	2-Pentanone	1.78	1.33	−0.02	−0.20	0.30	98	7.31	3.88	−0.95	0.72
19	2-Hexanone	2.32	1.34	−0.05	−0.21	0.30	116	7.41	3.22	−0.83	0.59
20	3-Hexanone	2.27	1.28	0.17	−0.23	0.11	115	8.07	3.13	−0.92	0.22
21	1-Fluorooctane	3.41	0.67	−0.05	−0.09	0.13	160	7.30	1.19	−0.26	0.19
22	1,1-Difluorotetrachloroethane	2.49	0.26	−0.48	0.10	0.82	133	5.60	0.59	0.37	1.53
23	1,2-Difluorotetrachloroethane	2.45	0.26	−0.49	0.09	0.85	132	5.56	0.60	0.34	1.60
24	Chloroform	1.26	0.13	0.59	0.43	0.64	83	8.61	0.48	2.59	1.93
25	Carbon tetrachloride	1.70	0.04	0.46	0.06	0.48	104	8.03	0.12	0.30	1.18
26	1-Chlorohexane	2.72	0.44	0.54	−0.05	0.07	135	9.00	0.93	−0.17	0.12
27	1,1,2,2-Tetrachloroethane	2.00	0.16	0.94	0.58	0.94	101	10.80	0.43	2.55	2.06
28	Ethyl bromide	0.91	0.35	0.77	0.03	0.09	73	8.49	1.56	0.22	0.33
29	1-Bromopentane	2.38	0.37	0.84	−0.05	0.02	122	9.87	0.87	−0.19	0.04
30	Methyl iodide	0.64	0.12	1.18	0.09	0.09	63	9.32	0.64	0.79	0.39
31	1-Iodobutane	2.13	0.23	1.24	−0.04	−0.10	112	11.05	0.59	−0.17	−0.21
32	2-Iodobutane	2.04	0.29	1.08	−0.05	−0.06	110	10.46	0.77	−0.22	−0.13
33	Propional	0.90	1.10	0.19	−0.08	0.22	69	7.30	4.94	−0.59	0.81

38	2-Ethylhexene	2.97	0.13	0.18	−0.03	0.05	150	7.64	0.26	−0.10	0.08
39	1-Octyne	2.66	0.25	0.31	0.12	0.31	134	8.19	0.54	0.42	0.55
40	2-Octyne	2.79	0.19	0.65	0.01	0.10	138	9.27	0.40	0.03	0.17
41	Nitromethane	0.58	1.20	−0.04	0.39	1.07	51	7.26	6.70	3.56	4.89
42	Nitroethane	0.98	1.32	0.17	0.13	0.74	65	8.10	5.65	0.91	2.59
43	Nitropropane	1.43	1.35	0.22	0.02	0.61	81	8.40	4.58	0.11	1.69
44	2-Methyl-2-nitropropane	1.83	1.45	−0.13	−0.16	0.54	98	7.14	4.15	−0.75	1.26
45	Acetonitrile	0.64	1.45	−0.11	0.24	0.70	54	6.99	7.74	2.10	3.06
46	Valeronitrile	2.08	1.52	−0.03	−0.04	0.46	104	7.72	3.96	−0.17	0.98
47	Pyridine	0.95	0.79	0.31	0.0	1.14	68	7.98	3.44	0.0	4.06
48	Thiophene	0.95	0.31	1.02	0.07	0.41	71	9.69	1.35	0.50	1.46
49	Propyl sulphide	2.74	0.46	0.77	−0.12	−0.07	134	9.77	0.97	−0.41	−0.12
50	Hexanethiol	2.90	0.30	0.88	0.0	−0.01	139	10.20	0.61	0.0	−0.02
51	Benzene	1.18	0.46	0.81	−0.04	0.28	80	9.14	1.76	−0.25	0.88
52	Toluene	1.74	0.51	0.74	−0.07	0.28	99	9.37	1.51	−0.34	0.68
53	Ethylbenzene	2.15	0.46	0.82	−0.08	0.25	113	9.84	1.17	−0.33	0.52
54	Ethynylbenzene	2.16	0.38	0.57	0.38	0.85	109	9.42	0.96	1.58	1.76
55	Mesitylene	2.84	0.53	0.53	−0.10	0.42	136	9.17	1.09	−0.34	0.71
56	Styrene	2.09	0.54	0.84	0.01	0.43	108	10.13	1.40	0.04	0.91
57	2,4-Dimethylpentane	2.55	0.01	−0.37	−0.02	0.35	141	5.71	0.02	−0.07	0.64
58	2-Methylheptane	3.27	0.07	−0.12	−0.01	0.05	163	6.73	0.13	−0.03	0.07
59	3-Methylheptane	3.28	0.06	−0.10	−0.01	0.07	163	6.80	0.11	−0.03	0.10
60	2,2,5-Trimethylhexane	3.47	0.13	−0.41	−0.02	0.19	171	5.90	0.23	−0.06	0.27
61	Butyl acetate	2.53	1.06	−0.28	−0.14	0.55	127	6.57	2.38	−0.51	1.01
62	Propyl butyrate	3.04	1.02	−0.14	−0.17	0.35	144	7.11	1.98	−0.54	0.56
63	Dibutyl ether	3.34	0.38	0.23	−0.10	−0.04	160	8.03	0.68	−0.29	−0.06
64	1,4-Dioxane	1.01	1.04	0.33	−0.21	0.71	71	7.99	4.37	−1.45	2.44
65	Anisole	1.92	0.69	0.72	0.0	0.69	100	9.86	1.91	0.0	1.56
66	Cyclohexane	2.18	−0.03	0.59	−0.05	−0.05	123	8.48	−0.08	−0.21	−0.10
67	Hydrindane	3.36	−0.04	0.93	−0.09	−0.04	159	10.22	−0.07	−0.26	−0.06
68	Decalin	3.91	−0.04	0.91	−0.09	0.01	177	10.34	−0.06	−0.23	0.01
69	Ethane	0.49	0.0	0.0	0.0	0.0	71	4.95	0.0	0.0	0.0
70	Butane	1.47	0.0	0.0	0.0	0.0	104	6.13	0.0	0.0	0.0
71	Hexane	2.44	0.0	0.0	0.0	0.0	136	6.74	0.0	0.0	0.0
72	Octane	3.42	0.0	0.0	0.0	0.0	168	7.13	0.0	0.0	0.0
73	Decane	4.40	0.0	0.0	0.0	0.0	200	7.38	0.0	0.0	0.0
74	Dodecane	5.37	0.0	0.0	0.0	0.0	232	7.57	0.0	0.0	0.0
75	Tetradecane	6.35	0.0	0.0	0.0	0.0	265	7.71	0.0	0.0	0.0

$$\left.\begin{array}{ll} V_b = 45\alpha + 33 & (r = 0.98,\ N = 75) \\ V_{20} = 33\alpha - 12\omega - 9\varepsilon - 9\pi - 5\beta + 55 & (r = 0.98,\ N = 75) \\ \delta_d = (2.6\varepsilon + 6.4)\ V_b/V_{20} & (r = 0.84,\ N = 25) \\ \delta_o = 330\omega/V_b & (r = 0.92,\ N = 25) \\ \delta_a = 540\pi/V_b & (r = 0.89,\ N = 25) \\ \delta_b = 270\beta/V_b & (r = 0.85,\ N = 25) \end{array}\right\} \quad (13)$$

The last four columns in Table IV show the numerical data we obtained with these equations for the 75 substances studied. Workers in thermodynamics should be able to say if these data seem precise. Theoretical adjustments could perhaps allow a new initiation of our program that is more accurate.

The first four factors proposed in this work are closely related to those of Laffort *et al.* ("1973 version"), as shown in Fig. 3. [We changed the letter ϱ (receptor of protons) into ω (orientation), which seems more appropriate.] The new factor β (of basicity) is not well correlated with any of the old factors.

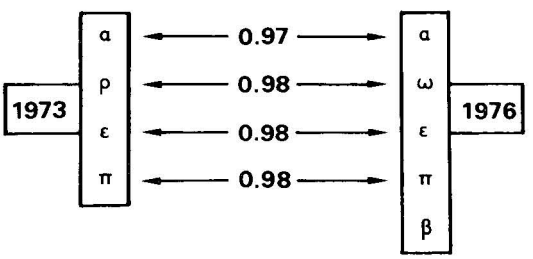


Fig. 3. Correlation coefficients (according to Pearson) between the 1973 version of molecular factors and the 1976 version for 75 substances.

APPLICATIONS IN BIOLOGY

Among the molecular properties used by some pharmacologists (Hansch[21]) for correlation with biological properties, only one is "polychromatic", *e.g.*, valid for various families of substances at once, namely the partition coefficient of octanol–water, P. This coefficient P, established for 31 of the 75 substances studied above, can be calculated from the five molecular factors with good accuracy ($r = 0.95$) by means of the equation

$$\log P = \alpha - 0.93\omega + 0.80\varepsilon - 0.29\pi - 0.22\beta + 0.38 \quad (14)$$

Therefore, the present work could perhaps be applied in pharmacology, but there is the limitation, inherent in GLC, that it cannot be used for substances of low volatility. We are now attempting to extrapolate the results obtained in gas chromatography to liquid chromatography, for the purpose of studying slightly volatile substances, but we have not yet achieved consistent results.

In fact, our general purpose is to attempt to identify the significant molecular characteristics for the neuroreceptors of the olfactory system. Highly significant cor-

relations have been established between experimental and calculated human olfactory thresholds, on the basis of the "1973 version" of molecular factors. Fig. 4 (according to Etcheto[22]) shows the results obtained so far. The accuracy is comparable to that of the experiment, except for three substances. Unfortunately, these three substances are not included in the set studied in the present work. Using a five-column system filled with the five phases described above, we are therefore measuring experimentally the retention indices of the 180 substances previously studied with only four phases. We are expecting that the three exceptions in Fig. 4 will disappear.

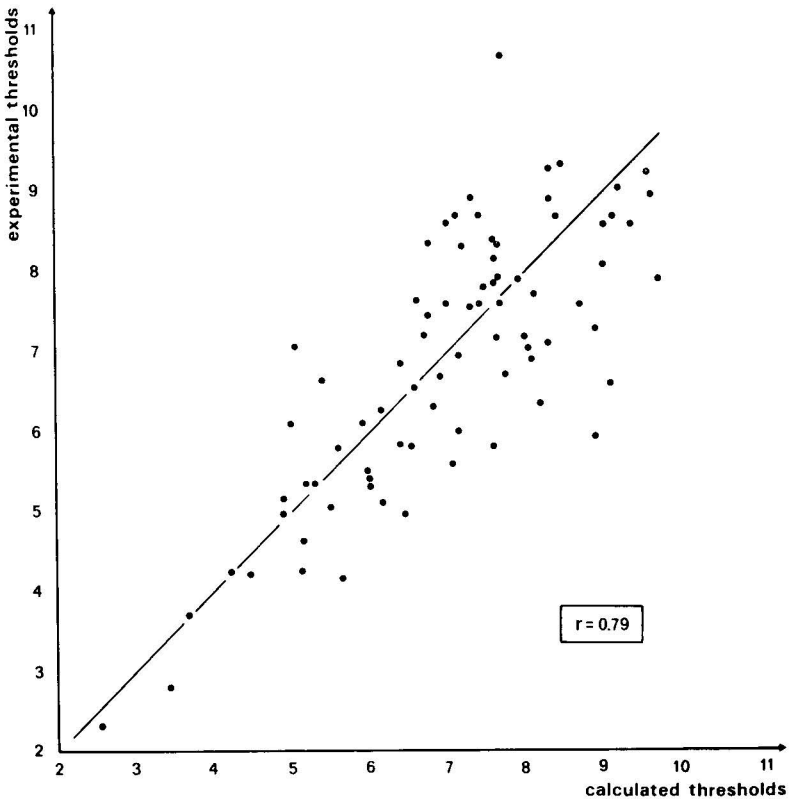


Fig. 4. Comparison between experimental and calculated human olfactory thresholds on the basis of the "1973 version" of molecular factors for 79 substances. Data are expressed as $-$(log molar fractions). (From Etcheto[22].)

Fig. 5 was proposed by Patte in 1974[23], and represents similarities and differences in the distribution of molecular factors (1973 version) for substances with various qualitative olfactory notes. It seems that a given distribution pattern can characterize only one qualitative note, even if the results are not numerous enough to be absolutely sure. We are also expecting that the taking into account of five factors will improve the correspondences.

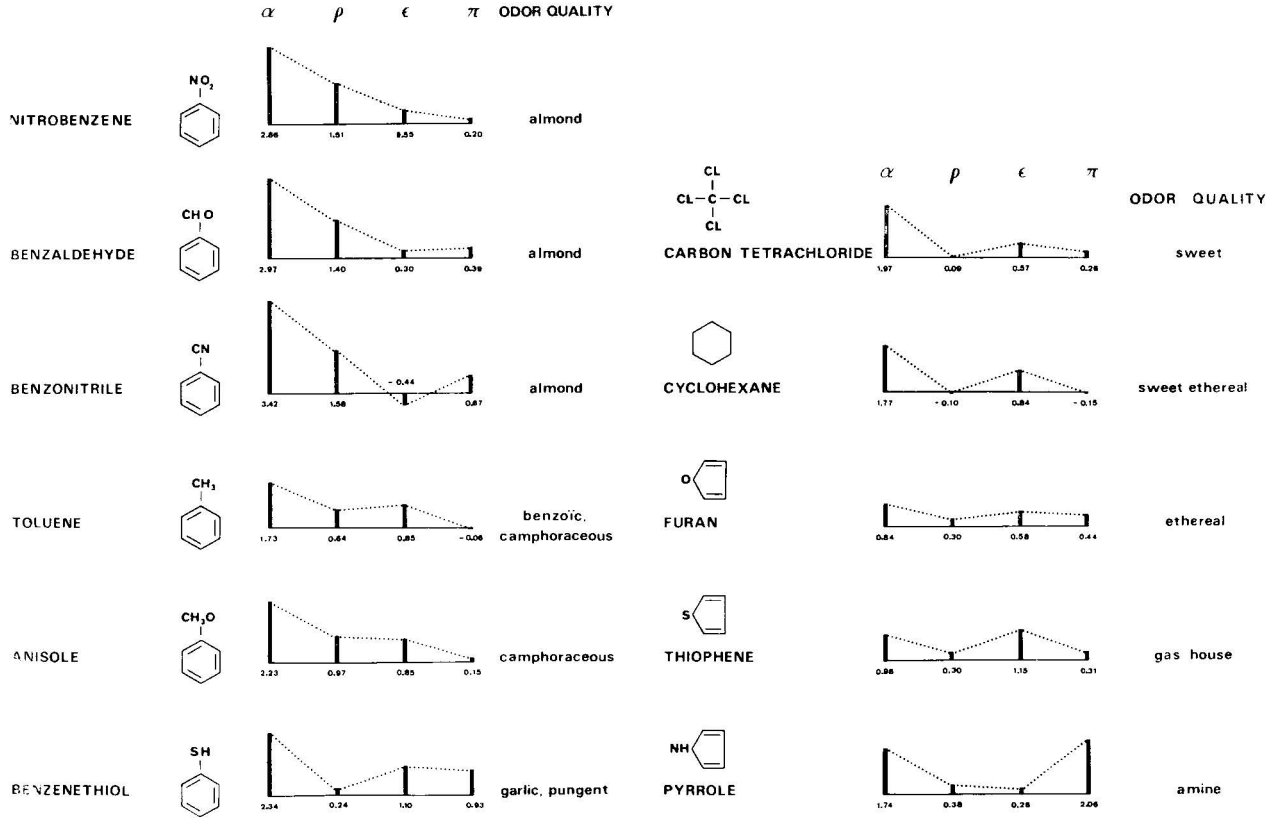


Fig. 5. Developed formulae, "physico-chemical patterns" and qualitative olfactory notes of 11 substances. It seems that similarity of odour is more related to a similarity of the "physico-chemical pattern" than to a similarity of shape (From Patte[23].)

CONCLUSION

The comparison between the semi-theoretical approach of Snyder and co-workers[10,11] and the empirical approach of Laffort *et al.*[7] indicates confidence in each and also a mutual improvement. It is clear that on the one hand the induction solubility parameter δ_{in} does not seem to be correctly defined, and that on the other hand five factors instead of four have to be considered. However, for the remaining factors, a very good correspondence has been established. On the basis of the overlapping observed, simple equations have been proposed in order to establish the numerical values of factors in both approaches from the retention indices compared on five polar phases.

We hope that this cooperation is only a first step. Workers in thermodynamics should now be able to further refine these data, and topologists to compare them with their own approach. It will, perhaps, be possible that working together in this way will be useful not only in olfaction, but also in other scientific fields.

ACKNOWLEDGEMENTS

The authors acknowledge Dr. W. O. McReynolds for his unpublished chromatographic data, without which this and other previous work could never have been carried out. They also thank Dr. P. Robin for his help in working out the computer program.

REFERENCES

1 L. Rohrschneider, *J. Chromatogr.*, 17 (1965) 1.
2 L. Rohrschneider, *J. Chromatogr.*, 22 (1966) 6.
3 W. O. McReynolds, *J. Chromatogr. Sci.*, 8 (1970) 685.
4 P. H. Weiner and D. G. Howery, *Can. J. Chem.*, 50 (1972) 448.
5 P. H. Weiner and D. G. Howery, *Anal. Chem.*, 44 (1972) 1189.
6 A. Dravnieks and P. Laffort, in D. Schneider (Editor), *Olfaction and Taste*, Vol. IV, Wiss. Verlagsges. mbH, Stuttgart, 1972, pp. 142–148.
7 P. Laffort, F. Patte and M. Etcheto, *Ann. N.Y. Acad. Sci.*, 237 (1974) 193.
8 F. Dupuis and A. Dijkstra, *Anal. Chem.*, 47 (1975) 379.
9 L. R. Snyder, in J. J. Kirkland (Editor), *Modern Practice of Liquid Chromatography*, Wiley, New York, 1971, pp. 125–157; Gauthier-Villars, Paris, 1973, (in French), pp. 103–128.
10 L. R. Snyder, B. L. Karger and C. H. Eon, *Anal. Chem.*, submitted for publication.
11 B. L. Karger, C. H. Eon and L. R. Snyder, *Anal. Chem.*, submitted for publication.
12 J. H. Hildebrand and R. L. Scott, *Regular Solutions*, Prentice-Hall, Englewood Cliffs, N.J., 1962.
13 J. H. Hildebrand and R. L. Scott, *The Solubility of Nonelectrolytes*, Dover Publications, New York, 3rd ed., 1964.
14 R. A. Keller, *J. Chromatogr. Sci.*, 11 (1973) 49.
15 G. Lenfant, M. Chastrette and J. E. Dubois, *J. Chromatogr. Sci.*, 9 (1971) 220.
16 W. O. McReynolds, Celanese Chemical Co., Bishop, Texas, personal communication, 1970.
17 P. Robin, CIRCE-CNRS, Orsay, France, personal communication, 1971.
18 J. R. Partington, *An Advanced Treatise on Physical Chemistry*, Vol. II, *The Properties of Liquids*, Longmans, Green and Co., London, 1951.
19 P. Laffort, in C. Pfaffman (Editor), *Olfaction and Taste*, Vol. III, Rockefeller University Press, New York, 1969, pp. 150–157.
20 P. Laffort and A. Dravnieks, *J. Theor. Biol.*, 38 (1973) 335.
21 C. Hansch, in C. J. Cavallito (Editor), *Structure–Activity Relationships*, Vol. I, Pergamon Press, Oxford, 1973, pp. 75–165.
22 M. Etcheto, *Diplôme de l'École Pratique des Hautes Études*, Paris, 1975.
23 F. Patte, *First Congress of ECRO (European Chemoreception Research Organization), Paris-Orsay July 3–5, 1974* (unpublished).

Journal of Chromatography, 126 (1976) 641–650
© Elsevier Scientific Publishing Company, Amsterdam — Printed in The Netherlands

CHROM. 9360

STRUCTURE–GAS CHROMATOGRAPHIC ELECTRON CAPTURE SENSITIVITY RELATIONSHIPS OF SOME SUBSTITUTED 17α-ACETOXYPROGESTERONES

K. T. KOSHY

The Upjohn Company, Kalamazoo, Mich. 49001 (U.S.A.)

SUMMARY

Structure–electron capture sensitivity relationships were established for underivatized 17α-acetoxyprogesterones. While progesterone was very insensitive, 17α-acetoxyprogesterone had a response of 4.8×10^2 C/mole. Methyl groups in the A or B ring of 17α-acetoxyprogesterone had no effect. A keto group at C-6 was 25 times more sensitive (1.2×10^4 C/mole). A double bond at C-6,7 enhanced the sensitivity sevenfold (3.5×10^3 C/mole), but double bonds at C-1,2 or C-9,11 had only slight effect. Substitution at C-16 was important. A methyl group at C-16 had two and three times the sensitivity in the 3-keto Δ^4 and 3-keto $\Delta^{4,6}$ series (1.1×10^3 and 1.1×10^4 C/mole), respectively. A methylene group at C-16, in contrast, showed a six- and twofold greater sensitivity over the C-16 methyl in the two series (7×10^3 and 2.2×10^4 C/mole), respectively. The most sensitive compound was 6-dehydro-6-methyl-16-methylene-17α-acetoxyprogesterone (melengestrol acetate). Its sensitivity was 2.2×10^4 C/mole, comparable to the most sensitive halo esters of steroid alcohols reported in the literature. Its electron capture coefficient was $3–7.6 \times 10^{10}$ l/mole. The coefficient was independent of the detector temperature, indicating low activation energy for electron absorption.

INTRODUCTION

It is well known that relatively few organic compounds respond to detection by an electron capture detector (ECD). Steroids generally are not considered to have any strong electron attachment properties. Lovelock *et al.*[1] determined the electron absorption coefficients of some underivatized steroid hormones using a tritium detector in conjunction with a cross-section ionization detector. Unsaturated keto steroids were shown to have some affinity for electrons and the most sensitive compound in their series was 1,4-androstadiene-3,11,17-trione. There are a large number of references on the analysis of steroids by electron capture gas chromatography (GC–ECD) after their convertion to more sensitive derivatives. Steroid alcohols are analyzed by GC–ECD after having been converted to their halo esters. Perfluorobutyrates are the most popular and sensitive among such derivatives. Recently, O-

pentafluorobenzyloximes were reported as very sensitive derivatives for several keto steroids[2].

The first report that has come to our attention on the practical utilization of GC–ECD for the analysis of underivatized steroids is on melengestrol acetate (6-dehydro-6-methyl-16-methylene-17α-acetoxyprogesterone, MGA®) in cattle feed supplements by Davis *et al.*[3]. Krzeminski and Cox[4] and Ryan and Dupont[5] have reported procedures for the residual level (2.5–10 ppb) determination of MGA in several bovine tissues. Because of the unusually high sensitivity of MGA to ECD, we have in this study determined its response quantitatively and compared it with several underivatized 17α-acetoxyprogesterones to elucidate structure–ECD response relationships of this class of steroids.

EXPERIMENTAL

Steroids

All the steroids were obtained from the Biological Screening Office of The Upjohn Company. They were first tested for purity by thin-layer and gas–liquid chromatography using a flame ionization detector (FID). Solutions for GC–ECD were prepared by dilution of a 1 mg/100 ml solution of each steroid in 10% benzene in cyclohexane. (The solvents were distilled in glass and of high purity). Dilutions were made with cyclohexane to obtain 40 and 100 pg/μl for the more sensitive compounds and 1 ng/μl for the less sensitive ones.

Glassware

All glassware was specially washed with chromic acid followed by cleaning in an ultrasonic cleaner. It was again rinsed with water and 3A alcohol, dried, and stored in a desiccator.

Gas–liquid chromatography and detection system

The gas chromatograph used was a Tracor Model MT 220 (Tracor, Austin, Texas, U.S.A.) equipped with a dual hydrogen FID and a ^{63}Ni (10 μCi) ECD. The operating parameters were: Column —1% OV-17 on Gas-Chrom Q 100–120 mesh, packed in a 3 mm I.D. glass U tube. The glass tube was silanized with dichlorodimethylsilane as described[6] prior to packing. The length of the column packing was 14 in. Temperatures —column, 235°; inlet, 250°; FID, 255°; ECD, 290°. Gas flow-rates —nitrogen for FID, 50 ml/min; nitrogen for ECD, 52.3 ml/min with no purge; hydrogen, 40 ml/min; air, 400 ml/min. Pulsed voltage parameters for ECD —applied voltage, 55 V; pulse rate, 270 μsec; pulse width, 9 μsec. Attenuation —10 $\times$ 64 (6.4×10^{-10} A.f.s.d.).

Initially, 1 mg/ml solutions of the steroids were subjected to GC using the FID (GC–FID) in order to establish chromatographic conditions. The diluted solutions (0.04–1.0 ng/μl) were then injected into the column connected to the ECD. The steroids under observation fell into two groups, *viz.* the highly sensitive ones, having a linear response for 40–500 pg injected onto the column, and the second group, having a lower sensitivity and falling in the linear range of 1–5 ng. Progesterone which was also included did not register any response for 5 ng. Of the steroids in the first group 40–500 pg were injected and the areas under the peak were measured using a

planimeter calibrated to represent 1 cm^2 for every ten counts. The areas were plotted against picomoles of the compound injected to find the linear dynamic range of response. The second group of steroids was treated in a similar manner except that the quantities injected into the GLC column were from 1 to 5 ng.

RESULTS

All the steroids gave good peaks on the OV-17 column with no indication of decomposition. Since the most important compound in the series was MGA, it was subjected to GLC–mass spectrometry (GLC–MS) (LKB 9000, LKB-Produkter AB, Stockholm, Bromma, Sweden) and found to chromatograph intact. The chromatographic conditions were the same for all and the retention times ranged from 2–6 min. Chromatograms of a few typical compounds and the amounts of each injected on the column are shown in Figs. 1 and 2. The structures of the steroids, their response

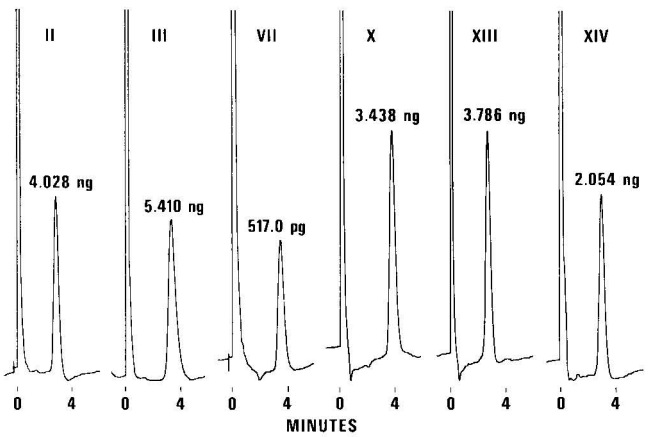


Fig. 1. Chromatograms of underivatized 17α-acetoxyprogesterones by GLC–ECD. The amounts injected onto the column are indicated for each steroid. For structural identification, see Table I.

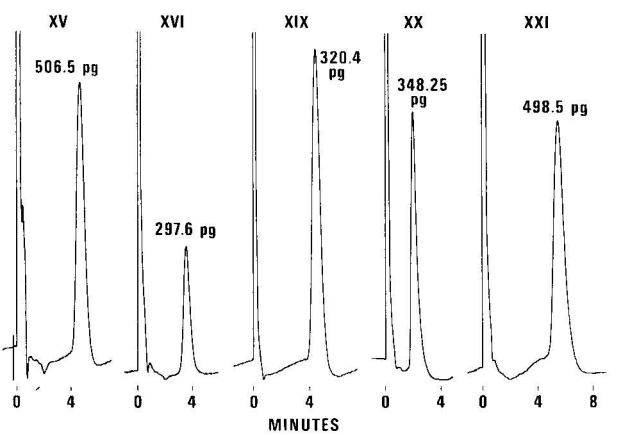
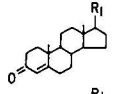
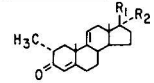
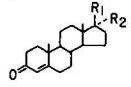
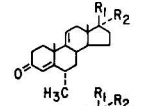
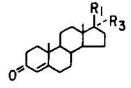
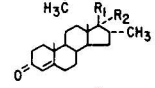
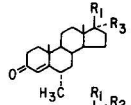
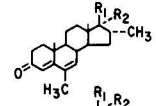
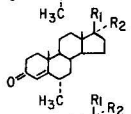
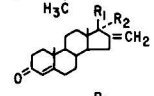
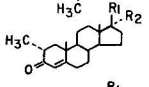
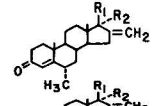
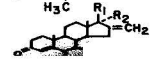


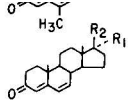
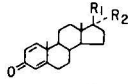
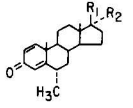
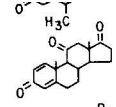
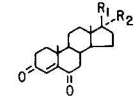
Fig. 2. Chromatograms of underivatized 17α-acetoxyprogesterones by GLC–ECD. The amounts injected onto the column are indicated for each steroid. For structural identification, see Table I.

TABLE I

STRUCTURES AND RESPONSES TO ELECTRON CAPTURE DETECTION OF SUBSTITUTED 17α-ACETOXYPROGESTERONES

$R_1 = -\overset{O}{\overset{\|}{C}}-CH_3$, $R_2 = -O-\overset{O}{\overset{\|}{C}}-CH_3$, $R_3 = -O-\overset{O}{\overset{\|}{C}}-CH_2CH_3$

Compound No.	*Structure*	*Electron capture response (C/mole)*	*Response relative to 17α-acetoxyprogesterone*	*Compound No.*	*Structure*	*Electron capture response (C/mole)*	*Response relative to 17α-acetoxyprogesterone*
I		—*	—	XII		6.7×10^2	1.4
II		4.8×10^2	1.0	XIII		6.7×10^2	1.4
III		5.47×10^2	1.14	XIV		1.1×10^3	2.3
IV		5.28×10^2	1.10	XV		1.1×10^4	22.9
V		6.4×10^2	1.3	XVI		6.5×10^3	13.5
VI		4.5×10^2	0.94	XVII		7.1×10^3	14.8
VII		3.5×10^3	7.3	XVIII		6.2×10^3	12.9

IX		2.7 × 10^3	5.6
X		9.3 × 10^2	1.9
XI		9.0 × 10^2	1.9
XX		8.1 × 10^3	16.9
XXI		1.2 × 10^4	25.0

* No response for 5 ng injected on the column.

to ECD in C/mole and the relative responses compared to 17α-acetoxyprogesterone (AP, II) are shown in Table I. The responses are the average of at least four points from the linear range of plots of concentrations *versus* response (peak areas). For MGA, the plot was linear from 40–300 pg injected onto the column and the *Y* intercept was zero. For all the other compounds, the *Y* intercept was negative. This deviation was minimal for those steroids which showed fair to good response in the picogram quantities and greater for those that had response only in the nanogram quantities.

DISCUSSION

The theories on the fundamental processes taking place in an ECD operated in the pulsed mode are well documented. Wentworth *et al.*[7,8] proposed a series of reactions taking place in the detector on the basis of kinetic derivations using steady-state approximations. They derived the following expression relating the concentration of capturing species and changes in plasma current

$$\frac{I_b - I_e}{I_e} = Ka \tag{1}$$

where

I_b = maximum initial current before addition of capturing species
I_e = current remaining after the introduction of a capturing species
K = capture coefficient
a = instantaneous concentration of capturing species

The capture coefficient K can be obtained by integration of eqn. 1 with respect to the volume of gas passing through the detector cell during the residence time of the peak and the following equation was derived[8]

$$K = \frac{I_b - I_e}{I_e} \cdot (W_{1/2}) \cdot \frac{Fr}{SMCs} \tag{2}$$

where

$W_{1/2}$ = peak width at half-height (in.)
Fr = flow-rate in the detector in l/min
S = sample size (μl)
M = molar concentration
Cs = chart speed (in./min).

Even though the capture coefficient is a useful figure to determine the temperature dependence of electron capture, activation energies, and other thermodynamic properties, the sensitivities of steroid derivatives to ECD are more commonly expressed in C/mole. In order to compare the response of MGA and the other steroids in this study with the reported values of steroid derivatives, the responses in C/mole were calculated knowing the electrometer specifications for the amount of current required for full scale deflection, the chart speed, the area of the peak, and the concentration of the sample.

Effect of 17α-esters

Progesterone showed no response when 5 ng were injected onto the column.

17α-Acetoxyprogesterone (AP, II) on the other hand, showed fair response and had a sensitivity of 4.8×10^2 C/mole (80 mm peak for 4 ng). C-17 α-propionates (III and IV) showed the same response as the acetate. Introduction of a methyl group at C-2 or C-6 of AP did not have any effect (V and VI).

Effect of additional double bonds

Lovelock *et al.*[1] in their study on the affinity of steroids for electrons with thermal energies had observed that only those steroids possessing the structure $-CO-CH=CR_1R_2$ had any marked electron absorption and that this structure conferred electron absorption provided that there was in the molecule an opportunity for further electronic interaction. In view of the above observations, one would expect a greater response for 6-dehydro AP (VII) than for AP. 6-Dehydro AP and 6-dehydro-6-methyl AP (VIII) indeed were seven times more sensitive (3.5×10^3 C/mole) than AP. 17β-Acetoxy-17-isoprogesterone (IX) had a response of 2.7×10^3 C/mole, not significantly lower than its 17 epimer (VII). A comparison of Δ^1 AP (X, 9.3×10^2 C/mole) and Δ^1-6α-methyl AP (XI, 9.0×10^2 C/mole) with the 3-keto $\Delta^{4,6}$-ones (VII–IX) having otherwise identical substituents on the D ring showed the $\Delta^{4,6}$ compounds had a more than threefold greater affinity for electrons than the $\Delta^{1,4}$ compounds. The 1,4-dien-3-ones were only about twice as sensitive as the 3-keto Δ^4 compounds (II–VI) in their affinity for electrons. This result is in agreement with the observations of Lovelock *et al.*[1]. The UV spectra of these two classes of steroids show greater conjugation in the 3-keto $\Delta^{4,6}$ systems than in the 3-keto $\Delta^{1,4}$ ones. The former have absorption maxima at $\approx$285 nm with an extinction coefficient of 27,000–29,000; the latter have absorption maxima at $\approx$245 nm and an extinction coefficient of $\approx$15,000. Therefore, the greater electron affinity by the 3-keto $\Delta^{4,6}$ steroids may be explained on the basis that the absorbed electron may be delocalized more readily in this system than in the 3-keto $\Delta^{1,4}$ system.

There were two 3-keto $\Delta^{4,9-11}$ compounds in the series, one with a methyl group at C-2 (XII) and the other with methyl at C-6 (XIII). These were included to determine the effect of an isolated double bond. The response values for these two compounds were intermediate between the AP type (II–VI) and the Δ^1 AP type of compounds (X and XI). Obviously, the electronic interaction in the 3-keto $\Delta^{4,9-11}$ compounds is more than in the 4-en-3-one systems, but less than the 1,4-dien-3-one systems.

Effect of substitution at C-16

It was pointed out earlier that a methyl group in the A or B ring did not affect the sensitivity, but when an α methyl was substituted at C-16 in AP (XIV), a twofold difference in sensitivity was observed (1.1×10^3 C/mole). In the 4,6-dien-3-one series, the effect of C-16 methyl substitution was even more pronounced. Thus, 6-dehydro-16α-methyl AP (XV) was thrice as sensitive (1.1×10^4 C/mole) as 6-dehydro AP (VII) and other similar compounds (VIII and IX). It is difficult to explain that while a methyl group at C-2 was immaterial, a methyl group at C-16 was so influential in the absorption of electrons.

The effect of C-16 methylene substitution was much greater than that of methyl substitution. The three 16-methylene AP tested (XVI–XVIII) were fourteen times as sensitive as the 16-nonsubstituted ones (II–VI) and about seven times as

sensitive as 16α-methyl AP (XIV). Among the 4,6-dien-3-one steroids, the C-16 methylene steroid (XIX, MGA) was twice as sensitive as the corresponding C-16 methyl one (XV) and about seven times more sensitive as the 16-nonsubstituted ones (VII–IX). Its response in C/mole was 2.2×10^4, a very high figure for an underivatized steroid.

Effect of additional keto groups

Lovelock *et al.*[1] had reported that the presence of even three isolated keto groups in a saturated steroid conferred little more electron absorption than the slight amount expected of a simple ketone. He had also pointed out that in a 4-en-3-one system, a keto group in the 11 position was important and the most active compound in his series was 4-androstene-3,11,17-trione (XX). Our results showed this compound to be fairly active, giving a response of 8.1×10^3 C/mole. This was only slightly better than the 16-methylene 17α-acetoxyprogesterones (XVI–XVIII). 6-Keto AP (XXI), however, was more sensitive than 4-androstene-3,11,17-trione. Its response of 1.2×10^4 C/mole can be attributed to the good electronic interaction of the C-6 keto group with the orbitals of the 4-en-3-one system.

The three steroids that had the highest responses were 6-dehydro-6β,16α-dimethyl AP (XV, 1.1×10^4 C/mole), 6-keto AP (XXI, 1.2×10^4 C/mole), and 6-dehydro-6-methyl-16-methylene AP (XIX, MGA, 2.2×10^4 C/mole). The responses for these underivatized steroids were very high: 10–20 pg were easily detectable. For comparison, the responses for these three steroids are shown in Table II alongside

TABLE II

COMPARISON OF ELECTRON CAPTURE RESPONSES OF UNDERIVATIZED MELENGESTROL ACETATE AND RELATED STEROIDS AND LITERATURE VALUES FOR STEROID HEPTAFLUOROBUTYRATES AND O-PENTAFLUOROBENZYLOXIMES

Steroid	*Electron capture response (C/mole)*			
	Underivatized steroids	*Heptafluorobutyrates*		*O-Pentafluorobenzyloxime (Ref. 2)*
		Ref. 9	*Ref. 10*	
MGA (XIX)	2.2×10^4			
6-Dehydro-6β,16α-dimethyl-17α-acetoxy-progesterone (XV)	1.1×10^4			
6-Keto-17α-acetoxy-progesterone (XXI)	1.2×10^4			
Testosterone		3-enol, mono 0.96×10^3		
Testosterone		3-enol, 17-di 4.5×10^3	3-enol, 17-di 3.9×10^4	4.7×10^4
Androstenedione		3-enol 4.0×10^3	3-enol 3.1×10^4	9.0×10^4
Progesterone		3-enol 2.9×10^3	3-enol 2.6×10^4	9.6×10^4
Androsterone		3-hydroxy, mono 1.7×10^2	–	1.5×10^4
Pregnenolone		3-hydroxy, mono 0.87×10^2	–	4.2×10^4

reported values for steroidal heptafluorobutyrates and O-pentafluorobenzyloximes. These three underivatized steroids have higher sensitivity than the values reported by Exley and Chamberlain[9] for heptafluorobutyrates and close to the values reported by Dehennin and Scholler[10]. The extremely high sensitivity of MGA to ECD was, as reported earlier, made use of in the analysis of cattle feed supplements and residual level determination in bovine tissues.

Mechanism of electron capture by MGA

It was of interest to calculate the value of the electron capture coefficient, K, for MGA and to determine the mechanism of electron capture, *i.e.* whether it was of the dissociative or nondissociative type. The values of K were calculated from eqn. 2. A plot of $(I_b - I_e)/(I_e)$ *versus* S was not linear even though other plots of response factors (peak heights, peak areas or C/mole) *versus* concentrations were linear up to 1.6 pmoles injected onto the column. Because of this deviation, the values for the electron capture coefficient were not constant; they varied from 3–7.6 $\times$ 10^{10} l/mole. In a recent paper on the theory and practice of the ECD, Lovelock[11] has stated that the well-known Wentworth equation, which served so well in the early days when less efficient ionization sources were used, does not apply when nearly all of the sample input is ionized. He has also shown that small changes in either the flow-rate of the carrier gas or the ionization current can significantly affect the proportion of molecules ionized and, hence, the detector response factor. These factors may explain the reason for the variation in the value of K.

The electron capture coefficient for MGA was independent of the detector temperature from 260–360°. The mechanism of electron capture is usually determined from a plot of ln $KT^{3/2}$ *versus* $1/T$. For MGA, such a plot had a zero slope and therefore the mechanism of electron capture did not clearly fall in the category of the nons dissociative or the dissociative type. This temperature independency also suggest-low activation energy for MGA-electron reaction in the detector cell.

CONCLUSIONS

A number of biologically active substituted 17α-acetoxyprogesterones were found to respond to a ^{63}Ni GC–ECD in their underivatized forms. The response was fair for 17α-acetoxyprogesterone (II) and excellent for 6-dehydro-6-methyl-16-methylene-17α-acetoxyprogesterone (XIX). The following structure–electron capture response relationships were established:

(1) 17α-acetate was an important functionality as progesterone showed practically no response to ECD (5 ng on-column).

(2) α- or β-methyl substituents in the A and B rings (2, 6, and 7 positions) had no effect in 4-en-3-one and 4,6-dien-3-one systems.

(3) 1,4-dien-3-one and 4,9–11-dien-3-one systems were better electron absorbers than 4-en-3-one systems, but 4,6-dien-3-one compounds were definitely more sensitive to ECD.

(4) C-16 α-methyl substitution doubled and tripled the sensitivity of the 4-en-3-one and 4,6-dien-3-one acetoxyprogesterones, respectively.

(5) C-16 methylene substitution gave the greatest increment in sensitivity of all groups tested. It increased the sensitivity of 17α-acetoxyprogesterone fourteen

times and that of Δ^6-17α-acetoxyprogesterone seven times. C-16 methylene-17α-acetoxyprogesterone was twice as sensitive as C-16 methyl-17α-acetoxyprogesterone. Similarly, C-16 methylene-Δ^6-17α-acetoxyprogesterone was twice as sensitive as C-16 methyl-Δ^6-17α-acetoxyprogesterone. The most sensitive compound in the series was 6-dehydro-6-methyl-16-methylene-17α-acetoxyprogesterone (melengestrol acetate). Its sensitivity was about the same as the steroid heptafluorobutyrates reported in the literature.

(6) A keto group at C-6 was an effective contributor to a 4-en-3-one system. Its sensitivity was 25 times greater than 17α-acetoxyprogesterone.

ACKNOWLEDGEMENTS

The author wishes to thank J. A. Campbell of The Upjohn Company for helpful suggestions in the selection of the steroids and in the preparation of the manuscript.

REFERENCES

1 J. E. Lovelock, P. G. Simmonds and W. J. A. VandenHeuvel, *Nature (London)*, 197 (1963) 249.
2 K. T. Koshy, D. G. Kaiser and A. L. VanDerSlik, *J. Chromatogr. Sci.*, 13 (1975) 97.
3 R. A. Davis, K. T. Koshy, M. L. Ogilvie, G. L. Stahl and W. A. Callahan, *J. Ass. Offic. Agr. Chem.*, 55 (1972) 103.
4 L. F. Krzeminski and B. L. Cox, *J. Ass. Offic. Agr. Chem.*, 56 (1973) 74.
5 J. J. Ryan and J. A. Dupont, *J. Agr. Food Chem.*, 23 (1975) 917.
6 *Gas-Chrom Newsletter*, Vol. 11, No. 3, Applied Science Labs., State College, Pa., May/June, 1970.
7 W. E. Wentworth, E. Chen and J. E. Lovelock, *J. Phys. Chem.*, 70 (1966) 445.
8 W. E. Wentworth, R. S. Baker and R. Tung, *J. Phys. Chem.*, 71 (1967) 1652.
9 D. Exley and J. Chamberlain, *Steroids*, 10 (1967) 509.
10 L. A. Dehennin and R. Scholler, *Steroids*, 13 (1969) 739.
11 J. E. Lovelock, *J. Chromatogr.*, 99 (1974) 3.

Journal of Chromatography, 126 (1976) 651–663
© Elsevier Scientific Publishing Company, Amsterdam — Printed in The Netherlands

CHROM. 9454

APPLICATION OF GAS–LIQUID CHROMATOGRAPHY AND HIGH-PERFORMANCE LIQUID CHROMATOGRAPHY TO THE ANALYSIS OF TRACE AMOUNTS OF SALICYLIC ACID, ACETYLSALICYLIC ANHYDRIDE AND ACETYLSALICYLSALICYLIC ACID IN ASPIRIN SAMPLES AND ASPIRIN FORMULATIONS

SYED LAIK ALI

Zentrallaboratorium Deutscher Apotheker, Ginnheimer Strasse 20, 6236 Eschborn/Ts (G.F.R.)

SUMMARY

The gas–liquid chromatographic (GLC) determination of salicylic acid (SA) in 12 commercial acetylsalicylic acid (aspirin, ASA) samples and 12 ASA formulations is reported. The GLC determination of SA as an impurity in ASA, utilising methylation with methyl iodide in the presence of potassium carbonate, requires a column chromatographic separation of SA prior to derivatization. Trace amounts of SA in ASA have also been determined by high-performance liquid chromatography (HPLC) on a Sil-X-I adsorption column using light petroleum–ethyl acetate–acetic acid as the mobile phase. Acetylsalicylic anhydride (ASN) and acetylsalicylsalicylic acid (ASSA) were determined by HPLC on a reversed-phase C_{18} column with water–methanol mixtures as the mobile phase. GLC was also applied to the determination of ASN as an impurity in ASA formulations.

INTRODUCTION

The determination of salicylic acid (SA) as an impurity in pure samples of aspirin or acetylsalicylic acid (ASA) is necessary, its presence being limited to 0.05–3% in various pharmacopeiae.

The gas–liquid chromatographic (GLC) determination of SA in ASA utilizes various reagents (HMDC, TMCS, BSTA, BSTFA) for derivitization prior to the actual measurement[1–4]. The use of methylation reagents for esterification such as diazomethane[5] and boron trifluoride[6] has also been reported. The technique used here permits a simple and elegant methylation of both acids, dissolved in a polar solvent such as acetone, with methyl iodide in the presence of potassium carbonate[7]. This method was originally used by Claisen and Eisleb[8] for the preparation of phenyl allyl ethers and has recently been applied for the derivatization of barbituric acids and fatty acids[9].

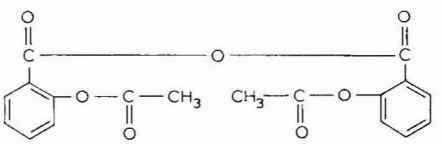
ASA and SA are easily converted quantitatively into their methyl esters in dilute solutions (0.001–0.1 *M*), which could also be confirmed by thin-layer chromatography (TLC) using the solvent system light petroleum (b.p. 40–60°)–ethyl acetate–

acetic acid (85:10:3) and silica gel GF_{254} plates. The method is suitable for the simultaneous determination of ASA and SA by GLC in dilute solutions (0.001 *M*). However, it was found that ASA samples, when analyzed for SA as an impurity, showed a higher SA content than those obtained by spectrophotometry. This result is due to the generation of SA by the slight hydrolysis of ASA during the methylation. The concentration of the ASA solution used here is about 2%, which ultimately leads to its slight hydrolysis on heating at 60–70° in the presence of potassium carbonate. One could not use dilute solutions of ASA, such as 0.001 *M*, for the determination of trace amounts of SA owing to the lack of sensitivity of the method.

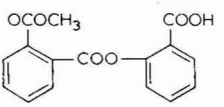
On account of this fact, a column chromatographic separation of trace amounts of SA from ASA is necessary prior to methylation and GLC determination[10]. An iron(III) chloride–urea reagent holds the SA back on a Celite 545 column, where it forms a violet-coloured complex compound with the iron(III) chloride–urea reagent. ASA is first eluted quantitatively with chloroform and later the SA is washed down quantitatively with a mixture of acetic acid and diethyl ether. The resulting solution is then methylated and subsequently gas chromatographed. In this work, this method has been applied to the GLC determination, using camphor as an internal standard, of SA as an impurity in 12 pure ASA samples and 12 ASA formulations containing phenacetin, salicylamide, *p*-acetaminophenol, ascorbic acid, glycocoll, sodium carbonate and salts of calcium and magnesium.

High-performance liquid chromatography (HPLC) is a very useful technique for the separation and detection of SA as an impurity in ASA, as the whole operation is carried out in cold solution without the application of chemical methods for previous separation or derivitization, etc. The sample is not exposed to high temperatures, which would lead to the slight hydrolysis of ASA and produce extra SA that was not previously present in the sample.

There have been reports about the simultaneous determination of aspirin, phenacetin and caffeine by HPLC[11,12]. Henry and Schmitt[13] and Schmitt[14] used an ion-exchange column and separated trace amounts of SA from ASA with an aqueous borate buffer solution of pH 9.2, the ionic strength being adjusted dy the addition of ammonium nitrate. The determination of trace amounts of SA in ASA by HPLC reported here by HPLC utilizes an Sil-X-I adsorption column and light petroleum (b.p. 40–60°)–ethyl acetate–glacial acetic acid (85:14:1) as the mobile phase. The determination was carried on with a Perkin-Elmer Model 1220 liquid chromatograph and an LC-55 UV detector at 306 nm. On a reversed-phase C_{18} column with water–methanol mixtures of different proportions as the mobile phase, SA could not be separated from the bulk of the ASA in order to allow its quantitative evaluation. The optimal conditions for the HPLC determination of SA with the adsorption column were chosen by changing the composition of the mobile phase, flow-rate, column temperature and detection wavelength.



(ASN)



(ASSA)

Acetylsalicylic anhydride (ASN) and acetylsalicylsalicylic acid (ASSA) are considered to be immunogenic impurities in ASA[15,16] and it has been suggested that the allergic reactions of ASA could be caused by ASN and ASSA impurities present in it[15,16]. These allergic reactions are attributed to the presence of antibodies of acetylsalicyloyl or salicyloyl specificity in man following ingestion of ASA. ASN and ASSA are considered to be capable of inducing the formation of acetylsalicyloyl/salicyloyl-specific antibodies in guinea-pigs and rabbits. According to De Weck[15], there is a relationship between the presence of such specific antibodies and the clinically observed allergic reactions.

A spectrophotometric determination of trace amounts of ASN in ASA[17] and a GC determination of ASSA[2] after its derivitization with N,O-bis(trimethylsilyl)-acetamide have been reported. It was reported earlier that the 12 commercial ASA samples analyzed by GLC contained 0.002–0.03% of ASN and 0.03–0.1% of ASSA[18]. In this work, ten ASA formulations were analyzed by GLC on a 3% OV-17 column.

ASN has been also determined in ASA formulations by HPLC after its separation on a reversed-phase C_{18} column with water–methanol (45:55) as the mobile phase and detection at 250 nm. In another experiment, ASN and ASSA were separated from the bulk of the ASA simultaneously by HPLC on a reversed-phase column isocratically with the mobile phase methanol (containing 1% of acetic acid)–water (48:52) and detection at 240 nm. The ASSA content of four ASA formulations was evaluated by the latter method and the results for ASN were also checked in a few instances with those obtained by the former.

EXPERIMENTAL

Chemicals

All chemicals were of pro analysi grade (Merck, Darmstadt, G.F.R.). Acetone, diethyl ether, chloroform and methanol were dried overnight over anhydrous sodium sulphate. Potassium carbonate was previously dried over phosphorus pentoxide at 170°; methyl iodide was distilled freshly. Iron(III) chloride–urea reagent was prepared freshly by adding 60 g of urea to a mixture of 8 ml of 60% iron(III) chloride solution and 42 ml of 0.05 *N* hydrochloric acid. Urea was dissolved by swirling and without the aid of heat and the pH of the resulting solution was adjusted to 3.2 by the addition of 6 *N* hydrochloric acid. Celite 545 of particle size 20–45 μm (Serva, Heidelberg, G.F.R.) was used for column chromatography.

Chromatographic column

About 3 g of Celite were intimately mixed in a mortar with 2 ml of iron(III) chloride–urea reagent and the siliceous mass was packed into a 20 × 1.5 cm I.D. chromatographic column, uniform packing being achieved with the aid of a column vibrator. A small piece of glass-wool was inserted previously at the bottom of the column. The chromatographic mass was covered with a small pad of cotton-wool so as to ensure uniform distribution of the solvent over the cross-section of the column.

Phosphate buffer solution, pH 8.0

A 68-g amount of potassium dihydrogen orthophosphate was dissolved in

240 ml of 2 *N* sodium hydroxide solution and the volume was made up with water to 1000 ml.

Phosphate buffer solution, pH 11.3

A 68-g amount of potassium dihydrogen orthophosphate was dissolved in 380 ml of 2 *N* sodium hydroxide solution and the volume was made up with water to 1000 ml.

ASN (m.p. 83°) and ASSA (m.p. 156–158°) were supplied by Bayer (Leverkusen, G.F.R.) and were found to be almost pure by TLC. ASN showed only a very faint spot of ASA. Stock solutions of SA (1 mg/ml in acetone) and ASN (1 mg/ml in benzene) were always freshly prepared. Methanolic solutions of SA, ASN and ASSA (each 1 mg/ml) were prepared for HPLC.

Procedure for GLC of SA in commercial ASA samples and ASA formulations

About 500 mg of ASA or an amount equivalent to 500 mg of ASA in ASA formulation, obtained by powdering and homogenizing 10 tablets, were extracted with cold chloroform for a few minutes, filtered (in the case of formulations) and the volume was made up with chloroform in a 50-ml calibrated flask. A 10-ml volume of this solution was pipetted into the chromatographic column, prepared as described above. The solution was allowed to pass through the column bed; an additional 75–100 ml of chloroform were passed through the column in order to remove ASA completely. This removal was checked by measuring the extinction of the last few millilitres of chloroform at 283 nm. The SA trapped on the column, which could be seen as a violet-coloured band, was then eluted with 15–20 ml of a 1:10 solution of glacial acetic acid in diethyl ether that had previously been saturated with water. The column was washed with an additional 30–50 ml of diethyl ether and the total volume of diethyl ether was extracted three or four times in a separating funnel with 50–75-ml aliquots of water so as to remove acetic acid and any urea present in the organic layer. The organic extract was then dried over anhydrous sodium sulphate, filtered and evaporated to dryness under vacuum at 30–40°. The residue was dissolved in 1 ml of acetone, 1 ml of methyl iodide and 30–50 mg of potassium carbonate were added and the solution was refluxed in a small round-bottomed flask for 20–30 min at 60–70°. The solution was decanted, washed with a small volume of acetone, camphor was added as an internal standard and the volume of the methylated solution was made up to 5 ml with acetone. Aliquots of 1 μl were withdrawn with a Hamilton micro-syringe and injected five or six times directly into the gas chromatograph. The GLC analysis was carried out on a Perkin-Elmer Model F 22 gas chromatograph equipped with a flame-ionization detector and a Hewlett-Packard Model 3380 recorder–integrator–calculator. The instrument contained a 2 m × 4 mm I.D. coiled glass column, packed with 3% OV-17 phenylmethylsilicone, which was coated on Chromosorb G, 80–100 mesh, acid washed and DMCS treated. Nitrogen was used as the carrier gas at a flow-rate of 30–40 ml/min and the column temperature was 110° (isothermal). The standard solutions of the SA were treated in exactly the same manner as the sample, in order to compensate for any losses of SA that occurred during the washing. The amounts of SA present in the pure ASA samples and ASA formulations were obtained from the calculator using the internal standard method. The results for SA in ASA formulations are presented in Table I, and a gas chromatogram is shown in Fig. 1.

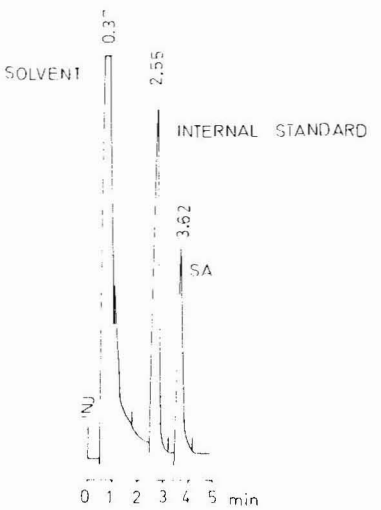


Fig. 1. Gas chromatographic determination of SA in ASA after its column chromatographic separation. Column, 2 m × 4 mm I.D. coiled glass, packed with 3% OV-17 on Chromosorb G AW DMCS, 80–100 mesh; column temperature, 110°, isothermal; injector temperature, 220°; detector temperature, 250°; carrier gas, nitrogen, 35 ml/min.

Procedure for HPLC determination of SA in pure ASA samples and formulations

Ten tablets of the ASA formulation were finely powdered and an amount equivalent to 500 mg of ASA was accurately weighed and extracted for 10 min with 2–3 ml of cold methanol in a stoppered reagent glass, filtered and the volume of the filtrate was made up to 5 ml with methanol. For pure ASA samples, 500 mg were weighed accurately and simply dissolved in 5 ml of methanol. A 5-μl volume of this solution was injected into the liquid chromatograph. After every injection of the sample, the solvent was injected two or three times in order to wash all traces of ASA from the septum and the column. The analysis was carried out on a Perkin-Elmer Model 1220 liquid chromatograph equipped with an LC-55 variable UV detector and a Perkin-Elmer FGI recorder (1–100 mV). The Sil-X-I adsorption column used had the dimensions 0.5 m × 2.6 mm I.D. and was packed with partly deactivated silica gel particles (37 μm). Other details of the chromatographic conditions are given in Fig. 3. The SA peak area was obtained from the height multiplied by the width at half-height and the SA content of the sample was calculated by the standard addition method.

Procedure for determination of ASN in ASA formulations by GLC

Ten tablets of ASA formulation were powdered and an amount equivalent to 500 mg of ASA was extracted with 40 ml of diethyl ether for 10 min. The ether extract was filtered in a 100-ml round-bottomed flask and the solvent was evaporated under vacuum at 30–40°. The residue was dissolved in 10 ml of phosphate buffer solution (pH 11.3) and the pH of the resulting solution was adjusted to 7.8–8.0. A 0.5-ml volume of benzene solution of ASN standard, containing 400 μg/ml of ASN, was added (the extraction was thereby facilitated). The test-tube was stoppered and shaken vigorously for 10 min and then set aside for few moments so as to permit the separa-

tion of the benzene layer. Each sample was extracted by the addition of further two different amounts of ASN standard solution (150 and 100 μg), but the volume of the benzene added always remained the same (0.5 ml). A 1-μl volume of the supernatant liquid was finally injected into the gas chromatograph. The column used was a 2 m $\times$ 4 mm I.D. coiled glass column, packed with 3% OV-17 on Varaport 30, acid washed and DMCS treated. The column was operated at 240° (isothermal).

In another experiment, 10 ml of the cold phosphate buffer solution (pH 8.0) were pipetted into each of three test-tubes, ASN standard benzene solution, containing 200, 150 and 100 μg, respectively, was added (the volume of benzene always being 0.5 ml). They were further treated in the same manner as described above. The amount of anhydride present in ASA formulations was evaluated by the difference of corresponding peak areas of the anhydride standard + 500 mg of sample and the standard solution alone. Reproducible results were obtained by selective extraction with the addition of 200 and 150 μg of ASN standard.

Procedure for HPLC determination of ASN in ASA formulations

An amount equivalent to 500 mg of ASA was extracted with 2–3 ml of methanol in a stoppered reagent glass, filtered and the volume made up to 5 ml with methanol. A 5-μl volume of this solution was injected into Perkin-Elmer Model 1220 liquid chromatograph. A reversed-phase C_{18} column, 0.25 m $\times$ 2.6 mm I.D., packed with silica gel SI-100 (10 μm, Merck), coated with chemically bonded C_{18} organic phase, was used for separation. Further details of the chromatographic conditions are presented in Fig. 4. The ASN content of the samples was calculated by the standard addition method. Solutions of the ASN standard were always prepared freshly in methanol.

RESULTS AND DISCUSSION

GLC of SA

Of three columns used (OV-17 on Varaport 30, SE-30 on Varaport 30 and OV-225 on Chromosorb W), the OV-17 column gave the optimal separation. The detection limit for SA lies between 10 and 20 ng. The hydroxyl functional group of the salicylic acid is weakly acidic ($K = 4 \cdot 10^{-14}$) and will not be changed under the experimental conditions to an OCH_3 group. The methylated solutions could be stored for several days provided that moisture is completely excluded.

The column chromatographic isolation of SA from bulk ASA is necessary prior to methylation. The SA thus isolated by the method of Weber and Levine[19,20] is generally determined spectrophotometrically. However, other phenolic compounds, such as salicylamide, *p*-aminophenol and acetaminophen, which also form coloured compounds with the iron(III) chloride–urea reagent, would also then contribute to the absorbance values when eluted from the column along with SA. The methylation of the SA and its subsequent GLC determination has the advantage over spectrophotometry that it is a specific method. Any other species present would not be methylated and, even if derivatized, would have different retention values.

The method applied here eliminates almost completely the possibility of hydrolysis of ASA during the methylation, and measures only the amount of SA present in the sample, not that generated during the course of the chemical operations.

Twelve pure ASA samples, obtained from different manufacturers, contained 0.02–0.05% of SA, which complies with the specifications of most of the pharmacopoeias. Twelve ASA formulations analyzed contained amounts of SA between 0.05 and 6.9% (Table I). The standard deviation of the method was found to be ±0.008 and the coefficient of variation was ±2.59%.

TABLE I

DETERMINATION OF SA CONTENT OF ASA FORMULATIONS

Product	*SA content (%)*	
	GLC	*HPLC*
A as calcium salt	0.13	0.10
B + salicylamide + phenacetin	6.90	6.15
C + salicylamide	6.24	5.87
D + magnesium oxide	3.11	3.23
E	0.06	0.07
F + vitamin C + sodium carbonate	1.67	1.38
G + *p*-acetaminophenol	0.23	0.15
H	0.15	0.13
I	0.25	0.30
K	0.05	0.05
L + glycocoll	0.04	0.05
M	0.43	0.44

HPLC of SA

There was good agreement between the results obtained by GLC and HPLC. With HPLC, it is a great advantage that the sample is simply dissolved in a cold solvent and injected directly. Under the experimental conditions used, the determination of trace amounts of SA in bulk ASA was not affected by the presence of salicylamide, phenacetin, ascorbic acid, *p*-acetaminophenol and salts of calcium and magnesium. The detection wavelength was chosen as 306 nm, where the SA has an absorption maximum. ASA, although present in bulk, would cause negligible absorption (Fig. 2). It is desirable for the minor component to be eluted before the major component in trace analysis. SA eluted from the column before ASA gave a higher accuracy and a greater ease of determination (Fig. 3a).

The important factor of the influence of the mobile phase on the selectivity of the system is evident here. As other columns packed with particles of smaller diameter or with different dimensions were not available, then instead of improving the column efficiency by increasing the number of theoretical plates, the selectivity factor has to be utilized maximally. Fig. 3a shows the separation of SA from bulk ASA after a small amount of acetic acid (1%) had been added to the mobile phase. A good separation was also obtained with formic acid as the strong solvent component of the mobile phase (Fig. 3b), but it was avoided owing to its unpleasent odour.

Without the addition of acetic or formic acid to the mobile phase (light petroleum + ethyl acetate), SA was not eluted or the separation was inadequate if methanol or propanol-2 was added to the solvent mixtures as the polar component. A strong solvent selectivity arises from the solute–solvent–adsorbent interactions, where acetic or formic acid acts as the strong solvent component. The effect of the

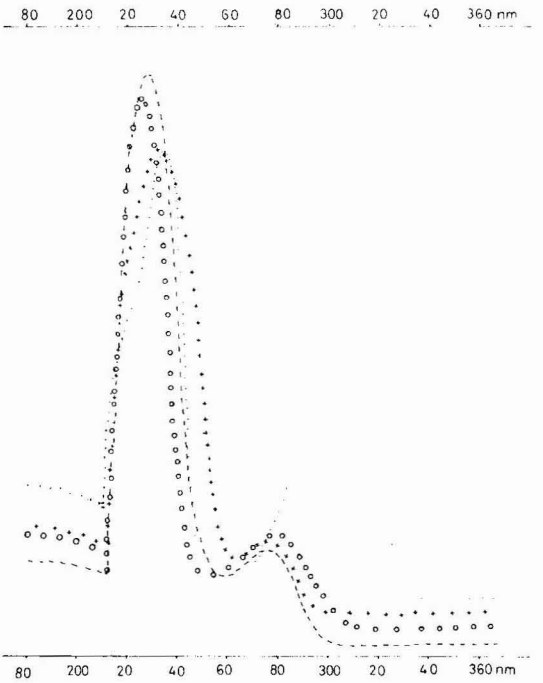


Fig. 2. UV spectra of SA (···), ASA (+++), ASN (○○○) and ASSA (---) taken with a Perkin-Elmer Model 124 recording double-beam UV–visible spectrophotometer. Ethanol was used as solvent to make 0.0004 *M* solutions of SA and ASA and 0.0002 *M* solutions of ASN and ASSA.

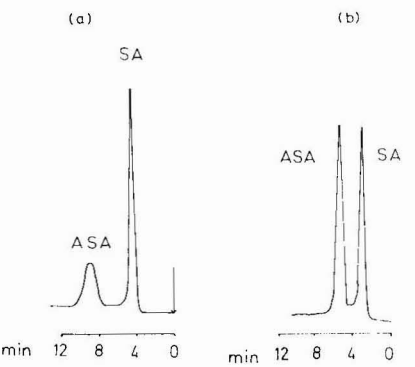


Fig. 3. HPLC separation of trace amounts of SA from bulk ASA. (a) Column, Sil-X-I, 0.5 m × 2.6 mm I.D., partially deactivated; pressure, 400 p.s.i.; flow-rate, 1 ml/min; wavelength, 306 nm; mobile phase, light petroleum (b.p. 40–60°)–ethyl acetate–glacial acetic acid (85:14:1); temperature, ambient; amount injected, 5 μl; recorder sensitivity, 5 mV; chart speed, 12 in./h. (b) Mobile phase, light petroleum (b.p. 40–60°)–ethyl acetate–formic acid (85:10:5); all other parameters as in Fig. 3a.

flow-rate on the elution and separation was also studied. With a flow-rate of 0.5 ml/min, broader peaks were obtained owing to diffusion effects and there was no significant increase in resolution. In order to achieve a rapid analysis with optimal separation, a flow-rate of 1 ml/min and ambient temperature were chosen.

Attempts to shorten the analysis time further by operating at 35 and 40° did not bring the desired results. Also, at higher temperatures hydrolysis of ASA is accelerated owing to its thermal instability. If the same sample had been allowed to stand for 12 h, an increase in SA peak height as a result of gradual hydrolysis was observed. This result was also confirmed by Henry and Schmitt[13] and Schmitt[14]. During the analysis of some of the ASA formulations, a rather rapid increase in SA peak height was noticed. This effect could be attributed to some unknown impurity (auxiliaries present in ASA formulations were not known) extracted along with SA + ASA and thus interacting with the adsorbent and leading to the adsorbent-catalyzed reaction of the sample during the separation process. This produces a minute amount of SA not previously present in the sample. Pure ASA samples analyzed for SA did not show this effect. However, in HPLC the sample is protected from air and light, and by utilizing shorter separation times the reaction time is greatly reduced[21]. It is recommended that the analysis should be performed as quickly as possible after the sample has been brought into solution.

Attempts to separate trace amounts of SA from bulk ASA and to determine it on a reversed-phase column were not successful. The separation of both components with water–methanol (55:45) as the mobile phase was inadequate.

Twelve pure ASA samples analyzed contained between 0.02 and 0.06% of SA; twelve ASA formulations analyzed contained between 0.03 and 6.9% of SA (Table I). The standard deviation was found to be ± 0.065 and the coefficient of variation was $\pm 3.62\%$. The detection limit for SA is about 100 ng, and could be further increased by injecting a larger sample and utilizing a more sensitive recorder setting.

GLC of ASN

The addition of a known amount of ASN standard to the sample solution prior to extraction allows a quantitative and selective extraction of ASN. It is necessary to extract the ASA formulations first with diethyl ether in order to remove other ingredients used as auxiliaries, which would otherwise form emulsions with benzene and might also disturb the GLC determination. On the other hand, pure ASA samples could be dissolved directly in phosphate buffer solution and extracted with benzene. Cold solutions (24°) must be used in order to avoid the hydrolysis of ASN. The flame-ionization detector has to be cleaned from time to time, as it becomes contaminated with carbon particles when using benzene as the solvent. On examining a number of organic solvents, benzene was found to be the most suitable from the viewpoint of solubility (ASN) and specific gravity. It is not miscible with aqueous solutions, and forms an upper layer, thus facilitating injections without separation from the aqueous layer.

Fig. 4 shows a gas chromatogram for an ASN determination. Ten ASA formulations were examined; in six instances ASN was not detectable and in the other four samples the ASN content was between 0.002 and 0.08%. The standard deviation was found to be ± 0.004 and the coefficient of variation was $\pm 3.20\%$.

HPLC of ASN

This method is simple and needs no previous extraction of trace amounts of ASN from the sample. The increase in the methanol content of the mobile phase causes early elution of ASN. The separation is not sufficient for the quantitative

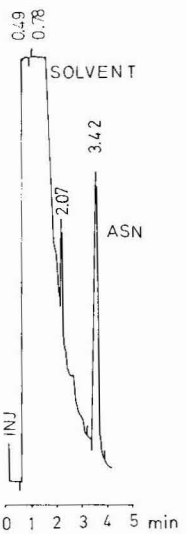


Fig. 4. Gas chromatographic determination of trace amounts of ASN in ASA. Column, 2 m × 4 mm I.D., coiled glass, packed with 3% OV-17 on Varaport 30 AW DMCS, 80–100 mesh; column temperature, 240°, isothermal; injector temperature, 280°; detector temperature, 300°; carrier gas, nitrogen, 30 ml/min.

evaluation of trace amounts of ASN. The resolution and retention are governed by the concentration of methanol in the mobile phase. It is well known from the viewpoint of column dynamics that a mobile phase of low viscosity should be chosen in order to achieve a rapid analysis at modest driving pressures. An increase in the water content of the mobile phase also enhanced its viscosity, but the desired resolution with an optimal analysis time was obtained only with a 45:55 mixture of water and methanol (Fig. 5).

Chromatographic packings with chemically bonded silicone phases provide excellent column efficiency and stability and eliminate the problems associated with the loss of partitioning phase from the support during the operation. Highly polar components such as water–methanol mixtures can be used to elute strongly retained sample components rapidly without effecting a change in the properties of the chromatographic column[22]. The use of a reversed-phase column coated with the chemically bonded C_{18} organic phase enabled the strongly retained trace amounts of ASN and ASSA to be separated from the bulk ASA.

The results of the ASN determination are presented in Table II; HPLC was not as sensitive as gas chromatography. The detection limit is about 0.01 %, and could be further increased as described for the SA determination. The standard deviation was found to be ± 0.075 and the coefficient of variation was $\pm 3.30\%$.

HPLC of ASSA

Optimal conditions were worked out for the simultaneous determination of ASSA and ASN impurities in ASA by HPLC. The separation was performed on a reversed-phase column isocratically with the mobile phase methanol (containing 1% glacial acetic acid)–water (48:52) with detection at 240 nm. Without the addition of

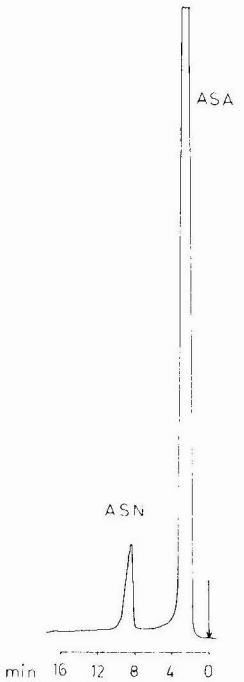


Fig. 5. HPLC separation of trace amounts of ASN from ASA on a reversed-phase column. Column, 0.25 m × 2.6 mm I.D., packed with silica gel SI-100 (10 μm, Merck), coated with chemically bonded organic phase C_{18}; mobile phase, water–methanol (45:55); pressure, 1200 p.s.i.; flow-rate, 1 ml/min; wavelength, 250 nm; temperature ambient; amount injected, 5 μl; recorder sensitivity, 5 mV; chart speed, 12 in./h.

TABLE II

DETERMINATION OF ASN IMPURITY IN ASA FORMULATIONS

Product	*ASN content (%)*	
	GLC	*HPLC*
A	Not detectable	Not detectable
D	0.081	0.06
E	Not detectable	Not detectable
F	0.003	Not detectable
G	0.01	0.01
H	Not detectable	Not detectable
I	Not detectable	Not detectable
K	0.002	0.01
L	Not detectable	Not detectable
M	0.038	0.031

acetic acid, a broad peak of poor resolution, not suitable for quantitative analysis, was obtained for ASSA and the analysis time was also prolonged. No separation of trace amounts of ASSA from ASA could be obtained on a Sil-X-I adsorption column with different solvent mixtures of diverse polarities (a, light petroleum–ethyl

acetate–glacial acetic acid, 77:20:3; b, ethyl acetate–glacial acetic acid, 97:3; c, cyclohexane–chloroform–methanol, 50:40:10).

The UV spectra of ASSA and ASN (Fig. 2) show a maximum in the region of 230 nm, but higher detection wavelengths were chosen in both instances on account of the absorption of some solvent impurities in the lower wavelength region where a zero baseline could not be obtained. The determination of trace amounts of ASN is to be preferred by the former method (Fig. 5) owing to the prolonged time of analysis (32 min) with the latter (Fig. 6).

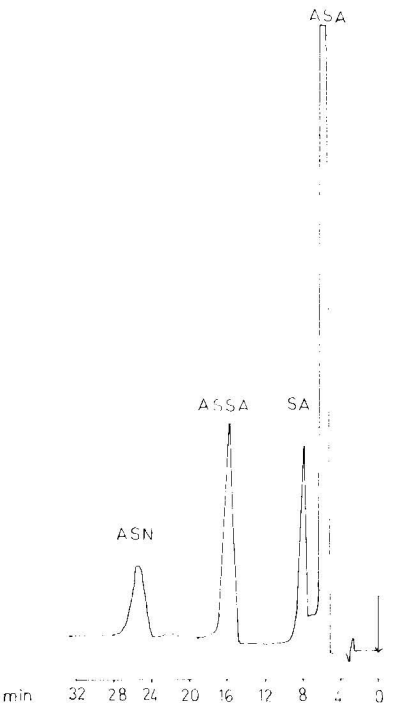


Fig. 6. Simultaneous separation of ASN and ASSA from ASA. Column, as in Fig. 5; mobile phase, water–methanol (containing 1% of acetic acid) (52:48); pressure, 1400 p.s.i.; flow-rate, 1 ml/min; wavelength, 240 nm; temperature, ambient; amount injected, 5 μl; recorder sensitivity, 5 mV; chart speed, 12 in./h.

In Fig. 6 a chromatogram is presented in which ASN, ASSA and partly SA are separated from ASA. The ASSA contents of four ASA formulations were determined quantitatively by the standard addition method. As for ASN, an amount equivalent to 500 mg of ASA was extracted with cold methanol, the volume made up to 5 ml with methanol and 5 μl of the solution were injected. Two samples showed ASSA contents of 0.028 and 0.05%, while in the other two formulations ASSA was not detectable.

ACKNOWLEDGEMENTS

The author thanks Mrs. Petra Grötsch for the experimental HPLC work and for making the drawings and Mr. Manfred Reinhard for valuable assistance with the GLC determinations.

REFERENCES

1 M. Rowland and S. Riegelman, *J. Pharm. Sci.*, 56 (1967) 717.
2 S. Patel, J. H. Perrin and J. J. Windheuser, *J. Pharm. Sci.*, 61 (1972) 1794.
3 B. H. Thomas, G. Solomonraj and B. B. Coldwell, *J. Pharm. Pharmacol.*, 25 (1973) 201.
4 M. J. Rance, B. J. Jordan and D. Nichols, *J. Pharm. Pharmacol.*, 27 (1975) 425.
5 J. R. Watson, P. Crescuolo and F. Matsui, *J. Pharm. Sci.*, 60 (1971) 454.
6 R. D. Crippen and H. D. Freimuth, *Anal. Chem.*, 36 (1964) 273.
7 S. L. Ali, *Chromatographia*, 6 (1973) 478.
8 L. Claisen and O. Eisleb, *Justus Liebigs Ann. Chem.*, 401 (1913) 29.
9 W. Dünges, *Chromatographia*, 6 (1973) 196.
10 S. L. Ali, *Chromatographia*, 7 (1974) 655.
11 D. Rosenbaum, *Anal. Chem.*, 46 (1974) 2226.
12 P. O. Ascione, *J. Pharm. Sci.*, 64 (1975) 1029.
13 R. A. Henry and J. A. Schmitt, *Chromatographia*, 3 (1870) 116.
14 J. A. Schmitt, in J. J. Kirkland (Editor), *Modern Practice of Liquid Chromatography*, Wiley-Interscience, New York, 1971, p. 388.
15 A. L. de Weck, *Int. Arch. Allergy*, 41 (1971) 393.
16 H. Bundgaard, *J. Pharm. Pharmacol.*, 26 (1974) 18.
17 H. Bundgaard and C. Bundgaard, *J. Pharm. Pharmacol.*, 25 (1973) 593.
18 S. L. Ali, *Z. Anal. Chem.*, 278 (1976) 365.
19 J. D. Weber and J. J. Levine, *J. Pharm. Sci.*, 55 (1966) 78.
20 J. D. Weber and J. J. Levine, *J. Pharm. Sci.*, 57 (1968) 631.
21 L. R. Snyder, in J. J. Kirkland (Editor), *Modern Practice of Liquid Chromatography*, Wiley-Interscience, New York, 1971, p. 226.
22 J. J. Kirkland, in J. J. Kirkland (Editor), *Modern Practice of Liquid Chromatography*, Wiley-Interscience, New York, 1971, p. 195.

Journal of Chromatography, 126 (1976) 665–677
© Elsevier Scientific Publishing Company, Amsterdam — Printed in The Netherlands

CHROM. 9424

POST-COLUMN FLUORESCENCE DERIVATIZATION OF PEPTIDES

PROBLEMS AND POTENTIAL IN HIGH-PERFORMANCE LIQUID CHROMATOGRAPHY

R. W. FREI, L. MICHEL and W. SANTI

Analytical Research and Development, Pharmaceutical Department, Sandoz Ltd., 4002 Basle (Switzerland)

SUMMARY

Some critical parameters such as the pumping system, mixing devices and detector design in instrumentation for post-column derivatization in high-performance liquid chromatography are discussed. The derivatization was studied with pharmaceutically important nona-peptides containing primary amino groups which react with Fluram® and reaction parameters such as pH, solvent and reagent concentration were investigated.

Both adsorption systems and reversed-phase systems were used to separate the peptides prior to the post-column reaction. Reversed-phase chromatography has the advantage of simpler sample preparation, better reaction control and optimization of solvent conditions. As a result, detection limits of between 5 and 10 ng per injection can be obtained and the reproducibility of the results is better than $\pm 2\%$ (relative standard deviation).

The method has been applied to the analysis of injection solutions (ampoules).

INTRODUCTION

The nona-peptides oxytocin (Ox), lysine^8-vasopressin (Lyp) and ornipressin (Orp) which were investigated in this study are important pharmaceutical substances and some of the techniques used for their physico-chemical determination have been discussed elsewhere[1]. None of these techniques is sufficiently accurate and sensitive to permit the analysis of these peptides and their by-products and degradation products in pharmaceutical formulations except for high-performance liquid chromatography (HPLC)[1,2]. Otherwise bioassay techniques are used to test the activity of these substances.

Direct separation on reversed-phase material and detection at 210–220 nm was shown to be very helpful for many problems in the analysis of pharmaceutical preparations. The limitation of this technique, however, is the critical detection conditions under low-wavelength UV radiation, which renders the quantitation of low dosage forms (<1 international unit) and particularly of the by-products difficult.

In this study, we therefore attempted to investigate the possibilities of carrying out chemical reactions after the chromatographic separation in order to render the peptides fluorescent prior to detection. The advantages and disadvantages of these post-column reaction techniques have been discussed elsewhere[3,4]. An ideal and selective reagent for this purpose has been developed by Udenfriend *et al.*[5]; the reagent Fluram® is selective for primary amino groups and has been used for amino acid analysis in conjunction with HPLC[4,6].

Preliminary results on adsorption systems have shown the potential of this reagent for post-column derivatization of the nona-peptides containing a primary amino group[3]. It was therefore decided to use Fluram as a fluorigenic reagent after reversed-phase separation according to Krummen and Frei[1] and to investigate extensively the various parameters involved in such a post-column reaction.

EXPERIMENTAL

Reagents

The structures of the peptides investigated are listed in Table I. Acetonitrile (Uvasol; Merck, Darmstadt, G.F.R.), tetrahydrofuran (THF; analytical grade, Merck) and doubly distilled water were used as chromatographic solvents.

Buffers for pH 7, 8 and 9 (Titrisol, Merck) and a 0.05 *N* solution of acetic acid were used. The reagent solution consisted of Fluram (Hoffman-La Roche, Nutley, N.J., U.S.A.) at various concentrations in acetonitrile (Uvasol quality). Other solvents used were dioxan, acetone and THF (analytical grade, Merck). The chromatographic supports were packed by slurry techniques[7,8]. Reversed-phase material RP 8 (Merck) of average particle size 10 μm was packed in a column of 25 cm length and 0.3 cm I.D.

For the adsorption system a similar column, packed with silica gel SI 60 (Merck), particle size 10 μm, was used. The exact batch conditions and chromatographic conditions are given in the legends of the appropriate figures and under Results and discussion.

Apparatus

A schematic diagram of the apparatus constructed for this work is given in Fig. 1. A Perkin-Elmer Model MPF 3 spectrofluorimeter was used for recording of spectra and some batch investigations.

RESULTS AND DISCUSSION

The general reaction of the primary amino group with Fluram has been discussed elsewhere[3,5]. An excitation maximum $\lambda_{ex} = 390$ nm and an emission maximum $\lambda_{em} = 470$ nm have been recorded. The spectra were not corrected.

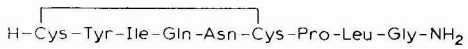
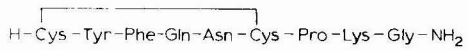
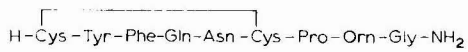
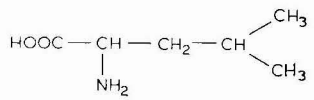
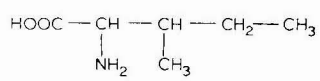
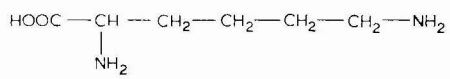
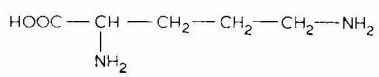
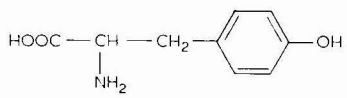
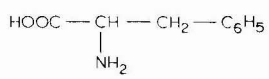
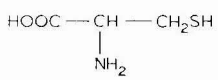
As virtually no information is available on the reaction of nona-peptides with Fluram, extensive *in vitro* studies of the reaction conditions were first undertaken, the effects of pH, solvent and Fluram concentration being investigated.

Effect of the solvent system

From data reported by other workers[9], it is known that the fluorescence of the Fluram derivatives and other derivatives[4] is strongly dependent on the type of organic

TABLE I

STRUCTURES OF THE NONA-PEPTIDES STUDIED

Nona-peptide	*Structure*
Oxytocin	
Lysine^8-vasopressin	
Ornipressin	
Leucine	
Isoleucine	
Lysine	
Ornithine	
Tyrosine	
Phenylalanine	
Cystine	

solvent used in the mobile phase of a chromatographic system or in the reagent solution. In addition to dielectric effects and heavy atom effects (with halogenated solvents), the kinetics of the derivatization reaction and the rate of hydrolysis of the Fluram also account for this dependence. Different solvents that are of interest as reagent solvents or mobile phases in adsorption or reversed-phase chromatography were tested. Fig. 2 shows the influence of organic solvents added in various amounts to an aqueous solution buffered at pH 9. In the batch experiments the volume was maintained constant in order to eliminate dilution effects. In Fig. 3 the net fluorescence (sample minus blank) has been plotted based on the results in Fig. 2.

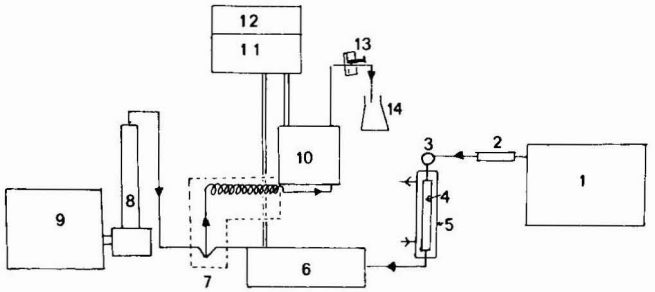


Fig. 1. Schematic diagram of the instrument used. 1 = Haskel pump (Haskel Engineering Co., Burbank, Calif., U.S.A.); 2 = pre-column, Si 60, 30 μm, 5 cm length, to remove impurities in solvent stream; 3 = injection system (loop, 20–150 μl) (Rheodyne Co., Berkeley, Calif., U.S.A.); 4 = analytical column; 5 = mantle for thermostating with water; 6 = PE LC 55 UV detector (Perkin-Elmer, Norwalk, Conn., U.S.A.); 7 = mixing device; 8 = Isco pump (Isco, Lincoln, Nebr., U.S.A.); 9 = electronic control for Isco pump; 10 = Aminco fluorescence detector (American Instrument Co., Silver Spring, Mo., U.S.A.); 11 = W + W two-pen recorder (W + W Electronic Inc., Basle, Switzerland); 12 = Hewlett-Packard HP 3352 integration system (Hewlett-Packard, Cupertino, Calif., U.S.A.); 13 = metal clamp for back-pressure; 14 = reagent reservoir (waste).

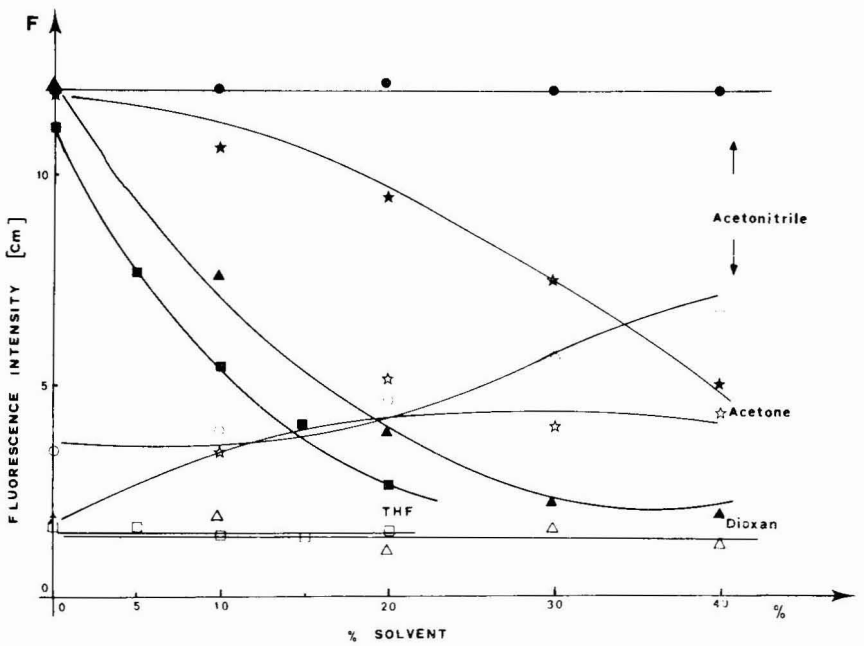


Fig. 2. Influence of different solvents on the fluorescence reaction of oxytocin at pH 9. Condition at 0%: 5 ml of buffer (pH 9) + 4 ml of water + 5 μl of oxytocin (200 I.U./ml) + 1 ml of Fluram (30 mg per 100 ml of acetonitrile). Closed symbols: assay, open symbols: blank. $\lambda_{excitation}$ = 390 nm, $\lambda_{emission}$ = 470 nm.

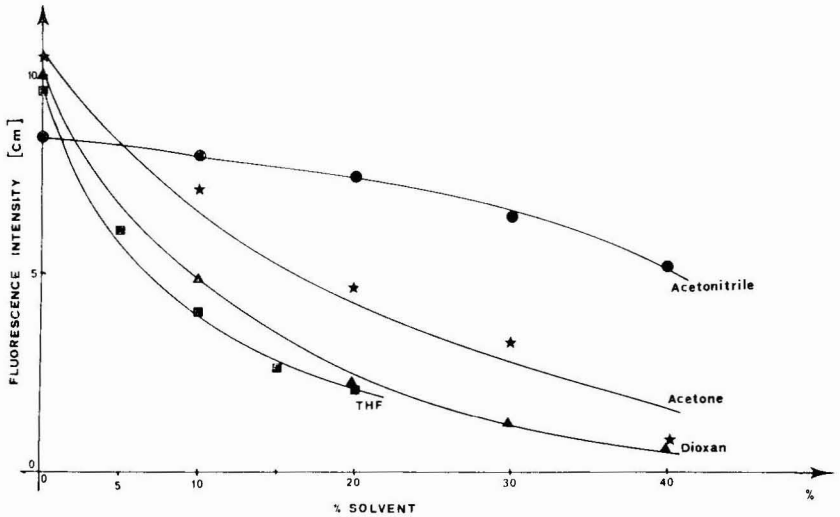


Fig. 3. Influence of different solvents on the fluorescence reaction of oxytocin at pH 9. Conditions as in Fig. 2. Net values (blank subtracted from assays).

In Figs. 2 and 3 a decrease in net fluorescence is observed with increasing proportions of organic solvent. This phenomenon is not simple to explain as it can be due to a mixed effect of solvent polarity (dielectric constant) and hydrolysis of Fluram. It is interesting that the net fluorescence decreases with a decrease in polarity in the order acetonitrile, acetone, dioxan and THF.

From Fig. 2, it is obvious that acetonitrile gives the best net fluorescence despite having also the largest increase in blank fluorescence (Fig. 2). This result is fortunate, as acetonitrile also happens to have very useful solvent properties for reversed-phase separations of these peptides and for the reagent solution[1].

Influence of pH

Studies on the effect of pH were carried out in water–acetonitrile (80:20) as this system was found to be the most promising for chromatographic purposes (see above). Such an investigation in the pH range 5–10 was carried out with Ox under the conditions that would occur in an actual analysis (for details, see legend to Fig. 4). From this study, an optimal pH range between 6 and 8 is obtained when considering the net fluorescence curve in Fig. 4. The effect of the percentage of acetonitrile added to the aqueous phase buffered to pH 7 is shown in Fig. 5. Results at pH 8 were similar or slightly inferior owing to a higher blank, resulting in higher noise (see also Fig. 4).

From these results, one can conclude that one should work at as low an acetonitrile content as possible in the mobile phase and add as little reagent solution as possible.

Effect of Fluram concentration

To study the effect of reagent concentration, solutions of various concentrations of Fluram in acetonitrile (0.1 to 30 mg per 100 ml) were added to aqueous solu-

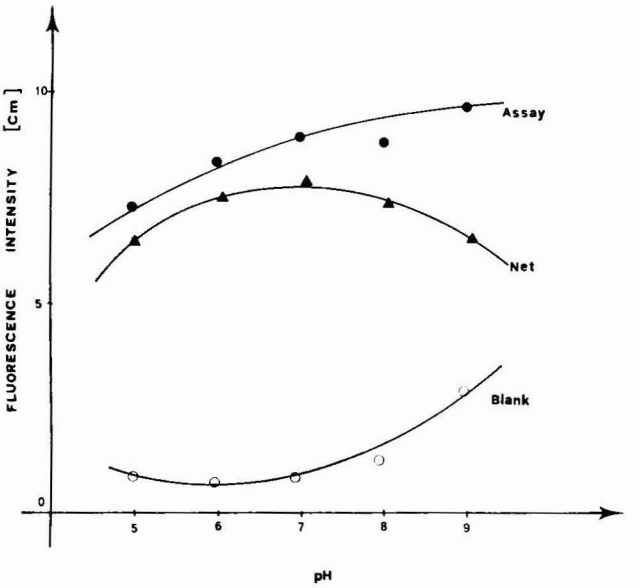


Fig. 4. Influence of pH on the fluorescence reaction with oxytocin. Conditions: phosphate buffer adjusted to appropriate pH with H_3PO_4 or NaOH; 3 ml of buffer mixture–acetonitrile (80:20, v/v) + 100 μl of oxytocin (5 I.U./ml) + 300 μl of Fluram (30 mg per 100 ml of acetonitrile).

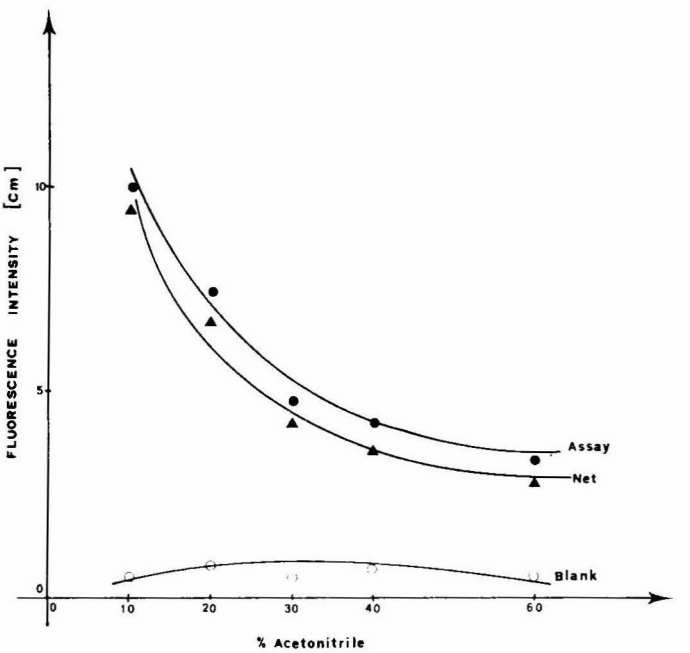


Fig. 5. Influence of acetonitrile concentration on the fluorescence reaction at pH 7 (phosphate buffer) with oxytocin. Conditions as in Fig. 4.

tions of Ox buffered to pH 7 with a phosphate buffer (Fig. 6) and to pH 8 with a borate buffer (Fig. 7). The optimal concentration seems to be reached with about 20 mg of Fluram per 100 ml of acetonitrile at both pH 7 and 8. The net fluorescence yield is inferior at pH 8 owing to the higher blank mentioned previously. The time needed for complete reaction under these conditions and at room temperature is about 50 sec.

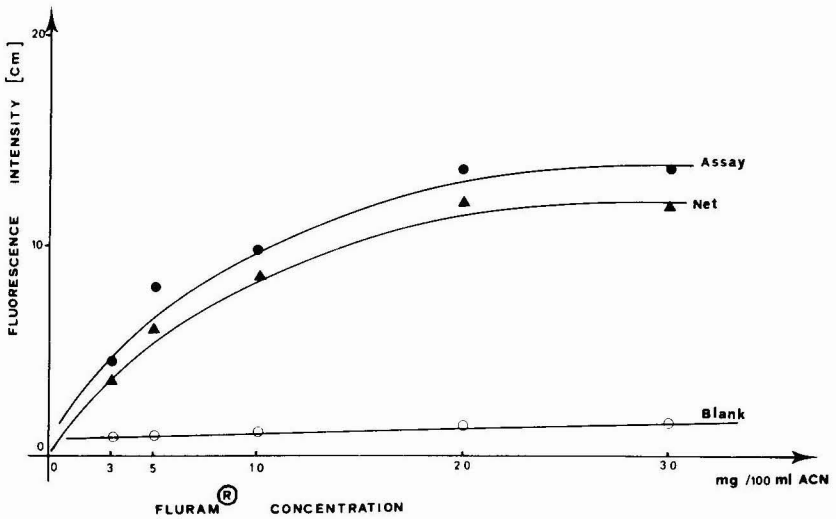


Fig. 6. Influence of Fluram concentration on the fluorescence reaction at pH 7 (phosphate buffer) with oxytocin. Conditions as in Fig. 4.

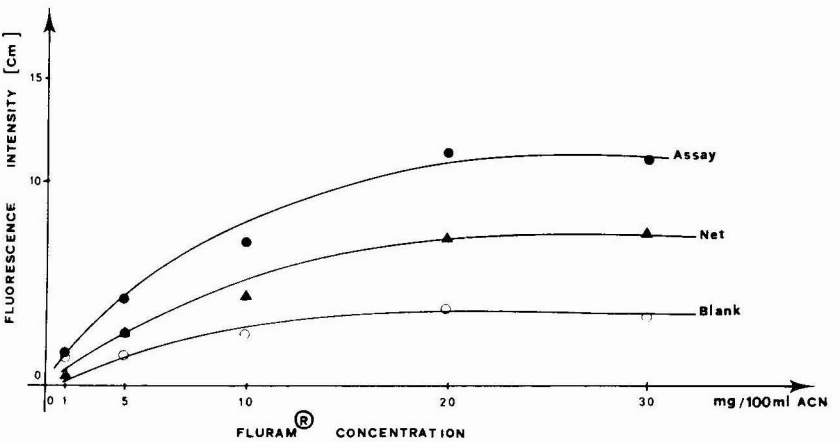


Fig. 7. Influence of Fluram concentration on the fluorescence reaction at pH 8 (borate buffer) with oxytocin. Conditions as in Fig. 4.

Instrument optimization

Mixing devices (Fig. 8). Modification c (Fig. 8) was optimal for the Fluram reaction, resulting in lowest band broadening. The instrument used is shown in Fig. 1. Such an apparatus is still relatively simple to construct from the different parts mentioned in the legend. It is approximately the same for adsorption and reversed-phase

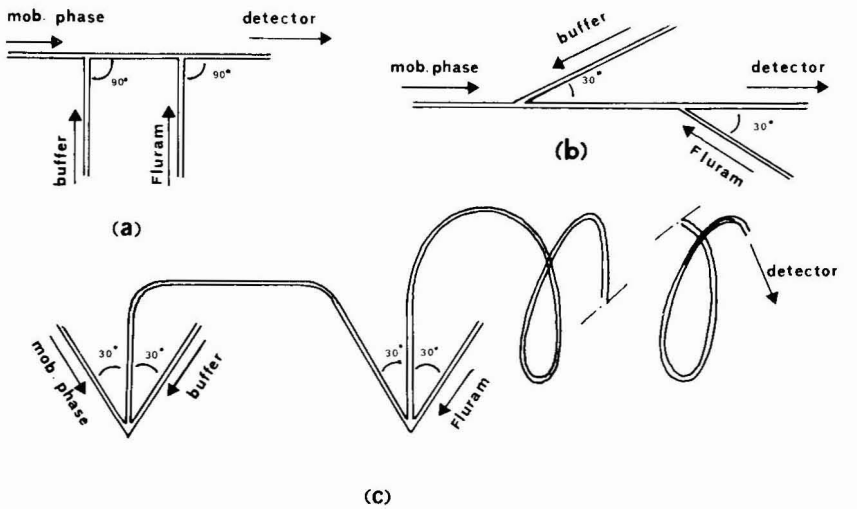


Fig. 8. Mixing devices studied for derivatization after the column. I.D. of tubes = 0.25 mm. Length of spiral (system c) ≈ 4.4 m.

systems except that only one mixing block is required on the latter, because the buffer is part of the mobile phase. Some rules have to be observed in the assembly of the instrument in order to avoid any pitfalls. Some of the more important parts are described below.

Pumping systems. As it has been observed that small variations in the organic solvent–water composition can strongly influence the fluorescence, the blank and the reaction conditions, it is not surprising that constancy of the flow-rate of the chromatographic effluent and of the reagent mixing is of prime importance. Piston pumps, even with good damping systems, are therefore not suitable for this work and pneumatic or syringe-type pumps have to be used. As can be seen in Fig. 1, a Haskel pneumatic amplifier pump and an Isco syringe-type pump were used in the optimal systems. Cheaper constant-displacement devices are currently being investigated.

Fluorescence detectors. Suitable commercial fluorescence detectors are still difficult to find. The modification of a Turner 111 fluorimeter has been described earlier[10] but its drawback is a relatively long response time. The LDC fluoro-monitor has also been used. The best results to date have been obtained with the Aminco fluoro-colorimeter and later the fluoro-monitor with cell volumes varying between 70 and 12 μl. These detectors permit the detection of, for example, quinine sulphate in the higher picogram concentration range. Fluorescence detector design is still far from optimal and as new and more efficient detectors (cell design, energy sources, focusing) become available, the detection limits might be decreased[11].

Chromatography and derivatization

Adsorption systems. The peptide derivatization after separation on an adsorption system has been mentioned briefly in an earlier paper[3]. The following conditions were used for the separation and derivatization of the peptides: mobile phase, THF–0.05 *M* acetic acid (2:1, v/v), flow-rate 0.7 ml/min; column, SI 60, 5 μm, length 25 cm, I.D. 3 mm, packed by a slurry technique[7]; buffer solution, pH 9 (Merck), flow-

rate 1.3 ml/min; Fluram solution, 30 mg per 100 ml acetonitrile, flow-rate 0.4 ml/min. Under these conditions, k' values of 0.4 for Ox, 3.8 for Orp and 4.0 for Lyp were obtained.

The flow-rates indicated are optimal with regard to fluorescence yield and reproducibility of fluorescence signals. The ratio of organic phase to water is about 0.6.

From the previous discussion, it has been shown that the proportion of organic solvent should be kept to a minimum. An increase in the flow-rate of the mobile phase containing THF therefore resulted, as expected, in a rapid decrease in the fluorescence signal.

The same phenomenon is observed with an increase in flow-rate of the reagent solution (acetonitrile). The decrease in signal intensity is of the same magnitude when increasing the flow-rate of Fluram solution from 0.4 to 0.7 ml/min or the eluent flow-rate from 0.3 to 1 ml/min. An increase in the rate of addition of buffer in order to optimize the ratio of water to organic solvent results in a decrease in the signal due to a dilution effect.

The chromatogram for Ox is shown in Fig. 9. Simultaneous detection by UV and, following derivatization, by fluorescence clearly demonstrates the advantage of post-column derivatization. Very little information can be obtained from the UV detection. The sensitivity is good enough (detection limit 40 ng at a signal-to-noise ratio of 3:1) to permit the analysis of injection solutions containing 5 international units (I.U.) of Ox (25 μl injected) and to see by-products at the 1% level (Fig. 10).

In principle, one can say that post-column Fluram derivatization of peptides is possible in an adsorption chromatographic system. There are several disadvantages, however. The need for mixing two solutions into the eluent stream makes the system more complicated and harder to control. The eluent composition containing acetic acid and particularly THF is less favourable for a good fluorescence yield, and finally sampling and removal of matrix interferences are more difficult with adsorption systems. The modification of the mobile phase to alter separation patterns and good reproducibility of retention data are more difficult to achieve.

As a result, the reproducibility of the data is inferior to 3% (relative standard deviation), for example for the analysis of samples as shown in Figs. 9 and 10, and by-products are difficult to separate and quantitate.

Reversed-phase systems. Based on the previous experience with reversed-phase separations of these peptides by Krummen and Frei[1] and based on the batch experiments discussed previously, separations were carried out with water–acetonitrile mixtures (Fig. 5) buffered to pH 7. The instrumental arrangement is depicted in Fig. 1. The formation of air bubbles in the detector can be eliminated by applying a small back-pressure (<5 atm). The optimal conditions with regard to separation and fluorescence signal were water (buffered at pH 7)–acetonitrile in the proportions 80:17.5 for Ox and 80:15 for Orp and Lyp.

From Fig. 6, it can be seen that reagent solutions of concentration $\approx$20–30 mg per 100 ml of acetonitrile are optimal. This concentration corresponds to a 300–400-fold excess of reagent and corresponds to previously reported data for amino acids[6]. In order to keep the organic solvent content low, this Fluram solution is added at relatively slow flow-rates. Fig. 11 shows the influence of flow-rate of the reagent solution on the detection signal for Lyp injection solution (10 I.U.). In going from a flow-rate of 0.16 to 1.4 ml/min, the signal is reduced 8-fold. A 3 mg per 100 ml con-

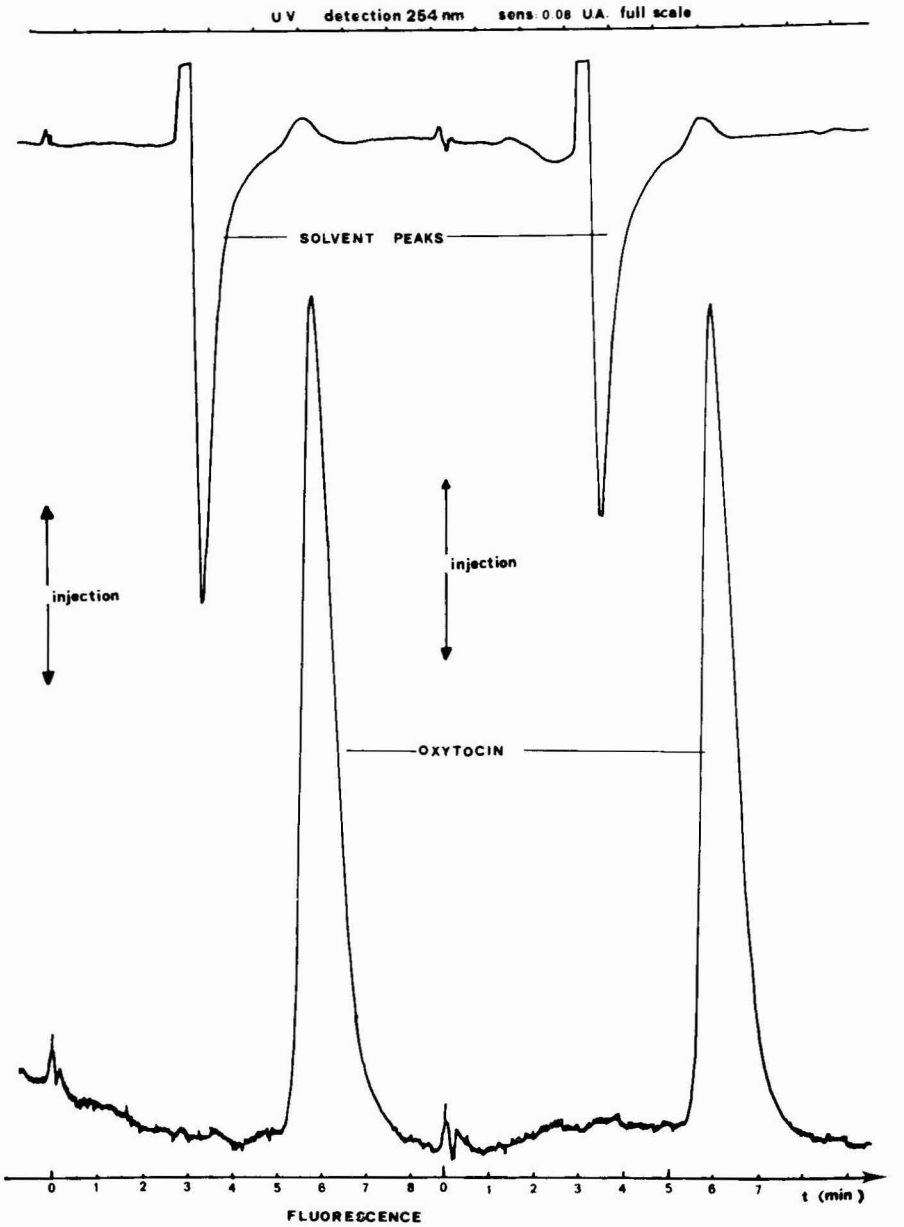


Fig. 9. Chromatogram of oxytocin (0.88 μg per injection of 2 μl). Comparison of UV (254 nm) and fluorescence after mixing with buffer and Fluram. Column, Si 60, 10 μm, I.D. 0.3 cm, length 25 cm; mobile phase, THF–0.05 *M* acetic acid (2:1, v/v), flow-rate 0.28 ml/min, Δp = 46 kg/cm^2; borate buffer (pH 9), flow-rate 0.85 ml/min; Fluram (30 mg per 100 ml of acetonitrile), flow-rate 0.43 ml/min.

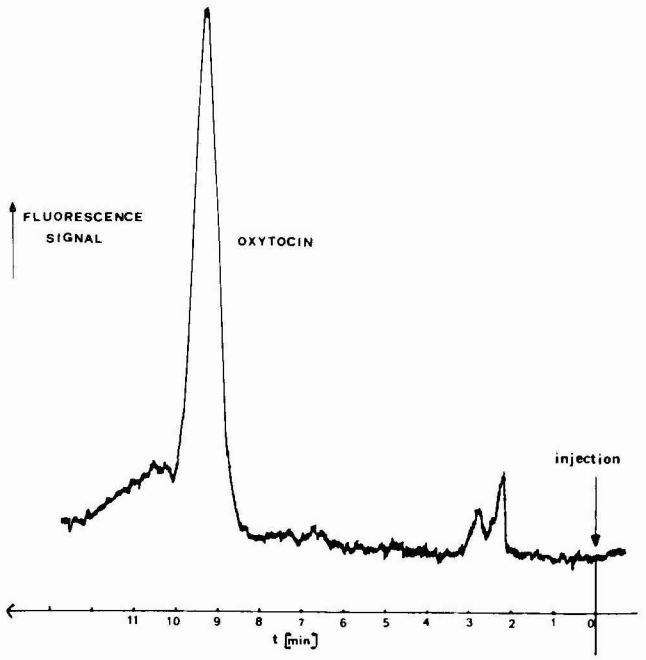


Fig. 10. Chromatogram of 25 μl of Syntocinon injection solution (5 I.U./ml). Stationary phase, Si 60 (Merck), 10 μm, length 25 cm, reaction with Fluram after the column; mobile phase, as in Fig. 9 but flow-rate 0.7 ml/min and Δp – 92 kg/cm^2; borate buffer (pH 9), flow-rate 1.3 ml/min; Fluram, (30 mg per 100 ml of acetonitrile), flow-rate 0.43 ml/min.

centration was used in this instance, but a similar decrease in signal can be observed for a 30 mg per 100 ml solution.

Fig. 11 also gives a comparison of the sensitivity of UV and fluorescence detection at comparable background noise. For optimal reaction conditions (*i.e.*, a 30 mg per 100 ml Fluram solution) this improvement in sensitivity is about 5-fold (in Fig. 11 it is 2-fold).

The detection limits for the three peptides Orp, Lyp and Ox at a signal-to-noise ratio of 3:1 and using an Aminco fluoro-colorimeter detector with a 30-μl flow cell are 5.5, 6.4 and 9.0 ng per injection, respectively. About a 3-fold improvement can be expected by using the Aminco fluoro-monitor with a 12-μl cell. The reproducibility at concentrations higher than 100 ng per injection is better than $\pm 2\%$ (relative standard deviation).

This reproducibility and sensitivity of the method permit an accurate analysis of these peptides in pharmaceutical formulations, for example injection solutions, down to 1 I.U. as well as the quantification of trace amounts of by-products containing a primary amino group.

A chromatogram for an injection solution of Ox (5 I.U. $\approx$11 μg/ml) is shown in Fig. 12. Comparison with Fig. 10 demonstrates the superior performance with the reversed-phase system.

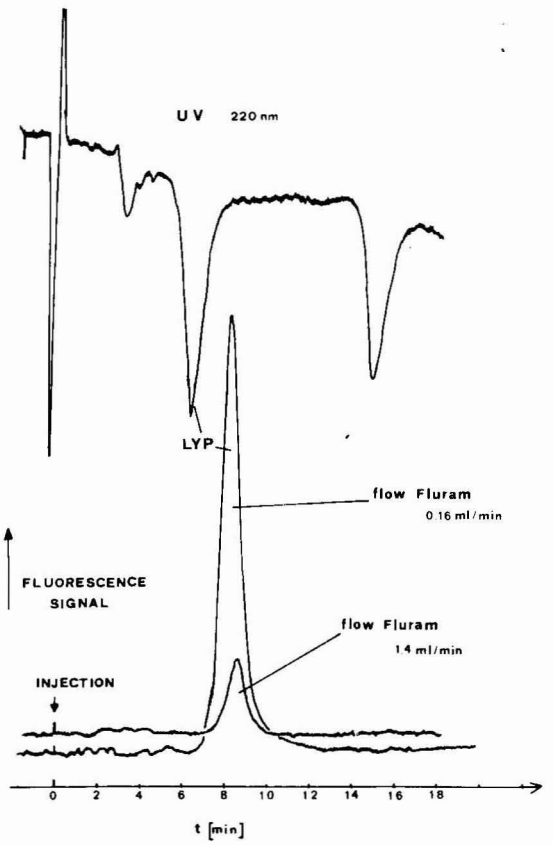


Fig. 11. Chromatogram of 25 μl lysine^8-vasopressin (10 I.U./ml). Influence of the flow-rate of Fluram on the fluorescence detection. Stationary phase, RP 8 (Merck), 10 μm, column I.D. 0.3 mm, length 25 cm; mobile phase, acetonitrile–phosphate buffer (pH 7) (15:80, v/v), flow-rate 1.58 ml/min, Δp = 130 kg/cm^2; Fluram, 3 mg per 100 ml of acetonitrile.

CONCLUSIONS

With proper instrument design and control it is possible to carry out quantitative determinations of the nona-peptides investigated and their by-products in 1 h. This was not possible previously owing to the lack of physico-chemical analytical techniques with sufficiently good selectivity and sensitivity. The bioassay techniques utilized for such systems are tedious, time consuming and costly and their replacement by physico-chemical methods could prove advantageous. The method developed by Krummen and Frei[1] gives results that are in agreement with these; the limitations of their method, however, become apparent when complicated matrices have to be handled or when trace amounts of by-products have to be quantitated.

The difficulties encountered with Fluram post-column reactions in conjunction with adsorption systems suggest that reversed-phase systems should be used whenever possible.

Further studies on the influence of dead volumes and reaction volumes, reaction temperatures, salt and buffer concentrations, and longer residence times due to

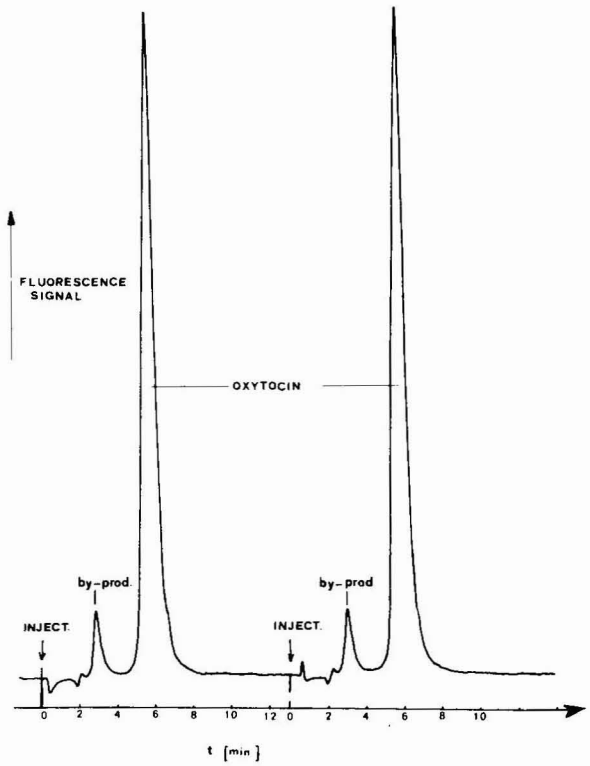


Fig. 12. Chromatogram of 100 μl of Syntocinon injection solution (5 I.U./ml). Stationary phase, RP 8 (Merck), 10 μm, column I.D. 0.3 mm, length 25 cm; mobile phase, phosphate buffer (pH 7)–acetonitrile (80:20, v/v), flow-rate 1.47 ml/min, Δp = 132 kg/cm^2; Fluram, 30 mg per 100 ml of acetonitrile, flow-rate 0.16 ml/min.

lower elution rates and pressures have to be investigated with regard to fluorescence yield and resolution.

Further instrumental improvements can be expected with pumping systems and fluorescence detectors to lower the cost and improve the sensitivity. Some of these studies are currently in progress.

REFERENCES

1 K. Krummen and R. W. Frei, *J. Chromatogr.*, submitted for publication.
2 K. Tsuji and J. H. Robertson, *J. Chromatogr.*, 112 (1975) 663.
3 R. W. Frei and W. Santi, *Z. Anal. Chem.*, 277 (1975) 303.
4 J. F. Lawrence and R. W. Frei, *Chemical Derivatization in Liquid Chromatography*, Elsevier, Amsterdam, 1976.
5 S. Udenfriend, S. Stein, S. Bohlen, P. Dairman, W. Leimgruber and M. Weigele, *Science*, 178 (1972) 871.
6 K. Zech and W. Woelter, *Chromatographia*, 8 (1975) 350.
7 R. M. Cassidy, D. le Gay and R. W. Frei, *Anal. Chem.*, 46 (1974) 340.
8 H. R. Linder, H. P. Keller and R. W. Frei, *J. Chromatogr. Sci.*, in press.
9 P. M. Fröhlich and T. D. Cunningham, *Anal. Chim. Acta*, 14 (1976) 234.
10 R. M. Cassidy and R. W. Frei, *J. Chromatogr.*, 72 (1972) 293.
11 R. J. Perchalski, B. J. Wilder and J. D. Winefordner, *Anal. Chem.*, 47 (1975) 1993.

Journal of Chromatography, 126 (1976) 679–691
© Elsevier Scientific Publishing Company, Amsterdam — Printed in The Netherlands

CHROM. 9425

EVALUATION OF MICROPARTICLE CHEMICALLY BONDED REVERSED-PHASE PACKINGS IN THE HIGH-PRESSURE LIQUID CHROMATOGRAPHIC ANALYSIS OF NUCLEOSIDES AND THEIR BASES*

RICHARD A. HARTWICK and PHYLLIS R. BROWN
Department of Chemistry, University of Rhode Island, Kingston, R.I. 02881 (U.S.A.)

SUMMARY

The reversed-phase partition mode of high-pressure liquid chromatography was used for the analysis of seven of the naturally occurring nucleosides and their bases. With microparticle chemically bonded packings, nucleosides and their bases can be quantitatively determined in the presence of nucleotides in 30 min with high sensitivity, accuracy, and reproducibility. Peaks in chromatograms of cell extracts were identified by absorbance ratios and enzymatic peak shift methods. Applications of this technique to biochemical studies are reported.

INTRODUCTION

Many procedures have been used for the analysis of nucleosides and bases by high-pressure liquid chromatography (HPLC)[1–17]. The majority of these techniques were used for the separation of hydrolysates of DNA and RNA; thus the only compounds of interest in the samples were either the nucleoside or base pairs. Other analyses were developed to separate all the UV absorbing constituents in urine[18–20]. However, the time required for these analyses prevents their use in metabolic studies involving multiple samples. Furthermore, in cell extracts large concentrations of nucleotides and other UV absorbing components may be present which interfere with the desired analyses. Therefore, these compounds either must be removed prior to the chromatographic analysis or have retention times which do not coincide with those of the nucleosides and bases. In addition, for routine work in studies of normal and abnormal metabolisms, the analytical technique must be reliable, rapid, quantitative, and sensitive and require a minimum of sample preparation.

While ion-exchange chromatography has been the method of choice for the separation of nucleic acid components, limitations have been encountered using the totally porous or pellicular anion or cation exchangers for nucleoside and base separations. The development of microparticle chemically bonded reversed-phase

* Abbreviations: Ade = adenine; Ado = adenosine, Gua = guanine; Guo = guanosine; Hyp = hypoxanthine; Ino = inosine; Thym = thymine; Ura = uracil; Urd = uridine; Xan = xanthine; Xao = xanthosine.

partition packings for HPLC has opened new possibilities for these analyses.

Since the nucleosides and bases do not possess the ionic phosphate groups which made possible the excellent HPLC separation of the nucleotides on micro-particle ion-exchange resins, the use of the partition mode for the separation of nucleosides and bases was investigated. Various applications of the partition mode of liquid–liquid chromatography have been applied to the nucleosides and bases[21–30]. However, prior to the development of chemically bonded packings, the partition mode was difficult to use because of column instability caused by bleeding of the liquid phase from the support. Thus, packings in which the liquid stationary phase is chemically bonded to an inert support have advantages over packings previously used because the stability of the packings makes it possible to obtain reproducible separations over a period of time. Furthermore, the use of microparticle packings was investigated, since it has been predicted by theory[31–35] and shown to be true in adsorption[36] and ion-exchange chromatography[37] that column efficiency increases with decreasing particle size.

Therefore, microparticle, chemically bonded reversed-phase partition packings were investigated for the development of a rapid, sensitive, and reliable analysis for the quantitative determination of the nucleosides adenosine, guanosine, xanthosine, inosine, cytidine, uridine and thymidine concomitantly with their bases in the presence of nucleotides in plasma and cell extracts.

EXPERIMENTAL

Apparatus

A Waters Assoc. Model ALC 202 liquid chromatograph (Waters Assoc., Milford, Mass., U.S.A.) with a micro UV detector with a fixed wavelength at 254 nm was used. Gradients were generated by a solvent programmer accessory.

Peak areas were electronically integrated using a Hewlett-Packard Model 3380-A integrator (Hewlett-Packard, Avondale, Pa., U.S.A.) and a Model SF-770 Spectro-flow Monitor variable-wavelength detector (Schoeffel Instrument, Westwood, N.J., U.S.A.), was used to obtain absorbance ratios for peak identification.

Columns

The columns used were 4 mm × 25 cm Partisil 10-ODS (Whatman, Clifton, N.J., U.S.A.) or 4 mm × 30 cm μBondapak C_{18} (Waters Assoc.). The columns were pre-packed with 10-μm, totally porous silica particles to which octadecyl groups were bonded through a Si–O–Si bond.

Chemicals

Aqueous buffers were prepared using reagent-grade potassium dihydrogen phosphate from Mallinckrodt (St. Louis, Mo., U.S.A.) and distilled water, which was first filtered through a membrane filter (Whatman). Unless otherwise indicated, the buffers were prepared in the concentrations of 0.010 *F*, after which the pH was adjusted to 5.5 using dilute potassium hydroxide.

Standards of the nucleosides adenosine, guanosine, inosine, xanthosine, thymidine, uridine, and cytidine, and the bases adenine, guanine, hypoxanthine, xanthine, thymine, uracil, and cytosine were obtained from Sigma (St. Louis, Mo.,

U.S.A.). Standard solutions were prepared at a concentration of 1 m*M* in a solution of 0.010 *F* KH_2PO_4. Before analysis, all cell extracts were filtered using a membrane filter, pore size GS, from Millipore (Bedford, Mass., U.S.A.).

Extraction procedure

For the cell extracts under Applications, the extraction procedure described by Khym[38] was used. The proteineous material was precipitated by the addition of two parts of cold trichloroacetic acid (TCA) (6% by weight). The solution was centrifuged and then filtered. To 1 ml of the supernatant fluid 1 ml of a solution of 0.5 *F* tri-N-octylamine in Freon was added. After vortexing and centrifuging the solution, the aqueous solution which was the top layer was withdrawn and stored at −4°.

Recovery experiments were carried out by adding known amounts of thymidine to a plasma matrix. These solutions were extracted according to the procedure outlined above, and per cent recovery was calculated to average 97%.

Peak identification

With cell extracts, initial peak identification was made on the basis of retention times. Standard solutions were run daily before and after the samples to monitor reproducibility of retention times. The standard addition method was also used to determine peak identities. A known quantity of a standard compound was added to the cell extract and a quantitative increase in the area of a specified peak was taken as further identification of the peak.

Some peaks in the chromatograms of cell extracts were identified by the enzymic peak-shift technique. Xanthine oxidase was used to characterize the peak with the retention time of xanthine and hypoxanthine in cell extracts. This enzyme catalyzes specifically the conversion of xanthine and hypoxanthine to uric acid.

$$\text{Hypoxanthine} + O_2 + H_2O \xrightarrow[\text{oxidase}]{\text{xanthine}} \text{xanthine} + H_2O_2$$

$$\text{Xanthine} + O_2 + H_2O \xrightarrow[\text{oxidase}]{\text{xanthine}} \text{uric acid} + H_2O_2$$

Thus both the xanthine and the hypoxanthine peak can be quantitatively moved in the chromatogram. A solution of standards and an erythrocyte sample were incubated with xanthine oxidase at 25° and a pH of 9.2 for 5 min. The reaction of the enzyme was stopped by the addition of TCA, which was subsequently removed by extraction with water-saturated diethyl ether.

Ratios of peak areas at various wavelengths were also employed to aid in identification. In such instances, triplicate runs were made at each wavelength used and the ratios of the unknown peaks in a cell extract were correlated to those of known compounds.

RESULTS

Optimal conditions

Optimal resolution of the seven nucleosides and their bases was achieved using

gradient elution, with 0.010 F KH_2PO_4, pH 5.5 as a low-strength eluent and a solution of methanol–water (80:20) as a high-concentration eluent. The slope of the linear gradient was from 0% of the methanol mixture to 25% over a period of 30 min and the flow-rate was 1.0 ml/min. The column temperature was ambient.

The separation of the seven nucleosides (in order of elution) cytidine, uridine, xanthosine, inosine, guanosine, thymidine, and adenosine is shown in Fig. 1A and that of the bases of these nucleosides in Fig. 1B. Under the conditions used the bases hypoxanthine, xanthine, and guanine are not completely resolved. A chromatogram of standard solutions of both the nucleosides and the bases is shown in Fig. 1C.

In most cell extracts the nucleotides will be present in substantially higher concentrations than the nucleosides and bases. Thus, either the nucleotides must be removed prior to the HPLC analysis, or it is important to be able to separate the bases

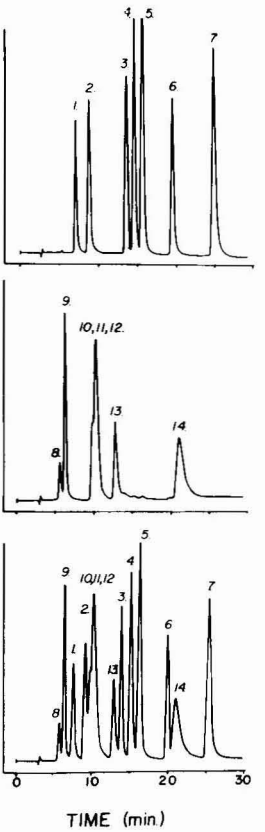


Fig. 1. (A) Separation of 5 nmoles each of the seven nucleosides cytidine (1), uridine (2), xanthosine (3), inosine (4), guanosine (5), thymidine (6), and adenosine (7). Column, μBondapak C_{18}; temperature, ambient; detector sensitivity, 0.02 a.u.f.s.; integrator setting at 254 nm, 64; eluents, (low) 0.010 F KH_2PO_4, pH 5.5, (high) methanol–water (80:20); gradient, linear, 0–25% of high-concentration eluent in 30 min; flow-rate, 1.5 ml/min. (B) Separation of 5 nmoles each of the corresponding bases under the same conditions as under (A). 8 = Cytosine; 9 = uracil; 10 = hypoxanthine; 11 = guanine; 12 = xanthine; 13 = thymine; 14 = adenine. (C) Separation of both the nucleosides and the bases.

and nucleosides in the presence of the nucleotides. Since it is preferable to have as few steps as possible in an analysis, we chose to investigate the latter possibility. The chromatogram in Fig. 2 shows the separation of 5 nmoles each of the seven nucleosides and bases in the presence of approximately 64 nmoles total of the mono-, di- and triphosphates of the seven nucleosides. The numbering of the peaks is the same as is used in Fig. 1C. As can be seen from the chromatogram, the nucleotides (peaks not numbered) were not retained on the column. For the nucleosides and bases, the capacity factors (k') were high enough for good separation from the nucleotides.

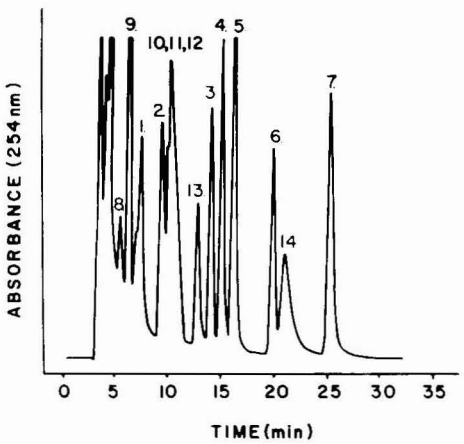


Fig. 2. Separation of 5 nmoles each of the nucleosides and bases in the presence of 64 nmoles of mono-, di-, and triphosphate nucleotides. All conditions are the same as in Fig. 1.

Reproducibility

The retention times and peak shapes were reproducible, and remained constant for sample sizes up to 100 nmoles. Variations in retention times over a month's time averaged 1.5%.

The reproducibility of peak areas is directly related to the precision of the injection and to the integration of the peak areas. Using standard solutions and syringe injection, the average variation in peak areas was 2%.

Sensitivity

Fig. 3 shows the detection of approximately 80 pmoles of each of the seven nucleosides. The lower limit of detection for the purine nucleosides, which have a higher molar absorptivity than the pyrimidines at 254 nm, was approximately 50 pmoles. The limit depends upon three parameters, *viz.* the sharpness of the peaks, the molar absorptivity of the compound of interest, and the noise of the system.

Efficiency

Because gradient elution is used for the separations, it is not possible to calculate the number of theoretical plates. However, because the time of analysis was

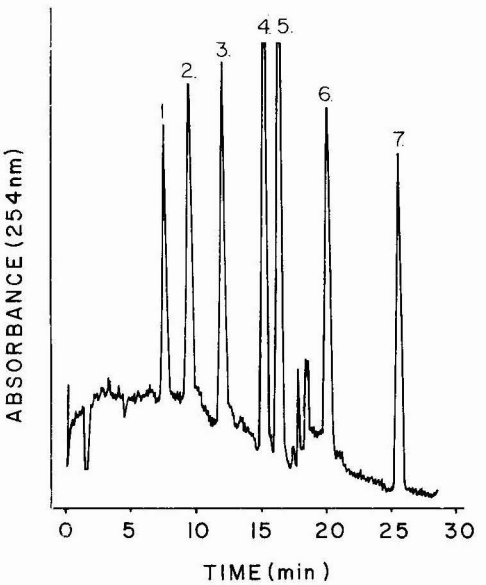


Fig. 3. Detection of approximately 80 pmoles each of the seven nucleosides. Detector sensitivity, 0.02 a.u.f.s.; integrator setting, 1. All conditions as in Fig. 1, but with the low-strength eluent at pH 5.8. Peak identification follows that in Fig. 1.

greatly shortened and the peaks decreased in width, a significant increase in efficiency was obtained over the same separation on totally porous conventional ion-exchange resins[17].

Methanol concentration

The effect of methanol concentration in the mobile phase upon the retention volumes $1/V_{R'}$ of the nucleosides and bases was investigated. Fig. 4 shows graphically the relationship between $1/V_{R'}$ and the molar concentration of methanol for the three nucleosides adenosine, guanosine, and xanthosine, and for the bases adenine and guanine. Each data point represents duplicate runs, with a precision of 2% or better. The retention volumes were obtained by multiplying the flow-rate by the retention times.

Ionic strength

In order to study the effect of ionic strength upon the separation of the nucleosides and bases, the ionic strength of the mobile phase was altered by the addition of known amounts of KCl. The pH of the mobile phase was held constant with 0.005 *F* potassium phosphate buffer. The ionic strength in a range from 0.01–0.10 Debye units had no effect upon the retention volumes of any of the nucleosides or bases. Therefore, the ionic strength of the mobile phase was not a critical factor in obtaining optimal resolution of these compounds within this range.

pH of the mobile phase

To observe the effect of pH changes, the ionic strength of the eluent was held

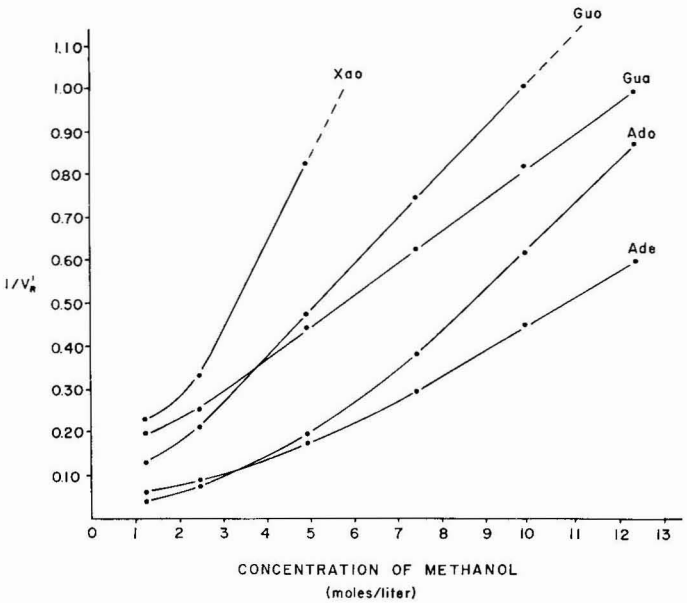


Fig. 4. Effect of increasing methanol concentration upon the retention volumes of several of the nucleosides and bases. Data were obtained under isocratic conditions. Retention volumes were calculated by multiplying the flow-rate (volumetrically measured) by the retention times.

approximately constant during isocratic elution by making all solutions 0.10 *F* in KCl and 0.005 *F* in KH_2PO_4. The pH of the system was then varied in the range of 2.8–6.8 by the addition of HCl or KOH.

The effect of pH changes on the nucleosides and bases is shown in Fig. 5. The retention volumes can be correlated with the pK_a and pK_b values of the solute molecules. There was little or no effect of pH on the bases uracil, xanthine, and hypoxanthine or on the nucleosides uridine, inosine and guanosine, whose pK_a or pK_b values are either above or below the pH range of the eluent.

Xanthosine, however, with a pK_a of 5.7, showed a marked decrease in retention volume in this pH region. At a pH of 6.8, xanthosine was eluted essentially in the void volume. However, it is interesting to note that the retention volume of xanthine did not change with pH. This is the only nucleoside–base pair studied in which the effect of pH on the retention volume of the base was significantly different from the effect of pH on the nucleoside. With adenosine and adenine, which have pK_b values of 3.50 and 4.15, respectively, the retention times were increased with increasing pH up to pH 5.8 although the slope of the rise was greater with adenosine than with adenine.

Applications

The reversed-phase partition mode was used in the HPLC analysis of nucleosides and bases in three biochemical studies. In a study of three samples of a substance which was isolated from a marine invertebrate extract, initial UV and thin-layer chromatographic data had indicated that the compound was thymine. However, it was suspected that impurities might be present.

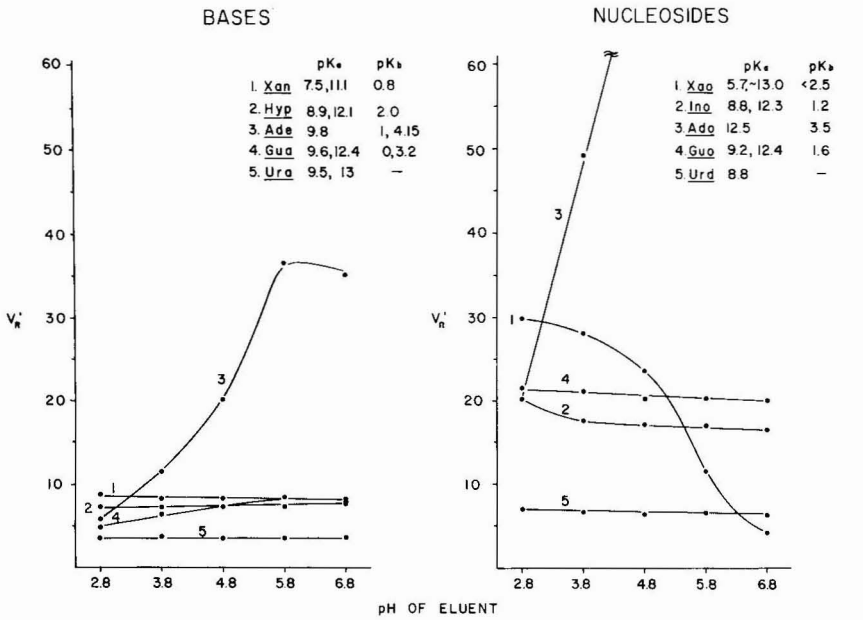


Fig. 5. Effect of pH changes on the nucleosides and bases. The data were obtained as in Fig. 4. The ionic strength of the mobile phase was held constant by making all eluents 0.10 *F* in KCl.

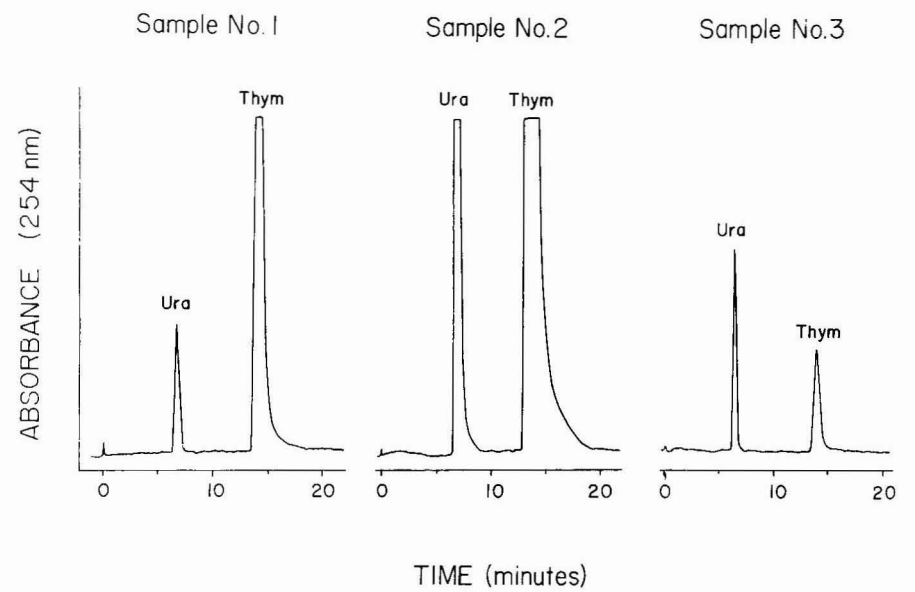


Fig. 6. Separation of components in marine invertebrate extract under the same chromatographic conditions as in Fig. 1. Instrument attenuation, 0.02 a.u.f.s.; integrator settings, 8, 16, and 32 for samples 1, 2, and 3, respectively; injection volume, 5 μl.

Using the HPLC conditions described in Methods, it was found that the samples actually contained two compounds, one with the retention time of thymine, and the other with the retention time of uracil (Fig. 6). The percentage of uracil varied from 2 to 38%.

In another study, the effect of the drug tubercidin upon the free nucleoside levels in the plasma of dogs (D-4) was observed. In the plasma of a control dog, one of the peaks present had the retention time of thymidine (Fig. 7). After treatment of the dog with tubercidin for three weeks, this peak was not present in the plasma although all the other peaks were unchanged. The total amount of thymidine contained under the peak in the control was 0.5 nmoles.

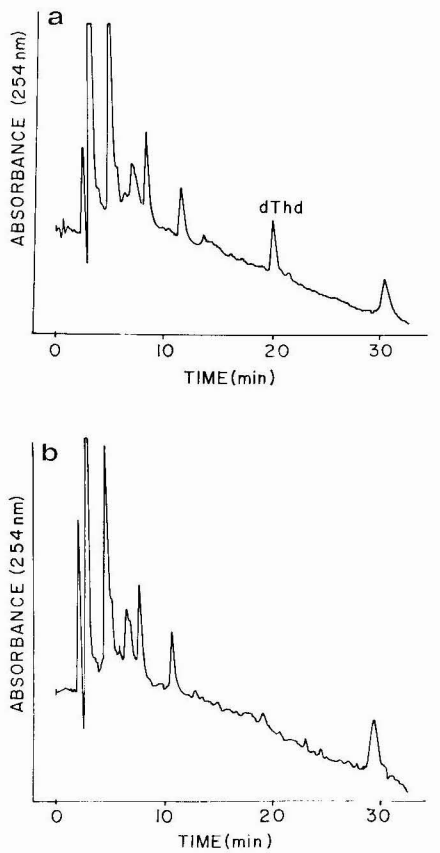


Fig. 7. Concentration of thymidine in the plasma of a control dog (D-4) (a) before and (b) after treating the dog for three weeks with the drug tubercidin. Injection volume, 25 μl; instrument attenuation, 0.02 a.u.f.s.; integrator setting, 4. All other conditions are the same as in Fig. 1.

In a third study, the levels of free nucleosides and bases from an extract of the erythrocytes of dogs (D-4) were investigated. It was found that one base or group of bases was present in significant quantities (Fig. 8a). This peak at 11 min had a retention time similar to that of guanine, hypoxanthine, or xanthine. In order to identify the

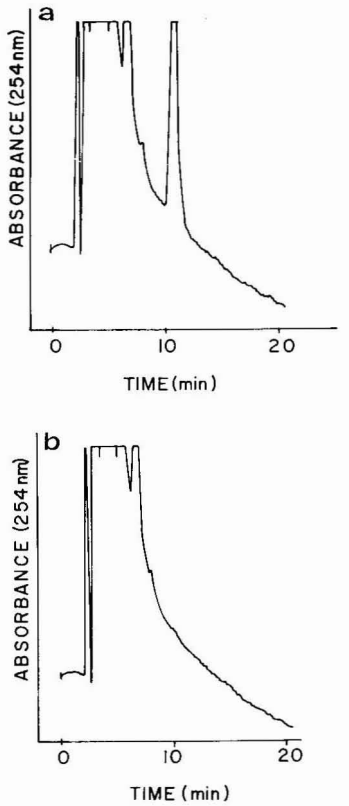


Fig. 8. (a) Detection of a peak tentatively identified as being either xanthine, hypoxanthine, or guanine. Injection volume, 25 μl; instrument attenuation, 0.02 a.u.f.s.; integrator setting, 4. All other conditions as in Fig. 1. (b) Separation of the same extract after incubation with the enzyme xanthine oxidase.

peak of interest, the enzymatic peak shift technique was used. An aliquot of the cell extract was incubated with xanthine oxidase, an enzyme which catalyzes the conversion of xanthine or hypoxanthine to uric acid. As may be seen in Fig. 8b, the peak at 11 min totally disappeared after incubation with xanthine oxidase, providing evidence that the peak was not guanine, but hypoxanthine or xanthine. To determine whether the peak was hypoxanthine or xanthine, the ratios of the peak areas at different wavelengths were determined. Using a variable-wavelength detector the area ratios (in triplicate) of standard solutions of hypoxanthine and xanthine were obtained at 260/230 nm and 250/230 nm. As shown in Table I, the ratio of the peak areas at 260/230 nm and 250/230 nm of the unknown peak was similar to that of hypoxanthine, and dissimilar to that of xanthine; thus evidence is obtained that the identity of the extract peak is that of hypoxanthine.

TABLE I

IDENTIFICATION OF THE UNKNOWN PEAK IN FIG. 8 USING AREA RATIOS OBTAINED AT 260/230 nm AND 250/230 nm

The area ratios of the unknown peaks match closely those of an authentic sample of hypoxanthine. Ratios were obtained by injecting samples in triplicate with a Schoeffel SF770 variable-wavelength detector. All other conditions as in Fig. 1.

Nucleoside	*Area ratio*	
	260 nm/230 nm	*250 nm/230 nm*
Xanthine	2.65 ± 0.04	1.98 ± 0.02
Hypoxanthine	0.67 ± 0.05	1.14 ± 0.03
Sample D-4 (1 h incubation)	0.65 ± 0.01	1.20 ± 0.07

DISCUSSION

The reversed-phase partition mode for the separation of nucleosides and bases offers several advantages over ion-exchange techniques used previously in HPLC. The majority of the naturally occurring nucleosides can be analyzed simultaneously with the bases in the presence of nucleotides in 30 min. Quantitative analyses were achieved at ambient temperatures with high sensitivity, selectivity, and efficiency. In addition, the eluents were very dilute salts and methanol which can be readily removed after fraction collections. The chromatograms were highly reproducible and column stability was good. In our laboratory columns have been used continuously for six months with no loss in efficiency.

As with all microparticle columns, proper care is essential to long life. Particulate matter must be removed from samples and solvents by membrane filtration. In addition, mechanical shock and extremes of pH and temperature must be avoided. The recommended pH range for silica-based packings is from 2 to 7.5. Due to the lyophobic nature of the stationary phase, trace organics in the solvents, as well as high-molecular-weight organics in the samples, tend to accumulate on the columns over a period of time. Unless the column is periodically flushed with a moderately polar eluent such as ethanol or acetonitrile, ghost peaks and a rising baseline during gradient elution may be encountered.

The enzymatic peak shift technique is a sensitive and accurate means of peak identification for certain nucleosides and bases. Either the disappearance of a particular peak, or the appearance of a newly formed peak, or both, may be used as a selective method of peak identification. In addition, interfering peaks may be removed by this technique.

With a variable-wavelength detector, absorbance ratios at different wavelengths can be used as a method for peak identification. A combination of absorbance ratios and enzymatic peak shift offers a selective technique for the identification of peaks in cell extracts.

Proper adjustment of pH of the samples is necessary for reproducible retention times for xanthosine. If a cell extract is very acidic, the retention times of xanthosine will vary (Fig. 5) due to small pH changes *in situ* within the column. Xanthosine is the only compound we found to be affected by small variations in pH.

Finally, reversed-phase columns from different manufacturers will produce

small differences in selectivity and retention times. For example, we found that columns from one manufacturer gave enhanced separation of xanthine–hypoxanthine–guanine, but decreased resolution of thymidine–adenine, whereas similar columns from another manufacturer gave the opposite results.

Therefore, graphs in which retention volumes are plotted against concentrations of methanol and pH are helpful for the rapid optimization of conditions for the particular column and the compounds of interest.

ACKNOWLEDGEMENTS

We thank Waters Associates, Inc. for the use of the Waters ALC 202 liquid chromatograph and for the μBondapak C_{18} columns, Whatman Inc. for the Partisil columns, the Schoeffel Instrument Co. for the Spectroflow SF-770 detector, Dr. Julian Jaffee and Dr. Henry Doremus of the Department of Pharmacology, the University of Vermont Medical School, for the samples of dog plasma and erythrocytes, Dr. George Constantine of the Oregon State University for the marine invertebrate extract, Anté Krstulóvic for his work with the enzyme peak shift and absorbance ratio methods, and Roberta Caldwell for help with the manuscript.

This work is supported by Grant No. CA-GM-17603-01 from the United States Public Health Service.

REFERENCES

1 A. Burtis, M. Munk and F. MacDonald, *Clin. Chem.*, 16 (1970) 667.
2 H. Breter and R. Zahn, *Anal. Biochem.*, 54 (1973) 346.
3 C. G. Horvath and S. R. Lipsky, *Anal. Chem.*, 39 (1967) 1922.
4 C. Horvath and S. Lipsky, *Anal. Chem.*, 41 (1969) 1227.
5 J. Mrochek, W. Butts, W. Rainey, Jr. and C. Burtis, *Clin. Chem.*, 17 (1971) 72.
6 F. Blattner and H. Erickson, *Anal Biochem.*, 18 (1967) 220.
7 J. Kirkland, *J. Chromatogr. Sci.*, 8 (1970) 72.
8 M. Uziel, C. Koh and W. Cohn, *Anal. Biochem.*, 25 (1968) 77.
9 F. Murakami, S. Rokushika and H. Hatano, *J. Chromatogr.*, 53 (1970) 584.
10 R. P. Singhal, *Biochim. Biophys. Acta*, 319 (1973) 11.
11 W. E Cohn, *Science*, 109 (1949) 377.
12 J. X. Khym, *J. Chromatogr.*, 97 (1974) 277.
13 R. Singhal and W. Cohn, *Anal. Biochem.*, 45 (1972) 585.
14 R. Singhal, *Eur. J. Biochem.*, 43 (1974) 245.
15 R. Singhal and W. Cohn, *Biochemistry*, 12 (1973) 1532.
16 R. Singhal and W. Cohn, *Biochim. Biophys. Acta*, 262 (1972) 565.
17 P. R. Brown, S. Bobick and F. L. Hanley, *J. Chromatogr.*, 99 (1974) 587.
18 C. D. Scott, R. L. Jolley and W. F. Johnson, *Amer. J. Clin. Pathol.*, 53 (1970) 701.
19 C. P. Scott, D. Chilcote, S. Katz and W. Pitt, Jr., *J. Chromatogr. Sci.*, 11 (1973) 96.
20 C. P. Scott, *Clin. Chem.*, 14 (1968) 521.
21 B. Pal, J. Regan and F. Hamilton, *Anal. Biochem.*, 67 (1975) 625.
22 J. Khym, *Anal. Biochem.*, 58 (1974) 638.
23 S. Ehrlich, J. Thiery and G. Bernardi, *Biochim. Biophys. Acta*, 246 (1971) 161.
24 E. H. Pfadenhauer *J. Chromatogr.*, 81 (1973) 85.
25 R. Holton, D. Spatz, E. VanTamelen and W. Wierenge, *Biochem. Biophys. Res. Commun.*, 58 (1974) 605.
26 G. Hoffman, *Anal. Biochem.*, 33 (1970) 209.
27 M. Carrara and G. Bernardi, *Biochim. Biophys. Acta*, 155 (1968) 1.
28 F. Kull and M. Soodack, *Anal. Biochem.*, 32 (1969) 10.

29 K.-W. Stahl, E. Schlimme and D. Bojanowski, *J. Chromatogr.*, 83 (1973) 395.
30 J. Greene, C. Nunley and N. Anderson, *Nat. Cancer Inst. Monogr.*, 21 (1966) 431.
31 R. E. Leitch and J. J. DeStefano, *J. Chromatogr. Sci.*, 11 (1973) 105.
32 J. J. van Deemter, F. J. Zuiderweg and A. Klinkenberg, *Chem. Eng. Sci.*, 5 (1956) 271.
33 J. C. Giddings, *Dynamics of Chromatography*, Marcel Dekker, New York, 1965.
34 J. F. K. Huber and J. Hulsman, *Anal. Chim. Acta*, 38 (1967) 305
35 I. Halász and M. Naefe, in A. Zlatkis (Editor), *Advances in Chromatography 1971*, Chromatography Symposium, Houston, Texas, 1971, p. 195.
36 L. R. Snyder, *J. Chromatogr. Sci.*, 7 (1969) 352.
37 R. A. Hartwick and P. R. Brown, *J. Chromatogr.*, 112 (1975) 651.
38 J. X. Khym, *Clin. Chem.*, 21 (1975) 1245.

Journal of Chromatography, 126 (1976) 693–703
© Elsevier Scientific Publishing Company, Amsterdam — Printed in The Netherlands

CHROM. 9527

HIGH-PERFORMANCE LIQUID CHROMATOGRAPHIC ANALYSIS OF THE ISOMERIZATION PRODUCTS OF CARBOHYDRATES

WOLFGANG VOELTER and HERMANN BAUER
Chemisches Institut der Universität, Auf der Morgenstelle, D-7400 Tübingen (G.F.R.)

SUMMARY

A high-performance liquid chromatographic system for the separation of complex mixtures of carbohydrates is described. The efficiency of the system is based on the application of anion-exchange resins (particle size 10–20 μm), a specially designed gradient chamber and a solution of orcinol in concentrated sulphuric acid as the detection reagent. On the basis of the chromatographic separations, a reaction mechanism for the molybdic acid-catalyzed isomerization of aldopyranoses is given.

INTRODUCTION

Column chromatographic separations of sugar isomers are among the most difficult tasks in chromatography. In connection with our work on the isomerization reactions of carbohydrates[1–7], it became necessary for our laboratory to develop an efficient and rapid separation system for this class of compounds.

More than 20 years ago, the first column chromatographic separations of carbohydrates were reported. Since then, three different principles have been applied: (1) adsorption chromatography[8–10]; (2) partition chromatography[11–13]; and (3) ion-exchange chromatography[14–17]. Ion-exchange chromatography of carbohydrates on anion-exchange resins in the borate form has been performed for years and the recent work has been surveyed in an excellent review[18].

The availability of anion-exchange resins of small particle size, the application of our specially designed gradient-generating system[17] and the use of a solution of orcinol in concentrated sulphuric acid as the detection reagent prompted us to develop an efficient and rapid separation apparatus for the separation of carbohydrates.

EXPERIMENTAL

Materials

Sugars of the highest available purity were obtained from E. Merck (Darmstadt, G.F.R.). Boric acid, sulphuric acid and orcinol were of analytical-reagent grade and were also purchased from Merck. Potassium tetraborate was obtained from Riedel-de Haen (Seelze-Hannover, G.F.R.).

For the separations, the anion-exchange resins DA-X4 and DA-X4F (Durrum, Palo Alto, Calif., U.S.A.), which are 4% cross-linked polystyrenes of particle size $20 \pm 5\ \mu m$ and $11 \pm 1\ \mu m$, respectively, were used. The pre-washing column was filled with Dowex 1-X4 resin (200–400 mesh).

Borate buffers were prepared by dissolving boric acid in doubly distilled water and adjusting the pH to the desired value with concentrated sodium hydroxide solution.

For regeneration of the resin, aqueous potassium tetraborate solution was used, 100 g of potassium tetraborate tetrahydrate being dissolved in 1 l of deionized water.

Orcinol–sulphuric acid reagent was prepared by dissolving 2.5 g of orcinol in 2.5 l of concentrated sulphuric acid.

Apparatus

Fig. 1 shows a schematic diagram of the carbohydrate analyzer constructed in our laboratory.

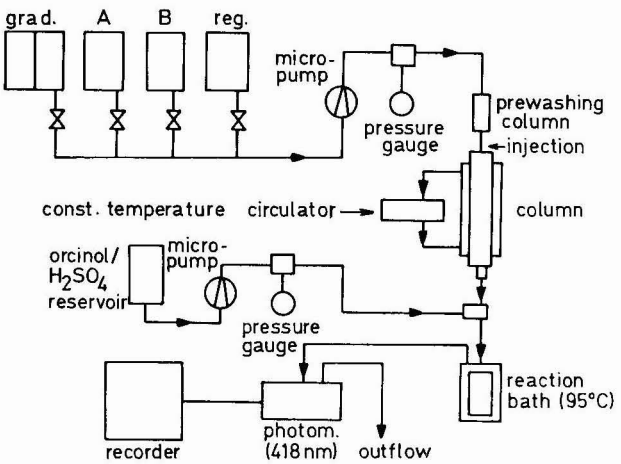


Fig. 1. Schematic diagram of the carbohydrate analyzer. grad. = Gradient-generating system; A,B = buffer reservoirs; reg. = regenerating buffer reservoir.

Borate complexes of carbohydrates specifically interact with anion-exchange resins and are therefore separable on columns filled with such material. A Milton Roy Dosapro micro-pump pumps borate buffer from a gradient-generating system (grad., Fig. 1)[7] and borate buffer reservoirs (A, B, Fig. 1) via a pre-washing column on a Biotronik (Frankfurt, G.F.R.) glass-jacketed high-performance liquid chromatographic column, filled with DA-X4 anion-exchange resin. To the effluent from the column, orcinol–sulphuric acid reagent is added and the mixture is passed through a 20 m × 0.7 mm PTFE coil that is situated in a heated (98–100°) water-bath. Under these conditions, sugars from furan derivatives react with orcinol to give a red-yellow dye which has an absorption maximum at 420 nm. A Biotronik BT 6620 spectrophotometer with an interference filter at 420 nm is used for photometric detection (path length of the optical cell, 1 cm; extinction ranges, 0.1, 0.2, 0.5, 1.0 and 2.0 absorbance units).

Preparation of the sugar mixtures

Pure carbohydrate (1 g) is dissolved in 100 ml of water or in 100 ml of methanol–water (30:70). To these solutions, 10 mg of molybdic acid are added and then the mixtures are heated for different periods of time. The reaction mixtures are cooled to room temperature, filtered and deionized with Dowex 1-X4 (OH^-).

RESULTS AND DISCUSSION

Chromatographic separations

The efficiency of our system[7] is demonstrated by the 16-component standard chromatogram in Fig. 2. The buffer gradient (Fig. 2, broken line) is produced by a specially designed two-chamber gradient genetaror. One of these chambers is filled with the diluted borate buffer A (0.1 mole/l) of pH 8.0 and the other with the concentrated borate buffer B (0.5 mole/l), adjusted to pH 10. Fig. 2 shows that a mixture of 16 mono- and disaccharides are well separated in about 5 h.

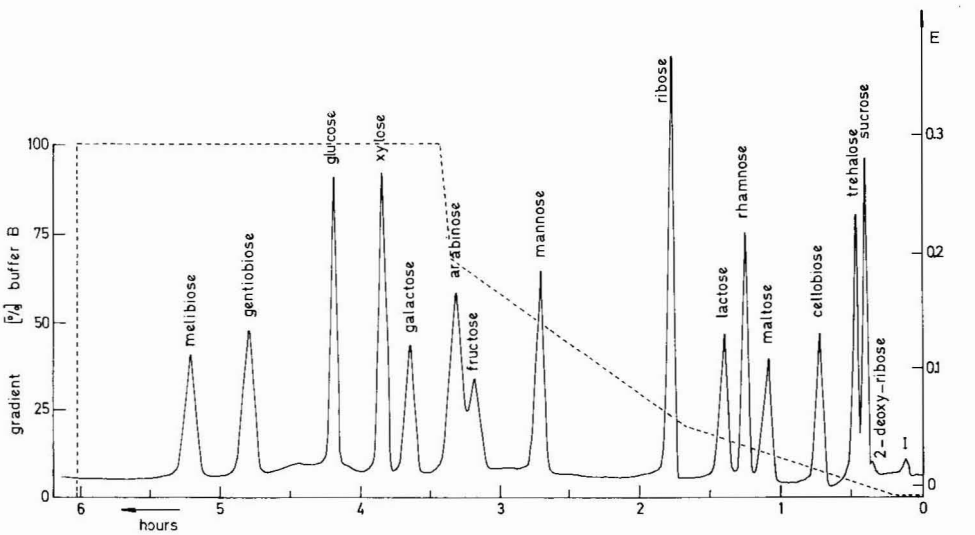


Fig. 2. Chromatogram of a 16-component standard. Gradient, 0.1–0.5 mmole/l H_3BO_3, pH 8.0–10.0; 280 × 6 mm column; DA-X4 resin; flow-rate, 1 ml/min; temperature, 50°; recorder range, 0–0.5 A. Each peak represents 80 nmole of monosaccharide or 40 nmole of disaccharide. I = Injection peak.

Separations with one-buffer elutions are more convenient. Using resins of small particle size, many of the liquid chromatographic problems in carbohydrate chemistry can be solved in a minimum of time, as demonstrated by Fig. 3. A mixture of six common monosaccharides is separated in less than 1 h by applying a 0.4 *M* H_3BO_3 buffer of pH 9.2 and a DA-X4F resin of particle size 11 $\pm$ 1 μm.

Relationship between peak area and sugar concentration

For several sugar analysis systems, the orcinol reagent is prepared from 70% sulphuric acid[15,19] [*e.g.*, 1 g of orcinol is dissolved in 1 l of 70% (v/v) sulphuric acid]. This orcinol reagent becomes brownish after storage for longer than 3 weeks in the

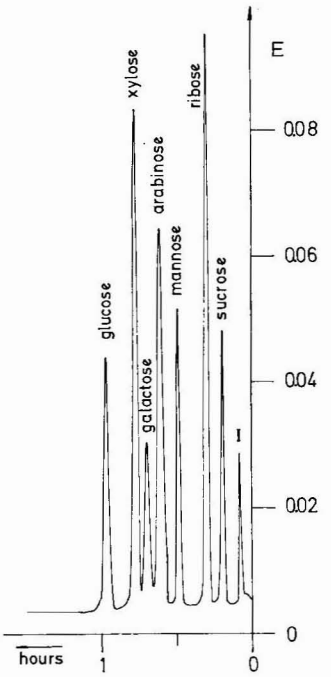


Fig. 3. Chromatogram of a seven-component standard. One-buffer elution with H_3BO_3 buffer (0.4 mole/l, pH 9.2); 190 × 6 mm column; DA-X4 resin; flow-rate, 1.3 ml/min; temperature, 60°; recorder range, 0–0.1 A. Each peak represents 1 μg per component. I = Injection peak.

cold, and higher blank values and lower colour yields are obtained with such a colorimetric reagent[19]. However, we found that the stability of the orcinol–sulphuric acid reagent can be improved considerably by dissolving 1 g of orcinol in 1 l of concentrated (95–97%) sulphuric acid. This 0.1% orcinol reagent is stable for several months without forming brownish by-products.

The coupled furan- and dye-forming reaction of carbohydrates in the presence of the ocrinol–sulphuric acid reagent is very dependent on the acid concentration, as demonstrated in Fig. 4. The highest colour yield is acieved with 50% sulphuric acid.

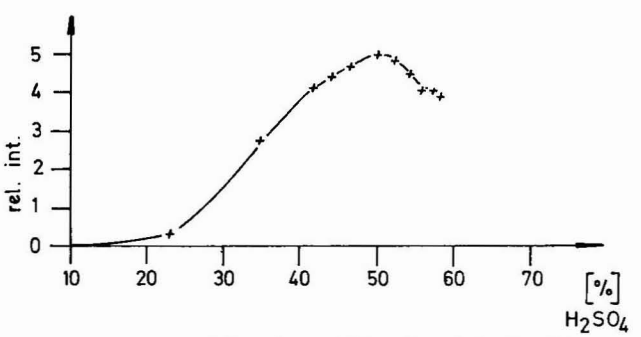


Fig. 4. Dependence of the colour yield on the sulphuric acid concentration for the reaction of sucrose with orcinol (0.1%)–sulphuric acid reagents of different sulphuric acid concentrations. The solutions were 0.01 *M* in sucrose and were measured after heating for 15 min in boiling water at a wavelength of 423 nm. The relative intensity refers to scale units for an optical path length of 1 cm.

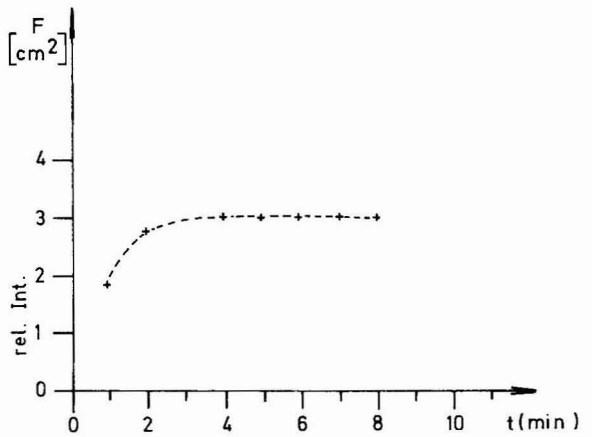


Fig. 5. Dye development for the reaction of sucrose with orcinol–sulphuric acid reagent in the sugar analyzer as a function of reaction time. Reaction-bath temperature, 100° (boiling water); borate buffer flow-rate, 60 ml/h; orcinol (0.1 %)–sulphuric acid (95–97 %) flow-rate, 66 ml/h; variation of the length of the mixing coil, 5.5–44 m; internal diameter of the mixing coil, 0.7 mm; t = flow-time of the sugar reagent mixture through the coil; rel. int. = relative intensity of the calculated peak areas, relative to $A = 0.0$–1.0.

The development of dye originating from sucrose as a function of time is shown in Fig. 5. The results were obtained with the sugar analyzer described above using reaction coils of different lengths. Fig. 5 shows that after a reaction time of 3–4 min the colour yields become constant.

The relationships between the peak areas and the concentrations of gentiobiose, lactose, mannose and glucose are given in Fig. 6. The results were ob-

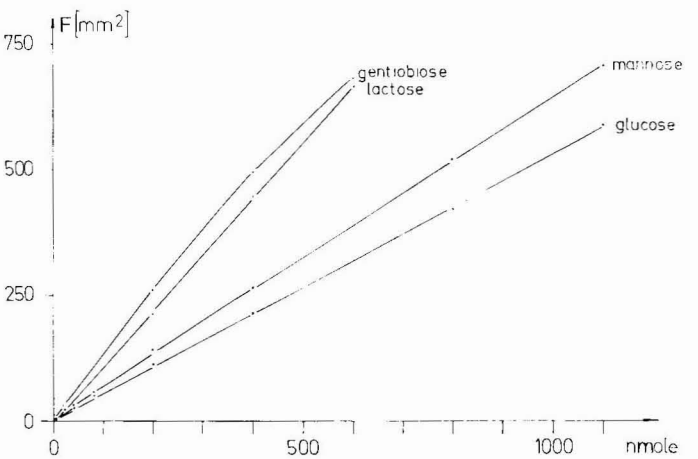


Fig. 6. Linearity of peak areas as a function of sugar concentration established with the sugar analyzer shown in Fig. 1. F = area (mm²) relative to $E = 1$; gradient, 0.1–0.5 mole/l H_3BO_4, pH 8.0–10.0; 280 × 6 mm column; DA-X4 resin; flow-rate, 1 ml/min; reagent flow-rate, 1.1 ml/min; temperature of separation column, 50°; temperature of heating bath, 100° (boiling water).

tained with the sugar analyzer, using a reaction coil of length 19 m and I.D. 0.7 mm. The limits of detection are in the range 0.1–2.0 nmole.

Under the experimental conditions, the relative elution times and the colour yields for a larger series of carbohydrates were established (Table I).

TABLE I

RELATIVE ELUTION TIMES AND MOLAR EXTINCTION COEFFICIENTS FOR SOME ORCINOL–SULPHURIC ACID DYES RESULTING FROM REACTIONS WITH SUGARS

Molar extinction coefficient $C_{HW} = HW/M$ (H = height of the peak in extinction units; W = half-width of the peak; M = amount of sugar in μmoles). Gradient, 0.1–0.5 mole H_3BO_3, pH 8.0–10.0; 280 × 6 mm column; DA-X4 resin; temperature of separation column, 60°.

Compound	*Relative elution time (glucose = 100)*	*Molar extinction coefficient*
Methyl β-arabinopyranoside	6.4	—
Methyl β-xylopyranoside	8.0	—
2-Deoxyribose	8.4	47.8
Sucrose	9.6	1056
Trehalose	11.2	912
Methyl α-mannopyranoside	12.0	—
Cellobiose	13.2	924
Methyl β-glucopyranoside	22.8	—
Maltose	26.4	864
Rhamnose	30.0	636
Lactose	33.6	1088
Erythrose	39.9	—
Ribose	42.8	963
Lyxose	42.0	—
Mannose	65.2	652
Tagatose	74.0	—
Fructose	76.4	506
Gulose	76.4	—
Lactulose	77.6	—
Allose	77.6	—
Arabinose	78.8	900
Fucose	78.8	
Epimelibiose	82.8	
Talose	85.3	—
Galactose	87.6	462
Altrose	89.0	—
Sorbose	89.2	—
Xylose	92.4	786
Glucose	100.0	684
Gentiobiose	114.4	1342
Melibiose	125.2	1336

Molybdic acid-catalyzed isomerization of aldopyranoses

Aldohexoses and aldopentoses from complexes with molybdate, as can be proved unequivocally by circular dichroism studies[20,21]. These sugars isomerize in the presence of catalytic amounts of molybdic acid upon heating in aqueous solutions[1,2,22].

In order to obtain greater insight into the reaction mechanism of these isomerizations, we investigated the reaction products with our carbohydrate analysis system.

Heating glucose solutions with catalytic amounts of molybdic acid causes epimerization and mannose can be isolated from the reaction mixture[23]. Fig. 7 shows a gradient chromatogram of an aqueous glucose solution treated for 14 days with catalytic amounts of molybdic acid. According to the peak intensities, about one third of the glucose has epimerized to mannose, but in addition small amounts of altrose, allose and disaccharides could also be detected.

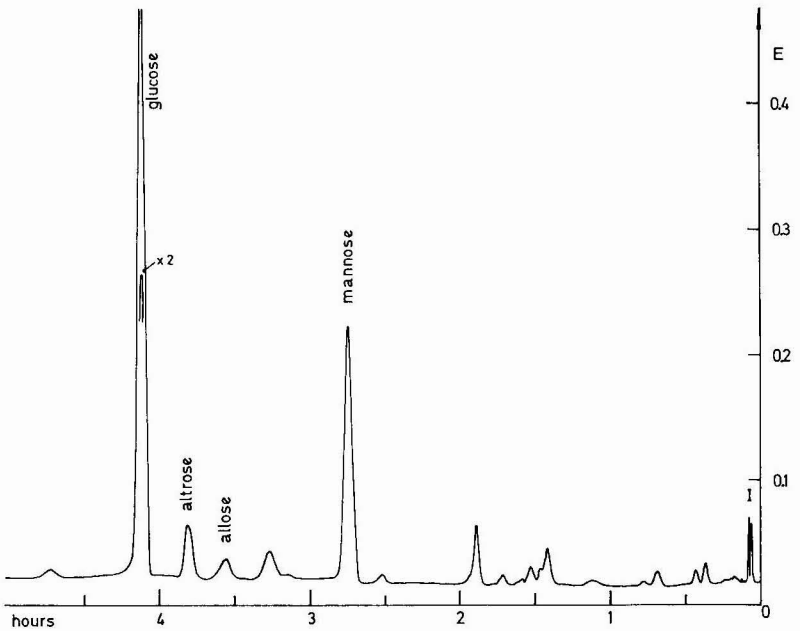
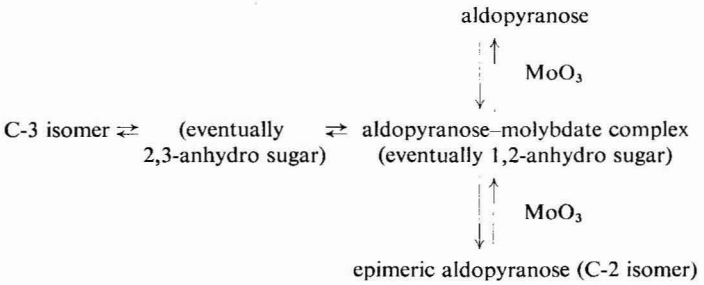


Fig. 7. Gradient chromatogram of the reaction mixture from an aqueous glucose solution heated for 14 days at 90° in the presence of catalytic amounts of molybdic acid. Gradient, 0.1–0.6 mole/l H_3BO_3, pH 8.0–10.0; 280 × 6 mm column; DA-X4 resin; flow-rate, 1 ml/min; temperature, 55°; injection of 50 μg. I = Injection peak.

Fig. 8 shows chromatograms of aqueous glucose and arabinose solutions heated with catalytic amounts of molybdic acid and obtained after 1–2 h and 140–190 h, respectively. The chromatograms demonstrate clearly that catalytic amounts of molybdic acid first cause epimerization and, after longer reaction times, isomerization at the C-3 position of aldopyranoses occurs. This conclusion was confirmed by the determination of the concentrations of the main products for several isomerization reactions as a function of time (Fig. 9).

On the basis of these chromatographic separations, the following reaction mechanism is suggested for the molybdic acid-catalyzed isomerization reaction:



The formation of oligosaccharides can be explained by the reaction of the intermediate with a second carbohydrate molecule.

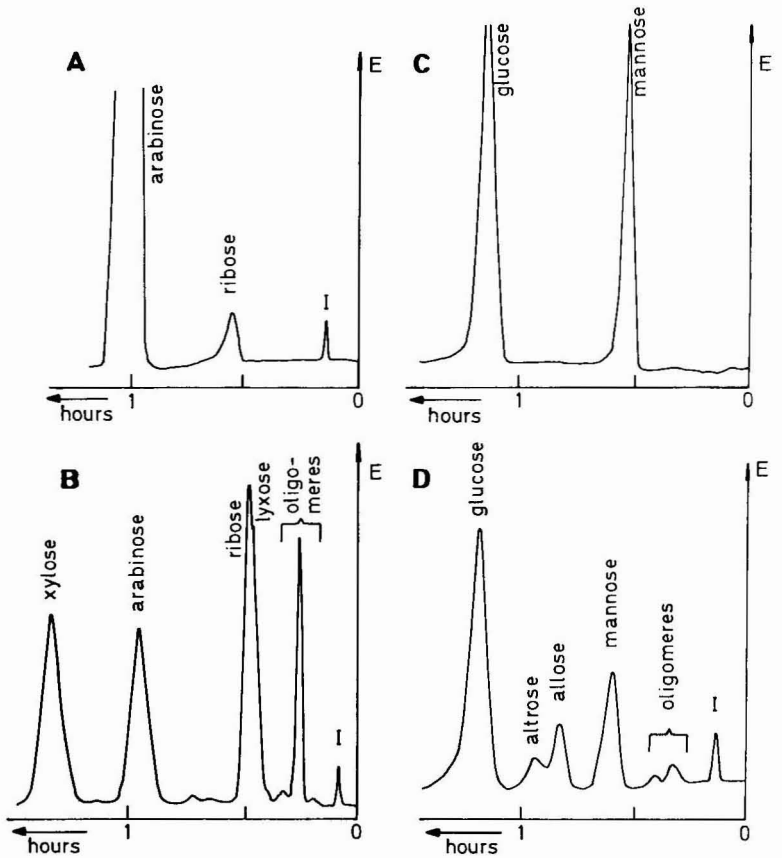


Fig. 8. Chromatograms of aqueous glucose and arabinose solutions heated with catalytic amounts of molybdic acid. A, starting material arabinose, reaction time 1.5 h; B, starting material arabinose, reaction time 188 h; C, starting material mannose, reaction time 2 h; D, starting material mannose, reaction time 141 h; one-buffer elution with H_3BO_3 buffer (0.4 mole/l, pH 9.0); 280 × 6 mm column (A and B)or 190 × 6 mm column (C and D); DA-X4 resin; flow-rate, 1 ml/min; temperature, 50°.

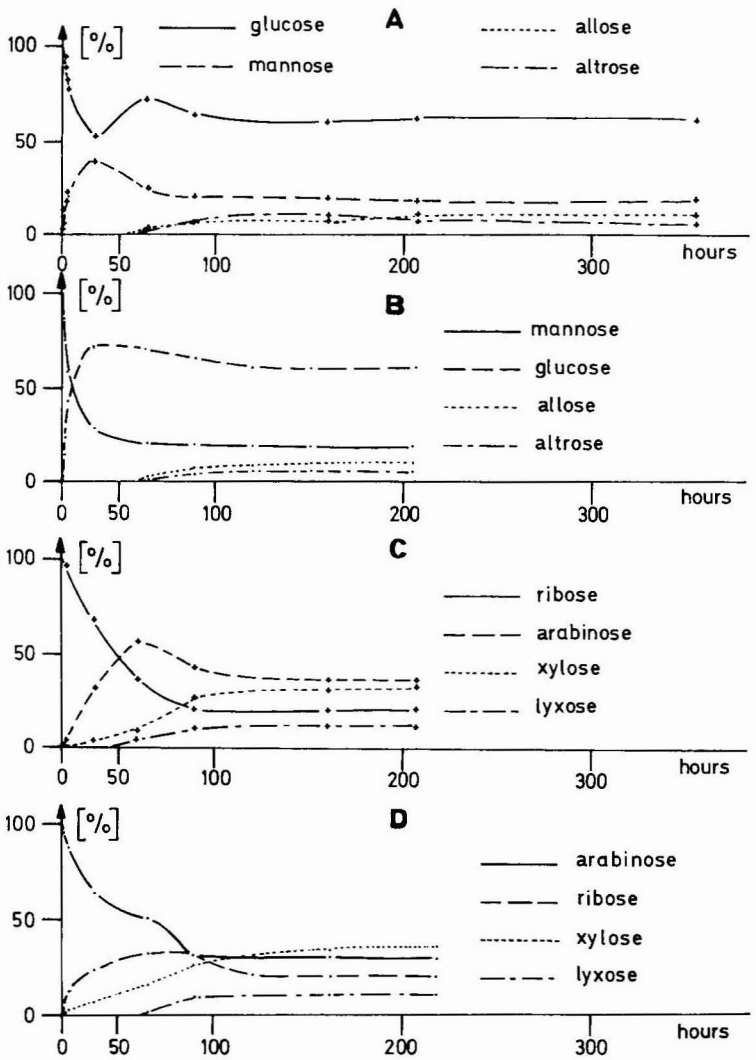


Fig. 9. Concentration of the components in molybdic acid-catalyzed isomerization reactions as a function of reaction time. Starting materials: A, glucose; B, mannose; C, ribose; D, arabinose. For separation technique, see legend to Fig. 8.

In the presence of methanol, the active intermediate forms a series of different methyl derivatives, which so far have not been identified. Fig. 10 shows the gradient chromatogram of the reaction mixture of glucose after heating for 14 days in methanol–water (3:7) at 90° in the presence of catalytic amounts of molybdic acid. The methylated carbohydrates are eluted from the column within 1–2 h.

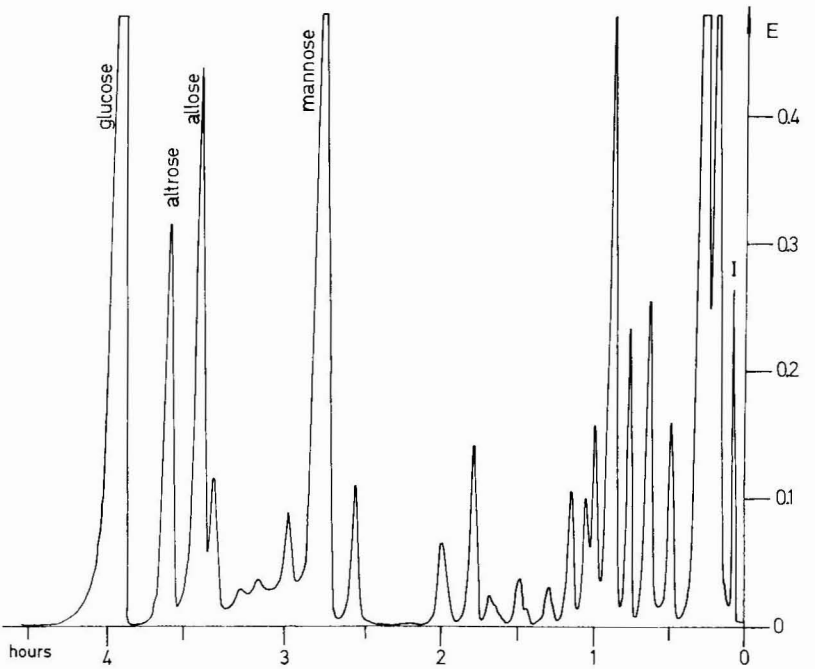


Fig. 10. Gradient chromatogram of the reaction mixture from a glucose solution heated for 14 days at 90° in the presence of catalytic amounts of molybdic acid and methanol–water (3:7). Gradient, 0.1–0.6 mole/l H_3BO_3, pH 8.0–10.0; 280 × 6 mm column; DA-X4 resin; flow-rate, 1 ml/min; temperature, 55°; injection of 50 μg. I = Injection peak.

ACKNOWLEDGEMENT

We sincerely thank the Deutsche Forschungsgemeinschaft for supporting part of this work.

REFERENCES

1 V. Bílik, W. Voelter and E. Bayer, *Angew. Chem.*, 83 (1971) 967; *Angew. Chem. Int. Ed. Engl.*, 10 (1971) 909.
2 V. Bílik, W. Voelter and E. Bayer, *Justus Liebigs Ann. Chem.*, 759 (1972) 189.
3 W. Voelter (Editor), *Abstracts of the "Tübingen Seminar", Methoden zur Trennung und Strukturaufklärung von Kohlenhydraten, Z. Naturforsch. B*, 29 (1974) 1.
4 V. Bílik, W. Voelter and E. Bayer, *Justus Liebigs Ann. Chem.*, (1974) 1162.
5 W. Voelter and H. Bauer, *Tetrahedron Lett.*, (1974) 3597.
6 W. Voelter, *Chem.-Ztg.*, 98 (1974) 493.
7 H. Bauer, *Thesis*, University of Tübingen, Tübingen, 1975.
8 F. Hyashi, *J. Biochem. (Tokyo)*, 16 (1932) 1.
9 W. H. McNeely, W. W. Binkley and M. L. Wolfrom, *J. Amer. Chem. Soc.*, 67 (1945) 527.
10 R. L. Whistler and D. F. Durso, *J. Amer. Chem. Soc.*, 72 (1950) 677.
11 H. Rückert and O. Samuelson, *Sätryck Sv. Kem. Tidskr.*, 66 (1954) 337.
12 J. K. N. Jones, R. A. Wall and A. P. Pittet, *Can. J. Chem.*, 38 (1960) 2285.
13 J. K. N. Jones and R. A. Wall, *Can. J. Chem.*, 38 (1960) 2290.
14 J. X. Khym and L. P. Zill, *J. Amer. Chem. Soc.*, 73 (1951) 2399.

15 R. B. Kesler, *Anal. Chem.*, 39 (1967) 1416.
16 D. D. Chilcote, C. D. Scott and W. W. Pitt, Jr., *J. Chromatogr.*, 75 (1973) 175.
17 W. Voelter and H. Bauer, *GIT Fachz. Lab.*, 17 (1973) 846.
18 P. Jandera and J. Churáček, *J. Chromatogr.*, 98 (1974) 55.
19 Y. C. Lee, J. F. McKelvy and D. Lang, *Anal. Biochem.*, 27 (1969) 567.
20 W. Voelter, G. Kuhfittig, G. Schneider and E. Bayer, *Justus Liebigs Ann. Chem.*, 734 (1970) 126.
21 W. Voelter, G. Kuhfittig, O. Oster and E. Bayer, *Chem. Ber.*, 104 (1971) 1234.
22 V. Bílik and J. Čaplovič, *Chem. Zvesti*, 27 (1973) 547.
23 V. Bílik, *Chem. Zvesti*, 26 (1972) 183.

Journal of Chromatography, 126 (1976) 705–716
© Elsevier Scientific Publishing Company, Amsterdam — Printed in The Netherlands

CHROM. 9420

SELECTIVE LIQUID CHROMATOGRAPHIC ISOLATION PROCEDURE FOR GAS CHROMATOGRAPHIC–MASS SPECTROMETRIC ANALYSIS OF 3-KETOSTEROIDS IN BIOLOGICAL MATERIALS

M. AXELSON and J. SJÖVALL

Department of Chemistry, Karolinska Institutet, Stockholm (Sweden)

SUMMARY

A method for the isolation of 3-ketosteroids based on the positive charge of their oximes is described. The biological extract is filtered through a column of sulphoethyl Sephadex LH-20 (H^+). Steroids in the filtrate are converted into oximes and the dried reaction mixture is filtered through a column of diethylaminohydroxypropyl Sephadex LH-20 (OH^-) in methanol. After evaporation of the solvent and hydroxylamine, the oximes are taken up by and separated on a column of sulphoethyl Sephadex LH-20 (H^+) in methanol. Following elution of other steroids, the oximes of 3-ketosteroids are eluted as a group with methanol–pyridine (20:1, v/v), and are converted into trimethylsilyl ethers. Removal of reagents and further purification of the sample is achieved by rapid filtration through Lipidex 5000 in *n*-hexane–pyridine–hexamethyldisilazane–dimethoxypropane (97:1:2:10). The derivatives are then analyzed by computerized gas chromatography–mass spectrometry using open-tubular glass capillary columns. Recoveries of picogram amounts of ^3H-labelled steroids carried through the entire isolation procedure are 80–90%. The purification achieved in analyses of plasma permits solid injection of the equivalent of 1–2 ml of plasma without overloading of the capillary column. The principle of the isolation procedure might be applicable to other groups of compounds that possess keto or aldehydo groups.

INTRODUCTION

Most of the biologically active neutral steroids possess a 3-keto group. Many methods exist for the analysis of individual 3-ketosteroids but there is no method which permits the isolation of this entire group of steroids for further analysis by procedures that separate the individual compounds. Such a method would be of obvious value as it would permit an unbiased analysis of 3-ketosteroid profiles in biological materials under different physiological conditions.

In the course of studies on the use of ion exchangers for the purification of steroids and steroid derivatives from biological materials[1,2], it was observed that the positive charge of O-methyloximes[3] of some 3-keto-Δ^4-steroids was sufficiently strong to permit sorption by a cation exchanger. This paper describes a quantitative isolation

and purification procedure for picogram amounts of 3-ketosteroids based on this principle. The final analytical step consists in repetitive scanning gas chromatography–mass spectrometry using open-tubular glass capillary columns.

EXPERIMENTAL

Glassware, solvents and reagents

All glassware was silanized with dimethyldichlorosilane in toluene. Cleaning was carried out in an ultrasonic bath.

All solvents were of reagent grade and were re-distilled twice in an all-glass system with 1-m distillation columns. Methanol was stored over sodium hydroxide prior to re-distillation to remove contaminating acids. Hexamethyldisilazane and trimethylchlorosilane (Applied Science Labs., State College, Pa., U.S.A.) were re-distilled, and trimethylsilylimidazole (Supelco, Bellefonte, Pa., U.S.A.) was used as supplied. Hydroxylammonium chloride (Fluka, Buchs, Switzerland) was recrystallized from 70% aqueous methanol.

Column packing materials

Amberlite XAD-2 (Rohm and Haas, Philadelphia, Pa., U.S.A.) was washed in the following way: 200 g was kept in 2 l of 2 *M* sodium hydroxide solution in 50% aqueous ethanol overnight at 39°; it was then washed in a chromatographic column with 2 l each of water, 2 *M* hydrochloric acid, water, acetone, ethanol and water, and was then refluxed for 4 h in ethanol and 4 h in water. Fines were removed by decantation or by back-washing of the column. The resin was finally washed with re-distilled ethanol and was stored in this solvent until used.

Lipidex® 5000 (Packard, Downers Grove, Ill., U.S.A.) was washed prior to use. Amounts of 50–100 g were stirred for 1 h at 70° in 1 l of 20% aqueous ethanol. After filtration on a Büchner funnel, similar extractions were carried out with 50% aqueous ethanol and ethanol. The gel was finally washed and stored in re-distilled methanol in dark bottles at 4°. Immediately before use, the appropriate amount of gel was washed on a Büchner funnel with absolute ethanol (20 ml per gram of gel) and *n*-hexane (20 ml/g), dried at 60° for 15 min and allowed to swell in the solvent used for chromatography.

Sulphoethyl Sephadex LH-20 (SE-LH-20) was prepared as described previously[4]. The capacity of the gel was about 0.10 mequiv./g. The Na^+ form of the gel was washed as described above for Lipidex 5000 and was stored at 4° in methanol. Prior to use, a few grams were washed on a Büchner funnel with 100 ml each of 0.3 *M* hydrochloric acid in 72% aqueous ethanol, 20% aqueous ethanol (until neutral), absolute ethanol and re-distilled methanol.

Diethylaminohydroxypropyl Sephadex LH-20 (DEAP-LH-20) was prepared and washed as described previously[4,5]. The Cl^- form of the gel, prepared by washing the gel with 0.25 *M* hydrochloric acid in 72% aqueous ethanol, was washed as described above for Lipidex 5000 and was then converted back into the acetate form and stored in a dry form at −20°. Prior to use, the gel was converted into the OH^- form by washing 1–3 g on a Büchner funnel with 100 ml each of 0.3 *M* sodium hydroxide solution in 72% ethanol, 20% aqueous ethanol (until neutral), absolute ethanol and re-distilled methanol.

Steroids

Unlabelled steroids were purchased from Ikapharm (Ramat-Gan, Israel) and kindly donated by Dr. J. Babcock (Upjohn, Kalamazoo, Mich., U.S.A.) and the MRC Reference Steroid Collection (Professor W. Klyne and Dr. D. N. Kirk).

Tritium-labelled steroids (1,2,6,7-$^3H_4$, 80–110 Ci/mmole except for 17α-hydroxyprogesterone, which was 7-^{3}H, 10 Ci/mmole) were obtained from the Radiochemical Centre (Amersham, Great Britain). Radioactivity was determined in a Packard Model 3003 liquid scintillation spectrometer using Instagel as the scintillation liquid.

Preparation of oximes

Oximes were prepared as described by Thenot and Horning[6,7]. A 5-mg amount of hydroxylammonium chloride and 50 μl of pyridine were added to the dried sample in a glass-stoppered centrifuge tube and heated at 60° for 30 min. The pyridine was then removed under a stream of nitrogen.

The residue was dissolved in 1 ml of methanol and applied to a column of DEAP-LH-20 (OH^-), *ca.* 400 mg, 150 × 4 mm packed in methanol under gravity flow. The sample was allowed to pass through the column at a flow-rate of 10 ml/h. The reaction tube was washed with 1-ml portions of methanol, which were also passed through the column until 5 ml of effluent had been collected in a round-bottomed flask. The solvent was removed *in vacuo*.

As an alternative to the DEAP-LH-20 column step, the reaction mixture can be diluted with 1 ml of water and extracted three times with 1 ml of ethyl acetate. However, in work with biological extracts, the DEAP-LH-20 filtration procedure is preferred as extraction losses do not occur and sample purification is achieved.

Chromatography of oximes on SE-LH-20

The residue from the DEAP-LH-20 column effluent was dissolved in 1 ml of methanol and applied to a column of SE-LH-20 (H^+), *ca.* 250 mg, 100 × 4 mm, packed in methanol under gravity flow. The flask was rinsed with methanol, which was also passed through the column, and elution with methanol was continued at a flow-rate of about 12 ml/h with collection of 0.5–1-ml fractions. When oximes of 3-ketosteroids were to be isolated as a group, the first 10 ml of effluent were discarded and the column was eluted with 3 ml of methanol–pyridine (20:1), to recover these steroids. The solvent was evaporated under a stream of nitrogen.

Preparation and purification of oxime trimethylsilyl ether derivatives

A 5-mg amount of hydroxylammonium chloride (as catalyst), 50 μl of pyridine and 50 μl of trimethylsilylimidazole were added to the sample of steroid oximes, and the mixture was heated at 100° for 2.5 h, as described by Thenot and Horning[6,7]. The solution was then diluted with 1.0 ml of *n*-hexane–pyridine–hexamethyldisilazane–dimethoxypropane (97:1:2:10) and rapidly filtered through a column of Lipidex 5000 by applying pressure of 0.5 kp/cm^2. The column, *ca.* 250 mg, 70 × 4 mm, was packed under gravity flow and washed with 10 ml of solvent prior to sample application. The reaction tube was rinsed with the same solvent in 0.5-ml portions and elution was continued at a flow-rate of 3 ml/min. The steroid derivatives were recovered in the first 2.5 ml of effluent, which were collected and stored at room

temperature in a stoppered centrifuge tube until required for analysis by gas chromatography and mass spectrometry.

As an alternative to this silylation procedure, when hindered hydroxyl groups are not present in the steroids, the oxime derivatives can be dissolved in pyridine–hexamethyldisilazane–trimethylchlorosilane (3:2:1), and left to react for 30 min at room temperature. The reagents are then removed under a stream of nitrogen.

Gas–liquid chromatography (GLC)

GLC was carried out using a Pye 104 gas chromatograph equipped with a flame-ionization detector, and housing a 20 m × 0.34 mm open-tubular glass capillary column coated with SE-30[8]. Solid injection in an all-glass system[9] was employed. Nitrogen was used as the carrier gas at an inlet pressure of 0.5 kp/cm^2, giving a flow-rate of about 1 ml/min. The oven temperature was 260°.

Computerized gas chromatography–mass spectrometry (GC–MS–COM)

GC–MS–COM was carried out using a modified LKB 9000 instrument[10]. A 25-m open-tubular glass capillary column coated with OV-1 was connected to the ion source via a single-stage adjustable jet separator. Other details of the connection between the capillary column and the ion source will be published elsewhere.

Methods for computerized evaluation of the mass spectral data recorded on tape have been described[11]. The temperature of the column was programmed from 235° to 275° at 0.6°/min, and the temperatures of the separator and ion source were 225° and 290°, respectively. The energy of the bombarding electrons was 22.5 eV, ionizing current 60 μA and accelerating voltage 3.5 kV. Spectra (*m/e* 0–800, 10 scans/min) were recorded after a suitable delay following injection of the sample.

Procedure for analysis of 3-ketosteroids in plasma

The steroids in 10 ml of plasma were extracted on a 4-g Amberlite XAD-2 column at 64° as described previously[2]. The column was packed in ethanol and was then washed with 50 ml of water prior to sample application. When the sample had passed through the column the latter was washed with 20 ml of water and 8 ml of *n*-hexane. The steroids were eluted according to the original procedure[2].

After evaporation of the solvents, the extract was dissolved in 1 ml of methanol and passed through a column of SE-LH-20 (H^+), *ca.* 500 mg, 200 × 4 mm, packed by gravity flow in methanol. A flow-rate of 7 ml/h was used. The flask containing the extract was rinsed with methanol, which was also passed through the column until 6 ml of effluent had been collected. The methanol was evaporated *in vacuo*.

The residue was transferred to a stoppered centrifuge tube and oximes were prepared using the DEAP-LH-20 column for purification. Oximes of 3-ketosteroids were isolated as a group by chromatography on SE-LH-20, and trimethylsilyl ether derivatives were prepared using trimethylsilylimidazole and purification on Lipidex 5000 as described above. The sample was then analyzed by GC–MS–COM.

RESULTS AND DISCUSSION

Separation of oximes of ketosteroids on sulphoethyl Sephadex LH-20

Originally, it was observed that the O-methyloxime of progesterone was taken

up by the strong cation exchanger Amberlyst A-15 (H^+) in methanol. However, O-methyloximes of more polar 3-keto-Δ^4-steroids were only incompletely sorbed, and quantitative conditions could not be achieved. Further studies were therefore carried out in which different ion exchangers, solvents and oxime derivatives were tested. It was found that a strong cation exchanger was required and that a non-aqueous solvent had to be used. Simple (unsubstituted) oximes were most strongly sorbed and the method was therefore based on this derivative. As an organic solvent had to be used, the lipophilic ion exchanger sulphoethyl Sephadex LH-20 was selected. Previous work has shown that adsorptive losses on lipophilic Sephadex derivatives are minimal and ion-exchange processes in organic solvents are rapid[12]. The selection of methanol as the solvent was based on the solubility properties of steroids, the swelling of lipophilic Sephadex and the chromatographic behaviour of the oximes.

The mobilities of the oximes of a number of steroids on columns of SE-LH-20 in methanol are given in Table I. Based on the elution volumes of their oximes, the monoketosteroids can be divided into three main groups in the following order of retention: 3-keto-Δ^4 > 3-keto (saturated) > 20-keto, 17-keto and 7-keto. The simultaneous presence of two oxime groups increases the retention. The elution volume is also influenced by the presence of neighbouring functional groups and by configuration. Thus, the oximes of 20-ketosteroids are less retarded when a 16,17-double bond or 17α- and 21-hydroxyl groups are present. In the absence of such effects, oximes of the 7-, 17- and 20-ketosteroids studied are eluted in this order.

As expected from previous work on simple and substituted oximes of ketosteroids[13,14], geometric isomers of the *syn/anti* type are formed from the 3-ketosteroids. The isomeric O-methyloximes of 3-keto-Δ^4-steroids can be separated by thin-layer chromatography[13] and the present study has shown that the isomeric oximes are well separated on SE-LH-20 columns in methanol. The latter separation seems to depend on the presence of a 4,5-double bond, as the two isomers formed from the saturated 3-ketosteroids were not separated. The influence of the double bond is also seen in the relative proportions of the two isomers formed (Table I). It was therefore of interest to study the effect of the presence of a hydroxyl group at C-2. It can be seen from Table I that there was no indication of the formation of two isomeric oximes from 2α-hydroxytestosterone, and one predominant isomer was formed from 2β-hydroxytestosterone. The oxime of 2α-hydroxytestosterone was retained much longer than the major oxime from 2β-hydroxytestosterone on the SE-LH-20 column, and the retention volumes of these two oximes were about the same as those of the *syn/anti* isomers formed from testosterone. However, the minor isomer of 2β-hydroxytestosterone was eluted rapidly and this isomer will therefore be lost in the procedure for the analysis of 3-ketosteroids in biological materials. As the separations are most likely based on an ion-exchange process, the differences in mobility of the isomers may be due to interactions between the hydroxyl group of the oxime and neighbouring functional groups, resulting in differences in the positive charge of the two isomers. As the *syn/anti* isomers of the oxime of testosterone can now be separated on a preparative scale, it may be possible to use NMR spectrometry to reveal interactions between the hydroxyl group of the oxime and neighbouring protons in the two isomers.

As mentioned above, the water content of the solvent used in the SE-LH-20 chromatography has to be kept low. The marked influence of the addition of water

TABLE I

ELUTION VOLUMES OF STEROID OXIMES ON COLUMNS OF SULPHOETHYL SEPHADEX LH-20 (CAPACITY ABOUT 0.10 mequiv./g) IN METHANOL AND RETENTION TIMES RELATIVE TO THAT OF CHOLESTANE OF THE OXIME TRIMETHYLSILYL ETHER DERIVATIVES ON AN OPEN-TUBULAR GLASS CAPILLARY COLUMN (SE-30) AT 260°

Position of oxime	*Steroid**	*Column length** (mm)*	*Peak elution volume*		*Relative retention time*	*Relative amounts of isomers (%)*
			ml	*Col. vols.****		
—	Cholesterol	100	1.0– 2.0	0.8– 1.6	—	—
—	Estradiol	100	1.0– 2.0	0.8– 1.6	—	—
C-20	5β-P-3α,11β,17α,21-ol-20-one	100	1.0– 2.0	0.8– 1.6	1.93	—
C-20	P^5-3β,17α-ol-20-one	100	1.5– 2.0	1.2– 1.6	1.49	—
C-20	$P^{5,16}$-3β-ol-20-one	100	1.5– 2.0	1.2– 1.6	1.16	—
C-7	C^5-3β-ol-7-one	100	2.0– 2.5	1.6– 2.0	3.30	—
C-17	A^5-3β-ol-17-one	100	3.0– 3.5	2.4– 2.8	0.78	—
C-20	5β-P-3α,21-ol-11,20-one§	100	4.0– 4.5	3.2– 3.6	1.79	—
C-20	P^5-3β-ol-20-one	100	4.5– 5.0	3.6– 4.0	1.24	—
C-3	5α-A-17β-ol-3-one	100	10.0–11.0	8.0– 8.8	0.88	49
			10.0–11.0	8.0– 8.8	0.84	51
C-3, C-17	5β-A-3,17-one	20	6.0– 7.0	24.0–28.0	0.89	48
			6.0– 7.0	24.0–28.0	0.86	52
C-3, C-20	5α-P-3,20-one	100	>30.0	>24.0	1.78	40
			>30.0	>24.0	1.68	60
C-3	A^4-17β-ol-3-one	100	25.0–30.0	20.0–24.0	0.91	70
			>30.0	>24.0	0.88	30
C-3	A^4-17β-ol-3-one	20	4.0– 5.0	16.0–20.0	0.91	70
			12.0–13.0	48.0–52.0	0.88	30
C-3	A^4-2β,17β-ol-3-one	20	1.0– 2.0	4.0– 8.0	1.32	15
			3.0– 4.0	12.0–16.0	1.17	85
C-3	A^4-2α,17β-ol-3-one	20	11.0–12.0	44.0–48.0	1.01	—
C-3	P^4-20α-ol-3-one	20	5.0– 6.0	20.0–30.0	1.50	70
			12.0–13.0	48.0–52.0	1.43	30
C-3, C-20	P^4-17α-ol-3,20-one	23	9.0–10.0	31.3–34.8	2.15	70
			>20.0	>69.6	1.96	30
C-3, C-20	P^4-11β,17α,21-ol-3,20-one	23	12.0–13.0	41.7–45.2	4.18	70
			>20.0	>69.6	3.99	30
C-3, C-17	A^4-3,17-one	25	14.0–15.0	44.8–48.0	1.13	70
			>20.0	>64.0	1.09	30
C-3, C-20	P^4-11β,21-ol-3,20-one	23	14.0–15.0	48.7–52.2	3.51§§	45
			>20.0	>69.6	3.51§§	40
					3.69	15
C-3, C-20	P^4-3,20-one	23	>20.0	>69.6	1.88	70
			>20.0	>69.6	1.81	30

* A = androstane; P = pregnane; C = cholestane; superscript indicates position of double bonds; Greek letter denotes configuration of hydroxyl groups.

** Column diameter 4 mm; a length of 100 mm corresponds to about 250 mg of SE-LH-20.

*** Elution volume (ml) divided by total column volume.

§ 11-Keto group underivatized. A minor isomer is not included.

§§ The major GC peak of corticosterone is eluted as two peaks on the SE-LH-20 column.

to the methanol on the mobility of the isomeric oximes of testosterone is shown in Table II. It is evident that the water content must be kept low for separations to occur. For comparison, mobilities in ethanol and acetone are also given. Although the oximes are retarded by the column, in acetone the peak is broad and no separation of the isomers is obtained.

If acids or bases are present in the methanol, there is no retention of the oximes. The addition of 5% of pyridine to the methanol provides a rapid means of recovering the oximes of 3-ketosteroids after the other steroids have been eluted.

TABLE II

EFFECT OF WATER ON THE MOBILITIES OF THE TWO ISOMERIC OXIMES OF TESTOSTERONE ON SE-LH-20 IN METHANOL

Mobilities in ethanol and acetone are given for comparison.

Solvent	*Water content (%)*	*Peak elution volume**	
		ml	*Col. vols.***
Methanol	<0.1	4.0– 5.0	16.0–20.0
		12.0–13.0	48.0–52.0
Methanol	0.1	3.0– 4.0	12.0–16.0
		>10	>40
Methanol	1.0	1.0– 2.0	4.0– 8.0***
		4.0– 5.0	16.0–20.0***
Methanol	5.0	0.0– 1.0	0.0– 4.0***
Ethanol	<1.0	1.0– 2.0	4.0– 8.0***
Acetone	<0.1	5.0– 6.0	20.0–24.0***

* The column was 20 × 4 mm, requiring 50 mg of gel in methanol or ethanol and 70 mg in acetone.

** See Table I.

*** Incomplete or no separation of the isomers.

Recoveries of tritiated steroids

The recoveries of steroids in the preparation of oximes and filtration through DEAP-LH-20, in the chromatography on SE-LH-20, and in the preparation of trimethylsilyl ether derivatives and filtration through Lipidex 5000 were tested with tracer amounts of ^{3}H-labelled steroids used individually or in mixtures. The results of experiments with a mixture of six 3-keto-Δ^4-steroids are shown in Table III. The mean recovery was 87% for the entire procedure, and experiments with individual steroids showed no selective losses.

A comment should be made concerning the purification of trimethylsilyl ethers of oxime and O-methyloxime derivatives of steroids on Lipidex 5000. In a previous study, difficulties were experienced when the O-methyloxime trimethylsilyl ether derivative of cortisol was filtered through a Lipidex 5000 column at a flow-rate of 6 ml/h, using as the solvent *n*-hexane–pyridine–hexamethyldisilazane (98:1:1). Filtration of the O-trimethylsilyl oxime trimethylsilyl ether derivative of the same steroid in this system gave a considerably higher yield (about 80%). The losses seem to be due to hydrolysis of trimethylsilyl ether groups in the derivatives. However, when dimethoxypropane was added to the solvent and the sample was rapidly filtered through the Lipidex column, hydrolysis was prevented. Trimethylsilyl ethers of oxime and O-

TABLE III

RECOVERIES OF ^{3}H-LABELLED 3-KETO-Δ^4-STEROIDS IN THE CONVERSION INTO OXIMES, FILTRATION THROUGH DEAP-LH-20, SEPARATION ON SE-LH-20, CONVERSION INTO TRIMETHYLSILYL ETHER DERIVATIVES AND FILTRATION THROUGH LIPIDEX 5000

*Steroid mixture**	*Amount added*		*Recovery from columns (%)**			*Loss in first 10 ml from SE-LH-20 (%)***
	pg	*cpm*	*DEAP-LH-20 + SE-LH-20*	*Lipidex 5000*	*Total*	
A^4-3,17-one	4	1000				
A^4-17β-ol-3-one	4	1000				
P^4-3,20-one	4	1000	92.2 ± 4.6	96.7 ± 2.8	87.4 ± 5.1	3.5 ± 0.4
P^4-17α-ol-3,20-one	40	1000	(n = 10)	(n = 10)	(n = 10)	(n = 10)
P^4-11β,17α,21-ol-3,20-one	4	1000				
P^4-17α,21-ol-3,11,20-one	4	1000				

* For abbreviations see Table I.

** Per cent of added radioactivity ± S.D.; n = number of experiments.

methyloxime derivatives of cortisol were recovered quantitatively and essentially the same purification of the sample was achieved.

Application to the analysis of 3-ketosteroids in plasma

The extraction of steroids in plasma using Amberlite XAD-2 at elevated temperature has been described previously[2]. Recoveries of 3-keto-Δ^4-steroids by this method were better than 90%. In order to remove cations that might have interfered in the subsequent separation of oximes and in the GC–MS analysis, the extract from Amberlite XAD-2 was filtered through a column of SE-LH-20 in methanol. Recoveries of ^{3}H-labelled steroids in this step were quantitative and a 500-mg column was sufficient for an extract of 10 ml of plasma.

If large amounts of non-polar lipids contaminate the sample, they can be removed by filtration through a column of Lipidex 5000 in the reversed-phase system methanol–water–chloroform (9:1:2)[1,2]. Hormonal steroids are eluted early, while cholesterol and neutral lipids are retained on this column.

After the reaction with hydroxylammonium chloride, the sample was filtered through a column of DEAP-LH-20. This step served two purposes: to remove chloride ions so that hydroxylamine could be evaporated, and to remove contaminating anions from the sample.

The separation of steroid oximes on SE-LH-20 has been discussed above. For the analysis of 3-ketosteroids, the oximes of these steroids were eluted as a group with methanol–pyridine following elution of other steroids with methanol. The selectivity of this purification step is high.

Final purification of the sample prior to GC–MS–COM analysis was achieved by filtration of the reaction mixture after formation of trimethylsilyl ether derivatives through a column of Lipidex 5000. This step served two purposes: to remove reagents and to remove interfering compounds that had not become non-polar in the silylation reaction.

The recoveries of ^{3}H-labelled steroids added to plasma and carried through the entire procedure were better than 78% in five experiments (mean: 82.3%).

The degree of purification achieved in the entire procedure was such that the equivalent of 1–2 ml of plasma could be injected without overloading of the glass capillary column in the GC–MS–COM analysis. A high degree of purification is necessary as analyses of steroid metabolite profiles require rapid repetitive scanning of the entire mass range, which reduces the sensitivity compared with detection by single or multiple ion monitoring. Obviously, the ability of the latter methods to detect low concentrations of steroids is also increased with improved sample purification.

The isolation procedure may appear tedious but it is in fact relatively easy to carry out as it is based on simple filtrations through a series of columns. The 3-keto-steroids in a plasma sample can be isolated for GC–MS analysis in 2 days and one technician can run four samples in parallel. Although the present study has been limited to ketosteroids, it should be pointed out that the principle of isolating oximes by cation-exchange chromatography in organic solvents might be more widely applicable to other groups of compounds that possess keto or aldehydo groups.

The GC–MS–COM analyses of 3-ketosteroids in plasma samples from two pregnant women (35th and 38th weeks) are shown in Fig. 1. Fragment (and molecular) ion current (FIC) chromatograms were constructed by the computer for *m/e* values typical of O-trimethylsilyloxime trimethylsilyl ether derivatives of various steroids possessing a 3-keto group. The selection of *m/e* values was based on spectra of reference compounds, the molecular weight of steroids, the known loss of 15 and 89 mass units from the molecular ion and the knowledge of ions typical of specific structural features in the molecules. Spectra of this type of steroid derivative have been discussed by Brooks and co-workers[14,15].

As expected, cortisol (scans 293 and 308, plasma sample 1) and progesterone (scans 60 and 69) are the major 3-ketosteroids in the analyses shown in Fig. 1. The spectrum of the derivative of progesterone is shown in Fig. 2. The molecular ion at *m/e* 488 is seen as well as the peak at *m/e* 211 typical of the derivative of the 3-keto-Δ^4-structure[15]. The peaks at *m/e* 145 and 158 arise from the derivatized 20-keto-21-deoxy structure[14]. A relatively large amount of 20α-hydroxy-4-pregnen-3-one (scans 14 and 21) is also seen. The spectrum of the derivative of this steroid is shown in Fig. 2. The molecular ion at *m/e* 475, the ion at *m/e* 211 and the intense ion at *m/e* 117, arising from the side-chain of the derivatized 20-hydroxy-21-deoxy structure, are seen.

In addition to these steroids, the presence of 17α-hydroxy-4-pregnene-3,20-dione (main isomer scan 85, plasma sample 2) and 16α-hydroxy-4-pregnene-3,20-dione (relative retention times 2.52 and 2.59, scans 100 and 107, plasma sample 2) was noted. 5α-Pregnane-3,20-dione has been identified in plasma from pregnant women[2,16] and its derivatives are seen to be eluted at scans 37 and 51 in plasma 1.

Recently, Murphy *et al.*[17] demonstrated the presence of cortisone in plasma of pregnant women, and the analyses shown in Fig. 1 confirm these results. Relatively large amounts of the derivatives of this compound (relative retention times 3.51 and 3.92) appear at scans 252 and 286 (plasma sample 1), and the spectrum of this steroid derivative is shown in Fig. 2. The concentrations of the different steroids can be calculated from the peak areas in appropriate FIC chromatograms by comparison with known amounts of reference compounds. The following approximate values were found in the analysis of plasma sample 1 shown in Fig. 1 (the equivalent of 0.3 ml plasma was injected): progesterone, 200 ng/ml; 20α-hydroxy-4-pregnen-3-one, 37 ng/ml; 5α-pregnane-3,20-dione, 35 ng/ml; 17α-hydroxy-4-pregnene-3,20-dione, *ca.* 1

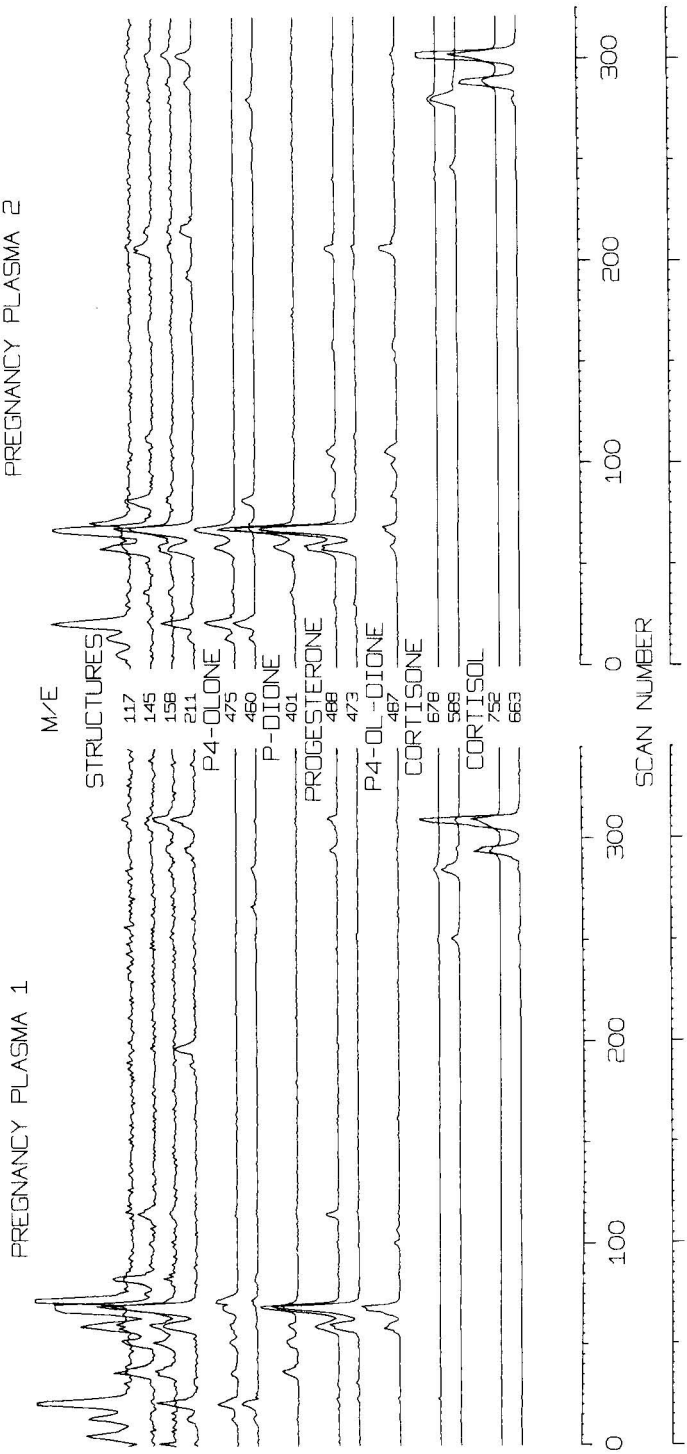


Fig. 1. Fragment ion current (FIC) chromatograms constructed by the computer in analyses of 3-ketosteroids in plasma from women in the 35th (pregnancy plasma 1) and 38th week (pregnancy plasma 2) of pregnancy. The equivalent of about 0.3 ml of plasma was injected into the glass capillary column. *m/e* values characteristic of O-trimethylsilyloxime trimethylsilyl ether derivatives of various steroids possessing a 3-keto group and ions given by specific structural features in the molecules were selected.

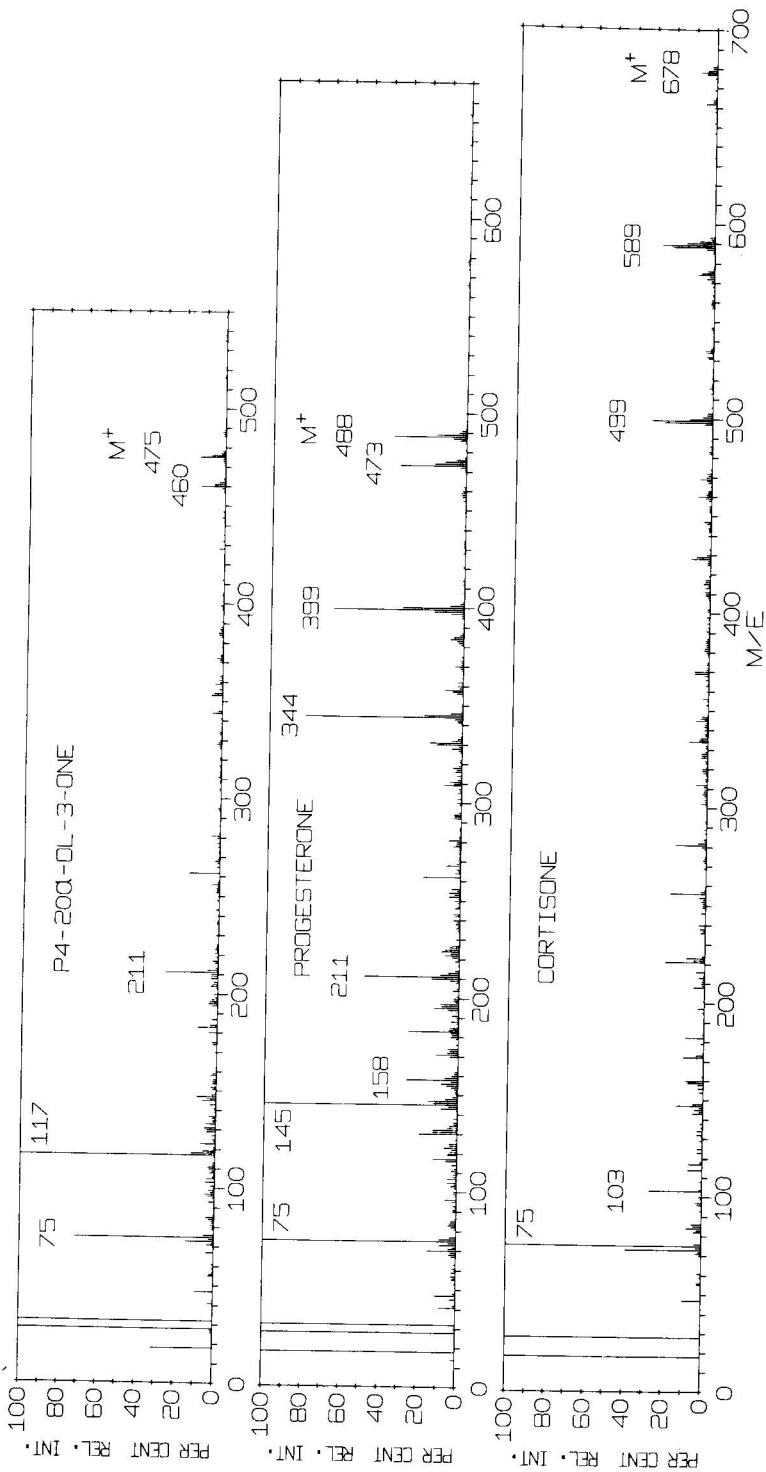


Fig. 2. Mass spectra of O-trimethylsilyloxime trimethylsilyl ether derivatives of steroids found in plasma from a pregnant woman. The spectra of 20α-hydroxy-4-pregnen-3-one, progesterone and cortisone were recorded from the analysis of pregnancy plasma 2, at scans 23, 68 and 280, respectively, shown in Fig. 1.

ng/ml; 16α-hydroxy-4-pregnene-3,20-dione, *ca.* 5 ng/ml; cortisol, 297 ng/ml; and cortisone, 57 ng/ml. These values are in agreement with published values for the concentrations of these steroids in late-pregnancy plasma.

The separation of *syn/anti* isomers of the oxime derivatives of 3-ketosteroids (see Table I) is evident in Fig. 1. This is a disadvantage in quantitative analyses, as it decreases the sensitivity and makes the GLC profiles more complex. However, the formation of two peaks may help to support the identification of the steroids.

The sensitivity of the repetitive scan method using electron-impact ionization and O-trimethylsilyloxime trimethylsilyl ether derivatives is not sufficiently high to detect steroids present in plasma at concentrations below 1 ng/ml. For example, the molecular ion of the progesterone derivative constitutes only 4.6% of the total ionization. In a test in which chemical ionization in isobutane was employed, the value for the quasimolecular ion was 6.5%, *i.e.*, only slightly higher. Attempts to make more suitable derivatives of the oxime groups were unsuccessful. However, recently it has become possible to convert the oximes into the more favourable O-methyloximes and this method is presently being studied[18]. Finally, increased sensitivity is obviously obtained if the ions to be monitored are selected prior to injection of the sample so that multiple ion detection can be employed.

ACKNOWLEDGEMENTS

The technical assistance of Mrs. B. Mörk, Mr. T. Pettersson and Mr. R. Reimendal is gratefully acknowledged. The chemical ionization spectra were kindly recorded by Dr. R. Ryhage. We are also grateful to Dr. R. Ryhage for providing us with drawings of the jet separator. This work was supported by grants from the Swedish Medical Research Council (No. 13X-219), Magnus Bergvalls Stiftelse, Karolinska Institutet and the World Health Organization.

REFERENCES

1 M. Axelson, G. Schumacher and J. Sjövall, *J. Chromatogr. Sci.*, 12 (1974) 535.
2 M. Axelson and J. Sjövall, *J. Steroid Biochem.*, 5 (1974) 733.
3 R. Breslow, *Organic Reaction Mechanisms*, W. A. Benjamin, New York, 1969, p. 190.
4 K. D. R. Setchell, B. Almé, M. Axelson and J. Sjövall, *J. Steroid Biochem.*, (1976) in press.
5 B. Almé and E. Nyström, *J. Chromatogr.*, 59 (1971) 45.
6 J. P. Thenot and E. C. Horning, *Anal. Lett.*, 4 (1971) 683.
7 J. P. Thenot and E. C. Horning, *Anal. Lett.*, 5 (1972) 21.
8 G. A. F. M. Rutten and J. A. Luyten, *J. Chromatogr.*, 74 (1972) 177.
9 P. M. J. van den Berg and T. P. H. Cox, *Chromatographia*, 5 (1972) 301.
10 R. Reimendal and J. Sjövall, *Anal. Chem.*, 44 (1972) 21.
11 M. Axelson, T. Cronholm, T. Curstedt, R. Reimendal and J. Sjövall, *Chromatographia*, 7 (1974) 502.
12 E. Nyström and J. Sjövall, *Methods Enzymol.*, 35 (1975) 378.
13 M. G. Horning, A. M. Moss and E. C. Horning, *Anal. Biochem.*, 22 (1968) 284.
14 C. J. W. Brooks and D. J. Harvey, *Steroids*, 15 (1970) 283.
15 C. J. W. Brooks and B. S. Middleditch, in E. Heftmann (Editor), *Modern Methods of Steroid Analysis*, Academic Press, New York, 1973, p. 140.
16 K. F. Støa and A. Bessesen, *J. Steroid Biochem.*, 6 (1975) 21.
17 B. E. P. Murphy, S. J. Clark, I. R. Donald, M. Pinsky and D. Vedady, *Amer. J. Obstet. Gynecol.*, 118 (1974) 538.
18 M. Axelson, in preparation.

Journal of Chromatography, 126 (1976) 717–722
© Elsevier Scientific Publishing Company, Amsterdam — Printed in The Netherlands

CHROM. 9478

ANALYSIS OF BENZOYLECGONINE IN URINE BY HIGH-PERFORMANCE LIQUID CHROMATOGRAPHY AND GAS CHROMATOGRAPHY–MASS SPECTROMETRY

ANTHONY P. GRAFFEO, DENIS C. K. LIN and RODGER L. FOLTZ
Battelle, Columbus Laboratories, 505 King Avenue, Columbus, Ohio 43201 (U.S.A.)

SUMMARY

Benzoylecgonine, a polar metabolite of cocaine, was extracted and purified from urine using a reversed-phase high-performance liquid chromatographic column. The portion of the eluent corresponding to elution of the drug was collected, derivatized, and quantified using gas chromatography–mass spectrometry with selected ion monitoring. Using this procedure, analysis of 1 ng/ml of benzoylecgonine in urine can be achieved.

INTRODUCTION

It is presently very difficult to detect and quantify cocaine in body fluids of the drug abuser. This is due primarily to the rapid and extensive metabolism of cocaine in the body to the metabolites benzoylecgonine and ecgonine. Only about 1 % of the parent drug is excreted in the urine[1]. Benzoylecgonine is excreted in higher concentration than ecgonine[2] and has been the metabolite of choice for drug monitoring. Benzoylecgonine has been analyzed by thin-layer chromatography[3,4], enzyme multiplied immunoassay[3], and gas chromatography with flame ionization[5,6], electron capture[7], and nitrogen detection[8]. A review has been published by Bastos and Hoffman[9].

A major problem in the analysis of benzoylecgonine is the difficulty of extracting the metabolite from biological media. Since the molecule contains both amine and carboxyl functions, it is amphoteric and therefore highly lipophobic. Solvent extraction from aqueous media requires exhaustive continuous extraction[10], or a salting out procedure[3], or liquid–solid extraction of previously lyophilized material[11]. These methods are cumbersome, inefficient, and relatively unselective.

We have developed a high-performance liquid chromatographic (HPLC) procedure which is capable of extracting and sufficiently purifying benzoylecgonine from urine to enable its analysis by gas chromatography–mass spectrometry (GC–MS) without further cleanup. This development has led to a simple analytical procedure for the analysis of benzoylecgonine in urine which shows promise of wide applicability to other drugs and their metabolites. By using the combination of HPLC and GC–MS with selected ion monitoring and and isotope-labeled variant as

an internal standard, analysis of benzoylecgonine has been achieved at concentrations as low as 1 ng/ml of urine.

EXPERIMENTAL

A reversed-phase HPLC column (μBondapak C_{18}, Waters Assoc., Milford, Mass., U.S.A.) was used to simultaneously extract and purify benzoylecgonine from urine. A 5-cm pre-column packed with pellicular reversed-phase particles was used to protect the analytical column. A solvent program* was generated by a Varian 8500 liquid chromatograph and the column eluent was monitored at 254 nm (DuPont, Model 837). One hundred ng of pentadeuterated benzoylecgonine were added to each of the 1-ml urine samples as internal standard. The 1-ml samples were then introduced onto the column via a large-volume loop injector (Rheodyne, Model 7105). The mobile phase flow-rate was maintained at 100 ml/h resulting in an initial column pressure drop of 1500 p.s.i. at room temperature. Distilled-in-glass methanol and distilled water were used as mobile phase solvents. The portion of the effluent (approx. 4 ml)

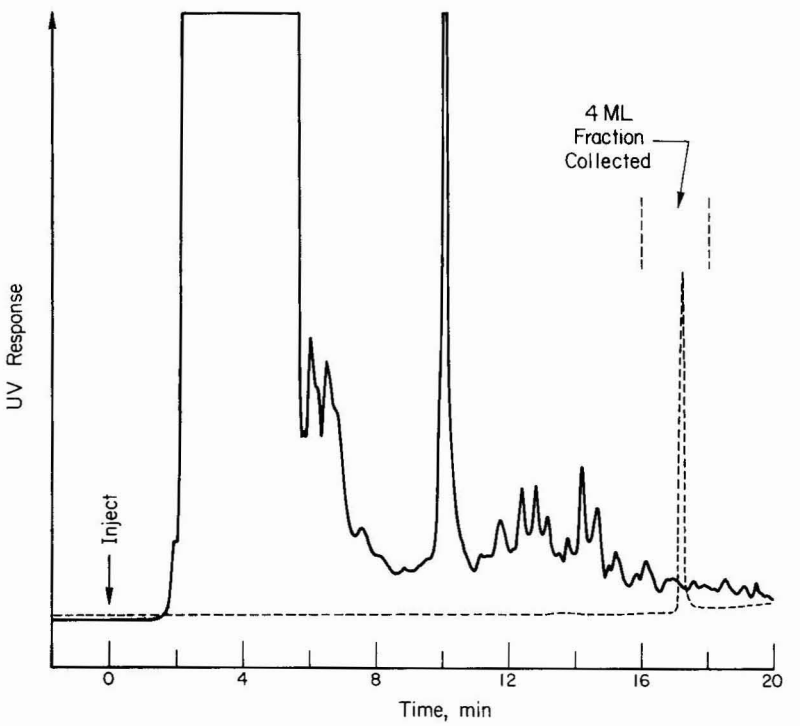


Fig. 1. Chromatograms of 1 ml of urine (———) and 3 μg of benzoylecgonine (– – –). Column, μBondapak C_{18}; solvent, 5 min isocratic, 5% methanol in water; 10 min gradient, 5% methanol/min; 5 min gradient, 10% methanol/min; flow-rate: 100 ml/h; UV attenuation: urine, absorbance 0.128; benzoylecgonine, absorbance 0.08.

* Solvent program: 5 min isocratic, 5% methanol in water; 10 min gradient, 5% methanol/min; 5 min gradient, 10% methanol/min; reset to initial conditions.

corresponding to where benzoylecgonine eluted (the window is as shown in Fig. 1) was collected. The effluent was evaporated at 40° under a gentle stream of nitrogen and then trimethylsilylated with 25 μl of bis(trimethylsilyl)trifluoroacetamide (Pierce, Rockford, Ill., U.S.A.). A 2- to 4-μl volume of the trimethylsilylated solution was injected onto a 6 ft. $\times$ 2 mm column packed with 3% OV-1. The column temperature was kept at 220°. Methane which was used as the carrier gas entered directly into the ion source. Ammonia (0.1 torr) was also bled into the ion source so that a mixture of methane and ammonia (8:1) was the chemical ionization reagent gas. The source pressure was approximately 1 torr. The protonated-molecule ions of trimethylsilyl benzoylecgonine (*m/e* 362) and the internal standard (*m/e* 366) were monitored by a Finnigan 3200 mass spectrometer (Fig. 2).

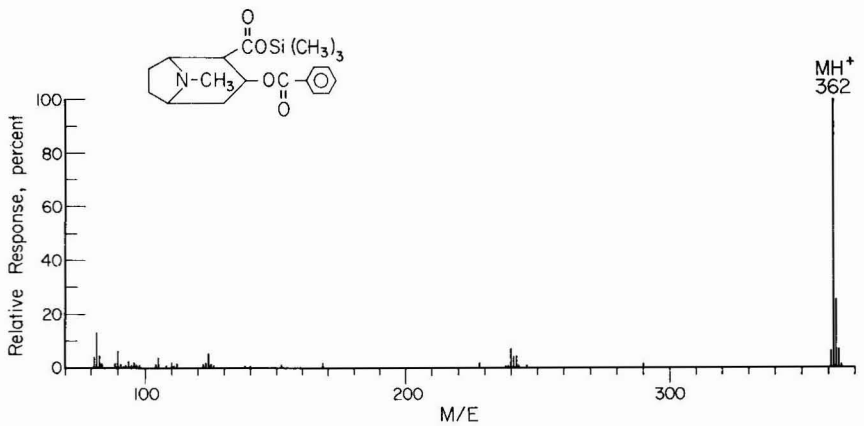


Fig. 2. The methane-ammonia chemical ionization mass spectrum of trimethylsilyl benzoylecgonine.

The ion source voltages were adjusted to give maximum sample ion intensities under methane chemical ionization conditions while unit resolution and symmetrically shaped peaks were maintained. Typical operating conditions were: ionization energy, 200 eV; ion repeller, 0 V; lens, −20 V; filament emission, 1 mA; ion source temperature, 130 to 160°; and electron multiplier gain, 5×10^4 to 7×10^5.

The pentadeuterated benzoylecgonine was obtained from National Institute on Drug Abuse. The mass spectrum of the deuterated compound shows that it is not isotopically pure. The most intense ion at the molecular ion region is for the d_4-variant (*m/e* 366); therefore, this ion was monitored as the internal standard.

RESULTS AND DISCUSSION

Reversed-phase liquid chromatography is a useful technique for extracting and purifying benzoylecgonine from urine prior to analysis by GC–MS. Although the metabolite benzoylecgonine is a polar compound, it is retained considerably longer on a reversed-phase column than most polar urinary constituents and therefore it can be effectively purified (Fig. 1). This has been verified by collecting the portion of the eluent (t_R = 16–18 min) corresponding to where benzoylecgonine elutes, silylating,

and analyzing for trimethylsilyl benzoylecgonine by GC–MS with selected ion monitoring. Fig. 3 shows the GC peak corresponding to 1 ng of benzoylecgonine collected from the HPLC column. Hardly any interferences from endogeneous compounds were observed while monitoring this mass number (*m/e* 362).

Before incorporating this HPLC procedure into an analysis method for benzoylecgonine, three important studies were performed: the reproducibility in HPLC retention, the lifetime of the reversed-phase column, and the quantification of benzoylecgonine by GC–MS.

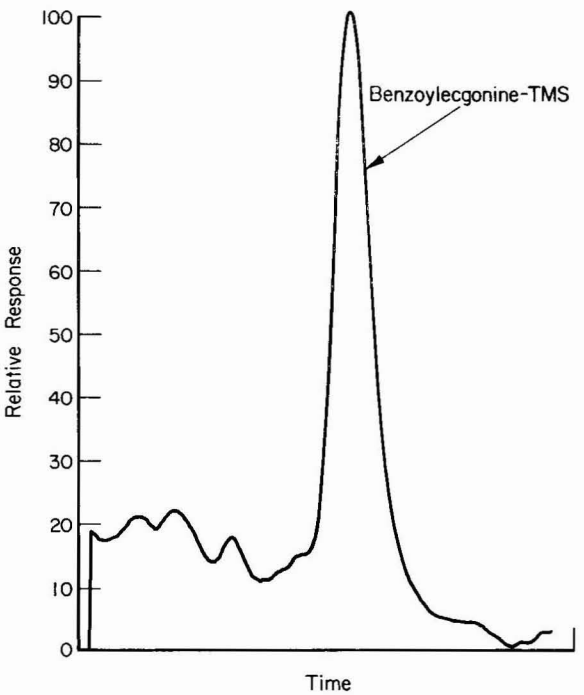


Fig. 3. Analysis of 1 ng of benzoylecgonine in 1 ml of urine by GC–MS with selected ion monitoring (*m/e* 362.4). Benzoylecgonine was extracted and purified by the method illustrated in Fig. 1.

Since the quantities of benzoylecgonine being analyzed are below the detection limit of the ultraviolet (UV) photometer, a time window corresponding to the elution of the drug is collected. It is therefore extremely important that the retention time of the drug remains constant. We monitor the reproducibility in retention by injecting 3 μg of standard benzoylecgonine before and after injection of urine samples. The relative standard deviation was 0.64% over 12 measurements in 20 days (retention time, 1011.33 $\pm$ 6.46 sec). The reproducibility in retention of later eluting peaks in gradient elution is more dependent on the reproducibility of the solvent gradient than on the initial solvent conditions. Column re-equilibration is therefore shortened (10 min). This allows a fast sample throughput time (30 min) while maintaining a reproducible retention time.

An additional concern was the ability of the reversed-phase column to maintain

its performance (*i.e.*, efficiency, permeability, and retention reproducibility) after injections of large quantities of biological fluids. To date over fifty 1-ml urine samples have been injected with essentially no change in column performance. Also, there has not yet been a need to replace the pre-column. Column performance is continually being measured to determine its useful lifetime.

Once the HPLC conditions had been determined, a GC–MS quantification procedure specific for benzoylecgonine was developed using selected ion monitoring. A 4-ml volume of water–methanol (1:1) (to approximate the collected eluent) was spiked with 100 ng of deuterated benzoylecgonine and 1, 3, 6, 10, and 50 ng of benzoylecgonine. These solutions were evaporated at 40° with a gentle stream of nitrogen, derivatized and analyzed by GC–MS (see Experimental). Fig. 4 shows the standard curve in which the correlation coefficient obtained was 1.000.

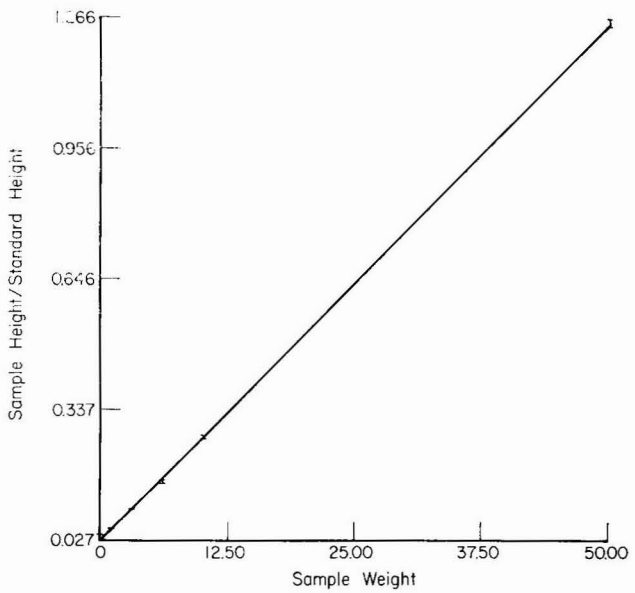


Fig. 4. Standard curve for the range 0–50 ng of benzoylecgonine using 100 ng of internal standard.

GC–MS with selected ion monitoring constitutes a highly specific and sensitive method for the analysis of many drugs and related compounds[12]. Nevertheless, the analysis of some drugs and their metabolites, especially the more polar ones, has been hampered due to poor extraction and cleanup techniques. Often, similar drugs require two entirely different extraction and purification steps to allow their analysis by GC–MS.

There are a number of advantages in using HPLC for the extraction and purification of drugs and their metabolites from body fluids prior to GC–MS analysis. Using benzoylecgonine as an example, we have demonstrated that a polar metabolite, previously very difficult to concentrate in biological fluids, can be easily extracted and purified using HPLC. Twitchett and Moffat[13] have listed retentions of a large

number of drugs, on reversed-phase columns, all of which behave similar to benzoylecgonine.

This approach, therefore, shows promise as a general method for the extraction and cleanup of drugs from body fluids. Additional advantages are: extraction selectivity can be enhanced for polar, ionic drugs by controlling the pH of the mobile phase[14]; several drugs can be extracted and purified in a single run; and the extraction and purification procedure can now be automated. The combination of HPLC and GC–MS with selected ion monitoring allows very sensitive drug analysis with minimum sample preparation.

ACKNOWLEDGEMENT

This work was supported by the National Institute on Drug Abuse, Contract ADM-45-74-140.

REFERENCES

1 L. A. Woods, F. G. McMahon and M. H. Seeves, *J. Pharmacol. Exp. Ther.*, 101 (1951) 200.
2 F. Fish and W. D. C. Wilson, *J. Pharm. Pharmacol.*, 21 (1969) Suppl. 135-S.
3 M. L. Bastos, D. Jukofsky and S. J. Mulé, *J. Chromatogr.*, 89 (1974) 335.
4 J. M. Meola and H. H. Brown, *Clin. Chem.*, 21 (1975) 945.
5 S. Koontz, D. Besemer, N. Mackey and R. Phillips, *J. Chromatogr.*, 85 (1973) 75.
6 J. M. Moore, *J. Chromatogr.*, 101 (1974) 215.
7 J. I. Javaid, H. Dekirmenjian, E. G. Brunngraber and J. M. Davis, *J. Chromatogr.*, 110 (1975) 141.
8 P. I. Jatlow and D. N. Bailey, *Clin. Chem.*, 21 (1975) 1918.
9 M. L. Bastos and D. B. Hoffman, *J. Chromatogr. Sci.*, 12 (1974) 269.
10 S. J. Mulé, M. L. Bastos, D. Jukofsky and E. Saffer, *J. Chromatogr.*, 63 (1971) 289.
11 D. B. Hoffman, C. J. Umberger, S. Goldner, S. Andryauskas, D. Mulligan and J. R. Broich, *J. Chromatogr.*, 66 (1972) 63.
12 F. C. Falkner, B. J. Sweetman and J. T. Watson, *Appl. Spectros. Rev.*, 10 (1975) 51.
13 P. J. Twitchett and A. C. Moffat, *J. Chromatogr.*, 111 (1975) 149.
14 A. P. Graffeo and B. L. Karger, *Clin. Chem.*, 22 (1976) 184.

Journal of Chromatography, 126 (1976) 723–730
© Elsevier Scientific Publishing Company, Amsterdam — Printed in The Netherlands

CHROM. 9518

IDENTIFICATION OF ORGANIC COMPOUNDS BY AN ELUTION GAS CHROMATOGRAPHY–REACTOR–FRONTAL GAS CHROMATOGRAPHY SYSTEM

VLASTIMIL REZL and JIŘÍ BURSA

Institute of Analytical Chemistry, Czechoslovak Academy of Sciences, Brno (Czechoslovakia)

SUMMARY

The on-line identification of gas chromatographic (GC) effluents is described using an automated elution GC–reactor–frontal GC instrumental system and exploiting a commercial gas chromatograph for this purpose. The identification is based on elemental analysis, *viz.*, the determination of the empirical formula without knowing the amount of the substances being analyzed. A detailed discussion is given of C,H,N,O determinations. With the system described, it is possible to analyze, with satisfactory precision, as little as 10 μg of a substance.

INTRODUCTION

During the rapid development of gas chromatography (GC) and its applications in organic chemistry, macromolecular chemistry, biochemistry and biology, a demand arose for the identification of components leaving the GC column after separation. A number of methods evolved gradually in this way, based essentially on the direct coupling of GC with mass spectrometry (MS), infrared spectrometry, Raman spectrometry, etc. In addition to the fact that these instrumental combinations are expensive, they usually require highly specialized operators, who are capable of interpreting the very complicated data that are produced.

Elemental analysis (EA), which is one of the most commonly employed identification methods in organic chemistry, has also been subjected to attempts to combine it with GC, particularly after the intensive development of automatic instrumentation[1–13]. Nevertheless, only one such technique has found a commercial application[14,15], and there are a number of difficulties that have to be overcome in the realization of a practically utilizable instrumental arrangement. As the data that can be obtained from this coupling are as useful as those obtained from GC–MS, it deserves greater attention.

Some problems associated with the realization of the GC–EA coupling have been discussed earlier[12]. They involve mainly the design of the elemental analyzer, the reaction section, arrangements for the isolation and/or conservation of the individually chromatographically separated components or fractions, and lastly the method of processing the data obtained. We shall restrict ourselves here to the description of

a relatively inexpensive automatic instrumental version that is suitable for use with most commercial gas chromatographs, on the reaction section, providing for the determination of C, H, N and O with the precision usually required in EA, and finally on, the calculation of the percentage composition and the determination of empirical formulae without knowing the amount of substance being analyzed.

EXPERIMENTAL

The design of the instrument was based on experience obtained with an elemental analyzer based on the principle of frontal chromatography[12,16–19]. Extensive alterations were made to the previously employed arrangement[12]. The operation of the elemental analyzer was completely automated, and the analyzer utilizes the column oven, detectors and katharometer of a Shimadzu GC-4APTF gas chromatograph. A stream splitter was connected to the outlet of the chromatographic column, by means of which a small fraction of the effluent from the column is led to a flame-ionization detector (FID) while the larger fraction is led by means of a system of diaphragm valves into the atmosphere or into the reactor of the elemental analyzer. The diaphragm valves in the system and in the face of the dilution chamber of the elemental analyzer are operated by the pressure of the carrier gas by means of three-way solenoid valves situated outside of the analyzer. The operation of the valves is automated according to a programme. A flow diagram of the equipment is shown in Fig. 1.

The carrier gas (helium) is led into the gas chromatograph via a pressure controller (1) and, after splitting the stream by flow controllers (2 and 3), it flows through chromatographic columns (4 and 5) into a dual FID (6). The components separated by GC enter a resistance splitter with pneumatic resistors (7 and 8), where 7 is much larger than 8. The smaller amount flows through resistor 7 into the FID, and the

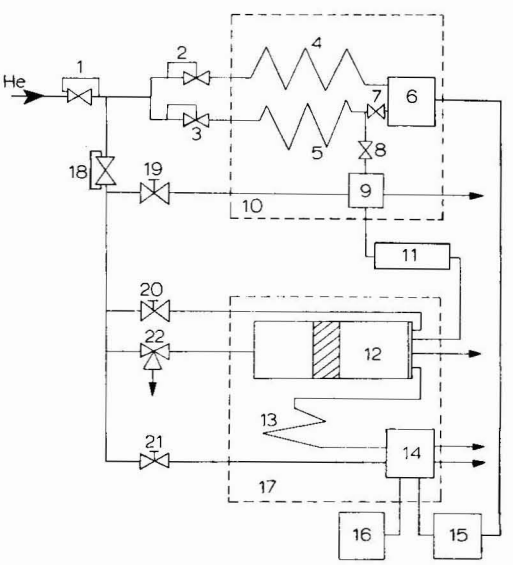


Fig. 1. Flow diagram of the equipment.

larger amount flows through resistor 8 into the system of diaphragm valves (9) and then either into the atmosphere or into a reactor (11) and a dilution chamber (12).

The dilution chamber serves to dilute and collect the reaction products. After homogenization, the products are pushed out by a piston into a chromatographic column (13) and the measuring part of the katharometer (14), which is connected to a recorder (15) and a digital voltmeter (16). The dual-channel recorder (15) is also connected to the FID. The second stream of carrier gas is led from the pressure controller (1) (*ca.* 5 kg/cm^2) into another pressure controller (18) (*ca.* 1.2 kg/cm^2), then via a needle valve (19) into the system of diaphragm valves (9), and, further, via another needle valve (20) into the diaphragm valve in the face of chamber 12, a three-way solenoid valve (22) and then into the space behind the piston of chamber 12 or into the atmosphere and, finally, via a needle valve (21) into the reference part of the katharometer (14). In the main thermostat (10) are situated chromatographic columns 4 and 5, the FID (6), resistors (7 and 8) and diaphragm valves (9). In the other thermostat (17), originally intended for thermostatting detectors, *i.e.*, the katharometer and the FID, are situated the basic elements of the frontal gas chromatograph: the dilution chamber (12), chromatographic column (13) and katharometer (14), the last item being part of the original gas chromatograph. The thermostat maintains the temperature with a precision of $\pm 0.1°$.

Columns 4 and 5 are 2 m × 3 mm I.D., packed with Chromosorb W, 60–80 mesh, coated with 10% of Apiezon L, and maintained at 100°. Resistors 7 and 8 are made of metal capillaries. The interconnections of the diaphragm valves 9 are indicated in Fig. 2.

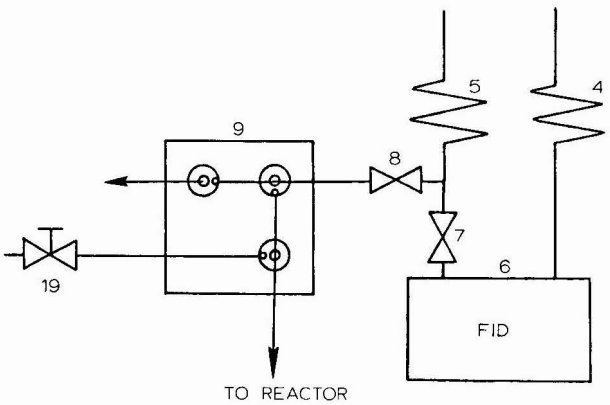


Fig. 2. Detailed scheme of the stream splitter and the valve system.

These valves, and also those in the face of the dilution chamber (12) are operated by three-way solenoid valves, which supply helium at a pressure of 2–3 kg/cm^2 to the membranes and/or release the helium into the atmosphere. Reactor 11 is a silica tube, 15 cm × 10 mm I.D., which in the case of C,H,N analysis is filled with a layer of about 10 cm of copper(II) oxide wire and a 5-cm layer of copper and kept at 850°. In the analysis of C and O, where use is made of the reduction conversion of organic compounds into methane and water, the tube is filled with a nickel catalyst[20] and maintained at 450°. Before entering the reactor, the helium is mixed with hydrogen in the ratio of about 2:1 (30 and 60 ml/min, respectively). The mixture of gases leaving

the reactor enters a capillary made of a melt of palladium and silver (1 m × 1 mm I.D.), coiled into a spiral and maintained at 500°, in order to remove hydrogen from the reaction mixture by diffusion. The dilution chamber (12) consists of a glass cylinder of volume 100 ml with a silanized inner surface, inside which is a stainless-steel piston with sealing rings of silicone rubber; the faces are made of brass. The chromatographic column (13) is 80 cm × 3 mm I.D., packed with Porapak Q, 80–100 mesh.

The course of the chromatographic analysis is as usual; after their separation, the components leave the column (5) and are detected with the FID (6) and recorded with a recorder (15). A large proportion of the components is vented via the diaphragm valves (9). At the moment when EA of some components leaving the GC column is to be carried out, upon pushing a button and holding it during the recording of the corresponding peak the component passes through system 9 and enters the reactor 11 and then the frontal chromatograph. Upon releasing the button, an automatic cycle of EA is started; the purging of the contents of the reaction space into the dilution chamber is carried out with helium directed by a valve (19) to flow through system 9. The other components leaving the column are vented through system 9. It is possible to include in this circuit a separator for the isolation of virtually all of the components of the chromatogram and gradually to provide their EA.

RESULTS AND DISCUSSION

The most frequent group of substances that come into consideration in GC are those which contain C, H, N and O. EA of these elements places specific requirements on the reaction section. Thus, C,H,N analysis is carried out after the complete oxidation of the sample, usually with the aid of a catalyst. The determination of O can be performed either after the conversion of the sample into carbon monoxide on a carbon catalyst or after its hydrogenation to water. We chose the second alternative, *i.e.*, hydrogenation on nickel, in which simultaneously all of the oxygen and carbon in the sample are converted into water and methane, respectively. As shown below, the simultaneous determination of O and C is very important in the determination of empirical formulae without knowledge of the amount of the sample.

A prerequisite in EA without knowledge of the amount of the sample is knowledge of the proportions of all of the elements in the sample being analyzed. The calculation proper is based on the determination of the relative proportions of the individual atoms[21]. If the empirical formula $C_aH_bN_cO_d$ is to be obtained, the percentage contents of the individual atoms are divided by the appropriate atomic weights. The results so obtained are then divided by the smallest of them and, if necessary, multiplied by a small integer (usually 2 or 3) so as to obtain the empirical formula in the form of integers. Further, the ratio of the atoms is related to a particular one of them, usually N (or C with substances that do not contain nitrogen).

Thus, in the case of C,H,N analysis, we obtain for the individual subscripts

$$a = \frac{\%C \cdot 14.0067}{12.01115 \cdot \%N}$$

$$b = \frac{\%H \cdot 14.0067}{1.00797 \cdot \%N}$$

$$c = 1$$

If we substitute for $\%X$, where X represents the individual atoms, from the relationship

$$\%X = \frac{K_X (H_X - h_X)}{w}$$

K_X is the response factor of the given element, which is obtained by means of a standard compound of known percentage composition, employing the relationship

$$K_X = \frac{\%X_{st} \cdot w_{st}}{(H_X - h_X)_{st}}$$

where H represents the height of the integral record and/or the area or height of the peak corresponding to the analysis of the unknown, h represents the same quantities corresponding to the blank experiment and w is the sample weight. In this way, we obtain for the individual subscripts

$$a = 1.1661 \cdot \frac{(H_C - h_C) K_C}{(H_N - h_N) K_N}$$

$$b = 13.896 \cdot \frac{(H_H - h_H) K_H}{(H_N - h_N) K_N}$$

$$c = 1$$

It follows from the previous relationships that

$$\frac{K_C}{K_N} = \frac{\%C_{st} (H_N - h_N)_{st}}{\%N_{st} (H_C - h_C)_{st}}$$

and

$$\frac{K_H}{K_N} = \frac{\%H_{st} (H_N - h_N)_{st}}{\%N_{st} (H_H - h_H)_{st}}$$

so that

$$a = 1.1661 \cdot \frac{(H_C - h_C) \cdot \%C_{st} (H_N - h_N)_{st}}{(H_N - h_N) \cdot \%N_{st} (H_C - h_C)_{st}}$$

$$b = 13.896 \cdot \frac{(H_H - h_H) \cdot \%H_{st} (H_N - h_N)_{st}}{(H_N - h_N) \cdot \%N_{st} (H_H - h_H)_{st}}$$

$$c = 1$$

We have obtained in this way the atomic ratios in the empirical formula for C,H,N without the necessity of knowing the weights of the charges of sample and standard.

An analogous procedure is followed if the substance does not contain nitrogen, *i.e.*, in C,H analysis. In this instance, the number of hydrogen atoms is usually related to the number of carbon atoms, so that

$$a = 1$$

$$b = 11.9162 \cdot \frac{(H_H - h_H) K_H}{(H_C - h_C) K_C}$$

As

$$\frac{K_H}{K_C} = \frac{\%H_{st}\,(H_C - h_C)_{st}}{\%C_{st}\,(H_H - h_H)_{st}}$$

we have

$$a = 1$$

$$b = 11.9162 \cdot \frac{(H_H - h_H) \cdot \%H_{st}\,(H_C - h_C)_{st}}{(H_C - h_C) \cdot \%C_{st}\,(H_H - h_H)_{st}}$$

As for the analysis of oxygen, this is based on an entirely different reaction principle compared with C,H,N analysis. If the ratio of O to C,H,N is to be determined, it is necessary to determine simultaneously with oxygen some of the other three elements. As carbon is virtually universal in this respect, we chose hydrogenolysis on nickel for the simultaneous determination of carbon and oxygen.

When proceeding in an analogous manner to the procedures considered above and relating the number of carbon atoms to those of oxygen, we obtain

$$a = 1.3320 \cdot \frac{(H_C - h_C)\,K_C}{(H_O - h_O)\,K_O}$$

$$d = 1$$

As

$$\frac{K_C}{K_O} = \frac{\%C_{st}\,(H_O - h_O)_{st}}{\%O_{st}\,(H_C - h_C)_{st}}$$

we have

$$a = 1.3320 \cdot \frac{(H_C - h_C) \cdot \%C_{st}\,(H_O - h_O)_{st}}{(H_O - h_O) \cdot \%O_{st}\,(H_C - h_C)_{st}}$$

$$d = 1$$

The determination of the empirical formula can suffer from an uncertainty in the value found, especially for hydrogen in C,H,N analysis. In this instance, the determination of the empirical formula is usually related to nitrogen, the atomic ratio of which to hydrogen is small. Therefore, in questionable cases it is expedient to complement the determination by another one referred to carbon, which is usually represented by a larger number of atoms in the molecule. Obviously, the corrected result for carbon from the first determination is used, rounded off to an integral value. At the same time, the rule is observed according to which a substance containing an even number of odd-valent atoms in the molecule cannot contain an odd number of hydrogen atoms.

Tables I and II give examples of C,H,N and C,H,O analyses for various types of compounds using the above procedures. Fig. 3 shows a record of EA of oxygen and carbon. This record differs from an exclusively frontal one, such as that in C,H,N analysis[18,19], for instance, in that it is a mixed frontal–elution record, obtained as a result of a shorter charging time (2 min).

TABLE I

EXAMPLE OF C,H,N ANALYSIS

Standard: pyridine (average of four determinations)

Compound	*Response (μV)*			*Number of atoms referred to N*			*Number of atoms referred to C*	
	N	*C*	*H*	*N*	*C*	*H*	*C*	*H*
Aniline (C_6H_7N)	90	1188	259	1	5.98	7.15	1	1.19
	99	1304	264	1	5.97	6.63	1	1.11
	83	1095	218	1	5.97	6.53	1	1.09
	99	1312	277	1	6.00	6.96	1	1.16
3-Picoline (C_6H_7N)	127	1658	346	1	5.91	6.77	1	1.14
	105	1382	302	1	5.96	7.15	1	1.20
	121	1593	361	1	5.98	7.41	1	1.23
	121	1607	367	1	6.02	7.53	1	1.25

TABLE II

EXAMPLE OF C,H,O ANALYSIS

Standard: acetone (average of two determinations)

Compound	*Response (μV)*		*Number of atoms referred to O*		*Response (μV)*		*Number of atoms referred to C*	
	C	*O*	*O*	*C*	*C*	*H*	*C*	*H*
Diethyl ketone	865	106	1	5.16	2933	1324	1	1.99
($C_5H_{10}O$)	905	112	1	5.11	3002	1370	1	2.02
	1105	139	1	5.03	3034	1374	1	2.00
	1026	130	1	4.99	3025	1373	1	2.00
Methyl isobutyl	2259	353	1	5.89	3181	1450	1	2.01
ketone ($C_6H_{12}O$)	2379	368	1	5.95	3250	1493	1	2.03
	2136	335	1	5.87	3230	1480	1	2.02
	2230	350	1	5.87	2977	1358	1	2.01

The method described for EA of GC effluents without knowing their amounts offers a number of possibilities. The possibility of rounding off the results to integral values in the determination of empirical formulae makes it possible, to a certain extent, to carry out the determination with a lower precision. The size of the sample is limited only by the detector sensitivity, stability of the conditions and/or the sorption properties of the analytical system with respect to some of the compounds being analyzed (water for instance). In our work, it was possible to analyze, with an acceptable precision, as little as 10 μg of a substance.

The extension of the method to other elements (sulphur for example) is a question of the choice of a suitable reaction system. However, the procedure would remain analogous to that described for the analysis of C,H,N and O,C.

The determination of the molecular formulae from empirical formulae (if they are not identical) is a matter of the use of the elution chromatographic data of the substances being analyzed.

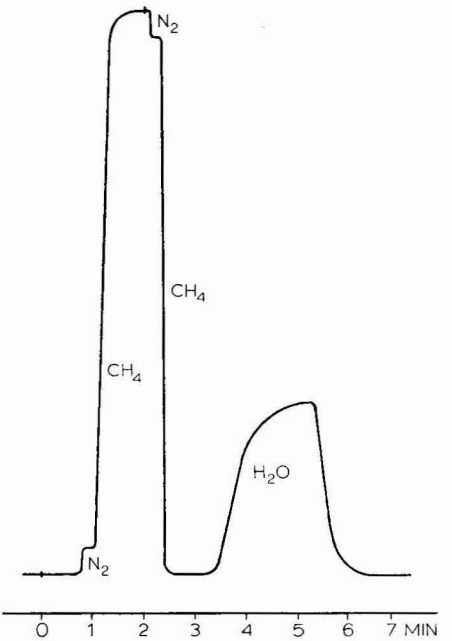


Fig. 3. Frontal elution record of an analysis of oxygen and carbon.

The practical utilization of the possibilities outlined above requires coupling of the analytical system described with a small computer and/or a programmable calculator with a digital output and record.

REFERENCES

1 F. Cacace, R. Cipollini and G. Perez, *Science*, 182 (1960) 1253.
2 F. Cacace, R. Cipollini, G. Perez and E. Possagno, *Gazz. Chim. Ital.*, 91 (1961) 804.
3 F. Cacace, R. Cipollini and G. Perez, *Anal. Chem.*, 35 (1963) 1348.
4 E. P. Skornyakov, *Aut. Cert. SSSR*, 155,026 (1962); *Byull. Izobr.*, No 11 (1963).
5 I. A. Revelśkii, R. I. Borodulina and T. D. Khokhlova, *Neftekhimiya*, 4 (1964) 624.
6 I. A. Revelśkii, R. I. Borodulina, T. M. Sovakova and V. G. Klimanova, *Dokl. Akad. Nauk SSSR*, 159 (1964) 861.
7 I. Klesment, *Izv. Akad. Nauk Est. SSR*, 15 (1966) 436.
8 R. H. Reitsema and N. L. Allphin, *Anal. Chem.*, 33 (1961) 355.
9 F. H. Huyten and G. W. A. Rijnders, *Z. Anal. Chem.*, 205 (1964) 244.
10 J. Franc and J. Pour, *J. Chromatogr.*, 32 (1968) 2.
11 S. A. Liebman, D. H. Ahlstrom, T. C. Creighton, G. D. Pruder, R. Averitt and E. J. Levy, *Anal. Chem.*, 44 (1972) 1411.
12 V. Rezl, B. Kaplanová and J. Janák, *J. Chromatogr.*, 65 (1972) 47.
13 V. G. Berezkin and V. S. Tatarinskii, *Zh. Anal. Khim.*, 25 (1971) 398.
14 S. A. Liebman, D. H. Ahlstrom, C. D. Nauman, G. D. Pruder, R. Averitt and E. J. Levy, *Res. Develop.*, 23 (1972) 24.
15 S. A. Liebman, D. H. Ahlstrom, T. C. Creighton, G. D. Pruder and E. J. Levy, *Thermochim. Acta*, 5 (1973) 403.
16 V. Rezl, *Microchem. J.*, 15 (1970) 381.
17 V. Rezl, *J. Chromatogr. Sci.*, 10 (1972) 419.
18 V. Rezl and B. Kaplanová, *Mikrochim. Acta*, i (1975) 493.
19 V. Rezl and J. Uhdeová, *Int. Lab.*, (1976) 11.
20 B. N. Dolgov, *Kataliz v Organicheskoi Khimii*, Goskhimizdat, Leningrad, 1959, p. 288.
21 E. Häberli, *Mikrochim. Acta*, (1973) 597.

Journal of Chromatography, 126 (1976) 731–740
© Elsevier Scientific Publishing Company, Amsterdam — Printed in The Netherlands

CHROM. 9441

SEPARATION OF CARBOHYDRATES ON A NEW POLAR BONDED PHASE MATERIAL

FREDRIC M. RABEL, ARTHUR G. CAPUTO and EDWARD T. BUTTS
Whatman Inc., Clifton, N.J. 07014 (U.S.A.)

SUMMARY

The separation of a number of carbohydrates on Partisil-10 PAC, a 10-μm silica gel with a permanently bonded polar phase, is described. The basic mobile phase is acetonitrile–water, but various acids or salts may be added to the aqueous portion to change the selectivity of the separation. A study of the effect of H_3PO_4, HCl, $HClO_4$, KH_2PO_4, and sodium acetate on the separation of mono-, di-, and trisaccharides is discussed and chromatograms of several real sample solutions are shown.

INTRODUCTION

For researchers involved in biochemistry or in the food industry, carbohydrate analysis continues to grow in importance. Previous analysis of this class of compounds was slow and quite unsatisfactory. Such separations were performed on cellulose or ion-exchange resins and frequently required detection by colorimetric derivatization after chromatography[1]. The most recent work with ion-exchange resins has involved the use of various counter-ions and elution with water or ethanol–water to accomplish partition separations of carbohydrates[2–6]. Fortunately for the analytical chemist of today, recent developments in the technology of packings for high-performance liquid chromatography (HPLC) have led to faster and more selective media for the carbohydrate separation. In the past two years researchers have been reporting on carbohydrate separations on these new, stable, siloxane-bonded media for HPLC[7–9]. Aside from a recent paper by Schwarzenbach[10], in which a 3-aminopropyl-bonded phase gave carbohydrate separations, very little information has been reported on the chemistry of these new packings or the mechanism of the separation. Indeed, reference is made to "reversed-phase partition" chromatography in such separations when, actually, normal-phase partition chromatography appears to be the mode of separation[9].

Because of the selectivity changes possible by varying the mobile phase, only one polar bonded phase is necessary for normal-phase partition chromatography. Historically, the most useful polar bonded phases have been ether, cyano, and amino; so, a complex bonded phase which would give the best features of each was developed. The product was named Partisil-10 PAC and is a most versatile packing for normal

partition LC. Much work is being done on this stationary phase to separate polar solutes by eluting with heptane modified with ethanol, acetonitrile, or chloroform. This study deals, however, with the novel separations possible on Partisil-10 PAC of a number of carbohydrates using combinations of acetonitrile and water as eluent.

EXPERIMENTAL

Apparatus and material

The liquid chromatograph used for this study consisted of the following components: a Varian Model 4000 cylinder pump (Palo Alto, Calif., U.S.A.); a Whatman LIC syringe septum injector (Clifton, N.J., U.S.A.); a Hamilton No. 702 (25-μl) syringe (Reno, Nev., U.S.A.); a Whatman Partisil-10 PAC PXS 10/25 column; a Laboratory Data Control refractive index detector (Riviera Beach, Fla., U.S.A.); and a Varian Model A-25 recorder.

The carbohydrate chromatographic standards were purchased from ICN Nutritional Biochemicals (Cleveland, Ohio, U.S.A.). Acetonitrile was distilled-in-glass, manufactured by Burdick and Jackson Labs. (Muskegon, Mich., U.S.A.). The salts and acids were from J. T. Baker (Phillipsburg, N.J., U.S.A.). The maple sugar sample was obtained from Laboratoire de Chimie, Complexe Scientifique (Ste. Foy, Quebec, Canada). The soybean extract was donated by Professor P. A. Sieb, Kansas State University. Hycal® is a product of Beecham Labs., Brentford, Great Britain. Coca-Cola® is a product of the Coca-Cola Bottling Co., Atlanta, Ga., U.S.A. Sweet 'n Low® is a product of the Cumberland Packing Corp., Brooklyn, N.Y., U.S.A. All other foodstuffs were obtained from local stores.

Preparation of the Partisil-10 PAC columns

The Partisil-10 PAC packing is made by reacting various organochlorosilanes with Partisil-10, but the details of this reaction are proprietary. To prepare properly packed columns, Partisil-10 PAC is slurried with chloroform–methanol (4:1) (1 g packing/10 ml) and pumped at 10,000 p.s.i. from a reservoir into a 25 cm $\times$ 1/4 in. O.D. $\times$ 4.6 mm I.D. seamless, smooth-bore, 316 stainless-steel column. The column fittings are zero dead volume (ZDV) fittings containing a removable 1/4-in. diameter, 2-μm porosity, 316 stainless-steel frit. Only columns reaching a minimum efficiency of 15,000 plates/m ($H = 0.067$ mm) with a standard test mixture of carbon tetrachloride, benzene, and naphthalene with a mobile phase of heptane are used in this study. All Partisil-10 PAC columns are activated with ethanol, acetone, ethyl acetate, 1,1,1-trichloroethane, and heptane before testing. Details of the drying procedure are given elsewhere[11].

RESULTS AND DISCUSSION

Initial separations of carbohydrate samples on Partisil-10 PAC showed poor separations of components with methanol–water mobile phases. It was considered that the less polar character of acetonitrile might be a better solvator of the bonded phase and allow greater selectivity. Acetonitrile–water combinations, indeed, did have much better selectivity, but with the disadvantage of peak tailing. Phosphoric acid was added to the mobile phase to bring its pH to 5.0, which eliminated much,

and sometimes all, of the tailing. Fig. 1 shows a variety of mono- and disaccharides separated with this mobile phase. High-molecular-weight saccharides were eluted by increasing the water content of the mobile phase (Fig. 2 and Table I), suggesting separation by normal-phase partition chromatography rather than reversed-phase partition chromatography. At any given mobile phase composition, a plot of k' *versus* chain-length of the carbohydrate produces a straight line. A similar relationship was reported by Havlicek and Samuelson[3], who also found the slope to be related to both the concentration of ethanol in the mobile phase and the type of glycosidic linkage.

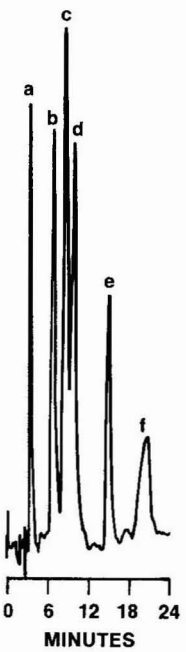


Fig. 1. Separation of mono- and disaccharides. Column, 25 cm × 4.6 mm I.D., Partisil-10 PAC PXS 10/25; mobile phase, acetonitrile–water (80:20), pH 5.0 with H_3PO_4; flow-rate, 1.3 ml/min; pressure, 350 p.s.i.; detection, refractive index, × 0.04. a = Solvent front; b = xylose; c = fructose; d = glucose; e = sucrose; f = lactose.

Because of the complex structure of the Partisil-10 PAC bonded phase, the effect of varying pH on the selectivity for the carbohydrate separation was studied. Table II shows the k' values of the carbohydrates when making pH changes on Partisil-10 PAC using phosphoric acid and potassium hydroxide. No apparent trend in the change of k' with pH was noted except that at a pH of 5.0, a minimum k' value was frequently encountered. The general peak shape was rated on a relative scale from excellent to poor (Table II) and was found to be best for the largest number of carbohydrates at a pH of 5.0. Accordingly, pH 5.0 is considered optimal and was used exclusively in this study.

Because various anions might interact with the Partisil-10 PAC bonded phase and with the carbohydrates (*i.e.*, borate), the effect of a number of acids and salts at

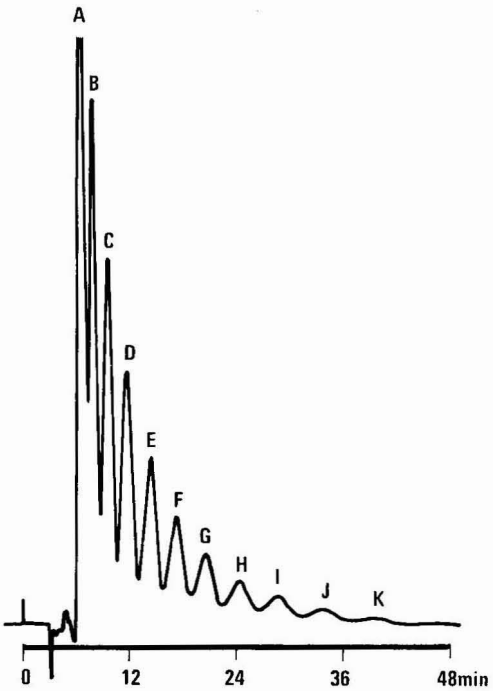


Fig. 2. Separation of oligosaccharides. Column, 250 mm × 4.6 mm I.D., Partisil-10 PAC; mobile phase, acetonitrile–0.0025 *M* $NaC_2H_3O_2$ (65:35), pH 5.0 with acetic acid. Flow-rate, 65 ml/h; pressure, 400 p.s.i.; detection, refractive index, 6.4×10^{-4}. Sample: Hycal; 25 μl of pure sample injected. A = Glucose (mono); B = maltose (di); C = trisaccharides; D = tetrasaccharides; E = pentasaccharides; F = hexasaccharides; G–K = higher saccharides.

TABLE I

CAPACITY FACTORS (k') OF OLIGOSACCHARIDES WITH CHANGES IN CONCENTRATION OF ACETONITRILE

All mobile phases are ratios of acetonitrile–0.0025 *M* sodium acetate, pH 5.0 with acetic acid.

Saccharide	*Mobile phase ratio*		
	70:30	*65:35*	*60:40*
Glucose (mono)	0.35	0.30	0.13
Maltose (di)	1.22	0.55	0.50
Trisaccharide	1.97	0.95	0.75
Tetrasaccharide	3.05	1.45	1.00
Pentasaccharide	4.51	1.95	1.25
Hexasaccharide	5.03	2.60	1.50
Heptasaccharide	7.92	3.30	1.88
Octasaccharide	*	4.15	2.13
Nonasaccharide	*	5.05	2.51
Decasaccharide	*	6.20	2.88

* Peaks too broad to measure accurately.

TABLE II

CAPACITY FACTORS (k') OF CARBOHYDRATES WITH CHANGE IN pH

All systems have a mobile phase of acetonitrile–water in the ratio 75:25. Key for peak evaluation: Ex = excellent, VG = very good, G = good, F = fair, P = poor.

Carbohydrate	*pH 3.0 with H_3PO_4*	*pH 5.0 with H_3PO_4*	*pH 6.1 distilled water*	*pH 7.1 with KOH*
Xylose	1.18 Ex	1.16 Ex	1.17 G	1.19 Ex
Arabinose	1.47 G	1.42 G	1.36 G	1.44 G
Ribose	0.94 Ex	0.89 Ex	0.86 Ex	0.88 Ex
Lyxose	1.02 Ex	1.12 Ex	1.06 Ex	1.00 Ex
Fucose	0.94 and 1.22 P	1.02 and 1.22 P	1.00 and 1.24 P	1.00 and 1.24 P
Fructose	1.59 Ex	1.53 Ex	1.42 Ex	1.44 Ex
Mannose	1.49 G	1.58 G	1.61 F	1.59 Ex
Glucose	1.83 F	1.84 G	1.91 F	1.83 F
Galactose	2.06 and 2.35 P	1.93 and 2.26 P	2.00 and 2.35 P	1.83 and 2.16 P
Sucrose	3.18 Ex	2.92 Ex	3.32 Ex	2.81 Ex
Maltose	3.67 P	3.47 G	3.60 P	3.67 P
Lactose	4.11 F	3.86 G	4.26 P	4.11 F
Melibiose	5.22 F	4.05 F	5.47 P	5.00 F
Cellobiose	3.55 F	3.47 G	3.63 P	3.50 F
Raffinose	6.94 G	7.26 VG	7.78 G	7.53 VG

a pH of 5.0 and at fixed ionic strength was investigated. The results of the acid-modified mobile phases are also summarized in Table III. Very small quantities of acid were necessary to adjust the pH (approximately 10^{-6} M). The water is pH adjusted with the acid before mixing with the acetonitrile. Again, no consistent trend with the various acids tested is observed except that nine of the fifteen carbohydrates have their greatest retention with the perchloric acid-modified mobile phase.

The effect of anions from the salts, KH_2PO_4 and sodium acetate, on the separation are noted in Table IV. As with the addition of different acids, these salts change the retention of the carbohydrates. Capacity factors are consistently equal to or less than those obtained with only phosphoric acid added to the mobile phase. In the case of the disaccharides, maltose, and cellobiose, dilute phosphoric acid in the mobile phase gives no separation. With KH_2PO_4 in the mobile phase, cellobiose elutes before maltose; however, with sodium acetate in the mobile phase, maltose elutes before cellobiose.

The most obvious trend, seen in Tables II–IV, is that each type of carbohydrate falls within a specific k' region with any given mobile phase. Martinsson and Samuelson[2] found a similar elution pattern from their partition separations on ion-exchange/ethanol–water systems. Thus, from Table II, the pentoses (xylose, arabinose, ribose, lyxose, fucose) have k' values between 0.94 and 1.47 at a pH of 3; the hexoses (fructose, mannose, glucose, galactose), between 1.49 and 2.35 at a pH of 3; and the disaccharides, between 3.18 and 5.22 at a pH of 3. Similar distinct ranges are noted with all of the mobile phases tried.

Goulding[5] reported the separation of α- and β-anomers of certain carbohydrates in his work. In this study, distinct doublets were noted for fucose and galactose and were attributed to the anomers (see Tables II–IV). Authentic samples

TABLE III

CAPACITY FACTORS (k') OF CARBOHYDRATES WITH CHANGES IN ACID USED TO ADJUST pH

All systems have a mobile phase of acetonitrile–water in the ratio 75:25, pH 5.0. Key for peak evaluation, see Table II.

Carbohydrate	H_3PO_4	$HClO_4$	HCl	$HOAc$*	H_3BO_3*
Xylose	1.16 Ex	1.11 G	1.12 Ex	1.13 Ex	1.07 Ex
Arabinose	1.42 G	1.39 F	1.22 G	1.38 G	1.36 Ex
Ribose	0.89 Ex	0.94 Ex	0.74 Ex	0.86 Ex	0.33 G
Lyxose	1.12 Ex	1.11 Ex	0.98 Ex	1.08 Ex	1.00 VG
Fucose	1.02 and	1.06 and	1.13 and	1.00 and	1.07 G
	1.22 P	1.28 P	1.34 P	1.21 P	
Fructose	1.53 Ex	1.53 Ex	1.44 Ex	1.44 Ex	–
Mannose	1.58 G	1.53 G	1.55 G	1.35 F	1.44 G
Glucose	1.84 G	2.06 F	1.78 F	1.53 Ex	1.54 Ex
Galactose	1.93 and	2.06 and	1.83 and	1.59 and	2.02 VG
	2.26 P	2.26 P	2.17 P	1.76 P	
Sucrose	2.92 Ex	3.06 Ex	3.02 Ex	2.40 Ex	2.80 Ex
Maltose	3.47 G	4.06 F	3.56 F	2.63 Ex	2.82 VG
Lactose	3.86 G	4.28 F	3.89 F	3.06 Ex	3.08 VG
Melibiose	4.05 F	5.28 F	4.89 F	3.55 G	3.47 F
Cellobiose	3.47 G	3.78 F	3.44 F	2.73 Ex	2.59 VG
Raffinose	7.26 VG	7.56 VG	7.06 VG	4.65 Ex	5.30 VG

* Added in proof.

TABLE IV

CAPACITY FACTORS (k') OF CARBOHYDRATES WITH ACETONITRILE WITH VARIOUS BUFFERS

All systems are 75% acetonitrile and 25% buffer. Key for peak evaluation, see Table II.

Carbohydrate	*0.0025 M* KH_2PO_4, *pH 5.0 with KOH*	*water, pH 5.0 with* H_3PO_4	*0.0025 M* $NaC_2H_3O_2$, *pH 5.0 with acetic acid*
Xylose	1.00 Ex	1.16 Ex	1.13 Ex
Arabinose	1.22 G	1.42 G	1.26 VG
Ribose	0.74 Ex	0.89 Ex	0.88 Ex
Lyxose	0.94 Ex	1.12 Ex	1.00 Ex
Fucose	0.94 and	1.02 and	0.94 and
	1.11 P	1.22 P	1.15 P
Fructose	1.26 Ex	1.53 Ex	1.40 Ex
Mannose	1.44 G	1.58 G	1.50 VG
Glucose	1.58 G	1.84 G	1.59 Ex
Galactose	1.89 and	1.93 and	1.93 P
	2.22 P	2.26 P	
Sucrose	2.61 Ex	2.92 Ex	2.28 Ex
Maltose	2.89 G	3.47 G	2.94 G
Lactose	3.59 G	3.86 G	3.35 VG
Melibiose	3.89 G	4.05 F	4.00 Ex
Cellobiose	2.60 Ex	3.47 G	3.13 Ex
Raffinose	6.00 Ex	7.26 VG	5.78 Ex

of anomers were not available for confirmatory studies, but other samples of these two carbohydrates exhibited the same doublet, with peak ratios being the same. Results of further work will be reported at a later date.

To demonstrate the range of application available for real carbohydrate samples on Partisil-10 PAC, a number of authentic samples which had been submitted for analysis were separated and their chromatograms given.

Lactose in whole milk is easily and reproducibly determined if the milk is first extracted with carbon tetrachloride to remove lipophilic material and a portion of the aqueous solution injected (Fig. 3). Samples of evaporated milk and low-fat milk gave similar chromatograms without this extraction step.

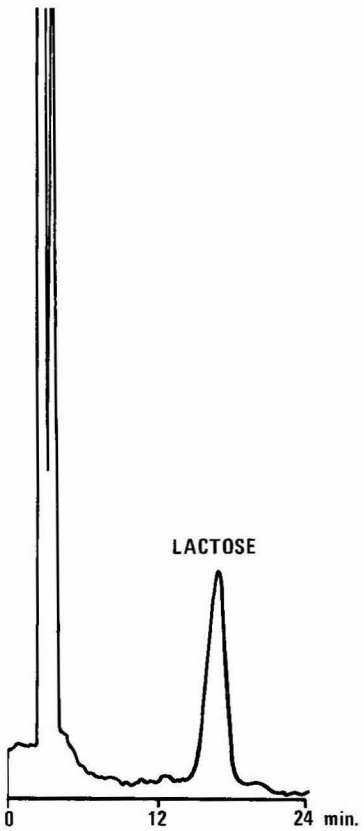


Fig. 3. Separation of lactose in whole milk. Column, 250 mm × 4.6 mm I.D., Partisil-10 PAC; mobile phase, acetonitrile–0.0025 *M* KH_2PO_4 (80:20), pH 5.0 with KOH; flow-rate 90 ml/h; pressure, 300 p.s.i.; detection, refractive index, × 0.02. Sample: Homogenized whole milk; fats removed by carbon tetrachloride extraction.

The quality control of beverages is simple, as exemplified in Fig. 4 by a sample of a cola, indicating the presence of fructose, glucose, and sucrose.

Natural products have to be closely monitored to detect dangerous or illegal adulterants, and the quality control of one such material is seen in Fig. 5, a sample

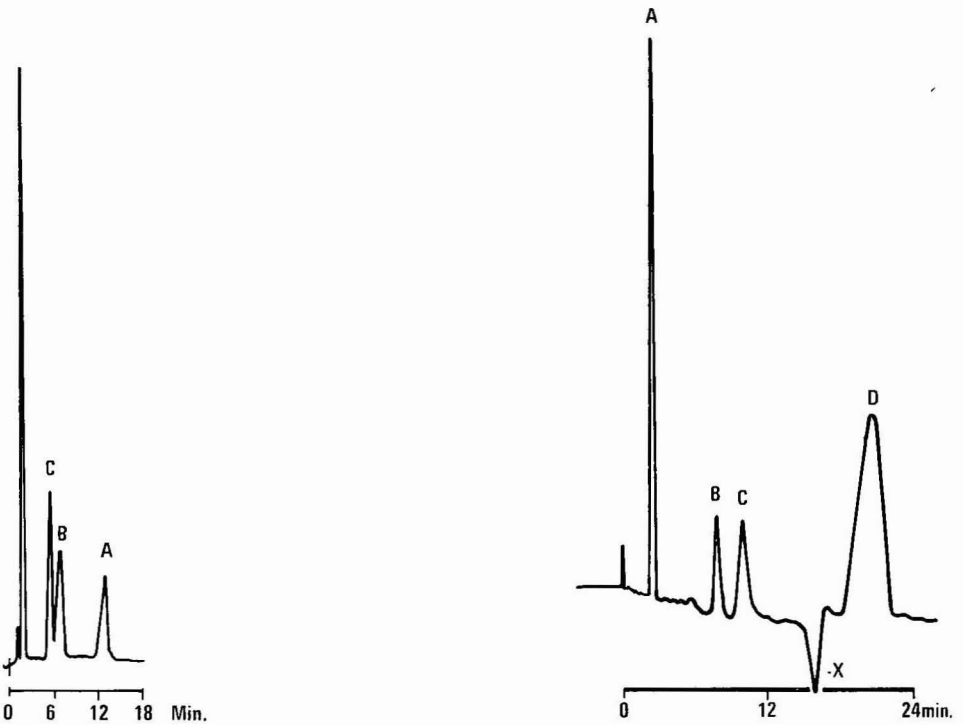


Fig. 4. Separation of carbohydrates in beverage. Column, 250 mm × 4.6 mm I.D., Partisil-10 PAC; mobile phase, acetonitrile–0.0025 *M* KH_2PO_4 (84:16), pH 5.0 with KOH; flow-rate, 110 ml/h; pressure, 375 p.s.i.; detector, refractive index, × 0.02. Amount injected: 7.0 μl. A = Sucrose; B = glucose; C = fructose.

Fig. 5. Separation of carbohydrates in maple sugar syrup. Column, 250 mm × 4.6 mm I.D., Partisil-10 PAC; mobile phase, acetonitrile–0.0025 *M* $NaC_2H_3O_2$, pH 5.0; flow-rate, 108 ml/h; pressure, 425 p.s.i.; detection, refractive index, 1.6×10^{-4}. Sample: pure maple sugar syrup; 25% of sample in water. A = Solvent front; B = fructose; C = glucose; D = sucrose; X = unidentified compound.

of pure maple sugar syrup. Component X is unidentified but is probably not a carbohydrate since it gives the only negative response on the refractive index detector that was observed throughout the study.

The food industry is supplementing traditional animal protein foods with vegetable protein in the form of soybean meal. The commonly occurring tetrasaccharide, stachyose, in soybean, however, causes gastric distress in humans and must be removed or reduced in concentration. The separation of a sample of soybean extract before any such removal is shown in Fig. 6.

Because people have to satisfy their "sweet tooth" yet want lower-calorie intakes, many artifical sweeteners have become available in recent years. Lactose is substituted for sucrose in such preparations. Fig. 7 shows the separation of lactose from saccharin in one commercially available artificial sweetener. A UV monitor placed in series with the refractive index monitor would allow for more sensitive detection of saccharin.

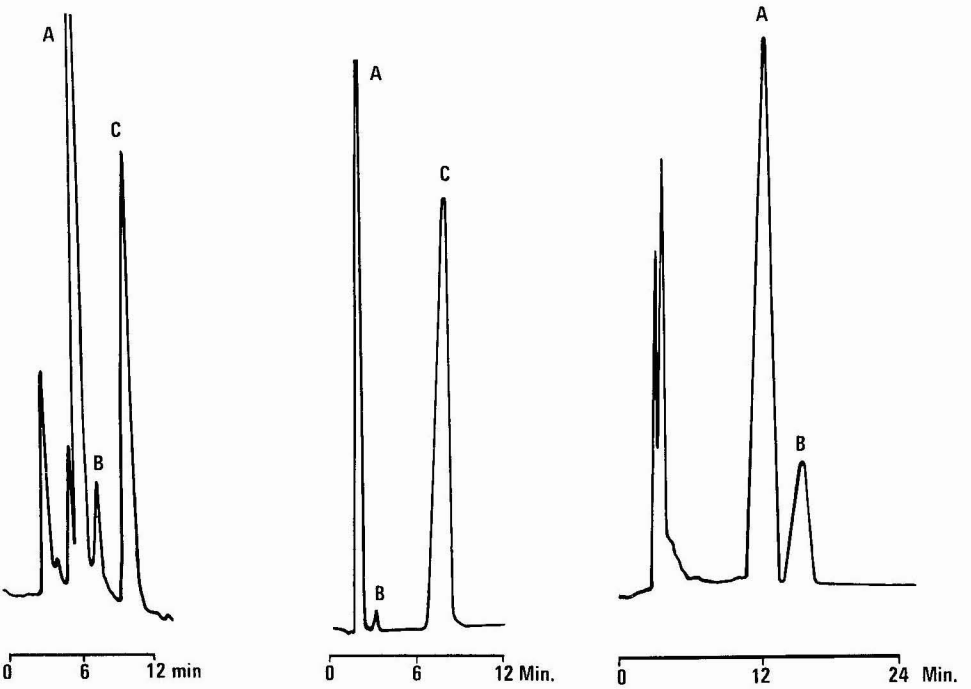


Fig. 6. Separation of carbohydrates in soybean extract. Column, 250 mm × 4.6 mm I.D., Partisil-10 PAC; mobile phase, acetonitrile–0.0025 *M* KH_2PO_4 (70:30), pH 5.0 with KOH; flow-rate, 70 ml/h; pressure, 300 p.s.i.; detector, refractive index, × 0.02. Sample: Soybean extract. A = Sucrose, 280 μg; B = raffinose, 84 μg; C = stachyose, 280 μg.

Fig. 7. Separation of carbohydrate in artificial sweetener. Column, 250 mm × 4.6 mm I.D., Partisil-10 PAC; mobile phase, acetonitrile–0.0025 *M* KH_2PO_4 (75:25), pH 5.0 with KOH; flow-rate, 92 ml/h; pressure, 465 p.s.i.; detector, refractive index, × 0.01–0.04. Sample: Sweet 'n Low®, 1 g/10 ml water. A = Solvent; B = saccharine, × 0.01; C = lactose, × 0.04.

Fig. 8. Separation of carbohydrates in intravenous high-calorie electrolyte solution. Column, 250 mm × 4.6 mm I.D., Partisil-10 PAC; mobile phase, acetonitrile–0.002 *M* KH_2PO_4, pH 5.0 with KOH; flow-rate, 90 ml/h; pressure, 250 p.s.i.; detection, refractive index, × 0.04; injected amount, 10 μl. A = Fructose; B = glucose.

Some hospitalized patients are given life-sustaining intravenous solutions; therefore, the quality control of such solutions is most important to pharmaceutical companies, the federal regulatory agencies, and the patients. Fig. 8 illustrates a separation, capable of precise quantitation and high reproducibility, of one such solution.

CONCLUSION

The separation of carbohydrates on Partisil-10 PAC with acid- or salt-modified acetonitrile/water combinations has been shown. This adjustment of pH or use of various anions in the mobile phase allows optimization of the separation but the mechanism of the observed changes with such modifiers is not clear, at present, since no distinct trends are noted. Complexation of the modifiers with the bonded phase or with the carbohydrates may be responsible, but further work will have to be per-

formed to furnish information upon which such a theory could be based. It was observed that the various classes of carbohydrates do fall within certain capacity factor ranges with any of the mobile phases used, as other researchers have found with similar chromatographic systems.

One of the advantages of performing separations in the partition mode is the improved column stability since interfering sample components seldom bond to the support. Filtration of samples is frequently the only clean-up step required in using the Partisil-10 PAC. The accompanying chromatograms show the applicability of this polar bonded phase to the separation of real samples containing carbohydrates using the refractive index detector. Only in the separation of the carbohydrate lactose in whole milk was an extra step (an extraction with carbon tetrachloride) used before sample injection.

ACKNOWLEDGEMENTS

We would like to thank Dr. I. Fagerson for his discussions about carbohydrates and D. Southern for his help with the manuscript.

REFERENCES

1 K. Čapek and J. Staněk, Jr., in Z. Deyl, K. Macek and J. Janák (Editors), *Liquid Column Chromatography —A Survey of Modern Techniques and Applications*, Elsevier, Amsterdam, Oxford, New York, 1975, p. 465.
2 E. Martinsson and O. Samuelson, *J. Chromatogr.*, 50 (1970) 429.
3 J. Havlicek and O. Samuelson, *Anal. Chem.*, 47 (1975) 1854.
4 J. Havlicek and O. Samuelson, *Carbohydr. Res.*, 22 (1972) 307; *Chromatographia*, 7 (1974) 361.
5 R. W. Goulding, *J. Chromatogr.*, 103 (1975) 229.
6 J. G. Lawrence, *Chimia*, 29 (1975) 367.
7 J. K. Palmer, *Anal. Lett.*, 8 (1975) 215.
8 J. C. Linden and C. L. Lawhead, *J. Chromatogr.*, 105 (1975) 125.
9 R. B. Meagher and A. Furst, *J. Chromatogr.*, 117 (1976) 211.
10 R. Schwarzenbach, *J. Chromatogr.*, 117 (1976) 206.
11 Whatman, *Care and Use of Partisil Columns*, Bulletin 112, Whatman, Clifton, N.J., 1976.

ENVIRONMENTAL APPLICATIONS OF GAS AND LIQUID CHROMATOGRAPHY

Journal of Chromatography, 126 (1976) 743–755
© Elsevier Scientific Publishing Company, Amsterdam — Printed in The Netherlands

CHROM. 9410

MICRODETERMINATION OF NITRATES AND NITRITES IN SALIVA, BLOOD, WATER, AND SUSPENDED PARTICULATES IN AIR BY GAS CHROMATOGRAPHY

JOHN W. TESCH, WILLIAM R. REHG and ROBERT E. SIEVERS
Department of Chemistry, University of Colorado, Boulder, Colo. 80309 (U.S.A.)

SUMMARY

A generally applicable method for the analysis of nitrates and nitrites has been used for a wide variety of samples, including human saliva, blood, drinking water, and airborne particulates. Aqueous nitrate ion is first converted to nitrobenzene by reaction with benzene (or another aromatic reactant) in the presence of a catalyst. The nitrobenzene is then quantitated by electron capture gas chromatography (GC–ECD). Nitrite ion and gaseous oxides of nitrogen can be determined also if such samples are treated appropriately prior to GC–ECD analysis. Other reactants such as 1,3,5-trimethoxybenzene can also be used in the place of benzene. The high sensitivity of ECD allows the quantitation of as little as 0.1 ppm (w/w) nitrate in a single drop of saliva or blood.

INTRODUCTION

It is well established that nitrites and secondary amines can react to form the highly carcinogenic nitrosamines, and that such reactions can occur under the conditions present in the human stomach[1]. For this reason the widespread use of nitrites and nitrates in meat processing is cause for concern; furthermore, a significant source of nitrites which find their way into the stomach is saliva itself[2]. Nitrate concentrations in human saliva are generally in the range of 5–60 ppm; and the presence of nitrate-reducing bacteria in the saliva causes nitrite to be formed, resulting in nitrite concentrations in the range of 6–10 ppm[2]. In view of the fact that the average person swallows approximately 1 l of saliva per day, these levels could be significant.

The presence of high concentrations of nitrate in drinking water can cause infant methemoglobinemia[3] and can also be correlated with high incidences of gastric cancer[4]. Furthermore, high levels of oxides of nitrogen in the ambient air in urban areas can be statistically correlated with high cancer rates; it is speculated that NO_x plays a role in the formation of atmospheric nitrosamines[5].

For these reasons and others, development of rapid, simple, and sensitive general techniques for the determination of nitrates and nitrites in a variety of matrices is essential. This paper details the extension and further development of the gas chro-

matographic (GC) technique for the analysis of nitrates that we and others have outlined in recent communications[6,7]. We have now refined and miniaturized the method so that determinations of sub-ppm levels of nitrate or nitrite can be performed with a single drop of saliva or blood. Furthermore, a sensitive method has been developed for measurement of nitrates and nitric acid present in and adsorbed on the surface of suspended particulates in ambient air.

EXPERIMENTAL

Apparatus

Chromatographic analyses were performed on Hewlett-Packard Models 402 and 5750 gas chromatographs, equipped with ^{63}Ni and titanium tritide electron capture detectors (ECD), respectively. The columns used contained 1.5% SE-30 coated on 80–100 mesh Chromosorb G, acid-washed, packed in either 76 cm × 4 mm I.D. glass tubing or 51 cm × 3 mm I.D. heavy-walled Teflon® tubing. Isothermal column temperatures between 100 and 150° were used for various experiments, and carrier gas flow-rates of 40–60 ml/min of argon–methane (90:10) were employed.

24-h airborne particulate samples were collected with a Precision Scientific Hi-Vol air sampler, which meets ASTM standard D2009. Specific ion electrode measurements were made using an Orion Model 93-07 nitrate ion electrode.

Reagents

Reagent grade sulfuric acid and thiophene-free reagent grade benzene were obtained from both Fisher Scientific (Pittsburgh, Pa., U.S.A.) and J. T. Baker (Phillipsburg, N.J., U.S.A.). Precautions noted in our previous paper with regard to sulfuric acid purity should be observed[7]. Both the benzene and the sulfuric acid were used without additional purification. Mallinckrodt (St. Louis, Mo., U.S.A.) Analytical Reagent grade 30% hydrogen peroxide, and nitrobenzene (Chem. Services, West Chester, Pa., U.S.A.) were employed. 1,3,5-Trimethoxybenzene (99%) (Aldrich, Milwaukee, Wisc., U.S.A.) was further purified by sublimation *in vacuo* at 40°. Reagent grade pentamethylbenzene was obtained from Eastman-Kodak (Rochester, N.Y., U.S.A.) and practical grade phenylmercuric acetate from Matheson, Coleman, and Bell (East Rutherford, N.J., U.S.A.). Potassium nitrate and nitrite, silver sulfate, sodium citrate, and urea were Analytical Reagent Chemicals from Mallinckrodt.

Other organic liquids were obtained from commercial sources and were distilled at least once prior to use. All other reagents were used without further purification.

Microanalysis procedure for nitrate and nitrite

The general procedure for microanalysis of nitrate and nitrite in aqueous media is as follows. For the determination of NO_3^-, a one-dram vial with a polyethylene stopper (Kimble No. 60975-L) was used as a reaction vessel. A 0.20-ml aliquot of aqueous sample was introduced into the vial, followed by 1.0 ml of benzene. The reaction was catalyzed by addition of 1.0 ml of concentrated sulfuric acid. The vial was then shaken for 10 min. The benzene layer was removed immediately from the reaction vial with a Pasteur pipette, placed in a separate vial, and analyzed by GC–ECD for the nitrobenzene concentration generated. Either 1- or 2-μl aliquots were injected. If the benzene is allowed to stand in contact with the acid for long periods, by-

products are formed and these appear in the chromatogram. Standard solutions of KNO_3 were treated in the same manner to generate a standard calibration plot relating nitrobenzene concentration to peak height. If higher precision is desired (approximately 4% relative standard deviation), 2,5-dimethylnitrobenzene can be added to the benzene prior to reaction as an internal standard (concentration 5×10^{-7} g/ml) to correct for differences in injection size, detector sensitivity, fluctuations, etc. When this internal standard was used, the peak heights of nitrobenzene were normalized to the peak heights of the standard before further data reduction.

Nitrite was determined by difference: a second identical sample was treated with an oxidant to convert NO_2^- to NO_3^-. Consequently, the concentration of nitrite plus nitrate is subsequently measured, so nitrite must be determined by difference. Specifically, the procedure used was to introduce 0.15 ml of the sample into the reaction vial, followed by addition of 0.05 ml of 0.1 *N* H_2O_2. The rest of the reaction procedure is the same as that for NO_3^-.

The general procedure outlined above, with appropriate modifications, was applied to the analysis of drop-sized biological samples. Analyses of drinking waters from several Colorado towns were also performed using the procedure above without modification. Because nitrate concentrations can be reduced by bacterial action, it is recommended that the drinking water samples be stabilized after collection by adding two drops of 1% phenylmercuric acetate per 100 ml of drinking water. As a demonstration of the efficacy of the GC–ECD method, identical drinking water samples were also analyzed for nitrate by standard ion-selective electrode procedures, described in the Orion instruction manual for the Model 93-07 nitrate ion electrode.

Saliva analysis

To analyze saliva for NO_3^-, 0.05 ml of 3×10^{-5} *M* phenylmercuric acetate was placed in a vial, which was then weighed. The subject expectorated directly into the vial and the vial was reweighed. The saliva was then diluted threefold with distilled water to obtain a more uniform sample and to lower the NO_3^- concentration to a range in which the ECD exhibits a more nearly linear response to the nitrobenzene generated. An aliquot (0.15 ml) of the saliva solution was then pipetted into the reaction vial, followed by 0.05 ml of saturated silver sulfate solution. The remainder of the procedure is identical to the general microtechnique described above. To analyze for NO_2^- plus NO_3^-, 0.05 ml of 0.1 *N* H_2O_2 was used in place of the silver sulfate above. By subtraction of the nitrate concentration determined without addition of H_2O_2, the nitrite concentration can be calculated.

Blood analysis

The following is a tentative method for the determination of nitrate in blood. A solution of 2% sodium citrate (0.05 ml) was placed in the bottom of a small test tube to prevent clotting of the blood. The test tube was then weighed. A drop of freshly drawn blood was placed directly into the test tube, and the test tube was reweighed. To the tube was added 0.1 ml of a 4% (w/v) $ZnSO_4$ solution followed by 0.5 g of solid Ag_2SO_4. The mixture was shaken well, and the tube was centrifuged for about 5 min. An aliquot (0.20 ml) of the supernatant liquid was transferred to the reaction vial and the general reaction procedure outlined above was followed.

Analysis for nitrate in airborne particulates

Particulate samples were collected on 20.3 × 25.4 cm glass fiber filter papers using a standard Hi-Vol air sampler. A cork borer (bore sizes Nos. 5–8) was used to cut out 0.90–1.72 cm^2 pieces of the glass fiber filter for NO_3^- analysis. This particulate "aliquot" was placed in a 125-ml glass-stoppered erlenmeyer flask, 2.0 ml of distilled water was added, followed by 10 ml of benzene and 10 ml of concentrated sulfuric acid and the flask was stoppered. The flask was shaken by hand one time (use eye protection), the stopper was carefully removed to relieve the pressure and then replaced. The flask was shaken for 10 min and the benzene layer was analyzed by chromatography by injection of 1- or 2-μl aliquots. For determination of nitrite plus nitrate, 2.0 ml of 0.1 *N* H_2O_2 should be used in place of the water above.

Use of organic reactants other than benzene

Other organic compounds such as toluene, *m*-xylene, *p*-xylene, anisole, 2,6-dimethylanisole, mesitylene, pentamethylbenzene, and 1,3,5-trimethoxybenzene (TMB) were also tested as possible reactants in preliminary experiments. Conditions were generally the same as those used with benzene, *i.e.*, 0.1–0.2 ml of sample was allowed to react with 1 ml of the organic compound and 1 ml of concentrated sulfuric acid (although in some cases less concentrated acid was used).

A suitable procedure for the determination of NO_3^- using TMB as a reactant has been developed. With this reactant a greater water:acid ratio can be used than with benzene; consequently, a larger aqueous sample can be taken, improving the effective sensitivity of the method. Equal volumes (0.5 ml) of aqueous sample and concentrated sulfuric acid were mixed in a 1-dram glass reaction vial and allowed to cool. TMB (0.1 g) was added and the vial held at 67° for 10 min in a bath. The vial was then shaken for 5 min while it cooled. One milliliter of benzene was added, the vial was shaken again for 5 min, and the benzene layer was drawn off with a pipette and analyzed by chromatography for the concentration of 1-nitro-2,4,6-trimethoxybenzene (NTMB). The identity of the NTMB peak was confirmed by comparison of retention times with a standard prepared according to Fukui *et al.*[8] and by gas chromatography–mass spectrometry. Under these conditions, none of the benzene used as an extractant is converted to nitrobenzene. Standard KNO_3 solutions treated in the same manner were used to generate a calibration plot.

RESULTS AND DISCUSSION

Microtechnique studies

The amount of benzene used for the microtechnique (1 ml) was chosen as being about the minimum amount that can be easily handled for separation and subsequent GC analysis. Although it must be carefully measured for quantitation, this amount is not a critical factor in the yield of nitrobenzene. The water:sulfuric acid ratio in the reaction is more important. Experiments in which the reaction yield was studied as a function of this ratio demonstrated the ratio 0.2 ml of water to 1.0 ml of sulfuric acid to be optimum. When volumes of water greater than 0.2 ml are used, the increased heat of mixing with the acid produces undesirable benzene pressure buildup inside the reaction vials. Although quantitative conversion of nitrate to nitrobenzene

can be obtained when water volumes up to 0.5 ml are used, it is necessary to secure the vial caps with tape to prevent them from being blown off.

It should be noted here that new, unused vials must be well cleaned prior to use. A suitable simple cleaning method is to put the vials through the same reaction procedure to be utilized later, substituting distilled water for the samples. The vials were then rinsed sequentially with hot water, distilled water, acetone, and distilled water, before introducing the samples to be analyzed.

The results of applying the microtechnique to the analysis of nitrate in several samples of drinking waters are summarized in Table I. In no case were detectable amounts of NO_2^- found. (The limit of detection for NO_2^- depends on the NO_3^- concentration, since NO_2^- is determined by difference. Generally a NO_2^- concentration which is 5% of the NO_3^- concentration can be detected.) In Table I the results are shown of a comparison study of the GC–ECD microtechnique *vs.* ion-selective electrode measurements (ISE). The close agreement (usually within 5%) of the totally independent methods used for the analysis of identical samples is an excellent demonstration of the efficacy of the methods. No significant interferences (such as high levels of chloride) were found in the drinking water samples. The EPA maximum allowable NO_3^- concentration in bottled drinking water is 45 ppm (w/v)[9].

TABLE I

COMPARISON OF ANALYSES OF DRINKING WATERS FOR NO_3^- CONCENTRATION BY GC–ECD AND ISE

Numerical designations refer to selected municipal water supplies in Crowley County, Colo., U.S.A. Unless otherwise specified, concentrations reported in this paper are expressed in ppm (w/w). Abbreviations: GC–ECD = electron capture gas chromatography; ISE = ion-selective electrode measurement.

Site	*Concentration NO_3^- (ppm)*	
	GC–ECD	*ISE*
Boulder, Colo.	0.40	—
TW0011	44	48
TW0012	42	46
TW0013	51	52
TW0014	16	16
TW0015	35	36
TW0016	12	13

The analysis of saliva and blood is complicated by the presence of known interferences, primarily chloride and thiocyanate ions, as well as possible interferences arising from the presence of peptides, proteins, and other nitrogen-containing compounds. Incidentally, high levels of chloride also interfere seriously with measurement of nitrate by ISE. Human saliva has been found to contain as much as 280 ppm (w/v) SCN^- and 630 ppm Cl^-, while blood serum may have as much as 3800 ppm Cl^-[10,11]. Both Cl^- and SCN^- can be removed by precipitation with Ag^+ prior to addition of the sulfuric acid. Analyses of saliva without this prior Ag^+ treatment gave NO_3^- values 15–30% lower than values obtained otherwise. Addition of quantities of Ag^+ in excess of that specified in Experimental did not affect the final result. Fig. 1

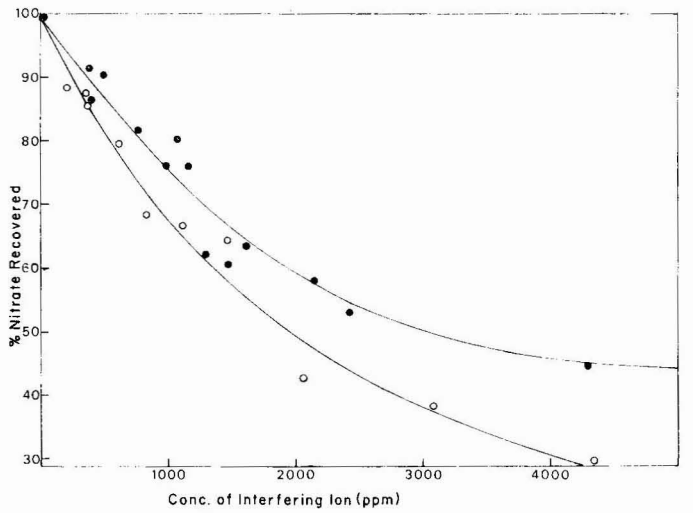


Fig. 1. Effect of interfering ions on the measurement of nitrate at the 2-ppm concentration level. The open circles are for the thiocyanate ion, the closed circles for the chloride ion.

is a plot of interfering ion concentration *vs.* NO_3^- recovery; this shows that appreciable concentrations of Cl^- and SCN^- will cause interference. The fact that this interference is irregular in nature precludes the use of a numerical correction.

Hydrogen peroxide has been demonstrated to inhibit the action of these interferences. Table II shows the results of treating solutions of known NO_3^- concentrations and known Cl^- concentrations with H_2O_2. Addition of H_2O_2 also prevents interference by SCN^-. For this reason the Ag^+ treatment is unnecessary in NO_2^- determinations. The fact that H_2O_2 alone or in conjunction with Cl^- does not produce a positive interference is also shown by the data in Table II obtained when no nitrate was present.

Other possible interferences were tested at the 1% (w/v) level in a 2-ppm standard solution of nitrate and found to produce less than 10% error in the value determined. These were: $ZnSO_4$, KF, Na_2CO_3, and sodium citrate.

The following were found not to interfere when present in quantities sufficient

TABLE II

EFFECT OF ADDITION OF HYDROGEN PEROXIDE IN REDUCING INTERFERENCE BY CHLORIDE

Cl^- concentration (ppm)	*H_2O_2 concentration (N)*	*NO_3^- concentration (ppm)*	
		Expected	*Found*
0	0	2.5	2.5
3000	0	2.5	1.2
3000	0.012	2.5	2.5
3000	0	0	0
0	0.012	0	0
3000	0.012	0	0

to produce saturated solutions: aspartic acid, glutamic acid, phenylalanine, and Ag_2SO_4. Tyrosine and tryptophan, when present at concentrations of 1000 ppm as free amino acids, appear to interfere with the nitrate determination.

In order to determine whether appreciable amounts of nitrobenzene are formed from nitrite in the absence of an oxidizing agent, the following test was made. A standard solution of KNO_2 containing 17.7 ppm of nitrite was subjected to the procedure for the analysis of nitrate. The benzene layer, which contained some nitrobenzene apparently resulting from nitrate impurities, was discarded and a fresh aliquot of benzene was added to the acidic nitrite solution. The solution was heated to simulate the heat arising from mixing the sulfuric acid with water, which would normally be generated, and the benzene layer was analyzed for nitrobenzene. No appreciable quantities of nitrobenzene were found; consequently, one may conclude that nitrite is not converted to nitrobenzene in the absence of an oxidant under the conditions specified in our method.

In the absence of a preservative, NO_3^- in saliva is rapidly reduced by microbial[2] and enzymatic activities[12]. Therefore, the saliva should be treated with a preservative immediately after collection. The NO_3^- concentrations in untreated samples were 90% lower after 2 h. Fig. 2a shows the chromatogram obtained from the analysis of a saliva sample. The absence of extraneous peaks is noteworthy. Table III shows some typical results. The GC–ECD method for saliva analysis is quite simple and was performed as a routine experiment by our undergraduate students.

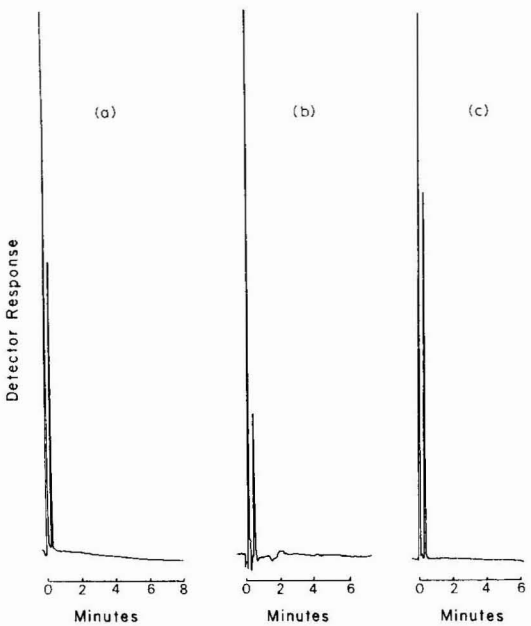


Fig. 2. (a) Chromatogram obtained from the analysis of 0.05 g of saliva containing 12 ppm NO_3^- (w/w). Attenuation, × 8. (b) Chromatogram obtained from the analysis of 0.1 ml of whole blood containing 1.8 ppm NO_3^- (w/w). Attenuation, × 4. (c) Chromatogram obtained from the analysis of particulate matter contained on a 1.45 cm^2 section of glass fiber filter. The suspended particulate nitrate concentration was found to be 0.8 $\mu g/m^3$. In each chromatogram the nitrobenzene generates the second peak.

TABLE III

TYPICAL NO_3^- AND NO_2^- CONCENTRATION LEVELS IN SALIVA AS DETERMINED BY GC–ECD

Subject	*NO_3^- concentration (ppm)*	*NO_2^- concentration (ppm)*
L. J.	15	<0.7
A. N.	12	4.6
R. S.	15	3.7
B. E.	12	12
P. L.	53	21
J. T.	46	5.0
S. S.	12	11
R. N.	7.9	1.5
J. C.	5.2	<0.2
C. H.	2.3	0.9
P. G.	12	6.0
A. R.	8.1	4.7
C. D.	16	9.5

Fig. 2b shows the chromatogram obtained from the analysis of a whole blood sample. The high chloride concentration in blood causes this matrix to be more difficult to analyze than drinking water. Also there is the possibility of other, as yet unidentified, interferences. The clean baseline shown in Fig. 2b suggests the utility of this method in the simple and rapid microanalysis of blood for nitrate concentration. These experiments demonstrate the feasibility of using this technique in the analysis of small whole blood samples obtained from finger pricks.

Airborne particulate analysis

The method used for the analysis of nitrates in airborne particulates is an extension and modification of the general method we previously reported[7]. The optimum amount of water used in the reaction was found in the present work to be 2 ml. The uniformity of collection on the 20 × 25 cm filter was checked by analyzing five different 1.45 cm^2 sections of a suspended particulate filter sample; results are shown in

TABLE IV

UNIFORMITY OF NO_3^- DISTRIBUTION ON A GLASS FIBER FILTER ON WHICH SUSPENDED PARTICULATES HAD BEEN COLLECTED

The size of the entire glass filter was 20 × 25 cm; individual samples taken for analysis from the filter measured 1.45 cm^2 (circular pieces 1.36 cm in diameter).

Position on filter analyzed	*NO_3^- concentration ($\mu g/m^3$ of air collected)*
Center	0.49
Front edge	0.43
Back edge	0.48
Front corner	0.48
Back corner	0.42
Mean	0.46
S.D.	± 0.03

TABLE V

TYPICAL NO_3^- CONCENTRATION LEVELS IN SUSPENDED PARTICULATE MATTER AS DETERMINED BY GC–ECD

Date	*Concentration of total suspended particulates in air ($\mu g/m^3$)* *	*Concentration of particulate NO_3^- in air ($\mu g/m^3$)*	*% (w/w) NO_3^- in particulates*
3-26-76	22.7	0.81	3.6
3-27-76	32.6	1.19	3.6
3-28-76	10.5	0.43	4.1
4-01-76	67.4	1.35	2.0
4-12-76	82.0	2.10	2.2
4-26-76	79.0	1.14	1.4
4-27-76	16.8	0.88	5.2
5-05-76	32.7	0.82	2.5

* Sampling station located at the University of Colorado, Boulder, Colo., U.S.A.

Table IV. Table V shows some typical data for airborne particulates while Fig. 2c shows a representative chromatogram, and Fig. 3 shows preparation of the sections.

Values previously reported for total suspended particulates in the Denver metropolitan area are in the range of 11–283 $\mu g/m^3$. The arithmetic mean of total suspended particulates in Boulder in 1967 was 49 $\mu g/m^3$ while the downtown Denver mean was 105 $\mu g/m^3$. Nitrate levels in the suspended particulates in the Denver metropolitan area were 0.4–5.8 $\mu g/m^3$ with a mean of 1.7 $\mu g/m^3$ (ref. 13).

As a check for possible interferences in the particulate analysis an 11 × 3 cm section was cut from a sampled filter and extracted according to the established EPA procedure[13]. The extract was then analyzed for NO_3^- using both the general microtechnique presented here and the nitrate ISE. Values obtained were 0.99 and 0.97 $\mu g/m^3$, respectively. These values compare well with the value of 0.94 $\mu g/m^3$ obtained from a 0.90 cm^2 section of the same filter analyzed according to the particulate procedure presented above in Experimental. NO_x can also be determined by GC–ECD[7].

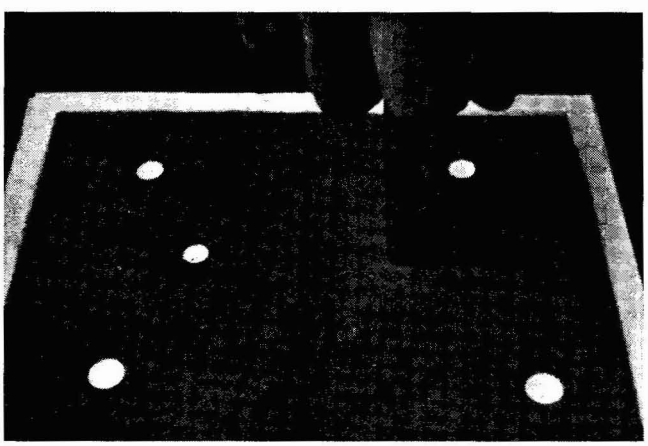


Fig. 3. Preparation of sections of glass fiber filters containing particulate samples from air prior to analysis for nitrate.

Use of trimethoxybenzene as a reactant

The advantages of benzene as a reactant are that chromatographically pure benzene is readily available and relatively inexpensive. Other reactants may be somewhat more reactive, but in general they are difficult to obtain in acceptable purity (and even difficult to purify), more expensive, and usually more susceptible to acid attack. Benzene, on the other hand, is toxic and is a volatile and flammable liquid. The volatility of benzene results in pressure buildup inside the reaction vessels due to the heat generated by the mixing of the aqueous nitrate sample and the acid, which causes one to take extra precautions.

One of the goals of this research was to find a reactant that would be more reactive than benzene so that more dilute final solutions of sulfuric acid would still be effective in catalyzing nitration. Of the other possible organic reactants considered, toluene, anisole, 2,6-dimethylanisole, *m*-xylene, *tert.*-butyl benzene, and cymene gave more than one reaction product, and no apparent advantage in reactivity was observed. Preliminary experiments with mesitylene, pentamethylbenzene, and TMB showed that the latter two compounds merited further investigation.

Of these two, pentamethylbenzene is more stable to heat and strong acid while TMB reacts better at lower acid concentrations. Both form mononitro derivatives which are easily chromatographed at 170° (see Experimental for other conditions). TMB has been more extensively studied to date, but both are under consideration as possible substitutes for benzene.

Figs. 4 and 5 are the results of the optimization of conditions in the TMB nitration reaction, using aqueous standard samples containing 2 ppm NO_3^-. The optimum acid concentration (after dilution with the aqueous NO_3^- sample) was found to be 50–60% (Fig. 4). Fig. 5 shows that the optimum reaction temperature is *ca.* 67°; at higher temperatures, undesirable pressure buildups occur in the vials. The narrow usable range of acid concentration displayed in Fig. 4 is striking; apparently, at higher

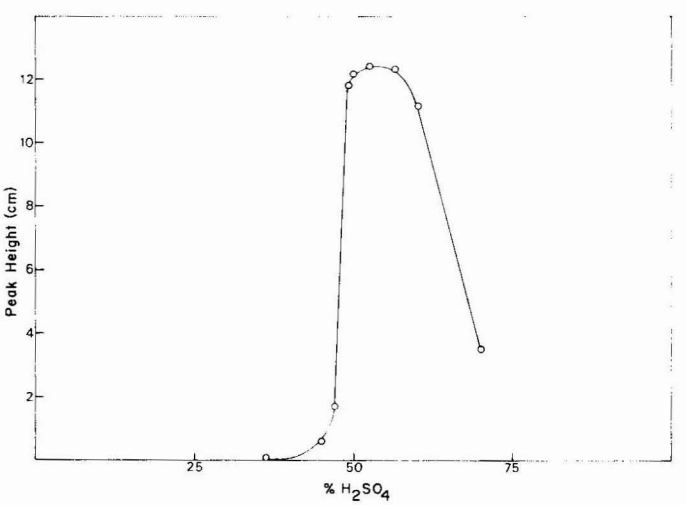


Fig. 4. Effect of the sulfuric acid concentration on the conversion of NO_3^- to NTMB. The NO_3^- concentration was 2 ppm.

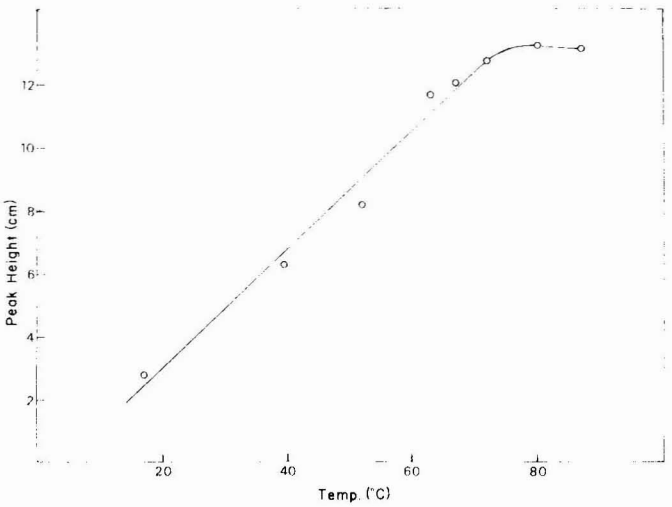


Fig. 5. Effect of the reaction temperature on the conversion of NO_3^- to NTMB. The NO_3^- concentration was 2 ppm. Each reaction was allowed to proceed for 10 min at the given temperature.

acid concentrations the yield is reduced by hydrolysis of TMB. The use of less than 0.1 g of TMB with 0.5 ml of aqueous sample and 0.5 ml of sulfuric acid results in incomplete reaction.

Table VI shows that the conversion efficiency of aqueous nitrate to NTMB is 81 $\pm$ 3%. The efficiency of the extraction of the TMB nitration product from the aqueous reaction mixture by shaking with benzene was found to be essentially quantitative (99%). One-milliliter aliquots of 1.06×10^{-6} g/ml and 2.57×10^{-7} g/ml of NTMB in benzene were each separately shaken with 1-ml portions of 50% sulfuric acid for 5 min, and in both cases 99% of the NTMB was determined to be still present in the benzene layer. Fig. 6 shows the chromatogram obtained using TMB as a reactant, with a 1-ppm NO_3^- sample.

The identity of the NTMB peak was confirmed by injection of a sample of independently synthesized NTMB and comparison of retention times. The last compound to be eluted in Fig. 6 is NTMB, while the second peak arises from much larger quantities of the reactant TMB, which has a lower ECD cross-section.

TABLE VI

EFFICIENCIES OF CONVERSION OF NO_3^- TO NTMB

NO_3^- concentration (ppm)*	*μg NTMB product*		*% Conversion*
	Theoretical	*Found*	
0.2	0.69	0.57	83
0.4	1.37	1.12	82
0.6	2.06	1.59	77

* The final concentration of sulfuric acid was 50% rather than 70% as in the experiments with benzene as reactant.

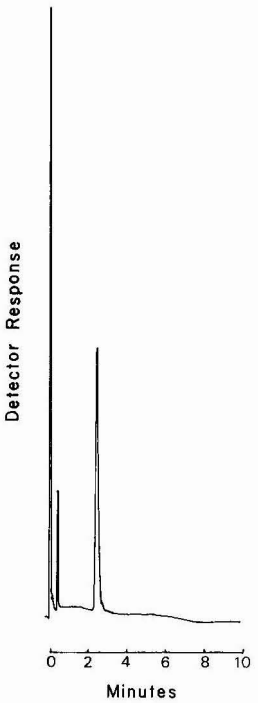


Fig. 6. Reaction products of NO_3^- with TMB. A 0.05-ml aliquot of 1 ppm NO_3^- was allowed to react.

CONCLUSION

A general microanalysis technique has been developed for the analysis of nitrate and nitrite in as little as one drop of sample, with a detection limit of 0.1 ppm NO_3^-. This technique, with slight modifications, has been applied successfully to the analysis of drinking water and biological fluids such as human saliva and whole blood, engendering the possibility of analyzing for nitrate and nitrite in blood samples obtained from small finger prick samples.

Suspended particulate samples collected from ambient air in Boulder, Colo. have been analyzed successfully for nitrates. The procedure presented here requires much less time than the EPA method, which involves an extraction step. Agreement between the EPA and our GC–ECD methods was found to be excellent.

TMB can be used as a suitable replacement for benzene as a reactant in the determination of trace levels of nitrate.

ACKNOWLEDGEMENTS

The authors are grateful to Dr. Theodora Ludington for providing the drinking water samples, to Gregory Hanna for performing many of the analyses, to Mark Rojec and Joseph Zufall for discovering the ability of hydrogen peroxide to prevent chloride and thiocyanate interferences, and to Kris Ottoson and Alfred Nitka for

their assistance in the preparation of the manuscript. This work was partially supported by the Air Force Office of Scientific Research under Contract F44620-76-C-0031.

REFERENCES

1 W. Lijinsky and S. S. Epstein, *Nature (London)*, 225 (1968) 21.
2 S. R. Tannenbaum, A. J. Sinskey, M. Weisman and W. Bishop *J. Nat. Cancer Inst.*, 53 (1974) 79.
3 D. H. Lee, *Environ. Res.*, 3 (1970) 484.
4 P. Correa, W. Haenszel, C. Cuello, S. Tannenbaum and M. Archer, *Lancet*, July 12 (1975) 58.
5 D. Shapley, *Science*, 191 (1976) 268.
6 D. J. Glover and J. C. Hoffsommer, *J. Chromatogr.*, 94 (1974) 334.
7 W. D. Ross, G. W. Buttler, T. G. Duffy, W. R. Rehg, M. T. Wininger and R. E. Sievers, *J. Chromatogr.*, 112 (1975) 719.
8 Y. Fukui, Y. Kuwahara, K. Saheki and M. Mori, *Yakugaku Zasshi*, 80 (1960) 1472.
9 Environmental Protection Agency, *Fed. Regist.*, 38, No. 226 (1973) 32558.
10 P. L. Altman, *Blood and Other Body Fluids*, Federation of American Societies for Experimental Biology, Washington, 1961, pp. 399–400.
11 P. B. Hawk, *Hawk's Physiological Chemistry*, McGraw-Hill, New York, 14th ed., 1965, p. 977.
12 P. W. Goaz and H. A. Biswell, *J. Dent. Res.*, 40 (1961) 355.
13 *Air Quality Data for 1967*, Rep. APTD-0741, Environmental Protection Agency, Research Triangle Park, N.C., 1971.

Journal of Chromatography, 126 (1976) 757–770
© Elsevier Scientific Publishing Company, Amsterdam — Printed in The Netherlands

CHROM. 9394

EVALUATION OF ORGANIC POLLUTANTS IN THE OPEN AIR AND ATMOSPHERES IN INDUSTRIAL SITES USING GRAPHITIZED CARBON BLACK TRAPS AND GAS CHROMATOGRAPHIC–MASS SPECTROMETRIC ANALYSIS WITH SPECIFIC DETECTORS

PAOLO CICCIOLI, GIULIANO BERTONI, ENZO BRANCALEONI, RINALDO FRATARCANGELI and FABRIZIO BRUNER*

Laboratorio sull'Inquinamento Atmosferico del C.N.R., Via Montorio Romano, 36-00131 Rome (Italy)

SUMMARY

A method for evaluating the organic content of the atmosphere, involving the use of personal samplers, is described. A comparison of the performances of Tenax GC and Carbopack B is given in terms of sample recovery. Apparatus including selective columns, specific detectors and combined gas chromatography–mass spectrometry is also described.

Practical examples of the analysis of organic air pollutants trapped in the open air and the atmosphere in a chemical plant are discussed. A comparison of the results of complete gas chromatography and of the total hydrocarbon content is also made.

INTRODUCTION

The evaluation of organic pollutants in air involves techniques of various degrees of complexity, depending on the nature of the compounds involved, from the total hydrocarbon content including methane (using a simple flame-ionization detector), through the measurement of organic substances other than methane, the determination of lower alkanes and alkenes, and finally to the individual analysis of single organic substances.

The last type of measurement is essential when the situation in industrial sites has to be evaluated, because one needs to know the health hazards that specific compounds may have for persons continuously exposed to polluted atmospheres. In this context, the use of "personal samplers" has been proposed in order to obtain a better knowledge of the nature and amounts of actual and potential poisons inhaled in particular environments such as chemical plants and laboratories and in industrial sites where volatile organic substances have to be used.

On the other hand, the occurrence of photochemical oxidants in the open air and the recognition of the important role played by reactive hydrocarbons and other

* To whom correspondence should be addressed.

organic substances in the formation of photochemical smog make measurements of specific air pollutants important for research purposes and for optimizing air pollution control.

Because of the low concentrations of each component usually found in the atmosphere, sample enrichment is necessary in both instances, and various workers have sought the best enrichment procedures, ensuring that trapping is as complete as possible and that there is complete release of the organic compounds from the traps. Different approaches have been followed, mainly the use of cold traps at very low temperatures[1–6] and of traps working at room temperature[7–13]. Different kinds of trapping materials have also been studied, such as porous polymers alone[6–10] or coated with liquid phases[14,15], strong adsorbents such as active charcoal and successive solvent extraction[11], or moderately strong adsorbents such as graphitized carbon black[12,13]. However, cold traps obviously cannot be used in personal samplers, while traps operated at room temperature are also much more useful for monitoring organic pollutants in the open air, especially if automatic sampling and analysis is desired. The main problem is to find an adsorbent that is capable of trapping the highest number of substances, even though large volumes of air have to be sampled, and at the same time that is able to release higher boiling compounds on heating at moderately high temperatures.

With such severe limitations, both strong and weak adsorbents should be excluded, and only intermediate adsorbents or porous polymers remain to be considered. From preliminary results, Tenax GC (Enka, Arnhem, The Netherlands) and Carbopack B (Supelco, Bellefonte, Pa., U.S.A.) appeared to be the best materials for such purposes.

GENERAL CHARACTERISTICS OF TENAX GC AND CARBOPACK B

Tenax GC (18.6 m^2/g) is a porous polymer based on 2,6-diphenyl-*p*-phenylene oxide, the most important properties of which are its high operating temperature without appreciable bleeding and the capability of eluting a large number of compounds with good transmission of even highly polar or basic molecules. However, the resolution of Tenax GC as a packing material for chromatographic columns is very low and the selectivity is also poor in comparison with other adsorbents. Water is readily eluted from Tenax. The most interesting feature of Tenax, however, is its capability of eluting many compounds of different natures and molecular weights in a relatively short time. This porous polymer has been used mainly as a trapping material for enriching air or water samples[16]. It should be noted that, owing to its peculiar characteristics, Tenax was chosen for the chromatographic column in the Viking project[17].

Carbopack B is a graphitized carbon black adsorbent (90 m^2/g) and has a large variety of applications as a column material in gas chromatography. It has been used in isotope separations[18] and in the analysis of sulphur compounds in air at the parts per billion level[19]. When suitably modified with small amounts of liquid phases, it shows a high selectivity for isomeric hydrocarbons[4] and complete transmission of alcohols, carboxylic acids and amines[20,21]. Columns made of Carbopack B offer good permeability and extremely high performance. The thermal stability of Carbopack B is without limit in practice and it does not show any bleeding, even at extremely high temperatures.

EXPERIMENTAL

Trapping procedure, measurement of breakthrough volumes and sample recovery

The traps are glass tubes, length 12 cm, I.D. 4 mm and O.D. 6 mm, with a 9-cm portion occupied by the trapping material, plugged with glass-wool on each side. The amount of material in each trap is 0.28 g of Tenax GC and 0.45 g of Carbopack B. Carbopack B is in the size range 80–100 mesh and Tenax GC 60–80 mesh.

Trapping in the open air is carried out with an electrically operated pump. Its pumping capacity is such that sampling with up to six traps simultaneously is possible, with a flow-rate in each trap of 30 ml/min. Sequential sampling is also possible for monitoring; a scheme of the trapping system is shown in Fig. 1. The sampling funnel is placed at about 10 m from the ground in the open air. A PTFE tube is used to connect the traps to the funnel.

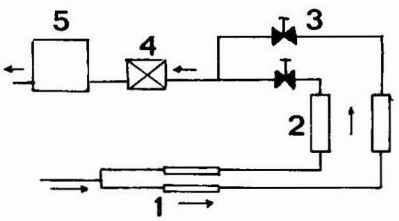


Fig. 1. Scheme of the trapping system. 1 = Traps; 2 = rotameters; 3 = needle valves; 4 = pump; 5 = flow counter.

Personal sampling is effected by using an Aircheck Personal Pump (SKC, Pittsburgh, Pa., U.S.A., Model 222-351). This pump is equipped with a digital flow meter and has a regulatable pumping capacity ranging from about 30 to 200 ml/min. The dimensions of the trap are as described above. Breakthrough volumes of test compounds are measured by injecting a known amount of the sample into the trap at room temperature, allowing extra-pure nitrogen to pass through the trap at the flow-rate desired until 0.5, 1.5 or 5.0 l have passed through, then closing the trap and heating it at 300° for 10 min.

A special four-way valve operating at temperatures up to 400° is used (Valco, Houston, Texas, U.S.A.). Injection is made by passing the carrier gas through the trap before entering the column. A scheme of the injection device that is also used when the organic compounds from traps have to be analyzed is shown in Fig. 2.

The chromatograms are compared for quantitative evaluation with that obtained by injecting the test mixture directly through the trap at 300°. In this way, one knows the amount lost or irreversibly retained by the trap. A Hewlett-Packard Model 3380A digital integrator is used for calculations.

Analytical equipment

It is important to note that with the device shown in Fig. 2, no loss of chromatographic resolution is observed for compounds scarcely retained in the column, as shown in Fig. 3.

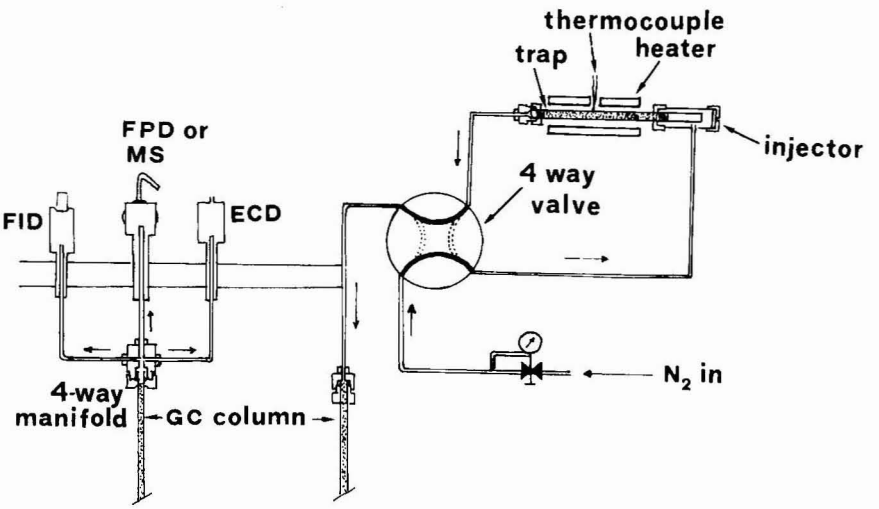


Fig. 2. Injection and detection system.

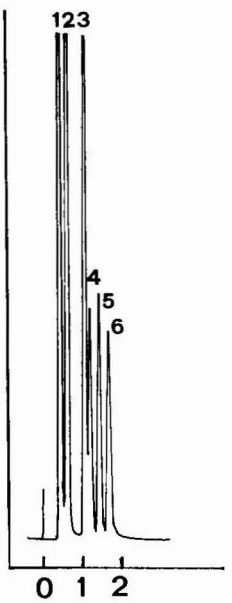


Fig. 3. Chromatogram obtained by injection through the trap, showing that dead volumes do not affect resolution. Peaks: 1 = methane + ethane; 2 = propane; 3 = isobutane; 4 = butene-1; 5 = *n*-butane; 6 = *trans*-butene-2.

A Carlo Erba Model GI gas chromatograph was modified at the injection port as described and a four-way manifold was used at the column exit to divide the gas stream into three portions, so that three detectors (flame-ionization, FID; electron-capture, ECD; and flame-photometric, FPD) could be used, as shown in Fig. 2. An analogous apparatus was used by McLeod *et al.*[22]. A similar chromatograph,

equipped with the same injection device, is coupled to an AEI MS12 mass spectrometer with an FID placed in parallel according to the technique described previously[23]. The apparatus for trapping and analyzing low-boiling compounds was shown in a previous paper[4].

The total organic content less methane is monitored using an automatic apparatus constructed in our laboratory. It consists of a modification of the apparatus described elsewhere[24] and is shown schematically in Fig. 4. One of the two detectors is directly fed with ambient air, sampled at the location of the traps, while the other is placed at the end of a chromatographic column (stainless steel, 2.0 m long, 4 mm I.D., 6 mm O.D., packed with Porapak Q, 80–100 mesh) where the same sample of air is injected every 5 min.

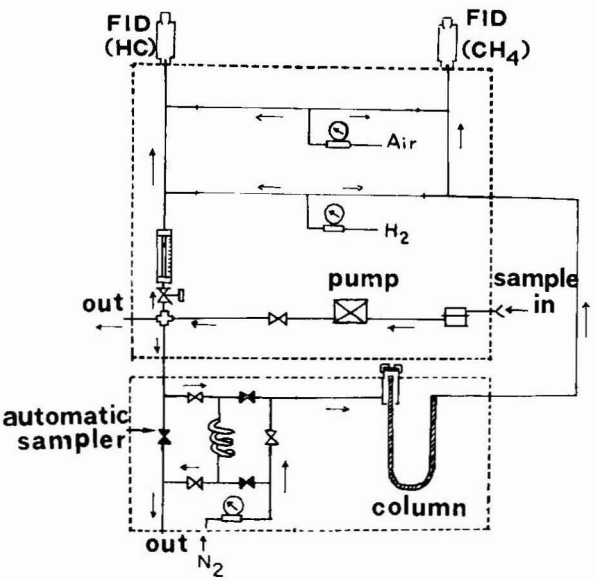


Fig. 4. Scheme of the apparatus for monitoring total hydrocarbon content and methane in air.

The column is operated at room temperature so that the methane peak is separated from any other peak. Further, owing to the large difference in the concentrations of methane and other single organic substances, it is possible to regulate the electrometer attenuation so as to detect the methane peak only. From calibration graphs, by subtracting the methane concentration, that of the total organic content is obtained.

A highly selective column was devised for the purposes of this work. The column should be able to work either at room temperature, yielding good separation factors for light compounds, or at higher temperatures to separate aromatic compounds up to C_{10}–C_{12}. It should also be able to elute polar compounds.

The column chosen was made of stainless steel, 1.80 m long and 2 mm I.D., packed with Carbopack C (Supelco), coated with 0.4% SP1000. Such a stationary phase, based on the unique properties of gas–liquid–solid chromatography, shows a pronounced selectivity for isomeric hydrocarbons and, owing to the polarity of the

liquid modifier, gives symmetrical peaks for hydrogen-bonding compounds. It should be noted that a polar liquid phase on graphitized carbon black enhances the separation of isomers and decreases the retention times[25]. The percentage of SP1000 is such that the first monolayer is incomplete, so that the separation is best for the effect of lateral interactions.

RESULTS AND DISCUSSION

Sample recovery

In Table I, the recoveries of various compounds attained with Carbopack B and Tenax GC are compared. The choice of the compounds examined was made with the aim of screening most of the types of organic compounds likely to be present in air pollutants. The list of compounds is obviously incomplete, but gives a fair idea of the trapping and releasing properties of the adsorbents considered.

There are two reasons why a particular compound injected in the trap could be incompletely recovered: (i) the compound is hardly adsorbed and is eluted from the trap by the air passing through it during the trapping step, or (ii) the compound is strongly adsorbed and is not released when the trap is heated. Thus, there is a critical region where the trap is most efficient for each adsorbent. The results in Table I show

TABLE I

RECOVERY (%) OF ORGANIC COMPOUNDS FROM AIR SAMPLES USING CARBOPACK B AND TENAX GC TRAPS

Compound	*Carbopack B*			*Tenax GC*		
	0.5-l sample	*1.5-l sample*	*5.0-l sample*	*0.5-l sample*	*1.5-l sample*	*5.0-l sample*
Methanol	3	0	0	1	0	0
Ethanol	3	0	0	1	0	0
Methyl chloride	1	0	0	3	1	0
Acetone	5	1	0	68	2	0
Chloroform	100	54	1	100	84	5
Diethylamine	100	80	50	80	50	1
Isobutanol	100	100	25	100	95	16
n-Pentane	100	100	100	100	50	9
Cyclohexane	100	100	100	100	50	9
n-Hexane	100	100	100	100	100	20
Ethyl acetate	100	100	100	100	100	35
n-Butanol	100	100	100	100	100	35
Benzene	100	100	100	100	100	35
Toluene	100	100	100	100	100	100
— *	—	—	—	—	—	—
n-C_{13}	65	65	65	100	100	100
n-C_{14}	46	46	46	100	100	100
n-C_{15}	25	25	25	100	100	100
n-C_{16}	8	8	8	100	100	100
n-C_{17}	1	1	1	100	100	100
n-C_{18}	0	0	0	100	100	100

* Styrene, ethylbenzene, xylene, pyridine, chlorophenol, alkanes, alkenes from C_7–C_{12} had 100% recovery in any case.

that Carbopack B and Tenax GC are comparable in this respect. However, benzene and *n*-hexane are completely retained by Carbopack B in the trapping step, but pass through Tenax GC, and the same occurs for the alkanes from *n*-pentane to isooctane. It is worth noting that significant differences are observed for light compounds. Acetone is recovered better from Tenax GC, while for butanol and diethylamine Carbopack B is more efficient.

Such differences may be explained by the strong retention of hydrocarbons on graphitized carbon black. For polar compounds, the specific active sites present on the carbon black surface increase the retention. The small number of carbon atoms and the low polarity are responsible for the low retention of acetone on Carbopack B. Tenax, which elutes amines linearly[17], *i.e.* without appreciable irreversible adsorption, allows these compounds to pass through the trap.

The same reasons that favour Carbopack B for the range C_4–C_8 favour Tenax GC if compounds above C_{12} are considered. However, it should be noted that such compounds are seldom present in the open air or in industrial sites, as will be shown later with examples of field measurements. They are, however, major constituents of the organic fraction of atmospheric dust, but this is a different problem.

For the sake of comparison in the real use of the adsorbents, the following experiment was carried out. Two traps of the same length and diameter, one of Tenax GC followed by Carbopack B according to the direction of the air stream, and the other of Carbopack B followed by Tenax GC, were used for parallel air sampling, 1.5 l of air being sampled in each trap. During the trapping step, the compounds that were not retained by Tenax GC passed into the second part of the trap and were retained by the Carbopack B. In a similar manner, in the other trap compounds that were not retained by Carbopack B were subsequently retained by Tenax GC.

The traps in tandem were then separated and their organic contents injected into the column, giving the four chromatograms shown in Fig. 5. Calculations were made by considering the total peak areas of chromatograms A + B and C + D as 100%. The two total areas were closely correlated, showing that the sampling and injection procedure is highly reproducible.

From this experiment, it was also found that Carbopack B behaves as a better trapping and releasing material than Tenax GC (83% recovery compared with 75%). Only acetone, as expected from the results in Table I, is better retained by Tenax GC, while cyclohexane and pentane are partly lost by Tenax GC and completely retained by Carbopack B in the trapping step.

In addition, the chromatograms in Fig. 5 show that there is a discrepancy between the breakthrough volumes measured with the method described and the actual retention and releasing properties of the adsorbents in field measurements. In fact, both of the materials lose some of the C_8–C_{10} fraction, and this could not be forecast from the results in Table I. A possible explanation of this effect is that sampling is carried out under extremely dilute conditions, which are completely different from those which occur when breakthrough volumes are being measured. In this instance, the samples injected in the traps are much more concentrated.

Sampling and analysis of atmospheric pollutants

A 5.0-l volume of air from suburban open air was sampled with a Carbopack B trap at a flow-rate of 30 ml/min. A cold trap[4] was used at the same time for the

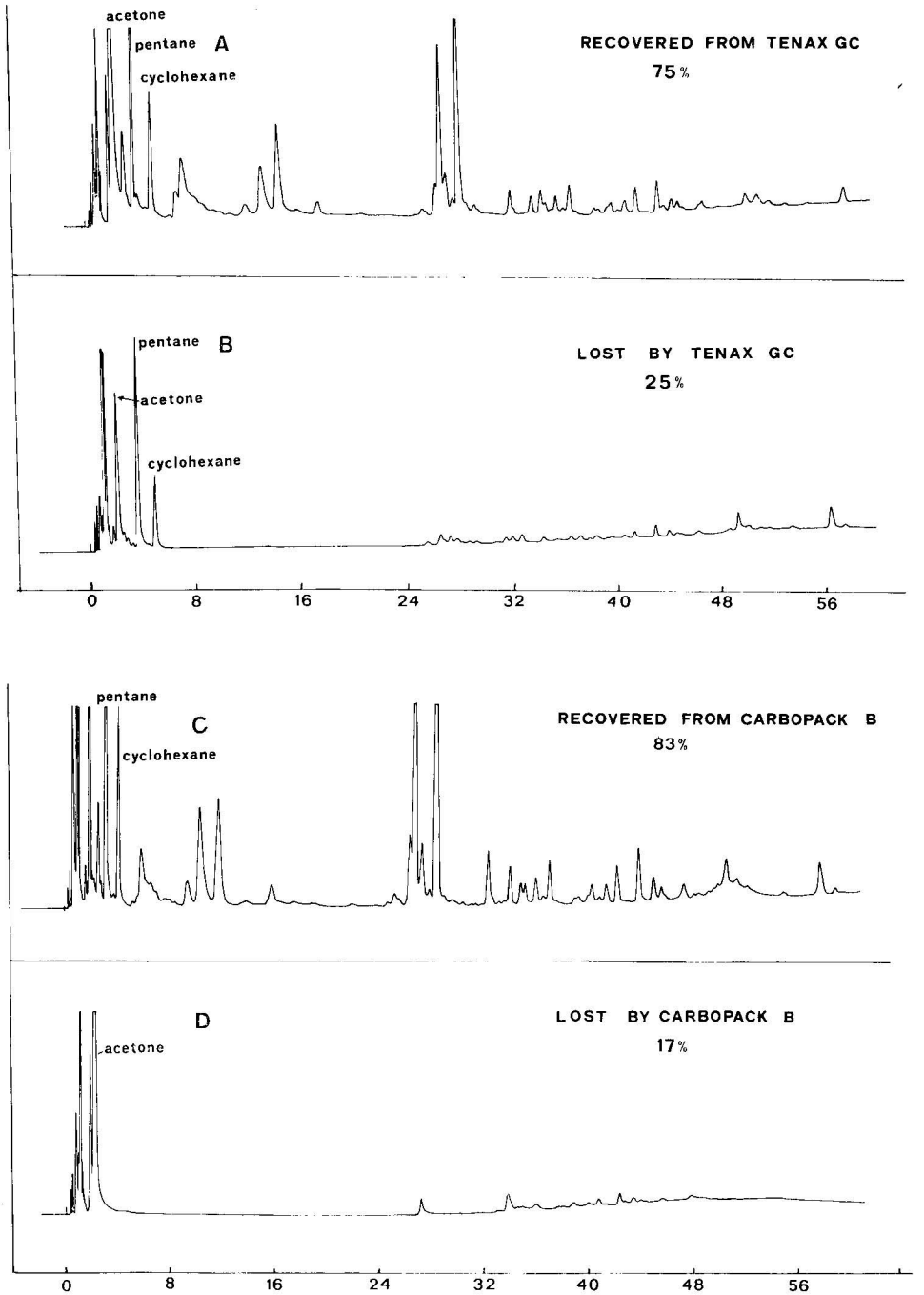


Fig. 5. Chromatograms showing losses and recovery from an actual air sample using Tenax GC and Carbopack B.

analysis of C_2–C_4 compounds and the total non-methane organic compounds (THC) were also monitored. The THC trace obtained is shown in Fig. 6 together with that obtained with a sample from an urban site. The area within the broken line corresponds to the time period when the traps were operated.

The analysis was then run using the FPD, ECD and FID as parallel detectors

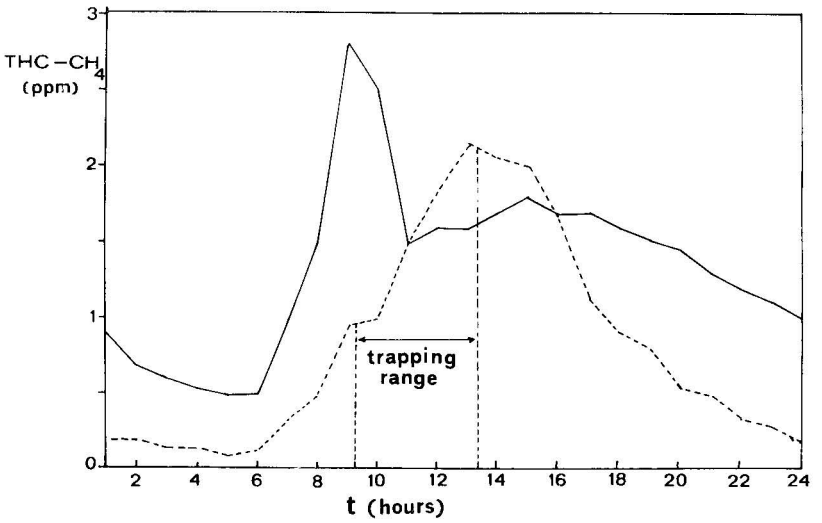


Fig. 6. Total hydrocarbon content during 24 h monitored in typical urban (———) and suburban (– – –) areas.

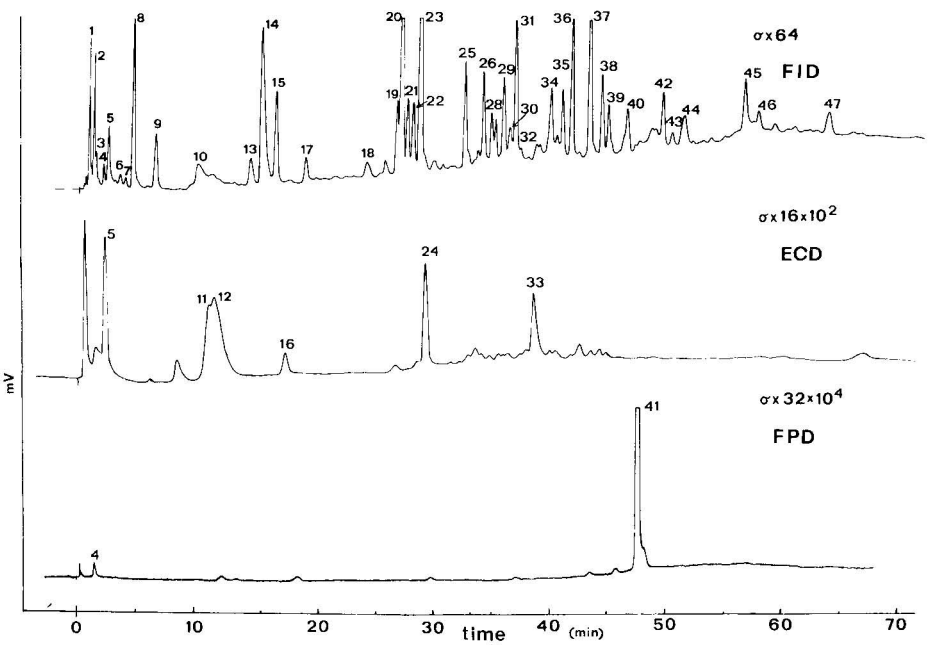


Fig. 7. Triple detector chromatogram showing the analysis of a sample of air taken in suburban open atmosphere. Peak Nos. as in Table II. Sampling material: Carbopack B.

and the resulting chromatogram is shown in Fig. 7. Most peaks were identified by MS. The potentiality of specific detection is shown by the identification of benzothiophene and halogenated compounds, which was effected on the basis of retention times. The amount of these compounds is so low that when other compounds were present in the same region of the chromatogram mass spectrometric identification was impossible.

Another feature of the chromatogram is that, in spite of its complexity, major peaks corresponding to single compounds were obtained, showing a high selectivity. This can also be seen from peaks Nos. 30, 31 and 32, which gave identical mass spectra, and which were identified as the three xylenes from the retention times. The separation achieved for the other aromatic compounds is also worthy of note. Only two pairs of peaks overlapped.

Table II lists the compounds identified, together with the approximate amounts found. The accuracy of the determinations was 10–20% based on the absolute amounts present.

Parallel sampling and analysis of the light fraction were also carried out, using a technique described elsewhere[4]. The analysis was effected with the triple detector system and the qualitative and quantitative results are reported in Table III.

It is interesting to note the noticeable amount of methylene chloride found, which indicates the importance of halogenated compounds in air pollution.

Table IV shows the results for the balance of the components. From a comparison of the data in Tables II and III, it can be seen that the C_2–C_5 fraction is only 26% of the total, showing that a complete analysis up to C_{10} is needed for a reasonable screening of air pollutants. The aromatic fraction is present in about the same percentage as the C_2–C_5 hydrocarbons, in good agreement with the data available from the literature[26]. The concentration of the heavier organic compounds is obtained by subtracting the peaks corresponding to the light fraction from the total integration of the chromatogram in Fig. 7.

The unidentified fraction is the sum of the minor peaks, present in low amounts, for which mass spectrometric identification was impossible. The fraction lost probably corresponds in part to compounds heavier than C_{10}, but the discrepancy may also be due to errors in the analytical measurements. However, repetitive measurements always gave a lower figure for the total amount found by gas chromatography with respect to the direct THC values, showing that the first hypothesis is more feasible. The non-hydrocarbon fraction comprises about 14% of the total organic compounds, confirming the strong prevalence of petroleum products in organic air pollutants.

No evidence for the presence of terpenes has been found; in fact, the suburban area where sampling was carried out is a long distance from forest areas. The presence of some ketones and halogenated compounds is probably due to some small factories located 1–2 km from the sampling point.

Sampling and analysis in industrial sites

Carbopack B traps were used for sampling organic substances in a chemical plant where solvents are used in process syntheses. A 1-l volume of air was sampled in the area of the plant where workers usually spend most of their working day, in order to obtain a representative sample of inhaled air. The sampling rate was ap-

TABLE II

ANALYSIS OF ORGANIC COMPOUNDS IN OPEN AIR

Peak No.	*Retention time (min)*	*Identified as (MS)*	*Amount (ppb CH_4)*
1	0.72	Butene-1 + *cis*-butene-2 + isobutane	25
2	1.13	*n*-Butane + *trans*-butene-2	16
3	1.35	1,3-Butadiene	7
4	2.02	Methyl mercaptan	4
5	2.37	Acetone + CH_2Cl_2*	16
6	3.42	C_5 unsaturated hydrocarbon	2
7	3.88	*i*-C_5 hydrocarbon	1
8	4.48	*n*-C_5 hydrocarbon	40
9	6.45	Cyclohexane	17
10	10.0	–	50
11	11.20	–*	5
12	11.80	Carbon tetrachloride*	5
13	14.66	Dietyl ketone	11
14	15.64	Benzene	74
15	16.88	C_6 unsaturated hydrocarbon	33
16	18.00	Trichloroethylene*	<1
17	19.54	*n*-C_6 hydrocarbon	8
18	25.03	Butanol	6
19	27.63	Methylcyclohexane	19
20	27.99	C_7 unsaturated hydrocarbon	90
21	28.55	C_7 unsaturated hydrocarbon	21
22	29.06	Toluene	20
23	29.61	C_7 hydrocarbon	100
24	29.80	1,3-Dichloropropane*	6
25	33.59	Dimethylcyclohexane	30
26	35.19	C_8 unsaturated	26
27	35.91	Ethyl butyl ketone	15
28	36.25	Styrene	13
29	36.96	Ethylbenzene	21
30	37.50	*m*-Xylene	11
31	37.98	*p*-Xylene + isopropylbenzene	41
32	38.44	*o*-Xylene	3
33	39.81	–*	4
34	41.04	*n*-C_9 hydrocarbon	20
35	42.07	Ethyltoluene	19
36	42.83	1,3,5-Trimethylbenzene	18
37	44.38	1,2,4-Trimethylbenzene	54
38	45.46	1,2,3-Trimethylbenzene	22
39	46.05	Ethyldimethylbenzene	18
40	47.67	Methylisopropylbenzene	18
41	48.67	Benzothiophene*	3
42	50.77	1,2,3,5-Tetramethylbenzene	13
43	51.57	1,2,3,4- + 1,2,4,5-Tetramethylbenzene	4
44	52.59	–	18
45	57.74		18
46	58.99		4
47	65.05		19
		Total:	988

* Detected with specific detectors and identified with standards.

TABLE III

ANALYSIS OF LIGHT ORGANIC COMPOUNDS IN THE OPEN AIR (COLD TRAP)

All peaks identified with standards.

Peak No.	*Retention time (min)*	*Identified as*	*Amount (ppb CH_4)*
1	3.00	Ethene	15
2	3.23	Ethane	7
3	7.45	Propene	8
4	7.84	Propane	5
5	21.07	Isobutane	10
6	35.08	*n*-Butane	35
7	32.12	1,3-Butadiene	10
8	37.0	*trans*-Butene	5
9	47.45	Dichloroethane*	150
10	50.82	—	35
11	61.25	2-Methylbutene	14
12	67.54	Isopentane	10
13	77.70	*n*-Pentane	40
14	80.25	-	35
15	90.20	*	1
			Total: 376

* Detected with ECD.

TABLE IV

BALANCE OF THE COMPONENTS IN THE OPEN AIR

Fraction	*Amount (ppb)*
THC (non-methane)	1550
Light organics (cold trap)	375 (26%)
Heavier organics trapped and recovered	1076 (74%)
Total organics trapped	1451
Unidentified (minor peaks)	336 (23.1%)
Lost	98 (6.3%)

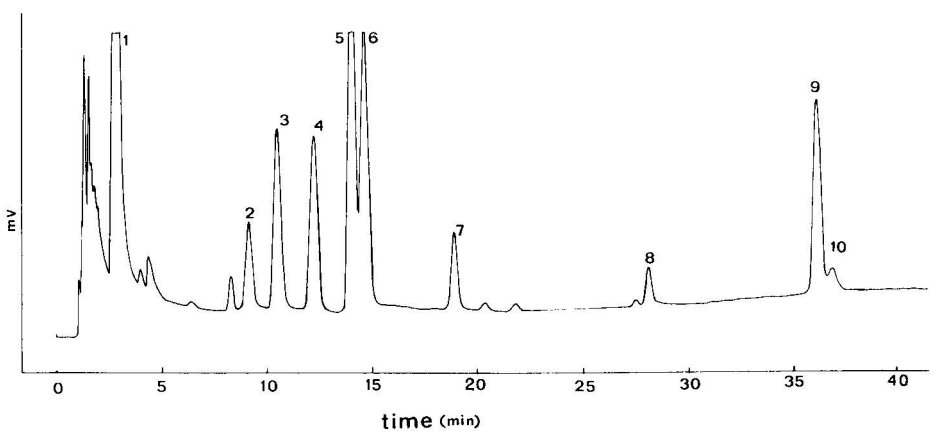


Fig. 8. Chromatographic analysis of an air sample taken inside a chemical plant. Peaks as in Table IV. Sampling material: Carbopack B.

proximately 100 ml/min. Particular emphasis was placed on a search for aromatic solvents. The chromatogram obtained is shown in Fig. 8 and peak identification is reported in Table V.

The GC–MS analysis was made 2 h after sampling, and a parallel sampling was made with an identical trap, which was processed 1 week later. The same chromatogram was obtained without significant changes, which indicates that traps can be stored prior to analysis without problems unless very reactive and unstable compounds are present in the trap. The trap was closed at the terminals during storage. The amount of acetone was estimated knowing that about 95% is lost during the trapping step.

TABLE V

ANALYSIS OF AIR SAMPLE FROM A CHEMICAL PLANT

Chromatograms in Fig. 7.

Peak No.	*Identified as*	*Amount (ppm)*
1	Acetone	≈50
2	C_6 unsaturated	1.0
3	C_6 unsaturated	2.2
4	Ethyl isopropyl ketone	2.0
5	Diethyl ketone	3.6
6	Benzene	2.9
7	Hexane	0.7
8	Toluene	0.3
9	Styrene	2.6
10	Ethylbenzene	0.12

CONCLUSION

The results show that the analytical procedure involving the use of Carbopack B or Tenax GC traps for sampling at room temperature can be used to evaluate the air quality with reliable results. It should be noted that the total amount of organic pollutants unidentified is relatively high (23%), but also that the practical value of this figure is limited, because it includes only very minor components.

REFERENCES

1 R. E. Kaiser, *Anal. Chem.*, 45 (1973) 965.
2 C. Nicotra, A. Cornu, R. Massot and Perilhon, in S. G. Perry (Editor), *Gas Chromatography 1972*, Applied Science Publ., Barking, 1973, p. 9.
3 C. Narain, P. J. Marron and J. H. Glover, in S. G. Perry (Editor), *Gas Chromatography 1972*, Applied Science Publ., Barking, 1973, p. 1.
4 F. Bruner, P. Ciccioli and F. di Nardo, *J. Chromatogr.*, 99 (1974) 661.
5 N. Brenner and L. S. Ettre, *Anal. Chem.*, 31 (1959) 1815.
6 B. Versino, M. de Groot and F. Geiss, *Chromatographia*, 6 (1974) 302.
7 A. Zlatkis, H. A. Lichtenstein and A. Tishbee, *Chromatographia*, 6 (1973) 67.
8 W. Bertoch, R. C. Chang and A. Zlatkis, *J. Chromatogr. Sci.*, 12 (1974) 175.
9 R. Jeltes, *Atmos. Environ.*, 3 (1969) 587.
10 J. W. Russel, *Environ. Sci. Technol.*, 8 (1974) 143.
11 K. Grob and G. Grob, *J. Chromatogr.*, 62 (1971) 1.
12 A. Raymond and G. Guiochon, *Analusis*, 5 (1973) 357.

13 A. Raymond and G. Guiochon, *Environ. Sci. Technol.*, 8 (1974) 143.
14 F. T. Eggersten and F. M. Nelsen, *Anal. Chem.*, 30 (1958) 1040.
15 W. A. Lonnemann, S. L. Kopczynski Darley and F. D. Sutterfield, *Environ. Sci. Technol.*, 8 (1974) 229.
16 B. Versino, M. de Groot and F. Geiss *Report of the COST Project 64B*, European Community, Brussels, 1975.
17 M. Novotný, J. M. Hayes, F. Bruner and P. G. Simmonds, *Science*, 189 (1975) 215.
18 F. Bruner, C. Canulli, A. di Corcia and A. Liberti, *Nature Phys. Sci.*, 231 (1971) 175.
19 F. Bruner, P. Ciccioli and F. di Nardo, *Anal. Chem.*, 47 (1975) 141.
20 A. di Corcia, A. Liberti and R. Samperi, *Anal. Chem.*, 45 (1973) 1228.
21 A. di Corcia and R. Samperi, *Anal. Chem.*, 45 (1974) 977.
22 H. A. McLeod, A. G. Butterfield, D. Lewis, W. E. J. Phillips and D. E. Cohin, *Anal. Chem.*, 47 (1975) 674.
23 F. Bruner, P. Ciccioli and S. Zelli, *Anal. Chem.*, 45 (1973) 1002.
24 F. Bruner and P. Ciccioli, *Proceedings of TECOMAP, Helsinki, 30 July–4 August, 1973*, WMO, Geneva, 1974, p. 324.
25 F. Bruner, P. Ciccioli, G. C. Crescentini and M. T. Pistolesi, *Anal. Chem.*, 45 (1973) 1851.
26 *Air Quality Criteria for Hydrocarbons*, NAPCA, Washington, D.C., 1970.

Journal of Chromatography, 126 (1976) 771–785

CHROM. 9494

GAS CHROMATOGRAPHIC–MASS SPECTROMETRIC EVALUATION OF EXHALED TOBACCO SMOKE

GUENTHER HOLZER and JOHN ORÓ

Department of Biophysical Sciences, University of Houston, Houston, Texas 77004 (U.S.A.)

and

WOLFGANG BERTSCH

Department of Chemistry, University of Alabama, University, Ala. 35486 (U.S.A.)

SUMMARY

The impact of cigarette smoking on the distribution of organic substances in ambient air has been determined for the intermediate volatility range. A simple sampling procedure was employed, involving gas–solid adsorption onto an organic polymer followed by direct thermal elution onto a glass capillary column.

Aliphatic and substituted aromatic hydrocarbons are predominant in urban atmospheres. Depending on location and weather conditions the total concentration of such volatiles can differ by as much as a factor of 20. This high background variation makes it difficult to analyze for trace substances with low odor threshold values, such as encountered in cigarette smoke.

Standard cigarettes were smoked in a relatively small room, having no air filtration system. Air samples of approximately 3.5 l were taken. The amount of volatiles added to air by cigarette smoking is insignificant. Substances were analyzed and identified by gas chromatography and gas chromatography–mass spectrometry with glass capillary columns. Many compounds reported in cigarette smoke condensate have been confirmed.

INTRODUCTION

Cigarette smoking is clearly hazardous to health. Several states in the U.S.A. have recently enacted legislation which prohibits smoking in public buildings, and separate facilities for non-smokers are required in some parts of the country.

The composition of cigarette smoke is relatively well known, in spite of its tremendous complexity. A great deal of research has been devoted to the analysis of tobacco products, due to its general importance, but little is known about the substances non-smokers are exposed to in the presence of smokers. The analytical problems lie in both sampling and analysis. Significant advances have recently been made in sampling technology, and the analytical chemist now has several routes for the concentration of trace volatiles from air. Specialized analytical instrumentation

for such detailed analysis has been available for several years, but its use is still not widely accepted and generally restricted to laboratories which specialize in high-resolution separations.

The composition of volatile trace contaminants in air, especially urban air, has been investigated only within the last few years due to these experimental difficulties. Besides the permanent gases, water is the predominant substance in air. For obvious reasons, a preconcentration step is necessary prior to analysis. Its presence often causes problems for the analyst.

Surprisingly, the composition of organic volatiles in urban air closely resembles gasoline vapors[1,2] in the intermediate volatility range to which this investigation has been directed. It is not clear to what extent loss of gasoline due to evaporation contributes or how much incomplete combustion in automobile engines is responsible. Alkanes and substituted aromatic hydrocarbons which make up the bulk of the organic material in urban air are relatively inert and only slowly undergo chemical change in the atmosphere. A higher reactivity, however, can be expected for unsaturates, oxygenated substances and similar labile compounds which take part in photochemical processes to various degrees. These substances are present only in relatively small concentrations, therefore, chromatographic profiles of urban air samples are relatively consistent.

Tobacco smoke can be expected to be much more reactive, and secondary reactions of sample components with each other, oxidation in air and photochemical reactions can produce many compounds which were not originally present in the smoke. On the other hand, other substances may be removed by absorption or may polymerize. The products obtained depend very much on the smoking conditions[3,4]. Factors such as puff volume, puff rate, puff frequency, length of butt, the nature and type of the tobacco product, its history, and pretreatment as well as other extraneous variables such as moisture content, additives, texture and porosity of paper all influence the amount and distribution of components in tobacco smoke. Tobacco smoke analysts have agreed on standard smoking conditions, nevertheless, considerable variations can be expected from batch to batch even with the same tobaccos.

The standardized conditions used for the production of smoke condensate are not easily applicable for the analysis of tobacco smoke in air. The sampling conditions which were chosen in this investigation therefore represent a compromise between reproducibility and convenience. Since many of the substances generated by pyrosynthesis from plant material possess low odor and taste threshold values, as opposed to most contaminants in air, it is difficult to distinguish between compounds which are significant from the standpoint of biological activity or nuisance and substances which are relatively inert and do not represent a nuisance or health hazard.

SAMPLING CONSIDERATIONS

The preparation of air samples must be matched to the analytical technique to be used. Although the physical separation of sample components is not absolutely required even for a detailed analysis (high-resolution mass spectrometry (MS), especially with low-fragmentation ionization methods is another possibility), it is clearly desirable. Gas chromatography (GC) with high-resolution capillary columns is, at present, the most powerful approach for the type of analysis considered. The use of

such instruments requires relatively small samples, usually in the low μl range, with preferably low water content.

The most important sampling requirements can be summarized as follows:

(a) Concentration in the desired volatility range with minimal interference from moisture

(b) Complete and nondiscriminatory collection

(c) Quantitative and unaltered regeneration

(d) Compatibility with the instrument used for analysis

(e) Simplicity

Several different approaches have been offered in the past. Syringe injection, or sample loops[5–10] are useful only for relatively concentrated samples, unless special selective and sensitive detection techniques are applied such as multiple ion detection by MS. Cryogenic condensation with containers or onto packed columns[11–26] is limited by the presence of water which will condense. On the other hand, this approach is well suited for gases and reactive substances and application of a temperature gradient ensures excellent recovery[27]. Drying agents have been used sometimes prior to condensation; their use, however, is questionable for less volatile substances, and labile or reactive compounds as found in tobacco smoke might be altered or absorbed.

Gas–solid adsorption onto carbonaceous adsorbents of high surface areas has been the most popular concentration method before synthetic polymers have become commercially available. Activated carbon[28–35] has been frequently used, often in combination with solvent extraction[1,36–41]. Carbon molecular sieve[42,43] has also been applied, however, excessive temperatures are required for sample regeneration by thermal desorption. Adsorption onto surface-modified siliceous supports[44] has been described, but these materials are commercially not available.

Synthetic polymers of hydrophobic nature have been introduced within the last few years and are now becoming increasingly popular for the enrichment of organic substances from dilute media. Several types of commercially available polymers have been applied to the concentration of trace organics from air[45–57]. Thermal elution has considerable advantages over solvent extraction methods, if the adsorbent can meet certain requirements. Besides adequate capacity for the compounds to be analyzed, avoidance of artifacts due to outgassing products and inertness are of prime importance. Not all organic adsorbents fulfill these requirements. Specially treated graphitized carbon blacks have also been applied for air sampling[58].

There are advantages and disadvantages to each principle which is applicable for the concentration of trace organics from air. Unfortunately, there is no universal method which can be used for a very wide volatility range. Methods must be combined to achieve some overlap. Cigarette smoke unfortunately falls into this category, sinse it includes a large variety of substances of various polarity, ranging from permanent gases to virtually involatile polymers and other high-molecular-weight substances. In dilute cigarette smoke in room air, semivolatile substances seem to account for the bulk of the material nonsmokers are exposed to. Our investigation has been directed towards this volatility range. The restriction however is not by choice but is rather dictated by the analytical tools, including both sampling methods and analytical instrumentation, which are currently available.

EXPERIMENTAL

Sampling

Air samples were taken in a room having a total volume of 60 m^3. The sampler consisted of a vacuum source, a flow meter and set of three parallel tubes containing the adsorbent. Pyrex glass tubes 115 × 7 mm O.D. × 5 mm I.D. were filled with Tenax GC 60–80 mesh (Applied Science, State College, Pa., U.S.A.) and Carbopack BHT (Supelco, Bellefonte, Pa., U.S.A.). Both adsorbents were also coated with 5% and 25% of OV-101 silicon fluid. The uncoated tubes were conditioned at 330° for 60 min with nitrogen as carrier gas, the coated tubes were conditioned overnight.

Cigerettes (standard reference cigarette, IRI, University of Kentucky, Lexington, Ky., U.S.A.) were smoked under standard conditions. Immediately after a cigarette had been smoked, an air sample of 3.5 l was taken in triplicate at a flow-rate of 220 ml/min per tube. Samples were usually analyzed immediately.

For comparison, cigarette smoke samples were taken with a simple sampler of our own design. The device (Fig. 1) consisted of three parallel adsorbent tubes connected to a vacuum source via a flow meter. A fine metering valve and a shut-off valve (Whitey, Oakland, Calif., U.S.A.) were located between vacuum source and flow meter. The conditions were adjusted to yield puffs of 35 ml volume and 2 sec duration. To obtain the desired amount of cigarette smoke from a 2-sec puff, one of the tubes, having a variable restriction, served as bypass. An aliquot of only 3 ml of the smoke was drawn through each of the two sampling tubes during a puff. The samples, as evidenced by their gas chromatograms were relatively reproducible, but no effort was made to study the variations. The air samples were taken in Houston, Texas, and Tuscaloosa, Ala., over a period of several weeks.

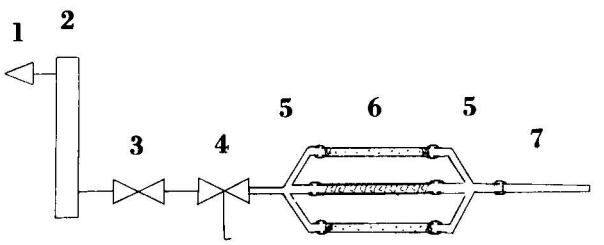


Fig. 1. Sampler for a small fraction of a standardized puff of fresh cigarette smoke. 1 = Vacuum source; 2 = flow meter; 3 = shutoff valve; 4 = fine metering valve; 5 = flow dividers and sample tube holders; 6 = adsorbent tubes and bypass tube; 7 = cigarette.

GC and GC–MS

A Hewlett-Packard GC 5830 with a flame ionization detector (FID), and a Hewlett-Packard GC 5720 with FID were used. Both instruments were modified to accept glass capillary columns. Additional injector ports were added to the instruments to accommodate the adsorbent tubes. Glass capillary columns of 0.35 mm I.D. and lengths between 25 and 55 m were drawn from soft glass, and either deactivated by Carbowax treatment according to Blomberg[59] or by standard silylation methods. OV-101 (Supelco, Bellefonte, Pa., U.S.A.) served as stationary phase. The columns were coated by either a modified plug method or the static procedure originally pro-

posed by Ilkova and Mistryukov[60]. In the latter procedure in which the filled glass capillary is screwed into a hot oven, a heated mercury interface has been added. Columns were tested for efficiency and absorptive behavior. Average efficiencies, measured for *n*-decane at 100° were 2000–2600 effective plates per meter. Standards of phenolic compounds and aromatic amines were used to test the acid/base behavior of the column surfaces. Trapping periods of 30 min at 270° were allowed to compensate for the relatively large volume of the injector port. The purge gas passed through the entire column. No breakthrough was observed. Liquid nitrogen served as coolant.

Identifications were performed on a LKB 9000 gas chromatograph–mass spectrometer as described previously[61]. The column in the gas chromatograph–mass spectrometer was flow-controlled and rather reproducible over a period of several months. Mass spectra were deducted by comparison with reference spectra kept in our laboratory in files and with the use of standard tables[62]. In some cases where standards were available, small amounts of the references were added to the adsorbent tube by direct injection.

RESULTS AND DISCUSSION

Tobacco smoke analysis is one of the most challenging tasks for an analyst. Difficulties are encountered in both sampling procedures and the analysis itself. Nevertheless tobacco smoke condensate has been thoroughly investigated and its composition is now fairly well established. Grob applied capillary columns to cigarette smoke as early as 1962[63] and provided a comprehensive discussion on the analytical aspects with respect to sampling and especially column requirements[64–66]. Others have also used capillary column GC–MS[67–71] and further extended identifications.

Tobacco smoke analysts divide the total smoke into several overlapping fractions which have been well characterized. Little, however, is known about the fate of cigarette smoke condensate, as it ages and is exposed to air. It can be expected that variations in the smoke are reflected in the composition of volatiles found in air. Since a pyrolytic process is involved in the generation of the smoke, samples are often difficult to reproduce. For analysis, fresh cigarette smoke is desirable, but sample reproducibility may be low. Tobacco smoke condensate generated by smoking machines under standardized conditions is more reproducible, but changes inevitably occur during storage. The analyst is faced with the decision whether to apply a sampling technique which does deliver fresh tobacco smoke but which may not be easily reproducible from laboratory to laboratory or to use a more standardized technique which may generate additional artifacts.

It is common to distinguish between volatiles, semivolatiles and nonvolatiles. For the purpose of this investigation, the term "volatiles" refers to the material which can be collected and regenerated on an adsorbent, regardless if it is a true gaseous form or associated with particulate matter. As a basic rule, stable substances having boiling points between benzene and *n*-pentacosane fall into that category. To determine if significant differences could be determined between cigarette smoke in room air, filtered through a glass fiber filter and between unfiltered air, a short experiment was undertaken. Two tubes were connected in parallel and a glass fiber filter, as used for the collection of air particulate matter, was placed before the orifice of one tube. No significant differences were found.

The purpose of this investigation was the determination of the nature and approximate quantity of volatiles non-smokers are exposed to in the presence of smokers. An investigation was therefore undertaken to determine the suitability of several adsorbents for the selective concentration of organics from air. Only adsorbents were considered which permit thermal elution of the substances of interest at a moderate temperature, without generation of artifacts or absorptive losses. These requirements eliminate most of the classical adsorbents, such as activated carbon or silica gel, because of high surface activity or high affinity for water. Our previous experiences with a number of different adsorbents also indicated that crosslinked DVB polymers would not be suitable for the purpose, due to their limited temperature stability and high background. Silica beads modified by surface esterification were excluded because of their small sample capacity and sensitivity towards hydrolysis.

Tenax GC and Carbopack fulfill more requirements. Unfortunately, the capacities of these adsorbents are quite small and usually insufficient for substances being more volatile than benzene, unless a large quantity of adsorbent is used. In principle, the trapping efficiency can be improved by this method. In practice, the acceptable amount of adsorbent however is limited, primarily by an increase in background contamination from the adsorbent and by water which does accumulate on both sample tube and adsorbent. During desorption, small amounts of water can then cause a physical obstruction in a small-bore capillary column, disrupting the transfer process.

For quantitative analysis, it is important to ensure that the adsorbent has adequate capacity for the substances under investigation. Sample recovery at trace levels must also be confirmed, since irreversible losses can easily occur, especially for adsorbents which are not completely homogeneous.

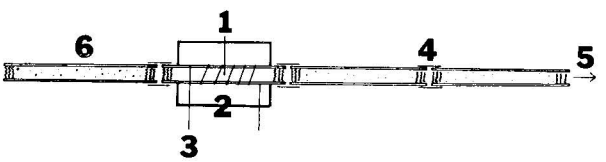


Fig. 2. Arrangement for the determination of breakthrough volumes and sample recoveries. 1 = Tube with small glass wool plug; 2 = thermal insulation; 3 = heating type; 4 = adsorbent tubes, in series; 5 = vacuum source; 6 = adsorbent tube for exclusion of air volatiles.

Fig. 2 shows the experimental arrangement which was used to evaluate breakthrough volumes and desorption efficiencies of some model compounds on Tenax GC. A standard was injected into a heated tube which preceeded two sampling tubes in series, and a constant volume of air was drawn through the tubes. After injection, an additional tube was placed in front of the injection tube to exclude air volatiles. The adsorbent tubes were relatively small in size, 88 × 2.5 mm I.D., and contained approximately 70 mg of Tenax GC. Results are summarized in Table I. It should be noted that adsorption efficiencies depend on several parameters, such as sample size, amount of adsorbent, flow-rate, temperature, geometrical arrangement, etc. Fortunately, adsorbent capacity does not seem to be influenced to any extent by the moisture in the air[72]. Losses were estimated by difference with direct injections.

TABLE I

RECOVERY OF SELECTED COMPOUNDS ON TWO ADSORBENT TUBES CONNECTED IN SERIES

Conditions: tube, 88 × 2.2 mm I.D.; filled with Tenax GC, 60–80 mesh; flow-rate, 80 ml/min for 12 min; sampling temperature, 22–26°; desorption temperature, 320°; amount of single component, 30–100 ng.

Compound	*MW*	*B.p. (°C)*	*Recovery (%)**		*Lost***
			Tube 1	*Tube 2*	
Alcohols					
Methanol	32	65	< 2	< 4	>90
Ethanol	46	79	< 3	< 5	>90
Isopropanol	60	82	55	20	25
1-Hexanol	103	158	>90	< 5	< 5
1-Octanol			>95	< 5	< 3
Ketones					
Acetone	58	56	35	25	40
Methyl isobutyl ketone	100	117	95	< 5	< 3
2-Octanone	128	173	95	< 5	< 3
Alkanes					
n-Pentane	72	36	35	30	35
n-Hexane	86	69	65	20	15
n-Octane	114	126	>95	< 5	< 3
n-Decane	143	174	>95	< 5	< 3
n-Tetradecane	198	254	>95	< 5	< 3
n-Octadecane	255	316	>95	< 5	< 3
Cyclohexane	84	81	75	15	10
Alkenes					
1-Octene	112	121	>95	< 5	< 3
Esters					
Ethyl acetate	88	77	65	25	10
Butyl acetate	116	126	>95	< 5	< 3
Halogenated hydrocarbons					
Dichloromethane	85	40	15	20	65
Chloroform	119	62	85	10	5
Bromoform	253	150	>95	< 5	< 3
Trichlorotrifluoroethane	187	478	15	15	20
Aromatic hydrocarbons					
Benzene	78	80	65	30	5
Toluene	92	111	>95	< 5	< 3
Ethylbenzene	106	136	>95	< 5	< 3
Cumene	120	152	>95	< 5	< 3
Mesitylene	120	165	>95	< 5	< 3

* Average results from 3 runs.

** Calculated by difference.

In another series of experiments, Tenax GC and Carbopack BHT, having surface areas of approximately 20 m^2/g and 90 m^2/g (ref. 73) were compared to each other. Data are summarized in Table II. It can be seen that Carbopack BHT retains low-molecular-weight compounds slightly better than Tenax GC. Additional coating of these adsorbents with a high-temperature liquid phase of low viscosity should extend

TABLE II

RELATIVE TRAPPING EFFICIENCIES FOR COATED *VERSUS* NONCOATED TENAX GC AND CARBOPACK BHT

	Tenax 60–80		*Tenax 5% OV-101*		*Tenax 25% OV-101*		*Carbopack BHT*		*Carbopack 5% OV-101*		*Carbopack 25% OV-101*	
	Outer	*Inner*	*Outer*	*Inner*	*Outer*	*Inner*	*Outer*	*Inner*	*Outer*	*Inner*	*Outer*	*Inner*
C_6H_5	100	100	100	45	100	80	100	100	100	170	≈100	≈100
C_6H_5–CH_3	100	<2	100	4	100	7	100	<5	100	<5	100	0
C_6H_5–C_2H_5	100	0	100	0	100	<3	100	≈0	100	30	100	≈0

the usefulness of either adsorbent towards more volatile compounds. The data obtained support this prediction, the improvement, however, is smaller than expected. In general, Carbopack BHT and Tenax GC are comparable in performance.

Selective concentration of trace organics from air at ambient temperature followed by direct desorption is an attractive sampling approach, but the method has some inherent contradictions which limit its usefulness. The adsorbent, on one hand, should provide adequate and nonspecific retentions for substances of a wide boiling point range. This requirement can be met by choosing an adsorbent with a larger surface area. On the other hand, desorption temperatures, necessary for complete sample regeneration, especially of less volatile compounds also increases with increasing adsorbent activity. Obviously, a compromise must be found.

It is conceivable that the overall usable range of such gas–solid adsorption–thermal elution processes could be extended by the use of several adsorbents having different surface areas or by multilayer traps. In the latter, high-molecular-weight substances would be adsorbed on a less active adsorbent in the front section of the sample tube and only the more volatile compounds would move to the more active adsorbent layers. Sample regeneration could be done under relatively mild conditions. Preliminary experiments are still unsatisfactory and more work is needed to establish this procedure for practical use.

Most volatiles in urban air are clearly associated with gasoline. The absolute levels vary considerably depending primarily on sample location and weather conditions. Samples were taken within a short time interval to avoid drastic changes of the background. The contribution of cigarette smoke to the volatiles already present in an urban atmosphere is smaller than may be expected from its general appearance and odor perception. It is difficult to distinguish between the relatively small additions of volatiles coming from tobacco smoke under such background variations, but no effort was made to suppress the hydrocarbon background or to enhance the concentration of the cigarette smoke beyond a level which would not relate to conditions usually encountered in practice. Cigarettes were smoked in relatively large rooms and the cigarette smoke was strongly diluted under these circumstances. No attempt was made to analyze tobacco smoke itself. Cigarette smoke samples were only taken for purposes of comparison.

Fig. 3 shows the total ion current monitor profiles obtained from a 3.5-l sample of urban air, from a sample of the same volume, after a cigarette had been smoked, and from a 3-ml puff of the cigarette used for the experiment. Differences between the air samples are primarily in the higher molecular weight range.

Table III lists the identifications of both volatiles in urban air and the additions which result from the action of cigarette smoking. The quantitations are only semiquantitative, since many of the peaks are composed of several unresolved substances. Some breakthrough of components has been observed over the entire range of the chromatogram, regardless of boiling point or substance type. This phenomenon still needs to be explained. Sample loss due to insufficient retention, however, is minor for the substances eluting after toluene (peak 42). For compounds eluting between benzene and toluene, adsorbent capacity might have been exceeded by a factor of 2 or 3. The picture gets progressively worse for the compounds eluting before benzene. These regions have therefore been omitted from quantitation.

It would be interesting to investigate the retention of tobacco smoke compo-

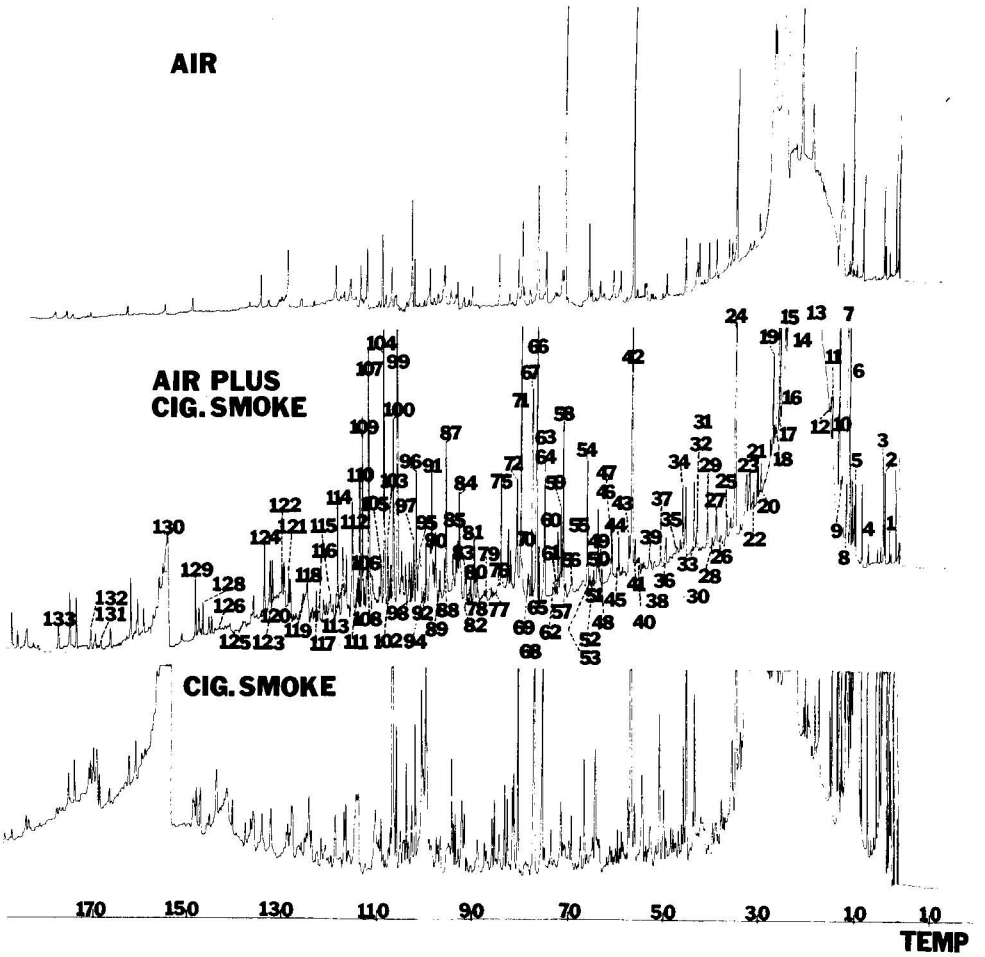


Fig. 3*. Total ion current chromatograms of urban air, air contaminated by cigarette smoke and cigarette smoke. Sample size of air samples, 3.5 l; sample size of cigarette puff, 3 ml; glass capillary column: 38 m × 0.35 mm I.D., coated with OV-101; carrier gas (helium) flow-rate, 3 ml/min; temperature program: 20° for 8 min, 20–200° at 2°/min. For identification of peaks, see Table III.

nents in lung tissue. Preliminary investigations indicate that compounds found in tobacco smoke are still exhaled for a considerable time after the smoking process. An investigation into aspects of selective retention of some smoke constituents is presently underway.

* *Editor's note:* Fig. 3 contains very valuable information. It compares 3.5 l of air from a room in which a cigarette was smoked to a 3.5-ml puff of cigarette smoke. The 3.5-l volume is approximately the vital capacity (*i.e.*, the average volume which a person inspires and expires during normal respiration). From comparing the two chromatograms, it is evident that a person breathing in a room where one cigarette was smoked inspires the equivalent of a 3.5-ml puff of cigarette smoke (with 10 to 12 respirations per minute). Thus, I cannot agree to the authors' statement that "the amount of volatiles added to air by cigarette smoking is insignificant". *Editor of J. Chromatogr.*

TABLE III

IDENTIFICATION OF VOLATILES IN AIR AND AIR CONTAMINATED BY TOBACCO SMOKE

Peak No.	*Compound*	*MW*	*Approximate concentration (ppb)*		*Method*
			In air without cigarette smoke	*In air with cigarette smoke*	
1	1-Pentene	70			MS
2	C_5H_{12}	72			MS
3	Acetaldehyde	44			MS
4	C_5H_{12}	72			MS
5	*n*-Pentane	72			GC–MS
6	Acrolein	46			MS
7	Isoprene	68			MS
8	C_6H_{12}	84			MS
9	2-Methylbutane	70			MS
10	Furan	68			GC–MS
11	Diethylether	74			MS
12	Dichloromethane	84			GC–MS
13	2-Methylpentane	86			MS
14	3-Methylpentane	86			MS
15	C_6H_{12}	84			GC–MS
16	*n*-Hexane	86			GC–MS
17	Dimethylbutene	84			MS
18	Chloroform	118			GC–MS
19	Ethylacetate	88			MS
20	4-Methyl-2-pentene	84			MS
21	2-Methylcyclopentane	84			MS
22	C_6H_{12}	84			MS
23	Dichloroethylene	96			MS
24	Benzene	78			GC–MS
25	C_8H_{12}	108			MS
26	C_6H_{10}	82			MS
27	Methylhexane	100			MS
28	1,5-Hexadiene	82			MS
29	C_7H_{16}	100			MS
30	Cyclohexene	82			MS
31	1,2-Dimethylcyclopentane	98			MS
32	C_7H_{14}	98			MS
33	Trichloroethylene	130			MS
34	*n*-Heptane	100			MS
35	*n*-C_7H_{14}	98			GC–MS
36	C_2-Alkylcyclopentane	98			MS
37	2-Methyl-2-hexene	98			MS
38	2,4-Dimethylhexane	114			MS
39	C_8H_{16}	112			
40	C_8H_{18}	114			MS
41	2-Methylheptane	114			MS
42	Toluene	92	40	45	GC–MS
43	C_8H_{18}	114		2	
44	2,5-Dimethylhexane	114	2	2	MS
45	3-Methylheptane	114		1	MS
46	1,1-Dimethylcyclohexane	112	2	4	MS

(Continued on p. 782)

TABLE III *(continued)*

Peak No.	*Compound*	*MW*	*Approximate concentration (ppb)*		*Method*
			In air without cigarette smoke	*In air with cigarette smoke*	
47	C_8H_{16}	112		4	MS
48	C_8H_{16}	112		1	MS
49	C_8H_{16}	112		8	MS
50	2,5-Dimethy-1,2-hexene	112	1	8	MS
51	1,3-Dimethylcyclohexane	112		1	MS
52	Tetrachloroethylene	164		1	GC–MS
53	C_8H_{18}	114		1	MS
54	C_8H_{16}	112	6	6	MS
55	C_8H_{18}	114		10	MS
56	C_2-Cyclohexane	106		1	
57	Trimethylcyclopentane	110		2	
58	C_8H_{16}	112	50	45	MS
59	C_3-Cyclopentane	112		7	MS
60	1,1,3-Trimethylcyclohexane	128		6	MS
61	C_9H_{18}	126		1	MS
62	C_3-Cyclohexane	126		3	MS
63	Ethylbenzene	106	5	12	GC–MS
64	C_3-Cyclohexane	126		12	MS
65	C_9H_{16}	124		5	MS
66	*m*-Xylene + *p*-xylene	106	18	50	GC–MS
67	Methyloctane	128		25	MS
68	C_9H_{18}	126	1	2	
69	3-Ethylheptane	128		4	MS
70	Diethylpentane	128	1		MS
71	Styrene	104	5	35	MS
72	*o*-Xylene	106	3	7	GC–MS
73	C_9H_{16}	124		3	GC–MS
74	C_9H_{18}	126		5	MS
75	*n*-Nonane	128		8	GC–MS
76	C_9H_{18}	126		1	MS
77	$C_{10}H_{20}$	140		1	
78	Cumene	120		2	GC–MS
79	*n*-Nonyne	124		2	MS
80	C_3-Benzene	120		2	MS
81	α-Pinene	136	2	7	GC–MS
82	$C_{10}H_{20}$	140		3	MS
83	C_3-Benzene	120	1	5	MS
84	C_3-Benzene	120	2	15	MS
85	C_3-Benzene	120		4	MS
86	$C_{10}H_{20}$	140	2	2	MS
87	$C_{10}H_{22}$	142	3	20	MS
88	β-Pinene	36	1	4	MS
89	5-Methyldecane	156	1	3	MS
90	Methylstyrene	118		6	MS
91	C_3-Benzene	156	3	12	MS
92	$C_{10}H_{20}$	190		7	MS
93	$C_{11}H_{24}$	156	1		MS
94	1,3-Dichlorobenzene	146		3	GC–MS
95	$C_{11}H_{24}$	156		7	MS
96	*n*-Decane	142	10	13	GC–MS
97	C_3-Benzene	120		6	MS

TABLE III *(continued)*

Peak No.	*Compound*	*MW*	*Approximate concentration (ppb)*		*Method*
			In air without cigarette smoke	*In air with cigarette smoke*	
98	C_4-Benzene	134		5	MS
99	Limonene	178		40	GC–MS
100	$C_{10}H_{26}$	170	5	18	MS
101	$C_{11}H_{22}$	154	2	1	MS
102	C_4-Benzene	134		5	MS
103	$C_{11}H_{22}$	154	6	2	MS
104	$C_{11}H_{24}$	156		25	MS
105	C_4-Benzene	134	1	6	MS
106	C_4-Benzene	134		4	MS
107	Undecane	156	6	23	GC–MS
108	C_4-Benzene	134		6	MS
109	$C_{12}H_{26}$	170	4	15	MS
110	Methyldecane	156		13	MS
111	C_4-Benzene	134		3	MS
112	$C_{12}H_{26}$	170	4	9	MS
113	C_4-Benzene	134		7	MS
114	2-Methyldecane	156		10	MS
115	C_4-Benzene	134		1	MS
116	$C_{12}H_{26}$	170		2	MS
117	1-Methylindane	132		3	MS
118	C_5-Benzene	148		5	MS
119	C_5-Benzene	148		4	MS
120	C_5-Benzene	148		1	MS
121	Naphthalene	128		3	MS
122	1-Methyl-(1,2,3,4-tetrahydronaphthalene)	156		3	MS
123	C_5-Benzene	148		3	MS
124	*n*-Dodecane	170		7	GC–MS
125	Phenylhexane	162		2	MS
126	2-Methylnaphthalene	142		1	MS
127	$C_{12}H_{24}$	168		2	MS
128	1-Methylnaphthalene	142		3	MS
129	Tridecane	184		7	GC–MS
130	Nicotine			40	MS
131	Phenyloctane	190		2	MS
132	Dimethylphthalate	194		2	MS
133	Diethylphthalate	222		3	MS

ACKNOWLEDGEMENT

We would like to thank E. Anderson and H. Mayfield for experimental assistance.

REFERENCES

1 K. Grob and G. Grob, *J. Chromatogr.*, 62 (1971) 1.
2 W. Bertsch, R. C. Chang and A. Zlatkis, *J. Chromatogr. Sci.*, 12 (1974) 175.
3 W. Wynder and D. Hoffman, *Tobacco and Tobacco Smoke*, Academic Press, New York, 1967.
4 I. Schmeltz, *The Chemistry of Tobacco and Tobacco Smoke*, Plenum Press, New York, 1972.

5 J. H. Simmons, in S. G. Perry and E. R. Adlard (Editors), *Gas Chromatography 1972*, Applied Science Publ., Barking, 1973, p. 17.
6 R. A. Rasmussen, *Air Pollut. Contr. Ass. J.*, 7 (1972) 537.
7 K. Bretschneider, R. Fahnert and J. Otto, *Z. Gesamte Hyg. Ihre Grenzgeb.*, 10 (1972) 18.
8 R. A. Rasmussen, *Environ. Sci. Technol.*, 4 (1970) 667.
9 R. A. Rasmussen and F. W. Went, *Proc. Nat. Acad. Sci. U.S.*, 53 (1965) 215.
10 A. P. Altshuller and C. A. Clemons, *Anal. Chem.*, 34, 4 (1962) 466.
11 C. Narrain, P. J. Marron and J. H. Glover, in S. G. Perry and E. R. Adlard (Editors), *Gas Chromatography 1972*, Applied Science Publ., Barking, 1973, p. 1.
12 L. S. Young, *Summary of Testing for Trace Contaminants in the Biosatellite III Spacecraft Atmosphere*, Ames Research Center, Moffett Field, Calif., Report N71-21510, Oct. 1970.
13 H. de Schmertzing, S. S. Nelson and H. G. Eaton, USAF School of Aerospace Medicine, Aerospace Medical Division (AFSC), Brooks Air Force Base, Texas, Report SAM-TR-67-68, August, 1967.
14 R. A. Rasmussen, H. H. Westberg and M. Holdren, *J. Chromatogr. Sci.*, 12 (1974) 80.
15 R. A. Rasmussen, *Amer. Lab.*, 4 (1972) 7.
16 K. H. Bergert, V. Betz and D. Pruggmair, *Chromatographia*, 7, 3 (1974) 115.
17 S. Pilar and W. F. Graydon, *Environ. Sci. Technol.*, 7 (1973) 628.
18 C. Vicotra, A. Cornu, R. Mossot and P. Perilhon, in S. G. Perry and E. R. Adlard (Editors), *Gas Chromatography 1972*, Applied Science Publ., Barking, 1973, p. 9.
19 B. Dimitriades and D. E. Seizinger, *Environ. Sci. Technol.*, 5 (1971) 223.
20 A. P. Altshuller, W. A. Lonneman, F. D. Sutterfield and S. L. Kopczynski, *Environ. Sci. Technol.*, 5 (1971) 1009.
21 W. A. Lonneman, T. A. Bellar and A. P. Altshuller, *Envron. Sci. Technol.*, 2 (1968) 1017.
22 D. A. McEwen, *Anal. Chem.*, 38 (1966) 1047.
23 I. H. Williams, *Anal. Chem.*, 37 (1965) 1723.
24 T. A. Bellar, M. F. Brown and J. E. Sigsby, Jr., *Anal. Chem.*, 35 (1963) 1924.
25 P. S. Farrington, R. L. Pecsok, R. L. Meeker and T. J. Olson, *Anal. Chem.*, 31 (1959) 1512.
26 L. Rohrschneider, A. Jaeschke and W. Kubik, *Chem.-Ing.-Tech.*, 43 (1971) 1010.
27 R. E. Kaiser, *Anal. Chem.*, 45 (1973) 965.
28 R. Herbolsheimer, L. Funk and H. Drasche, *Staub—Reinhalt. Luft.*, 32 (1972) 31.
29 R. Herbolsheimer, *Staedtehygiene*, 12 (1972) 280.
30 F. E. Saalfeld, F. W. Williams and R. Saunders, *Amer. Lab.*, 3 (1971) 8.
31 R. A. Saunders and R. H. Gammon, *The Sealab II Trace Contaminant Profile*, NRL Report 6636, 1967.
32 R. A. Saunders, M. E. Umstead, W. D. Smith and R. H. Gammon, *The Atmospheric Trace Contaminant Pattern of Sealab II, Proceedings of the 3rd Annual Conference on Atmospheric Contamination in Confined Spaces*, AMRL-TR-67-200 (1967).
33 A. J. Chiantella, W. D. Smith, M. E. Umstead and J. E. Johnson, *Amer. Ind. Hyg. Assoc., J.*, 27 (1966) 186.
34 R. A. Saunders, *Atmospheric Contamination in Sealab I, Proceedings of the Conference on Atmospheric Contamination in Confined Spaces*, AMRL-TR-65-230 (1965).
35 R. A. Saunders, *Analysis of Spacecraft Atmospheres*, NRL Report 5316, 1962.
36 F. X. Mueller and T. A. Miller, *Amer. Lab.*, 5 (1974) 49.
37 Th. zur Muehlen, *Zentralbl. Arbeitsmed. Arbeitsschutz*, 22, 9 (1072) 264.
38 G. Jennings and H. E. Nursten, *Anal. Chem.*, 39 (1967) 521.
39 S. M. Rappaport and D. A. Fraser, *Anal. Chem.*, 48 (1976) 476.
40 B. Levadie and S. MacAskill, *Anal. Chem.*, 47 (1975) 1851.
41 B. Levadie and S. MacAskill, *Anal. Chem.*, 48 (1976) 76.
42 A. Raymond and G. Guiochon, *Analusis*, (1973) 357.
43 A. Raymond and G. Guiochon, *Environ. Sci. Technol.*, 8 (1974) 143.
44 W. A. Aue and P. M. Teli, *J. Chromatogr.*, 62 (1971) 15.
45 A. Dravnieks, B. K. Krotosznski, J. Whitfield, A. O'Donnell and T. Burgwald, *Environ. Sci. Technol.*, 5 (1971) 1220.
46 F. W. Williams and M. E. Umstead, *Anal. Chem.*, 40 (1969) 2232.
47 B. Versino, M. de Groot and F. Geiss, *Chromatographia*, 7, 6 (1974) 302.
48 J. P. Mieure and M. W. Dietrich, *J. Chromatogr. Sci.*, 11 (1973) 559.

49 W. V. Ligon and R. L. Johnson, *Anal. Chem.*, 48 (1976) 481.
50 E. D. Pellizzari, T. E. Bunch, R. E. Berkley and T. McRae, *Anal. Chem.*, 48 (1976) 803.
51 D. Ellgehausen, *Anal. Chem.*, 272 (1974) 284.
52 L. S. Frankel and R. F. Black, *Anal. Chem.*, 48 (1976) 732.
53 J. W. Russell, *Environ. Sci. Technol.*, 9 (1975) 1175.
54 K. P. Evans, A. Mathias, N. Mellor, R. Sylvester and A. E. Williams, *Anal. Chem.*, 47 (1975) 821.
55 T. S. Fritz and R. C. Chang, *Anal. Chem.*, 46 (1974) 938.
56 W. Bertsch, A. Zlatkis, H. M. Liebich and H. T. Schneider, *J. Chromatogr.*, 99 (1974) 673.
57 H. M. Liebich, W. Bertsch, A. Zlatkis and H. T. Schneider, *Aviat. Space Environ. Med.*, 46 (1975) 1002.
58 F. Bruner, P. Ciccioli and F. Di Nardo, *J. Chromatogr.*, 99 (1974) 661.
59 L. Blomberg, *J. Chromatogr.*, 115 (1975) 365.
60 E. L. Ilkova and E. A. Mistryukov, *J. Chromatogr. Sci.*, 9 (1971) 569.
61 W. Bertsch, E. Anderson and G. Holzer, *J. Chromatogr.*, 112 (1975) 701.
62 *Eight Peak Index of Mass Spectral Data*, Mass Spectrometry Data Centre, Aldermaston, 2nd ed., 1970.
63 K. Grob, *Beitr. Tabakforsch.*, 9 (1962) 315.
64 K. Grob, *J. Gas Chromatogr.*, 3 (1965) 52.
65 K. Grob, *Beitr. Tabakforsch.*, 3 (1966) 403.
66 K. Grob and J. A. Voellmin, *Beitr. Tabakforsch.*, 5 (1969) 52.
67 L. Blomberg and G. Widmark, *J. Chromatogr.*, 106 (1975) 59.
68 K. D. Bartle, L. Bergstedt, M. Novotný and G. Widmark, *J. Chromatogr.*, 45 (1969) 256.
69 C. R. Enzell, E. Bergstedt, T. Dalhamn and W. H. Johnson, *Beitr. Tabakforsch.*, 6 (1971) 41.
70 D. Schueller, C. J. Drews and H. P. Harke, *Beitr. Tabakforsch.*, 6 (1971) 84.
71 G. Neurath, M. Duenger and I. Kuestermann, *Beitr. Tabakforsch.*, 6 (1971) 12.
72 J. Janák, J. Růžičková and J. Novák, *J. Chromatogr.*, 99 (1974) 689.
73 K. Sakodynskii, L. Panina and N. Klinskaya, *Chromatographia*, 7 (1974) 339.

Journal of Chromatography, 126 (1976) 787–794
© Elsevier Scientific Publishing Company, Amsterdam — Printed in The Netherlands

CHROM. 9419

APPLICATION OF HIGH-SPEED LIQUID CHROMATOGRAPHY TO THE ANALYSIS OF POLYOXYETHYLENE SURFACTANTS AND THEIR DECOMPOSITION PRODUCTS IN INDUSTRIAL PROCESS WATERS

R. M. CASSIDY and C. M. NIRO

General Chemistry Branch, Atomic Energy of Canada Limited, Chalk River Nuclear Laboratories, Chalk River, Ontario K0J 1J0 (Canada)

SUMMARY

Complementary high-speed liquid chromatographic techniques have been combined with infrared spectroscopy for the characterization and analysis of polyoxyethylene fatty acid surfactants and their decomposition products in industrial process waters. The combination of molecular sieve chromatography and infrared spectroscopy offers a selective and simple method for the analysis of trace concentrations (detection limit approx. 0.05–0.1 ppm) of these surfactants. Liquid–solid and reversed-phase chromatography have proven useful for the characterization and analysis of free fatty acids. Some of the parameters that affect the reversed-phase separation of fatty acids are discussed.

INTRODUCTION

Fatty acid esters of polyoxyethylenes (POE), a common class of non-ionic surfactants, are used extensively in industry. In GS heavy water-plants, based on a dual temperature process for the exchange of deuterium between water and hydrogen sulfide, *i.e.* the so-called Girdler-Sulfide process, these surfactants are used in formulations, such as antifoams, that are used to help control processes that affect the hydrogen–deuterium isotopic exchange. Large concentrations of these surfactants and/or their decomposition products (mainly fatty acids) can cause excessive foaming and also decrease oil coalescer efficiency. Consequently, it has been important to have analytical methods for the surfactants and their decomposition products that can be applied to process waters (hydrogen sulfide-saturated water containing large amounts of oil, organosulfur compounds, and other organics), effluent water, and bulk oil.

A wide variety of analytical methods for POE non-ionic surfactants is available and these have been reviewed recently[1]. The analysis of non-ionic surfactants is very difficult[1] and most of the methods developed have been applied only to the analysis of commercial formulations and are not selective enough for the determination of small concentrations in complex matrices. Recent applications of high-speed liquid chromatography (HSLC)[2–7] have illustrated its potential for the characterization of POE surfactants. Both liquid–solid and liquid–liquid systems have been used. For

liquid–solid systems we found irreversible absorption occurred on silica gel and eventually the column changed to a liquid–liquid system. Strong absorption of POE surfactants on silica gel has also been observed elsewhere[4]. For both liquid–solid and liquid–liquid systems a portion of the POE surfactants studied in this work was sterically excluded from the pores of the support causing rapid elution of the large molecules followed by broad tailing peaks. Consequently, these HSLC techniques are not suitable for the analysis of these surfactants. Molecular sieve chromatography (MSC) should not have these problems of steric exclusion and adsorption. However, a problem of sensitive and selective detection still exists since these compounds exhibit no apprecialbe UV adsorption. We felt that a combination of MSC and infrared (IR) spectroscopy might prove suitable for the analysis of these surfactants.

In the presence of heat and acids, fatty acid esters hydrolyze to give free POE and fatty acids. Fatty acids are foaming agents and it is important to be able to follow their concentration with time. Methods for fatty acid analysis can also be used to characterize the fatty acids used for the manufacture of these surfactants, important information which is often not available. The separation of fatty acids by HSLC has been reviewed recently[8]. Most studies have used derivatization to improve UV detection, but direct analysis does offer some advantages[9]. Since our initial studies had indicated that the concentrations of fatty acids were sufficient for refractive index (RI) detection, it was felt that a reversed-phase system could be used for the separation and analysis of fatty acids.

EXPERIMENTAL

Reagents and materials

High-purity solvents were used where possible (Burdick and Jackson, Muskegon, Mich., U.S.A.). All other chemicals were reagent grade except for fatty acid standards, which were high-purity reagents (Chromatographic Specialties, Brockville, Ont., Canada). Two main formulations of fatty acid POE esters were studied in this work, *viz.* MYRJ (mono fatty acid ester), and a mixture of disubstituted fatty acid esters (linoleic, linolelaidic, oleic, and elaidic acids). The molecular sieve columns were standardized with C_5–C_{40} *n*-hydrocarbons (Chromatographic Specialties) and polystyrene and polypropylene standards (Waters Assoc., Milford, Mass., U.S.A.). The molecular sieve packings (15–37 μm) were styrene-divinylbenzene copolymers (Styragel; Waters Assoc.). This small-particle packing (15–37 μm) was slurry packed into 90 cm $\times$ 4.8 mm I.D. stainless-steel columns as described previously[10]. The 10 cm $\times$ 4.8 mm clean-up column was slurry packed with 20 μm silica gel (LiChrosorb SI-60; Brinkmann, Rexdale, Ont., Canada). A C_{18} μBondapak column (Waters Assoc.) was used for reversed-phase separations.

The liquid chromatographs were custom-built from commercial components and have been described elsewhere[10]. Samples were introduced by syringe injection into a modified sample loop[10]. IR spectra were recorded in microcells (2.5 or 4.5 μl, Perkin-Elmer, Montreal, Quebec, Canada) with a Perkin-Elmer Model 467 spectrophotometer.

Surfactant standardization

Known amounts of the surfactant were added to a mixture of 0.5 ml pump-seal

oil (a C_{25} hydrocarbon oil and the major organic component present in the process water) and 100 ml water. The final concentrations of the surfactant were normally 2, 5, 8, and 10 μg/ml. These mixtures were extracted with 10 ml of chloroform and 3-ml aliquots of the extracts were evaporated to dryness under nitrogen. These residues were separated by MSC and the high-molecular-weight fraction that contained the emulsifier was collected and evaporated to dryness. This fraction was dissolved in carbon tetrachloride (10–50 μl) and the absorption at 1740 cm^{-1} was measured using a IR micro cell.

Fatty acid clean-up

Oil samples and dried extracts from chloroform or methylene chloride extractions from water samples were dissolved in the mobile phase (20% chloroform in hexane, sample volume approx. 2.5 ml) and injected into a 10-ml sample loop. The sample was then washed onto the column at a flow-rate of 7–8 ml/min and the oil and other non-polar components were eluted (10–15 ml wash). Then the sample loop was filled with 10% methanol in chloroform and this was used to elute the fatty acids. The first 5–8 ml of eluate, which contained the acids, were collected and saved for the reversed-phase separation. The column was then reconditioned with approx. 30 ml of the original mobile phase.

RESULTS AND DISCUSSION

Surfactant characterization

Before the analysis results for POE surfactants or their decomposition products can be interpreted sensibly, the chemical composition of the surfactant must be known. Our experience has shown that MSC is valuable for rapid, routine monitoring of surfactant formulations. Total sample analysis is one of its main advantages and since the surfactants are relatively large molecules, any imputiries (normally free POE or fatty acids) present are usually well separated. If desired, fractions are easily obtained for IR spectra to tell if the surfactants are mono- or disubstituted POE (presence or absence of characteristic R–OH frequency for terminal OH group) or if the impurities are mainly POE (OH stretch) and/or fatty acids (C=O stretch and hydrogen bonded OH). Fig. 1 illustrates the usefulness of MSC. The surfactant was autoclaved with hydrogen sulfide to study its decomposition under plant conditions but other acids, such as hydrochloric, could be used if only surfactant characterization is of interest. From this chromatogram the extent of decomposition could be easily determined and IR spectra of peaks A and B showed these components were POE and carboxylic acids, respectively. The acids were further separated by reversed-phase chromatography (see below) and found to be a mixture of linoleic, linolelaidic, oleic, and elaidic acids. All C_{18} acids gave molecular sizes equivalent to C_{23} *n*-hydrocarbons, possibly due to solvation effects. From this information it was possible to reasonably estimate the chemical composition of the surfactant.

Surfactant analysis

The analysis of POE surfactants is complicated by the fact that they contain large numbers of telomers and the distribution of these can vary. Consequently, the

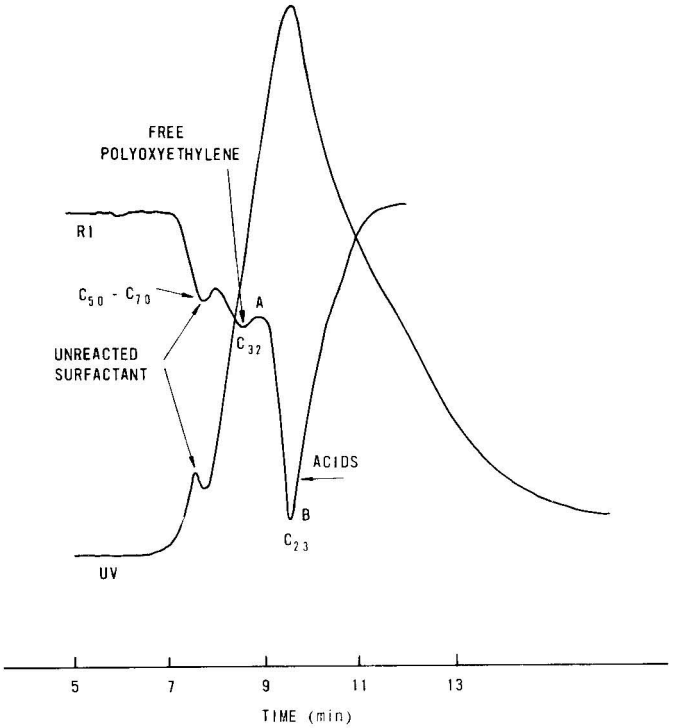


Fig. 1. Molecular sieve separation of surfactant after contact with hydrogen sulfide and water at 150° for 110 h. Experimental conditions: column, 1 m × 4.5 mm I.D. Styragel 100; mobile phase, chloroform; flow-rate, 1 ml/min; sample, 100 μl of approx. 2 mg/ml solution; refractive index and UV detection. Equivalent molecular sizes in terms of *n*-hydrocarbons are indicated on the curves.

choice of a standard is difficult. For this work samples of commercial products were used and their purity was checked by MSC.

MSC has two main attractive features for the preliminary separation of POE surfactants. Firstly, it is not too selective and the majority of the telomers can be collected quickly and in a small volume. Secondly, it quickly separates the high-molecular-weight surfactant molecules from the bulk of the other organics (C_{25} oil in this case). For some samples the ratio of organic to POE surfactant was approx. 3000:1. These features are illustrated in Fig. 2, which is representative of most of the process water samples analyzed. The dotted line shows the position at which the surfactant is eluted.

Due to the poor sensitivity of LC detectors for these fatty acid esters, detection is not possible on the shoulder of the peak due to the other organics, but this fraction can be collected for further analysis. The peak at 15 min is elemental sulfur[10]. For simple and rapid analysis of the surfactant in this fraction it was felt that IR offered the best choice of selectivity and sensitivity. The detection limits were found to be approx. 10 μg for a 100-ml water sample (0.1 ppm) and this could be reduced if larger water samples were extracted. Standard curves were linear and the relative standard deviation for 100-ml, 2-ppm standards, containing 0.5 ml oil, was 10%.

A large number of water and oil samples have been analyzed for POE surfactants and the results are considered satisfactory. Further improvements in reprodu-

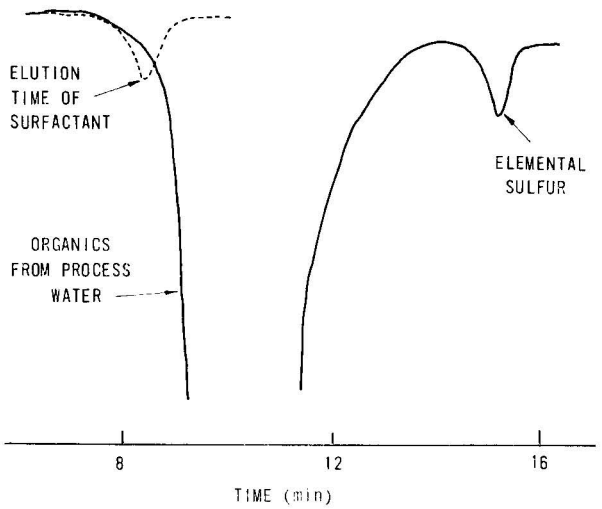


Fig. 2. Molecular sieve separation of surfactant from process water extract. Experimental conditions: column, 1 m × 4.8 mm I.D. Styragel 100; mobile phase, chloroform; flow-rate, 1 ml/min; samples 250 μl (1/4 of total) of extract from 100 ml water; refractive index detection.

ibility are not considered warranted due to the problem of choice of standard. Selectivity is good and the large concentrations of fatty acids (up to 4 mg/ml oil) and free POE do not interfere. Plastic bottles are not recommended for sample storage. Not only can plastic adsorb and/or absorb trace organics but it will also contaminate samples with phthalate plasticizers which can interfere with the analysis of lower-molecular-weight POE surfactants.

If more than one type of POE surfactant is present, then this method will give only semi-quantitative results, unless the molecular weights of the two surfactants are significantly different so as to permit their separation by MSC. Since the fatty acid content of POE surfactants is often different for different formulations, it appears that the best method for the analysis of mixtures might be a combination of MSC clean-up with gas chromatographic analysis of the fatty acids via transesterification.

Fatty acid analysis

Free POE and fatty acids were the two main decomposition products found for POE surfactants under GS process conditions. The concentration of free POE was not of direct interest and the analysis of this component was not studied.

For fatty acid analysis, clean-up on silica gel gave good recoveries (>98%) and reproducibility (relative standard deviation, approx. 1% for 0.7–4 mg/ml oil). Most of the samples studied were bulk oil and for these it is important to wash all the oil off the column prior to elution of the acids. Small volumes of oil in the eluate will extract the acids and cause low results. The effectiveness of the clean-up procedure was reflected by the steady baselines and reproducible retention times for the reversed-phase separation of the acids discussed below.

For the reversed-phase separation of fatty acids (only C_{12}–C_{18} acids were of

interest in this work) the choice of mobile phase was an important factor. With solvents less polar than water, such as acetonitrile or methanol, long retention times and very broad peaks and unreproducible results were observed (Fig. 3a). The addition of small amounts of water gave better results (Fig. 3b) but small concentrations of acetic acid were much more effective (Fig. 3c). Increases in the acetic acid concentration (0.1–0.8%) caused only a slight reduction in capacity factors (k')*. When the series C_3, C_4, C_7, C_9, and C_{10} *n*-carboxylic acids was used in place of acetic acid there was a small increase in k' up to C_9 and then a decrease with C_{10}. When C_9 and C_{10} acids were used as modifiers, they were desorbed on sample injection and observed as peaks in the chromatogram.

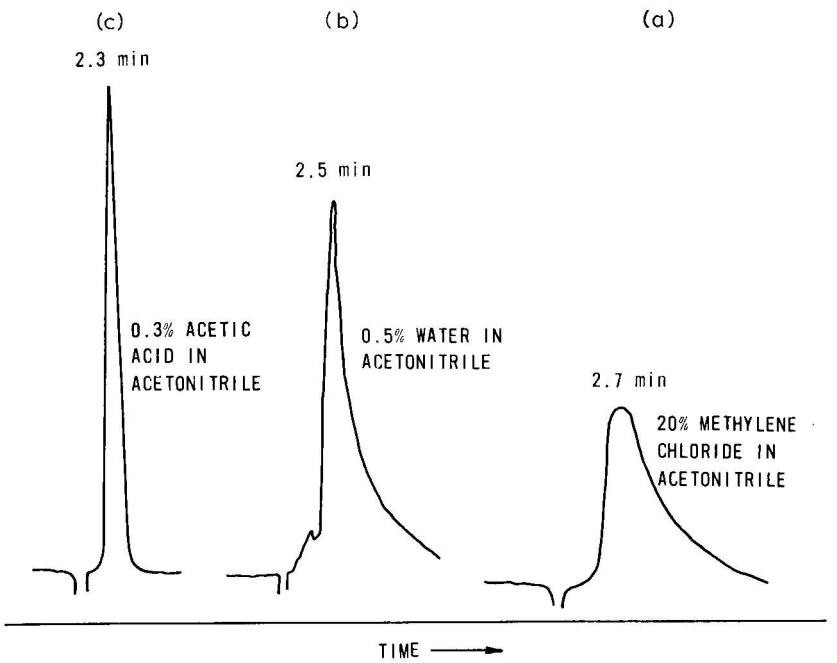


Fig. 3. Effect of polar modifiers on peak symmetry. Experimental conditions: column, 30 cm C_{18} μBondapak; flow-rate, 2.0 ml/min; sample, 100 μl of an approx. 1 mg/ml solution of dodecanoic acid in the mobile phase; refractive index detection.

The mechanism by which these acids improve reproducibility and peak symmetry is not completely understood. Deactivation of free silanol groups on the reversed-phase packing is not likely important since with the solvent used, fatty acids are eluted at the solvent front on silica gel columns and peak symmetry is good. Deactivation of impurities introduced during the preparation of the packing[11] could play a role but the importance of this is uncertain. Carboxylic acids form dimers and this type of interaction between the acid modifier and sample could be important. This interaction would cause a reduction in k' and explain the increase in k' with

* k' = (peak retention time − inert peak retention time)/ (inert peak retention time).

chain length of the acid modifier. The maximum in k' at C_9 is likely a result of overloading of the support with modifiers larger than C_9.

The effect of basic modifiers was examined briefly. Pyridine, a weak base, gave only slight improvements. Diethylamine, a much stronger base, gave symmetrical peaks but reduced k' to approx. 0 for all components of interest.

Various mixtures of acetonitrile or methanol with methylene chloride and/or water were examined as mobile phases. The best solvent system was a mixture of methanol (major component) with methylene chloride and water plus 0.1–0.3% acetic acid. This was a better solvent for the fatty acids than acetonitrile-based solvents. The k' of the acids was easily controlled through variations in the water and methanol content. Fig. 4 shows the separation of four acids with one of the solvent systems used. With this mixed solvent system evaporation in the solvent reservoir caused small changes in solvent composition and baseline shift was severe unless a long narrow reservoir was used.

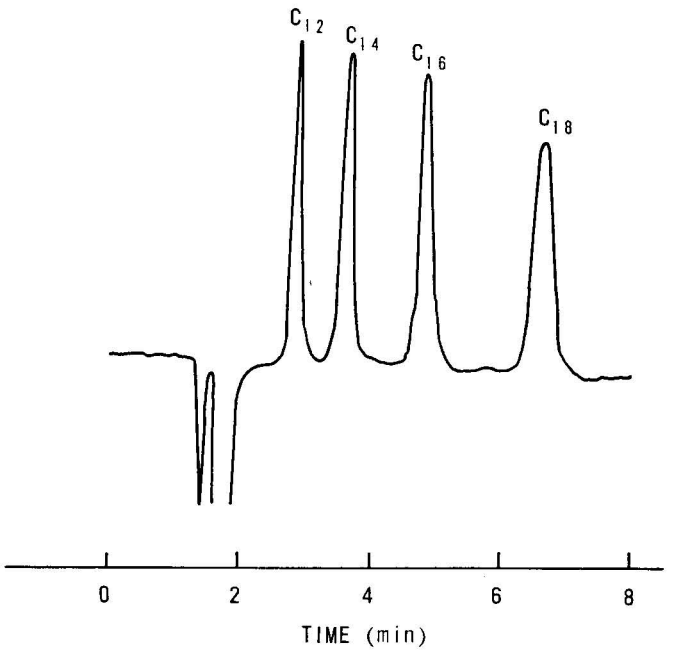


Fig. 4. Reversed-phase separation of straight-chain saturated fatty acids. Experimental conditions: column, 30 cm C_{18} μBondapak; flow-rate, 2.0 ml/min; mobile phase, 68% methanol, 16% methylene chloride, 16% water, 0.2% acetic acid; sample, 100 μl of approx. 1 mg/ml solution of fatty acids; refractive index detection.

The combination of liquid–solid clean-up and reversed-phase analysis of fatty acids has proven valuable for monitoring fatty acid concentration changes which are related to changes in POE surfactant formulations and for the identification of the fatty acids obtained when the surfactants are hydrolyzed. Fig. 5 shows the separation of the decomposition products from one of the surfactants studied. For this surfactant the HSLC identification of linolelaidic and elaidic acids, the *trans* isomers of linoleic and oleic acids, respectively, was more definitive than were mass spectrometric results.

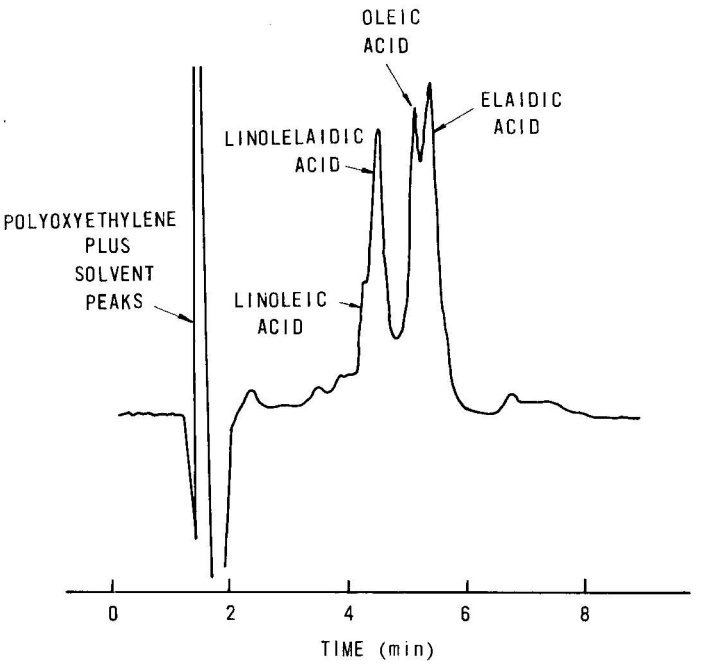


Fig. 5. Reversed-phase separation of surfactant after contact with hydrogen sulfide and water at 150° for 110 h. Experimental conditions, as for Fig. 4.

CONCLUSIONS

A combination of HSLC techniques and IR spectroscopy offers rapid and selective methods for the routine monitoring of POE fatty acid surfactants and free fatty acids in industrial process waters. These techniques can also be used to characterize unknown POE surfactants.

REFERENCES

1 G. F. Longman, *Talanta*, 22 (1975) 621.
2 K. J. Bombaugh, *J. Chromatogr.*, 53 (1970) 27.
3 K. J. Bombaugh, R. E. Levangie, R. N. King and L. Abrahams, *J. Chromatogr. Sci.*, 8 (1970) 657.
4 J. F. K. Huber, F. F. M. Kolder and J. M. Miller, *Anal. Chem.*, 44 (1972) 105.
5 M. Krejci, M. Rounda and Z. Vavrouch, *J. Chromatogr.*, 91 (1974) 549.
6 C. F. Allen and L. I. Rice, *J. Chromatogr.*, 110 (1975) 151.
7 J. H. van Dijk, R. R. Lamping, C. Slagt and A. W. J. Raaijmakers, *Tenside Deterg.*, 12 (1975) 261.
8 M. J. Cooper and M. W. Anders, *J. Chromatogr. Sci.*, 13 (1975) 407.
9 B. A. Bidling-Meyer, R. V. Vivilecchia and D. C. Clark, Jr., *Pittsburgh Conf. Anal. Chem. Appl. Spectrosc., 27th, Cleveland, Ohio, March 1976.*
10 R. M. Cassidy, *J. Chromatogr.*, 117 (1976) 71.
11 D. C. Locke, *J. Chromatogr. Sci.*, 11 (1973) 120.

Author Index

Abbott, S. R.
——, Berg, J. R., Achener, P. and Stevenson, R.
Chromatographic reproducibility in high-performance liquid chromatographic gradient elution 421
Achener, P., see Abbott, S. R. 421
Alexander, G., see Maskarinec, M. P. 559
Alexander, J., see Jellum, E. 487
Ali, S. L.
Application of gas–liquid chromatography and high-performance liquid chromatography to the analysis of trace amounts of salicylic acid, acetylsalicylic anhydride and acetylsalicylsalicylic acid in aspirin samples and aspirin formulations 651
Anderson, E., see Bertsch, W. 213
Annino, R.
——, Curren, Jr., J., Kalinowiski, R., Karas, E., Lindquist, R. and Prescott, R.
Totally pneumatic gas chromatographic process stream analyzer 301
Asai, K.
——, Kanno, Y.-I., Nakamoto, A. and Hara, T.
A flow controller for high-performance liquid chromatography and its applications 369
Asmus, P. A.
——, Jorgenson, J. W. and Novotný, M.
Fluorescence enhancement. New selective detection principle for liquid chromatography 317
Axelson, M.
—— and Sjövall, J.
Selective liquid chromatographic isolation procedure for gas chromatographic–mass spectrometric analysis of 3-ketosteroids in biological materials 705
Badger, C. M. A.
——, Harris, J. A., Scott, K. F., Walker, M. J. and Phillips, C. S. G.
Heater-displacement chromatography 11
Bakalyar, S. R.
—— and Henry, R. A.
Variables affecting precision and accuracy 327
in high-performance liquid chromatography
Bauer, H., see Voelter, W. 693
Berg, J. R., see Abbott, S. R. 421
Bertoni, G., see Ciccioli, P. 757
Bertsch, W.
——, Anderson, E. and Holzer, G.
Characterization of coal-derived fluids by capillary column gas chromatography–mass spectrometry 213
——, see Holzer, G. 771
Boksányi, L.
—— and Kováts, E. sz.
A study of column performances in gas chromatography. A C_{87} hydrocarbon on chemically modified supports 87
Boshoff, P. R.
——, Hopkins, B. J. and Pretorius, V.
Thin-layer chromatographic transport detector for high-performance liquid chromatography 35
Brancaleoni, E., see Ciccioli, P. 757
Brooks, C. J. W., see Gaskell, S. J. 591
Broś, E.
—— and Page, F. M.
Continuous stirred reactor model as basis for optimisation of electron capture detector operation in coulometric and constant current modes 271
Brown, III, A. C., see Cram, S. P. 279
Brown, P. R., see Hartwick, R. A. 679
Bruner, F., see Ciccioli, P. 757
Bursa, J., see Rezl, V. 723
Butts, E. T., see Rabel, F. M. 731
Caputo, A. G., see Rabel, F. M. 731
Cassidy, R. M.
—— and Niro, C. M.
Application of high-speed liquid chromatography to the analysis of polyoxyethylene surfactants and their decomposition products in industrial process waters 787
Chambaz, E. M., see Madani, C. 161
Chebroux, P., see Madani, C. 161
Chesler, S. N., see Cram, S. P. 279
Chrétien, J. R.
—— and Dubois, J.-É.
New perspectives in the prediction of Kováts indices 171
Ciccioli, P.
——, Bertoni, G., Brancaleoni, E., Fratarcangeli, R. and Bruner, F.
Evaluation of organic pollutants in the open air and atmospheres in industrial sites using graphitized carbon black traps and gas chromatographic–mass spectrometric analysis with specific detectors 757
Colin, H.
—— and Guiochon, G.
Development and use of carbon adsorbents in high-performance liquid–solid chromatography. I. Carbon-coated silica particles 43
Colomé, J., see Sánchez, M. C. 601

Comba, M. E., see Onuska, F. I. 133
Cotter, R. L., see Little, J. N. 439
Cram, S. P.
——, Chesler, S. N. and Brown, III, A. C.
Effects of digital filters on chromatographic signals 279
Curren, Jr., J., see Annino, R. 301
Curtius, H. Ch.
——, Mettler, M. and Ettlinger, L.
Study of the intestinal tyrosine metabolism using stable isotopes and gas chromatography–mass spectrometry 569
Dessy, R. E.
——, Reynolds, W. D., Nunn, W. G., Titus, C. A. and Moler, G. F.
New mini-computer automated linear photodiode array spectrometer system for high-resolution liquid chromatography 347
Dimitrova, Z. St., see Vitenberg, A. G. 205
Dubois, J.-É., see Chrétien, J. R. 171
Durand, J., see Madani, C. 161
Ebel, S.
—— and Hocke, J.
Computer-controlled evaluation in thin-layer chromatography. Results and possibilities 449
Edmonds, C. G., see Gaskell, S. J. 591
Ettlinger, L., see Curtius, H. Ch. 569
Feibush, B., see Weinstein, S. 97
Foltz, R. L., see Graffeo, A. P. 717
Franken, J. J.
——, Rutten, G. A. F. M. and Rijks, J. A.
Preparation of glass capillary columns coated with polar phase for high-temperature gas chromatography. I. Study of roughening of the glass surface 117
Fratarcangeli, R., see Ciccioli, P. 757
Frei, R. W.
——, Michel, L. and Santi, W.
Post-column fluorescence derivatization of peptides. Problems and potential in high-performance liquid chromatography 665
Fritz, D., see Riedo, F. 63
Gaskell, S. J.
——, Edmonds, C. G. and Brooks, C. J. W.
Applications of boronate derivatives in the study of ceramides by gas–liquid chromatography–mass spectrometry 591
Gelpí, E., see Sánchez, M. C. 601
Giese, R. W., see Petersen, B. A. 503
Gil-Av, E., see Weinstein, S. 97
Graffeo, A. P.
——, Lin, D. C. K. and Foltz, R. L.
Analysis of benzoylecgonine in urine by high-performance liquid chromatography and gas chromatography–mass spectrometry 717
Grushka, E., see Mott, S. D. 191
Guiochon, G., see Colin, H. 43
Haegele, K. D.
——, Skrdlant, H. B., Robie, N. W., Lalka, D. and McNay, Jr., J. L.
Determination of hydralazine and its metabolites by gas chromatography–mass spectrometry 517
Haken, J. K.
—— and Ho, D. K. M.
Quantitative pyrolysis studies of styrene, acrylate ester systems, and their α-methyl-substituted homologs 239
Halász, I.
——, Schmidt, H. and Vogtel, P.
Particle size, pressure and analysis time in routine high-performance liquid chromatography 19
Hanson, R. N., see Petersen, B. A. 503
Hara, T., see Asai, K. 369
Harris, J. A., see Badger, C. M. A. 11
Hartwick, R. A.
—— and Brown, P. R.
Evaluation of microparticle chemically bonded reversed-phase packings in the high-pressure liquid chromatographic analysis of nucleosides and their bases 679
Helland, P., see Jellum, E. 487
Henderson, D. E., see Uden, P. C. 225
Henry, R. A., see Bakalyar, S. R. 327
Ho, D. K. M., see Haken, J. K. 239
Hocke, J., see Ebel, S. 449
Holzer, G.
——, Oró, J. and Bertsch, W.
Gas chromatographic–mass spectrometric evaluation of exhaled tobacco smoke 771
——, see Bertsch, W. 213
Hopkins, B. J., see Boshoff, P. R. 35
Horning, E. C., see Pfaffenberger, C. D. 535
Horning, M. G., see Stafford, M. 495
Horvath, C.
—— and Lin, H.-J.
Movement and band spreading of unsorbed solutes in liquid chromatography 401
Hsu, F., see Shanfield, H. 457
Huesgen, G., see Liebich, H. M. 465
Ioffe, B. V., see Vitenberg, A. G. 205
Janiga, Š., see Krupčík, J. 147
Jellum, E.
——, Størseth, P., Alexander, J., Helland, P., Stokke, O. and Teig, E.
Application of glass capillary-column gas chromatography–mass spectrometry to the studies of human diseases 487
Jorgenson, J. W., see Asmus, P. A. 317
Kaiser, R. E., see Ševčík, J. 263
Kalinowiski, R., see Annino, R. 301

Kaljurand, M., see Küllik, E. 249
Kanno, Y.-I., see Asai, K. 369
Karas, E., see Annino, R. 301
Karger, B. L., see Petersen, B. A. 503
Karmen, A., see Lehrer, M. 615
Kim, K., see Zlatkis, A. 475
Koel, M., see Küllik, E. 249
Koshy, K. T.
Structure–gas chromatographic electron capture sensitivity relationships of some substituted 17α-acetoxyprogesterones 641
Kováts, E. sz., see Riedo, F. 63
——, see Boksányi, L. 87
Kristín, M., see Krupčík, J. 147
Krupčík, J.
——, Kristín, M., Valachovičová, M. and Janiga, Š.
Effect of etching with gaseous hydrogen chloride on the quality of glass capillary columns 147
Küllik, E.
——, Kaljurand, M. and Koel, M.
Analysis of pyrolysis gas chromatograms using pattern recognition techniques 249
Laffort, P.
—— and Patte, F.
Solubility factors in gas–liquid chromatography. Comparison between two approaches and application to some biological studies 625
Lalka, D., see Haegele, K. D. 517
Lehrer, M.
—— and Karmen, A.
Chemical ionization mass spectrometry for rapid assay of drugs in serum 615
Liebich, H. M.
—— and Huesgen, G.
Rapid quantitative microanalysis of ketones in urine by gas chromatography–mass fragmentography 465
Lin, D. C. K., see Graffeo, A. P. 717
Lin, H.-J., see Horvath, C. 401
Lindquist, R., see Annino, R. 301
Little, J. N.
——, Cotter, R. L., Prendergast, J. A. and McDonald, P. D.
Preparative liquid chromatography using radially compressed columns 439
Lloyd, R. J., see Uden, P. C. 225
Lovelock, A. J., see Simmonds, P. G. 3
Lovelock, J. E., see Simmonds, P. G. 3
McDonald, P. D., see Little, J. N. 439
McNay, Jr., J. L., see Haegele, K. D. 517
Madani, C.
——, Chambaz, E. M., Rigaud, M., Durand, J. and Chebroux, P.
New method for the preparation of highly stable polysiloxane-coated glass open-tubular capillary columns and application to the analysis of hormonal steroids 161
Martin, A. J. P., see Shanfield, H. 457
Maskarinec, M. P.
——, Alexander, G. and Novotný, M.
Analysis of the acidic fraction of marijuana smoke condensate by capillary gas chromatography–mass spectrometry 559
Mathews, R. G., see Schwartz, R. D. 113
Mettler, M., see Curtius, H. Ch. 569
Michel, L., see Frei, R. W. 665
Middleditch, B. S.
Aldehyde condensation products as derivatives for the vapor phase analysis of biogenic amines 581
Moler, G. F., see Dessy, R. E. 347
Mott, S. D.
—— and Grushka, E.
Chromatographic solute identification using peak shape analysis 191
Nakamoto, A., see Asai, K. 369
Niro, C. M., see Cassidy, R. M. 787
Novotný, M., see Asmus, P. A. 317
——, see Maskarinec, M. P. 559
Nunn, W. G., see Dessy, R. E. 347
Onuska, F. I.
—— and Comba, M. E.
Preparation and application of surface-modified high-resolution wall-coated open tubular columns 133
Oró, J., see Holzer, G. 771
Page, F. M., see Broś, E. 271
Patte, F., see Laffort, P. 625
Petersen, B. A.
——, Hanson, R. N., Giese, R. W. and Karger, B. L.
Picogram analysis of free triiodothyronine and free thyroxine hormones in serum by equilibrium dialysis and electron capture gas chromatography 503
Pfaffenberger, C. D.
——, Szafranek, J. and Horning, E. C.
Gas chromatographic study of free polyols and aldoses in cataractous human lens tissue 535
Phillips, C. S. G., see Badger, C. M. A. 11
Prendergast, J. A., see Little, J. N. 439
Prescott, R., see Annino, R. 301
Pretorius, V., see Boshoff, P. R. 35
Rabel, F. M.
——, Caputo, A. G. and Butts, E. T.
Separation of carbohydrates on a new polar bonded phase material 731
Rehg, W. R., see Tesch, J. W. 743
Reynolds, W. D., see Dessy, R. E. 347
Rezl, V.
—— and Bursa, J.
Identification of organic compounds by an elution gas chromatography–reactor–frontal gas chromatography system 723

Rieder, R., see Ševčík, J. 263
Riedo, F.
——, Fritz, D., Tarján, G. and Kováts, E. sz.
A tailor-made C_{87} hydrocarbon as a possible non-polar standard stationary phase for gas chromatography 63
Rigaud, M., see Madani, C. 161
Rijks, J. A., see Franken, J. J. 117
Robie, N. W., see Haegele, K. D. 517
Rutten, G. A. F. M., see Franken, J. J. 117
Sakodynski, K. I.
——, Sokolovski, R. I., Tunitzki, N. I. and Volkov, S. A.
Possibility of increasing the selectivity of chromatographic separation under the action of laser radiation 257
Sánchez, M. C.
——, Colomé, J. and Gelpí, E.
Electron capture and multiple ion detection of benzodiazepine esters in pharmacokinetic studies 601
Santi, W., see Frei, R. W. 665
Schmidt, H., see Halász, I. 19
Schwartz, R. D.
—— and Mathews, R. G.
"Selectivity" of high-temperature liquid phases for gas chromatography 113
Scott, C. D.
——, Spence, R. D. and Sisson, W. G.
Pressurized, annular chromatograph for continuous separations 381
Scott, K. F., see Badger, C. M. A. 11
Ševčík, J.
——, Kaiser, R. E. and Rieder, R.
A semi-specific flame-ionization detection system 263
Shanfield, H.
——, Hsu, F. and Martin, A. J. P.
Use of a gaseous electrical discharge to induce fluorescence in organic compounds separated by thin-layer chromatography 457
Sievers, R. E., see Tesch, J. W. 743
Simmonds, P. G.
——, Lovelock, A. J. and Lovelock, J. E.
Continuous and ultrasensitive apparatus for the measurement of air-borne tracer substances 3
Sisson, W. G., see Scott, C. D. 381
Sjövall, J., see Axelson, M. 705
Skrdlant, H. B., see Haegele, K. D. 517
Sokolovski, R. I., see Sakodynski, K. I. 257
Spence, R. D., see Scott, C. D. 381
Stafford, M.
——, Horning, M. G. and Zlatkis, A.
Profiles of volatile metabolites in body fluids 495
Stevenson, R. L., see Abbott, S. R. 421
Stillwell, R. N.
—— and Stillwell, W. G.
Gas chromatographic–mass spectrometric–computer methods in the study of drug metabolism 547
Stillwell, W. G., see Stillwell, R. N. 547
Stokke, O., see Jellum, E. 487
Størseth, P., see Jellum, E. 487
Strukova, T. P., see Vitenberg, A. G. 205
Szafranek, J., see Pfaffenberger, C. D. 535
Tarján, G., see Riedo, F. 63
Teig, E., see Jellum, E. 487
Tesch, J. W.
——, Rehg, W. R. and Sievers, R. E.
Microdetermination of nitrates and nitrites in saliva, blood, water, and suspended particulates in air by gas chromatography 743
Titus, C. A., see Dessy, R. E. 347
Tunitzki, N. I., see Sakodynski, K. I. 257
Uden, P. C.
——, Henderson, D. E. and Lloyd, R. J.
Comprehensive interfaced pyrolysis gas chromatographic peak identification system 225
Valachovičová, M., see Krupčík, J. 147
Vitenberg, A. G.
——, Ioffe, B. V., Dimitrova, Z. St. and Strukova, T. P.
Application of gas chromatographic headspace analysis to the characterization of chemical equilibria in solutions 205
Voelter, W.
—— and Bauer, H.
High-performance liquid chromatographic analysis of the isomerization products of carbohydrates 693
Vogtel, P., see Halász, I. 19
Volkov, S. A., see Sakodynski, K. I. 257
Walker, M. J., see Badger, C. M. A. 11
Weinstein, S.
——, Feibush, B. and Gil-Av, E.
N-Acyl derivatives of chiral amines as novel, readily prepared phases for the separation of optical isomers by gas chromatography 97
Zlatkis, A.
—— and Kim, K.
Column elution and concentration of volatile compounds in biological fluids 475
——, see Stafford, M. 495

PUBLICATION SCHEDULE FOR 1976

Journal of Chromatography (incorporating *Chromatographic Reviews*)

MONTH	D 1975	J	F	M	A	M	J	J	A	S	O	N	D
JOURNAL	115/1 115/2	116/1 116/2	117/1 117/2	118/1 118/2	118/3 119	120/1 120/2	121/1 121/2	122 123/1	123/2	124/1 124/2 125/1	125/2 125/3	126 128/1	128/2 129
REVIEWS*					127/1				127/2			127/3	

* Volume 127 will consist of *Chromatographic Reviews*. The issues comprising this volume will not be published consecutively, but will appear at various times in the course of the year.

GENERAL INFORMATION

(A leaflet *Instructions to Authors* can be obtained by application to the publisher.)

Types of Contributions. (a) Original research work not previously published in a generally accessible language in other periodicals (Full-length papers). (b) Review articles. (c) Short communications and Notes. (d) Book reviews; News; Announcements. (e) Bibliography of Paper Chromatography, Thin-Layer Chromatography, Column Chromatography, Gas Chromatography and Electrophoretic Techniques. (f) Chromatographic Data.

Submission of Papers. Three copies of manuscripts in English, French or German should be sent to: Editorial office of the Journal of Chromatography, P.O. Box 681, Amsterdam, The Netherlands. For *Review articles*, an outline of the proposed article should first be forwarded to the Editorial office for preliminary discussion prior to preparation.

Manuscripts. The manuscript should be typed with double spacing on pages of uniform size and should be accompanied by a separate title page. The name and the complete address of the author to whom proofs are to be sent should be given on this page. Authors of papers in French or German are requested to supply an English translation of the title. A short running title of not more than 50 letters (including spaces between the words) is also required for Full-length papers and Review articles. All illustrations, photographs, tables, etc., should be on separate sheets.

Heading. The title of the paper should be concise and informative. The title should be followed by the authors' full names, academic or professional affiliations, and addresses.

Summary. Full-length papers and Review articles should have a summary of 50–100 words. In the case of French or German articles an additional summary in English, headed by an English translation of the title, should also be provided. (Short communications and Notes will be published without a summary.)

Illustrations. The figures should be submitted in a form suitable for reproduction, drawn in Indian ink on drawing or tracing paper. Particular attention should be paid to the size of the lettering to ensure that it does not become unreadable after reduction. Sharp, glossy photographs are required to obtain good halftones. Each illustration should have a legend, all the *legends* being typed together on a *separate sheet*. Coloured illustrations are reproduced at the author's expense.

References. References should be numbered in the order in which they are cited in the text and listed in numerical sequence on a separate sheet at the end of the article. The numbers should appear in the text at the appropriate places using superscript numerals. In the reference list, periodicals[1], books[2], and multi-author books[3] should be cited in accordance with the following examples:

1 A. T. James and A. J. P. Martin, *Biochem. J.*, 50 (1952) 679.
2 L. R. Snyder, *Principles of Adsorption Chromatography*, Marcel Dekker, New York, 1968, p. 201.
3 R. D. Marshall and A. Neuberger, in A. Gottschalk (Editor), *Glycoproteins*, Vol. 5, Part A, Elsevier, Amsterdam, 2nd ed., 1972, Ch. 3, p. 251.

Abbreviations for the titles of journals should follow the system used by *Chemical Abstracts*.

Proofs. Two sets of proofs will be sent to the author to be carefully checked for printer's errors. Corrections must be restricted to instances in which the proof is at variance with the manuscript. "Extra corrections" will be inserted at the author's expense.

Reprints. Fifty reprints of Full-length papers, Short communications and Notes will be supplied free of charge. Additional reprints can be ordered by the authors. An order form containing price quotations will be sent to the authors together with the proofs of their article.

News. News releases of new products and developments, and information leaflets of meetings should be addressed to: The Editor of the News Section, Journal of Chromatography, Elsevier Scientific Publishing Company, P.O. Box 330, Amsterdam, The Netherlands.

Subscription orders. Subscription orders should be sent to: Elsevier Scientific Publishing Company, P.O. Box 211, Amsterdam, The Netherlands.

Publication. The *Journal of Chromatography* (including *Chromatographic Reviews*) appears fortnightly and has 14 volumes in 1976. The subscription price for 1976 [Vols. 115–128 and Supplementary Vol. 5 (Bibliography of Paper and Thin-Layer Chromatography 1970–1973)] is Dfl. 1470.00 plus Dfl. 180.00 (postage) (total US$ 660.00). Subscribers in the U.S.A., Canada and Japan receive their copies by air mail. Additional charges for air mail to other countries are available on request. Back volumes of the *Journal of Chromatography* (Vols. 1 through 114) are available at Dfl. 100.00 plus postage. Claims for issues not received should be made within three months of publication of the issues. If not, they cannot be honoured free of charge.

Advertisements. Advertisement rates are available from the publisher on request. **The Editor of the journal accepts no responsibility for the content of the advertisements.**



CAMAG HPTLC

High Performance Thin-Layer Chromatography with the new CAMAG U-Chamber System

according to R. E. Kaiser

- This system provides controlled development of thin-layer (circular) chromatograms using the new type of high performance thin-layer chromatography plates for nano TLC.
- All phases of chromatography (stationary, mobile and gas) are kept under control.
- With this system, chromatography is fast and economical: The time required for chromatogram development ranges from 1 to 4 minutes and solvent consumption is only between 0.07 and 0.2 ml.
- For the first time this system provides correct experimental conditions for direct transfer of information from TLC to column chromatography (HPLC).
- Reproducibility of retention data is better than in HPLC.
- As in all TLC analyses, several samples (12 and more) can be chromatographed simultaneously.
- Extremely efficient enrichment procedures are easily employed without losing resolution.

Ask for complete HPTLC information from

CAMAG

4132 Muttenz/Schweiz
Homburgerstrasse 24
Tel. (061) 61 34 34

1000 Berlin 41
Bismarckstrasse 27–29
Tel. (030) 795 10 91

United States Affiliate, Main-Offices and Warehouse:
CAMAG Inc. 16229 West Ryerson, New Berlin, Wisconsin 53151

ref. no. 120

10 JUN 2